

ΦSX

Advanced Topics of Theoretical Physics I

Introduction to Solid-State Theory

Peter E. Blöchl

Caution! This is an unfinished draft version
Mistakes are unavoidable!

Institute of Theoretical Physics; Clausthal University of Technology;
D-38678 Clausthal Zellerfeld; Germany;
<http://www.pt.tu-clausthal.de/atp/>

don't panic!

© Peter Blöchl, 2000-February 27, 2024

Source: <https://phisx.org/>

Permission to make digital or hard copies of this work or portions thereof for personal or classroom use is granted provided that copies are not made or distributed for profit or commercial advantage and that copies bear this notice and the full citation. To copy otherwise requires prior specific permission by the author.

1

¹To the title page: What is the meaning of ΦSX ? Firstly, it sounds like "Physics". Secondly, the symbols stand for the three main pillars of theoretical physics: "X" is the symbol for the coordinate of a particle and represents Classical Physics. "Φ" is the symbol for the wave function and represents Quantum Physics "S" is the symbol for the entropy and represents Statistical Physics.

Foreword and outlook

This book is work in progress. This book is not completed and not proofread. You can use this book currently as a basis for following through the material presented in the course. However, you should never blindly copy formulas and apply them. The chances that there are still errors is too large.

This book provides an introduction into solid-state theory. This course concentrates on non-interacting particles, while interacting many-particle systems are considered in a following course “Advanced Solid-State Theory”.

The lecture has the following goals:

- **Electron-nuclear systems:** The students shall understand how to divide the description for a system of electrons and nuclei into one for electrons and one for nuclei. The students know the main approximations such as classical and Born-Oppenheimer approximation. They understand non-adiabatic effects and the relaxation process through conical intersections connecting excited states with the ground state.
- **Non-interacting electrons:** Students understand how non-interacting many-electron systems can be mapped onto a one-particle Schrödinger equation. Students are familiar with dispersion relations and their information content for particles and waves. Students understand Bloch theorem, are able to construct a band structure using the tight-binding method and can interpret a band structure. Students are familiar with the most important thermodynamic relations.
- **Non-interacting phonons:** Students are familiar how the concept of phonons emerges from a the classical nuclear dynamics. They understand the dispersion relation of phonons and typical approximations. Analogous to the case of electrons, students will understand to derive the main thermodynamic properties of non-interacting phonons.
- **Transport:** Students are familiar with the Boltzmann equation. Given the large variety of formulations of the Boltzmann equation, I will show how the Boltzmann equation is obtained from a minimum set of assumptions as theory relying on empirical parameters. Students will be familiar with the main approximations and understand the concept of quasi-Fermi level.

There are important omissions. To name a few, I do not cover phase transitions, microstructure and lattice defects in solids. I barely touch on magnetism and optical properties.

This lecture does not replace a course on solid-state physics, which covers the wide range of phenomena in solids, material-specific behavior, as well as experimental probes of solids. Rather, the present book concentrates on the main concepts underlying the theoretical description of processes in materials. Thus, it shall clarify the precise meaning of terms and the underlying assumptions.

My aim is to include all proofs in a comprehensive and hopefully water-tight manner. I am also avoiding special systems of units. I consider this important in view of a large variety of notations, differing definitions etc. While the proofs have the advantage to train the student to perform the typical operations, it clutters the course with material far from applications. Therefore, I have placed many of the more detailed derivations into appendices. On the graduate level, the student should be able to follow the proofs without problem. It is strongly recommended to follow through the derivations.

In the online version, there are many hyperreferences that allow to jump to the relevant information in the book. To avoid the additional cost for color printouts just for the references they are not visible. They still work, when you click on them. Here is a list of links set:

- List of contents
- references to equation numbers, figures, tables, sections, appendices, etc.
- citations will take you to the corresponding position in the list of references

Editor: TODO: The following are notes of the author to the author about planed modifications:

- Place the exercise about the Landau-Zener model into the appendix.
- Move the section on the H-Theorem in the chapter on the Boltzmann equation into the appendix. Leave the Boltzmann entropy, though.
- Discuss energy and momentum conservation for the intrinsic scattering probabilities in the chapter on the Boltzmann equation.

Contents

I	Lecture notes	15
1	The standard model of solid-state physics	17
1.1	The standard model	17
1.2	Home study and practice	20
1.2.1	Linear algebra of 2×2 matrices	21
1.2.2	Dirac's bra-ket notation	29
1.2.3	Dirac atom	32
1.2.4	Thermodynamics	34
1.2.5	Eigenvalue decomposition of non-hermitian matrices	37
2	Born-Oppenheimer approximation and beyond	43
2.1	Separation of electronic and nuclear degrees of freedom	44
2.1.1	Born-Oppenheimer wave functions and Born-Oppenheimer surfaces	44
2.1.2	Born-Huang Ansatz for the electronic-nuclear wave function	45
2.1.3	Nuclear Schrödinger equation	47
2.2	Born-Oppenheimer approximation	51
2.3	Non-adiabatic effects	52
2.3.1	Off-diagonal derivative couplings	53
2.3.2	Diagonal derivative couplings (optional)	54
2.4	Conical intersections	55
2.4.1	Non-crossing theorem and conical intersections	55
2.4.2	Poor man's demonstration of the non-crossing theorem	56
2.4.3	Jahn-Teller model	57
2.5	Outlook: trajectories	58
2.6	Summary	59
2.7	Home study and practice	59
2.7.1	Landau-Zener Formula (Optional)	59
2.7.2	Holstein model	62
2.7.3	Molecular dynamics	77
3	Many-particle wave functions	85
3.1	Spin orbitals	85
3.2	Symmetry and quantum mechanics	90
3.3	Identical particles	93
3.3.1	Levi-Civita symbol or the fully-antisymmetric tensor	94
3.3.2	Permutation operator	94

3.3.3	Antisymmetrize wave functions	95
3.3.4	Slater determinants	96
3.3.5	Bose wave functions	97
3.3.6	General many-fermion wave function	97
3.4	Occupation-number representation	98
3.5	Non-interacting electrons and one-particle wave functions	99
3.5.1	The one-particle view on many-particle wave functions	99
3.6	Home study and practice	103
3.6.1	Two Fermions in a 1d-box	103
3.6.2	Expectation values with a Slater determinant	115
4	Band structure of non-interacting electrons	121
4.1	Dispersion relations	121
4.1.1	Quasiparticles:	121
4.1.2	Free particles	122
4.1.3	Band structure of real systems	124
4.1.4	Correspondence principle	125
4.2	Crystal lattices	127
4.2.1	Reciprocal space revisited	127
4.2.2	Bloch theorem	129
4.2.3	Non-interacting electrons in an external potential (optional)	131
4.2.4	Zone schemes	132
4.3	Orbitals and Slater-Koster matrix elements	135
4.3.1	Orbitals	135
4.3.2	Slater-Koster matrix elements	136
4.3.3	Sign of $h_{pp\sigma}$ and $h_{pp\pi}$	136
4.4	Bands and orbitals	138
4.5	Calculating band structures in the tight-binding model	140
4.5.1	Bloch orbitals as basis functions (optional)	141
4.5.2	Worked example: alternating linear chain	142
4.6	Home study and practice	145
4.6.1	Tight-binding calculation of graphene	145
4.6.2	Band structure of high- T_C superconductors	151
4.6.3	Canonical p-band for the fcc structure	157
4.6.4	Local and itinerant states	166
4.6.5	Manganites	169
5	Expectation values and density of states	173
5.1	Brillouin-zone integrations	173
5.1.1	Periodic boundary conditions	173
5.1.2	Sum over states	174
5.2	Density of states	176
5.2.1	Density-of-states operator in the solid	179
5.3	Home study and practice	179
5.3.1	Jellium model	179
6	Thermodynamics of non-interacting electrons	183

6.1	A brief tour from statistical physics to thermodynamics	183
6.2	Fundamental relations of thermodynamics	185
6.3	Many-particle states of non-interacting electrons	186
6.4	Fermi distribution	188
6.4.1	Fermi-, Bose- and Boltzmann distribution	190
6.5	Thermodynamic integrations	191
6.5.1	Thermal smoothing of the density of states	192
6.5.2	Metals: Sommerfeld expansion	194
6.5.3	Insulators: expansion for $ \epsilon - \mu > k_B T$:	195
6.6	Thermodynamics of non-interacting electrons	196
6.7	Home study and practice	203
6.7.1	Free-electron gas	203
7	Phonons	213
7.1	Phonons as quasi particles	213
7.2	Connection to the Born-Oppenheimer framework	213
7.3	Harmonic oscillator revisited	220
7.4	Bloch theorem for phonons	223
7.4.1	Lattice-translation symmetry	223
7.4.2	Eigenstates of the lattice translation:	226
7.4.3	Block diagonalization of the dynamical matrix	227
7.4.4	Energies and Lagrangian in normal coordinates	229
7.5	Phonons	231
7.5.1	One-dimensional harmonic oscillator	232
7.5.2	Back to the normal modes of displacement fields	235
7.5.3	Comparison to the Schrödinger equation	242
7.5.4	Interaction picture in classical mechanics	242
7.5.5	Energy and momentum conservation of phonons	243
7.5.6	Left-and right-moving plane waves	243
7.6	Phonon band structures	245
7.6.1	Example for a phonon band structure	245
7.6.2	Acoustic branches	245
7.6.3	Optic branches of the phonon band structure	246
7.7	Thermodynamics of phonons	247
7.7.1	Thermodynamics: Models for the density of states	247
7.7.2	Grand potential	251
7.7.3	Internal energy	251
7.8	Worked Example: Phonon band structure of the two-site linear chain	251
7.8.1	Tasks	252
7.9	Worked example: phonon band structure of the hanging linear chain	255
7.9.1	Tasks	256
7.9.2	Discussion	256
8	Boltzmann equation	259
8.1	General form of the Boltzmann equation	259
8.1.1	Demonstration of the principle in real space	259

8.1.2	From coordinate space to phase space	260
8.1.3	Nature of Hamilton's functions	261
8.1.4	Many bands	261
8.1.5	Sources and Sinks	261
8.1.6	Boltzmann equation	262
8.1.7	Normalization	262
8.1.8	Combined index for bands and momentum	263
8.2	Collisions	264
8.2.1	Scattering of classical particles	264
8.2.2	Correlations and coherence	264
8.2.3	Energy and momentum conservation	265
8.2.4	Exclusion principle	265
8.2.5	Types of collisions	266
8.2.6	General form of the collision term	267
8.3	Thermal equilibrium	268
8.3.1	Boltzmann entropy	268
8.3.2	Equilibrium distributions	270
8.3.3	Detailed balance	271
8.3.4	Bare particles and quasi-particles	273
8.3.5	Summary	276
8.4	Inherent approximations	277
8.4.1	Molecular chaos	277
8.4.2	Classical versus quantum	277
8.4.3	Decoherence	277
8.5	Linearized Boltzmann equation	278
8.6	Relaxation-time approximation	280
8.7	Dynamics in the linearized Boltzmann equation	281
8.7.1	Dynamics in the relaxation-time approximation	284
8.8	Linear response	285
8.8.1	Linear response of the distribution to external forces	285
8.8.2	Transport coefficients	287
8.8.3	Transport coefficients in the relaxation time approximation	289
8.8.4	Examples	290
8.8.5	Response to temperature gradients	291
8.9	Quasi Fermi level	292
8.9.1	Quasi Fermi level	292
8.9.2	Boltzmann equation in terms of quasi Fermi levels:	292
8.10	Home study and practice	293
8.10.1	Electric conductivity and Seebeck coefficient of the free-electron gas	293
8.10.2	Thermal conductivity	298
8.10.3	No title yet	299
9	Tour of band structures and densities of states of real materials	301
9.1	Free-electron like metals	302
9.2	Noble metals	303
9.3	Transition metals	305

9.4	Diamond, zinc-blende and wurtzite-type semiconductors	308
9.5	Simple oxides	312
9.6	Graphene	313
9.7	Parent compound of high-temperature superconductors	315
9.8	What band structures are good for	317
9.8.1	Chemical stability	317
9.9	Home study and practice	317
9.9.1	Bandstructure and lifetime broadening	317
9.9.2	Peierls transition	320
II	Additional topics	323
10	Phonon scattering	327
10.1	Sketch of the derivation of the collision term of the Boltzmann equation for phonons	327
10.2	Equation of motion for the phonon amplitudes	328
10.3	Momentum and energy conservation	331
10.3.1	Momentum conservation	331
10.3.2	Energy conservation	332
10.4	Scattering	332
10.4.1	Compact notation	332
10.4.2	Perturbation theory	334
10.4.3	Density matrix	335
10.4.4	Initial random-phase approximation	336
10.4.5	Repeated random-phase approximation	340
10.4.6	Long-time limit, energy conservation and Fermi's golden rule	342
10.4.7	Phonon scattering without lattice expansion	345
10.4.8	Phonons coupling to elastic distortions	347
10.5	Kinetic equation	347
10.5.1	Units of quantities	350
10.6	Quantum derivation of the collision term	351
10.6.1	From the Lagrangian to ladder operators	351
10.6.2	The phonon Hamiltonian	353
10.6.3	Random-phase approximation and rate equation	355
10.6.4	Classical limit	360
10.6.5	Linearized Boltzmann equation	360
11	Density-functional theory	365
11.1	One-particle and two-particle densities	366
11.1.1	N-particle density matrix	366
11.1.2	One-particle reduced density matrix	366
11.1.3	Two-particle density	369
11.1.4	Two-particle density of the free-electron gas	372
11.1.5	Pair-correlation function and hole function	374
11.2	Self-made density functional	375
11.3	Constrained search	380
11.4	Self-consistent equations	382

11.4.1	Universal functional	382
11.4.2	Exchange-correlation functional	383
11.4.3	The self-consistency condition	383
11.4.4	Flow chart for a conventional self-consistency loop	386
11.4.5	Another minimum principle	386
11.5	Adiabatic connection	387
11.5.1	Screened interaction	389
11.5.2	Hybrid functionals	390
11.6	Functionals	391
11.7	X_α method	392
11.8	Local density functionals	393
11.9	Local spin-density approximation	394
11.10	Non-collinear local spin-density approximation	394
11.11	Generalized gradient functionals	394
11.12	Additional material	399
11.12.1	Relevance of the highest occupied Kohn-Sham orbital	399
11.12.2	Correlation inequality and lower bound of the exact density functional	399
11.13	Functionals	399
11.14	Reliability of DFT	399
11.15	Deficiencies of DFT	400
12	Magnetism	401
12.1	Charged particles in a magnetic field	401
12.2	Dirac equation and magnetic moment	401
12.3	Magnetism of the free-electron gas	401
12.4	Magnetic order	401
III	Appendices	403
A	Organization	405
A.1	Some ideas on the examination	405
A.2	Timing	408
B	More on the Born-Huang Ansatz	409
B.1	Combined systems	409
B.1.1	Coupled systems	409
B.1.2	Brackets and real-space wave functions	410
B.2	Non-uniqueness of the nuclear wave function	410
B.3	Diabatic picture	414
C	Non-crossing theorem	417
C.1	Proof of the non-crossing theorem	417
D	Adiabatic decoupling in the Born-Oppenheimer approximation	423
D.1	Adiabatic theorem	423
D.2	Justification for the Born-Oppenheimer approximation	424

E	Trajectories and non-adiabatic effects	427
E.1	Nuclear trajectories	427
E.1.1	Born-Oppenheimer dynamics	428
E.1.2	Electron dynamics for nuclear trajectories	429
E.1.3	Ehrenfest dynamics	431
E.1.4	Surface hopping	432
E.1.5	Statistical mixtures	432
E.2	Further reading	434
E.3	Ehrenfest dynamics	435
E.3.1	Lagrangian for the Schrödinger equation	435
E.3.2	Lagrangian for Ehrenfest dynamics	435
E.3.3	Ehrenfest dynamics in terms of the Born-Oppenheimer framework	436
E.4	Quasi-classical approximation for the nuclear wave functions	438
E.5	Diagonal terms of the derivative couplings	440
E.5.1	Example: Jahn-Teller model	443
E.6	Geometric phase	444
E.6.1	Aharonov-Bohm effect	444
E.6.2	Geometric phase	444
E.6.3	Generalization to more than three dimensions	447
E.6.4	Berry phase and polarization	447
E.7	Exact factorization	449
F	Landau-Zener formula	453
F.1	Landau-Zener formula	453
F.1.1	Relation to the Landau-Zener formula	455
F.2	Size of a conical intersection	456
F.2.1	Landau-Zener formula in terms of Born-Oppenheimer states	460
G	Optical excitations in the Holstein dimer	463
G.1	Optic transitions	463
H	Jahn-Teller model	467
H.1	Jahn-Teller model as minimal model with a conical intersection	467
H.2	Jahn-Teller model and manganites	468
H.3	Jahn-Teller model	469
H.3.1	Jahn-Teller model	470
H.3.2	Born-Oppenheimer Hamiltonian and Born-Oppenheimer surfaces	471
H.3.3	Born-Oppenheimer wave functions: real-valued, but discontinuous	472
H.3.4	Continuous, but complex-valued Born-Oppenheimer wave functions	474
H.3.5	Nuclear Schrödinger equation	478
H.4	Nuclear wave function of the Jahn-Teller model	479
H.4.1	Nuclear Schrödinger equation of the Jahn-Teller model	479
H.4.2	Relation of stationary wave functions for m and $-m - 1$	482
H.4.3	Behavior of the radial nuclear wave function at the origin	485
H.4.4	Optimization of the radial wave functions	487
H.4.5	Integration of the Schrödinger equation for the radial nuclear wave functions	489
H.4.6	FORTTRAN code	491

H.5	From a conical intersection to an avoided crossing	499
H.5.1	Conical intersection as limit of an avoided intersection	500
I	Quick peek on creation and annihilation operators	503
I.1	Creation and annihilation operators, the language of second quantization	503
I.1.1	Hamilton operator with creation and annihilation operators (Optional)	505
J	Some group theory for symmetries	509
J.1	Definition of a group	509
J.2	Symmetry class	509
K	Thermodynamic relations	511
K.1	Thermal expectation values from the grand potential	511
K.2	Sommerfeld expansion	512
L	Why is the effective mass of semiconductors much smaller than that of metals?	515
M	Brillouin-zone integrations	519
M.1	Solid in a box	519
N	Minimal models for phonon-phonon scattering	521
N.1	Anharmonic oscillator	521
N.2	First- and second-order approximation	522
O	Boltzmann equation	525
O.1	Boltzmann equation constructed from a specified equilibrium distribution	525
O.2	Self energy from a density-matrix functional	527
O.3	Wigner functions	529
O.4	Generating functional:	530
O.5	Functional form of Boltzmann's entropy	530
O.6	H-theorem	533
O.6.1	The drift term conserves the Boltzmann entropy	533
O.6.2	Entropy growth for scattering at obstacles	534
O.6.3	Entropy growth for complicated scattering processes	536
P	Time integrals for the phonon-phonon scattering elements	539
P.1	Integrations have only two arguments	539
P.2	Integrations relevant for the occupations	540
Q	Additional material for the Phonon Boltzmann equation	543
Q.1	Sketch of the derivation of the Phonon Boltzmann equation	543
Q.2	Equations of motion of phonon amplitudes	544
Q.2.1	Obtain Lagrangian in terms of phonon amplitudes	544
Q.3	Comparison of formulas	545
Q.3.1	Comparison with Peierls work	545
Q.3.2	Equation of motion of the phonon amplitudes	546
R	Slater determinants for parallel and antiparallel spins	547

R.1	Spatial symmetry for parallel and antiparallel spins	548
R.2	An intuitive analogy for particle with spin	550
S	Lagrange formalism and action principle	551
T	Recommended reading	555
U	Additional notes for the chapter on phonons	557
U.1	Vibrational amplitudes	557
U.2	Backup material on phonon amplitudes	559
U.2.1	Left- and right-moving waves	559
U.2.2	From normal coordinates to phonon amplitudes	559
V	Dictionary	567
V.1	Explanations	567
V.2	Symbols	567
W	Greek Alphabet	571
X	Philosophy of the ΦSX Series	573
X.1	Todo	574
Y	About the Author	575

Part I

Lecture notes

Chapter 1

The standard model of solid-state physics

1.1 The standard model

Solid-state physics deals with only few different types of particles and interactions. The particles are electrons and nuclei¹ and their interaction is described by electromagnetism. In contrast, gravitation is such a weak force at atomic distances that it is completely dominated by the electromagnetic interaction. The strong force, which is active inside the nucleus, has such a short range that it does not affect the relative motion of electrons and nuclei.

While the constituents of solids are simple, the complexity emerges from the interaction of many of these simple particles. The simple constituents act together to form an entire zoo of phenomena with fascinating complexity. The concept of emergent phenomena has been described by the Nobel laureate Phil Anderson in his famous article "More is different"[1].

Let me start with describing the theoretical basis of solid-state theory, which also serves to introduce my notation.

The dynamics of a system of particles is described by the Schrödinger equation:

$$i\hbar\partial_t|\Phi\rangle = \hat{H}|\Phi\rangle \quad (1.1)$$

where the wave function depends on the coordinates of all electrons and nuclei in the system. In addition, the wave function depends on the spin degrees of freedom of the electrons. Thus, a wave function for N electrons and M nuclei has the form

$$\Phi_{\sigma_1, \dots, \sigma_N}(\vec{r}_1, \dots, \vec{r}_N, \vec{R}_1, \dots, \vec{R}_M)$$

where we denote the electronic coordinates by a lower-case \vec{r} and the nuclear positions by an uppercase \vec{R} . The symbols σ_j are the spin indices, which may assume values $\sigma_j \in \{-\frac{1}{2}, +\frac{1}{2}\}$. We will also use the notation $\sigma_j \in \{\downarrow, \uparrow\}$. The spin quantum number in z-direction is $s_z = \hbar\sigma$.

I will combine position and spin index of the electrons in the form $\vec{x} = (\vec{r}, \sigma)$, so that

$$\Phi(\vec{x}_1, \dots, \vec{x}_N, \vec{R}_1, \dots, \vec{R}_M) \stackrel{\text{def}}{=} \Phi_{\sigma_1, \dots, \sigma_N}(\vec{r}_1, \dots, \vec{r}_N, \vec{R}_1, \dots, \vec{R}_M) \quad (1.2)$$

¹The cautious reader may object that the nuclei are objects that are far from being fully understood. However, the only properties that are relevant for us are their charge, their mass, and their size.

For the integrations and summations, we use the short-hand notation

$$\int d^4x \stackrel{\text{def}}{=} \sum_{\sigma \in \{\uparrow, \downarrow\}} \int d^3r \quad (1.3)$$

The electrons are Fermions. Therefore, the wave function is antisymmetric with respect to interchange of two electrons. This antisymmetry is the cause for the **Pauli principle**

PAULI PRINCIPLE

$$\Phi(\dots, \vec{x}_i, \dots, \vec{x}_j, \dots, \vec{R}_1, \dots, \vec{R}_M) = -\Phi(\dots, \vec{x}_j, \dots, \vec{x}_i, \dots, \vec{R}_1, \dots, \vec{R}_M) \quad (1.4)$$

An electronic many-particle wave function for Fermions is antisymmetric under particle exchange. As a consequence, no two electrons with the same spin can occupy the same point in space or the same one-particle orbital.

Standard model of solid-state physics

Now, we arrive at the most important equation: This equation forms the basis of all that will be said in this book. This equation specifies the many-particle Hamiltonian of our standard model of solid-state physics.

HAMILTONIAN OF THE STANDARD MODEL

The Hamiltonian for a many-particle system, such as a molecule or a solid, is

$$\begin{aligned} \hat{H} = & \underbrace{\sum_{j=1}^M \frac{-\hbar^2}{2M_j} \nabla_{\vec{R}_j}^2}_{E_{kin,nuc}} + \underbrace{\sum_{i=1}^N \frac{-\hbar^2}{2m_e} \nabla_{\vec{r}_i}^2}_{E_{kin,e}} \\ & + \underbrace{\frac{1}{2} \sum_{i \neq j}^M \frac{e^2 Z_i Z_j}{4\pi\epsilon_0 |\vec{R}_i - \vec{R}_j|}}_{E_{C,nuc-nuc}} - \underbrace{\sum_{i=1}^N \sum_{j=1}^M \frac{e^2 Z_j}{4\pi\epsilon_0 |\vec{r}_i - \vec{R}_j|}}_{E_{C,e-nuc}} \\ & + \underbrace{\frac{1}{2} \sum_{i \neq j}^N \frac{e^2}{4\pi\epsilon_0 |\vec{r}_i - \vec{r}_j|}}_{E_{C,e-e}} \end{aligned} \quad (1.5)$$

The electrons are characterized by their charge $-e$, their mass m_e , their position \vec{r}_j and spin-components σ_j . The nuclei are characterized by their masses M_j , their atomic numbers Z_j and their positions \vec{R}_j . The first term, denoted by $E_{kin,nuc}$, describes the kinetic energy of the nuclei. The second term, denoted by $E_{kin,e}$, describes the kinetic energy of the electrons. The third term, denoted by $E_{C,nuc-nuc}$, describes the electrostatic repulsion between the nuclei. The fourth term, denoted by $E_{C,e-nuc}$, describes the electrostatic attraction between electrons and nuclei. The last term, denoted by $E_{C,e-e}$, describes the electrostatic repulsion between the electrons.

Deficiencies of the standard model

No model is perfect. Therefore, let me discuss what I consider its main deficiencies. The following effects are missing:

- **Relativistic effects** are important for the heavier elements, because the deep Coulomb potential of the nuclei results in relativistic velocities for the electrons near the nucleus. Relativistic effects are important for magnetic effects such as the **magnetic anisotropy**.
- **Magnetic fields** have only a small effect on solids. The dominant magnetic properties of materials do not originate from magnetic interactions, but they are a consequence of Pauli's principle and the electrostatic interaction. Important are, however, **stray fields**, which tend to force the magnetization at a surface to be in-plane. Magnetic effects are also important for NMR or Mössbauer experiments, which are sensitive to the magnetic interaction of nuclei and electrons.
- **Size, shape and spin of the nuclei** play a role in certain nuclear experiments which measure isomer shifts, electric-field gradients and magnetic hyperfine parameters.
- **Photons**. The use of electrostatics –as opposed to electrodynamics– is justified, because the electrons and nuclei are moving sufficiently slow that the electrostatic field responds instantaneously. Excitations by photons can be treated explicitly.

These effects are not necessarily ignored, but can be incorporated into the standard model, when required.

Dimensional bottleneck

It is immediately clear that the standard model, as simple as it can be stated, is impossible to solve as such. To make this argument clear, let us estimate the amount of storage needed to store the wave function of a simple molecule such as N_2 . In order to store the wave function on the grid, we discretize each coordinate into 100 grid points. For 2 nuclei and 14 electrons, we need $100^{(3 \cdot 16)}$ grid points. In addition, we need to consider the 2^{14} sets of spin indices. Thus, we need to store about $2^{14} \cdot 100^{3 \cdot 16} \approx 10^{100}$ numbers. One typical hard disk can hold about 1 TByte = 10^{15} Bytes, which corresponds to 10^{14} complex numbers. A complex number occupies 16 byte. This implies that we would need 10^{86} hard discs to store a single wave function. A hard-disc occupies a volume of $5 \text{ cm} \times 5 \text{ cm} \times 0.5 \text{ cm} = 1.25 \times 10^{-5} \text{ m}^3$. The volume occupied by the hard discs with our wave function would be 10^{81} m^3 corresponding to a sphere with a radius of 10^{27} m or 10^{11} light years! This is about the size of our universe. I hope that this consideration convinced you that there is a problem...

The problem described here is called the **dimensional bottle-neck**.

In order to make progress, we need to simplify the problem. That is, we have to make approximations: We will develop simpler models that can be understood in detail. This is what solid-state physics is about. In the following, I will lead you through a set of common approximations, and their origins and their limitations.

Quasi particles

The standard model describes basic entities, namely nuclei, electrons and photons, which strongly interact with each other.

One of the major lessons is the surprising observation, that many properties of solids can be described in terms of weakly interacting **quasi-particles**. These quasi-particles are themselves complicated objects, which may consist of one of the basic entities combined with a deformation of its environment. The environment are the surrounding electrons and nuclei. Quasi-particles may also emerge from elementary excitations of the solid, which are not directly related to one of the basic entities of the theory.

Quasi-particles have properties, which differ from the basic entities: They have a **effective mass**, which differs from the mass of the bare particle because the deformation of the environment is tied to it. Quasi-particles interact differently with each other, because the environment screens the interaction resulting in a **screened interaction**. Quasi-particles may have a finite **lifetime** and fall apart after a while. In many cases, the interaction between quasi-particles is sufficiently weak, so that they can be approximated by non-interacting particles.

It may be helpful to consider some everyday analogy of quasi-particles.

- Consider a boat on a lake. To predict the motion of the boat, we rarely consider the lake. The interaction between boat and the water of the lake is, however, very strong: Without the water, the boat would fall immediately to the bottom of the lake. On the other hand, the water surface without the boat is flat, while it is strongly deformed when the boat is there. Thus, when we consider a boat on the lake, we do not have in mind the boat alone, but the boat combined with the deformation of the water surface. Considering boat and lake as two individual, but strongly interacting systems would not make much sense. What we have in mind is a quasi-boat in analogy of a quasi-particle.
- Another analogy is a VIP (very important person) in a crowd of people. If a VIP passes the crowded room, she will attract people nearby wishing to talk to her. The smalltalk takes a little time, so that she will be slowed down, in analogy to a quasi-particle attaining additional mass through the deformation of the environment. Being surrounded by a dense crowd, she will be less visible to people being further away. This is analogous to **screening**, resulting in an effective shortranged effective interaction between quasi-particles. As the VIP walks through the room, she is not surrounded by the same people all the time. Rather some people ahead of her will approach her, as they become aware of her. Others at their back will loose contact with her and will interact with themselves. Thus it is the deformation of the crowd that moves along with here, rather than individual people.

The remaining interaction between quasi-particles results in a plethora of additional effects: Quasi-particles may form combined entities, which themselves may act as quasi-particles. The arrangement of quasi-particles may undergo phase transitions with radical changes of the properties. On example are superconductors, which carry electrical current without any resistance.

The central topic of the present lecture notes "Introduction to Solid State Theory" is the description of quasi-particles.

1.2 Home study and practice

I have a take on exercises that is not common. Let me explain it:

I consider exercises crucial, to ensure that one captures the quantities one deals with and to be able to apply the knowledge in real life.

I do supply the solutions together with the problem set. This requires some discipline from the students, not to look up the solutions before at least doing an attempt to solve the problem. On the other hand, it is probably efficient to look up a solution if one gets severely stuck. There is a balance to be found.

The solutions are not only solutions but they also add to the teaching material. I usually provide more material than what one would expect from a student. The main motivation for this is that students often deliver a result without contemplating what it actually means. This last step is, however, crucial in research. By supplying additional context, I try to show the student that the result is "more than a number".

The problem sets are often not suitable for an examination. This is because examinations, while necessary, do not reflect well the challenges one encounters in real life.

The problem sets are not adapted to the expected workload of a student. The student is free to select her own set of problems.

1.2.1 Linear algebra of 2×2 matrices

Introduction

2×2 matrices are the smallest non-trivial matrices and they can be used concentrate on the relevant degrees of freedom of more complicated matrix problems. Therefore, every scientist should be able to do all elementary matrix problems in two dimensions without effort.

The two-by-two problems shall also serve to remind us of some general matrix properties.

PROPERTIES OF MATRIX DIAGONALIZATION

Consider an eigenvalue problem of a hermitean matrix $\mathbf{H} = \mathbf{H}^\dagger$

$$\sum_j H_{i,j} c_{j,n} = c_{i,n} \epsilon_n \tag{1.6}$$

with eigenvectors \vec{c}_n and eigenvalues ϵ_n .

- Eigenvalues of hermitian matrices (Observables) are real valued.
- Eigenvectors of hermitian matrices with distinct eigenvalues are orthogonal.

$$\vec{c}_n^* \vec{c}_{n'} = 0 \quad \text{if} \quad \lambda_n \neq \lambda_{n'} \tag{1.7}$$

The eigenvalues can always be orthonormalized so that $\vec{c}_n^* \vec{c}_{n'} = \delta_{n,n'}$. In that case, the eigenvectors form a unitary matrix $\mathbf{c}^\dagger \mathbf{c} = \mathbf{1}$ respectively $\sum_j c_{j,n}^* c_{j,n'} = \delta_{n,n'}$.

- **Level repulsion:** An increase of an off-diagonal element $H_{i,j}$ of a Hermitean matrix increases the distance between its eigenvalues ϵ_i and ϵ_j .
- **Trace sum rule:** The sum of the eigenvalues of a hermitean matrix equals the sum of its diagonal elements, i.e. its trace.

$$\sum_j \epsilon_j = \sum_j H_{j,j} \tag{1.8}$$

- **Orbital sum rule:** The projections $c_{j,n}^* c_{j,n}$ onto a component j sum up to one.

$$\sum_n c_{j,n}^* c_{j,n} = 1 \tag{1.9}$$

For non-hermitean matrices, see section 1.2.5 below.

The **generalized eigenvalue problem** has the form

$$\sum_j (H_{i,j} - \epsilon_n \mathbf{O}_{i,j}) c_{j,n} = 0 \tag{1.10}$$

with an overlap matrix \mathbf{O} . It is not discussed here.

Problem

- 1 **Matrix inversion:** Invert a general (complex-valued) 2×2 matrix

$$\mathbf{A} = \begin{pmatrix} a & b \\ c & d \end{pmatrix} \quad (1.11)$$

No derivation is required. Verify that your result is correct.

- 2 **Diagonalization:** Diagonalize the most general hermitian 2×2 matrix. Express the matrix by its eigenvalues and eigenvectors. Verify that the following statements hold for your result.

- The eigenvalues are real valued.
- The presence of non-zero off-diagonal elements always increases the spacing between the eigenvalues. This is called “**level-repulsion**”.
- verify the **orbital sum rule** for a hermitean 2×2 matrix \mathbf{A} with eigenvectors \vec{c}_n .

$$\sum_n c_{j,n}^* c_{j,n} = 1 \quad (1.12)$$

- verify the **trace sum rule** for a hermitean 2×2 matrix \mathbf{A} with eigenvalues λ_n .

$$\sum_n A_{n,n} = \sum_n \lambda_n \quad (1.13)$$

The reader may also consult chapter 1 in Φ SX: Advanced Solid-State Theory[2] and the corresponding exercises on the hydrogen molecule and the general diatomic molecule. More background on the chemical bond can be found in Φ SX: Quantum mechanics of the chemical bond[3].

- 3 **Unitary matrix from orthonormal vectors:** Show, how the most general unitary matrix in two dimensions can be set up using a set of normalized and orthogonal vectors.

Solution

- 1 **Matrix inversion:** Invert a general (complex-valued) 2×2 matrix

$$\mathbf{A} = \begin{pmatrix} a & b \\ c & d \end{pmatrix} \quad (1.14)$$

No derivation is required. Verify that your result is correct.

$$\mathbf{A} = \begin{pmatrix} a & b \\ c & d \end{pmatrix} \quad \Rightarrow \quad \mathbf{A}^{-1} = \frac{1}{\det[\mathbf{A}]} \begin{pmatrix} d & -b \\ -c & a \end{pmatrix} = \frac{1}{ad - bc} \begin{pmatrix} d & -b \\ -c & a \end{pmatrix} \quad (1.15)$$

INVERT A GENERAL 2×2 MATRIX

The rule to memorize this result is:

- interchange the diagonal elements.
- revert the sign of the off-diagonal elements.
- divide by the determinant.

Test:

$$\mathbf{A}\mathbf{A}^{-1} = \begin{pmatrix} a & b \\ c & d \end{pmatrix} \frac{1}{ad-bc} \begin{pmatrix} d & -b \\ -c & a \end{pmatrix} = \frac{1}{ad-bc} \begin{pmatrix} ad-bc & -ab+ba \\ cd-dc & -cb+da \end{pmatrix} = \begin{pmatrix} 1 & 0 \\ 0 & 1 \end{pmatrix} \quad (1.16)$$

2 **Diagonalization:** Diagonalize the most general hermitian 2×2 matrix. Express the matrix by its eigenvalues and eigenvectors. Verify that the following statements hold for your result. (See box on p. 21)

- The eigenvalues are real valued.
- The presence of non-zero off-diagonal elements always increases the spacing between the eigenvalues. This is called “**level-repulsion**”.
- verify the **orbital sum rule** for a hermitean 2×2 matrix \mathbf{A} with eigenvectors \vec{c}_n .

$$\sum_n c_{j,n}^* c_{j,n} = 1 \quad (1.17)$$

- verify the **trace sum rule** for a hermitean 2×2 matrix \mathbf{A} with eigenvalues λ_n .

$$\sum_n A_{n,n} = \sum_n \lambda_n \quad (1.18)$$

The most general hermitian 2×2 matrix has real valued diagonal elements and a complex-valued off-diagonal element. The two complex-valued off-diagonal elements are complex conjugates of each other. The Hamilton matrix has the form.

$$\mathbf{H} = \begin{pmatrix} \bar{\epsilon}_1 & -t \\ -t^* & \bar{\epsilon}_2 \end{pmatrix} \quad (1.19)$$

with real-valued $\bar{\epsilon}_1, \bar{\epsilon}_2$ and complex-valued hopping parameter t .

Some caution is required regarding the sign of the **hopping parameter** t , which is not defined in a unique manner. (And it may not yet be consistent in my lecture notes!) I follow the definition that the hopping parameter is the negative of the upper-left off-diagonal element of the Hamilton matrix, i.e. $H_{1,2} = -t$. For real-valued orbitals, the sign of the hopping parameter corresponds to the overlap between the two orbitals.

- two s-orbitals in a bond have a positive overlap matrix-element and, thus, a positive hopping parameter. The orbitals in the bonding orbital have the same sign, so that the electron density accumulates in the bond center. This accumulation of the electron density reflects the delocalization of electrons across the bond. ²

²The bond energy should not be attributed (exclusively) to the electrostatic of the nuclei to the build-up of charge density in the bond center. Rather, it is related to the lowering of the kinetic energy. The kinetic energy is related to the squared gradient of the wave function. Thus, a vanishing gradient of the wave function in the bond center is a sign of low kinetic energy. Another way is relating it to Heisenberg's uncertainty principle, which relates the zero-point energy to the space available to the particle.

- two p-orbitals oriented along the bond axis have a negative overlap matrix element and thus a negative hopping parameter. This ensures that the two p-orbitals contribute with opposite sign to the bonding orbital, so that the electron density builds up in the bond center.

The sign of the hopping parameter is discussed in more detail in section 4.3.3 on p. 136.

The **characteristic equation** provides the eigenvalues:

$$\begin{aligned}\det[\mathbf{H} - \mathbf{1}\epsilon] &= 0 \\ (\bar{\epsilon}_1 - \epsilon)(\bar{\epsilon}_2 - \epsilon) - |t|^2 &= 0 \\ \epsilon^2 - \underbrace{(\bar{\epsilon}_1 + \bar{\epsilon}_2)}_{\text{Tr}[\mathbf{H}]} \epsilon + \underbrace{\bar{\epsilon}_1 \bar{\epsilon}_2}_{\det[\mathbf{H}]} - |t|^2 &= 0\end{aligned}$$

We name the lower eigenvalue ϵ_- and the upper ϵ_+ . In order to reduce typing, I combine both solutions by using the symbols \pm and $\mp = -\pm$. The upper symbols belong together and the lower symbols belong to each other. The two eigenvalues are

$$\epsilon_{\pm} = \frac{\bar{\epsilon}_1 + \bar{\epsilon}_2}{2} \pm \sqrt{\left(\frac{\bar{\epsilon}_1 - \bar{\epsilon}_2}{2}\right)^2 + |t|^2} \quad (1.20)$$

By inspection we can verify the following:

- The sum of the eigenvalues equals the trace \mathbf{H} , i.e. $\epsilon_- + \epsilon_+ = \bar{\epsilon}_1 + \bar{\epsilon}_2$.
- The eigenvalues are real.
- The presence of non-zero off-diagonal elements always increases the spacing between the eigenvalues.

A general effect is **level repulsion**: As the off-site Hamilton matrix element, the hopping parameter, is increased in size, the affected eigenstates repel each other. This level repulsion is largest in the degenerate case, when the diagonal matrix elements of the Hamiltonian are initially degenerate. The effect is smaller, when diagonal matrix elements are already well separated.

The degenerate case describes typical **covalent bonds**, such as the bond in the hydrogen atom. The energy gain in a covalent bond is due to the delocalization of the orbital over two sites, which lowers its kinetic energy.

The non-degenerate case describes typically a **ionic bond**. Here the energy gain is predominantly due to the electron transfer to the lower-lying orbital. However, every ionic bond also has a covalent contribution, which further lowers the energy.

A very helpful observation is that **for orthonormal orbitals, the sum of the eigenvalues is identical to the trace of the Hamiltonian**.³ The origin of this statement is that the trace is invariant under unitary transformation. It implies that bonds and antibonds compensate.

Eigenvectors: The equation defining the eigenvectors $\vec{c}_{\pm} = (c_{1,\pm}, c_{2,\pm})$ is

$$(\bar{\epsilon}_1 - \epsilon_{\pm})c_{1,\pm} - tc_{2,\pm} = 0 \quad (1.22)$$

³For an orthonormal basisset with $\langle \chi_{\alpha} | \chi_{\beta} \rangle = \delta_{\alpha,\beta}$, the eigenvectors $U_{\alpha,n} \stackrel{\text{def}}{=} \langle \chi_{\alpha} | \psi_n \rangle$ form a unitary matrix, i.e. $U^{\dagger}U = 1$, so that

$$\begin{aligned}\sum_n \epsilon_n &= \sum_n \langle \psi_n | \hat{H} | \psi_n \rangle = \sum_n \langle \psi_n | \underbrace{\sum_{\alpha} \chi_{\alpha} \langle \chi_{\alpha} |}_{=1 \text{ for } \langle \chi_{\alpha} | \chi_{\beta} \rangle = \delta_{\alpha,\beta}} \hat{H} \underbrace{\sum_{\beta} \chi_{\beta} \langle \chi_{\beta} |}_{=1 \text{ for } \langle \chi_{\alpha} | \chi_{\beta} \rangle = \delta_{\alpha,\beta}} | \psi_n \rangle \\ &= \sum_n \sum_{\alpha,\beta} \underbrace{\langle \psi_n | \chi_{\alpha} \rangle}_{U_{\alpha,n}^*} \underbrace{\langle \chi_{\alpha} | \hat{H} | \chi_{\beta} \rangle}_{H_{\alpha,\beta}} \underbrace{\langle \chi_{\beta} | \psi_n \rangle}_{U_{\beta,n}} = \text{Tr}[U^{\dagger}HU] = \text{Tr}[\underbrace{UU^{\dagger}}_{\mathbf{1}}H] = \text{Tr}[H] = \sum_{\alpha} H_{\alpha,\alpha}\end{aligned} \quad (1.21)$$

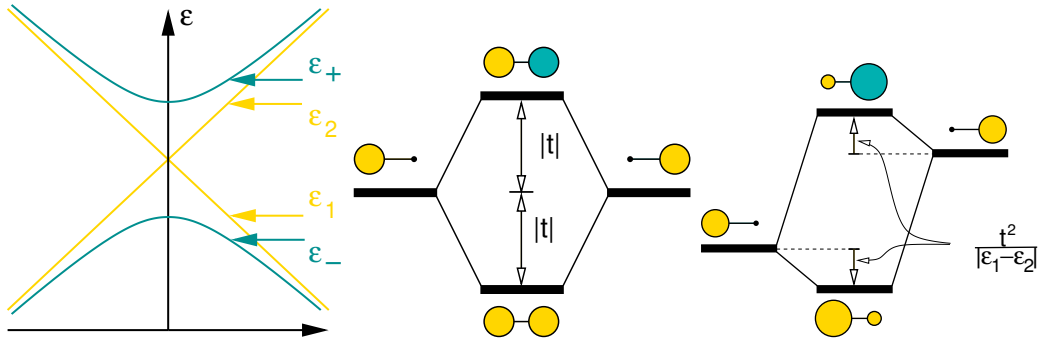


Fig. 1.1: Left: Demonstration of level repulsion. Energy levels ϵ_+ , ϵ_- as function of some parameter, which tunes the diagonal elements ϵ_1, ϵ_2 of the Hamiltonian while the hopping parameter t remains fixed. Middle: Energy-level and orbital scheme for a two-center bond in the degenerate limit. Right: Energy-level and orbital scheme for a two-center bond in the non-degenerate limit.

I find it often convenient to directly incorporate the orthonormalization by expressing the coefficients in terms of cosine and sine functions. For a hopping parameter $t = |t|e^{i\varphi}$, I parameterize the eigenvectors as

$$(c_{1,\pm}, c_{2,\pm}) = \begin{cases} (\cos(\alpha), \sin(\alpha)e^{-i\varphi}) & \text{for } \pm = - \\ (-\sin(\alpha)e^{i\varphi}, \cos(\alpha)) & \text{for } \pm = + \end{cases} \quad (1.23)$$

I name the parameter α the **orbital-mixing angle**.

Whatever the value of α is, the normalization of the two states and their orthogonality is automatically satisfied because of $\cos^2(\alpha) + \sin^2(\alpha) = 1$.

- When $\alpha = 45^\circ$, the ground state \bar{c}_- has the same coefficients on both sides, i.e. $c_{1,-} = c_{2,-} = 1/\sqrt{2}$, and the excited state \bar{c}_+ has opposite coefficients, i.e. $c_{1,+} = -c_{2,+}$.
- A mixing angle of $\alpha = 0$ implies that the ground state is the first basis orbital, i.e. $c_{1,-} = 1$, and the excited state is the second orbital, i.e. $c_{2,+} = 1$.

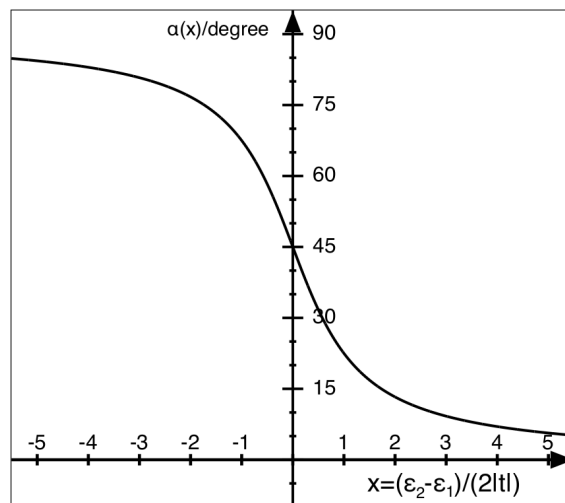
What needs to be done, is to determine the orbital-mixing angle α . We insert the Ansatz Eq. 1.23 into the defining equation Eq. 1.22

$$(\bar{\epsilon}_1 - \epsilon_-) \underbrace{\cos(\alpha)}_{c_{1,-}} - \underbrace{|t|e^{i\varphi}}_t \underbrace{\sin(\alpha)e^{-i\varphi}}_{c_{2,-}} = 0 \quad (1.24)$$

which yields α as

$$\begin{aligned} \tan(\alpha) &= \frac{\sin(\alpha)}{\cos(\alpha)} = \frac{\bar{\epsilon}_1 - \epsilon_-}{|t|} = \frac{\bar{\epsilon}_1 - \frac{\bar{\epsilon}_1 + \bar{\epsilon}_2}{2} + \sqrt{\left(\frac{\bar{\epsilon}_1 - \bar{\epsilon}_2}{2}\right)^2 + |t|^2}}{|t|} \\ &= -\frac{\bar{\epsilon}_2 - \bar{\epsilon}_1}{2|t|} + \sqrt{\left(\frac{\bar{\epsilon}_2 - \bar{\epsilon}_1}{2|t|}\right)^2 + 1} \\ \alpha &= \text{atan} \left(-\frac{\bar{\epsilon}_2 - \bar{\epsilon}_1}{2|t|} + \sqrt{1 + \left(\frac{\bar{\epsilon}_2 - \bar{\epsilon}_1}{2|t|}\right)^2} \right) \end{aligned} \quad (1.25)$$

The orbital-mixing parameter $\alpha(x)$ depends only on $x = (\bar{\epsilon}_2 - \bar{\epsilon}_1)/(2|t|)$.



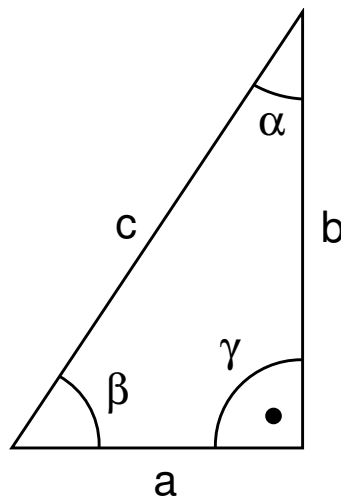
$\alpha(x)$ is a function that falls off monotonically with x from $\alpha(-\infty) = \pi/2$ to $\alpha(+\infty) = 0$. The function $\alpha(x) - \pi/4$ is odd, i.e. $\alpha(x) - \pi/4 = -(\alpha(-x) - \pi/4)$.

The sign of the offsite matrix elements does not affect the energies but it changes the relative sign of the coefficients. With the “wrong” sign, bonding and antibonding orbitals are interchanged.

- degenerate limit $(\epsilon_2 - \epsilon_1)/(2|t|) = 0$: Bonding and antibonding states are separated by $2|t|$. The (lower) bonding orbital accumulates electron density in the bond center. The antibonding state has a node in the bond center.
- non-degenerate limit $(\epsilon_2 - \epsilon_1)/(2|t|) = +\infty$: The (lower) bonding orbital is predominantly localized on the lower atomic orbital, while the (upper) antibonding orbital is localized on the upper atomic orbital

A more detailed discussion is given in Φ SX: Quantum mechanics of the chemical bond.[3] The curious reader may look into section R.4 in Φ SX: Quantum Physics[4] for another derivation relying on Pauli matrices.

Some trigonometry In this exercise we required the trigonometric functions of the arcus tangens of something. These formulas can be recovered using a few basic geometric relations for rectangular triangles.



c , the side opposite to the right angle γ , is called the **hypotenuse**. The side a is the **adjacent**⁴ of angle β , while b is the **opposite** of the angle β .

We will use the basic geometric relations of rectangular triangles

$$\begin{aligned} a^2 + b^2 &= c^2 && \text{Pythagorean theorem} \\ \cos(\beta) &= \frac{a}{c} \\ \sin(\beta) &= \frac{b}{c} \\ \tan(\beta) &= \frac{\sin(\beta)}{\cos(\beta)} = \frac{b}{a} \quad \Rightarrow \quad \beta = \text{atan}\left(\frac{b}{a}\right) \end{aligned} \tag{1.26}$$

Let us choose $a = 1$ and $b = f(x)$, so that we can identify the arcus tangens of $f(x)$ with the angle β

$$\beta = \text{atan}\left(\frac{b}{a}\right) = \text{atan}(f(x)) \tag{1.27}$$

To determine the cosine and sine of β , we still need the hypotenuse c , which we obtain with the Pythagorean theorem.

$$c = \sqrt{a^2 + b^2} = \sqrt{1 + (f(x))^2} \tag{1.28}$$

Now we determine the cosine

$$\begin{aligned} \cos\left(\text{atan}(f(x))\right) &= \cos(\beta) = \frac{a}{c} = \frac{1}{\sqrt{1 + (f(x))^2}} \\ \sin\left(\text{atan}(f(x))\right) &= \sin(\beta) = \frac{b}{c} = \frac{f(x)}{\sqrt{1 + (f(x))^2}} \end{aligned} \tag{1.29}$$

3 Unitary matrix from orthonormal vectors: Show, how the most general unitary matrix in two dimensions can be set up using a set of normalized and orthogonal vectors.

Let $\vec{u} = (u_1, u_2)$ and $\vec{v} = (v_1, v_2)$ be two orthonormal vectors, i.e. $\vec{u}\vec{u}^* = 1$, $\vec{u}\vec{v}^* = 0$, and $\vec{v}\vec{v}^* = 1$. Then the matrix

$$\mathbf{U} = \begin{pmatrix} u_1 & v_1 \\ u_2 & v_2 \end{pmatrix} \tag{1.30}$$

is unitary. This identity can be generalized to higher dimensions than two.

In order to show that \mathbf{U} is unitary, I need to show that its adjunct is equal to its inverse.

$$\mathbf{U}^\dagger \mathbf{U} = \begin{pmatrix} u_1^* & u_2^* \\ v_1^* & v_2^* \end{pmatrix} \begin{pmatrix} u_1 & v_1 \\ u_2 & v_2 \end{pmatrix} = \begin{pmatrix} u_1^* u_1 + u_2^* u_2 & u_1^* v_1 + u_2^* v_2 \\ v_1^* u_1 + v_2^* u_2 & v_1^* v_1 + v_2^* v_2 \end{pmatrix} = \mathbf{1} \tag{1.31}$$

The derivation also shows that the orthonormality is the only condition for a unitary matrix. Namely, we can consider u_1, u_2, v_1, v_2 without conditions as notation for the four matrix elements. Then we see that the condition $\mathbf{U}^\dagger \mathbf{U} = \mathbf{1}$ can only be satisfied if the orthonormality conditions are obeyed.

⁴In German adjacent=Ankathete, Hypotenuse=hypotenuse and opposite= Gegenkathete.

Eigenvalue problems: This representation of unitary matrices is used for eigenvalue problems. Because eigenvalue problems are so important, it is worth while to become used to efficient notations: A matrix \mathbf{H} is diagonalized by the eigenvectors u_n with eigenvalues E_n

$$\begin{aligned} (\mathbf{H} - E_n \mathbf{1}) \vec{u}_n &= 0 \\ \Rightarrow \mathbf{H} \vec{u}_n &= \vec{u}_n E_n \\ \Rightarrow \vec{u}_m^* \mathbf{H} \vec{u}_n &= \underbrace{\vec{u}_m^* \vec{u}_n}_{\delta_{m,n}} E_n = E_m \delta_{m,n} \end{aligned} \quad (1.32)$$

Using the unitary matrix \mathbf{U} formed by the eigenvectors \vec{u}_n , and the diagonal matrix \mathbf{E} formed by the eigenvalues E_n , we can express the same in the form

$$\begin{aligned} \mathbf{H} \mathbf{U} &= \mathbf{U} \mathbf{E} \\ \Rightarrow \mathbf{U}^\dagger \mathbf{H} \mathbf{U} &= \mathbf{U}^\dagger \mathbf{U} \mathbf{E} = \mathbf{E} \\ \Rightarrow \mathbf{H} &= \mathbf{U} \mathbf{E} \mathbf{U}^\dagger \end{aligned} \quad (1.33)$$

Use dyadic products: Another representation of unitary matrices uses dyadic products of two orthonormal sets of vectors. Let $\{\vec{a}_n\}$ with $\vec{a}_m^* \vec{a}_n = \delta_{m,n}$ be one orthonormal set of vectors and let $\{\vec{b}_n\}$ with $\vec{b}_m^* \vec{b}_n = \delta_{m,n}$ be another orthonormal set of vectors, then a unitary matrix is obtained as

$$\mathbf{U} = \sum_{n=1}^d \vec{b}_n \otimes \vec{a}_n^* \quad (1.34)$$

The property that \mathbf{U} is unitary is shown below:

$$\mathbf{U}^\dagger \mathbf{U} = \underbrace{\sum_{m=1}^d \vec{a}_m \otimes \vec{b}_m^*}_{\mathbf{U}^\dagger} \underbrace{\sum_{n=1}^d \vec{b}_n \otimes \vec{a}_n^*}_{\mathbf{U}} = \sum_{n=1}^d \vec{a}_n \otimes \vec{a}_n^* = \mathbf{1} \quad (1.35)$$

To show that the last matrix is the unit matrix, we apply it to a general vector $\sum_{n=1}^d \vec{a}_n c_n$ with some arbitrary coefficients c_n . If the set $\{\vec{a}_n\}$ is complete every vector can be represented in this form.

$$\left(\sum_{n=1}^d \vec{a}_n \otimes \vec{a}_n^* \right) \left(\sum_{m=1}^d \vec{a}_m c_m \right) = \sum_{n,m=1}^d \vec{a}_n \underbrace{(\vec{a}_n^* \vec{a}_m)}_{\delta_{m,n}} c_m = \sum_{n=1}^d \vec{a}_n c_n \quad (1.36)$$

Thus, the matrix reproduces the same vector it is applied to, which proves that it is the identity.

In bra-ket notation: These vector identities are easily translated into a bra-ket notation. For two orthonormal sets of states with $\langle a_n | a_m \rangle = \delta_{m,n}$ and $\langle b_n | b_m \rangle = \delta_{m,n}$, a unitary matrix is

$$\begin{aligned} \hat{U} &= \sum_n |a_n\rangle \langle b_n| \\ \hat{U}^\dagger &= \sum_n |b_n\rangle \langle a_n| \\ \hat{U}^\dagger \hat{U} &= \sum_{m,n} |b_m\rangle \langle a_m | a_n \rangle \langle b_n| = \sum_n |b_n\rangle \langle b_n| = \mathbf{1} \quad \text{because } \langle b_m | b_n \rangle = \delta_{m,n} \end{aligned} \quad (1.37)$$

Any hermitian matrix \hat{H} can be represented by its eigenstates $|u_n\rangle$ and eigenvalues E_n as

$$\hat{H} = \hat{U} \hat{E} \hat{U} = \sum_n |u_n\rangle E_n \langle u_n| \quad (1.38)$$

1.2.2 Dirac's bra-ket notation

Introduction

I make extensive use of Dirac's bracket notation. I find it a mathematically rigorous, intuitive and very efficient notation. Therefore, I consider it important to be comfortable with it and to grasp the meaning of expressions without effort. This problem sheet shall remind you of the most important relations.

One source to look up the material are the lecture notes $\Phi SX: Quantum Theory$, section 6.5 "From bras and kets to wave functions" available online at <https://www2.pt.tu-clausthal.de/atp/phix.html>.

Before starting, let me put down some definitions:

- Numbers can be obtained from Dirac's notation only! as scalar product $\langle \phi | \psi \rangle$.
- The real-space basis is defined by the following set of equations.

$$\begin{aligned} \hat{r}|\vec{r}\rangle &= |\vec{r}\rangle \vec{r} && \text{eigenvalue equation} \\ \langle \vec{r} | \vec{r}' \rangle &= \delta(\vec{r} - \vec{r}') && \text{orthonormality} \\ \hat{1} &= \int d^3r |\vec{r}\rangle \langle \vec{r}| && \text{completeness} \end{aligned} \quad (1.39)$$

- The momentum-space basis can be introduced by the following set of equations

$$|\vec{p}\rangle = \int d^3r |\vec{r}\rangle e^{i\vec{p}\vec{r}} \quad (1.40)$$

Other authors define the momentum eigenstates with a different scale factor.⁵ Both notations have their own virtues.

The basis functions are eigenstates of the momentum operator

$$\hat{p}|\vec{p}\rangle = |\vec{p}\rangle \vec{p} \quad \text{eigenvalue equation} \quad (1.42)$$

Problem

- 1 What is the wave function $\psi(\vec{r})$ expressed in bras and kets. What is the wave function $\phi(\vec{r})$ obtained by applying an operator such as $\hat{p} \hat{=} \frac{\hbar}{i} \vec{\nabla}$ to a wave function $\psi(\vec{r})$ expressed in terms of bras and kets.
- 2 Determine the orthonormality relation for the momentum eigenstates $|\vec{p}\rangle$ defined above. (Be prepared to encounter conventions that you are not used to.)

You can use the improper integral

$$\int_{-\infty}^{\infty} dx \frac{\sin x}{x} = \pi \quad (1.43)$$

- 3 Work out the kinetic energy operator $\hat{p}^2/(2m)$ in a real-space representation. Represent it once as differential operator and once as abstract operator in the bra-ket notation.

⁵Often the momentum basis is defined in the form

$$|\vec{p}\rangle = \int d^3r |\vec{r}\rangle e^{i\vec{p}\vec{r}} \frac{1}{\sqrt{2\pi\hbar}} \quad (1.41)$$

while we use a convention that is often used in statistical physics, where the factor $\frac{1}{\sqrt{2\pi\hbar}}$ is absent.

Solution

1 What is the wave function $\psi(\vec{r})$ expressed in bra's and kets.

$$\psi(\vec{r}) = \langle \vec{r} | \psi \rangle \quad (1.44)$$

Similarly,

$$\hat{A}\psi(\vec{r}) = \langle \vec{r} | \hat{A} | \psi \rangle \quad (1.45)$$

The operator \hat{A} on the left-hand side is a transformation of functions, while the one on the right-hand side is an abstract operator. Strictly speaking, they are completely different objects even though they are represented by the same symbol.

2 determine the orthonormality relation for the momentum eigenstates $|\vec{p}\rangle$ defined above. (Be prepared to encounter conventions that you are not used to.)

You can use the improper integral

$$\int_{-\infty}^{\infty} dx \frac{\sin x}{x} = \pi \quad (1.46)$$

$$\begin{aligned} \langle \vec{p} | \vec{p}' \rangle &= \int d^3 r \int d^3 r' e^{-\frac{i}{\hbar} \vec{p} \vec{r}} \langle \vec{r} | \vec{r}' \rangle e^{\frac{i}{\hbar} \vec{p}' \vec{r}'} \\ &= \int d^3 r e^{\frac{i}{\hbar} (\vec{p}' - \vec{p}) \vec{r}} \\ &= \prod_{j=1}^3 \lim_{L \rightarrow \infty} \int_{-L}^L dx_j e^{\frac{i}{\hbar} (p'_j - p_j) x_j} \\ &= \prod_{j=1}^3 \lim_{L \rightarrow \infty} \frac{1}{\frac{i}{\hbar} (p'_j - p_j)} \left(e^{\frac{i}{\hbar} (p'_j - p_j) L} - e^{-\frac{i}{\hbar} (p'_j - p_j) L} \right) \\ &= \prod_{j=1}^3 \lim_{L \rightarrow \infty} \frac{2\hbar \sin((p'_j - p_j)L/\hbar)}{(p'_j - p_j)} \\ &\stackrel{?}{=} (2\pi\hbar)^3 \delta(\vec{p} - \vec{p}') \end{aligned} \quad (1.47)$$

In order to prove the last step, we need to show that

$$\lim_{Q \rightarrow \infty} \frac{\sin(xQ)}{x} = \pi \delta(x) \quad (1.48)$$

Dirac's δ -function is defined by the identity

$$\int dx \delta(x) f(x) = f(0) \quad (1.49)$$

which holds for any fully differentiable function $f(x)$.

In order to prove Eq. 1.48, I will show that

$$\lim_{Q \rightarrow \infty} \int_{-\infty}^{\infty} dx \frac{\sin(xQ)}{x} f(x) = \pi f(0) . \quad (1.50)$$

This is done in the following

$$\begin{aligned}
 \lim_{Q \rightarrow \infty} \int_{-\infty}^{\infty} dx \frac{\sin(xQ)}{x} f(x) &\stackrel{y=Qx}{=} \lim_{Q \rightarrow \infty} \int_{-\infty}^{\infty} \frac{dy}{Q} \frac{\sin(y)}{y/Q} f(y/Q) \\
 &= \lim_{Q \rightarrow \infty} \int_{-\infty}^{\infty} dy \frac{\sin(y)}{y} f(y/Q) \\
 &= f(0) \underbrace{\int_{-\infty}^{\infty} dy \frac{\sin(y)}{y}}_{=\pi \text{ (See Eq. 1.43)}} \\
 &= \pi f(0) \quad \text{q.e.d}
 \end{aligned} \tag{1.51}$$

3 Work out the kinetic-energy operator $\hat{p}^2/(2m)$ in a real-space representation. Represent it once as differential operator and once as abstract operator in the bra-ket notation.

From the problem above, we obtained

$$\langle \vec{p} | \vec{p}' \rangle = (2\pi\hbar)^3 \delta(\vec{p} - \vec{p}') \tag{1.52}$$

Together with the completeness of the momentum eigenstates this yields

$$\int \frac{d^3 p}{(2\pi\hbar)^3} |\vec{p}\rangle \langle \vec{p}| = \hat{1} \tag{1.53}$$

This expression can be used to rewrite the kinetic energy operator

$$\begin{aligned}
 \hat{T} &= \frac{\hat{p}^2}{2m} = \frac{\hat{p}^2}{2m} \underbrace{\int \frac{d^3 p}{(2\pi\hbar)^3} |\vec{p}\rangle \langle \vec{p}|}_{\hat{1}} \\
 &= \int \frac{d^3 p}{(2\pi\hbar)^3} |\vec{p}\rangle \frac{\vec{p}^2}{2m} \langle \vec{p}| \\
 &= \int \frac{d^3 p}{(2\pi\hbar)^3} \underbrace{\int d^3 r |\vec{r}\rangle \langle \vec{r}|}_{\hat{1}} |\vec{p}\rangle \frac{\vec{p}^2}{2m} \langle \vec{p}| \underbrace{\int d^3 r' |\vec{r}'\rangle \langle \vec{r}'|}_{\hat{1}} \\
 &= \int d^3 r \int d^3 r' |\vec{r}\rangle \left(\int \frac{d^3 p}{(2\pi\hbar)^3} \langle \vec{r} | \vec{p} \rangle \frac{\vec{p}^2}{2m} \langle \vec{p} | \vec{r}' \rangle \right) \langle \vec{r}' | \\
 &= \int d^3 r \int d^3 r' |\vec{r}\rangle \left(\int \frac{d^3 p}{(2\pi\hbar)^3} e^{-\frac{i}{\hbar} \vec{p}(\vec{r}' - \vec{r})} \frac{\vec{p}^2}{2m} \right) \langle \vec{r}' | \\
 &= \int d^3 r \int d^3 r' |\vec{r}\rangle \left(\int \frac{d^3 p}{(2\pi\hbar)^3} \frac{-\hbar^2}{2m} \vec{\nabla}^2 e^{-\frac{i}{\hbar} \vec{p}(\vec{r}' - \vec{r})} \right) \langle \vec{r}' |
 \end{aligned} \tag{1.54}$$

I purposely introduced the gradient $\vec{\nabla}$ acting on \vec{r} rather than the gradient $\vec{\nabla}'$ acting on \vec{r}' . Using $\vec{\nabla}'$, I would have to ensure that the derivatives of $\langle \vec{r}' |$ are treated properly.

$$\begin{aligned}
 \hat{T} &= \int d^3 r \int d^3 r' |\vec{r}\rangle \frac{-\hbar^2}{2m} \vec{\nabla}^2 \underbrace{\left(\int \frac{d^3 p}{(2\pi\hbar)^3} e^{-\frac{i}{\hbar} \vec{p}(\vec{r}' - \vec{r})} \right)}_{\delta(\vec{r} - \vec{r}')} \langle \vec{r}' | \\
 &= \int d^3 r \int d^3 r' |\vec{r}\rangle \frac{-\hbar^2}{2m} \vec{\nabla}^2 \delta(\vec{r} - \vec{r}') \langle \vec{r}' | \\
 &= \int d^3 r |\vec{r}\rangle \frac{-\hbar^2}{2m} \vec{\nabla}^2 \int d^3 r' \delta(\vec{r} - \vec{r}') \langle \vec{r}' | \\
 &= \int d^3 r |\vec{r}\rangle \frac{-\hbar^2}{2m} \vec{\nabla}^2 \langle \vec{r} |
 \end{aligned} \tag{1.55}$$

This is the abstract version of the kinetic-energy operator.

The differential operator is obtained by evaluating the wave function resulting from applying the kinetic-energy operator onto a state.

$$\begin{aligned}
 \langle \vec{r} | \hat{T} | \psi \rangle &= \langle \vec{r} | \int d^3 r' | \vec{r}' \rangle \frac{-\hbar^2}{2m} \nabla'^2 \langle \vec{r}' | \psi \rangle \\
 &= \int d^3 r' \langle \vec{r} | \vec{r}' \rangle \frac{-\hbar^2}{2m} \nabla'^2 \psi(\vec{r}') \\
 &= \frac{-\hbar^2}{2m} \nabla^2 \psi(\vec{r})
 \end{aligned} \tag{1.56}$$

This shows the differential operator acting on the wave function $\psi(\vec{r})$.

1.2.3 Dirac atom

Introduction

This exercise is meant to introduce the **Dirac atom**. The Dirac atom is a minimal one-dimensional model for an atom. The bound-state wave function falls off exponentially with distance like that of the 3-dimensional hydrogen atom.

A solid formed from Dirac atoms, the **Dirac comb**, is used as a model for wave functions in a solid.

Problem

- 1 Determine all! wave functions and eigenvalues of the Dirac atom, which satisfies the one-dimensional Schrödinger equation

$$\left[\frac{-\hbar^2}{2m_e} \partial_x^2 - U\delta(x) \right] \psi(x) = \psi(x)E \tag{1.57}$$

Solution

Away from the origin, the electrons experience a constant potential with energy zero. For each side of the atom, i.e. for $x > 0$ and for $x < 0$, we obtain plane waves as solution for positive energies and exponentials for negative energies. For negative energies, we can furthermore exclude a contribution of partial solutions, which grow exponentially towards infinity.

Away from the origin, the solutions have the form

$$\psi(x) = \begin{cases} A_{\pm} \cos(k(E)x - \varphi_{\pm}(E)) & \text{for } E > 0 \\ B_{\pm} e^{-\lambda(E)|x|} & \text{for } E < 0 \end{cases} \tag{1.58}$$

where the indices $\pm \in \{+, -\}$ specify the parameters for the left side, $-$ for $x < 0$, and the right side, $+$ for $x > 0$.

Insertion into the differential equation for $x \neq 0$ yields

$$\begin{aligned}
 \frac{\hbar^2 k^2(E)}{2m} = E &\quad \Rightarrow \quad k(E) = \pm \frac{1}{\hbar} \sqrt{2mE} \\
 \frac{-\hbar^2 \lambda^2(E)}{2m} = E &\quad \Rightarrow \quad \lambda(E) = \pm \frac{1}{\hbar} \sqrt{2m|E|}
 \end{aligned} \tag{1.59}$$

Let me now investigate the differential equation next to the origin.

$$\begin{aligned}
 \left[\frac{-\hbar^2}{2m} \partial_x^2 - U\delta(x) \right] \psi(x) &= \psi(x)E \\
 \Rightarrow \partial_x^2 \psi(x) &= -\frac{2m}{\hbar^2} \left(U\delta(x)\psi(x) + \psi(x)E \right) \\
 \Rightarrow \partial_x|_{x=+\epsilon} \psi - \partial_x|_{x=-\epsilon} \psi &= -\frac{2m}{\hbar^2} \int_{-\epsilon}^{\epsilon} dx \left(U\delta(x)\psi(x) + \psi(x)E \right) \\
 &= -\frac{2mU}{\hbar^2} \psi(0) \quad \text{for } \epsilon \rightarrow 0
 \end{aligned} \tag{1.60}$$

- Bound states $E < 0$: The condition that the wave function is continuous requires $B := B_- = B_+$ in the Ansatz Eq. 1.58.

$$\begin{aligned}
 -\lambda(E)B - \lambda(E)B &\stackrel{\text{Eq. 1.60}}{=} -\frac{2mU}{\hbar^2}B \quad \Rightarrow \quad \lambda(E) = \frac{mU}{\hbar^2} \\
 \Rightarrow \psi(x) &\stackrel{\text{Eq. 1.58}}{=} B e^{-\frac{mU}{\hbar^2}|x|}
 \end{aligned} \tag{1.61}$$

Only one bound state exists. Its energy is

$$E = \frac{-\hbar^2 \lambda^2}{2m} = \frac{-\hbar^2 m^2 U^2}{2m \hbar^4} = \frac{-mU^2}{2\hbar^2} \tag{1.62}$$

- Scattering states:

We exploit that the Dirac atom has an inversion symmetry. Therefore, one can divide the solutions into ones that are symmetric and others, that are antisymmetric under inversion.

- Antisymmetric scattering states:

Let me start with the antisymmetric solutions. The condition that the solution is continuous determines this solution as

$$\psi(x) = A \sin(k(E)x) \tag{1.63}$$

The differential equation at the origin is automatically satisfied.

- Symmetric scattering states:

$$\psi(x) = A \cos(k(E)|x| - \varphi(E)) \tag{1.64}$$

Being symmetric under inversion automatically ensures that the solution is continuous.

$$\begin{aligned}
 \partial_x|_{0+} \psi(x) - \partial_x|_{0-} \psi(x) &= -\frac{2m_e U}{\hbar^2} \psi(0) \\
 Ak(E) \left(-\sin(-\varphi(E)) - \sin(-\varphi(E)) \right) &= -\frac{2mU}{\hbar^2} A \cos(-\varphi(E)) \\
 \tan(\varphi_+(E)) &= \frac{mU}{\hbar^2 k(E)} = \frac{mU}{\hbar \sqrt{2mE}} \\
 \varphi_+(E) &= \text{atan} \left(\frac{mU}{\hbar \sqrt{2mE}} \right) = \text{atan} \left(\sqrt{\frac{mU^2}{2\hbar^2 E}} \right)
 \end{aligned} \tag{1.65}$$

The phase-shift is shown in figure 1.2.

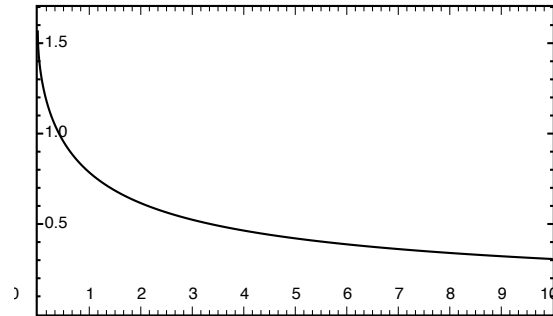


Fig. 1.2: Phaseshift $\varphi_+(E)$ of the Dirac atom as function of energy.

This provides the wave function of the scattering states, which are symmetric under inversion.

$$\psi(x) \stackrel{\text{Eq. 1.58}}{=} A \cos \left(\frac{\hbar}{\sqrt{2mE}} |x| - \text{atan} \left(\sqrt{\frac{m_e U^2}{2E \hbar^2}} \right) \right) \quad (1.66)$$

The prefactor A must be determined according to the normalization condition, and that depends on the boundary conditions chosen.

1.2.4 Thermodynamics

Introduction

Let us revisit some basic identities for the example of the harmonic oscillator and the two-state system. These two systems lead us to the thermodynamics of non-interacting Bosons and Fermions.

Problem

- 1 Determine the partition function for the quantum harmonic oscillator. Use it to write down the free energy as function of temperature.
- 2 Determine the partition function for a two-state system. Use it to write down the free energy as function of temperature.
- 3 Determine from the free energies calculated above (1) the internal energy as function of temperature, (2) the entropy as function of temperature. Plot the results. (A qualitative sketch is sufficient.)
- 4 Calculate the specific heat as function of temperature for the two-state system and the harmonic oscillator.

Solution

- 1 Determine the partition function for the quantum harmonic oscillator. Use it to write down the free energy as function of temperature.

- Energy levels: $E_n = \hbar\omega(n + \frac{1}{2})$. $\frac{1}{2}\hbar\omega$ is the zero-point energy and $\hbar\omega$ is the excitation energy.
- Partition function:

$$\begin{aligned} Z(T) &:= \sum_{n=0}^{\infty} e^{-\beta E_n} = \sum_{n=0}^{\infty} e^{-\beta\hbar\omega/2} (e^{-\beta\hbar\omega})^n \\ &= e^{-\beta\hbar\omega/2} \frac{1}{1 - e^{-\beta\hbar\omega}} \end{aligned} \quad (1.67)$$

We use the geometric series $\sum_{n=0}^{\infty} q^n = (1 - q)^{-1}$.

- Free energy:

$$\begin{aligned} F(T) &= -k_B T \ln[Z(T)] = -k_B T \ln \left[e^{-\beta\hbar\omega/2} \frac{1}{1 - e^{-\beta\hbar\omega}} \right] \\ &= \frac{1}{2} \hbar\omega + k_B T \ln [1 - e^{-\beta\hbar\omega}] \end{aligned} \quad (1.68)$$

2 Determine the partition function for a two-state system. Use it to write down the free energy as function of temperature.

- Energy levels $E_n = E_0 + \hbar\omega n$, with $n \in \{0, 1\}$. E_0 is the ground-state energy and $\hbar\omega$ is the excitation energy.
- Partition sum:

$$Z(T) = \sum_{n=0}^1 e^{-\beta E_n} = e^{-\beta E_0} (1 + e^{-\beta\hbar\omega}) \quad (1.69)$$

- Free energy:

$$\begin{aligned} F(T) &= -k_B T \ln[Z(T)] = -k_B T \ln [e^{-\beta E_0} (1 + e^{-\beta\hbar\omega})] \\ &= E_0 - k_B T \ln [1 + e^{-\beta\hbar\omega}] \end{aligned} \quad (1.70)$$

3 Determine from the free energies calculated above (1) the internal energy as function of temperature, (2) the entropy as function of temperature. Plot the results. (A qualitative sketch is sufficient.)

Relations used:

$$F(T) := \text{stat}_S (U(S) - TS) \quad \Leftrightarrow \quad U(S) = \text{stat}_T (F(T) + TS) \quad (1.71)$$

The operation stat_x means “vary x until you find the stationary point”. It is a generalization of \min_x and \max_x to saddle points and general extrema. In contrast to \min and \max there may be several stationary points.

The expression for the Legendre transform given above is unconventional. It combines two equations, namely

$$F = U - TS \quad \text{and} \quad \frac{\partial U}{\partial S} = T \quad (1.72)$$

in one expression. Similarly I obtain the back transform

$$U = F + TS \quad \text{and} \quad \frac{\partial F}{\partial T} = -S \quad (1.73)$$

Harmonic oscillator: We start with the free energy from the first question and calculate the entropy

$$\begin{aligned} F(T) &= \frac{1}{2}\hbar\omega + k_B T \ln [1 - e^{-\beta\hbar\omega}] \\ S(T) &= -\frac{\partial F}{\partial T} = -k_B \ln [1 - e^{-\beta\hbar\omega}] - k_B T \frac{1}{1 - e^{-\beta\hbar\omega}} \left((-1) \left(-\frac{-1}{k_B T^2} \right) \hbar\omega e^{-\beta\hbar\omega} \right) \\ &= -k_B \ln [1 - e^{-\beta\hbar\omega}] + k_B \beta \hbar\omega \frac{e^{-\beta\hbar\omega}}{1 - e^{-\beta\hbar\omega}} \\ &= k_B \left\{ -\ln [1 - e^{-\beta\hbar\omega}] + \beta \hbar\omega \frac{1}{e^{+\beta\hbar\omega} - 1} \right\} \end{aligned} \quad (1.74)$$

The entropy can be used to obtain the internal energy U .

$$\begin{aligned} U &= F + TS \\ &= \underbrace{\frac{1}{2}\hbar\omega + k_B T \ln [1 - e^{-\beta\hbar\omega}]}_F + \underbrace{\left(-k_B T \ln [1 - e^{-\beta\hbar\omega}] + k_B T \beta \hbar\omega \frac{1}{e^{+\beta\hbar\omega} - 1} \right)}_{TS} \\ &= \frac{1}{2}\hbar\omega + \hbar\omega \frac{1}{e^{+\beta\hbar\omega} - 1} \end{aligned} \quad (1.75)$$

The function

$$b_{T,\mu}(\epsilon) = \frac{1}{e^{+\beta(\epsilon-\mu)} - 1} \quad (1.76)$$

is the Bose distribution function, which specifies the occupations of energy levels with non-interacting bosons.

- Two-state system: We proceed analogously to the previous problem using the free energy calculated in the second question.

$$\begin{aligned} F(T) &= E_0 - k_B T \ln [1 + e^{-\beta\hbar\omega}] \\ S(T) &= -\frac{\partial F}{\partial T} = k_B \ln [1 + e^{-\beta\hbar\omega}] + k_B T \frac{1}{1 + e^{-\beta\hbar\omega}} \left((+1) \left(-\frac{-1}{k_B T^2} \right) \hbar\omega e^{-\beta\hbar\omega} \right) \\ &= k_B \ln [1 + e^{-\beta\hbar\omega}] + k_B \beta \hbar\omega \frac{e^{-\beta\hbar\omega}}{1 + e^{-\beta\hbar\omega}} \\ &= k_B \left\{ \ln [1 + e^{-\beta\hbar\omega}] + \frac{\beta \hbar\omega}{1 + e^{+\beta\hbar\omega}} \right\} \end{aligned} \quad (1.77)$$

$$\begin{aligned} U &= F + TS \\ &= \underbrace{E_0 - k_B T \ln [1 + e^{-\beta\hbar\omega}]}_F + \underbrace{\left(k_B T \ln [1 + e^{-\beta\hbar\omega}] + k_B T \beta \hbar\omega \frac{1}{1 + e^{+\beta\hbar\omega}} \right)}_{TS} \\ &= E_0 + \hbar\omega \frac{1}{1 + e^{+\beta\hbar\omega}} \end{aligned} \quad (1.78)$$

The function

$$f_{T,\mu}(\epsilon) = \frac{1}{1 + e^{+\beta(\epsilon-\mu)}} \quad (1.79)$$

is the **Fermi distribution function**, which specifies the occupations of energy levels with non-interacting fermions (See Fig. 6.3 on p. 191).

4 Calculate the specific heat as function of temperature for the two-state system and the harmonic oscillator.

Specific heat: The specific heat is the amount of energy required to heat the substance by one unit of temperature.

$$c(T) = \frac{dU}{dT} \quad (1.80)$$

Specific heat of the harmonic oscillator

$$\begin{aligned} U &= \frac{1}{2}\hbar\omega + \hbar\omega \frac{1}{e^{\beta\hbar\omega} - 1} \\ c(T) &= \frac{dU}{dT} = \hbar\omega \frac{-1}{(e^{\beta\hbar\omega} - 1)^2} \left(-\frac{\beta\hbar\omega}{T} e^{\beta\hbar\omega} \right) \\ &= k_B \frac{(\beta\hbar\omega)^2}{(e^{\beta\hbar\omega} - 1)(1 - e^{-\beta\hbar\omega})} \\ &= k_B \frac{\frac{1}{2}(\beta\hbar\omega)^2}{\cosh(\beta\hbar\omega) - 1} \end{aligned} \quad (1.81)$$

Specific heat of the two-state system

$$\begin{aligned} U &= E_0 + \hbar\omega \frac{1}{e^{\beta\hbar\omega} + 1} \\ c(T) &= \frac{dU}{dT} = \hbar\omega \frac{-1}{(e^{\beta\hbar\omega} + 1)^2} \left(-\frac{\beta\hbar\omega}{T} e^{\beta\hbar\omega} \right) \\ &= k_B \frac{(\beta\hbar\omega)^2}{(e^{\beta\hbar\omega} + 1)(1 + e^{-\beta\hbar\omega})} \\ &= k_B \frac{\frac{1}{2}(\beta\hbar\omega)^2}{1 + \cosh(\beta\hbar\omega)} \end{aligned} \quad (1.82)$$

The specific heats are shown in Fig. 1.3. The specific heat at low temperatures are almost identical. This is because the second and higher states of the harmonic oscillator are out of reach for thermal excitations. At high temperatures, the specific heat of the harmonic oscillator approaches the classical result, namely k_B . The high-temperature specific heat of the two-state system vanishes: Once both states are equally occupied, the energy can not more be raised by raising the temperature.

1.2.5 Eigenvalue decomposition of non-hermitian matrices

Introduction

The problem described here is closely related to the problem 1.2.1 on the linear algebra of 2×2 matrices. As a physicist one rarely encounters the eigenvalue problems of non-hermitian matrices. They are important, though, to exploit symmetry. Symmetry transformations are unitary but rarely hermitian. In this lecture, I will exploit the symmetry of crystals, and this is where we encounter eigenvalue problems of non-hermitian matrices.

In physics we are very much accustomed to eigenvalue problems for hermitian matrices or operators. We easily forget that the diagonalization of non-hermitian matrices is more complex. The eigenvalue problem of unitary operators is relevant for exploiting symmetry. This is because transformation operators are, in general, non-hermitian.

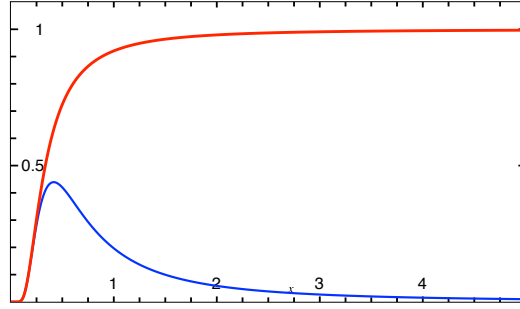


Fig. 1.3: Specific heat in units of k_B for a harmonic oscillator (red) and a two-state system (blue) as function of the temperature $1/(\beta\hbar\omega)$.

For a general square matrix, the eigenvalues can be complex-valued, and we need to distinguish **left- and right-handed eigenvectors**.

Let me describe the general square eigenvalue problem: Let \mathbf{A} be a complex-valued square matrix. There are two square matrices, \mathbf{U} and \mathbf{V} , as well as a diagonal matrix \mathbf{a} , which satisfy the following eigenvalue equations.

$$\begin{aligned} \mathbf{A}\mathbf{U} &= \mathbf{U}\mathbf{a} && \text{right eigenvalue equation} \\ \mathbf{V}^\dagger\mathbf{A} &= \mathbf{a}\mathbf{V}^\dagger && \text{left eigenvalue equation} \end{aligned} \quad (1.83)$$

The eigenvalues for the left and right eigenvalue problems are the same. The eigenvalues of non-hermitian matrices are usually complex-valued, even if the matrix is real-valued. The eigenvectors of non-hermitian matrices are not orthogonal to each other. As shown below, left and right eigenvectors can, however, be chosen bi-orthonormal to each other. [Editor: Describe that the eigenvectors have been combined to \$\mathbf{U}\$ etc.](#)

The left eigenvectors of \mathbf{A} are closely related to the right eigenvectors of the hermitian conjugate \mathbf{A}^\dagger :

$$(\mathbf{V}^\dagger\mathbf{A})^\dagger = (\mathbf{a}\mathbf{V}^\dagger)^\dagger \Rightarrow \mathbf{A}^\dagger\mathbf{V} = \mathbf{V}\mathbf{a}^* \quad (1.84)$$

The eigenvectors of left- and right eigenvalue equations can be chosen such that they obey the **bi-orthonormality** condition $\mathbf{V}^\dagger\mathbf{U} = \mathbf{1}$, which is shown as follows.

$$\begin{aligned} \mathbf{A}\mathbf{U} &= \mathbf{U}\mathbf{a} \quad \text{and} \quad \mathbf{V}^\dagger\mathbf{A} = \mathbf{a}\mathbf{V}^\dagger \\ \mathbf{a}\mathbf{V}^\dagger\mathbf{U} &= \mathbf{V}^\dagger\mathbf{A}\mathbf{U} = \mathbf{V}^\dagger\mathbf{U}\mathbf{a} \\ \Rightarrow a_m(\mathbf{V}^\dagger\mathbf{U})_{m,n} &= (\mathbf{V}^\dagger\mathbf{U})_{m,n} a_n \\ \Rightarrow (a_m - a_n)(\mathbf{V}^\dagger\mathbf{U})_{m,n} &= 0 \\ \Rightarrow (\mathbf{V}^\dagger\mathbf{U})_{m,n} &= 0 \quad \text{for } a_m \neq a_n \end{aligned} \quad (1.85)$$

Thus, if the diagonal elements of \mathbf{a} are non-degenerate, $\mathbf{V}^\dagger\mathbf{U}$ is a diagonal matrix. For degenerate multiplets, the orthogonality can be imposed by a Gram-Schmidt orthogonalization. By rescaling the eigenvectors, the product can be made equal to the unit matrix, which results in a **bi-orthonormality condition**

$$\mathbf{V}^\dagger\mathbf{U} = \mathbf{1} \quad (1.86)$$

Let us make the normalization above part of the definition of \mathbf{U} and \mathbf{V} .

Diagonalization:

$$\mathbf{AU} = \mathbf{U}\mathbf{a}\mathbf{V}^\dagger \mathbf{AU} = \mathbf{V}^\dagger \mathbf{U}\mathbf{a} = \mathbf{a}$$

$$\mathbf{AU} = \mathbf{U}\mathbf{a} \Rightarrow \mathbf{A} = \underbrace{\mathbf{A}\mathbf{U}\mathbf{V}^\dagger}_\mathbf{1} = \mathbf{U}\mathbf{a}\mathbf{V}^\dagger \tag{1.87}$$

- Real-valued matrices, that are not symmetric have complex-valued eigenvalues, but they come in complex-conjugate pairs.
- Hermitian matrices have real-valued eigenvalues. Left and right eigenvectors are identical, that is, $\mathbf{U} = \mathbf{V}$.

Outlook: Singular value problem We can also extend the problem of diagonalization to matrices that are not square. In that case one speaks of a singular-value decomposition. A typical problem for a singular value decomposition is the fitting of a data set by a superposition of a set of functions. This shall be mentioned on a side. Because it is not used in this lecture, I do not elaborate on it.

Problem

Consider a 2×2 matrix \mathbf{A} , that describes a counter-clock-wise rotation by 45° .

- 1 determine the matrix \mathbf{A}
- 2 determine the eigenvalues of \mathbf{A}
- 3 determine the right eigenvectors of \mathbf{A}
- 4 determine the left eigenvectors of \mathbf{A}
- 5 construct the matrices \mathbf{U} , \mathbf{V}^\dagger and the diagonal matrix \mathbf{a} holding the eigenvalues.
- 6 confirm that the bi-orthogonality holds
- 7 reconstruct the matrix \mathbf{A} from \mathbf{U} , \mathbf{V}^\dagger and \mathbf{a}

Solution

Consider a 2×2 matrix \mathbf{A} , that describes a counter-clock-wise rotation by 45° .

- 1 determine the matrix \mathbf{A}

Let us consider a rotation in two dimensions by an angle of $45^\circ = \pi/4$

$$\mathbf{A} = \begin{pmatrix} \cos(\alpha) & \sin(\alpha) \\ -\sin(\alpha) & \cos(\alpha) \end{pmatrix} \stackrel{\alpha=\pi/4}{=} \frac{1}{\sqrt{2}} \begin{pmatrix} 1 & 1 \\ -1 & 1 \end{pmatrix} \tag{1.88}$$

- 2 determine the eigenvalues of \mathbf{A}

The eigenvalues a_\pm result from the characteristic equation

$$0 = \det |\mathbf{A} - a_\pm \mathbf{1}| = \frac{1}{2} \left((1 - \sqrt{2}\lambda)^2 + 1 \right) \Rightarrow a_\pm = \frac{1}{\sqrt{2}} (1 \pm i) = e^{\pm i\pi/4} \tag{1.89}$$

Because the matrix \mathbf{A} is real-valued, the eigenvalues a_{\pm} come in complex-conjugate pairs. Because the matrix A is unitary, the absolute values $|a_{\pm}|$ of the eigenvalues are unity.

3 determine the right eigenvectors of \mathbf{A}

The right-handed eigenvectors are obtained from

$$\begin{aligned}
 0 &= (\mathbf{A} - a_{\pm} \mathbf{1}) \vec{c}_{\pm}^{(r)} \\
 0 &= (A_{11} - a_{\pm})c_{1,\pm} + A_{12}c_{2,\pm} = \frac{1}{\sqrt{2}} \left[(1 - 1 \mp i)c_{1,\pm} + c_{2,\pm} \right] \\
 c_{2,\pm}^{(r)} &= \pm i c_{1,\pm}^{(r)} \\
 \vec{c}_{\pm}^{(r)} &= \frac{1}{\sqrt{2}} \begin{pmatrix} 1 \\ \pm i \end{pmatrix} \tag{1.90}
 \end{aligned}$$

4 determine the left eigenvectors of \mathbf{A}

The left-handed eigenvalues are

$$\begin{aligned}
 0 &= \vec{c}_{\pm}^{(l)} (\mathbf{A} - a_{\pm} \mathbf{1}) \quad \left[\Rightarrow \quad 0 = (\mathbf{A}^{\dagger} - a_{\pm}^* \mathbf{1}) \vec{c}_{\pm}^{(l)*} \right] \\
 0 &= \vec{c}_{1,\pm}^{(l)} (A_{11} - a_{\pm}) + c_{2,\pm}^{(l)} U_{21} = \frac{1}{\sqrt{2}} \left[(1 - 1 \mp i)c_{1,\pm}^{(l)} - c_{2,\pm}^{(l)} \right] \\
 c_{2,\pm}^{(l)} &= \mp i c_{1,\pm}^{(l)} \\
 \vec{c}_{\pm}^{(l)} &= \frac{1}{\sqrt{2}} \begin{pmatrix} 1 \\ \mp i \end{pmatrix} \tag{1.91}
 \end{aligned}$$

5 construct the matrices \mathbf{U} , \mathbf{V}^{\dagger} and the diagonal matrix \mathbf{a} holding the eigenvalues.

Let me combine the eigenvectors and eigenvalues into matrices

$$\mathbf{U} = \frac{1}{\sqrt{2}} \begin{pmatrix} 1 & 1 \\ i & -i \end{pmatrix} \quad \text{and} \quad \mathbf{V}^{\dagger} = \frac{1}{\sqrt{2}} \begin{pmatrix} 1 & -i \\ 1 & i \end{pmatrix} \quad \text{and} \quad \mathbf{a} = \frac{1}{\sqrt{2}} \begin{pmatrix} 1+i & 0 \\ 0 & 1-i \end{pmatrix} \tag{1.92}$$

6 confirm that the bi-orthogonality holds

Let me test the bi-orthonormality

$$\mathbf{1} \stackrel{?}{=} \mathbf{V}^{\dagger} \mathbf{U} = \frac{1}{\sqrt{2}} \begin{pmatrix} 1 & -i \\ 1 & +i \end{pmatrix} \frac{1}{\sqrt{2}} \begin{pmatrix} 1 & 1 \\ +i & -i \end{pmatrix} = \frac{1}{2} \begin{pmatrix} 2 & 0 \\ 0 & 2 \end{pmatrix} = \mathbf{A} \tag{1.93}$$

7 reconstruct the matrix \mathbf{A} from \mathbf{U} , \mathbf{V}^{\dagger} and \mathbf{a}

Let me reconstruct the matrix \mathbf{A} from the eigenvalues and the two bi-orthogonal matrices \mathbf{U} and

V.

$$\begin{aligned}
 \mathbf{A} &\stackrel{?}{=} \mathbf{UaV}^\dagger = \frac{1}{\sqrt{2}} \begin{pmatrix} 1 & 1 \\ +i & -i \end{pmatrix} \frac{1}{\sqrt{2}} \begin{pmatrix} 1+i & 0 \\ 0 & 1-i \end{pmatrix} \frac{1}{\sqrt{2}} \begin{pmatrix} 1 & -i \\ 1 & +i \end{pmatrix} \\
 &= \frac{1}{2\sqrt{2}} \begin{pmatrix} 1; & 1 \\ +i; & -i \end{pmatrix} \begin{pmatrix} 1+i; & 1-i \\ 1-i; & 1+i \end{pmatrix} = \frac{1}{2\sqrt{2}} \begin{pmatrix} 1+i+1-i & 1-i+1+i \\ i-1-i-1 & i+1-i+1 \end{pmatrix} \\
 &= \frac{1}{2\sqrt{2}} \begin{pmatrix} 2 & 2 \\ -2 & 2 \end{pmatrix} = \mathbf{1} \tag{1.94}
 \end{aligned}$$

Chapter 2

Born-Oppenheimer approximation and beyond

In this chapter, the problem of describing nuclei, electrons and photons will be divided up into two simpler problems, one for electrons and one for atoms.¹ This division, which I will call the **Born-Huang framework**, separates out the electronic-structure problem, which describes electrons in the presence of frozen atom configurations, from the atom dynamics. By exploring electrons in all conceivable, albeit frozen, atom distributions, one can rigorously extract their effect on moving atoms. This will lead to an effective Schrödinger equation Eq. 2.27 for the atoms that evolve under the influence of the electronic structure. The full wave function of electrons and nuclei is obtained finally by combining electronic and atomic wave functions.

Later, in chapter 7, I will use the Born-Huang framework to introduce **phonons**, the quasi-particles describing lattice vibrations, in a rigorous and unambiguous fashion.

Once we arrived at the Schrödinger equation for the atoms, we can make approximations to it: widely known is the **Born-Oppenheimer approximation** [5, 6] or adiabatic approximation, which omits transitions between electronically excited states.

Non-adiabatic effects, which are discarded in the Born-Oppenheimer approximation, are discussed in section 2.3. Non-adiabatic effects describe transitions between excited electronic states under the influence of the atom dynamics. They are responsible for the dissipation of the energy of an excited state and they form the basis for photochemistry². I will introduce the famous **non-crossing theorem**, which plays an important role also in a different context of topological materials. The non-crossing theorem implies that electronic transitions occur “usually” at **conical intersections**. The transitions at a conical intersection will be demonstrated using the **Jahn-Teller model**.

Finally, I will briefly touch the semi-classical approximation of the atomic Schrödinger equation, which replaces the quantum-mechanical wave functions for the atoms by classical atomic trajectories. This approximation forms the basis of **molecular dynamics**, a simulation technique for the atom dynamics. Because of the large atom masses, this is usually a well justified approximation.

In this chapter, I emphasize the rigorous derivation and I will discuss approximations that are made to this theory. The reason is that there are many misleading or even incorrect statements on this topic in the literature. One goal of this chapter is to enable you to verify the arguments by yourself.

¹The atoms are the quasiparticles made from nuclei together with their deformation of the surrounding electron gas.

²Photochemistry describes light-induced chemical reactions.

2.1 Separation of electronic and nuclear degrees of freedom

The ultimate goal is to determine the wave function $\Phi(\vec{x}_1, \dots, \vec{x}_N, \vec{R}_1, \dots, \vec{R}_M, t)$, which describes the electronic degrees of freedom $\vec{x}_1, \dots, \vec{x}_N$ and the atomic positions $\vec{R}_1, \dots, \vec{R}_M$ on the basis of the time-dependent Schrödinger equation Eq. 1.1

$$i\hbar\partial_t|\Phi(t)\rangle \stackrel{\text{Eq. 1.1}}{=} \hat{H}|\Phi(t)\rangle \quad (2.1)$$

The Hamiltonian \hat{H} is the one given in Eq. 1.5.

The **Born-Huang framework**, which separates the electronic-structure problem from the atom dynamics consists of the following two steps:

1. First, one determines the electronic eigenstates for frozen atomic positions. The corresponding Born-Oppenheimer equation Eq. 2.4 defines the **Born-Oppenheimer wave functions** and **Born-Oppenheimer surfaces**, which are the basic ingredient for the atom dynamics. This step does not make any assumptions on the electron dynamics. Rather, it merely defines a set of auxiliary quantities required in the next step.
2. Using the Born-Oppenheimer wave functions and -surfaces, a time-dependent Schrödinger equation Eq. 2.27 for the dynamics of the nuclei is derived. This step does not introduce any approximations: The electron dynamics is properly included via the Born-Oppenheimer surfaces and wave functions, once they are combined with the wave functions of the nuclei.

2.1.1 Born-Oppenheimer wave functions and Born-Oppenheimer surfaces

Firstly, we define the Born-Oppenheimer Hamiltonian \hat{H}^{BO} by removing all terms from the Hamiltonian \hat{H} , which depend on the momenta of the nuclei Eq. 1.5.

$$\begin{aligned} \hat{H}^{BO}(\vec{R}_1, \dots, \vec{R}_M) = & \underbrace{\sum_{i=1}^N \frac{-\hbar^2}{2m_e} \nabla_{\vec{r}_i}^2}_{E_{kin,e}} + \underbrace{\frac{1}{2} \sum_{i \neq j}^M \frac{e^2 Z_i Z_j}{4\pi\epsilon_0 |\vec{R}_i - \vec{R}_j|}}_{E_{C,nuc-nuc}} - \underbrace{\sum_{i=1}^N \sum_{j=1}^M \frac{e^2 Z_j}{4\pi\epsilon_0 |\vec{r}_i - \vec{R}_j|}}_{E_{C,e-nuc}} \\ & + \underbrace{\frac{1}{2} \sum_{i \neq j}^N \frac{e^2}{4\pi\epsilon_0 |\vec{r}_i - \vec{r}_j|}}_{E_{C,e-e}} \end{aligned} \quad (2.2)$$

The full Hamiltonian of Eq. 1.5, namely

$$\hat{H} = \sum_{j=1}^M \frac{-\hbar^2}{2M_j} \nabla_{\vec{R}_j}^2 + \hat{H}^{BO}(\vec{R}_1, \dots, \vec{R}_M), \quad (2.3)$$

is obtained by adding the nuclear kinetic energy to the Born-Oppenheimer Hamiltonian \hat{H}^{BO} . The unit operator $\hat{1}$ acts on the electronic Hilbert space.

The Born-Oppenheimer Hamiltonian acts in the Hilbert space of electronic wave functions, and it depends parametrically on the nuclear positions. In other words, the Born-Oppenheimer Hamiltonian does not contain any gradients acting on the nuclear positions.

In order to simplify the equations, I combine

- the electronic coordinates and spin indices into a vector $\vec{x} = (\vec{x}_1, \dots, \vec{x}_N)$ and
- the nuclear positions into a $3M$ -dimensional vector $\vec{R} = (\vec{R}_1, \dots, \vec{R}_M)$.

Thus, the wave function for electrons and nuclei will be written as $\Phi(\vec{x}, \vec{R}, t) = \langle \vec{x}, \vec{R} | \Phi(t) \rangle$. I combine the nuclear masses into a diagonal matrix \mathbf{M} with dimension $3M$.

In addition, I introduce another notation, where the wave function is a regular function of the atomic positions but a quantum state $|\Phi(\vec{R}, t)\rangle$ in the Hilbert space for the electrons, so that $\Phi(\vec{x}, \vec{R}, t) = \langle \vec{x} | \Phi(\vec{R}, t) \rangle$.

The Born-Oppenheimer wave functions $|\Psi_n^{BO}(\vec{R})\rangle$ and the Born-Oppenheimer surfaces $E_n^{BO}(\vec{R})$ are obtained from the **Born-Oppenheimer equation**

$$\left[\hat{H}^{BO}(\vec{R}) - E_n^{BO}(\vec{R}) \right] |\Psi_n^{BO}(\vec{R})\rangle = 0. \quad (2.4)$$

Eq. 2.4 corresponds to a Schrödinger equation for the electrons feeling the static potential from the nuclei, which are fixed in space. The **Born-Oppenheimer surfaces** $E_n^{BO}(\vec{R})$ are the position-dependent energy eigenvalues of the Born-Oppenheimer Hamiltonian. For each atomic configuration, we obtain a ground-state Born-Oppenheimer surface and infinitely many excited-state Born-Oppenheimer surfaces, which are labeled by the quantum number n . Similarly, the **Born-Oppenheimer wave functions** $\Psi_n^{BO}(\vec{x}, \vec{R}) = \langle \vec{x} | \Psi_n^{BO}(\vec{R}) \rangle$ ³ depend parametrically on the nuclear positions \vec{R} . Note, however, that the Born-Oppenheimer wave functions are time-independent.

The Born-Oppenheimer wave functions are chosen⁴ to be orthogonal for each set of atomic positions, i.e.

$$\langle \Psi_m^{BO}(\vec{R}) | \Psi_n^{BO}(\vec{R}) \rangle = \int d^{4N}x \Psi_m^{BO*}(\vec{x}, \vec{R}) \Psi_n^{BO}(\vec{x}, \vec{R}) = \delta_{m,n} \quad (2.5)$$

2.1.2 Born-Huang Ansatz for the electronic-nuclear wave function

Now, we are ready to write down the Born-Huang ansatz for the wave function of a system of electrons and nuclei:

BORN-HUANG EXPANSION

$$\Phi(\vec{x}, \vec{R}, t) = \sum_n \langle \vec{x} | \Psi_n^{BO}(\vec{R}) \rangle \Theta_n(\vec{R}, t) \quad (2.6)$$

The multi-valued nuclear wave function $(\Theta_0(\vec{R}, t), \Theta_1(\vec{R}, t), \Theta_2(\vec{R}, t), \dots)$ with one component $\Theta_n(\vec{R}, t)$ for every Born-Oppenheimer surface, obeys the normalization condition

$$\sum_n \int d^{3M}R \Theta_n^*(\vec{R}, t) \Theta_n(\vec{R}, t) \stackrel{\text{Eq. 2.9}}{=} 1. \quad (2.7)$$

The Born-Oppenheimer states $|\Psi_n^{BO}(\vec{R})\rangle$ are electronic wave functions defined by the Born-Oppenheimer equation

$$\left[\hat{H}^{BO}(\vec{R}) - E_n^{BO}(\vec{R}) \right] |\Psi_n^{BO}(\vec{R})\rangle \stackrel{\text{Eq. 2.4}}{=} 0 \quad (2.8)$$

and the orthonormalization condition

$$\langle \Psi_m^{BO}(\vec{R}) | \Psi_n^{BO}(\vec{R}) \rangle \stackrel{\text{Eq. 2.5}}{=} \delta_{m,n}.$$

The normalization of the electron-nuclear wave function $\Phi(\vec{x}, \vec{R}, t)$ leads to the norm of the

³ $\Psi_n^{BO}(\vec{x}_1, \dots, \vec{x}_N, \vec{R}_1, \dots, \vec{R}_M) = \langle \vec{x}_1, \dots, \vec{x}_N | \Psi_n^{BO}(\vec{R}_1, \dots, \vec{R}_M) \rangle$

⁴They are orthogonal whenever the energies differ, and each set of degenerate states can be orthonormalized.

nuclear wave function used in Eq. 2.7 above.

$$\begin{aligned}
1 &\stackrel{!}{=} \int d^{4N}x \int d^{3M}R \Phi^*(\vec{x}, \vec{R}, t) \Phi(\vec{x}, \vec{R}, t) = \int d^{3M}R \langle \Phi(\vec{R}, t) | \Phi(\vec{R}, t) \rangle \\
&= \int d^{3M}R \left(\sum_m \Theta_m^*(\vec{R}, t) \langle \Psi_m^{BO}(\vec{R}) | \right) \left(\sum_n |\Psi_n^{BO}(\vec{R})\rangle \Theta_n(\vec{R}, t) \right) \\
&= \int d^{3M}R \sum_{m,n} \Theta_m^*(\vec{R}, t) \underbrace{\langle \Psi_m^{BO}(\vec{R}) | \Psi_n^{BO}(\vec{R}) \rangle}_{\delta_{m,n}} \Theta_n(\vec{R}, t) \\
&= \sum_n \int d^{3M}R \Theta_n^*(\vec{R}, t) \Theta_n(\vec{R}, t) \tag{2.9}
\end{aligned}$$

The nuclear-electronic wave function $\Phi(\vec{x}, \vec{R}, t)$ is expressed as a sum of products of the Born-Oppenheimer wave functions $|\Psi_n^{BO}(\vec{R})\rangle$ and time-dependent nuclear wave functions $\Theta_n(\vec{R}, t)$. It is better to think of the nuclear wave functions as multi-valued wave functions with a component for ground state and one for each excited state. The nuclear wave functions $\Theta_n(\vec{R}_1, \dots, \vec{R}_M, t)$ do no more refer to the electronic positions, except through the state index n .

Some caution is required to keep the symbols for the different types of wave functions apart

$\Phi(\vec{x}, \vec{R}, t)$	wave function of electrons and nuclei
$\Psi_n^{BO}(\vec{x}, \vec{R})$	Born-Oppenheimer wave function of electrons
$\Theta_n(\vec{R}, t)$	n -th component of the nuclear wave function

Physical meaning of the Born-Huang expansion: In order to convey some of the physical meaning of the quantities defined in the Born-Huang ansatz, let me anticipate a few observations that will be derived and stated more rigorously in the following sections.

- One Born-Oppenheimer surface $E_n^{BO}(\vec{R})$ can be considered as the potential-energy surface governing the motion of the nuclei. The forces $\vec{F}_n = -\vec{\nabla}_R E_n^{BO}$ acting on the atoms are the negative gradients of the Born-Oppenheimer surface. The Born-Oppenheimer surface is the object that is parameterized in classical molecular-dynamics simulations.
- The squared nuclear wave function describes the probability density $p_n(\vec{R}, t) \stackrel{\text{def}}{=} \Theta_n^*(\vec{R}, t) \Theta_n(\vec{R}, t)$ for the nuclei to be at positions \vec{R} and for the electrons to be in the n -th excited state.
- If the electrons remain in the ground state, only the first component of the nuclear wave function $\Theta_{n=0}(\vec{R}, t)$ differs from zero, and the atomic motion is entirely determined by the single-valued potential energy $E_0^{BO}(\vec{R})$.
- An optical absorption event is usually sufficiently rapid, that the nuclei do not move by any appreciable distance during that process. This is the **Franck-Condon principle**. When it holds, the absorption energy can be estimated as the energy difference between two Born-Oppenheimer surfaces for the same nuclear coordinates.

The Born-Huang expansion is a non-restrictive ansatz: In contrast to the Born-Oppenheimer approximation, the Born-Huang expansion is not an approximation. The Born-Huang expansion is an Ansatz for the electron-nuclear wave function, which does not pose any restriction. This becomes evident, when we insert this ansatz into the electron-nuclear Schrödinger equation: With the proper choice of the nuclear wave function $\Theta_n(\vec{R}, t)$, it can be satisfied exactly.

Let me demonstrate now, that the Born-Huang expansion is non-restrictive: For any given position vector \vec{R} and time t , the wave function $\Phi(\vec{x}, \vec{R}, t)$ is a function of the electronic coordinates \vec{x} . This function can be expanded into any complete, orthonormal basisset $\{|\tilde{\Psi}_n\rangle\}$ in the form

$$\Phi(\vec{x}, \vec{R}, t) = \sum_n \langle \vec{x} | \tilde{\Psi}_n \rangle \bar{c}_n(\vec{R}, t) \tag{2.10}$$

with complex-valued coefficients $\bar{c}_n(\vec{R}, t) = \langle \bar{\Psi}_n | \Phi(\vec{R}, t) \rangle$. Because the wave function changes with \vec{R} and t , the coefficients depend on nuclear positions and time.

With the same right, one can choose a different complete, orthonormal basisset $\{|\tilde{\Psi}_n(\vec{R})\rangle\}$ for every set of nuclear coordinates, so that

$$\Phi(\vec{x}, \vec{R}, t) = \sum_n \langle \vec{x} | \tilde{\Psi}_n(\vec{R}) \rangle \bar{c}_n(\vec{R}, t) \quad (2.11)$$

with complex-valued coefficients $\bar{c}_n(\vec{R}, t) = \langle \tilde{\Psi}_n(\vec{R}) | \Phi(\vec{R}, t) \rangle$.

The eigenstates of the Born-Oppenheimer equation Eq. 2.8 form such a complete basisset. Thus, we can replace $|\tilde{\Psi}_n(\vec{R})\rangle \rightarrow |\Psi_n^{BO}(\vec{R})\rangle$ by the Born-Oppenheimer wave functions and the coefficients $\bar{c}_n(\vec{R}, t) \rightarrow \Theta_n(\vec{R}, t)$ by the nuclear wave functions

$$\Phi(\vec{x}, \vec{R}, t) = \sum_n \langle \vec{x} | \Psi_n^{BO}(\vec{R}) \rangle \Theta_n(\vec{R}, t) \quad (2.12)$$

which is nothing but the Born-Huang expansion Eq. 2.6.

Thus, any physical wave function can be expressed by the Born-Huang expansion without restriction. This is discussed in more detail in appendix B.2.

2.1.3 Nuclear Schrödinger equation

In the following, I will insert the Born-Huang Ansatz Eq. 2.6 into the Schrödinger equation for electrons and nuclei. This will lead to a Schrödinger equation for the nuclear wave function $\Theta(\vec{R}, t)$ alone. The electrons will effectively be “hidden away” and occur only in the form of (scalar and vector) potentials acting on the nuclei.

When the Born-Huang Ansatz Eq. 2.6 is inserted into the Schrödinger equation Eq. 2.1 for electrons and nuclei with the full Hamiltonian Eq. 2.3, we obtain

$$\begin{aligned} i\hbar\partial_t \left[\sum_n |\Psi_n^{BO}(\vec{R})\rangle \Theta_n(\vec{R}, t) \right] &\stackrel{\text{Eq. 2.6}}{=} \hat{H} \left[\sum_n |\Psi_n^{BO}(\vec{R})\rangle \Theta_n(\vec{R}, t) \right] \\ &\stackrel{\text{Eq. 2.3}}{=} \left[\frac{1}{2} \left(\frac{\hbar}{i} \vec{\nabla}_R \right) \mathbf{M}^{-1} \left(\frac{\hbar}{i} \vec{\nabla}_R \right) + \hat{H}^{BO}(\vec{R}) \right] \left[\sum_n |\Psi_n^{BO}(\vec{R})\rangle \Theta_n(\vec{R}, t) \right] \\ &\stackrel{\text{Eq. 2.4}}{=} \sum_n |\Psi_n^{BO}(\vec{R})\rangle \left[\frac{1}{2} \left(\frac{\hbar}{i} \vec{\nabla}_R \right) \mathbf{M}^{-1} \left(\frac{\hbar}{i} \vec{\nabla}_R \right) + E_n^{BO}(\vec{R}) \right] \Theta_n(\vec{R}, t) \\ &\quad + \sum_n \left\{ \left[\left(\frac{\hbar}{i} \vec{\nabla}_R \right) |\Psi_n^{BO}(\vec{R})\rangle \right] \mathbf{M}^{-1} \left(\frac{\hbar}{i} \vec{\nabla}_R \right) + \frac{1}{2} \left[\left(\frac{\hbar}{i} \vec{\nabla}_R \right) \mathbf{M}^{-1} \left(\frac{\hbar}{i} \vec{\nabla}_R \right) |\Psi_n^{BO}(\vec{R})\rangle \right] \right\} \Theta_n(\vec{R}, t) \end{aligned} \quad (2.13)$$

Note, that the gradients inside the square brackets indicated in blue do **not** act beyond the square bracket onto the nuclear wave function.

Now, we multiply Eq. 2.13 from the left with the bra $\langle \Psi_m^{BO}(\vec{R}) |$ of the Born-Oppenheimer wave function and integrate over the electronic coordinates. Hereby, we exploit the orthonormality Eq. 2.5 of the Born-Oppenheimer wave functions.

As the result, we obtain a Schrödinger equation for the nuclear motion alone.

$$\begin{aligned} i\hbar\partial_t \Theta_m(\vec{R}, t) &\stackrel{\text{Eqs. 2.13, 2.5}}{=} \left[\frac{1}{2} \frac{\hbar}{i} \vec{\nabla}_R \mathbf{M}^{-1} \frac{\hbar}{i} \vec{\nabla}_R + E_m^{BO}(\vec{R}) \right] \Theta_m(\vec{R}, t) \\ &\quad + \underbrace{\sum_n \left[\underbrace{\bar{A}_{m,n}(\vec{R})}_{\langle \Psi_m^{BO} | \frac{\hbar}{i} \vec{\nabla}_R | \Psi_n^{BO} \rangle} \mathbf{M}^{-1} \frac{\hbar}{i} \vec{\nabla}_R + \frac{1}{2} \underbrace{B_{m,n}(\vec{R})}_{\langle \Psi_m^{BO} | \frac{\hbar}{i} \vec{\nabla}_R \mathbf{M}^{-1} \frac{\hbar}{i} \vec{\nabla}_R | \Psi_n^{BO} \rangle} \right]}_{\text{non-adiabatic terms}} \Theta_n(\vec{R}, t) \end{aligned} \quad (2.14)$$

The **first-derivative couplings** $\vec{A}_{m,n}(\vec{R})$ and the **second-derivative couplings** $B_{m,n}(\vec{R})$ are defined as (see Eq. 2.14)

$$\vec{A}_{m,n}(\vec{R}) \stackrel{\text{def}}{=} \left\langle \Psi_m^{BO}(\vec{R}) \left| \frac{\hbar}{i} \vec{\nabla}_R \right| \Psi_n^{BO}(\vec{R}) \right\rangle \quad (2.15)$$

$$B_{m,n}(\vec{R}) \stackrel{\text{def}}{=} \left\langle \Psi_m^{BO}(\vec{R}) \left| \left(\frac{\hbar}{i} \vec{\nabla}_R \right) \mathbf{M}^{-1} \left(\frac{\hbar}{i} \vec{\nabla}_R \right) \right| \Psi_n^{BO}(\vec{R}) \right\rangle \quad (2.16)$$

Note, that the brackets $\langle \dots \rangle$ are evaluated by integrating over the electronic degrees of freedom only. Thus, the matrix elements still depend explicitly on the nuclear coordinates.

Up to now, we did not introduce any approximations to arrive at the nuclear Schrödinger equation Eq. 2.14. We are still on solid ground. Let us now spend some time to bring this equation into a more convenient form.

Second-derivative couplings from first-derivative couplings: The first- and the second-derivative couplings are not independent. Rather, the second-derivative coupling $B_{m,n}(\vec{R})$ can be calculated from the first-derivative couplings $\vec{A}_{m,n}(\vec{R})$. This is shown as follows (see [7]):

$$\begin{aligned} & \frac{\hbar}{i} \vec{\nabla}_R \mathbf{M}^{-1} \vec{A}_{m,n}(\vec{R}) \stackrel{\text{Eq. 2.15}}{=} \frac{\hbar}{i} \vec{\nabla}_R \mathbf{M}^{-1} \left\langle \Psi_m^{BO}(\vec{R}) \left| \frac{\hbar}{i} \vec{\nabla}_R \right| \Psi_n^{BO}(\vec{R}) \right\rangle \\ &= \frac{\hbar}{i} \left\{ + \left\langle \vec{\nabla}_R \Psi_m^{BO}(\vec{R}) \left| \mathbf{M}^{-1} \frac{\hbar}{i} \vec{\nabla}_R \right| \Psi_n^{BO}(\vec{R}) \right\rangle + \left\langle \Psi_m^{BO}(\vec{R}) \left| \left(\vec{\nabla}_R \right) \mathbf{M}^{-1} \left(\frac{\hbar}{i} \vec{\nabla}_R \right) \right| \Psi_n^{BO}(\vec{R}) \right\rangle \right\} \\ &= \left\langle -\frac{\hbar}{i} \vec{\nabla}_R \Psi_m^{BO}(\vec{R}) \left| \mathbf{M}^{-1} \frac{\hbar}{i} \vec{\nabla}_R \right| \Psi_n^{BO}(\vec{R}) \right\rangle + \underbrace{\left\langle \Psi_m^{BO}(\vec{R}) \left| \left(\frac{\hbar}{i} \vec{\nabla}_R \right) \mathbf{M}^{-1} \left(\frac{\hbar}{i} \vec{\nabla}_R \right) \right| \Psi_n^{BO}(\vec{R}) \right\rangle}_{B_{m,n}(\vec{R})} \\ & \stackrel{\text{Eq. 2.16}}{=} - \left\langle \frac{\hbar}{i} \vec{\nabla}_R \Psi_m^{BO}(\vec{R}) \left| \underbrace{\left(\sum_k \left| \Psi_k^{BO}(\vec{R}) \right\rangle \left\langle \Psi_k^{BO}(\vec{R}) \right| \right)}_{=\hat{1}} \right| \mathbf{M}^{-1} \frac{\hbar}{i} \vec{\nabla}_R \right| \Psi_n^{BO}(\vec{R}) \right\rangle + B_{m,n}(\vec{R}) \\ &= - \sum_k \left\langle \frac{\hbar}{i} \vec{\nabla}_R \Psi_m^{BO}(\vec{R}) \left| \Psi_k^{BO}(\vec{R}) \right\rangle \mathbf{M}^{-1} \left\langle \Psi_k^{BO}(\vec{R}) \left| \frac{\hbar}{i} \vec{\nabla}_R \right| \Psi_n^{BO}(\vec{R}) \right\rangle + B_{m,n}(\vec{R}) \right. \\ &= - \sum_k \underbrace{\left\langle \Psi_k^{BO}(\vec{R}) \left| \frac{\hbar}{i} \vec{\nabla}_R \right| \Psi_m^{BO}(\vec{R}) \right\rangle^*}_{\vec{A}_{k,m}^*(\vec{R})} \mathbf{M}^{-1} \underbrace{\left\langle \Psi_k^{BO}(\vec{R}) \left| \frac{\hbar}{i} \vec{\nabla}_R \right| \Psi_n^{BO}(\vec{R}) \right\rangle}_{\vec{A}_{k,n}(\vec{R})} + B_{m,n}(\vec{R}) \\ &= - \sum_k \vec{A}_{k,m}^*(\vec{R}) \mathbf{M}^{-1} \vec{A}_{k,n}(\vec{R}) + B_{m,n}(\vec{R}) \end{aligned}$$

so that

$$\Rightarrow B_{m,n}(\vec{R}) = \frac{\hbar}{i} \vec{\nabla}_R \mathbf{M}^{-1} \vec{A}_{m,n}(\vec{R}) + \sum_k \vec{A}_{k,m}^*(\vec{R}) \mathbf{M}^{-1} \vec{A}_{k,n}(\vec{R}) \quad (2.17)$$

We have already reached our main goal, namely to express the second-derivative couplings $B_{m,n}$ by the first-derivative couplings $A_{m,n}$. However, the result is not yet in the desired form, because we refer to the hermitian conjugate of the first-derivative couplings.

Derivative couplings are hermitian: We exploit that the first-derivative couplings $\vec{A}_{m,n}$ are hermitian in the band indices, i.e. $\vec{A}_{k,m}^*(\vec{R}) = \vec{A}_{m,k}(\vec{R})$, which can be shown as follows: We start from the orthonormality condition Eq. 2.5 of the Born-Oppenheimer wave functions. Because the orthonormality conditions Eq. 2.5 hold for all \vec{R} , the nuclear gradients of the overlap matrix elements

vanish⁵

$$\begin{aligned}
 0 &\stackrel{\text{Eq. 2.5}}{=} \vec{\nabla}_R \overbrace{\langle \Psi_m^{BO} | \Psi_n^{BO} \rangle}^{\delta_{m,n}} \\
 &= \langle \vec{\nabla}_R \Psi_m^{BO} | \Psi_n^{BO} \rangle + \langle \Psi_m^{BO} | \vec{\nabla}_R \Psi_n^{BO} \rangle \\
 &= \langle \Psi_n^{BO} | \vec{\nabla}_R \Psi_m^{BO} \rangle^* + \langle \Psi_m^{BO} | \vec{\nabla}_R \Psi_n^{BO} \rangle \\
 \Rightarrow 0 &= -\langle \Psi_n^{BO} | \frac{\hbar}{i} \vec{\nabla}_R \Psi_m^{BO} \rangle^* + \langle \Psi_m^{BO} | \frac{\hbar}{i} \vec{\nabla}_R \Psi_n^{BO} \rangle \\
 \Rightarrow \vec{A}_{k,m}^*(\vec{R}) &= \langle \Psi_k^{BO} | \frac{\hbar}{i} \vec{\nabla}_R \Psi_m^{BO} \rangle^* = \langle \Psi_m^{BO} | \frac{\hbar}{i} \vec{\nabla}_R \Psi_k^{BO} \rangle = \vec{A}_{m,k}(\vec{R}) \quad (2.18)
 \end{aligned}$$

DERIVATIVE COUPLINGS ARE HERMITIAN

$$\vec{A}_{m,n}^* = \vec{A}_{n,m} \quad (2.19)$$

This allows us to rewrite Eq. 2.17 in the form

$$B_{m,n}(\vec{R}) = \frac{\hbar}{i} \vec{\nabla}_R \mathbf{M}^{-1} \vec{A}_{m,n}(\vec{R}) + \sum_k \vec{A}_{m,k}(\vec{R}) \mathbf{M}^{-1} \vec{A}_{k,n}(\vec{R}) \quad (2.20)$$

Thus, we only need to evaluate the first-derivative couplings, while the second-derivative couplings can be obtained from the former via Eq. 2.20.

Towards the final form for the nuclear Schrödinger equation

The general structure of the nuclear Schrödinger equation Eq. 2.14 is

$$i\hbar \partial_t \Theta_m(\vec{R}, t) \stackrel{\text{Eq. 2.14}}{=} \left[\frac{1}{2} \vec{P} \mathbf{M}^{-1} \vec{P} + E_m^{BO}(\vec{R}) \right] \Theta_m(\vec{R}, t) + \sum_n \left[\vec{A}_{m,n}(\vec{R}) \mathbf{M}^{-1} \hat{P} + \frac{1}{2} B_{m,n}(\vec{R}) \right] \Theta_n(\vec{R}, t) \quad (2.21)$$

where $\vec{P} = \frac{\hbar}{i} \vec{\nabla}_R$ is the momentum vector of the nuclear coordinates.

Insertion of the second-derivative couplings \mathbf{B} from Eq. 2.20 into the nuclear Schrödinger equation Eq. 2.21 will bring it into the final form Eq. 2.27.

Let me sketch here the line of thought schematically and, for the sake of clarity, let me drop here the matrix structure of the equations. The terms in Eq. 2.21 related to momenta $\hat{P} \triangleq \frac{\hbar}{i} \vec{\nabla}$ and derivative couplings have the form

$$\left(\frac{1}{2} \hat{P} \mathbf{M}^{-1} \hat{P} + \vec{A} \mathbf{M}^{-1} \hat{P} + \frac{1}{2} B \right) \stackrel{\text{Eq. 2.20}}{=} \frac{1}{2} \left(\hat{P} \mathbf{M}^{-1} \hat{P} + 2 \vec{A} \mathbf{M}^{-1} \hat{P} + \overbrace{(\hat{P} \mathbf{M}^{-1} \vec{A}) + \vec{A} \mathbf{M}^{-1} \vec{A}}^B \right) \quad (2.22)$$

Special care is needed to distinguish conventional expressions from those in operator equations. The left-hand side is an operator and part of the effective nuclear Hamiltonian. Eq. 2.20, on the other hand, is not an operator equation but a simple relation between functions. When we import Eq. 2.20 into the operator expressions, we need to place parentheses around the expression $(\hat{P} \mathbf{M}^{-1} \vec{A})$. The parentheses prevent the momentum operator from acting on a function written to the right of the

⁵Note, that we make use of natural or periodic boundary conditions. Without boundary conditions such as these, we would not be able to apply Gauss' theorem as done below.

expression. Considered as operators, we can use the identity⁶

$$(\hat{P}\mathbf{M}^{-1}\vec{A}) = \hat{P}\mathbf{M}^{-1}\vec{A} - (\mathbf{M}^{-1}\vec{A})\hat{P} = \hat{P}\mathbf{M}^{-1}\vec{A} - \vec{A}\mathbf{M}^{-1}\hat{P} \quad (2.24)$$

which should be read like

$$(\hat{P}\mathbf{M}^{-1}\vec{A})|\Theta\rangle = \hat{P}\mathbf{M}^{-1}\vec{A}|\Theta\rangle - \vec{A}\mathbf{M}^{-1}\hat{P}|\Theta\rangle \quad (2.25)$$

Thus, we obtain from Eq. 2.22 the operator identity

$$\begin{aligned} \left(\frac{1}{2}\hat{P}\mathbf{M}^{-1}\hat{P} + \vec{A}\mathbf{M}^{-1}\hat{P} + \frac{1}{2}B\right) &\stackrel{\text{Eq. 2.22, Eq. 2.24}}{=} \frac{1}{2}\left(\hat{P}\mathbf{M}^{-1}\hat{P} + 2\vec{A}\mathbf{M}^{-1}\hat{P} + \overbrace{\hat{P}\mathbf{M}^{-1}\vec{A} - \vec{A}\mathbf{M}^{-1}\hat{P}}^{(\hat{P}\mathbf{M}^{-1}\vec{A})} + \vec{A}\mathbf{M}^{-1}\vec{A}\right) \\ &= \frac{1}{2}\left(\hat{P}\mathbf{M}^{-1}\hat{P} + \vec{A}\mathbf{M}^{-1}\hat{P} + \hat{P}\mathbf{M}^{-1}\vec{A} + \vec{A}\mathbf{M}^{-1}\vec{A}\right) \\ &= \frac{1}{2}\left(\hat{P} + \vec{A}\right)\mathbf{M}^{-1}\left(\hat{P} + \vec{A}\right) \end{aligned} \quad (2.26)$$

which leads from Eq. 2.21 to Eq. 2.27 below.

SCHRÖDINGER EQUATION FOR THE NUCLEAR WAVE FUNCTIONS IN TERMS OF BORN-OPPENHEIMER WAVE FUNCTIONS

In this manner, we arrive at our final form Eq. 2.27 for the nuclear Schrödinger equation.

$$i\hbar\partial_t\Theta_m(\vec{R}, t) = \sum_n \left[\frac{1}{2} \sum_k \left(\delta_{m,k} \frac{\hbar}{i} \vec{\nabla}_R + \vec{A}_{m,k}(\vec{R}) \right) \mathbf{M}^{-1} \left(\delta_{k,n} \frac{\hbar}{i} \vec{\nabla}_R + \vec{A}_{k,n}(\vec{R}) \right) + \delta_{m,n} E_m^{BO}(\vec{R}) \right] \Theta_n(\vec{R}, t) \quad (2.27)$$

This equation can be written in a more compact form, combining the components of the nuclear wave functions in a vector-matrix notation – using a single underline to denote a vector and a double underline for a matrix –

$$i\hbar\partial_t\underline{\Theta}(\vec{R}, t) = \left[\frac{\left(\underline{\hat{P}} + \underline{\vec{A}}(\vec{R})\right)^2}{2\mathbf{M}} + \underline{\underline{E}}^{BO}(\vec{R}) \right] \underline{\Theta}(\vec{R}, t) \quad (2.28)$$

$\underline{\underline{E}}^{BO}$ denotes the diagonal matrix with the Born-Oppenheimer energies E_n^{BO} as diagonal elements and $\underline{\hat{P}} = \frac{\hbar}{i}\vec{\nabla}_R$ is the $3M$ -dimensional momentum operator of the nuclei.

Strictly speaking, the kinetic-energy expression in Eq. 2.28 is mathematically not allowed, because I wrote a vector-matrix-vector expression as vector-squared-divided-by-matrix. I used it here to allude to the corresponding equation from electrodynamics so that it can be memorized more easily. Because the matrix \mathbf{M} is diagonal, the expression can be evaluated component by component.

The first-derivative couplings $\vec{A}_{m,k}(\vec{R})$ are defined in Eq. 2.15.

$$\vec{A}_{m,n}(\vec{R}) \stackrel{\text{Eq. 2.15}}{=} \left\langle \Psi_m^{BO}(\vec{R}) \left| \frac{\hbar}{i} \vec{\nabla}_R \right| \Psi_n^{BO}(\vec{R}) \right\rangle = \left\langle \Psi_m^{BO}(\vec{R}) \left| \hat{P} \right| \Psi_n^{BO}(\vec{R}) \right\rangle \quad (2.29)$$

As shown in Eq. 2.18, each vector component of the first-derivative couplings is a hermitian matrix in the indices m, n .

⁶We used product rule for \hat{P} , which is a gradient operator.

$$\frac{\hbar}{i} \vec{\nabla} F(\vec{R}) = \hat{P}F(\vec{R}) = \left(\hat{P}F(\vec{R}) \right) + F(\vec{R})\hat{P} \Rightarrow \left(\hat{P}F(\vec{R}) \right) = \hat{P}F(\vec{R}) - F(\vec{R})\hat{P} \quad (2.23)$$

This form of the nuclear Schrödinger equation, i.e. Eq. 2.28, has been mentioned⁷ already in 1969 by F. Smith[8].

Some caution is required when comparing the expressions above with the literature, because my notation deviates from the common use in the literature. I have done this on purpose in order to group the expressions into physically meaningful terms. Combining the gradients with $\frac{\hbar}{i}$ to form a momentum operator for the nuclei is not common. One result of this is that the first-derivative couplings are hermitian in my notation, but anti-hermitian in the literature.

We have not introduced any approximations to bring Eq. 2.14 into the new form given by Eq. 2.28. That is, we are still on solid grounds.

Relation to electrodynamics

Interesting is the formal similarity of the nuclear Hamilton function in Eq. 2.15 with that of a charged particle in a electromagnetic field, which has the form

$$H(\vec{p}, \vec{r}) = \frac{1}{2m} (\vec{p} - q\vec{A}(\vec{r}))^2 + q\Phi(\vec{r})$$

This analogy shows that the diagonal terms (in the band indices) of the derivative couplings act like a magnetic field \vec{B} expressed by the vector potential \vec{A} as $\vec{B} = \vec{\nabla} \times \vec{A}$ and an electric potential Φ . This analogy is discussed in somewhat more detail in the appendix E.5.

2.2 Born-Oppenheimer approximation

The essence of the famous **Born-Oppenheimer approximation** is the neglect of the derivative couplings in the nuclear Schrödinger equation Eq. 2.27.

BORN-OPPENHEIMER APPROXIMATION FOR THE NUCLEAR WAVE FUNCTION

$$i\hbar\partial_t\Theta_n(\vec{R}, t) = \left[\sum_{j=1}^M \frac{-\hbar^2}{2M_j} \nabla_{R_j}^2 + E_n^{BO}(\vec{R}) \right] \Theta_n(\vec{R}, t) \quad (2.30)$$

This equation describes nuclei that move on a specific total-energy surface $E_n^{BO}(\vec{R})$, which is called the **Born-Oppenheimer surface**. Transitions between different Born-Oppenheimer surfaces are completely suppressed in the Born-Oppenheimer approximation.

What are the limitations of the Born-Oppenheimer approximation? There are two arguments, which are relevant in different situations.

- One argument emphasizes that the derivative couplings diverge when Born-Oppenheimer surfaces touch as shown below in Eq. 2.31. Where Born-Oppenheimer surfaces touch, is where (radiation-less) electronic transitions take place. After removing the derivative couplings, all relaxation processes, which may bring the electrons into the ground state or into thermal equilibrium are completely suppressed. In order to describe electronic transitions, we need to include **non-adiabatic effects**, i.e. we need to take into account the derivative couplings again.
- The original argument of Born and Oppenheimer considers the coupling of atomic vibrations and electronic excitations. If two systems have very different frequencies, they are out of resonance and, therefore, exchange only small amounts of energy. As a consequence the dynamics of the two subsystem is nearly independent. This is the essence of the **adiabatic principle**. In a colloquial way, this is usually rephrased by saying that the the “electrons are fast compared

⁷see his Eq. 10. His $\vec{P}(R)$ are the first-derivative couplings.

to the nuclear motion". The frequencies of the lattice vibrations are linked to the nuclear masses and the electronic excitation energies $\hbar\omega$ are linked to the electron mass m_e . Thus, the adiabatic principle is satisfied well in the limit of a vanishing ratio of electron mass to the nuclear masses. The mass ratio can thus be used as a small parameter in a perturbation expansion.

The adiabatic principle is relevant in the absence of electronic transitions, where the system evolves on the lowest Born-Oppenheimer approximation. The dominant "error" of the Born-Oppenheimer approximation in this case is probably the neglect of friction and fluctuation forces for the atom dynamics caused by the electronic system.

I wish to emphasize, that the adiabatic principle, which is often quoted, does not explain the breakdown of the Born-Oppenheimer approximations at crossings of Born-Oppenheimer surfaces and that this qualitative failure is fairly independent of the ratio of electronic and nuclear masses.

Interestingly, the separation of nuclear and electronic degrees of freedom have already been in use before the original Born-Oppenheimer approximation (see [9]). Born and Oppenheimer [5] gave a justification for neglecting the non-adiabatic effects.

The Born-Oppenheimer approximation is the prerequisite for treating the nuclei as classical particles. In section 2.5 below, I will give a brief outlook on trajectory based formulations.

2.3 Non-adiabatic effects

While the Born-Oppenheimer approximation is a widely used and tremendously successful approach, its limitations are important for relaxation processes, photochemistry, charge transfer processes and many more interesting processes. They shall be briefly discussed here.

Non-adiabatic effects are relevant firstly for electronic relaxation processes of excited states. An excitation produced, for example, by an optical excitation dissipates its energy by transferring energy and momentum into other forms of energy, which can be other electronic excitations, the emission of photons, or the creation of phonons.

Non-adiabatic effects also play a role for the atom dynamics, because lattice vibrations can exchange energy with the electronic system. This results in an effective friction for the atoms and random forces, which act on the atoms as the electronic excitations decay and transfer their energy back to the atom dynamics. Electronic excitations are not the only source of friction. Another one is the coupling of atomic vibrations among each other. Electronic friction is relevant in particular in metals, which have many low-energy excitations, that are in the energy range of lattice vibrations $\Delta E_{\text{electrons}} \sim \hbar\omega_{\text{phonon}}$.

All these effects are of great technological importance. In a solar cell, for example, it is important to avoid the uncontrolled dissipation before the energy can be harvested. Friction is often an undesired side effect leading to energy-inefficient processes. On the other hand, friction can also be desirable to avoid the uncontrolled vibration due to a resonance, which can destroy a material structure.

We will see that the derivative couplings governing the non-adiabatic effects are singular where two Born-Oppenheimer surface meet. Unfortunately, these are exactly the points of physical interest, namely those where a system makes a **non-radiative transition**⁸ from one Born-Oppenheimer surface to another. Even worse, these singular points have non-local consequences, so-called topological effects.

Interesting is a close formal similarity between non-adiabatic effects and field theory[10]. Related topics are the **Aharonov-Bohm effect**[11] and **Yang-Mills fields**[12].

Under normal circumstances, the diagonal terms of the derivative couplings are of secondary importance. The diagonal term of the derivative couplings are discussed in the appendix E.5.

⁸A non-radiative transition is one where the energy of the transition is not emitted in the form of light. Rather, the energy is used for internal excitations of the material such as phonons.

2.3.1 Off-diagonal derivative couplings

The off-diagonal elements of the first-derivative couplings defined in Eq. 2.29 can be brought into the form

OFF-DIAGONAL DERIVATIVE COUPLINGS

$$\vec{A}_{m,n}(\vec{R}) = \frac{\left\langle \Psi_m^{BO}(\vec{R}) \left| \left[\frac{\hbar}{i} \vec{\nabla}_R, \hat{H}^{BO}(\vec{R}) \right]_- \right| \Psi_n^{BO}(\vec{R}) \right\rangle}{E_n^{BO}(\vec{R}) - E_m^{BO}(\vec{R})} \quad \text{for } E_m^{BO} \neq E_n^{BO} \quad (2.31)$$

The gradient acts only on the Born-Oppenheimer Hamiltonian but not further to the state on the right.

This expression makes it evident that non-adiabatic effects are important when two Born-Oppenheimer surfaces become degenerate, i.e. when $E_m^{BO} = E_n^{BO}$.

The diagonal derivative couplings are purely real-valued, i.e. $\text{Im}(\vec{A}_{n,n}) = 0$, which follows from the hermitean property Eq. 2.18. Other than this, there is no analogous simplification as in the off-diagonal derivative couplings.

Derivation of Eq. 2.31 The off-diagonal elements of $\vec{A}_{n,m}(\vec{R})$ of the first-derivative couplings are obtained as follows: We begin with the Schrödinger equation for the Born-Oppenheimer wave function

$$\left(\hat{H}^{BO}(\vec{R}) - E_n^{BO}(\vec{R}) \right) |\Psi_n^{BO}(\vec{R})\rangle \stackrel{\text{Eq. 2.4}}{=} 0$$

Because this equation is valid for all atomic positions, the gradient of the above expression vanishes.

$$\begin{aligned} 0 &= \vec{\nabla}_R \left(\hat{H}^{BO}(\vec{R}) - E_n^{BO}(\vec{R}) \right) |\Psi_n^{BO}(\vec{R})\rangle \\ &= \left[\vec{\nabla}_R, \hat{H}^{BO}(\vec{R}) \right]_- |\Psi_n^{BO}(\vec{R})\rangle - |\Psi_n^{BO}(\vec{R})\rangle \vec{\nabla}_R E_n^{BO}(\vec{R}) + \left(\hat{H}^{BO}(\vec{R}) - E_n^{BO}(\vec{R}) \right) \vec{\nabla}_R |\Psi_n^{BO}(\vec{R})\rangle \end{aligned}$$

The commutator is used to express the gradient of the Hamiltonian.⁹ Now, we multiply from the left with the bra $\langle \Psi_m^{BO} |$ and form the scalar products in the electronic Hilbert space.¹⁰

$$\begin{aligned} 0 &= \langle \Psi_m^{BO} | \left[\vec{\nabla}_R, \hat{H}^{BO} \right]_- | \Psi_n^{BO} \rangle - \langle \Psi_m^{BO} | \Psi_n^{BO} \rangle \vec{\nabla}_R E_n^{BO} + \langle \Psi_m^{BO} | \left(\hat{H}^{BO} - E_n^{BO} \right) \vec{\nabla}_R | \Psi_n^{BO} \rangle \\ &= \langle \Psi_m^{BO} | \left[\vec{\nabla}_R, \hat{H}^{BO} \right]_- | \Psi_n^{BO} \rangle - \underbrace{\delta_{m,n} \vec{\nabla}_R E_n^{BO}}_{=0 \text{ for } m \neq n} + \left(\hat{E}_m^{BO} - E_n^{BO} \right) \langle \Psi_m^{BO} | \vec{\nabla}_R | \Psi_n^{BO} \rangle \end{aligned}$$

The middle term, containing the gradient of the Born-Oppenheimer surfaces, vanishes for $m \neq n$. If, furthermore, the energies E_m^{BO}, E_n^{BO} differ, we divide by their difference, which brings us to the

⁹Consider the following identities for a two functions A and B .

$$\begin{aligned} \vec{\nabla}(AB) &= B\vec{\nabla}A + A\vec{\nabla}B \\ \vec{\nabla}(AB) &= \vec{\nabla}AB - A\vec{\nabla}B + A\vec{\nabla}B = \left[\vec{\nabla}, A \right]_- B + A\vec{\nabla}B \end{aligned} \quad (2.32)$$

The first identity is sufficient for functions. However, if A is an position-dependent operator that also acts on B , we cannot place it to the right of the term B as in the first equation. In that case, only the second expression is suitable. In our case, A is the Hamiltonian and B is the state.

¹⁰The Born-Oppenheimer wave functions depend on electronic and nuclear coordinates. The nuclear coordinates, however, play a different role, because they are treated like external parameters.

desired result.

$$\vec{A}_{m,n}(\vec{R}) \stackrel{\text{Eq. 2.15}}{=} \langle \Psi_m^{BO} | \frac{\hbar}{i} \vec{\nabla}_R | \Psi_n^{BO} \rangle = \frac{\langle \Psi_m^{BO} | \left[\frac{\hbar}{i} \vec{\nabla}_R, \hat{H}^{BO}(\vec{R}) \right]_- | \Psi_n^{BO} \rangle}{\hat{E}_n^{BO} - E_m^{BO}} \quad \text{for } E_n \neq E_m \quad (2.33)$$

This is the proof for Eq. 2.31 given above. Unfortunately, no information can be extracted for the diagonal elements of the first-derivative couplings.

2.3.2 Diagonal derivative couplings (optional)

I added this section on the diagonal derivative couplings, because it seemed an omission relative to the more important off-diagonal derivative couplings. It can be omitted without harm, because I will not build on it. Nevertheless it is of interest in its own right because of the many hidden connections to other fields of physics.

Because derivative couplings are hermitian according to Eq. 2.19, the diagonal derivative couplings $\vec{A}_{n,n}(\vec{R})$ are real-valued vector fields.

The Born-Oppenheimer wave functions are determined only up to a global¹¹ phase factor $e^{i\chi(\vec{R})}$ for each Born-Oppenheimer surface and each atomic configuration \vec{R} . Multiplication with such a phase factor is a **gauge transformation**.

$$|\tilde{\Psi}_n^{BO}(\vec{R})\rangle = |\Psi_n^{BO}(\vec{R})\rangle e^{i\chi_n(\vec{R})} \quad (2.34)$$

This gauge transformation leaves the Born-Oppenheimer surfaces unchanged, but it affects the derivative couplings.

$$\begin{aligned} \tilde{E}_n^{BO}(\vec{R}) &= E_n^{BO}(\vec{R}) \\ \vec{\tilde{A}}_{n,n}(\vec{R}) &= \vec{A}_{n,n}(\vec{R}) + \vec{\nabla}\chi_n(\vec{R}) \end{aligned} \quad (2.35)$$

The gauge transformation also affects the nuclear wave functions resulting from the transformed nuclear Schrödinger equation.

Ideally, one would like to use the gauge transformation to remove the derivative couplings altogether. Unfortunately, this is only possible for systems with a single nuclear coordinate. The best we can do is to turn the derivative couplings into a divergence-free vector field.

$$\vec{\nabla} \cdot \vec{\tilde{A}}_{n,n}(\vec{R}) \stackrel{!}{=} 0 \quad \Rightarrow \quad \vec{\nabla}^2 \chi_n(\vec{R}) = -\vec{\nabla} \cdot \vec{A}_{n,n}(\vec{R}) \quad (2.36)$$

This is a Poisson equation in $3M$ dimensions for the phase $\chi_n(\vec{R})$.

The quantity, which is independent of the gauge transformations is the curl

$$F_{ij}^{(n)} = \partial_i A_{j,n,n} - \partial_j A_{i,n,n} \quad (2.37)$$

The observable information must be gauge invariant, because the complete electronic-nuclear wave function is invariant under a gauge transformation. Thus, the only physical information contained in the derivative couplings is also contained in the curl $F_{ij}^{(n)}$.

The components of the curl act like generalized magnetic fields and $F_{ij}^{(n)}$ has close similarity to the **field-strength tensor** of electrodynamics. [Editor: refer to phisx-electrodynamics](#)

The gauge transformations discussed here are only a small subset of the possible transformations of the nuclear and electronic wave functions. The gauge transformations, discussed here, are special because they do not change the general structure of the nuclear Schrödinger equation with a diagonal potential-energy term.

The most general transformations are presented in appendix B.2 on p. 410. Among the resulting different representations, there is the **adiabatic representation** discussed in appendix B.3 on p. 414.

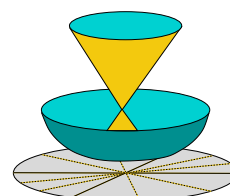
¹¹In the electronic Hilbert space.

In the diabatic representation the derivative couplings vanish, while the diagonal matrix holding the Born-Oppenheimer surfaces is turned into a non-diagonal matrix, which couples the electronic states. Unfortunately, a non-trivial¹² transformation on diabatic states is not always possible.[13]

2.4 Conical intersections

We need to understand crossings of Born-Oppenheimer surfaces, because these are the points where off-diagonal non-adiabatic effects Eq. 2.31 become important. These are the points where the Born-Oppenheimer approximation (not the Born-Oppenheimer framework) fails in a fundamental way.

It turns out that most crossings of Born-Oppenheimer surfaces are conical intersections. **Conical intersections** are crossings of Born-Oppenheimer surfaces, that touch at a point in two (or three) dimensions, rather than on a line. That is, if the dimension of the nuclear degrees of freedom is d , the conical intersection is a $d - 2$ -dimensional (or $d - 3$ -dimensional) hypersurface.



As shown by Truhlar and Mead[14], conical intersections of Born-Oppenheimer surfaces are much more frequent than avoided crossings. Thus, they are critical for an understanding electronic relaxation processes in materials.

For a review on conical intersections, see for example the paper of Yarkony [15]. For studies on the conical intersection see also Mead[16] and Hader et al.[17].

2.4.1 Non-crossing theorem and conical intersections

The fact that Born-Oppenheimer surfaces cross at conical intersections has been unexpected initially. The famous non-crossing theorem, discussed in this section, could show that this is a generic topological property of eigenvalue problems, which depend on external parameters, such as the atomic positions. Therefore, the non-crossing theorem is relevant in a variety of different quantum problems.

The most important information on the topology of surface crossings is provided by the **non-crossing theorem** of von Neumann and Wigner[18]. It is derived in appendix C on p. 417.

NON-CROSSING THEOREM

Consider a Hamiltonian $\hat{H}(Q_1, \dots, Q_m)$ which depends on m parameters Q_1, \dots, Q_m .

- For each accidental crossing of two eigenvalues, there is a three-dimensional subspace of the parameter space in which the degeneracy is lifted except for a single point.
- If the Hamiltonian is real-valued for all parameters, the subspace where the degeneracy is lifted has two dimensions.

- In our case, the Hamiltonian is the Born-Oppenheimer Hamiltonian and the parameters are the nuclear positions.
- Two energy surfaces that meet in a point within a two-dimensional hypersurface form two cones. Therefore, the crossing is called a **conical intersection**.
- The $m - 2$, respectively $m - 3$ dimensional, hypersurface, for which the two energy surfaces are degenerate, is called the **degenerate seam**. It is spanned by “unimportant” degree's of freedom, which shift the conical intersection around within the 2- or 3-dimensional space of relevant degrees of freedom, but which themselves do not lift the degeneracy.

¹²A *trivial* diabatic representation has electronic wave functions that do not depend on the nuclear positions.

- The Hamiltonian is usually¹³ real-valued in the absence of magnetic fields and relativistic effects. Spin-orbit coupling, a relativistic effect, and magnetic fields that act on the orbital motion of charged particles introduce complex-valued contributions. The absence of imaginary parts in the Hamiltonian is a consequence of **time-inversion symmetry**, which is violated by the presence of magnetic fields. Time-inversion symmetry is discussed in Appendix H of Φ SX: Quantum Theory[4].
- The limitation of the non-crossing theorem to accidental crossings implies that there are no limitations on crossings that occur because two states have different symmetry.
- The non-crossing theorem implies that there are no accidental crossings for dimeric molecules.¹⁴

Let me consider a conical intersection related to the motion of a single atom in a molecule or solid. Let me furthermore consider real-valued Hamiltonians. For this example, the conical intersection would form a one-dimensional line in a three-dimensional space. The two displacements perpendicular to this line lift the degeneracy. If we plot the energy surfaces in the plane of these two distortions, the Born-Oppenheimer surfaces would have the shape of a double cone, a **conical intersection**. A change of a coordinate along the line will change the shape and the position of the cone, but it will not affect the qualitative cone-like topology.

More generally, there is a two-dimensional plane of coordinates relevant to the conical intersection. Distortions of distant nuclei will not affect the general shape of the conical intersection, while they do have an effect on the total energy.

2.4.2 Poor man's demonstration of the non-crossing theorem

Consider a **real-valued** (2×2) -Hamiltonian

$$H(\vec{Q}) = \begin{pmatrix} \bar{\epsilon}_1(\vec{Q}) & -t(\vec{Q}) \\ -t(\vec{Q}) & \bar{\epsilon}_2(\vec{Q}) \end{pmatrix} \quad (2.38)$$

which depends parametrically on a vector \vec{Q} of generalized coordinates \vec{Q} . In the context of the Born-Oppenheimer approach, the Hamiltonian is the Born-Oppenheimer Hamiltonian and \vec{Q} are the nuclear positions.

In order to form a degeneracy, the hopping parameter $t(\vec{Q})$ has to vanish and the two diagonal elements must be equal. This is a direct consequence of the eigenvalue equation,

$$\epsilon_{\pm} \stackrel{\text{Eq. 1.20}}{=} \frac{\bar{\epsilon}_1 + \bar{\epsilon}_2}{2} \pm \sqrt{\left(\frac{\bar{\epsilon}_1 - \bar{\epsilon}_2}{2}\right)^2 + |t|^2}, \quad (2.39)$$

with the requirement that both eigenvalues are equal.

Thus, the two conditions

$$\begin{aligned} t(\vec{Q}) &= 0 \\ \bar{\epsilon}_2(\vec{Q}) - \bar{\epsilon}_1(\vec{Q}) &= 0 \end{aligned} \quad (2.40)$$

need to be satisfied.

For the sake of simplicity, we have restricted ourselves to a real-valued Hamiltonian, so that the hopping $t(\vec{Q})$ is real-valued. When we allow also complex-valued Hamiltonians, we have to satisfy an additional requirement, namely that also the imaginary part of the hopping parameter vanishes. This is the origin of the non-crossing theorem for complex-valued Hamiltonian. Let us now return to real-valued Hamiltonians.

¹³There are other interactions that are similar to a magnetic field. They are, however, not very important for solid-state physics.

¹⁴Dimeric molecules have only a one-dimensional configuration space. The five other dimensions do not count, because they are related by exact symmetry operations of the system, rotations and translations. For a one-dimensional configuration space the crossing would have $1 - 2 = -1$ dimensions.

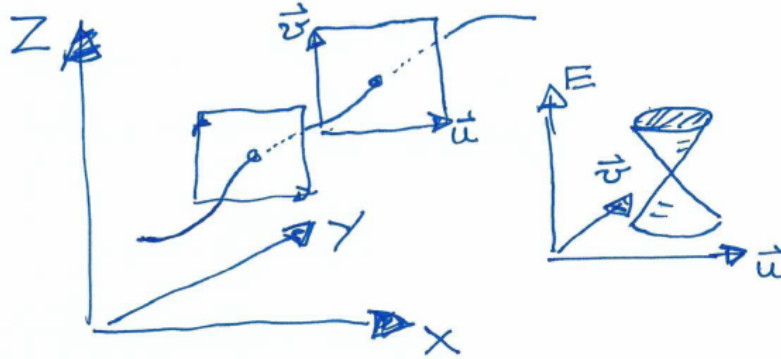


Fig. 2.1: Sketch of a degenerate seam of a conical intersection for real-valued Born-Oppenheimer Hamiltonians in a three-dimensional space of nuclear coordinates. The line is the degenerate seam. The planes are spanned by the two independent vectors \vec{u} and \vec{v} pointing away from the degenerate seam. The degeneracy is lifted within this plane, except for a point where the degenerate seam passes through the plane.

In order to leave the degeneracy intact, we need to proceed in coordinate space perpendicular to $\vec{u} \stackrel{\text{def}}{=} \vec{\nabla}_Q t(\vec{Q})$ and perpendicular to $\vec{v} \stackrel{\text{def}}{=} \vec{\nabla}_Q (\bar{\epsilon}_2(\vec{Q}) - \bar{\epsilon}_1(\vec{Q}))$. This is sketched in figure 2.1.

Any displacement of \vec{Q} away from a point \vec{Q}_0 with the intact degeneracy, which has a projection onto \vec{u} or \vec{v} , violates the conditions for the degeneracy. In three dimensions, i.e. $\vec{Q} \in \mathbb{R}^3$, there is only one direction, namely $\vec{u} \times \vec{v}$, which leaves the degeneracy intact¹⁵. The conical intersection in the plane through \vec{Q}_0 perpendicular to $\vec{u} \times \vec{v}$ is a point. In three dimensions, the conical intersection forms a line, $Q_0(s)$ with $s \in \mathbb{R}^1$. This line is called the **degenerate seam**.

In an M -dimensional space of nuclear coordinates, the degenerate seam for real-valued Hamiltonians has $M - 2$ dimensions. For a one-dimensional path lying within the degenerate seam of a M -dimensional system, the planes perpendicular to the degenerate seam exhibit a conical intersection, which changes its shape, (position, energy, slopes) as one proceeds along the path. Nevertheless, the system will remain to be a point-like conical intersection in a two-dimensional subspace of the nuclear position space.

To go beyond the poor-man's version of the non-crossing theorem, see appendix C on p. 417.

2.4.3 Jahn-Teller model

The minimal model for a conical intersection is the **Jahn-Teller model**. It describes two Born-Oppenheimer surfaces in a two-dimensional configuration space. The Jahn-Teller model is described in some detail in the appendix H on p. 467.

One interesting feature, which becomes evident, is the presence of a non-vanishing **geometric phase**. Even though the Hamiltonian is real valued, the wave functions cannot be chosen real-valued and, at the same time, continuous. If one follows the real-valued wave functions on a path surrounding the conical intersection, the wave function does not match to itself after one full turn, but it changes its sign.

The problem of a discontinuous phase can be avoided by adding a position-dependent phase factor, which makes the wave function continuous at the price that it becomes complex valued.

The energy eigenstates of have a nuclear wave function, which has contributions both on the upper and the lower Born-Oppenheimer surface. The nuclear wave function of the Jahn-Teller model is circular symmetric. Therefore, the nuclear wave functions Θ_{\pm} can be decomposed into angular momentum eigenstates. For each angular momentum one obtains a system of two ordinary

¹⁵The vector product $\vec{u} \times \vec{v}$ is perpendicular to, both, \vec{u} and \vec{v} .

differential equation for the radial parts of the nuclear wave function on the upper and the lower Born-Oppenheimer surface. Interestingly the Born-Oppenheimer wave functions (for the electrons) carry themselves two angular momenta, so that the final electron-nuclear wave function has two angular-momentum coefficients.

Editor: This summary needs to be extended.

While the phase of the wave function is not an observable, the geometric phase is physically relevant.

Mention behavior of the wave functions at the center.

The problem appears related to the behavior of a half-integer spin.

2.5 Outlook: trajectories

Within the Born-Huang framework, we arrived at a Schrödinger equation for the nuclei. Because nuclei are fairly heavy, quantum effects for nuclei are often secondary. A nucleon, proton or neutron, is about 2000 times heavier than an electron. The main quantum effects related to the nuclear motion are the zero-point energy of vibrations and the tunneling through barriers. It should also be noted that quantum effects tend to become invisible at higher temperatures, where thermal fluctuations dominate over quantum fluctuations.

Therefore, it is often desirable to describe nuclei as classical point particles and, thus, to avoid the complexity of a quantum-mechanical treatment. There is a huge number of different approaches towards this goal. The topic is an active and still emerging research area.

To provide an orientation, let me just mention a few of them:

1. **Born-Oppenheimer dynamics** Based on the Born-Oppenheimer approximation, i.e. the neglect of the derivative couplings, one can make the classical approximation for the nuclei. The electrons are limited to the ground state and the forces acting on the atoms are obtained from the gradients of the lowest Born-Oppenheimer surface.

$$M_j \ddot{R}_j = -F_j \quad \text{with} \quad \vec{F} = -\vec{\nabla}_R E_0^{BO} \quad (2.41)$$

The Born-Oppenheimer surface $E^{BO}(\vec{R})$ can either be parameterized or calculated on-the-fly from an electronic structure calculation. The simulation technique is called **molecular dynamics**. The variant using forces from an explicit electronic structure method is called **ab-initio molecular dynamics**.

2. **Ehrenfest dynamics**: Ehrenfest dynamics does not restrict the electrons to a particular Born-Oppenheimer surface. Rather it propagates the electronic wave functions under the action of a time-dependent Hamiltonian $\hat{H}_e(t) = \hat{H}^{BO}(\vec{R}(t))$, which changes as the atoms move around. Ehrenfest dynamics suffers from the fact that different Born-Oppenheimer surfaces produce different forces that split a wave packet. A single trajectory cannot capture the splitting of a wave packet. Instead, the trajectory follows the averaged forces, that often do not represent any individual Born-Oppenheimer surfaces.
3. **Landau-Zener formula**[19]: Within Ehrenfest dynamics, the transition probability P between two Born-Oppenheimer surfaces can be evaluated as shown in appendix F.

$$P \stackrel{\text{Eq. F.14}}{=} \exp\left(-2\pi \underbrace{\frac{|H_{12}|}{\hbar}}_{\text{Rabi frequency}} \underbrace{\frac{|H_{12}|}{V|F_1 - F_2|}}_{\tau}\right) \quad (2.42)$$

where V is the velocity and H_{12} is the coupling between the two crossing total-energy surfaces. ω_{12} is the **Rabi frequency** at the crossing point and τ is a measure for the duration of the interaction between the surfaces.

4. **Surface hopping:** John Tully is the father of the surface hopping approach. In this technique, the system is constrained to a single Born-Oppenheimer surface at a time, but it may make sudden transitions from one Born-Oppenheimer surface to another.

2.6 Summary

- Born-Huang Ansatz
- Born-Oppenheimer equation, Born-Oppenheimer surfaces, multi-valued Born-Oppenheimer wave functions, derivative couplings
- Nuclear Schrödinger equation
- Non-adiabatic effects, derivative couplings, divergence at degenerate states
- Non-crossing theorem, conical intersections, real-valued and complex-valued Hamiltonians, poor man's proof of the non-crossing theorem, accidental crossings, degenerate seam
- Conical intersections are the usual type of band crossings and dominate radiation-less relaxation processes.

2.7 Home study and practice

2.7.1 Landau-Zener Formula (Optional)

Editor: This exercise is optional because many aspects turn up again in the exercise on the Holstein dimer.

Introduction

The Landau-Zener formula is the most elementary expression for the transition probability between two Born-Oppenheimer surfaces.

It approximates the nuclear system by a single coordinate representing a trajectory. The velocity of the trajectory is constant. The electronic system is represented by two crossing energy surfaces, with a offsite Hamilton matrix element lifting the degeneracy. The result is an avoided crossing.

The resulting transition probability is

$$P = e^{-2\pi\omega_{Rabi}\tau} \quad (2.43)$$

where ω_{Rabi} is the **Rabi frequency** $\hbar\omega_{Rabi} = |\Delta|$ and $\tau = |\frac{\Delta}{V(F_1 - F_2)}|$ is the duration of the contact to both energy surfaces. The description is kept in appendix F.

A derivation[20] of the Landau-Zener formula is provided in appendix F on p. 453.

The purpose of this section is to demonstrate that derivative couplings become important at points where two Born-Oppenheimer nearly cross each other. This is best investigated for a one-dimensional problem.

Often, the symmetries that are responsible for a degeneracy, which is a surface crossing, are only approximately present. A small matrix element lifts the degeneracy "a little". This is called an **avoided crossing**. Due to an avoided crossing two Born-Oppenheimer sheets may come so close that the non-adiabatic effects can no more be ignored. Thus, regions with avoided crossings are important for the relaxation of the system to a Born-Oppenheimer surface with lower energy.

What is an avoided crossing? Let me start with a position-dependent Hamiltonian for a one-dimensional nuclear coordinate R , for which the energy levels cross for a certain position $R_0 = 0$. In addition we add non-diagonal terms Δ .

Problem

Consider nuclear-electronic Hamiltonian

$$\hat{H} = \frac{\hat{P}^2}{2M} + \begin{pmatrix} |a\rangle \\ |b\rangle \end{pmatrix} \begin{pmatrix} \bar{\epsilon} + F\hat{Q} & -\Delta \\ -\Delta & \bar{\epsilon} - F\hat{Q} \end{pmatrix} \begin{pmatrix} \langle a| \\ \langle b| \end{pmatrix} \quad (2.44)$$

with two electronic states $|a\rangle$ and $|b\rangle$ and a one dimensional nuclear coordinate \hat{Q} with the momentum \hat{P} . The parameters of the model are M , $\bar{\epsilon}$, F , Δ .

- 1 Determine the Born-Oppenheimer Hamiltonian.
- 2 Determine the Born-Oppenheimer surfaces $E_{\pm}^{BO}(Q)$
- 3 Determine the derivative couplings as function of Q .
- 4 Determine the nuclear Schrödinger equation. Resolve the state indices for the electrons. You need not resolve $A_{+,+}(Q)$, $A_{+,-}(Q)$, $A_{-,+}(Q)$, $A_{-,-}(Q)$, E_{+}^{BO} , E_{-}^{BO} .

Discussion

- 1 Determine the Born-Oppenheimer Hamiltonian.

The Hamiltonian has the form

$$\hat{H} = \frac{\hat{P}^2}{2M} + \underbrace{\begin{pmatrix} |a\rangle \\ |b\rangle \end{pmatrix} \begin{pmatrix} \bar{\epsilon} + F\hat{Q} & -\Delta \\ -\Delta & \bar{\epsilon} - F\hat{Q} \end{pmatrix} \begin{pmatrix} \langle a| \\ \langle b| \end{pmatrix}}_{\hat{H}_{BO}} \quad (2.45)$$

The Born-Oppenheimer Hamiltonian is obtained by stripping away the nuclear kinetic energy and by converting the coordinate operator \hat{Q} into a parameter.

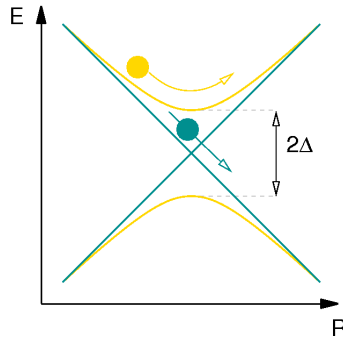
$$\hat{H}^{BO}(Q) = \begin{pmatrix} |a\rangle \\ |b\rangle \end{pmatrix} \begin{pmatrix} \bar{\epsilon} + FQ & -\Delta \\ -\Delta & \bar{\epsilon} - FQ \end{pmatrix} \begin{pmatrix} \langle a| \\ \langle b| \end{pmatrix} \quad (2.46)$$

- 2 Determine the Born-Oppenheimer surfaces $E_{\pm}^{BO}(Q)$

Diagonalization of the Born-Oppenheimer Hamiltonian yields the two Born-Oppenheimer surfaces

$$E_{\pm}^{BO}(Q) = \bar{\epsilon} \pm \Delta \sqrt{1 + \left(\frac{F}{\Delta}Q\right)^2} \quad (2.47)$$

where the minus sign applies for the lower and the plus sign for the upper Born-Oppenheimer surface.



3 Determine the derivative couplings as function of Q .

The eigenstates of the Born-Oppenheimer Hamiltonian, the Born-Oppenheimer states are

$$|\Psi_+^{BO}(Q)\rangle = \begin{pmatrix} |a\rangle \\ |b\rangle \end{pmatrix} \begin{pmatrix} -\sin(\gamma(Q)) \\ \cos(\gamma(Q)) \end{pmatrix} \quad \text{and} \quad |\Psi_-^{BO}(Q)\rangle = \begin{pmatrix} |a\rangle \\ |b\rangle \end{pmatrix} \begin{pmatrix} \cos(\gamma(Q)) \\ \sin(\gamma(Q)) \end{pmatrix} \quad (2.48)$$

where

$$\gamma(Q) = \arctan \left(\frac{F}{\Delta} Q + \sqrt{1 + \left(\frac{F}{\Delta} Q \right)^2} \right) = \frac{\pi}{4} + \frac{1}{2} \arctan \left(\frac{F}{\Delta} Q \right) \quad (2.49)$$

is shown in Fig. 2.2.

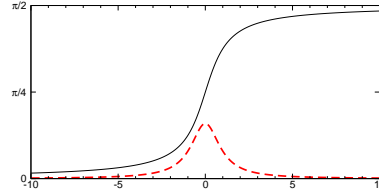


Fig. 2.2: $\gamma(Q)$ determining the eigenstates and derivative couplings for the avoided crossing. The coordinate is drawn in units of $\frac{\Delta}{F}$. The dashed line is the derivative of $\gamma(Q)$ in units of $\frac{F}{\Delta}$.

The non-diagonal derivative couplings are¹⁶

$$\begin{aligned} A_{+,-} &\stackrel{\text{Eq. 2.29}}{=} \langle \Psi_+^{BO}(Q) | \frac{\hbar}{i} \partial_Q | \Psi_-^{BO}(Q) \rangle \\ &\stackrel{\text{Eq. 2.48}}{=} \left[\begin{pmatrix} -\sin(\gamma(Q)) \\ \cos(\gamma(Q)) \end{pmatrix} \begin{pmatrix} \langle a| \\ \langle b| \end{pmatrix} \right] \left[\begin{pmatrix} |a\rangle \\ |b\rangle \end{pmatrix} \begin{pmatrix} -\sin(\gamma(Q)) \\ \cos(\gamma(Q)) \end{pmatrix} \right] \frac{\hbar}{i} \frac{d\gamma}{dQ} = \frac{\hbar}{i} \frac{d\gamma}{dQ} \\ &= \frac{\hbar}{i} \frac{1}{2} \frac{F}{\Delta} \frac{1}{1 + \left(\frac{F}{\Delta} Q \right)^2} \\ A_{-,+} &\stackrel{\text{Eq. 2.19}}{=} A_{+,-}^* = -A_{+,-} = -\frac{\hbar}{i} \frac{d\gamma(Q)}{dQ} \\ &= -\frac{\hbar}{i} \frac{1}{2} \frac{F}{\Delta} \frac{1}{1 + \left(\frac{F}{\Delta} Q \right)^2} \end{aligned} \quad (2.50)$$

and the diagonal derivative couplings vanish. From the red dashed line in Fig. 2.2, it is evident that the derivative couplings are large near the avoided crossing. The reason for this is that the wave function changes its character from one side of the avoided crossing to the other: The character of the wave function seems to ignore the (avoided) crossing and thus follow the straight line. This means that the changes strongly along lower band, which exhibits a kink. (And similar for the upper band.)

For $|F| \gg |\Delta|$, the first-derivative couplings turn into a delta function $A_{+,-}(Q) \rightarrow \frac{\hbar}{i} \frac{\pi}{2} \delta(Q)$.

4 Determine the nuclear Schrödinger equation. Resolve the state indices for the electrons. You need not resolve $A_{+,+}(Q)$, $A_{+,-}(Q)$, $A_{-,+}(Q)$, $A_{-,-}(Q)$, E_+^{BO} , E_-^{BO} .

¹⁶ $\partial_x \text{atan}(x) = \frac{1}{1+x^2}$ and $\text{atan}(\infty) - \text{atan}(-\infty) = \pi$

$$\begin{aligned}
i\hbar\partial_t\Theta_m(Q, t) &= \sum_{n\in\{+,-\}} \left\{ \frac{1}{2M} \sum_{k\in\{+,-\}} \left(\delta_{m,k} \frac{\hbar}{i} \partial_Q + A_{m,k}(Q) \right) \left(\delta_{k,n} \frac{\hbar}{i} \partial_Q + A_{k,n}(Q) \right) + \delta_{m,n} E_m^{BO}(Q) \right\} \Theta_n(Q, t) \\
i\hbar\partial_t\Theta_-(Q, t) &= \left\{ \frac{1}{2M} \left(\frac{\hbar}{i} \partial_Q \right)^2 + \frac{1}{2M} A_{-,+}(Q) A_{+,-}(Q) + E_-^{BO}(Q) \right\} \Theta_-(Q, t) \\
&\quad + \left\{ \frac{\hbar}{i} \partial_Q A_{-,+}(Q) + A_{-,+}(Q) \frac{\hbar}{i} \partial_Q \right\} \Theta_+(Q, t) \\
i\hbar\partial_t\Theta_+(Q, t) &= \left\{ \frac{1}{2M} \left(\frac{\hbar}{i} \partial_Q \right)^2 + \frac{1}{2M} A_{+,-}(Q) A_{-,+}(Q) + E_+^{BO}(Q) \right\} \Theta_+(Q, t) \\
&\quad + \left\{ \frac{\hbar}{i} \partial_Q A_{+,-}(Q) + A_{+,-}(Q) \frac{\hbar}{i} \partial_Q \right\} \Theta_-(Q, t)
\end{aligned} \tag{2.51}$$

2.7.2 Holstein model

Introduction

Holstein monomer

The Holstein model is the standard model for small polarons.[21, 22] A good description of the Holstein model is given in the paper by Firsov[23].

The Holstein model describes a lattice of Holstein monomers. The Holstein monomer is the minimal problem for a system with **electron-phonon coupling**. It consists of one electronic degree of freedom and one phonon, which interact via a coupling term.

A good example for a Holstein monomer is a hydrogen molecule to which an electron can be added to form H_2^- anion. The Holstein monomer is shown schematically in Fig. 2.3.

The two electrons of the H_2 molecule enter the bonding orbital and the bond has a certain equilibrium bond-length d_0 . The bonding orbital will not be represented in the Holstein model, because it is always occupied.

When the H_2 molecule is perturbed, the bond distance $d(t) = d_0 + Z(t)$ vibrates about its equilibrium value d_0 with a circular frequency $\omega_0 = \sqrt{\frac{C}{M}}$. This can be described by a harmonic oscillator. The vibration represents a **phonon**¹⁷

The molecule can accept an additional electron. Upon adding an electron into the antibonding orbital $|\chi\rangle$ of the hydrogen molecule, the bond expands. The molecule distorts in order to reduce the energy of this additional electron. A new equilibrium distance is reached when the forces from electron and the restoring force from the phonon are in balance. Thus, a bound electron-phonon pair is formed, which is called **polaron**. The energy gain from the distortion induced by the additional electron is the **polaron binding energy** E_P .

The Holstein monomer is described by the model Hamiltonian

$$\hat{H} = \underbrace{\frac{\hat{P}^2}{2M}}_{\text{vibration}} + \underbrace{\frac{1}{2}C\hat{Z}^2}_{\text{electron}} + \underbrace{|\chi\rangle\bar{\epsilon}\langle\chi| - |\chi\rangle\gamma\hat{Z}\langle\chi|}_{\text{e-ph coupling}} \tag{2.52}$$

The orbital $|\chi\rangle$ is the antibonding orbital of the H_2 molecule with energy $\bar{\epsilon}$.¹⁸ The bond-length distortion is $\hat{Z} \stackrel{\text{def}}{=} \hat{d} - d_0\hat{1}$ and its momentum is \hat{P} .

¹⁷A phonon is a lattice vibration. It is considered as a quasi-particle like the electron in a solid.

¹⁸When the electron is not on the hydrogen molecule, its energy is equal to the vacuum level. We set the energy zero to the vacuum level, so that the energy of the electron is zero. If the electron is on the molecule, i.e. in the antibonding orbital $|\chi\rangle$, the electronic energy is $\langle\psi|(|\chi\rangle\bar{\epsilon}\langle\chi| - |\chi\rangle\gamma\hat{Z}\langle\chi|)|\psi\rangle = \bar{\epsilon} - \gamma\hat{Z}$

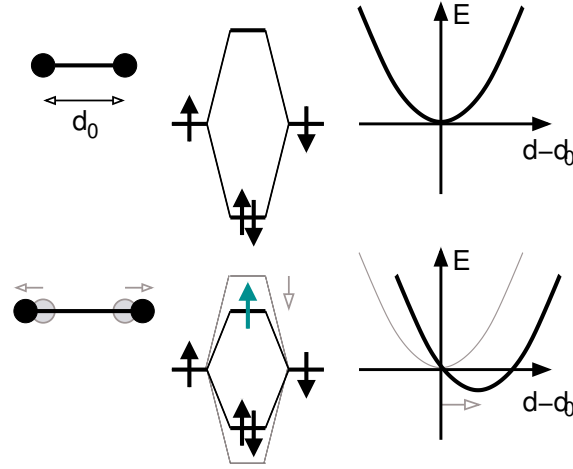


Fig. 2.3: Scheme to illustrate the Holstein monomer, the monomer of the Holstein model. Left: atomic structure. Middle: atomic and molecular energy levels. Right: potential energy for the bond vibration. The top line shows a hydrogen molecule, while the bottom line shows an H_2^- ion obtained after adding an electron into the antibonding orbital.

Without the electron in the antibonding orbital, the Hamiltonian describes a simple harmonic oscillator with circular frequency $\omega_0 = \sqrt{\frac{c}{M}}$. With the electron added, also the energy $\bar{\epsilon}$ of the electron in the antibonding orbital and the electron-phonon coupling needs to be considered.

The corresponding Born-Oppenheimer surfaces are

$$E_0^{BO}(Z) = \frac{1}{2}CZ^2 \quad \text{without additional electron} \quad (2.53)$$

$$E_1^{BO}(Z) = \frac{1}{2}CZ^2 + \bar{\epsilon} - \gamma Z \quad \text{with additional electron} \quad (2.54)$$

The **polaron binding energy** E_P is the energy gained when the electron-phonon coupling is switched on. For the Holstein model, we obtain the polaron binding energy as

$$E_P = \left(E_1^{BO}(Z_{opt}) - E_1^{BO}(Z = 0) \right) = \frac{\gamma^2}{2C}, \quad (2.55)$$

where Z_{opt} minimizes the energy $E_1^{BO}(Z)$.

Holstein dimer

The Holstein dimer is a pair of two Holstein monomers. The Holstein dimer is the minimal problem for **self-localization** and for **polaron hopping**.

The Holstein dimer consists of two Holstein monomers, which share one electron. The electron can jump from one Holstein monomer to the next. The Holstein dimer is described by the model Hamiltonian

$$\hat{H} = \underbrace{-|\chi_1\rangle t \langle \chi_2| - |\chi_2\rangle t \langle \chi_1|}_{\text{hopping}} + \sum_{j=1}^2 \left\{ \hat{1}_e \underbrace{\frac{\hat{p}_j^2}{2M} + \frac{1}{2}cZ_j^2}_{\text{phonons}} + \underbrace{|\chi_j\rangle \bar{\epsilon} \langle \chi_j|}_{\text{electrons}} - \underbrace{|\chi_j\rangle \gamma \hat{Z}_j \langle \chi_j|}_{\text{e-ph coupling}} \right\} \quad (2.56)$$

where $\hat{1}_e \stackrel{\text{def}}{=} \sum_{k=1}^2 |\chi_k\rangle \langle \chi_k|$ is the identity in the electronic Hilbert space.¹⁹ The parameter t is the

¹⁹We do not consider the vacuum level, mentioned in the Holstein monomer.

hopping parameter. The orbitals $|\chi_j\rangle$ are considered orthogonal to each other.²⁰

The hopping parameter $t = -\langle\chi_1|\hat{H}|\chi_2\rangle$ is the Hamilton matrix element between the antibonding orbitals $|\chi_j\rangle$ of both Holstein monomers. The Born-Oppenheimer wave functions of the dimer have the form

$$|\Psi_{\pm}^{BO}(Z_1, Z_2)\rangle = |\chi_1\rangle c_{1,\pm}(Z_1, Z_2) + |\chi_2\rangle c_{2,\pm}(Z_1, Z_2) \quad (2.57)$$

There will be a lower wave function $|\psi_{-}^{BO}\rangle$, which will accept the electron of the dimer, and an upper wave function $|\psi_{+}^{BO}\rangle$, which will remain empty²¹. The two states can be characterized as bonding and antibonding superposition of the two (antibonding) molecular orbitals of the two monomers. If the two monomers are undistorted, (or distorted in the same way), the resulting electron density will be equally distributed over both sites. If the Holstein monomers distort, the electron-phonon coupling may also shift the electron orbitals of the monomers relative to each other. As a result, the electron density is transferred towards one or the other of the two monomers.

The Holstein dimer can be separated into two independent systems: (1) a simple phonon, the symmetric vibration, which does not affect the electron dynamics, and (2) the antisymmetric vibration, which is strongly coupled to the two electron levels. The energy of the two subsystems is additive and the wave function is a product of wave functions of the subsystems.

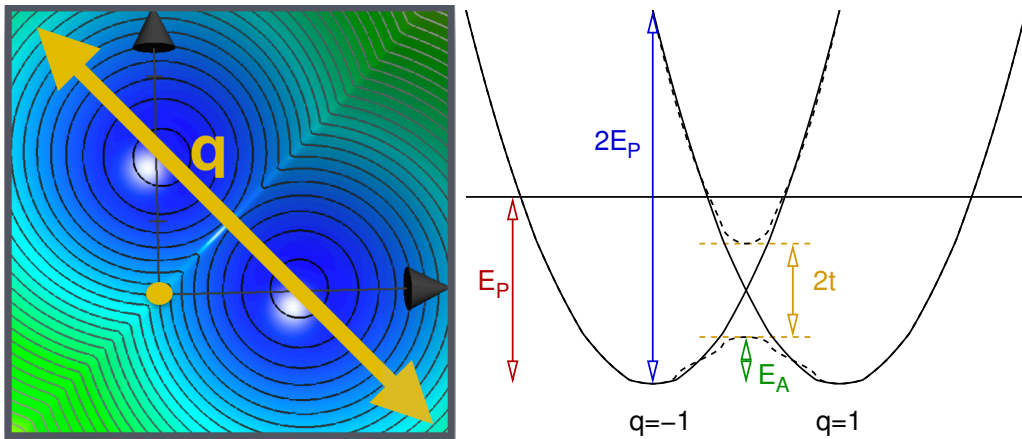


Fig. 2.4: Left: lower Born-Oppenheimer surface of the Holstein dimer without electronic hopping. The horizontal and vertical axes represent the expansion of the left and right Holstein monomer, respectively. Right: Born-Oppenheimer surface of the two Holstein monomers (filled black line) and those of the Holstein dimer (dashed lines) as function of the antisymmetric vibration coordinate q . E_P is the polaron binding energy. $2E_P$ is the optical excitation energy. The thermal barrier for the polaron motion is $E_A = \frac{1}{2}E_P - t$. The point where this barrier vanishes marks the transition from a small to a large polaron.

After splitting off the symmetric vibration, the two Born-Oppenheimer surfaces are shown on the right of Fig. 2.4. The lower potential-energy surface has two degenerate minima separated by a barrier $E_A = \frac{1}{2}E_P - t$. This barrier must be overcome before the electron migrates from one Holstein monomer to the other. This indicates that the motion of polarons in this limit is due to thermally activated hopping. Thermal motion can be expected²² to follow an **Arrhenius law**²³ with

²⁰The orthogonality condition requires a basis transformation analogous to that of the Wannier orbitals.[24]

²¹Note, that the Born-Oppenheimer wave functions are many-electron wave functions. In this special case, there is exactly one electron so that we can use the language of one-particle quantum mechanics.

²²This is a simple estimate, that can be understood from **transition-state theory** and Einstein's formula for diffusion. Transition-state theory is discussed in chapter 1 of Φ SX: The statistical properties of matter[25]

²³Arrhenius law says that the rate of thermally activated processes grows with temperature like $\Gamma e^{-\frac{1}{k_B T} E_A}$. Arrhenius law is an idealization and deviations are observed.

conductivity proportional to $e^{-\frac{1}{k_B T} E_A}$ with the activation energy E_A .

Small and large polarons: Up to now we discussed the **small-polaron** case, in which the electron localizes on one site and the polaron moves by thermally activated hopping over a barrier. Thus, the conductivity has a strong temperature dependence.

If the hopping is so large that the barrier vanishes, $t \gg \frac{1}{2} E_P$, the two minima merge in the middle. The result is a rather flat potential-energy surface with a minimum in the center. This is the **large-polaron** case.

Let me return to the small-polaron case:

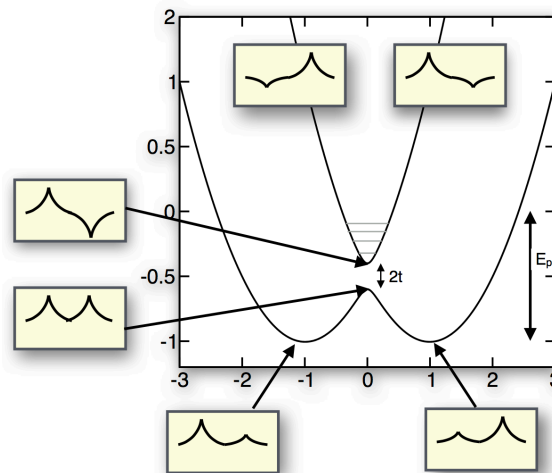


Fig. 2.5: Schematic Born-Oppenheimer wave functions at different points of the Born-Oppenheimer surfaces. The horizontal axis is the antisymmetric vibration coordinate q and the vertical axis is the energy axis. The (antibonding) orbital of a monomer is sketched as atomic hydrogen wave function. Each inset shows an orbital delocalized over two sites.

In figure 2.5, the Born-Oppenheimer wave functions related to the different Born-Oppenheimer surfaces are shown. Next to the avoided crossing, the states can be described as bonding and antibonding states. For $q = -1$ the lower surface describes an electron on the left Holstein monomer, while the upper surface describes an electron on the other, unfavorable site.

The derivative coupling $A_{1,2}(q)$ is shown in figure 2.8. It is a scalar, because the nuclear coordinate space is one-dimensional. The diagonal derivative couplings vanish, because we have chosen real-valued Born-Oppenheimer wave functions. The derivative couplings are strongly peaked at the avoided crossing. This is where the Born-Oppenheimer wave functions depend strongly on the nuclear coordinates, because the wave functions change their character from one side of the avoided crossing to the other.

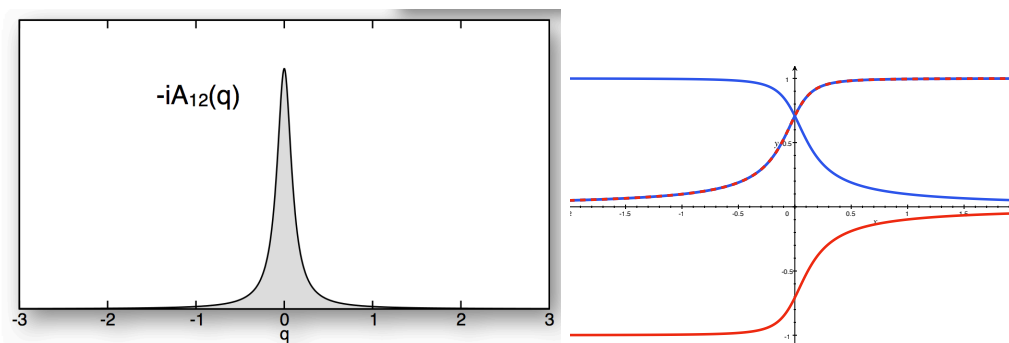


Fig. 2.6: Left: Off-diagonal derivative coupling $-iA_{1,2}(q)$ as function of the antisymmetric vibration coordinate q of the Holstein dimer. Right: wave-function coefficients $\langle \chi_j | \Psi_{\pm}^{BO} \rangle$ of the Born-Oppenheimer wave function as function of the antisymmetric vibration coordinate q .

This exercise aims to practice the Born-Oppenheimer framework of dividing up the electron-nuclear problem into a position dependent Hamiltonian for the electrons and a multi-valued wave function describing the nuclear motion.

Problem

The Hamiltonian of the Holstein dimer is

$$\hat{H} = \underbrace{-|\chi_1\rangle t \langle \chi_2| - |\chi_2\rangle t \langle \chi_1|}_{\text{electrons}} + \underbrace{\hat{1}_e \sum_{j=1}^2 \left(\frac{\hat{P}_j^2}{2M} + \frac{1}{2} C \hat{Z}_j^2 \right)}_{\text{vibration}} - \underbrace{\sum_{j=1}^2 |\chi_j\rangle \gamma \hat{Z}_j \langle \chi_j|}_{\text{electron-phonon coupling}} , \quad (2.58)$$

where $\hat{1}_e \stackrel{\text{def}}{=} \sum_{j=1}^2 |\chi_j\rangle \langle \chi_j|$ is the identity in the electronic Hilbert space. The parameter t is the hopping parameter. γ is the electron-phonon coupling. M is the effective mass of the vibrational coordinate and C is its force constant. $|\chi_j\rangle$ is the electronic energy level of the j -th monomer, which can receive or give an electron. Z_j is the nuclear vibrational coordinate on the j -th monomer and $\hat{P}_j := \frac{\hbar}{i} \partial_{Z_j}$ is the corresponding momentum. The electron energy $\bar{\epsilon}$ used previously has been set to zero.

Important note: The goal of this problem is to practice the Born-Oppenheimer framework as described in the lecture notes. The problem at hand is simple enough to be solved by other means as well, but that is not desired.

- 1 Make yourself familiar with the Hamiltonian of the Holstein dimer
- 2 Use the following transformation of the nuclear coordinates (Z_1, Z_2) to a new set (s, q)

$$s = \frac{C}{\gamma} (Z_1 + Z_2) - 1 \quad \text{and} \quad q = \frac{C}{\gamma} (Z_1 - Z_2) . \quad (2.59)$$

to extract the one-dimensional Hamiltonian for the electron-phonon coupling.

This task demands for the transformation of the momenta based on the prescribed coordinate transformation. Make evident, which rules are used for the transformation of the momenta. In the new coordinates, the Hamiltonian can be separated into a simple harmonic oscillator for the coordinate s , and a one-dimensional Hamiltonian for the coordinate q , which describes the electron-phonon coupling.

All the following questions apply only to the one-dimensional Hamiltonian containing the electron-phonon coupling.

- 3 Determine the Born-Oppenheimer Hamiltonian $\hat{H}^{BO}(\vec{R})$.
- 4 Extract the Born-Oppenheimer surfaces $E^{BO}(\vec{R})$. Calculate the expression and sketch them. Describe the qualitative differences between large and small electron-phonon couplings by sketching the surfaces.
- 5 Determine the Born-Oppenheimer states $|\Phi^{BO}(\vec{R})\rangle$ and describe them qualitatively.
- 6 Calculate the first-derivative coupling $\vec{A}_{m,n}(\vec{R})$.
- 7 (Optional) Write down the Hamiltonian for the nuclear coordinates.

Discussion

- 1 Make yourself familiar with the Hamiltonian of the Holstein dimer

Let us first inspect the Hamiltonian

$$\hat{H} = \underbrace{-|\chi_1\rangle t \langle \chi_2| - |\chi_2\rangle t \langle \chi_1|}_{\text{electrons}} + \underbrace{\hat{1}_e \sum_{j=1}^2 \left(\frac{\hat{P}_j^2}{2M} + \frac{1}{2} c \hat{Z}_j^2 \right)}_{\text{vibration}} - \underbrace{\sum_{j=1}^2 |\chi_j\rangle \gamma \hat{Z}_j \langle \chi_j|}_{\text{electron-phonon coupling}} \quad (2.60)$$

Notation: The Hamilton operator acts on a Hilbert space spanned by $\{|\chi_j, Z_1, Z_2\rangle\}$ with $j \in \{1, 2\}$ and $(Z_1, Z_2) \in \mathbb{R}^2$. $|\chi_1\rangle$ is the electronic orbital centered at one and $|\chi_2\rangle$ is the orbital on the other Holstein monomer.²⁴ $(Z_1, Z_2) \in \mathbb{R}^2$ describes the two nuclear degrees of freedom, one for each Holstein monomer.

A state $|\chi_j, Z_1, Z_2\rangle = |\chi_j\rangle \otimes |Z_1\rangle \otimes |Z_2\rangle$ is product state, respectively a the tensor product.

The basis obeys

$$\begin{aligned} \langle \chi_j, Z_1, Z_2 | \chi_k, Z'_1, Z'_2 \rangle &= \delta_{j,k} \delta(Z_1 - Z'_1) \delta(Z_2 - Z'_2) && \text{orthonormality} \\ \hat{1} &= \sum_j \int dZ_1 \int dZ_2 |\chi_j, Z_1, Z_2\rangle \langle \chi_j, Z_1, Z_2| && \text{completeness} \end{aligned} \quad (2.61)$$

The general state, on which the electron-nuclear Hamiltonian acts, has the form

$$|\Phi(t)\rangle = \sum_{j=1}^2 \int dZ_1 \int dZ_2 |\chi_j, Z_1, Z_2\rangle \Theta_j(Z_1, Z_2, t) \quad (2.62)$$

where $\Theta_j(Z_1, Z_2, t)$ is the nuclear wave function. Note, that in this case the nuclear wave function is not linked to the Born-Oppenheimer wave functions, but to the orbitals $|\chi_j\rangle$.

The Schrödinger equation can be rewritten as a partial differential equation for the double-valued wave function with components $\Theta_j(Z_1, Z_2, t)$, when we use

$$\begin{aligned} \hat{P}_k |\chi_j, Z_1, Z_2\rangle \Theta_j(Z_1, Z_2, t) &= |\chi_j, Z_1, Z_2\rangle \frac{\hbar}{i} \partial_{Z_k} \Theta_j(Z_1, Z_2, t) \\ \hat{Z}_k |\chi_j, Z_1, Z_2\rangle \Theta_j(Z_1, Z_2, t) &= |\chi_j, Z_1, Z_2\rangle Z_k \Theta_j(Z_1, Z_2, t) \end{aligned} \quad (2.63)$$

Multiplication of the Schrödinger equation from the left with $\langle \chi_j, Z_1, Z_2|$ yields

$$\begin{aligned} \langle \chi_j, Z_1, Z_2 | i\hbar \partial_t | \Phi(t) \rangle &= \langle \chi_j, Z_1, Z_2 | \hat{H} | \Phi(t) \rangle \\ \stackrel{\text{Eq. 2.60}}{\Rightarrow} i\hbar \partial_t \Theta_j(Z_1, Z_2, t) &= \underbrace{\left[\sum_{k=1,2} \left(\frac{-\hbar^2}{2M} \partial_{Z_k}^2 + \frac{1}{2} c Z_k^2 \right) \right]}_{\text{vibration}} \Theta_j(Z_1, Z_2, t) \\ &\quad - \underbrace{\gamma Z_j \Theta_j(Z_1, Z_2, t)}_{\text{electron-phonon coupling}} + \underbrace{\begin{cases} t \Theta_2(Z_1, Z_2, t) & \text{for } j = 1 \\ t \Theta_1(Z_1, Z_2, t) & \text{for } j = 2 \end{cases}}_{\text{electrons}} \end{aligned} \quad (2.64)$$

Qualitative behavior of the potential energy: Before we start, we should have an understanding of the Hamiltonian. For the following discussion, it may be helpful to inspect fig. 2.4 on p. 64.

Let us approach the physical system by first considering certain limiting cases that can easily be worked out:

One limiting case is to set the hopping parameter t to zero. In that case, the two components $\Theta_j(Z_1, Z_2)$ with $j \in \{1, 2\}$ of the nuclear wave function are independent. I.e. the nuclear

²⁴In this specific example, we consider only a single electron rather than many. And we limit the electronic Hilbert space to only two orbitals.

Schrödinger equation does not connect the two components. Thus, we obtain one potential-energy surface $V_1(Z_1, Z_2)$ for one component and another potential-energy surface $V_2(Z_1, Z_2)$ for second component. This limiting case is identical to constraining the electron once to the left and once to the right side of the dimer.

$$V_j(Z_1, Z_2) = \frac{C}{2}(Z_1^2 + Z_2^2) - \gamma Z_j = \begin{cases} \frac{C}{2} \left(\left(Z_1 - \frac{\gamma}{C} \right)^2 + Z_2^2 \right) - \frac{\gamma^2}{2C} & \text{for } j = 1 \\ \frac{C}{2} \left(Z_1^2 + \left(Z_2 - \frac{\gamma}{C} \right)^2 \right) - \frac{\gamma^2}{2C} & \text{for } j = 2 \end{cases} \quad (2.65)$$

The potential $V_1(Z_1, Z_2)$ is obtained when the electron is on the first Holstein monomer. In that case the minimum describes a state with $Z_1 = \gamma/C$, that implies that the first monomer is distorted. The second monomer is undistorted. The potential is a spherical parabola.

The potential $V_2(Z_1, Z_2)$ is obtained by interchanging the two coordinates Z_1, Z_2 in $V_1(Z_1, Z_2)$, i.e. $V_2(Z_1, Z_2) = V_1(Z_2, Z_1)$.

The two parabola intersect in the midplane of the two points, $(\gamma/C, 0)$ and $(0, \gamma/C)$. This means that the two potential surfaces are degenerate. This suggests that the line

$$Z_1 + Z_2 = \frac{\gamma}{C} \quad (2.66)$$

is a mirror plane of the problem. The midplane of the two minima, the line where both potentials are degenerate, is $Z_1 = Z_2$.

2 Use the following transformation of the nuclear coordinates

$$s = \frac{C}{\gamma}(Z_1 + Z_2) - 1 \quad \text{and} \quad q = \frac{C}{\gamma}(Z_1 - Z_2). \quad (2.67)$$

to extract the one-dimensional Hamiltonian for the electron-phonon coupling.

This task demands for the transformation of the momenta based on the prescribed coordinate transformation. Make evident, which rules are used for the transformation of the momenta. In the new coordinates, the Hamiltonian can be separated into a simple harmonic oscillator for the coordinate s , and a one-dimensional Hamiltonian for the coordinate q , which describes the electron-phonon coupling.

Transformed momenta from commutator relation: In quantum mechanics, the canonical momentum of a variable obey the canonical commutator relation

$$[\hat{p}_j, \hat{q}_k]_- = \frac{\hbar}{i} \delta_{j,k}. \quad (2.68)$$

For a wave function in coordinate space \vec{q} , this implies that the momentum operator can be written as differential operator

$$\hat{p}_j = \frac{\hbar}{i} \partial_{q_j} \quad (2.69)$$

because it automatically satisfies the required commutator relation.

Consider now a variable transform

$$Q_j = F_j(\vec{q}) \quad \text{and} \quad q_j = f_j(\vec{Q}) \quad (2.70)$$

so that

$$\psi(\vec{Q}) = \psi(\vec{F}(\vec{q})) = \bar{\psi}(\vec{q}). \quad (2.71)$$

We obtain the momenta as the corresponding gradient operator

$$\begin{aligned} \frac{\hbar}{i} \partial_{q_j} \bar{\psi}(\vec{q}) &= \frac{\hbar}{i} \partial_{q_j} \psi(\vec{F}(\vec{q})) = \sum_k \frac{\hbar}{i} \frac{\partial \psi}{\partial Q_k} \frac{\partial F_k}{\partial q_j} = \sum_k \frac{\partial F_k(\vec{q})}{\partial q_j} \frac{\hbar}{i} \partial_{Q_k} \psi(\vec{Q}) \\ \Rightarrow \hat{p}_j &= \sum_k \frac{\partial F_k(\vec{q})}{\partial q_j} \hat{P}_k \end{aligned} \quad (2.72)$$

Transformed momenta from action principle: Here, I use an alternative description based on classical mechanics.

Given the **Lagrange function** $\mathcal{L}(\vec{q}, \vec{v}, t)$, the **canonical momenta** are defined as

$$p_j \stackrel{\text{def}}{=} \frac{\partial \mathcal{L}}{\partial v_j}, \quad (2.73)$$

where q_j are generalized coordinates and $v_j \stackrel{\text{def}}{=} \dot{q}_j$ are their velocities.

A simple coordinate transform from coordinates \vec{q} to the new coordinates \vec{Q} can be expressed as

$$q_j = f_j(\vec{Q}) \quad \text{respectively} \quad Q_j = F_j(\vec{q}). \quad (2.74)$$

We assume that the coordinate transform is invertible. The coordinate transform used here is more restricted than the most general **canonical transform**: Namely, the new coordinates do not depend on the old velocities and vice versa.

The **action** $S[\vec{q}(t)] = \int dt \mathcal{L}(\vec{q}, \dot{\vec{q}}, t)$ for a given path $q(t)$ expressed in old or new coordinates must be the same, except for a total time integral.²⁵ The functional form of the Lagrangian is, however, different. The value of the Lagrangian expressed in old and new coordinates is the same up to a total derivative of a function, that is

$$\begin{aligned} \mathcal{L}'(\vec{Q}, \dot{\vec{Q}}, t) &= \mathcal{L}(\vec{q}, \dot{\vec{q}}, t) \\ &= \mathcal{L}\left(\vec{f}(\vec{Q}), \frac{d\vec{f}(\vec{Q})}{dt}, t\right) = \mathcal{L}\left(\vec{f}(\vec{Q}), \sum_k \frac{\partial \vec{f}(\vec{Q})}{\partial Q_k} \dot{Q}_k, t\right) \\ \Rightarrow \mathcal{L}'(\vec{Q}, \vec{V}, t) &= \mathcal{L}\left(\vec{f}(\vec{Q}), \sum_k \frac{\partial \vec{f}(\vec{Q})}{\partial Q_k} v_k, t\right) \end{aligned} \quad (2.75)$$

where $\vec{V} = \dot{\vec{Q}}$ is the velocity of the new coordinate \vec{Q} .

This condition yields the new momenta as

$$\begin{aligned} P_j &\stackrel{\text{Eq. 2.73}}{=} \frac{\partial \mathcal{L}'}{\partial V_j} \stackrel{\text{Eq. 2.75}}{=} \frac{\partial}{\partial V_j} \mathcal{L}\left(\vec{f}(\vec{Q}), \sum_k \frac{\partial \vec{f}}{\partial Q_k} v_k, t\right) = \sum_k \frac{\partial \mathcal{L}}{\partial v_k} \frac{\partial f_k}{\partial Q_j} \\ &\stackrel{\text{Eq. 2.73}}{=} \sum_k p_k \frac{\partial f_k}{\partial Q_j} \end{aligned} \quad (2.76)$$

Special transformation of momenta: In our case, the transformation has been given in Eq. 2.67 as

$$\begin{aligned} s &= f_s(Z_1, Z_2) = \frac{C}{\gamma} (Z_1 + Z_2) - 1 \\ q &= f_q(Z_1, Z_2) = \frac{C}{\gamma} (Z_1 - Z_2) \end{aligned} \quad (2.77)$$

²⁵Because the end-points of the path are fixed during the variation of the action in Hamilton's principle, a total time integral of the action does not affect the "optimum" path. See e.g. section ?? in Φ SX:Klassische Mechanik[?].

The back transformation is

$$\begin{aligned} Z_1 &= F_1(s, q) = \frac{\gamma}{2C} (1 + s + q) \\ Z_2 &= F_2(s, q) = \frac{\gamma}{2C} (1 + s - q) \end{aligned} \quad (2.78)$$

which allows replace the old coordinates by the new ones.

The next goal is to express the momenta P_1, P_2 by the conjugate momenta of the new coordinates.

$$\begin{aligned} P_1 &\stackrel{\text{Eq. 2.76}}{=} p_s \frac{\partial f_s}{\partial Z_1} + p_q \frac{\partial f_q}{\partial Z_1} \stackrel{\text{Eq. 2.77}}{=} p_s \frac{C}{\gamma} + p_q \frac{C}{\gamma} = \frac{C}{\gamma} (p_s + p_q) \\ P_2 &= p_s \frac{\partial f_s}{\partial Z_2} + p_q \frac{\partial f_q}{\partial Z_2} = p_s \frac{C}{\gamma} - p_q \frac{C}{\gamma} = \frac{C}{\gamma} (p_s - p_q) \end{aligned} \quad (2.79)$$

Notice the subtle difference between classical momenta used in the Lagrange formalism above and the momentum operators used in the Hamiltonian below.

This result is inserted into the Hamiltonian Eq. 2.67

$$\begin{aligned} \hat{H} &= \underbrace{-|\chi_1\rangle\langle\chi_2| - |\chi_2\rangle\langle\chi_1|}_{\text{electrons}} + \underbrace{\sum_{j=1}^2 \left(\frac{\hat{p}_j^2}{2M} + \frac{1}{2} C \hat{Z}_j^2 \right)}_{\text{vibration}} - \underbrace{\sum_{j=1,2} |\chi_j\rangle\gamma\hat{Z}_j\langle\chi_j|}_{\text{electron-phonon coupling}} \\ &= \underbrace{-|\chi_1\rangle\langle\chi_2| - |\chi_2\rangle\langle\chi_1|}_{\text{electrons}} + \underbrace{\frac{C^2}{M\gamma^2} (\hat{p}_s^2 + \hat{p}_q^2) + \frac{\gamma^2}{4C} ((1 + \hat{s})^2 + \hat{q}^2)}_{\text{vibration}} \\ &\quad - \underbrace{\frac{\gamma^2}{2C} (1 + \hat{s}) - \frac{\gamma^2}{2C} \hat{q} (|\chi_1\rangle\langle\chi_1| - |\chi_2\rangle\langle\chi_2|)}_{\text{electron-phonon coupling}} \\ &= -|\chi_1\rangle\langle\chi_2| - |\chi_2\rangle\langle\chi_1| + \frac{C^2}{M\gamma^2} \hat{p}_q^2 + \frac{\gamma^2}{4C} \hat{q}^2 - \frac{\gamma^2}{4C} - \frac{\gamma^2}{2C} \hat{q} (|\chi_1\rangle\langle\chi_1| - |\chi_2\rangle\langle\chi_2|) \\ &\quad + \frac{C^2}{M\gamma^2} \hat{p}_s^2 + \frac{\gamma^2}{4C} (1 + \hat{s})^2 - \frac{\gamma^2}{2C} (1 + \hat{s}) + \frac{\gamma^2}{4C} \\ &= \underbrace{\frac{C^2}{M\gamma^2} \hat{p}_q^2 + \frac{\gamma^2}{4C} (\hat{q}^2 - 1) + \left(\begin{array}{c} |\chi_1\rangle \\ |\chi_2\rangle \end{array} \right) \left(\begin{array}{cc} -\gamma^2 \hat{q}/(2C) & -t \\ -t & \gamma^2 \hat{q}/(2C) \end{array} \right) \left(\begin{array}{c} \langle\chi_1| \\ \langle\chi_2| \end{array} \right)}_{\hat{H}_q} \\ &\quad + \underbrace{\frac{C^2}{M\gamma^2} \hat{p}_s^2 + \frac{\gamma^2}{4C} \hat{s}^2}_{\hat{H}_s} \end{aligned} \quad (2.80)$$

From the first to the second step above, we used for the electron-phonon coupling

$$\begin{aligned} \sum_{j=1}^2 |\chi_j\rangle\gamma\hat{Z}_j\langle\chi_j| &= |\chi_1\rangle\gamma\hat{Z}_1\langle\chi_1| + |\chi_2\rangle\gamma\hat{Z}_2\langle\chi_2| \\ &= \gamma \underbrace{\frac{\hat{Z}_1 + \hat{Z}_2}{2}}_{\frac{\gamma}{2C}(1+s)} \underbrace{(|\chi_1\rangle\langle\chi_1| + |\chi_2\rangle\langle\chi_2|)}_{\hat{I}_e} + \gamma \underbrace{\frac{\hat{Z}_1 - \hat{Z}_2}{2}}_{\frac{\gamma}{2C}q} (|\chi_1\rangle\langle\chi_1| - |\chi_2\rangle\langle\chi_2|) \\ &= \frac{\gamma^2}{2C} (1 + s) + \frac{\gamma^2}{2C} q (|\chi_1\rangle\langle\chi_1| - |\chi_2\rangle\langle\chi_2|) \end{aligned} \quad (2.81)$$

Thus, the Hamiltonian can be split into two parts. One, \hat{H}_q , only depends on the coordinate q , its momentum p_q and the electronic Hamiltonian. The other only depends on the coordinate s and

its momentum p_s . This second Hamiltonian is a one-dimensional harmonic oscillator. We shift the constant energy term so that the minimum of the potential energy in \hat{H}_s lies at zero.

$$\begin{aligned}\hat{H}_q &= -|\chi_1\rangle t \langle \chi_2| - |\chi_2\rangle t \langle \chi_1| + \frac{C^2}{M\gamma^2} \hat{p}_q^2 + \frac{\gamma^2}{4C} (\hat{q}^2 - 1) - \frac{\gamma^2}{2C} \hat{q} (|\chi_1\rangle \langle \chi_1| - |\chi_2\rangle \langle \chi_2|) \\ &= \frac{C^2}{M\gamma^2} \hat{p}_q^2 + \frac{\gamma^2}{4C} (\hat{q}^2 - 1) + \begin{pmatrix} \langle \chi_1| \\ \langle \chi_2| \end{pmatrix} \begin{pmatrix} -\gamma^2 \hat{q}/(2C) & -t \\ -t & \gamma^2 \hat{q}/(2C) \end{pmatrix} \begin{pmatrix} \langle \chi_1| \\ \langle \chi_2| \end{pmatrix} \\ \hat{H}_s &= \frac{C^2}{M\gamma^2} \hat{p}_s^2 + \frac{\gamma^2}{4C} \hat{s}^2\end{aligned}\quad (2.82)$$

New parameters: Let us introduce new parameters, namely the effective mass m_q for the coordinates s and q and the **polaron binding energy** E_b .

$$\begin{aligned}m_q &\stackrel{\text{def}}{=} \frac{M\gamma^2}{2C^2} \\ E_b &\stackrel{\text{def}}{=} \frac{\gamma^2}{2C}\end{aligned}\quad (2.83)$$

$$\begin{aligned}\hat{H}_q &= \frac{\hat{p}_q^2}{2m_q} + \frac{1}{2} E_b (\hat{q}^2 - 1) + \begin{pmatrix} \langle \chi_1| \\ \langle \chi_2| \end{pmatrix} \begin{pmatrix} -E_b \hat{q} & -t \\ -t & E_b \hat{q} \end{pmatrix} \begin{pmatrix} \langle \chi_1| \\ \langle \chi_2| \end{pmatrix} \\ \hat{H}_s &= \frac{\hat{p}_s^2}{2m_q} + \frac{1}{2} E_b \hat{s}^2\end{aligned}\quad (2.84)$$

Note, that q and s are dimension-less quantities.

Drop symmetric vibrations: In the following, we proceed only with the Hamiltonian \hat{H}_q . The subscript q is dropped.

All the following questions apply only to the one-dimensional Hamiltonian containing the electron-phonon coupling.

3 Determine the Born-Oppenheimer Hamiltonian $\hat{H}^{BO}(\vec{R})$.

The Born-Oppenheimer Hamiltonian is obtained by stripping all terms related to the nuclear momenta and by replacing the nuclear position operators by parameters

$$\hat{H}^{BO}(q) = \frac{1}{2} E_b (q^2 - 1) + \begin{pmatrix} \langle \chi_1| \\ \langle \chi_2| \end{pmatrix} \begin{pmatrix} -E_b q & -t \\ -t & E_b q \end{pmatrix} \begin{pmatrix} \langle \chi_1| \\ \langle \chi_2| \end{pmatrix}\quad (2.85)$$

The Born-Oppenheimer is an operator acting on the electronic degrees of freedom. That is, it acts on the two-dimensional Hilbert space spanned by the orbitals $|\chi_1\rangle$ and $|\chi_2\rangle$. The Born-Oppenheimer Hamiltonian depends on nuclear coordinates.

4 Extract the Born-Oppenheimer surfaces $E^{BO}(\vec{R})$. Calculate the expression and sketch them. Describe the qualitative differences between large and small electron-phonon couplings by sketching the surfaces.

The Born-Oppenheimer surfaces are obtained by diagonalizing the BO Hamiltonian for each set of nuclear coordinates.

The eigenvalues are obtained from the **secular equation**²⁶. We determine the eigenvalues of the electronic operator first and add the remainder later.

$$\begin{aligned} (-E_b q - \epsilon_{\pm})(E_b q - \epsilon_{\pm}) - t^2 &= 0 \\ \Rightarrow \epsilon_{\pm}^2 - (E_b q)^2 &= t^2 \\ \Rightarrow \epsilon_{\pm} &= \pm \sqrt{t^2 + (E_b q)^2} \end{aligned} \quad (2.86)$$

We add the part containing only the nuclear coordinates

$$E_{\pm}^{BO}(q) = \frac{1}{2} E_b (q^2 - 1) \pm \sqrt{t^2 + (E_b q)^2} \quad (2.87)$$

The result is shown in fig. 2.4 on p. 64.

5 Determine the Born-Oppenheimer states $|\Phi^{BO}(\vec{R})\rangle$ and describe them qualitatively.

The Born-Oppenheimer $|\Psi_{\pm}^{BO}\rangle$ states are obtained from

$$\left[\hat{H}^{BO}(q) - E_{\pm}^{BO}(q) \right] |\Psi_{\pm}^{BO}\rangle = 0 \quad (2.88)$$

where

$$|\Psi_{\pm}^{BO}\rangle = \sum_{j=1}^2 |\chi_j\rangle c_{j,\pm} \quad (2.89)$$

It is sufficient to use the condition

$$\begin{aligned} \langle \chi_1 | \left[\hat{H}^{BO}(q) - E_{\pm}^{BO}(q) \right] |\Psi_{\pm}^{BO}\rangle &= 0 \\ \stackrel{\text{Eqs. 2.85, 2.87}}{\Rightarrow} \left[\frac{1}{2} E_b (q^2 - 1) - E_b q - E_{\pm}^{BO}(q) \right] c_{1,\pm} - t c_{2,\pm} &= 0 \\ \Rightarrow \left[-E_b q \mp \sqrt{t^2 + (E_b q)^2} \right] c_{1,\pm} - t c_{2,\pm} &= 0 \end{aligned} \quad (2.90)$$

With the ansatz²⁷

$$\begin{aligned} c_{1,\pm}(q) &= \cos(\gamma_{\pm}(q)) \\ c_{2,\pm}(q) &= \sin(\gamma_{\pm}(q)) \end{aligned} \quad (2.91)$$

we fulfill the normalization automatically because $\cos^2(x) + \sin^2(x) = 1$. The problem is mapped on one unknown, namely $\gamma_{\pm}(q)$.

One could now evaluate γ_+ and γ_- independently. However, also the conditions that the two Born-Oppenheimer wave functions are orthonormal allows one to link $\gamma_+(q)$ and $\gamma_-(q)$

$$\begin{aligned} c_{1,+}^* c_{1,-} + c_{2,+}^* c_{2,-} &= 0 \\ \Rightarrow \cos(\gamma_+(q)) \cos(\gamma_-(q)) + \sin(\gamma_+(q)) \sin(\gamma_-(q)) &= 0 \\ \Rightarrow \cot(\gamma_+(q)) &= -\tan(\gamma_-(q)) \\ \cot(x) = -\tan(x + \pi(j+1/2)) \Rightarrow \gamma_-(q) &= \gamma_+(q) + \pi(j + \frac{1}{2}) \end{aligned} \quad (2.92)$$

²⁶“Secular equation” is another word for the characteristic equation, respectively the eigenvalue equation $\det[\mathbf{H} - \epsilon \mathbf{1}] = 0$

²⁷The coefficients can be chosen real-valued, because the Hamiltonian is real-valued. Therefore, the complex conjugate of any eigenvector is itself an eigenvector with the same energy. Any superposition of these two eigenvectors is again an eigenvector with the same energy. Hence also real and imaginary part of the original eigenvector. These two are real.

The integer j is an arbitrary integer. We can set it to zero, because the other solutions lead to equivalent wave functions Eq. 2.91, except for insignificant sign changes of the wave function.

Now, we are left with evaluating either $\gamma_+(q)$ or $\gamma_-(q)$. For this purpose, I insert the ansatz Eq. 2.91 into the equation Eq. 2.90 for the eigenvectors.

$$\begin{aligned}
& 0 \stackrel{\text{Eqs. 2.90,2.91}}{=} \left[-E_b q \mp \sqrt{t^2 + (E_b q)^2} \right] \cos(\gamma_{\pm}(q)) - t \sin(\gamma_{\pm}(q)) \\
\Rightarrow \gamma_{\pm}(q) &= \arctan \left[\frac{-E_b q \mp |t| \sqrt{1 + (E_b q/t)^2}}{t} \right] \\
&= -\arctan \left[\underbrace{\frac{E_b q}{t} \pm \frac{|t|}{t} \sqrt{1 + \left(\frac{E_b q}{t}\right)^2}}_{=x \pm \text{sgn}(t) \sqrt{1+x^2} \quad \text{see below}} \right] \\
&= -\frac{1}{2} \left[\arctan \left(\frac{E_b q}{t} \right) \pm \frac{\pi}{2} \text{sgn}(t) \right] \tag{2.93}
\end{aligned}$$

In the last line, I used the **tangent half-angle formula**²⁸ Let me demonstrate the relevant steps:

$$\begin{aligned}
x \pm \sqrt{1+x^2} &\stackrel{x=\tan(y)}{=} \frac{\sin(y)}{\cos(y)} \pm \sqrt{1 + \frac{\sin^2(y)}{\cos^2(y)}} \stackrel{\sin^2 + \cos^2 = 1}{=} \frac{\sin(y)}{\cos(y)} \pm \sqrt{\frac{1}{\cos^2(y)}} \\
&= \frac{\sin(y)}{\cos(y)} \pm \frac{1}{|\cos(y)|} = \frac{\sin(y) \pm \text{sgn}(\cos(y))}{\cos(y)} \\
&\stackrel{\text{Eq. 2.95}}{=} \tan \left(\frac{1}{2} (y \pm \frac{\pi}{2} \text{sgn}(\cos(y))) \right) \\
&\stackrel{\text{Eq. 2.95}}{=} \tan \left(\frac{1}{2} (\arctan(x) \pm \frac{\pi}{2} \text{sgn}(\cos(\tan(x)))) \right) \\
\Rightarrow \arctan(x \pm \sqrt{1+x^2}) &= \frac{1}{2} \left[\arctan(x) \pm \frac{\pi}{2} \underbrace{\text{sgn}(\cos(\tan(x)))}_{=+1 \text{ for } y \in -\frac{\pi}{2}, \frac{\pi}{2}} \right] \tag{2.96}
\end{aligned}$$

When we restrict y to the interval $y \in]-\frac{\pi}{2}, \frac{\pi}{2}]$, we can use $\text{sgn}(\cos(y)) = 1$. This should suffice to get to the last line of Eq. 2.93.

To obtain an graph of the coefficients as function of generalized nuclear coordinate q , we use $\tan(0) = 0$, $\tan(\frac{\pi}{4}) = 1$, $\tan(\frac{\pi}{2}) = \infty$.

$\frac{ E_b }{t} q$	$-\infty$	-1	0	1	∞
$\gamma_+(q)$	0	$-\frac{1}{8}\pi$	$-\frac{1}{4}\pi$	$-\frac{3}{8}\pi$	$-\frac{1}{2}\pi$
$\gamma_-(q)$	$+\frac{1}{2}\pi$	$+\frac{3}{8}\pi$	$+\frac{1}{4}\pi$	$+\frac{1}{8}\pi$	0

- The wave function $|\Psi_+^{BO}\rangle$ at the excited state Born-Oppenheimer surface have coefficients with opposite signs indicative of an antibond.
- The wave function $|\Psi_-^{BO}\rangle$ at the groundstate Born-Oppenheimer surface have coefficients with the same signs indicative of an bonding orbital

²⁸I forgot how I arrived at it, but then I found it in Wikipedia https://en.wikipedia.org/wiki/Tangent_half-angle_formula. The tangent half-angle formula is

$$\tan \left(\frac{1}{2} (\alpha + \beta) \right) = \frac{\sin(\alpha) + \sin(\beta)}{\cos(\alpha) + \cos(\beta)}. \tag{2.94}$$

With the choice $\beta = \pm \frac{\pi}{2}$ this results in

$$\tan \left(\frac{1}{2} (\alpha \pm \frac{\pi}{2}) \right) = \frac{\sin(\alpha) \pm 1}{\cos(\alpha)}. \tag{2.95}$$

- for the symmetric case, i.e. $q = 0$ the absolute values of the coefficients are the same, which tells us that the electron is delocalized over both Holstein monomers, both in the ground and the excited state.

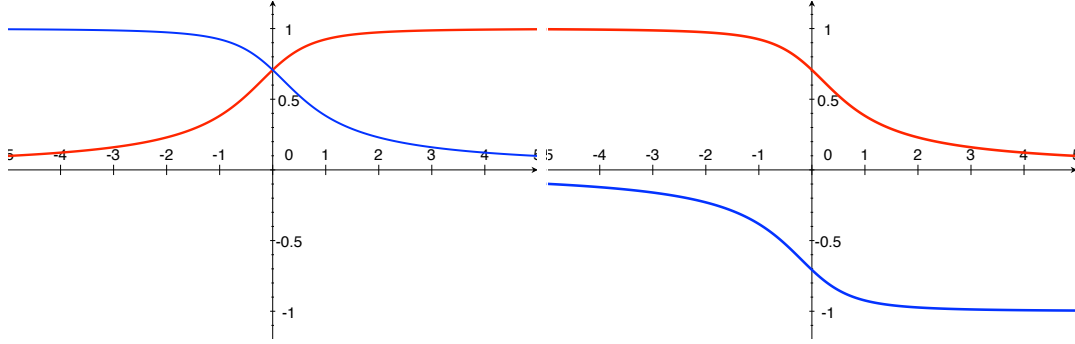


Fig. 2.7: Wave-function coefficients $c_{1/2,\pm}$ of the Holstein dimer as function of the nuclear coordinate q . Left: lower BO state (blue: $c_{1,-}$, red: $c_{2,-}$). Right: upper Born-Oppenheimer wave function (blue: $c_{1,+}$, red: $c_{2,+}$). The lower Born-Oppenheimer state has bonding character and therefore the two coefficients have the same sign, while for the antibonding, upper Born-Oppenheimer surface, they have opposite sign. For negative q , the lower Born-Oppenheimer state is mostly on the left side (blue line, in the left graph), while the upper Born-Oppenheimer state has its dominant weight on the right side of the dimer (red line, right graph). For positive q , this is the other way around.

6 Calculate the first-derivative coupling $\vec{A}_{m,n}(\vec{R})$.

The derivative couplings are defined

$$\vec{A}_{m,n}(\vec{R}) = \left\langle \Psi_m^{BO}(\vec{R}) \left| \frac{\hbar}{i} \vec{\nabla}_{\vec{R}} \right| \Psi_n^{BO}(\vec{R}) \right\rangle \quad (2.97)$$

For $m, n \in \{+, -\}$ we obtain

$$\begin{aligned} A_{m,n}(q) &= \left[\cos(\gamma_m(q)) \langle \chi_1 | + \sin(\gamma_m(q)) \langle \chi_2 | \right] \\ &\quad \times \frac{\hbar}{i} \partial_q \left[|\chi_1\rangle \cos(\gamma_n(q)) + |\chi_2\rangle \sin(\gamma_n(q)) \right] \\ &= \cos(\gamma_m(q)) \frac{\hbar}{i} \partial_q \cos(\gamma_n(q)) + \sin(\gamma_m(q)) \frac{\hbar}{i} \partial_q \sin(\gamma_n(q)) \\ &= \cos(\gamma_m(q)) \left[-\sin(\gamma_n(q)) \right] \frac{\hbar}{i} \partial_q \gamma_n(q) + \sin(\gamma_m(q)) \cos(\gamma_n(q)) \frac{\hbar}{i} \partial_q \gamma_n(q) \\ &= \frac{\hbar}{i} \partial_q \gamma_n(q) \underbrace{\left(-\cos(\gamma_m(q)) \sin(\gamma_n(q)) + \sin(\gamma_m(q)) \cos(\gamma_n(q)) \right)}_{=:\sin(\gamma_m(q) - \gamma_n(q)) =: Y_{m,n}} \end{aligned} \quad (2.98)$$

- $m = n$: The sum of cosines and sines cancels and the result vanishes. I.e. $A_{++}(q) = A_{--}(q) = 0$.
- $m \neq n$: We exploit Eq. 2.93, i.e. $\gamma_-(q) = \gamma_+(q) + \frac{\pi}{2}$, and $\sin(\pm\pi/2) = \pm 1$, so that

$$Y_{m,n} = \begin{cases} -1 & \text{for } (m, n) = (+, -) \\ +1 & \text{for } (m, n) = (-, +) \end{cases} \quad (2.99)$$

Thus, we obtain

$$A_{+,-} = -\frac{\hbar}{i}\partial_q\gamma_-(q) \quad \text{and} \quad A_{-,+} = +\frac{\hbar}{i}\underbrace{\partial_q\gamma_+(q)}_{=\partial_q\gamma_-(q)} \quad (2.100)$$

The derivatives of γ_+ and γ_- are identical because, as shown in Eq. 2.93, the functions γ_+ and γ_- differ only by a constant.

We can verify that the derivative couplings are hermitian, i.e. $A_{+,-} = A_{-,+}^*$.

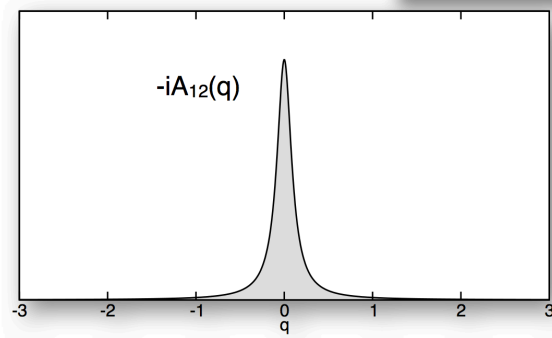


Fig. 2.8: Off-diagonal derivative coupling $-iA_{1,2}(q)$ as function of the antisymmetric vibration coordinate q of the Holstein dimer.

Let me introduce a new symbol, namely

$$a(q) \stackrel{\text{def}}{=} \partial_q\gamma_-(q) \quad (2.101)$$

so that

$$\mathbf{A}(q) = \begin{pmatrix} A_{++} & A_{+-} \\ A_{-+} & A_{--} \end{pmatrix} \stackrel{\text{Eqs. 2.100, 2.101}}{=} \frac{\hbar}{i} \begin{pmatrix} 0 & -a(q) \\ a(q) & 0 \end{pmatrix} \quad (2.102)$$

The vector index of the derivative couplings refers to the one-dimensional nuclear configuration space. Therefore, the derivative couplings of this problem have only one component.

7 (Optional) Write down the Hamiltonian for the nuclear coordinates.

In the lecture notes the nuclear Schrödinger equation has been given in the compact form Eq. 2.28 on p. 50, namely

$$i\hbar\partial_t\tilde{\Theta}(\vec{R}, t) = \left[\frac{(\mathbf{1}\hat{P} + \vec{A}(\vec{R}))^2}{2M} + E^{BO}(\vec{R}) \right] \tilde{\Theta}(\vec{R}, t) \quad (2.103)$$

This expression is compact but also ambiguous because one has to know the vector spaces in which the individual objects (matrices, vectors, operators) operate. The detailed form is Eq. 2.27 on p. 50, namely

$$i\hbar\partial_t\Theta_m(\vec{R}, t) = \sum_n \left[\frac{1}{2} \sum_k \left(\delta_{m,k} \frac{\hbar}{i} \vec{\nabla}_R + \vec{A}_{m,k}(\vec{R}) \right) \frac{1}{M_k} \left(\delta_{k,n} \frac{\hbar}{i} \vec{\nabla}_R + \vec{A}_{k,n}(\vec{R}) \right) + \delta_{m,n} E_m^{BO}(\vec{R}) \right] \Theta_n(\vec{R}, t) \quad (2.104)$$

In our example, the nuclear wave function has two components, one for the upper and one for the lower BO surface.

$$\vec{\Theta}(q, t) = \begin{pmatrix} \Theta_+(q) \\ \Theta_-(q) \end{pmatrix} \quad (2.105)$$

The nuclear coordinates are one-dimensional with $R_1 = q$.

The matrix $\mathbf{E}^{BO}(\vec{R})$ is a diagonal matrix holding the two Born-Oppenheimer surfaces.

$$\mathbf{E}^{BO}(q) = \begin{pmatrix} E_+^{BO}(q) & 0 \\ 0 & E_-^{BO}(q) \end{pmatrix} \quad (2.106)$$

The derivative couplings are given in Eq. 2.102.

The momenta are combined in the matrix

$$\mathbf{1}\hat{P} = \frac{\hbar}{i} \begin{pmatrix} \partial_q & 0 \\ 0 & \partial_q \end{pmatrix} \quad (2.107)$$

so that

$$\mathbf{1}\vec{P} + \vec{\mathbf{A}}^{BO}(q) = \frac{\hbar}{i} \begin{pmatrix} \partial_q & -a(q) \\ a(q) & \partial_q \end{pmatrix} \quad (2.108)$$

and

$$\begin{aligned} \frac{1}{2m_q} \left[\mathbf{1}\vec{P} + \vec{\mathbf{A}}^{BO}(q) \right]^2 &= \frac{-\hbar^2}{2m_q} \begin{pmatrix} \partial_q & -a(q) \\ a(q) & \partial_q \end{pmatrix}^2 \\ &= \frac{-\hbar^2}{2m_q} \begin{pmatrix} \partial_q^2 - (a(q))^2 & -\partial_q a(q) - a(q)\partial_q \\ \partial_q a(q) + a(q)\partial_q & \partial_q^2 - (a(q))^2 \end{pmatrix} \end{aligned} \quad (2.109)$$

Thus, the desired nuclear Schrödinger equation is

$$\begin{aligned} i\hbar\partial_t\Theta_+(q, t) &= \left[\frac{-\hbar^2}{2m_q}\partial_q^2 + \frac{(\hbar a(q))^2}{2m_q} + E_+^{BO}(q) \right] \Theta_+(q, t) \\ &\quad + \frac{\hbar^2}{2m_q} \left[a(q) + 2a(q)\partial_q \right] \Theta_-(q, t) \\ i\hbar\partial_t\Theta_-(q, t) &= \left[\frac{-\hbar^2}{2m_q}\partial_q^2 + \frac{(\hbar a(q))^2}{2m_q} + E_-^{BO}(q) \right] \Theta_-(q, t) \\ &\quad - \frac{\hbar^2}{2m_q} \left[a(q) + 2a(q)\partial_q \right] \Theta_+(q, t) \end{aligned} \quad (2.110)$$

2.7.3 Molecular dynamics

Introduction

The classical approximations for the nuclei in combination with the Born-Oppenheimer approximation is the basis for **molecular-dynamics (MD) simulations**. In this exercise, we will study the basics of this approach for a simple model system, namely the Holstein dimer.

The goal of this exercise is to make you familiar with the basic concepts behind molecular-dynamics simulations. For this purpose, you will become familiar with a simple code and you will perform some small calculations and investigate the results.

The notions developed here can be tried out using a more realistic description of the Born-Oppenheimer surface using available codes such as Avogadro. (See <http://avogadro.cc/docs/>)

Verlet algorithm: Newton's equations can be discretized using Verlet's algorithm. Verlet's algorithm is the most simple and robust technique for discretizing Newton's equations of motion. It has one important property, namely that is time-inversion symmetric. As a consequence, it does not introduce an artificial drift of the total energy. This feature is important for simulations of thermodynamic quantities. Despite its simplicity, the Verlet algorithm is today the method of choice.

For an equation of motion of the nuclei in a potential $E_{pot}(\vec{R})$ with a friction coefficient αM_i on the i -th coordinate,

$$M_i \ddot{R}_i = - \left. \frac{dE_{pot}(\vec{R})}{dR_i} \right|_{\vec{R}(t)} - \alpha M_i \dot{R}_i(t) = F_i(\vec{R}(t)) - \alpha M_i \dot{R}_i(t), \quad (2.111)$$

we replace the time derivatives by the discrete differential quotient for a given time step Δ .

$$\begin{aligned} \dot{R}_i &= \frac{R_i(t + \Delta) - R_i(t - \Delta)}{2\Delta} + O(\Delta^2) \\ \ddot{R}_i &= \frac{R_i(t + \Delta) - 2R_i(t) + R_i(t - \Delta)}{\Delta^2} + O(\Delta^2) \end{aligned} \quad (2.112)$$

After inserting the differential quotients into the equation of motion Eq. 2.111, we resolve for $R(t + \Delta)$ and use the definition $a = \frac{\alpha\Delta}{2}$

$$R_i(t + \Delta) = R_i(t) \frac{2}{1+a} - R_i(t - \Delta) \frac{1-a}{1+a} + F_i(\vec{R}(t)) \frac{\Delta^2}{M_i(1+a)} \quad (2.113)$$

Do not use the one-sided differential quotient for the first derivative!

Now, we introduce a time grid $t_j = \Delta \cdot j$. With the knowledge of the positions at t_j and t_{j-1} , one can evaluate the force at t_j and thus predict the position at t_{j+1} . This is repeated in order to iteratively construct the trajectory of the atoms.

The friction coefficient is used in practice to find the ground state. The special form of the friction coefficient as αM_i has been introduced for convenience. In practice, we choose one common parameter α for all coordinates.

Stability and convergence The convergence and stability of the Verlet algorithm can be estimated from a model of a harmonic oscillator, for which the correct and the discretized trajectories can be determined analytically. From this analysis the following rules have been extracted:

The Verlet algorithm becomes unstable, if the time step is chosen too large. In order to stay sufficiently far away from the stability limit and to keep the numerical error on the frequencies below 1 %, the time step Δ should be smaller than one-tenths of the period of the fastest vibration (having circular frequency ω_X) of the system. This implies $\Delta < \frac{2\pi}{10\omega_{max}}$.

A common mistake while searching for the minimum of the potential-energy surface is to use a friction that is too large. For a friction that brings the vibrations into the overdamped regime, the convergence rate becomes extremely slow. The system can hardly move, that is, it is almost frozen in. This is often mistaken for convergence. Rather, the optimum convergence is right at the boundary between damped and overdamped vibration, which is at $a = \alpha\Delta/2 = \omega\Delta$. For a system with several vibrations, the friction parameter should be chosen according to the smallest vibrational frequency in the system.

Potential energy of the Holstein model The potential energy of the simulation is the lower Born-Oppenheimer surface of the Holstein dimer. The ground-state Born-Oppenheimer surface of the Holstein dimer has the form

$$\begin{aligned} E_{pot}(\vec{R}) &= E_{-}^{BO}(s(\vec{R}), q(\vec{R})) \\ E_{-}^{BO}(s, q) &= \frac{1}{2} E_b (q^2 + s^2 - 1) - \sqrt{t^2 + (E_b q)^2} \end{aligned} \quad (2.114)$$

with $E_b = \gamma^2/(2C)$ and

$$\begin{aligned} s(\vec{R}) &= \frac{C}{\gamma} (R_1 + R_2) - 1 \\ q(\vec{R}) &= \frac{C}{\gamma} (R_1 - R_2) \end{aligned} \quad (2.115)$$

The energy and the corresponding derivatives are evaluated in the code below in the subroutine `energyandforce`.

The Lagrangian of the system is

$$\mathcal{L}(\vec{R}, \vec{V}) = \frac{1}{2M} \vec{V}^2 - E_{pot}(\vec{R}) \quad (2.116)$$

The equations of motion are the Euler-Lagrange equations

$$\frac{d}{dt} \frac{\partial \mathcal{L}}{\partial V_j} = \frac{\partial \mathcal{L}}{\partial R_j} \quad \text{with} \quad \dot{\vec{R}} = \vec{V} \quad (2.117)$$

The minima of the potential energy lie approximately²⁹ at $\vec{R} = (1., 0.)$ and $\vec{R} = (0., 1.)$.

Recipe to run the code

The commands below refer to a UNIX operating system and in particular the bash shell.

Compile the code: If the file `md.f90` has been uploaded, use it. Otherwise cut and paste the code below, in section 2.7.3 into a file `md.f90`. (Cutting from a pdf file may produce errors.) Then compile the code with

```
gfortran -o md.x md.f90
```

`gfortran` is an open source FORTRAN compiler. It needs to be installed on your system. `gfortran` takes the FORTRAN code `md.f90` and produces a executable code `md.x`.

Prepare input file: Create an input file `state.in`

```
1.d0 1.d-1 0. 1000
1.d0 2.d0 1.d0 2.d0 0
'tra.out' 'state.out'
```

The data are

- first line:
 - mass,
 - time step Δ ,
 - friction parameter $a = \alpha\Delta/2$,
 - number of iterations
- second line:
 - initial coordinates $\vec{R}(t=0)$ (two values),
 - coordinates in the previous time step $R(t=-\Delta) \approx -\Delta \dot{\vec{R}}$ (two values)

²⁹for small hopping

- The last value is the iteration number of the first time step of this simulation.

- third line:
 - name of the file holding the trajectory $(t_j, \vec{R}(t_j))$ for $t_j = j\Delta$;
 - new input file for the simulation. Holds the last coordinates $\vec{R}(t_n), \vec{R}(t_{n-1})$ and can be used as input file to continue the calculation.

Perform the simulation: Execute the `md.x` with

```
md.x < state.in > e.dat
```

We supply the input data with `< state.in`, which feeds the contents of the file `state.in` to the standard input channel. The standard input is what, normally, is typed to the terminal. The output from the standard output channel, whatever is otherwise written to the terminal, is directed into the file `e.dat`.

The simulation can be continued with

```
md.x < state.out >>e.dat
```

which reads in the final coordinates from the file `state.out` of previous run. Before continuing a simulation, the input file may be adjusted. The `>>` symbol ensures that existing data in `e.dat` are not deleted, but the new data is appended. The data of `tra.out` is always appended. If you remove the old data you need to delete it before the simulation.

Inspect the results: The data can be inspected using for example with the open source program `xmgrace` <http://plasma-gate.weizmann.ac.il/Grace/>.

```
xmgrace -free -noask -nxy e.dat
```

`xmgrace` has been written to efficiently make xy-plots in publication-ready form. It also allows simple analysis of data, such as fits Fourier transforms, simple computation etc.

The file `e.dat` has a four-column format, where in each line the first column is the time of the corresponding time step, the second line is the kinetic energy, the third is the potential energy and the fourth line is the total energy.

Inspect the coordinates as function of time with

```
xmgrace -free -noask -nxy tra.out
```

The file `tra.out` has a three-column format where in each line, the first column is the time of the corresponding time step, which is followed by the two coordinates \vec{R} in this iteration.

Problem

- 1 In the code in section 2.7.3 below, identify the formulas that are calculated and write them down. Draw a flow diagram of the code. (Do not be surprised, if some of the equations have been given in the background material above.)
- 2 make yourself familiar with the potential-energy surface. Describe the main qualitative features. (symmetries, position of minima, saddle points, etc.)
- 3 Follow the recipe given above to compile the code, execute it and inspect the output. Verify that the total energy is conserved and how well. Measure a typical period of the atomic simulation from the trajectories and convert it into angular frequency.
- 4 Set the initial coordinates so that once, only the free phonon coordinate s is excited, and once, only the coordinate q . In the second case, set the initial coordinates on the barrier and give it a tiny velocity towards one of the two minima by displacing $\vec{R}(-\Delta)$ in the input file by about 10^{-6} in the q coordinate. Describe the trajectory and the energies as function of time.
- 5 Determine the stability limit by increasing the time step Δ . What is the maximum time step that can be used? Compare with the result given above.
- 6 Find the friction parameter that allows you to reach the minimum with the least number of time steps.
- 7 Play around: Explore the behavior of the trajectories by modifying the input parameters. Try to make a few observations, which you can describe to others. (It is up to you, whether you write them down.) The goal is to practice the typical process of a simulation: (1) Guess how the system will behave. (2) Inspect the outcome of a simulation and note its behavior without bias. (3) Analyze any unexpected behavior. (4) Make additional simulations to understand the unexpected behavior. (5) Select interesting findings. (6) Explore the dependence of the conclusions on the approximations in the simulation.

Example code in FORTRAN

The code md.f90 follows:

```

Program main
implicit none
integer(4),parameter :: n=2      ! dimension of nuclear coordinates
real(8)                :: mass    ! mass
real(8)                :: delta   ! time step
real(8)                :: afric   ! friction parameter a=alpha*delta/2
real(8)                :: rp(n),r0(n),rm(n) ! positions
real(8)                :: force(n)
real(8)                :: etot,epot,ekin
real(8)                :: time
integer(4)             :: niter    ! number of iterations
integer(4)             :: iter0
integer(4)             :: nfilt=10 ! fortran unit for trajectory file
integer(4)             :: nfils=11 ! fortran unir for state file
character(64)         :: trajectoryfile
character(64)         :: statefile
real(8)               :: svar1,svar2,svar3
integer(4)            :: iter,i

```

```

! *****
!
! =====
! == variables set here are overwritten by the content of the state file==
! =====
mass=1.d0
delta=1.d-1
afric=0.d-1
niter=1000
r0(:)=(/1.d0,2.d0/)
rm(:)=r0(:)
trajectoryfile='tra.out'
statefile='state.out'
iter0=0
!
! =====
! == read state file ==
! =====
read(*,*)mass,delta,afric,niter
read(*,*)r0,rm,iter0
read(*,*)trajectoryfile,statefile
!
! =====
! == start molecular dynamics loop ==
! =====
! == connect trajectoryfile to fortran unit nfile
OPEN(NFILE,FILE=TRAJECTORYFILE,ACTION='WRITE',ACCESS='APPEND')
do iter=1,niter
  time=delta*real(iter0+iter,kind=8)
!
! == calculate potential energy and forces =====
call energyandforce(n,r0,epot,force)
!
! == propagate: determine position of next time step =====
svar1=2.d0/(1.d0+afric)
svar2=-(1.d0-afric)/(1.d0+afric)
svar3=delta**2/(mass*(1.d0+afric))
do i=1,n
  rp(i)=r0(i)*svar1+rm(i)*svar2+force(i)*svar3
enddo
!
! == kinetic energy =====
ekin=0.d0
do i=1,n
  ekin=ekin+0.5d0*mass*( (rp(i)-rm(i))/(2.d0*delta) )**2
enddo
!
! == print information =====
write(*,fmt='(4f10.5)')time,ekin,epot,ekin+epot
write(nfile,*)time,r0
!
! == switch =====
do i=1,n
  rm(i)=r0(i)

```

```

        r0(i)=rp(i)
    enddo
enddo
close(nfilt) ! disconnect trajectory file
!
! =====
! == write state file ==
! =====
open(nfils,file=statefile)
write(nfils,*)mass,delta,afric,niter
write(nfils,*)r0,rm,iter0+niter
write(nfils,*)"'"//trim(trajectoryfile)//"' ' '//trim(statefile)//'"'"
close(nfils)
stop
end
!
! .....
subroutine energyandforce(n,r,epot,force)
! *****
! ** calculates potential energy and forces for positions r **
! *****
implicit none
real(8) ,parameter :: c=1.d0 ! force constant
real(8) ,parameter :: gamma=1.d0 ! electron-phonon coupling
real(8) ,parameter :: t=0.1d0 ! hopping parameter
real(8) ,parameter :: eb=gamma**2/(2*c) ! polaron binding energy
integer(4),intent(in) :: n ! number of atomic positions
real(8) ,intent(in) :: r(n) ! atomic coordinates
real(8) ,intent(out):: epot ! potential energy
real(8) ,intent(out):: force(n) ! forces
real(8) :: s,q ! symmetry-adapted coordinates
real(8) :: deds,dedq ! derivative of Epot wrt s,q
real(8) :: dsdr1,dsdr2,dqdr1,dqdr2
! *****
! == transform r to symmetry adapted coordinates (s,q) =====
s=c/gamma*(r(1)+r(2))-1.d0
q=c/gamma*(r(1)-r(2))
! == evaluate potential energy =====
epot=0.5d0*Eb*(q**2-1.d0)-sqrt((Eb*q)**2+t**2) + 0.5d0*eb*s**2
! == derivatives wrt (s,q) =====
deds=eb*s
dedq=eb*q-0.5d0/sqrt( (Eb*q)**2+t**2 )*2.d0*eb**2*q
! == forces F=-depot/dr =====
dsdr1=c/gamma
dsdr2=c/gamma
dqdr1=c/gamma
dqdr2=-c/gamma
force(1)=-dedq*dqdr1-deds*dsdr1
force(2)=-dedq*dqdr2-deds*dsdr2
return
end

```

Solution

The input data below leave the free oscillator in the ground state, while the bistable potential is explored such that the barrier is just overcome. (in1.dat)

```
1.d0 1.d-1 0. 1000
-0.394096d0 1.394096d0 -0.394096d0 1.394096d0 0
'tra_1.out' 'state.out'
```

Optimization: For a time step of $\Delta = 0.1$, good convergence is obtained with a friction parameter $a = 0.1$

```
1. 0.1 0.1 1000
-0.394096d0 0.605904 -0.394096d0 0.605904 0
'tra_2.out' 'state.out'
```

Plotting $\ln(E(t) - E(\infty))$ shows that the convergence is exponential. The coordinates of the minimum is (0.041742430502215801, 0.95825756949759489).

The input data file below excites only the symmetric vibration s . The vibration passes through the minimum $\vec{R} = (1, 0)$ and has the same amplitude as the previous example.

```
1.0 0.1 0. 1000
0.141742430502215801 1.05825756949759489 0.141742430502215801 1.05825756949759489 0
'tra_3.out' 'state.out'
```

We find a period of $T = 8.95$.

Stability limit: for the free oscillation, the stability limit is reached at $\Delta = 2.8285$, i.e. $\omega\Delta = 2$. This is verified by decreasing and increasing the time step.

```
1.d0 2.83 0. 20
0.141742430502215801 1.05825756949759489 0.141742430502215801 1.05825756949759489 0
'tra_4.out' 'state.out'
```

With a time step of $\Delta = 2.82$ the trajectory alternates approximately between two values.

```
1.d0 2.82 0. 20
0.141742430502215801 1.05825756949759489 0.141742430502215801 1.05825756949759489 0
'tra_5.out' 'state.out'
```

The kinetic energy is nearly zero, which is because the coordinates essentially jump back and forth between two values, so that $\vec{R}(t + 2\Delta) \approx \vec{R}(t)$. In the discretized expression for the velocity this yields almost zero.

The following input file places the initial coordinate at the top of the barrier and give the system a tiny velocity towards one of the stable states.

```
1.d0 0.1d0 0. 10000
0.5 0.5 0.5000001 0.49999999 0
'tra_6.out' 'state.out'
```

The system makes a one-dimensional motion along the q -coordinate and repeatedly overcomes the barrier. Because of the small kinetic energy, it spends most of its time on-top of the barrier. Such back-crossings are rare in more complicated systems, because the energy from the barrier crossing is quickly distributed over many other modes, so that there is too little energy left in the same mode to overcome the barrier immediately.

Chapter 3

Many-particle wave functions

In the previous section we have shown how we can split the description into two parts, one for the electrons and another one for the nuclei. The dynamics of the nuclei requires the knowledge of the electronic problem, namely the Born-Oppenheimer surfaces $E_n^{BO}(\vec{R})$ and the derivative couplings $\vec{A}_{m,n}(\vec{R})$ obtained from the Born-Oppenheimer wave functions $|\Psi_n^{BO}(\vec{R})\rangle$. The Born-Oppenheimer wave functions are states in the electronic Hilbert space and the atomic positions \vec{R} , as arguments of the Born-Oppenheimer wave functions, are parameters as opposed to quantum variables.

The next difficulty is to obtain the Born-Oppenheimer surfaces and wave functions. For non-interacting electrons, this is of the same complexity as a one-particle problem, while the interaction makes this problem usually intractable without further approximations. Therefore, we will start with non-interacting electrons before we turn to the more complicated interacting systems.

In the present section, I will describe the basics of many-particle wave functions in order to prepare the context for the following sections. I will start out with one-particle wave functions with position and spin degrees of freedom. Then, I will describe the underlying symmetry of identical particles, which results in the concept of **Fermions** and **Bosons**. Finally, I will return to one-particle wave functions, by showing how the wave function of a noninteracting system of fermions and bosons can be expressed in terms of one-particle wave functions.

This will form the basis of the following sections that address non-interacting electrons.

3.1 Spin orbitals

Before I continue with many-particle wave functions, let me discuss one-particle orbitals. I will introduce a notation for treating the electron spin which, on the one hand, simplifies the expressions, and on the other hand, it is more rigorous.

When I first learned about spins and magnetic moments, I was puzzled by the special role, which was attributed to the z-coordinate. I learned that an electron can have a spin pointing parallel or antiparallel to the z-axis. The direction of the z-axis, however, is arbitrary. It seemed as if the physics changed, when I turned my head.

Indeed, there is nothing special about the z-coordinate. Here, I present a more general formulation, which describes electrons by two-component spinor wave functions. With this formulation, one can form wave functions with a spin pointing in an arbitrary direction in each point in space. This description restores the rotational symmetry that appears to be broken in the simple-minded formulation used commonly.

We use here **two-component spinor wave functions**, which are also called **spin orbitals**

$$\phi(\vec{x}) = \phi(\vec{r}, \sigma) = \langle \vec{r}, \sigma | \phi \rangle \quad (3.1)$$

Spin-orbitals actually consists of two complex-valued wave functions, one for the spin-down $\phi(\vec{r}, \downarrow)$

and one for the spin up contribution $\phi(\vec{r}, \uparrow)$. One can write the spin orbitals also as two-component spinor

$$\begin{pmatrix} \phi(\vec{r}, \uparrow) \\ \phi(\vec{r}, \downarrow) \end{pmatrix} \stackrel{\text{def}}{=} \begin{pmatrix} \langle \vec{r}, \uparrow | \phi \rangle \\ \langle \vec{r}, \downarrow | \phi \rangle \end{pmatrix} \quad (3.2)$$

PHYSICAL MEANING OF A SPIN WAVEFUNCTION

The square of a component of a spin wavefunction is the probability density $P_\sigma(\vec{r})$ for finding a particle with the specified spin orientation at a specific position \vec{r} .

This rule is completely analogous to the rule that the absolute square of a scalar wave function is the probability density $P(\vec{r}) = \psi^*(\vec{r})\psi(\vec{r})$ of finding a particle at a given position \vec{r} .

Dirac equation and Pauli equation

The two-component spinor description follows from the **Pauli equation**¹. The Pauli equation is the non-relativistic limit of the **Dirac equation**, the relativistic one-particle equation for electrons. In the Dirac equation, each particle has four components. Two components describe spin-up and spin-down electrons, and the two other components describe spin-up and spin-down positrons. The **positron**[26] is the anti-particle of the electron. In the non-relativistic limit, the electronic and positronic components become independent of each other, so that the electrons can be described by a two-component spinor wave function.

For further background on the Dirac equation, relativistic effects and the Pauli equation see section 14 of $\Phi\text{SX:Quantum Physics}$ [4]

Spin expectation values and spin eigenstates

Note, however, that the wave function contains much more information than that just mentioned. Below, we will see that the spin wave function does not only provide the information on the probabilities for the spin projection on the z-axis but also for any other axis. This notation is a little puzzling at first, because one usually works with spin-eigenfunctions, for which one of the components vanishes.

The **spin** is defined as

$$\hat{S} = \frac{\hbar}{2} \hat{\sigma} \quad (3.3)$$

where the three components of the vector $\hat{\sigma}$ are

$$\hat{\sigma}_i = \int d^3r \sum_{\sigma, \sigma'=1}^2 |\vec{r}, \sigma\rangle \sigma_{i, \sigma, \sigma'} \langle \vec{r}, \sigma' |$$

Somewhat confusing are the different indices for the different vector spaces: The index i can have the values x, y, z and refers to the components of the vector $\vec{\sigma}$. Each component of the vector $\hat{\sigma}$ is a scalar operator, which acts on a two-dimensional Hilbert space. The indices σ, σ' of $\sigma_{i, \sigma, \sigma'}$ can assume the values \uparrow or \downarrow , which are the coordinates of the two-dimensional spinor space. That is, σ_i is a (2×2) matrix for each value of i . These (2×2) matrices are the **Pauli matrices**²

$$\sigma_x = \begin{pmatrix} 0 & 1 \\ 1 & 0 \end{pmatrix}, \quad \sigma_y = \begin{pmatrix} 0 & -i \\ i & 0 \end{pmatrix}, \quad \sigma_z = \begin{pmatrix} 1 & 0 \\ 0 & -1 \end{pmatrix} \quad (3.4)$$

¹See section 14 and in particular 14.9 of $\Phi\text{SX:Quantum Theory}$ [4]

²The matrices are made of the matrix elements $\sigma_{i, \sigma, \sigma'} = \langle \sigma | \hat{\sigma}_i | \sigma' \rangle$ of the operator $\hat{\sigma}_i$ with $\sigma \in \{\uparrow, \downarrow\}$, $\sigma' \in \{\uparrow, \downarrow\}$ and $i \in \{x, y, z\}$.

As a worked example, let us determine the expectation value of the operator \hat{S}_x for a one-particle state $|\phi\rangle$. The states $|\vec{r}, \uparrow\rangle$ and $|\vec{r}, \downarrow\rangle$ are still eigenstates of \hat{S}_z .

$$\begin{aligned} \langle\phi|\hat{S}_x|\phi\rangle &= \langle\phi|\left[\frac{\hbar}{2}\int d^3r\sum_{\sigma,\sigma'=1}^2|\vec{r},\sigma\rangle\sigma_{x,\sigma,\sigma'}\langle\vec{r},\sigma'|\right]|\phi\rangle \\ &= \frac{\hbar}{2}\int d^3r\left[\sum_{\sigma,\sigma'=1}^2\langle\phi|\vec{r},\sigma\rangle\sigma_{x,\sigma,\sigma'}\langle\vec{r},\sigma'|\phi\rangle\right] \\ &= \frac{\hbar}{2}\int d^3r\left[\begin{pmatrix}\langle\phi|\vec{r},\uparrow\rangle \\ \langle\phi|\vec{r},\downarrow\rangle \end{pmatrix}\begin{pmatrix}0 & 1 \\ 1 & 0 \end{pmatrix}\begin{pmatrix}\langle\vec{r},\uparrow|\phi\rangle \\ \langle\vec{r},\downarrow|\phi\rangle \end{pmatrix}\right] \\ &= \frac{\hbar}{2}\int d^3r[\langle\phi|\vec{r},\uparrow\rangle\langle\vec{r},\downarrow|\phi\rangle + \langle\phi|\vec{r},\downarrow\rangle\langle\vec{r},\uparrow|\phi\rangle] \\ &= \frac{\hbar}{2}\int d^3r[\phi^*(\vec{r},\uparrow)\phi(\vec{r},\downarrow) + \phi^*(\vec{r},\downarrow)\phi(\vec{r},\uparrow)] \end{aligned}$$

We obtain the spin density, that is the probability that we find a particle at position \vec{r} multiplied with the average spin expectation value in x-direction of that particle.

For a spin orbital that is an eigenstate of S_z , one of the spinor components vanishes.

$$\hat{S}_z|\phi_\uparrow\rangle = |\phi_\uparrow\rangle\left(+\frac{\hbar}{2}\right) \Rightarrow \begin{pmatrix}\langle\vec{r},\uparrow|\phi_\uparrow\rangle \\ \langle\vec{r},\downarrow|\phi_\uparrow\rangle \end{pmatrix} = \begin{pmatrix}\phi_\uparrow(\vec{r},\uparrow) \\ 0 \end{pmatrix} = \begin{pmatrix}1 \\ 0 \end{pmatrix} f_\uparrow(\vec{r}) \quad (3.5)$$

$$\hat{S}_z|\phi_\downarrow\rangle = |\phi_\downarrow\rangle\left(-\frac{\hbar}{2}\right) \Rightarrow \begin{pmatrix}\langle\vec{r},\uparrow|\phi_\downarrow\rangle \\ \langle\vec{r},\downarrow|\phi_\downarrow\rangle \end{pmatrix} = \begin{pmatrix}0 \\ \phi_\downarrow(\vec{r},\downarrow) \end{pmatrix} = \begin{pmatrix}0 \\ 1 \end{pmatrix} f_\downarrow(\vec{r}) \quad (3.6)$$

$$\hat{S}_x|\phi_\rightarrow\rangle = |\phi_\rightarrow\rangle\left(+\frac{\hbar}{2}\right) \Rightarrow \begin{pmatrix}\langle\vec{r},\uparrow|\phi_\rightarrow\rangle \\ \langle\vec{r},\downarrow|\phi_\rightarrow\rangle \end{pmatrix} = \frac{1}{\sqrt{2}}\begin{pmatrix}1 \\ 1 \end{pmatrix} f_\rightarrow(\vec{r}) \quad (3.7)$$

$$\hat{S}_x|\phi_\leftarrow\rangle = |\phi_\leftarrow\rangle\left(-\frac{\hbar}{2}\right) \Rightarrow \begin{pmatrix}\langle\vec{r},\uparrow|\phi_\leftarrow\rangle \\ \langle\vec{r},\downarrow|\phi_\leftarrow\rangle \end{pmatrix} = \frac{1}{\sqrt{2}}\begin{pmatrix}1 \\ -1 \end{pmatrix} f_\leftarrow(\vec{r}) \quad (3.8)$$

$$\hat{S}_y|\phi_\circ\rangle = |\phi_\circ\rangle\left(+\frac{\hbar}{2}\right) \Rightarrow \begin{pmatrix}\langle\vec{r},\uparrow|\phi_\circ\rangle \\ \langle\vec{r},\downarrow|\phi_\circ\rangle \end{pmatrix} = \frac{1}{\sqrt{2}}\begin{pmatrix}1 \\ i \end{pmatrix} f_\circ(\vec{r}) \quad (3.9)$$

$$\hat{S}_y|\phi_\bullet\rangle = |\phi_\bullet\rangle\left(-\frac{\hbar}{2}\right) \Rightarrow \begin{pmatrix}\langle\vec{r},\uparrow|\phi_\bullet\rangle \\ \langle\vec{r},\downarrow|\phi_\bullet\rangle \end{pmatrix} = \frac{1}{\sqrt{2}}\begin{pmatrix}1 \\ -i \end{pmatrix} f_\bullet(\vec{r}) \quad (3.10)$$

The spatial wave functions $\phi_\uparrow(\vec{r}, \uparrow)$, $\phi_\downarrow(\vec{r}, \downarrow)$, $f_\rightarrow(\vec{r})$, $f_\leftarrow(\vec{r})$, $f_\circ(\vec{r})$, and $f_\bullet(\vec{r})$ are square normalized. The indices $\uparrow, \downarrow, \leftarrow, \rightarrow, \circ$, and \bullet are the quantum numbers, while the spin indices \uparrow, \downarrow are treated as argument together with the spatial argument. In this way, the spinor indices are clearly distinguished from the quantum numbers. The quantum number indicates that the orbital is an eigenstate to some symmetry operator.

The spin-orbitals have the advantage that they allow to describe orbitals, for which the spin does not point along the z-axis, but it can also point, for example, to the right or in any other direction. For a spin orbital, the spin direction can actually vary in space. Such an orbital is called **non-collinear**, because the spins are not aligned.

Spin indices and spin quantum numbers

In the literature, one usually uses another notation, namely

$$\phi_\sigma(\vec{r}) \stackrel{\text{def}}{=} \phi(\vec{r}, \sigma)$$

Here, it is difficult to distinguish the **role of σ as a coordinate and its role as quantum number**. One usually uses one-particle orbitals with only one spin component, for which σ is a quantum number. In our notation this would be – for a spin-up particle –

$$\phi_{\uparrow}(\vec{r}, \sigma) = \langle \vec{r}, \sigma | \phi_{\uparrow} \rangle \hat{=} \begin{pmatrix} \langle \vec{r}, \uparrow | \phi_{\uparrow} \rangle \\ 0 \end{pmatrix}$$

The orbital still has two components, but one of them, namely $\phi_{\uparrow}(\vec{r}, \downarrow)$, vanishes. With the common notation, it is difficult to write down expressions that do not break the rotational symmetry for the spin direction.

Magnetization

So-far, we used the spin operator to determine the expectation value of the spin. Now, we would like to obtain the spin density and the magnetization, that is the spatial distribution of angular momentum and magnetic moment.

In order to clarify the principles, let me work out the charge density as a trivial example: The projector $\hat{P}(\vec{r})$ onto a certain point in space \vec{r} is

$$\hat{P}(\vec{r}) \stackrel{\text{def}}{=} \sum_{\sigma \in \{\uparrow, \downarrow\}} |\vec{r}, \sigma\rangle \langle \vec{r}, \sigma| = |\vec{r}, \downarrow\rangle \langle \vec{r}, \downarrow| + |\vec{r}, \uparrow\rangle \langle \vec{r}, \uparrow| \quad (3.11)$$

We obtain the charge density as expectation value of $\hat{P}(\vec{r})$, multiplied with the electron charge $q_e = -e$.

$$\begin{aligned} \rho(\vec{r}) &= \langle \phi | [q\hat{P}(\vec{r})] | \phi \rangle = q \langle \phi | \left[\sum_{\sigma} |\vec{r}, \sigma\rangle \langle \vec{r}, \sigma| \right] | \phi \rangle \\ &= q \sum_{\sigma} \langle \phi | \vec{r}, \sigma \rangle \langle \vec{r}, \sigma | \phi \rangle \\ &= q \left(\langle \phi | \vec{r}, \downarrow \rangle \langle \vec{r}, \downarrow | \phi \rangle + \langle \phi | \vec{r}, \uparrow \rangle \langle \vec{r}, \uparrow | \phi \rangle \right) \end{aligned} \quad (3.12)$$

Hence, the charge density is, up to the factor q , the sum of the spin-up and spin-down densities. After this introduction, we can analogously determine the magnetization.

The **magnetic moment** \vec{M} of an electron is given by its **g-factor**[27] $g_e = -2.00231930436182$ and its spin \vec{S} by

$$\vec{M} = g_e \frac{e}{2m_e} \vec{S} = |g_e| \frac{q_e}{2m_e} \vec{S} \quad (3.13)$$

where e is the (positive) elementary charge and m_e is the electron mass. (see Eq. 102 of [27] and following.) The energy of a particle in the magnetic field is $E = -\vec{M}\vec{B}$ (see Eq. 102 of [27]) The g-factor for the electron is close to -2 and $g = -2$ is often implied. The definition of the g-factor for the electron differs from that for other particles such as nucleons. Note that the g-factor is often given as positive quantity. In order to avoid this ambiguities due to the choice of the sign, I provide also the second form in Eq. 3.13, which uses the absolute value of the g-factor and the charge $q_e = -e$ of the electron instead of the elementary charge e . The elementary charge is a fundamental constant defined as positive quantity.

The magnetization operator is obtained as product of the factor³ $\frac{q}{m}$, the spin operator and the

³The classical ratio of magnetic moment and angular momentum is $\frac{q}{2m}$, which however assumes a constant ratio the mass- and charge distribution in space. While the "distribution" of electrons leads to such a constant ratio, the properties of a single electron may differ in a classical picture. In a quantum-mechanical description the electron is point-like with a certain gyro-magnetic ratio, that follows directly from the relativistic Dirac equation.

projection operator onto a point in space.

$$\begin{aligned}
\hat{m}_i(\vec{r}) &\stackrel{\text{def}}{=} \frac{|g|}{2} \frac{q}{m} \hat{P}(\vec{r}) \hat{S}_i \stackrel{\text{Eq. 3.3}}{=} \frac{|g|}{2} \frac{q\hbar}{2m} \hat{P}(\vec{r}) \hat{\sigma}_i \\
&= \frac{|g|}{2} \frac{q\hbar}{2m} \left[\underbrace{\sum_{\sigma} |\vec{r}, \sigma\rangle \langle \vec{r}, \sigma|}_{\hat{P}(\vec{r})} \right] \left[\underbrace{\int d^3r' \sum_{\sigma', \sigma''} |\vec{r}', \sigma'\rangle \sigma_{i, \sigma', \sigma''} \langle \vec{r}', \sigma''|}_{\hat{\sigma}_i} \right] \\
&= \frac{|g|}{2} \frac{q\hbar}{2m} \sum_{\sigma} \int d^3r' \sum_{\sigma', \sigma''} |\vec{r}, \sigma\rangle \underbrace{\langle \vec{r}, \sigma | \vec{r}', \sigma' \rangle}_{\delta(\vec{r}-\vec{r}')\delta_{\sigma, \sigma'}} \sigma_{i, \sigma', \sigma''} \langle \vec{r}', \sigma''| \\
&= \frac{|g|}{2} \frac{q\hbar}{2m} \sum_{\sigma, \sigma''} |\vec{r}, \sigma\rangle \sigma_{i, \sigma, \sigma''} \langle \vec{r}, \sigma''| \tag{3.14}
\end{aligned}$$

The factor $\mu_B \stackrel{\text{def}}{=} \frac{e\hbar}{2m_e}$ is the **Bohr magneton**, which is approximately equal to the magnetic moment of an electron. Spin and magnetic moment of the electron point in opposite directions due to the negative charge of the electron.

MAGNETIZATION OPERATOR

$$\hat{m}(\vec{r}) = \frac{|g|}{2} \frac{q\hbar}{2m} \sum_{\sigma, \sigma'} |\vec{r}, \sigma\rangle \vec{\sigma}_{\sigma, \sigma'} \langle \vec{r}, \sigma'| \tag{3.15}$$

with the Pauli matrices $\vec{\sigma}$ defined in Eq. 3.4.

For an electron, the g-factor is $g_e \approx -2$ and $q_e = -e$. Because the energy is $E = - \int d^3r \vec{m}(\vec{r}) \vec{B}(\vec{r})$, the magnetization will align preferably parallel to the magnetic field and the electron spin density will align preferably antiparallel to the magnetic field.

More explicitly, we obtain

$$\begin{aligned}
\rho(r) &= q \begin{pmatrix} \langle \phi | \vec{r}, \uparrow \rangle \\ \langle \phi | \vec{r}, \downarrow \rangle \end{pmatrix} \begin{pmatrix} 1 & 0 \\ 0 & 1 \end{pmatrix} \begin{pmatrix} \langle \vec{r}, \uparrow | \phi \rangle \\ \langle \vec{r}, \downarrow | \phi \rangle \end{pmatrix} \\
&= q \left[\phi^*(\vec{r}, \uparrow) \phi(\vec{r}, \uparrow) + \phi^*(\vec{r}, \downarrow) \phi(\vec{r}, \downarrow) \right] \tag{3.16}
\end{aligned}$$

$$\begin{aligned}
m_x(r) &= \frac{q\hbar}{2m} \begin{pmatrix} \langle \phi | \vec{r}, \uparrow \rangle \\ \langle \phi | \vec{r}, \downarrow \rangle \end{pmatrix} \begin{pmatrix} 0 & 1 \\ 1 & 0 \end{pmatrix} \begin{pmatrix} \langle \vec{r}, \uparrow | \phi \rangle \\ \langle \vec{r}, \downarrow | \phi \rangle \end{pmatrix} \\
&= \frac{q\hbar}{2m_e} \left[\phi^*(\vec{r}, \uparrow) \phi(\vec{r}, \downarrow) + \phi^*(\vec{r}, \downarrow) \phi(\vec{r}, \uparrow) \right] \tag{3.17}
\end{aligned}$$

$$\begin{aligned}
m_y(r) &= \frac{q\hbar}{2m} \begin{pmatrix} \langle \phi | \vec{r}, \uparrow \rangle \\ \langle \phi | \vec{r}, \downarrow \rangle \end{pmatrix} \begin{pmatrix} 0 & -i \\ i & 0 \end{pmatrix} \begin{pmatrix} \langle \vec{r}, \uparrow | \phi \rangle \\ \langle \vec{r}, \downarrow | \phi \rangle \end{pmatrix} \\
&= -i \frac{q\hbar}{2m} \left[\phi^*(\vec{r}, \uparrow) \phi(\vec{r}, \downarrow) - \phi^*(\vec{r}, \downarrow) \phi(\vec{r}, \uparrow) \right] \tag{3.18}
\end{aligned}$$

$$\begin{aligned}
m_z(r) &= \frac{q\hbar}{2m} \begin{pmatrix} \langle \phi | \vec{r}, \uparrow \rangle \\ \langle \phi | \vec{r}, \downarrow \rangle \end{pmatrix} \begin{pmatrix} 1 & 0 \\ 0 & -1 \end{pmatrix} \begin{pmatrix} \langle \vec{r}, \uparrow | \phi \rangle \\ \langle \vec{r}, \downarrow | \phi \rangle \end{pmatrix} \\
&= \frac{q\hbar}{2m} \left[\phi^*(\vec{r}, \uparrow) \phi(\vec{r}, \uparrow) - \phi^*(\vec{r}, \downarrow) \phi(\vec{r}, \downarrow) \right] \tag{3.19}
\end{aligned}$$

3.2 Symmetry and quantum mechanics

In the following, we will be concerned with the symmetry of the Hamilton operator under permutation of particles. Therefore, I will revisit the main **symmetry** arguments discussed in section 9 of *ΦSX:Quantum Theory*[4]. The sequence of arguments are worthwhile to keep in mind:

A symmetry of an object is a transformation, that leaves the appearance of the object unchanged. For example, a square is symmetric under four-fold rotation.

A physical system is characterized⁴ by its Hamiltonian, which determines the dynamics of the system by the Schrödinger equation. The system is symmetric under a given transformation, if every time-dependent solution $|\psi(t)\rangle$ of the Schrödinger equation is transformed by a symmetry transformation into another solution of the same Schrödinger equation.

Let me formalize this:

1. Definition of a **transformation operator**: An operator \hat{S} can be called a transformation, if it conserves the norm for any state, that is if

$$\forall_{|\psi\rangle} \quad \langle\psi|\psi\rangle \stackrel{|\phi\rangle=\hat{S}|\psi\rangle}{=} \langle\phi|\phi\rangle \quad (3.20)$$

2. A transformation operator \hat{S} is **unitary**, that is

$$\hat{S}^\dagger \hat{S} = 1 \quad (3.21)$$

Proof:

$$\forall_{|\psi\rangle} \quad \langle\psi|\hat{S}^\dagger \hat{S}|\psi\rangle \stackrel{\text{Eq. 3.20}}{=} \langle\psi|\psi\rangle \quad \Rightarrow \quad \hat{S}^\dagger \hat{S} = 1$$

3. Definition of a **symmetry**: A system is called symmetric under the transformation \hat{S} , if, for any solution of the Schrödinger equation describing that system, also $\hat{S}|\Psi\rangle$ is a solution of the same Schrödinger equation. That is, if

$$\left(i\hbar\partial_t|\Psi(t)\rangle = \hat{H}|\Psi(t)\rangle \right) \stackrel{|\Phi(t)\rangle\stackrel{\text{def}}{=} \hat{S}|\Psi(t)\rangle}{\Rightarrow} \left(i\hbar\partial_t|\Phi(t)\rangle = \hat{H}|\Phi(t)\rangle \right) \quad (3.22)$$

4. The **commutator** of the Hamilton operator with its symmetry operator vanishes, that is $[\hat{H}, \hat{S}]_- = 0$:

Proof:

$$\begin{aligned} i\hbar\partial_t|\Phi\rangle &= \hat{H}|\Phi\rangle \\ \stackrel{|\Phi\rangle\stackrel{\text{def}}{=} \hat{S}|\Psi\rangle}{\Rightarrow} i\hbar\partial_t\hat{S}|\Psi\rangle &= \hat{H}\hat{S}|\Psi\rangle \\ \stackrel{\partial_t\hat{S}=0}{\Rightarrow} \hat{S}(i\hbar\partial_t|\Psi\rangle) &= \hat{H}\hat{S}|\Psi\rangle \\ \stackrel{i\hbar\partial_t|\Psi\rangle=\hat{H}|\Psi\rangle}{\Rightarrow} \hat{S}\hat{H}|\Psi\rangle &= \hat{H}\hat{S}|\Psi\rangle \\ \underbrace{(\hat{H}\hat{S} - \hat{S}\hat{H})}_{[\hat{H}, \hat{S}]_-} |\Psi\rangle &= 0 \end{aligned}$$

Because this equation holds for any solution of the Schrödinger equation, it holds for any wave function, because any function can be written as superposition of solutions of the Schrödinger equation. (The latter form a complete set of functions.) Therefore,

⁴The argument is not limited to quantum systems. The Schrödinger equation can be replaced by any other equation of motion governing the dynamics or other properties.

SYMMETRY AND COMMUTATOR

The commutator between the Hamilton operator \hat{H} with its (time-independent^a) symmetry operators \hat{S} vanishes.

$$[\hat{H}, \hat{S}]_- = 0$$

Thus, one usually identifies a symmetry by working out the commutator with the Hamiltonian.

^aFor time-dependent symmetry operators, the more general rule is $[\hat{H}, \hat{S}]_- = i\hbar\partial_t\hat{S}$. An example for a time-dependent symmetry is that between two relatively moving frames of inertia.

5. The matrix elements of the Hamilton operator between two eigenstates of the symmetry operator with different eigenvalues vanish. That is

$$(\hat{S}|\Psi_s\rangle = |\Psi_s\rangle s \quad \wedge \quad \hat{S}|\Psi_{s'}\rangle = |\Psi_{s'}\rangle s' \quad \wedge \quad s \neq s') \Rightarrow \langle\Psi_s|\hat{H}|\Psi_{s'}\rangle = 0$$

Thus, the Hamilton operator is block diagonal in a representation of eigenstates of its symmetry operators. The eigenstates of the Hamilton operator can be obtained for each block individually. Because the effort to diagonalize a matrix increases rapidly with the matrix size, a block-diagonalization simplifies the calculation of Hamilton eigenstates substantially, both for analytical and for numerical calculations.

If the Hamiltonian is block diagonal, the time-dependent Schrödinger equation does not mix states from different blocks. A wave function that starts out as an eigenstate of a symmetry operator with a given eigenvalue, will always be an eigenstate with the same eigenvalue.

$$\hat{S}|\psi(0)\rangle = |\psi(0)\rangle s_j \Rightarrow \hat{S}|\psi(t)\rangle = |\psi(t)\rangle s_j \quad (3.23)$$

In other words, the eigenvalue of the symmetry operator is a conserved quantity. (Note, however, that the eigenvalue of a symmetry operator is usually complex-valued.)

The eigenvalues of the symmetry operators are related to the **quantum numbers**.

Proof: In the following, we will need an expression for the bra $\langle\psi_s|\hat{S}$, where $|\psi_s\rangle$ is a symmetry eigenstate.

- We start by showing that the absolute value of an eigenvalue of a unitary operator is equal to one, that is $s = e^{i\phi}$ where ϕ is real. With an eigenstate $|\psi_s\rangle$ of \hat{S} we obtain

$$\begin{aligned} s^* \langle\psi_s|\psi_s\rangle s &\stackrel{\hat{S}|\psi_s\rangle = |\psi_s\rangle s}{=} \langle\hat{S}\psi_s|\hat{S}\psi_s\rangle = \langle\psi_s|\underbrace{\hat{S}^\dagger\hat{S}}_{\hat{1}}|\psi_s\rangle \stackrel{\text{Eq. 3.21}}{=} \langle\psi_s|\psi_s\rangle \\ \Rightarrow |s| &= 1 \Rightarrow s = e^{i\phi} \quad \text{with real-valued } \phi \end{aligned} \quad (3.24)$$

- Next, we show that the eigenvalues of the hermitian conjugate operator \hat{S}^\dagger of a unitary operator \hat{S} are the complex conjugates of the eigenvalues of \hat{S} .

$$\begin{aligned} &\Rightarrow |\psi_s\rangle \stackrel{\text{Eq. 3.21}}{=} \underbrace{\hat{S}^\dagger\hat{S}}_{\hat{1}}|\psi_s\rangle \stackrel{\hat{S}|\psi_s\rangle = |\psi_s\rangle s}{=} \hat{S}^\dagger|\psi_s\rangle s \\ \Rightarrow \hat{S}^\dagger|\psi_s\rangle s &\stackrel{\text{Eq. 3.24}}{=} |\psi_s\rangle \underbrace{s^*s}_{=1} \\ \Rightarrow \hat{S}^\dagger|\psi_s\rangle &= |\psi_s\rangle s^* \\ \Rightarrow \langle\psi_s|\hat{S} &= s\langle\psi_s| \end{aligned}$$

- With this, we are ready to show that the matrix elements of the Hamilton operator between two eigenstates of the symmetry operator with different eigenvalues vanish.

$$\begin{aligned}
0 & \stackrel{[\hat{H}, \hat{S}]_- = 0}{=} \langle \Psi_s | [\hat{H}, \hat{S}]_- | \Psi_{s'} \rangle = \langle \Psi_s | \hat{H} \hat{S} | \Psi_{s'} \rangle - \langle \Psi_s | \hat{S} \hat{H} | \Psi_{s'} \rangle \\
& \stackrel{\hat{S} |\Psi_s\rangle = |\Psi_s\rangle_{s, \text{etc.}}}{=} \langle \Psi_s | \hat{H} | \Psi_{s'} \rangle s' - s \langle \Psi_s | \hat{H} | \Psi_{s'} \rangle = \langle \Psi_s | \hat{H} | \Psi_{s'} \rangle (s' - s) \\
& \stackrel{s \neq s'}{\Rightarrow} \langle \Psi_s | \hat{H} | \Psi_{s'} \rangle = 0
\end{aligned}$$

q.e.d

With the findings above, we can set up a construction method for eigenstates of a symmetry operator. This operation allows one to block diagonalize a Hamiltonian.

SYMMETRY EIGENSTATES OF CYCLIC SYMMETRIES

A transformation operator \hat{S} is cyclic with period N , when $\hat{S}^N = \hat{1}$.
The eigenvalues of a cyclic transformation are

$$s_\alpha = e^{i \frac{2\pi}{N} \alpha} . \quad (3.25)$$

where α is an integer between zero and $N - 1$.

The eigenstates $|\psi_\alpha\rangle$ of \hat{S} with eigenvalue s_α can be constructed by applying the following formula to an arbitrary wave function $|\phi\rangle$.

$$|\psi_\alpha\rangle = \frac{1}{N} \sum_{n=0}^{N-1} \hat{S}^n |\chi\rangle s_\alpha^{-n} = \frac{1}{N} \sum_{n=0}^{N-1} (\hat{S}^\dagger)^n |\phi\rangle s_\alpha^{+n} \quad (3.26)$$

The two equations are equivalent.

The operation acts like a filter that removes any component from the “wrong” eigenvalues. Thus, if the state $|\phi\rangle$ does not have any projection onto an eigenstate with the “right” eigenvalue s_α , the resulting state is the null state $|\emptyset\rangle$.

A complete set of eigenstates of a given eigenvalue s_α can be obtained by applying the operation Eq. 3.26 to a complete set of states $|\phi\rangle$.

Let me give a brief derivation of Eq. 3.26: Consider a state $|\phi\rangle = \sum_\beta |\beta\rangle c_\beta$, which is a superposition of eigenstates of the symmetry operator \hat{S} , so that

$$\hat{S} |\beta\rangle = |\beta\rangle s_\beta \quad (3.27)$$

where s_β is one of the eigenvalues of \hat{S} . Every state can be represented in this form. Thus

$$\frac{1}{N} \sum_{j=0}^{N-1} \hat{S}^j |\phi\rangle s_\alpha^{-j} = \frac{1}{N} \sum_{j=0}^{N-1} \hat{S}^j \left(\sum_\beta |\beta\rangle c_\beta \right) s_\alpha^{-j} = \sum_\beta |\beta\rangle c_\beta \left(\frac{1}{N} \sum_{j=0}^{N-1} s_\beta^j s_\alpha^{-j} \right) = |\alpha\rangle c_\alpha \quad (3.28)$$

This shows that the result of Eq. 3.26 is a simple projection onto the sub-Hilbert space spanned by the eigenstates of \hat{S} with the selected eigenvalue s_α . We exploited that the geometric series in the equation above has, for $\beta \in \{0, 1, \dots, N - 1\}$, the form

$$\frac{1}{N} \sum_{j=0}^{N-1} \left(e^{i \frac{2\pi}{N} \beta} \right)^j = \begin{cases} \frac{1 - (e^{i \frac{2\pi}{N} \beta})^N}{1 - (e^{i \frac{2\pi}{N} \beta})} = 0 & \text{for } \beta \neq 0 \\ = \frac{1}{N} \sum_{j=1}^{N-1} 1 = 1 & \text{for } \beta = 0 \end{cases} \quad (3.29)$$

Because of the cyclic property of the symmetry operation, the equation $(s_\beta)^N = 1$ holds for all eigenvalues. Finally, we make use that $s_\beta / s_\alpha = e^{i \frac{2\pi}{N} (\beta - \alpha)}$, which is a special property of the eigenvalues given by Eq. 3.25.

3.3 Identical particles

Electrons with the same spin are indistinguishable. This says that there is no conceivable experiment that discriminates between two electrons. Thus, there is a symmetry with respect to exchange of two particles, and the Hamiltonian for indistinguishable particles commutes with the permutation operator of two particles.

The **two-particle permutation operator** is defined as

$$\hat{P}_{ij}^{(2)}\Psi(\dots, \vec{x}_i, \dots, \vec{x}_j, \dots) = \Psi(\dots, \vec{x}_j, \dots, \vec{x}_i, \dots)$$

The eigenstates of the Hamiltonian are eigenstates of the permutation operator. Because $(\hat{P}_{ij}^{(2)})^2 = \hat{1}$, the permutation operator has the two eigenvalues, namely +1 and -1. Thus, the wave functions are fully symmetric or fully antisymmetric with respect to the permutation of two particle coordinates. Particles with a symmetric wave function are called **Bosons** and particles with an antisymmetric wave function are called **Fermions**. Bosons are particles with integer spin such as photons, mesons, gluons, gravitons, etc, which are usually related to an interaction, while Fermions are particles with half-integer spin such as electrons, protons, neutrons, quarks, etc.

Unlike other symmetries, this symmetry is not a property of a specific Hamiltonian, but it is a property of the particles themselves. If the particles are indistinguishable, there is no conceivable Hamiltonian, that is not symmetric under permutation of two of these particles. If we could construct only one Hamiltonian that is not symmetric, we could design an experiment, just by realizing this Hamiltonian, that distinguishes two of such particles

The electron exchange is illustrated in Fig. 3.1. Except for the color, which distinguishes the two electrons, left and right situations are identical. Note, that for the particle exchange both spatial and spin-indices have to be exchanged simultaneously. Since the electrons are indistinguishable, no distinguishing property like the color indicated can exist.

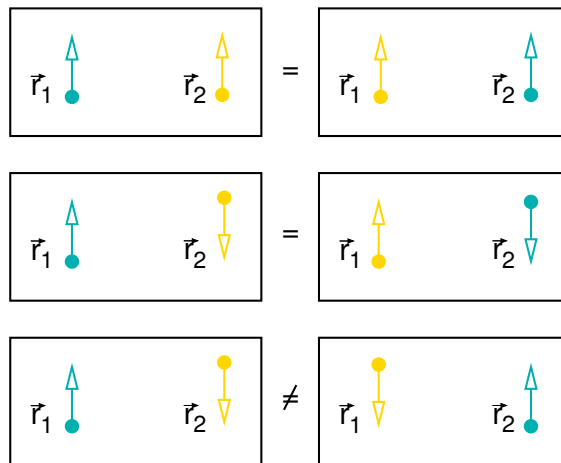


Fig. 3.1: Demonstration of the particle exchange. For the two figures at the top, left and right situations are identical except for a color of the particles. For identical particles there is no property such as the color that allows one to distinguish them. Thus $\Psi(\vec{x}_1, \vec{x}_2) = -\Psi(\vec{x}_2, \vec{x}_1)$ or $\Psi(\vec{r}_1, \sigma_1, \vec{r}_2, \sigma_2) = -\Psi(\vec{r}_2, \sigma_2, \vec{r}_1, \sigma_1)$. In the bottom figure, the particle positions are exchanged but not their spin. Thus, the two configurations are not identical. In this case we may also view electrons with up and down spin as distinguishable particles, because they have different spin.

Fermions, such as electrons, have an antisymmetric wave function, that is

$$\hat{P}_{ij}^{(2)}|\Psi\rangle = -|\Psi\rangle$$

3.3.1 Levi-Civita symbol or the fully-antisymmetric tensor

In the following, I will represent wave functions by determinants. In order to work with determinants, the Levi-Civita symbol, also called the fully-antisymmetric tensor, will be introduced. Here, I define the fully-antisymmetric tensor and derive some formulas, which will be needed later.

Definition

The **Levi-Civita symbol**⁵, also called the **fully-antisymmetric tensor** is a **rank**⁶ N Tensor defined by the following properties

- For ascending indices the Levi-Civita symbol has the value one:

$$\epsilon_{1,2,3,\dots,N} = 1$$

- The Levi-Civita symbol changes sign with any pairwise permutation of its indices
- The Levi-Civita symbol vanishes whenever at least two indices are pairwise identical

Relation to determinants

The determinant of a $N \times N$ matrix \mathbf{A} is defined by the Levi-Civita symbol $\epsilon_{i,j,k,l,\dots}$ as

$$\det[\mathbf{A}] = \sum_{i,j,k,\dots} \epsilon_{i,j,k,\dots} A_{1,i} A_{2,j} A_{3,k} \dots$$

Vector product (not needed)

A common and useful application of the Levi-Civita Symbol is to express the vector product in three dimensions by its components.

$$\vec{a} = \vec{b} \times \vec{c} \quad \Leftrightarrow \quad a_i = \sum_{j,k} \epsilon_{i,j,k} b_j c_k$$

3.3.2 Permutation operator

The most simple way to construct a many-particle wave function, is to take the product of **one-particle wave functions** $\phi_j(\vec{x})$, such as

$$\Psi(\vec{x}_1, \vec{x}_2, \dots) = \phi_a(\vec{x}_1) \phi_b(\vec{x}_2) \dots$$

This is a **product wave function**.

Such a product wave function is neither symmetric nor antisymmetric with respect to permutation. Therefore, we need to antisymmetrize it. We use the N -particle **permutation operator** $\hat{P}_{i_1, \dots, i_N}$ that is defined as follows

⁵Tullio Levi-Civita (1873-1941): Italian mathematician. Invented the covariant derivative. Made tensor-algebra popular, which was used in Einstein's theory of general relativity.

⁶The rank is the number of indices that define a tensor element. Note, that there is another more limited definition of the word rank.

N-PARTICLE PERMUTATION OPERATOR

$$\hat{\mathcal{P}}_{i_1, \dots, i_N} := \int d^4 x_1 \cdots \int d^4 x_N |\vec{x}_{i_1}, \dots, \vec{x}_{i_N}\rangle \langle \vec{x}_1, \dots, \vec{x}_N| \quad (3.30)$$

$$\Leftrightarrow \hat{\mathcal{P}}_{i_1, \dots, i_N}^\dagger := \int d^4 x_1 \cdots \int d^4 x_N |\vec{x}_1, \dots, \vec{x}_N\rangle \langle \vec{x}_{i_1}, \dots, \vec{x}_{i_N}| \quad (3.31)$$

The permutation operator reorders the coordinates so that the first particle is placed onto the position of the particle i_1 and so on. This implies that the coordinates of the i_1 -th particle are placed on the first position, which is the one of the first particle.

In order to make more transparent, how the operator works, let us rewrite it as an operator of real-space functions. Consider a state $|\vec{y}_1, \dots, \vec{y}_N\rangle$, which describes a particle distribution where the first particle is at position \vec{y}_1 , the second at \vec{y}_2 and so on.

It turns out that the argument is shown easier for the adjoint permutation operator Eq. 3.31, which yields

$$\begin{aligned} \hat{\mathcal{P}}_{i_1, \dots, i_N}^\dagger \Psi(\vec{y}_1, \dots, \vec{y}_N) &= \langle \vec{y}_1, \dots, \vec{y}_N | \hat{\mathcal{P}}_{i_1, \dots, i_N}^\dagger | \Psi \rangle \\ &\stackrel{\text{Eq. 3.31}}{=} \int d^4 x_1 \cdots \int d^4 x_N \underbrace{\langle \vec{y}_1, \dots, \vec{y}_N | \vec{x}_1, \dots, \vec{x}_N \rangle}_{\delta(\vec{y}_1 - \vec{x}_1) \cdots \delta(\vec{y}_N - \vec{x}_N)} \underbrace{\langle \vec{x}_{i_1}, \dots, \vec{x}_{i_N} | \Psi \rangle}_{\Psi(\vec{x}_{i_1}, \dots, \vec{x}_{i_N})} \\ &= \Psi(\vec{y}_{i_1}, \dots, \vec{y}_{i_N}) \end{aligned} \quad (3.32)$$

Because the permutation operator is unitary, its adjoint is also its inverse. Using this, we extract how the permutation vector $\hat{\mathcal{P}}_{i_1, \dots, i_N}$ itself acts on a wave function.

$$\begin{aligned} \hat{\mathcal{P}}_{i_1, \dots, i_N} \underbrace{\Psi(\vec{x}_{i_1}, \dots, \vec{x}_{i_N})}_{\stackrel{\text{Eq. 3.32}}{=} \hat{\mathcal{P}}_{i_1, \dots, i_N}^\dagger \Psi(\vec{x}_1, \dots, \vec{x}_n)} &= \underbrace{\hat{\mathcal{P}}_{i_1, \dots, i_N} \hat{\mathcal{P}}_{i_1, \dots, i_N}^\dagger}_{=\hat{1}} \Psi(\vec{x}_1, \dots, \vec{x}_n) = \Psi(\vec{x}_1, \dots, \vec{x}_n) \\ \Rightarrow \hat{\mathcal{P}}_{i_1, \dots, i_N} \Psi(\vec{x}_{i_1}, \dots, \vec{x}_{i_N}) &= \Psi(\vec{x}_1, \dots, \vec{x}_n) \end{aligned} \quad (3.33)$$

In the new state $\hat{\mathcal{P}}_{i_1, \dots, i_N} |\Psi\rangle$, the wave function amplitude $\langle \vec{x}_{i_1}, \dots, \vec{x}_{i_N} | \hat{\mathcal{P}}_{i_1, \dots, i_N} |\Psi\rangle$ at the permuted positions $(\vec{x}_{i_1}, \dots, \vec{x}_{i_N})$ has the same values as the old state $|\Psi\rangle$, at the original positions $(\vec{x}_1, \dots, \vec{x}_N)$. This is the content of Eq. 3.30, which has now been demonstrated on the wave-function level.

3.3.3 Antisymmetrize wave functions

The exchange or permutation operator $\hat{\mathcal{P}}_{i_1, \dots, i_N}$ applied to a fermionic wave function has the eigenvalue -1 if the sequence i_1, \dots, i_N is obtained by an odd number of permutations from regular order $1, 2, 3, \dots, N$, and it has the eigenvalue $+1$ for an even number of permutations. These values are those of the fully-antisymmetric tensor or the Levi-Civita symbol.

EIGENVALUES OF THE PERMUTATION OPERATOR

A many-fermion state is an eigenstate of the permutation operators

$$\hat{\mathcal{P}}_{i_1, \dots, i_N} |\Psi^F\rangle = |\Psi^F\rangle \epsilon_{i_1, \dots, i_N} \quad (3.34)$$

with eigenvalues given by the fully-antisymmetric tensor $\epsilon_{i_1, \dots, i_N}$ defined in section 3.3.1.

A many-boson state can be defined similarly, but the eigenvalues are +1 for any permutation of the particle coordinates.

$$\hat{\mathcal{P}}_{i_1, \dots, i_N} |\Psi^B\rangle = |\Psi^B\rangle \epsilon_{i_1, \dots, i_N}^2 \quad (3.35)$$

Editor: Here we need a derivation of the permutation eigenstates from Eq. 3.26. There is a complication because the permutations do not commute with each other. I have started an appendix on symmetry groups with a set of non-abelian (non-commutating) symmetry operators for that purpose.

The Fermionic eigenstates of the permutation operators can be constructed from an arbitrary wave function $|\chi\rangle$ as

$$|\Phi^F\rangle = \sum_{i_1, \dots, i_N=1}^N \hat{\mathcal{P}}_{i_1, \dots, i_N}^\dagger |\chi\rangle \epsilon_{i_1, \dots, i_N} \quad (3.36)$$

3.3.4 Slater determinants

The most simple many-particle wave function is a **product state** $|\phi_1, \dots, \phi_N\rangle$, which can be written as

$$\langle \bar{x}_1, \dots, \bar{x}_N | \phi_1, \dots, \phi_N \rangle = \langle \bar{x}_1 | \phi_1 \rangle \cdots \langle \bar{x}_N | \phi_N \rangle = \phi_1(\bar{x}_1) \cdots \phi_N(\bar{x}_N) \quad (3.37)$$

A product state is not yet antisymmetric with respect to particle exchange, but with Eq. 3.36 it can be antisymmetrized. Using the N-particle permutation operator $\hat{\mathcal{P}}_{i_1, \dots, i_N}$ and the fully-antisymmetric tensor $\epsilon_{i_1, \dots, i_N}$ we can antisymmetrize a product wave function.

$$|\Phi^F\rangle = \frac{1}{\sqrt{N!}} \sum_{i_1, \dots, i_N=1}^N \hat{\mathcal{P}}_{i_1, \dots, i_N}^\dagger |\phi_1, \phi_2, \dots, \phi_N\rangle \epsilon_{i_1, \dots, i_N} \quad (3.38)$$

The pre-factor $1/\sqrt{N!}$ is the required normalization for an orthonormal set of one-particle wave functions: there are $N!$ distinct permutations of the N orbitals. Product states that differ by a permutation are orthonormal, if the one-particle states are orthonormal.

The corresponding wave function is

$$\begin{aligned} \Phi^F(\bar{x}_1, \bar{x}_2, \dots, \bar{x}_N) &\stackrel{\text{Eq. 3.38}}{=} \frac{1}{\sqrt{N!}} \sum_{i_1, \dots, i_N} \epsilon_{i_1, \dots, i_N} \hat{\mathcal{P}}_{i_1, \dots, i_N}^\dagger \phi_1(\bar{x}_1) \cdots \phi_N(\bar{x}_N) \\ &\stackrel{\text{Eq. 3.32}}{=} \frac{1}{\sqrt{N!}} \sum_{i_1, \dots, i_N} \phi_1(\bar{x}_{i_1}) \cdots \phi_N(\bar{x}_{i_N}) \epsilon_{i_1, \dots, i_N} \end{aligned} \quad (3.39)$$

where $\epsilon_{i,j,k,\dots}$ is the fully-antisymmetric tensor defined in Sec. 3.3.1. When one exploits the connection between Levi-Civita Symbol and the determinant discussed in section 3.3.1, the wave function

Eq. 3.39 can also be written as a **Slater determinant** [28, 29]⁷

$$\Psi^F(\vec{x}_1, \dots, \vec{x}_N) \stackrel{\text{Eq. 3.39}}{=} \frac{1}{\sqrt{N!}} \det \begin{vmatrix} \phi_1(\vec{x}_1) & \phi_1(\vec{x}_2) & \dots & \phi_1(\vec{x}_N) \\ \phi_2(\vec{x}_1) & \phi_2(\vec{x}_2) & \dots & \phi_2(\vec{x}_N) \\ \vdots & \vdots & \ddots & \vdots \\ \phi_N(\vec{x}_1) & \phi_N(\vec{x}_2) & \dots & \phi_N(\vec{x}_N) \end{vmatrix} \quad (3.40)$$

The Slater determinant exploits the property of the determinant, that it changes its sign under permutation of two columns of a matrix. In the Slater determinant the exchange of two columns corresponds to the exchange of two particle coordinates.

An antisymmetric wave function can be constructed even from a non-orthogonal set of one-particle orbitals by forming the corresponding determinant. However, unless the one-particle orbitals are orthonormal, the evaluation of matrix elements between Slater determinants is a nearly hopelessly difficult undertaking. Therefore, Slater determinants are usually built from an orthonormal set of one-particle orbitals.

As an example, the two-particle Slater determinant $|S_{a,b}\rangle$ of two one-particle states $\phi_a(\vec{x})$ and $\phi_b(\vec{x})$ is

$$S_{a,b}(\vec{x}_1, \vec{x}_2) = \langle \vec{x}_1, \vec{x}_2 | S_{a,b} \rangle = \frac{1}{\sqrt{2}} \left(\phi_a(\vec{x}_1) \phi_b(\vec{x}_2) - \phi_b(\vec{x}_1) \phi_a(\vec{x}_2) \right)$$

3.3.5 Bose wave functions

Analogous to the Slater determinant, we can represent symmetrized product wave functions as a **permanent**. The permanent of a matrix $[A]$ can be written as

$$\text{perm}[A] = \sum_{i_1, \dots, i_N=1}^N \epsilon_{i_1, \dots, i_N}^2 A_{1, i_1} A_{2, i_2} \dots A_{N, i_N}$$

We see from Eq. 3.35 that the permanent plays for bosons the same role as the determinant for Fermions.

A Bose wave function obtained by symmetrization of a product wave function has the form

$$\Psi^B(\vec{x}_1, \dots, \vec{x}_N) = \frac{1}{\sqrt{N!}} \sum_{i_1, \dots, i_N=1}^N \epsilon_{i_1, \dots, i_N}^2 \phi_1(\vec{x}_{i_1}) \dots \phi_N(\vec{x}_{i_N})$$

If the one-particle states are orthonormal, also the resulting “Permanent-wave functions” built from the same one-particle basis set are orthonormal.

3.3.6 General many-fermion wave function

It is important to realize that not every antisymmetric wave function can be represented as a Slater determinant. Slater determinants are derived from product wave functions and thus have a rather restricted form.

However, the Slater determinants that can be constructed from a complete, orthonormal set of one-particle wave functions $\{|\phi_1\rangle, |\phi_2\rangle, \dots\}$ form a complete orthonormal basis for antisymmetric many-particle states. (without proof)⁸

An attempt to visualize the restrictions of product state is given in fig. 3.2.

⁷According to a remark on Wikipedia, Heisenberg and Dirac proposed already in 1926 to write the antisymmetric wave function in a form of a determinant.

⁸The one-particle states need not be orthonormal to fulfill the completeness condition. The requirement of orthonormal wave functions is a convenience to make the evaluation of matrix elements for many-particle states constructed from these one-particle states efficient. These will become clear later when the Slater-Condon rules are derived.

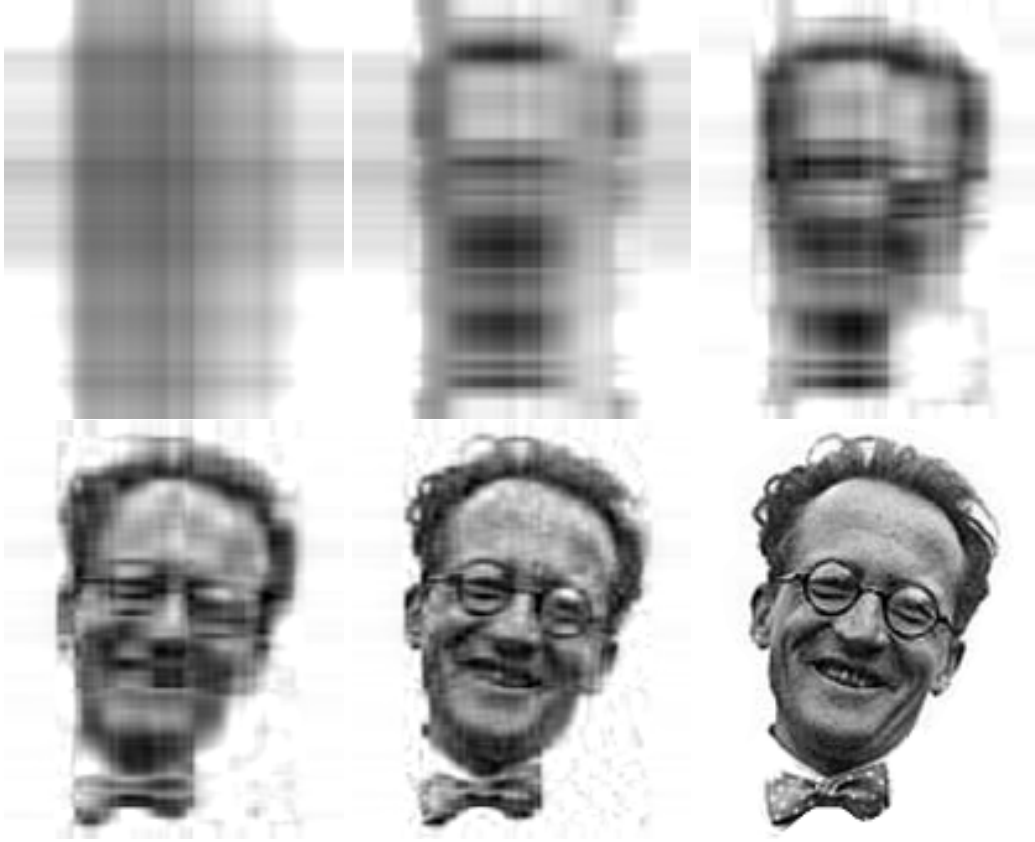


Fig. 3.2: Demonstration of product states and the superposition of product states. The grey-scale values $F(x, y)$ of the picture of Erwin Schrödinger is approximated by finite sums of product wave functions in the form $F(x, y) = \sum_{j=1}^M f_j(x)g_j(y)$ for $M = 1, 2, 4$ in the top row and for $M = 8, 16$ and the original figure in the bottom row. The functions $f_j(x)$ and $g_j(y)$ have been optimized individually to minimize the mean square deviation from the grey-scale values.

A general N -particle state can be constructed as follows: Let us consider a complete and orthonormal one-particle basis set $|\phi_1\rangle, |\phi_2\rangle, \dots$. A subset of N such basis functions, namely $|\phi_{i_1}\rangle, |\phi_{i_2}\rangle, \dots, |\phi_{i_N}\rangle$ defines a particular Slater determinant $|S_{i_1, i_2, \dots, i_N}\rangle$. A general antisymmetric N -particle state $|\Psi\rangle$ can be written as a sum⁹ over all Slater determinants

$$|\Psi\rangle = \sum_{i_1, i_2, \dots, i_N=1; i_1 < i_2 < \dots}^{\infty} |S_{i_1, i_2, \dots}\rangle c_{i_1, i_2, \dots}$$

where the $c_{i_1, i_2, \dots}$ are the (complex-valued) expansion coefficients.

3.4 Occupation-number representation

We have learned that a Slater determinant is defined by a subset of N states from a given one-particle basis. Thus, we can form a vector with one component for each one-particle orbital. If we set the components equal to one for the orbitals in the set and equal to zero for all orbitals not in the set,

⁹The sum goes over all N -tuples (i_1, \dots, i_N) with $1 \leq i_1 < i_2 < \dots < i_N$. The indices can go up to infinity.

we arrive at the **occupation-number representation** for Slater determinants

$$|S_{i_1, \dots, i_n}\rangle = |0, 0, \underbrace{1}_{\text{pos } i_1}, 0, 0, 0, \underbrace{1}_{\text{pos } i_2}, \underbrace{1}_{\text{pos } i_3}, 0, \dots\rangle \quad (3.41)$$

This allows to write a general fermionic state in the form

$$|\Psi\rangle = \sum_{\sigma_1=0}^1 \sum_{\sigma_2=0}^1 \dots \sum_{\sigma_\infty=0}^1 |\sigma_1, \sigma_2, \dots, \sigma_\infty\rangle c_{\sigma_1, \sigma_2, \dots, \sigma_\infty} = \sum_{\vec{\sigma}} |\vec{\sigma}\rangle c_{\vec{\sigma}} \quad (3.42)$$

It is important, not to confuse the occupation number with a spin index, even though both are denoted by the same symbol σ . The only connection is that both can assume two values, namely $\{0, 1\}$ for occupation numbers and $\{\uparrow, \downarrow\}$ for spins.

3.5 Non-interacting electrons and one-particle wave functions

Because the electrons interact strongly by their Coulomb repulsion, their description is a very difficult quantum-mechanical problem.

Before we enter into the difficulties of many-particle physics, let us ignore the interaction and study problems with non-interacting particles.

At first, this sounds like intolerable approximation. However, the particles, we describe here, are not bare electrons but **quasi-particles** that carry a distortion of the surrounding electrons along with them. If this distortion is taken into account, the interaction becomes screened. As a result, the interaction becomes sufficiently small that the picture of non-interacting quasi electrons becomes appropriate for most physical systems.

This picture of almost non-interacting quasi particles breaks down in a fundamental way for materials with so-called **strong correlations**. Examples of materials with strong correlations are the High- T_c superconductors, manganites which exhibit colossal magnetoresistance, heavy Fermion systems, and many more.

A system of non-interacting electrons is relatively simple, because its Hamilton eigenstates can be expressed by one-particle wave functions. In this section, I want to clarify the connection to one-particle wave functions.

3.5.1 The one-particle view on many-particle wave functions

FERMIONIC EIGENSTATES OF A NON-INTERACTING HAMILTONIAN ARE SLATER DETERMINANTS

All eigenstates of a Hamiltonian $\hat{H} = \sum_{j=1}^N \hat{h}_j$ without interactions are Slater determinants formed by the one-particle eigenstates of the Hamiltonian \hat{h} . Here \hat{h}_j is always the same Hamilton operator acting on the coordinates of the j th particle.

One-particle (at-a-time) operators

The Hamiltonian for independent particles is a one-particle operator. An interaction, in contrast, depends on, at least, two particles. The Coulomb interaction, for example, depends on the relative positions of two particles.

Let me consider any **one-particle operator** \hat{A} . A one-particle operator acts on a many-particle wave function, but only on one particle at a time: It is a sum of operators each of which acts only

on the coordinates (or momenta) of one particle.

$$\hat{A} = \sum_{j=1}^N \hat{a}_j \quad (3.43)$$

In other words: $\hat{a}_j = a(\hat{x}_j, \hat{p}_j)$.

An example for a one-particle operator is the one-particle Hamiltonian

$$\hat{H} = \sum_{j=1}^N \hat{h}_j = \sum_{j=1}^N \left(\frac{\hat{p}_j^2}{2m} + v(\hat{x}_j) \right) \quad (3.44)$$

where \hat{p}_j and \hat{x}_j are momentum and position operators for the j -th particle coordinate.

Eigenstates of a non-interacting Hamiltonian

Let us consider the Hamiltonian for a system with N non-interacting particles

$$\hat{H} = \sum_{j=1}^N \hat{h}_j \quad (3.45)$$

Because the electrons are independent, the method of **separation of variables** can be used to break the problem up into the eigenvalue problems for individual particles. Let us assume that the one-particle eigenstates $|\varphi_n\rangle$ and the eigenvalues ϵ_n of \hat{h} are known, i.e.

$$\hat{h}|\varphi_n\rangle = |\varphi_n\rangle\epsilon_n \quad \text{with } \langle\varphi_m|\varphi_n\rangle = \delta_{m,n}. \quad (3.46)$$

The eigenstates of the Hamiltonian \hat{H} for *independent*¹⁰ particles are product states of these one-particle orbitals $|\varphi_n\rangle$ and the eigenvalues of the Hamiltonian H are sums of the one-particle energies ϵ_n .

For *identical* particles, these product states need to be symmetrized (for Bosons) or antisymmetrized (for Fermions). For Fermions, this results in Slater determinants. They can be represented as

$$|\vec{\sigma}\rangle = |\sigma_1, \sigma_2, \dots, \sigma_\infty\rangle \quad (3.47)$$

in the occupation-number representation for the basis $\{|\varphi_n\rangle\}$ of eigenstates of the one-particle Hamiltonian \hat{h} .

The energy eigenvalues $E_{\vec{\sigma}}$ of \hat{H} and the particle-number eigenvalues $N_{\vec{\sigma}}$ are

$$E_{\vec{\sigma}} = \sum_{n=1}^{\infty} \epsilon_n \sigma_n \quad \text{and} \quad N_{\vec{\sigma}} = \sum_{n=1}^{\infty} \sigma_n, \quad \text{respectively.} \quad (3.48)$$

The expectation value of any other one-particle operator $\hat{A} = \sum_{j=1}^N \hat{a}_j$ is¹¹

$$\langle A \rangle = \langle \vec{\sigma} | \hat{A} | \vec{\sigma} \rangle = \sum_{n=1}^{\infty} \langle \varphi_n | \hat{a} | \varphi_n \rangle \sigma_n = \text{Tr} \left[\underbrace{\sum_j |\varphi_n\rangle \sigma_n \langle \varphi_n|}_{\hat{\rho}^{(1)}} \hat{a} \right] = \text{Tr} \left[\hat{\rho}^{(1)} \hat{a} \right] \quad (3.49)$$

Thus, for a non-interacting system, it is, for most purposes, sufficient to know the eigenvalues and eigenstates one-particle Hamiltonian \hat{h} well.

¹⁰not necessarily identical

¹¹This statement, one of the Slater-Condon rules, is given here without proof. The Slater-Condon rules are given for example in section 3.5 in *ΦSX: Advanced Solid-State Theory*[2]

We introduced here the **one-particle reduced density matrix**

$$\hat{\rho}^{(1)} = \sum_n |\varphi_n\rangle f_n \langle \varphi_n| \quad (3.50)$$

The eigenstates of the one-particle Hamiltonian are also the **natural orbitals** of the system. The full meaning of the term *natural orbitals* will become clear only later. The natural orbitals have a well defined meaning for many-particle states (interacting or not) and also for their ensembles. They are the eigenstates of the one-particle reduced density matrix. The eigenvalues of the one-particle reduced density matrix are called **occupations**. For the many-particle eigenstates of a Hamiltonian for independent electrons, the natural orbitals are the eigenstates of the one-particle Hamiltonian \hat{h} . For a Slater determinant of natural orbitals, the occupations are equal to the occupation numbers, which can only be zero or one. For an arbitrary many-particle state or an ensemble of many-particle states, the occupations f_n are the averaged occupation numbers σ_n . Thus, the occupations can have any value between zero and one.

Ensembles

In many cases, such as finite temperatures, the state is not uniquely determined. Rather, an ensemble is specified. An **ensemble** $\{(P_q, |\Phi_q\rangle), q = 1, 2, \dots\}$ of states is specified by a set of normalized wave functions $|\Phi_q\rangle$ and their probabilities P_q , which obey $P_q \geq 0$ and $\sum_q P_q = 1$.

The ensemble expectation value is the weighted sum over the states in the ensemble

$$\langle A \rangle = \sum_q P_q \langle \Phi_q | \hat{A} | \Phi_q \rangle \quad (3.51)$$

Thermal equilibrium and Fermi distribution

Thermal ensembles are a special type of ensembles, namely those that describe a system in thermal equilibrium. In thermal equilibrium, the ensemble is specified¹² by the eigenstates and eigenvalues of the Hamiltonian and particle number.¹³ The probabilities $P_{\vec{\sigma}}$ for the eigenstates $|\vec{\sigma}\rangle$ of a non-interacting Hamiltonian are given by the Boltzmann factor

$$P_{\vec{\sigma}} = \frac{1}{Z(T, \mu)} e^{-\beta(E_{\vec{\sigma}} - \mu N_{\vec{\sigma}})} \quad (3.52)$$

where T is the temperature, $\beta = 1/(k_B T)$, and μ the chemical potential.

$$Z(T, \mu) = \sum_{\vec{\sigma}} e^{-\beta(E_{\vec{\sigma}} - \mu N_{\vec{\sigma}})} \quad (3.53)$$

is the partition sum. The corresponding grand potential is $\Omega(T, \mu) = -k_B T \ln(Z(T, \mu))$.

The expectation value of a one-particle operator \hat{A} for a thermal ensemble of a non-interacting Hamiltonian is¹⁴

$$\langle A \rangle = \sum_{\vec{\sigma}} P_{\vec{\sigma}} \langle \vec{\sigma} | \hat{A} | \vec{\sigma} \rangle = \sum_{j=1}^{\infty} \langle \varphi_j | \hat{a} | \varphi_j \rangle \underbrace{\left(\sum_{\vec{\sigma}} P_{\vec{\sigma}} \sigma_j \right)}_{f_n} = \sum_{j=1}^{\infty} f_n \langle \varphi_j | \hat{a} | \varphi_j \rangle \quad (3.54)$$

The thermal expectation value of the occupation number is, for Fermions, the **Fermi distribution** $f_{T, \mu}(\epsilon)$

$$f_n = \left(\sum_{\vec{\sigma}} P_{\vec{\sigma}} \sigma_j \right) = \frac{1}{1 + e^{\beta(\epsilon_j - \mu)}} = f_{T, \mu}(\epsilon_j) \quad (3.55)$$

¹²This is a consequence of the maximum-entropy principle.

¹³This statement is not valid in full generality, but it applies to the problems studied here.

¹⁴without proof

See Fig. 6.3 on p. 191 The proof of this equation is a good exercise for the reader.

MANY-PARTICLE AND ONE-PARTICLE VIEW ON INDEPENDENT ELECTRONS

<p>ensemble: $\{(P_q, \Phi_q\rangle)\}$ <small>probabilities and microstates</small></p> <p>$\sum_q P_q = 1$ and $0 \leq P_q$ and $\langle \Phi_q \Phi_q \rangle = 1$</p> <p>$\hat{\rho}^{vN} = \sum_q \Phi_q\rangle P_q \langle \Phi_q$ <small>von-Neumann density matrix</small></p> <p>$\langle \hat{A} \rangle = \sum_q P_q \langle \Phi_q \hat{A} \Phi_q \rangle = \text{Tr} [\hat{\rho}^{vN} \hat{A}]$ <small>for any (many-particle) operator \hat{A}</small></p>	<p>$\{(f_n, \varphi_n\rangle)\}$ <small>occupations and natural orbitals</small></p> <p>$\sum_n f_n = N$ and $0 \leq f_n \leq 1$</p> <p>$\hat{\rho}^{(1)} = \sum_n \varphi_n\rangle f_n \langle \varphi_n$ <small>one-particle reduced density matrix</small></p> <p>$\langle \hat{A} \rangle = \sum_n f_n \langle \varphi_n \hat{a} \varphi_n \rangle = \text{Tr} [\hat{\rho}^{(1)} \hat{a}]$ <small>only for one-particle (at-a-time) operators \hat{A}</small></p>
---	---

Non-interacting particles

<p>$\hat{H} \vec{\sigma}\rangle = \vec{\sigma}\rangle \left(\underbrace{\sum_n \epsilon_n \sigma_n}_{E_{\vec{\sigma}}} \right)$</p> <p>$\hat{N} \vec{\sigma}\rangle = \vec{\sigma}\rangle \left(\underbrace{\sum_n \sigma_n}_{N_{\vec{\sigma}}} \right)$</p> <p>$\langle \vec{\sigma} \vec{\sigma}' \rangle = \delta_{\vec{\sigma}, \vec{\sigma}'}$</p> <p>$P_{T, \mu, \vec{\sigma}} = \frac{1}{Z_{T, \mu}} e^{-\beta(E_{\vec{\sigma}} - \mu N_{\vec{\sigma}})}$ <small>thermal probabilities</small></p>	<p>$\hat{h} \varphi_n\rangle = \varphi_n\rangle \epsilon_n$</p> <p>$\sum_n f_n = N$</p> <p>$\langle \varphi_m \varphi_n \rangle = \delta_{m, n}$</p> <p>$f_{T, \mu, n} = f_{T, \mu}(\epsilon_n) = \frac{1}{1 + e^{\beta(\epsilon_n - \mu)}}$ <small>Fermi distribution</small></p>
--	--

I am using $\beta = 1/(k_B T)$.

For ensembles, the ensemble may be chosen so that the micro states $|\Phi_q\rangle$ are the eigenstates $|\vec{\sigma}\rangle$ of the Hamiltonian. Then, the index q is equivalent to $q \rightarrow \vec{\sigma}$, so that the probabilities are $P_q \rightarrow P_{\vec{\sigma}}$ and the microstates are $|\Phi_q\rangle \rightarrow |\vec{\sigma}\rangle$. Thermal probabilities $P_{T, \mu, \vec{\sigma}}$ need to be expressed in terms of eigenstates of particle number and Hamiltonian, which, for non-interacting systems, are the Slater determinants $|\vec{\sigma}\rangle$ defined above.

Summary

- The fermionic eigenstates of a non-interacting Hamiltonian for non-interacting particles are Slater determinants. This differs from the eigenstates of an interacting Hamiltonian for which the eigenstate is a superposition of many Slater determinants.
- The thermal expectation value of a one-particle operator \hat{A} is a weighted sum over the expectation values with one-particle eigenstates of the Hamiltonian. The weight is the Fermi distribution function $f_{T, \mu}(\epsilon)$.

$$\langle A \rangle = \sum_{j=1}^{\infty} f_{T, \mu}(\epsilon_j) \langle \varphi_j | \hat{a} | \varphi_j \rangle \tag{3.56}$$

See Fig. 6.3 on p. 191.

3.6 Home study and practice

3.6.1 Two Fermions in a 1d-box

Introduction and background

This exercise explores one-dimensional Fermions in a box. It is closely related to the **jellium model** describing free electrons. The jellium model is a minimal model system for a metal. It removes the complexity of the potential acting on the electrons.

Here, I remove the complexity of the infinite system by introducing a finite box size L . This allows one to inspect individual wave functions. The jellium model is regained in a controlled manner by making the limit of infinite box size and infinite particle number.

By furthermore using a one-dimensional system, the two-particle wave function can still be drawn in all its complexity on a piece of paper.

The goal of this exercise is to provide an understanding of many-particle wave functions of identical particles. The exercise also covers Bosons and distinguishable particles to provide additional context.

Tasks

- 1 Determine the wave functions and energy eigenvalues for a particle with mass m in a N -dimensional square box with side-length L .
Use the result to determine the wave functions and the spectrum for N distinguishable particles in a one-dimensional box.
- 2 Calculate the density of the first particle as function of the one-dimensional particle position x for the ground state of two spin-less^a one-dimensional Fermions in a box. Plot this density for particle numbers $N = 1, 2, 10$. (Use the computer or do a hand-drawn sketch.)
- 3 Calculate the two-particle wave functions for two non-interacting 1-dimensional particles. Sketch the result in a contour plot in the plane of the two particle coordinates and indicate positive and negative regions.
 - (a) ground state of two bosons
 - (b) ground state for two fermions with like spin.
 - (c) ground state for two electrons with opposite spin.
- 4 Consider the ground state of two 1-dimensional spin-less Fermions in a box of sidelength L . Sketch the (conditional) particle density of the second particle given that the first electron is
 - (a) close o the left border,
 - (b) at $x = 0.4L$
 - (c) in the center of the box,
 - (d) close to the right border.
- 5 Rationalize **Hund's rule** for the specific example for two interacting 1-d electrons. (For the sake of the argument use a short-ranged repulsive potential instead of the Coulomb interaction.) Discuss why two non-interacting Fermions have opposite spin in the ground state. Discuss why two interacting electrons with a large short-ranged interaction favors spin-aligned electrons. (Hint: argue on the level of first-order perturbation theory in the interaction.)
- 6 Discuss under the guidance of the tutor the following puzzles: (1) What is the wave function of a zero-particle state? (2) What is the scalar product of two states with different particle numbers.
- 7 The real-space basis functions for two particles is $\{|x_1, x_2\rangle\}$, where x_1, x_2 denote the two coordinates of the particles. (In this case x is the coordinate of a 1-dimensional particle as opposed to the combined position-and-spin coordinate.)

$$\begin{aligned} \langle x_1, x_2 | x'_1, x'_2 \rangle &= \delta(x_1 - x'_1) \delta(x_2 - x'_2) \\ \hat{1} &= \int dx_1 \int dx_2 |x_1, x_2\rangle \langle x_1, x_2| \end{aligned} \quad (3.57)$$

The particle-permutation operator for two one-dimensional particles is

$$\hat{P}_{1,2} = \int dx_1 \int dx_2 |x_2, x_1\rangle \langle x_1, x_2| \quad (3.58)$$

Show that the particle-permutation operator is unitary. Determine the eigenvalues and eigenstates of the particle-permutation operator.

^aA spin-less particle is a scalar particle without a spin index. This concept is often used to simplify the description of Fermions. The concept violates the spin-statistics theorem, which says that Fermions have half-integer spin. The physical situation would be that of a ferromagnetic material, where only one spin direction is of interest.

Discussion

- 1 Determine the wave functions and energy eigenvalues for a particle with mass m in a N -dimensional square box with side-length L .

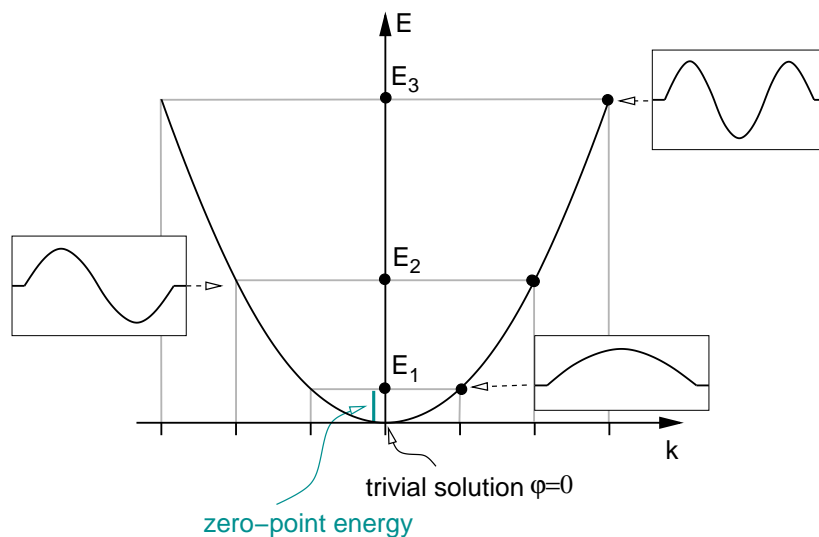
Use the result to determine the wave functions and the spectrum for N distinguishable particles in a one-dimensional box.

1. Particle in a one-dimensional box: The energy eigenstates for a single particle in a one-dimensional box are

$$\varphi_n^{(1)}(x) = \sqrt{\frac{2}{L}} \sin\left(\frac{n\pi}{L}x\right) \quad (3.59)$$

The energy of this state is

$$\epsilon_n = \frac{\hbar^2 \pi^2}{2m_e L^2} n^2 \quad (3.60)$$



The graph shows how the energies are related to the dispersion relation. The dispersion relation $\epsilon(k) = \frac{\hbar^2 k^2}{2m}$ connects the energy with the wave vector¹⁵ $k_n = n\pi/L$, respectively to the momentum $p = \hbar k$. The wave vector is quantized by the boundary conditions. The allowed values of the wave vector lie on an equidistant grid. When the box size is increased, the spacing of the wave vectors shrinks.

Notice the presence of a finite zero-point energy in the finite system. For an infinite system the zero-point energy approaches zero. Caution is required, if a finite zero-point energy makes a qualitative difference, however small it is. It actually makes a difference for the Bose-Einstein condensation.

The insets in the graph show the wave functions.

2. Particle in a two-dimensional box: Notice that the wave functions are single product wave functions formed from one-particle wave functions.

The two-dimensional box with side-length L covers the area $[0, L] \times [0, L]$.

¹⁵In one dimension, the wave vector is a number. It is nevertheless called a vector.

The wave functions for a particle in a 2-dimensional box are of the form

$$\varphi_{n,m}(x,y) = \varphi_n(x)\varphi_m(y) = \frac{2}{L} \sin\left(\frac{n\pi}{L}x\right) \sin\left(\frac{m\pi}{L}y\right) \quad (3.61)$$

The energy of such a state is due to the kinetic energy. It is

$$E_{n,m} = \epsilon_n + \epsilon_m = \frac{\hbar^2\pi^2}{2m_eL^2}(n^2 + m^2) \quad (3.62)$$

3. Particle in a N -dimensional box:

$$\begin{aligned} \varphi_{n_1, n_2, \dots, n_N}(x_1, x_2, \dots, x_N) &= \prod_{j=1}^N \varphi_{n_j}(x_j) = \left(\frac{2}{L}\right)^{\frac{N}{2}} \prod_{j=1}^N \sin\left(\frac{n_j\pi}{L}x_j\right) \\ E_{n_1, n_2, \dots, n_N} &= \sum_{j=1}^N \epsilon_j = \frac{\hbar^2\pi^2}{2m_eL^2} \sum_{j=1}^N n_j^2 \end{aligned}$$

4. N distinguishable particles 1-dimensional box: The wave function for two distinguishable particles is the product of one-particle wave functions. Thus, the wave functions for N one-dimensional particles are identical to those for a single particle in a N dimensional box obtained above.

$$\varphi_{n_1, n_2, \dots, n_N}(x_1, x_2, \dots, x_N) \stackrel{\text{Eq. 3.63}}{=} \prod_{j=1}^N \varphi_{n_j}(x_j) = \left(\frac{2}{L}\right)^{\frac{N}{2}} \prod_{j=1}^N \sin\left(\frac{n_j\pi}{L}x_j\right) \quad (3.63)$$

$$E_{n_1, n_2, \dots, n_N} = \sum_{j=1}^N \epsilon_j \stackrel{\text{Eq. 3.63}}{=} \frac{\hbar^2\pi^2}{2m_eL^2} \sum_{j=1}^N n_j^2 \quad (3.64)$$

2 Calculate the density of the first particle as function of the one-dimensional particle position x for the ground state of two spin-less one-dimensional Fermions in a box. Plot this density for a particle numbers $N = 1, 2, 10$. (Use the computer or do a hand-drawn sketch.)

The total particle density $n^{(1)}(x)$ can be determined from the one-particle wave functions in the Slater determinant as

$$\begin{aligned} n^{(1)}(x) &\stackrel{\text{for } |\vec{\sigma}\rangle}{=} \sum_{n=1}^{\infty} \sigma_n |\varphi_n^{(1)}(x)|^2 \\ &\stackrel{\text{ground state}}{=} \sum_{n=1}^N |\varphi_n^{(1)}(x)|^2 \end{aligned} \quad (3.65)$$

where the σ_n are the occupation numbers. The one-particle states are ordered according to increasing energy. The Fermionic ground state with N particles has occupation numbers $\sigma_n = 1$ for $n \leq N$ and $\sigma_n = 0$ for $n > N$.

The density $n^{(1)}(x)$ is a one-particle-at-a-time density and integrates to the number of particles. The superscript (1) above the density distinguishes the one-particle density from, e.g., the two-particle density.

Because the particles are indistinguishable, the density of each particle is the same as that of any other particle. Thus, the particle density of the first particle is the electron density of all particles

divided by the particle number.

$$\begin{aligned}
 \frac{1}{N} n^{(1)}(x) &= \frac{1}{N} \sum_{n=1}^N |\varphi_n^{(1)}(x)|^2 \\
 &= \frac{1}{N} \frac{2}{L} \sum_{n=1}^N \sin^2\left(\frac{n\pi}{L}x\right) \quad \text{for } 0 < x < L \\
 &= \frac{1}{L} \left(1 + \frac{1}{N}\right) - \frac{1}{N} \frac{1}{L} \sum_{n=0}^N \cos\left(\frac{2n\pi}{L}x\right) \quad \text{for } 0 < x < L
 \end{aligned} \tag{3.66}$$

The last step has not been necessary. It shows the relation to a Fourier transform of a δ -function. The densities per particle are shown in Fig. 3.3.

The oscillations of the particle density are so-called **Friedel oscillations**. They occur around any perturbation of the metallic systems at sufficiently low temperatures. Friedel oscillations are a consequence of the abrupt step in the occupations as function of wave vector.

- 3 Calculate the two-particle wave functions for two non-interacting 1-dimensional particles. Sketch the result in a contour plot in the plane of the two particle coordinates and indicate positive and negative regions.
- (a) ground state of two bosons
 - (b) ground state for two fermions with like spin.
 - (c) ground state for two electrons with opposite spin.

The wave functions for two distinguishable particles

$$\varphi_{n_1, n_2}(x_1, x_2) \stackrel{\text{Eq. 3.63}}{=} \frac{2}{L} \sin\left(\frac{n_1\pi}{L}x_1\right) \sin\left(\frac{n_2\pi}{L}x_2\right) \tag{3.67}$$

$$E_{n_1, n_2} = \stackrel{\text{Eq. 3.63}}{=} \frac{\hbar^2\pi^2}{2mL^2} (n_1^2 + n_2^2) \tag{3.68}$$

To obtain Bosonic and Fermionic wave functions the product state needs to be symmetrized and antisymmetrized, respectively.

- Bosonic ground state: For Bosons in the ground state, both particles occupy the same one-particle orbital. Thus, one needs to symmetrize the state with quantum numbers $n_1 = 1$ and $n_2 = 1$.

$$\begin{aligned}
 \psi^B(x_1, x_2) &= C \left(\varphi_{1,1}(x_1, x_2) + \varphi_{1,1}(x_2, x_1) \right) \\
 &= \varphi_{1,1}(x_1, x_2)
 \end{aligned} \tag{3.69}$$

The constant C is the normalization factor, which is not required. In occupation-number representation, this state is $\vec{\sigma}$ with $\vec{\sigma} = (2, 0, 0, \dots)$. The wave function is shown in the top row of Fig. 3.4.

- Fermionic ground state with two particles with the same spin: For two Fermions with like spin only one of the electrons can occupy the lowest spatial orbital, while the second occupies the second-lowest spatial one-particle orbital. The spatial wave function is the anti-symmetrized orbital $|\varphi_{1,2}\rangle$.

$$\begin{aligned}
 \psi^F(x_1, x_2) &= \frac{1}{\sqrt{2}} \left(\varphi_{1,2}(x_1, x_2) - \varphi_{1,2}(x_2, x_1) \right) \\
 &= \frac{\sqrt{2}}{L} \left(\sin\left(\frac{\pi x_1}{L}\right) \sin\left(\frac{2\pi x_2}{L}\right) - \sin\left(\frac{2\pi x_1}{L}\right) \sin\left(\frac{\pi x_2}{L}\right) \right)
 \end{aligned} \tag{3.70}$$

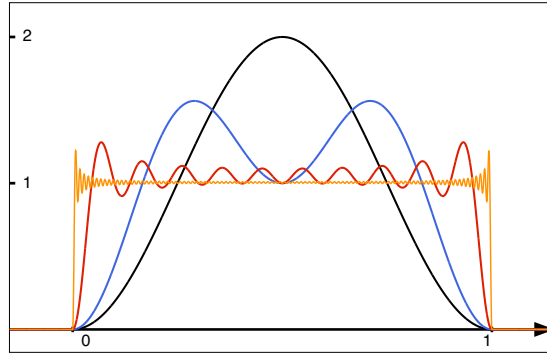


Fig. 3.3: Unconditional density of a single particle in the ground state for N one-dimensional spin-less fermions in a box of sidelength $L = 1$. The density is shown for particle numbers $N = 1$ (black), $N = 2$ (blue), $N = 10$ (red) and $N = 100$ (orange). The oscillations are so-called **Friedel oscillations**. They reflect the wave length of electrons at the Fermi surface. The black line is also the unconditional particle density for bosons in the ground state for arbitrary particle number. It is also the unconditional electron density of two Fermions with opposite spin.

Treating only the spatial dependence results in the wave function for spin-less fermions. Let us now consider the spin degrees-of-freedom as well. As spin orbital, the two-particle wave function has four spin components. The wave function for two Fermions with both spins in the positive z -direction is

$$\psi^{F,\uparrow,\uparrow}(x_1, \sigma_1, x_2, \sigma_2) = \begin{cases} \frac{\sqrt{2}}{L} \left(\sin\left(\frac{\pi x_1}{L}\right) \sin\left(\frac{2\pi x_2}{L}\right) - \sin\left(\frac{2\pi x_1}{L}\right) \sin\left(\frac{\pi x_2}{L}\right) \right) & \text{for } \sigma_1 = \sigma_2 = \uparrow \\ 0 & \text{for } \sigma_1 = \downarrow \text{ and } \sigma_2 = \uparrow \\ 0 & \text{for } \sigma_1 = \uparrow \text{ and } \sigma_2 = \downarrow \\ 0 & \text{for } \sigma_1 = \sigma_2 = \downarrow \end{cases} \quad (3.71)$$

In occupation-number representation, this state is $\vec{\sigma}$ with $\vec{\sigma} = (1, 0, 1, 0, \dots)$. The spin orbitals shall be arranged for the occupation number representation in the order $\underbrace{(1, \uparrow)}_1, \underbrace{(1, \downarrow)}_2, \underbrace{(2, \uparrow)}_3, \underbrace{(2, \downarrow)}_4, \dots$, where the first number identifies the spatial one-particle orbital and the second is the spin quantum number.

The wave function is shown at the bottom row of Fig. 3.4.

- Fermionic ground state for two electrons with opposite spin: For two Fermions with like opposite spin, both electrons may occupy the lowest spatial one-particle orbital, because they have opposite spin

Now we need to consider the antisymmetry of the wave function. Let us start with one-particle spin orbitals

$$\begin{aligned} \psi_{1,\uparrow}(x, \sigma) &= \begin{cases} \sqrt{\frac{2}{L}} \sin\left(\frac{\pi x}{L}\right) & \text{for } \sigma = \uparrow \\ 0 & \text{for } \sigma = \downarrow \end{cases} \\ \psi_{1,\downarrow}(x, \sigma) &= \begin{cases} 0 & \text{for } \sigma = \uparrow \\ \sqrt{\frac{2}{L}} \sin\left(\frac{\pi x}{L}\right) & \text{for } \sigma = \downarrow \end{cases} \end{aligned} \quad (3.72)$$

$$\begin{aligned}
 \psi^F(x_1, \sigma_1, x_2, \sigma_2) &= \frac{1}{\sqrt{2}} \left(\psi_{1,\uparrow}(x_1, \sigma_1) \psi_{1,\downarrow}(x_2, \sigma_2) - \psi_{1,\downarrow}(x_1, \sigma_1) \psi_{1,\uparrow}(x_2, \sigma_2) \right) \\
 &= \begin{cases} 0 & \text{for } \sigma_1, \sigma_2 = \uparrow \\ -\frac{1}{\sqrt{2}} \psi_{1,\downarrow}(x_1, \downarrow) \psi_{1,\uparrow}(x_2, \uparrow) & \text{for } \sigma_1 = \downarrow \text{ and } \sigma_2 = \uparrow \\ +\frac{1}{\sqrt{2}} \psi_{1,\uparrow}(x_1, \uparrow) \psi_{1,\downarrow}(x_2, \downarrow) & \text{for } \sigma_1 = \uparrow \text{ and } \sigma_2 = \downarrow \\ 0 & \text{for } \sigma_1, \sigma_2 = \downarrow \end{cases} \\
 &= \varphi_1^{(1)}(x_1) \varphi_1^{(1)}(x_2) \frac{1}{\sqrt{2}} (|\downarrow, \uparrow\rangle - |\uparrow, \downarrow\rangle) \quad (3.73)
 \end{aligned}$$

4 Consider the ground state of two 1-dimensional spin-less Fermions in a box of sidelength L . Sketch the (conditional) particle density of the second particle given that the first electron is

- (a) close o the left border,
- (b) at $x = 0.4L$
- (c) in the center of the box,
- (d) close to the right border.

We begin with the two-particle wave function obtained above

$$\psi^F(x_1, \uparrow, x_2, \uparrow) = \frac{\sqrt{2}}{L} \left(\sin\left(\frac{\pi x_1}{L}\right) \sin\left(\frac{2\pi x_2}{L}\right) - \sin\left(\frac{2\pi x_1}{L}\right) \sin\left(\frac{\pi x_2}{L}\right) \right) \quad (3.74)$$

The other spin components of this wave function vanish.

The conditional density $n_X(x)$ of particle 2 given that particle 1 is at a given position X is the probability that particle 1 is at X and particle 2 is at x , divided by the probability that particle 1 is at X independent of the position of particle 2.

$$\begin{aligned}
 n_{x_1}(x_2) &= \frac{n^{(2)}(x_1, x_2)}{n^{(1)}(x_1)} \\
 &= \frac{|\psi^F(x_1, \uparrow, x_2, \uparrow)|^2}{\int dx'_1 |\psi^F(x'_1, \uparrow, x_2, \uparrow)|^2} \\
 n^{(2)}(x_1, x_2) &= \frac{2}{L^2} \left(\underbrace{\sin^2\left(\frac{\pi x_1}{L}\right)}_{\frac{1}{2} - \frac{1}{2} \cos(2\pi x/L)} \sin^2\left(\frac{2\pi x_2}{L}\right) - \underbrace{\sin\left(\frac{\pi x_1}{L}\right) \sin\left(\frac{2\pi x_1}{L}\right)}_{\frac{1}{2} \cos(\pi x/L) + \frac{1}{2} \cos(3\pi x/L)} \sin\left(\frac{\pi x_2}{L}\right) \sin\left(\frac{2\pi x_2}{L}\right) \right. \\
 &\quad \left. - \underbrace{\sin\left(\frac{2\pi x_1}{L}\right) \sin\left(\frac{\pi x_1}{L}\right)}_{\frac{1}{2} \cos(\pi x/L) + \frac{1}{2} \cos(3\pi x/L)} \sin\left(\frac{\pi x_2}{L}\right) \sin\left(\frac{2\pi x_2}{L}\right) + \underbrace{\sin^2\left(\frac{2\pi x_1}{L}\right)}_{\frac{1}{2} - \frac{1}{2} \cos(4\pi x/L)} \sin^2\left(\frac{\pi x_2}{L}\right) \right) \quad (3.75)
 \end{aligned}$$

The electron density is one half of the total density. The total density is obtained by adding up the densities of the two one-particle orbitals.

$$n^{(1)}(x) = \frac{2}{L} \left(\sin^2\left(\frac{\pi x}{L}\right) + \sin^2\left(\frac{2\pi x}{L}\right) \right) = \frac{2}{L} \left(1 - \frac{1}{2} \cos\left(\frac{\pi x}{L}\right) - \frac{1}{2} \cos\left(\frac{4\pi x}{L}\right) \right) \quad (3.76)$$

The conditional densities are shown in Fig. 3.5. Notice that the conditional density vanishes at the position of the first electron. The difference between the conditional density and the total density is the so-called **exchange-correlation hole**. The exchange-correlation hole integrates to -1 .

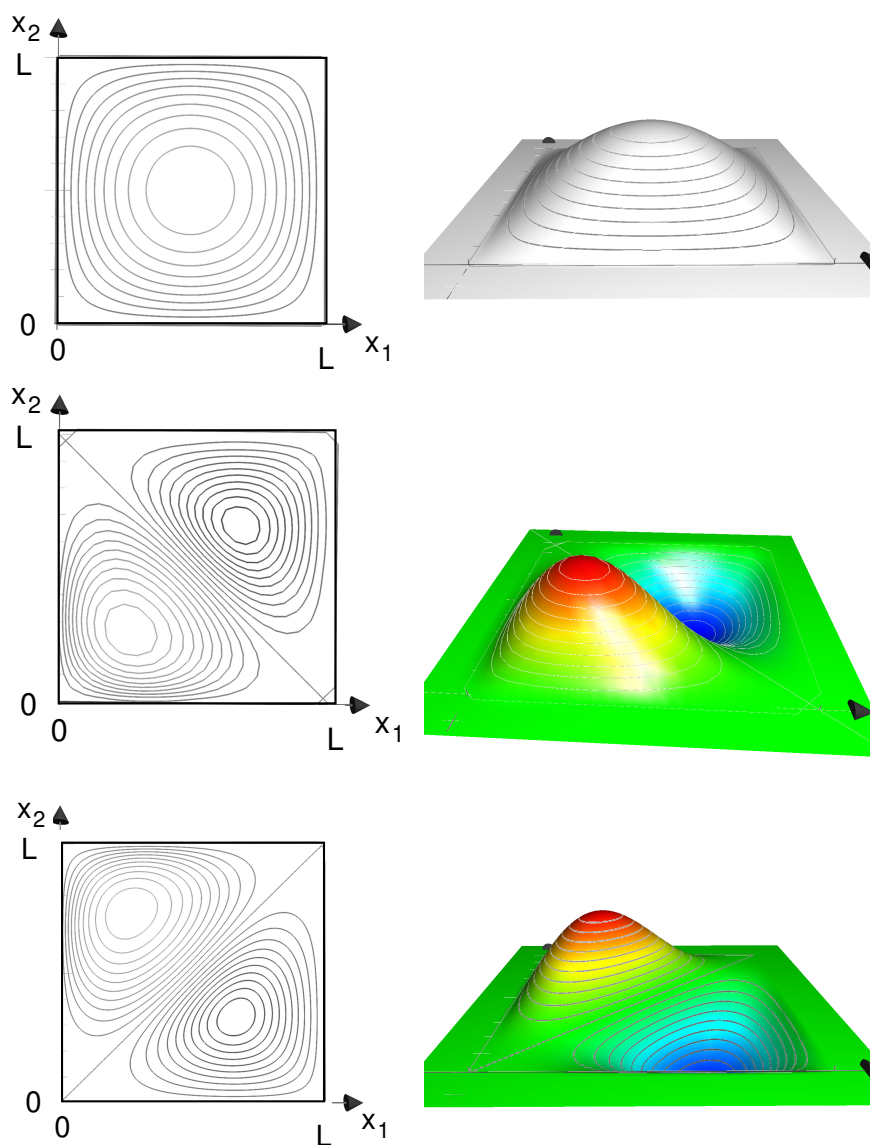


Fig. 3.4: Top. Bosonic ground-state wave function of two particles in box. Middle. Bosonic function of two particles in box of which one is in the lowest one-particle orbital and the other is in the first excited state. Bottom: Fermionic ground state wave function. [Editor: Add labels and the box to the figures.](#)

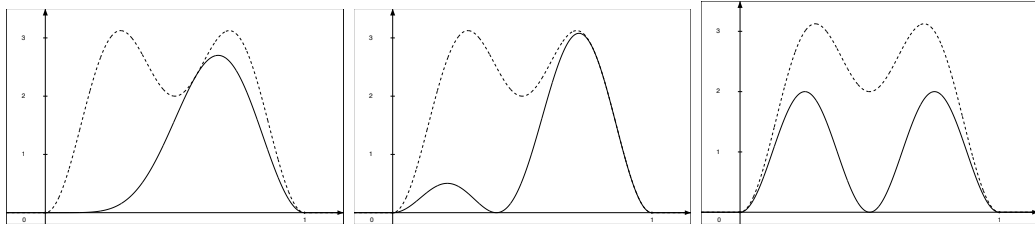


Fig. 3.5: Conditional density of the second electron given that the first electron is at position 0, 0.4, 0.5 for two Fermions in a box in the ground state. The dashed line is the total particle density.

It acts like a negative particle density surrounding one-electron, making the electron together with its exchange-correlation hole a neutral object.

6 Discuss under the guidance of the tutor the following puzzles: (1) What is the wave function of a zero particle state? (2) What is the scalar product of two states with different particle numbers.

There is no zero-particle wave function, because it would not have any arguments. The zero-particle state, however, has a phase. Therefore, the zero particle state is a complex-valued number.

A common mistake is to describe the zero particle state as a function of some particle coordinates, albeit with constant value. This mistake happens usually when trying to add a zero particle state and a one-particle state. The result cannot be simplified to a single function.

The scalar product of two states with different particle numbers can not be formed in real space, because the two functions have different numbers of arguments.

The scalar product can be given in the Fock space, because then the particle number is not a parameter but an observable represented by a hermitian operator. Since eigenstates of a hermitian operator to different eigenvalues are orthogonal, the scalar product of states with different particle numbers is zero.

4 The real-space basis functions for two particles is $\{|x_1, x_2\rangle\}$, where x_1, x_2 denote the two coordinates of the particles. (In this case x is the coordinate of a 1-dimensional particle as opposed to the combined position-and-spin coordinate.)

$$\langle x_1, x_2 | x'_1, x'_2 \rangle = \delta(x_1 - x'_1) \delta(x_2 - x'_2)$$

$$\hat{1} = \int dx_1 \int dx_2 |x_1, x_2\rangle \langle x_1, x_2| \tag{3.77}$$

The particle-permutation operator for two one-dimensional particles is

$$\hat{P}_{1,2} = \int dx_1 \int dx_2 |x_2, x_1\rangle \langle x_1, x_2| \tag{3.78}$$

Show that the particle-permutation operator is unitary. Determine the eigenvalues and eigenstates of the particle-permutation operator.

1. **Show that the particle permutation operator is unitary:** The permutation operator is

$$\hat{P}_{12} = \int dx_1 \int dx_2 |x_2, x_1\rangle \langle x_1, x_2| \tag{3.79}$$

This implies for wave functions

$$\begin{aligned} |\Psi'\rangle &\stackrel{\text{def}}{=} \hat{P}_{12}|\Psi\rangle \\ \Psi'(x_1, x_2) &= \langle x_1, x_2 | \hat{P}_{12} | \Psi \rangle = \langle x_2, x_1 | \Psi \rangle = \Psi(x_2, x_1) \end{aligned} \quad (3.80)$$

An operator is unitary, if its adjoint is its inverse. That is, it is unitary if $\hat{P}\hat{P}^\dagger = \hat{1}$.

The adjoint can be obtained by exchanging bra's and kets.

$$\hat{P}_{12}^\dagger = \int dx_1 \int dx_2 |x_1, x_2\rangle \langle x_2, x_1| \quad (3.81)$$

The equation above also shows that the permutation operator is furthermore hermitean, i.e.

$$\hat{P}_{12}^\dagger = \hat{P}_{12} \quad (3.82)$$

Now we can show that particle permutation operator is unitary

$$\begin{aligned} \hat{P}_{12}\hat{P}_{12}^\dagger &\stackrel{?}{=} \hat{1} \\ \hat{P}_{12}\hat{P}_{12}^\dagger &= \underbrace{\int dx_1 \int dx_2 |x_2, x_1\rangle \langle x_1, x_2|}_{\hat{P}_{12}} \underbrace{\int dx'_1 \int dx'_2 |x'_1, x'_2\rangle \langle x'_2, x'_1|}_{\hat{P}_{12}^\dagger} \\ &= \int dx_1 \int dx_2 \int dx'_1 \int dx'_2 |x_2, x_1\rangle \underbrace{\langle x_1, x_2 | x'_1, x'_2 \rangle}_{\delta(x_1-x'_1)\delta(x_2-x'_2)} \langle x'_2, x'_1| \\ &= \int dx_1 \int dx_2 |x_2, x_1\rangle \langle x_2, x_1| = \hat{1} \quad \text{q.e.d} \end{aligned} \quad (3.83)$$

Thus, the permutation operator is unitary.

2. Eigenvalues of the permutation operator: As shown above, the permutation operator is unitary and hermitian. Hence, the permutation operator is cyclic $\hat{P}_{12}^2 = \hat{1}$.

Because $\hat{P}_{12}^2 = \hat{1}$, the eigenvalues of \hat{P}_{12} are +1 and -1.

3. Eigenstates of the permutation operator:

- The eigenstates $|\Psi^B\rangle$ for eigenvalue +1 are bosonic states

$$\begin{aligned} |\Psi^B\rangle &\stackrel{\text{Eq. 3.36}}{=} |\Psi^D\rangle + \hat{P}_{12}|\Psi^D\rangle \\ \Psi^B(x_1, x_2) &= \Psi^D(x_1, x_2) + \Psi^D(x_2, x_1) \end{aligned} \quad (3.84)$$

where $\Psi^D(x_1, x_2)$ is an arbitrary wave function (for two distinguishable particles). The resulting state is not normalized. It can occur that symmetrized wave function vanishes. (This occurs when Ψ is antisymmetric.)

- The eigenstates Ψ^F for eigenvalue -1 are Fermionic states

$$\begin{aligned} |\Psi^F\rangle &= |\Psi^D\rangle - \hat{P}_{12}|\Psi^D\rangle \\ \Psi^F(x_1, x_2) &= \Psi^D(x_1, x_2) - \Psi^D(x_2, x_1) \end{aligned} \quad (3.85)$$

where $\Psi^D(x_1, x_2)$ is an arbitrary wave function (for two distinguishable particles). The resulting state is not normalized. It can occur that antisymmetrized wave function vanishes. (This occurs when Ψ is symmetric.)

- 5 Determine the wave functions and spectra for two Fermions in a 1-d box and for two Bosons. From the multiplicity of the states, respectively the spectra argue, why two identical Fermions cannot be in one orbital (Pauli principle) and why Bosons are preferably in the same orbital. That is, show that the probability to find two particles in the same orbital is higher for bosons than for distinguishable particles. (Bunching and anti-bunching.)

1. **Construct the Fermionic (anti symmetric) and Bosonic (symmetric) eigenstates of the Hamiltonian**

Fermions:

$$\begin{aligned}
 |\Psi_{n,m}^F\rangle &= \frac{1}{\sqrt{2}} \left(|\Psi_{n,m}^D\rangle - \hat{P}_{12} |\Psi_{n,m}^D\rangle \right) \\
 \psi_{n,m}^F(x,y) &= \frac{\sqrt{2}}{L} \left(\sin\left(\frac{n\pi}{L}x\right) \sin\left(\frac{m\pi}{L}y\right) - \sin\left(\frac{m\pi}{L}x\right) \sin\left(\frac{n\pi}{L}y\right) \right) \quad \text{for } n > m
 \end{aligned} \tag{3.86}$$

If a fermionic two-particle wave function $|\Psi_{nm}\rangle$ is constructed from two one-particle states $|\varphi_n\rangle$, $|\Psi_{n,m}\rangle$ is a Slater determinant.

$$\Psi_{n,m}^F(x,y) = \frac{\sqrt{2}}{L} \det \begin{vmatrix} \sin\left(\frac{n\pi}{L}x\right) & \sin\left(\frac{m\pi}{L}x\right) \\ \sin\left(\frac{n\pi}{L}y\right) & \sin\left(\frac{m\pi}{L}y\right) \end{vmatrix} \tag{3.87}$$

We find that the wave function with two electrons in the same orbital vanishes, $|\Psi_{n,n}^F\rangle = |\emptyset\rangle$, which says that there is no Fermionic state with two identical Fermions in the same one-particle state. This is one consequence of the Pauli principle.

We find $|\Psi_{n,m}^F\rangle = -|\Psi_{m,n}^F\rangle$. Interchanging the quantum numbers of a Fermionic state does not produce a new state.

The energies are

$$E_{n,m} = \sum_{j=1}^2 \epsilon_j = \frac{\hbar^2 \pi^2}{2m_e L^2} (n^2 + m^2) \quad \text{for } n > m \tag{3.88}$$

Note that the states with $n < m$ are, up to a phase factor identical to the one with exchanged quantum numbers. States with two equal quantum numbers are zero states and therefore excluded from the sum. This indicates that Fermions try to stay away from each other (anti-bunching).

Bosons:

$$\begin{aligned}
 |\psi_{n,m}^B\rangle &= \begin{cases} |\psi_{n,n}^D\rangle & \text{for } n = m \\ \frac{1}{\sqrt{2}} (|\Psi_{n,m}^D\rangle + \hat{P}_{12} |\Psi_{n,m}^D\rangle) & \text{for } m < n \end{cases} \\
 \psi_{n,m}^B(x,y) &= \begin{cases} \frac{2}{L} \sin\left(\frac{n\pi}{L}x\right) \sin\left(\frac{n\pi}{L}y\right) & \text{for } n = m \\ \frac{\sqrt{2}}{L} \left(\sin\left(\frac{n\pi}{L}x\right) \sin\left(\frac{m\pi}{L}y\right) + \sin\left(\frac{m\pi}{L}x\right) \sin\left(\frac{n\pi}{L}y\right) \right) & \text{for } m < n \end{cases}
 \end{aligned} \tag{3.89}$$

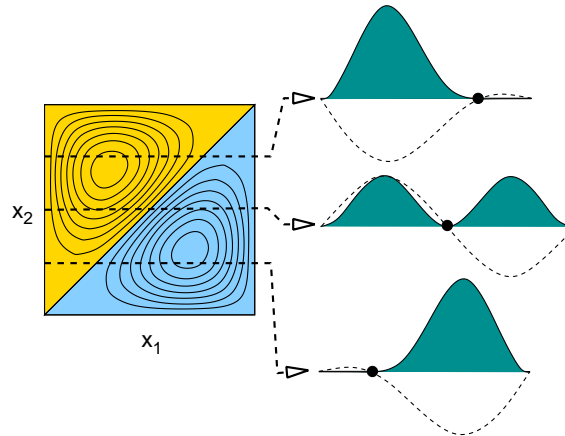


Fig. 3.6: Ground state wave function of two spin-less fermions in a 1d-box. The coordinates of the two electrons are x_1 and x_2 . (Note, that x does not refer to the combined position-and-spin representation.) The colors indicate the sign of the wave function. On the right, the density (filled area) and wave function (dashed line) of the first electron is shown for specific frozen positions of the second electron.

The energies are

$$E_{n,m} = \sum_{j=1}^2 \epsilon_j = \frac{\hbar^2 \pi^2}{2m_e L^2} (n^2 + m^2) \quad \text{for } m \leq n \quad (3.90)$$

Note here, that the states with equal quantum numbers are present. Per state with unequal quantum numbers, there are twice as many states with equal quantum numbers as in the case of distinguishable particles. This is an indication that bosons prefer to be next to each other (bunching).

Gnuplot example

Fig. 3.6 has been drawn by graphical tool Gnuplot. Here, a small script is provided for gnuplot. Simply paste it into a file 'boxtwoparticle.gnu' and run the command 'gnuplot boxtwoparticle.gnu'

```
#Set terminal postscript
#set output "boxtwoparticle.eps"
set terminal png
set output "boxtwoparticle.png"
#set terminal latex
#set terminal fig
#set output "boxtwoparticle.fig"
#set size 1.0,1.0
set size ratio 1.0
set nokey
set contour
set view 30, 20
#set view 0, 0
set contour surface
set hidden3d
set isosamples 40, 40
set ticslevel -0.5
```

```
#unset surface
unset xtics
unset ytics
unset ztics
set cntrparam cubicspline
set cntrparam levels auto 20
splot[0:1][0:1](-sin(x*pi)*sin(2*y*pi)+sin(2*x*pi)*sin(y*pi))
```

3.6.2 Expectation values with a Slater determinant

Introduction and background

The energy eigenstates of non-interacting electrons are Slater-determinants. This allows one to represent the expectation values of one-particle operators in terms of one-particle wave functions. This makes the description of non-interacting electrons much simpler than that of interacting electrons.

Non-interacting electrons experience a one-particle Hamilton operator $\hat{h} = \frac{\hat{p}^2}{2m_e} + \hat{v}$. The Hamilton operator of N electrons is $\hat{H} = \sum_{j=1}^N \hat{h}_j$, where \hat{h}_j is the operator \hat{h} acting on the momenta and coordinates of the j -th electron.

The one-particle eigenstates $|\varphi_n\rangle$ of \hat{h} and its eigenvalues ϵ_n obey

$$\hat{h}|\varphi_n\rangle = |\varphi_n\rangle\epsilon_n \quad (3.91)$$

Tasks

1 Form the Slater-determinant from two one-particle states (e.g. eigenstates of \hat{h}) with indices n_1 and n_2 as function of the coordinates of the two electrons $\vec{x}_j \stackrel{\text{def}}{=} (\vec{r}_j, \sigma_j)$ with $j = 1, 2$.

2 Evaluate the electron density^a

$$n(\vec{r}) = \langle \Phi | \left\{ \sum_{\sigma} \int d^4x' (|\vec{x}, \vec{x}'\rangle \langle \vec{x}, \vec{x}'| + |\vec{x}', \vec{x}\rangle \langle \vec{x}', \vec{x}|) \right\} | \Phi \rangle \quad (3.92)$$

where $\vec{x} = (\vec{r}, \sigma)$ and $\vec{x}' = (\vec{r}', \sigma')$, for the wave function $|\Phi\rangle$, which is the Slater determinant described above.

3 Exploit the analogy with the previous exercise to provide the expressions for the total energy, the number of electrons and the electron density. (Do not guess, but check the validity of the analogy step-by-step.)

4 Express the Coulomb energy of a two-particle Slater determinant in terms of matrix elements of one-particle orbitals. Exploit orthonormality of the one-particle orbitals. Identify Hartree and exchange energy.

^aDistinguish the electron density from the charge density.

Discussion

1 Form the Slater-determinant from two one-particle states (e.g. eigenstates of \hat{h}) with indices n_1 and n_2 as function of the coordinates of the two electrons $\vec{x}_j \stackrel{\text{def}}{=} (\vec{r}_j, \sigma_j)$ with $j = 1, 2$.

The state $|\vec{x}, \vec{x}'\rangle = |\vec{x}\rangle \otimes |\vec{x}'\rangle$ is a product state of $|\vec{x}\rangle$ and $|\vec{x}'\rangle$.

Therefore, the orthogonality condition is

$$\begin{aligned}\langle \vec{x}_1, \vec{x}_2 | \vec{x}'_1, \vec{x}'_2 \rangle &= \delta(\vec{x}_1 - \vec{x}'_1) \delta(\vec{x}_2 - \vec{x}'_2) \\ &= \delta_{\sigma_1, \sigma'_1} \delta(\vec{r}_1 - \vec{r}'_1) \delta_{\sigma_2, \sigma'_2} \delta(\vec{r}_2 - \vec{r}'_2)\end{aligned}\quad (3.93)$$

where $\vec{x}_1 = (\vec{r}_1, \sigma_1)$, $\vec{x}_2 = (\vec{r}_2, \sigma_2)$, $\vec{x}'_1 = (\vec{r}'_1, \sigma'_1)$, $\vec{x}'_2 = (\vec{r}'_2, \sigma'_2)$, and the completeness relation is

$$\int d^4 x_1 \int d^4 x_2 |\vec{x}_1, \vec{x}_2\rangle \langle \vec{x}_1, \vec{x}_2| = \hat{1}\quad (3.94)$$

Where $\hat{1}$ is the unit operator in the two-particle Hilbert space.

$$\begin{aligned}\langle \vec{x}, \vec{x}' | \Phi \rangle &= \frac{1}{\sqrt{2}} \left(\langle \vec{x}, \vec{x}' | n_1, n_2 \rangle - \langle \vec{x}, \vec{x}' | n_2, n_1 \rangle \right) \\ &= \frac{1}{\sqrt{2}} \left(\langle \vec{x} | n_1 \rangle \langle \vec{x}' | n_2 \rangle - \langle \vec{x} | n_2 \rangle \langle \vec{x}' | n_1 \rangle \right) \\ &= \frac{1}{\sqrt{2}} \left(\varphi_{n_1}(\vec{x}) \varphi_{n_2}(\vec{x}') - \varphi_{n_2}(\vec{x}) \varphi_{n_1}(\vec{x}') \right)\end{aligned}\quad (3.95)$$

2 evaluate the electron density

$$n(\vec{r}) = \langle \Phi | \left\{ \sum_{\sigma} \int d^4 x' (|\vec{x}, \vec{x}'\rangle \langle \vec{x}, \vec{x}'| + |\vec{x}', \vec{x}\rangle \langle \vec{x}', \vec{x}|) \right\} | \Phi \rangle \quad (3.96)$$

where $\vec{x} = (\vec{r}, \sigma)$ and $\vec{x}' = (\vec{r}', \sigma')$, for the wave function $|\Phi\rangle$, which is the Slater determinant described above.

$$\begin{aligned}n(\vec{r}) &= \langle \Phi | \sum_{\sigma} \int d^4 x' (|\vec{x}, \vec{x}'\rangle \langle \vec{x}, \vec{x}'| + |\vec{x}', \vec{x}\rangle \langle \vec{x}', \vec{x}|) | \Phi \rangle \\ &= \sum_{\sigma} \int d^4 x' \\ &\times \left\{ \frac{1}{\sqrt{2}} \left(\underbrace{\varphi_{n_1}^*(\vec{x}) \varphi_{n_2}^*(\vec{x}')}_{A} - \underbrace{\varphi_{n_2}^*(\vec{x}) \varphi_{n_1}^*(\vec{x}')}_{B} \right) \frac{1}{\sqrt{2}} \left(\underbrace{\varphi_{n_1}(\vec{x}) \varphi_{n_2}(\vec{x}')}_{C} - \underbrace{\varphi_{n_2}(\vec{x}) \varphi_{n_1}(\vec{x}')}_{D} \right) \right. \\ &\quad \left. + \frac{1}{\sqrt{2}} \left(\underbrace{\varphi_{n_1}^*(\vec{x}') \varphi_{n_2}^*(\vec{x})}_{B} - \underbrace{\varphi_{n_2}^*(\vec{x}') \varphi_{n_1}^*(\vec{x})}_{A} \right) \frac{1}{\sqrt{2}} \left(\underbrace{\varphi_{n_1}(\vec{x}') \varphi_{n_2}(\vec{x})}_{D} - \underbrace{\varphi_{n_2}(\vec{x}') \varphi_{n_1}(\vec{x})}_{C} \right) \right\}\end{aligned}\quad (3.97)$$

In total there are 8 terms. For N-particle Slater determinant the number of terms is $N(N!)^2$.

The first line is the density of the first electron, while the second line is the density of the second electron. These two densities are identical, because the two particles are indistinguishable. This property is hidden in the antisymmetrization. The letters in the equation above identify identical terms. It shows that the first and the second line, the densities of first and second electron, are identical.

Therefore, we proceed with the first line and multiply it by two.

$$\begin{aligned}
 n(\vec{r}) &= \sum_{\sigma} \int d^4 x' \\
 &\times \underbrace{\left(\varphi_{n_1}^*(\vec{x}) \varphi_{n_2}^*(\vec{x}') - \varphi_{n_2}^*(\vec{x}) \varphi_{n_1}^*(\vec{x}') \right)}_A \underbrace{\left(\varphi_{n_1}(\vec{x}) \varphi_{n_2}(\vec{x}') - \varphi_{n_2}(\vec{x}) \varphi_{n_1}(\vec{x}') \right)}_B \\
 &= \sum_{\sigma} \int d^4 x' \\
 &\times \left(\underbrace{\varphi_{n_1}^*(\vec{x}) \varphi_{n_2}^*(\vec{x}') \varphi_{n_1}(\vec{x}) \varphi_{n_2}(\vec{x}')}_A - \underbrace{\varphi_{n_1}^*(\vec{x}) \varphi_{n_2}^*(\vec{x}') \varphi_{n_2}(\vec{x}) \varphi_{n_1}(\vec{x}')}_A \right. \\
 &\quad \left. - \underbrace{\varphi_{n_2}^*(\vec{x}) \varphi_{n_1}^*(\vec{x}') \varphi_{n_1}(\vec{x}) \varphi_{n_2}(\vec{x}')}_B + \underbrace{\varphi_{n_2}^*(\vec{x}) \varphi_{n_1}^*(\vec{x}') \varphi_{n_2}(\vec{x}) \varphi_{n_1}(\vec{x}')}_B \right) \\
 &= \sum_{\sigma} \\
 &\times \left(\varphi_{n_1}^*(\vec{x}) \varphi_{n_1}(\vec{x}) \underbrace{\int d^4 x' \varphi_{n_2}^*(\vec{x}') \varphi_{n_2}(\vec{x}')}_{=\langle \varphi_{n_2} | \varphi_{n_2} \rangle = 1} - \varphi_{n_1}^*(\vec{x}) \varphi_{n_2}(\vec{x}) \underbrace{\int d^4 x' \varphi_{n_2}^*(\vec{x}') \varphi_{n_1}(\vec{x}')}_{=\langle \varphi_{n_2} | \varphi_{n_1} \rangle = 0} \right. \\
 &\quad \left. - \varphi_{n_2}^*(\vec{x}) \varphi_{n_1}(\vec{x}) \underbrace{\int d^4 x' \varphi_{n_1}^*(\vec{x}') \varphi_{n_2}(\vec{x}')}_{=\langle \varphi_{n_1} | \varphi_{n_2} \rangle = 0} + \varphi_{n_2}^*(\vec{x}) \varphi_{n_2}(\vec{x}) \underbrace{\int d^4 x' \varphi_{n_1}^*(\vec{x}') \varphi_{n_1}(\vec{x}')}_{=\langle \varphi_{n_1} | \varphi_{n_1} \rangle = 1} \right) \\
 &= \sum_{\sigma} \left(\varphi_{n_1}^*(\vec{x}) \varphi_{n_1}(\vec{x}) + \varphi_{n_2}^*(\vec{x}) \varphi_{n_2}(\vec{x}) \right) \quad \text{for } n_1 \neq n_2 \tag{3.98}
 \end{aligned}$$

The result is the sum of the densities of the two one-particle orbitals. One might argue that there is one electron in each of the orbitals. This is not so. Both electrons are in both orbitals with the same probability.

Now, the number of terms for N electrons is simply N , a tremendous simplification compared to the $N(N!)^2$ terms, we had before. This was only possible by choosing an orthonormal basis set. If the Slater determinant would have been built from two non-orthonormal orbitals, the number of terms would not be lowered. This simplification is the main reason for choosing orthonormal basis sets in many-particle physics.

The density of two electrons in the same orbital vanishes, because then the two terms with the negative sign cancel those with positive sign.

3 Exploit the analogy with the previous exercise to provide the expressions for the total energy, the number of electrons and the electron density. (Do not guess, but check the validity of the analogy step-by-step.)

$$\begin{aligned}
 E &= \langle \Phi | \hat{h}_1 + \hat{h}_2 | \Phi \rangle = \langle \varphi_{n_1} | \hat{h} | \varphi_{n_1} \rangle + \langle \varphi_{n_2} | \hat{h} | \varphi_{n_2} \rangle = \epsilon_{n_1} + \epsilon_{n_2} \\
 N &= \langle \Phi | \hat{1}_1 + \hat{1}_2 | \Phi \rangle = \langle \varphi_{n_1} | \hat{1} | \varphi_{n_1} \rangle + \langle \varphi_{n_2} | \hat{1} | \varphi_{n_2} \rangle = 2 \tag{3.99}
 \end{aligned}$$

This result can be generalized to

$$\begin{aligned}
 E &= \sum_n f_n \epsilon_n \\
 N &= \sum_n f_n \\
 n(\vec{r}) &= \sum_{\sigma \in \{\uparrow, \downarrow\}} \sum_{n=1}^{\infty} \varphi_n^*(\vec{r}, \sigma) f_n \varphi_n(\vec{r}, \sigma) \tag{3.100}
 \end{aligned}$$

where $f_n \in \{0, 1\}$ are the occupations of the orbitals in the Slater determinant.

The vector $|f_1, f_2, f_3, \dots\rangle$ is the occupation number representation of the Slater determinant. If one averages over several Slater determinants, the occupations are replaced by their averages $\langle f_j \rangle$. This yields fractional occupations for ensembles of Slater determinants.

Occupations can also be defined for interacting many-particle wave functions. Then, they are the eigenvalues of the one-particle reduced density matrix.

4 Express the Coulomb energy of a two-particle Slater determinant in terms of matrix elements of one-particle orbitals. Exploit orthonormality of the one-particle orbitals. Identify Hartree and exchange energy.

Let us start with the Coulomb-interaction operator

$$\hat{W}_{i,j} = \frac{e^2}{4\pi\epsilon_0|\hat{r}_i - \hat{r}_j|} \quad (3.101)$$

where \hat{r}_i is the position operator for the i -th electron and \hat{r}_j is the position of the j -th electron.

The Slater determinant for which we evaluate the expectation value is formed from the two one-particle orbitals $|\varphi_a\rangle$ and $|\varphi_b\rangle$.

The expectation value of the Coulomb interaction is

$$\begin{aligned} E_{int} &= \langle \Psi | \hat{W} | \Psi \rangle = \langle \Psi | \frac{1}{2} \sum_{\substack{i,j=1 \\ i \neq j}}^2 \hat{W}_{i,j} | \Psi \rangle \\ &= \int d^4x_1 \int d^4x_2 \Psi^*(\vec{x}_1, \vec{x}_2) \frac{1}{2} [W(\vec{x}_1, \vec{x}_2) + W(\vec{x}_2, \vec{x}_1)] \Psi(\vec{x}_1, \vec{x}_2) \\ &\stackrel{\Psi(\vec{x}_1, \vec{x}_2) = -\Psi(\vec{x}_2, \vec{x}_1)}{=} \int d^4x_1 \int d^4x_2 \Psi^*(\vec{x}_1, \vec{x}_2) W(\vec{x}_1, \vec{x}_2) \Psi(\vec{x}_1, \vec{x}_2) \\ &\stackrel{\text{Eq. ??}}{=} \int d^4x_1 \int d^4x_2 \frac{1}{\sqrt{2}} [\varphi_a(\vec{x}_1)\varphi_b(\vec{x}_2) - \varphi_a(\vec{x}_2)\varphi_b(\vec{x}_1)]^* \\ &\quad \cdot W(\vec{x}_1, \vec{x}_2) \frac{1}{\sqrt{2}} [\varphi_a(\vec{x}_1)\varphi_b(\vec{x}_2) - \varphi_a(\vec{x}_2)\varphi_b(\vec{x}_1)] \\ &= \frac{1}{2} \int d^4x_1 \int d^4x_2 \varphi_a^*(\vec{x}_1)\varphi_b^*(\vec{x}_2) W(\vec{x}_1, \vec{x}_2) \varphi_a(\vec{x}_1)\varphi_b(\vec{x}_2) \\ &\quad - \frac{1}{2} \int d^4x_1 \int d^4x_2 \varphi_a^*(\vec{x}_1)\varphi_b^*(\vec{x}_2) W(\vec{x}_1, \vec{x}_2) \varphi_a(\vec{x}_2)\varphi_b(\vec{x}_1) \\ &\quad - \frac{1}{2} \int d^4x_1 \int d^4x_2 \varphi_a^*(\vec{x}_2)\varphi_b^*(\vec{x}_1) W(\vec{x}_1, \vec{x}_2) \varphi_a(\vec{x}_1)\varphi_b(\vec{x}_2) \\ &\quad + \frac{1}{2} \int d^4x_1 \int d^4x_2 \varphi_a^*(\vec{x}_2)\varphi_b^*(\vec{x}_1) W(\vec{x}_1, \vec{x}_2) \varphi_a(\vec{x}_2)\varphi_b(\vec{x}_1) \\ &= \underbrace{\int d^4x_1 \int d^4x_2 \varphi_a^*(\vec{x}_1)\varphi_b^*(\vec{x}_2) \frac{1}{2} [W(\vec{x}_1, \vec{x}_2) + W(\vec{x}_2, \vec{x}_1)] \varphi_a(\vec{x}_1)\varphi_b(\vec{x}_2)}_{\text{Hartree}} \\ &\quad - \underbrace{\int d^4x_1 \int d^4x_2 \varphi_a^*(\vec{x}_1)\varphi_b^*(\vec{x}_2) \frac{1}{2} [W(\vec{x}_1, \vec{x}_2) + W(\vec{x}_2, \vec{x}_1)] \varphi_a(\vec{x}_2)\varphi_b(\vec{x}_1)}_{\text{exchange}} \end{aligned} \quad (3.102)$$

There are two distinct terms. The first is the **Hartree energy**

$$E_H = \frac{1}{2} \int d^3r \int d^3r' \frac{e^2 n^{(1)}(\vec{r}) n^{(1)}(\vec{r}')}{4\pi\epsilon_0|\vec{r} - \vec{r}'|} \quad (3.103)$$

which is equivalent to the Coulomb self energy of the electron density $n^{(1)}(\vec{r})$. The superscript (1) indicates that this is the one-particle density of the electrons.¹⁶

The second term, which is called the **exchange energy**, has the opposite sign and acts like an attraction between the electrons. This term describes the Pauli principle. The antisymmetry of the many-particle wave function under exchange of two particles results in a correlation¹⁷ between the electrons: Two electrons with like spin tend to stay away from each other.

The consequence of the Pauli principle is that electrons prefer to align their spins and form a ferromagnetic system. Because electrons with the same spin keep a distance, their Coulomb repulsion is smaller than that of electron pairs with opposite spin. Thus, it is more favorable for electrons to align their spins. This is the origin of **Hund's rule**, which says that spins in the same angular momentum shell of an atom tend to align their spins such that the spin is maximized. One may wonder why not all materials are ferromagnets. The reason is that there is a competition between kinetic energy and Coulomb repulsion: Because electrons stay at a distance, their accessible space is reduced, which, in the spirit of Heisenberg's principle, increases the momentum fluctuations and therefore the kinetic energy. The simple picture using Heisenberg's principle is very simplified and a more rigorous argument would start from a system of non-interacting particles and compare the changes of Coulomb and kinetic energy as function of interaction strength.

¹⁶The (classical) **self energy** of a charge density is the energy obtained by moving infinitesimally small charges, which initially are infinitely far separated from each other to the final position where they form the charge density. It is termed classical, because no charge quantization is considered.

¹⁷There are two distinct conventions for the spatial correlation between electrons. In one case, used here, the uncorrelated state is the product of the electron densities. In the other, more common notation, the uncorrelated state is the distribution of non-interacting electrons. In this latter notation, a Slater determinant would describe a system which has exchange but no correlation. When both are meant, one speaks of "*exchange-and-correlation*".

Chapter 4

Band structure of non-interacting electrons

Dispersion relations, the relation between energy and momentum, are a very simple but extremely versatile tool to describe the properties of quasi-particles. The starting point is the translation symmetry in space and time, which results in the conservation laws for momentum and energy. Energy and momentum conservation strongly limit the scattering processes between particles. Dispersion relations are valid both for particles and for waves. Thus, they often provide a simple classical description of complicated quantum processes, which nevertheless capture their essential physics.

4.1 Dispersion relations

In solid-state physics, we often deal with crystals, which exhibit discrete translation symmetry. As a consequence of Bloch's theorem, this is sufficient to make the momentum a conserved quantity for non-interacting electrons. Thus, we can characterize the states by their crystal momentum or wave vector.

The one-particle energy as function of the crystal momentum or the wave vector is the **dispersion relation** or the **band structure**.

4.1.1 Quasiparticles:

The dispersion relation is a very general concept in solid-state physics, which applies to

- electrons, as free particles or in a material, also as specifically as "additional electrons in the conduction band"
- holes, i.e. "missing electrons in the valence band",
- excitons, i.e. electron-hole pairs,
- Cooper pairs, i.e. electron pairs which are responsible for superconductivity.
- magnons, i.e. oscillations of the magnetization,
- phonons, i.e. lattice vibrations,
- polariton, i.e. a photon interacting with bosonic particles such as phonons, excitons, etc.,
- polarons, i.e. electron-phonon pairs
- photons, i.e. light,

- polaritons, i.e. photon-phonon pair, photon-exciton pair, photon-plasmon pair, etc.
- plasmons, i.e. charge oscillations,

All these entities are called **quasiparticles**, which behave as particles with a defined energy and momentum. While we deal in solid-state physics with a small number of basic particles, electrons, nuclei with their electrodynamic interactions, the interplay between them produces a large zoo of quasiparticles, which exceeds the complexity of real particles by far.

4.1.2 Free particles

Let us consider a free relativistic particle, which has the dispersion relation given by $E^2 - p^2c^2 = m_0^2c^4$, that is

$$E_{\pm}(\vec{p}) = \pm \sqrt{(m_0c^2)^2 + (pc)^2} \quad (4.1)$$

which is shown in Fig. 4.1 alongside with the bandstructure of electrons in silicon.

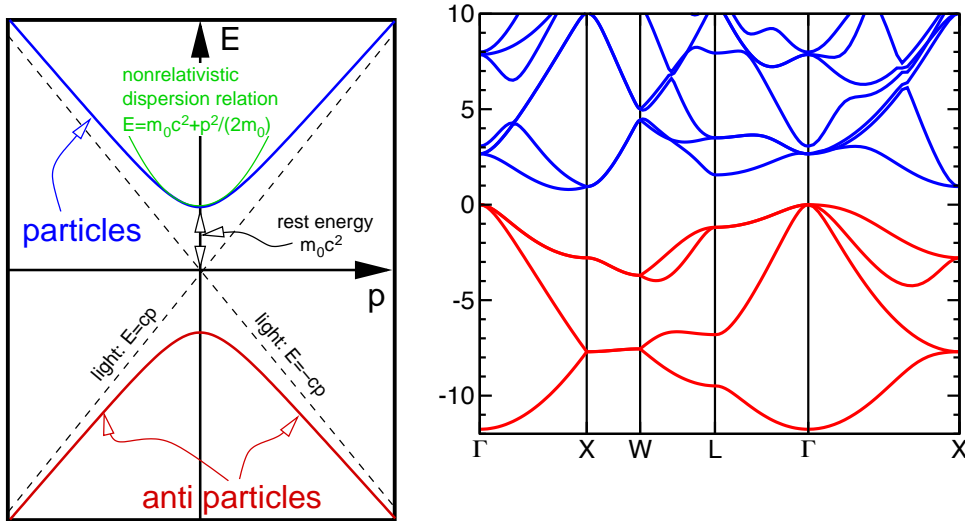


Fig. 4.1: Left: Dispersion relation of a relativistic particle. Right: bandstructure of electrons in silicon as calculated with density-functional theory. (CP-PAW and PBE functional)

The dispersion relation of a relativistic particle has two branches, one for particles and one for antiparticles. For small momenta, the non-relativistic dispersion relation is obtained by a Taylor expansion at $\vec{p} = 0$ to quadratic order in \vec{p} . After subtraction the rest energy m_0c^2 , this is the non-relativistic dispersion relation $E = \frac{p^2}{2m}$ of a free particle. For large momenta, the dispersion relation approaches a straight line with slope equal to the speed of light. This reflects that no particle can move faster than the speed of light.

The energy as function of momentum can be considered as the **Hamilton function** $H(\vec{p}, \vec{r})$ of the corresponding particle¹. Because of translation symmetry of the free particle the Hamilton function has no spatial dependence. We can use **Hamilton's equations**

$$\dot{\vec{r}} = \vec{v} = \vec{\nabla}_{\vec{p}} H(\vec{p}, \vec{r}) \quad (4.2a)$$

$$\dot{\vec{p}} = \vec{F} = -\vec{\nabla}_{\vec{r}} H(\vec{p}, \vec{r}) \quad (4.2b)$$

¹Position and momenta are three dimensional.

Thus, we can obtain the **velocity** v of the particle with a given momentum graphically as the slope of the dispersion relation. We observe that

- the particle is at rest for zero momentum, and that
- the velocity approaches the speed of light c for large momenta, but never exceeds it.

Observe also that the slope in the anti-particle branch, that is the velocity, is opposite to the direction of the momentum. This is something to be taken seriously.²

The second Hamilton's equation is Newton's law. If the system is translationally symmetric, there are no forces and the momentum is a constant of motion, i.e. it does not change with time. However, we may also consider external forces. A constant **force** implies that the momentum changes linearly with time. By observing the change of the slope, that is the velocity, over time while the momentum is shifted to the right, we can extract the dynamics of the system under a constant force.

As an example, we may follow a skyrocket, which accelerates under the constant thrust created by its rocket engines. Initially, that is for small momenta, the dispersion relation is quadratic, so that the velocity changes linearly with momentum. Under a constant force, the velocity increases linearly with time with an acceleration a obtained from $\vec{F} = m_0 \vec{a}$. The curvature of the dispersion relation is the inverse **mass**. As the rocket continues to accelerate, its speed grows less and less, while the momentum still grows continuously. This captures that the speed of light is the absolute maximum velocity for particles.

The dispersion relation of the relativistic particle has two branches. The upper one is identified with particles and the other is identified with antiparticles. In order to avoid the problem, that an antiparticle could accelerate indefinitely while emitting light, the concept of the **Dirac sea** has been introduced. The problem finds a more satisfactory solution in the context of quantum field theory. However, here we employ it, because it is analogous to the conventional view in solid-state physics. The idea is that all states of the antiparticle band are filled with electrons under normal circumstances. Due to the Pauli principle, a fermionic particle cannot lower its energy by occupying an already filled state of the antiparticle band. Thus, an antiparticle is a "missing electron in the antiparticle band" or a hole.

A particle-antiparticle pair can annihilate by emitting quanta of light, which carry away energy and momentum of the particle-antiparticle pair. This is an example of the interplay of two band structures, one for electrons and one for photons, i.e. light. Their only difference is the mass, which is zero for photons. Let us consider the process in detail. Initially there is a particle, say with momentum zero and a "hole" in the antiparticle branch. The particle can drop into the hole. In that process, the rest energy $2m_0c^2$ of both particles and the total momentum $\vec{p} = 0$ needs to be carried away. Therefore, we turn to the bandstructure for photons, that is for mass-less particles. We observe that the energy cannot be placed into a single photon, because that would also absorb a finite momentum. However, the energy can be placed into two photons with opposite momentum and each having an energy equal to the rest mass of the annihilated particle.

This is the underlying principle of **positron annihilation**. When positrons implanted into a solid, annihilate by combining with electrons, their momentum is picked up by the two emitted photons. Hence the angle of the emitted photons is a measure of the momentum of the electron-positron pair.

While electron-positron annihilation occurs on a large energy scale, $m_e c^2 \approx 511$ keV, the **electron-hole recombination** is a similar process in solids which occurs on a energy scale of a few eV. However, the solid has more possibilities to dispose of the energy of the electron-hole-pair. Radiative recombination emits light and phonons, but other processes such as the excitation of other electron-hole pairs, excitation of lattice vibrations are possible.

²However, the interpretation of antiparticles can be changed so that the energies are positive.

4.1.3 Band structure of real systems

The interpretation of the band structure of a real material is analogous to that of the dispersion relation of the free particle. Therefore, the band structure of electrons in silicon are shown in Fig. 4.1 alongside the dispersion relation of the free particle.

There are two apparent difference to the free particle:

- there are even more **more branches** than just the particle and the antiparticle branches.
- the axis for the momenta is divided into several finite sections. The letters indicate high-symmetry points in reciprocal space.³

The reason for the complicated dispersion relation of electrons in a solid is due to the reduced symmetry compared vacuum. The dispersion relation of a free particle is isotropic, so that it is sufficient to draw it in one direction. In a crystal, the bands depend on the direction of the momentum.

Because the translational symmetry of a lattice is discrete, the coordinate axis for the momentum is folded up⁴ into a finite region. The resulting region of momentum space is thus finite. Furthermore, the folded bands add to the bands already present in this finite region. Each segment describes the band structure along a so-called high-symmetry line in momentum space.

Now, we can translate the observations made for the free particle to the band structure of silicon:

- The bands below the **Fermi level**⁵ (at negative energies), which are shown in red in Fig. 4.1, describe the valence electrons. These bands are filled with electrons like the antiparticle bands in the **Dirac sea**.
- The bands above the Fermi level (at positive energies) shown in blue in Fig. 4.1 describe the **conduction electrons**.
- Valence and conduction states are separated by a **band gap**, a region where no electrons can exist in a perfect lattice. The presence of a band gap is specific for this particular example, which is a semiconductor. The band gap vanishes for metals.
- By heating up the crystal, a small number of electrons are created in the conduction band and a small number of holes, i.e. missing electrons, are formed in the valence band. In the following, we often simply refer to electrons and **holes**. The electrons will relax towards the minima of the conduction band, near the point X .
- The curvature of the energy band at the minimum is related to the inverse **effective mass** of the conduction electron.

$$\begin{aligned} \epsilon(\vec{p}) &\approx \frac{1}{2} \vec{p} m_{\text{eff}}^{-1} \vec{p} \\ m_{\text{eff}} &= \hbar^2 \left(\vec{\nabla}_k \otimes \vec{\nabla}_k \Big|_{\vec{k}_0} \epsilon \right)^{-1} \end{aligned} \quad (4.3)$$

The derivative is taken at the band extremum and for the band that forms it. This effective mass is anisotropic, which can be seen from the curvature in $\Gamma - X$ direction and the perpendicular direction $X - W$. The holes are located at the maximum of the valence band, which lies at Γ . Flat bands indicate that the particle is heavy, while bands with large curvature indicate light particles. The effective masses of holes are obtained analytically, with the only difference that the sign in the definition changes.

³The letters specifying the high-symmetry points are well-defined for each crystallographic point group. They can be found in the International Tables for Crystallography[30].

⁴The concept of folding a band structure into the unit cell is not yet clear. It describes that, in a solid, there are many bands in a finite reciprocal unit cell, while, in vacuum, there may just be one (spin-degenerate) band extending over all space. The concept will become clearer in the context of extended, periodic and reduced zone schemes as shown in Fig. 4.4.

⁵The Fermi level is the chemical potential μ for electrons. Like in the present figure, the zero of the energy axis is often chosen equal to the Fermi level, but this is not a necessity.

- For metals, the slope of the bands at the Fermi level is a measure for the velocity of n electron, the **Fermi velocity**.

$$v^{\text{Fermi}}(\vec{k}) = \frac{1}{\hbar} \vec{\nabla}_{\vec{k}} \epsilon(\vec{k}) \tag{4.4}$$

The Fermi velocity depends strongly on the particular band and the position at the Fermi surface. Typical Fermi velocities are 10^6 m/sec, which is only a factor 300 slower than the speed of light.⁶

- The number of thermally created holes and electrons and their effective masses determine the **electrical conductivity**.
- A photon can be absorbed by the formation of electron-hole pairs, if its energy exceeds the band gap. Silicon is transparent to infrared radiation, but it reflects visible light. The band gap of silicon is about $E_g = 1.17$ eV, while the photon energy of visible light ranges from 1.65 to 3.26 eV. Therefore, visible light is partially absorbed and reflected by silicon. This is why silicon has a metallic appearance.

Because of the large speed of light, the dispersion relation of light has nearly infinite slope. Thus, an optical excitation or recombination is a **vertical process**, which means that the momentum transfer during the process is negligibly small.

- **Lifetime:** Because quasi-particles interact with their environment, they may scatter at inhomogeneities or at other quasi-particles. This is described in terms of loss of particles with one set of quantum numbers (energy and momentum) and the conversion into quasi-particles with different quantum numbers. As a result, the energy for a given momentum is not sharp, but broadened by the so-called **lifetime broadening**.
- **Interfaces:** The transition through an interface between two materials can be understood via dispersion relations. An ideal interface maintains the translational symmetry in the interface plane. Therefore, the momentum \vec{p}_{\parallel} parallel to the interface and the energy ϵ must be preserved when a quasi-particle encounters the interface. The dispersion relation allows one to look up, which quasi-particles with the given conserved quantities are available, if any. The problem is analogous to partial reflection of light at the surface of a material.

4.1.4 Correspondence principle

So far we have argued on the basis of classical particles. However, what has been said, applies (within certain limits) to quantum particles as well.

Namely, the wave packets of the Schrödinger equation behave analogously to classical particles.^{7,8} For waves, the dispersion relation is expressed in terms of frequency $\omega(\vec{k})$ as function of the wave vector \vec{k} .

⁶Consider a free-electron gas with dispersion relation $\epsilon(\vec{p}) = \frac{p^2}{2m_e}$. As shown below the particle number N in a volume V is given by $N = V \sum_{\sigma} \int_{|\vec{k}| < k_F} \frac{d^3k}{(2\pi)^3} = \frac{1}{3\pi^2} k_F^3 V$, so that $k_F = \sqrt[3]{3\pi^3 \frac{N}{V}}$. The velocity is $v_F = (\hbar |k_F|) / m_e = \frac{\hbar}{m_e} \sqrt[3]{3\pi^3 \frac{N_e}{V}}$. Let us estimate the quantities: Aluminium has a lattice constant of $a_{\text{lat}} = 4.05 \text{ \AA}$. Aluminium has the face centered cubic structure, with 4 atoms in the cubic unit cell. Each Al atom contributes three valence electrons. Thus, the electron density is $N/V = 12 a_{\text{lat}}^{-3} = 0.18 \times 10^{30} \text{ m}^{-3}$. With the electron mass of $0.911 \times 10^{-30} \text{ kg}$. Thus, we obtain

$$v_F = \frac{\hbar}{m_e} \sqrt[3]{3\pi^3 \frac{N_e}{V}} \approx 2 \times 10^6 \frac{m}{s} \tag{4.5}$$

⁷See Chapter 3 of “ΦSX: Quantum Theory.”[4]

⁸The argument is closely related to Ehrenfest theorem, which says that the expectation values of a quantum system obey the classical equations of motion.

- the **group velocity** \vec{v}_g of a wave packet is given as the slope of the dispersion relation

$$\vec{v}_g = \vec{\nabla}_k \omega(\vec{k}) \quad (4.6)$$

- For a system with time-translation invariance, the frequency remains constant over time. If we now consider a dispersion relation $\omega(\vec{k}, \vec{r})$ with a weak spatial dependence, we can investigate the motion of a wave packet centered at $\vec{r}(t)$ having a wave vector $\vec{k}(t)$

$$0 = \frac{d}{dt} \omega(\vec{k}(t), \vec{r}(t)) = \underbrace{\dot{\vec{k}} \vec{\nabla}_k \omega(\vec{k}, \vec{r}) + \dot{\vec{r}} \vec{\nabla}_r \omega(\vec{k}, \vec{r})}_{\dot{\vec{r}} \left(\dot{\vec{k}} + \vec{\nabla}_r \omega(\vec{k}, \vec{r}) \right)}$$

$$\Leftrightarrow \dot{\vec{k}} = -\vec{\nabla}_r \omega(\vec{k}, \vec{r}) \quad (4.7)$$

Remark⁹

Thus, we arrive at equations of motion for a wave packet that is completely analogous to Hamilton's equations for particles.

$$\dot{\vec{r}} = \vec{\nabla}_k \omega(\vec{k}, \vec{r}) \quad (4.8a)$$

$$\dot{\vec{k}} = -\vec{\nabla}_r \omega(\vec{k}, \vec{r}) \quad (4.8b)$$

which compares to Hamilton's equations

$$\dot{\vec{r}} = \vec{\nabla}_p H(\vec{p}, \vec{r}) \quad (4.9a)$$

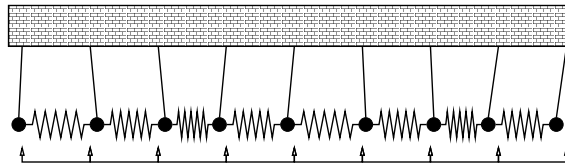
$$\dot{\vec{p}} = -\vec{\nabla}_r H(\vec{p}, \vec{r}) \quad (4.9b)$$

This is the basis for the **correspondence principle**, which says that localized wave packets behave like classical particles with energy and momentum given by

$$E = \hbar \omega \quad \text{and} \quad \vec{p} = \hbar \vec{k} \quad (4.10a)$$

The constant \hbar is at first an arbitrary constant. Experiments determine it for quantum particles to be equal to Planck's quantum. The correspondence principle, i.e. the analogy of particles and wave packets can be considered as one of the main pillars for the formulation of quantum physics.

Hanging linear chain: An example, which is often useful to compare classical and quantum systems is the hanging linear chain. The hanging linear chain is a set of pendula coupled by springs. In the continuous limit, the hanging linear chain has the same dispersion relation as the relativistic particle shown in Fig. 4.1.



Stability

So-far we considered properties that can be extracted from a dispersion relation. They are considered with transpory and (optical) excitations.

⁹In the last line, we could have added any vector such as $\vec{a} \times \dot{\vec{r}}$, which is perpendicular to the velocity $\dot{\vec{r}}$. With the correspondence principle we can assign $-\hbar \vec{\nabla}_r \omega(\vec{k})$ with the force $\vec{F} = -\vec{\nabla}_r H(\vec{p}, \vec{r})$. A force, that is perpendicular to the velocity, does not change the total energy and, therefore, cannot be obtained starting from energy conservation.

However, the band structure also contains information about **stability**, because the sum over the energies of occupied one-particle states is an important part of the total energy. (For non-interacting particles, it even is the complete energy.)

If one can predict how a change of the atomic positions affects the band structure, we can also predict whether such a change lowers the energy. Thus we can predict structural changes.

4.2 Crystal lattices

In solid-state physics, one deals mostly with materials that are periodic in space, so-called crystals. Crystals exhibit a discrete translational symmetry

$$V(\vec{r} + \vec{t}) = V(\vec{r}) \quad (4.11)$$

where the translation vectors \vec{t} form a regular lattice. More specifically, we should require for the one-particle Hamilton operator acting on the electrons

$$\langle \vec{r} + \vec{t} | \hat{H} | \vec{r} + \vec{t} \rangle = \langle \vec{r} | \hat{H} | \vec{r} \rangle \quad (4.12)$$

In addition to the discrete translation symmetry, a crystal has also a **point-group symmetry**, which allows to divide lattices into 230 **crystallographic space groups**. A set of useful tools for crystallography can be found on the Bilbao crystallographic server <http://www.cryst.ehu.es>.

Besides crystals, there are also solids without translational symmetry. Among them are quasicrystals, amorphous material and glasses. Even crystals are rarely perfect.

They usually have

- **point defects** such as substitutional defects (foreign atoms), vacancies (missing atoms), interstitials (additional atoms)
- **line defects** that are so-called **dislocations**
- **planar defects** such as **grain boundaries**, twin boundaries and interfaces
- other defects such as **precipitates**, i.e. small crystallites within another material.

4.2.1 Reciprocal space revisited

Shortened version of section 6.3.2 of ΦSX : *Quantum mechanics of the chemical bond*[3].

Let me explain my notation and remind you of some of the concepts related to real and reciprocal lattices.

Fig. 4.2.1 demonstrates the concepts developed in the following. Corresponding to the three spatial directions there are now three primitive lattice vectors, which we denote by $\vec{T}_1, \vec{T}_2, \vec{T}_3$. Note that in two or three dimensions there is no unique choice of primitive lattice vectors. The three primitive lattice vectors span the **primitive unit cell**.

A general lattice vector $\vec{t}_{i,j,k}$ can be expressed by the **primitive lattice vectors** $\vec{T}_1, \vec{T}_2, \vec{T}_3$ as

$$\vec{t}_{i,j,k} = i\vec{T}_1 + j\vec{T}_2 + k\vec{T}_3 \hat{=} \underbrace{\begin{pmatrix} T_{x,1} & T_{x,2} & T_{x,3} \\ T_{y,1} & T_{y,2} & T_{y,3} \\ T_{z,1} & T_{z,2} & T_{z,3} \end{pmatrix}}_{\mathbf{T}} \begin{pmatrix} i \\ j \\ k \end{pmatrix}$$

where i, j, k are arbitrary integers.

It is often convenient to combine the lattice vectors into a 3×3 matrix \mathbf{T} as shown above. Often the atomic positions \vec{R}_n are provided in **relative coordinates** \vec{X} which are defined as

$$\vec{R}_n = \mathbf{T}\vec{X}_n \quad \Leftrightarrow \quad \vec{X}_n = \mathbf{T}^{-1}\vec{R}_n$$

A potential is called periodic with respect to these lattice translations, if $V(\vec{r} + \vec{t}_{i,j,k}) = V(\vec{r})$.

RECIPROCAL LATTICE

The reciprocal lattice is given by those values of the wave vector \vec{G} , for which the corresponding plane waves $e^{i\vec{G}\vec{r}}$ have the same periodicity as the real-space lattice.

The primitive reciprocal-lattice vectors \vec{g}_n for $n = 1, 2, 3$ are defined in three dimensions as

$$\vec{g}_n \vec{T}_m = 2\pi\delta_{n,m} \quad (4.13)$$

The **reciprocal lattice vectors** can be obtained as

$$\vec{g}_1 = 2\pi \frac{\vec{T}_2 \times \vec{T}_3}{\vec{T}_1 (\vec{T}_2 \times \vec{T}_3)} \quad , \quad \vec{g}_2 = 2\pi \frac{\vec{T}_3 \times \vec{T}_1}{\vec{T}_2 (\vec{T}_3 \times \vec{T}_1)} \quad , \quad \vec{g}_3 = 2\pi \frac{\vec{T}_1 \times \vec{T}_2}{\vec{T}_3 (\vec{T}_1 \times \vec{T}_2)} \quad (4.14)$$

The general reciprocal lattice vectors $\vec{G}_{i,j,k}$ are multiples of the primitive lattice vectors $\vec{g}_1, \vec{g}_2, \vec{g}_3$.

$$\vec{G}_{i,j,k} = i\vec{g}_1 + j\vec{g}_2 + k\vec{g}_3 \quad (4.15)$$

- The reciprocal lattice vectors are perpendicular to the lattice planes of the real-space lattice.

$$\vec{g}_1 \parallel \vec{t}_2 \times \vec{t}_3 \quad \text{and} \quad \vec{g}_2 \parallel \vec{t}_3 \times \vec{t}_1 \quad \text{and} \quad \vec{g}_3 \parallel \vec{t}_1 \times \vec{t}_2$$

- The length of the *primitive* reciprocal lattice vectors is 2π divided by the distance Δ_n of the lattice planes.

$$|\vec{g}_n| = \frac{2\pi}{\Delta_n}$$

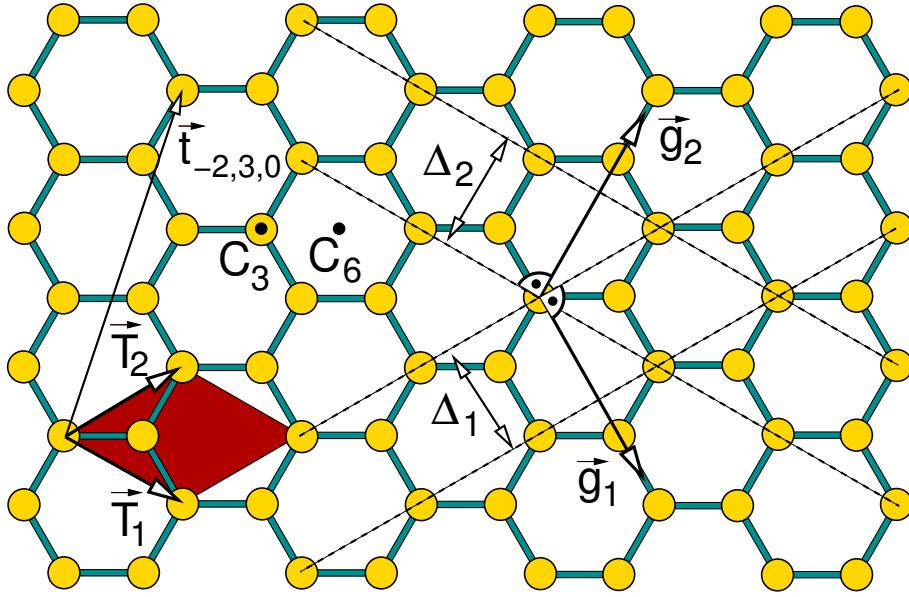


Fig. 4.2: Translational and rotational symmetry of a single graphite sheet and demonstration of reciprocal lattice vectors. Graphite is a layered material, which consists of sheets as the one shown. The yellow balls indicate the carbon atoms and the blue sticks represent the bonds. In graphite these two-dimensional sheets are stacked on top of each other, where every second sheet is shifted such that an atom falls vertically below the point indicated by C_6 . Here, we only consider the symmetry of a single sheet. The elementary unit cell is indicated by the red parallelogram, which is spanned by the elementary lattice vectors \vec{T}_1 and \vec{T}_2 . The third lattice vector points perpendicular to the sheet towards you. An example for a general lattice vector is $\vec{t}_{3,-2,0} = 3\vec{T}_1 - 2\vec{T}_2 + 0\vec{T}_3$. The lattice planes indicated by the dashed lines. The lattice planes are perpendicular to the sheet. The distance of the lattice planes are indicated by Δ_1 and Δ_2 . The elementary reciprocal lattice vectors are \vec{g}_1 and \vec{g}_2 . The third reciprocal lattice vector points perpendicular out of the plane towards you. Note that the reciprocal lattice vectors have the unit “inverse length”. Thus, their length is considered irrelevant in this real-space figure. The axis through C_3 standing perpendicular to the plane is a three-fold rotation axis of the graphite crystal. The axis through C_6 perpendicular to the plane is a 6-fold rotation axis of the graphite sheet, but only a three-fold rotation axis of the graphite crystal. (Note that a rotation axis for the graphite crystal must be one for both sheets of the crystal). In addition there is a mirror plane lying in the plane. Furthermore, there are several mirror planes perpendicular to the plane: One passing through every atom with one of the three bonds lying in the plane and one perpendicular each bond passing through the bond center.

4.2.2 Bloch theorem

From section 10.5.3 of Φ SX: *Quantum Theory*[4].

Symmetry: For every lattice-translation vector \vec{t} , we define a lattice-translation operator

$$\hat{S}(\vec{t}) \stackrel{\text{def}}{=} \int d^3 r |\vec{r}\rangle \langle \vec{r} - \vec{t}| \quad (4.16)$$

which satisfies

$$\langle \vec{r} | \hat{S}(\vec{t}) | \psi \rangle = \langle \vec{r} - \vec{t} | \psi \rangle. \quad (4.17)$$

Let us investigate the eigenstates of the translation operator. Because the lattice-translation operator is unitary, the absolute value of the eigenvalue is one, that is

$$\hat{S}(\vec{t})|\psi_{\varphi(\vec{t})}\rangle = |\psi_{\varphi(\vec{t})}\rangle e^{i\varphi(\vec{t})} \quad (4.18)$$

where the phase shift depends on the translation vector.

How can we express the simultaneous eigenstates of all lattice translation vectors \vec{t} ? First, we find the simultaneous eigenstates for the three primitive lattice translation vectors

$$\begin{aligned} \hat{S}(\vec{T}_1)|\psi_{\varphi_1, \varphi_2, \varphi_3}\rangle &= |\psi_{\varphi_1, \varphi_2, \varphi_3}\rangle e^{i\varphi_1} \\ \hat{S}(\vec{T}_2)|\psi_{\varphi_1, \varphi_2, \varphi_3}\rangle &= |\psi_{\varphi_1, \varphi_2, \varphi_3}\rangle e^{i\varphi_2} \\ \hat{S}(\vec{T}_3)|\psi_{\varphi_1, \varphi_2, \varphi_3}\rangle &= |\psi_{\varphi_1, \varphi_2, \varphi_3}\rangle e^{i\varphi_3} \end{aligned} \quad (4.19)$$

With the help of

$$\hat{S}(\vec{t}_1 + \vec{t}_2) = \hat{S}(\vec{t}_2)\hat{S}(\vec{t}_1) \quad (4.20)$$

one can show that the eigenstates of the three primitive lattice translations are also the eigenstates for all other translations on the lattice.

$$\begin{aligned} \hat{S}(n_1\vec{T}_1 + n_2\vec{T}_2 + n_3\vec{T}_3)|\psi_{\varphi_1, \varphi_2, \varphi_3}\rangle &= \hat{S}^{n_3}(\vec{T}_3)\hat{S}^{n_2}(\vec{T}_2)\hat{S}^{n_1}(\vec{T}_1)|\psi_{\varphi_1, \varphi_2, \varphi_3}\rangle \\ &= |\psi_{\varphi_1, \varphi_2, \varphi_3}\rangle e^{in_1\varphi_1} e^{in_2\varphi_2} e^{in_3\varphi_3} \\ &= |\psi_{\varphi_1, \varphi_2, \varphi_3}\rangle e^{i(n_1\varphi_1 + n_2\varphi_2 + n_3\varphi_3)} \end{aligned} \quad (4.21)$$

In order to arrive at the common conventions, we define **Bloch vector** or simply wave vector or k-point \vec{k} by

$$\vec{k} \stackrel{\text{def}}{=} -\mathbf{T}^{-1}\vec{\varphi} \quad \Leftrightarrow \quad \varphi_j = -\vec{k}\vec{T}_j \quad (4.22)$$

Thus, the eigenvalue equation for the lattice-translation operator is (see also Eq. 10.1 of [4])

$$\hat{S}(\vec{t})|\psi_{\vec{k}}\rangle = |\psi_{\vec{k}}\rangle e^{-i\vec{k}\vec{t}} \quad (4.23)$$

From now on, we use the wave vector \vec{k} as quantum number of the wave function rather than the angle $\vec{\varphi}$.

Two eigenvalues $e^{i\sum_{j=1}^3 \varphi_j n_j}$ are identical if the phases φ_j differ only by a multiple of 2π . Therefore we need to choose the phases from $\varphi_k \in [0, 2\pi]$. This implies that the wave vectors need to be chosen from one reciprocal unit cell.¹⁰

Let us now construct the eigenstates of the lattice translation operator:

$$\langle \vec{r} | \hat{S}(\vec{t}) | \psi_{\vec{k}} \rangle \stackrel{\text{Eq. 4.23}}{=} \langle \vec{r} | \psi_{\vec{k}} \rangle e^{-i\vec{k}\vec{t}} \quad (4.24)$$

$$\begin{aligned} &\stackrel{\text{Eq. 4.17}}{\Rightarrow} \langle \vec{r} - \vec{t} | \psi_{\vec{k}} \rangle = \langle \vec{r} | \psi_{\vec{k}} \rangle e^{-i\vec{k}\vec{t}} \\ \cdot e^{-i\vec{k}(\vec{r}-\vec{t})} &\Rightarrow \underbrace{\langle \vec{r} + \vec{t} | \psi_{\vec{k}} \rangle e^{-i\vec{k}(\vec{r}-\vec{t})}}_{=: u_{\vec{k}}(\vec{r}-\vec{t})} = \underbrace{\langle \vec{r} | \psi_{\vec{k}} \rangle e^{-i\vec{k}\vec{r}}}_{=: u_{\vec{k}}(\vec{r})} \end{aligned} \quad (4.25)$$

Thus, the function

$$u_{\vec{k}}(\vec{r}) \stackrel{\text{def}}{=} \psi_{\vec{k}}(\vec{r}) e^{-i\vec{k}\vec{r}} \quad (4.26)$$

¹⁰The unit cell can be displaced in reciprocal space, but we must not allow wave vectors that differ from each other by a reciprocal lattice vector.

which is defined for an eigenstate of the lattice translation operator $\hat{S}(\vec{t})$ with eigenvalue $e^{-i\vec{k}\vec{t}}$, is invariant under the lattice translations. That is

$$u_{\vec{k}}(\vec{r} - \vec{t}) = u_{\vec{k}}(\vec{r}). \quad (4.27)$$

Hence the eigenstates of the lattice-translation operators can be written as product of a periodic function and a plane wave. Without limitation of generality, this Bloch vector can be chosen from within the first reciprocal unit cell.

Lattice symmetry implies that the eigenstates of the lattice Hamiltonian can be chosen to be eigenstates of the lattice-translation operator, which immediately implies Bloch theorem.

BLOCH THEOREM

The eigenstates of a system with lattice symmetry can be written as product of a periodic function $u_{\vec{k}}(\vec{r})$, i.e.

$$u_{\vec{k}}(\vec{r} + \vec{t}) = u_{\vec{k}}(\vec{r}), \quad (4.28)$$

and a modulating plane wave $e^{i\vec{k}\vec{r}}$, that is

$$\psi_{\vec{k}}(\vec{r}) = u_{\vec{k}}(\vec{r})e^{i\vec{k}\vec{r}} \quad (4.29)$$

where the wave vector \vec{k} , the Bloch vector, is a good quantum number of the system.

4.2.3 Non-interacting electrons in an external potential (optional)

Another way to obtain the Bloch theorem is to set up the Hamiltonian in a plane wave basis. On the one hand, this approach to the problem connects to some of the principles used in a **plane-wave pseudopotential method**. On the other hand, it shows that lattice potential leads to a coupling between points in the reciprocal space, which are separated by reciprocal lattice vectors.

Let us now consider the consequences of a weak external potential.

$$V(\vec{r}) = \sum_{\vec{G}} V_{\vec{G}} e^{i\vec{G}\vec{r}} \quad (4.30)$$

Since the potential shall be periodic, only reciprocal lattice vectors \vec{G} occur in the sum. The Hamiltonian can be written as

$$\hat{H} = \sum_{\sigma} \int d^3r |\vec{r}, \sigma\rangle \left(\frac{-\hbar^2}{2m_e} \vec{\nabla}^2 + \sum_{\vec{G}} V_{\vec{G}} e^{i\vec{G}\vec{r}} \right) \langle \vec{r}, \sigma | \quad (4.31)$$

Let us now work out the matrix elements of the Hamiltonian between two plane waves¹¹ $\phi_{\vec{k},\sigma}$,

$$\phi_{\vec{k},\sigma}(\vec{r}, \sigma') = \langle \vec{r}, \sigma' | \phi_{\vec{k},\sigma} \rangle = \frac{\delta_{\sigma,\sigma'}}{\sqrt{\Omega}} e^{i\vec{k}\vec{r}}. \quad (4.32)$$

The subscript σ is the spin quantum number, while σ' in the argument list is the “spin-coordinate”. Plane waves are the eigenstates of the free-electron gas, and they are eigenstates of the (any) spatial translation operator.

¹¹Usually, the term “plane wave” refers only to the spatial part. Here, we use the term to denote the specific basisfunctions including the spin dependence.

The Hamilton matrix elements are

$$\begin{aligned}
H_{\sigma,\sigma'}(\vec{k}, \vec{k}') &:= \langle \phi_{\vec{k},\sigma} | \hat{H} | \phi_{\vec{k}',\sigma'} \rangle \\
&\stackrel{\text{Eq. 4.31}}{=} \sum_{\sigma''} \int_{\Omega} d^3r \underbrace{\langle \phi_{\vec{k},\sigma} | \vec{r}, \sigma'' \rangle}_{\phi_{\vec{k},\sigma}^*(\vec{r},\sigma'')} \left(\frac{-\hbar^2}{2m_e} \nabla^2 + \sum_{\vec{G}} V_{\vec{G}} e^{i\vec{G}\vec{r}} \right) \underbrace{\langle \vec{r}, \sigma'' | \phi_{\vec{k}',\sigma'} \rangle}_{\phi_{\vec{k}',\sigma'}(\vec{r},\sigma'')} \\
&\stackrel{\text{Eq. 4.32}}{=} \frac{\delta_{\sigma,\sigma'}}{\Omega} \int_{\Omega} d^3r e^{-i\vec{k}\vec{r}} \left(\frac{-\hbar^2}{2m_e} \nabla^2 + \sum_{\vec{G}} V_{\vec{G}} e^{i\vec{G}\vec{r}} \right) e^{i\vec{k}'\vec{r}} \\
&= \frac{(\hbar\vec{k})^2}{2m_e} \delta_{\sigma,\sigma'} \underbrace{\frac{1}{\Omega} \int_{\Omega} d^3r e^{i(\vec{k}'-\vec{k})\vec{r}}}_{\delta_{\vec{k}',\vec{k}}} + \sum_{\vec{G}} V_{\vec{G}} \delta_{\sigma,\sigma'} \underbrace{\frac{1}{\Omega} \int_{\Omega} d^3r e^{-i\vec{k}\vec{r}} e^{i\vec{G}\vec{r}} e^{i\vec{k}'\vec{r}}}_{\delta_{\vec{k}'+\vec{G},\vec{k}}} \\
&= \delta_{\sigma,\sigma'} \sum_{\vec{G}} \left[\frac{(\hbar\vec{k})^2}{2m_e} \delta_{\vec{G},\vec{0}} + V_{\vec{G}} \right] \delta_{\vec{k}'+\vec{G},\vec{k}} \tag{4.33}
\end{aligned}$$

We have used here the normalization condition¹² corresponding to a finite, even though very large, volume Ω with side-lengths L_x, L_y, L_z . Correspondingly, the spectrum is discrete with wave vectors $\vec{k}_{i,j,k} = \frac{2\pi}{L_x}i + \frac{2\pi}{L_y}j + \frac{2\pi}{L_z}k$.

Thus, there is only a coupling between states that are separated by a reciprocal lattice vector. This is one way to prove **Bloch's theorem**.

BLOCH'S THEOREM

Bloch's theorem says that the eigenstates in a periodic potential can be written as a product of a function $u_{\vec{k},\sigma}(\vec{r}, \sigma')$ that is periodic with the periodicity of the potential and a phase factor $e^{i\vec{k}\vec{r}}$.

This can be shown as follows: Once we diagonalize the Hamiltonian, the eigenstates will be a superposition of the basis states, the plane waves, that are connected by a Hamiltonian matrix element. Thus, the final wave function has the general form

$$\psi_{\vec{k}}(\vec{r}) = \sum_{\vec{G}} e^{i(\vec{k}+\vec{G})\vec{r}} c_{\vec{k},\vec{G}} = \underbrace{\left[\sum_{\vec{G}} e^{i\vec{G}\vec{r}} c_{\vec{k},\vec{G}} \right]}_{u_{\vec{k}}(\vec{r})} e^{i\vec{k}\vec{r}} = u_{\vec{k}}(\vec{r}) e^{i\vec{k}\vec{r}} \tag{4.34}$$

Because the function $u_{\vec{k}}(\vec{r})$ has only Fourier components at the reciprocal lattice vectors, it is periodic with the real-space lattice symmetry.

4.2.4 Zone schemes

The Hamiltonian Eq. 4.33 in the plane wave basis is instructive to understand how the crystal lattice deforms the free-electron parabola $\epsilon(\vec{k}, \sigma) = (\hbar\vec{k})^2/2m_e$ so that a non-trivial band structure emerges.

Level repulsion

At this point we should be familiar with some generic features of diagonalizing a Hamiltonian. They have been discussed in section 1.2.1 on p. 21. In particular, one should inspect fig. 1.1.

A more detailed discussion is given in Φ SX: Quantum mechanics of the chemical bond.[3].

We will use the principle of **level repulsion**:

¹²Other choices would normalize the wave function within the unit cell, or they would set the average density equal to one.

- If we consider the eigenvalues as function of the separation of the diagonal values, the hopping leads to a repulsion of the eigenvalues, when they come close.
- When the diagonal elements are well separated, the displacement of the energy eigenvalues from the diagonal elements becomes small.

Gaps at zone boundaries

When we consider the crystal potential as a small perturbation of the free-electron gas, the dominant effect is that band gaps open at the boundary of the Brillouin zone. In more than one dimension, these band gaps do not always imply the transition to an insulator, because these band gaps refer to specific k-points.

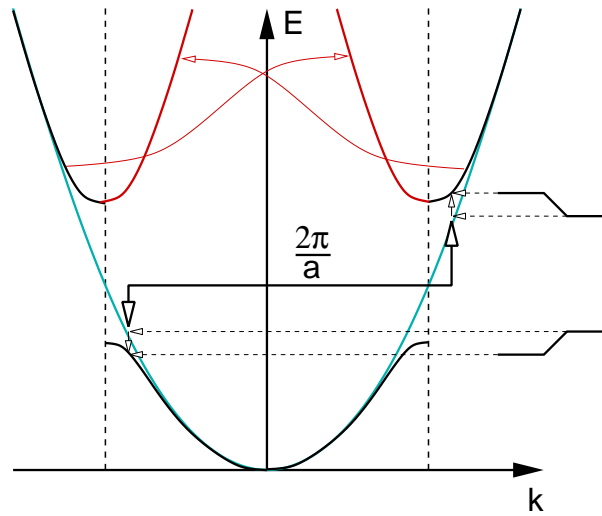


Fig. 4.3: Schematic demonstration how a periodic potential results in a coupling between states with the same wave vector in the reduced zone scheme

Let me discuss the band-gap opening using fig. 4.3.

1. According to Eq. 4.33, the crystal potential couples plane waves with wave vectors that differ by a reciprocal lattice vector \vec{G} .
2. In order to simplify the discussion, I consider the Hamiltonian only for two plane waves

$$H \approx \begin{pmatrix} (\hbar k_1)^2/(2m_e) & V_G \\ V_G^* & (\hbar k_2)^2/(2m_e) \end{pmatrix} \tag{4.35}$$

and one potential matrix element V_G with a primitive lattice vector $G = 2\pi/a_{\text{lat}}$, where a_{lat} is the real-space lattice constant. The coupling is nonzero only if $k_2 = k_1 + G$, where \vec{G} is a reciprocal lattice vector.

3. The dominant effect will be the level repulsion between the energy levels of plane waves with similar energies. The diagonal elements become degenerate at $k_1 = -\frac{1}{2}G$ and $k_2 = +\frac{1}{2}G$, which are the boundaries of the Brillouin zone. Therefore, we consider the band structure on this region. The level with $k_1 \approx -\frac{1}{2}G$ but $k_1 \geq \frac{1}{2}G$ will be shifted downward, while the state near $k_2 \approx +\frac{1}{2}G$ and $k_2 \geq +\frac{1}{2}G$ will be shifted upward. According to Eq. 1.20, the final energy levels at the zone boundary will be separated by $2|V_G|$. For wave vectors k_1 and k_2 far from the zone boundary, the raw plane waves have very different energies, so that the level-repulsion is small.

4. Once the states are hybridized, the wave vector of the original plane waves lose their relevance. If one draws all energy levels of plane waves that can hybridize due to the crystal potential on-top of each other, the different branches of the band structure are shifted into the first Brillouin zone. This also makes the near-degeneracy of plane waves, which are coupled by the crystal potential more obvious. It also leads us from the **extended zone scheme** to the **reduced zone scheme**.

Extended and reduced zone scheme

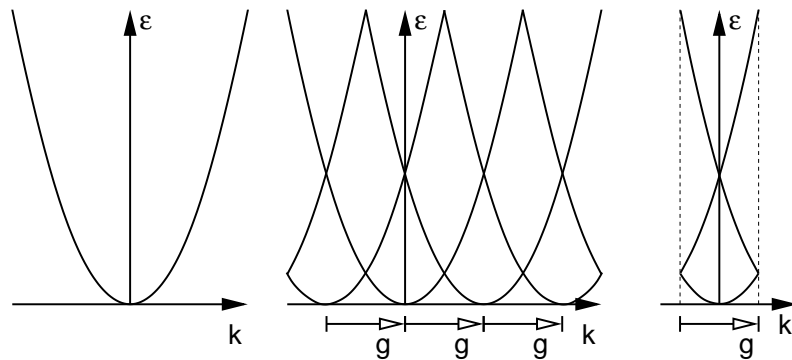


Fig. 4.4: Extended, periodic and reduced zone scheme for a one-dimensional free particle.

This is the reason why band structures are not represented in an **extended zone scheme** but in a **reduced zone scheme**.

- in the extended zone scheme the band structure of free electrons is a single parabola, and extends to infinity in reciprocal space.
- in the **periodic zone scheme**, the free electron consists of many parabola centered at the reciprocal lattice points. Thus, the reciprocal zone scheme is periodic with the periodicity of the reciprocal lattice.
- in the reduced zone scheme, only the irreducible part of the periodic zone scheme is shown, that is one single repeat unit. The band structures shown in Fig. 5.1 are in a reduced zone scheme. There are several choices for the repeat units of the reciprocal lattice. One choice is simply the primitive unit cell of the reciprocal lattice. However, the shape of the unit cell does not have the point-group symmetry of the reciprocal lattice. Therefore, one instead chooses the **Wigner Seitz cell**¹³ of the reciprocal lattice, which is called the **Brillouin zone**.

In the reduced zone scheme, all wave vectors connected by a reciprocal lattice vector, fall on top of the same point in the Brillouin zone. Thus, a Hamiltonian that has lattice periodicity couples all points that lie at the same point in the Brillouin zone. This is demonstrated in Fig. 4.3.

From perturbation theory we know that the splitting of two interacting states is large when the two states are close or even degenerate. Thus the largest effect in the band structure occurs right at the boundary of the irreducible zone, where the degeneracy of the free-electron gas is lifted by the periodic potential. Thus, local band gaps appear at the surface of the Brillouin zone. This band gap, however, is usually warped, so that there is no energy window, that completely lies in all local band gaps. In that case the material remains a metal.

¹³The Wigner Seitz cell of a lattice consists of all points that are closer to the origin than to any other lattice point. Thus, it is enclosed by planes perpendicular to the lattice vectors cutting the lattice vector in half.

4.3 Orbitals and Slater-Koster matrix elements

4.3.1 Orbitals

In order to understand the electronic structure of real materials, one can approach the problem using as starting point either the free-electron gas or isolated atoms. Typically physicists tend to focus on plane waves, while chemists start from atomic orbitals. Nowadays, it is rarely sufficient to focus on one point of view.

When one starts from atoms, one can use the nature of the atomic eigenstates that are readily available. The energy eigenstates of an atom are classified by their spin main quantum number n , angular quantum numbers ℓ, m and the spin quantum number σ .

The main angular momenta are denoted as

$\ell = 0$	s	s
$\ell = 1$	p	p_x, p_z, p_y
$\ell = 2$	d	$d_{xy}, d_{xz}, d_{yz}, d_{x^2-y^2}, d_{3z^2-r^2}$
$\ell = 3$	f	

The angular momentum eigenstates are represented by the spherical harmonics. In practice we use real spherical harmonics or cubic harmonics, which are superpositions of spherical harmonics with the same ℓ eigenvalue and the same absolute value of m , but which mix $+m$ and $-m$ spherical harmonics.

The orbitals are often represented in polar coordinates, where they have the form in fig. 4.5.

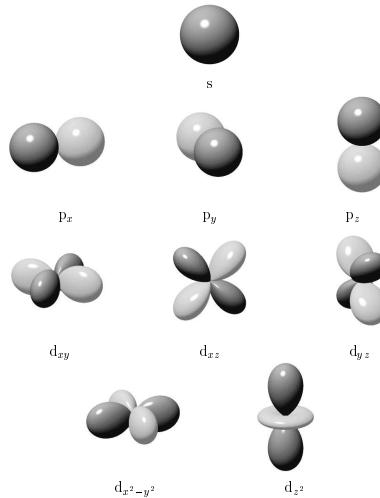


Fig. 4.5: Real spherical harmonics: the representation is a surface defined by $|\frac{1}{|r|} \bar{Y}_{\ell,m}(\vec{r})| = 1$. For a given direction, the distance of the surface from the origin is the absolute value of the cubic spherical harmonics. The different values of grey reflect to the signs of the function.

- The first approach towards an orbital based description has been the (Linear combination of atomic orbitals) **LCAO method**. [31] The underlying idea is to simply use atomic orbitals as basisset.
- The tight-binding approach uses orbitals that short ranged. They have obtained a justification from Andersen's **ab-initio tight-binding orbitals**. [32]
- Local orbitals, which are strictly orthonormal and describe the complete band structure precisely, are the **Wannier orbitals** [24].

4.3.2 Slater-Koster matrix elements

In the following, we will need to have an idea of orbital shapes and matrix elements of orbitals between different sites.

Orbitals are labeled by their main angular momentum as s for $\ell = 0$, p for $\ell = 1$, d for $\ell = 2$, f for $\ell = 3$. Instead of spherical harmonics defined as eigenstates of \hat{L}^2 and \hat{L}_z , we use their real and imaginary parts, the so-called cubic harmonics or real spherical harmonics. The real spherical harmonics are $s, p_x, p_y, p_z, d_{3z^2-r^2}, d_{x^2-y^2}, d_{xy}, d_{xz}, d_{yz}$.

As we characterize orbitals by their total angular momentum we can characterize bond orbital by the angular momentum along the bond. Thus we exploit the cylindrical symmetry. The eigenstates are denoted as σ, π, δ for $m = 0, 1, 2$ along the bond axis respectively.

Slater and Koster[31] showed how the Hamilton matrix elements for arbitrary bond directions can be constructed from 10 basic matrix elements, which are shown in figure 4.6. They exploited that orbitals having distinct angular momenta along the bond have nearly vanishing matrix elements.

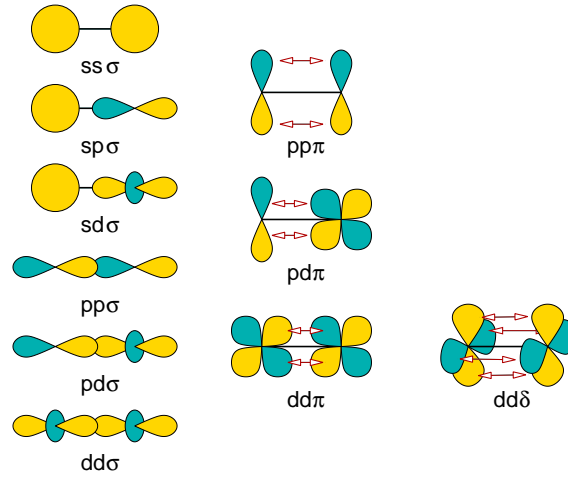


Fig. 4.6: Non-vanishing tight-binding matrix elements along their bond

4.3.3 Sign of $h_{pp\sigma}$ and $h_{pp\pi}$

For a σ -bond of two p states, the orbitals must contribute to the energetically lower (bonding) state with opposite sign. With this opposite sign, the two orbitals add up in the bonding region. In the energetically higher (antibonding) state, the two orbitals have equal sign in order which results in a node in the bonding region in between the atoms.

By inspecting the eigenstates of a two-by-two matrix with positive and negative off-site elements, we can relate the sequence of the state with and without node to the sign of the off-site Hamilton matrix element. If the off-site Hamilton matrix element is positive, the eigenvector of the energetically lower (bonding) state has components with opposite sign and vice versa, i.e.

$$c_{1,bond} \langle \chi_1 | \hat{H} | \chi_2 \rangle c_{2,bond} < 0 \quad (4.36)$$

In order to obtain the correct order of the states with and without node, the Hamilton matrix element for a σ -bond of p -states must be positive. For two s -orbitals, on the other hand, the Hamilton matrix element is negative.

There is another way to estimate the matrix element: We consider two atoms with atomic orbitals χ_1 for atom 1 and $|\chi_2\rangle$ for atom 2. The potentials of the atom are \hat{v}_1 and \hat{v}_2 and the atomic energies

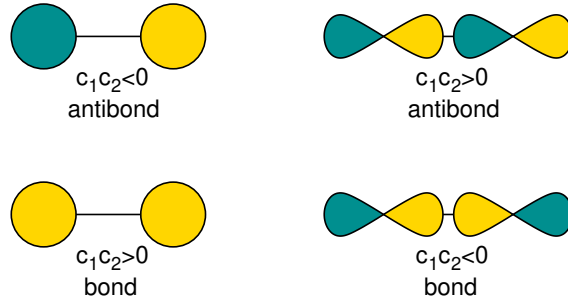


Fig. 4.7: Relation of the relative sign of orbital coefficients of bonding and antibonding orbitals for different angular momenta. For s-type orbitals the relative sign for the bonding orbital is negative and positive for the antibonding orbital. For p-type orbitals, for example, the rule is different. Bonding orbitals have in common that they have the same sign in the region where they overlap, because this lowers the kinetic energy, compared to the antibond which has a node-plane in the overlap region.

are ϵ_1 and ϵ_2 .

$$\begin{aligned}
 H_{1,2} &\stackrel{\text{def}}{=} \langle \chi_1 | \frac{\hat{p}^2}{2m_e} + \hat{v} | \chi_2 \rangle \\
 &= \frac{1}{2} \left(\langle \chi_1 | \frac{\hat{p}^2}{2m_e} + \hat{v}_2 | \chi_2 \rangle + \langle \chi_1 | \frac{\hat{p}^2}{2m_e} + \hat{v}_1 | \chi_2 \rangle \right) + \langle \chi_1 | \hat{v} - \frac{1}{2}(\hat{v}_1 + \hat{v}_2) | \chi_2 \rangle \\
 &= \frac{1}{2} \left(\epsilon_2 + \epsilon_1 \right) \langle \chi_1 | \chi_2 \rangle + \langle \chi_1 | \hat{v} - \frac{1}{2}(\hat{v}_1 + \hat{v}_2) | \chi_2 \rangle \\
 &\approx \underbrace{\left[\frac{1}{2}(\epsilon_2 + \epsilon_1) + v(\vec{r}_B) - \frac{1}{2}(v_1(\vec{r}_B) + v_2(\vec{r}_B)) \right]}_{\text{probably negative}} \langle \chi_1 | \chi_2 \rangle
 \end{aligned} \tag{4.37}$$

In the last line, we introduced \vec{r}_B , which marks the approximate “position of the bond” where the overlap $2\text{Re}[\chi_1^*(\vec{r})\chi_2(\vec{r})]$ of the orbitals is large.

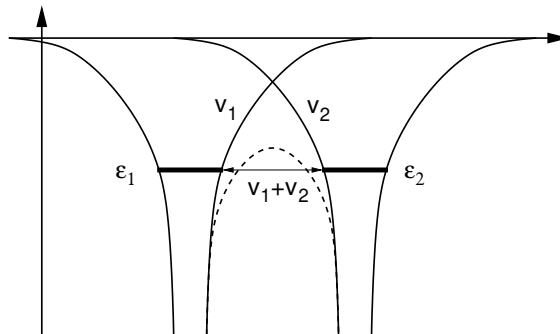


Fig. 4.8: Demonstration for the rule of thumb that the offsite Hamilton matrix element for a basis of quasi-atomic orbitals has opposite sign as the overlap matrix element, i.e. $\langle \chi_1 | \hat{H} | \chi_2 \rangle / \langle \chi_1 | \chi_2 \rangle < 0$. Assume that the vacuum level as the zero of the energy scale. Then the atomic orbitals are negative, as they are bound atomic states. Thus, $\frac{1}{2}(\epsilon_1 + \epsilon_2) < 0$. When the potential is approximated by the superposition of the atomic potentials, $v - \frac{1}{2}(v_1 + v_2) = \frac{1}{2}(v_1 + v_2) < 0$ which is negative because both atomic potentials are negative individually.

Now, we need to make educated guesses. We follow the consideration in figure 4.8:

$$\begin{aligned}
 v(\vec{r}_B) &\leq v_1(\vec{r}_B) \\
 v(\vec{r}_B) &\leq v_2(\vec{r}_B) \\
 \Rightarrow v(\vec{r}_B) &= \frac{1}{2} \left(v(\vec{r}_B) + v(\vec{r}_B) \right) \leq \frac{1}{2} \left(v_1(\vec{r}_B) + v_2(\vec{r}_B) \right) \\
 \epsilon_{1/2} &\leq 0
 \end{aligned} \tag{4.38}$$

If we insert these estimates into the approximate equation above, they indicate that the Hamilton matrix element has the opposite sign as the overlap matrix element $\langle \chi_1 | \chi_2 \rangle$.

4.4 Bands and orbitals

From section 6.6 of Φ SX:Quantum mechanics of the chemical bond[3]

So far we discussed the band structures as a variation of the dispersion relation of the free-electron bands. However, this point of view obscures the relation to chemical binding and the local picture of the wave functions.

The band structure can also be constructed starting from local orbitals. This is demonstrated here for the two-dimensional square lattice with atoms having s- and p-orbitals in the plane.

In order to simplify the work, we restrict ourselves to the high-symmetry points Γ , X and M of the two-dimensional reciprocal unit cell.

The real-space lattice vectors are

$$\vec{T}_1 = \begin{pmatrix} 1 \\ 0 \end{pmatrix} a \quad \text{and} \quad \vec{T}_2 = \begin{pmatrix} 0 \\ 1 \end{pmatrix} a$$

The corresponding reciprocal-space lattice vectors are

$$\vec{g}_1 = \begin{pmatrix} 1 \\ 0 \end{pmatrix} \frac{2\pi}{a} \quad \text{and} \quad \vec{g}_2 = \begin{pmatrix} 0 \\ 1 \end{pmatrix} \frac{2\pi}{a}$$

Because of rotational symmetry of the crystal, only a part of the states in the Brillouin zone are independent. The region containing an independent region of reciprocal space is called the **irreducible zone** of the reciprocal lattice. The states for the remaining reciprocal lattice can be generated from those in the irreducible zone by the symmetry operations, point group operations and lattice translations.

Usually, the boundaries of the irreducible zone have a higher symmetry than the center of the irreducible zone. The symmetry of the corners is typically even higher. One calls them **high-symmetry points**. Because of the larger symmetry, the states and energy levels at high-symmetry points are easier to compute and to comprehend.

The high-symmetry points are

$$k_\Gamma = 0 = \begin{pmatrix} 0 \\ 0 \end{pmatrix} \frac{2\pi}{a} \quad ; \quad k_X = \frac{1}{2} \vec{g}_1 = \begin{pmatrix} 1 \\ 0 \end{pmatrix} \frac{\pi}{a} \quad \text{and} \quad k_M = \frac{1}{2} (\vec{g}_1 + \vec{g}_2) = \begin{pmatrix} 1 \\ 1 \end{pmatrix} \frac{\pi}{a}$$

The first step is to construct Bloch waves out of the atomic orbitals, by multiplying them with $e^{i\vec{k}\vec{t}}$, where \vec{t} is the lattice translation of the atom relative to the original unit cell. This is illustrated in Fig. 4.9 on page 139.

- At the Γ , the phase factor for a lattice translation of the orbital is one. Thus, we repeat the orbital from the central unit cell in all other unit cells.

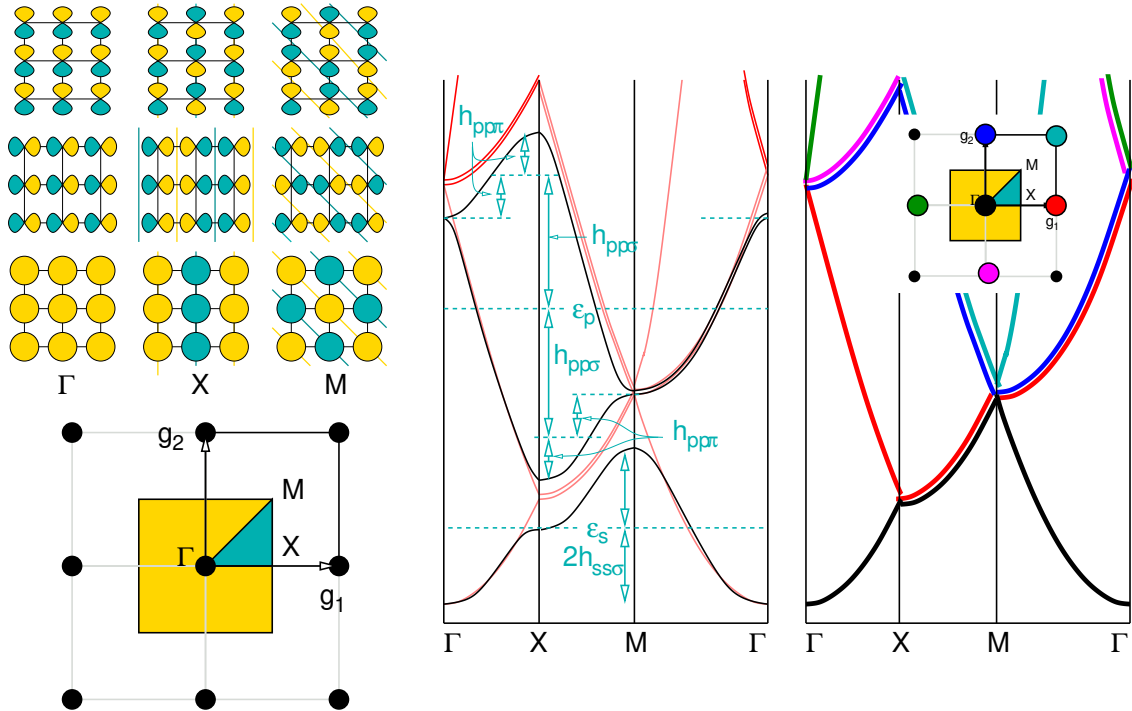


Fig. 4.9: Illustration of a band structure in real and reciprocal space for a planar square lattice. Bottom left: The reciprocal lattice is spanned by the reciprocal lattice vectors \vec{g}_1 and \vec{g}_2 . The yellow square is the corresponding Brillouin zone. The green inset is the Brillouin zone, whose corners are the high-symmetry points Γ , X and M . On the top left, the corresponding basis functions made from one s-orbital and two p-orbitals in a Bloch-basis are shown. These states are also eigenstates of the Hamiltonian, because the coupling vanishes due to point group symmetry at the high-symmetry points. The graph in the middle is a schematic band structure (black lines). Only the absolute values of the Slater-Koster parameters are considered. The red lines are free-electron bands for comparison. On the right, the free-electron bands are color coded according to the reciprocal lattice vector (inset), at which the corresponding parabolic free-electron band is centered.

- At the X point, the phase factor for a lattice translation along the first lattice vector is $e^{i\vec{k}_x\vec{T}_1} = e^{i\pi} = -1$ and the phase factor for the lattice translation along the second lattice vector \vec{T}_2 is $e^{i\vec{k}_x\vec{T}_2} = +1$. Thus, if we go to the right the sign of the orbital alternates, while in the vertical direction the orbital remains the same.
- At the M point, the phase factor alternates in each lattice direction, resulting in a checkerboard pattern.

Next we need to set up the Hamilton matrix elements for each k -point, using the Slater-Koster parameters. For a back-on-the envelope estimate the nearest neighbor matrix elements will be sufficient. The matrix elements are firstly ϵ_s and ϵ_p , the energies of the orbitals without any hybridization. Secondly, we need the hopping matrix elements $h_{ss\sigma}$, $h_{pp\sigma}$, $h_{pp\pi}$. In principle we would also need $h_{s p\sigma}$, but that matrix element will not be needed in our example.

In our simple example, the Bloch states are already eigenstates of the Hamiltonian so that we only need to calculate their energy. We obtain¹⁴

¹⁴Note, that the hopping matrix elements have the opposite sign than the overlap matrix elements. Thus, a positive overlap leads to a lowering of the energy level of the bond. In order to avoid confusion, I am introducing explicitly the absolute value of the hopping matrix elements, which have the same sign as the corresponding overlap matrix elements.

Γ	X	M
$\epsilon_p + h_{pp\sigma} - h_{pp\pi} $	$\epsilon_p + h_{pp\sigma} + h_{pp\pi} $	$\epsilon_p - h_{pp\sigma} + h_{pp\pi} $
$\epsilon_p + h_{pp\sigma} - h_{pp\pi} $	$\epsilon_p - h_{pp\sigma} - h_{pp\pi} $	$\epsilon_p - h_{pp\sigma} + h_{pp\pi} $
$\epsilon_s - 2 h_{ss\sigma} $	ϵ_s	$\epsilon_s + 2 h_{ss\sigma} $

If there is a band structure available, we can estimate the Hamilton matrix elements from that. Otherwise we just make an educated guess.

4.5 Calculating band structures in the tight-binding model

From section 6.7 of Φ SX:Quantum mechanics of the chemical bond[3]

Now, we wish to calculate the band structure. Let us begin with a tight-binding basisset with the usual assumption that the tight-binding orbitals shall be orthogonal. The tight-binding orbitals shall be represented by kets $|\alpha, \vec{t}\rangle$, where \vec{t} denotes a discrete lattice-translation vector and α denotes the type of the orbital such as s, p_x, p_y, p_z, \dots and a spin quantum number, as well as a site index R of an atom in the first unit cell of the lattice.

A Bloch wave can be represented in terms of local (orthonormal) tight binding orbitals $|\alpha, \vec{t}\rangle$ as

$$\begin{aligned}
|\Psi_{\vec{k},n}\rangle &= \sum_{\alpha,\vec{t}} |\alpha, \vec{t}\rangle \langle \alpha, \vec{t} | \Psi_{\vec{k},n}\rangle \\
&\stackrel{\text{Eq. 4.29}}{=} \sum_{\alpha,\vec{t}} |\alpha, \vec{t}\rangle \langle \alpha, \vec{t} | \int d^4x |\vec{x}\rangle \underbrace{e^{i\vec{k}\vec{r}} \langle \vec{x} | u_{\vec{k},n}\rangle}_{\psi_{\vec{k}}(\vec{x})=u_{\vec{k}}(\vec{x})e^{i\vec{k}\vec{r}}} \\
&= \sum_{\alpha,\vec{t}} |\alpha, \vec{t}\rangle e^{i\vec{k}\vec{t}} \langle \alpha, \vec{t} | \int d^4x |\vec{x}\rangle e^{i\vec{k}(\vec{r}-\vec{t})} \langle \vec{x} | u_{\vec{k},n}\rangle \\
&\stackrel{u(\vec{x})=u(\vec{r}-\vec{t},\sigma)}{=} \sum_{\alpha,\vec{t}} |\alpha, \vec{t}\rangle e^{i\vec{k}\vec{t}} \langle \alpha, \vec{t} | \sum_{\sigma} \int d^3r |\vec{r}, \sigma\rangle e^{i\vec{k}(\vec{r}-\vec{t})} \underbrace{\langle \vec{r}-\vec{t}, \sigma | u_{\vec{k},n}\rangle}_{=\langle r,\sigma | u_{\vec{k},n}\rangle} \\
&\stackrel{\vec{r}\rightarrow\vec{r}+\vec{t}}{=} \sum_{\alpha,\vec{t}} |\alpha, \vec{t}\rangle e^{i\vec{k}\vec{t}} \sum_{\sigma} \int d^3r \underbrace{\langle \alpha, \vec{t} | \vec{r} + \vec{t}, \sigma\rangle}_{\langle \vec{0}, \alpha | \vec{r}, \sigma\rangle} e^{i\vec{k}\vec{r}} \underbrace{\langle \vec{r}, \sigma | u_{\vec{k},n}\rangle}_{\langle \vec{r}, \sigma | \Psi_{\vec{k},n}\rangle} \\
&= \sum_{\alpha,\vec{t}} |\alpha, \vec{t}\rangle e^{i\vec{k}\vec{t}} \langle \alpha, \vec{0} | \psi_{\vec{k},n}\rangle \tag{4.39}
\end{aligned}$$

This shows us, how we can represent the entire wave function with a vector $\vec{c}_n(\vec{k})$ with elements $c_{\alpha,n}(\vec{k}) = \langle \alpha, \vec{0} | \Psi_{\vec{k},n}\rangle$, which has the dimension of the number of orbitals in the elementary unit cell.

Editor: Here could be more...

Our next goal is to find an equation for this vector. We will use the matrix elements of the Hamilton operator in the basis of tight-binding orbitals

$$\langle \alpha, \vec{t} | \hat{H} | \beta, \vec{t}' \rangle = h_{\alpha, \vec{t}; \beta, \vec{t}'} \tag{4.40}$$

Let me insert the ansatz Eq. 4.39 into the Schrödinger equation

$$\begin{aligned}
 \hat{H}|\Psi_{k,n}\rangle &= |\Psi_{k,n}\rangle\epsilon_{k,n} \\
 \stackrel{\text{Eq. 4.39}}{\Rightarrow} \hat{H} \sum_{\alpha, \vec{t}} |\alpha, \vec{t}\rangle e^{i\vec{k}\vec{t}} \langle \alpha, \vec{0} | \Psi_{k,n} \rangle &= \sum_{\vec{t}, \alpha} |\alpha, \vec{t}\rangle e^{i\vec{k}\vec{t}} \langle \alpha, \vec{0} | \Psi_{k,n} \rangle \epsilon_{k,n} \\
 \stackrel{\langle \beta, \vec{0} |}{\Rightarrow} \sum_{\alpha, \vec{t}} \underbrace{\langle \beta, \vec{0} | \hat{H} | \alpha, \vec{t} \rangle}_{h_{\vec{0}, \beta; \alpha, \vec{t}}} e^{i\vec{k}\vec{t}} \langle \alpha, \vec{0} | \Psi_{k,n} \rangle &= \sum_{\alpha, \vec{t}} \underbrace{\langle \beta, \vec{0} | \alpha, \vec{t} \rangle}_{\delta_{\vec{0}, \vec{t}} \delta_{\alpha, \beta}} e^{i\vec{k}\vec{t}} \langle \alpha, \vec{0} | \Psi_{k,n} \rangle \epsilon_{k,n} \\
 \Rightarrow \sum_{\alpha} \left[\underbrace{\sum_{\vec{t}} h_{\beta, \vec{0}; \alpha, \vec{t}} e^{i\vec{k}\vec{t}}}_{h_{\beta, \alpha}(\vec{k})} \right] \underbrace{\langle \vec{0}, \alpha | \Psi_{k,n} \rangle}_{c_{\alpha, n}(\vec{k})} &= \underbrace{\langle \beta, \vec{0} | \Psi_{k,n} \rangle}_{c_{\beta, n}(\vec{k})} \epsilon_{k,n} \\
 \Rightarrow \mathbf{h}(\vec{k}) \vec{c}_n(\vec{k}) &= \vec{c}_n(\vec{k}) \epsilon_n(\vec{k}) \tag{4.41}
 \end{aligned}$$

Thus, we obtain

SCHRÖDINGER EQUATION IN K-SPACE

$$\mathbf{h}(\vec{k}) \vec{c}_n(\vec{k}) = \vec{c}_n(\vec{k}) \epsilon_n(\vec{k}) \tag{4.42}$$

with $c_{\alpha, n}(\vec{k}) \stackrel{\text{def}}{=} \langle \alpha, \vec{0} | \Psi_{\vec{k}, n} \rangle$, respectively $|\Psi_{\vec{k}, n}\rangle \stackrel{\text{Eq. 4.39}}{=} \sum_{\vec{t}, \alpha} |\alpha, \vec{t}\rangle e^{i\vec{k}\vec{t}} c_{\alpha, n}(\vec{k})$ (4.43)

and

$$h_{\alpha, \beta}(\vec{k}) \stackrel{\text{def}}{=} \sum_{\alpha, \vec{t}} h_{\alpha, \vec{0}; \beta, \vec{t}} e^{i\vec{k}\vec{t}} \tag{4.44}$$

Thus, we obtained a k-dependent eigenvalue equation in matrix form with a finite and usually small size. The size is given by the number of basis orbitals considered in the first unit cell. This problem can be broken down into smaller subproblems, if we exploit the symmetry arguments that we used earlier for the molecules. Symmetry can be used especially at the high-symmetry points and lines in reciprocal space, where the band structure is usually represented.

4.5.1 Bloch orbitals as basis functions (optional)

The Hamiltonian $\mathbf{h}(\vec{k})$ can also be expressed as Hamilton matrix element with the basis orbitals

$$h_{\alpha, \beta}(\vec{k}) = \langle \alpha, \vec{k} | \hat{H} | \beta, \vec{k} \rangle \tag{4.45}$$

with

$$|\alpha, \vec{k}\rangle \stackrel{\text{def}}{=} \sum_{\vec{t}} |\alpha, \vec{t}\rangle e^{i\vec{k}\vec{t}} \frac{1}{\sqrt{\sum_{\vec{t}} 1}} \tag{4.46}$$

The Bloch orbital is defined by a sum over lattice translation vectors \vec{t} , which involves an infinite sum. In order to deal with these expressions, I consider the number of lattice translations as macroscopically large, but still finite. The finite number of translations defines a region, which represent the physical size of the piece of material at hand. If I want to describe, that this region extends over distances larger than any other physical length scale, I call it the “universe”. This trick, makes the sums finite and avoids the complexities related to continuous energy spectra such as different

normalizations for local and extended states. This trick is not commonly used and must be therefore used with caution.

Let me now show that the orbitals are normalized with the specified normalization factor.

$$\langle \alpha, \vec{k} | \beta, \vec{k}' \rangle = \frac{1}{\sqrt{\sum_{\vec{r}} 1}} \sum_{\vec{r}, \vec{r}'} e^{-i\vec{k}\vec{r}} \underbrace{\langle \alpha, \vec{r} | \beta, \vec{r}' \rangle}_{\delta_{\alpha, \beta} \delta_{\vec{r}, \vec{r}'}} e^{i\vec{k}'\vec{r}'} \frac{1}{\sqrt{\sum_{\vec{r}} 1}} = \delta_{\alpha, \beta} \frac{1}{\sum_{\vec{r}} 1} \underbrace{\sum_{\vec{r}} e^{-i\vec{k}\vec{r}} e^{i\vec{k}'\vec{r}}}_{\delta_{\vec{k}, \vec{k}'}} = \delta_{\alpha, \beta} \delta_{\vec{k}, \vec{k}'} \quad (4.47)$$

The Bloch orbitals $|\alpha, \vec{k}\rangle$ are not eigenstates of the Hamiltonian but they are eigenstates of the lattice translation operator $\hat{S}(\vec{t})$, Eq. 4.16, defined by $\langle \vec{r} | \hat{S}(\vec{t}) | \psi \rangle \stackrel{\text{Eq. 4.17}}{=} \langle \vec{r} - \vec{t} | \psi \rangle$.

$$\hat{S}_{\vec{t}} |\alpha, \vec{k}\rangle = \hat{S}_{\vec{t}} \sum_{\vec{r}} |\alpha, \vec{r}\rangle e^{i\vec{k}\vec{r}} \frac{1}{\sqrt{\sum_{\vec{r}} 1}} = \sum_{\vec{r}} \underbrace{|\alpha, \vec{r} + \vec{t}\rangle}_{\hat{S}_{\vec{t}} |\alpha, \vec{r}\rangle} e^{i\vec{k}(\vec{r} + \vec{t})} \frac{1}{\sqrt{\sum_{\vec{r}} 1}} e^{-i\vec{k}\vec{r}} = |\alpha, \vec{k}\rangle e^{-i\vec{k}\vec{t}} \quad (4.48)$$

Because the basis functions $|\alpha, \vec{k}\rangle$ are eigenstates of a symmetry operator the Hamiltonian becomes block diagonal. The Hamilton matrix elements are non-zero only when bra and ket belong to the same k-point.

$$\begin{aligned} \langle \alpha, \vec{k} | \hat{H} | \beta, \vec{k}' \rangle &= \frac{1}{\sqrt{\sum_{\vec{r}} 1}} \sum_{\vec{r}, \vec{r}'} e^{-i\vec{k}\vec{r}} \underbrace{\langle \alpha, \vec{r} | \hat{H} | \beta, \vec{r}' \rangle}_{h_{\alpha, \beta, \vec{r}, \vec{r}'}} e^{i\vec{k}'\vec{r}'} \frac{1}{\sqrt{\sum_{\vec{r}} 1}} \\ &= \frac{1}{\sum_{\vec{r}} 1} \underbrace{\sum_{\vec{r}} e^{-i(\vec{k} - \vec{k}')\vec{r}}}_{\delta_{\vec{k}, \vec{k}'}} \underbrace{\sum_{\vec{r}'} h_{\alpha, \beta, \vec{r}, \vec{r}'}}_{h_{\alpha, \beta}(\vec{k}')} e^{i\vec{k}'(\vec{r}' - \vec{r})} \\ &= \delta_{\vec{k}, \vec{k}'} h_{\alpha, \beta}(\vec{k}) \end{aligned} \quad (4.49)$$

This shows that the Hamilton matrix elements $h_{\alpha, \beta}(\vec{k})$ can be related to a well defined set of basis orbitals, namely the Bloch orbitals from Eq. 4.46.

Note that we have a Kronecker delta for the k-points, which, in principle, are continuous quantities. This is a consequence of considering a finite region, the “universe”. Because the region considered is finite, the wave vectors become discrete.

4.5.2 Worked example: alternating linear chain

Let us consider the example of a linear chain atoms with one s-type orbital. There shall be two atoms per unit cell. The lattice constant shall be a_{lat} . The orbitals are denoted by $(t/a_{\text{lat}}, \alpha)$, where $\alpha \in \{1, 2\}$ denote the two orbitals and t/a_{lat} is the number of lattice displacements.

The two atoms have orbital energies $\bar{\epsilon}_2$ and $\bar{\epsilon}_1$. We denote the hopping matrix element between orbitals $(i, 1)$ and $(i, 2)$ by t and the one between $(i, 2)$ and $(i + 1, 1)$ by t' . In the context of Slater-Koster matrix elements, both are matrix elements of the type $-t = h_{ss\sigma}$.

The difference of the atomic energy levels $\bar{\epsilon}_2 - \bar{\epsilon}_1$ describes relative **electronegativity** of the two atoms. The atom with the lower electron level is more electronegative than the one with the higher level. Without hopping, the electrons would accumulate at the more electronegative atom. This is analogous to rock salt (NaCl), where the sodium atom holds on only weakly to its valence electron, while the lowest unoccupied orbital of the chlorine atom is much stronger bound to the atom core. Therefore, sodium donates its electron to the chlorine atom, so that two ions Na^+ and Cl^- are formed.

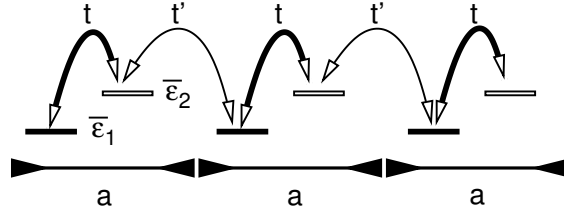


Fig. 4.10: Scheme to demonstrate the Hamiltonian of the alternating linear chain. It describes a chain with two atoms per unit cell with different ionicity, that is atomic energy levels $\bar{\epsilon}_1$ and $\bar{\epsilon}_2$. The atoms are connected by weak and strong bonds as characterized by the two hopping parameters t and t' . With a I denote the lattice constant.

The different hopping parameters describe that two of the atoms are pairwise closer together. That is, we describe a chain of molecules.

For the sake of simplicity, we only consider wave functions with one spin direction. The bands of the two spin direction are identical, because there is no magnetic field. When we consider one spin direction, the wave-function component of the other spin direction is zero.

The infinite Hamiltonian has the form

$$\mathbf{h} = \begin{pmatrix} \vdots & \vdots & \vdots & & & \\ \dots & \bar{\epsilon}_1 & -t & 0 & 0 & \dots \\ \dots & -t & \bar{\epsilon}_2 & -t' & 0 & \dots \\ \dots & 0 & -t' & \bar{\epsilon}_1 & -t & 0 & 0 & \dots \\ \dots & 0 & 0 & -t & \bar{\epsilon}_2 & -t' & 0 & \dots \\ & & \dots & 0 & -t' & \bar{\epsilon}_1 & -t & \dots \\ & & \dots & 0 & 0 & -t & \bar{\epsilon}_2 & \dots \\ & & & \vdots & \vdots & \vdots & \vdots & \end{pmatrix}$$

The Hamilton matrix elements can also be written as

$$\mathbf{h}_{i,j} = \begin{pmatrix} \bar{\epsilon}_1 & -t \\ -t & \bar{\epsilon}_2 \end{pmatrix} \delta_{i,j} + \begin{pmatrix} 0 & 0 \\ -t' & 0 \end{pmatrix} \delta_{i+1,j} + \begin{pmatrix} 0 & -t' \\ 0 & 0 \end{pmatrix} \delta_{i-1,j} \quad (4.50)$$

where i and j are the indices of the lattice translations $\vec{t}_j = a_{\text{lat}} \cdot j$. The components of the 2×2 matrices $\mathbf{h}_{i,j}$ refer to the orbital indices in the primitive unit cell, while i, j identify a particular unit cell.

When we transform the Hamiltonian into the Bloch representation using Eq. 4.44, we obtain the k -dependent Hamiltonian with $\vec{t}_j = a_{\text{lat}} j$

$$\mathbf{h}(\vec{k}) \stackrel{\text{Eq. 4.44}}{=} \sum_j \mathbf{h}(0, j) e^{i k a j} = \begin{pmatrix} \bar{\epsilon}_1 & -t - t' e^{-i k a} \\ -t - t' e^{i k a} & \bar{\epsilon}_2 \end{pmatrix}$$

The eigenvalues $\epsilon_n(k)$ and eigenvectors $c_\alpha(k)$ are obtained from the characteristic equation

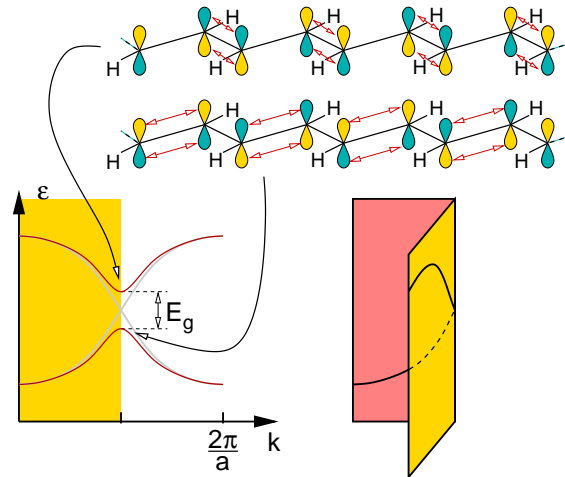


Fig. 4.12: Folding back of the band structure into the reciprocal cell of a doubled real-space unit cell. The example is shown for the one-dimensional molecule acetylene, which undergoes a Peierls distortion, which doubles the unit cell. Only the p-orbitals perpendicular to the molecular plane are considered.

4.6 Home study and practice

4.6.1 Tight-binding calculation of graphene

From ΦSX:Quantum mechanics of the chemical bond[3]

Introduction and background

A **graphene** sheet is a two-dimensional honeycomb lattice of carbon atoms. **Graphite** is a modification of carbon, made of stacked graphene sheets. The Nobel Prize in Physics 2010 was awarded jointly to Andre Geim and Konstantin Novoselov "*for groundbreaking experiments regarding the two-dimensional material graphene*". Rolled-up graphene sheets are the so-called **carbon nanotubes**. By introducing some five-membered rings into the graphene sheet, it will be curved and eventually forms closed cages, the **fullerenes**. The most famous fullerene is the the **bucky ball** C_{60} , which has the shape of a soccer ball. The Nobel Prize in Chemistry 1996 was awarded jointly to Robert F. Curl Jr., Sir Harold W. Kroto and Richard E. Smalley "*for their discovery of fullerenes*".

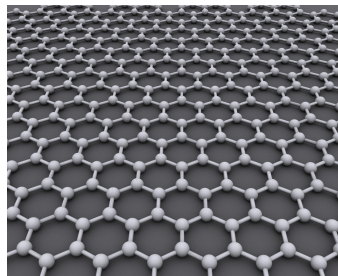


Fig. 4.13: The ideal crystalline structure of graphene is a hexagonal grid.

Image taken from <http://de.wikipedia.org/w/index.php?title=Datei:Graphen.jpg>, Author: AlexanderAIUS.

Further information can be found in section 9.6 on p. 313 below.

Some easy-to-read background information on graphene can be found on the web page of the Nobel foundation at

www.nobelprize.org/nobel_prizes/physics/laureates/2010/popular-physicsprize2010.pdf
and
www.nobelprize.org/nobel_prizes/physics/laureates/2010/advanced-physicsprize2010.pdf.

Tasks

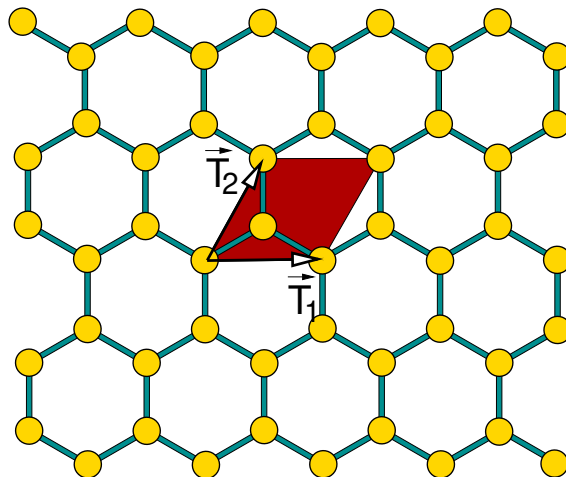
Determine the band structure of the π -orbitals of a graphene sheet[33].
Given the hexagonal structure of the 2d graphene lattice,

- 1 determine atomic positions and lattice vectors.
- 2 construct the reciprocal lattice
- 3 set up the real-space Hamiltonian (as opposed to the reciprocal-space Hamiltonian). Consider here and in the following, only the p-orbitals perpendicular to the graphene sheet. These are the orbitals that form the states near the interesting region near the Fermi level. Consider a single hopping parameter t between nearest neighbors and place the atomic orbital energy at zero. The orbitals shall be orthonormal.
- 4 set up the Bloch orbitals and transform the Hamiltonian into reciprocal space.
- 5 diagonalize the Hamiltonian in reciprocal space.
- 6 plot the band structure along the symmetry lines $\Gamma - M - K - \Gamma$. M is the midpoint between the extrema of the band structure. K is the k-point with the Dirac cone.

Solution

- 1 Determine atomic positions and lattice vectors.

The honeycomb lattice is built up from equilateral hexagons.



The carbon atoms are divided into two groups. All atoms within one group are related to each other by a simple translation. Therefore, the unit cell must contain at least two atoms, namely one from each group. The lattice vectors connect atoms from the same group. The unit cell drawn consists of two equilateral triangles, one with a carbon atom in the center and the other empty. The angles in an equilateral triangle are 60° . Using the sine and cosine of 60° , we construct the second lattice vector \vec{T}_2 .

$$\begin{aligned}\vec{T}_1 &= (1, 0)a_{\text{lat}} \\ \vec{T}_2 &= (\cos(60^\circ), \sin(60^\circ))a_{\text{lat}} = \left(\frac{1}{2}, \frac{1}{2}\sqrt{3}\right)a_{\text{lat}}\end{aligned}\quad (4.54)$$

The position of the second carbon atom in the unit cell is the center of the first triangle mentioned above

$$\vec{R}_2 = \frac{1}{3}(\vec{0} + \vec{T}_1 + \vec{T}_2) = \left(\frac{1}{2}, \frac{1}{6}\sqrt{3}\right)a_{\text{lat}}\quad (4.55)$$

The lattice vectors and atomic positions of graphene are at

\vec{T}_1	a	0	0
\vec{T}_2	$\frac{1}{2}a_{\text{lat}}$	$\frac{1}{2}\sqrt{3}a_{\text{lat}}$	0
\vec{T}_3	0	0	∞
\vec{R}_1	0	0	0
\vec{R}_1	$\frac{1}{2}a_{\text{lat}}$	$\frac{1}{6}\sqrt{3}a_{\text{lat}}$	0

where a_{lat} is the lattice constant.

2 construct the reciprocal lattice

In the following, “ \times ” denotes the vector product.

$$\begin{aligned}\vec{g}_1 &= 2\pi \frac{\vec{T}_2 \times \vec{T}_3}{\vec{T}_1(\vec{T}_2 \times \vec{T}_3)} = \frac{2\pi}{a_{\text{lat}}} \begin{pmatrix} 1 \\ -1/\sqrt{3} \\ 0 \end{pmatrix} \\ \vec{g}_2 &= 2\pi \frac{\vec{T}_3 \times \vec{T}_1}{\vec{T}_1(\vec{T}_2 \times \vec{T}_3)} = \frac{2\pi}{a_{\text{lat}}} \begin{pmatrix} 0 \\ 2/\sqrt{3} \\ 0 \end{pmatrix} \\ \vec{g}_3 &= 2\pi \frac{\vec{T}_1 \times \vec{T}_2}{\vec{T}_1(\vec{T}_2 \times \vec{T}_3)} = \frac{2\pi}{\infty} \begin{pmatrix} 0 \\ 0 \\ 1 \end{pmatrix}\end{aligned}$$

3 set up the real-space Hamiltonian (as opposed to the reciprocal-space Hamiltonian). Consider here and in the following, only the p-orbitals perpendicular to the graphene sheet. These are the orbitals that form the states near the interesting region near the Fermi level. Consider a single hopping parameter t between nearest neighbors and place the atomic orbital energy at zero. The orbitals shall be orthonormal.

We only consider the π states, which are the p-orbitals standing perpendicular to the graphene plane.

Each carbon atom has three neighbors that need to be considered. Considering all bonds per unit cell, we obtain the following matrix elements for the real-space Hamiltonian.

left atom	right atom	matrix element
\vec{R}_1	\vec{R}_2	$h_{pp\pi}$
\vec{R}_1	$\vec{R}_2 - \vec{T}_2$	$h_{pp\pi}$
\vec{R}_1	$\vec{R}_2 - \vec{T}_1$	$h_{pp\pi}$
\vec{R}_2	\vec{R}_1	$h_{pp\pi}$
\vec{R}_2	$\vec{R}_1 + \vec{T}_2$	$h_{pp\pi}$
\vec{R}_2	$\vec{R}_1 + \vec{T}_1$	$h_{pp\pi}$

The Hamilton matrix element is $h_{pp\pi} = -t$. The “atomic level” is $\bar{\epsilon}_p$.

The Hamiltonians can be split into blocks, one for each lattice translation vector $\vec{t}_{m,n} = \vec{T}_1 m + \vec{T}_2 n$. We define them as

$$\mathbf{H}_{m,n} = \begin{pmatrix} \langle \chi_{\vec{R}_1} | \hat{H} | \chi_{\vec{R}_1 + \vec{t}_{m,n}} \rangle & \langle \chi_{\vec{R}_1} | \hat{H} | \chi_{\vec{R}_2 + \vec{t}_{m,n}} \rangle \\ \langle \chi_{\vec{R}_2} | \hat{H} | \chi_{\vec{R}_1 + \vec{t}_{m,n}} \rangle & \langle \chi_{\vec{R}_2} | \hat{H} | \chi_{\vec{R}_2 + \vec{t}_{m,n}} \rangle \end{pmatrix} \quad (4.56)$$

$$\begin{aligned} \mathbf{H}_{0,0} &= \begin{pmatrix} \bar{\epsilon}_p & h_{pp\pi} \\ h_{pp\pi} & \bar{\epsilon}_p \end{pmatrix} & \mathbf{H}_{0,-1} &= \begin{pmatrix} 0 & h_{pp\pi} \\ 0 & 0 \end{pmatrix} & \mathbf{H}_{0,1} &= \begin{pmatrix} 0 & 0 \\ h_{pp\pi} & 0 \end{pmatrix} \\ \mathbf{H}_{-1,0} &= \begin{pmatrix} 0 & h_{pp\pi} \\ 0 & 0 \end{pmatrix} & \mathbf{H}_{(1,0)} &= \begin{pmatrix} 0 & 0 \\ h_{pp\pi} & 0 \end{pmatrix} \end{aligned}$$

As an example: For $H_{1,0}$, the second orbital interacts with the first orbital of the unit cell displaced along \vec{T}_1 (along the $+x$ direction). Therefore, the $h_{pp\pi}$ -parameter enters in the (2, 1) (lower-left) matrix element of $\mathbf{H}_{1,0}$.

Check that the Hamiltonian is hermitian.

4 set up the Bloch orbitals and transform the Hamiltonian into reciprocal space.

The Bloch orbitals are

$$\begin{aligned} |\bar{\chi}_{\vec{R}_1}(\vec{k})\rangle &= \sum_{m,n} |\chi_{\vec{R}_1 + \vec{t}_{m,n}}\rangle e^{i\vec{k}\vec{t}_{m,n}} \frac{1}{\sqrt{\sum_{m,n} 1}} \\ |\bar{\chi}_{\vec{R}_2}(\vec{k})\rangle &= \sum_{m,n} |\chi_{\vec{R}_2 + \vec{t}_{m,n}}\rangle e^{i\vec{k}\vec{t}_{m,n}} \frac{1}{\sqrt{\sum_{m,n} 1}} \end{aligned} \quad (4.57)$$

The Hamiltonian in the new basis

$$\begin{aligned} \mathbf{H}(\vec{k}) &= \frac{1}{\sum_{m,n}} \begin{pmatrix} \langle \chi_{\vec{R}_1}(\vec{k}) | \hat{H} | \chi_{\vec{R}_1}(\vec{k}) \rangle & \langle \chi_{\vec{R}_1}(\vec{k}) | \hat{H} | \chi_{\vec{R}_2}(\vec{k}) \rangle \\ \langle \chi_{\vec{R}_2}(\vec{k}) | \hat{H} | \chi_{\vec{R}_1}(\vec{k}) \rangle & \langle \chi_{\vec{R}_2}(\vec{k}) | \hat{H} | \chi_{\vec{R}_2}(\vec{k}) \rangle \end{pmatrix} = \sum_{m,n} \mathbf{H}_{m,n} e^{i\vec{k}\vec{t}_{m,n}} \\ &= \begin{pmatrix} \bar{\epsilon}_p & h_{pp\pi} (1 + \exp(-i\vec{k}\vec{T}_2) + \exp(-i\vec{k}\vec{T}_1)) \\ h_{pp\pi} (1 + \exp(+i\vec{k}\vec{T}_2) + \exp(+i\vec{k}\vec{T}_1)) & \bar{\epsilon}_p \end{pmatrix} \\ &= \begin{pmatrix} \bar{\epsilon}_p & -\bar{t}(\vec{k}) \\ -\bar{t}^*(\vec{k}) & \bar{\epsilon}_p \end{pmatrix} \end{aligned}$$

where

$$\bar{t}(\vec{k}) \stackrel{\text{def}}{=} -h_{pp\pi} (1 + \exp(-i\vec{k}\vec{T}_2) + \exp(-i\vec{k}\vec{T}_1)) \quad (4.58)$$

5 diagonalize the Hamiltonian in reciprocal space.

The eigenvalues are obtained from the characteristic equation $(\bar{\epsilon}_p - \epsilon_{\pm})^2 - |t(\vec{k})|^2 = 0$ as

$$\begin{aligned}
 \epsilon_{\pm} &= \bar{\epsilon}_p \pm |\bar{t}(\vec{k})| \\
 &= \bar{\epsilon}_p \pm h_{pp\pi} \sqrt{\left(1 + \exp(i\vec{k}\vec{T}_2) + \exp(i\vec{k}\vec{T}_1)\right)\left(1 + \exp(-i\vec{k}\vec{T}_2) + \exp(-i\vec{k}\vec{T}_1)\right)} \\
 &= \bar{\epsilon}_p \pm h_{pp\pi} \sqrt{3 + e^{-i\vec{k}\vec{T}_2} + e^{-i\vec{k}\vec{T}_1} + e^{i\vec{k}\vec{T}_2} + e^{i\vec{k}(\vec{T}_2 - \vec{T}_1)} + e^{i\vec{k}\vec{T}_1} + e^{i\vec{k}(\vec{T}_1 - \vec{T}_2)} } \\
 &= \bar{\epsilon}_p \pm h_{pp\pi} \sqrt{3 + 2 \cos(\vec{k}\vec{T}_1) + 2 \cos(\vec{k}\vec{T}_2) + 2 \cos(\vec{k}(\vec{T}_1 - \vec{T}_2))} \\
 &= \bar{\epsilon}_p \pm h_{pp\pi} \sqrt{3 + 2 \cos(k_x a) + 2 \cos\left(\frac{1}{2} k_x a_{\text{lat}} + \frac{1}{2} \sqrt{3} k_y a_{\text{lat}}\right) + 2 \cos\left(-\frac{1}{2} k_x a_{\text{lat}} + \frac{1}{2} \sqrt{3} k_y a_{\text{lat}}\right)}
 \end{aligned}
 \tag{4.59}$$

Thus, the band structure is

$$\epsilon_{\pm}(\vec{k}) = \bar{\epsilon}_p \pm h_{pp\pi} \sqrt{3 + 2 \cos(k_x a_{\text{lat}}) + 2 \cos\left(\frac{1}{2} k_x a_{\text{lat}} + \frac{1}{2} \sqrt{3} k_y a_{\text{lat}}\right) + 2 \cos\left(\frac{1}{2} k_x a_{\text{lat}} - \frac{1}{2} \sqrt{3} k_y a_{\text{lat}}\right)}
 \tag{4.60}$$

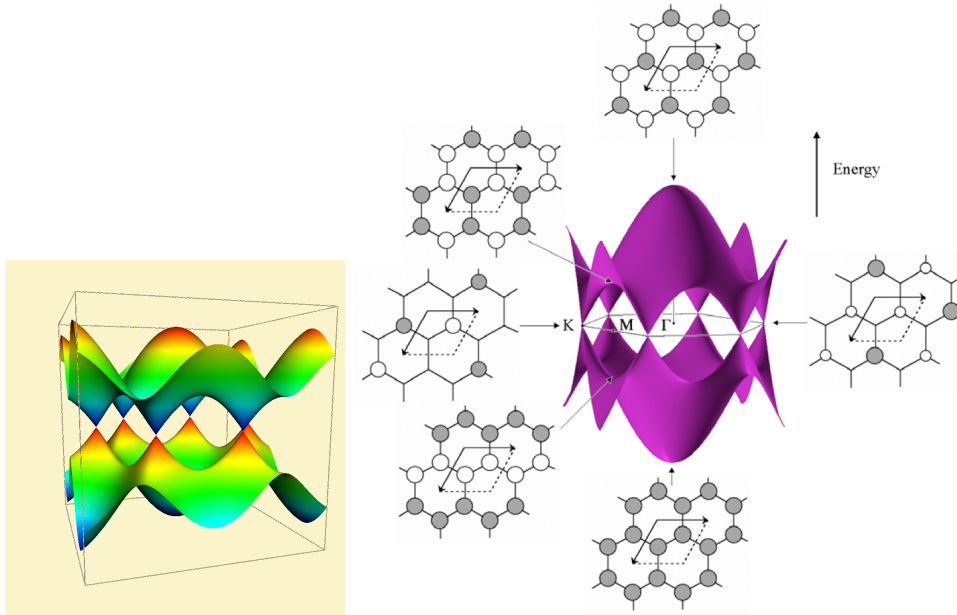


Fig. 4.14: Energy bands of the π electrons in graphene in the tight-binding model. Figure on the right with kind permission from Prof. T. Hughbanks, Texas A&M University.

Source of right figure: http://www.chem.tamu.edu/rxgroup/hughbanks/courses/673/handouts/translation_groups3.pdf

6 plot the band structure along the symmetry lines $\Gamma - M - K - \Gamma$. M is the midpoint between the extrema of the band structure. K is the k-point with the Dirac cone.

To locate the high-symmetry points, we can plot the band structure in the 2-dimensional reciprocal space as shown in fig. 4.15

Another approach is to construct the Brillouin-zone. For each vector to a reciprocal lattice point, we construct the mid-plane (in 2 dimensions, the mid-line), as the plane passing through $\frac{1}{2}\vec{G}$ which is vertical to \vec{G} . \vec{G} is any reciprocal lattice vector. The Brillouin zone is the resulting hexagon. The Γ point is the center of the hexagon. The M -point is the mid-point of one of its sides and the point K is one of its corners.

There are several possible choices for the high-symmetry points, because they are themselves related to equivalent high-symmetry points by point-group operations, i.e. a rotational symmetry operation.

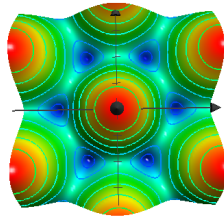


Fig. 4.15: Contour plot of the band structure of the π -bands of graphene in the 2-dimensional reciprocal unit cell.

The high-symmetry points are

$$\Gamma = \vec{0} \quad M = \frac{1}{2}\vec{g}_2 = \frac{2\pi}{a_{\text{lat}}} \begin{pmatrix} 0 \\ 1/\sqrt{3} \end{pmatrix} \quad K = \frac{1}{3}\vec{g}_1 + \frac{2}{3}\vec{g}_2 = \frac{2\pi}{a_{\text{lat}}} \begin{pmatrix} 1/3 \\ 1/\sqrt{3} \end{pmatrix} \quad (4.61)$$

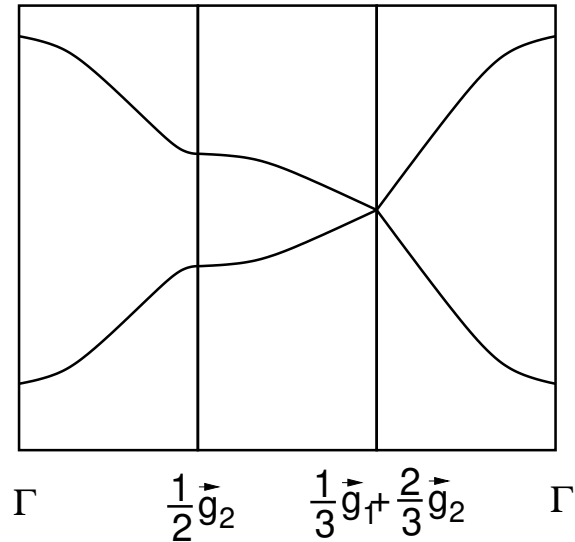


Fig. 4.16: Band structure of the π -bands of graphene along the high-symmetry lines.

4.6.2 Band structure of high- T_c superconductors

Introduction and background

Until 1986, superconductivity was believed to be an effect that takes place only in metals. Furthermore, it was believed that the transition temperatures would never exceed 30 K.

In 1986 Alex Müller und Georg Bednorz from the IBM Research Laboratory in Ruschlikon, Switzerland showed that there are superconducting ceramics, which, furthermore, have a transition temperatures of 35 K,[34] much higher than the 23 K achieved before for conventional superconductors. Now, there are many variants of these ceramics with transition temperatures up to 133 K. For obvious reasons, these materials are called **high- T_c superconductors**. Already in 1987, Müller and Bednorz, received the Nobel Price for the discovery of superconductivity in ceramics.

The material studied by Müller and Bednorz is a hole-doped La_2CuO_4 .

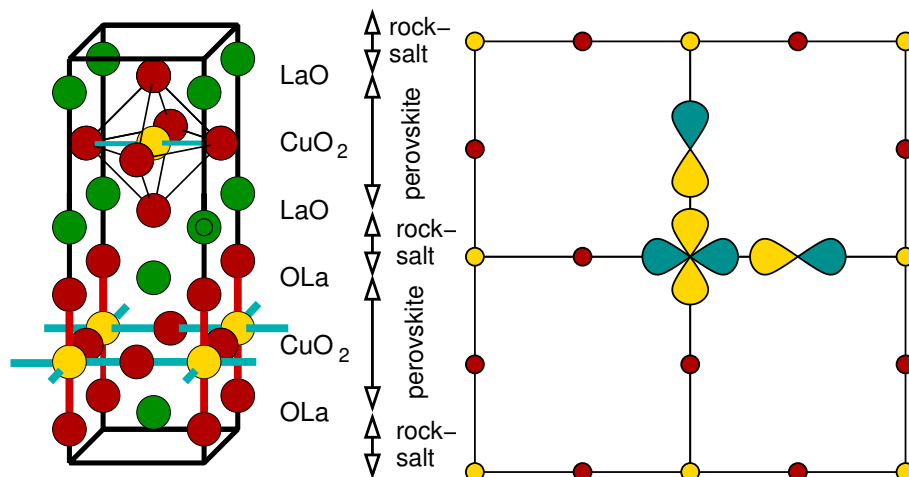


Fig. 4.17: Left: Atomic structure of the parent compound La_2CuO_4 of the cuprate superconductors. Cu atoms are drawn in yellow, oxygen atoms in red and La ions in green. The unit cell contains two identical, but shifted, CuO_2 planes. For the upper one, I emphasized the octahedra as structural element, while for the lower one the CuO_2 plane. The structure can be envisaged as a layered material formed from layers with perovskite and rock-salt structure. Right: sketch of the CuO_2 plane with the relevant basis orbitals, $d_{x^2-y^2}$ on Cu, and one p -orbital on each of the two oxygen ions in the unit cell. The blue side of the orbital stands for positive and the yellow one for negative values of the orbital.

The atomic structure of La_2CuO_4 is shown in figure 4.17. The common important element of the cuprate superconductors are CuO_2 planes, in which the Cu^{2+} ions form a two-dimensional square lattice. Oxygen ions are located in between the nearest Cu neighbors. Relevant are the $d_{x^2-y^2}$ orbitals on the Cu ions and the oxygen- p orbitals pointing towards the neighboring Cu sites.

Tasks

- 1 Identify the lattice vectors and atomic positions of the CuO_2 plane. Determine the reciprocal lattice and the high-symmetry points and lines.
- 2 Calculate the Hamiltonian in real space in the basis of the relevant orbitals specified above. The Cu-d level $\bar{\epsilon}_d$ lies above the O-p-level $\bar{\epsilon}_p$.
- 3 Calculate the k-dependent Hamiltonian for the Bloch states.
- 4 Determine the k-dependent eigenvalues of the Hamiltonian
- 5 Evaluate the band structure along a path from the Γ -point, via the X point and the M-point back to Γ .

$$\Gamma = \left(0, 0\right) \frac{2\pi}{a_{\text{lat}}} \quad \text{and} \quad X = \left(\frac{1}{2}, 0\right) \frac{2\pi}{a_{\text{lat}}} \quad \text{and} \quad M = \left(\frac{1}{2}, \frac{1}{2}\right) \frac{2\pi}{a_{\text{lat}}}$$

- 6 Sketch the band structure $\Gamma - X - M - \Gamma$.

Solution

- 1 Identify the lattice vectors and atomic positions of the CuO_2 plane. Determine the reciprocal lattice and the high-symmetry points and lines.

real-space lattice vectors

\vec{T}_1/a_{lat}	1	0	0
\vec{T}_2/a_{lat}	0	1	0
\vec{T}_3/a_{lat}	0	0	∞
$\vec{R}_{\text{Cu}}/a_{\text{lat}}$	0	0	0
$\vec{R}_{\text{O1}}/a_{\text{lat}}$	0.5	0	0
$\vec{R}_{\text{O2}}/a_{\text{lat}}$	0	0.5	0

reciprocal space lattice vectors

$\vec{g}_1/(2\pi/a_{\text{lat}})$	1	0	0
$\vec{g}_2/(2\pi/a_{\text{lat}})$	0	1	0
$\vec{g}_3/(2\pi/a_{\text{lat}})$	0	0	0

High-symmetry points

$\Gamma/(2\pi/a_{\text{lat}})$	0	0	0
$X/(2\pi/a_{\text{lat}})$	1/2	0	0
$M/(2\pi/a_{\text{lat}})$	1/2	1/2	0

- 2 Calculate the Hamiltonian in real space in the basis of the relevant orbitals specified above.

The relevant orbitals are shown in figure 4.17. In the following, we choose the x-axis in the figure pointing to the right and the y-axis vertically upwards on the page. The orbitals are the $d_{x^2-y^2}$ orbital

on the Cu-ion, the p_x on oxygen ion O_1 to the right of the Cu ion, and the p_y on oxygen ion O_2 above the Cu ion. We will keep the **orbitals in this order**.

The Hamilton matrix elements are of the same magnitude, but they differ in sign. I will **define the hopping parameter** t via the matrix element between the Cu- $d_{x^2-y^2}$ and the p_y orbital in the same unit cell. The overlap between these orbitals is positive, and the Hamilton matrix element is therefore negative. I define the hopping parameter to be equal in magnitude to the Hamilton matrix element, but opposite in sign, that is

$$t \stackrel{\text{def}}{=} -\langle d_{x^2-y^2, \vec{0}} | \hat{H} | p_{y, \vec{0}} \rangle = |\langle d_{x^2-y^2, \vec{0}} | \hat{H} | p_{y, \vec{0}} \rangle| \quad (4.62)$$

For the sign of the offsite Hamilton matrix elements, see the related discussion on p. 136.

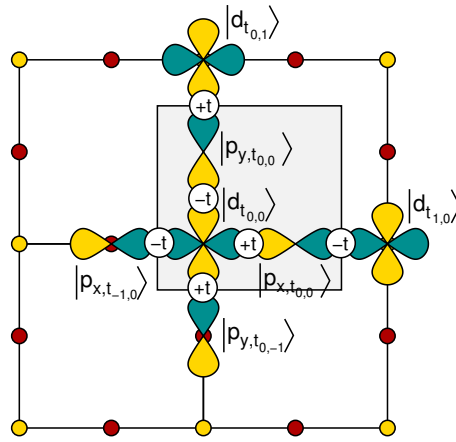


Fig. 4.18: Sketch of the orbitals in the first unit cell and those connected to orbitals in the first unit cell. In the white circles, the offsite Hamilton matrix elements of the corresponding bond are given in terms of the hopping parameter t . See figure 4.17 for further explanations.

The real-space Hamiltonians $\hat{H}_{\vec{0}, \vec{\tau}_{m,n}}$ for the second orbital displaced by $\vec{\tau}_{m,n} = (m, n)_{\text{lat}}$ is

$$\begin{aligned} \hat{H}_{\vec{0}, \vec{0}} &= \begin{pmatrix} |d_{x^2-y^2, \vec{0}}\rangle \\ |p_{x, \vec{0}}\rangle \\ |p_{y, \vec{0}}\rangle \end{pmatrix} \begin{pmatrix} \bar{\epsilon}_d + t - t \\ +t \bar{\epsilon}_p & 0 \\ -t & 0 & \bar{\epsilon}_p \end{pmatrix} \begin{pmatrix} \langle d_{x^2-y^2, \vec{0}} | \\ \langle p_{x, \vec{0}} | \\ \langle p_{y, \vec{0}} | \end{pmatrix} \\ \hat{H}_{\vec{0}, \vec{\tau}_{1,0}} &= |p_{x, \vec{0}}\rangle \underbrace{\langle p_{x, \vec{0}} | \hat{H} | d_{x^2-y^2, \vec{\tau}_{1,0}} \rangle}_{-t} \langle d_{x^2-y^2, \vec{\tau}_{1,0}} | = \begin{pmatrix} |d_{x^2-y^2, \vec{0}}\rangle \\ |p_{x, \vec{0}}\rangle \\ |p_{y, \vec{0}}\rangle \end{pmatrix} \begin{pmatrix} 0 & 0 & 0 \\ -t & 0 & 0 \\ 0 & 0 & 0 \end{pmatrix} \begin{pmatrix} \langle d_{x^2-y^2, \vec{\tau}_{1,0}} | \\ \langle p_{x, \vec{\tau}_{1,0}} | \\ \langle p_{y, \vec{\tau}_{1,0}} | \end{pmatrix} \quad \text{and} \\ \hat{H}_{\vec{0}, \vec{\tau}_{-1,0}} &= |d_{x^2-y^2, \vec{0}}\rangle \underbrace{\langle d_{x^2-y^2, \vec{0}} | \hat{H} | p_{x, \vec{\tau}_{-1,0}} \rangle}_{-t} \langle p_{x, \vec{\tau}_{-1,0}} | = \begin{pmatrix} |d_{x^2-y^2, \vec{0}}\rangle \\ |p_{x, \vec{0}}\rangle \\ |p_{y, \vec{0}}\rangle \end{pmatrix} \begin{pmatrix} 0 & -t & 0 \\ 0 & 0 & 0 \\ 0 & 0 & 0 \end{pmatrix} \begin{pmatrix} \langle d_{x^2-y^2, \vec{\tau}_{-1,0}} | \\ \langle p_{x, \vec{\tau}_{-1,0}} | \\ \langle p_{y, \vec{\tau}_{-1,0}} | \end{pmatrix} \\ \hat{H}_{\vec{0}, \vec{\tau}_{0,1}} &= |d_{x^2-y^2, \vec{0}}\rangle \underbrace{\langle d_{x^2-y^2, \vec{0}} | \hat{H} | p_{y, \vec{\tau}_{0,1}} \rangle}_{+t} \langle p_{y, \vec{\tau}_{0,1}} | = \begin{pmatrix} |d_{x^2-y^2, \vec{0}}\rangle \\ |p_{x, \vec{0}}\rangle \\ |p_{y, \vec{0}}\rangle \end{pmatrix} \begin{pmatrix} 0 & 0 & 0 \\ 0 & 0 & 0 \\ +t & 0 & 0 \end{pmatrix} \begin{pmatrix} \langle d_{x^2-y^2, \vec{\tau}_{0,1}} | \\ \langle p_{x, \vec{\tau}_{0,1}} | \\ \langle p_{y, \vec{\tau}_{0,1}} | \end{pmatrix} \quad \text{and} \\ \hat{H}_{\vec{0}, \vec{\tau}_{0,-1}} &= |d_{x^2-y^2, \vec{0}}\rangle \underbrace{\langle d_{x^2-y^2, \vec{0}} | \hat{H} | p_{y, \vec{\tau}_{0,-1}} \rangle}_{+t} \langle p_{y, \vec{\tau}_{0,-1}} | = \begin{pmatrix} |d_{x^2-y^2, \vec{0}}\rangle \\ |p_{x, \vec{0}}\rangle \\ |p_{y, \vec{0}}\rangle \end{pmatrix} \begin{pmatrix} 0 & 0 & +t \\ 0 & 0 & 0 \\ 0 & 0 & 0 \end{pmatrix} \begin{pmatrix} \langle d_{x^2-y^2, \vec{\tau}_{0,-1}} | \\ \langle p_{x, \vec{\tau}_{0,-1}} | \\ \langle p_{y, \vec{\tau}_{0,-1}} | \end{pmatrix} \quad (4.63) \end{aligned}$$

3 Calculate the k-dependent Hamiltonian for the Bloch states.

Hamiltonian in k-space:

$$\begin{aligned} H(\vec{k}) &\stackrel{\text{Eq. 4.44}}{=} \sum_{m,n} H_{\vec{0},\vec{t}_{m,n}} e^{i\vec{k}\vec{t}_{m,n}} \\ &= \begin{pmatrix} \bar{\epsilon}_d & +t[1 - \exp(-ik_x a_{\text{lat}})] & -t[1 - \exp(-ik_y a_{\text{lat}})] \\ +t[1 - \exp(ik_x a_{\text{lat}})] & \bar{\epsilon}_p & 0 \\ -t[1 - \exp(ik_y a_{\text{lat}})] & 0 & \bar{\epsilon}_p \end{pmatrix} \end{aligned} \quad (4.64)$$

Further Remarks:

The structure of the Hamiltonian for each k-point is that of a three-center bond: Consider the Hamiltonian for one atom in the center, with a hybridization to a neighboring atom on either side. The neighbors themselves do not hybridize directly. The structure of this Hamiltonian with zero off-diagonal elements between two of the orbitals is the same as the Hamiltonian for the CuO_2 plane above.

This observation can be exploited by forming a superposition of the two p-orbitals such that they does not couple to the d-orbital.

$$t[1 - \exp(-ik_x a_{\text{lat}})]c_2 - t[1 - \exp(-ik_y a_{\text{lat}})]c_3 = 0 \quad (4.65)$$

Because the two oxygen orbitals do not couple directly, the state satisfying the condition above would be an eigenstate. In our example

4 Determine the k-dependent eigenvalues of the Hamiltonian

It is possible to determine all eigenvalues analytically: The characteristic equation is

$$\begin{aligned} 0 &= (\bar{\epsilon}_d - \epsilon)(\bar{\epsilon}_p - \epsilon)^2 - t[1 - \exp(-ik_x a_{\text{lat}})]t[1 - \exp(ik_x a_{\text{lat}})](\bar{\epsilon}_p - \epsilon) \\ &\quad - t[1 - \exp(-ik_y a_{\text{lat}})]t[1 - \exp(ik_y a_{\text{lat}})](\bar{\epsilon}_p - \epsilon) \\ 0 &= (\bar{\epsilon}_d - \epsilon)(\bar{\epsilon}_p - \epsilon) - t^2[2 - 2\cos(-ik_x a_{\text{lat}})] - t^2[2 - 2\cos(-ik_y a_{\text{lat}})] = 0 \quad \text{or } \epsilon = \bar{\epsilon}_p \\ 0 &= \epsilon^2 - (\bar{\epsilon}_p + \bar{\epsilon}_d)\epsilon + \bar{\epsilon}_p \bar{\epsilon}_d - 4t^2 \sin^2(k_x a_{\text{lat}}/2) - 4t^2 \sin^2(k_y a_{\text{lat}}/2) \quad \text{or } \epsilon = \bar{\epsilon}_p \\ \epsilon &= \frac{\bar{\epsilon}_p + \bar{\epsilon}_d}{2} \pm \sqrt{\left(\frac{\bar{\epsilon}_p - \bar{\epsilon}_d}{2}\right)^2 + 4t^2 \left[\sin^2\left(\frac{1}{2}k_x a_{\text{lat}}\right) + \sin^2\left(\frac{1}{2}k_y a_{\text{lat}}\right)\right]} \quad \text{or } \epsilon = \bar{\epsilon}_p \end{aligned} \quad (4.66)$$

Thus, we obtain one pure p-band with $\epsilon = \bar{\epsilon}_p$ for the entire Brillouin zone. The other two states hybridize. Level-repulsion shifts the Cu-d-level higher up and the second p-state further down. The top of the highest band is at $\vec{k} = \frac{\pi}{a_{\text{lat}}}(1, 1)$.

5 Evaluate the band structure along a path from the Γ -point, via the X point and the M-point back to Γ .

$$\Gamma = \left(0, 0\right) \frac{2\pi}{a_{\text{lat}}} \quad \text{and} \quad X = \left(\frac{1}{2}, 0\right) \frac{2\pi}{a_{\text{lat}}} \quad \text{and} \quad M = \left(\frac{1}{2}, \frac{1}{2}\right) \frac{2\pi}{a_{\text{lat}}}$$

Editor: Previously, the point of this task was to exploit the increased symmetry at the high-symmetry lines to diagonalize the Hamiltonian. Now the Hamiltonian is diagonalized already. The Solution needs to be adapted accordingly.

- Γ - X :

The bands from Γ to X are scanned by a one-dimensional parameter s so that $\vec{k}(0) = \Gamma$ and $\vec{k}(1) = X$

$$\vec{k}(s) = (1-s)\vec{\Gamma} + s\vec{X} = \left(s \frac{\pi}{a_{\text{lat}}}, 0, 0 \right) \quad \text{for } s = [0, 1] \quad (4.67)$$

The k-vector at a high-symmetry point is denoted here by the symbol for that point with an vector arrow, such as $\vec{\Gamma}$. Another notation would be to label the k-point by the symbol as in \vec{k}_{Γ} .

The eigenvalues are

$$\begin{aligned} \epsilon_1(s) &= \bar{\epsilon}_p - \frac{\bar{\epsilon}_d - \bar{\epsilon}_p}{2} \left\{ \sqrt{1 + \left(\frac{4t \sin\left(s \frac{\pi}{2}\right)}{\bar{\epsilon}_d - \bar{\epsilon}_p} \right)^2} - 1 \right\} \\ \epsilon_2(s) &= \bar{\epsilon}_p \\ \epsilon_3(s) &= \bar{\epsilon}_d + \frac{\bar{\epsilon}_d - \bar{\epsilon}_p}{2} \left\{ \sqrt{1 + \left(\frac{4t \sin\left(s \frac{\pi}{2}\right)}{\bar{\epsilon}_d - \bar{\epsilon}_p} \right)^2} - 1 \right\} \end{aligned} \quad (4.68)$$

One band is dispersion-less. Its character is the p_y orbital on the O(2) ion.

At the Γ -point the three states are the pure Cu-d orbital with energy $\bar{\epsilon}_d$ and the two degenerate O-p orbitals at $\bar{\epsilon}_p$.

Let me consider the case with $\bar{\epsilon}_d > \bar{\epsilon}_p$. Towards the X -point the d-level shifts upwards towards

- Γ - M

$$\vec{k} = (1-s)\vec{\Gamma} + s\vec{M} = \left(s \frac{\pi}{a_{\text{lat}}}, s \frac{\pi}{a_{\text{lat}}}, 0 \right) \quad \text{for } s = [0, 1] \quad (4.69)$$

$$\begin{aligned} \epsilon_1(s) &= \bar{\epsilon}_p - \frac{\bar{\epsilon}_d - \bar{\epsilon}_p}{2} \left\{ \sqrt{1 + 2 \left(\frac{4t \sin\left(s \frac{\pi}{2}\right)}{\bar{\epsilon}_d - \bar{\epsilon}_p} \right)^2} - 1 \right\} \\ \epsilon_2(s) &= \bar{\epsilon}_p \\ \epsilon_3(s) &= \bar{\epsilon}_d + \frac{\bar{\epsilon}_d - \bar{\epsilon}_p}{2} \left\{ \sqrt{1 + 2 \left(\frac{4t \sin\left(s \frac{\pi}{2}\right)}{\bar{\epsilon}_d - \bar{\epsilon}_p} \right)^2} - 1 \right\} \end{aligned} \quad (4.70)$$

- $X - M$

$$\vec{k} = (1-s)\vec{X} + s\vec{M} = \left(\frac{\pi}{a_{\text{lat}}}, s \frac{\pi}{a_{\text{lat}}}, 0 \right) \quad \text{for } s = [0, 1] \quad (4.71)$$

$$\begin{aligned}
\epsilon_1(s) &= \bar{\epsilon}_p - \frac{\bar{\epsilon}_d - \bar{\epsilon}_p}{2} \left\{ \sqrt{1 + \left(\frac{4t}{\bar{\epsilon}_d - \bar{\epsilon}_p} \right)^2 \left[1 + \sin^2 \left(s \frac{\pi}{2} \right) \right]} - 1 \right\} \\
\epsilon_2(s) &= \bar{\epsilon}_p \\
\epsilon_3(s) &= \bar{\epsilon}_d + \frac{\bar{\epsilon}_d - \bar{\epsilon}_p}{2} \left\{ \sqrt{1 + \left(\frac{4t}{\bar{\epsilon}_d - \bar{\epsilon}_p} \right)^2 \left[1 + \sin^2 \left(s \frac{\pi}{2} \right) \right]} - 1 \right\}
\end{aligned} \tag{4.72}$$

6 Sketch the band structure $\Gamma - X - M - \Gamma$.

The sketch of the band structure is shown in figure 4.19.

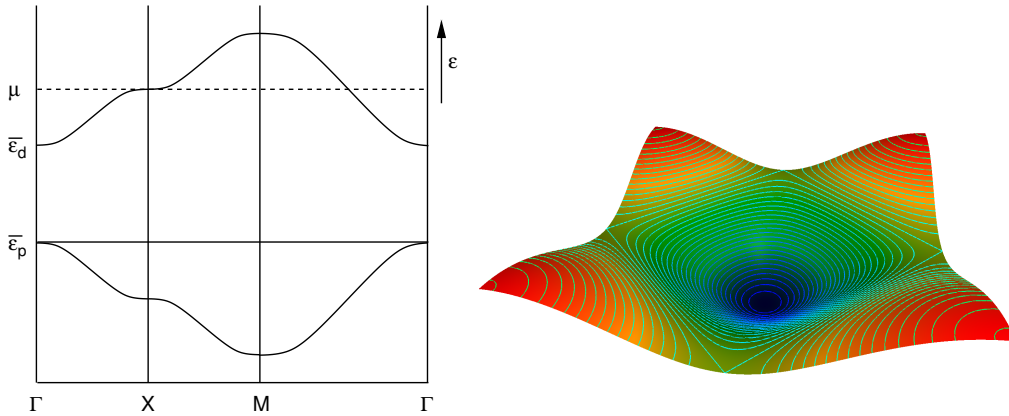


Fig. 4.19: Left: Sketch of the band structure of three-band model for CuO_2 . Right: graph of the upper band in the two-dimensional band structure. The Gamma point is in the center and the sides proceed parallel and perpendicular to Γ - X .

The observation in figure 4.19, that the oxygen p-band is completely flat, is an artifact of the model. A better description is obtained, when direct hopping parameters between the oxygen p-states are included, which are second-nearest neighbors of each other.

In the upper band is half filled. In figure 4.19 one sees that the Fermi surface forms a perfect square. This leads to a **nesting condition**. A perturbation of the potential, which includes a component with $\vec{G} = \frac{1}{2}(\vec{g}_1 + \vec{g}_2)$ and one with $\vec{G} = \frac{1}{2}(\vec{g}_1 - \vec{g}_2)$ is able to open a band gap. In the cuprates, this is accomplished by a phase transition to an antiferromagnet, which turns the cuprate into an insulator. This phase transition competes with the superconducting phase transition. Attempts to form superconductors in this class of materials use doping to suppress the antiferromagnetic transition.

4.6.3 Canonical p-band for the fcc structure

The anion lattice of most ionic materials form a closed-packed lattice, while the cations enter the octahedral and tetrahedral voids between the anions. The two most prominent closed packed lattices are the face-centered-cubic (fcc) and the hexagonally-closed-packed (hcp) structures. Because of this common structural principle, the valence band of many ionic materials looks alike.

Here we determine the tight-binding model for p-orbitals of atoms that form an fcc lattice. This band structure can be compared with the valence band of many oxides.

The lattice vectors of the fcc lattice are

$$\begin{aligned}\vec{T}_1 &= \left(0, \frac{1}{2}, \frac{1}{2}\right) a_{\text{lat}} \\ \vec{T}_2 &= \left(\frac{1}{2}, 0, \frac{1}{2}\right) a_{\text{lat}} \\ \vec{T}_3 &= \left(\frac{1}{2}, \frac{1}{2}, 0\right) a_{\text{lat}}\end{aligned}\quad (4.73)$$

Only the three p-states of the anion are considered and the cation orbitals are neglected. The parameters defining the band structure are Hamilton matrix elements $h_{pp\sigma}$, $h_{pp\pi}$ for σ and π bonds, as well as the “atomic” orbital energy $\bar{\epsilon}_p$.

In order to use the parameters, we will have to represent a p-orbital with a specific direction in space by the orbitals $|p_x\rangle$, $|p_y\rangle$, $|p_z\rangle$ of our basis set, which are oriented along the Cartesian coordinate axes. This relation is as follows: For a unit vector $\vec{e} = (e_x, e_y, e_z)$ defining the orientation of the p-orbital $|p_{\vec{e}}\rangle$, the orbital has the form

$$|p_{\vec{e}}\rangle = |p_x\rangle e_x + |p_y\rangle e_y + |p_z\rangle e_z \quad (4.74)$$

Tasks

- 1 calculate the Hamiltonian in real space in the basis of $|p_{x,\vec{t}}\rangle$, $|p_{y,\vec{t}}\rangle$, $|p_{z,\vec{t}}\rangle$ considering only nearest-neighbor hopping. Use the parameters given above. The vector \vec{t} indicates the lattice translation identifying a particular atom of the lattice.
- 2 Calculate the k-dependent Hamiltonian for the Bloch states.
- 3 In order to calculate the band structure from^a $\Gamma = (0, 0, 0)$ to $X = (\frac{1}{2}, 0, 0)$ $\frac{2\pi}{a_{\text{lat}}}$, calculate the Hamiltonian as function of the parameter s varying linearly from Γ to X .
- 4 Calculate the band structure from Γ to X . Draw the band structure.
- 5 Describe how the parameters $\bar{\epsilon}_p$, $h_{pp\sigma}$ and $h_{pp\pi}$ can be extracted from a band structure plot. Exploit that the dispersion from Γ to X of the singly-degenerate band is 2.4 eV and that of the doubly-degenerate state is 0.8 eV. The top of the band is at 0 eV.
- 6 Discuss the sign of $h_{pp\sigma}$ and $h_{pp\pi}$. The goal is not a rigorous proof, which is probably not possible. Rather the goal is qualitative reasoning. It is about visualizing wave functions and potentials with the aim to find qualitative arguments. Thus, there is not a single true or false answer.

Hint: this problem is rather involved unless you make extensive use of the symmetry of the problem. Furthermore, make sure that you have the trigonometric formulas at hand.

^aThe scale factor $2\pi/a_{\text{lat}}$ for the X-point rather than π/a_{lat} is correct. See below in Eq. 4.102 on p. 163.

Solution

This is a sketch for the solution and needs to be checked and niced up.

1 calculate the Hamiltonian in real space in the basis of $|\rho_x, \vec{t}\rangle$, $|\rho_y, \vec{t}\rangle$, $|\rho_z, \vec{t}\rangle$ considering only nearest-neighbor hopping. Use the parameters given above. The vector \vec{t} indicates the lattice translation identifying a particular atom of the lattice.

To clarify the notation, let us divide the Hamiltonian into contributions for pairs of unit cells.

$$\hat{H} = \sum_{\alpha, \vec{t}, \vec{\beta}, \vec{t}'} |\alpha, \vec{t}\rangle H_{\alpha, \vec{t}, \beta, \vec{t}'} \langle \beta, \vec{t}'| = \sum_{\vec{t}, \vec{t}'} \hat{H}_{\vec{t}, \vec{t}'} \quad (4.75)$$

The matrix elements for a pair operator $\hat{H}_{\vec{t}, \vec{t}'}$ are combined into the matrix $\mathbf{H}_{\vec{t}, \vec{t}'}$.

Because of translational invariance, we can use $\mathbf{H}_{\vec{t}, \vec{t}'} = \mathbf{H}_{\vec{0}, \vec{t}' - \vec{t}}$. Caution! The identity does not hold for the pair contribution of the Hamilton-operator $\hat{H}_{\vec{t}, \vec{t}'} \neq \hat{H}_{\vec{0}, \vec{t}' - \vec{t}}$.

The onsite Hamiltonian is easily set up as

$$\hat{H}_{\vec{0}, \vec{0}} = \begin{pmatrix} |\rho_x, \vec{0}\rangle \\ |\rho_y, \vec{0}\rangle \\ |\rho_z, \vec{0}\rangle \end{pmatrix} \underbrace{\begin{pmatrix} \bar{\epsilon}_p & 0 & 0 \\ 0 & \bar{\epsilon}_p & 0 \\ 0 & 0 & \bar{\epsilon}_p \end{pmatrix}}_{\mathbf{H}_{\vec{0}, \vec{0}}} \begin{pmatrix} \langle \rho_x, \vec{0}| \\ \langle \rho_y, \vec{0}| \\ \langle \rho_z, \vec{0}| \end{pmatrix} \quad (4.76)$$

The 12 nearest-neighbor vectors \vec{t} in units of $\frac{1}{2}a_{\text{lat}}$ are,

	$\vec{t}_1 =$	$\vec{t}_2 =$	$\vec{t}_3 =$	$\vec{t}_4 =$	$\vec{t}_5 =$	$\vec{t}_6 =$
$+\vec{t}$	(+1,+1,0)	(1,-1,0)	(+1,0,+1)	(-1,0,+1)	(0,+1,+1)	(0,-1,+1)
$-\vec{t}$	(-1,-1,0)	(-1,1,0)	(-1,0,-1)	(+1,0,-1)	(0,-1,-1)	(0,+1,-1)
	$= -\vec{t}_1$	$= -\vec{t}_2$	$= -\vec{t}_3$	$= -\vec{t}_4$	$= -\vec{t}_5$	$= -\vec{t}_6$

where a_{lat} is the real-space lattice constant. Below, I will refer to the nearest-neighbor pairs via the lattice translation vectors with the indices defined here. Notice that I can use the lattice vectors to identify the nearest-neighbor pairs only, because there is only one site per unit cell.

In the following, we will need to obtain p-orbitals that are oriented along a specific axis \vec{e} , rather than along one of the Cartesian coordinates. \vec{e} is normalized, i.e. $\vec{e}^2 = 1$. I use real spherical harmonics¹⁵

$$Y_{\rho_x}(\vec{r}) = \sqrt{\frac{3}{4\pi}} \frac{x}{|\vec{r}|} \quad \text{and} \quad Y_{\rho_y}(\vec{r}) = \sqrt{\frac{3}{4\pi}} \frac{y}{|\vec{r}|} \quad \text{and} \quad Y_{\rho_z}(\vec{r}) = \sqrt{\frac{3}{4\pi}} \frac{z}{|\vec{r}|} \quad (4.79)$$

Thus, a real spherical harmonic along \vec{e} has the form

$$Y_{\rho, \vec{e}}(\vec{r}) = \sqrt{\frac{3}{4\pi}} \frac{\vec{e} \cdot \vec{r}}{|\vec{r}|} = e_x Y_{\rho_x}(\vec{r}) + e_y Y_{\rho_y}(\vec{r}) + e_z Y_{\rho_z}(\vec{r}) \quad (4.80)$$

¹⁵The prefactor of the p-type real spherical harmonics can be obtained from the normalization condition

$$\int d\Omega Y_{p_j}^*(\vec{r}) Y_{p_j}(\vec{r}) = 1 \quad (4.77)$$

where the integration is performed over all directions in three dimensions. Let us start with the form $Y_{p_j} = C x_j / |\vec{r}|$.

$$1 \stackrel{!}{=} \int d\Omega Y_{p_j}^*(\vec{r}) Y_{p_j}(\vec{r}) = \frac{1}{3} \sum_{j=1}^3 \int d\Omega Y_{p_j}^*(\vec{r}) Y_{p_j}(\vec{r}) = \frac{1}{3} \int_{4\pi} d\Omega |C|^2 \underbrace{\frac{x_1^2 + x_2^2 + x_3^2}{r^2}}_{=1} = \frac{4\pi}{3} |C|^2$$

$$\Rightarrow C = \sqrt{\frac{3}{4\pi}} \quad \Rightarrow \quad Y_{p_j} = \sqrt{\frac{3}{4\pi}} \frac{x_j}{|\vec{r}|} \quad (4.78)$$

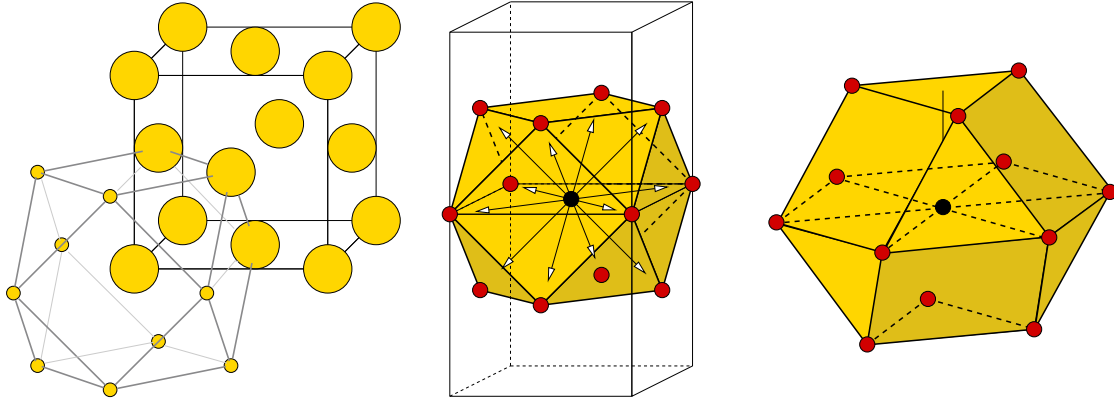


Fig. 4.20: Face-centered cubic (fcc) structure. Shown are the atomic positions at the corners and face centers of the cube. Furthermore the cubo-octahedron of the twelve nearest neighbors is shown. In the middle, the cubo-octahedron is shown in the same orientation as on the left hand side, while on the right side the cubo-octahedron is shown in an orientation with horizontal triangular planes.

Because the p-orbitals in the same shell have the same radial dependence, we obtain

$$|\vec{p}_{\vec{e}}\rangle = |\rho_x\rangle e_x + |\rho_y\rangle e_y + |\rho_z\rangle e_z \quad (4.81)$$

Let me first work out the off-site Hamiltonian for the first lattice-translation vector in our list, namely

$$\vec{t}_1 \stackrel{\text{def}}{=} \left(\frac{1}{2}, \frac{1}{2}, 0 \right) a_{\text{lat}}. \quad (4.82)$$

We express the Hamiltonian terms for this nearest-neighbor pair in terms of the orbitals with σ -character¹⁶ $|\rho_{(110)}\rangle$ and the two orbitals with π -character, namely $|\rho_{(1\bar{1}0)}\rangle$ and $|\rho_{(001)}\rangle$. They are defined as follows

$$\begin{aligned} |\rho_{(110)}\rangle &= \left(|\vec{p}_x\rangle + |\vec{p}_y\rangle \right) \frac{1}{\sqrt{2}} \\ |\rho_{(1\bar{1}0)}\rangle &= \left(|\vec{p}_x\rangle - |\vec{p}_y\rangle \right) \frac{1}{\sqrt{2}} \\ |\rho_{(001)}\rangle &= |\vec{p}_z\rangle \end{aligned} \quad (4.83)$$

Caution is required regarding the notation:

- to identify the orbitals I do not write the normalized direction vector \vec{e} for the orbital as index, but just a vector with the same direction, such as $|\rho_{(1,1,0)}\rangle$.
- In order to tighten the notation I am using $\bar{1} = -1$. Using the bar onto of the number to describe the negative number is a common notation in crystallography, which I am borrowing here. The bar is the “minus sign”, which is placed on-top of the number rather than in front of it.

The Hamiltonian for this atom pair connected by \vec{t}_1 is

$$\hat{H}_{\vec{0},\vec{t}_1} = \begin{pmatrix} |\rho_{(110),\vec{0}}\rangle \\ |\rho_{(1\bar{1}0),\vec{0}}\rangle \\ |\rho_{(001),\vec{0}}\rangle \end{pmatrix} \begin{pmatrix} h_{pp\sigma} & 0 & 0 \\ 0 & h_{pp\pi} & 0 \\ 0 & 0 & h_{pp\pi} \end{pmatrix} \begin{pmatrix} \langle \rho_{(110),\vec{t}_1} | \\ \langle \rho_{(1\bar{1}0),\vec{t}_1} | \\ \langle \rho_{(001),\vec{t}_1} | \end{pmatrix} \quad (4.84)$$

¹⁶ σ and π denote the angular momentum relative to this bond axis.

Next, we express the off-site Hamiltonian in terms of our basis states, $|\rho_x\rangle$, $|\rho_y\rangle$ and $|\rho_z\rangle$.

$$\begin{pmatrix} |\rho_{(110)}\rangle \\ |\rho_{(1\bar{1}0)}\rangle \end{pmatrix} = \begin{pmatrix} |\rho_x\rangle \\ |\rho_y\rangle \end{pmatrix} \begin{pmatrix} 1 & 1 \\ 1 & -1 \end{pmatrix} \frac{1}{\sqrt{2}} \Rightarrow \begin{pmatrix} |\rho_x\rangle \\ |\rho_y\rangle \end{pmatrix} = \begin{pmatrix} |\rho_{(110)}\rangle \\ |\rho_{(1\bar{1}0)}\rangle \end{pmatrix} \begin{pmatrix} 1 & 1 \\ 1 & -1 \end{pmatrix} \frac{1}{\sqrt{2}}$$

The $|\rho_{(001)}\rangle = |\rho_z\rangle$ state can be added simply.

$$\begin{pmatrix} |\rho_x\rangle \\ |\rho_y\rangle \\ |\rho_z\rangle \end{pmatrix} = \begin{pmatrix} |\rho_{(110)}\rangle \\ |\rho_{(1\bar{1}0)}\rangle \\ |\rho_{(001)}\rangle \end{pmatrix} \begin{pmatrix} 1 & 1 & 0 \\ 1 & -1 & 0 \\ 0 & 0 & \sqrt{2} \end{pmatrix} \frac{1}{\sqrt{2}} \quad (4.85)$$

Now, the transformation is inserted. We also consider the site, at which the orbital is centered, as one of the orbital indices.

$$\begin{aligned} \hat{H}_{\vec{0},\vec{\epsilon}_1} &= \begin{pmatrix} |\rho_{(110),\vec{0}}\rangle \\ |\rho_{(1\bar{1}0),\vec{0}}\rangle \\ |\rho_{(001),\vec{0}}\rangle \end{pmatrix} \begin{pmatrix} h_{pp\sigma} & 0 & 0 \\ 0 & h_{pp\pi} & 0 \\ 0 & 0 & h_{pp\pi} \end{pmatrix} \begin{pmatrix} \langle \rho_{(110),\vec{\epsilon}_1} | \\ \langle \rho_{(1\bar{1}0),\vec{\epsilon}_1} | \\ \langle \rho_{(001),\vec{\epsilon}_1} | \end{pmatrix} \\ &= \begin{pmatrix} |\rho_{x,\vec{0}}\rangle \\ |\rho_{y,\vec{0}}\rangle \\ |\rho_{z,\vec{0}}\rangle \end{pmatrix} \begin{pmatrix} 1 & 1 & 0 \\ 1 & -1 & 0 \\ 0 & 0 & \sqrt{2} \end{pmatrix} \frac{1}{\sqrt{2}} \begin{pmatrix} h_{pp\sigma} & 0 & 0 \\ 0 & h_{pp\pi} & 0 \\ 0 & 0 & h_{pp\pi} \end{pmatrix} \\ &\quad \times \begin{pmatrix} 1 & 1 & 0 \\ 1 & -1 & 0 \\ 0 & 0 & \sqrt{2} \end{pmatrix} \frac{1}{\sqrt{2}} \begin{pmatrix} \langle \rho_{x,\vec{\epsilon}_1} | \\ \langle \rho_{y,\vec{\epsilon}_1} | \\ \langle \rho_{z,\vec{\epsilon}_1} | \end{pmatrix} \\ &= \begin{pmatrix} |\rho_{x,\vec{0}}\rangle \\ |\rho_{y,\vec{0}}\rangle \\ |\rho_{z,\vec{0}}\rangle \end{pmatrix} \begin{pmatrix} (h_{pp\sigma} + h_{pp\pi})/2 & (h_{pp\sigma} - h_{pp\pi})/2 & 0 \\ (h_{pp\sigma} - h_{pp\pi})/2 & (h_{pp\sigma} + h_{pp\pi})/2 & 0 \\ 0 & 0 & h_{pp\pi} \end{pmatrix} \begin{pmatrix} \langle \rho_{x,\vec{\epsilon}_1} | \\ \langle \rho_{y,\vec{\epsilon}_1} | \\ \langle \rho_{z,\vec{\epsilon}_1} | \end{pmatrix} \end{aligned} \quad (4.86)$$

With this we have obtained one offsite Hamiltonian.

Next we construct the other off-site Hamiltonians. We do not repeat the calculation. Instead, we use symmetry considerations to convert the result for the first nearest-neighbor vector.

- The Hamiltonian is invariant under a sign change of the nearest-neighbor vector $\vec{\epsilon}$: Both p-orbitals change their sign under inversion, which leaves the result invariant.

$$\mathbf{H}_{\vec{0},-\vec{\epsilon}} = \mathbf{H}_{\vec{0},\vec{\epsilon}} \quad (4.87)$$

How can one show this? Let us introduce the inversion centered on the left atom (at $\vec{0}$) as symmetry operator \hat{S} . For $j \in \{x, y, z\}$, the orbitals transform as follows

$$\begin{aligned} \hat{S}|\rho_{j,\vec{0}}\rangle &= -|\rho_{j,\vec{0}}\rangle \\ \hat{S}|\rho_{j,\vec{\epsilon}_1}\rangle &= -|\rho_{j,-\vec{\epsilon}_1}\rangle \end{aligned} \quad (4.88)$$

Thus, the matrix element remains invariant

$$\langle \rho_{i,\vec{0}} | \hat{H} | \rho_{j,\vec{\epsilon}_1} \rangle = \underbrace{\langle \rho_{i,\vec{0}} | \hat{S}^\dagger}_{-\langle \rho_{i,\vec{0}} |} \underbrace{\hat{S} \hat{H} \hat{S}^\dagger}_{\hat{H}} \underbrace{\hat{S} | \rho_{j,\vec{\epsilon}_1} \rangle}_{-\langle \rho_{j,-\vec{\epsilon}_1} |} = \langle \rho_{i,\vec{0}} | \hat{H} | \rho_{j,-\vec{\epsilon}_1} \rangle \quad (4.89)$$

- The Hamiltonian for the third lattice translation vector in our list $\vec{\epsilon}_3 = (1, 0, 1)\frac{1}{2}a_{\text{lat}}$ is obtained from that for $\vec{\epsilon}_1 = (1, 1, 0)\frac{1}{2}a_{\text{lat}}$ by interchanging the components for ρ_y and ρ_z . The orbital

pointing along the bond axis is $|\rho_{(101)}\rangle$, and the orbitals perpendicular to the bond axis are $|\rho_{(010)}\rangle$ and $|\rho_{(10\bar{1})}\rangle$.

The transformation is therefore

$$\begin{pmatrix} |\rho_{(101)}\rangle \\ |\rho_{(001)}\rangle \\ |\rho_{(10\bar{1})}\rangle \end{pmatrix} = \begin{pmatrix} |\rho_x\rangle \\ |\rho_y\rangle \\ |\rho_z\rangle \end{pmatrix} \begin{pmatrix} 1 & 0 & 1 \\ 0 & \sqrt{2} & 0 \\ 1 & 0 & -1 \end{pmatrix} \frac{1}{\sqrt{2}} \quad (4.90)$$

The inverse transformation is obtained by matrix inversion. We can simplify this step noticing that we deal with a unitary transformation. The inverse is thus the transpose.

$$\begin{pmatrix} |\rho_x\rangle \\ |\rho_y\rangle \\ |\rho_z\rangle \end{pmatrix} = \begin{pmatrix} |\rho_{(101)}\rangle \\ |\rho_{(010)}\rangle \\ |\rho_{(10\bar{1})}\rangle \end{pmatrix} \begin{pmatrix} 1 & 0 & 1 \\ 0 & \sqrt{2} & 0 \\ 1 & 0 & -1 \end{pmatrix} \frac{1}{\sqrt{2}} \quad (4.91)$$

We transform the diagonal Hamiltonian in the basis of the rotated orbital into our basis-orbitals and obtain

$$\hat{H}_{\vec{0}, \vec{t}_3} = \begin{pmatrix} |\rho_{x,\vec{0}}\rangle \\ |\rho_{y,\vec{0}}\rangle \\ |\rho_{z,\vec{0}}\rangle \end{pmatrix} \begin{pmatrix} (h_{pp\sigma} + h_{pp\pi})/2 & 0 & (h_{pp\sigma} - h_{pp\pi})/2 \\ 0 & h_{pp\pi} & 0 \\ (h_{pp\sigma} - h_{pp\pi})/2 & 0 & (h_{pp\sigma} + h_{pp\pi})/2 \end{pmatrix} \begin{pmatrix} \langle \rho_{x,\vec{t}_3} | \\ \langle \rho_{y,\vec{t}_3} | \\ \langle \rho_{z,\vec{t}_3} | \end{pmatrix} \quad (4.92)$$

- The Hamiltonian for the vector $\vec{t}_5 = (0, 1, 1)\frac{1}{2}a_{\text{lat}}$ is obtained analogously by interchanging the components for ρ_x and ρ_z .

$$\hat{H}_{\vec{0}, \vec{t}_5} = \begin{pmatrix} |\rho_{x,\vec{0}}\rangle \\ |\rho_{y,\vec{0}}\rangle \\ |\rho_{z,\vec{0}}\rangle \end{pmatrix} \begin{pmatrix} h_{pp\pi} & 0 & 0 \\ 0 & (h_{pp\sigma} + h_{pp\pi})/2 & (h_{pp\sigma} - h_{pp\pi})/2 \\ 0 & (h_{pp\sigma} - h_{pp\pi})/2 & (h_{pp\sigma} + h_{pp\pi})/2 \end{pmatrix} \begin{pmatrix} \langle \rho_{x,\vec{t}_5} | \\ \langle \rho_{y,\vec{t}_5} | \\ \langle \rho_{z,\vec{t}_5} | \end{pmatrix} \quad (4.93)$$

- For $-t_2 = (-1, 1, 0)\frac{1}{2}a_{\text{lat}}$, we can use the same transformation as for $\vec{t}_1 = (1, 1, 0)\frac{1}{2}a_{\text{lat}}$, but the Hamiltonian in the transformed basis has the first two diagonal matrix elements, namely $h_{pp\sigma}$ and $h_{pp\pi}$, interchanged. This is because the σ -bond is formed by the orbitals $|\rho_{1,1,0}\rangle$ and $|\rho_{1,1,0}\rangle$ forms a π -bond. In the original basis this reverts the sign of the off-diagonal elements.

$$\hat{H}_{\vec{0}, -\vec{t}_2} = \begin{pmatrix} |\rho_{x,\vec{0}}\rangle \\ |\rho_{y,\vec{0}}\rangle \\ |\rho_{z,\vec{0}}\rangle \end{pmatrix} \begin{pmatrix} (h_{pp\sigma} + h_{pp\pi})/2 & -(h_{pp\sigma} - h_{pp\pi})/2 & 0 \\ -(h_{pp\sigma} - h_{pp\pi})/2 & (h_{pp\sigma} + h_{pp\pi})/2 & 0 \\ 0 & 0 & h_{pp\pi} \end{pmatrix} \begin{pmatrix} \langle \rho_{x,-\vec{t}_2} | \\ \langle \rho_{y,-\vec{t}_2} | \\ \langle \rho_{z,-\vec{t}_2} | \end{pmatrix} \quad (4.94)$$

- Similarly, we obtain the Hamiltonian for $-\vec{t}_4 = (1, 0, -1)\frac{1}{2}a_{\text{lat}}$ from that for $\vec{t}_3 = (1, 0, 1)\frac{1}{2}a_{\text{lat}}$ by changing the sign of the off-diagonal elements.

$$\hat{H}_{\vec{0}, \vec{t}_4} = \begin{pmatrix} |\rho_{x,\vec{0}}\rangle \\ |\rho_{y,\vec{0}}\rangle \\ |\rho_{z,\vec{0}}\rangle \end{pmatrix} \begin{pmatrix} (h_{pp\sigma} + h_{pp\pi})/2 & 0 & -(h_{pp\sigma} - h_{pp\pi})/2 \\ 0 & h_{pp\pi} & 0 \\ -(h_{pp\sigma} - h_{pp\pi})/2 & 0 & (h_{pp\sigma} + h_{pp\pi})/2 \end{pmatrix} \begin{pmatrix} \langle \rho_{x,-\vec{t}_4} | \\ \langle \rho_{y,-\vec{t}_4} | \\ \langle \rho_{z,-\vec{t}_4} | \end{pmatrix} \quad (4.95)$$

- Finally, we obtain the Hamiltonian for $-\vec{t}_6 = (0, 1, -1)\frac{1}{2}a_{\text{lat}}$ from that for $\vec{t}_5 = (0, 1, 1)\frac{1}{2}a_{\text{lat}}$ by changing the sign of the off-diagonal elements.

$$\hat{H}_{\vec{0}, -\vec{t}_6} = \begin{pmatrix} |\rho_{x,\vec{0}}\rangle \\ |\rho_{y,\vec{0}}\rangle \\ |\rho_{z,\vec{0}}\rangle \end{pmatrix} \begin{pmatrix} h_{pp\pi} & 0 & 0 \\ 0 & (h_{pp\sigma} + h_{pp\pi})/2 & -(h_{pp\sigma} - h_{pp\pi})/2 \\ 0 & -(h_{pp\sigma} - h_{pp\pi})/2 & (h_{pp\sigma} + h_{pp\pi})/2 \end{pmatrix} \begin{pmatrix} \langle \rho_{x,-\vec{t}_6} | \\ \langle \rho_{y,-\vec{t}_6} | \\ \langle \rho_{z,-\vec{t}_6} | \end{pmatrix} \quad (4.96)$$

2 Calculate the k-dependent Hamiltonian for the Bloch states.

Next, we set up the Hamiltonian in k-space.

$$\begin{aligned}
H(\vec{k}) &= \sum_{\vec{t}} H_{\vec{0},\vec{t}} e^{i\vec{k}\vec{t}} \\
&= H_{\vec{0},\vec{0}} \\
&\quad + 2H_{\vec{0},\vec{t}_1} \cos(k_x + k_y) + 2H_{\vec{0},\vec{t}_2} \cos(k_x - k_y) \\
&\quad + 2H_{\vec{0},\vec{t}_3} \cos(k_y + k_z) + 2H_{\vec{0},-\vec{t}_3} \cos(k_y - k_z) \\
&\quad + 2H_{\vec{0},\vec{t}_4} \cos(k_x + k_z) + 2H_{\vec{0},-\vec{t}_4} \cos(k_x - k_z)
\end{aligned} \tag{4.97}$$

The first line of Eq. 4.97 is the onsite Hamiltonian. The following three lines can be attributed each to a plane in reciprocal space, namely the (k_x, k_y) -plane in the first line, the (k_y, k_z) -plane in the second line, and the (k_x, k_z) -plane in the third line.

First, I consider all vectors in the (k_x, k_y) -plane. In this plane the four translation vectors $\vec{t}_1, \vec{t}_2, -\vec{t}_1, -\vec{t}_2$ contribute. I obtain

$$\begin{aligned}
&2H_{\vec{0},\vec{t}_1} \cos(k_x + k_y) + 2H_{\vec{0},\vec{t}_2} \cos(k_x - k_y) \\
&= \left(H_{\vec{0},\vec{t}_1} + H_{\vec{0},\vec{t}_2} \right) \left(\cos(k_x + k_y) + \cos(k_x - k_y) \right) \\
&\quad + \left(H_{\vec{0},\vec{t}_1} - H_{\vec{0},\vec{t}_2} \right) \left(\cos(k_x + k_y) - \cos(k_x - k_y) \right) \\
&= \left(H_{\vec{0},\vec{t}_1} + H_{\vec{0},\vec{t}_2} \right) 2 \cos(k_x) \cos(k_y) \\
&\quad - \left(H_{\vec{0},\vec{t}_1} - H_{\vec{0},\vec{t}_2} \right) 2 \sin(k_x) \sin(k_y) \\
&= 2 \cos(k_x) \cos(k_y) \begin{pmatrix} h_{pp\sigma} + h_{pp\pi} & 0 & 0 \\ 0 & h_{pp\sigma} + h_{pp\pi} & 0 \\ 0 & 0 & 2h_{pp\pi} \end{pmatrix} \\
&\quad - 2 \sin(k_x) \sin(k_y) \begin{pmatrix} 0 & -(h_{pp\sigma} - h_{pp\pi}) & 0 \\ -(h_{pp\sigma} - h_{pp\pi}) & 0 & 0 \\ 0 & 0 & 0 \end{pmatrix}
\end{aligned} \tag{4.98}$$

Finally, we can add the results for all three planes. The result for the yz and the xz -planes are obtained from that for the xy plane by interchanging the x, y and z components. To make the result more compact, I introduce

$$\begin{aligned}
u &\stackrel{\text{def}}{=} 2(h_{pp\sigma} + h_{pp\pi}) \\
v &\stackrel{\text{def}}{=} 2(h_{pp\sigma} - h_{pp\pi}) \\
w &\stackrel{\text{def}}{=} 4h_{pp\pi} .
\end{aligned} \tag{4.99}$$

$$\begin{aligned}
 \mathbf{H}(\vec{k}) = & \begin{pmatrix} \bar{\epsilon}_p & 0 & 0 \\ 0 & \bar{\epsilon}_p & 0 \\ 0 & 0 & \bar{\epsilon}_p \end{pmatrix} \\
 & + \cos(k_x) \cos(k_y) \begin{pmatrix} u & 0 & 0 \\ 0 & u & 0 \\ 0 & 0 & w \end{pmatrix} + \sin(k_x) \sin(k_y) \begin{pmatrix} 0 & v & 0 \\ v & 0 & 0 \\ 0 & 0 & 0 \end{pmatrix} \\
 & + \cos(k_x) \cos(k_z) \begin{pmatrix} u & 0 & 0 \\ 0 & w & 0 \\ 0 & 0 & u \end{pmatrix} + \sin(k_x) \sin(k_z) \begin{pmatrix} 0 & 0 & v \\ 0 & 0 & 0 \\ v & 0 & 0 \end{pmatrix} \\
 & + \cos(k_y) \cos(k_z) \begin{pmatrix} w & 0 & 0 \\ 0 & u & 0 \\ 0 & 0 & u \end{pmatrix} + \sin(k_y) \sin(k_z) \begin{pmatrix} 0 & 0 & 0 \\ 0 & 0 & v \\ 0 & v & 0 \end{pmatrix} \quad (4.100)
 \end{aligned}$$

3 In order to calculate the band structure from^a $\Gamma = (0, 0, 0) \frac{2\pi}{a_{\text{lat}}}$ to $X = (\frac{1}{2}, 0, 0) \frac{2\pi}{a_{\text{lat}}}$, calculate the Hamiltonian as function of the parameter s varying linearly from Γ to X .

^aThe scale factor $2\pi/a_{\text{lat}}$ for the X-point rather than π/a_{lat} is correct. See below in Eq. 4.102 on p. 163.

The reciprocal lattice vectors are

$$\mathbf{g} = \frac{2\pi}{a_{\text{lat}}} \begin{pmatrix} -1 & 1 & 1 \\ 1 & -1 & 1 \\ 1 & 1 & -1 \end{pmatrix} \quad (4.101)$$

The reciprocal lattice vector in x-direction is $\vec{g}_2 + \vec{g}_3 = \frac{2\pi}{a_{\text{lat}}}(2, 0, 0)$ so that

$$X = \frac{1}{2}(\vec{g}_2 + \vec{g}_3) = (1, 0, 0) \frac{2\pi}{a} \quad (4.102)$$

To get the band structure from Γ to X , I set $k_y = k_z = 0$

$$\begin{aligned}
 \mathbf{H}(\vec{k}) = & \begin{pmatrix} \bar{\epsilon}_p & 0 & 0 \\ 0 & \bar{\epsilon}_p & 0 \\ 0 & 0 & \bar{\epsilon}_p \end{pmatrix} + \cos(k_x) \begin{pmatrix} u & 0 & 0 \\ 0 & u & 0 \\ 0 & 0 & w \end{pmatrix} + \cos(k_x) \begin{pmatrix} u & 0 & 0 \\ 0 & w & 0 \\ 0 & 0 & u \end{pmatrix} + \begin{pmatrix} w & 0 & 0 \\ 0 & u & 0 \\ 0 & 0 & u \end{pmatrix} \\
 = & \begin{pmatrix} \bar{\epsilon}_p + w & 0 & 0 \\ 0 & \bar{\epsilon}_p + u & 0 \\ 0 & 0 & \bar{\epsilon}_p + u \end{pmatrix} + \cos(k_x) \begin{pmatrix} 2u & 0 & 0 \\ 0 & u + w & 0 \\ 0 & 0 & u + w \end{pmatrix} \\
 = & (\bar{\epsilon}_p + 2u + w) \begin{pmatrix} 1 & 0 & 0 \\ 0 & 1 & 0 \\ 0 & 0 & 1 \end{pmatrix} + (\cos(k_x) - 1) \begin{pmatrix} 2u & 0 & 0 \\ 0 & u + w & 0 \\ 0 & 0 & u + w \end{pmatrix} \quad (4.103)
 \end{aligned}$$

4 Calculate the band structure from Γ to X . Draw the band structure.

$$\begin{aligned}
2u + w &= 4h_{pp\sigma} + 8h_{pp\pi} \\
u + w &= 2h_{pp\sigma} + 6h_{pp\pi} \\
2u &= 4(h_{pp\sigma} + h_{pp\pi})
\end{aligned} \tag{4.104}$$

$$\begin{aligned}
\epsilon_1(k_x) &= \bar{\epsilon}_p + 4(h_{pp\sigma} + 2h_{pp\pi}) + (\cos(k_x) - 1)4(h_{pp\sigma} + h_{pp\pi}) \\
\epsilon_{2/3}(k_x) &= \bar{\epsilon}_p + 4(h_{pp\sigma} + 2h_{pp\pi}) + (\cos(k_x) - 1)2(h_{pp\sigma} + 3h_{pp\pi})
\end{aligned} \tag{4.105}$$

The bands are degenerate at the Γ -point, where the top of the band is. Towards the X -point, the bands fall off in energy. There are two degenerate upper bands and one lower band.

$$\begin{aligned}
\epsilon_{1/2/3}(\Gamma) &= \bar{\epsilon}_p + 4h_{pp\sigma} + 8h_{pp\pi} \\
\epsilon_1(X) &= \bar{\epsilon}_p - 4h_{pp\sigma} = \epsilon_{1/2/3}(\Gamma) - 8h_{pp\sigma} - 8h_{pp\pi} \\
\epsilon_{2/3}(X) &= \bar{\epsilon}_p - 4h_{pp\pi} = \epsilon_{1/2/3}(\Gamma) - 4h_{pp\sigma} - 12h_{pp\pi}
\end{aligned} \tag{4.106}$$

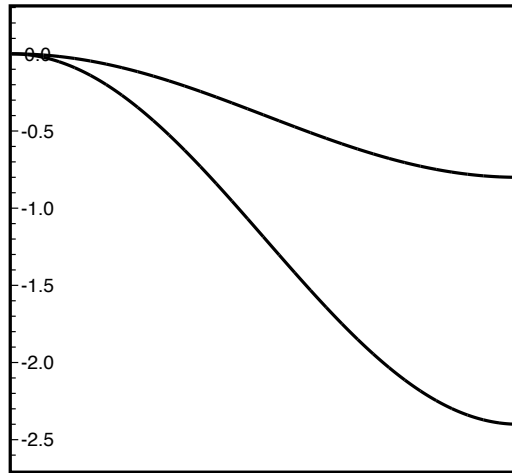


Fig. 4.21: Band structure of a p-type tight-binding band in the fcc structure from Γ to X . $\epsilon_{1/2/3}(\Gamma) = 0$ eV, $\epsilon_1(X) = -2.4$ eV and $\epsilon_{2/3}(X) = -0.8$ eV. (Values estimated for MgO.)

5 Describe how the parameters $\bar{\epsilon}_p$, $h_{pp\sigma}$ and $h_{pp\pi}$ can be extracted from a band structure plot.

Now, we can estimate the hopping parameters from the band structure.

A simple oxide such as MgO, exhibits an fcc-sublattice of oxygen atoms. The cations, namely Mg enter the octahedral voids in this fcc lattice, which results in the rock-salt (NaCl) structure. The valence band of a simple oxide is well represented by a p-type band in an fcc-arrangement. Such a band is shown in figure 9.13 on p. 312.

Let us assume that the dispersion of the singly degenerate band is 2.4 eV and that of the doubly degenerate bands is 0.8 eV. This yields $h_{pp\sigma} = 0.35$ eV and $h_{pp\pi} = -0.05$ eV.

6 Discuss the sign of $h_{pp\sigma}$ and $h_{pp\pi}$. The goal is not a rigorous proof, which is probably not possible. Rather the goal is qualitative reasoning. It is about visualizing wave functions and potentials with the aim to find qualitative arguments. Thus, there is not a single true or false answer.

The offsite Hamilton matrix elements are approximately related to the overlap matrix element. The sign of Hamilton matrix element is usually opposite to that of the overlap matrix element.

- The overlap of two p-orbitals along the orbital axis is negative. Therefore $h_{pp\sigma} > 0$.
- The overlap of two p-orbitals oriented orthogonal to the bond axis is positive. Therefore $h_{pp\pi} < 0$.

4.6.4 Local and itinerant states

Editor: write more background. Relate to Anderson impurity model

The following example demonstrates an itinerant band and a band of localized states. The local orbital could be the d- or f-electrons of a transition metal ion or a rare-earth ion. The itinerant electrons, on the other hand, represent the loosely bound s- and p-like electrons.

The model[35, 36] describes so-called **heavy-fermion materials**. Heavy fermions describe one class of electron-correlation phenomena. One example for a heavy-electron material is SmB_6 . The large Coulomb repulsion between the f-electrons of Sm split up the f-shell into a multiplet of filled f-electrons below the Fermi level and another multiplet of empty f-states above the Fermi level.¹⁷ When the filled f-band intersects the conduction band, the crossing of the two bands is turned into an avoided crossing. A small band gap occurs between the two bands. If the Fermi level is within the band gap a very large resistance shows up at low temperatures. When the Fermi level is close to, but outside the band gap, it gets pinned in the portions with f-character. As a result the conduction electrons have a very large effective mass, which explains the name heavy fermions.

In this minimal model, only one localized orbital and one itinerant orbital is considered.

Such models are relevant for the study of interacting electrons, because local orbitals with little coupling to the environment tend to experience large Coulomb interactions. Thus, they are dominated by “atomic physics”.

The Hamiltonian has the form

$$\hat{H} = \sum_j \left\{ |\chi_{s,j}\rangle \bar{\epsilon}_s \langle \chi_{s,j}| + |\chi_{d,j}\rangle \bar{\epsilon}_d \langle \chi_{d,j}| - (|\chi_{s,j}\rangle |t_{sd}| \langle \chi_{d,j}| + |\chi_{d,j}\rangle |t_{sd}| \langle \chi_{s,j}|) \right. \\ \left. - (|\chi_{s,j}\rangle |t_{ss}| \langle \chi_{s,j+1}| + |\chi_{s,j+1}\rangle |t_{ss}| \langle \chi_{s,j}|) \right\} \quad (4.107)$$

To make you familiar with the notation of second quantization let me express the same Hamiltonian in terms of creation and annihilation operators.

$$\hat{H} = \sum_j \left\{ \bar{\epsilon}_s \hat{c}_{s,j}^\dagger \hat{c}_{s,j} + \bar{\epsilon}_d \hat{c}_{d,j}^\dagger \hat{c}_{d,j} - |t_{sd}| (\hat{c}_{s,j}^\dagger \hat{c}_{d,j} + \hat{c}_{d,j}^\dagger \hat{c}_{s,j}) - |t_{ss}| (\hat{c}_{s,j}^\dagger \hat{c}_{s,j+1} + \hat{c}_{s,j+1}^\dagger \hat{c}_{s,j}) \right\} \quad (4.108)$$

The difference of this Hamiltonian from the first version is that the second form is a Hamiltonian in Fock space, while the first version acts in the one-particle Hilbert space.

Solution

Write down the real-space Hamilton matrices for the various lattice translation vectors

$$H_0 = \begin{pmatrix} \bar{\epsilon}_s & -|t_{sd}| \\ -|t_{sd}| & \bar{\epsilon}_d \end{pmatrix} \quad \text{and} \quad H_1 = \begin{pmatrix} -|t_{ss}| & 0 \\ 0 & 0 \end{pmatrix} \quad \text{and} \quad H_{-1} = \begin{pmatrix} -|t_{ss}| & 0 \\ 0 & 0 \end{pmatrix} \quad (4.109)$$

Write down the k-space Hamilton $H(k)$ Hamiltonian in k -space

$$H(k) = \sum_m H_m e^{ikt_m} = \begin{pmatrix} \bar{\epsilon}_s - 2|t_{ss}| \cos(ka_{\text{lat}}) & -|t_{sd}| \\ -|t_{sd}| & \bar{\epsilon}_d \end{pmatrix} = \begin{pmatrix} \tilde{\epsilon}_s(k) & -|t_{sd}| \\ -|t_{sd}| & \bar{\epsilon}_d \end{pmatrix} \quad (4.110)$$

The Hamiltonian looks like that of a di-atomic molecule with a k -dependent atomic level

$$\tilde{\epsilon}_s(k) \stackrel{\text{def}}{=} \bar{\epsilon}_s - 2|t_{ss}| \cos(ka_{\text{lat}}) \quad (4.111)$$

¹⁷The splitting of filled and empty states can be attributed to exchange energy, which is described on the level of the Hartree-Fock theory.

Determine the band structure

$$\begin{aligned}
 0 &= (\tilde{\epsilon}_s(k) - \epsilon)(\bar{\epsilon}_d - \epsilon) - |t_{sd}|^2 \\
 &= \epsilon^2 - (\bar{\epsilon}_d + \tilde{\epsilon}_s(k))\epsilon + \bar{\epsilon}_d\tilde{\epsilon}_s(k) - |t_{sd}|^2 \\
 &= \left[\epsilon - \frac{\bar{\epsilon}_d + \tilde{\epsilon}_s(k)}{2} \right]^2 + \bar{\epsilon}_d\tilde{\epsilon}_s(k) - \left(\frac{\bar{\epsilon}_d + \tilde{\epsilon}_s(k)}{2} \right)^2 - |t_{sd}|^2 \\
 \epsilon &= \frac{\bar{\epsilon}_d + \tilde{\epsilon}_s(k)}{2} \pm \sqrt{\left(\frac{\tilde{\epsilon}_s(k) - \bar{\epsilon}_d}{2} \right)^2 + |t_{sd}|^2}
 \end{aligned} \tag{4.112}$$

Thus, the band structure is

$$\epsilon_{\pm}(k) = \frac{\bar{\epsilon}_d + \bar{\epsilon}_s - 2|t_{ss}|\cos(ka_{\text{lat}})}{2} \pm \sqrt{|t_{sd}|^2 + \left(\frac{\bar{\epsilon}_s - 2|t_{ss}|\cos(ka_{\text{lat}}) - \bar{\epsilon}_d}{2} \right)^2} \tag{4.113}$$

with the band indices $-$ and $+$.

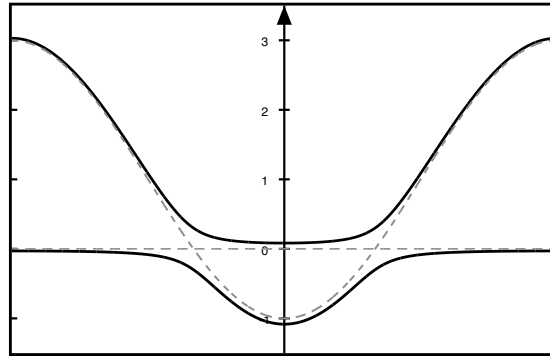


Fig. 4.22: Band structure of a system with one itinerant and one localized orbital. $|t_{ss}| = 1$, $|t_{sd}| = 0.3$, $\bar{\epsilon}_s = 1$, $\bar{\epsilon}_d = 0$. The dashed lines show the unhybridized bands, i.e. for $t_{sd} = 0$. The vertical axis is the energy axis and the horizontal axis is reciprocal space from $-\pi/a_{\text{lat}}$ to $+\pi/a_{\text{lat}}$.

Eigenstates

$$|\psi_n(k)\rangle = \sum_j \left(|\chi_{s,j}\rangle c_{s,n}(k) + |\chi_{p,j}\rangle c_{p,n}(k) \right) e^{ik a_{\text{lat}}} \tag{4.114}$$

where $n \in \pm$.

$$\begin{aligned}
 c_{s,-}(k) &= \cos(\gamma(k)) & \text{and} & & c_{d,-}(k) &= \sin(\gamma(k)) \\
 c_{s,+}(k) &= -\sin(\gamma(k)) & \text{and} & & c_{d,+}(k) &= \cos(\gamma(k))
 \end{aligned} \tag{4.115}$$

The first line of the eigenvalue equation is

$$\begin{aligned}
 & (\tilde{\epsilon}_s(k) - \epsilon_-) c_{s,-}(k) - |t_{sd}| c_{d,-}(k) = 0 \\
 & (\tilde{\epsilon}_s(k) - \epsilon_-) \cos(\gamma(k)) - |t_{sd}| \sin(\gamma(k)) = 0 \\
 \tan(\gamma(k)) &= \frac{1}{|t_{sd}|} (\tilde{\epsilon}_s(k) - \epsilon_-) \\
 &= \frac{1}{|t_{sd}|} \left[\tilde{\epsilon}_s(k) - \frac{\bar{\epsilon}_d + \tilde{\epsilon}_s(k)}{2} + \sqrt{\left(\frac{\tilde{\epsilon}_s(k) - \bar{\epsilon}_d}{2} \right)^2 + |t_{sd}|^2} \right] \\
 &= \frac{\tilde{\epsilon}_s(k) - \bar{\epsilon}_d}{2|t_{sd}|} + \sqrt{\left(\frac{\tilde{\epsilon}_s(k) - \bar{\epsilon}_d}{2|t_{sd}|} \right)^2 + 1} \tag{4.116}
 \end{aligned}$$

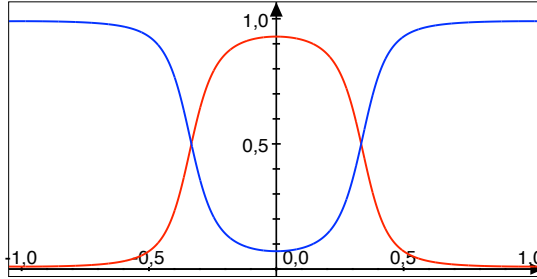


Fig. 4.23: Weight $\cos^2(\gamma(k))$ of the s-orbital (red) in the lower band as function of k_{lat}/π . The weight of the d-orbital is shown in blue. For the upper band the weight of the s-orbital is blue and that of the d-orbital is red. Note that the character of the wave functions changes as the itinerant band merges into the localized band.

4.6.5 Manganites

Editor: This is an unfinished sketch

In the manganites such as $\text{La}_{1-x}\text{Sr}_x\text{MnO}_3$ the Mn ions form a approximately simple cubic sublattice.

In this exercise, we consider only the e_g electrons of the majority spin direction of ferromagnetic manganites. Editor: Certain antiferromagnetic orderings can be obtained from this solution with small variations: For example the A-type structure, which consists of ferromagnetic xy planes, which are antiferromagnetically coupled in z direction, can be approximated by setting the hopping in z direction to zero and to adjust the onsite term to the sum of the non-zero offsite hopping terms.

We consider the (2×2) Hamiltonian for the two e_g orbitals $d_{x^2-y^2}$ and $d_{3z^2-r^2}$. I denote the onsite term with T_0 , the one for the nearest neighbor displacement along the x-axis with T_x . The notation for the other two Cartesian coordinates are identical. The hopping matrices for positive and negative lattice vectors are identical. The hopping matrix elements are given, for example in Sotoudeh, Rajpurohit et al.[37].

$$\begin{aligned} T_0 &= +t \begin{pmatrix} 3 & 0 \\ 0 & 3 \end{pmatrix} \\ T_x &= -t \begin{pmatrix} 3/4 & -\sqrt{3}/4 \\ -\sqrt{3}/4 & 1/4 \end{pmatrix} \\ T_y &= -t \begin{pmatrix} 3/4 & \sqrt{3}/4 \\ \sqrt{3}/4 & 1/4 \end{pmatrix} \\ T_z &= -t \begin{pmatrix} 0 & 0 \\ 0 & 1 \end{pmatrix} \end{aligned} \tag{4.117}$$

In this exercise, we consider only one site per unit cell. The real manganites have a more complicated unit cell with four Mn-sites. Thus, the band structure, we obtain, needs to be folded into the smaller reciprocal unit cell of the real manganites.

Hamiltonian in real space

The manganese ions are arranged on simple cubic sublattice

\vec{T}_1	(1, 0, 0)	a_{lat}
\vec{T}_2	(0, 1, 0)	a_{lat}
\vec{T}_3	(0, 0, 1)	a_{lat}
\vec{R}	(0, 0, 0)	a_{lat}

I represent the Hamilton matrix in terms of sub-matrices $H_{\vec{r},\vec{r}'}$ for each pair of lattice translation vectors \vec{r} and \vec{r}' .

The lattice-translation symmetry implies

$$H_{\vec{r},\vec{r}'} = H_{\vec{0},\vec{r}'-\vec{r}} \tag{4.118}$$

From the symmetry of the d-orbitals one can deduce that the matrix elements in the positive and negative directions are equal.

$$H_{\vec{0},\vec{r}} = H_{\vec{0},-\vec{r}} \tag{4.119}$$

This is not obvious and must be carefully derived and confirmed using the orbital shape and lattice symmetry at hand.

Finally I can exploit the underlying assumption that the Hamilton matrix elements vanish, except for onsite and nearest neighbor terms.

$$\begin{aligned}
H_{\vec{0},\vec{0}} &= T_0 = +t \begin{pmatrix} 3 & 0 \\ 0 & 3 \end{pmatrix} \\
H_{\vec{0},\pm\vec{T}_1} &= T_x = -t \begin{pmatrix} 3/4 & -\sqrt{3}/4 \\ -\sqrt{3}/4 & 1/4 \end{pmatrix} \\
H_{\vec{0},\pm\vec{T}_2} &= T_y = -t \begin{pmatrix} 3/4 & +\sqrt{3}/4 \\ +\sqrt{3}/4 & 1/4 \end{pmatrix} \\
H_{\vec{0},\pm\vec{T}_3} &= T_z = -t \begin{pmatrix} 0 & 0 \\ 0 & 1 \end{pmatrix}
\end{aligned} \tag{4.120}$$

k-dependent Hamiltonian

The k-dependent Hamiltonian is obtained from

$$H(\vec{k}) = \sum_{\vec{T}} H_{\vec{0},\vec{T}} e^{i\vec{k}\vec{T}} \tag{4.121}$$

Let me now determine the k-dependent Hamiltonian.

$$\begin{aligned}
H(\vec{k}) &= 3t - \frac{1}{2}t \begin{pmatrix} 3(\cos(k_x a_{lat}) + \cos(k_y a_{lat})) & \sqrt{3}(-\cos(k_x a_{lat}) + \cos(k_y a_{lat})) \\ \sqrt{3}(-\cos(k_x a_{lat}) + \cos(k_y a_{lat})) & 4\cos(k_z a_{lat}) + (\cos(k_x a_{lat}) + \cos(k_y a_{lat})) \end{pmatrix} \\
&= 3t - \frac{1}{2}t \begin{pmatrix} 3a & -\sqrt{3}b \\ -\sqrt{3}b & 4c + a \end{pmatrix}
\end{aligned} \tag{4.122}$$

Let me introduce the short-hand notation a, b, c

$$\begin{aligned}
a(k_x, k_y) &\stackrel{\text{def}}{=} \cos(k_x a_{lat}) + \cos(k_y a_{lat}) \\
b(k_x, k_y) &\stackrel{\text{def}}{=} \cos(k_x a_{lat}) - \cos(k_y a_{lat}) \\
c(k_z) &\stackrel{\text{def}}{=} \cos(k_z a_{lat})
\end{aligned} \tag{4.123}$$

Eigenvalues

$$\begin{aligned}
0 &= (3a - \lambda)(4c + a - \lambda) - 3b^2 \\
&= \lambda^2 - 4(a + c)\lambda + 12ac + 3a^2 - 3b^2 \\
&= \left(\lambda - 2\underbrace{(a + c)}_C \right)^2 - 4\underbrace{(a + c)}_C^2 + \underbrace{12ac}_B + \underbrace{3a^2 - 3b^2}_A
\end{aligned} \tag{4.124}$$

We need some side calculation to simplify the expressions.

$$\begin{aligned}
A &= 3(a^2 - b^2) = 3(a + b)(a - b) = 12 \cos(k_x a_{lat}) \cos(k_y a_{lat}) \\
B &= 12ac = 12 \cos(k_x a_{lat}) \cos(k_z a_{lat}) + 12 \cos(k_y a_{lat}) \cos(k_z a_{lat}) \\
C &= a + c = \cos(k_x a_{lat}) + \cos(k_y a_{lat}) + \cos(k_z a_{lat}) = Q_x + Q_y + Q_z \\
-4C + B + A &= -4(a + c)^2 + 12ac + 3a^2 - 3b^2 \\
&= -4(Q_x + Q_y + Q_z)^2 + 12(Q_x Q_y + Q_y Q_z + Q_x Q_z) \\
&= -4(Q_x^2 + Q_y^2 + Q_z^2) + 4(Q_x Q_y + Q_y Q_z + Q_x Q_z)
\end{aligned} \tag{4.125}$$

Let me introduce another short-hand notation

$$\vec{Q} = \begin{pmatrix} \cos(k_x a_{lat}) \\ \cos(k_y a_{lat}) \\ \cos(k_z a_{lat}) \end{pmatrix} \quad (4.126)$$

$$\lambda_{\mp} = 2(Q_x + Q_y + Q_z) \pm 2\sqrt{(Q_x^2 + Q_y^2 + Q_z^2) - (Q_x Q_y + Q_y Q_z + Q_x Q_z)} \quad (4.127)$$

The energy levels are therefore

$$\begin{aligned} \epsilon_{\pm} &= 3t - \frac{1}{2}t\lambda_{\mp} \\ &= 3t - t(Q_x + Q_y + Q_z) \pm t\sqrt{(Q_x^2 + Q_y^2 + Q_z^2) - (Q_x Q_y + Q_y Q_z + Q_x Q_z)} \\ &= 3t - t(\cos(k_x a_{lat}) + \cos(k_y a_{lat}) + \cos(k_z a_{lat})) \\ &\pm t \left\{ \left(\cos^2(k_x a_{lat}) + \cos^2(k_y a_{lat}) + \cos^2(k_z a_{lat}) \right) \right. \\ &\quad \left. - \left(\cos(k_x a_{lat}) \cos(k_y a_{lat}) + \cos(k_y a_{lat}) \cos(k_z a_{lat}) + \cos(k_z a_{lat}) \cos(k_x a_{lat}) \right) \right\}^{\frac{1}{2}} \end{aligned} \quad (4.128)$$

Position of conical intersections

Editor: This sub-part may not be an interesting question for students. I am curious about it to understand the nature of band intersectiond better.

I am looking for the intersections of the two bands $\epsilon_{\pm}(\vec{k})$, where $\epsilon_+(\vec{k}) = \epsilon_-(\vec{k})$.

We can simplify the expression for the bands using the identity

$$(x - y)^2 + (y - z)^2 + (x - z)^2 = 2(x^2 + y^2 + z^2 - xy - yz - xz) \quad (4.129)$$

so that

$$\begin{aligned} \epsilon_{\pm} &= 3t - t(Q_x + Q_y + Q_z) \pm t\sqrt{(Q_x^2 + Q_y^2 + Q_z^2) - (Q_x Q_y + Q_y Q_z + Q_x Q_z)} \\ &= 3t - t(Q_x + Q_y + Q_z) \pm \frac{t}{\sqrt{2}}\sqrt{(Q_x - Q_y)^2 + (Q_y - Q_z)^2 + (Q_x - Q_z)^2} \end{aligned} \quad (4.130)$$

The two bands are degenerate only when $Q_x = Q_y = Q_z$. Because the cosine is an even function under inversion, this implies $k_x = \pm k_z$, $k_y = \pm k_z$. The degenerate seams are given by

$$\begin{aligned} \vec{k}_1(\lambda) &= \frac{2\pi}{a_{lat}}(1, +1, +1)\lambda \\ \vec{k}_2(\lambda) &= \frac{2\pi}{a_{lat}}(1, +1, -1)\lambda \\ \vec{k}_3(\lambda) &= \frac{2\pi}{a_{lat}}(1, -1, +1)\lambda \\ \vec{k}_4(\lambda) &= \frac{2\pi}{a_{lat}}(1, -1, -1)\lambda \end{aligned} \quad (4.131)$$

with $\lambda \in \mathbb{R}$. The lines are the four main diagonals of a cube.

Bandstructure

- the line Γ -X.

$$\begin{aligned}\epsilon_{\pm} &= 3t - t(\cos(k_x a_{lat}) + 2) \pm t\sqrt{(\cos^2(k_x a_{lat}) + 2) - (2\cos(k_x a_{lat}) + 1)} \\ &= -t(\cos(k_x a_{lat}) - 1) \pm t\sqrt{(\cos(k_x a_{lat}) - 1)^2} \\ &= \begin{cases} 2t(1 - \cos(k_x a_{lat})) & \text{for } \pm = + \\ 0 & \text{for } \pm = - \end{cases} \end{aligned} \tag{4.132}$$

Chapter 5

Expectation values and density of states

5.1 Brillouin-zone integrations

In order to evaluate expectation values or the density of states, it is necessary to sum over all Bloch states. Because the wave vector \vec{k} is continuous, it is not a-priori clear how the states need to be weighted, that is how the transition from discrete states to a continuum is performed. The corresponding concepts are described in the following.

5.1.1 Periodic boundary conditions

For a solid in its pure sense, the description of a finite piece of material is inconvenient, because the surfaces distract from the essence of the bulk material. One of the inconveniences is that the eigenstates of a finite chunk of a material are standing waves and not propagating waves¹. The ability to act as medium for currents is, however, essential for the description.²

Therefore, **periodic boundary conditions**³ have been introduced. Periodic boundary conditions imply that we connect the wave functions on the right side of the box with the left side, the back with the front and the bottom with the top. In other words, we consider wave functions that extend over all space, but they repeat after a certain distance in each direction.

In the following, we use the matrix \mathbf{T} of primitive real-space lattice vectors of the crystal, and the matrix \mathbf{g} of primitive reciprocal-space lattice vectors. They obey the relation $\mathbf{g}^\dagger \mathbf{T} = 2\pi \mathbf{1}$ so that $\det(\mathbf{g}) \det(\mathbf{T}) = (2\pi)^3$.

We form a **supercell**⁴ Ω , which is defined by the lattice vectors $\vec{T}_1 N_1$, $\vec{T}_2 N_2$, and $\vec{T}_3 N_3$. A supercell thus contains $N_1 N_2 N_3$ unit cells of the crystal.

For the sake of counting states, we require true periodicity of the wave function with the lattice

¹The statement is true at zero temperature. Thermal excitations can still carry currents inside the material.

²Such a description is also possible using particles in the box, but requires extra measures such as alternating and spatially varying currents.

³For periodic boundary conditions see also chapter 8 of Φ SX: Statistical Physics[38]

⁴The term supercell has been used to exploit Bloch's theorem for systems that do not have translational symmetry. An example is a point defect in a material. In that case, a super-crystal is formed with a lattice constant that is larger than the correlation length of the material. In that case, the artificial translational symmetry becomes "irrelevant" for the properties of interest. Here, I use the same term for the purpose of making the limit towards an infinite crystal explicitly.

vectors of the supercell.

$$\begin{aligned}\psi_{\vec{k},n}(\vec{r} + N_1 \vec{T}_1, \sigma) &= \psi_{\vec{k},n}(\vec{r}, \sigma) \\ \psi_{\vec{k},n}(\vec{r} + N_2 \vec{T}_2, \sigma) &= \psi_{\vec{k},n}(\vec{r}, \sigma) \\ \psi_{\vec{k},n}(\vec{r} + N_3 \vec{T}_3, \sigma) &= \psi_{\vec{k},n}(\vec{r}, \sigma)\end{aligned}\quad (5.1)$$

While the wave functions are not necessarily periodic with the unit cell of the lattice, the wave function is forced to be periodic with the much larger supercell.

For Bloch states, the periodic boundary conditions within the supercell Ω restrict the wave vectors to a discrete set

$$\vec{k}_{i,j,k} = \frac{\vec{g}_1}{N_1} i + \frac{\vec{g}_2}{N_2} j + \frac{\vec{g}_3}{N_3} k \quad (5.2)$$

with integer i, j, k .

In the following, we will need the reciprocal-space volume V_k related to a given k-point.

$$V_k = \frac{\det |\mathbf{g}|}{N_1 N_2 N_3} = \frac{(2\pi)^3}{N_1 N_2 N_3 \det |\mathbf{T}|} = \frac{(2\pi)^3}{|\Omega|} \quad (5.3)$$

In order not to duplicate wave functions, we furthermore need to restrict the k-points into one reciprocal unit cell, that is

$$0 \leq i \leq N_1 - 1 \quad \text{and} \quad 0 \leq j \leq N_2 - 1 \quad \text{and} \quad 0 \leq k \leq N_3 - 1. \quad (5.4)$$

Below, we will remove the constraint of periodicity in the supercell by letting N_1, N_2, N_3 go to infinity, which results into a continuous set of wave vectors.

5.1.2 Sum over states

In order to evaluate the expectation value of a one-particle-at-a-time operator \hat{A} with a many-particle state, we need to sum over the expectation values⁵ of the one-particle operator \hat{A} with all **natural orbitals** $|\psi_{\vec{k},n}\rangle$, weighted by the **occupations** $f_{\vec{k},n}$.

$$\langle A \rangle = \sum_n \sum_{\vec{k}} f_{\vec{k},n} \frac{\langle \psi_{\vec{k},n} | \hat{A} | \psi_{\vec{k},n} \rangle}{\langle \psi_{\vec{k},n} | \psi_{\vec{k},n} \rangle} \quad (5.5)$$

The index n is a band index.

For a Slater determinant, the occupations are identical to the occupation numbers. The occupation numbers are either one or zero, and they select those one-particle states in the basisset that contribute to the Slater determinant. These orbitals are also the natural orbitals.

The concept of natural orbitals and occupations is, however, not limited to Slater determinants. The one-particle reduced density matrix Eq. 3.50 is a well defined object also for general many-particle wave functions.⁶ The eigenvalues of the one-particle reduced density matrix are the occupations and the eigenstates are the natural orbitals.

⁵ I included the normalization in the expectation value to avoid the ambiguity of different choices for the normalization volume.

⁶ The one-particle reduced density matrix

$$\hat{\rho}^{(1)} \stackrel{\text{def}}{=} \sum_{\alpha,\beta} |\chi_\alpha\rangle \langle \Phi | \hat{c}_\beta^\dagger \hat{c}_\alpha | \Phi \rangle \langle \chi_\beta|, \quad (5.6)$$

where Φ is the many-particle wave function describing the state of the system and $|\chi_\alpha\rangle$ are the one-particle orbitals, which are consistent with the creation and annihilation operators \hat{c}_α^\dagger and \hat{c}_α . Natural orbitals $|\psi_n\rangle$ and occupations f_n are the eigenstates and eigenvalues of the one-particle reduced density matrix

$$\hat{\rho} |\psi_n\rangle = |\psi_n\rangle f_n \quad (5.7)$$

The limitation to expectation values of one-particle(-at-a-time) operators is important, because it implies that the weighted sum given above cannot be used to calculate, for example, the interaction between particles, because the latter is a two-particle operator.

Next, we exploit $\det |\mathbf{T}| \det |\mathbf{g}| = (2\pi)^3$ and that the reciprocal-space volume of a k-point V_k given in Eq. 5.3 approaches the infinitesimal volume element of a reciprocal-space integration.

$$\begin{aligned}
 \langle A \rangle &\stackrel{\text{Eq. 5.5}}{=} \sum_n \underbrace{\sum_{i=1}^{N_1} \sum_{j=1}^{N_2} \sum_{k=1}^{N_3}}_{=\sum_{\vec{k} \rightarrow \int_{V_g}}} \overbrace{\frac{\det |\mathbf{g}|}{N_1 N_2 N_3} \frac{N_1 N_2 N_3 \det |\mathbf{T}|}{(2\pi)^3}}^{=1} f_{\vec{k}_{i,j,k},n} \frac{\langle \psi_{\vec{k}_{i,j,k},n} | \hat{A} | \psi_{\vec{k}_{i,j,k},n} \rangle}{\underbrace{\langle \psi_{\vec{k}_{i,j,k},n} | \psi_{\vec{k}_{i,j,k},n} \rangle}_{A_n(\vec{k}_{i,j,k})}} \\
 &\stackrel{N_j \rightarrow \infty}{=} \Omega \sum_n \int_{V_g} \frac{d^3 k}{(2\pi)^3} f_n(\vec{k}) \underbrace{\frac{\langle \psi_{\vec{k},n} | \hat{A} | \psi_{\vec{k},n} \rangle}{\langle \psi_{\vec{k},n} | \psi_{\vec{k},n} \rangle}}_{A_n(\vec{k})} \quad (5.8)
 \end{aligned}$$

where V_g is the primitive reciprocal unit cell and the occupations $f_n(\vec{k}) = f_{\vec{k},n}$ and matrix elements $A_n(\vec{k})$ are written as functions in reciprocal space.

The matrix elements are

$$A_n(\vec{k}) \stackrel{\text{def}}{=} \langle \psi_{\vec{k},n} | \hat{A} | \psi_{\vec{k},n} \rangle = \sum_{\sigma \in \{\uparrow, \downarrow\}} \int_{\Omega} d^3 r \psi_{\vec{k},n}^*(\vec{r}, \sigma) \hat{A} \psi_{\vec{k},n}(\vec{r}, \sigma) \quad \text{with} \quad \langle \psi_{\vec{k},n} | \psi_{\vec{k},n} \rangle = 1 \quad (5.9)$$

The integration for the expectation value is performed over the volume of the supercell Ω , which is, at the same time, the volume used for the normalization.

Using the supercell Ω as integration volume for the scalar products and the expectation values becomes inconvenient in the limit $\Omega \rightarrow \infty$. In order to eliminate the dependence on the integration volume, the matrix elements are written as ratio of matrix element and norm, which allows one to replace the supercell as integration volume by the volume V_T of the primitive unit cell of the lattice.

$$A_n(\vec{k}) = \frac{\sum_{\sigma} \int_{\Omega} d^3 r \psi_{\vec{k},n}^*(\vec{r}, \sigma) \hat{A} \psi_{\vec{k},n}(\vec{r}, \sigma)}{\sum_{\sigma} \int_{\Omega} d^3 r \psi_{\vec{k},n}^*(\vec{r}, \sigma) \psi_{\vec{k},n}(\vec{r}, \sigma)} = \frac{\sum_{\sigma} \int_{V_T} d^3 r \psi_{\vec{k},n}^*(\vec{r}, \sigma) \hat{A} \psi_{\vec{k},n}(\vec{r}, \sigma)}{\sum_{\sigma} \int_{V_T} d^3 r \psi_{\vec{k},n}^*(\vec{r}, \sigma) \psi_{\vec{k},n}(\vec{r}, \sigma)} \quad (5.10)$$

This implies that the matrix elements can also be written as integral over the primitive unit cell of the lattice

$$A_n(\vec{k}) = \sum_{\sigma} \int_{V_T} d^3 r \psi_{\vec{k},n}^*(\vec{r}, \sigma) \hat{A} \psi_{\vec{k},n}(\vec{r}, \sigma) \quad (5.11)$$

if the wave functions are normalized within the primitive unit cell, i.e.

$$\sum_{\sigma} \int_{V_T} d^3 r \psi_{\vec{k},n}^*(\vec{r}, \sigma) \psi_{\vec{k},n}(\vec{r}, \sigma) = 1 \quad (5.12)$$

If energy-dependent occupations $f_n(\vec{k}) = f(\epsilon_n(\vec{k}))$ are used, we arrive at the expression for the expectation value as Brillouin-zone integral: <

BRILLOUIN-ZONE INTEGRAL

The expectation value of a one-particle operator can be obtained by an **Brillouin-zone integration**

$$\langle A \rangle \stackrel{\text{Eq. 5.8}}{=} \Omega \sum_n \int_{V_g} \frac{d^3k}{(2\pi)^3} f(\epsilon_n(\vec{k})) A_n(\vec{k}) \quad (5.13)$$

where Ω is the integration volume which defines the normalization of the one-particle states and the matrix elements. V_g is the reciprocal unit cell of the lattice, having volume $\det |\mathbf{g}|$. $f(\epsilon)$ is the Fermi distribution function^a, which equals the step function $\theta(\epsilon_F - \epsilon)$ for low temperature.

$$A_n(\vec{k}) = \frac{\langle \psi_n(\vec{k}) | \hat{A} | \psi_n(\vec{k}) \rangle}{\langle \psi_n(\vec{k}) | \psi_n(\vec{k}) \rangle} \quad (5.14)$$

are the matrix elements.^b

Remember, that there are usually two degenerate states per spin quantum number, which need to be summed over.

^aSee Fig. 6.3 on p. 191.

^bStrictly speaking, the "matrix element" is only the numerator. The denominator has been included here to avoid the ambiguity related to the normalization volume. For normalized wave functions, the numerator equals unity.

For the reader, who is concerned that the periodic boundary conditions produce artifacts in the counting of states not present in a real system, appendix M.1 investigates the state counting for a large but finite system.

5.2 Density of states

Here we introduce the **density of states** often abbreviated as DoS. A more detailed description can be found in section 8.4 of ΦSX : Statistical Physics[38].

Consider the sum over one-particle states $|\psi_n\rangle$ to evaluate the expectation value of a one-particle operator. Let us assume that the occupations $f_n = f(\epsilon_n)$ are a function of the one-particle energies ϵ_n . In thermal equilibrium the occupations would be the Fermi function.

$$\begin{aligned} \langle \hat{A} \rangle &= \sum_n f_{T,\mu}(\epsilon_n) \langle \psi_n | \hat{A} | \psi_n \rangle \\ &= \sum_n \underbrace{\int d\epsilon \delta(\epsilon - \epsilon_n) f_{T,\mu}(\epsilon_n)}_{=1} \langle \psi_n | \hat{A} | \psi_n \rangle \\ &= \int d\epsilon f_{T,\mu}(\epsilon) \text{Tr} \left[\sum_n \delta(\epsilon - \epsilon_n) \langle \psi_n | \hat{A} | \psi_n \rangle \right] \\ &= \int d\epsilon f_{T,\mu}(\epsilon) \text{Tr} \left[\underbrace{\sum_n |\psi_n\rangle \delta(\epsilon - \epsilon_n) \langle \psi_n|}_{\hat{D}(\epsilon)} \hat{A} \right] \\ &= \int d\epsilon f_{T,\mu}(\epsilon) \text{Tr} \left[\hat{D}(\epsilon) \hat{A} \right] \end{aligned} \quad (5.15)$$

Thus, the density of states, more precisely $\text{Tr} \left[\hat{D}(\epsilon) \hat{A} \right]$ provides the energy-resolved information on the contribution to an expectation value. A more rigorous derivation of Eq. 5.15 is given in appendix K.1.

DENSITY OF STATES OPERATOR

The **density of states operator** is defined as

$$\hat{D}(\epsilon) = \sum_n |\psi_n\rangle \delta(\epsilon - \epsilon_n) \langle \psi_n| \quad (5.16)$$

Matrix elements of the density-of-states operator

I have introduced here a rather general definition of the density of states, namely the density of states as operator. This operator is the most flexible definition, which allows to derive a number of more special quantities.

It is convenient to express the density of states in terms of its matrix elements with a convenient basisset. This basisset is chosen depending on the question to be addressed. In order to understand the local electronic structure one often uses tight-binding orbitals or Wannier orbitals.

In order to divide the density of states into its components we need to insert a unit operator into the matrix elements. Let me elaborate in the unit operator so that we can formulate it with non-orthonormal basisfunctions χ_α , that is for $O_{\alpha,\beta} \stackrel{\text{def}}{=} \langle \chi_\alpha | \chi_\beta \rangle \neq \delta_{\alpha,\beta}$. The unit operator is

$$\hat{1} = \sum_{\alpha,\beta} |\chi_\alpha\rangle O_{\alpha,\beta}^{-1} \langle \chi_\beta| = \sum_{\alpha} |\chi_\alpha\rangle \langle \pi_\alpha| \quad (5.17)$$

where I introduced the **projector functions**

$$\langle \pi_\alpha| \stackrel{\text{def}}{=} \sum_{\beta} O_{\alpha,\beta}^{-1} \langle \chi_\beta| \quad (5.18)$$

In practice one has to pay attention whether to write the projector function on the left or the right-hand side. This is a problem that is analogous to the distinction of ko- and kontravariant vectors in a system with oblique axes.

This allows me to rewrite the trace in Eq. 5.15 in the form⁷

$$\begin{aligned} \text{Tr} \left[\hat{D}(\epsilon) \hat{A} \right] &\stackrel{\text{Eq. 5.17}}{=} \text{Tr} \left[\underbrace{\sum_{\alpha} |\chi_\alpha\rangle \langle \pi_\alpha|}_{\hat{1}} \hat{D}(\epsilon) \underbrace{\sum_{\beta} |\pi_\beta\rangle \langle \chi_\beta|}_{\hat{1}} \hat{A} \right] \\ &\stackrel{\text{Eq. 5.17}}{=} \sum_{\alpha,\beta} \underbrace{\langle \pi_\alpha | \hat{D}(\epsilon) | \pi_\beta \rangle}_{D_{\alpha,\beta}(\epsilon)} \underbrace{\langle \chi_\beta | \hat{A} | \chi_\alpha \rangle}_{A_{\beta,\alpha}} \\ &= \sum_{\alpha,\beta} D_{\alpha,\beta}(\epsilon) A_{\beta,\alpha} = \text{Tr} \left[\mathbf{D}(\epsilon) \mathbf{A} \right] \end{aligned} \quad (5.19)$$

A general expectation value expressed in terms of the density of states matrix has the form

$$\langle A \rangle = \int d\epsilon f_{T,\mu}(\epsilon) \sum_{\alpha,\beta} D_{\alpha,\beta}(\epsilon) A_{\beta,\alpha} \quad (5.20)$$

⁷I exploit that the trace is invariant under cyclic permutation of the terms in the product. This is shown by introducing an arbitrary orthonormal basisset $\{|n\rangle\}$

$$\begin{aligned} \text{Tr} \left[\sum_{\alpha,\beta} |\chi_\alpha\rangle D_{\alpha,\beta} \langle \chi_\beta| \hat{A} \right] &= \sum_{n,\alpha,\beta} \langle n | \chi_\alpha \rangle D_{\alpha,\beta} \langle \chi_\beta | \hat{A} | n \rangle = \sum_{n,\alpha,\beta} D_{\alpha,\beta} \langle \chi_\beta | \hat{A} | n \rangle \langle n | \chi_\alpha \rangle \\ &= \sum_{\alpha,\beta} D_{\alpha,\beta} \langle \chi_\beta | \hat{A} \underbrace{\sum_n |n\rangle \langle n|}_{\hat{1}} \chi_\alpha \rangle = \sum_{\alpha,\beta} D_{\alpha,\beta} \underbrace{\langle \chi_\beta | \hat{A} | \chi_\alpha \rangle}_{A_{\beta,\alpha}} = \text{Tr} \left[\mathbf{D} \mathbf{A} \right] \end{aligned}$$

where the density-of-states matrix elements are

$$D_{\alpha,\beta}(\epsilon) \stackrel{\text{def}}{=} \langle \pi_\alpha | \hat{D}(\epsilon) | \pi_\beta \rangle = \sum_n \langle \pi_\alpha | \psi_n \rangle \delta(\epsilon - \epsilon_n) \langle \psi_n | \pi_\beta \rangle \quad (5.21)$$

The matrix elements of the observable \hat{A} are obtained with the orbitals as $A_{\alpha,\beta} = \langle \chi_\alpha | \hat{A} | \chi_\beta \rangle$.

Special types of density of states

- The **total density of states** is simply the trace of the density of states operator

$$D_{\text{tot}}(\epsilon) \stackrel{\text{def}}{=} \text{Tr}[\hat{D}(\epsilon)] = \sum_n \delta(\epsilon - \epsilon_n) \quad (5.22)$$

The total density of states is the quantity relevant for the calculation of thermodynamic properties.

- The **projected density of states** selects the contribution of a specific orbital $|\chi_\alpha\rangle$ to the density of states.

$$D_{\alpha,\alpha}(\epsilon) \stackrel{\text{def}}{=} \langle \pi_\alpha | \hat{D}(\epsilon) | \pi_\alpha \rangle = \sum_n \delta(\epsilon - \epsilon_n) |\langle \pi_\alpha | \psi_n \rangle|^2 \quad (5.23)$$

For a complete set of orthonormal orbitals $\{|\chi_\alpha\rangle\}$, the total density of states is the sum over all projected density of states, because in this case $\text{Tr}[\mathbf{D}(\epsilon)\mathbf{S}] = \text{Tr}[\mathbf{D}(\epsilon)]$. The overlap matrix \mathbf{S} defined as $S_{\alpha,\beta} \stackrel{\text{def}}{=} \langle \chi_\alpha | \chi_\beta \rangle$ for orthonormal orbitals $|\chi_\alpha\rangle$ is the unit matrix.

- **Orbital populations**[39, 40, 41] The offsite matrix elements of the density of states are useful for analyzing chemical bonds. Orbital populations are frequently used in the form of **crystal-orbital overlap populations (COOP)**

$$\text{COOP}_{\alpha,\beta} = D_{\alpha,\beta}(\epsilon) O_{\beta,\alpha} \quad (5.24)$$

or as **crystal-orbital Hamilton populations (COHP)**

$$\text{COHP}_{\alpha,\beta} = D_{\alpha,\beta}(\epsilon) H_{\beta,\alpha} \quad (5.25)$$

COOPs and COHPs differ only by a factor, the matrix element of overlap matrix or Hamiltonian, but they have the same energy dependence.

The sum over all COOPs integrate up to the number of electrons, when multiplied with the Fermi function. Thus, one can divide the charge into orbital charges, the diagonal elements, and bond charges, the off-diagonal elements.

The sum over all COHPs integrate up to the total energy, when multiplied with the Fermi function.

$$\begin{aligned} E &= \sum_n f_{T,\mu}(\epsilon_n) \epsilon_n = \sum_{\alpha,\beta} \int d\epsilon f(\epsilon) D_{\alpha,\beta}(\epsilon) H_{\beta,\alpha} \\ &= \sum_\alpha \int d\epsilon f_{T,\mu}(\epsilon) D_{\alpha,\alpha}(\epsilon) H_{\alpha,\alpha} + \sum_{\alpha,\beta;\beta>\alpha} \int d\epsilon f_{T,\mu}(\epsilon) 2\text{Re}[D_{\alpha,\beta}(\epsilon) H_{\beta,\alpha}] \end{aligned} \quad (5.26)$$

We have already divided the energy into the diagonal and the off-diagonal terms.

Editor: include a figure describing the orbital populations

The diagonal terms are related to the projected density of states. They describe the ionic contribution of the bonding, namely the energy gained by redistributing electrons from more electropositive atoms to more electronegative atoms.

The off-diagonal elements describe the covalent bond energy in a bond.

$$E_{\alpha,\beta}^{bond} = \int d\epsilon f_{T,\mu}(\epsilon) 2\text{Re} [D_{\alpha,\beta}(\epsilon) H_{\beta,\alpha}] \quad (5.27)$$

However, in practice it is not the energy integral that is of interest, but also its energy dependence. The energy dependence tells how bonding will be affected by shifting orbitals in energy. They tell how robust a material is against external perturbation or chemical modifications. There is practical use of stable materials as well as for unstable materials. The latter can be used as switches.

5.2.1 Density-of-states operator in the solid

For a solid we can translate this result into a Brillouin-zone integral and a sum over bands.

$$\hat{D}(\epsilon) = \Omega \sum_n \int \frac{d^3k}{(2\pi)^3} |\psi_n(\vec{k})\rangle \delta(\epsilon - \epsilon_n(\vec{k})) \langle \psi_n(\vec{k})| \quad (5.28)$$

The density of states is defined as an extensive quantity⁸, that is, it is proportional to the volume Ω . This is understandable, because the energy levels come closer together as the system size is increased until the discrete spectrum is converted at infinite volume into a continuous spectrum. A little inconvenient is that the density of states is multiplied with an, in principle, infinite volume. This can be avoided by defining the **density of states per volume** $g(\epsilon)$

$$g(\epsilon) \stackrel{\text{def}}{=} \frac{1}{\Omega} D(\epsilon) \stackrel{\text{Eq. 5.28}}{=} \sum_n \int \frac{d^3k}{(2\pi)^3} \delta(\epsilon(\vec{k}, \sigma) - \epsilon_0) \quad (5.29)$$

I strongly recommend reading of the section 8.4 entitled “One-particle density of states” of ΦSX: Statistical Physics [38].

5.3 Home study and practice

5.3.1 Jellium model

Editor: Turn this into an exercise! It needs to be completed.

Introduction

We use model systems to understand the qualitative behavior of a system before we attempt to describe a real system in all its complexity. For the electron gas, the model system is the **free-electron gas** or the **jellium model**. The jellium model consists of electrons and a spatially constant, positive charge background, which ensures overall charge neutrality.

⁸The notion of extensive and intensive quantities originates from thermodynamics. An extensive quantity scales with the size of the system, while an intensive does not.

Problem

- 1 Determine the band structure $\epsilon(\vec{k})$ and the wave functions of the free-electron gas.
- 2 Determine the density of states of the jellium model. Hint: Calculate first the number of states as function of the Fermi level. Obtain then the density of states as derivative of the number of states function.
- 3 The density of states have a characteristic shape near band edges in each dimension. Compare the density of states for one, two and three dimensions. Specify the functional forms up to a pre-factor factor. Make schematic drawings.
- 4 **Editor:** The following needs to be completed. In order to construct a wire that behaves like a one-dimensional material, its width must be so small that only the lowest of the lateral modes of the wire are occupied. This requires the lowest energy of the first excited lateral mode lies a certain distance above the chemical potential. This distance is given by thermal energies.

Solution**Wave functions**

The wave functions of free electrons have, in the extended zone scheme, the form

$$\psi_{\vec{k},\sigma}(\vec{r},\sigma') = \delta_{\sigma,\sigma'} \frac{1}{\sqrt{\Omega}} e^{i\vec{k}\vec{r}} \quad (5.30)$$

where Ω is the normalization volume.

Band structure of the free-electron gas

The **dispersion relation** of free electrons forms a parabola

$$\epsilon_{\vec{k},\sigma} = \epsilon_0 + \frac{(\hbar\vec{k})^2}{2m_e} \quad (5.31)$$

where ϵ_0 is the value of the constant potential. The dispersion relation of electrons in a solid is often called the **band structure**.

In Fig. 5.1, the band structure of free and non-interacting electron gas is compared to that of a real material, namely aluminium. We observe that the free-electron gas already provides a fairly good description of some realistic systems.

The jellium model approximates real metals surprisingly well, even though the potential of the nuclei is far from being a constant. In a hand-waving manner we can say that the valence electrons are expelled from the nuclear region by the Pauli repulsion of the core electrons, so that they move around in a region with fairly constant potential.

Density of states of the free-electron gas

Now, we can calculate the density of states for the free, non-interacting electron gas.

$$D(\epsilon) \stackrel{\text{Eq. 5.28}}{=} \frac{\Omega}{(2\pi)^3} \underbrace{\sum_{\sigma}}_2 \int d^3k \delta\left(\underbrace{\epsilon_0 + \frac{(\hbar\vec{k})^2}{2m_e}}_{\epsilon_{\vec{k},\sigma}} - \epsilon\right) \quad (5.32)$$

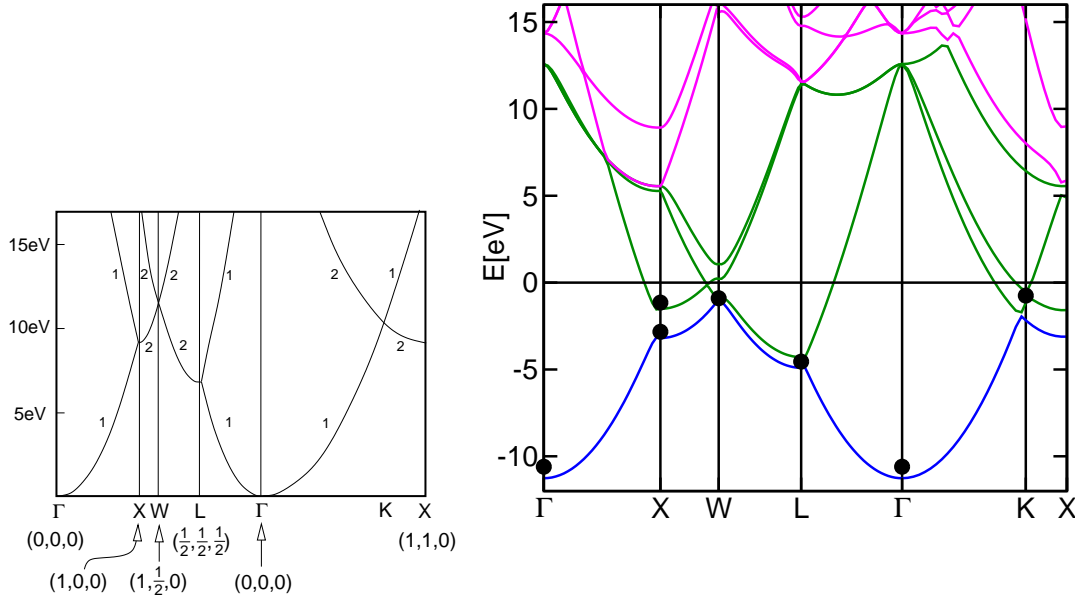


Fig. 5.1: Band structure of free, non-interacting electrons. The lattice is an fcc-cell with a lattice constant of 4.05 \AA corresponding to aluminium. The high-symmetry points are given in units of $\frac{2\pi}{a_{\text{lat}}}$. The numbers indicate the degeneracy beyond spin-degeneracy. Below the band structure of aluminium calculated by density functional theory is shown in comparison.

The integral is performed over the entire reciprocal space rather than being limited to a reciprocal unit cell. This is because the system has full translation symmetry, which results in a infinitesimally small real-space lattice vectors. This in turn leads to an infinite reciprocal unit cell covering all reciprocal space.

It is convenient to exploit that the delta function is the derivative of the Heaviside step function and to determine the density of states as derivative of the number of states at zero temperature.

$$\begin{aligned}
 N(T = 0, \mu) &= \int_{-\infty}^{\infty} d\epsilon D(\epsilon) f_{T=0, \mu}(\epsilon) = \int_{-\infty}^{\mu} d\epsilon D(\epsilon) \\
 \Rightarrow D(\epsilon) &= \left. \frac{\partial N(T = 0, \mu)}{\partial \mu} \right|_{\mu=\epsilon}
 \end{aligned} \tag{5.33}$$

The number of states function for the free-electron gas can be calculated independently from the density of states as expectation value of the unit operator. We use the Brillouin-zone integral Eq. 5.13 for expectation values

$$\begin{aligned}
 N(T = 0, \mu) &\stackrel{\text{Eq. 5.13}}{=} \Omega \underbrace{\left(\sum_{\sigma \in \{\uparrow, \downarrow\}} \right)}_{=2} \int \frac{d^3 k}{(2\pi)^3} \theta \left(\mu - \epsilon_0 - \frac{(\hbar \vec{k})^2}{2m_e} \right) \\
 &= \Omega \underbrace{\left(\sum_{\sigma \in \{\uparrow, \downarrow\}} \right)}_{=2} \frac{1}{(2\pi)^3} \frac{4\pi}{3} k_F^3 = \Omega \underbrace{\left(\sum_{\sigma \in \{\uparrow, \downarrow\}} \right)}_{=2} \frac{4\pi}{3} \left(\frac{2m_e(\mu - \epsilon_0)}{(2\pi\hbar)^2} \right)^{\frac{3}{2}}
 \end{aligned} \tag{5.34}$$

where

$$k_F(\mu) \stackrel{\text{def}}{=} \frac{1}{\hbar} \sqrt{2m_e(\mu - \epsilon_0)} \quad (5.35)$$

is the **Fermi wave vector**. $\hbar k_F$ is the **Fermi momentum**.⁹

Thus, we obtain the density of states of the free-electron gas

DENSITY OF STATES OF THE FREE-ELECTRON GAS

$$D(\epsilon) \stackrel{\text{Eqs. 5.33, 5.34}}{=} 2\pi\Omega \underbrace{\left(\sum_{\sigma \in \{\uparrow, \downarrow\}} \right)}_{=2} \left(\frac{2m_e}{(2\pi\hbar)^2} \right)^{\frac{3}{2}} \sqrt{\epsilon - \epsilon_0} \quad \text{for } \epsilon \geq \epsilon_0 \quad (5.36)$$

The density of states vanishes for $\epsilon < \epsilon_0$, because ϵ_0 is the lower band edge.

Editor: Include a graph with the density of states of the free-electron gas.

The Fermi momentum is very useful as upper cutoff for the energy integration for the zero-temperature results. It can directly be related to the electron density $n = \frac{N}{\Omega}$. From Eq. 5.34 we obtain

$$\begin{aligned} n &= \frac{N}{\Omega} \stackrel{T=0}{=} \frac{N(T=0, \mu)}{\Omega} \stackrel{\text{Eq. 5.34}}{=} \underbrace{\left(\sum_{\sigma \in \{\uparrow, \downarrow\}} \right)}_{=2} \frac{1}{(2\pi)^3} \frac{4\pi}{3} k_F^3 \\ \Rightarrow \quad k_F(n) &= \sqrt[3]{\frac{6\pi^2 n}{\sum_{\sigma \in \{\uparrow, \downarrow\}}}} = \sqrt[3]{3\pi^2 n} \end{aligned} \quad (5.37)$$

With the Fermi momentum from Eq. 5.37, we can determine the **Fermi energy**

$$\epsilon_F = \epsilon_0 + \frac{(\hbar k_F)^2}{2m_e} = \epsilon_0 + \frac{(3\pi^2 \hbar^3)^{\frac{2}{3}}}{2m_e} n^{\frac{2}{3}} \quad (5.38)$$

The Fermi energy of the free-electron gas depends on the mass, the potential and the electron-electron interaction. In contrast, the Fermi-momentum of a free-electron gas only depends on the density. The reason is that the dispersion relation of a free-electron gas is isotropic, and the volume of the volume inside the Fermi surface is determined by the number of states.

The density of the electron gas is often represented by a r_s , which is the radius of a sphere which occupies the mean volume per electron. If the electron density is $n = \frac{N}{\Omega}$, we obtain

$$n = \frac{1}{\frac{4\pi}{3} r_s^3} \quad \Rightarrow \quad r_s = \sqrt[3]{\frac{3}{4\pi n}} \quad (5.39)$$

The **electron-gas parameter** or **Seitz radius**¹⁰ The Seitz radius r_s is in common use because it provides a characteristic length scale of the system.

⁹In Hartree atomic units $\hbar = 1$ so that the difference between Fermi momentum and Fermi wave vector is not apparent. Therefore, the distinction between Fermi wave vector and Fermi momentum is rarely made explicit.

¹⁰I found the name Seitz radius in [42].

Chapter 6

Thermodynamics of non-interacting electrons

What makes the many-electron problem so complicated is the interaction between the electrons. A similar problem is known from classical mechanics. While the Kepler problem, a two-body problem, can be solved analytically, no such solution exists for the three-body problem, where the gravitational attraction between the planets is considered as well.

Similarly the thermodynamics of non-interacting systems is fairly simple to understand in comparison to an interacting many-particle theory. This is why one attempts to map the problem to one of non-interacting quasi electrons.

6.1 A brief tour from statistical physics to thermodynamics

Let us remind ourselves of the main relations in thermodynamics. A more detailed account can be found in Φ SX:Statistical Physics[38].

The definition of thermodynamic quantities appears at times unnatural or inconvenient. This is because thermodynamics developed as an empirical theory long before an atomistic understanding of the processes has been found. A solid theoretical foundation of the theory has been found much later, starting with Boltzmann. At this point, however, the quantities of the theory had to be linked into an already existing framework of definitions.

Thermodynamics is a theory of macroscopic quantities such as energy volume, and particle numbers. It describes systems in thermal equilibrium. The link to microscopic world is given by statistical physics.

The starting point is the concept of an **ensemble**. An ensemble is a set of wave functions $|\Psi_q\rangle$ with their probabilities P_q . The wave functions are general many-particle wave functions. The probabilities obey $\sum_q P_q = 1$ and $P_q \geq 0$. The wave functions are possible states of the system and the probabilities are the likelihood that the system is in the corresponding state.

The ensemble can be described by a **density operator** also called (von-Neumann) **density matrix**

$$\hat{\rho} = \sum_q |\Psi_q\rangle P_q \langle\Psi_q| \quad (6.1)$$

The **thermal expectation value** $\langle X \rangle$ of an observable \hat{X} is the weighted sum of quantum-mechanical expectation values

$$\langle X \rangle = \sum_q P_q \langle\Psi_q|\hat{X}|\Psi_q\rangle = \text{Tr}[\hat{\rho}\hat{X}] \quad (6.2)$$

The thermal equilibrium state is obtained by the **maximum-entropy principle** of Jaynes[43, 44]. It rests on the interpretation of the entropy S as basic concept of information theory.[45] Its quantum-mechanical expression is called the **von-Neumann entropy**.

$$S = -k_B \text{Tr}[\hat{\rho} \ln(\hat{\rho})] \quad (6.3)$$

If the wave functions $|\Psi_q\rangle$ in Eq. 11.1 are orthonormal, they are the eigenstates of the density matrix. In a basisset of orthonormal eigenstates, the von-Neumann entropy Eq. 6.3 has the form of Shannon's entropy eq:shannonentropy obtained from information theory¹

$$S = -k_B \sum_q P_q \ln(P_q) \quad (6.4)$$

Let me now become more specific and select the case that will be relevant in the following. We choose a system with a volume-dependent Hamilton operator $\hat{H}(V)$, which commutes with the particle-number operator \hat{N} . The Hamilton operator may be many-particle operator with or without interaction between particles.

The maximum-entropy principle requires to find the ensemble that maximizes the entropy under the constraints the thermal expectation values have certain values.

$$S(E, V, N) = \text{stat}_{T, \mu} \max_{\hat{\rho}} \left\{ S[\hat{\rho}] - \frac{1}{T} (\text{Tr}[\hat{\rho} \hat{H}(V)] - E) + \frac{\mu}{T} (\text{Tr}[\hat{\rho} \hat{N}] - N) \right\} \quad (6.5)$$

The intensive variables, the temperature T and the chemical potential μ act as Lagrange multipliers to enforce the constraints. The search for the maximum entropy must obey the conditions for a valid density operator.

The ensemble maximum of Eq. 6.5 can be done without thermodynamic constraints² for a fixed set of Lagrange multipliers $1/T$ and μ/T , so that

$$S(E, V, N) = \text{stat}_{T, \mu} \frac{1}{T} \left\{ -\Omega(T, V, \mu) + E - \mu N \right\} \quad (6.6)$$

using the **grand potential** $\Omega(T, V, N)$ defined as

$$\Omega(T, V, N) \stackrel{\text{def}}{=} \min_{\hat{\rho}} \left\{ -TS[\hat{\rho}] + \text{Tr}[\hat{\rho}(\hat{H}(V) - \mu\hat{N})] \right\} \quad (6.7)$$

The stationary condition leads to Boltzmann weights as probabilities, respectively, the equilibrium density operator

$$\hat{\rho}^{\text{eq}}(T, V, \mu) = \frac{1}{Z(T, V, \mu)} e^{-\beta(\hat{H}(V) - \mu\hat{N})} = \frac{1}{Z(T, V, \mu)} \sum_n |\Psi_n\rangle e^{-\beta(E_n(V) - \mu N_n)} \langle \Psi_n| \quad (6.8)$$

where $|\Psi_n(V)\rangle$ are eigenstates of the Hamiltonian $\hat{H}(V)$ and the particle-number operator \hat{N} with eigenvalues $E_n(V)$ and N_n .

The normalization constant is the **partition function**

$$Z(T, V, \mu) = \sum_n e^{-\beta(E_n(V) - \mu N_n)} = \text{Tr} \left[e^{-\beta(\hat{H}(V) - \mu\hat{N})} \right] \quad (6.9)$$

The partition function plays a fundamental role, because it establishes the link between statistical physics and thermodynamics. It links the description based on the quantum states of a system with the macroscopic description using only few thermodynamic variables such as T, V, μ .

¹Shannon used a different prefactor, namely $1/\ln(2)$, instead of k_B . With this prefactor the Shannon entropy of a message is the number of bits required to represent a message.

²The constraints required to limit the search to allowed density operators still need to be observed.

The **grand potential** can be expressed directly by the partition function as

$$\Omega(T, V, \mu) = -k_B T \ln[Z(T, V, \mu)] \quad (6.10)$$

It is important to note that thermodynamics is restricted to equilibrium ensembles given in Eq. 6.8. This is the price to pay for a very simple description in terms of few thermodynamic variables, such as energy, volume, particle number, etc., and their intrinsic partners temperature, pressure, chemical potential, etc. Thermodynamics is not able to say anything about general non-equilibrium states. It is assumed that a system relaxes, when left alone, into an equilibrium state. This is an important assumption about the dynamics of physical processes. Thus, it can describe quasi-static processes. The approach to thermal equilibrium is often very rapid on the time scale of human perception. Thus, thermodynamics machines can often be well described by quasi-static processes.

6.2 Fundamental relations of thermodynamics

From the grand potential, we can

$$S(T, V, \mu) \stackrel{\text{Eq. 6.7}}{=} -\frac{\partial \Omega}{\partial T} \quad (6.11)$$

$$N(T, V, \mu) \stackrel{\text{Eq. 6.7}}{=} -\frac{\partial \Omega}{\partial \mu} \quad (6.12)$$

$$U(T, V, \mu) \stackrel{\text{Eq. 6.7}}{=} \Omega(T, V, \mu) + TS(T, V, \mu) + \mu N(T, V, \mu) \quad (6.13)$$

These three equations can be combined into one, namely³

$$U(S, V, N) = \text{stat}_{T, \mu} \left(\Omega(T, V, \mu) + TS + \mu N \right) \quad (6.15)$$

which is a **Legendre transform** from the grand potential Ω to the internal energy $U(S, V, N)$.

The **pressure** acting on the system is defined as

$$p \stackrel{\text{def}}{=} -\frac{\partial U(S, V, N)}{\partial V} \quad (6.16)$$

Let us now consider a thermodynamic process, which is defined by a sequence of thermodynamic states. The process may be described by a path

$$\left(T(t), V(t), \mu(t) \right) \quad (6.17)$$

as function of time t .

Let us investigate the change of the internal energy $U(S, V, N)$

$$\begin{aligned} \frac{dU}{dt} &= \underbrace{\frac{dU}{dS}}_T \frac{dS}{dt} + \underbrace{\frac{dU}{dV}}_{-p} \frac{dV}{dt} + \underbrace{\frac{dU}{dN}}_{\mu} \frac{dN}{dt} \\ dU &= \underbrace{T dS}_{\text{heat}} - \underbrace{p dV + \mu dN}_{\text{Work}} = dQ + dW \end{aligned} \quad (6.18)$$

The **heat** dQ is the thermal energy transferred to the system. The **work** dW is the mechanical or other non-thermal energy transferred to the system.

3

$$U(T, V, \mu) = U(S(T, V, \mu), V, N(T, V, \mu)) \quad (6.14)$$

6.3 Many-particle states of non-interacting electrons

Let me start with the most simple case, namely the non-interacting electron gas. The Hamiltonian for a non-interacting electron gas with N electrons in a potential $v(\vec{r})$ has the form

$$\hat{H} = \sum_{i=1}^N \hat{h}_i = \sum_{i=1}^N \frac{\hat{p}_i^2}{2m_e} + v(\hat{r}_i) \quad (6.19)$$

and and, in Fock space,

$$\hat{H} = \sum_{N=0}^{\infty} \sum_{i=1}^N \int d^4x_1 \cdots \int d^4x_N |\vec{x}_1, \dots, \vec{x}_N\rangle \left(\frac{-\hbar^2}{2m_e} \vec{\nabla}_i^2 + v(\vec{r}_i) \right) \langle \vec{x}_1, \dots, \vec{x}_N| \quad (6.20)$$

Here, \hat{p}_i is the momentum operator acting on the i -th particle, and \hat{r}_i is the position operator of the i -th particle.

Even though the electrons do not interact, they do not move completely independently. The reason is, again, the Pauli-principle or the antisymmetry requirement for the wave function. If one electron is at a certain position, no other electron with the same spin can approach it. There is no repulsive potential. The two electrons simply do not “like” each other.

In practice, this means that we have to use an antisymmetric wave function. Luckily, the eigenstates of a system of non-interacting electrons (with a non-degenerate ground state) is a single **Slater determinant**. In contrast, the wave function for interacting electrons is, in general, a superposition of many Slater determinants.

Here, we mention a few facts about the states of non-interacting electrons without proving them:

Hamilton eigenstates: The eigenstates are Slater determinants made of eigenstates $\varphi_n(\vec{x})$ of the one-particle Hamiltonian $\hat{h} = \frac{\hat{p}^2}{2m} + v(\hat{r})$

$$\underbrace{\left[\frac{-\hbar^2}{2m} \vec{\nabla}^2 + v(\vec{r}) \right] \varphi_n(\vec{x})}_{\langle \vec{x} | \hat{h} | \varphi_n \rangle} = \varphi_n(\vec{x}) \epsilon_n \quad (6.21)$$

The Slater determinant, which is an eigenstate of the many-particle system, can be represented by its **number representation**. The **occupations numbers**, which may be zero or one, are combined into a vector $\vec{\sigma}$. The i -th element of $\vec{\sigma}$ vector is the occupation number of the i -th eigenstate of the one-particle Hamiltonian.

Thus, the eigenstates of the many-particle Hamiltonian can be labeled by the vector $\vec{\sigma}$

$$|\Phi_{\vec{\sigma}}\rangle = |\sigma_1, \sigma_2, \dots\rangle \quad (6.22)$$

Energy eigenvalues: A Slater determinant $|\Phi_{\vec{\sigma}}\rangle$ has the energy

$$E_{\vec{\sigma}} = \sum_{n=1}^{\infty} \sigma_n \epsilon_n$$

where the ϵ_n are the one-particle energies defined above in Eq. 6.21.

Particle number: A Slater determinant $|\Phi_{\vec{\sigma}}\rangle$ has the particle number

$$N_{\vec{\sigma}} = \sum_{n=1}^{\infty} \sigma_n$$

Grand potential: The **grand canonical ensemble** describes a system in thermal equilibrium which is in contact with a heat bath and a particle reservoir. A heat bath is characterized by a temperature T and the particle reservoir is characterized by a **chemical potential** μ . The temperature is often represented by the **thermodynamic beta** $\beta = \frac{1}{k_B T}$. k_B is the **Boltzmann constant**.

The thermodynamic potential for the grand-canonical ensemble is the **grand potential**. The grand potential for a system of non-interacting fermions is⁴

$$\begin{aligned}
\Omega(T, \mu) &\stackrel{\text{Eq. 6.7}}{=} -k_B T \ln \text{Tr}[e^{-\beta(\hat{H} - \mu \hat{N})}] \\
&= -k_B T \ln \left[\underbrace{\sum_{\vec{\sigma}} \exp\left(-\beta(E_{\vec{\sigma}} - \mu N_{\vec{\sigma}})\right)}_{\text{partition sum}} \right] \\
&= -k_B T \ln \left[\sum_{\vec{\sigma}} e^{-\beta \sum_{i=1}^{\infty} \sigma_i (\epsilon_i - \mu)} \right] \\
&= -k_B T \ln \left[\prod_{i=1}^{\infty} \sum_{\sigma_i=0}^1 e^{-\beta \sigma_i (\epsilon_i - \mu)} \right] \\
&= -k_B T \ln \left[\prod_{i=1}^{\infty} (1 + e^{-\beta(\epsilon_i - \mu)}) \right] \\
&= -k_B T \sum_{i=1}^{\infty} \ln(1 + e^{-\beta(\epsilon_i - \mu)}) \tag{6.23}
\end{aligned}$$

The interesting observation is that the thermodynamic potential of non-interacting particles, here electrons, is a sum over one-particle states.

If the density of states introduced in section 5.2 is known, we can rewrite the grand potential in the form

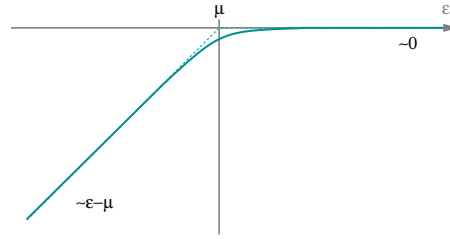
$$\begin{aligned}
\Omega(T, \mu) &= \sum_{i=1}^{\infty} \underbrace{\int d\epsilon \delta(\epsilon - \epsilon_i)}_{=1} \left[-k_B T \ln(1 + e^{-\beta(\epsilon_i - \mu)}) \right] \\
&= \int d\epsilon \underbrace{\sum_{i=1}^{\infty} \delta(\epsilon - \epsilon_i)}_{D_{tot}(\epsilon)} \left[-k_B T \ln(1 + e^{-\beta(\epsilon - \mu)}) \right] \\
&= \int d\epsilon D_{tot}(\epsilon) \left[-k_B T \ln(1 + e^{-\beta(\epsilon - \mu)}) \right] \tag{6.24}
\end{aligned}$$

GRAND POTENTIAL OF NON-INTERACTING ELECTRONS

$$\Omega(T, \mu) = \int_{-\infty}^{\infty} d\epsilon D_{tot}(\epsilon) \left[-k_B T \ln(1 + e^{-\beta(\epsilon - \mu)}) \right] \tag{6.25}$$

The shape of the function $-k_B T \ln(1 + e^{-\beta(\epsilon - \mu)})$ in the integral is shown in the following graph

⁴Caution: In the derivation we implicitly interchange a sum and a product. This is only possible in this special case.



Its characteristic features are captured by the following limiting cases

$$-k_B T \ln(1 + e^{-\beta(\epsilon - \mu)}) \approx \begin{cases} \epsilon - \mu & \text{for } \epsilon - \mu \ll -k_B T \\ -k_B T \ln(2) + \frac{1}{2}\beta(\epsilon - \mu) & \text{for } |\epsilon - \mu| \ll k_B T \\ 0 & \text{for } \epsilon - \mu \gg k_B T \end{cases} \quad (6.26)$$

Because the grand potential as function of all intrinsic variables T , μ , p , etc. contains the complete thermodynamics potential, all other thermodynamic quantities can be derived using the one-particle density of states. One caveat is that these expressions are only valid for non-interacting electrons. Furthermore, any dependence of the density of states on the intrinsic variables, such as a pressure dependence, need to be known as well.

With Eq. 6.25, we achieved a separation into a system dependent quantity, that is independent of temperature and thermodynamics, on the one hand, and, on the other hand, a system-independent quantity that captures all system-independent information on the thermodynamics.

6.4 Fermi distribution

With the grand potential Eq. 6.25 obtained above, we can evaluate with Eq. 6.13 the internal energy, or with Eq. 6.12 the particle number of non-interacting electrons. In both cases, we obtain an energy integral of a product of density of states $D(\epsilon)$, an occupation $f_{T,\mu}(\epsilon)$, and another term that is specific for the physical quantity at hand.

$$\begin{aligned} N &\stackrel{\text{Eq. 6.11}}{=} -\frac{\partial \Omega}{\partial \mu} \stackrel{\text{Eq. 6.25}}{=} -\int_{-\infty}^{\infty} d\epsilon D_{tot}(\epsilon) \frac{d}{d\mu} \left[-k_B T \ln(1 + e^{-\beta(\epsilon - \mu)}) \right] \\ &= \int_{-\infty}^{\infty} d\epsilon D_{tot}(\epsilon) \frac{1}{1 + e^{+\beta(\epsilon - \mu)}} \\ &\stackrel{\text{Eq. 6.28}}{=} \int_{-\infty}^{\infty} d\epsilon f_{T,\mu}(\epsilon) D_{tot}(\epsilon) \end{aligned} \quad (6.27)$$

where

FERMI FUNCTION

$$f_{T,\mu}(\epsilon) \stackrel{\text{def}}{=} \frac{1}{1 + e^{\beta(\epsilon - \mu)}} \quad (6.28)$$

is the **Fermi-distribution function** $f(\epsilon)$. (see sections 7.1 and 8.5 of “*FSX: Statistical Physics*”[38])

The Fermi distribution $f_{T,\mu}(\epsilon)$ is the mean occupation of a one-particle state at energy ϵ for a given temperature T and chemical potential μ .

- The Fermi function is shown in Fig. 6.1. In the absence of temperature effects we set the temperature to zero, so that the Fermi distribution function is turned into a step function.

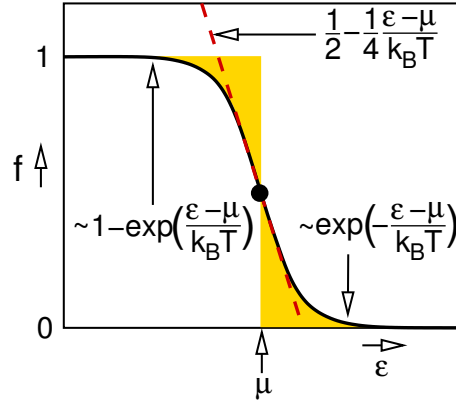


Fig. 6.1: Fermi distribution $f_{T,\mu}(\epsilon) = (1 + e^{\beta(\epsilon-\mu)})^{-1}$.

- Far away from the chemical potential, the Fermi function becomes similar to the Boltzmann distribution $e^{-\beta(\epsilon-\mu)}$. For holes, the occupation is analogously $1 - f_{T,\mu}(\epsilon) = e^{-\beta(-\epsilon+\mu)}$. The simple Boltzmann factor is characteristic for distinguishable particles. The finding seems to suggest that, far away from the chemical potential, the statistics of fermions is similar to that of distinguishable particles. The physical reason is that the likelihood that two electrons occupy the same state is insignificant already for the Boltzmann distribution, so that the Pauli principle becomes insignificant. This is a general observation that the distribution functions for bosons, fermions become identical to that, the Boltzmann distribution, of distinguishable particles for dilute gases.
- Near the Fermi level, the function switches approximately within $4k_B T$ from occupation one to occupation zero. (As obtained from the straight-line approximation.)

The chemical potential of the electrons is often called[46] the **Fermi energy** or **Fermi level**. While I will use the term in this way, it should be noted that the Fermi energy is sometimes[47] defined as the chemical potential at zero temperature.

Derivatives of the Fermi function: In the following, we will also need the derivatives of the Fermi distribution with respect to temperature and chemical potential. They can be expressed by the energy derivative of the Fermi function.⁵

$$\partial_T f_{T,\mu}(\epsilon) = -\frac{\epsilon - \mu}{T} \partial_\epsilon f_{T,\mu}(\epsilon) \quad (6.30)$$

$$\partial_\mu f_{T,\mu}(\epsilon) = -\partial_\epsilon f_{T,\mu}(\epsilon) \quad (6.31)$$

In the low-temperature limit, the energy derivative of the Fermi function approaches the negative

⁵

$$\begin{aligned} \partial_\epsilon [1 + e^{\beta(\epsilon-\mu)}]^{-1} &= \beta \left[\frac{d}{dx} \Big|_{x=\beta(\epsilon-\mu)} [1 + e^{\beta(\epsilon-\mu)}]^{-1} \right] \\ \partial_\mu [1 + e^{\beta(\epsilon-\mu)}]^{-1} &= -\beta \left[\frac{d}{dx} \Big|_{x=\beta(\epsilon-\mu)} [1 + e^{\beta(\epsilon-\mu)}]^{-1} \right] = -\partial_\epsilon f_{T,\mu}(\epsilon) \\ \partial_T [1 + e^{\beta(\epsilon-\mu)}]^{-1} &= \left(-\frac{1}{T} \beta(\epsilon - \mu) \right) \left[\frac{d}{dx} \Big|_{x=\beta(\epsilon-\mu)} [1 + e^{\beta(\epsilon-\mu)}]^{-1} \right] = -\frac{\epsilon - \mu}{T} \partial_\epsilon f_{T,\mu}(\epsilon) \end{aligned} \quad (6.29)$$

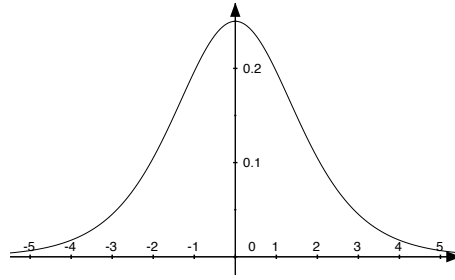


Fig. 6.2: (Negative) derivative of the Fermi distribution with respect to the chemical potential. Vertical axis $-\beta \partial_\mu f_{T,\mu}$, horizontal axis $\beta(\epsilon - \mu)$. With lowering temperatures the function becomes larger but more narrow. The integral equals always 1. For large arguments the function approaches $\beta \exp(-\beta|\epsilon - \mu|)$. For low temperatures it approaches the δ -function.

delta function at the Fermi level. ⁶

$$\lim_{T \rightarrow 0} \partial_\epsilon f_{T,\mu}(\epsilon) = -\delta(\epsilon - \mu) \quad (6.32)$$

6.4.1 Fermi-, Bose- and Boltzmann distribution

Fermi-, Bose- and Boltzmann distributions describe non-interacting particles in thermal equilibrium for a given temperature T and chemical potential μ . Fermi- and Bose distributions describe indistinguishable particles, while the Boltzmann distribution is adequate for distinguishable particles, i.e. it does not consider the symmetry under particle exchange. The Fermi distribution describes Fermions, that is particles with wave functions that are antisymmetric under particle exchange, while the Bose distribution describes Bosons, that is particles with wave functions that are symmetric under particle exchange.

$$f_{T,\mu}(\epsilon) = \frac{1}{e^{\beta(\epsilon-\mu)} + \eta} = \begin{cases} \frac{1}{e^{\beta(\epsilon-\mu)} + 1} & \text{Fermi distribution} \\ \frac{1}{e^{\beta(\epsilon-\mu)} - 1} & \text{Bose distribution} \\ \frac{1}{e^{\beta(\epsilon-\mu)} + 0} = e^{-\beta(\epsilon-\mu)} & \text{Boltzmann distribution} \end{cases} \quad (6.33)$$

All distributions can be described by one formula using $\eta = -1, +1, 0$ for Fermions, Bosons and distinguishable particles, respectively.

For dilute systems, that is for $\epsilon - \mu \gg k_B T$, Fermi-, Bose-, and Boltzmann distributions become indistinguishable. This implies that the Boltzmann distribution is appropriate for dilute gases.

The term **“degenerate Fermi gas”** describes a dense system of Fermions, that is for systems where the Fermi level lies within energy spectrum of the one-particle states. The term *“degenerate”* does not refer to *“degenerate states”* but to *“degenerated”* or *“shabby”*.

For Bosons, the Fermi-level lies always outside of the energy spectrum, because the singularity at $\epsilon = \mu$ in its functional form would otherwise lead an infinite number of particles. This notion is crucial for the understanding of the **Bose-Einstein condensation**.

For particles without a particle-number conservation, we cannot define a particle reservoir. This makes the concept of a chemical potential meaningless in this context. In the absence of a particle reservoir, the chemical potential is eliminated from the expressions by setting it to zero.

⁶The delta function is the negative derivative of the Heaviside step function.

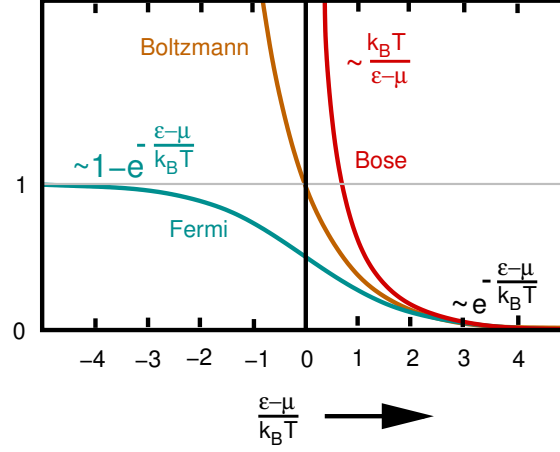


Fig. 6.3: Fermi distribution (green), Bose-distribution (red) and Boltzmann distribution (brown). Approximate limits forms are specified.

6.5 Thermodynamic integrations

In order to derive thermodynamic quantity, we will encounter integrations involving the product of the Fermi-distribution and some other energy dependent function $Q(\epsilon) = \text{Tr} [\hat{D}(\epsilon)\hat{A}]$ such as

$$\langle \hat{A} \rangle_{T,\mu} = \int_{-\infty}^{\infty} d\epsilon f_{T,\mu}(\epsilon) \text{Tr} [\hat{D}(\epsilon)\hat{A}] \quad (6.34)$$

$\hat{D}(\epsilon)$ is the density of states operator defined in Eq. 5.16 and \hat{A} is an arbitrary one-particle operator. This equation has been given earlier in Eq. 5.15. That result was given *ad hoc*. A more rigorous derivation based on the thermodynamic formalism is given in appendix K.1 on 511.

If the operator \hat{A} is the Hamiltonian, there is a more convenient form than Eq. 6.34 given above, namely⁷

$$\langle \hat{H} \rangle_{T,\mu} = \int_{-\infty}^{\infty} d\epsilon f_{T,\mu}(\epsilon) \underbrace{D_{tot}(\epsilon)}_{\text{Tr}[\hat{D}(\epsilon)]} \epsilon \quad (6.35)$$

In both cases, the general the expectation value has the form

$$\langle \hat{A} \rangle_{T,\mu} = \int_{-\infty}^{\infty} d\epsilon f_{T,\mu}(\epsilon) Q(\epsilon) \quad (6.36)$$

where $Q(\epsilon) = \text{Tr}[\hat{D}(\epsilon)\hat{A}]$ or, for the Hamiltonian, $Q(\epsilon) = D_{tot}(\epsilon)\epsilon$.

In this section, we will consider integrations of this sort.

- Temperature effects on thermal expectation values can be expressed by a thermal smoothing of the density of states $D(\epsilon)$. This shows that thermal effects are limited to a small energy region near the Fermi level.
- If there are states near the Fermi level, we can make an expansion in $\beta(\epsilon - \mu)$.

⁷1 use $\hat{D}(\epsilon)\hat{H} = \sum_n |\psi_n\rangle \delta(\epsilon - \epsilon_n) \langle \psi_n | \hat{H} = \sum_n |\psi_n\rangle \delta(\epsilon - \epsilon_n) \epsilon_n \langle \psi_n | = \sum_n |\psi_n\rangle \delta(\epsilon - \epsilon_n) \epsilon \langle \psi_n | = \hat{D}(\epsilon)\epsilon$.

- if the Fermi level lies within a band gap and far from the next states, one can make an expansion in $e^{-\beta|\epsilon-\mu|}$

6.5.1 Thermal smoothing of the density of states

Compared to finite temperatures, the thermal expectation value Eq. 6.34 has a much more intuitive form at zero temperature

$$\langle A \rangle_{T,\mu} \stackrel{T=0}{=} \int_{-\infty}^{\mu} d\epsilon \operatorname{Tr} [\hat{D}(\epsilon) \hat{A}] \quad (6.37)$$

At finite temperature, we can rewrite the equation above such that it attains the form of the equation below, albeit with a thermal smoothing of the integrand. This is what will be shown here.

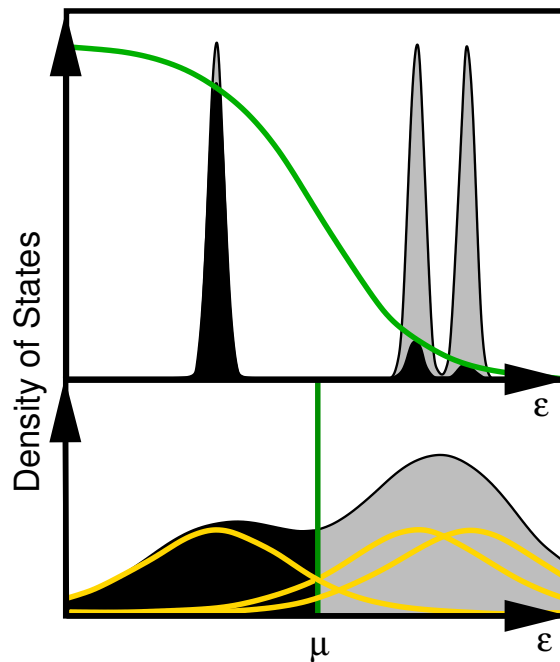


Fig. 6.4: Demonstration of the thermal smoothing of Eq. 6.41 and Eq. 6.42 for the example of three discrete states. The horizontal axis denotes the one-particle energy ϵ and μ is the electron chemical potential. Top: The density of states (grey and black) of three discrete states, represented here by narrow Gaussians, can be weighted by the Fermi function to select the occupied part (black) of the spectrum. Bottom: Alternatively, the states can be smoothed as in Eq. 6.42. Contribution of individual states are shown in yellow, their sum in grey/black. Thermal expectation values can then be obtained with the step-like zero-temperature Fermi function. The black areas in the top and bottom figures are identical.

An expression of interest for numerical calculation is

$$\begin{aligned}
 \langle A \rangle_{T,\mu} &\stackrel{\text{Eq. 6.34}}{=} \int_{-\infty}^{\infty} d\epsilon \text{Tr} [\hat{D}(\epsilon) \hat{A}] f_{T,\mu}(\epsilon) \\
 &= \underbrace{\int_{-\infty}^{\mu} d\mu'}_{\text{"=1"}} \partial_{\mu'} \int_{-\infty}^{\infty} d\epsilon \text{Tr} [\hat{D}(\epsilon) \hat{A}] f_{T,\mu'}(\epsilon) \\
 &= \int_{-\infty}^{\mu} d\mu' \text{Tr} \left[\underbrace{\int_{-\infty}^{\infty} d\epsilon \hat{D}(\epsilon) \overbrace{(-\partial_{\epsilon} f_{T,\mu'}(\epsilon))}^{\partial_{\mu'} f_{T,\mu'}(\epsilon)}}_{=: \hat{D}_T(\mu')} \hat{A} \right] \\
 &= \int_{-\infty}^{\mu} d\epsilon \text{Tr} [\hat{D}_T(\epsilon) \hat{A}] \tag{6.38}
 \end{aligned}$$

The thermally smoothed density of states $\hat{D}_T(\epsilon)$ is obtained by a convolution

$$\hat{D}_T(\epsilon) \stackrel{\text{def}}{=} \int_{-\infty}^{\infty} d\epsilon' K_T(\epsilon - \epsilon') \hat{D}(\epsilon') \tag{6.39}$$

with a kernel

$$K_T(\epsilon - \epsilon') = -\partial_{\epsilon} f_{T,\epsilon}(\epsilon') = \frac{\beta}{\left(e^{\beta(\epsilon - \epsilon')/2} + e^{-\beta(\epsilon - \epsilon')/2} \right)^2} = 4\beta \cosh^{-2}(\beta(\epsilon - \epsilon')/2) \tag{6.40}$$

Thus, we can smoothen the density of states $\hat{D}(\epsilon)$ using Eq. 6.39. Expectation values can be obtained with the smoothened density of states $\hat{D}_T(\epsilon)$ as if the temperature were zero. The disadvantage is that \hat{D}_T depends on temperature. The advantage is, however, two-fold: Firstly, we can “think” in terms of zero-temperature expressions after having done the smoothing. These zero-temperature expressions are easier to comprehend. Secondly, noise from experiment or numerical calculations is averaged over by the smoothing.

THERMAL SMOOTHING

The thermal expectation value

$$\langle \hat{A} \rangle_{T,\mu} = \int_{-\infty}^{\mu} d\epsilon \text{Tr} [\hat{D}_T(\epsilon) \hat{A}] \tag{6.41}$$

can be expressed by the zero-temperature Fermi function and the thermally smoothed density of states

$$\hat{D}_T(\epsilon) \stackrel{\text{Eq. 6.39}}{=} \int_{-\infty}^{\infty} d\epsilon' \frac{\beta}{\left(e^{\beta(\epsilon - \epsilon')/2} + e^{-\beta(\epsilon - \epsilon')/2} \right)^2} \hat{D}(\epsilon') \tag{6.42}$$

Expectation value of the energy: The internal energy U can be calculated either as expectation value of the Hamiltonian $U = \int d\epsilon f_{T,\mu}(\epsilon) \text{Tr} [\hat{D}(\epsilon) \hat{H}]$ or as first energy moment $U = \int d\epsilon f_{T,\mu}(\epsilon) D_{tot}(\epsilon) \epsilon$ of the occupied density of states. The “trick” of combining a smoothed density of states with a zero-temperature occupation, which has shown above, cannot trivially be carried over to the second form of the energy.⁸

⁸An analogous trick can be used yielding a smoothed version of the energy-weighted density of states $D_{tot}(\epsilon)\epsilon$.

In order to alert the reader to this problem, let me show the corresponding derivation.

$$\begin{aligned}
U(T, \mu) &= \langle \hat{H} \rangle_{T, \mu} = \int_{-\infty}^{\infty} d\epsilon f_{T, \mu}(\epsilon) \text{Tr} [\hat{D}_T(\epsilon) \hat{H}] = \int_{-\infty}^{\infty} d\epsilon f_{T, \mu}(\epsilon) [\hat{D}_{tot}(\epsilon) \epsilon] \\
&= \int_{-\infty}^{\mu} d\mu' \partial_{\mu'} \int_{-\infty}^{\infty} d\epsilon f_{T, \mu'}(\epsilon) [\hat{D}_{tot}(\epsilon) \epsilon] = \int_{-\infty}^{\mu} d\mu' \int_{-\infty}^{\infty} d\epsilon \overbrace{(-\partial_{\epsilon} f_{T, \mu'}(\epsilon))}^{\partial_{\mu'} f_{T, \mu'}(\epsilon)} \hat{D}_{tot}(\epsilon) \epsilon \\
&\stackrel{\text{Eq. 6.40}}{=} \int_{-\infty}^{\mu} d\mu' \int_{-\infty}^{\infty} d\epsilon K_T(\mu' - \epsilon) \hat{D}_{tot}(\epsilon) \epsilon \\
&\stackrel{K_T(x) = K_T(-x)}{=} \int_{-\infty}^{\mu} d\epsilon \int_{-\infty}^{\infty} d\epsilon' K_T(\epsilon - \epsilon') \hat{D}_{tot}(\epsilon') \epsilon' \\
&= \int_{-\infty}^{\mu} d\epsilon \int_{-\infty}^{\infty} d\epsilon' K_T(\epsilon - \epsilon') \hat{D}_{tot}(\epsilon') (\epsilon + (\epsilon' - \epsilon)) \\
&= \int_{-\infty}^{\mu} d\epsilon \underbrace{\left[\int_{-\infty}^{\infty} d\epsilon' K_T(\epsilon - \epsilon') D_{tot}(\epsilon') \right]}_{\tilde{D}_{tot}(\epsilon)} \epsilon - \int_{-\infty}^{\mu} d\epsilon \left[\int_{-\infty}^{\infty} d\epsilon' (\epsilon - \epsilon') K_T(\epsilon - \epsilon') D_{tot}(\epsilon') \right] \\
&= \int_{-\infty}^{\mu} d\epsilon \tilde{D}_{tot}(\epsilon) \epsilon - \int_{-\infty}^{\mu} d\epsilon \left[\int_{-\infty}^{\infty} d\epsilon' (\epsilon - \epsilon') K_T(\epsilon - \epsilon') D_{tot}(\epsilon') \right] \tag{6.43}
\end{aligned}$$

The left-hand side is what would be expected, but the calculation shows that there is also the right-hand side. In the low-temperature limit, the right-hand side can be related to the density of states at the Fermi level.⁹

6.5.2 Metals: Sommerfeld expansion

In order to evaluate the integrals involving the Fermi function for metals one can use the **Sommerfeld expansion** derived in appendix K.2 on p. 512.

The Sommerfeld expansion is useful if the integrand at the Fermi level is finite. It furthermore is a low-temperature expansion.

The underlying idea is a Taylor expansion of

$$G(\epsilon) = \int_{-\infty}^{\epsilon} d\epsilon' g(\epsilon') \tag{6.44}$$

where $g(\epsilon)$ may be $g(\epsilon) = \text{Tr}[\hat{D}(\epsilon)\hat{A}]$ or $g(\epsilon) = D_{tot}(\epsilon)\epsilon$.

⁹This has not been proven explicitly. The idea is that $xK_T(x)$ is a localized antisymmetric function its integral with a function picks up the derivative of the function as dominant term. If then, this derivative is integrated to the Fermi level, the result is expected to be related to the density of states at the Fermi level.

We start with a partial integration

$$\begin{aligned}
 \int_{-\infty}^{\infty} d\epsilon f_{T,\mu}(\epsilon)g(\epsilon) &= \int_{-\infty}^{\infty} d\epsilon f_{T,\mu}(\epsilon)\partial_{\epsilon}G(\epsilon) = \int_{-\infty}^{\infty} d\epsilon \left[\underbrace{\partial_{\epsilon} \left(f_{T,\mu}(\epsilon)G(\epsilon) \right)}_{\sim 0} - G(\epsilon)\partial_{\epsilon}f_{T,\mu}(\epsilon) \right] \\
 &= 0 - \int_{-\infty}^{\infty} d\epsilon \underbrace{\left[\sum_{n=0}^{\infty} \frac{1}{n!} (\epsilon - \mu)^n \partial_{\epsilon}^n \Big|_{\mu} G \right]}_{G(\epsilon)} \partial_{\epsilon}f_{T,\mu}(\epsilon) \\
 &= \sum_{n=0}^{\infty} \left[\partial_{\epsilon}^n \Big|_{\mu} G \right] \frac{-1}{n!} \underbrace{\int_{-\infty}^{\infty} d\epsilon (\epsilon - \mu)^n \partial_{\epsilon}f_{T,\mu}(\epsilon)}_{(k_B T)^n \int_{-\infty}^{\infty} dx x^n \partial_x \frac{1}{1+e^x}} \\
 &= \sum_{n=0}^{\infty} \left[\partial_{\epsilon}^n \Big|_{\mu} G \right] \frac{(k_B T)^n}{n!} \underbrace{\int_{-\infty}^{\infty} dx \frac{x^n}{(1+e^x)(1+e^{-x})}}_{\text{vanishes for odd } n} \\
 &= \underbrace{\int_{-\infty}^{\mu} d\epsilon g(\epsilon)}_{n=0} + \underbrace{0}_{n=1} + \underbrace{\left[\partial_{\epsilon} \Big|_{\mu} g \right] \frac{(k_B T)^2}{2} \int_{-\infty}^{\infty} dx \frac{x^2}{(1+e^x)(1+e^{-x})}}_{n=2} + \underbrace{0}_{n=3} + \dots
 \end{aligned} \tag{6.45}$$

Notice that the derivative of the Fermi function is strongly peaked close to the Fermi level and that its width is proportional to the temperature. The function is plotted in figure 6.2.

SOMMERFELD EXPANSION

$$\int_{-\infty}^{\infty} d\epsilon g(\epsilon)f(\epsilon) = \left(\int_{-\infty}^{\mu} d\epsilon g(\epsilon) \right) + \frac{(\pi k_B T)^2}{6} \overbrace{\left(\partial_{\epsilon} \Big|_{\mu} g \right)}^{\frac{\partial^2 G}{\partial \epsilon^2}} + O((k_B T)^4) \tag{6.46}$$

Note however, that the Sommerfeld expansion is a low-temperature expansion, which breaks down if the function to be integrated is not analytical within a few $k_B T$ away from the chemical potential.

6.5.3 Insulators: expansion for $|\epsilon - \mu| > k_B T$:

For insulators, another expansion is of use. If the Fermi level lies outside the energy spectrum, only the exponential tails of the Fermi function are relevant beyond the zero-temperature integral.

Thus, we expand the Fermi distribution function into powers of Boltzmann factors¹⁰ $e^{-\beta(\epsilon-\mu)}$.

$$f_{T,\mu}(\epsilon) = \begin{cases} \sum_{n=1}^{\infty} (-1)^{n+1} \left[e^{-\beta(\epsilon-\mu)} \right]^n & \text{for } \epsilon - \mu \gg k_B T \\ 1 - \sum_{n=1}^{\infty} (-1)^{n+1} \left[e^{\beta(\epsilon-\mu)} \right]^n & \text{for } \epsilon - \mu \ll -k_B T \end{cases} \tag{6.48}$$

This implies that the Fermi distribution approaches the Boltzmann distribution far from the chemical potential. If the Fermi level lies outside the energy spectrum, the electrons form a very dilute gas.

¹⁰We use the Taylor expansion in terms of e^{-x} :

$$\frac{1}{1+e^x} = e^{-x} \frac{1}{1+e^{-x}} = e^{-x} \sum_{n=0}^{\infty} (-e^{-x})^n = \sum_{n=0}^{\infty} (-1)^n (e^{-x})^{n+1} = \sum_{n=1}^{\infty} (-1)^{n+1} (e^{-x})^n \tag{6.47}$$

Because the probability that two particles come close together is then vanishingly small, it does not matter whether the particles are identical or distinct. Thus, the Fermi-distribution describing identical particles and the Boltzmann distribution describing distinguishable particles become similar in a dilute gas.

In the following, we will often have to do with integrals of the form

$$\int_{\epsilon_0}^{\infty} d\epsilon f_{T,\mu}(\epsilon) \sqrt{\epsilon - \epsilon_0} \quad (6.49)$$

which can be addressed as follows ¹¹:

$$\begin{aligned} \int_{\epsilon_0}^{\infty} d\epsilon f_{T,\mu}(\epsilon) \sqrt{\epsilon - \epsilon_0} &= \sum_{n=1}^{\infty} (-1)^{n+1} \int_{\epsilon_0}^{\infty} d\epsilon \sqrt{\epsilon - \epsilon_0} \left[e^{-\beta(\epsilon - \mu)} \right]^n \\ &= \sum_{n=1}^{\infty} (-1)^{n+1} \int_{\epsilon_0}^{\infty} d\epsilon \sqrt{\epsilon - \epsilon_0} \left[e^{-\beta(\epsilon - \epsilon_0) - \beta(\epsilon_0 - \mu)} \right]^n \\ &= \sum_{n=1}^{\infty} (-1)^{n+1} \left[e^{-\beta(\epsilon_0 - \mu)} \right]^n \underbrace{\left(\frac{1}{\beta n} \right)^{\frac{3}{2}} \int_0^{\infty} dx \sqrt{x} e^{-x}}_{\frac{1}{2}\sqrt{\pi}} \\ &= \frac{\sqrt{\pi}}{2} (k_B T)^{\frac{3}{2}} \sum_{n=1}^{\infty} \frac{(-1)^{n+1}}{n^{\frac{3}{2}}} \left[e^{-\beta(\epsilon_0 - \mu)} \right]^n \end{aligned} \quad (6.50)$$

NUMBER OF ELECTRONS IN A DILUTE ELECTRON GAS WITH A GIVEN EFFECTIVE MASS

$$\begin{aligned} N(T) &\stackrel{\text{Eq. 5.36}}{=} \int_{\epsilon_0}^{\infty} d\epsilon f_{T,\mu}(\epsilon) \frac{2\pi\Omega}{(2\pi\hbar)^3} \left(\sum_{\sigma \in \{\uparrow, \downarrow\}} \right) (2m^*)^{\frac{3}{2}} \sqrt{\epsilon - \epsilon_0} \\ &= 2\Omega \left(\frac{2\pi m^* k_B T}{(2\pi\hbar)^2} \right)^{\frac{3}{2}} e^{-\beta(\epsilon_0 - \mu)} + O\left(\left[e^{-\beta(\epsilon_0 - \mu)} \right]^2 \right) \end{aligned} \quad (6.51)$$

Here Ω is the volume considered. m^* is the effective mass, and ϵ_0 is the band-minimum.

6.6 Thermodynamics of non-interacting electrons

Editor: Can this entire section be made into an exercise?

As shown in section 8.5 of “*FSX: Statistical Physics*”[38], we can express the thermodynamic quantities of non-interacting Fermions by the density of states

Particle number and chemical potential for a metal

We have seen that the grand potential for non-interacting electrons has a fairly simple form. Typical problems however, require an ensemble with a fixed particle number N rather than a specific chemical potential μ . Therefore, one of the first tasks is to evaluate the chemical potential μ for a given particle number N .

¹¹ $\int_0^{\infty} dx x^n e^{-x} = \Gamma(n+1)$, where $\Gamma(x)$ is the Gamma function. $\Gamma(1) = 1$, $\Gamma(\frac{1}{2}) = \sqrt{\pi}$. From $\Gamma(x+1) = x\Gamma(x)$ we obtain $\Gamma(\frac{3}{2}) = \frac{1}{2}\Gamma(\frac{1}{2}) = \frac{1}{2}\sqrt{\pi}$. (see Bronstein[48]).

Furthermore, many of the relevant thermodynamic quantities are obtained as temperature derivatives at given particle number, rather than at fixed chemical potential. For this reason we also need to know, how the chemical potential changes with temperature.

In order to extract the chemical potential one needs to evaluate the particle number as function of chemical potential and find that value for which $N(T, \mu) = N$.

Because of its practical value we consider here the special case of a metal, where we can use the Sommerfeld expansion Eq. 6.46 to obtain the particle number.

$$\begin{aligned}
 N(T, \mu) &\stackrel{\text{Eq. 6.27}}{=} \int_{-\infty}^{\infty} d\epsilon D(\epsilon) f_{T, \mu}(\epsilon) \\
 &\stackrel{\text{Eq. 6.46}}{=} \underbrace{\left(\int_{-\infty}^{\mu} d\epsilon D(\epsilon) \right)}_{N(T=0, \mu)} + \frac{(\pi k_B T)^2}{6} (\partial_{\epsilon}|_{\mu} D) + O((k_B T)^4)
 \end{aligned} \tag{6.52}$$

The requirement that the particle number remains unchanged gives us an expression for the temperature shift of the chemical potential.

$$\begin{aligned}
 0 &= \overbrace{\frac{dN}{dT}}^{\text{total derivative}} \Big|_{T=0, \mu(T=0)} = \overbrace{\frac{\partial N}{\partial T}}^{\text{partial derivative}} \Big|_{T=0, \mu(T=0)} + \frac{d\mu}{dT} \frac{\partial N}{\partial \mu} \Big|_{T=0, \mu(T=0)} \\
 &\stackrel{\text{Eq. 6.52}}{=} \pi k_B \frac{(\pi k_B T)^2}{3} (\partial_{\epsilon}|_{\mu} D) + \frac{d\mu}{dT} D(\mu) + O((k_B T)^2) \\
 \frac{d\mu}{dT} &= -\frac{(\pi k_B)^2}{3} \frac{(\partial_{\epsilon}|_{\mu} D)}{D(\epsilon_F)} T + O(T^2)
 \end{aligned} \tag{6.53}$$

Thus, the chemical potential moves quadratically away from its low-temperature value. This equation is only valid for metals, which have a finite density of states at the Fermi level.

Entropy

The entropy is a quantity that is often hard to comprehend. It is important because it determines thermodynamic stability at finite temperatures. Therefore, I will derive a relation that is easy to comprehend.

$$\begin{aligned}
 S(T, \mu) &\stackrel{\text{Eq. 6.11}}{=} -\frac{\partial \Omega(T, \mu)}{\partial T} \\
 &\stackrel{\text{Eq. 6.25}}{=} \int_{-\infty}^{\infty} d\epsilon D(\epsilon) \left[-\partial_T \left(-k_B T \ln \left(1 + e^{-\beta(\epsilon - \mu)} \right) \right) \right] \\
 &= \int_{-\infty}^{\infty} d\epsilon D(\epsilon) \left[\underbrace{\left(k_B \ln \left(1 + e^{-\beta(\epsilon - \mu)} \right) \right)}_{\frac{1}{1-f}} + \left(k_B T \frac{1}{1 + e^{+\beta(\epsilon - \mu)}} \underbrace{\left(\frac{1}{k_B T^2} (\epsilon - \mu) \right)}_{\frac{1}{T} \ln(f^{-1} - 1)} \right) \right] \\
 &= \int_{-\infty}^{\infty} d\epsilon D(\epsilon) \left[k_B \left(-\ln(1 - f) + f \ln \left(\frac{1 - f}{f} \right) \right) \right] \\
 &= \int_{-\infty}^{\infty} d\epsilon D(\epsilon) \left[-k_B \left(f \ln(f) + (1 - f) \ln(1 - f) \right) \right]
 \end{aligned} \tag{6.54}$$

The entropy can be obtained from the occupations $f = f_{T, \mu}(\epsilon)$.

Eq. 6.54 tells us that completely filled or completely empty orbitals do not contribute to the entropy of a system. A half-occupied orbital contributes $k_B \ln(2)$ to the entropy. This is exactly the entropy of a yes-no decision, because the orbital can be either filled or empty with equal probability.

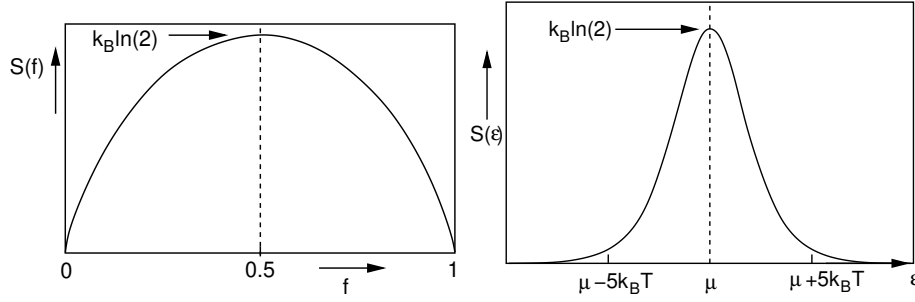


Fig. 6.5: Entropy per state $S(f) = -k_B \{f \ln(f) + (1-f) \ln(1-f)\}$ (left) as function of occupation f and (right) as function of one-particle energy, i.e. $S(\epsilon) = -k_B \{f(\epsilon) \ln[f(\epsilon)] + [1-f(\epsilon)] \ln[1-f(\epsilon)]\}$.

The expression for the entropy of non-interacting fermions expressed by the occupations

$$S[\{f_n\}] = -k_B \sum_n [f_n \ln(f_n) + (1-f_n) \ln(1-f_n)] \quad (6.55)$$

is very useful to estimate the electronic entropy of a system, when, for example, the occupation of a given defect state is known.

The expression Eq. 6.55 is actually not limited to specific ensembles. It can be used to derive the Fermi distribution by minimizing $U - TS = \sum_n f_n \epsilon_n - TS[\{f_n\}] - \mu N$ with respect to occupations.

Internal energy

The internal energy U is the expectation value of the energy of the system.

Before we continue, we express the grand potential by the occupations, because that will simplify the equations.

$$\Omega(T, \mu) = \int_{-\infty}^{\infty} d\epsilon D(\epsilon) \left[-k_B T \ln \left(1 + e^{-\beta(\epsilon-\mu)} \right) \right] = \int_{-\infty}^{\infty} d\epsilon D(\epsilon) \left[k_B T \ln (1 - f_{T,\mu}(\epsilon)) \right] \quad (6.56)$$

Now, we evaluate the internal energy from the fundamental thermodynamic relations Eq. 6.13 summarized earlier

$$\begin{aligned} U(T, \mu) &\stackrel{\text{Eq. 6.13}}{=} \Omega(T, \mu) + TS(T, \mu) + \mu N(T, \mu) \\ &= \int_{-\infty}^{\infty} d\epsilon D(\epsilon) \left[\underbrace{k_B T \ln (1 - f)}_{\leftarrow \Omega} - \underbrace{k_B T (f \ln(f) + (1-f) \ln(1-f))}_{\leftarrow TS} + \mu f \right] \\ &= \int_{-\infty}^{\infty} d\epsilon D(\epsilon) \left[f \cdot \underbrace{\left[k_B T \ln \left(\frac{1-f}{f} \right) + \mu \right]}_{\substack{\beta(\epsilon-\mu) \\ \epsilon}} \right] \\ &= \int_{-\infty}^{\infty} d\epsilon D(\epsilon) f_{T,\mu}(\epsilon) \epsilon \end{aligned} \quad (6.57)$$

where, again, $f = f_{T,\mu}(\epsilon)$. The internal energy has a simple interpretation: it is the sum of the energies of the occupied states.

The temperature dependent term can be separated out as follows

$$\begin{aligned}
 U(T, N) &= \int_{-\infty}^{\infty} d\epsilon D(\epsilon) f_{T,\mu(T,N)}(\epsilon) \epsilon \\
 &= \underbrace{\int_{-\infty}^{\infty} d\epsilon D(\epsilon) f_{T=0,\mu(T=0)}(\epsilon) \epsilon}_{U(T=0,N)} + \int_{-\infty}^{\infty} d\epsilon D(\epsilon) \left(f_{T,\mu(T)}(\epsilon) - f_{T=0,\mu(T=0)}(\epsilon) \right) \epsilon \quad (6.58)
 \end{aligned}$$

The weight function for the temperature dependent term is shown in Fig. 6.6.

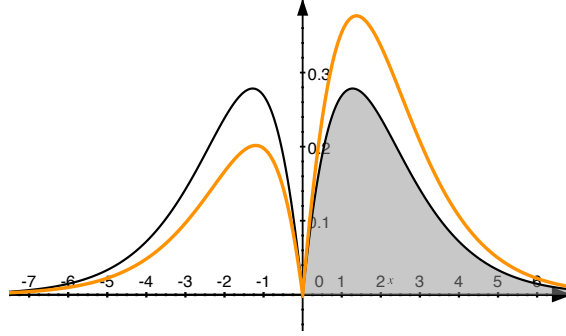


Fig. 6.6: Weight function of the thermal part to the internal energy. $\epsilon(f_{T,\mu(T,N)}(\epsilon) - f_{T=0,\mu(T=0,N)}(\epsilon))$ as function of the deviation from the zero-temperature chemical potential in units of $k_B T$. The one-sided integral of this function (shaded area) is $\pi^2/12$. The orange line shows a function for a temperature-dependent chemical potential.

Heat capacity

The **heat capacity** is the amount of energy required to raise the temperature by one unit.

$$C_V \stackrel{\text{def}}{=} \frac{\partial U(T, V, N)}{\partial T} \quad (6.59)$$

When calculating the heat capacity from $U(T, V, \mu)$ we need to account for the shift of the chemical potential with temperature

$$\begin{aligned}
 c_V &\stackrel{\text{Eq. 6.59}}{=} \frac{\partial U(T, V, N)}{\partial T} = \frac{d}{dT} U(T, V, \mu(T, V, N)) \\
 &= \frac{\partial U(T, V, \mu)}{\partial T} + \frac{\partial U(T, V, \mu)}{\partial \mu} \frac{d\mu(T, V, N)}{dT} \\
 &\stackrel{\text{Eq. 6.57}}{=} \int_{-\infty}^{\infty} d\epsilon D(\epsilon) \frac{\partial f_{T,\mu}(\epsilon)}{\partial T} \epsilon + \int_{-\infty}^{\infty} d\epsilon D(\epsilon) \frac{\partial f_{T,\mu}(\epsilon)}{\partial \mu} \epsilon \frac{d\mu(T, V, N)}{dT} \\
 &\stackrel{\text{Eq. 6.30}}{=} \int_{-\infty}^{\infty} d\epsilon D(\epsilon) \frac{\epsilon - \mu}{T} \frac{\partial f_{T,\mu}(\epsilon)}{\partial \mu} \epsilon + \int_{-\infty}^{\infty} d\epsilon D(\epsilon) \frac{\partial f_{T,\mu}(\epsilon)}{\partial \mu} \epsilon \frac{d\mu(T, V, N)}{dT} \\
 &= \frac{1}{T} \int_{-\infty}^{\infty} d\epsilon D(\epsilon) \frac{\partial f_{T,\mu}(\epsilon)}{\partial \mu} \epsilon \left[\epsilon - \mu + T \frac{d\mu(T, V, N)}{dT} \right] \\
 &= \frac{1}{T} \int_{-\infty}^{\infty} d\epsilon D(\epsilon) \frac{\partial f_{T,\mu}(\epsilon)}{\partial \mu} \left[\epsilon - \mu + T \frac{d\mu(T, V, N)}{dT} \right]^2 \\
 &+ \left[\mu - T \frac{d\mu(T, V, N)}{dT} \right] \underbrace{\frac{1}{T} \int_{-\infty}^{\infty} d\epsilon D(\epsilon) \frac{\partial f_{T,\mu}(\epsilon)}{\partial \mu} \left[\epsilon - \mu + T \frac{d\mu(T, V, N)}{dT} \right]}_{(A)=0 \text{ for } N(T)=\text{const. Eq. 6.61}} \quad (6.60)
 \end{aligned}$$

The last term has been split off in order to show that the heat capacity depends approximately on the density of states multiplied approximately¹² with the squared energetic distance from the Fermi level.

The particle-number conservation provides us with $d\mu/dT$. It turns out that we even do not need to evaluate it explicitly, if we proceed as follows:

$$\begin{aligned}
 0 &= \frac{dN}{dT} = \int d\epsilon D(\epsilon) \left[\frac{\partial f_{T,\mu}(\epsilon)}{\partial T} + \frac{\partial f_{T,\mu}(\epsilon)}{\partial \mu} \frac{d\mu}{dT} \right] \\
 &\stackrel{\text{Eq. 6.30,6.31}}{=} \int d\epsilon D(\epsilon) \left[\frac{(\epsilon - \mu)}{T} \frac{\partial f_{T,\mu}(\epsilon)}{\partial \mu} + \frac{\partial f_{T,\mu}(\epsilon)}{\partial \mu} \frac{d\mu}{dT} \right] \\
 &= \frac{1}{T} \int d\epsilon D(\epsilon) \underbrace{\frac{\partial f_{T,\mu}(\epsilon)}{\partial \mu}}_{(A)} \left[\epsilon - \mu + T \frac{d\mu}{dT} \right] \tag{6.61}
 \end{aligned}$$

Thus, the second term in the specific heat Eq. 6.60 denoted as (A) vanishes completely, so that

$$c_V \stackrel{\text{Eq. 6.60}}{=} \frac{1}{T} \int_{-\infty}^{\infty} d\epsilon D(\epsilon) \frac{\partial f_{T,\mu}(\epsilon)}{\partial \mu} \left[\epsilon - \mu + T \frac{d\mu(T, V, N)}{dT} \right]^2 \tag{6.62}$$

where

$$T \frac{d\mu}{dT} = - \frac{\int d\epsilon D(\epsilon) \frac{\partial f_{T,\mu}(\epsilon)}{\partial \mu} (\epsilon - \mu)}{\int d\epsilon D(\epsilon) \frac{\partial f_{T,\mu}(\epsilon)}{\partial \mu}} \tag{6.63}$$

The function used to obtain the specific heat from an integration over the density of states is shown in Fig. 6.7.

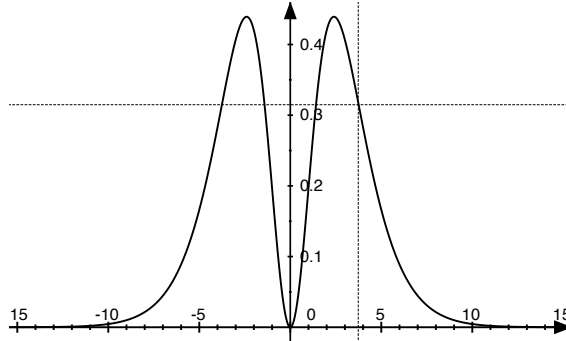


Fig. 6.7: Weight function $g(\epsilon) = \beta \frac{\partial f}{\partial \mu} (\epsilon - \mu)^2$ which yields the specific heat $c_V = k_B \int d\epsilon D(\epsilon) g(\epsilon)$ without a thermal shift of the chemical potential.

If the density of states is approximately constant with $k_B T$ from the chemical potential, we can approximate the expression by

$$\begin{aligned}
 c_V &\approx \frac{1}{T} D(\mu) \int_{-\infty}^{\infty} d\epsilon (\epsilon - \mu)^2 \left(-\partial_\epsilon f(\epsilon) \right) \\
 &= \frac{1}{T} D(\mu) (k_B T)^2 \left(- \int_{-\infty}^{\infty} dx x^2 \partial_x \frac{1}{1 + e^x} \right) \\
 &= \underbrace{\left(\frac{(\pi k_B)^2}{3} D(\mu) \right)}_{\gamma} T \tag{6.64}
 \end{aligned}$$

¹²It is only approximate because of the opposite sign of the $T d\mu/dT$ -term

In the last step we used an integral out of the Sommerfeld expansion, which is described in appendix K.2.

The parameter

$$\gamma \stackrel{\text{def}}{=} \lim_{T \rightarrow 0} \frac{1}{T} c_V \quad \Rightarrow \quad c_V \approx \gamma T + O(T^2) \quad (6.65)$$

is called the **Sommerfeld coefficient of the specific heat**. We learned that, the heat capacity is proportional to the temperature at low temperatures, with a coefficient proportional to the density of states at the electron chemical potential. The Sommerfeld coefficient γ of the specific heat can readily be measured and it provides a direct measure for the electronic density of states at the Fermi level. Vibrations contribute to the specific heat enter only with a higher power of the temperature and therefore do not show up in the low-temperature result.

Pressure

The **pressure** p is defined as the derivative of the total energy upon contraction.

$$p \stackrel{\text{Eq. 6.16}}{=} - \frac{\partial U(S, V, N)}{\partial V} \quad (6.66)$$

Note, that it is not allowed to calculate the pressure as derivative of $U(T, V, \mu)$! The pressure is the derivative of the total energy with fixed occupations.

Nevertheless, we can also calculate the pressure from the grand potential

$$\begin{aligned} p &\stackrel{\text{Eq. 6.69}}{=} - \frac{\partial \Omega(T, V, \mu)}{\partial V} \\ &= \int_{-\infty}^{\infty} d\epsilon \frac{dD(\epsilon)}{dV} \left[+k_B T \ln \left(1 + e^{-\beta(\epsilon - \mu)} \right) \right] \end{aligned} \quad (6.67)$$

Why does this give the same result as the derivative of $U(S, V, N)$?

The grand potential describes the energy of the system and the reservoirs. This fact is expressed by the Legendre transform

$$\Omega(T, V, \mu) = \text{stat}_{S, N} \left[U(S, V, N) - TS - \mu N \right] \quad (6.68)$$

The term $-TS$ can be identified with the energy of the heat bath and the energy $-\mu N$ is the energy of the volume reservoir. Both energies are expressed by the entropy S and particle number N of the system. Because the total entropy and particle number are conserved for a closed system¹³, any change of the particle number or of the entropy must be canceled by a corresponding change of these quantities in the reservoirs. Therefore a change of the particle number dN in the system implies a change of of the particle number by $-dN$ in the particle reservoir. The analogous holds for the entropy.

The stationary condition with respect to S and N provide relations for temperature and chemical potential as derivatives of the internal energy.

$$\begin{aligned} \frac{\partial \Omega(T, V, \mu)}{\partial V} &= \frac{\partial U(S, V, N)}{\partial V} + \underbrace{\left(\frac{\partial U(S, V, N)}{\partial S} - T \right)}_{=0} \frac{dS(T, V, \mu)}{dV} + \underbrace{\left(\frac{\partial U(S, V, N)}{\partial N} - \mu \right)}_{=0} \frac{dN(T, V, \mu)}{dV} \\ &= \frac{\partial U(S, V, N)}{\partial V} \end{aligned} \quad (6.69)$$

If the volume expansion changes the entropy or the particle number of the system, the corresponding energy change is exactly balanced to first order by an opposite energy change of the reservoirs. Thus, including the energies of the reservoirs produces the same energy change as keeping entropy and particle number fixed.

¹³Processes, which obey the stationary conditions, are remain in thermal equilibrium. Thus, they do not generate entropy, i.e. they are adiabatic processes.

Bulk modulus

The **bulk modulus** is the measure of how a material can resist compression.

$$B_0 = -V \frac{\partial P}{\partial V} = V \frac{\partial^2 U(S, V, N)}{\partial V^2} \quad (6.70)$$

Thus, it is a second derivative of the internal energy.

Magnetic susceptibility

In a magnetic field, the energy of an electron is shifted by an energy

$$\Delta E = -\vec{m} \vec{B}, \quad (6.71)$$

where \vec{m} is the **magnetic moment** of the electron and \vec{B} is the magnetic field. The magnetic moment of an electron is related to its spin by its **gyro-magnetic ratio** γ_e , that is

$$\vec{m} = \gamma_e \vec{S} = \gamma_e \frac{1}{2} \hbar \vec{e}_S = \frac{1}{2} g_e \mu_B \vec{e}_S \quad (6.72)$$

The factor $g_e = -2.0023 \dots$ is the **g-factor** of the free electron. The **Bohr magneton** $\mu_B = \frac{e\hbar}{2m_e}$ is a unit for the magnetic moment. The Bohr magneton is nearly (up to a factor $\frac{1}{2}g_e$) identical to the magnetic moment of the electron.

Depending on the spin alignment with respect to the magnetic field the electron is raised or decreased. This is the so-called **Zeeman splitting**.

The Zeeman splitting between the energies of spin-up and spin-down electrons in the field of 1 Tesla corresponding to a strong permanent magnet is approximately 0.1 meV.¹⁴

When the Zeeman energy is added to the dispersion relation, the band structure of the spin up-electrons is shifted by a small amount with respect to that of the down spin electrons. If the electron number is initially the same for both spin directions, the system can reduce its energy by changing the spin of some of its electrons. Thus, the total energy depends, via the Zeeman splitting, on the magnetic field.

The magnetization is

$$\begin{aligned} \vec{M} &= \underbrace{\left(\frac{1}{2} g_e \mu_B \right)}_{\text{magnetic moment}} \underbrace{\frac{1}{2V} \left(N(T, \mu - \frac{1}{2} g_e \mu_B |\vec{B}|) - N(T, \mu + \frac{1}{2} g_e \mu_B |\vec{B}|) \right)}_{\text{spin density}} \\ &= \left(\frac{|g_e \mu_B|}{2} \right)^2 \frac{D(\mu)}{V} B + O(|\vec{B}|^2) \end{aligned} \quad (6.73)$$

where $N(T, \mu)$ is the total electron number, including both spin directions.

From the field dependence of the magnetic susceptibility, we obtain the **magnetic susceptibility** of a free-electron gas

$$\chi = \frac{d|\vec{M}|}{d|\vec{B}|} = \left(\frac{|g_e \mu_B|}{2} \right)^2 \frac{D(\mu)}{V} \quad (6.74)$$

, which is the **Pauli spin susceptibility** . .

¹⁴ I used the value electron magnetic moment $\approx -9.284 \times 10^{-24}$ J/T from https://en.wikipedia.org/wiki/Electron_magnetic_moment and the conversion from eV to Joule $1 \text{ eV} \approx 1.602 \times 10^{-19}$ J from <https://de.wikipedia.org/wiki/Elektronenvolt>, retrieved 27.04.2020

6.7 Home study and practice

6.7.1 Free-electron gas

The free-electron gas is a model for a solid, where the charge of atomic cores (nuclei and core electrons) are smeared out into a homogeneous, positively charged background. Thus, the generic properties of electrons can be studied without any additional complications due to the lattice structure.

Metals are described by a **degenerate electron gas**,¹⁵ for which the Fermi level cuts through a non-zero density of states. The conduction electrons and the holes of a semiconductor can be reasonably described by a dilute electron gas.

The one-particle Hamiltonian acting on each of the free electrons is

$$\hat{h} = \frac{\hat{p}^2}{2m} + \epsilon_0 \quad (6.75)$$

m is the effective mass of the electron. If the electrons are truly free, this mass equals the electron mass m_e . In a crystal, the effective mass is extracted from the band structure. A constant potential ϵ_0 has been added to the kinetic energy.

In order to extract material-specific information, we will consider aluminium as example for a metal and silicon as example for an semiconductor or an insulator.

- Aluminium forms a face-centered cubic (fcc) crystal with a lattice constant of $a_{\text{lat}} = 4.05 \text{ \AA}$. Only the three valence electrons per atom are considered for the free-electron gas. (The low-lying core states form an entity with the core states and are directly not relevant for transport questions.)

The band structure of aluminium is described in section 9.1 on p. 302.

- Silicon has the diamond structure with two atoms per unit cell. It has the unit cell of an fcc crystal, albeit with two atoms in it. The lattice constant is 5.431 \AA . Each silicon has four valence electrons.

The band structure of silicon is discussed in section 9.4 and shown in Fig. 9.11 on p.309. Use the information on silicon given in that section, in particular, on the conduction band minima, valence band maxima and their effective masses.¹⁶

Silicon has a band gap of 1.12 eV.

Silicon has six equivalent conduction-band minima that lie near the X point. Each conduction band minimum has one small curvature in k_x -direction and a large curvature in the two perpendicular directions. This results in a longitudinal mass of $0.98 m_e$ and two transversal masses of $0.19 m_e$. These three values form the three diagonal elements of the effective-mass tensor for one conduction-band minimum.

The valence-band top is formed by three nearly degenerate bands for each spin. The valence band top is at the Γ -point. The three bands at the valence band top, shown in Fig. 9.12 are called the **heavy-hole band** with an effective mass of $0.49 m_e$, the **light-hole band** with effective mass $0.16 m_e$ and the split-off hole band with mass $0.29 m_e$.

The expression for the density of states is generalized to non-isotropic effective mass tensors \mathbf{m}^* by replacing the scalar mass m^* by $m^* = \sqrt[3]{\det[\mathbf{m}^*]}$.

¹⁵Degenerate in this context means defective, that is, differing from the Boltzmann statistics. A "regular", non-degenerate, electron gas is very dilute so that electron collisions are rare and the particle exchange becomes irrelevant. For a dilute electron gas the Fermi level lies far below the lower band edge, so that, within the band, Fermi and Boltzmann distribution become identical, i.e. $1/(e^{\beta(\epsilon-\mu)} + 1) \approx e^{-\beta(\epsilon-\mu)}$.

¹⁶Information on silicon effective masses from <http://ecee.colorado.edu/~bart/book/effmass.htm>.

In the following, a number of physical quantities shall be extracted from the free-electron gas

- Determine the **Fermi velocity** of aluminium (velocity of an electron at the Fermi level.) Express the result in km/h and in m/s.
- Compare the Fermi velocity to other typical velocities^a Choose about three from the following list.
 1. speed of light,
 2. speed of sound in iron
 3. speed of sound in air,
 4. thermal velocity of a nitrogen molecule in air,
 5. maximum velocity of an iron atom oscillating about a lattice site (assume a single harmonic oscillator)
 6. velocity of an aircraft
 7. speed of a point on the earth surface due to the earth rotation.

The comparison can be in a table containing all these velocities.

- Determine the **Seitz radius** r_s , also called **electron-gas parameter**. The Seitz radius is the radius of a sphere with the volume equal to the volume per electron. It is used to characterize the electron density and it is a rough measure for the average distance between electrons. Calculate the Seitz radius considering only the valence electrons for aluminium.
- Calculate the one-particle density of states of the free-electron gas. The intention is to recover the derivation.
- Determine the **heat capacity per volume** of the free-electron gas at low temperatures. Use the expression to determine the heat capacity
 - for a metal such as Al, and
 - for a semi-conductor such as silicon.

(Note, that a semi-conductor or an insulator can not be approximated by a (single) free-electron gas!)

... cont'd

^aSearch the internet, for example.

cont'ing...

- Determine the static **magnetic susceptibility** χ and the **permeability** $\mu_r = 1 + \chi$ of the free-electron gas. The magnetic susceptibility is the derivative of the magnetization \vec{M} (magnetic moment per volume) with respect to the magnetic field B .

An electron has a magnetic moment \vec{m} ,

$$\vec{m} = \gamma_e \vec{S} = \underbrace{g_e}_{-2.0023\dots} \underbrace{\left(\frac{-e\hbar}{2m_e}\right)}_{-\mu_B} \underbrace{\frac{1}{\hbar} \vec{S}}_{\frac{1}{2} \vec{e}_S} = \frac{g_e}{2} \mu_B \vec{e}_S \quad (6.76)$$

where γ_e is the **gyro-magnetic ratio** of the electron, which relates the electron magnetic moment to its spin $\vec{S} = \frac{1}{2} \hbar \vec{e}_S$. We describe the direction of the electron spin by the unit vector \vec{e}_S . The dimension-less quantity $g_e = 2.0023\dots$ is the g -factor^a of the free electron. The **Bohr magneton** $\mu_B = \frac{e\hbar}{2m_e}$ is a unit for the magnetic moment. The Bohr magneton is approximately equal to the magnetic moment μ_e of a free electron.

In a magnetic field \vec{B} , an electron receives an additional energy $\Delta E = -\vec{\mu} \cdot \vec{B}$. This shifts the energy for the electrons parallel to the magnetic field down and the energy for the electrons antiparallel to the field is shifted upward. This is the so-called **Zeeman splitting**. In a magnetic field the Zeeman splitting needs to be added to the band structure.

Calculate the magnetization as function of magnetic field B and number of electrons, and derive from that the magnetic susceptibility and the permeability.

- Determine the pressure of the free-electron gas.

^aFor classical particles orbiting about a center the ratio of magnetic moment to angular momentum is $\frac{q}{2m}$, i.e. $\vec{m} = \frac{q}{2m} \vec{L}$. The g -factor is used to account for deviations from this classical value.

In the following the solutions are provided.

Determine the **Fermi velocity** of aluminium (velocity of an electron at the Fermi level.) Express the result in km/h and in m/s.

The Fermi velocity v_F of a free-electron gas is velocity at the Fermi surface.

$$v_F = |\vec{\nabla}_p \epsilon| = \frac{p_F}{m_e} = \frac{\hbar}{m_e} k_F \quad (6.77)$$

where m_e is the electron mass and $p_F = \hbar k_F$ is the Fermi momentum of the free-electron gas.

The electron density n in aluminium is given by the number ($N = 3$) of electrons per unit cell and the volume $V = \frac{1}{4} a_{\text{lat}}^3$ of the fcc unit cell with lattice constant $a_{\text{lat}} = 4.05 \text{ \AA}$ of aluminium.

- The fcc lattice vectors are

$$\mathbf{T} = (\vec{T}_1, \vec{T}_2, \vec{T}_3) = \begin{pmatrix} 0.0 & 0.5 & 0.5 \\ 0.5 & 0.0 & 0.5 \\ 0.5 & 0.5 & 0.0 \end{pmatrix} a_{\text{lat}} \quad (6.78)$$

The volume of the unit cell is $V = \det[\mathbf{T}] = \frac{1}{4} a_{\text{lat}}^3$.

- As an alternative, we could have started the cubic unit cell with

$$\mathbf{T}' = (\vec{T}'_1, \vec{T}'_2, \vec{T}'_3) = \begin{pmatrix} 1 & 0 & 0 \\ 0 & 1 & 0 \\ 0 & 0 & 1 \end{pmatrix} a_{\text{lat}} \quad (6.79)$$

The volume of this unit cell is $V' = \det[\mathbf{T}'] = a_{\text{lat}}^3$. This unit cell however contains four atoms instead of one: one at the corner and three at the distinct faces of the cube. Thus, we obtain the same volume per atom as when we use the fcc unit cell.

Only the valence electrons are considered in the electron number N , because the free-electron parabola $\epsilon(\vec{k})$ is formed only by the valence electrons. The core electrons are tightly bound to the nucleus and are absorbed in the positive charge background. Thus, the electron density of the jellium model for aluminium is

$$n = \frac{N}{V} = \frac{3}{\frac{1}{4}(4.05 \text{ \AA})^3} \quad (6.80)$$

The spacing of k-vectors is $\Delta_k = \frac{2\pi}{L}$, where L is the side length of the box (supercell) defining the periodic boundary conditions. By enforcing periodicity of the Bloch waves for the supercell, the k-points are discretized. The reciprocal space volume of such a k-point is therefore $\Delta_k^3 = \frac{(2\pi)^3}{L^3}$. Each reciprocal-space point corresponds to two one-particle states of the free-electron gas, namely one for each spin direction.

The electron density is thus

$$\begin{aligned} n &= \frac{N}{V} = \sum_{\substack{\sigma \in \{\uparrow, \downarrow\} \\ =2}} \cdot \frac{4\pi}{3} k_F^3 \frac{1}{\Delta_k^3} \frac{1}{V} = \frac{8\pi k_F^3}{3(2\pi)^3} L^3 \frac{1}{V} = \frac{8\pi k_F^3}{3(2\pi)^3} \\ \Rightarrow k_F &= \sqrt[3]{\frac{3(2\pi)^3 n}{8\pi}} = \sqrt[3]{3\pi^2 n} = \sqrt[3]{3\pi^2 \cdot \frac{3 \cdot 4}{(4.05 \text{ \AA})^3}} = \frac{\sqrt[3]{(6\pi)^2}}{4.05 \text{ \AA}} \approx 1.75 \text{ \AA}^{-1} \quad (6.81) \end{aligned}$$

This corresponds to a wave length of $2\pi/k_F \approx 3.6 \text{ \AA}$

We use the reduced Planck quantum $\hbar \approx 1.054 \times 10^{-34} \text{ Js}$ and the electron mass $m_e = 9.1 \times 10^{-31} \text{ kg}$.

Thus, the Fermi velocity is

$$v_F = \frac{\hbar}{m_e} k_F = \frac{\hbar}{m_e} \frac{\sqrt[3]{(6\pi)^2}}{4.05 \text{ \AA}} = 2.029 \times 10^6 \frac{\text{m}}{\text{s}} \approx 7.3 \times 10^6 \text{ km/h} \quad (6.82)$$

Relate the Fermi velocity of aluminium, as calculated before, to other typical velocities^a Choose about three from the following list.

1. speed of light,
2. speed of sound in iron
3. speed of sound in air,
4. thermal velocity of a nitrogen molecule in air,
5. maximum velocity of an iron atom oscillating about a lattice site (assume a single harmonic oscillator)
6. velocity of an aircraft
7. speed of a point on the earth surface due to the earth rotation.

The comparison can be in a table containing all these velocities.

^aSearch the internet for example.

	m/s	km/hour
Fermi velocity of Al	2.029×10^6	7.3×10^6
speed of light	3×10^8	1.08×10^9
speed of sound in air	343	1235
speed of sound in iron	5130	18468
avg. velocity of nitrogen molecule at room temp.	510	1839
velocity of an aircraft	242	870
speed of equatorial point on earth due to rotation	466	1677

Determine the **Seitz radius** r_s , also called **electron-gas parameter**. The Seitz radius is the radius of a sphere with the volume equal to the volume per electron. It is used to characterize the electron density and it is a rough measure for the average distance between electrons. Calculate the Seitz radius considering only the valence electrons for aluminium.

The electron density for aluminium is

$$n = \frac{3}{\frac{1}{4}(4.05\text{\AA})^3} = 0.18064\text{\AA}^{-3} = 0.18064 \times 10^{30} \text{ m}^{-3} \quad (6.83)$$

where an Angstrom is defined as $1 \text{\AA} \stackrel{\text{def}}{=} 10^{-10} \text{ m}$.

The electron density of aluminium consists of the same number of spin-up and spin-down electrons. The electron density with same spin is $\frac{\text{No. of electrons}}{\text{volume}} = \frac{n}{2}$

I estimate the average distance between the electrons considering a model where the electrons form a closed-packed lattice.

The volume per electron in aluminium is $\frac{1}{n}$, which is also the volume $4\pi/3 \cdot r_s^3$ of the Seitz sphere.

$$\frac{4\pi}{3} r_s^3 = \frac{1}{n} \Rightarrow r_s = \sqrt[3]{\frac{3}{4\pi n}} = 1.32 \quad (6.84)$$

The average distance between electrons is about $2r_s = 2.64 \text{\AA}$.

Calculate the one-particle density of states of the free-electron gas. The intention is to recover the derivation.

The density of states $D(\epsilon)$ of the free-electron gas has been derived earlier in section 5.3.1. The result is given in Eq. 5.36 as

$$\frac{1}{\Omega} D(\epsilon) \stackrel{\text{Eq. 5.36}}{=} 2\pi \underbrace{\left(\sum_{\sigma \in \{\uparrow, \downarrow\}} \right)}_{=2} \left(\frac{2m_e}{(2\pi\hbar)^2} \right)^{\frac{3}{2}} \sqrt{\epsilon - \epsilon_0} \quad \text{for } \epsilon \geq \epsilon_0 \quad (6.85)$$

Editor: decide whether the following derivation of the density of states simply duplicates what is already in the main text.

The derivation is as follows: Calculate first the number of states at zero temperature

$$\begin{aligned} N(T=0, \mu) &= \Omega \underbrace{\left(\sum_{\sigma \in \{\uparrow, \downarrow\}} \right)}_{=2} \int \frac{d^3k}{(2\pi)^3} \theta \left(\mu - \epsilon_0 - \frac{(\hbar\vec{k})^2}{2m_e} \right) = \Omega \cdot 2 \cdot \frac{1}{(2\pi)^3} \frac{4\pi}{3} k_F^3 \\ &= \Omega \frac{8\pi}{3} \left(\frac{2m_e(\mu - \epsilon_0)}{(2\pi\hbar)^2} \right)^{\frac{3}{2}} \end{aligned} \quad (6.86)$$

$\mu_B = \frac{e\hbar}{2m_e}$ is a unit for the magnetic moment. The Bohr magneton is approximately equal to the magnetic moment μ_e of a free electron.

In a magnetic field \vec{B} , an electron receives an additional energy $\Delta E = -\vec{\mu}\vec{B}$. This shifts the energy for the electrons parallel to the magnetic field down and the energy for the electrons antiparallel to the field is shifted upward. This is the so-called **Zeeman splitting**. In a magnetic field the Zeeman splitting needs to be added to the band structure.

Calculate the magnetization as function of magnetic field B and number of electrons, and derive from that the magnetic susceptibility and the permeability.

Magnetic susceptibility as derived in the lecture notes (eq. 4.104),

$$\begin{aligned}\chi &= \left(\frac{|g_e\mu_B|}{2}\right)^2 \frac{D(\epsilon_F)}{\Omega} = \left(\frac{2.0023 \times 9.274 \times 10^{-24} \text{JT}^{-1}}{2}\right)^2 \times \frac{D(\epsilon_F)}{\Omega} \\ &= 8.62 \times 10^{-47} \text{J}^2\text{T}^{-2} \times \frac{D(\epsilon_F)}{\Omega}\end{aligned}$$

Determine the pressure of the free-electron gas.

The pressure due to a free-electron gas is

$$p = -\frac{\partial U(S, V, N)}{\partial V}$$

The internal energy is

$$\begin{aligned}U &= \int_0^\infty d\epsilon \epsilon D(\epsilon) f(\epsilon) = \frac{4\pi(2m)^{\frac{3}{2}}}{h^3} V \underbrace{\int_0^\infty d\epsilon \epsilon^{\frac{3}{2}} f(\epsilon)}_{\frac{\epsilon_F^{5/2}}{5/2} + \frac{(\pi k_B T)^2}{4} + \mathcal{O}(k_B T)^4} \\ &= \frac{4\pi}{h^3} (2m)^{\frac{3}{2}} V \left[\frac{\hbar^5 (3\pi^2 N)^{\frac{5}{3}}}{(5/2)(2m)^{5/2}} V^{-5/3} + \frac{(\pi k_B T)^2}{4} \times \frac{\hbar (3\pi^2 N)^{1/3}}{(2m)^{1/2}} V^{-1/3} \right] + \mathcal{O}(k_B T)^4 \\ &= \frac{4\pi}{h^3} (2m)^{\frac{3}{2}} \left[\frac{\hbar^5 (3\pi^2 N)^{\frac{5}{3}}}{(5/2)(2m)^{5/2}} V^{-2/3} + \frac{(\pi k_B T)^2}{4} \times \frac{\hbar (3\pi^2 N)^{1/3}}{(2m)^{1/2}} V^{2/3} \right] + \mathcal{O}(k_B T)^4\end{aligned}$$

Thus, the pressure due to a free-electron gas is

$$\begin{aligned}p &= -\frac{\partial U}{\partial V} = \frac{4\pi}{h^3} (2m)^{\frac{3}{2}} \left[\frac{\hbar^5 (3\pi^2 N)^{\frac{5}{3}}}{(5/2)(2m)^{5/2}} \frac{2}{3} V^{-5/3} - \frac{(\pi k_B T)^2}{4} \times \frac{\hbar (3\pi^2 N)^{1/3}}{(2m)^{1/2}} \frac{2}{3} V^{-1/3} \right] \\ &= \frac{4\pi}{h^3} (2m)^{\frac{3}{2}} \left[\frac{\hbar^5 (3\pi^2 N)^{\frac{5}{3}}}{(5/2)(2m)^{5/2}} \frac{2}{3} V^{-5/3} - \frac{(\pi k_B T)^2}{4} \times \frac{\hbar (3\pi^2 N)^{1/3}}{(2m)^{1/2}} \frac{2}{3} V^{-1/3} \right] + \mathcal{O}(k_B T)^4 \\ &= \frac{4\pi}{h^3} (2m)^{\frac{3}{2}} \frac{\hbar (3\pi^2 n)^{1/3}}{(2m)^{1/2}} \left[\frac{\hbar^4 (3\pi^2 n)^{\frac{4}{3}}}{(2m)^2} \frac{4}{15} - \frac{(\pi k_B T)^2}{6} \right] + \mathcal{O}(k_B T)^4 \\ &= \frac{4m}{h^2} (3\pi^2 n)^{1/3} \left[\frac{\hbar^4 (3\pi^2 n)^{\frac{4}{3}}}{(2m)^2} \frac{4}{15} - \frac{(\pi k_B T)^2}{6} \right] + \mathcal{O}(k_B T)^4\end{aligned}$$

Electron pressure in aluminium:

$$\begin{aligned}
 p &= \frac{4 \times 9.1 \times 10^{-31} \text{kg}}{(6.626 \times 10^{-34} \text{Js})^2} \times (3 \times 3.14^2 \times 1.806 \times 10^{29} \text{m}^{-3})^{1/3} \times \\
 &\left[\frac{(1.0536 \times 10^{-34} \text{Js})^4 \times (3 \times 3.14^2 \times 1.806 \times 10^{29} \text{m}^{-3})^{4/3}}{(2 \times 9.1 \times 10^{-31} \text{kg})^2} \times \frac{4}{15} - \frac{(3.14 \times 1.38 \times 10^{-23} \text{J/K})^2}{6} T^2 \right] \\
 &= (1.347 \times 10^{11} - T^2 \times 45.5455 \text{K}^{-1}) \text{Jm}^{-3}
 \end{aligned}$$

Electron pressure in silicon:

$$\begin{aligned}
 p &= \frac{4 \times 9.1 \times 10^{-31} \text{kg}}{(6.626 \times 10^{-34} \text{Js})^2} \times (3 \times 3.14^2 \times 4.994 \times 10^{28} \text{m}^{-3})^{1/3} \times \\
 &\left[\frac{(1.0536 \times 10^{-34} \text{Js})^4 \times (3 \times 3.14^2 \times 4.994 \times 10^{28} \text{m}^{-3})^{4/3}}{(2 \times 9.1 \times 10^{-31} \text{kg})^2} \times \frac{4}{15} - \frac{(3.14 \times 1.38 \times 10^{-23} \text{J/K})^2}{6} T^2 \right] \\
 &= (1.581 \times 10^{10} - T^2 \times 29.67 \text{K}^{-1}) \text{Jm}^{-3}
 \end{aligned}$$

Chapter 7

Phonons

A recommended reading is chapter 3 of the 1st Volume *Theoretical Solid-state physics* by Jones and March.[49]

7.1 Phonons as quasi particles

Just as electrons in a lattice can be described as entities with a given energy and momentum, also the vibrations of the atoms about their equilibrium positions can be combined into vibrational modes with a given momentum $\vec{p} = \hbar\vec{k}$ and energy $\epsilon(\vec{k}) = \hbar\bar{\omega}(\vec{k})$. Thus, the vibrations can be characterized by a dispersion relation, the **phonon band structure**.

The Hamiltonian for each vibrational mode has the form of a harmonic oscillator. If the vibrations are quantized, the intensity of the vibrations increases in discrete steps $E_{j,\vec{k}}(n) = \hbar\omega_j(\vec{k})(n + \frac{1}{2})$, where j is the band index and n is the number of excitations of this vibration. Thus, the vibrations are quanta with specific energy and momentum. Therefore, one describes these entities as quasiparticles. These quasi particles are named **phonons**

The study of phonons provides insight into the ladder of quantization, namely

1. We can consider phonons as classical particles with a given energy and momentum. This is how one looks at phonons in the Boltzmann equation.
2. We can consider phonons as vibrational modes or distortion fields. This description follows when one treats the atoms as classical particles. The “distortion fields” are analogous to the wave function of the Schrödinger equation of quantum mechanics. For this reason one often talks of the first quantization as a classical field theory.
3. When the quantum-mechanical nature of the atoms is considered, we obtain a **quantum field theory**. This is what is described as **second quantization**.

The second quantization of electrons is at the center of the course on Φ SX:Advanced Solid-State Theory[2]. The analogies from moving up and down the ladder of quantization is very useful to understand many-particle physics.

In contrast to electrons, phonons are bosons. They are thus a model for the description of other bosonic quasi particles such as photons.

7.2 Connection to the Born-Oppenheimer framework

In the Born-Oppenheimer framework of chapter 2, we arrived on p. 50 at a Schrödinger equation Eq. 2.28 for the nuclear wave function. This nuclear Schrödinger equation requires the Born-Oppenheimer surfaces $E_n^{BO}(\vec{R})$ and the derivative couplings $\vec{A}_{m,n}(\vec{R})$ as input.

At sufficiently low temperature, the nuclei remain close to the global minimum of the ground-state Born-Oppenheimer surface. Therefore, we expand the Born-Oppenheimer surfaces in the displacements $\delta\vec{R} \stackrel{\text{def}}{=} \vec{R} - \vec{R}_0$ from this minimum \vec{R}_0 .

In order to disentangle the electronic and phononic degrees of freedom, let me introduce the operator $|\Psi_0^{BO}\rangle\langle\Psi_0^{BO}|$, which projects the electronic wave function to the ground state $|\Psi_0^{BO}(\vec{R})\rangle$. I rewrite it as unity operator minus the projection onto all other electronic states:

$$|\Psi_0^{BO}\rangle\langle\Psi_0^{BO}| = \hat{1} - \sum_{n \neq 0} |\Psi_n^{BO}\rangle\langle\Psi_n^{BO}| \quad (7.1)$$

This allows one to write down the Born-Oppenheimer Hamiltonian energy as a sum of (1) the energy of the lowest Born-Oppenheimer surface and (2) corrections due to excited states.

The Born-Oppenheimer Hamiltonian, which acts on the electronic degrees of freedom is

$$\begin{aligned} \hat{H}^{BO}(\vec{R}) &= \sum_{n=0}^{\infty} |\Psi_n^{BO}(\vec{R})\rangle E_n^{BO}(\vec{R}) \langle\Psi_n^{BO}(\vec{R})| \\ &\stackrel{\text{Eq. 7.1}}{=} E_0^{BO}(\vec{R}) + \sum_{n>0}^{\infty} |\Psi_n^{BO}(\vec{R})\rangle (E_n^{BO}(\vec{R}) - E_0^{BO}(\vec{R})) \langle\Psi_n^{BO}(\vec{R})| \\ &= \underbrace{E_0^{BO}(\vec{R}_0)}_{\text{ground state energy}} + \underbrace{(E_0^{BO}(\vec{R}) - E_0^{BO}(\vec{R}_0))}_{\text{phonons}} \\ &+ \underbrace{\sum_{n>0}^{\infty} |\Psi_n^{BO}(\vec{R}_0)\rangle (E_n^{BO}(\vec{R}_0) - E_0^{BO}(\vec{R}_0)) \langle\Psi_n^{BO}(\vec{R}_0)|}_{\text{electronic excitations}} \\ &+ \sum_{n>0}^{\infty} \left[\underbrace{|\Psi_n^{BO}(\vec{R})\rangle (E_n^{BO}(\vec{R}) - E_0^{BO}(\vec{R})) \langle\Psi_n^{BO}(\vec{R})|}_{\text{electron-phonon coupling (part 1, distorted)}} \right. \\ &\quad \left. - \underbrace{|\Psi_n^{BO}(\vec{R}_0)\rangle (E_n^{BO}(\vec{R}_0) - E_0^{BO}(\vec{R}_0)) \langle\Psi_n^{BO}(\vec{R}_0)|}_{\text{electron-phonon coupling (part 2; undistorted)}} \right] \end{aligned} \quad (7.2)$$

where the Born-Oppenheimer surfaces $E^{BO}(\vec{R})$ and Born-Oppenheimer states $|\Psi^{BO}(\vec{R})\rangle$ are defined in Eq. 2.4 on p. 45 and where $\vec{A}_{m,n}$ are the derivative couplings defined in Eq. 2.29 on p. 50

Eq. 7.2 divides the Born-Oppenheimer Hamiltonian into the

- the **ground-state energy**,
- the energy due phonons,
- the energy of electronic excitations, and
- the **electron-phonon coupling**, which couples phonons and electronic excitations

I use the term “phonon” here as synonym for a distortion of the atomic configuration in the electronic ground state.

The electron-phonon couplings vanish for $\vec{R} = \vec{R}_0$.

Where is the zero-point energy, the energy of zero-point vibrations of the nuclei? This energy “must not be included” at this point. It is not part of the Born-Oppenheimer Hamiltonian, which is divided here into its parts. Rather, it enters via the Schrödinger equation Eq. 2.27 for the nuclei, which combines the Born-Oppenheimer Hamiltonian with the kinetic energy of the nuclei.

Per definition, the Born-Oppenheimer Hamiltonian describes only one part of the complete electron-nuclear Hamiltonian, because the kinetic energy of the nuclei has been stripped off. The nuclear kinetic energy will be considered later and as part of the nuclear Schrödinger equation Eq. 2.27. Nevertheless, the division Eq. 7.2 of the Born-Oppenheimer Hamiltonian is exact.

In the next step, a Taylor expansion about the equilibrium positions is introduced, and truncation of the Taylor expansion introduces approximations. This divides the phonon term into a term of non-interacting phonons and the phonon-phonon interaction, which contains the anharmonic terms that are responsible for phonon-phonon scattering. The electron-phonon coupling is only expanded up to first order in the deviation from the equilibrium positions.

BORN-OPPENHEIMER HAMILTONIAN QUADRATIC IN PHONONS AND EXCITATIONS

A Taylor expansion of the Born-Oppenheimer Hamiltonian in $\delta\vec{R} \stackrel{\text{def}}{=} \vec{R} - \vec{R}_0$

$$\begin{aligned}
\hat{H}^{BO}(\vec{R}) \stackrel{\text{Eq. 7.2}}{=} & \underbrace{E_0^{BO}(\vec{R}_0)}_{\text{ground-state energy}} + \underbrace{\frac{1}{2} \sum_{i,j} \delta R_i \frac{\partial^2 E_0^{BO}}{\partial R_i \partial R_j} \delta R_j}_{\text{free phonons}} + \underbrace{\frac{1}{3!} \sum_{i,j,k} \frac{\partial^3 E_0^{BO}}{\partial R_i \partial R_j \partial R_k} \delta R_i \delta R_j \delta R_k}_{\text{phonon-phonon scattering}} + O(\delta\vec{R}^4) \\
& + \underbrace{\sum_{n>0} |\Psi_n^{BO}(\vec{R}_0)\rangle \left(E_n^{BO}(\vec{R}_0) - E_0^{BO}(\vec{R}_0) \right) \langle \Psi_n^{BO}(\vec{R}_0) |}_{\text{electronic excitations}} \\
& + \sum_i \delta R_i \underbrace{\left\{ \sum_{n>0} |\Psi_n^{BO}(\vec{R}_0)\rangle \left(\frac{\partial E_n^{BO}}{\partial R_i} \Big|_{\vec{R}_0} - \frac{\partial E_0^{BO}}{\partial R_i} \Big|_{\vec{R}_0} \right) \langle \Psi_n^{BO}(\vec{R}_0) | \right\}}_{\text{electron-phonon coupling/adiabatic}} \\
& + \underbrace{\sum_{m,n=0, m \neq n}^{\infty} |\Psi_m^{BO}(\vec{R}_0)\rangle \langle \Psi_m^{BO}(\vec{R}_0) | \left(\frac{\partial \hat{H}^{BO}}{\partial R_i} \Big|_{\vec{R}_0} \right) |\Psi_n^{BO}(\vec{R}_0)\rangle \langle \Psi_n^{BO}(\vec{R}_0) |}_{\text{electron-phonon coupling/non-adiabatic (Eq. 7.5)}} \\
& + O(\delta\vec{R}^2) \tag{7.3}
\end{aligned}$$

The last term of Eq. 7.3 is divided into

- a term from the change of the Born-Oppenheimer surfaces with displacement, the adiabatic electron-phonon coupling, and
- two terms from a change in the Born-Oppenheimer wave functions with displacement, the non-adiabatic electron-phonon coupling.

The derivation of the non-adiabatic electron-phonon coupling in Eq. 7.3 is not straightforward. Let me elaborate it: Consider the last term in Eq. 7.2, which I expand to first order in the displacement from the reference configuration. This involved (1) gradients of the Born-Oppenheimer surfaces, which produce the adiabatic electron-phonon coupling, and (2) gradients of the wave functions,

which will produce the non-adiabatic terms in Eq. 7.3. I start with the gradient of the wave function.

$$\begin{aligned}
|\delta\Psi_n^{BO}\rangle &= \delta\vec{R}\vec{\nabla}_R\Big|_{\vec{R}_0}\Big|\Psi_n^{BO}(\vec{R})\rangle = \delta\vec{R}\underbrace{\sum_{m=0}^{\infty}\Big|\Psi_m^{BO}(\vec{R}_0)\rangle\langle\Psi_m^{BO}(\vec{R}_0)\Big|\vec{\nabla}_R\Big|_{\vec{R}_0}\Big|\Psi_n^{BO}(\vec{R})\rangle}_{\hat{1}} \\
&= \sum_{m=0}^{\infty}\Big|\Psi_m^{BO}(\vec{R}_0)\rangle\frac{i}{\hbar}\delta\vec{R}\underbrace{\langle\Psi_m^{BO}(\vec{R}_0)\Big|\frac{\hbar}{i}\vec{\nabla}_R\Big|_{\vec{R}_0}\Big|\Psi_n^{BO}(\vec{R})\rangle}_{\vec{A}_{m,n}(\vec{R}_0)} \\
&\stackrel{\text{Eq. 2.29}}{=} \sum_{m=0}^{\infty}\Big|\Psi_m^{BO}(\vec{R}_0)\rangle\frac{i}{\hbar}\delta\vec{R}\vec{A}_{m,n}(\vec{R}_0) \tag{7.4}
\end{aligned}$$

where $\vec{A}_{m,n}(\vec{R})$ are the first-derivative couplings defined in Eq. 2.29 on p. 50.

Thus, I obtain for the nonadiabatic electron-phonon coupling (last term of Eq. 7.2 after removing the adiabatic term depending on the gradients of the energy surfaces.)

$$\begin{aligned}
&\sum_{n>0}^{\infty}\left(\Big|\delta\Psi_n^{BO}\rangle\left(E_n^{BO}(\vec{R}_0) - E_0^{BO}(\vec{R}_0)\right)\langle\Psi_n^{BO}(\vec{R}_0)\Big| + \Big|\Psi_n^{BO}(\vec{R}_0)\rangle\left(E_n^{BO}(\vec{R}_0) - E_0^{BO}(\vec{R}_0)\right)\langle\delta\Psi_n^{BO}\Big|\right) \\
&\stackrel{\text{Eq. 7.4}}{=} \delta\vec{R}\sum_{m,n=0}^{\infty}\Big|\Psi_m^{BO}(\vec{R}_0)\rangle\left(\frac{i}{\hbar}\vec{A}_{m,n}\left(E_n^{BO} - E_0^{BO}\right) + \frac{-i}{\hbar}\underbrace{\vec{A}_{n,m}^*}_{=\vec{A}_{m,n}}\left(E_m^{BO} - E_0^{BO}\right)\right)\langle\Psi_n^{BO}(\vec{R}_0)\Big| \\
&\stackrel{\text{Eq. 2.18}}{=} \delta\vec{R}\sum_{m,n=0;m\neq n}^{\infty}\Big|\Psi_m^{BO}(\vec{R}_0)\rangle\frac{i}{\hbar}\vec{A}_{m,n}(\vec{R}_0)\underbrace{\left(E_n^{BO}(\vec{R}_0) - E_m^{BO}(\vec{R}_0)\right)}_{=0 \text{ for } m=n}\langle\Psi_n^{BO}(\vec{R}_0)\Big| \\
&\stackrel{\text{Eq. 2.31}}{=} \delta\vec{R}\sum_{m,n=0;m\neq n}^{\infty}\Big|\Psi_m^{BO}(\vec{R}_0)\rangle\langle\Psi_m^{BO}(\vec{R}_0)\Big|\left[\vec{\nabla}_R\Big|_{\vec{R}_0}, \hat{H}^{BO}\right]_-\Big|\Psi_n^{BO}(\vec{R}_0)\rangle\langle\Psi_n^{BO}(\vec{R}_0)\Big| \tag{7.5}
\end{aligned}$$

I expanded the sum over states in the first step of Eq. 7.5, so that it includes also the ground state. This is allowed because the additional term vanishes due to the factor $E_m^{BO} - E_0^{BO}$.

The expansion can be carried further to higher orders¹.

1. **Ground-state energy:** The constant $E_0^{BO}(\vec{R}_0) = \langle\Psi_0^{BO}(\vec{R}_0)|\hat{H}^{BO}|\Psi_0^{BO}(\vec{R}_0)\rangle$ is the ground-state energy of the system.
2. **No forces:** The first-order term in the displacements of the nuclei vanishes, because the expansion starts at a minimum of the Born-Oppenheimer surface.
3. **Free phonons:** The quadratic term of in the displacements corresponds to a harmonic oscillator. The vibrational modes of this harmonic oscillator are independent of each other and will be attributed to phonons.
4. **Anharmonic terms, phonon-phonon coupling:** The third and higher-order terms in the atomic displacements $\delta\vec{R}$ will be interpreted in terms of phonon-phonon scattering. They describe the interaction between phonons. The dominant term for phonons is due to the third-order expansion coefficients. The scattering processes of the third order involve three phonons: Either two phonons combine into a third one, or one phonon splits up into two phonons.

Fourth-order terms involve four phonons: One phonon can split into three, two phonons scatter and emerge as two other phonons, or three phonons combine into one.

¹The expansion up to third order in $\delta\vec{R}$ produces an energy surface that is not bounded from below. This causes problems for methods searching for an energy minimum. For the sake of simplicity, I will nevertheless not go beyond the third order.

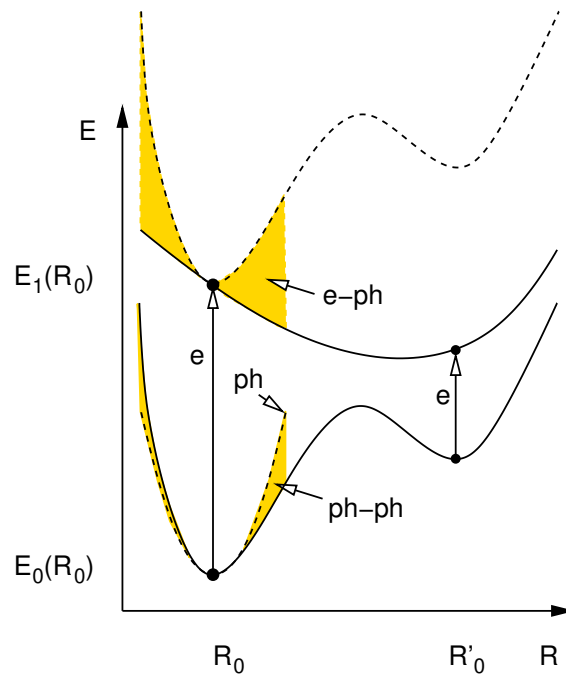


Fig. 7.1: Sketch for the electronic and phononic energy contribution to the Born-Oppenheimer Hamiltonian. Equilibrium configuration \vec{R}_0 . Ground-state energy $E_0(\vec{R}_0)$. Excited-state energy $E_1(\vec{R}_0)$. The parabolic term indicated by “ph” describes phonons. Deviations from the parabola, indicate phonon-phonon scattering terms. The dashed line indicated by $ph - ph$ is the third order polynomial describes the phonon energy plus lowest-order anharmonic terms. b The dashed vertical line indicate by “e” describes an electronic excitation. The slope indicated by “e-ph” is the first-order adiabatic electron-phonon term.

5. **Electronic excitations:** In addition to the atomic displacements, the energy depends on the electronic excitations. The first term describes excitations at the ideal ground-state atomic structure.
6. **Adiabatic electron-phonon coupling:** The excited-state Born-Oppenheimer surface depends differently on the atomic displacements than the ground-state Born-Oppenheimer surface. This is accounted for by the **adiabatic electron-phonon coupling**. The adiabatic electron-phonon couplings do not induce transitions between different excited states.
7. **Non-adiabatic electron-phonon coupling:** the last term, which we call **non-adiabatic electron-phonon coupling** describes electronic transitions between different excited states due to the motion of the atoms. The term listed results in a position-independent derivative coupling, which has no impact on the classical trajectories.

Editor: The following is unclear: The higher-order terms, on the other hand, affect the entropy² of the electronic excitations and are expected to describe a friction term for the nuclear motion.

Taken together, the total energy can be written as the ground-state energy, the energy of phonons, the energy of electronic excitation and interactions between phonons and electronic excitations.

²When we speak of the entropy of electronic excitations, we interpret the absolute square of the nuclear wave function of a specific Born-Oppenheimer surface as probability P_n to be in the specified electronic states. The corresponding entropy is then $S = -k_B \sum_n P_n \ln(P_n)$ is then attributed to the electronic excitations.

The ground-state energy and that of the electronic excitations are usually treated together as the electronic energy.

The electronic excitations can be divided up further into electron and hole excitations, magnons, and other elementary excitations.

Let me introduce the symbols, which we will use for the force constants $C_{\alpha,\beta}$ and the anharmonic coefficients $W_{\alpha,\beta,\gamma}$

$$\begin{aligned} C_{\alpha,\beta} &\stackrel{\text{def}}{=} \left. \frac{\partial^2 E_0^{BO}}{\partial R_\alpha \partial R_\beta} \right|_{\vec{R}_0} \\ W_{\alpha,\beta,\gamma} &\stackrel{\text{def}}{=} \left. \frac{\partial^3 E_0^{BO}}{\partial R_\alpha \partial R_\beta \partial R_\gamma} \right|_{\vec{R}_0} \end{aligned} \quad (7.6)$$

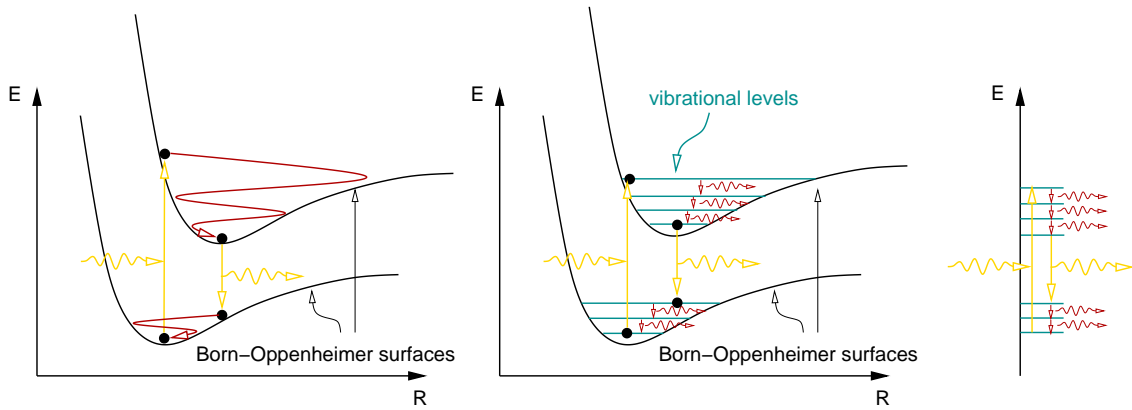


Fig. 7.2: Schematic for the optical absorption and desorption of a photon. Let R be one spatial coordinate for the nuclei, such as a bond distance. A photon excites an electron from the ground-state sheet of the total-energy surface to an excited-state sheet. The atoms vibrate around the equilibrium structure of the excited energy surface. During that process the system dissipates energy. In other words, it thermalizes by emitting phonons. At some point the electron drops again on the ground-state energy surface, while emitting a photon. The emitted photon has a lower energy than the absorbed photon, because some of the energy has been lost by creating for example phonons, i.e. heat. The system vibrates again about the equilibrium structure until it has dissipated its energy. Note that the transition proceeds between different energy levels of the total energy, which also include the vibrational levels. Thus vibrations or phonons are excited as well. Thus, to determine the absorption probability not only the optical transition matrix elements of the electronic subsystem must be considered, but also the overlap of the nuclear part of the wave function. Note that the figure describes the case at zero temperature. At finite temperature, the system can be initially already in an excited vibrational level. The left figure is appropriate for a classical description of the nuclear motion, while the right figure is an abstract energy level diagram appropriate for a quantum description.

Derivative couplings

Once we have obtained the approximate Born-Oppenheimer Hamiltonian Eq. 7.3, we can use it to extract the corresponding approximate Born-Oppenheimer surfaces and derivative couplings.

The approximate Born-Oppenheimer Hamiltonian Eq. 7.3 depends on the nuclear position. Thus, we can work out the derivative couplings of this approximate Born-Oppenheimer Hamiltonian. This may be of use, in order to set up the nuclear Schrödinger equation consistent with the limited Taylor expansion inherent to Eq. 7.3.

Editor: Work out the Born-Oppenheimer surfaces and ensure that the derivative couplings are fully consistent with the approximate Hamiltonian, without additional approximations such as first-order perturbation theory

The derivative couplings are obtained from Eq. 2.31 on p. 53 are

$$\begin{aligned} \vec{A}_{m,n}^{\text{approx}}(\vec{R}) &\stackrel{\text{Eq. 2.31}}{=} \frac{\left\langle \Psi_m^{BO,\text{approx}}(\vec{R}) \left| \left[\frac{\hbar}{i} \vec{\nabla}_R, \hat{H}^{BO,\text{approx}}(\vec{R}) \right]_- \right| \Psi_n^{BO,\text{approx}}(\vec{R}) \right\rangle}{E_n^{BO,\text{approx}}(\vec{R}) - E_m^{BO,\text{approx}}(\vec{R})} \quad \text{for } E_m^{BO} \neq E_n^{BO} \\ &\stackrel{\text{Eq. 7.3}}{=} \frac{\left\langle \Psi_m^{BO}(\vec{R}_0) \left| \left(\frac{\hbar}{i} \vec{\nabla}_R \right)_{\vec{R}_0} \hat{H}^{BO}(\vec{R}) \right| \Psi_n^{BO}(\vec{R}_0) \right\rangle}{E_n^{BO}(\vec{R}_0) - E_m^{BO}(\vec{R}_0)} + O(\delta\vec{R}) \quad \text{for } E_m^{BO} \neq E_n^{BO} \quad (7.7) \end{aligned}$$

The position dependent terms $O(\delta\vec{R})$ are ignored, when the Hamiltonian is restricted to quadratic terms³ in positions and excitations.

When we limit the Born-Oppenheimer Hamiltonian to the terms quadratic in phonons and excitations as indicated in Eq. 7.3, the derivative couplings $\vec{A}_{m,n}(\vec{R})$ are position-independent vectors. The vectors become non-zero only, when the electronic state is in a superposition of two Born-Oppenheimer states. Thus, they contribute to the nuclear motion only during an electronic transition.

Editor: Are the non-adiabatic effects important for effects such as a friction acting on nuclei due to dissipation of nuclear kinetic energy into electronic excitations.

Limitation of the decomposition into elementary excitations

One may think of extending the scheme sketched above and introduce phonon-phonon scattering terms and electron-phonon scattering terms to increasingly high order. This approach, however, has limitations, simply because the number of terms to be considered would be exceedingly large.

On a more fundamental level, we need to consider the finite convergence radius of the Taylor expansion. Beyond the convergence radius, the results of the Taylor expansion are invalid. Beyond the convergence radius, the Taylor expansion does not converge or it converges to an arbitrary value.⁴

If several minima of the Born-Oppenheimer surface contribute, it may be more convenient to consider a few minima of the Born-Oppenheimer surfaces and use those as center of the expansions. This would automatically lead to an ensemble of different configurations, namely minima of the BO surfaces. Each configuration would have its own set of phonons and excitations. Each configuration would contribute with a weight, which is given approximately by the Boltzmann factor $e^{-\beta\Delta E}$ of the energy difference of the meta-stable minima from the ground state energy. This weight describes the probability that the system is next to a specific local minimum of the ground state Born-Oppenheimer surface.⁵

Treating several meta-stable state simultaneously, has limitations: There is a danger that the same states are counted twice. This happens when the same configuration has an appreciable statistical weight in the expansions about both minima, that is, when when the probability distributions from both minima overlap. Because the thermal broadening of the probability distribution shrinks with decreasing temperature, this approximation is expected to be reasonable at sufficiently low temperatures. In this limit, one only needs to include those minima that have energies within a few $k_B T$ from the ground state.

³One excitation and one phonon form such a quadratic term.

⁴Such an expansion would be a **conditionally convergent series**. The **Riemann series theorem** says that, by rearranging the terms, the series can be made divergent or convergent to any value. Editor: This need verification.

⁵To make this point a bit more concise, consider the configuration space to be divided into regions, which are attributed to a specific local minimum A of the ground-state Born-Oppenheimer surface. Each point of configuration space can be attributed exactly to one local minimum, by following the forces until a local minimum is reached. This defines a region Ω_A in configuration space for each local minimum. Next, we can evaluate the partition function for each region Ω_A individually. From the corresponding phase-space integration we can extract the probability that the system is in one of the local regions Ω_A .

Another concern is that an energy surface, which is represented by polynomial of odd order, is not bounded from below. This is a severe limitation for all applications related to thermodynamics. Thermodynamics relies on the maximization of the entropy, respectively the minimization of a thermodynamic potential such as the grand potential. The minimization fails when the thermodynamic potential is not bounded from below. The problem can, however, be remedied by including terms of the next higher even order.

7.3 Harmonic oscillator revisited

The **harmonic oscillator** has the Hamilton function

$$H(\vec{P}, \vec{X}, t) = \frac{1}{2}\vec{P}\mathbf{M}^{-1}\vec{P} + \frac{1}{2}\vec{X}\mathbf{C}\vec{X} \quad (7.8)$$

where $\vec{X} \stackrel{\text{def}}{=} \delta\vec{R}$ is a $3M$ dimensional vector of the atomic displacements from the equilibrium⁶ position \vec{R}_0 and \vec{P} is the $3M$ -dimensional vector of canonical momenta. \mathbf{M} is the mass tensor, which is a diagonal matrix with the atomic masses on the diagonal. \mathbf{C} is the force-constant matrix formed from the second derivatives of the potential energy.

Newton's equation of motion of the harmonic oscillator

$$\mathbf{M}\ddot{\vec{X}} = -\mathbf{C}\vec{X} \quad (7.9)$$

are obtained from the Hamilton function via the Hamilton's equation of motion.

Reminder: action principle

Below, I will use the action principle, which is why I want to turn to Lagrange functions. The Lagrange function for the harmonic oscillator is⁷

$$\mathcal{L}(\vec{V}, \vec{X}, t) = \text{stat}_{\vec{P}} \left[\vec{P}\vec{V} - H(\vec{P}, \vec{X}, t) \right] = \frac{1}{2}\vec{V}\mathbf{M}\vec{V} - \frac{1}{2}\vec{X}\mathbf{C}\vec{X} \quad (7.10)$$

where $\vec{V}(t) = \partial_t \vec{X}(t)$ is the velocity.

The **action principle** yields the Euler-Lagrange equation

$$\frac{d}{dt} \underbrace{\frac{\partial \mathcal{L}}{\partial V_\alpha}}_{P_\alpha} = \underbrace{\frac{\partial \mathcal{L}}{\partial X_\alpha}}_{-\partial H / \partial X_\alpha} \quad \text{and} \quad \frac{d}{dt} X_\alpha = \underbrace{V_\alpha}_{\partial H / \partial P_\alpha} \quad (7.11)$$

which are equivalent to Hamilton's equations.⁸

The Hamilton function is obtained from the Lagrange function as

$$H(\vec{P}, \vec{X}, t) = \text{stat}_{\vec{V}} \left[\vec{P}\vec{V} - \mathcal{L}(\vec{V}, \vec{X}, t) \right] \quad (7.12)$$

The stationary condition defines the canonical momentum as

$$P_\alpha \stackrel{\text{def}}{=} \frac{\partial \mathcal{L}}{\partial V_\alpha} \quad (7.13)$$

⁶The term "equilibrium" refers here to the balance of forces acting on the nuclei and not to thermal equilibrium.

⁷I denote with $\text{stat}_{\vec{P}}$ the stationary point of the following expression against variations of \vec{P} . This condition $V_\alpha = \partial H / \partial P_\alpha$ defines $\vec{P}(\vec{V}, \vec{X}, t)$, which is inserted to eliminate the explicit dependence on \vec{P} .

⁸The last equation is the definition of \vec{V} as the velocity. It is usually suppressed by treating $\dot{\vec{X}}$ itself as a variable. I prefer to make this explicit.

Solve equations of motion of the harmonic oscillator

The harmonic oscillator is solved by two variable transformations:

1. The first transformation introduces mass-weighted coordinates

$$\vec{Y}(t) = \sqrt{\mathbf{M}}\vec{X}(t) \quad (7.14)$$

which yields

$$\begin{aligned} \mathcal{L} &\stackrel{\text{Eq. 7.10}}{=} \frac{1}{2}(\sqrt{\mathbf{M}}\dot{\vec{X}})^2 - \frac{1}{2}(\sqrt{\mathbf{M}}\vec{X}) \underbrace{\left(\frac{1}{\sqrt{\mathbf{M}}}\mathbf{C}\frac{1}{\sqrt{\mathbf{M}}}\right)}_D (\sqrt{\mathbf{M}}\vec{X}) \\ &= \frac{1}{2}\dot{\vec{Y}}^2 - \frac{1}{2}\vec{Y}D\vec{Y} \end{aligned} \quad (7.15)$$

where

$$D \stackrel{\text{def}}{=} \frac{1}{\sqrt{\mathbf{M}}}\mathbf{C}\frac{1}{\sqrt{\mathbf{M}}} \quad (7.16)$$

is the **dynamical matrix**.

2. The second transformation requires the eigenvectors of the dynamical matrix. The dynamical matrix is diagonalized yielding eigenvalues d_n and eigenvectors \vec{U}_n

$$D\vec{U}_n = \vec{U}_n d_n \quad (7.17)$$

Because the dynamical matrix is hermitian, the eigenvalues are real-valued and the eigenvectors can be chosen orthonormal.

The eigenvectors \vec{U}_n can be combined in a unitary matrix \mathbf{U} with matrix elements $U_{i,n}$, which are the components of the eigenvectors \vec{U}_n . The orthonormality of the eigenvectors $\vec{U}_m^* \vec{U}_n = \delta_{m,n}$ translates into the requirement that \mathbf{U} is unitary, i.e. $\mathbf{U}^\dagger \mathbf{U} = \mathbf{1}$.

Thus, the dynamical matrix has the form

$$D = \mathbf{U}d\mathbf{U}^\dagger \quad (7.18)$$

The second variable transform

$$\vec{Z}(t) = \mathbf{U}^\dagger \vec{Y}(t) = \mathbf{U}^\dagger \sqrt{\mathbf{M}}\vec{X}(t) \quad (7.19)$$

yields

$$\begin{aligned} \mathcal{L} &= \frac{1}{2}(\mathbf{U}^\dagger \sqrt{\mathbf{M}}\dot{\vec{X}})^* (\mathbf{U}^\dagger \sqrt{\mathbf{M}}\dot{\vec{X}}) - \frac{1}{2}(\mathbf{U}^\dagger \sqrt{\mathbf{M}}\vec{X})^* d (\mathbf{U}^\dagger \sqrt{\mathbf{M}}\vec{X}) \\ &= \sum_{n=1}^{3M} \left[\frac{1}{2}|\dot{Z}_n|^2 - \frac{1}{2}d_n|Z_n|^2 \right] \end{aligned} \quad (7.20)$$

Thus, the Lagrangian decomposes into a set of decoupled one-dimensional harmonic oscillators.

The Euler-Lagrange equations are⁹

$$\frac{d}{dt} \frac{\partial \mathcal{L}}{\partial \dot{Z}_n^*} - \frac{\partial \mathcal{L}}{\partial Z_n^*} = 0 \quad \Rightarrow \quad \ddot{Z}_n = d_n Z_n \quad (7.21)$$

⁹We use Wirtinger derivatives.

The resulting trajectories are

$$Z_n(t) \stackrel{\text{Eq. 7.20}}{=} A_n e^{-i\omega_n t} + A_n^* e^{i\omega_n t} \quad (7.22)$$

with the circular frequency

$$\omega_n = +\sqrt{d_n} \quad (7.23)$$

and the complex-valued amplitudes A_n .

In summary, coordinate transform, that has brought us to this point, is

$$\vec{Z} \stackrel{\text{def}}{=} \mathbf{U}^\dagger \sqrt{\mathbf{M}} \vec{X} \quad \Leftrightarrow \quad \vec{X} = \frac{1}{\sqrt{\mathbf{M}}} \mathbf{U} \vec{Z} \quad (7.24)$$

The back transform of the trajectory yields our final result,

$$\vec{X}(t) \stackrel{\text{Eq. 7.24}}{=} \sum_n \frac{1}{\sqrt{\mathbf{M}}} \vec{U}_n Z_n(t) \stackrel{\text{Eq. 7.22}}{=} \sum_n \frac{1}{\sqrt{\mathbf{M}}} \vec{U}_n (A_n e^{-i\omega_n t} + A_n^* e^{i\omega_n t}) \quad (7.25)$$

In the problem at hand, the variables $X_\alpha(t)$ describe the atomic displacements $R_\alpha(t)$.

MULTIDIMENSIONAL HARMONIC OSCILLATOR

The multidimensional harmonic oscillator can be mapped onto independent harmonic oscillators using the following recipe:

1. start from a Lagrangian

$$\mathcal{L}(\dot{\vec{X}}, \vec{X}) = \frac{1}{2} \dot{\vec{X}} \mathbf{M} \dot{\vec{X}} - \frac{1}{2} \vec{X} \mathbf{C} \vec{X} \quad (7.26)$$

2. transform to mass-weighted coordinates

$$\vec{Y} = \sqrt{\mathbf{M}} \vec{X} \quad (7.27)$$

3. set up the dynamical matrix

$$D_{\alpha,\beta} = \frac{1}{\sqrt{M_\alpha}} C_{\alpha,\beta} \frac{1}{\sqrt{M_\beta}} \quad (7.28)$$

4. diagonalize the dynamical matrix

$$\sum_{\beta} D_{\alpha,\beta} U_{\beta,n} = U_{\alpha,n} \omega_n^2 \quad \text{with} \quad \sum_{\alpha} U_{\alpha,n}^* U_{\alpha,m} = \delta_{m,n} \quad (7.29)$$

5. transform to normal coordinates Z_n

$$\vec{Z} = \mathbf{U}^\dagger \vec{Y} \quad (7.30)$$

6. express the Lagrangian in normal coordinates

$$\mathcal{L} = \sum_{n=1}^{3M} \left[\frac{1}{2} \dot{Z}_n^2 - \frac{1}{2} \omega_n^2 Z_n^2 \right] \quad (7.31)$$

7. solve the Euler-Lagrange equations and transform the trajectory back into displacements $\vec{X}(t)$.

$$\begin{aligned} \vec{X}(t) &= \mathbf{M}^{-\frac{1}{2}} \vec{Y}(t) = \mathbf{M}^{-\frac{1}{2}} \mathbf{U} \vec{Z}(t) \\ X_\alpha(t) &= \frac{1}{\sqrt{M_\alpha}} \sum_n U_{\alpha,n} \left(e^{i\omega_n t} A_n^* + e^{-i\omega_n t} A_n \right) \quad \text{with} \quad A_n = \frac{1}{2} \left(Z_n(0) + i \frac{1}{\omega_n} \dot{Z}_n(0) \right) \end{aligned} \quad (7.32)$$

7.4 Bloch theorem for phonons

7.4.1 Lattice-translation symmetry

In the following, I will show how to deal with a Lagrangian of the form

$$\mathcal{L}(\vec{V}, \dot{\vec{X}}, t) = \frac{1}{2} \vec{V} \mathbf{M} \dot{\vec{V}} - \frac{1}{2} \vec{X} \mathbf{C} \vec{X} - \frac{1}{3!} \sum_{\alpha,\beta,\gamma} W_{\alpha,\beta,\gamma} X_\alpha X_\beta X_\gamma \quad (7.33)$$

where $(\vec{X} \stackrel{\text{def}}{=} \delta\vec{R})$ are the atomic displacements. In a lattice, the goal is to exploit translation symmetry. We will proceed analogously to the description of electrons in a lattice by using Bloch's theorem.

Lattice vectors, periodic boundary conditions and k-point grid: Let me remind us of the notation: The lattice is characterized by the primitive lattice vectors $\vec{T}_1, \vec{T}_2, \vec{T}_3$, which can be combined into a the matrix \mathbf{T} . A general lattice vector is denoted by a lowercase \vec{t} , and is an integer multiple of the primitive lattice vectors.

	primitive lattice vectors	general lattice vectors
real space	$\vec{T}_1, \vec{T}_2, \vec{T}_3$ or \mathbf{T}	$\vec{t}_j = \vec{T}_1 j_1 + \vec{T}_2 j_2 + \vec{T}_3 j_3 = \mathbf{T}\vec{j}$
reciprocal space	$\vec{g}_1, \vec{g}_2, \vec{g}_3$ or \mathbf{g}	$\vec{G}_j = \vec{g}_1 j_1 + \vec{g}_2 j_2 + \vec{g}_3 j_3 = \mathbf{g}\vec{j}$

The primitive reciprocal lattice vectors are denoted as $\vec{g}_1, \vec{g}_2, \vec{g}_3$, which can be combined into the matrix \mathbf{g} . The general reciprocal lattice vectors are denoted by the uppercase symbol \vec{G} and is an integer multiple of the primitive reciprocal lattice vectors.

Real-space and reciprocal lattice vectors are related by

$$\vec{g}_i \vec{T}_j = 2\pi\delta_{i,j} \quad (7.34)$$

As for the description of electrons, I will introduce in the following periodic boundary conditions on a **supercell**. Furthermore, we will perform the sums only over one supercell, rather than summing the energy terms over the infinite lattice, As a consequence of the periodic boundary conditions, we only need to consider a discrete lattice of k-points.

We denote the primitive lattice-translation vectors by \vec{T}_j and the ones of the supercell by $\vec{T}_j^{(S)}$. The lattice vectors of the supercell are multiples of those of the real lattice, i.e.

$$\vec{T}_j^{(S)} = \vec{T}_j \mathcal{N}_j \quad \text{for } j = 1, 2, 3 \quad (7.35)$$

The restriction imposed by the periodic boundary conditions can be removed by performing the limit $\mathcal{N}_j \rightarrow \infty$.

The reciprocal lattice of the supercell define a grid of k-points. We denote the reciprocal lattice vectors of the supercell by $\vec{g}_j^{(S)}$. They are obtained as

$$\vec{g}_j^{(S)} = \vec{g}_j \frac{1}{\mathcal{N}_j} \quad \text{for } j = 1, 2, 3 \quad (7.36)$$

which is easily shown by

$$\vec{g}_i^{(S)} \vec{T}_j^{(S)} = \frac{1}{\mathcal{N}_i} \underbrace{\vec{g}_i \vec{T}_j}_{2\pi\delta_{i,j}} \mathcal{N}_j = 2\pi\delta_{i,j} \quad (7.37)$$

A sum over k-points includes all reciprocal lattice vectors of the super cell in the **first Brillouin zone** Ω_G of the reciprocal lattice of the crystal.

$$\vec{k}_{i,j,k} = \vec{g}_1^{(S)} i + \vec{g}_2^{(S)} j + \vec{g}_3^{(S)} k \quad (7.38)$$

we denote the sum as

$$\sum_{\vec{k} \in \Omega_G} \quad (7.39)$$

The sum has $\mathcal{N} = \mathcal{N}_1 \mathcal{N}_2 \mathcal{N}_3$ terms, that is the number of real-space unit cells of the crystal within a supercell.

In the limit of a very large supercell, the sum over k-points becomes an integral.

$$\sum_{k \in \Omega_G} = \sum_{\vec{k}} \underbrace{\frac{1}{\mathcal{N}} \det |\mathbf{G}|}_{(\Delta k)^3} \underbrace{\mathcal{N} \frac{\det |\mathbf{T}|}{(2\pi)^3}}_{\Omega/(2\pi)^2} = \Omega \sum_{\vec{k}} \frac{(\Delta k)^3}{(2\pi)^3} \rightarrow \Omega \int_{\Omega_G} \frac{d^3 k}{(2\pi)^3} \quad (7.40)$$

where $\Omega = \mathcal{N} \det |\mathbf{T}|$ is the size of the supercell for which all extensive quantities are calculated.

Instead of the Brillouin zone, which is centered at the Γ -point, we could also have chosen the first reciprocal crystal unit cell. In that case, for example, the reverted k-point $-\vec{k}$ lies outside the first unit cell. We exploit the periodicity in the reciprocal lattice and bring it back into the first unit cell by adding an appropriate reciprocal lattice vector which leads to $-\vec{k} + \vec{g}_1 + \vec{g}_2 + \vec{g}_3$.

Notation for displacement vectors The displacements are grouped according to specific unit cells of the lattice. The unit cell can be characterized by a translation vector \vec{t} which describes its position relative to the origin. A specific displacement is specified by an index (α, \vec{t}) , of which α characterizes a particular atom in the unit cell and a Cartesian direction for the corresponding displacement, and \vec{t} , which is the lattice translation vector.

PHONON LAGRANGIAN AND TRANSLATIONAL SYMMETRY

The Lagrangian of an anharmonic crystal with \mathcal{N} unit cells has the form

$$\begin{aligned} \mathcal{L}(\vec{V}, \vec{X}) = & \frac{1}{2} \sum_{\alpha, \vec{t}} M_{\alpha} V_{\alpha, \vec{t}}^2 - \frac{1}{2} \sum_{\alpha, \beta, \vec{t}, \vec{t}'} C_{\alpha, \vec{t}, \beta, \vec{t}'} X_{\alpha, \vec{t}} X_{\beta, \vec{t}'} \\ & - \frac{1}{3!} \sum_{\alpha, \beta, \gamma, \vec{t}, \vec{t}', \vec{t}''} W_{\alpha, \vec{t}, \beta, \vec{t}', \gamma, \vec{t}''} X_{\alpha, \vec{t}} X_{\beta, \vec{t}'} X_{\gamma, \vec{t}''} \end{aligned} \quad (7.41)$$

where $V_{\alpha, \vec{t}} = \dot{X}_{\alpha, \vec{t}}$ is the velocity of the displacement $X_{\alpha, \vec{t}} \stackrel{\text{def}}{=} \delta R_{\alpha, \vec{t}}$.
If the lattice has a translational symmetry, we can exploit

$$\begin{aligned} C_{\alpha, \vec{t}, \beta, \vec{t}'} &= C_{\alpha, \vec{0}, \beta, \vec{t}' - \vec{t}} \quad \text{and} \\ W_{\alpha, \vec{t}, \beta, \vec{t}', \gamma, \vec{t}''} &= W_{\alpha, \vec{0}, \beta, \vec{t}' - \vec{t}, \gamma, \vec{t}'' - \vec{t}} \end{aligned} \quad (7.42)$$

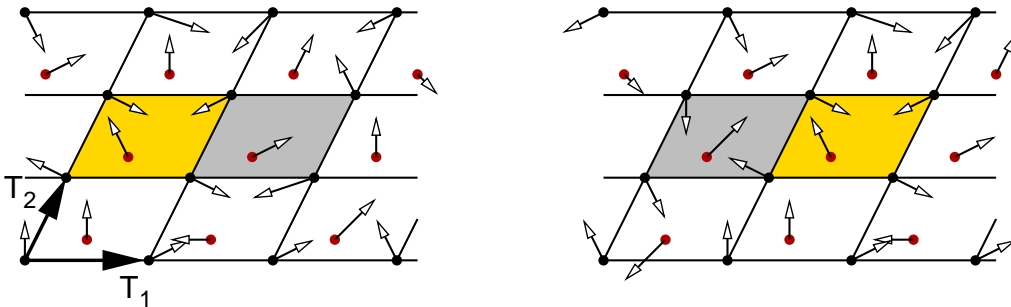


Fig. 7.3: Demonstration of a shifted displacement vector. The displacement vector $\vec{X}' = \delta \vec{R}'$, shown in the graph on the right side, is obtained by shifting \vec{X} , the one in the left graph, by \vec{T}_1 . I.e. $X'_{\alpha, \vec{t}} = X_{\alpha, \vec{t} - \vec{T}_1}$. The unit cell is spanned by the two primitive lattice vectors \vec{T}_1 and \vec{T}_2 . The unit cell has two atoms, one marked as black and the other as red bullets.

7.4.2 Eigenstates of the lattice translation:

The lattice translation operator \hat{S}_j is defined so that it shifts the entire displacement vector by one primitive lattice vector \vec{T}_j . It transforms the displacement vector $\vec{X} \stackrel{\text{def}}{=} \delta\vec{R}$ having components $X_{\alpha,\vec{r}}$ into the shifted displacement vector \vec{X}' with components $X'_{\alpha,\vec{r}} = X_{\alpha,\vec{r}-\vec{T}_j}$.¹⁰

The lattice translation operator is represented as a matrix acting on the displacement vector $\delta\vec{R}$.

$$\vec{X}' = \mathbf{S}(\vec{T}_j)\vec{X} \quad \text{with} \quad S_{\alpha,\vec{r};\beta\vec{r}'}(\vec{T}_j) = \delta_{\alpha,\beta}\delta_{\vec{r}-\vec{T}_j,\vec{r}'} \quad (7.43)$$

so that

$$X'_{\alpha,\vec{r}} = \sum_{\beta,\vec{r}'} S_{\alpha,\vec{r};\beta\vec{r}'} X_{\beta,\vec{r}'} \stackrel{\text{Eq. 7.43}}{=} \sum_{\beta,\vec{r}'} \delta_{\alpha,\beta}\delta_{\vec{r}-\vec{T}_j,\vec{r}'} X_{\beta,\vec{r}'} = X_{\alpha,\vec{r}-\vec{T}_j} \quad (7.44)$$

In order to arrive at Bloch's theorem for lattice displacements, we need to determine the eigenstates of the symmetry operator. The procedure is analogous to the derivation of Bloch's theorem for electronic wave functions.

A simultaneous eigenvector of the translations $\mathbf{S}(\vec{T}_j)$ along the three primitive lattice translation vectors $\vec{T}_1, \vec{T}_2, \vec{T}_3$ obeys the eigenvalue equations¹¹ (see also Eq. 10.1 of [4]) with eigenvalues $e^{-i\vec{k}\vec{T}_j}$

$$\begin{aligned} \underbrace{\mathbf{S}(\vec{T}_j)\vec{X}}_{X_{\alpha,\vec{r}-\vec{T}_j}} &= \vec{X}e^{-i\vec{k}\vec{T}_j} & (7.45) \\ \Rightarrow X_{\alpha,\vec{r}-\vec{T}_j} &\stackrel{\text{Eq. 7.44}}{=} X_{\alpha,\vec{r}}e^{-i\vec{k}\vec{T}_j} \quad \text{for } j = 1, 2, 3 \\ \times \exp\left(\frac{-i\vec{k}(\vec{r}-\vec{T}_j)}{\Rightarrow}\right) X_{\alpha,\vec{r}-\vec{T}_j} &e^{-i\vec{k}(\vec{r}-\vec{T}_j)} \stackrel{\text{Eq. 7.44}}{=} X_{\alpha,\vec{r}}e^{-i\vec{k}\vec{r}} \quad \text{for } j = 1, 2, 3 \\ \Rightarrow X_{\alpha,\vec{r}}e^{-i\vec{k}\vec{r}} &\stackrel{\text{transl.invariant}}{\Rightarrow} X_{\alpha,\vec{r}}e^{-i\vec{k}\vec{r}} = X_{\alpha,\vec{0}} & (7.46) \end{aligned}$$

The product $X_{\alpha,\vec{r}}e^{-i\vec{k}\vec{r}}$ is the same in every unit cell, i.e. it is translationally invariant.

Hence, an eigenstate of the lattice translation vector has the form of a Bloch state, namely a product of a displacement vector having lattice periodicity and a phase factor.

$$X_{\alpha,\vec{r}} = \underbrace{X_{\alpha,\vec{0}}}_{\text{periodic}} \underbrace{e^{i\vec{k}\vec{r}}}_{\text{phase factor}} \quad (7.47)$$

BLOCH THEOREM FOR LATTICE VIBRATIONS

The eigenmodes Eq. 7.32 of a lattice are eigenstates of the lattice translation. Thus, they have the form given in Eq. 7.47, namely^a

$$X_{\alpha,\vec{r}} = \frac{1}{\sqrt{M_\alpha}} U_\alpha(\vec{k}) e^{i\vec{k}\vec{r}} \quad (7.48)$$

which is the product of a displacement vector $M^{-\frac{1}{2}}\vec{U}_n(\vec{k})$, which is periodic with the lattice, and a phasefactor $e^{i\vec{k}\vec{r}}$.

This theorem is analogous to the Bloch theorem for electrons Eq. 4.29 given on p. 131 and to Eq. 4.43 on p. 141.

^aThe mass weighting at this point is not essential but has been included for the sake of consistency of symbols.

¹⁰Note that the lattice translation is not added to the displacement \vec{X} , but to the unit-cell index \vec{r} , so that different components of \vec{X} are exchanged.

¹¹In order to bring the eigenvalues into this form, I exploited that the eigenvalue of a unitary matrix is complex-valued and has the absolute value 1. Thus, the eigenvalues can be written $e^{i\phi_j}$ with real-valued phases ϕ_j . From $\vec{k}\vec{T}_j = \phi_j$ we can obtain directly the wave vector $\vec{k} = \vec{\phi}\vec{T}^{-1}$.

7.4.3 Block diagonalization of the dynamical matrix

Let us now consider the Lagrangian in terms of eigenstates of the translation operator

$$\delta R_{\alpha, \vec{\tau}} = \sum_{\vec{k} \in \Omega_G, n} \frac{1}{\sqrt{M_\alpha}} U_{\alpha, n}(\vec{k}) e^{i\vec{k}\vec{\tau}} Q_n(\vec{k}) \quad (7.49)$$

The variables $Q_n(\vec{k}, t)$ are called **normal coordinates**.

The sum in Eq. 7.49 is performed over all k-points on the grid defined above as the reciprocal-lattice vectors of the supercell. We already did the mass weighting. The vectors $\vec{U}_n(\vec{k})$ remain undetermined at the moment except for their orthonormality¹²

$$\vec{U}_m^*(\vec{k}) \vec{U}_n(\vec{k}) = \delta_{m,n} \quad (7.50)$$

and that they are complete within the space of distortions in one unit cell.

$$\begin{aligned} E_{\text{harm}} &\stackrel{\text{Eq. 7.41}}{=} \frac{1}{2} \sum_{\vec{\tau}, \vec{\tau}'} \delta \vec{R}_{\vec{\tau}} \mathbf{C}_{\vec{\tau}, \vec{\tau}'} \delta \vec{R}_{\vec{\tau}'} \\ &\stackrel{\text{Eq. 7.49}}{=} \frac{1}{2} \sum_{\vec{\tau}, \vec{\tau}'} \sum_{\vec{k}, \vec{k}'} \sum_{m, n} Q_m^*(\vec{k}) e^{-i\vec{k}\vec{\tau}} \vec{U}_m^*(\vec{k}) \underbrace{\frac{1}{\sqrt{M}} \mathbf{C}_{\vec{\tau}, \vec{\tau}'}}_{\mathbf{C}_{\vec{\tau}, \vec{\tau}' - \vec{\tau}}} \frac{1}{\sqrt{M}} \vec{U}_n(\vec{k}') e^{i\vec{k}'\vec{\tau}'} Q_n(\vec{k}') \\ &= \frac{1}{2} \sum_{\vec{k}, \vec{k}'} \underbrace{\left[\sum_{\vec{\tau}} e^{i(\vec{k}' - \vec{k})\vec{\tau}} \right]}_{\mathcal{N} \sum_{\vec{G}} \delta_{\vec{k} - \vec{k}' - \vec{G}}} \sum_{m, n} Q_m^*(\vec{k}) \vec{U}_m^*(\vec{k}) \underbrace{\left[\sum_{\vec{\tau}'} \frac{1}{\sqrt{M}} \mathbf{C}_{\vec{\tau}, \vec{\tau}' - \vec{\tau}} \frac{1}{\sqrt{M}} e^{i\vec{k}'(\vec{\tau}' - \vec{\tau})} \right]}_{\mathbf{D}(\vec{k}')} \vec{U}_n(\vec{k}') Q_n(\vec{k}') \\ &= \frac{1}{2} \mathcal{N} \sum_{\vec{k} \in \Omega_G} \sum_{m, n} Q_m^*(\vec{k}) \underbrace{\vec{U}_m^*(\vec{k}) \mathbf{D}(\vec{k}) \vec{U}_n(\vec{k})}_{\sim d_n(\vec{k}) \delta_{m,n} \text{ (Eq. 7.55 below)}} Q_n(\vec{k}) \end{aligned} \quad (7.51)$$

where $\mathcal{N} = \mathcal{N}_1 \mathcal{N}_2 \mathcal{N}_3$.

We used the identity

$$\left[\sum_{\vec{\tau}} e^{i(\vec{k}' - \vec{k})\vec{\tau}} \right] = \mathcal{N} \sum_{\vec{G}} \delta_{\vec{k} - \vec{k}' - \vec{G}} \quad (7.52)$$

Within the supercell containing \mathcal{N} primitive unit cells, two plane waves $e^{i\vec{k}\vec{\tau}}$ from the k-point grid are orthogonal (in the sense of Eq. 7.52). If the difference of the wave vectors $\vec{k} - \vec{k}'$ vanishes modulo a reciprocal lattice vector, the product of the plane waves is unity, i.e. $e^{i(\vec{k} - \vec{k}')\vec{\tau}} = 1$ for $\vec{k} = \vec{k}'$, and the sum over $\vec{\tau}$ adds up to \mathcal{N} .

For the following argument, we will require that the k-points are taken from the first Brillouin zone rather than from a box spanned by the reciprocal lattice vectors $\vec{g}_1, \vec{g}_2, \vec{g}_3$.¹³ Because the two wave vectors, \vec{k} and \vec{k}' , within first Brillouin zone can not add up to reciprocal lattice vector other than $\vec{G} = 0$, the sum over reciprocal lattice vectors in Eq. 7.52 can be removed. We will see below, that the reciprocal lattice vectors will become important for the evaluation of anharmonic terms.

In Eq. 7.51, we obtain the expected result, namely that the contributions from different wave vectors are completely independent of each other, and that the harmonic energy can be expressed as a sum over contributions from k-points.

We introduced here the k-dependent **dynamical matrix**¹⁴

$$D_{\alpha, \beta}(\vec{k}) \stackrel{\text{def}}{=} \sum_{\vec{\tau}} D_{\alpha, \vec{\tau}, \beta, \vec{\tau}} e^{i\vec{k}\vec{\tau}} \quad (7.53)$$

¹²This requirement is imposed to simplify the kinetic energy contribution to the Lagrangian.

¹³Because the k-points of the first Brillouin zone and the primitive unit cell spanned by the lattice translation vectors are related by a reciprocal lattice vectors, the essence of the argument is independent of this choice. It is only slightly less obvious.

¹⁴Compare the equation for the k-dependent dynamical matrix with the one, Eq. 4.44 for the k-dependent Hamilton matrix.

Up to this point, the matrices $\mathbf{U}(\vec{k})$ were free parameters of the Ansatz Eq. 7.49. Now, we specify them in terms of the eigenvectors of the dynamical matrix. We diagonalize the k-dependent dynamical matrix¹⁵, which then determines the eigenvalues d_n and the eigenvectors \vec{U}_n , i.e.

$$\sum_{\beta} D_{\alpha,\beta}(\vec{k}) U_{\beta,n}(\vec{k}) = U_{\alpha,n}(\vec{k}) d_n(\vec{k}) \quad \text{with} \quad \sum_{\alpha} U_{\alpha,m}^*(\vec{k}) U_{\alpha,n}(\vec{k}) \stackrel{\text{Eq. 7.50}}{=} \delta_{m,n} \quad (7.55)$$

The eigenvalues $d_n(\vec{k})$ are identified with the squared frequencies.¹⁶

Thus, we obtain a **dispersion relation for phonons**

$$\omega_n(\vec{k}) = \sqrt{d_n(\vec{k})} \quad (7.56)$$

The dynamical matrices for wave vectors \vec{k} and $-\vec{k}$ are related, i.e.

$$D_{\alpha,\beta}(-\vec{k}) \stackrel{\text{Eq. 7.53}}{=} D_{\alpha,\beta}^*(\vec{k}) \quad \text{and} \quad (7.57)$$

$$\omega_n(-\vec{k}) = \omega_n(\vec{k}) \quad \text{and} \quad (7.58)$$

$$U_{\alpha,n}(-\vec{k}) = U_{\alpha,n}^*(-\vec{k}). \quad (7.59)$$

With these definitions, namely Eq. 7.49 with Eq. 7.55, the harmonic potential energy obtains the simple form

$$E_{\text{harm}} \stackrel{\text{Eq. 7.51}}{=} \frac{1}{2} \mathcal{N} \sum_{\vec{k} \in \Omega_G} \sum_n \omega_n^2(\vec{k}) Q_n^*(\vec{k}) Q_n(\vec{k}) \quad (7.60)$$

As shown below in Eq. 7.64, also the kinetic energy is a sum over the states introduced above. This shows that the eigenmodes of the harmonic problem have the form of Bloch waves.

LATTICE VIBRATIONS IN TERMS OF NORMAL COORDINATES

The displacements $\delta \vec{R}_{\alpha,\vec{\tau}}$ can be expressed in terms of lattice eigenmodes and the **normal coordinates**^a $Q_n(\vec{k})$ as

$$\delta R_{\alpha,\vec{\tau}} \stackrel{\text{Eq. 7.49}}{=} \sum_{\vec{k}} \sum_n \frac{1}{\sqrt{M_{\alpha}}} U_{\alpha,n}(\vec{k}) e^{i\vec{k}\vec{\tau}} Q_n(\vec{k}) \quad (7.61)$$

$$\Leftrightarrow Q_n(\vec{k}) \stackrel{\text{Eq. 7.61}}{=} \frac{1}{\mathcal{N}} \sum_{\alpha,\vec{\tau}} e^{-i\vec{k}\vec{\tau}} U_{\alpha,n}^*(\vec{k}) \sqrt{M_{\alpha}} \delta R_{\alpha,\vec{\tau}} \quad (7.62)$$

The matrices $\mathbf{U}(\vec{k})$ are built from the eigenvectors $\vec{u}_n(\vec{k})$ of the dynamical matrix

$$D_{\alpha,\beta}(\vec{k}) \stackrel{\text{Eqs. 7.16, 7.53}}{=} \frac{1}{\sqrt{M_{\alpha}}} \left[\sum_{\vec{\tau}} C_{\alpha,\vec{\tau},\beta,\vec{\tau}} e^{i\vec{k}\vec{\tau}} \right] \frac{1}{\sqrt{M_{\beta}}} \quad (7.63)$$

This is a complete Ansatz for the displacements and therefore it involves no approximation. The eigenmodes and frequencies are, nevertheless, defined solely through the harmonic terms.

^aCompare Eq. 3.2.10 of Jones and March[49]. Our definitions for the normal coordinates differ by a factor $\sqrt{\mathcal{N}}$.

¹⁵The eigenvectors are orthonormal and the eigenvalues are real-valued, because the k-dependent dynamical matrix is hermitian. The latter property is shown as follows:

$$D(\vec{k}) \stackrel{\text{Eq. 7.53}}{=} \sum_{\vec{\tau}} D_{\vec{\tau},\vec{\tau}} e^{i\vec{k}\vec{\tau}} = \left(\sum_{\vec{\tau}} D_{\vec{\tau},\vec{\tau}} e^{-i\vec{k}\vec{\tau}} \right)^{\dagger} = \left(\sum_{\vec{\tau}} D_{\vec{\tau},-\vec{\tau}} e^{-i\vec{k}\vec{\tau}} \right)^{\dagger} = \left(\sum_{\vec{\tau}} D_{\vec{\tau},\vec{\tau}} e^{i\vec{k}\vec{\tau}} \right)^{\dagger} \stackrel{\text{Eq. 7.53}}{=} D^{\dagger}(\vec{k}) \quad (7.54)$$

where we used translational invariance and that the dynamical matrix is symmetric and real-valued, i.e. $D_{\alpha,\vec{\tau},\beta,\vec{\tau}} = D_{\beta,\vec{\tau},\alpha,\vec{\tau}}^*$

¹⁶This identification rests on the equations of motion derived below.

The transformation Eq. 7.62 to normal coordinates can be applied within the context of the Born-Huang framework (section 2.1.2 on p. 45) either to the Schrödinger equation for the nuclear wave function¹⁷ $\Theta_0(\{\vec{R}_{\alpha,\vec{r}}\}, t)$, or to the classical equations of motion for the nuclear trajectories $\delta\vec{R}_{\alpha,\vec{r}}(t)$ in the context of a classical approximation.

If the transformation Eq. 7.62 is applied to the nuclear Schrödinger equation, the theory will arrive at a quantum field theory for the phonon amplitudes. When the nuclei are treated as classical particles, we will arrive at a classical field theory for the phonon amplitudes. This classical field theory is on the same level of quantization as the one-particle Schrödinger equation for an electron.

7.4.4 Energies and Lagrangian in normal coordinates

For the sake of completeness let us calculate the kinetic energy and the anharmonic terms in terms of normal coordinates $Q_n(\vec{k}, t)$.

$$\begin{aligned}
E_{kin} &\stackrel{\text{Eq. 7.41}}{=} \frac{1}{2} \sum_{\vec{r}, \vec{r}'} \delta\vec{R}_{\vec{r}} \mathbf{M}_{\vec{r}, \vec{r}'} \delta\dot{\vec{R}}_{\vec{r}'} \\
&\stackrel{\text{Eq. 7.49}}{=} \frac{1}{2} \sum_{\vec{r}, \vec{r}'} \sum_{\vec{k}, \vec{k}'} \sum_{m,n} \dot{Q}_m^*(\vec{k}) e^{-i\vec{k}\vec{r}} \underbrace{\frac{1}{\sqrt{M}} \mathbf{M}_{\vec{r}, \vec{r}'} \frac{1}{\sqrt{M}}}_{\mathbf{1}\delta_{\vec{r}, \vec{r}'}} \bar{U}_n(\vec{k}') e^{i\vec{k}'\vec{r}'} \dot{Q}_n(\vec{k}') \\
&= \frac{1}{2} \sum_{\vec{k}, \vec{k}'} \underbrace{\left[\sum_{\vec{r}} e^{i(\vec{k}' - \vec{k})\vec{r}} \right]}_{\mathcal{N}\delta_{\vec{k}, \vec{k}'}} \sum_{m,n} \dot{Q}_m^*(\vec{k}) \underbrace{\bar{U}_m^*(\vec{k}) \bar{U}_n(\vec{k}')}_{=\delta_{m,n} \text{ Eq. 7.50}} \dot{Q}_n(\vec{k}') \\
&= \frac{1}{2} \mathcal{N} \sum_{\vec{k} \in \Omega_G} \sum_n \dot{Q}_n^*(\vec{k}) \dot{Q}_n(\vec{k}) \tag{7.64}
\end{aligned}$$

$$\begin{aligned}
E_{anharm} &\stackrel{\text{Eq. 7.41}}{=} \frac{1}{3!} \sum_{\vec{r}, \vec{r}', \vec{r}''} \sum_{\alpha, \beta, \gamma} W_{\alpha, \vec{r}, \beta, \vec{r}', \gamma, \vec{r}''} \delta R_{\alpha, \vec{r}} \delta R_{\gamma, \vec{r}'} \delta R_{\beta, \vec{r}''} \\
&\stackrel{\text{Eq. 7.49}}{=} \frac{1}{3!} \sum_{\vec{r}, \vec{r}', \vec{r}''} \sum_{\alpha, \beta, \gamma} \underbrace{W_{\alpha, \vec{r}, \beta, \vec{r}', \gamma, \vec{r}''}}_{=W_{\alpha, \delta, \beta, \vec{r} - \vec{r}, \gamma, \vec{r}'' - \vec{r}}} \sum_{\vec{k}, \vec{k}', \vec{k}'' \in \Omega_G} \sum_{l, m, n} \\
&\quad \frac{1}{\sqrt{M_\alpha}} U_{\alpha, l}(\vec{k}) e^{i\vec{k}\vec{r}} Q_l(\vec{k}) \frac{1}{\sqrt{M_\beta}} U_{\beta, m}(\vec{k}') e^{i\vec{k}'\vec{r}'} Q_m(\vec{k}') \frac{1}{\sqrt{M_\gamma}} U_{\gamma, n}(\vec{k}'') e^{i\vec{k}''\vec{r}''} Q_n(\vec{k}'') \\
&= \frac{1}{3!} \sum_{\vec{k}, \vec{k}', \vec{k}'' \in \Omega_G} \sum_{l, m, n} \underbrace{\sum_{\vec{r}} e^{i(\vec{k} + \vec{k}' + \vec{k}'')\vec{r}}}_{\mathcal{N} \sum_{\vec{c}} \delta_{\vec{k} + \vec{k}' + \vec{k}'' - \vec{c}}} \left[\sum_{\alpha, \beta, \gamma} \left[\sum_{\vec{r}, \vec{r}'} \frac{W_{\alpha, \delta, \beta, \vec{r} - \vec{r}, \gamma, \vec{r}'' - \vec{r}}}{\sqrt{M_\alpha M_\beta M_\gamma}} e^{i\vec{k}'(\vec{r}' - \vec{r})} e^{i\vec{k}''(\vec{r}'' - \vec{r})} \right] \right. \\
&\quad \left. \times U_{\alpha, l}(\vec{k}) U_{\beta, m}(\vec{k}') U_{\gamma, n}(\vec{k}'') \right] Q_l(\vec{k}) Q_m(\vec{k}') Q_n(\vec{k}'') \\
&= \frac{1}{3!} \mathcal{N} \sum_{\vec{k}, \vec{k}', \vec{k}'' \in \Omega_G} \sum_{l, m, n} X_{l, m, n}(\vec{k}, \vec{k}', \vec{k}'') Q_l(\vec{k}) Q_m(\vec{k}') Q_n(\vec{k}'') \tag{7.65}
\end{aligned}$$

with

¹⁷The nuclear wave function is a multicomponent wave function with one component for each Born-Oppenheimer surface. In the present discussion, we have excluded electronic excitations, so that we need to consider only the component from the lowest Born-Oppenheimer surface. In the more general case the very same transformation, derived from the lowest Born-Oppenheimer sheet, is applied to all components of the nuclear wave function.

ANHARMONIC SCATTERING TERMS

a

$$X_{l,m,n}(\vec{k}, \vec{k}', \vec{k}'') \stackrel{\text{def}}{=} \left(\sum_{\vec{G}} \delta_{\vec{k} + \vec{k}' + \vec{k}'' - \vec{G}} \right) \times \sum_{\alpha, \beta, \gamma} \left[\sum_{\vec{t}, \vec{t}', \vec{t}''} \frac{W_{\alpha, \vec{0}, \beta, \vec{t}, \gamma, \vec{t}''}}{\sqrt{M_\alpha M_\beta M_\gamma}} e^{i\vec{k}\vec{t}} e^{i\vec{k}'\vec{t}'} \right] U_{\alpha, l}(\vec{k}) U_{\beta, m}(\vec{k}') U_{\gamma, n}(\vec{k}'') \quad (7.66)$$

^acompare with Eq. (3.13.17) of Jones and March, Vol.1[49].

The first term in Eq. 7.66 expresses momentum conservation, which is described in detail below in section 10.3.1 on p. 331.

Why is there is a reciprocal lattice vector appearing in $\sum_{\vec{t}} e^{i(\vec{k} + \vec{k}' + \vec{k}'')\vec{t}} = \mathcal{N} \sum_{\vec{G}} \delta_{\vec{k} + \vec{k}' + \vec{k}'' - \vec{G}}$, when three phonons take part in a collision, while no reciprocal lattice vector is considered, when only two wave vectors are involved? The reason is that the difference of two wave vectors \vec{k} in the primitive reciprocal unit cell can never become equal to a reciprocal lattice vector \vec{G} . Therefore, the sum over \vec{G} in $\sum_{\vec{G}} \delta_{\vec{k} - \vec{k}' - \vec{G}}$ is superfluous. The sum of three wave vectors, on the other hand, can add up to a reciprocal lattice vector.

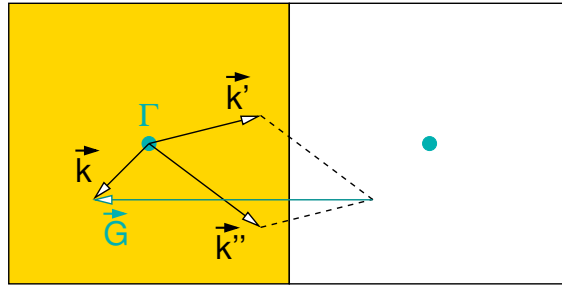


Fig. 7.4: Sketch to show that three wave vectors in the Brillouin zone can add up to a reciprocal lattice vector $\vec{G} = \vec{k} - \vec{k}' - \vec{k}''$. Scattering processes, which involve reciprocal lattice vectors \vec{G} to conserve momentum, are called **umklapp processes**.

From Eqs. 7.64, 7.60, and 7.65, we obtain the Lagrangian

$$\mathcal{L} = \mathcal{N} \left\{ \sum_{\vec{k} \in \Omega_{G,n}} \left(\frac{1}{2} \dot{Q}_n^*(\vec{k}) \dot{Q}_n(\vec{k}) - \frac{1}{2} \omega_n^2(\vec{k}) Q_n^*(\vec{k}) Q_n(\vec{k}) \right) - \sum_{\vec{k}, \vec{k}', \vec{k}'' \in \Omega_G} \sum_{l,m,n} \frac{1}{3!} X_{l,m,n}(\vec{k}, \vec{k}', \vec{k}'') Q_l(\vec{k}) Q_m(\vec{k}') Q_n(\vec{k}'') \right\} \quad (7.67)$$

Real-valued displacements: The Lagrangian Eq. 7.67 does not seem to be purely real-valued. The real-valued property of the Lagrangian, however, is hidden in the requirement that the distortions are purely real-valued.

The ansatz Eq. 7.49

$$\delta R_{\alpha, \vec{t}}(t) \stackrel{\text{Eq. 7.49}}{=} \sum_{\vec{k} \in \Omega_{G,n}} \frac{1}{\sqrt{M_\alpha}} U_{\alpha, n}(\vec{k}) e^{i\vec{k}\vec{t}} Q_n(\vec{k}, t) \quad (7.68)$$

can be made real-valued by requiring

$$Q_n(\vec{k}, t) = Q_n^*(-\vec{k}, t) \quad (7.69)$$

$$U_{\alpha,n}(\vec{k}) = U_{\alpha,n}^*(-\vec{k}) \quad (7.70)$$

The second relation follows from the fact that the dynamical matrix $D_{\alpha,\vec{\tau},\beta,\vec{\tau}}$ is real-valued. A consequence of this property is that inverting the wave vector of the \mathbf{k} -dependent dynamical matrix $\mathbf{D}(\vec{k})$ is the same as taking the complex conjugate of it.

$$\mathbf{D}(\vec{k}) \stackrel{\text{Eq. 7.53}}{=} \sum_{\vec{\tau}} \mathbf{D}_{\vec{0},\vec{\tau}} e^{i\vec{k}\vec{\tau}} = \left(\sum_{\vec{\tau}} \mathbf{D}_{\vec{0},\vec{\tau}} e^{-i\vec{k}\vec{\tau}} \right)^* = \mathbf{D}^*(-\vec{k}) \quad (7.71)$$

This property directly produces complex-conjugate eigenvectors for the inverted wave vector.

We use the relation between the amplitudes with opposite wave vector to express the Lagrangian without referring to the complex conjugates.

$$\begin{aligned} \mathcal{L} \stackrel{\text{Eq. 7.67}}{=} \mathcal{N} \left\{ \sum_{\vec{k},n} \left(\frac{1}{2} \dot{Q}_n(-\vec{k}) \dot{Q}_n(\vec{k}) - \frac{1}{2} \omega_n^2(\vec{k}) Q_n(-\vec{k}) Q_n(\vec{k}) \right) \right. \\ \left. - \sum_{\vec{k},\vec{k}',\vec{k}'' \in \Omega_G} \sum_{l,m,n} \frac{1}{3!} X_{l,m,n}(\vec{k}, \vec{k}', \vec{k}'') Q_l(\vec{k}) Q_m(\vec{k}') Q_n(\vec{k}'') \right\} \quad (7.72) \end{aligned}$$

Euler-Lagrange equations: The Euler-Lagrange equations are obtained as

$$\begin{aligned} 0 &= \frac{d}{dt} \frac{\partial \mathcal{L}}{\partial \dot{Q}_n(-\vec{k})} - \frac{\partial \mathcal{L}}{\partial Q_n(-\vec{k})} \\ &\stackrel{\text{Eq. 7.72}}{=} \mathcal{N} \left\{ \ddot{Q}_n(\vec{k}) + \omega_n^2(\vec{k}) Q_n(\vec{k}) + \sum_{\vec{k}',\vec{k}'' \in \Omega_G} \sum_{l,m} \frac{1}{2} X_{n,l,m}(-\vec{k}, \vec{k}', \vec{k}'') Q_l(\vec{k}') Q_m(\vec{k}'') \right\} \quad (7.73) \end{aligned}$$

so that

EQUATIONS OF MOTION IN NORMAL COORDINATES

$$\ddot{Q}_n(\vec{k}) = -\omega_n^2(\vec{k}) Q_n(\vec{k}) - \sum_{\vec{k}',\vec{k}'' \in \Omega_G} \sum_{l,m} \frac{1}{2} X_{n,l,m}(-\vec{k}, \vec{k}', \vec{k}'') Q_l(\vec{k}') Q_m(\vec{k}'') \quad (7.74)$$

The requirement that displacements are real-valued translates into the condition

$$Q_n(\vec{k}, t) \stackrel{\text{Eq. 7.69}}{=} Q_n^*(-\vec{k}, t) \quad (7.75)$$

This is now the starting point of the discussion of lattice vibrations.

7.5 Phonons

In the previous section, we became familiar with Bloch states for the lattice vibrations, which lead us to the dispersion relation $\hbar\omega_n(\vec{k})$. This dispersion relation is analogous to that for electrons discussed in the earlier chapters. The atom-displacements can be identified with displacement fields¹⁸ with the corresponding values at the equilibrium positions.

¹⁸A field is a function of space (and time) as opposed to coordinates such as atomic positions.

We still have a second-order differential equation in time for the real-valued displacements. This is in contrast to the Schrödinger equation, which is a first-order differential equation in time for a complex-valued field.

The “normal” approach to teaching this subject is to proceed directly to quantized atomic positions and from there to quantum field theory. This mingles up concepts with those from quantum field theory. I prefer to proceed in two steps: First, I prepare the terminology within a classical field theory. The step to a quantum field theory is then fairly straight-forward.

Besides clarifying the evolution between classical (point) theory, classical field theory, quantum (point) theory and quantum field theory, we will become familiar with classical equations of motion for the lattice distortions that are analogous to the Schrödinger equation.

The analogies described above are of conceptual nature. Another aspect of this section is to define the ingredients quasiparticle scattering entering the phonon-Boltzmann equation. The derivation of the scattering terms of the Boltzmann equation is described in a later chapter (chapter 10), that, unfortunately, goes beyond what I can cover in a course.

7.5.1 One-dimensional harmonic oscillator

The phonon amplitudes are closely related to the ladder operators of the quantum-mechanical harmonic oscillator. In a quantum description of the nuclei, each vibrational mode is identified with one harmonic oscillator. The ladder operators of this harmonic oscillator create or annihilate the phonons with a specific wave vector and particle index.

We will translate the creation and annihilation operators into classical variables and explore their physical meaning.

Quantum harmonic oscillator: We start with the quantum mechanical theory: The Hamilton operator of the harmonic oscillator with eigenfrequency ω_0 .

$$\begin{aligned}
 H(\hat{p}, \hat{x}) &= \frac{\hat{p}^2}{2m} + \frac{1}{2}m\omega_0^2\hat{x}^2 = \frac{1}{2m} \{ \hat{p}^2 + m^2\omega_0^2\hat{x}^2 \} \\
 &= \frac{1}{2m} \left\{ (-i\hat{p} + m\omega_0\hat{x})(+i\hat{p} + m\omega_0\hat{x}) + m\hbar\omega_0 \frac{i}{\hbar} [\hat{p}, \hat{x}]_- \right\} \\
 &= \hbar\omega_0 \underbrace{\left(\frac{-i\hat{p} + m\omega_0\hat{x}}{\sqrt{2m\hbar\omega_0}} \right)}_{\hat{b}^\dagger} \underbrace{\left(\frac{+i\hat{p} + m\omega_0\hat{x}}{\sqrt{2m\hbar\omega_0}} \right)}_{=\hat{b}} + \frac{1}{2}\hbar\omega_0 \underbrace{\frac{i}{\hbar} [\hat{p}, \hat{x}]_-}_{=1} \\
 &= \hbar\omega_0 \left(\hat{b}^\dagger \hat{b} + \frac{1}{2} \right) \tag{7.76}
 \end{aligned}$$

The eigenvalues of $\hat{b}^\dagger \hat{b}$ are non-negative integers, which is the number of energy quanta $\hbar\omega_0$.

In the case of phonons, this expression will be translated into the number of phonons. Let me already use the terminology of phonons, considering the harmonic oscillator as a system with a single normal mode. I will call the observable $\hat{b}^\dagger \hat{b}$ the **phonon number** and \hat{b} the **phonon amplitude**. The phonon amplitude is not hermitian and therefore not an observable.

Classical harmonic oscillator: Now, we translate the quantum harmonic oscillator into classical mechanics. The purpose is to obtain a better understanding of a terms, that seem inseparably interwoven with the terminology of quantum theory. In a classical description, (1) the Hamilton operator Eq. 7.76 is turned into the Hamilton function $H(p, x)$, (2) the momenta and coordinates are translated into numbers, and, correspondingly, (3) the commutators vanish.

The classical (non-quantum) version of the harmonic oscillator described in Eq. 7.76 has the Hamilton function

$$H(p, x) = \frac{p^2}{2m} + \frac{1}{2}m\omega_0^2x^2 = \hbar\omega_0 b^*(p, x)b(p, x), \tag{7.77}$$

where the phonon amplitude is a function in phase space

$$b(p, x) = \frac{ip + m\omega_0 x}{\sqrt{2m\hbar\omega_0}}. \quad (7.78)$$

Let me emphasize the point that the phonon amplitude is usually only used in the context of quantum mechanical problems. In quantum mechanics it is a key quantity for what is called **second quantization**, which leads to quantum field theory. Here we have introduced the phonon amplitude for a purely classical problem. This allows one to understand the underlying physics in a much simpler context.

Positions and momenta can be recovered from the phonon amplitude b via

$$\begin{aligned} p &= -\frac{i}{2}\sqrt{2m\hbar\omega_0}(b - b^*) \\ x &= \frac{1}{2m\omega_0}\sqrt{2m\hbar\omega_0}(b + b^*) \end{aligned} \quad (7.79)$$

Thus, the full information of the real-valued trajectory $(p(t), x(t))$ is contained in one complex-valued trajectory $b(t)$.

The equation of motion is obtained using Hamilton's equations of motion.

$$\begin{aligned} \partial_t b(p, x) &= \frac{\partial b}{\partial p} \dot{p} + \frac{\partial b}{\partial x} \dot{x} \\ &= \frac{\partial b}{\partial p} \left(-\frac{\partial H}{\partial x} \right) + \frac{\partial b}{\partial x} \left(\frac{\partial H}{\partial p} \right) \\ &= \frac{i}{\sqrt{2m\hbar\omega_0}} \cdot (-m\omega_0^2 x) + \frac{m\omega_0}{\sqrt{2m\hbar\omega_0}} \cdot \left(\frac{p}{m} \right) \\ &= -i\omega_0 \frac{ip + m\omega_0 x}{\sqrt{2m\hbar\omega_0}} = -i\omega_0 b(p, x) \end{aligned} \quad (7.80)$$

Rather than a differential equation of second order for the real-valued coordinate $x(t)$, I obtain a first-order differential equation of motion

$$i\hbar\partial_t b(t) = \hbar\omega_0 b(t) \quad (7.81)$$

for the complex-valued phonon amplitude $b(t)$.

Analogy with Schrödinger's equation: There is a close analogy between the equation of motion Eq. 7.81 for the phonon amplitude b and Schrödinger's equation.

$$i\hbar\partial_t |\psi(t)\rangle = \underbrace{\sum_n |\varphi_n\rangle \epsilon_n \langle \varphi_n|}_{\hat{H}} |\psi(t)\rangle \quad \Rightarrow \quad i\hbar\partial_t \underbrace{\langle \varphi_n |}_{c_n(t)} |\psi(t)\rangle = \epsilon_n \underbrace{\langle \varphi |}_{c_n(t)} |\psi(t)\rangle \quad (7.82)$$

where ϵ_n are the eigenvalues and $|\varphi_n\rangle$ are the eigenstates of the one-particle Hamiltonian. The phonon amplitude is translated into the coefficients $\langle \varphi_n | \psi(t) \rangle$ of a quantum mechanical wave function. On this level of the theory, the Schrödinger equation is a classical field theory on the same level as the field theory of distortion waves of the nuclear positions. A full quantum theory turns the classical phonon amplitude b into an operator \hat{b} and similarly the wave function $\psi(\vec{x})$ into an field operator $\hat{\psi}(\vec{x})$. The result is that the excitations will become quantized with the energy quantum $\hbar\omega_0$ or ϵ_n respectively. This is where the **particle concept**, which we take for granted in classical mechanics, emerges naturally from a field theory.

Trajectories: Let me return to the equations of motion for the phonon amplitude. The trajectory of the phonon amplitude is

$$b(t) = e^{-i\omega_0 t} b(0) \quad (7.83)$$

In the harmonic system, the excitation number b^*b is a constant of motion. This is seen in Eq. 7.83. The reason is that the Hamiltonian is proportional to b^*b and therefore commutes with it. If the Hamiltonian is more complicated, the “excitation number” b^*b will change with time. This change can be described as a scattering process.

Using the definition of the excitation amplitude $b(t)$, Eq. 7.78, and Hamilton’s first equation of motion $\dot{x} = \frac{\partial H}{\partial p} = p/m$, we can track the excitation amplitude $b(t)$ as function of time, for any given trajectory $x(t)$ in coordinate space

$$b(p, x) = \frac{ip + m\omega_0 x}{\sqrt{2m\hbar\omega_0}} \quad (7.84)$$

$$\stackrel{p=m\dot{x}}{\Rightarrow} b(t) = \frac{im\dot{x} + m\omega_0 x}{\sqrt{2m\hbar\omega_0}} = \sqrt{\frac{m}{2\hbar\omega_0}} (i\partial_t + \omega_0)x(t) \quad (7.85)$$

Thus, for any given trajectory $x(t)$ we can extract $b(t)$.

From Newton’s equations of motion to that of phonon trajectories: Newton’s equation of motion are a second-order differential equation

$$m\ddot{x} = -m\omega_0^2 x \quad \stackrel{x \in \mathbb{R}}{\Rightarrow} x(t) = A^* e^{i\omega t} + A e^{-i\omega t} \quad (7.86)$$

As a consequence, there are two linearly independent solutions.

The phonon amplitude selects one out of these two solutions

$$\begin{aligned} b(t) &\stackrel{\text{Eq. 7.85}}{=} \sqrt{\frac{m}{2\hbar\omega_0}} (i\partial_t + \omega_0) \underbrace{(A^* e^{i\omega_0 t} + A e^{-i\omega_0 t})}_{x(t)} \\ &= \sqrt{\frac{m}{2\hbar\omega_0}} \left(A^* e^{i\omega t} \underbrace{(-\omega_0 + \omega_0)}_{=0} + A e^{-i\omega t} (\omega_0 + \omega_0) \right) \\ &= \sqrt{\frac{2m\omega_0}{\hbar}} A e^{-i\omega t} \end{aligned} \quad (7.87)$$

This is the essence of the fact that the equation of motion Eq. 7.81 for the phonon amplitude is a first-order differential equation, rather than a second-order differential equation like Newton’s equation of motion Eq. 7.86.

Hamilton and Lagrange function in terms of phonon amplitudes: With the total-energy expression

$$E(p, x) = \hbar\omega_0 b^*(p, x)b(p, x) \quad (7.88)$$

we do not have a Hamilton function, which is a function of a generalized coordinate (in this case b) and its canonical conjugate momentum. Thus, we need to find the expression for the canonical momentum for the phonon amplitude.

We construct a Hamilton function by “reverse engineering”. We require that the equation of motion Eq. 7.81 has the form of a Hamilton equation.

$$\dot{b} = \frac{\partial H}{\partial \pi} \quad \Leftrightarrow \quad \dot{b} \stackrel{\text{Eq. 7.81}}{=} \frac{1}{i\hbar} \hbar\omega_0 b \quad (7.89)$$

With the Ansatz $\pi = i\hbar b^*$ for the canonical momentum of the phonon amplitude, we obtain the Hamilton function consistent with the energy

$$H(\pi, b) = -i\omega_0 \pi b \stackrel{!}{=} \hbar\omega_0 b^* b \quad \Leftarrow \quad \pi = i\hbar b^* \quad (7.90)$$

This Hamilton function produces the desired equations of motion

$$\begin{aligned} \dot{b} &= \frac{\partial H}{\partial \pi} = -i\omega_0 b \\ \dot{\pi} &= -\frac{\partial H}{\partial b} = +i\omega_0 \pi \quad \Rightarrow \quad \dot{b}^* = +i\omega_0 b^* \end{aligned} \quad (7.91)$$

Now we can construct the Lagrange function by a Legendre transform

$$\begin{aligned} \mathcal{L}(v, x) &= \text{stat}_{\pi} (\pi v - H(\pi, v)) = \text{stat}_{\pi} (\pi v - [-i\omega_0 \pi b]) \quad \Rightarrow \quad v = -i\omega_0 b (= \dot{b}) \\ &= \underbrace{i\hbar b^*}_{\pi} (\dot{b} + i\omega_0 b) \\ &= b^* (i\hbar \dot{b} - \hbar\omega_0 b) \end{aligned} \quad (7.92)$$

The corresponding Euler-Lagrange equations are

$$\begin{aligned} 0 &= \frac{d}{dt} \frac{\partial \mathcal{L}}{\partial \dot{b}} - \frac{\partial \mathcal{L}}{\partial b} = i\hbar \dot{b}^* + \hbar\omega b^* \\ 0 &= \frac{d}{dt} \frac{\partial \mathcal{L}}{\partial \dot{b}^*} - \frac{\partial \mathcal{L}}{\partial b^*} = -(i\hbar \dot{b} - \hbar\omega b) \end{aligned} \quad (7.93)$$

which are identical to the Hamilton's equation of motion.

Quantization condition:

$$[\hat{\pi}, \hat{b}]_- = \frac{\hbar}{i} \quad \Rightarrow \quad [\hat{b}, \hat{b}^\dagger]_- = 1 \quad (7.94)$$

7.5.2 Back to the normal modes of displacement fields

Let us now generalize the steps from the previous section on the one-dimensional harmonic oscillator to lattice vibrations. The first step is the generalization from the one-dimensional harmonic oscillator to the multi-dimensional harmonic oscillator. The second step will be the introduction of Bloch waves.

From one to many dimensions

We use again the variable $\vec{X} \stackrel{\text{def}}{=} \delta\vec{R}$.

$$\begin{aligned} H(\vec{P}, \vec{X}) &= \frac{1}{2} \vec{P} \frac{1}{\mathbf{M}} \vec{P} + \frac{1}{2} \vec{X} \mathbf{C} \vec{X} \\ &= \frac{1}{2} \left\{ \vec{P} \frac{1}{\sqrt{\mathbf{M}}} \frac{1}{\sqrt{\mathbf{M}}} \vec{P} + \vec{X} \sqrt{\mathbf{M}} \underbrace{\mathbf{D}}_{U\omega^2 U^\dagger} \sqrt{\mathbf{M}} \vec{X} \right\} \\ &= \frac{1}{2} \left\{ \left(-i\vec{P} \frac{1}{\sqrt{\mathbf{M}}} + \vec{X} \sqrt{\mathbf{M}} \sqrt{\mathbf{D}} \right) \left(+i \frac{1}{\sqrt{\mathbf{M}}} \vec{P} + \sqrt{\mathbf{D}} \sqrt{\mathbf{M}} \vec{X} \right) \right\} \\ &= \frac{1}{2} \left\{ \left(-i\vec{P} \frac{1}{\sqrt{\mathbf{M}}} \mathbf{D}^{-\frac{1}{4}} + \vec{X} \sqrt{\mathbf{M}} \mathbf{D}^{\frac{1}{4}} \right) \sqrt{\mathbf{D}} \left(+i \mathbf{D}^{-\frac{1}{4}} \frac{1}{\sqrt{\mathbf{M}}} \vec{P} + \mathbf{D}^{\frac{1}{4}} \sqrt{\mathbf{M}} \vec{X} \right) \right\} \end{aligned} \quad (7.95)$$

Next we diagonalize the dynamical matrix $\mathbf{D} = \mathbf{U}\boldsymbol{\omega}^2\mathbf{U}^\dagger$, where $\boldsymbol{\omega}^2$ is a diagonal matrix holding the eigenvalues of \mathbf{D} , and \mathbf{U} is the unitary matrix with its eigenvectors. The normalization region for the eigenvectors is the entire system, i.e. $\mathbf{U}^\dagger\mathbf{U} = \mathbf{1}$. As the system becomes larger, the size of the eigenvectors at a given atomic site shrinks.

$$\begin{aligned}
H(\vec{P}, \vec{X}) &= \frac{1}{2} \left\{ \left(-i\vec{P} \frac{1}{\sqrt{M}} \mathbf{D}^{-\frac{1}{4}} + \vec{X} \sqrt{M} \mathbf{D}^{\frac{1}{4}} \right) \mathbf{U} \boldsymbol{\omega} \mathbf{U}^\dagger \left(+i\mathbf{D}^{-\frac{1}{4}} \frac{1}{\sqrt{M}} \vec{P} + \mathbf{D}^{\frac{1}{4}} \sqrt{M} \vec{X} \right) \right\} \\
&= \frac{1}{2} \left\{ \underbrace{\left(-i\vec{P} \frac{1}{\sqrt{M}} \mathbf{U} \frac{1}{\sqrt{\boldsymbol{\omega}}} + \vec{X} \sqrt{M} \mathbf{U} \sqrt{\boldsymbol{\omega}} \right)}_{\sqrt{2\hbar b^*}} \boldsymbol{\omega} \underbrace{\left(+i \frac{1}{\sqrt{\boldsymbol{\omega}}} \mathbf{U}^\dagger \frac{1}{\sqrt{M}} \vec{P} + \sqrt{\boldsymbol{\omega}} \mathbf{U}^\dagger \sqrt{M} \vec{X} \right)}_{\sqrt{2\hbar b}} \right\} \\
&= \vec{b}^* \hbar \boldsymbol{\omega} \vec{b} \\
\text{with } \vec{b} &= \frac{1}{\sqrt{2\hbar}} \left(i \frac{1}{\sqrt{\boldsymbol{\omega}}} \mathbf{U}^\dagger \frac{1}{\sqrt{M}} \vec{P} + \sqrt{\boldsymbol{\omega}} \mathbf{U}^\dagger \sqrt{M} \vec{X} \right) \\
b_n &= \frac{1}{\sqrt{2\hbar\omega_n}} \sum_{\alpha, \vec{\tau}} \left(\underbrace{U_{n, \alpha, \vec{\tau}}^\dagger}_{U_{\alpha, \vec{\tau}, n}^*} \frac{1}{\sqrt{M_\alpha}} iP_{\alpha, \vec{\tau}} + \omega_n \underbrace{U_{n, \alpha, \vec{\tau}}^\dagger}_{U_{\alpha, \vec{\tau}, n}^*} \sqrt{M_\alpha} X_{\alpha, \vec{\tau}} \right) \quad (7.96)
\end{aligned}$$

Bloch waves

Editor: Some of the derivations can be placed into an appendix

Finally, we introduce eigenstates of the translation in order to block-diagonalize the dynamical matrix (and \mathbf{U}). To avoid confusion, I will indicate the k-dependent variables by a tilde as long as transformed and untransformed variables are used in the same expression.

We use ¹⁹

$$\begin{aligned}
X_{\alpha, \vec{\tau}} &= \sum_{\vec{k}} \tilde{X}_\alpha(\vec{k}) e^{i\vec{k}\vec{\tau}} \Leftrightarrow \tilde{X}_\alpha(\vec{k}) = \frac{1}{\mathcal{N}} \sum_{\vec{\tau}} X_{\alpha, \vec{\tau}} e^{-i\vec{k}\vec{\tau}} \\
U_{\alpha, \vec{\tau}, n} &= \frac{1}{\sqrt{\mathcal{N}}} \tilde{U}_{\alpha, \vec{n}}(\vec{k}) e^{i\vec{k}\vec{\tau}} \Leftrightarrow \tilde{U}_{\alpha, \vec{n}}(\vec{k}) = \frac{1}{\sqrt{\mathcal{N}}} \sum_{\vec{\tau}} U_{\alpha, \vec{\tau}, n} e^{-i\vec{k}\vec{\tau}} \quad (7.98)
\end{aligned}$$

The factors $\sqrt{\mathcal{N}}$ result from the different normalization conditions. In the first case, the sum is performed over the entire system, while in the second case, the sum extends only over the displacements in one unit cell.

$$\sum_{\alpha, \vec{\tau}} U_{\alpha, \vec{\tau}, n}^* U_{\alpha, \vec{\tau}, n'} = \delta_{n, n'} \quad \text{and} \quad \sum_{\alpha} \tilde{U}_{\alpha, \vec{n}}^*(\vec{k}) \tilde{U}_{\alpha, \vec{n}'}(\vec{k}) = \delta_{\vec{n}, \vec{n}'} \quad (7.99)$$

The index $n \hat{=} (\vec{k}, \vec{n})$ labeling the eigenmodes is now replaced by (\vec{k}, \vec{n}) , a wave vector \vec{k} and a band index \vec{n} . The band index \vec{n} runs up to the number of displacements in one unit cell.

$$b_{\vec{n}}(\vec{k}) = b_n \stackrel{\text{Eq. 7.96}}{=} \frac{1}{\sqrt{2\hbar\omega_{\vec{n}}(\vec{k})}} \sum_{\alpha, \vec{\tau}} \left(\overbrace{\frac{1}{\sqrt{\mathcal{N}}} \tilde{U}_{\alpha, \vec{n}}^*(\vec{k}) e^{-i\vec{k}\vec{\tau}}}^{U_{\alpha, \vec{\tau}, n}^*}} \frac{1}{\sqrt{M_\alpha}} iP_{\alpha, \vec{\tau}} + \omega_{\vec{n}}(\vec{k}) \overbrace{\frac{1}{\sqrt{\mathcal{N}}} \tilde{U}_{\alpha, \vec{n}}^*(\vec{k}) e^{-i\vec{k}\vec{\tau}}}^{U_{\alpha, \vec{\tau}, n}^*}} \sqrt{M_\alpha} X_{\alpha, \vec{\tau}} \right) \quad (7.100)$$

¹⁹

$$\sum_{\vec{\tau}} e^{-i\vec{k}\vec{\tau}} X_{\alpha, \vec{\tau}} = \sum_{\vec{\tau}} e^{-i\vec{k}\vec{\tau}} \underbrace{\sum_{\vec{k}'} X_{\alpha, n}(\vec{k}') e^{i\vec{k}'\vec{\tau}}}_{X_{\alpha, \vec{\tau}}} = \sum_{\vec{k}'} X_{\alpha, n}(\vec{k}') \underbrace{\sum_{\vec{\tau}} e^{i(\vec{k}' - \vec{k})\vec{\tau}}}_{\mathcal{N} \delta_{\vec{k}, \vec{k}'}} = \mathcal{N} X_{\alpha, n}(\vec{k}) \quad (7.97)$$

These are the desired phonon amplitudes

$$\hat{H} = \sum_{\vec{k}} \sum_{\vec{n}} \hbar \omega_{\vec{n}}(\vec{k}) b_{\vec{n}}^*(\vec{k}) b_{\vec{n}}(\vec{k}) \quad (7.101)$$

Backtransformation

$$\begin{aligned} b_{\vec{n}}(\vec{k}) + b_{\vec{n}}^*(-\vec{k}) &= \frac{1}{\sqrt{2\mathcal{N}\hbar\omega_{\vec{n}}(\vec{k})}} \sum_{\alpha, \vec{t}} \left(\tilde{U}_{\alpha, \vec{n}}^*(\vec{k}) e^{-i\vec{k}\vec{t}} \frac{1}{\sqrt{M_{\alpha}}} i P_{\alpha, \vec{t}} + \omega_{\vec{n}}(\vec{k}) \tilde{U}_{\alpha, \vec{n}}^*(\vec{k}) e^{-i\vec{k}\vec{t}} \sqrt{M_{\alpha}} X_{\alpha, \vec{t}} \right) \\ &+ \frac{1}{\sqrt{2\mathcal{N}\hbar\omega_{\vec{n}}(\vec{k})}} \sum_{\alpha, \vec{t}} \left(\underbrace{\tilde{U}_{\alpha, \vec{n}}^*(\vec{k})}_{= (\tilde{U}_{\alpha, \vec{n}}^*(-\vec{k}))^*} \underbrace{e^{-i\vec{k}\vec{t}}}_{=(e^{i\vec{k}\vec{t}})^*} \frac{1}{\sqrt{M_{\alpha}}} (-i) P_{\alpha, \vec{t}} + \omega_{\vec{n}}(\vec{k}) \underbrace{\tilde{U}_{\alpha, \vec{n}}^*(\vec{k})}_{= (\tilde{U}_{\alpha, \vec{n}}^*(-\vec{k}))^*} e^{-i\vec{k}\vec{t}} \sqrt{M_{\alpha}} X_{\alpha, \vec{t}} \right) \\ &= 2 \frac{1}{\sqrt{2\mathcal{N}\hbar\omega_{\vec{n}}(\vec{k})}} \sum_{\alpha, \vec{t}} \omega_{\vec{n}}(\vec{k}) \tilde{U}_{\alpha, \vec{n}}^*(\vec{k}) e^{-i\vec{k}\vec{t}} \sqrt{M_{\alpha}} X_{\alpha, \vec{t}} \quad (7.102) \end{aligned}$$

$$\begin{aligned} &\Rightarrow \sqrt{\frac{\mathcal{N}\hbar}{2\omega_{\vec{n}}(\vec{k})}} (b_{\vec{n}}(\vec{k}) + b_{\vec{n}}^*(-\vec{k})) = \sum_{\alpha, \vec{t}} \tilde{U}_{\alpha, \vec{n}}^*(\vec{k}) e^{-i\vec{k}\vec{t}} \sqrt{M_{\alpha}} X_{\alpha, \vec{t}} \\ \Rightarrow \sum_{\vec{n}} U_{\beta, \vec{n}}(\vec{k}) \sqrt{\frac{\mathcal{N}\hbar}{2\omega_{\vec{n}}(\vec{k})}} (b_{\vec{n}}(\vec{k}) + b_{\vec{n}}^*(-\vec{k})) &= \sum_{\alpha} \underbrace{\sum_{\vec{n}} U_{\beta, \vec{n}}(\vec{k}) \tilde{U}_{\alpha, \vec{n}}^*(\vec{k})}_{\delta_{\alpha\beta}} \sum_{\vec{t}} e^{-i\vec{k}\vec{t}} \sqrt{M_{\alpha}} X_{\alpha, \vec{t}} \\ &= \sum_{\vec{t}} e^{-i\vec{k}\vec{t}} \sqrt{M_{\beta}} X_{\beta, \vec{t}} \\ \Rightarrow \sum_{\vec{k}} e^{i\vec{k}\vec{t}} \frac{1}{\sqrt{M_{\beta}}} \sum_{\vec{n}} U_{\beta, \vec{n}}(\vec{k}) \sqrt{\frac{\mathcal{N}\hbar}{2\omega_{\vec{n}}(\vec{k})}} (b_{\vec{n}}(\vec{k}) + b_{\vec{n}}^*(-\vec{k})) &= \sum_{\vec{t}'} \underbrace{\sum_{\vec{k}} e^{-i\vec{k}(\vec{t}'-\vec{t})}}_{\mathcal{N}\delta_{\vec{t}'\vec{t}}} X_{\beta, \vec{t}'} = \mathcal{N} X_{\beta, \vec{t}} \quad (7.103) \end{aligned}$$

which provides the coordinates as function of the phonon amplitudes.

Analogously, we obtain the momenta

$$P_{\beta, \vec{t}} = -i \sum_{\vec{k}} e^{i\vec{k}\vec{t}} \sqrt{M_{\beta}} \sum_{\vec{n}} U_{\beta, \vec{n}}(\vec{k}) \sqrt{\frac{\hbar\omega_{\vec{n}}(\vec{k})}{2\mathcal{N}}} (b_{\vec{n}}(\vec{k}) - b_{\vec{n}}^*(-\vec{k})) \quad (7.104)$$

PHONON AMPLITUDES

$$b_{\vec{n}}(\vec{k}) \stackrel{\text{Eq. 7.100}}{=} \frac{1}{\sqrt{2\mathcal{N}\hbar\omega_{\vec{n}}(\vec{k})}} \sum_{\alpha, \vec{\tau}} e^{-i\vec{k}\vec{\tau}} \left(\tilde{U}_{\alpha, \vec{n}}^*(\vec{k}) \frac{1}{\sqrt{M_{\alpha}}} iP_{\alpha, \vec{\tau}} + \omega_{\vec{n}}(\vec{k}) \tilde{U}_{\alpha, \vec{n}}^*(\vec{k}) \sqrt{M_{\alpha}} X_{\alpha, \vec{\tau}} \right) \quad (7.105)$$

This expression provides the phonon amplitude as function over the phase space. The knowledge of all the phonon amplitudes (real and imaginary part) contains all information to recover the positions and momenta.

$$X_{\alpha, \vec{\tau}} = \frac{1}{\sqrt{\mathcal{N}}} \sum_{\vec{k}} \sum_{\vec{n}} e^{i\vec{k}\vec{\tau}} \frac{1}{\sqrt{M_{\alpha}}} U_{\alpha, \vec{n}}(\vec{k}) \sqrt{\frac{\hbar}{2\omega_{\vec{n}}(\vec{k})}} (b_{\vec{n}}(\vec{k}) + b_{\vec{n}}^*(-\vec{k})) \quad (7.106)$$

$$P_{\alpha, \vec{\tau}} = \frac{-i}{\sqrt{\mathcal{N}}} \sum_{\vec{k}} \sum_{\vec{n}} e^{i\vec{k}\vec{\tau}} \sqrt{M_{\alpha}} U_{\alpha, \vec{n}}(\vec{k}) \sqrt{\frac{\hbar\omega_{\vec{n}}(\vec{k})}{2}} (b_{\vec{n}}(\vec{k}) - b_{\vec{n}}^*(-\vec{k})) \quad (7.107)$$

Canonical momenta

Now comes a point that is easily overlooked: The origin of the problem is due to the complex-valued prefactor

$$e^{-i\vec{k}\vec{\tau}} \tilde{U}_{\alpha, \vec{n}}^*(\vec{k}) \quad (7.108)$$

which is complex conjugate to its value with inverted wave vector

$$e^{-i\vec{k}\vec{\tau}} \tilde{U}_{\alpha, \vec{n}}^*(\vec{k}) = \left(e^{-i(-\vec{k})\vec{\tau}} \tilde{U}_{\alpha, \vec{n}}^*(-\vec{k}) \right)^* \quad (7.109)$$

Therefore the canonical momentum of the phonon amplitude is in analogy to Eq. 7.90

$$\pi_{\vec{n}}(\vec{k}) = i\hbar b_{\vec{n}}^*(-\vec{k}) \quad (7.110)$$

rather than the complex conjugate for the same wave vector. **Editor:** At this point I can argue that the commutator relations between positions and momenta carry over to the phonon amplitudes and their momenta, if the prefactors are the same. I need to find a better argument. (Canonical transformation?)

$$\begin{aligned} b_{\vec{n}}(\vec{k}) &\rightsquigarrow \hat{b}_{\vec{n}}(\vec{k}) \\ b_{\vec{n}}^*(\vec{k}) &\rightsquigarrow \hat{b}_{\vec{n}}^{\dagger}(-\vec{k}) \end{aligned} \quad (7.111)$$

Let me define a short-hand notation, by adding an additional index $\sigma \in \{+, -\}$

$$\begin{aligned} b_{\vec{n}, -}(\vec{k}) &\stackrel{\text{def}}{=} b_{\vec{n}}(\vec{k}) \rightsquigarrow \hat{b}_{\vec{n}}(\vec{k}) \\ b_{\vec{n}, +}(\vec{k}) &\stackrel{\text{def}}{=} b_{\vec{n}}^*(-\vec{k}) \rightsquigarrow \hat{b}_{\vec{n}}^{\dagger}(\vec{k}) \end{aligned} \quad (7.112)$$

PHONON AMPLITUDES

$$b_{\tilde{n},\sigma}(\vec{k}) \stackrel{\text{Eq. 7.100}}{=} \frac{1}{\sqrt{2\mathcal{N}\hbar\omega_{\tilde{n}}(\vec{k})}} \sum_{\alpha,\vec{\tau}} e^{-i\vec{k}\vec{\tau}} \left(\tilde{U}_{\alpha,\tilde{n}}^*(\vec{k}) \frac{1}{\sqrt{M_{\alpha}}} i\sigma P_{\alpha,\vec{\tau}} + \omega_{\tilde{n}}(\vec{k}) \tilde{U}_{\alpha,\tilde{n}}^*(\vec{k}) \sqrt{M_{\alpha}} X_{\alpha,\vec{\tau}} \right) \quad (7.113)$$

This expression provides the phonon amplitude as function over the phase space.

The knowledge of all the phonon amplitudes (real and imaginary part) contains all information to recover the positions and momenta.

$$X_{\alpha,\vec{\tau}} = \frac{1}{\sqrt{\mathcal{N}}} \sum_{\vec{k}} \sum_{\tilde{n}} e^{i\vec{k}\vec{\tau}} \frac{1}{\sqrt{M_{\alpha}}} U_{\alpha,\tilde{n}}(\vec{k}) \sqrt{\frac{\hbar}{2\omega_{\tilde{n}}(\vec{k})}} \sum_{\sigma \in \{+,-\}} b_{\tilde{n},\sigma}(\vec{k}) \quad (7.114)$$

$$P_{\alpha,\vec{\tau}} = \frac{-i}{\sqrt{\mathcal{N}}} \sum_{\vec{k}} \sum_{\tilde{n}} e^{i\vec{k}\vec{\tau}} \sqrt{M_{\alpha}} U_{\alpha,\tilde{n}}(\vec{k}) \sqrt{\frac{\hbar\omega_{\tilde{n}}(\vec{k})}{2}} \sum_{\sigma \in \{+,-\}} \sigma b_{\tilde{n},\sigma}(\vec{k}) \quad (7.115)$$

Phonon amplitudes and normal coordinates

Editor: do not read what is marked in red

$$\delta R_{\alpha,\vec{\tau}} \stackrel{\text{Eq. 7.49}}{=} \sum_{\vec{k}} \sum_n \frac{1}{\sqrt{M_{\alpha}}} U_{\alpha,n}(\vec{k}) e^{i\vec{k}\vec{\tau}} Q_n(\vec{k}) \quad (7.116)$$

$$\Leftrightarrow Q_n(\vec{k}) \stackrel{\text{Eq. 7.61}}{=} \frac{1}{\mathcal{N}} \sum_{\alpha,\vec{\tau}} e^{-i\vec{k}\vec{\tau}} U_{\alpha,n}^*(\vec{k}) \sqrt{M_{\alpha}} \delta R_{\alpha,\vec{\tau}} \quad (7.117)$$

The matrices $\mathbf{U}(\vec{k})$ are built from the eigenvectors $\vec{u}_n(\vec{k})$ of the dynamical matrix

$$D_{\alpha,\beta}(\vec{k}) \stackrel{\text{Eqs. 7.16,7.53}}{=} \frac{1}{\sqrt{M_{\alpha}}} \left[\sum_{\vec{\tau}} C_{\alpha,\beta,\vec{\tau}} e^{i\vec{k}\vec{\tau}} \right] \frac{1}{\sqrt{M_{\beta}}} \quad (7.118)$$

$$Q_n(\vec{k}) = \sqrt{\frac{\hbar}{2\mathcal{N}\omega_{\tilde{n}}(\vec{k})}} \left(b_{\tilde{n}}(\vec{k}) + b_{\tilde{n}}^*(-\vec{k}) \right) \quad (7.119)$$

With $P = M\dot{X}$ we obtain

$$b_{\tilde{n}}(\vec{k}) \stackrel{\text{Eq. 7.100}}{=} \sqrt{\frac{\mathcal{N}}{2\hbar\omega_{\tilde{n}}(\vec{k})}} \left(i\partial_t + \omega_{\tilde{n}}(\vec{k}) \right) \underbrace{\frac{1}{\mathcal{N}} \sum_{\alpha,\vec{\tau}} e^{-i\vec{k}\vec{\tau}} \tilde{U}_{\alpha,\tilde{n}}^*(\vec{k}) \sqrt{M_{\alpha}} X_{\alpha,\vec{\tau}}}_{Q_n(\vec{k})} \quad (7.120)$$

Trajectories: Let us inspect the trajectory of the phonon amplitudes, as the atoms proceed according to Hamilton's equations of motion.

Eq. 7.113

$$\begin{aligned}
\frac{d}{dt} b_{\bar{n}}(\vec{k}) &\stackrel{\text{Eq. 7.113}}{=} \frac{1}{\sqrt{2\mathcal{N}\hbar\omega_{\bar{n}}(\vec{k})}} \sum_{\alpha, \vec{t}} e^{-i\vec{k}\vec{t}} \left(\omega_{\bar{n}}(\vec{k}) \tilde{U}_{\alpha, \bar{n}}^*(\vec{k}) \sqrt{M_{\alpha}} \overbrace{\frac{1}{M_{\alpha}} P_{\alpha, \vec{t}}}^{\dot{X}_{\alpha, \vec{t}}} \right. \\
&\quad \left. + \tilde{U}_{\alpha, \bar{n}}^*(\vec{k}) \frac{1}{\sqrt{M_{\alpha}}} i \left[- \sum_{\beta, \vec{t}'} C_{\alpha, \vec{t}, \beta, \vec{t}'} X_{\beta, \vec{t}'} - \frac{1}{2!} \sum_{\beta, \vec{t}', \gamma, \vec{t}''} W_{\alpha, \vec{t}, \beta, \vec{t}', \gamma, \vec{t}''} X_{\beta, \vec{t}'} X_{\gamma, \vec{t}''} \right] \right) \\
&= -i\omega_{\bar{n}}(\vec{k}) \frac{1}{\sqrt{2\mathcal{N}\hbar\omega_{\bar{n}}(\vec{k})}} \sum_{\alpha, \vec{t}} e^{-i\vec{k}\vec{t}} \left(\tilde{U}_{\alpha, \bar{n}}^*(\vec{k}) \frac{1}{\sqrt{M_{\alpha}}} i P_{\alpha, \vec{t}} \right. \\
&\quad \left. + \tilde{U}_{\alpha, \bar{n}}^*(\vec{k}) \frac{1}{\sqrt{M_{\alpha}}} \frac{1}{\omega_{\bar{n}}(\vec{k})} \left[\sum_{\beta, \vec{t}'} C_{\alpha, \vec{t}, \beta, \vec{t}'} X_{\beta, \vec{t}'} + \frac{1}{2!} \sum_{\beta, \vec{t}', \gamma, \vec{t}''} W_{\alpha, \vec{t}, \beta, \vec{t}', \gamma, \vec{t}''} X_{\beta, \vec{t}'} X_{\gamma, \vec{t}''} \right] \right)
\end{aligned} \tag{7.121}$$

Side calculation for the harmonic potential energy in the preceding equation

$$\begin{aligned}
&\sum_{\alpha, \vec{t}} e^{-i\vec{k}\vec{t}} \tilde{U}_{\alpha, \bar{n}}^*(\vec{k}) \frac{1}{\sqrt{M_{\alpha}}} \frac{1}{\omega_{\bar{n}}(\vec{k})} \sum_{\beta, \vec{t}'} \underbrace{\frac{C_{\alpha, \vec{t}, \beta, \vec{t}'}}{\sqrt{M_{\alpha}} D_{\alpha, \vec{t}, \beta, \vec{t}'}}}_{\sqrt{M_{\alpha}} \sum_{n'} U_{\alpha, \vec{t}, n'} \omega_{n'}^2 U_{\beta, \vec{t}', n'}^* \sqrt{M_{\beta}}} X_{\beta, \vec{t}'} \\
&\quad \underbrace{\sqrt{M_{\alpha}} \frac{1}{\mathcal{N}} \sum_{\vec{k}', \vec{n}'} U_{\alpha, \vec{n}'}(\vec{k}') e^{i\vec{k}'\vec{t}} \omega_{\vec{n}'}^2(\vec{k}') U_{\beta, \vec{n}'}^*(\vec{k}') e^{-i\vec{k}'\vec{t}'}}_{\sqrt{M_{\alpha}} \frac{1}{\mathcal{N}} \sum_{\vec{k}', \vec{n}'} U_{\alpha, \vec{n}'}(\vec{k}') e^{i\vec{k}'\vec{t}} \omega_{\vec{n}'}^2(\vec{k}') U_{\beta, \vec{n}'}^*(\vec{k}') e^{-i\vec{k}'\vec{t}'}} \sqrt{M_{\beta}}} \\
&= \sum_{\beta, \vec{t}'} \sum_{\vec{k}', \vec{n}'} \underbrace{\left(\frac{1}{\mathcal{N}} \sum_{\vec{t}} e^{i(\vec{k}' - \vec{k})\vec{t}} \right)}_{\delta_{\vec{k}, \vec{k}'}} \underbrace{\sum_{\alpha} \tilde{U}_{\alpha, \bar{n}}^*(\vec{k}) \tilde{U}_{\alpha, \vec{n}'}(\vec{k}')}_{\delta_{\vec{n}, \vec{n}'}, \text{ for } \vec{k} = \vec{k}'} \frac{1}{\omega_{\bar{n}}(\vec{k})} \omega_{\vec{n}'}^2(\vec{k}') \tilde{U}_{\beta, \vec{n}'}^*(\vec{k}') e^{-i\vec{k}'\vec{t}'} \sqrt{M_{\beta}} X_{\beta, \vec{t}'} \\
&= \sum_{\beta, \vec{t}'} \frac{1}{\omega_{\bar{n}}(\vec{k})} \omega_{\bar{n}}^2(\vec{k}) \tilde{U}_{\beta, \bar{n}}^*(\vec{k}) e^{-i\vec{k}\vec{t}} \sqrt{M_{\beta}} X_{\beta, \vec{t}'} \\
&= \sum_{\alpha, \vec{t}} \omega_{\bar{n}}(\vec{k}) \tilde{U}_{\alpha, \bar{n}}^*(\vec{k}) e^{-i\vec{k}\vec{t}} \sqrt{M_{\alpha}} X_{\alpha, \vec{t}}
\end{aligned} \tag{7.122}$$

When we insert this into \dot{b} , it completes b on the right-hand side.

$$\begin{aligned}
i\hbar\partial_t b_{\bar{n}}(\vec{k}) &= \hbar\omega_{\bar{n}}(\vec{k}) b_{\bar{n}}(\vec{k}) \\
&\quad + \underbrace{\frac{\hbar}{\sqrt{2\mathcal{N}\hbar\omega_{\bar{n}}(\vec{k})}} \sum_{\alpha, \vec{t}} e^{-i\vec{k}\vec{t}} \tilde{U}_{\alpha, \bar{n}}^*(\vec{k}) \frac{1}{\sqrt{M_{\alpha}}} \frac{1}{2!} \sum_{\beta, \vec{t}', \gamma, \vec{t}''} W_{\alpha, \vec{t}, \beta, \vec{t}', \gamma, \vec{t}''} X_{\beta, \vec{t}'} X_{\gamma, \vec{t}''}}_A
\end{aligned} \tag{7.123}$$

Finally we express the displacements $X_{\alpha,\bar{\tau}}$ by phonon amplitudes using Eq. 7.114

$$\begin{aligned}
\mathcal{A} &= \frac{\hbar}{\sqrt{2\mathcal{N}\hbar\omega_{\bar{n}}(\vec{k})}} \sum_{\alpha,\bar{\tau}} e^{-i\vec{k}\bar{\tau}} \tilde{U}_{\alpha,\bar{n}}^*(\vec{k}) \frac{1}{\sqrt{M_{\alpha}}} \frac{1}{2!} \sum_{\beta,\bar{\tau}',\gamma,\bar{\tau}''} W_{\alpha,\bar{\tau},\beta,\bar{\tau}',\gamma,\bar{\tau}''} X_{\beta,\bar{\tau}'} X_{\gamma,\bar{\tau}''} \\
&\stackrel{\text{Eq. 7.114}}{=} \frac{\hbar}{\sqrt{2\mathcal{N}\hbar\omega_{\bar{n}}(\vec{k})}} \sum_{\alpha,\bar{\tau}} \sum_{\beta,\bar{\tau}',\gamma,\bar{\tau}''} e^{-i\vec{k}\bar{\tau}} \tilde{U}_{\alpha,\bar{n}}^*(\vec{k}) \frac{1}{2!} \frac{W_{\alpha,\bar{\tau},\beta,\bar{\tau}',\gamma,\bar{\tau}''-\bar{\tau}}}{\sqrt{M_{\alpha}M_{\beta}M_{\gamma}}} \\
&\quad \times \underbrace{\frac{1}{\sqrt{\mathcal{N}}} \sum_{\vec{k}'} \sum_{\bar{n}'} e^{i\vec{k}'\bar{\tau}'} U_{\beta,\bar{n}'}(\vec{k}') \sqrt{\frac{\hbar}{2\omega_{\bar{n}'}(\vec{k}')}} (b_{\bar{n}'}(\vec{k}') + b_{\bar{n}'}^*(-\vec{k}'))}_{\sqrt{M_{\beta}}X_{\beta,\bar{\tau}'}} \quad (\text{Eq. 7.114}) \\
&\quad \times \underbrace{\frac{1}{\sqrt{\mathcal{N}}} \sum_{\vec{k}''} \sum_{\bar{n}''} e^{i\vec{k}''\bar{\tau}''} U_{\gamma,\bar{n}''}(\vec{k}'') \sqrt{\frac{\hbar}{2\omega_{\bar{n}''}(\vec{k}'')}} (b_{\bar{n}''}(\vec{k}'') + b_{\bar{n}''}^*(-\vec{k}''))}_{\sqrt{M_{\gamma}}X_{\gamma,\bar{\tau}''}} \quad (\text{Eq. 7.114}) \\
&= \frac{1}{2!} \sum_{\vec{k}',\vec{k}'',\bar{n}',\bar{n}''} \underbrace{\left(\sum_{\bar{\tau}} e^{i(-\vec{k}-\vec{k}'+\vec{k}'')\bar{\tau}} \right)}_{\mathcal{N} \sum_{\bar{\tau}} \delta_{\vec{k}-\vec{k}'+\vec{k}''+\bar{\tau}}} \left(\frac{\hbar}{2\mathcal{N}} \right)^{\frac{3}{2}} \frac{1}{\sqrt{\omega_{\bar{n}}(\vec{k})\omega_{\bar{n}'}(\vec{k}')\omega_{\bar{n}''}(\vec{k}'')}} \\
&\quad \times \left\{ \sum_{\alpha,\beta,\gamma} \left[\sum_{\bar{\tau},\bar{\tau}'} \frac{W_{\alpha,\bar{\tau},\beta,\bar{\tau}',\gamma,\bar{\tau}''-\bar{\tau}}}{\sqrt{M_{\alpha}M_{\beta}M_{\gamma}}} e^{i\vec{k}'(\bar{\tau}'-\bar{\tau})} e^{i\vec{k}''(\bar{\tau}''-\bar{\tau})} \right] \tilde{U}_{\alpha,\bar{n}}^*(\vec{k}) U_{\beta,\bar{n}'}(\vec{k}') U_{\gamma,\bar{n}''}(\vec{k}'') \right\} \\
&\quad \times (b_{\bar{n}'}(\vec{k}') + b_{\bar{n}'}^*(-\vec{k}')) (b_{\bar{n}''}(\vec{k}'') + b_{\bar{n}''}^*(-\vec{k}'')) \\
&= \sum_{\vec{k}',\vec{k}'',\bar{n}',\bar{n}''} Y_{\bar{n},\bar{n}',\bar{n}''}(-\vec{k},\vec{k}',\vec{k}'') (b_{\bar{n}'}(\vec{k}') + b_{\bar{n}'}^*(-\vec{k}')) (b_{\bar{n}''}(\vec{k}'') + b_{\bar{n}''}^*(-\vec{k}'')) \\
\end{aligned} \tag{7.124}$$

Thus, the equation of motion for the phonon amplitudes has the form

EQUATION OF MOTION FOR PHONON AMPLITUDES

$$\begin{aligned}
i\hbar\partial_t b_{\bar{n}}(\vec{k}) &= \hbar\omega_{\bar{n}}(\vec{k}) b_{\bar{n}}(\vec{k}) \\
&\quad + \sum_{\vec{k}',\vec{k}'',\bar{n}',\bar{n}''} Y_{\bar{n},\bar{n}',\bar{n}''}(-\vec{k},\vec{k}',\vec{k}'') (b_{\bar{n}'}(\vec{k}') + b_{\bar{n}'}^*(-\vec{k}')) (b_{\bar{n}''}(\vec{k}'') + b_{\bar{n}''}^*(-\vec{k}'')) \\
\Leftrightarrow i\hbar\sigma\partial_t b_{\bar{n},\sigma}(\vec{k}) &= \hbar\omega_{\bar{n}}(\vec{k}) b_{\bar{n},\sigma}(\vec{k}) \\
&\quad + \sum_{\vec{k}',\vec{k}'',\bar{n}',\bar{n}''} \sum_{\sigma',\sigma'' \in \{+,-\}} Y_{\bar{n},\bar{n}',\bar{n}''}(\sigma\vec{k},\vec{k}',\vec{k}'') b_{\bar{n}',\sigma'}(\vec{k}') b_{\bar{n}'',\sigma''}(\vec{k}'') \tag{7.125}
\end{aligned}$$

with

$$\begin{aligned}
Y_{\bar{n},\bar{n}',\bar{n}''}(\vec{k},\vec{k}',\vec{k}'') &\stackrel{\text{def}}{=} \frac{\mathcal{N}}{2} \sum_{\bar{\tau}} \delta_{\vec{k}-\vec{k}'+\vec{k}''+\bar{\tau}} \left(\frac{\hbar}{2\mathcal{N}} \right)^{\frac{3}{2}} \frac{1}{\sqrt{\omega_{\bar{n}}(\vec{k})\omega_{\bar{n}'}(\vec{k}')\omega_{\bar{n}''}(\vec{k}'')}} \\
&\quad \times \left\{ \sum_{\alpha,\beta,\gamma} \left[\sum_{\bar{\tau},\bar{\tau}'} \frac{W_{\alpha,\bar{\tau},\beta,\bar{\tau}',\gamma,\bar{\tau}''-\bar{\tau}}}{\sqrt{M_{\alpha}M_{\beta}M_{\gamma}}} e^{i\vec{k}'\bar{\tau}'} e^{i\vec{k}''\bar{\tau}''} \right] \tilde{U}_{\alpha,\bar{n}}(\vec{k}) \tilde{U}_{\beta,\bar{n}'}(\vec{k}') \tilde{U}_{\gamma,\bar{n}''}(\vec{k}'') \right\} \tag{7.126}
\end{aligned}$$

Once the trajectories of the phonon amplitudes are obtained, the displacements of the nuclei from the equilibrium position are obtained via Eq. 7.114

7.5.3 Comparison to the Schrödinger equation

The significance of the equation above is that is very similar to the Schrödinger equation.

$$\begin{aligned} |\psi(t)\rangle &= \sum_{n, \vec{k}} |\varphi_n(\vec{k})\rangle \langle \varphi_n(\vec{k}) | \psi(t)\rangle \\ i\hbar \partial_t \langle \varphi_n(\vec{k}) | \psi(t)\rangle &= \epsilon_n(\vec{k}) \langle \varphi_n(\vec{k}) | \psi(t)\rangle \end{aligned} \quad (7.127)$$

Nevertheless, this Eq. 7.125 has the same content as Newton's equation of motion.

By including quantum effects for the nuclei, positions and momenta of the nuclei would turn from numbers into operators. Accordingly, also the phonon-amplitudes will turn into operators, namely the **creation** and **annihilation operators** of phonons.

The non-linear terms describe the interaction. Thus, an interacting system would be captured by a non-linear Schrödinger equation. The Hamiltonian in quantum field theory has the very same structure. Nevertheless the resulting equations of motion are linear in the field, the quantum field, onto which the operators act.

7.5.4 Interaction picture in classical mechanics

Let me enter the classical pendant to the **interaction picture**. The interaction picture is a representation, which is widely used in quantum field theory. I indicate the quantities in the interaction picture with a subscript I . In order to make it evident that the "normal" quantities are considered I will include a subscript S , which stands for Schrödinger picture.

The phonon amplitudes evolve in the absence of anharmonic terms, according to

$$b_{\vec{n}, \sigma}(t) = e^{-i\sigma\omega_n(\vec{k})t} b_{\vec{n}, \sigma}(0) \quad (7.128)$$

Let me now introduce the interaction picture. The quantities in the interaction picture are marked by a subscript I , while quantities in the "normal" representation are marked by a subscript S , which stands for Schrödinger picture.

$$b_{S, \vec{n}, \sigma}(t) = e^{-i\sigma\omega_n(\vec{k})t} b_{I, \vec{n}, \sigma}(t) \quad \Leftrightarrow \quad b_{I, \vec{n}, \sigma}(t) = e^{i\sigma\omega_n(\vec{k})t} b_{S, \vec{n}, \sigma}(t) \quad (7.129)$$

so that

$$\begin{aligned} i\hbar\sigma\partial_t b_{I, \vec{n}, \sigma}(\vec{k}, t) &\stackrel{\text{Eq. 7.129}}{=} e^{i\sigma\omega_n(\vec{k})t} \left(-\hbar\omega_{\vec{n}}(\vec{k}) + i\hbar\sigma\partial_t \right) b_{S, \vec{n}, \sigma}(t) \\ &\stackrel{\text{Eq. 7.125}}{=} e^{i\omega_n(\vec{k})t} \left(-\hbar\omega_{\vec{n}}(\vec{k}) b_{S, \vec{n}, \sigma}(\vec{k}) + \hbar\omega_{\vec{n}}(\vec{k}) b_{S, \vec{n}, \sigma}(\vec{k}) \right) \\ &\quad + \sum_{\vec{k}', \vec{k}''} \sum_{\vec{n}', \vec{n}''} \sum_{\sigma', \sigma'' \in \{+1, -1\}} Y_{\vec{n}, \vec{n}', \vec{n}''}(-\vec{k}, \vec{k}', \vec{k}'') b_{S, \vec{n}', \sigma'}(\vec{k}') b_{S, \vec{n}'', \sigma''}(\vec{k}'') \\ &\stackrel{\text{Eq. 7.129}}{=} \sum_{\vec{k}', \vec{k}''} \sum_{\vec{n}', \vec{n}''} \sum_{\sigma', \sigma'' \in \{+1, -1\}} Y_{\vec{n}, \vec{n}', \vec{n}''}(-\vec{k}, \vec{k}', \vec{k}'') e^{i[\sigma\omega_{\vec{n}}(\vec{k}) - \sigma'\omega_{\vec{n}'}(\vec{k}') - \sigma''\omega_{\vec{n}''}(\vec{k}'')]t} \\ &\quad \times b_{I, \vec{n}', \sigma'}(\vec{k}') b_{I, \vec{n}'', \sigma''}(\vec{k}'') \end{aligned} \quad (7.130)$$

Now the advantages of the interaction picture becomes evident.

- The interaction picture suggests an expansion in the scattering term Y . Inserting the zeroth order, we obtain a first-order differential equation for the first order, which can solved by a simple integration. With the zeroth and first order at hand, we obtain a similar differential equation for the second order.
- In the absence of anharmonic terms the phonon amplitudes in the interaction picture are time independent.

- The phase factor oscillates rapidly, when incoming and outgoing phonons are out of resonance. In that case the anharmonic terms are averaged out and contribute only little. As shown below, the resonance condition is equivalent to the energy conservation of phonons.

7.5.5 Energy and momentum conservation of phonons

Let us consider now a case where the anharmonic terms are small. The phonon amplitudes in the interaction picture change only slowly. If the phonon amplitudes can be considered constant on a time scale on which the term $e^{i[\omega_{\tilde{n}}(\vec{k}) - \omega_{\tilde{n}'}(\vec{k}') - \omega_{\tilde{n}''}(\vec{k}'')]t}$ changes rapidly, the result is averaged out.

However, a large effect of the anharmonic terms is expected when

$$\omega_{\tilde{n}}(\vec{k}) - \omega_{\tilde{n}'}(\vec{k}') - \omega_{\tilde{n}''}(\vec{k}'') = 0 \quad (7.131)$$

This is an expression for energy conservation of phonons: Scattering events are efficient if the energy does not change. Note, however, that this energy, namely $\hbar\omega_{\tilde{n}}(\vec{k})$ has nothing to do with the energy of the nuclei.

7.5.6 Left- and right-moving plane waves

$$\begin{aligned} X_{\alpha, \vec{k}} &\stackrel{\text{Eq. 7.114}}{=} \frac{1}{\sqrt{\mathcal{N}}} \sum_{\vec{k}} \sum_{\tilde{n}} e^{i\vec{k}\vec{r}} \frac{1}{\sqrt{M_{\alpha}}} U_{\alpha, \tilde{n}}(\vec{k}) \sqrt{\frac{\hbar}{2\omega_{\tilde{n}}(\vec{k})}} \sum_{\sigma \in \{+1, -1\}} b_{S, \tilde{n}, \sigma}(\vec{k}) \\ &= \frac{1}{\sqrt{\mathcal{N}}} \sum_{\vec{k}} \sum_{\tilde{n}} \frac{1}{\sqrt{M_{\alpha}}} U_{\alpha, \tilde{n}}(\vec{k}) \sqrt{\frac{\hbar}{2\omega_{\tilde{n}}(\vec{k})}} e^{i\vec{k}\vec{r}} \sum_{\sigma \in \{+1, -1\}} e^{-i\sigma\omega_{\tilde{n}}(\vec{k})t} b_{l, \tilde{n}}(\vec{k}) \\ &= \frac{1}{\sqrt{\mathcal{N}}} \sum_{\vec{k}} \sum_{\tilde{n}} \frac{1}{\sqrt{M_{\alpha}}} U_{\alpha, \tilde{n}}(\vec{k}) \sqrt{\frac{\hbar}{2\omega_{\tilde{n}}(\vec{k})}} \\ &\quad \times \left(\left(e^{i(\vec{k}\vec{r} - \omega_{\tilde{n}}(\vec{k})t)} b_{\tilde{n}}^{(W)}(\vec{k}) \right) + \left(e^{-i(\vec{k}\vec{r} - \omega_{\tilde{n}}(\vec{k})t)} b_{\tilde{n}}^{(W)}(-\vec{k}) \right)^* \right) \end{aligned} \quad (7.132)$$

The phase velocity is $\vec{k} \frac{\omega}{k^2}$. Thus, the phonons consist of plane waves that move in the positive direction of the wave vector.

This property is important for the use of $\hbar\omega_{\tilde{n}}(\vec{k})$ in the drift term of a Boltzmann equation. This is one advantage of phonon amplitudes over normal coordinates, because the latter describe waves moving in the forward and the backward direction.

Phonon-interaction energy

For the sake of completeness, let me convert also the energy resulting from the anharmonic terms into a representation of phonon amplitudes.

We begin with the expression Eq. 7.67 using normal coordinates

$$Q_n(\vec{k}) \stackrel{\text{Eq. U.24}}{=} \frac{\hbar}{\sqrt{2\mathcal{N}\hbar\omega_n(\vec{k})}} \sum_{\sigma \in \pm} b_{n, \sigma}(\vec{k}) e^{i\sigma\omega_n(\vec{k})t} \quad (7.133)$$

We obtain

$$\begin{aligned}
 E^{an harm} &\stackrel{\text{Eq. 7.67}}{=} \mathcal{N} \sum_{\vec{k}, \vec{k}', \vec{k}'' \in \Omega_G} \sum_{l, m, n} \frac{1}{3!} X_{l, m, n}(\vec{k}, \vec{k}', \vec{k}'') Q_l(\vec{k}) Q_m(\vec{k}') Q_n(\vec{k}'') \Big\} \\
 &\stackrel{\text{Eq. U.24}}{=} \mathcal{N} \sum_{\vec{k}, \vec{k}', \vec{k}'' \in \Omega_G} \sum_{l, m, n} \frac{1}{3!} \left(\frac{\hbar}{2\mathcal{N}} \right)^{\frac{3}{2}} \frac{X_{l, m, n}(\vec{k}, \vec{k}', \vec{k}'')}{\sqrt{\omega_l(\vec{k}) \omega_m(\vec{k}') \omega_n(\vec{k}'')}} \\
 &\quad \times \sum_{\sigma, \sigma', \sigma'' \in \pm} b_{l, \sigma}(\vec{k}) b_{m, \sigma'}(\vec{k}') b_{n, \sigma''}(\vec{k}'') e^{i[\sigma \omega_l(\vec{k}) + \sigma' \omega_m(\vec{k}') + \sigma'' \omega_n(\vec{k}'')]t} \quad (7.134)
 \end{aligned}$$

This expression may be useful to derive the equations of motion for the phonon amplitudes in the presence of anharmonic terms.

7.6 Phonon band structures

7.6.1 Example for a phonon band structure

In Fig. 7.5 the phonon band structures of gold and silicon are shown.

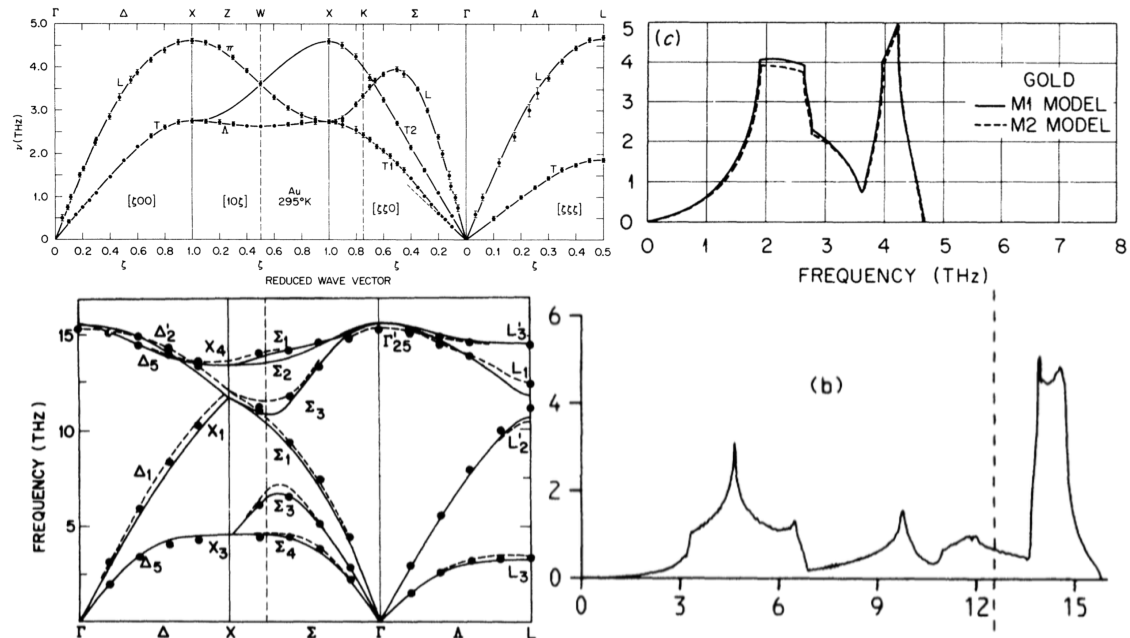


Fig. 7.5: Top: Phonon band structure and density of states of gold.[50]. Bottom: Phonon band structure and density of states of silicon[51] (Copyright Physical Review B)

7.6.2 Acoustic branches

Acoustic and optical branches All phononic band structures in three dimensions have three branches with a frequencies that vanish at the Γ -point, i.e. for $\vec{k} = 0$, and that, for small enough wave vectors, grow approximately linearly with increasing wave vectors. They are called **acoustic branches** of the phonon band structure. The other branches have a finite frequency at the Γ -point and are called **optic branches** of the phonon band structure.

The number of acoustic branches is identical to the dimension of the of the system.

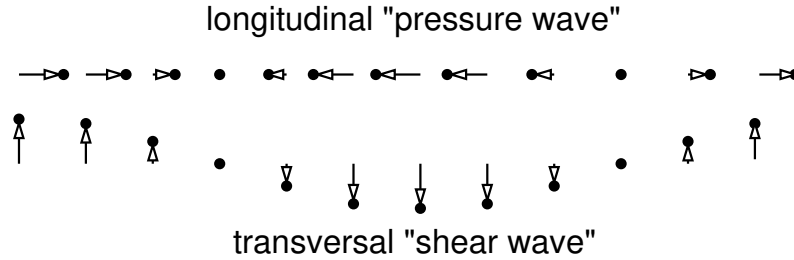
The acoustic branches, namely branches which have zero frequency at long wave length, result from the fact that a global translations of the entire lattice does not cost any energy. **Editor: formulate this in a clearer fashion.** Such a translation could be described an equal displacement of all atoms into any spatial direction. Thus, there are three eigenvectors of the dynamical matrix at the Γ -point, i.e. at $\vec{k} = \vec{0}$, with zero frequency.

It is important to exclude these modes from the sum, because they are not vibrations and thus must not be represented by anharmonic oscillators. Thermodynamically, these modes would be treated as the translational motion of the macroscopic crystal.

Longitudinal and transversal acoustic branches: The three acoustic modes can be classified²⁰ as longitudinal and transversal acoustic waves. For **longitudinal waves**, the displacement vector points

²⁰given sufficiently high symmetry

parallel to the wave vector, while for **transversal waves**, the displacement is orthogonal to the wave vector. The transversal wave is a shear wave.



Sound: In the long-wavelength limit, the distortions of the material can be described by the theory of elasticity. The elastic distortions are described by a displacement field $\vec{u}(\vec{r})$, which gives the displacement of an atom with equilibrium position at \vec{r} .

The frequency spectrum of the acoustic modes near the Γ -point can be approximated

$$\omega_n(\vec{k}) = \sqrt{\vec{k} \mathbf{A}_n \vec{k}} \quad (7.135)$$

where the index n refers to a particular acoustic branch, and the matrix A is a second derivative of the corresponding eigenvalue $d_n(\vec{k})$ of the dynamical matrix.

Propagating elastic waves are called **sound waves**. Their (group) velocity is

$$\vec{v}_n = \vec{\nabla}_{\vec{k}} \omega(\vec{k}) = \frac{\mathbf{A}_n \vec{k}}{\omega_n(\vec{k})} \quad (7.136)$$

Each acoustic branch has its own **speed of sound**. The speed of sound of the transversal modes is often a factor two smaller than that of the longitudinal modes.

In seismology, the study of earth quakes, one calls the longitudinal modes waves **P-waves, pressure waves** or primary waves. The transversal modes are called **S-waves, shear waves** or secondary waves. The lower speed of sound of transversal modes explains why the transversal modes of an earth quake are called "secondary".

Elasticity: [Editor: This needs to be done](#)

An elastic distortion of a material can be described by a transformation of all coordinates according to

$$x'_j = x_j + \epsilon_{j,k} x_k \quad (7.137)$$

where $\epsilon_{j,k}$ is the strain tensor. The strain tensor is symmetric. An antisymmetric contribution to the strain tensor would describe a rotation, which does not distort the material. The diagonal elements of the strain tensor describe a stretching along a specified direction, while the off-diagonal elements describe shear distortions.

7.6.3 Optic branches of the phonon band structure

Reststrahl absorption

(see Optical Properties of Ions in Solids, by Baldassare Di Bartolo)

An example for the interaction of quasi-particles is the conversion of light into vibrations. The absorption of light by a one-phonon process is called **reststrahl absorption**.

This process can be investigated by superimposing the one-particle band structures of phonons with those of light. Where the band structures of photons and phonons intersect, a conversion satisfies energy and momentum conservation.

The speed of light is $c = 3 \times 10^8$ m/s, while the speed of sound is of the order of $c_s = 10^3 - 10^4$ m/s, which is about 10^5 times smaller than the speed of light. Because of the large speed of light, the photon bands are very steep, so that they intersect the phonon band structure very close to the Γ -point. This tells us that the reststrahl absorption takes place at the energy of the optical phonons at (near) the Γ point.

In addition to energy and momentum conservation, the transformation requires a non-vanishing matrix element. For the optical transition, it is an electrostatic dipole, which couples to the electric field of the photon. The dipole is due to the displacement of positive and negative ions. (This implies that the reststrahl absorption for non-ionic materials will be small.) Because the electric field of the light wave is perpendicular to the wave vector, it will couple to the transversal optical phonons with frequency ω_{TO} .

In the crystal, the photon and phonon bands will create an avoided crossing of the band structures of phonon and photon. That is, near the crossing the light will travel as a **phonon-polariton**, which is a mixed photon-phonon quasi-particle. In general, a polariton is a quasi-particle, which is a combination of a strong electric field with an excitation of a material.

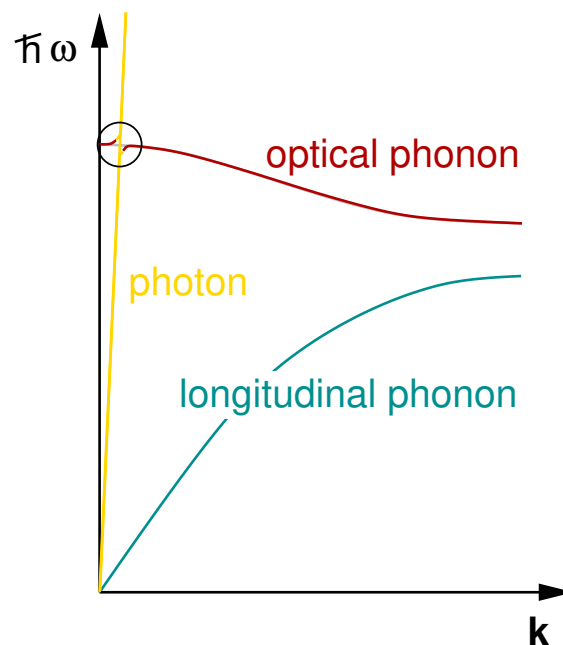


Fig. 7.6: Sketch of a polariton. Dispersion relation of a photon and phonons. The coupling of the optical phonon of a polar crystal to the electric field of a light-wave a photon leads to an avoided crossing, where phonon and photon are strongly coupled. Such a state is called a **phonon-polariton**. Note that the slope of the photon dispersion relation is reduced artificially. The true photon dispersion relation would look vertical on this scale. The speed of light $c_{light} = 3 \times 10^8$ m/s, while the speed of sound in materials is typically of order $c_{sound} = 5 \times 10^3$ m/s or less.

7.7 Thermodynamics of phonons

7.7.1 Thermodynamics: Models for the density of states

As shown for the thermodynamic properties of non-interacting Fermions one can extract analogously the thermodynamic properties of non-interacting phonons from a given density of states.

Einstein model for the density of states:

The most simple model for the density of states is the Einstein Model, which replaces the phononic density of states by delta function at the so-called **Einstein frequency** ω_E .

$$\omega_n(\vec{k}) = \omega_E \quad \text{for } n \in \{1, \dots, 3n_{at}\} \quad (7.138)$$

where n_{at} is the number of atoms in the unit cell.

Historically, the Einstein frequency has been fitted to measured specific heats as function of temperature. It has been interpreted as an average frequency, i.e. the mean value of the phononic band structure $\omega(\vec{k})$. The Einstein frequency is ²¹

$$\omega_E = \frac{1}{\sum_{\vec{k}, \alpha} \omega_{\alpha}(\vec{k})} \sum_{\vec{k}, \alpha} \omega_{\alpha}(\vec{k}) \quad (7.141)$$

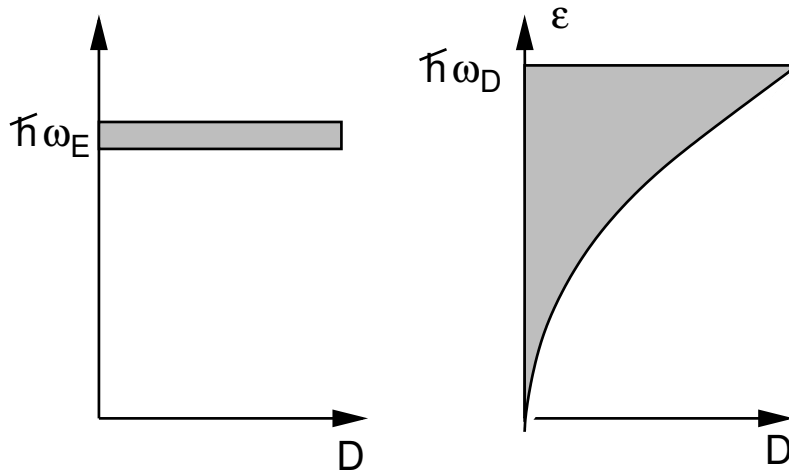


Fig. 7.7: Phonon density of states D (vertical axis) as function of phonon energy $\epsilon = \hbar\omega$ (horizontal axis) of the Einstein model (left) and the Debye model (right). ω_E is the Einstein frequency and ω_D is the Debye frequency.

²¹Editor: This is a sketch: One might also define the Einstein frequency differently: As shown in Eq. 7.23 of ΦSX: Statistical Physics[38], the high-temperature or classical limit of the vibrational free energy depends on the determinant of the dynamical matrix. Choosing the Einstein frequency as geometric mean of the eigenvalues preserves this limit

$$(\omega_E^2)^{3N-6} = \det(D) \quad (7.139)$$

The Einstein frequency defined in this manner is obtained from the average logarithm of the frequencies.

$$\ln(\beta\hbar\omega_E) = \frac{1}{3N-6} \sum_{j=1}^{3N-6} \ln(\beta\hbar\omega_j) \quad (7.140)$$

As a result, the low-frequency modes, which are less frequent, obtain a larger weight. Potentially, this explains the overestimation of the Einstein frequency by Einstein himself. [52, 53]

DENSITY OF STATES OF THE EINSTEIN MODEL

The density of states of the Einstein model is (see also fig. 7.7)

$$D^E(\epsilon) = \Omega \frac{\sum_{\alpha} \delta(\epsilon - \hbar\omega_{\alpha})}{\det |\mathbf{T}|} \quad (7.142)$$

where $\sum_{\alpha} = 3n_{at}$ is the number of degrees of freedom in one unit cell and Ω is the volume of the supercell. We used here that the number of modes is $\mathcal{N} \sum_{\alpha}$ and $\mathcal{N} = \Omega / \det |\mathbf{T}|$.

Debye model for the density of states

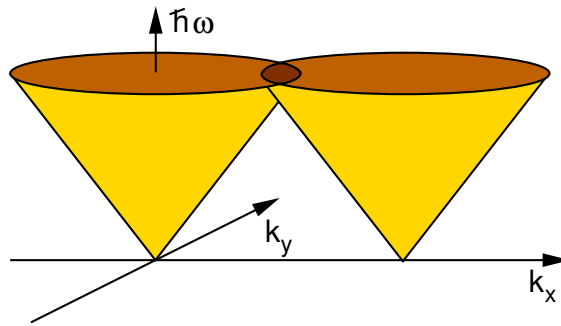


Fig. 7.8: Bands of the Debye model in the k_x, k_y -plane of reciprocal space. Each cone is centered at a reciprocal lattice vector \vec{G} and belongs to one unit cell. Only two of the cones are shown. I show two cones to demonstrate that (1) the unit cell is approximated itself by a sphere to enforce spherical symmetry and (2), that, as a result, the cones may overlap in reciprocal space. The cones are cut off at $\hbar\omega_D$, which is the highest phonon energy in the model.

The Debye model uses a model of a linear dispersion relation

$$\omega_n(\vec{k}) = c_s |\vec{k}| \theta(\omega_D - c_s |\vec{k}|) \quad \text{for } n = 1, 2, 3 \quad (7.143)$$

which is simply cut off [49] beyond a so-called **Debye frequency** ω_D . c_s is the speed of sound. The Debye frequency can be identified roughly with the highest frequency in the phonon dispersion. Thus, it is large for a material such as diamond, which has strong bonds and light atoms, while it is very low for a material like gold, with heavy atoms and relatively weak metallic bonds.

Editor: Include a table for Debye frequencies and sound speeds.

The Debye model considers only one speed of sound c_s . The different speed of sound between the longitudinal and the transversal modes is not accounted for. The linear dispersion relation is a consequence of assuming the same group velocity throughout the Brillouin zone.

A second implicit assumption of the Debye model is that it treats all atoms as identical. Therefore, there are only three branches of the phonon band structure Eq. 7.143 in the extended zone scheme.

The density of states $D(\epsilon) = \partial_{\epsilon} N(\epsilon)$ is obtained as derivative of the number-of-states function $N(\epsilon)$. We consider three branches of the phonon band structure, one for each polarization, each having a slope determined by the speed of sound c_s .

- For energies $\epsilon = \hbar\omega$ below the Debye energy $\hbar\omega_D$ the number of states $N^D(\epsilon)$ of the Debye model is

$$N^D(\epsilon) = 3\Omega \int \frac{d^3k}{(2\pi)^3} \theta(\hbar c_s |\vec{k}| - \epsilon) = 3\Omega \frac{1}{(2\pi)^3} \frac{4\pi}{3} \left(\frac{\epsilon}{\hbar c_s} \right)^3 \quad \text{for } \epsilon \leq \hbar\omega_D \quad (7.144)$$

where Ω is the volume of the supercell. The volumetric phonon density of states is $N(\epsilon)/\Omega$.

- Above the Debye energy, there are no further states, so that the number of states is constant for $\epsilon > \hbar\omega_D$. On the one hand we can calculate the number of states by integrating the density of states Eq. 7.144 up to the Debye energy.

$$N^D(\epsilon) \stackrel{\epsilon \geq \hbar\omega_D}{=} N^D(\hbar\omega_D) \stackrel{\text{Eq. 7.144}}{=} 3\Omega \frac{1}{(2\pi)^3} \frac{4\pi}{3} \left(\frac{\hbar\omega_D}{\hbar c_s} \right)^3 \quad \text{for } \epsilon \geq \hbar\omega_D \quad (7.145)$$

On the other hand, the total number of states equals the total number of degrees of freedom, that is three times the number of atoms. For M atoms in the unit cell of the crystal, the volume density of atoms is $n_{at} \stackrel{\text{def}}{=} \frac{M}{\det|\mathbf{T}|}$. This allows one to estimate the Debye frequency.

$$\int_0^\infty d\epsilon' D(\epsilon') = 3\Omega \frac{M}{\det|\mathbf{T}|} = 3n_{at}\Omega \quad (7.146)$$

By comparing the two expressions, we obtain the Debye energy as

$$4\pi\Omega \left(\frac{\hbar\omega_D}{2\pi\hbar c_s} \right)^3 = 3n_{at}\Omega \quad \Rightarrow \quad \hbar\omega_D = 2\pi\hbar c_s \sqrt[3]{\frac{3n_{at}}{4\pi}} \quad (7.147)$$

Remember that, in this case, c_s is the speed of sound and not the speed of light. Thus, the parameters of the model are reduced to the speed of sound c_s and the volume-density n_{at} of the atoms.

DENSITY OF STATES OF THE DEBYE MODEL

The density of states $D(\epsilon)$ of the Debye model is (see also fig. 7.7)

$$D^D(\epsilon) = \frac{12\pi\Omega}{(2\pi\hbar c_s)^3} \epsilon^2 \theta(\hbar\omega_D - \epsilon) = \Omega \frac{9n_{at}}{\hbar\omega_D} \left(\frac{\epsilon}{\hbar\omega_D} \right)^2 \theta(\hbar\omega_D - \epsilon) \quad (7.148)$$

where $n_{at} = M/\det|\mathbf{T}|$ is the number of atoms per volume.

We provide here the density of states defined as number of states per unit energy interval for the sake of consistency with the description of Fermions. In the present case it may seem more natural to use the number of states per unit frequency interval.

Debye temperature: The Debye frequency is often expressed[49] by the **Debye temperature** via the relation

$$k_B T_D = \hbar\omega_D \quad (7.149)$$

Thus, the density of states of the Debye model is, in terms of the Debye temperature,

$$D^D(\epsilon) = \Omega \frac{9n_{at}}{k_B T_D} \left(\frac{\epsilon}{k_B T_D} \right)^2 \theta(k_B T_D - \epsilon) \quad (7.150)$$

Combination of Einstein and Debye model

A side remark is, that a reasonable description of the density of states may be achieved using a combination of the Debye model for the acoustic modes and the Einstein model for the optical modes. The Debye model can furthermore be modified by distinguishing longitudinal and transversal bands.

7.7.2 Grand potential

In order to extract thermodynamic properties we start with the partition function and the grand potential. In contrast to the previous case of electrons we need to consider here bosons.

In contrast to the previous discussion, we switch now to the quantum-mechanical description. This implies that we add the zero-point energy and discretize the energy levels.

The energy of the phonons is

$$E_{ph}[\{n_\lambda\}] = \sum_\lambda \hbar\omega_\lambda(n_\lambda + \frac{1}{2}) \quad (7.151)$$

where n_λ is the number of phonons with index λ . $\lambda = (n_\lambda, \vec{k}_\lambda)$ combines the wave vector and the band index, i.e. $\omega_\lambda = \omega_n(\vec{k})$. Each eigenstate of the phonon Hamiltonian can be characterized by a vector of occupation numbers \vec{n} with components n_λ .

The partition sum is

$$Z(T, \mu) = \sum_{\vec{n}} e^{-\beta[E(\vec{n}) - \mu N(\vec{n})]} \quad (7.152)$$

The total number of excitations is $N(\vec{n}) = \sum_\lambda n_\lambda$

Because phonons do not satisfy particle conservation, there is no such a thing as a phonon reservoir. Therefore, the chemical potential is set to zero. Nevertheless, despite the value $\mu = 0$, I will carry the symbol for the chemical potential along, so that the reader remains familiar with the general formula.²²

$$Z(T, \mu) = \prod_\lambda \sum_{n_\lambda=0}^{\infty} e^{-\beta(\epsilon_\lambda - \mu)n_\lambda} = \prod_\lambda \frac{1}{1 - e^{-\beta(\epsilon_\lambda - \mu)}} \quad (7.153)$$

Thus, we obtain the grand potential as

$$\Omega(T, \mu) = -k_B T \ln[Z(T, \mu)] = \sum_\lambda k_B T \ln[1 - e^{-\beta(\epsilon_\lambda - \mu)}] \quad (7.154)$$

7.7.3 Internal energy

$$U(T, \mu) = \int_0^\infty d\epsilon D(\epsilon)\epsilon b(\epsilon) \quad (7.155)$$

where

$$b_{T,\mu} = \frac{1}{e^{\beta(\epsilon - \mu)} - 1} \quad (7.156)$$

is the **Bose distribution**.

7.8 Worked Example: Phonon band structure of the two-site linear chain

The linear chain is a minimal model for a phonon bandstructure with an acoustical and an optical mode. Here we consider the extension with two atoms per unit cell. It consists of two atoms per unit cell, which are connected by harmonic springs C_1 and C_2 , and which have masses M_1 and M_2 . The equilibrium distance between two adjacent beads is a .

²²On the one hand, there is, strictly speaking, no particle reservoir and, therefore, no chemical potential. On the other hand, setting the chemical potential to zero has the same effect.

7.8.1 Tasks

- 1 Set up the Lagrange or the Hamilton function for this system
- 2 Set up the dynamical matrix in real space
- 3 Determine the k -dependent dynamical matrix
- 4 Determine the band structure $\omega(k)$ of the system, and determine the values at the Γ -point and at the zone boundary.
- 5 Calculate the speed of sound for this system
- 6 Calculate the band structure for identical beads and plot it schematically.
- 7 Describe the main changes of the band structure when the two masses and spring constants become different. (A qualitative description of the effects is sufficient.)

Discussion

- 1 Set up the Lagrange or the Hamilton function for this system

$$\begin{aligned}
 \mathcal{L}(\vec{X}, \vec{V}, t) &= \sum_j \left\{ \underbrace{\frac{1}{2} \sum_{\alpha=1}^2 M_{\alpha} V_{\alpha j}^2}_{\text{kinetic energy}} - \underbrace{\frac{1}{2} C_1 (X_{2j} - X_{1j})^2 - \frac{1}{2} C_2 (X_{1j+1} - X_{2j})^2}_{\text{springs}} \right\} \\
 \mathcal{H}(\vec{X}, \vec{P}, t) &= \sum_j \left\{ \underbrace{\frac{1}{2} \sum_{\alpha=1}^2 \frac{\vec{P}_{\alpha j}^2}{M_{\alpha}}}_{\text{kinetic energy}} + \underbrace{\frac{1}{2} C_1 (X_{2j} - X_{1j})^2 + \frac{1}{2} C_2 (X_{1j+1} - X_{2j})^2}_{\text{springs}} \right\} \quad (7.157)
 \end{aligned}$$

The position of the atom with indices (α, j) is $\vec{R}_{\alpha j} = \vec{e}_x a (2j - 3 + \alpha) + X_{\alpha j} \vec{e}_x$ where \vec{e}_x is the unit vector along the chain direction and a is the distance between the beads. The lattice constant of the problem would be $2a$, and the lattice vector is $\vec{T} = 2a\vec{e}_x$.

The Hamilton function must be expressed in terms of momenta. If the momenta are expressed by velocities, the result will still be the total energy, but it is not a Hamilton function which allows to extract the equations of motion.

- 2 Set up the dynamical matrix in real space

The dynamical matrix is

$$\begin{aligned}
D_{\alpha,i,\beta,j} &\stackrel{\text{Eq. 7.16}}{=} \frac{1}{\sqrt{M_\alpha}} \frac{\partial^2 E_{pot}}{\partial X_{\alpha,i} \partial X_{\beta,j}} \frac{1}{\sqrt{M_\beta}} \\
&= \delta_{i,j} \begin{pmatrix} \frac{1}{\sqrt{M_1}} & 0 \\ 0 & \frac{1}{\sqrt{M_2}} \end{pmatrix} \begin{pmatrix} C_1 + C_2 & -C_1 \\ -C_1 & C_1 + C_2 \end{pmatrix} \begin{pmatrix} \frac{1}{\sqrt{M_1}} & 0 \\ 0 & \frac{1}{\sqrt{M_2}} \end{pmatrix} \\
&+ \delta_{i,j+1} \begin{pmatrix} \frac{1}{\sqrt{M_1}} & 0 \\ 0 & \frac{1}{\sqrt{M_2}} \end{pmatrix} \begin{pmatrix} 0 & -C_2 \\ 0 & 0 \end{pmatrix} \begin{pmatrix} \frac{1}{\sqrt{M_1}} & 0 \\ 0 & \frac{1}{\sqrt{M_2}} \end{pmatrix} \\
&+ \delta_{i,j-1} \begin{pmatrix} \frac{1}{\sqrt{M_1}} & 0 \\ 0 & \frac{1}{\sqrt{M_2}} \end{pmatrix} \begin{pmatrix} 0 & 0 \\ -C_2 & 0 \end{pmatrix} \begin{pmatrix} \frac{1}{\sqrt{M_1}} & 0 \\ 0 & \frac{1}{\sqrt{M_2}} \end{pmatrix} \tag{7.158}
\end{aligned}$$

3 Determine the k-dependent dynamical matrix

We start expanding the displacements $X_{\alpha,j}$ in Bloch waves

$$X_{\alpha,j} = \sum_j X_\alpha(\vec{k}) e^{i\vec{k}\vec{r}_j} \tag{7.159}$$

The dynamical matrix in k-space is

$$\begin{aligned}
D_{\alpha,\beta}(\vec{k}) &\stackrel{\text{Eq. 7.53}}{=} \sum_t D_{\alpha,0,\beta,j} e^{i\vec{k}\vec{r}_j} \\
\mathbf{D}(\vec{k}) &= \begin{pmatrix} \frac{1}{\sqrt{M_1}} & 0 \\ 0 & \frac{1}{\sqrt{M_2}} \end{pmatrix} \begin{pmatrix} C_1 + C_2 & -C_1 - C_2 e^{-2i\vec{k}a} \\ -C_1 - C_2 e^{+2i\vec{k}a} & C_1 + C_2 \end{pmatrix} \begin{pmatrix} \frac{1}{\sqrt{M_1}} & 0 \\ 0 & \frac{1}{\sqrt{M_2}} \end{pmatrix} \tag{7.160}
\end{aligned}$$

4 Determine the band structure $\omega(k)$ of the system, and determine the values at the Γ -point and at the zone boundary.

Below, we use the identities

$$\begin{aligned}
\frac{1}{2}(1 + \cos(2x)) &= \cos^2(x) \\
\frac{1}{2}(1 - \cos(2x)) &= \sin^2(x) \tag{7.161}
\end{aligned}$$

To obtain the dispersion relation, we diagonalize the dynamical matrix. The eigenvalues of the

dynamical matrix are denoted as d_j .

$$\begin{aligned}
& \left(\frac{C_1 + C_2}{M_1} - d \right) \left(\frac{C_1 + C_2}{M_2} - d \right) - \frac{C_1^2 + C_2^2 + 2C_1C_2 \cos(2ka)}{M_1M_2} = 0 \\
\Rightarrow & \left(\frac{C_1 + C_2}{M_1} - d \right) \left(\frac{C_1 + C_2}{M_2} - d \right) - \frac{(C_1 + C_2)^2 - 2C_1C_2[1 - \cos(2ka)]}{M_1M_2} = 0 \\
\Rightarrow & \left(\frac{C_1 + C_2}{M_1} - d \right) \left(\frac{C_1 + C_2}{M_2} - d \right) - \frac{(C_1 + C_2)^2 - 4C_1C_2 \sin^2(ka)}{M_1M_2} = 0 \\
& (x - a)(x - b) - c = \left(x - \frac{a+b}{2} \right)^2 - \left(\frac{a+b}{2} \right)^2 + ab - c \\
d = & \frac{1}{2} \left(\frac{C_1 + C_2}{M_1} + \frac{C_1 + C_2}{M_2} \right) \pm \sqrt{\frac{1}{4} \left(\frac{C_1 + C_2}{M_1} + \frac{C_1 + C_2}{M_2} \right)^2 - \frac{4C_1C_2 \sin^2(ka)}{M_1M_2}} \\
= & \frac{C_1 + C_2}{2M_{rel}} \pm \sqrt{\left(\frac{C_1 + C_2}{2M_{rel}} \right)^2 - \frac{4C_1C_2 \sin^2(ka)}{M_{tot}M_{rel}}} \\
= & \frac{C_1 + C_2}{2M_{rel}} \left\{ 1 \pm \sqrt{1 - \frac{M_{rel}}{M_{tot}} \frac{C_1C_2}{(C_1 + C_2)^2} [4 \sin(ka)]^2} \right\} \\
\omega = \sqrt{d} = & \sqrt{\frac{C_1 + C_2}{2M_{rel}}} \sqrt{1 \pm \sqrt{1 - \frac{M_{rel}}{M_{tot}} \frac{C_1C_2}{(C_1 + C_2)^2} [4 \sin(ka)]^2}} \quad (7.162)
\end{aligned}$$

with $M_{rel} = (M_1^{-1} + M_2^{-1})^{-1}$ and $M_{tot} = M_1 + M_2$.

Editor: include a sketch of the band structure!

5 Calculate the speed of sound for this system

The speed of sound is the group velocity at the Γ -point, that is for infinite long wave length.

$$\begin{aligned}
c &= \left| \frac{\partial \omega}{\partial k} \right|_{k=0} \\
&= \partial_k \left\{ \sqrt{\frac{C_1 + C_2}{2M_{rel}}} \sqrt{1 - \sqrt{1 - \frac{M_{rel}}{M_{tot}} \frac{C_1C_2}{(C_1 + C_2)^2} [4 \sin(ka)]^2}} \right\} \\
&= \sqrt{\frac{C_1 + C_2}{2M_{rel}}} \partial_k \left\{ \sqrt{1 - \left(1 - \frac{1}{2} \frac{M_{rel}}{M_{tot}} \frac{C_1C_2}{(C_1 + C_2)^2} [4 \sin(ka)]^2 + O(k^4) \right)} \right\} \\
&= \sqrt{\frac{C_1 + C_2}{2M_{rel}}} \partial_k \left\{ \sqrt{\frac{1}{2} \frac{M_{rel}}{M_{tot}} \frac{C_1C_2}{(C_1 + C_2)^2} [4 \sin(ka)]^2 + O(k^4)} \right\} \\
&= 4a \sqrt{\frac{C_1 + C_2}{2M_{rel}} \frac{1}{2} \frac{M_{rel}}{M_{tot}} \frac{C_1C_2}{(C_1 + C_2)^2}} \\
&= 2a \sqrt{\frac{1}{M_{tot}} \left(\frac{1}{C_1} + \frac{1}{C_2} \right)^{-1}} \quad (7.163)
\end{aligned}$$

We observe that the smaller of the two spring constants dominates the speed of sound. To rationalize this, consider a molecular crystal where the higher of spring constant holds the molecules together. In that case we can consider the molecules as entities, which themselves form a linear chain of molecules, with equilibrium distance $2a$, mass M_{tot} and the smaller of the two force constants holding together different molecules.

If the two atoms are identical $M_1 = M_2 = M$ and the spring constants $C_1 = C_2 = C$ are the same, the speed of sound is $c_s = a_{\text{lat}} \sqrt{\frac{C}{M}}$

6 Calculate the band structure for identical beads and plot it schematically.

In order to rationalize the dispersion relation obtained above, let us investigate the special case with identical beads. This case could be described with only one bead per unit cell. Doing the more complicated two-bead case shows the folding of the band structure into the smaller reciprocal unit cell of two atoms. The degeneracies, which will lift in the two beads actually become different, provide indications how the band structure changes for more complicated systems.

For $C_1 = C_2 (= C)$ and $M_1 = M_2 (= M)$ we obtain the following result:

$$\begin{aligned} M_{\text{rel}} &= \frac{1}{2}M \\ M_{\text{tot}} &= 2M \\ \omega &= \sqrt{\frac{C}{M_{\text{rel}}}} \sqrt{1 \pm \sqrt{1 - \sin^2(ka)}} = \sqrt{2\frac{C}{M}} \sqrt{1 \pm \sqrt{\cos^2(ka)}} = \sqrt{2\frac{C}{M}} \sqrt{1 \pm |\cos(ka)|} \\ &= \sqrt{\frac{C}{M}} \begin{cases} 2\sin(ka/2) & \text{for } \pm = - \\ 2\cos(ka/2) & \text{for } \pm = + \end{cases} \end{aligned} \quad (7.164)$$

We already recognize the acoustic and the optic branch of the band structure. Because we restricted the displacement into one direction, there are no transversal modes as in a real material.

At the zone boundary, the acoustic and optic branches of the band structure are degenerate.

7 Describe the main changes of the band structure when the two masses and spring constants become different. (A qualitative description of the effects is sufficient.)

Editor: to be done. (1) band ‘folding’ (2) lifting of the degeneracy 3) in the large reciprocal-space unit cell: band discontinuity.

7.9 Worked example: phonon band structure of the hanging linear chain

The hanging linear chain is a one-dimensional chain of pendula connected by springs. In contrast to the conventional linear chain, the bandstructure of the hanging linear chain does not have **linear** acoustic modes.

The hanging linear chain is a model for a relativistic spin-0 particle, which is described by the Klein-Gordon equation. If the hanging linear chain is made continuous, the dispersion relation turns into that of a relativistic particle. Thus, we have a mechanical analogue for a quantum-mechanical wave function of a relativistic particle.

The hanging linear chain is also a model for the band structure in a quasi-one-dimensional system such as an interface. At an interface, the translational invariance is violated in one direction, but it is preserved in the two directions parallel to the interface. As a result the wave vector components \vec{k}_{\parallel} parallel to the interface is a conserved quantity and the dynamical matrix remains block diagonal with respect to different values of \vec{k}_{\parallel} . In order to describe a three-dimensional interface problem, it is necessary to solve many one-dimensional problems. For $\vec{k}_{\parallel} \neq \vec{0}$, the one-dimensional dispersion relation does not have any acoustic phonon modes with (nearly) zero energy. This effect is described by the pendula of the hanging linear chain. In a very hand-waving manner we can say the pendulum describes the coupling of a single linear chain in a three dimensional material relative to the atoms surrounding it.

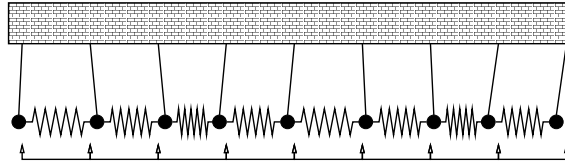
7.9.1 Tasks

- 1 write down the Lagrangian for the hanging linear chain. (Spring constant C and force constant of the pendulum U)
- 2 Determine the equations of motion from the Lagrangian.
- 3 Determine the dynamical matrix in real space
- 4 Determine the dynamical matrix in k-space
- 5 Plot the phonon bandstructure $\omega(k)$, once for $U = 0$ and once for $U \neq 0$.
- 6 Compare the dispersion relation of the linear chain in the continuum limit with that of a relativistic particle $E^2 = m_0c^2 + p^2c^2$. Translate the parameters of the linear chain into those of the relativistic particle.

7.9.2 Discussion

- 1 write down the Lagrangian for the hanging linear chain. (Spring constant C and force constant of the pendulum U)

Let me start with a sketch of the hanging linear chain



$$\mathcal{L}(\vec{X}, \vec{V}, t) = \sum_j \left\{ \underbrace{\frac{1}{2} M V_j^2}_{\text{kinetic energy}} - \underbrace{\frac{1}{2} C (X_j - X_{j+1})^2}_{\text{springs}} - \underbrace{\frac{1}{2} U X_j^2}_{\text{pendula}} \right\} \quad (7.165)$$

The position of the atom with index j is $\vec{R}_j = a_{\text{lat}} \vec{e}_x \cdot j + \vec{e}_x X_j$ where \vec{e}_x is the unit vector pointing along the chain direction and a is the distance between the beads. The primitive lattice vector is $\vec{T} = a \vec{e}_x$.

I am using uppercase symbols C and U for the spring constant and the force constant of the pendulum to avoid a conflict with the symbol c for the speed of light, which I will use in the discussion.

- 2 Determine the equations of motion from the Lagrangian.

$$0 = \frac{d}{dt} \frac{\partial \mathcal{L}}{\partial V_j} \Big|_{V_j = \dot{X}_j} - \frac{\partial \mathcal{L}}{\partial X_j} \Big|_{V_j = \dot{X}_j} = M \ddot{X}_j - C(X_{j+1} - 2X_j + X_{j-1}) + UX_j$$

$$\Rightarrow M \ddot{X} = +C(X_{j+1} - 2X_j + X_{j-1}) - UX_j \quad (7.166)$$

- 3 Determine the dynamical matrix in real space

The dynamical matrix has the matrix elements

$$D_{i,j} = \frac{1}{\sqrt{M}} \frac{\partial^2 E_{pot}}{\partial X_i \partial X_j} \frac{1}{\sqrt{M}} = \delta_{i,j} \frac{2C + U}{M} + \delta_{i+1,j} \frac{-C}{M} + \delta_{i-1,j} \frac{-C}{M} \quad (7.167)$$

4 Determine the dynamical matrix in k-space

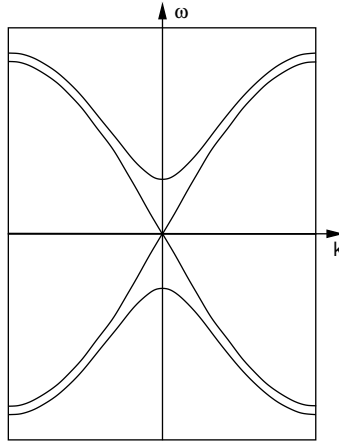
The k-dependent dynamical matrix is a simple number, because the one-dimensional hanging linear chain has only one degree of freedom per unit cell.

$$\begin{aligned} D(\vec{k}) &= \sum_{\vec{r}} D_{0,\vec{r}} e^{i\vec{k}\vec{r}} = \sum_j D_{0,j} e^{i\vec{k}\vec{r}_j} = \frac{1}{M} (U + 2C - 2C \cos(ka)) \\ &= \frac{1}{M} \left(U + 4C \sin^2 \left(\frac{1}{2} ka \right) \right) \end{aligned} \quad (7.168)$$

5 Plot the phonon bandstructure $\omega(k)$, once for $U = 0$ and once for $U \neq 0$.

$$\omega(k) = \sqrt{D(\vec{k})} = \sqrt{\frac{U}{M} + \frac{C}{M} \left(2 \sin \left(\frac{1}{2} ka \right) \right)^2} \quad (7.169)$$

The dispersion relation is sketched below.



For $U = 0$ the dispersion relation reaches $\omega = 0$ at the Γ point, while for $U > 0$ the dispersion relation starts at a value $\omega = \sqrt{U/M}$.

6 Compare the dispersion relation of the linear chain in the continuum limit with that of a relativistic particle $E^2 = m_0 c^2 + p^2 c^2$. Translate the parameters of the linear chain into those of the relativistic particle.

The dispersion relation of the hanging linear chain is closely related to that of a relativistic particle, namely

$$E(\vec{p}) = \pm \sqrt{(m_0 c^2)^2 + (\vec{p}c)^2} \quad (7.170)$$

where $E = \hbar\omega$ is the energy, m_0 is the rest mass, c is the speed of light, and $\vec{p} = \hbar\vec{k}$ is the momentum.

In order to make the comparison clear, let me do the continuum limit $a \rightarrow 0$ of the hanging linear chain.

$$\hbar\omega(k) = \sqrt{\hbar^2 \frac{U}{M} + \left(a \sqrt{\frac{C}{M}} \hbar k \right)^2} \quad (7.171)$$

The general behavior is identical to the dispersion relation of a relativistic particle, if we identify the constants as follows

- the speed of light/sound is $c = a \sqrt{\frac{C}{M}}$ and
- the rest mass is $m_0 = \frac{\hbar}{aC} \sqrt{UM}$.

Chapter 8

Boltzmann equation

The Boltzmann equation is one of the key equations for transport problems. It links Onsager's macroscopic transport coefficients[54, 55] of irreversible thermodynamics to a microscopic description. The Onsager coefficients link the forces and a temperature gradient to the current densities they produce.¹

The Boltzmann equation can be derived in many possible ways, and each derivation may rest on its own set of assumptions. I will therefore emphasize the generic underlying principles in order to prepare a common ground for several formulations. On the one hand, this approach shows, why the Boltzmann equation is so general. On the other hand, the derivation is a good example, how an empirical theory can be developed, and, how fundamental principles enter into empirical theories in a non-trivial manner.

8.1 General form of the Boltzmann equation

8.1.1 Demonstration of the principle in real space

Consider a particle-conservation law² of the form

$$\partial_t \rho(\vec{r}, t) + \vec{\nabla} \cdot \vec{j}(\vec{r}, t) = 0 \quad (8.2)$$

where $\rho(\vec{r}, t)$ is the particle density and $\vec{j}(\vec{r}, t)$ is the particle-current density.

The particle-current density of particles, that follow ³ a given velocity field $\vec{v}(\vec{r}, t)$, is

$$\vec{j}(\vec{r}, t) = \rho(\vec{r}, t) \vec{v}(\vec{r}, t) \quad (8.3)$$

which brings the particle-conservation law into the form

$$\partial_t \rho + \vec{v} \cdot \vec{\nabla} \rho + \rho \left(\vec{\nabla} \cdot \vec{v} \right) = 0 \quad (8.4)$$

¹siehe Wikipedia: Onsagersche Reciprozitaetsbeziehungen.

²This is the general form for a (differential) conservation law. It is obtained from the more intuitive integral conservation law, which says that the conserved quantity in a spatial region Ω changes only due to the current through its surface $\partial\Omega$.

$$\frac{d}{dt} \underbrace{\int_{\Omega} d^3 r \rho(\vec{r}, t)}_{\text{quantity inside the volume } \Omega} = - \underbrace{\int_{\partial\Omega} d\vec{A} \vec{j}(\vec{r}, t)}_{\text{current out of the volume}} \quad (8.1)$$

³This implies particle trajectories which obey $\dot{\vec{r}}(t) = \vec{v}(\vec{r}(t), t)$.

If we add another assumption, namely that the **flow** $\vec{v}(\vec{r}, t)$ is **incompressible**, that is $\vec{\nabla} \cdot \vec{v} = 0$, we obtain

$$\partial_t \rho + \vec{v} \cdot \vec{\nabla} \rho = 0 \quad (8.5)$$

A violation of the particle-number conservation can be described by **sources** and **sinks**. A source produces particles, while a sink removes them. In the presence of sources and sinks, the density evolves according to

$$\partial_t \rho(\vec{r}, t) + \vec{v}(\vec{r}, t) \cdot \vec{\nabla} \rho(\vec{r}, t) = Q(\vec{r}, t) \quad (8.6)$$

where $Q(\vec{r}, t)$ is the **source density**⁴, to which sources and sinks contribute with opposite sign. When Eq. 8.6 is combined with the equations of state, which determines the velocity field $\vec{v}(\vec{r}, t)$ and the source term $Q(\vec{r}, t)$, one obtains an equation of motion for the density.⁵

8.1.2 From coordinate space to phase space

The state of a classical particle is characterized by its position and momentum. Both span the six-dimensional **phase space**.

Therefore, we generalize the principle of the previous section from the three-dimensional configuration space to the six-dimensional phase space. That is, we start with a particle-conservation law in phase space, show that the flow in phase space is incompressible, and introduce source terms.

$$\rho(\vec{r}, t) \rightarrow f(\vec{r}, \vec{p}, t) \quad \text{and} \quad \vec{v}(\vec{r}) \rightarrow \begin{pmatrix} \vec{v}(\vec{r}, \vec{p}) \\ \vec{F}(\vec{r}, \vec{p}) \end{pmatrix} \quad \text{and} \quad \vec{\nabla} \rightarrow \begin{pmatrix} \vec{\nabla}_r \\ \vec{\nabla}_p \end{pmatrix} \quad (8.7)$$

The particle dynamics is governed by Hamilton's equations of motion

$$\begin{pmatrix} \dot{\vec{r}} \\ \dot{\vec{p}} \end{pmatrix} = \begin{pmatrix} \vec{\nabla}_p H(\vec{r}, \vec{p}) \\ -\vec{\nabla}_r H(\vec{r}, \vec{p}) \end{pmatrix} \quad (8.8)$$

with the Hamilton function $H(\vec{r}, \vec{p})$. With $\vec{\nabla}_r$, we denote the gradient with respect to the position and with $\vec{\nabla}_p$ the gradient with respect to the momentum of the particle.

Because the particle dynamics is described in phase space, let me translate the particle-conservation law Eq. 8.6 for an incompressible flow into phase space. For this purpose, we need (1) to define a 6-dimensional flow in phase space and (2) to show that this flow is incompressible:

1. The phase-space flow (\vec{v}, \vec{F}) is given by the Hamilton function $H(\vec{p}, \vec{r})$.

$$\begin{pmatrix} \vec{v}(\vec{r}, \vec{p}) \\ \vec{F}(\vec{r}, \vec{p}) \end{pmatrix} \stackrel{\text{def}}{=} \begin{pmatrix} \vec{\nabla}_p H(\vec{p}, \vec{r}) \\ -\vec{\nabla}_r H(\vec{p}, \vec{r}) \end{pmatrix} \quad (8.9)$$

The six-dimensional flow in phase space is made up of the three-dimensional velocity field $\vec{v}(\vec{r}, \vec{p})$ and the three-dimensional force field $\vec{F}(\vec{r}, \vec{p})$.

2. **Liouville's theorem** says that the flow in phase space is incompressible. It is proven by expressing the divergence of the flow in phase space by the Hamilton function.

$$\underbrace{\begin{pmatrix} \vec{\nabla}_r \\ \vec{\nabla}_p \end{pmatrix} \begin{pmatrix} \vec{\nabla}_p H(\vec{p}, \vec{r}) \\ -\vec{\nabla}_r H(\vec{p}, \vec{r}) \end{pmatrix}}_{\text{divergence of phase-space flow}} = \vec{\nabla}_r \cdot \vec{\nabla}_p H - \vec{\nabla}_p \cdot \vec{\nabla}_r H = 0 \quad (8.10)$$

⁴I use the symbol Q reminding of the German word *Quelle* for *source*. I avoid the symbol S to avoid a conflict with the entropy.

⁵The equation of motion and its initial conditions specify the density for all future times.

When we generalize Eq. 8.6 into phase space, we obtain

$$\partial_t f(\vec{r}, \vec{p}, t) + \underbrace{\vec{v}(\vec{r}, \vec{p})}_{\vec{\nabla}_p H(\vec{r}, \vec{p})} \cdot \vec{\nabla}_r f(\vec{r}, \vec{p}, t) + \underbrace{\vec{F}(\vec{r}, \vec{p})}_{-\vec{\nabla}_r H(\vec{r}, \vec{p})} \cdot \vec{\nabla}_p f(\vec{r}, \vec{p}, t) = Q(\vec{r}, \vec{p}, t) \quad (8.11)$$

where the phase-space density $f(\vec{r}, \vec{p}, t)$ replaces the density $\rho(\vec{r}, t)$ in Eq. 8.6.

Thus, we arrived at the equation of motion for a distribution of non-interacting particles in phase space.

8.1.3 Nature of Hamilton's functions

We will identify the Hamilton function with the dispersion relation (the band structure) $\epsilon(\vec{k}, \vec{r})$ discussed in the previous chapters. Thus, the Hamilton function is $H(\vec{r}, \hbar\vec{k}) = \epsilon(\vec{k}, \vec{r})$.

A typical application would be to start with a homogeneous material having a band structure $\epsilon(\vec{k})$ and to add a potential $v(\vec{r})$, which locally shifts the band structure.

$$H(\vec{r}, \hbar\vec{k}) = \epsilon(\vec{k}) + v(\vec{r}) \quad (8.12)$$

The potential may be an external potential acting on the electrons or, in a mean-field electrostatic potential from the other electrons.

Hamilton's equations are not limited to classical particles. Position \vec{r} and wave vector \vec{k} of extended wave packets obey similar equations of motion, which are related to Hamilton's equation through the **correspondence principle**⁶ $\epsilon = \hbar\omega$ and $\vec{p} = \hbar\vec{k}$. Therefore, we may use Hamilton's equations of motion also for quantum wave packets as long as the Hamiltonian varies slowly on the length scale of the wave length.

In the following, I will treat the Hamilton function as time independent. This is not a requirement but a convenient choice, if we consider the Hamiltonian to be a materials property. The generalization to time-dependent Hamilton functions is straightforward and is done when needed.

8.1.4 Many bands

Usually, a real band structure has several bands $\epsilon_n(\vec{r}, \vec{p})$. Each band acts like a separate quasi-particle type, which is characterized by the band index n and which has its own dispersion relation. Thus, each band is described by its own Hamilton function $H_n(\vec{r}, \vec{p})$.

$$\partial_t f_n(\vec{r}, \vec{p}, t) + \underbrace{\vec{v}_n(\vec{r}, \vec{p})}_{\vec{\nabla}_p H_n(\vec{r}, \vec{p})} \cdot \vec{\nabla}_r f_n(\vec{r}, \vec{p}, t) + \underbrace{\vec{F}_n(\vec{r}, \vec{p})}_{-\vec{\nabla}_r H_n(\vec{r}, \vec{p})} \cdot \vec{\nabla}_p f_n(\vec{r}, \vec{p}, t) = Q_n(\vec{r}, \vec{p}, t) \quad (8.14)$$

8.1.5 Sources and Sinks

The sources and sinks $Q_n(\vec{r}, \vec{p})$ in Boltzmann equation, describe scattering of particles. When two particles with momenta \vec{p}_1 and \vec{p}_2 exchange momentum \vec{q} , the particles with the previous momenta disappear into the sink, while two particles with new momenta $\vec{p}_1 - \vec{q}/2$ and $\vec{p}_2 + \vec{q}/2$ emerge from the source. The source densities $Q_n(\vec{r}, \vec{p})$ depend themselves on the distribution of particles that are

⁶The correspondence principle $\vec{p} = \hbar\vec{k}$ and $E = \hbar\omega$ is a general property of wave packets and is not limited to quantum systems. The velocity of a wave packet is the group velocity $\vec{v} = \vec{\nabla}_k \omega(\vec{k}, \vec{r})$, which translates into Hamilton's first equation $\dot{\vec{r}} = -\vec{\nabla}_p H(\vec{p}, \vec{r})$. Hamilton's second equation follows from the "frequency conservation",

$$0 = \partial_t \omega(\vec{r}(t), \vec{k}(t)) = \dot{\vec{k}} \cdot \vec{\nabla}_k \omega + \dot{\vec{r}} \cdot \vec{\nabla}_r \omega = \dot{\vec{r}} \cdot \left(\dot{\vec{k}} + \vec{\nabla}_r \omega \right) \quad (8.13)$$

which translates into $\dot{\vec{p}} = -\vec{\nabla}_r H(\vec{p}, \vec{r})$. Specific to quantum mechanics is only the value of Planck's constant \hbar as proportionality constant. For a more detailed explanation, see chapter 3 in Φ SX: Quantum Physics[4].

available for a scattering event. The source density is a functional $Q[\vec{f}]$ of the particle distributions \vec{f} .

$$Q_n(\vec{r}, \vec{p}) = Q_n([\vec{f}], \vec{r}, \vec{p}) \quad (8.15)$$

We will discuss these scattering events in more detail below.

8.1.6 Boltzmann equation

When the source and sink terms describe collisions with external obstacles or with other particles, we arrive at the **Boltzmann equation**.

BOLTZMANN EQUATION

$$\left[\partial_t + \underbrace{\vec{v}_n(\vec{r}, \vec{p})}_{\vec{\nabla}_p H_n(\vec{r}, \vec{p})} \vec{\nabla}_r + \underbrace{\vec{F}_n(\vec{r}, \vec{p})}_{-\vec{\nabla}_r H_n(\vec{r}, \vec{p})} \vec{\nabla}_p \right] f_n(\vec{r}, \vec{p}, t) = \underbrace{Q_n([\vec{f}], \vec{r}, \vec{p}, t)}_{\left(\frac{\partial f_n(\vec{r}, \vec{p}, t)}{\partial t} \right)_{\text{coll}}} \quad (8.16)$$

The left-hand side of the equation is called the **drift term**, while the right-hand side is the **collision term**.

Usually, the collision term is denoted as

$$\left(\frac{\partial f_n(\vec{r}, \vec{p}, t)}{\partial t} \right)_{\text{coll}} \stackrel{\text{def}}{=} Q_n(\vec{r}, \vec{p}, t) \quad (8.17)$$

meaning “*growth of the phase-space distribution due to collisions*”. I will not use this notation, because I find it misleading. One should, however, be familiar with it because it is often used in the literature.

Memory hook

A compact way of writing the Boltzmann equation Eq. 8.16 is

$$\frac{d}{dt} f_n(\vec{r}_n(t), \vec{p}_n(t), t) = Q_n(\vec{r}_n(t), \vec{p}_n(t)) \quad \text{with} \quad \underbrace{\dot{\vec{r}}_n = \vec{v}_n \quad \text{and} \quad \dot{\vec{p}}_n = \vec{F}_n}_{\text{Hamilton's equations of motion}} \quad (8.18)$$

which folds up to the full Boltzmann equation, if we insert Hamilton's equations of motion for the trajectories. For the mental organization, this form simplifies Boltzmann's equation and places the mental load on memorizing Hamilton's equations of motion. For more than one band H_n , the form Eq. 8.18 is of limited use (none), because each particle follows its own trajectory.

For a single band, this notation considers a frame of reference that moves along with the phase-space trajectory. Considering a phase-space volume element moving along with the trajectories, maintains its size as a consequence of Liouville theorem Eq. 8.10. Particles enter and leave this volume element only through collisions. Therefore, the collision term Q provides directly the change of the the distribution. This is the literal meaning of Eq. 8.18.

8.1.7 Normalization

The normalization of the distribution $f_n(\vec{r}, \vec{p}, t)$ is defined such that the phase-space integral

$$\sum_n \int d^3r \int \frac{d^3p}{(2\pi\hbar)^3} f_n(\vec{r}, \vec{p}, t) = N \quad (8.19)$$

is the particle number N .

As described below, the factor $(2\pi\hbar)^3$ is the phase-space volume of a one-particle state. Thus, $f_n(\vec{r}, \vec{p}, t)$ is unit less. It is the fractional occupation of the one-particle state characterized by the band index n and the position (\vec{r}, \vec{p}) in phase space.

How do I know that $(2\pi\hbar)^3$ is the phase-space volume of a one-particle state? The arguments are analogous to those in section 5.1 on p. 173. Let us consider a material with volume $\Omega = L^3$ and sidelength L . The quantization condition of plane waves with periodic boundary conditions determines the spacing of wave vectors in each direction as $\Delta k = \frac{2\pi}{L}$. Thus, a state occupies a momentum-space volume of $\Delta p^3 = (\hbar\Delta k)^3 = \frac{(2\pi\hbar)^3}{\Omega}$ and a real-space volume of Ω . The phase-space volume of a state is therefore $\Delta p^3 \Delta r^3 = (2\pi\hbar)^3$.

With the normalization Eq. 8.19, the spatial particle density $\rho(\vec{r}, t)$ is given by the phase-space distribution $f_n(\vec{r}, \vec{p}, t)$ as

$$\rho(\vec{r}, t) = \sum_n \int \frac{d^3 p}{(2\pi\hbar)^3} f_n(\vec{r}, \vec{p}, t) . \quad (8.20)$$

8.1.8 Combined index for bands and momentum

As a matter of convenience, one can combine the band and momentum indices into a single, combined index $\lambda = (\vec{p}, n)$. I will often resort to this compact notation, where the extended notation would clutter the derivation and thus hide it's essence.

In this compact notation, the Boltzmann equation Eq. 8.16 has the form

$$\left[\partial_t + \vec{v}_\lambda(\vec{r}) \vec{\nabla}_r + \vec{F}_\lambda(\vec{r}) \vec{\nabla}_p \right] f_\lambda(\vec{r}, t) \stackrel{\text{Eq. 8.16}}{=} \underbrace{Q_\lambda(\vec{r}, t)}_{\left(\frac{\partial f_\lambda(\vec{r})}{\partial t} \right)_{\text{coll}}} \quad (8.21)$$

and the normalization Eq. 8.19 is

$$\sum_\lambda \int d^3 r f_\lambda(\vec{r}) \stackrel{\text{Eq. 8.19}}{=} N \quad (8.22)$$

The density in real space is according to Eq. 8.20

$$\rho(\vec{r}, t) \stackrel{\text{Eq. 8.20}}{=} \sum_\lambda f_\lambda(\vec{r}, t) \quad (8.23)$$

The general rule to translate expressions into the compact notation is

$$\begin{aligned} (n, \vec{p}_n) &\rightarrow \lambda \\ \sum_n \int \frac{d^3 p_n}{(2\pi\hbar)^3} &\rightarrow \sum_\lambda \\ (2\pi\hbar)^3 \delta(\vec{p} - \vec{p}') \delta_{n,n'} &\rightarrow \delta_{\lambda,\lambda'} \\ f_n(\vec{r}, \vec{p}, t) &\rightarrow f_\lambda(\vec{r}, t) \end{aligned} \quad (8.24)$$

The true payoff from this notation becomes evident in the multiple momentum-space integrations of the collision term discussed below. I will adhere to the explicit notation for some time, to make the reader familiar with the true meaning. The reader may, however, already practice the grouping of indices.

8.2 Collisions

8.2.1 Scattering of classical particles

A particle may collide with an obstacle and thus change its momentum. This collision can be described as an annihilation of a particle with the initial quantum numbers and the simultaneous creation of a particle with the final quantum numbers. The annihilation is described by the sink term (negative source term) and the creation by a source term.

The form of the collision term depends on the physical interaction. Usually, the collisions are assumed to be local: In a scattering event, two particles may collide at a given position in space.⁷

In the most simple scattering term, so-called **impurity scattering**, the source term has the form

$$Q_n(\vec{r}, \vec{p}, t) = \sum_a \int \frac{d^3 p_a}{(2\pi\hbar)^3} L^*_a(\vec{p}, \vec{p}_a) f_a(\vec{r}, \vec{p}_a, t) - \sum_b \int \frac{d^3 p_b}{(2\pi\hbar)^3} L^*_b(\vec{p}_b, \vec{p}) f_n(\vec{r}, \vec{p}, t) \quad (8.25)$$

The **intrinsic scattering probability per unit time** $L^*_a(\vec{p}_b; \vec{p}_a)$ is the probability per unit time that a particle of band a with momentum \vec{p}_a is scattered into band b with momentum \vec{p}_b . The first term describes the increase of the particle number of the state (\vec{p}, n) under consideration, due to scattering from another state (\vec{p}_a, a) and the second term describes the decrease of the particle number due to scattering the state (\vec{p}, n) under consideration into another state (\vec{p}_b, b) .

Conceptual origin of scattering: The underlying assumption for the chosen form of the collision term is that the source term can be written as a functional of the distribution function. This functional is then expanded in a Taylor series about the distribution $f_{\lambda}^{eq}(\vec{r})$ in thermal equilibrium. The deviation from the equilibrium distribution is

$$\delta f_{\lambda}(\vec{r}, t) \stackrel{\text{def}}{=} f_{\lambda}(\vec{r}, t) - f_{\lambda}^{eq}(\vec{r}) \quad (8.26)$$

We use the compact notation described in section 8.1.8. Each sum over the combined index λ expands into a sum over bands and a momentum integration.

$$Q_{\lambda}[f(\vec{r}, t)] = Q_{\lambda}[f^{eq}(\vec{r}, t)] + \sum_{\lambda'} \left. \frac{\partial Q_{\lambda}}{\partial f_{\lambda'}} \right|_{f^{eq}} \delta f_{\lambda'}(\vec{r}, t) + \frac{1}{2} \sum_{\lambda', \lambda''} \left. \frac{\partial^2 Q_{\lambda}}{\partial f_{\lambda'} \partial f_{\lambda''}} \right|_{f^{eq}} \delta f_{\lambda'}(\vec{r}, t) \delta f_{\lambda''}(\vec{r}, t) + \dots \quad (8.27)$$

The Taylor expansion is truncated at a certain order. The form used previously, Eq. 8.25, is obtained when the deviations δf_{λ} are expressed again in terms of f_{λ} and f_{λ}^{eq} . The prefactors of the powers of the distribution f_{λ} are the so-called **intrinsic scattering probabilities**.

Limiting the source term to a dependence on the local distribution only, has historical origin. It appears also to be physically reasonable, but I do not yet have a stringent argument for it. The generalization to non-local dependence would be straightforward. It would, however, make solving the problem considerably harder.

There may also be an additional dependence of the source term on space and time, as in $Q([f], \vec{r}, t)$, which is suppressed and which is also rarely used.

8.2.2 Correlations and coherence

The reader may object that the collision term should involve the probabilities of the initial many-particle state, that is $f_{n_1, \dots, n_M}(\vec{r}_1, \dots, \vec{r}_M, \vec{p}_1, \dots, \vec{p}_M, t)$, rather than the product of one-particle occupations $f_{n_1}(\vec{r}_1, \vec{p}_1, t) f_{n_2}(\vec{r}_2, \vec{p}_2, t) \dots f_{n_M}(\vec{r}_M, \vec{p}_M, t)$. Breaking up the probability into a product of

⁷The notion of local collisions emerged from the classical picture of point particles. For quantum-mechanical wave packets, the collision process has a more complicated interpretation.

one-particle probabilities discards the information on correlations between particles. This is the assumption of **molecular chaos**, which is one of the central approximations of the Boltzmann equation. It is discussed below in section 8.4.1.

8.2.3 Energy and momentum conservation

During a collision, the total momentum and the total energy of the participating particles is conserved. Therefore, the intrinsic probabilities of collisions have the form

$$L^{\alpha_1, \dots, \alpha_N}_{i_1, \dots, i_M} = M^{\alpha_1, \dots, \alpha_N}_{i_1, \dots, i_M} \delta\left(\sum_{n=1}^N \vec{k}_{\alpha_n} - \sum_{m=1}^M \vec{k}_{i_m}\right) \delta\left(\sum_{n=1}^N \epsilon_{\alpha_n} - \sum_{m=1}^M \epsilon_{i_m}\right) \quad (8.28)$$

The tensor M has no specific meaning. It has been introduced to demonstrate that the intrinsic scattering probabilities contain the delta-functions, which ensure energy and momentum conservation. Energy and momentum conservation of a quantum collision results from Fermi's golden rule. Hence, the limitations of Fermi's golden rule enter also the Boltzmann equation.

8.2.4 Exclusion principle

A scattering event, which creates a Fermion in a state that is already occupied, is forbidden by the **Pauli (exclusion) principle**. This is a quantum effect that does not emerge from a classical description.

The exclusion principle is not incorporated into the intrinsic scattering probabilities $L^b_a(\vec{p}_b; \vec{p}_a)$, but described, for Fermions, by an additional factor $1 - f_{n_b}(\vec{p}_b, \vec{r}, t)$ for each final state (n_b, \vec{p}_n) of the collision.⁸ The additional factor is the probability for the final state of the scattering process to be unoccupied.

For Bosons, the factor is $1 + f_{n_b}(\vec{p}_b, \vec{r}, t)$. I will not derive it here. The scattering probability for Bosons is increased, if the final state is already occupied. While the exclusion principle for Fermions acts like a repulsion, the one for Bosons acts like an attraction. The origin of this effect is, however, not a force but mere statistics.

A consistent description for Fermions, Bosons and distinguishable particles is obtained by defining the parameter η

$$\eta \stackrel{\text{def}}{=} \begin{cases} -1 & \text{for Fermions} \\ 0 & \text{for distinguishable particles} \\ +1 & \text{for Bosons} \end{cases} \quad (8.29)$$

The factors to be introduced for each outgoing particle index of the **intrinsic scattering probability** are

$$1 + \eta f_n(\vec{p}, \vec{r}, t) \stackrel{\text{def}}{=} \begin{cases} 1 - f_n(\vec{p}, \vec{r}, t) & \text{for Fermions} \\ 1 & \text{for distinguishable particles} \\ 1 + f_n(\vec{p}, \vec{r}, t) & \text{for Bosons} \end{cases} \quad (8.30)$$

Thus, the impurity-scattering term has the form

$$Q_n(\vec{r}, \vec{p}, t) = \sum_a \int \frac{d^3 p_a}{(2\pi\hbar)^3} \left(1 + \eta f_n(\vec{r}, \vec{p}, t)\right) L^n_a(\vec{p}, \vec{p}_a) f_a(\vec{r}, \vec{p}_a, t) \\ - \sum_b \int \frac{d^3 p_b}{(2\pi\hbar)^3} \left(1 + \eta f_b(\vec{r}, \vec{p}_b, t)\right) L^b_n(\vec{p}_b, \vec{p}) f_n(\vec{r}, \vec{p}, t)$$

By comparison, we see that classical particles act like distinguishable particles with $\eta = 0$.

⁸The factors emerges from the quantum mechanical scattering matrix elements between many-particle states.

8.2.5 Types of collisions

Up to now, I discussed the principles of the collision term for the most simple scattering term, namely impurity scattering. Here, I will summarize the most important contributions for the collision term.

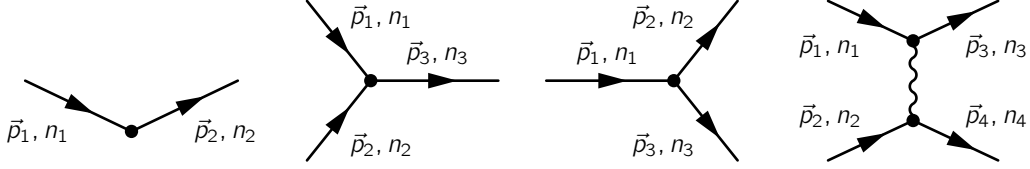


Fig. 8.1: Schematic representation of different scattering terms. From left to right: Impurity scattering, two three-particle processes, particle-particle scattering. The three-particle processes are relevant for phonons or photons, which do not have a particle-conservation law. The particle-particle scattering would describe the Coulomb interaction between electrons.

- **Impurity scattering** discussed above:

$$Q_n(\vec{r}, \vec{p}, t) = \sum_a \int \frac{d^3 p_a}{(2\pi\hbar)^3} \left(1 + \eta f_n(\vec{r}, \vec{p}, t)\right) L^n_a(\vec{p}, \vec{p}_a) f_a(\vec{r}, \vec{p}_a, t) - \sum_b \frac{d^3 p_b}{(2\pi\hbar)^3} \left(1 + \eta f_b(\vec{r}, \vec{p}_b, t)\right) L^n_b(\vec{p}_b, \vec{p}) f_n(\vec{r}, \vec{p}, t) \quad (8.31)$$

- The scattering terms involving three one-particle states violate particle-number conservation and are forbidden for particles that obey a particle-conservation law. Such terms do not exist for electrons. They are, however, allowed for bosons such as phonons or photons. Phonon scattering events with three sets of quantum numbers are due to anharmonic terms in the potential-energy surface.

There are two different scattering terms involving three one-particle states, namely one ($L^{c,d}_a$), where one particle is consumed and two particles emerge, and another one ($L^c_{a,b}$), where two particles (a, \vec{p}_a) and (b, \vec{p}_b) are consumed and one particle (c, \vec{p}_c) emerges. The collision term is

$$Q_n(\vec{r}, \vec{p}, t) = \sum_{a,b} \int \frac{d^3 p_a}{(2\pi\hbar)^3} \int \frac{d^3 p_b}{(2\pi\hbar)^3} \left(1 + \eta f_n(\vec{r}, \vec{p}, t)\right) L^n_{a,b}(\vec{p}; \vec{p}_a, \vec{p}_b) f_a(\vec{r}, \vec{p}_a, t) f_b(\vec{r}, \vec{p}_b, t) - 2 \sum_{a,c} \int \frac{d^3 p_a}{(2\pi\hbar)^3} \int \frac{d^3 p_c}{(2\pi\hbar)^3} \left(1 + \eta f_c(\vec{r}, \vec{p}_c, t)\right) L^c_{a,n}(\vec{p}_c; \vec{p}_a, \vec{p}) f_a(\vec{r}, \vec{p}_a, t) f_n(\vec{r}, \vec{p}, t) + 2 \sum_{a,c} \int \frac{d^3 p_a}{(2\pi\hbar)^3} \int \frac{d^3 p_c}{(2\pi\hbar)^3} \times \left(1 + \eta f_n(\vec{r}, \vec{p}, t)\right) \left(1 + \eta f_c(\vec{r}, \vec{p}_c, t)\right) L^{n,c}_a(\vec{p}, \vec{p}_c; \vec{p}_a) f_a(\vec{r}, \vec{p}_a, t) - \sum_{b,c} \int \frac{d^3 p_b}{(2\pi\hbar)^3} \int \frac{d^3 p_c}{(2\pi\hbar)^3} \times \left(1 + \eta f_b(\vec{r}, \vec{p}_b, t)\right) \left(1 + \eta f_c(\vec{r}, \vec{p}_c, t)\right) L^{b,c}_n(\vec{p}_b, \vec{p}_c; \vec{p}) f_n(\vec{r}, \vec{p}, t) \quad (8.32)$$

The Fermionic case $\eta = -1$ is nonphysical because Fermions obey a particle-conservation law.

- two-particle scattering has four sets of quantum numbers as indices. It is the dominant collision term for electrons, because the particle-number conservation law excludes a collision term

involving three indices. The scattering rate⁹ $L^{c,d}_{a,b}(\vec{p}_c, \vec{p}_d; \vec{p}_a, \vec{p}_b)$ describes the probability per unit time that two particles (a, \vec{p}_a) and (b, \vec{p}_b) collide and emerge as particles (c, \vec{p}_c) and (d, \vec{p}_d).

$$\begin{aligned}
Q_n(\vec{r}, \vec{p}, t) &= 2 \sum_{a,b,d} \int \frac{d^3 p_a}{(2\pi\hbar)^3} \int \frac{d^3 p_b}{(2\pi\hbar)^3} \int \frac{d^3 p_d}{(2\pi\hbar)^3} \\
&\quad \left(1 + \eta f_n(\vec{r}, \vec{p}, t)\right) \left(1 + \eta f_d(\vec{r}, \vec{p}_d, t)\right) L^{n,d}_{a,b}(\vec{p}, \vec{p}_d; \vec{p}_a, \vec{p}_b) f_a(\vec{r}, \vec{p}_a, t) f_b(\vec{r}, \vec{p}_b, t) \\
&\quad - 2 \sum_{a,c,d} \int \frac{d^3 p_a}{(2\pi\hbar)^3} \int \frac{d^3 p_c}{(2\pi\hbar)^3} \int \frac{d^3 p_d}{(2\pi\hbar)^3} \\
&\quad \left(1 + \eta f_c(\vec{r}, \vec{p}_c, t)\right) \left(1 + \eta f_d(\vec{r}, \vec{p}_d, t)\right) L^{c,d}_{a,n}(\vec{p}_c, \vec{p}_d, \vec{p}_a, \vec{p}) f_a(\vec{r}, \vec{p}_a, t) f_n(\vec{r}, \vec{p}, t)
\end{aligned} \tag{8.33}$$

8.2.6 General form of the collision term

For the sake of completeness, let me now write down the collision term in the most general form. In order to simplify the expression, let me use the combined index $\lambda = (\vec{p}, n)$ introduced in section 8.1.8 and let me use the factor η from Eq. 8.29, which is $\eta = -1, 0, 1$ for Fermions, distinguishable particles and Bosons, respectively.

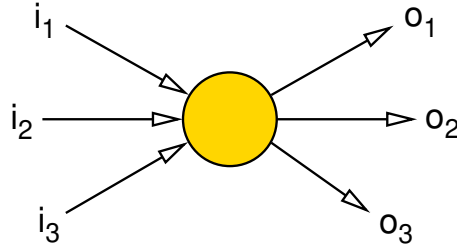


Fig. 8.2: Sketch for a collision term with $M = 3$ colliding (incoming) particles having quantum numbers i_1, i_2, i_3 and $N = 3$ emerging (outgoing) particles having quantum numbers o_1, o_2, o_3 .

With the short-hand notation $\lambda = (\vec{p}, n)$, the collision term has the general form¹⁰

$$\begin{aligned}
Q_\lambda &= \sum_{N,M=1}^{\infty} \sum_{o_1, \dots, o_N} \sum_{i_1, \dots, i_M} \left(\sum_{u=1}^N \delta_{\lambda, o_u} - \sum_{v=1}^M \delta_{\lambda, i_v} \right) \left[\prod_{j=1}^N (1 + \eta f_{o_j}) \right] L^{o_1, \dots, o_N}_{i_1, \dots, i_M} \left[\prod_{k=1}^M f_{i_k} \right] \\
&= \sum_{N,M=1}^{\infty} \sum_{o_1, \dots, o_N} \sum_{i_1, \dots, i_M} (N \delta_{\lambda, o_1} - M \delta_{\lambda, i_1}) \left[\prod_{j=1}^N (1 + \eta f_{o_j}) \right] L^{o_1, \dots, o_N}_{i_1, \dots, i_M} \left[\prod_{k=1}^M f_{i_k} \right]
\end{aligned} \tag{8.34}$$

In the last step, I exploited that the intrinsic collision probability is symmetric under exchange of the upper, outgoing indices among themselves, and under exchange of the lower outgoing indices among themselves.

In the most general case, we may also consider scattering between Fermions and Bosons. An example for such a term is electron-phonon coupling, where an electron may change its momentum by absorbing or emitting a phonon. We may describe it by giving each particle an individual value for η .

⁹For particles such as phonons without particle number conservation, there would also be terms describing collisions that consume one particle, while three particles emerge.

¹⁰Terms with $N = 0$ or $M = 0$ have been ignored for no special reason. They describe the spontaneous creation or annihilation of particles, which seems to violate energy conservation.

Expression Eq. 8.34 is daunting. Because it is, typical applications deal only with a very small set of intrinsic collision probabilities. I have written down the general expression Eq. 8.34 to place these simplified cases into a broader context.

8.3 Thermal equilibrium

The distribution of the Boltzmann equation approaches, over time, a stationary equilibrium state. The nature of the equilibrium distribution is important to make contact to the microscopic formulation.

Historically, the Boltzmann equation is central in the puzzle of the **second law of thermodynamics**, which says that the entropy increases with time until it reaches a state of maximum entropy. The problem is that the second law of thermodynamics seems to be in contradiction with the microscopic equations of motion, classical or quantum. Because the microscopic equations of motion are time-inversion symmetric, a quantity that only increases with time should not exist. [Editor: The article\[56\] by Ehrenfest may be useful in this context. Paul Ehrenfest has been a PhD Student of Boltzmann.](#)

Nevertheless, the second law of thermodynamics can be observed in our everyday life. Boltzmann derived the Boltzmann equations from the microscopic equations of motion and the equation, he arrived at, has an entropy which increases with time, namely the Boltzmann entropy. The derivation¹¹ rests on the assumption of **molecular chaos** and **decoherence**, which is inherent in Boltzmann's equation. Molecular chaos and decoherence discard information, which is responsible for the increase of the entropy. Therefore, one should carefully analyze the implications of the assumption of molecular chaos, and its validity.

In my personal view, the key to the understanding of the second law of thermodynamics is (probably) related to decoherence in open systems. The attempt to derive the second law of thermodynamics via Boltzmann's equation is probably indirect and only of historical relevance.

8.3.1 Boltzmann entropy

The description of thermodynamic equilibrium states requires some background on the entropy. In particular, it is important to distinguish between different entropy concepts[57] and to understand how they are related.

Shannon's entropy[45] is the conceptual starting point of the entropy concept. Shannon's entropy has been derived from information theory as a measure for the uncertainty of a probabilistic experiment with possible outcomes q , which occur with probabilities P_q .

$$S[P_q] = -k_B \sum_q P_q \ln(P_q) \quad (8.35)$$

Shannon's entropy corresponds, up to a factor¹², to the number of yes-no questions, that need to be asked on average until the specific outcome q is been identified. (See for example Φ SX: Statistical Physics[38] chapter 1 and in particular section 1.4)

Von-Neumann's entropy[58] is the ultimate underlying form for the entropy of physical systems. It is identical to Shannon's entropy applied to ensembles of quantum states. An ensemble $\{P_q, |\Phi_q\rangle\}$ of quantum states is described by a set of normalized many-particle wave functions $|\Phi_q\rangle$ and their probabilities P_q . The ensemble defines the **von-Neumann density matrix**¹³

$$\hat{\rho} = \sum_q |\Phi_q\rangle P_q \langle \Phi_q| \quad (8.36)$$

¹¹See also appendix O.6 on p. 533.

¹²Shannon used a different prefactor, namely $(1/\ln(2))$ instead of the Boltzmann constant k_B .

¹³It is important to distinguish the von-Neumann density matrix $\hat{\rho}$ (or $\hat{\rho}^{vN}$) from the one-particle reduced density matrix $\hat{\rho}^{(1)}$.

which contains the complete information of the ensemble: The expectation values of all observables \hat{A} can be obtained as $\langle \hat{A} \rangle = \text{Tr}[\hat{\rho}\hat{A}]$.

The von-Neumann entropy

$$S[\hat{\rho}] = -k_B \text{Tr}[\hat{\rho} \ln(\hat{\rho})] . \quad (8.37)$$

is a functional of the von-Neumann density matrix. In a representation of eigenstates of the von-Neumann density matrix, von-Neumann's entropy Eq. 8.37 turns into Shannon's entropy Eq. 8.35 with the probabilities P_q being the eigenvalues of the von-Neumann density matrix.

Other forms of the entropy are derived from von-Neumann's entropy via the **maximum-entropy principle**. [43, 44] (see section 1.5 in Φ SX: Statistical Physics[38]) The maximum-entropy principle determines the most unbiased choice of an ensemble given a specified set of prior knowledge. The prior knowledge is built into the search for the maximum entropy as constraints.

For the maximum entropy principle, the ensembles are divided into subsets, which are characterized by some chosen set of observables. Let me consider an example, where a subset contains all ensembles of many-particle states with a thermal expectation value of the energy $U \stackrel{\text{def}}{=} \text{Tr}[\hat{\rho}\hat{H}]$ and of the particle number $N \stackrel{\text{def}}{=} \text{Tr}[\hat{\rho}\hat{N}]$. Then, the maximum-entropy principle will define an entropy

$$S(U, N) = \max_{\hat{\rho}} \text{stat}_{\mu, T, \lambda} \left\{ \underbrace{-k_B \text{Tr}[\hat{\rho} \ln(\hat{\rho})]}_{S[\hat{\rho}]} - \frac{1}{T} (\text{Tr}[\hat{\rho}\hat{H}] - U) + \frac{\mu}{T} (\text{Tr}[\hat{\rho}\hat{N}] - N) + \lambda \underbrace{(\text{Tr}[\hat{\rho}] - 1)}_{\text{normalization}} \right\} \quad (8.38)$$

for each set of macroscopic expectation values U and N .

Boltzmann's entropy¹⁴ results from an analogous procedure: Under the assumption of molecular chaos and decoherence, the ensemble of states can be characterized entirely by a set of one-particle occupations, which corresponds to the distribution function $f_n(\vec{r}, \vec{p}, t)$. All other information is discarded.

Therefore, Boltzmann's entropy $S^B[\vec{f}]$ is defined as the maximum entropy for a specific distribution $f_n(\vec{r}, \vec{p})$.

$$S^B[\vec{f}] = \max_{\hat{\rho}} \text{stat}_{\vec{\gamma}, \Lambda} \left\{ \underbrace{-k_B \text{Tr}[\hat{\rho} \ln(\hat{\rho})] - \sum_{\lambda} k_B \gamma_{\lambda} (\text{Tr}[\hat{\rho} \hat{c}_{\lambda}^{\dagger} \hat{c}_{\lambda}] - f_{\lambda}) - k_B \Lambda (\text{Tr}[\hat{\rho}] - 1)}_{S(\hat{\rho}, \vec{f}, \vec{\gamma}, \Lambda)} \right\} \quad (8.39)$$

For the sake of simplicity, the set of occupations is represented by a vector \vec{f} with coefficients f_{λ} . The γ_{λ} are the Lagrange multipliers for the occupation constraint $\text{Tr}[\hat{\rho} \hat{c}_{\lambda}^{\dagger} \hat{c}_{\lambda}] = f_{\lambda}$ and Λ is the one for the normalization constraint $\text{Tr}[\hat{\rho}] = 1$.

The functional form of Boltzmann's entropy S^B for Fermions $\eta = -1$, Bosons $\eta = +1$ or distinguishable particles $\eta = 0$ is

$$S^B[\vec{f}] \stackrel{\text{Eq. 8.41}}{\text{def}} -k_B \sum_{\lambda} \left\{ f_{\lambda} \ln(f_{\lambda}) - \eta (1 + \eta f_{\lambda}) \ln(1 + \eta f_{\lambda}) + (\eta^2 - 1) f_{\lambda} \right\} \quad (8.40)$$

The derivation is shown in appendix O.5 on p. 530.

For a phase-space distribution $f_n(\vec{r}, \vec{p})$ this yields

$$S^B[f_n(\vec{r}, \vec{p})] \stackrel{\text{def}}{=} -k_B \sum_n \int d^3r \int \frac{d^3p}{(2\pi\hbar)^3} \times \left\{ f_n(\vec{r}, \vec{p}) \ln(f_n(\vec{r}, \vec{p})) - \eta (1 + \eta f_n(\vec{r}, \vec{p})) \ln(1 + \eta f_n(\vec{r}, \vec{p})) + (\eta^2 - 1) f_n(\vec{r}, \vec{p}) \right\} \quad (8.41)$$

¹⁴Take the term "Boltzmann entropy" with a grain of salt. The terminology may not be uniform. Take this as "my" definition of the Boltzmann entropy.

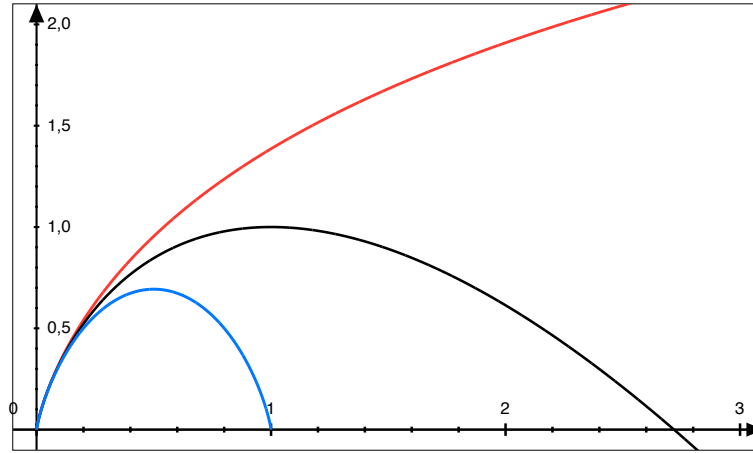


Fig. 8.3: Entropy contribution from a one-particle state in units of k_B as function of occupation f_n for Fermions (blue) Bosons (red) and distinguishable particles (black) from Eq. ???. (Repeated as fig. 8.3).

Boltzmann used the classical version of Eq. 8.40 and Eq. 8.41 with $\eta = 0$. This version is obtained from the expression for Fermions and Bosons in the dilute limit, which retains for the second, η -dependent term only the contribution linear in f_n .

As shown (for elastic collisions) in appendix O.6, Boltzmann's entropy increases with time, which is consistent with the second law of thermodynamics, when the distribution evolves under Boltzmann's equation. For a more extended discussion, see appendix O.6 on p. 533. The way this loss of information is linked to the microscopic quantum dynamics bears the essence of the second law of thermodynamics. For the Boltzmann equation it is the assumption of molecular chaos, i.e. the specific form of the collisions, which discards all phase relations between the outgoing particles. This loss of information is responsible for the increase of the entropy.

8.3.2 Equilibrium distributions

The criterion for a distribution to be in thermal equilibrium is that it maximizes the entropy¹⁵[43]. For a system in contact with a heat-bath and a particle-reservoir, the entropy S is maximized where the **grand potential**

$$\Omega_{T,\mu} = \min_{S,N} (U(S) - TS - \mu N) \quad (8.42)$$

of the system is minimized.

Now we determine the (Boltzmann) grand potential $\Omega_{T,\mu}^B$, using Boltzmann's entropy instead of von-Neumann's entropy.¹⁶ Rather than varying the entropy, as in Eq. 8.42 above, I vary the distribution function $f_n(\vec{r}, \vec{p})$, because Boltzmann's entropy and the particle number are themselves

¹⁵For the maximum-entropy principle, see section 1.5 in *ΦSX: Statistical Physics*[38].

¹⁶Notice the subtle difference of the grand potential obtained from Boltzmann's entropy rather than von-Neumann's entropy

functionals of the distribution $\vec{f} \triangleq \{f_n(\vec{r}, \vec{p})\}$.

$$\Omega_{T,\mu}[H] = \min_{f_n(\vec{r}, \vec{p})} \left\{ \underbrace{-TS^B[f] + \sum_n \int d^3r \int \frac{d^3p}{(2\pi\hbar)^3} f_n(\vec{r}, \vec{p}) (H_n(\vec{r}, \vec{p}) - \mu)}_{\Omega^B[\vec{f}]} \right\} \quad (8.43)$$

The equilibrium distributions for non-interacting particles with energies $\epsilon_n(\vec{r}, \vec{p})$ are the Boltzmann, the Bose and the Fermi distribution.¹⁷ Thus, with the prefactors from section 8.1.7, the equilibrium distributions of non-interacting electrons with energies $H_n(\vec{r}, \vec{p})$ are

$$f_n^{eq}(\vec{r}, \vec{p}) = f_{T,\mu}(H_n(\vec{r}, \vec{p})) \quad (8.44)$$

where $f_{T,\mu}(\epsilon)$ is Fermi-, Bose- or Boltzmann distribution defined by

$$f_{T,\mu}(\epsilon) \stackrel{\text{def}}{=} \left(e^{\beta(\epsilon-\mu)} - \eta \right)^{-1} = \begin{cases} \left(e^{\beta(\epsilon-\mu)} + 1 \right)^{-1} & \text{for Fermions} \\ e^{-\beta(\epsilon-\mu)} & \text{for distinguishable particles} \\ \left(e^{\beta(\epsilon-\mu)} - 1 \right)^{-1} & \text{for Bosons} \end{cases} \quad (8.45)$$

The distribution functions, which emerge from the maximum-entropy principle with the Boltzmann entropy are identical to the equilibrium occupations of non-interacting particles obtained with the von-Neumann entropy. Nevertheless, we did not make any reference to non-interacting particles. The reason is that the energy of non-interacting particles can be specified entirely by the one-particle occupations. Therefore, the minimum grand potential expressed by the von-Neumann entropy coincides with that expressed by the Boltzmann entropy. This changes in the presence of an interaction: An interaction may lead to correlations, which, for the same set of occupations, result in a lower maximum von-Neumann entropy as compared to that obtained with the Boltzmann entropy.

8.3.3 Detailed balance

The principle of **detailed balance** says that for every process, the reverse process occurs in thermal equilibrium with equal probability.¹⁸

The principle of detailed balance is a rather fundamental concept. It is a consequence of the fact that thermodynamic processes are driven¹⁹ by the increase of entropy. Let me dig a little deeper: The entropy is a measure of the uncertainty regarding in which microstate²⁰ the system actually is. A thermodynamic state is an ensemble of microstates with their probabilities. A thermodynamic state, which contains more microstates than another one, is more likely to occur. The entropy is constructed such that such a state also has a higher entropy. Thus, the system will evolve from a state with lower entropy to one with higher entropy. This is true under two important assumptions: (1) The dynamics of the micro-states does not favor specific microstates. (2) The dynamics involves loss of information on the system.²¹ Hence, every (spontaneous) net flux between two thermodynamic states is accompanied by an entropy increase. In thermal equilibrium, the entropy is already maximized

¹⁷see *ΦSX:Statistical Physics*[38]

¹⁸See Jones and March, *Theoretical Solid-State Physics Vol.1*, Appendix 4.2 "In thermal equilibrium any process must have reverse process occurring with equal probability"

¹⁹This is a colloquial way of phrasing that the system tends to become more random, and that the entropy increases with increasing randomness. The phrase originates in the way of thinking in irreversible thermodynamics.

²⁰A microstate is a quantum (or classical) state of the system. A macro state is an ensemble of microstates. A macrostate is what we call a thermodynamic state.

²¹The two assumptions are not formulated with mathematical rigor. They shall alert that we make use of the microscopic equations of motion. Both, Newton's equations of motion and the Schrödinger equation are deterministic and, hence, do not involve loss of information. The Boltzmann equation is not deterministic and thus describes loss of information, i.e. growth of entropy.

and can not grow any further, which implies that there can be no net fluxes. This also forbids circular fluxes between more than two states, even if they leave the distribution invariant. [Editor: include here a sketch with a circular flux between three states](#)

Let me switch to the compact notation described in section 8.1.8.

Detailed balance introduces a requirement for the intrinsic transition probabilities in Eq. 8.34, namely that forward and backward scattering probabilities Eq. 8.34 are identical between each pair of states. This implies

$$\left[\prod_{j=1}^N (1 + \eta f_{o_j}^{eq}) \right] L^{o_1, \dots, o_N, i_1, \dots, i_M} \left[\prod_{k=1}^M f_{i_k}^{eq} \right] = \left[\prod_{k=1}^M (1 + \eta f_{i_k}^{eq}) \right] L^{i_1, \dots, i_M, o_1, \dots, o_N} \left[\prod_{j=1}^N f_{o_j}^{eq} \right] \quad (8.46)$$

$$\Rightarrow L^{o_1, \dots, o_N, i_1, \dots, i_M} = L^{i_1, \dots, i_M, o_1, \dots, o_N} \left[\prod_{k=1}^M \frac{(1 + \eta f_{i_k}^{eq})}{f_{i_k}^{eq}} \right] \left[\prod_{j=1}^N \frac{f_{o_j}^{eq}}{1 + \eta f_{o_j}^{eq}} \right] \quad (8.47)$$

As shown below, this expression does not depend on a specific form of the equilibrium distribution f_n^{eq} .

With the representation of the equilibrium distribution in Eq. 8.45, we can use the identity

$$\frac{1 + \eta f_{\lambda}^{eq}(\vec{r})}{f_{\lambda}^{eq}(\vec{r})} \stackrel{\text{Eq. 8.45}}{=} e^{\beta(H_{\lambda}(\vec{r}) - \mu)} \quad \text{which implies}$$

$$\left[\prod_{k=1}^M \frac{(1 + \eta f_{i_k}^{eq})}{f_{i_k}^{eq}} \right] \left[\prod_{j=1}^N \frac{f_{o_j}^{eq}}{1 + \eta f_{o_j}^{eq}} \right] = \exp \left(-\beta \underbrace{\left(\sum_{j=1}^N (H_{o_j}(\vec{r}) - \mu) - \sum_{k=1}^M (H_{i_k}(\vec{r}) - \mu) \right)}_{\Delta E - \mu \Delta N} \right) \quad (8.48)$$

Insertion of this result into Eq. 8.47 yields

$$L^{o_1, \dots, o_N, i_1, \dots, i_M} = L^{i_1, \dots, i_M, o_1, \dots, o_N} e^{-\beta(\Delta E - \mu \Delta N)} \quad (8.49)$$

$$\text{with } \Delta E = \sum_{j=1}^N H_{o_j}(\vec{r}) - \sum_{k=1}^M H_{i_k}(\vec{r}) \quad \text{and} \quad \Delta N = N - M$$

[Editor: Caution: I am using the symbol \$N\$ twice. Once as summation bound similar to \$M\$ and once as particle number in \$\Delta N\$.](#) Detailed balance imposes a strong condition on the intrinsic scattering conditions, namely that they are symmetric under exchange of incoming (lower) and outgoing (upper) indices. It will be used, for example, to show that the entropy grows with time under Boltzmann's equation. (See appendix O.6 on p. 533.) It furthermore indicates that the collision terms of the Boltzmann equation can be written as derivatives of a generating functional as discussed in appendix O.4 on p. 530.

Collisions can be **elastic** or **inelastic**.²² An elastic process is, per definition, energy conserving $\Delta E = 0$. During inelastic scattering, energy can also be absorbed or emitted.

When the intrinsic scattering probabilities are calculated from the microscopic equations of motion, the conservation laws, such as energy conservation or particle-number conservation, are automatically built into the intrinsic scattering probabilities. (See also section 8.2.3)

Therefore, usually only elastic collisions $\Delta E = 0$ are considered. Furthermore ΔN vanishes for particles with particle-number conservation such as electrons. For particles without particle number conservation, such as phonons and photons, there is no meaningful particle reservoir, so that the chemical potential can be set to zero²³, i.e. $\mu = 0$. Thus, under the above-mentioned assumption

²²**Inelastic processes** come into play when internal degrees of freedom can absorb or emit energy during a collision. An example may be impurity scattering at an impurity that can exist in two states with different energies. Each of the two states exist with certain probabilities. A particle colliding with such an impurity may gain or lose energy. Another example is the scattering of electrons at phonons, where the phonons are not treated explicitly but as an effective medium. For further information on inelastic collisions in the context of Boltzmann's equation see the reviews[59, 60] by Cedric Villani, holder of the Fields Medal 2010.

²³The choice $\mu = 0$ removes all terms relating to the particle reservoir.

$\Delta E - \mu \Delta N = 0$, the intrinsic scattering probabilities $L_{\vec{i}}$ obey detailed balance Eq. 8.49 in the simple form

INTRINSIC SCATTERING PROBABILITIES WITH DETAILED BALANCE

$$L_{i_1, \dots, i_M}^{o_1, \dots, o_N} = L_{o_1, \dots, o_N}^{i_1, \dots, i_M} \quad (8.50)$$

Detailed balance does not only ensure that the net source term Q_n due to collisions vanishes for the equilibrium distribution, but it also suppresses fluxes, which do not affect the equilibrium distribution. The absence of fluxes distinguishes thermal equilibrium from another, non-thermal stationary distribution.

The principle of detailed balance for the intrinsic scattering probabilities says that (1) there is a set of energies $H_\lambda(\vec{r})$, which is unique up to a common shift **Editor: explain what that means!**, and (2) that this set of energies links the forward and backward scattering processes.

When the intrinsic scattering probabilities satisfy detailed balance, their contribution to the source and sink terms vanish in thermal equilibrium.

8.3.4 Bare particles and quasi-particles

Editor: This section is under construction! Do not read!

I based the Boltzmann equation on fairly general principles. It is not completely clear, what type of particles the Boltzmann equation describes, bare particles or screened quasi particles. Often a theory is built starting with a non-interacting Hamiltonian to which the interaction is added. The natural expectation is that the drift term describes the dynamics of non-interacting (bare²⁴) particles, while the collision term captures the interactions.

Following this line of argumentation leads to a conceptual problem: On the one hand, the drift term does not depend on the strength of the interaction. On the other hand, the equilibrium distribution of particles must depend on the interaction. The equilibrium distribution is, however, given by the same Hamilton function, which is also responsible for the drift term.

1. In order to unravel this problem, let me introduce a bare Hamiltonian $H_n^{bare}(\vec{r}, \vec{p})$, which is responsible for the drift term of non-interacting particles

$$\vec{v}^{bare}(\vec{r}, \vec{p}) = \vec{\nabla}_p H^{bare}(\vec{r}, \vec{p}) \quad \text{and} \quad \vec{F}^{bare}(\vec{r}, \vec{p}) = -\vec{\nabla}_r H^{bare}(\vec{r}, \vec{p}) \quad (8.51)$$

2. The equilibrium distribution is still specified by the interacting Hamilton function $H_n = H_n^{bare} + \Sigma_n$

$$f^{eq}(\vec{r}, \vec{p}) = f_{T, \mu} \left(H_n^{bare}(\vec{r}, \vec{p}) + \Sigma_n(\vec{r}, \vec{p}) \right) \quad (8.52)$$

where $\Sigma_n(\vec{r}, \vec{p})$ is called a **self-energy correction**²⁵. It captures the effects of the interaction on the particle distribution. $f_{T, \mu}(\epsilon)$ is the Fermi, Bose or Boltzmann distribution function Eq. 8.65.

In practice, one may have information on the equilibrium distribution $f^{eq}(\vec{r}, \vec{p})$ rather than the energy $H_n + \Sigma_n$. In that case, Σ_λ is obtained for a given equilibrium distribution as

$$\Sigma_n(\vec{r}, \vec{p}) \stackrel{\text{Eq. 8.45}}{=} \mu - H_n^{bare}(\vec{r}, \vec{p}) + k_B T \ln \left(\frac{1 + \eta f_n^{eq}(\vec{r}, \vec{p})}{f_n^{eq}(\vec{r}, \vec{p})} \right) \quad (8.53)$$

We take this as a definition of $\Sigma_n(\vec{r}, \vec{p})$.

²⁴The term "bare" refers to the picture that a particle with interaction polarized its environment, and thus is **dressed** by a polarization cloud. The particle with its polarization cloud is called a **quasi-particle**. In contrast, a non-interacting particle is not dressed by a polarization cloud and is, therefore, **bare**.

²⁵The term self-energy correction is borrowed from the many-particle Green's function approach, where it has a precise meaning. Its connection to the Boltzmann equation is, at least to me, not yet obvious.

3. Furthermore, I will need add a diffuse scattering term $Q_n^\Sigma(\vec{r}, \vec{p})$ in addition to the collision term $Q_n^{coll}(\vec{r}, \vec{p})$, that we discussed earlier. The diffuse scattering term is chosen so that the interacting equilibrium distribution Eq. 8.52 is stationary

The resulting Boltzmann equation has the form

$$\left(\partial_t + \vec{v}_n^{bare}(\vec{r}, \vec{p}) \vec{\nabla}_r + \vec{F}_n^{bare}(\vec{r}, \vec{p}) \vec{\nabla}_p \right) f_n(\vec{r}, \vec{p}) = Q_n^\Sigma(\vec{r}, \vec{p}) + Q_n^{coll}(\vec{r}, \vec{p}) \quad (8.54)$$

It differs only by the diffuse scattering term.

The requirement that the equilibrium distribution is stationary, determines the diffuse scattering term $Q_n^\Sigma(\vec{r}, \vec{p})$:

$$\begin{aligned} 0 &\stackrel{!}{=} \partial_t f_n^{eq}(\vec{r}, \vec{p}, t) \\ &\stackrel{\text{Eq. 8.54}}{=} -\vec{v}_n^{bare} \vec{\nabla}_r f_n^{eq} - \vec{F}_n^{bare} \vec{\nabla}_p f_n^{eq} + Q_n^\Sigma + Q_n^{coll} \\ &\stackrel{\text{Eq. 8.52}}{=} \underbrace{-\beta f_n^{eq} (1 + \eta f_n^{eq})}_{df_{T,\mu}(\epsilon)/d\epsilon = -\beta f_{T,\mu}(1 + \eta f_{T,\mu})} \left(-\vec{v}_n^{bare} \vec{\nabla}_r (H_n^{bare} + \Sigma_n) - \vec{F}_n^{bare} \vec{\nabla}_p (H_n^{bare} + \Sigma_n) \right) + Q_n^\Sigma + \underbrace{Q_n^{coll}}_{= 0 \text{ for } f^{eq} \text{ Eq. 8.49}} \\ \Rightarrow Q_n^\Sigma &= \underbrace{-\beta f_n^{eq} (1 + \eta f_n^{eq})}_{df_{T,\mu}(\epsilon)/d\epsilon = -\beta f_{T,\mu}(1 + \eta f_{T,\mu})} \left(\vec{v}_n^{bare} \vec{\nabla}_r (H_n^{bare} + \Sigma_n) + \vec{F}_n^{bare} \vec{\nabla}_p (H_n^{bare} + \Sigma_n) \right) \quad (8.55) \end{aligned}$$

The pure collision term Q_n^{coll} , Eq. 8.34, vanishes for the equilibrium distribution as a consequence of detailed balance Eq. 8.49: Detailed balance requires that there is no net flux between any two states in the equilibrium distribution due to pure collisions.

The drift term in Eq. 8.55 can be simplified using Liouville theorem Eq. 8.10 for the non-interacting particles, namely

$$\underbrace{(\vec{\nabla}_p H_n^{bare})}_{\vec{v}_n^{bare}} (\vec{\nabla}_r H_n^{bare}) + \underbrace{(-\vec{\nabla}_r H_n^{bare})}_{\vec{F}_n^{bare}} (\vec{\nabla}_p H_n^{bare}) \stackrel{\text{Eq. 8.10}}{=} 0, \quad (8.56)$$

which leads to non-collisional term

$$Q_n^\Sigma(\vec{r}, \vec{p}) = -\beta f_n^{eq}(\vec{r}, \vec{p}) \left(1 + \eta f_n^{eq}(\vec{r}, \vec{p}) \right) \left(\vec{v}_n^{bare} \vec{\nabla}_r \Sigma_n(\vec{r}, \vec{p}) + \vec{F}_n^{bare} \vec{\nabla}_p \Sigma_n(\vec{r}, \vec{p}) \right) \quad (8.57)$$

Insertion of the diffuse scattering Eq. 8.57 into the Boltzmann equation Eq. 8.54 yields

$$\left\{ \partial_t + \underbrace{\vec{v}_n^{eff}(\vec{r}, \vec{p})}_{\vec{\nabla}_p H_n^{eff}(\vec{r}, \vec{p})} \vec{\nabla}_r + \underbrace{\vec{F}_n^{eff}(\vec{r}, \vec{p})}_{-\vec{\nabla}_r H_n^{eff}(\vec{r}, \vec{p})} \vec{\nabla}_p \right\} f_n(\vec{r}, \vec{p}) = Q_n^{eff}(\vec{r}, \vec{p}) \quad (8.58)$$

where diffuse scattering is incorporated into the drift term by redefining \vec{v}_n and \vec{F}_n .

$$\begin{aligned} H_n^{eff}(\vec{r}, \vec{p}) &= H_n^{bare}(\vec{r}, \vec{p}) + \Sigma_n(\vec{r}, \vec{p}) \\ \vec{v}_n^{eff}(\vec{r}, \vec{p}) &= \vec{\nabla}_p \left(H_n^{bare}(\vec{r}, \vec{p}) + \Sigma_n(\vec{r}, \vec{p}) \right) \\ \vec{F}_n^{eff}(\vec{r}, \vec{p}) &= -\vec{\nabla}_r \left(H_n^{bare}(\vec{r}, \vec{p}) + \Sigma_n(\vec{r}, \vec{p}) \right) \\ Q_n^{eff}(\vec{r}, \vec{p}) &= Q_n^{bare}(\vec{r}, \vec{p}) - Q_n^{\Sigma, eff}(\vec{r}, \vec{p}) = Q_n^{coll}(\vec{r}, \vec{p}) \quad (8.59) \end{aligned}$$

The pure collision term Q_n^{coll} is obtained using the instantaneous distribution $f_n(\vec{r}, \vec{p})$ together with the intrinsic scattering probabilities²⁶ $L_{\alpha_1, \dots, \alpha_N}^{i_1, \dots, i_M}$.

This amounts to a shift of perspective. Whereas we previously took the point of view that the drift term describes non-interacting particles, now, it describes **quasi-particles** that have part of the interaction already built in.

The Boltzmann equation depends now entirely on the effective Hamilton function $H_n^{eff}(\vec{r}, \vec{p}) = H_n(\vec{r}, \vec{p}) + \Sigma_n(\vec{r}, \vec{p})$, which determines now (1) the drift term, (2) the equilibrium distribution and (3) detailed balance. The diffuse scattering term has disappeared, which is in line with other textbooks.

The important message is that the drift term is determined entirely by a band structure $\epsilon_n(\vec{k})$ that includes a quasi-particle shift $\Sigma_n(\vec{r}, \vec{p})$ stemming from the interaction. This implies that the drift term is obtained from the **spectral function**, which is accessible to experiments via e.g. photo-emission spectra.

The distinction between non-interacting and effective terms is, however, important, when setting up Boltzmann's equation from first principles.

²⁶In a first approximation the intrinsic scattering probabilities could be taken from the non-interacting system.

8.3.5 Summary

FINAL FORM OF THE BOLTZMANN EQUATION

The **Boltzmann equation** requires the following ingredients:

- a Hamilton function $H_n(\vec{r}, \vec{p})$ defining the drift term, respectively the phase-space flow $(\vec{v}_n(\vec{r}, \vec{p}), \vec{F}_n(\vec{r}, \vec{p}))$. The Hamilton function reflects the band structure, which may become spatially dependent by adding an additional potential.
- the intrinsic collision probabilities $L^{o_1, \dots, o_N}_{i_1, \dots, i_M}$, which satisfy detailed balance^a (Eq. 8.49),

The Boltzmann equation is given in Eq. 8.16

$$\left(\partial_t + \vec{v}_n(\vec{r}, \vec{p}) \vec{\nabla}_r + \vec{F}_n(\vec{r}, \vec{p}) \vec{\nabla}_p \right) f_n(\vec{r}, \vec{p}, t) \stackrel{\text{Eq. 8.16}}{=} Q_n(\vec{r}, \vec{p}) \quad (8.60)$$

with the velocities \vec{v}_n and forces \vec{F}_n Eq. 8.9

$$\vec{v}_n(\vec{r}, \vec{p}) = \vec{\nabla}_p H_n(\vec{r}, \vec{p}) \quad \text{and} \quad \vec{F}_n(\vec{r}, \vec{p}) = -\vec{\nabla}_r H_n(\vec{r}, \vec{p}) \quad (8.61)$$

and a source term Q_n as specified in Eq. 8.34. It is expressed in the compact notation (see section 8.1.8 on p. 263), where each incoming or outgoing index (i_j or o_j) contains both, a momentum and a band index.

$$Q_\lambda(\vec{r}) \stackrel{\text{Eq. 8.34}}{=} \sum_{N, M} \sum_{o_1, \dots, o_N} \sum_{i_1, \dots, i_M} (N \delta_{\lambda, o_1} - M \delta_{\lambda, i_1}) \left[\prod_{j=1}^N (1 + \eta f_{o_j}(\vec{r}, t)) \right] L^{o_1, \dots, o_N}_{i_1, \dots, i_M} \left[\prod_{k=1}^M f_{i_k}(\vec{r}, t) \right] \quad (8.62)$$

Under the assumption of elastic collisions $\Delta E - \mu \Delta N = 0$, the intrinsic scattering probabilities are symmetric under exchange of the sets of the incoming i_j and outgoing o_j indices, i.e.

$$L^{o_1, \dots, o_N}_{i_1, \dots, i_M} \stackrel{\text{Eq. 8.50}}{=} L^{i_1, \dots, i_M}_{o_1, \dots, o_N} \quad (8.63)$$

The resulting equilibrium distribution is

$$f_n^{eq}(\vec{r}, \vec{p}) = f_{T, \mu}(H_n(\vec{r}, \vec{p})) \quad (8.64)$$

where

$$f_{T, \mu}(\epsilon) = \left(e^{\beta(\epsilon - \mu)} - \eta \right)^{-1} \quad (8.65)$$

which is the Fermi distribution for fermions ($\eta = -1$), the Bose distribution for bosons ($\eta = +1$), and the Boltzmann distribution for distinguishable particles ($\eta = -0$).

^aThe test of the principle of detailed balance requires the knowledge of the equilibrium distribution. The equilibrium distribution can be determined from the Hamilton function and the equilibrium source term alone.

8.4 Inherent approximations

8.4.1 Molecular chaos

In order to determine the collision probability, we assumed that the probability of the initial state is given by the one-particle distribution $f_n(\vec{r}, \vec{p}, t)$. This implies that the particles taking part in the scattering event are uncorrelated. A correct description would use a many-particle distribution function

$$f_{n_1, \dots, n_M}^M(\vec{r}_1, \vec{p}_1, \dots, \vec{r}_M, \vec{p}_M, t) \quad (8.66)$$

to determine the probability of the initial state

One of the key approximations of the Boltzmann equation is the **molecular chaos hypothesis**. It assumes that the particle distributions are uncorrelated before and after the collision, that is

$$f_{n_1, \dots, n_M}^M(\vec{r}_1, \vec{p}_1, \dots, \vec{r}_M, \vec{p}_M, t) \approx \prod_{j=1}^M f_{n_j}(\vec{r}_j, \vec{p}_j, t). \quad (8.67)$$

Also the correlations, which build up during the collision, are ignored.

The assumption of molecular chaos before and after the collision is important for introducing irreversible behavior into the Boltzmann equation, when obtaining the collision probabilities from the microscopic equations of motion.

8.4.2 Classical versus quantum

I derived the Boltzmann equation from a particle-conservation law and the notion that there is some incompressible dynamics in phase space. Specifically, I have used the classical equations of motion, which suggests that the Boltzmann equation is restricted to classical systems.

Despite the limitations of our derivation, the Boltzmann equation is not limited to classical systems.

The general idea of the Boltzmann equation is that the drift term includes only functions $\vec{v}_n(\vec{r}, \vec{p})$ and $\vec{F}_n(\vec{r}, \vec{p})$, which are indeed slowly varying in space. If this variation is negligible over the width of a wave packet, quantum effects can be ignored. This is a “mild” classical approximation. All terms that are abrupt, and which could split a wave packet, are included in the collision term. Splitting a wave packet is an inherent quantum effect.

8.4.3 Decoherence

The collision term contains the severe approximation of the Boltzmann equation. Namely, the Boltzmann equation discards the information of the phase of the wave functions after each individual collision. As a consequence, the Boltzmann equation deals only with a scalar probability density. It does not contain information about the phase of the wave packets. In the Boltzmann equation, each collision is described by a scattering process followed by an average over the relative phases of all particles. This loss of phase information is the “severe” approximation of the Boltzmann equation. I call this the **random-phase approximation**.

The random-phase approximation rests on the representation of the one-center reduced density matrix

$$\rho_{\alpha, \beta}^{(1)} = \sum_n C_{\alpha, n} f_n C_{\beta, n}^* \quad (8.68)$$

where the natural orbitals $|\psi_n\rangle = \sum_{\alpha} |\chi_{\alpha}\rangle C_{\alpha, n}$ are expressed in some one-particle basisset $\{|\chi_{\alpha}\rangle\}$. In the random-phase approximation the wave-function coefficients obtain an additional phase factor

$e^{i\phi_\alpha}$.

$$\tilde{C}_{\alpha,n}(\vec{\phi}) = C_{\alpha,n} e^{i\phi_\alpha} \quad (8.69)$$

and the new reduced density matrix

$$\tilde{\rho}_{\alpha,\beta}^{(1)}(\vec{\phi}) = \rho_{\alpha,\beta}^{(1)}(\vec{0}) e^{i(\phi_\alpha - \phi_\beta)} \quad (8.70)$$

is then averaged over the phases $\{\phi_\alpha\}$:

$$\int_0^{2\pi} \frac{d\phi_1}{2\pi} \cdots \int_0^{2\pi} \frac{d\phi_\infty}{2\pi} \tilde{\rho}_{\alpha,\beta}^{(1)}(\vec{\phi}) = \rho_{\alpha,\beta}^{(1)}(\vec{0}) \delta_{\alpha,\beta} \quad (8.71)$$

The average over the phases removes the offsite matrix elements of the reduced density matrix. This describes the effect of decoherence, which is caused by the coupling the system to an environment. The one-particle basis $|\varphi_\alpha\rangle$ are the eigenstates of this coupling operator. (see for example ΦSX: The statistical properties of matter. [Editor: complete reference with chapter](#))

The random-phase approximation of the Boltzmann equation implies that **multiple-scattering** events are not considered.²⁷ In a multiple-scattering event, a particle could scatter back into its original state and thus interfere with the incoming wave packet.

The random-phase approximation is expected to be good when collisions are rare. Consider a **coherence time** after which particles lose their phase information. The random-phase approximation would be valid if collisions occur on time scales larger than this coherence time.

This discussion on decoherence is not meant to be complete, nor will the implications be fully transparent. It is a topic of large interest, with still conflicting points of view.

Note, that there is also another well-known approximation with the name "random-phase approximation", which describes the screening of the electrostatic interaction by electron-hole pairs of an electron gas[61]. I am not aware of any relation between these two approximations.

8.5 Linearized Boltzmann equation

The Boltzmann equation is a non-linear integro-differential equation, which is hard to solve in its generality. The nonlinearity is entirely due to the collision terms. The natural first step towards a simplification is to avoid the nonlinear terms by linearizing the collision term around some reference distribution $f_n^{(0)}(\vec{r}, \vec{p}, t)$.

The linearized collision term has the form

$$Q_n(\vec{r}, \vec{p}, t) = Q_n^{(0)}(\vec{r}, \vec{p}, t) + \sum_m \int \frac{d^3 p'}{(2\pi\hbar)^3} B_{n,m}(\vec{p}, \vec{p}', \vec{r}, t) \left(f_m(\vec{r}, \vec{p}', t) - f_m^{(0)}(\vec{r}, \vec{p}', t) \right) + O\left((f - f^{(0)})^2\right) \quad (8.72)$$

where²⁸

$$B_{n,m}(\vec{p}, \vec{p}', \vec{r}, t) = \left. \frac{\partial Q_n(\vec{r}, \vec{p}, t)}{\partial f_m(\vec{r}, \vec{p}', t)} \right|_{\{f_n^{(0)}(\vec{r}, \vec{p}, t)\}} \quad (8.73)$$

with the source term Q defined in Eq. 8.62.

It is convenient to formulate the linearized Boltzmann equation in terms of deviations $\delta f_n(\vec{r}, \vec{p}, t)$ from the reference distribution, i.e.

$$\delta f_n(\vec{r}, \vec{p}, t) \stackrel{\text{def}}{=} f_n(\vec{r}, \vec{p}, t) - f_n^{(0)}(\vec{r}, \vec{p}, t) . \quad (8.74)$$

²⁷Multiple scattering events can nevertheless combined into an own, intrinsic scattering amplitude.

²⁸ B has only one spatial argument, because collisions are assumed to be local. This is a common assumption, which can be relaxed in a straightforward manner. The remaining space argument is used to describe different materials.

LINEARIZED BOLTZMANN EQUATION

The linearized Boltzmann equation describes the deviation $\delta f_n(\vec{r}, \vec{p}, t)$ from some reference distribution $f_n^{(0)}(\vec{r}, \vec{p}, t)$.

$$\begin{aligned} \left[\partial_t + \vec{v}_n(\vec{r}, \vec{p}, t) \vec{\nabla}_r + \vec{F}_n(\vec{r}, \vec{p}, t) \vec{\nabla}_p \right] \delta f_n(\vec{r}, \vec{p}, t) &= \sum_m \int \frac{d^3 p'}{(2\pi\hbar)^3} B_{n,m}(\vec{p}, \vec{p}', \vec{r}, t) \delta f_m(\vec{r}, \vec{p}', t) \\ &+ \underbrace{Q_n^{(0)}(\vec{r}, \vec{p}, t) - \left[\partial_t + \vec{v}_n(\vec{r}, \vec{p}, t) \vec{\nabla}_r + \vec{F}_n(\vec{r}, \vec{p}, t) \vec{\nabla}_p \right] f_n^{(0)}(\vec{r}, \vec{p}, t)}_{\text{inhomogeneity } I_n(\vec{r}, \vec{p}, t)} \end{aligned} \quad (8.75)$$

with \mathbf{B} defined in Eq. 8.73.

In this expression, I left more flexibility than usual so that one can linearize about any reference distribution, which is close to the one of interest.

- Usually, the reference distribution $f^{(0)}$ is the equilibrium distribution. In that case, the inhomogeneity I_n vanishes and we obtain a purely linear, homogeneous equation for the deviation δf . Using a static reference such as the equilibrium distribution ensures that the collision matrix \mathbf{B} is time independent.
- $f_n^{(0)}$ may be an initial distribution, if one is interested in the initial dynamics of a relaxation process.
- $f^{(0)}$ may be a non-equilibrium distribution.
- One may even use the time-dependent solution $f_n^{(0)}(\vec{r}, \vec{p}, t)$ of an approximation, such as the relaxation-time Ansatz.

Collision term

Let me now work out the collision matrix $B_{m,n}(\vec{p}, \vec{p}') = \frac{\partial Q_m}{\partial f_n}$, which is the derivative of the source term with respect to the occupations at the reference distribution.

Let me switch to the compact notation described in section 8.1.8 with $\lambda = (n, \vec{p})$ and $\lambda' = (m, \vec{p}')$. The space and time dependence is suppressed because the expressions are local.

$$\begin{aligned} Q_\lambda[\vec{f}] &= \underbrace{Q_\lambda^{(0)}}_{Q_\lambda[\vec{f}^{(0)}]} + \sum_{\lambda'} \frac{\partial Q_\lambda[\vec{f}]}{\partial f_{\lambda'}} \Big|_{\vec{f}^{(0)}} \delta f_{\lambda'} + O(\delta f_\lambda^2) \\ Q_\lambda &\stackrel{\text{Eq. 8.34}}{=} \sum_{N,M} \sum_{o_1, \dots, o_N} \sum_{i_1, \dots, i_M} \left(\sum_{j=1}^N \delta_{\lambda, o_j} - \sum_{k=1}^M \delta_{\lambda, i_k} \right) \left[\prod_{j=1}^N (1 + \eta f_{o_j}) \right] L^{o_1, \dots, o_N}_{i_1, \dots, i_M} \left[\prod_{k=1}^M f_{i_k} \right] \\ \Rightarrow \frac{\partial Q_\lambda}{\partial f_{\lambda'}} &= \sum_{N,M} \sum_{o_1, \dots, o_N} \sum_{i_1, \dots, i_M} \underbrace{\left[\prod_{j=1}^N (1 + \eta f_{o_j}^{(0)}) \right] L^{o_1, \dots, o_N}_{i_1, \dots, i_M} \left[\prod_{k=1}^M f_{i_k}^{(0)} \right]}_{=: A_{\vec{\sigma}, \vec{i}} = A_{\vec{r}, \vec{\sigma}}} \\ &\quad \times \underbrace{\left(\sum_{j=1}^N \delta_{\lambda, o_j} - \sum_{k=1}^M \delta_{\lambda, i_k} \right)}_{=: B_{\vec{\sigma}, \vec{i}} = -B_{\vec{r}, \vec{\sigma}}} \underbrace{\left(\sum_{j=1}^N \frac{\eta \delta_{o_j, \lambda'}}{1 + \eta f_{o_j}^{(0)}} + \sum_{k=1}^M \frac{\delta_{i_k, \lambda'}}{f_{i_k}^{(0)}} \right)}_{=: C_{\vec{\sigma}, \vec{i}}} \end{aligned} \quad (8.76)$$

This expression can be simplified:

- Because the intrinsic collision probabilities satisfy detailed balance, Eq. 8.46, the term $A_{\vec{\sigma}, \vec{\tau}}$ is symmetric under exchange of the set of incoming and with that of outgoing indices, i.e. $A_{\vec{\sigma}, \vec{\tau}} = A_{\vec{\tau}, \vec{\sigma}}$.
- The term B changes sign under an exchange of incoming and outgoing indices, i.e. $B_{\vec{\sigma}, \vec{\tau}} = -B_{\vec{\tau}, \vec{\sigma}}$.
- Because of the antisymmetry of $A_{\vec{\sigma}, \vec{\tau}} B_{\vec{\sigma}, \vec{\tau}} = -A_{\vec{\tau}, \vec{\sigma}} B_{\vec{\tau}, \vec{\sigma}}$, only the antisymmetric contribution of the term C contributes.

$$\begin{aligned}
\frac{1}{2} (C_{\vec{\tau}}^{\vec{\sigma}} - C_{\vec{\sigma}}^{\vec{\tau}}) &= \frac{1}{2} \left[\left(\sum_{j=1}^N \frac{\eta \delta_{o_j, \lambda'}}{1 + \eta f_{o_j}^{(0)}} + \sum_{k=1}^M \frac{\delta_{i_k, \lambda'}}{f_{i_k}^{(0)}} \right) - \left(\sum_{k=1}^M \frac{\eta \delta_{i_k, \lambda'}}{1 + \eta f_{i_k}^{(0)}} + \sum_{j=1}^N \frac{\delta_{o_j, \lambda'}}{f_{o_j}^{(0)}} \right) \right] \\
&= \frac{1}{2} \left[\sum_{j=1}^N \left(\frac{\eta \delta_{o_j, \lambda'}}{1 + \eta f_{o_j}^{(0)}} - \frac{\delta_{o_j, \lambda'}}{f_{o_j}^{(0)}} \right) + \sum_{k=1}^M \left(\frac{\delta_{i_k, \lambda'}}{f_{i_k}^{(0)}} - \frac{\eta \delta_{i_k, \lambda'}}{1 + \eta f_{i_k}^{(0)}} \right) \right] \\
&= \frac{1}{2} \frac{1}{(1 + \eta f_{\lambda'}^{(0)}) f_{\lambda'}^{(0)}} \left[- \sum_{j=1}^N \delta_{o_j, \lambda'} + \sum_{k=1}^M \delta_{i_k, \lambda'} \right] \tag{8.77}
\end{aligned}$$

Insertion of the antisymmetrized term C into the expression above yields

$$\begin{aligned}
\frac{\partial Q_\lambda}{\partial f_{\lambda'}} &= -\frac{1}{2} \frac{1}{(1 + \eta f_{\lambda'}^{(0)}) f_{\lambda'}^{(0)}} \sum_{N, M} \sum_{o_1, \dots, o_N} \sum_{i_1, \dots, i_M} \left[\prod_{j=1}^N (1 + \eta f_{o_j}^{(0)}) \right] L^{o_1, \dots, o_N}_{i_1, \dots, i_M} \left[\prod_{k=1}^M f_{i_k}^{(0)} \right] \\
&\quad \times \left(\sum_{j=1}^N \delta_{\lambda, o_j} - \sum_{k=1}^M \delta_{\lambda, i_k} \right) \left(\sum_{j=1}^N \delta_{o_j, \lambda'} - \sum_{k=1}^M \delta_{i_k, \lambda'} \right) \\
&= -\frac{1}{2} \frac{1}{(1 + \eta f_{\lambda'}^{(0)}) f_{\lambda'}^{(0)}} \sum_{N, M} \sum_{o_1, \dots, o_N} \sum_{i_1, \dots, i_M} \left[\prod_{j=1}^N (1 + \eta f_{o_j}^{(0)}) \right] L^{o_1, \dots, o_N}_{i_1, \dots, i_M} \left[\prod_{k=1}^M f_{i_k}^{(0)} \right] \\
&\quad \times \begin{cases} \left(N \delta_{\lambda, o_1} - M \delta_{\lambda, i_1} \right)^2 & \text{for } \lambda = \lambda' \\ \left(N \delta_{\lambda, o_1} - M \delta_{\lambda, i_1} \right) \left(N \delta_{\lambda', o_2} - M \delta_{\lambda', i_2} \right) & \text{for } \lambda \neq \lambda' \end{cases} \tag{8.78}
\end{aligned}$$

(R): We exploited that the intrinsic collision probability is symmetric under exchange of the upper, outgoing indices among each other and under exchange of the lower outgoing indices among each other.

Editor: Exercise: Use the equation above to evaluate the collision term for two-particle scattering for a specified intrinsic scattering probability $L_{c,d}^{a,b}$. Expand the indices from λ to (\vec{r}, \vec{p})

8.6 Relaxation-time approximation

The evaluation of the collision term $B_{m,n}(\vec{p}, \vec{p}')$ is possible but difficult. Therefore, a common further approximation is to approximate the collision matrix B by a diagonal matrix, which define the **relaxation times** $\tau_n(\vec{p})$ via ²⁹

$$B_{m,n}(\vec{p}, \vec{p}') \approx -\frac{1}{\tau_n(\vec{p})} (2\pi\hbar)^3 \delta(\vec{p} - \vec{p}') \delta_{m,n} \tag{8.79}$$

²⁹A better choice is probably to first evaluate the inverse K of B and to identify the relaxation times with the diagonal elements of $-K$, i.e. $\tau_\lambda = K_{\lambda,\lambda}$.

BOLTZMANN EQUATION IN THE RELAXATION-TIME APPROXIMATION

$$\left[\partial_t + \vec{v}_n(\vec{r}, \vec{p}, t) \vec{\nabla}_r + \vec{F}_n(\vec{r}, \vec{p}, t) \vec{\nabla}_p + \frac{1}{\tau_n(\vec{p})} \right] \delta f_n(\vec{r}, \vec{p}, t) = \underbrace{Q_n^{(0)}(\vec{r}, \vec{p}, t) - \left[\partial_t + \vec{v}_n(\vec{r}, \vec{p}, t) \vec{\nabla}_r + \vec{F}_n(\vec{r}, \vec{p}, t) \vec{\nabla}_p \right] f_n^{(0)}(\vec{r}, \vec{p}, t)}_{\text{inhomogeneity } I_n(\vec{r}, \vec{p}, t)} \quad (8.80)$$

The relaxation-time approximation builds on top of the linearization of the Boltzmann equation as preceding approximation.

To understand the physical meaning of the relaxation-time ansatz, let me consider the Boltzmann equation with a trivial drift term, namely one with $\vec{v} = 0$ and $\vec{F} = 0$. Furthermore, I choose the equilibrium distribution as reference so that the inhomogeneity vanishes. Then, we obtain a simple dynamical picture, namely

$$\delta f_n(\vec{r}, \vec{p}, t) = e^{-t/\tau_n(\vec{p})} \delta f_n(\vec{r}, \vec{p}, 0) \quad (8.81)$$

The non-equilibrium distribution approaches the equilibrium exponentially. A simple physical picture emerges, in which a particle with a given momentum channel has a **finite lifetime**, after which it typically “collides” with other particles. In this picture, the scattering event “thermalizes” the particle instantly.

The relaxation-time approximation comes in many flavors having different quality: For example, instead of using one relaxation time for each momentum and band, one often uses one single common relaxation time. This approximation is fairly severe, but often, there is not sufficient information on the state-dependent relaxation times. The approximation of one common relaxation time is typically employed, when one has to rely on limited experimental information.

8.7 Dynamics in the linearized Boltzmann equation

In this section, a framework is provided, which allows one to discuss the dynamics of an distribution within the linearized Boltzmann equation. The results from this section will be used for the linear response.

Bracket notation for classical distributions in phase space Let me introduce a notation similar to the bracket notation for quantum states, but now for distributions in phase space.

$$\delta f_n(\vec{r}, \vec{p}) = \langle \vec{r}, \vec{p}, n | \delta f \rangle \quad (8.82)$$

I define a scalar product

$$\langle a | b \rangle = \sum_n \int d^3r \int \frac{d^3p}{(2\pi\hbar)^3} a_n^*(\vec{r}, \vec{p}) b_n(\vec{r}, \vec{p}) \quad (8.83)$$

an identity

$$\hat{1} = \sum_n \int d^3r \int \frac{d^3p}{(2\pi\hbar)^3} | \vec{r}, \vec{p}, n \rangle \langle \vec{r}, \vec{p}, n | \quad (8.84)$$

and

$$\langle \vec{r}, \vec{p}, n | \vec{r}', \vec{p}', n' \rangle = \delta(\vec{r} - \vec{r}') (2\pi\hbar)^3 \delta(\vec{p} - \vec{p}') \delta_{n,n'} \quad (8.85)$$

Ingredients of the linearized Boltzmann equation In order to bring the linearized Boltzmann equation Eq. 8.75 into a more compact form, let me introduce the operator $\hat{Q}(t)$ ³⁰ defined for an arbitrary phase-space function $a_n(\vec{r}, \vec{p})$ as

$$\underbrace{\langle \vec{r}, \vec{p}, n | \hat{Q}(t) | a \rangle}_{\hat{Q}(t) a_n(\vec{r}, \vec{p})} \stackrel{\text{def}}{=} \left[\vec{v}_n^{(0)}(\vec{r}, \vec{p}) \vec{\nabla}_r + \vec{F}_n^{(0)}(\vec{r}, \vec{p}) \vec{\nabla}_p \right] a_n(\vec{r}, \vec{p}) - \sum_m \int \frac{d^3 p'}{(2\pi\hbar)^3} B_{n,m}(\vec{p}, \vec{p}', \vec{r}, t) a_m(\vec{r}, \vec{p}') \quad (8.86)$$

In addition, we will also use the inhomogeneity Eq. 8.75

$$\langle \vec{r}, \vec{p}, n | I(t) \rangle = I_n(\vec{r}, \vec{p}, t) \stackrel{\text{Eq. 8.75}}{=} Q_n^{(0)}(\vec{r}, \vec{p}, t) - \left[\partial_t + \vec{v}_n(\vec{r}, \vec{p}, t) \vec{\nabla}_r + \vec{F}_n(\vec{r}, \vec{p}, t) \vec{\nabla}_p \right] f_n^{(0)}(\vec{r}, \vec{p}, t) \quad (8.87)$$

Restriction to time-independent collisions: In the following discussion of the dynamics, I will make the simplifying assumption that we linearize about a time-independent problem so that Q is a time-independent operator. Nevertheless, we treat the inhomogeneity as time dependent, because we will later encounter problems with this property.

The generalization to time-independent problems is possible. However, the generality is rarely exploited and it obscures the view onto the basic insights.

Linearized Boltzmann equation and its solution: The linearized Boltzmann equation can formally be written in the form

$$\left[\partial_t + \hat{Q} \right] |\delta f\rangle = |I(t)\rangle \quad (8.88)$$

where $|I(t)\rangle$ accounts for the inhomogeneity. It can, again formally, be solved in the form

$$|\delta f(t)\rangle = e^{-\hat{Q}t} \left\{ |\delta f(0)\rangle + \int_0^t dt' e^{+\hat{Q}t'} |I(t')\rangle \right\} \quad (8.89)$$

which can be verified by insertion.

In order to work out the exponential of the operator $-\hat{Q}t$, we determine the eigenstates

$$\hat{Q} |\phi_\gamma\rangle = |\phi_\gamma\rangle \lambda_\gamma \quad (8.90)$$

The operator is not hermitian, which implies that its eigenvalues can be complex-valued and the left and right-handed eigenstates are not complex conjugates of each other.³¹ The left-handed eigenstates obey

$$\langle \pi_\gamma | \hat{Q} = \lambda_\gamma \langle \pi_\gamma | \quad (8.91)$$

Left and right-handed eigenvalues are identical. Left and right-handed eigenvectors obey the bi-orthogonality condition $\langle \pi_\gamma | \phi_{\gamma'} \rangle = \delta_{\gamma, \gamma'}$.

With the eigenvalues and the left- and right-handed eigenvectors we obtain

$$\hat{Q} = \sum_\gamma |\phi_\gamma\rangle \lambda_\gamma \langle \pi_\gamma | \quad \text{and} \quad e^{-\hat{Q}t} = \sum_\gamma |\phi_\gamma\rangle e^{-\lambda_\gamma t} \langle \pi_\gamma | \quad (8.92)$$

³⁰This operator is closely related, but not identical to the **Liouville operator**, which lacks the scattering term.

³¹A matrix \mathbf{A} is **diagonalizable**, if there exists a matrix \mathbf{U} so that $\mathbf{D} = \mathbf{U}^{-1} \mathbf{A} \mathbf{U}$ is diagonal. The diagonal elements $\lambda_n \stackrel{\text{def}}{=} D_{n,n}$ of \mathbf{D} are the eigenvalues of \mathbf{A} . The columns of \mathbf{U} are the **right-handed eigenvectors** \vec{u}_n of \mathbf{A} and the rows of \mathbf{U}^{-1} are the **left-handed eigenvectors** \vec{v}_n of \mathbf{A} . They obey $\mathbf{A} \vec{u}_n = \vec{u}_n \lambda_n$ and $\vec{v}_n \mathbf{A} = \lambda_n \vec{v}_n$. Right- and left-handed eigenvectors obey a **bi-orthogonality condition** $\vec{v}_m \vec{u}_n = \delta_{m,n}$

so that

$$|\delta f(t)\rangle \stackrel{\text{Eq. 8.89}}{=} \sum_{\gamma} |\Phi_{\gamma}\rangle \left\{ e^{-\lambda_{\gamma}t} \langle \pi_{\gamma} | \delta f(0) \rangle + \int_0^t dt' e^{-\lambda_{\gamma}(t-t')} \langle \pi_{\gamma} | I(t') \rangle \right\} \quad (8.93)$$

When we expand about thermal equilibrium, the inhomogeneity vanishes. In this case, the deviation from thermal equilibrium falls off exponentially with time. The eigenvalues λ_{γ} can be complex-valued, which also allows a decay with damped oscillations.

The real part of the eigenvalues must be non-negative for the dynamics to remain stable. Interesting are eigenvalues for which the real part vanishes. These contribute to deviation from equilibrium, which remain stationary or which oscillate for ever.

A permanent oscillation, implies that there is a mode that does not dissipate. This is a rare situation, which usually is due to oversimplified model assumptions in setting up Boltzmann equation.

Eigenvalues that vanish require special attention. When vanishing eigenvalues exist, we must not neglect contributions from the far past, if they have a projection onto a zero eigenvalue. They will be discussed in the following section.

Stability and conservation laws For the system to be stable, the real part of all eigenvalues λ_{γ} must be positive. The smallest eigenvalues λ_{γ} determine the long-time behavior. An eigenvalue with a vanishing real part indicates the presence of stationary states that differ from thermal equilibrium.

Each conservation law contributes to one eigenvector of \hat{Q} with zero eigenvalue. Examples are

- energy conservation: The energy is

$$E = \langle H | f \rangle = \sum_{\lambda} \int d^3r f_{\lambda}(\vec{r}, t) H_{\lambda}(\vec{r}) \quad (8.94)$$

Energy conservation can be expressed as follows (with $|I(t)\rangle = 0$)

$$\partial_t E = \langle H | \partial_t f \rangle = -\langle H | \hat{Q} | f \rangle = -\sum_{\gamma} \langle H | \Phi_{\gamma} \rangle \lambda_{\gamma} \langle \pi_{\gamma} | f \rangle \stackrel{!}{=} 0 \quad (8.95)$$

This requires one eigenvalue $\lambda_{\gamma_0} = 0$ to vanish. The eigenvectors have the properties

$$\begin{aligned} \langle H | \Phi_{\gamma} \rangle &= 0 \quad \text{for } \gamma \neq \gamma_0 \text{ and} \\ \langle \pi_{\gamma_0} | &\sim \langle H | \end{aligned} \quad (8.96)$$

- particle-number conservation

$$N = \langle 1 | f \rangle = \sum_{\lambda} \int d^3r f_{\lambda}(\vec{r}) \quad (8.97)$$

- momentum conservation

$$\vec{P} = \langle \vec{p} | f \rangle = \sum_{\lambda} \int d^3r \int \frac{d^3p}{(2\pi\hbar)^3} f_n(\vec{r}, \vec{p}) \vec{p} \quad (8.98)$$

- angular momentum conservation

$$L = \langle \vec{r} \times \vec{p} | f \rangle = \sum_{\lambda} \int d^3r f_{\lambda} = \sum_{\lambda} \int d^3r \int \frac{d^3p}{(2\pi\hbar)^3} f_n(\vec{r}, \vec{p}) (\vec{r} \times \vec{p}) \quad (8.99)$$

8.7.1 Dynamics in the relaxation-time approximation

In the relaxation-time approximation the operator \hat{Q} has the form Eq. 8.86

$$\hat{Q} \stackrel{\text{Eq. 8.86}}{=} \sum_n \int d^3r \int \frac{d^3p}{(2\pi\hbar)^3} |\vec{r}, \vec{p}, n\rangle \left(\vec{v}_n^{(0)}(\vec{r}, \vec{p}) \vec{\nabla}_r + \vec{F}_n^{(0)}(\vec{r}, \vec{p}) \vec{\nabla}_p + \frac{1}{\tau_n(\vec{r}, \vec{p})} \right) \langle \vec{r}, \vec{p}, n| \quad (8.100)$$

which we restrict further to spatially homogeneous problems, i.e. $\vec{F}_n^{(0)} = 0$, $\vec{\nabla}_r \tau_n = 0$ and $\vec{\nabla}_r \otimes \vec{v}_n = 0$.

$$\hat{Q} \stackrel{\text{Eq. 8.86}}{=} \sum_n \int d^3r \int \frac{d^3p}{(2\pi\hbar)^3} |\vec{r}, \vec{p}, n\rangle \left(\vec{v}_n^{(0)}(\vec{p}) \vec{\nabla}_r + \frac{1}{\tau_n(\vec{p})} \right) \langle \vec{r}, \vec{p}, n| \quad (8.101)$$

The spatial translation symmetry suggests to choose a new basisset of eigenstates of the space-translation operator. In other words, we use plane waves rather than position eigenstates.³²

$$|\vec{G}, \vec{p}, n\rangle \stackrel{\text{def}}{=} \int d^3r |\vec{r}, \vec{p}, n\rangle e^{i\vec{G}\vec{r}} \quad (8.104)$$

$$|\vec{r}, \vec{p}, n\rangle = \int \frac{d^3G}{(2\pi)^3} |\vec{G}, \vec{p}, n\rangle e^{-i\vec{G}\vec{r}} \quad (8.105)$$

$$\langle \vec{G}, \vec{p}, n | \vec{G}', \vec{p}', n' \rangle = (2\pi)^3 \delta(\vec{G} - \vec{G}') (2\pi\hbar)^3 \delta(\vec{p} - \vec{p}') \delta_{n,n'} \quad (8.106)$$

$$\hat{1} = \sum_n \int \frac{d^3G}{(2\pi)^3} \int \frac{d^3p}{(2\pi\hbar)^3} |\vec{G}, \vec{p}, n\rangle \langle \vec{G}, \vec{p}, n| \quad (8.107)$$

$$\langle \vec{r}, \vec{p}, n | \vec{G}', \vec{p}', n' \rangle = \int d^3r' \langle \vec{r}, \vec{p}, n | \vec{r}', \vec{p}', n' \rangle e^{i\vec{G}'\vec{r}'} = e^{i\vec{G}'\vec{r}} (2\pi\hbar)^3 \delta(\vec{p} - \vec{p}') \delta_{n,n'} \quad (8.108)$$

The operator \hat{Q} is reexpressed in this new basisset

$$\begin{aligned} \hat{Q} &\stackrel{\text{Eq. 8.101}}{=} \sum_n \int d^3r \int \frac{d^3p}{(2\pi\hbar)^3} |\vec{r}, \vec{p}, n\rangle \left(\vec{v}_n^{(0)}(\vec{p}) \vec{\nabla}_r + \frac{1}{\tau_n(\vec{p})} \right) \overbrace{\int \frac{d^3G}{(2\pi)^3} e^{i\vec{G}\vec{r}} \langle \vec{G}, \vec{p}, n|}^{\substack{= \langle \vec{r}, \vec{p}, n | \text{ see Eq. 8.105} \\ = |\vec{G}, \vec{p}, n\rangle \text{ see Eq. 8.104}}} \quad (8.109) \\ &= \sum_n \int \frac{d^3p}{(2\pi\hbar)^3} \int \frac{d^3G}{(2\pi)^3} \underbrace{\int d^3r |\vec{r}, \vec{p}, n\rangle e^{i\vec{G}\vec{r}}}_{= |\vec{G}, \vec{p}, n\rangle \text{ see Eq. 8.104}} \left(i\vec{G} \vec{v}_n^{(0)}(\vec{p}) + \frac{1}{\tau_n(\vec{p})} \right) \langle \vec{G}, \vec{p}, n| \end{aligned}$$

This implies that the states $|\vec{G}, \vec{p}, n\rangle$ are the eigenstates of the operator \hat{Q} .

The solution of the time-dependent Boltzmann equation is obtained via Eq. 8.89

$$|\delta f(t)\rangle \stackrel{\text{Eq. 8.89}}{=} \underbrace{\sum_n \int \frac{d^3p}{(2\pi\hbar)^3} \int \frac{d^3G}{(2\pi)^3} |\vec{G}, \vec{p}, n\rangle e^{-\frac{t-t'}{\tau_n(\vec{p})}} e^{-i\vec{G} \vec{v}_n^{(0)}(\vec{p})(t-t')} \langle \vec{G}, \vec{p}, n|}_{e^{-\hat{Q}t}} \delta f(0) \rangle \quad (8.110)$$

Thus, a perturbation of the distribution relaxes back to equilibrium on a time scale given by the relaxation time. In addition, a perturbation undergoes oscillations with frequency $\vec{G} \vec{v}_n^{(0)}(\vec{p})$. The origin of this oscillating term is simple: the particles have velocity $\vec{v}^{(0)}$ and this is also the velocity of the spatial perturbation of the distribution. When a plane wave moves in space, its amplitude at a given point undergoes oscillations with $\omega = \vec{G} \vec{v}$, which is the origin of the term.

32

$$\int \frac{dG}{2\pi} e^{ikx} = \delta(x) \quad (8.102)$$

$$\begin{aligned} \text{Proof: } \lim_{L \rightarrow \infty} \int dx f(x) \int_{-L}^L \frac{dG}{2\pi} e^{ikx} &= \lim_{L \rightarrow \infty} \int dx f(x) \left[\frac{e^{iLx}}{2\pi i x} \right]_{-L}^L = \lim_{L \rightarrow \infty} \int dx f(x) \frac{\sin(Lx)}{\pi x} \\ &= \lim_{L \rightarrow \infty} \int dy f\left(\frac{y}{L}\right) \frac{1}{\pi} \frac{2\sin(y)}{y} = f(0) \frac{1}{\pi} \int dy \frac{2\sin(y)}{y} = f(0) \quad (8.103) \end{aligned}$$

8.8 Linear response

External fields, which act on a material produce currents.

An example is the induced current in response to an electric field. The proportionality between electric current and electric field is the electric conductivity σ , a transport coefficient. It connects the linear response of the charge current to the electric field as stimulus. The linear relation is **Ohm's law**³³

$$\vec{J}_q = \sigma \vec{E} \quad (8.111)$$

The transport coefficients lead us into the field of irreversible thermodynamics, respectively non-equilibrium thermodynamics[54, 55].

In this section, we will derive general transport coefficients from the Boltzmann equation.

Editor: This section should be generalized to frequency and k -dependent response function. Instead one could use a unperturbed system with translational symmetry in space and time. Then,

$$\delta f(\vec{k}, \vec{\omega}) = \left(i\omega + \hat{Q}(\vec{k}) \right)^{-1} |I(k, \omega)\rangle \quad (8.112)$$

8.8.1 Linear response of the distribution to external forces

Consider the Boltzmann equation Eq. 8.16 with a perturbation of the Hamilton function $H_n^{(1)}(\vec{p}, \vec{q}, t)$ and the corresponding velocity and force fields.

$$\left(\partial_t + \left(\vec{v}_n^{(0)} + \vec{v}_n^{(1)} \right) \vec{\nabla}_r + \left(\vec{F}_n^{(0)} + \vec{F}_n^{(1)} \right) \vec{\nabla}_p \right) f_n = Q_n \quad (8.113)$$

- Subtract the Boltzmann equation of the equilibrium distribution $f^{(0,eq)}$ of the unperturbed system

$$\left(\partial_t + \vec{v}_n^{(0)} \vec{\nabla}_r + \vec{F}_n^{(0)} \vec{\nabla}_p \right) f_n^{(0,eq)} = Q_n^{(0,eq)}. \quad (8.114)$$

- The perturbed distribution f_λ is expressed by the unperturbed equilibrium and a deviation $\delta f_\lambda = f_\lambda - f_\lambda^{(0,eq)}$ from it.
- The source term Q_λ is expanded about the value $Q_\lambda^{(0,eq)}$ for unperturbed equilibrium in δf_λ .
- contributions to second and higher order in the perturbation $\vec{v}_\lambda^{(1)}, \vec{F}_\lambda^{(1)}$ and the response δf_λ are neglected.

³³Ohm's law is often remembered as $U = RI$. The voltage $U_{B,A} = \phi_B - \phi_A = - \int_A^B d\vec{r} \vec{E} \hat{=} - E\ell$ is the difference of the electric potential between two points A and B along a wire. The charge current through the wire with crosssection A is $I = \int d\vec{A} \vec{j}_q \hat{=} \vec{j}_q \vec{A}$. R is the **electric resistance** of the wire. The resistance R is related to the **resistivity** ρ by $R = \rho\ell/A$, where ℓ is the length of the wire and A is its crosssection. The **electric conductivity** $\sigma = 1/\rho$ is the inverse of the resistivity ρ . I introduced the simplified version of the expressions with " $\hat{=}$ ". **Editor:** Work out the mess with the minus sign.

Spatial translation symmetry Here, I introduce a further limitation, namely that to problems with spatial translation symmetry. While I omit forces in the unperturbed Hamiltonian, I will allow forces as perturbation, even though this requires a space-dependent perturbing Hamiltonian $H_\lambda^{(1)}(\vec{r})$

Editor: This discussion may be extended to time/frequency dependent stimuli $F_n^{(1)}(\vec{p}, \omega)$ and linear response $\delta f_n(\vec{p}, \omega)$. That is one relaxes the condition $\partial_t \delta f_n(\vec{p}) = 0$.

With a time and space independent Hamiltonian $H_n^{(0)}(\vec{p})$ of the unperturbed system the forces vanish

$$\vec{F}_n^{(0)} = -\vec{\nabla}_r H_n^{(0)}(\vec{p}) = 0 \quad (8.121)$$

and with a distribution that is stationary and constant in space the following terms vanish.

$$\begin{aligned} \vec{\nabla}_r f_n^{(0)}(\vec{p}) &= 0 \\ \partial_t \delta f_n(\vec{p}) &= 0 \\ \vec{\nabla}_r \delta f_n(\vec{p}) &= 0 \end{aligned} \quad (8.122)$$

The linear-response equation Eq. 8.115 simplifies considerably, because we need to work only in momentum space

$$0 = \underbrace{\sum_n \int \frac{d^3 p'}{(2\pi\hbar)^3} \frac{\partial Q_n(\vec{p})}{\partial f_m(\vec{p}')} \Big|_{f^{(0),eq}}}_{-\langle \vec{r}, \vec{p}, n | \hat{Q}^{(0)} | \delta f \rangle} \delta f_m(\vec{p}') \underbrace{- \vec{F}^{(1)}(\vec{p}) \vec{\nabla}_p f_n^{(0),eq}(\vec{p})}_{-\langle \vec{r}, \vec{p}', n | I \rangle} \quad (8.123)$$

Let me define ³⁴ the inverse \mathbf{K} of the \mathbf{B}

$$\sum_j \int \frac{d^3 p''}{(2\pi\hbar)^3} K_{m,j}(\vec{p}, \vec{p}'') B_{j,n}(\vec{p}'', \vec{p}') = (2\pi\hbar)^3 \delta(\vec{p} - \vec{p}') \delta_{m,n} \quad (8.125)$$

We obtain the response from

$$\begin{aligned} \delta f_n(\vec{p}) &= \sum_m \int \frac{d^3 p'}{(2\pi\hbar)^3} K_{n,m}(\vec{p}, \vec{p}') \vec{F}_m^{(1)}(\vec{p}') \vec{\nabla}_{p'} f_m^{(0),eq}(\vec{p}') \\ &= \sum_m \int \frac{d^3 p'}{(2\pi\hbar)^3} K_{n,m}(\vec{p}, \vec{p}') \underbrace{\left(-\vec{v}_m^{(0)}(\vec{p}') \right)}_{\vec{\nabla}_{p'} f_m^{(0),eq}(\vec{p}')} \frac{\partial f_m^{(0),eq}(\vec{p}')}{\partial \mu} \vec{F}_m^{(1)}(\vec{p}') \end{aligned} \quad (8.126)$$

There are again some subtleties to be taken care of in the spirit of Eq. 8.120. They are related to the vanishing eigenvalues of the collision matrix \mathbf{B} . While forming the inverse, their eigenvectors need to be projected out. This is usually done when inverting the matrix using **singular-value decomposition**.

8.8.2 Transport coefficients

Our intention is to evaluate current density of quantity X induced by an external field that acts on quantity Y and a temperature gradient.

³⁴In the relaxation-time approximation, the operator \hat{Q} can be inverted.

$$\Rightarrow \hat{Q}^{-1} \stackrel{\text{Eq. 8.109}}{=} \sum_n \int \frac{d^3 p}{(2\pi\hbar)^3} \int \frac{d^3 G}{(2\pi)^3} |\vec{G}, \vec{p}, n\rangle \left(\frac{\tau_n(\vec{p})}{1 + i\vec{G}\vec{v}_n^{(0)}(\vec{p})\tau_n(\vec{p})} \right) \langle \vec{G}, \vec{p}, n | \quad (8.124)$$

Because the perturbation is space-translation symmetric, only the projection onto the states with $\vec{G} = 0$ contribute.

The induced current density is obtained from the response of the distribution Eq. 8.126 and the external forces \vec{F} acting on the particles are expressed by an external field, which couples to a specific observable Y .

$$\begin{aligned}\vec{j}_X &= \sum_n \int \frac{d^3p}{(2\pi\hbar)^3} X_n(\vec{p}) \vec{v}_n^{(0)}(\vec{p}) \delta f_n(\vec{p}) \\ \vec{F}_n^{(1)}(\vec{p}) &= Y_n(\vec{p}) \vec{E}_Y\end{aligned}\quad (8.127)$$

Instead of one observable \hat{Y} , a set of several such variables can be introduced simultaneously.

- the perturbation is described by a field \vec{E}_Y acting onto a variable \hat{Y} . That is, the forces are

$$\vec{F}_\lambda^{(1)} = Y_\lambda \vec{E}_Y \quad (8.128)$$

where Y_λ is the one-particle expectation value of the operator Y .

$$Y_n(\underbrace{\hbar\vec{k}}_{\vec{p}}) = \langle \psi_n(\vec{k}) | \hat{Y} | \psi_n(\vec{k}) \rangle \quad (8.129)$$

- In section 8.8.5 below, it will be shown that a temperature gradient contributes a term in which

$$\vec{F}_n^{(1)} \frac{\partial f_n^{(0)}(\vec{p})}{\partial \mu} \vec{v}_n^{(0)}(\vec{p}) \quad \text{is replaced by} \quad - \frac{\partial f_n^{(0)}(\vec{p})}{\partial T} \vec{v}_n^{(0)} \vec{\nabla}_r T \quad (8.130)$$

- the induced current density of a quantity X is

$$\vec{j}_X = \sum_\lambda X_\lambda \vec{v}_\lambda^{(0)} \delta f_\lambda = \sum_n \int \frac{d^3p}{(2\pi\hbar)^3} X_n(\vec{p}) \vec{v}_n^{(0)}(\vec{p}) \delta f(\vec{p}) \quad (8.131)$$

where X_λ is the one-particle expectation value of the observable X .

$$X(\underbrace{\hbar\vec{k}}_{\vec{p}}) = \langle \psi_n(\vec{k}) | \hat{X} | \psi_n(\vec{k}) \rangle \quad (8.132)$$

- the induced current densities are related to the fields or the temperature gradient via the transport coefficients σ_{XY} and $\kappa_{X,Y}$

$$\vec{j}_X = \sigma_{XY} \vec{E}_Y - \kappa_X \vec{\nabla} T(\vec{r}) \quad (8.133)$$

With Eq. 8.126, we obtain the

$$\begin{aligned}\vec{j}_X \stackrel{\text{Eq. 8.126}}{=} & \underbrace{\sum_{n,m} \int \frac{d^3p d^3p'}{(2\pi\hbar)^6} \left(X_n(\vec{p}) K_{n,m}(\vec{p}, \vec{p}') Y_m(\vec{p}') \right) \left(\vec{v}_n^{(0)}(\vec{p}) \otimes \vec{v}_m^{(0)}(\vec{p}') \right) \frac{\partial f_m^{(0),eq}(\vec{p}')}{\partial \mu}}_{\sigma_{XY}} \vec{E}_Y \\ & + \underbrace{\sum_{n,m} \int \frac{d^3p d^3p'}{(2\pi\hbar)^6} X_n(\vec{p}) K_{n,m}(\vec{p}, \vec{p}') \left(\vec{v}_n^{(0)}(\vec{p}) \otimes \vec{v}_m^{(0)}(\vec{p}') \right) \frac{\partial f_m^{(0),eq}(\vec{p}')}{\partial T}}_{-\kappa_X} \vec{\nabla} T\end{aligned}\quad (8.134)$$

The symbol \otimes stands for dyadic product (outer product).

We can make the two terms look more similar by using Eq. 6.30 and Eq. 6.31 from p. 189.

$$\partial_T f_{T,\mu}(\epsilon) = \frac{\epsilon - \mu}{T} \partial_\mu f_{T,\mu}(\epsilon) \quad (8.135)$$

LINEAR TRANSPORT COEFFICIENTS

The current density of an observable \hat{X} induced by a field acting on observable \hat{Y} and a temperature gradient is

$$\vec{j}_X = \sigma_{XY} \vec{E}_Y - \kappa_X \vec{\nabla} T \quad (8.136)$$

When there are several fields acting onto different observables Y , they will be added, and there will be one transport coefficient for each. Similarly, there may be one or more than one observable X . There will be one equation Eq. 8.136 for each current density.

The generalized conductivity σ_{XY} is

$$\sigma_{XY} = - \sum_{n,m} \int_{\Omega_T} \frac{d^3 p d^3 p'}{(2\pi\hbar)^6} \left(X_n(\vec{p}) K_{n,m}(\vec{p}, \vec{p}') Y_m(\vec{p}') \right) \left(\vec{v}_n^{(0)}(\vec{p}) \otimes \vec{v}_m^{(0)}(\vec{p}') \right) \frac{\partial f_m^{(0),eq}(\vec{p}')}{\partial \mu} \quad (8.137)$$

and κ_X is

$$\kappa_X = - \sum_{n,m} \int_{\Omega_T} \frac{d^3 p d^3 p'}{(2\pi\hbar)^6} \left(X_n(\vec{p}) K_{n,m}(\vec{p}, \vec{p}') \frac{\epsilon_m(\vec{p}') - \mu}{T} \right) \left(\vec{v}_n^{(0)}(\vec{p}) \otimes \vec{v}_m^{(0)}(\vec{p}') \right) \frac{\partial f_m^{(0),eq}(\vec{p}')}{\partial \mu} \quad (8.138)$$

The kernel $K_{m,n}(\vec{p}, \vec{p}')$ is defined in Eq. 8.125. The matrix elements of the observables are defined in Eq. 8.129 and Eq. 8.133. The momentum integration is performed over the reciprocal unit cell Ω_T .

8.8.3 Transport coefficients in the relaxation time approximation

In the relaxation time approximation we can use

$$K_{m,n}(\vec{p}, \vec{p}') = -(2\pi\hbar)^3 \delta(\vec{p} - \vec{p}') \delta_{m,n} \tau_n(\vec{p}) \quad (8.139)$$

so that Eq. 8.136 transforms into

TRANSPORT COEFFICIENTS IN THE RELAXATION-TIME APPROXIMATION

The current density of an observable \hat{X} induced by a field acting on observable \hat{Y} and a temperature gradient is

$$\begin{aligned} \vec{j}_X &= \underbrace{\sum_n \int_{\Omega_T} \frac{d^3 p}{(2\pi\hbar)^3} \left(X_n(\vec{p}) Y_n(\vec{p}) \right) \left(\vec{v}_n^{(0)}(\vec{p}) \otimes \vec{v}_n^{(0)}(\vec{p}) \right) \tau_n(\vec{p}) \frac{\partial f_n^{(0),eq}(\vec{p})}{\partial \mu}}_{\sigma_{XY}} \vec{E}_Y \\ &\quad - \underbrace{\sum_n \int_{\Omega_T} \frac{d^3 p}{(2\pi\hbar)^3} \left(X_n(\vec{p}) \frac{\epsilon_n(\vec{p}) - \mu}{T} \right) \left(\vec{v}_n^{(0)}(\vec{p}) \otimes \vec{v}_n^{(0)}(\vec{p}) \right) \tau_n(\vec{p}) \frac{\partial f_n^{(0),eq}(\vec{p})}{\partial \mu}}_{\kappa_X} \vec{\nabla} T \end{aligned} \quad (8.140)$$

8.8.4 Examples

Ohm's law

The most famous example for a linear-response relation is **Ohm's law**: electrical conductivity σ_{qq} connects the charge current density \vec{J}_q with the to the electric field \vec{E}_q

$$\vec{J}_q = \sigma_{qq} \vec{E}_q \quad (8.141)$$

where both observables X and Y in Eq. 8.137 and Eq. 8.140 are the charge q .

The electrical conductivity in the relaxation-time approximation is

$$\sigma_{qq} \stackrel{\text{Eq. 8.140}}{=} q^2 \sum_n \int \frac{d^3p}{(2\pi\hbar)^3} \left(\vec{v}_n^{(0)}(\vec{p}) \otimes \vec{v}_n^{(0)}(\vec{p}) \right) \tau_n(\vec{p}) \underbrace{\beta f_n^{(0,eq)}(\vec{p}) \left(1 + f_n^{(0,eq)}(\vec{p}) \right)}_{\frac{\partial f_n^{(0,eq)}(\vec{p})}{\partial \mu}} \quad (8.142)$$

Heat conductivity

The thermal conductivity κ_Q connects the heat-current density \vec{J}_Q with the temperature gradient.

$$\vec{J}_Q = -\kappa_Q \vec{\nabla} T \quad (8.143)$$

The heat-current density is identical to the the energy-current density. Therefore, the observable $X_\lambda = H_\lambda$ is the Hamilton function.

The thermal conductivity is

$$\kappa_Q \stackrel{\text{Eq. 8.140}}{=} \sum_n \int \frac{d^3p}{(2\pi\hbar)^3} \underbrace{H_n(\vec{p}) \frac{\partial f_n^{(0,eq)}(\vec{p})}{\partial T}}_{C_n(\vec{p})} \left(\vec{v}_n^{(0)}(\vec{p}) \otimes \vec{v}_n^{(0)}(\vec{p}) \right) \tau_n(\vec{p}) \quad (8.144)$$

$C_n(\vec{p})$ can be considered as a heat capacity of a given state. The **heat capacity** describes the amount of energy required to change the temperature by one unit. $\Delta E = C \Delta T$.

$$C_{T,\mu}(\epsilon) \stackrel{\text{def}}{=} \epsilon \frac{\partial f_{T,\mu}(\epsilon)}{\partial T} = \epsilon \frac{\epsilon - \mu}{k_B T^2} \frac{e^{\beta(\epsilon - \mu)}}{(e^{\beta(\epsilon - \mu)} - \eta)^2} = k_B \frac{\epsilon}{k_B T} \frac{\epsilon - \mu}{k_B T} \frac{1/2}{\cosh(\beta(\epsilon - \mu) - \eta)} \quad (8.145)$$

The heat capacity is shown in figure 8.4.

Thermoelectric force

The **Seebeck coefficient** (Thermoelectric force) is defined as $S = \Delta V / \Delta T$, where ΔV is a voltage difference and ΔT is a temperature difference (Wikipedia). This implies that a temperature gradient produces and electric field.³⁵

$$\vec{E} = S \vec{\nabla} T \quad (8.146)$$

The electric field, in turn produces a charge current which is proportional to the electric field

$$\vec{J}_q = \sigma_{qq} S \vec{\nabla} T = \kappa_q \vec{\nabla} T \quad (8.147)$$

Thus, the product of electric conductivity and thermoelectric force is the transport coefficient, which links the charge current to a temperature gradient, and which is given by

$$\kappa_q \text{ eq : transport coefficient in relaxation time} = -q \sum_n \int \frac{d^3p}{(2\pi\hbar)^3} \left(\vec{v}_n^{(0)}(\vec{p}) \otimes \vec{v}_n^{(0)}(\vec{p}) \right) \tau_n(\vec{p}) \frac{\partial f_n^{(0,eq)}(\vec{p})}{\partial T} \quad (8.148)$$

³⁵Compare with Marder-Eq.17.77[62]

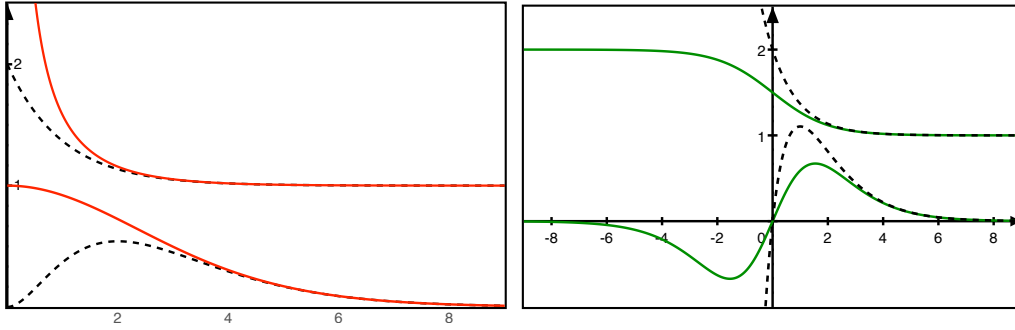


Fig. 8.4: Heat capacity in units of k_B and distribution function $f_{T,\mu}(\epsilon)$ as function of $(\epsilon - \mu)/k_B T$ (displaced upwards by 1 for better visibility) for Bosons (left, red) and Fermions (right, green). The results for the Boltzmann distribution are shown as dashed lines for comparison. For Fermions the heat capacity has been drawn for $\mu \rightarrow \infty$ and scaled by $3k_B T/\mu$. For Bosons $y(x) = x^2(e^x - \eta)e^x$ and for Fermions $y(x) = 3x(e^x - \eta)e^x$.

8.8.5 Response to temperature gradients

In order to investigate a temperature gradient, let me describe the perturbed distribution as a spatially uniform contribution δf and, in addition, the spatially varying changes of thermal excitations due to the temperature gradient. We consider a particular position \vec{r}_0 in space and consider, to first order, the changes of the thermal excitations relative to \vec{r}_0 .

$$f_n(\vec{r}, \vec{p}) = f_n^{(0)}(\vec{p}, \vec{r}_0) + \frac{\partial f_n^{(0)}(\vec{p}, \vec{r}_0)}{\partial T} (\vec{r} - \vec{r}_0) \vec{\nabla}_r T + \overbrace{\frac{\delta f(\vec{p}, \vec{r})}{\delta f_n(\vec{p}, \vec{r}_0)} \delta f(\vec{p}, \vec{r}_0)}^{\delta f(\vec{p}, \vec{r})} \quad (8.149)$$

In the following, I will use $\vec{r}_0 = 0$ and I will drop the argument \vec{r}_0 from the argument list.

Let me insert this ansatz into the Boltzmann equation Eq. 8.80.

$$\left(\partial_t + \vec{v}_n^{(0)} \vec{\nabla}_r + \vec{v}_n^{(1)} \vec{\nabla}_r + \vec{F}_n^{(0)} \vec{\nabla}_p + \vec{F}_n^{(1)} \vec{\nabla}_p \right) \left(f_n^{(0,eq)}(\vec{p}) + \frac{\partial f_n^{(0)}(\vec{p})}{\partial T} \vec{r} \vec{\nabla}_r T + \delta f_n(\vec{p}) \right) = Q_n[f] \quad (8.150)$$

When I discard all terms of higher than first order in the perturbation $\vec{F}^{(1)}$ and $\vec{\nabla}_r T$, I obtain

$$\underbrace{\left(\partial_t + \vec{v}_n^{(0)} \vec{\nabla}_r + \vec{F}_n^{(0)} \vec{\nabla}_p \right) f_n^{(0,eq)}(\vec{p})}_{Q_n^{(0)}(\vec{r}, \vec{p}, t)} + \vec{F}_n^{(1)} \vec{\nabla}_p f_n^{(0,eq)}(\vec{p}) + \frac{\partial f_n^{(0)}(\vec{p})}{\partial T} \vec{v}_n^{(0)} \vec{\nabla}_r T + \left(\partial_t + \vec{v}_n^{(0)} \vec{\nabla}_r + \vec{F}_n^{(0)} \vec{\nabla}_p \right) \delta f_n(\vec{p}) = Q_n[f] \quad (8.151)$$

Thus, the temperature gradient contributes an additional term to the inhomogeneity of the linear Boltzmann equation.

$$\begin{aligned} & \left(\partial_t + \vec{v}_n^{(0)} \vec{\nabla}_r + \vec{F}_n^{(0)} \vec{\nabla}_p \right) \delta f_n(\vec{p}) - \left(Q_n[f] - Q^{(0)} \right) \\ & \stackrel{\text{Eq. 8.151}}{=} -\vec{F}_n^{(1)} \vec{\nabla}_p f_n^{(0,eq)}(\vec{p}) - \frac{\partial f_n^{(0)}(\vec{p})}{\partial T} \vec{v}_n^{(0)} \vec{\nabla}_r T \\ & = \vec{F}_n^{(1)} \frac{\partial f_n^{(0)}(\vec{p})}{\partial \mu} \underbrace{\vec{\nabla}_p H_n^{(0)}}_{\vec{v}_n^{(0)}(\vec{p})} - \frac{\partial f_n^{(0)}(\vec{p})}{\partial T} \vec{v}_n^{(0)} \vec{\nabla}_r T \end{aligned} \quad (8.152)$$

Thus, we obtain the response to a temperature gradient, when we replace

$$\vec{F}_n^{(1)} \frac{\partial f_n^{(0)}(\vec{p})}{\partial \mu} \underbrace{\vec{\nabla}_p H_n^{(0)}}_{\vec{v}_n^{(0)}(\vec{p})} \quad (8.153)$$

in Eq. 8.126 by

$$-\frac{\partial f_n^{(0)}(\vec{p})}{\partial T} \vec{v}_n^{(0)} \vec{\nabla}_r T \quad (8.154)$$

8.9 Quasi Fermi level

The intrinsic variables are well defined for thermal equilibrium states. If systems come into contact, they exchange quantities (Energy, particles, Volume) until the corresponding intrinsic variables (temperature, chemical potential, pressure) become identical. By saying this, we have already extended the notion of intrinsic thermodynamic variables to non-equilibrium states. In order to distinguish these variables from the strict quantities in thermodynamic equilibrium, we call them quasi-temperature, quasi-Fermi level etc.

Here we will introduce these quantities in the context of the Boltzmann equation.

8.9.1 Quasi Fermi level

A convenient way to represent the distribution $f_n(\vec{r}, \vec{p}, t)$ is to express it by a **quasi Fermi level** $\varphi_n(\vec{r}, \vec{p}, t)$

$$\begin{aligned} f_n(\vec{r}, \vec{p}, t) &= f_{T, \varphi}^{eq}(\vec{r}, \vec{p}, t) (H_n(\vec{r}, \vec{p}) + \Sigma_n(\vec{r}, \vec{p})) \\ &= \left(e^{\beta[H_n(\vec{r}, \vec{p}) + \Sigma_n(\vec{r}, \vec{p}) - \varphi_n(\vec{r}, \vec{p}, t)]} - \eta \right)^{-1} \\ &= \begin{cases} \left[e^{\beta[H_n(\vec{r}, \vec{p}) + \Sigma_n(\vec{r}, \vec{p}) - \varphi_n(\vec{r}, \vec{p}, t)]} + 1 \right]^{-1} & \text{for Fermions} \\ e^{-\beta[H_n(\vec{r}, \vec{p}) + \Sigma_n(\vec{r}, \vec{p}) - \varphi_n(\vec{r}, \vec{p}, t)]} & \text{for distinguishable particles} \\ \left[e^{\beta[H_n(\vec{r}, \vec{p}) + \Sigma_n(\vec{r}, \vec{p}) - \varphi_n(\vec{r}, \vec{p}, t)]} - 1 \right]^{-1} & \text{for Bosons} \end{cases} \end{aligned} \quad (8.155)$$

The quasi Fermi level simply encodes the distribution. It is a mere variable transform from occupations as fundamental variable to quasi-Fermi levels

$$\varphi_n(\vec{r}, \vec{p}, t) \stackrel{\text{def}}{=} H_n(\vec{r}, \vec{p}) + \Sigma_n(\vec{r}, \vec{p}) - k_B T \ln \left(\frac{1 + \eta f_n(\vec{r}, \vec{p}, t)}{f_n(\vec{r}, \vec{p}, t)} \right) \quad (8.156)$$

The ansatz Eq. 8.155 is easily mistaken for an assumption of thermal equilibrium. This is not so. In contrast, the Ansatz does not limit or bias the solutions. Important is, that there is an individual quasi-Fermi level for each one-particle state, rather than one common value for all states. In thermal equilibrium, all quasi-Fermi levels are identical and equal to the true Fermi level.

8.9.2 Boltzmann equation in terms of quasi Fermi levels:

Let me start from the Boltzmann equation Eq. 8.16

$$\left[\partial_t + \underbrace{\vec{v}_n(\vec{r}, \vec{p})}_{\vec{\nabla}_p H_n(\vec{r}, \vec{p})} \vec{\nabla}_r + \underbrace{\vec{F}_n(\vec{r}, \vec{p})}_{-\vec{\nabla}_r H_n(\vec{r}, \vec{p})} \vec{\nabla}_p \right] f_n(\vec{r}, \vec{p}, t) = \underbrace{Q_n(\vec{r}, \vec{p}, t)}_{\left(\frac{\partial f_n(\vec{r}, \vec{p}, t)}{\partial t} \right)_{\text{coll}}} \quad (8.157)$$

and express the occupations in terms of quasi Fermi levels.

With the distribution expressed in terms of quasi Fermi levels Eq. 8.155, the Boltzmann equation obtains the form

$$\begin{aligned} \frac{\partial f_n(\vec{r}, \vec{p}, t)}{\partial \varphi} \left[\partial_t \varphi_n(\vec{r}, \vec{p}, t) + \vec{v}_n(\vec{r}, \vec{p}) \left(\vec{\nabla}_r \varphi_n(\vec{r}, \vec{p}, t) - \underbrace{\vec{\nabla}_r H_n(\vec{r}, \vec{p})}_{\vec{F}_n(\vec{r}, \vec{p})} \right) \right. \\ \left. + \vec{F}_n(\vec{r}, \vec{p}) \left(\vec{\nabla}_p \varphi_n(\vec{r}, \vec{p}, t) - \underbrace{\vec{\nabla}_p H_n(\vec{r}, \vec{p})}_{\vec{v}_n(\vec{r}, \vec{p})} \right) \right] = Q_n(\vec{r}, \vec{p}, t) \end{aligned} \quad (8.158)$$

The two gradients of the one-particle levels $H_n(\vec{r}, \vec{p})$ drop out because of Liouville's theorem $\vec{v}_n \vec{\nabla}_r H_n + \vec{F}_n \vec{\nabla}_p H_n = -\vec{v}_n \vec{F}_n + \vec{F}_n \vec{v}_n = 0$.

We move the prefactor³⁶ on the left-hand side of Eq. 8.158 to the right-hand side to obtain a differential equation for the quasi Fermi level.

BOLTZMANN EQUATION IN TERMS OF QUASI FERMI LEVELS

$$\left(\partial_t + \underbrace{\vec{v}_n(\vec{r}, \vec{p})}_{\vec{\nabla}_p H_n(\vec{r}, \vec{p})} \vec{\nabla}_r + \underbrace{\vec{F}_n(\vec{r}, \vec{p})}_{-\vec{\nabla}_r H_n(\vec{r}, \vec{p})} \vec{\nabla}_p \right) \varphi_n(\vec{r}, \vec{p}, t) = \underbrace{\left(\frac{\partial f_{T,\mu}^{eq}(\epsilon_n)}{\partial \mu} \Big|_{\mu=\varphi_n(\vec{r}, \vec{p}, t)} \right)^{-1}}_{k_B T / [f_n(1+\eta f_n)]} Q_n(\vec{r}, \vec{p}, t) \quad (8.160)$$

The division by the factors $f_n(1 + \eta f_n)$, which is often close to zero, is unproblematic, because each true collision term contains exactly this factor in the numerator.

Interestingly, the drift term has the same shape as before, when we used the distribution f rather than the quasi Fermi-levels. The main change is the shape of the collision term.

The collision term depends in a complicated manner on the quasi Fermi levels, because each distribution must be expressed by the quasi Fermi level using Eq. 8.155.

Once the quasi Fermi levels have been found, the distribution $f_n(\vec{r}, \vec{p}, t)$ is recovered with the help of Eq. 8.155

The Boltzmann equation Eq. 8.160 expressed in term of quasi Fermi levels is identical in content to the original Boltzmann equation Eq. 8.16.

8.10 Home study and practice

8.10.1 Electric conductivity and Seebeck coefficient of the free-electron gas

Introduction

In this and the following exercises, we will evaluate the transport coefficients for free electrons and for free phonons in the relaxation-time approximation. Specifically, we determine the charge and heat current densities in response to an electric field and a temperature gradient. This problem is relevant for thermoelectric devices, where one wishes to extract electrical energy from a temperature gradient.

³⁶

$$\frac{\partial f_n(\vec{r}, \vec{p}, t)}{\partial \varphi} \stackrel{\text{def}}{=} \frac{\partial \left(e^{\beta(\epsilon_n(\vec{r}, \vec{p}) - \mu)} - \eta \right)^{-1}}{\partial \mu} \Big|_{\mu=\varphi_n(\vec{r}, \vec{p}, t)} = \beta f_n(\vec{r}, \vec{p}, t) (1 + \eta f_n(\vec{r}, \vec{p}, t)) \quad (8.159)$$

We do not yet have access to the relaxation times. Therefore, we assume that there is one constant relaxation time τ_e for electrons and one, τ_{ph} for phonons. Each is state independent. Later, we will extract the relaxation times by comparing the calculated with measured transport coefficients.

The generic equation for the induced currents in the relaxation-time approximation is Eq. 8.140.

$$\begin{aligned} \vec{j}_X = & \sum_n \int_{\Omega_T} \frac{d^3 p}{(2\pi\hbar)^3} \left(X_n(\vec{p}) Y_n(\vec{p}) \right) \left(\vec{v}_n(\vec{p}) \otimes \vec{v}_n(\vec{p}) \right) \tau_n(\vec{p}) \frac{\partial f_{T,\mu}(\epsilon_n(\vec{p}))}{\partial \mu} \vec{E}_Y \\ & - \sum_n \int_{\Omega_T} \frac{d^3 p}{(2\pi\hbar)^3} X_n(\vec{p}) \left(\epsilon_n(\vec{p}) - \mu \right) \left(\vec{v}_n(\vec{p}) \otimes \vec{v}_n(\vec{p}) \right) \tau_n(\vec{p}) \frac{\partial f_{T,\mu}(\epsilon_n(\vec{p}))}{\partial \mu} \frac{1}{T} \vec{\nabla} T \end{aligned} \quad (8.161)$$

The dispersion relation of free electrons is

$$\epsilon_\sigma(\vec{k}) = \frac{(\hbar\vec{k})^2}{2m_e} + V_0 \quad \text{with the spin indices } \sigma \in \{\uparrow, \downarrow\} \quad (8.162)$$

The potential V_0 is the lower band edge of the free-electron gas. It is often set to zero for the sake of convenience. However, for practical problems, it may describe a band edge, that has physical meaning.

Hint: Use the Sommerfeld expansions from section 6.5.2 on p. 194 with the Sommerfeld coefficients from appendix K.2. on p. 512.

$$- \int_{-\infty}^{\infty} dx \partial_x \left(e^x + 1 \right)^{-1} = 1 \quad (8.163)$$

$$- \frac{1}{2!} \int_{-\infty}^{\infty} dx x^2 \partial_x \left(e^x + 1 \right)^{-1} \stackrel{\text{Eq. K.13}}{=} \frac{\pi^2}{6} \quad (8.164)$$

$$- \frac{1}{4!} \int_{-\infty}^{\infty} dx x^4 \partial_x \left(e^x + 1 \right)^{-1} \stackrel{\text{Eq. K.13}}{=} \frac{7\pi^4}{360} \quad (8.165)$$

Problem

Determine the **electric conductivity** σ and the **Seebeck coefficient** S of the degenerate free-electron gas, i.e. $\mu > V_0$. Determine the leading order of the coefficients in a low-temperature expansion. The electric conductivity relates the electric current density \vec{j}_q to the electric field \vec{E} . A temperature gradient induces a **thermo-electric current**. In the absence of a current, an electric field builds up instead. The Seebeck coefficient links this electric field to the temperature gradient.

$$\vec{j}_q = \sigma \left(\vec{E} - S \vec{\nabla} T \right) \quad (8.166)$$

The product σS is the **thermoelectric coefficient** K .

Note, that the intention is to use the expressions developed for general band structures. The free-electron gas has been chosen only as an example for which the integrations are simpler.

As an extension, one may perform the calculation for a non-degenerate electron gas, i.e. $\mu < V_0$, which would describe, for example, the conduction electrons in a semiconductor.

Solution:

Editor: Caution! These solutions are not completed nor are they checked, yet.

In the solution below, the temperature expansion is carried to higher orders than required.

We start from the expression for the transport coefficients Eq. 8.140 on p. 289.

$$\begin{aligned} \vec{J}_X \stackrel{\text{Eq. 8.140}}{=} & \sum_n \int_{\Omega_T} \frac{d^3 p}{(2\pi\hbar)^3} \left(X_n(\vec{p}) Y_n(\vec{p}) \right) \left(\vec{v}_n(\vec{p}) \otimes \vec{v}_n(\vec{p}) \right) \tau_n(\vec{p}) \frac{\partial f_{T,\mu}(\epsilon_{\sigma,n}(\vec{p}))}{\partial \mu} \vec{E}_V \\ & - \sum_n \int_{\Omega_T} \frac{d^3 p}{(2\pi\hbar)^3} X_n(\vec{p}) \left(\epsilon_n(\vec{p}) - \mu \right) \left(\vec{v}_n(\vec{p}) \otimes \vec{v}_n(\vec{p}) \right) \tau_n(\vec{p}) \frac{\partial f_{T,\mu}(\epsilon_n(\vec{p}))}{\partial \mu} \frac{1}{T} \vec{\nabla} T \end{aligned} \quad (8.167)$$

- The dispersion relation of the free-electron gas is

$$\epsilon_{\sigma}(\vec{p}) \stackrel{FEG}{=} \frac{\vec{p}^2}{2m_e} + V_0 \quad (8.168)$$

I introduced a finite value V_0 of the band edge of the free-electron gas.

The free-electron gas is special in that the dispersion relation is particularly simple in the extended zone scheme. For real systems, one would have to resort to the reduced zone scheme. Let me, therefore, compare the two different points of view:

- In the **reduced zone scheme**, the band structure of the free-electron gas is

$$\epsilon_{n,\sigma}(\vec{p}) = \frac{(\vec{p} - \hbar \vec{G}_n)^2}{2m_e} + V_0 \quad \text{for } \vec{k} = \vec{p}/\hbar \in \Omega_T \text{ (reduced zone scheme)} \quad (8.169)$$

Each reciprocal lattice vector \vec{G}_n contributes one band to the band structure. The integration over all states includes only the Brillouin zone Ω_T .

- In the **extended zone scheme**, we need to consider only a single band, but the Brillouin-zone integration must be replaced an integration over the entire reciprocal space.

$$\epsilon_{\sigma}(\vec{p}) = \frac{\vec{p}^2}{2m_e} + V_0 \quad \text{for } \vec{p} \in \infty^3 \text{ (extended zone scheme)} \quad (8.170)$$

- For the electrical current, the transported quantity is the charge of electrons $q = -e$

$$X_{\alpha}(\vec{p}) = q \quad (8.171)$$

- The electron velocity is

$$\vec{v}_{\sigma}(\vec{p}) = \vec{\nabla}_{\vec{p}} \epsilon(\vec{p}) \stackrel{FEG}{=} \frac{\vec{p}}{m} \quad (8.172)$$

We have used the extended zone scheme.

According to Eq. 8.140 on p. 289, and with the extended zone scheme, the electric current density \vec{J}_q is

$$\begin{aligned} \vec{J}_q \stackrel{\text{Eq. 8.140}}{=} & \sum_{\sigma \in \{\uparrow, \downarrow\}} \int_{\infty^3} \frac{d^3 p}{(2\pi\hbar)^3} q^2 \underbrace{\frac{(\vec{p} \otimes \vec{p})}{m^2}}_{\vec{v}_n(\vec{p}) \otimes \vec{v}_m(\vec{p})} \tau^e(\vec{p}) \frac{\partial f_{T,\mu}(\epsilon(\vec{p}))}{\partial \mu} \vec{E} \\ & - \sum_{\sigma \in \{\uparrow, \downarrow\}} \int \frac{d^3 p}{(2\pi\hbar)^3} q \underbrace{\frac{(\vec{p} \otimes \vec{p})}{m^2}}_{\vec{v}_n(\vec{p}) \otimes \vec{v}_m(\vec{p})} \tau^e(\vec{p}) \frac{\partial f_{T,\mu}(\epsilon(\vec{p}))}{\partial \mu} \left(\epsilon(\vec{p}) - \mu \right) \frac{1}{T} \vec{\nabla} T \\ = & \sum_{\sigma \in \{\uparrow, \downarrow\}} \int \frac{d^3 p}{(2\pi\hbar)^3} \left(\frac{\vec{p}}{|\vec{p}|} \otimes \frac{\vec{p}}{|\vec{p}|} \right) \frac{\partial f_{T,\mu}(\epsilon(\vec{p}))}{\partial \mu} \underbrace{\tau^e(\vec{p})}_{\Rightarrow \tau_e} \frac{\vec{p}^2}{m^2} \left(q^2 \vec{E} - q \left(\epsilon(\vec{p}) - \mu \right) \frac{1}{T} \vec{\nabla} T \right) \\ = & \underbrace{\left\langle \frac{\vec{p}}{|\vec{p}|} \otimes \frac{\vec{p}}{|\vec{p}|} \right\rangle_{\text{angles}}}_{\frac{1}{3} \mathbf{1}} \sum_{\sigma \in \{\uparrow, \downarrow\}} \frac{\tau^e}{(2\pi\hbar)^3} \underbrace{4\pi \int_0^{\infty} dp_r p_r^2}_{\int_{\infty^3} d^3 p} \frac{\partial f_{T,\mu}(\epsilon(p_r))}{\partial \mu} \frac{p_r^2}{m^2} \left(q^2 \vec{E} - q \left(\epsilon(p_r) - \mu \right) \frac{1}{T} \vec{\nabla} T \right) \end{aligned} \quad (8.173)$$

In the last step,

- the momentum integral has been divided into a radial momentum integration and an angular integration.

$$\int_{\infty^3} \frac{dp^3}{(2\pi\hbar)^3} \rightarrow \int_0^\infty dp_r p_r^2 \underbrace{\int_0^\pi d\theta \sin\theta \int_0^{2\pi} d\varphi}_{\sim 4\pi} \quad (8.174)$$

- The angular average is defined as

$$\langle X(\theta, \phi) \rangle_{\text{angles}} \stackrel{\text{def}}{=} \frac{1}{4\pi} \int_0^\pi d\theta \sin\theta \int_0^{2\pi} d\varphi X(\theta, \phi), \text{ and} \quad (8.175)$$

- the state-dependent relaxation time $\tau_e(\vec{p})$ has been replaced by a global one, namely τ_e .

In order to apply the Sommerfeld coefficients Eq. 8.164 and Eq. 8.165 provided above, I need to convert the radial momentum integration into an energy integration

$$\epsilon(p_r) = \frac{p_r^2}{2m} + V_0 \Rightarrow \frac{d\epsilon(p_r)}{dp_r} = \frac{p_r}{m} \Rightarrow dp_r = \frac{m}{p_r} d\epsilon = \frac{m}{\sqrt{2m(\epsilon - V_0)}} d\epsilon \quad (8.176)$$

Now, I return to our previous result for the charge current

$$\begin{aligned} \vec{J}_q &= \underbrace{\left\langle \frac{\vec{p}}{|\vec{p}|} \otimes \frac{\vec{p}}{|\vec{p}|} \right\rangle_{\text{angles}}}_{\frac{1}{3}\mathbf{1}} \sum_{\sigma \in \{\uparrow, \downarrow\}} \frac{4\tau^e}{(2\pi\hbar)^3} 4\pi \int dp_r \frac{\partial f_{T,\mu}(\epsilon(p_r))}{\partial \mu} \underbrace{\frac{p_r^4}{4m^2}}_{(\epsilon_\sigma(p_r) - V_0)^2} \left(q^2 \vec{E} - q(\epsilon(p_r) - \mu) \frac{1}{T} \vec{\nabla} T \right) \\ &= \frac{1}{3}\mathbf{1} \sum_{\sigma \in \{\uparrow, \downarrow\}} \frac{16\pi\tau^e}{(2\pi\hbar)^3} \int_{V_0}^\infty d\epsilon \underbrace{\sqrt{\frac{m}{2(\epsilon - V_0)}}}_{dp_r} \frac{\partial f_{T,\mu}(\epsilon)}{\partial \mu} (\epsilon - V_0)^2 \left(q^2 \vec{E} - q(\epsilon - \mu) \frac{1}{T} \vec{\nabla} T \right) \\ &\stackrel{\epsilon' = \epsilon - V_0}{=} \sum_{\sigma \in \{\uparrow, \downarrow\}} \frac{16\pi\tau^e}{3(2\pi\hbar)^3} \sqrt{\frac{m}{2}} \int_0^\infty d\epsilon' \frac{\partial f_{T,\mu}(\epsilon' + V_0)}{\partial \mu} (\epsilon')^3 \left(q^2 \vec{E} - q(\epsilon' + V_0 - \mu) \frac{1}{T} \vec{\nabla} T \right) \\ &\stackrel{\mu' \stackrel{\text{def}}{=} \mu - V_0}{=} \sum_{\sigma \in \{\uparrow, \downarrow\}} \frac{4\tau^e}{(2\pi\hbar)^3} \frac{4\pi}{3} \sqrt{\frac{m}{2}} \int_0^\infty d\epsilon' \frac{\partial f_{T,\mu'}(\epsilon')}{\partial \mu} \left(q^2 \vec{E} - q(\epsilon' - \mu') \frac{1}{T} \vec{\nabla} T \right) \\ &\quad \times \underbrace{(\mu')^{\frac{3}{2}} \left(1 + \frac{3}{2} \left(\frac{\epsilon' - \mu'}{\mu'} \right) + \frac{3}{8} \left(\frac{\epsilon' - \mu'}{\mu'} \right)^2 - \frac{1}{16} \left(\frac{\epsilon' - \mu'}{\mu'} \right)^3 + \frac{3}{128} \left(\frac{\epsilon' - \mu'}{\mu'} \right)^4 + O(\epsilon' - \mu')^5 \right)}_{\epsilon^{\frac{3}{2}}} \end{aligned} \quad (8.177)$$

I used $\epsilon' = \mu' \left(1 + \frac{\epsilon' - \mu'}{\mu'} \right)$. The new, primed, chemical potential is measured relative to the band edge, i.e.

$$\mu' \stackrel{\text{def}}{=} \mu - V_0 \quad (8.178)$$

Now, I exploit that only the even orders in $\epsilon - \mu$ contribute, because $\partial f_{T,\mu}/\partial \mu$ is itself an even function of $\epsilon - \mu$. The integrals are resolved using the Sommerfeld coefficients Eq. 8.163, Eq. 8.164 and Eq. 8.165 provided in the formulation of the current problem.

Furthermore, I extend the energy integration over the complete energy axis. The derivative of the Fermi function is sizable only next to the chemical potential so that the integration bounds become

irrelevant, as long as they lie sufficiently far from the chemical potential.

$$\begin{aligned}
\vec{j}_q &= \sum_{\sigma \in \{\uparrow, \downarrow\}} \frac{\tau_e}{m} \frac{1}{(2\pi\hbar)^3} \frac{4\pi}{3} (2m\mu')^{\frac{3}{2}} \\
&\times \left\{ q^2 \vec{E} \left(\underbrace{\int_{-\infty}^{\infty} d\epsilon' \frac{\partial f_{T, \mu'}(\epsilon')}{\partial \mu}}_{=1} + \frac{3}{8\mu'^2} \underbrace{\int_{-\infty}^{\infty} d\epsilon' \frac{\partial f_{T, \mu'}(\epsilon')}{\partial \mu} (\epsilon' - \mu')^2}_{(\pi k_B T)^2/3} + \frac{3}{128\mu'^4} \underbrace{\int_{-\infty}^{\infty} d\epsilon' \frac{\partial f_{T, \mu'}(\epsilon')}{\partial \mu} (\epsilon' - \mu')^4}_{7 \cdot 4! (\pi k_B T)^4 / 360 = 7(\pi k_B T)^4 / 15} + \dots \right) \right. \\
&+ \left. \frac{q}{T} \vec{\nabla} T \left(\frac{3}{2\mu'} \underbrace{\int_{-\infty}^{\infty} d\epsilon' \frac{\partial f_{T, \mu'}(\epsilon')}{\partial \mu} (\epsilon' - \mu')^2}_{(\pi k_B T)^2/3} + \frac{1}{16\mu'^3} \underbrace{\int_{-\infty}^{\infty} d\epsilon' \frac{\partial f_{T, \mu'}(\epsilon')}{\partial \mu} (\epsilon' - \mu')^4}_{7 \cdot 4! (\pi k_B T)^4 / 360 = 7(\pi k_B T)^4 / 15} + \dots \right) \right\} \\
&= \frac{\tau_e}{m} \underbrace{\sum_{\sigma \in \{\uparrow, \downarrow\}} \frac{1}{(2\pi\hbar)^3} \frac{4\pi}{3} (2m\mu')^{\frac{3}{2}}}_n \left\{ q^2 \vec{E} \left(1 + \frac{1}{8} \left(\frac{\pi k_B T}{\mu'} \right)^2 + \frac{21}{128 \cdot 15} \left(\frac{\pi k_B T}{\mu'} \right)^4 + \dots \right) \right. \\
&\quad \left. + \mu' \frac{q}{T} \vec{\nabla} T \left(\frac{1}{2} \left(\frac{\pi k_B T}{\mu'} \right)^2 + \frac{7}{15 \cdot 16} \left(\frac{\pi k_B T}{\mu'} \right)^4 + \dots \right) \right\} \tag{8.179}
\end{aligned}$$

Chemical potential: The result shall be expressed in terms of the electron density instead of the chemical potential.

The electron density is related to the chemical potential by

$$n = \sum_{\sigma \in \{\uparrow, \downarrow\}} \int \frac{d^3p}{(2\pi\hbar)^3} f_{T, \mu}(\epsilon_{\sigma}(\vec{p})) \tag{8.180}$$

At zero temperature, the Fermi distribution function turns into a step function, which cuts out the Fermi sphere from reciprocal space.

$$\begin{aligned}
n &\stackrel{T=0}{=} \sum_{\sigma \in \{\uparrow, \downarrow\}} \frac{1}{(2\pi\hbar)^3} \frac{4\pi}{3} \underbrace{(\sqrt{2m\mu'})^3}_{\hbar k_f} \\
\Rightarrow \mu_0 &\stackrel{\text{def}}{=} \mu(T=0) = V_0 + \underbrace{\frac{(2\pi\hbar)^2}{2m} \left(\frac{3n}{4\pi \sum_{\sigma \in \{\uparrow, \downarrow\}}} \right)^{\frac{2}{3}}}_{\mu'} \tag{8.181}
\end{aligned}$$

The temperature dependence of the chemical potential needs to be considered to ensure that it does not affect the leading order of the final results, the electric current and Seebeck coefficient. However, in the leading order in $k_B T$, only the zero-temperature value of the chemical potential enters. Linear and higher-order terms of μ in $k_B T$ only contribute in the higher orders of the current density.

Electric current density in leading order of the temperature expansion

To simplify the problem, let me limit myself to the leading order in temperature

$$\begin{aligned}
\vec{j}_q &= \frac{\tau_e}{m} \underbrace{\sum_{\sigma \in \{\uparrow, \downarrow\}} \frac{1}{(2\pi\hbar)^3} \frac{4\pi}{3} (2m\mu')^{\frac{3}{2}}}_n \left\{ q^2 \vec{E} + \frac{\pi^2 q}{2} \left(\frac{k_B T}{\mu'} \right) k_B \vec{\nabla} T \right\} \\
&= \frac{n\tau_e}{m} \left\{ q^2 \vec{E} + \frac{\pi^2 q k_B T}{2} \underbrace{\frac{2m}{(2\pi\hbar)^2} \left(\frac{3n}{4\pi \sum_{\sigma \in \{\uparrow, \downarrow\}}} \right)^{-\frac{2}{3}}}_{1/\mu} k_B \vec{\nabla} T \right\} \\
&= \frac{nq^2\tau_e}{m} \vec{E} + \frac{n^{\frac{1}{3}}\tau_e q k_B T}{\hbar^2} \underbrace{\left(\frac{\pi \sum_{\sigma \in \{\uparrow, \downarrow\}}}{6} \right)^{\frac{2}{3}}}_{\approx 1.031} k_B \vec{\nabla} T \tag{8.182}
\end{aligned}$$

This gives us the **electric conductivity** of a free-electron gas in the relaxation-time approximation³⁷

$$\sigma_q = \frac{q^2 n \tau^e}{m} \tag{8.183}$$

which is identical to the Drude conductivity. Note, that the mass is the effective mass of the respective quasi particle, which may differ from the free-electron mass.

The second term shows that a electric current can be created by a temperature gradient. This current the **thermoelectric current**

The **thermoelectric coefficient** κ_q links the electric current to the temperature gradient

$$\kappa_q = \frac{n^{\frac{1}{3}} \tau_e q k_B T}{\hbar^2} \underbrace{\left(\frac{\pi \sum_{\sigma \in \{\uparrow, \downarrow\}}}{6} \right)^{\frac{2}{3}}}_{\approx 1.031} k_B \tag{8.184}$$

Editor: The thermoelectric coefficient needs to be checked! See Marder-Eq.17.78 [62] and Ashcrof-Mermin-Eq.13.51

The Seebeck coefficient is

$$\mathbf{S} = \boldsymbol{\sigma}^{-1} \boldsymbol{\kappa}_q = \frac{m}{q^2 n \tau^e} \cdot \frac{n^{\frac{1}{3}} \tau_e q k_B T}{\hbar^2} \underbrace{\left(\frac{\pi \sum_{\sigma \in \{\uparrow, \downarrow\}}}{6} \right)^{\frac{2}{3}}}_{\approx 1.031} k_B = \frac{m k_B T}{\hbar^2 q n^{\frac{2}{3}}} \underbrace{\left(\frac{\pi \sum_{\sigma \in \{\uparrow, \downarrow\}}}{6} \right)^{\frac{2}{3}}}_{\approx 1.031} k_B \tag{8.185}$$

The Seebeck coefficient obtained here is independent of the relaxation time. Unfortunately, this is a consequence of our approximation of a single relaxation time for all electrons. As mentioned by Marder[62], however, the Seebeck effect is extremely sensitive to an energy-dependence of the relaxation time, which makes it very hard to interpret measured Seebeck coefficients.

The origin of the electric conductivity is that an electric field produces a force $F = q\vec{E}$ with $q = -e$ acting on the electrons. According to Hamilton's equation $\dot{\vec{p}} = -\vec{\nabla} H(\vec{p}, \vec{r}) =: \vec{F}$, the wave vectors of the electrons moves along the direction of the force \vec{F} . Scattering events interrupt this motion, and distribute the wave vector randomly to the available one-particle states. In the steady state, the electron distribution is displaced in reciprocal space by a finite amount. The resulting imbalance of electrons moving in different directions is the origin of the electric current.

Consider a hot and a cold region of a material to be in contact. In the hot region, there are thermal electron-hole pairs, moving in all directions. This causes a net current of charge carriers moving from the hot to the cold region, because there are less charge carriers in the cold region. If there is an imbalance of the thermally induced current of electrons and holes, a net charge current results, the so-called thermo-electric current.

The thermoelectric current can be compensated by applying an external electric field. This produces a situation, where there is no net electric current, but a constant electric field. This field is related to the temperature gradient by the Seebeck coefficient.

8.10.2 Thermal conductivity

Editor: To be done...

This exercise is concerned with the thermal conductivity of an elastic medium due to phonons. We use the Debye model for the phonon dispersion $\omega(\vec{k}) = c_s |\vec{k}| \theta(k_D - |\vec{k}|)$, where $\theta(x)$ is the Heaviside function and c_s is the speed of sound. As material we consider iron which has a speed of sound of approximately $c_s = 5 \text{ km/s}$. The lattice constant of bcc iron is $a_{\text{lat}} = 2.87 \text{ \AA}$.

³⁷Compare Ashcroft-Mermin-Eq. 13.30

The generic equation for the induced currents in the relaxation-time approximation is Eq. 8.140.

$$\begin{aligned} \vec{j}_X = & \sum_n \int_{\Omega_T} \frac{d^3 p}{(2\pi\hbar)^3} \left(X_n(\vec{p}) Y_n(\vec{p}) \right) \left(\vec{v}_n(\vec{p}) \otimes \vec{v}_n(\vec{p}) \right) \tau_n(\vec{p}) \frac{\partial f_{T,\mu}(\epsilon_n(\vec{p}))}{\partial \mu} \vec{E}_Y \\ & - \sum_n \int_{\Omega_T} \frac{d^3 p}{(2\pi\hbar)^3} X_n(\vec{p}) \left(\epsilon_n(\vec{p}) - \mu \right) \left(\vec{v}_n(\vec{p}) \otimes \vec{v}_n(\vec{p}) \right) \tau_n(\vec{p}) \frac{\partial f_{T,\mu}(\epsilon_n(\vec{p}))}{\partial \mu} \frac{1}{T} \vec{\nabla} T \end{aligned} \quad (8.186)$$

The dispersion relation for free phonons in the Debye model is

$$\omega_\sigma(\vec{k}) = c_s |\vec{k}| \theta\left(|\vec{k}| - \omega_{\text{debye}}/c\right) \quad \text{with the polarizations } \sigma \in \{x, y, z\} \quad (8.187)$$

The phonon dispersion is cut off at the so-called Debye frequency. In contrast to electrons, phonons have a maximum frequency.

Solutions for thermal conductivity

Editor: Answer the question why the energy is the observable for the heat transport. (The heat current is a form of energy current. There are two forms of energy changes, which are distinguished in thermodynamics, namely heat and work. An energy current induced by a temperature gradient is therefore clearly a heat flow. An energy current can also be induced, for example, by an electric field. Would one call this energy current also a heat current or is this a form of work?)

- For the heat current of phonons in the Debye model (DM) in three dimensions we use

$$X_n(\vec{p}) = \hbar \omega_n \stackrel{DM}{=} c_s |\vec{p}| \theta(\hbar \omega_D - \hbar \omega) \quad \text{for } n = 1, 2, 3 \quad (8.188)$$

where n sums over the three acoustic branches. c_s is the speed of sound.

- velocity of phonons

$$\vec{v}_\alpha(\vec{p}) = \vec{\nabla}_{\vec{p}} \epsilon(\vec{p}) \stackrel{DM}{=} c_s \frac{\vec{p}}{|\vec{p}|} \quad (8.189)$$

Editor: To be done...

1.

8.10.3 No title yet

Editor: This problem is no more than a placeholder for an idea. Do not try!

This exercise is concerned with the thermal conductivity of a elastic medium due to phonons. We use the Debye model for the phonon dispersion $\omega(\vec{k}) = c |\vec{k}| \theta(k_D - |\vec{k}|)$, where $\theta(x)$ is the Heaviside function and c is the speed of sound. As material we consider iron which has a speed of sound of approximately $c = 5 \text{ km/s}$. The lattice constant of bcc iron is $a_{\text{lat}} = 2.87 \text{ \AA}$.

1. Revisit the section 8.8.3 on the "Transport coefficients in the relaxation-time approximation"
2. What are the units of the thermal current density, heat conductivity tensor, the heat capacity, and the heat capacity per state used in the derivation of the heat conductivity tensor.
3. calculate the size of the reciprocal unit cell of bcc iron. Determine the Debye wave vector so that the volume of the sphere with radius k_D is identical to the reciprocal space volume for one atom.

4. Plot the specific heat as function of the band energy. Describe and rationalize its behavior.
5. Discuss the number of branches in the phonon dispersion relation. Each degree of freedom per unit cell is reflected by one branch.
6. calculate the thermal conductivity of iron using the model above in the relaxation-time approximation with a yet unknown relaxation time.
7. extract the relaxation time from the known thermal conductivity of $79.5 \text{ W}/(\text{m K})$. (<http://hyperphysics.phy-astr.gsu.edu/hbase/Tables/thrcn.html>.)

Chapter 9

Tour of band structures and densities of states of real materials

In this chapter I will show the band structure and the density of states of a number of materials classes. I hope that I can cover the most relevant materials. The true intent of this lecture is to provide some insight into the patterns of band structures and density of states, that allow one to “read” band structures and density of states.

A list of concepts that will be discussed are

- free-electron band structure
- canonical band structures[63]
- avoided crossing
- Van Hove singularities [Editor: To be done!](#)

[Editor: The concepts and patterns shall be described in the text as they have been described in the lecture.](#)

9.1 Free-electron like metals

The free-electron like metals are the main group elements with a valence of one, two or three. This includes the **alkali metals**, the **alkaline earth** metals and tri-valent metals such as aluminium.

Fig. 9.1: Location of free-electron like metals in the periodic table marked in green.

The free-electron-like metals form structures with close-packed spheres such as face-centered cubic (fcc), hexagonally close-packed structures or body-centered cubic structures. The number of neighbors is larger than expected for directional bonds.

The band structure of these materials is very similar to that of the free-electron gas. The main difference is the lifted degeneracies at the zone boundaries, where the free-electron bands cross each other. The density of states shows the typical square-root-like behavior of the free-electron gas.

The valence of the element determines the number of electrons per unit cell, and thus the position of the Fermi level. The free-electron gas is characterized by the effective mass of the electron. When the lattice constant of the same material is increased, its effective mass is increased too.

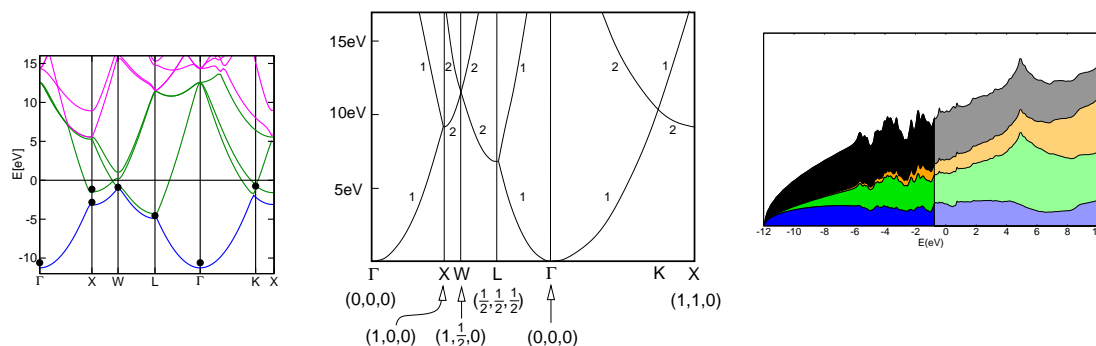


Fig. 9.2: Band structure (left) and density of states (right) of the free-electron-like metal aluminium. For comparison, the band structure (middle) of the free-electron gas in an fcc-cell with a lattice constant of 4.05 \AA corresponding to aluminium is shown. The bands are colored blue, green magenta for the bands derived from s, p and d -bands of a corresponding tight-binding model. The high-symmetry points marked in the free-electron band structure are given in units of $\frac{2\pi}{a_{\text{lat}}}$. The numbers indicate the degeneracy beyond spin-degeneracy. The function marked in black in on the right-hand side is the total density of states of aluminium. The blue, green yellow areas on top of the total density of states are the projections on s, p and d -type orbitals inside an atom-centered sphere. The band structure and density of states of Al has been calculated with density-functional theory using the CP-PAW code. Parts of this figure are identical to Fig. 5.1.

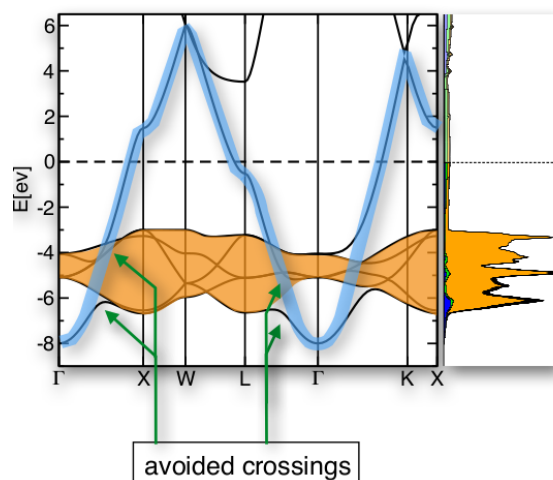


Fig. 9.5: Sketch of how the band structure of silver derives from a canonical s-type band (blue), which is intersected by the five d-bands (orange). During an avoided crossing of an s-band with a d-band, the character of the wave function changes from s-type to d-type for the lower band, and from d-type to s-type for the upper band and vice versa. The graph attached to the right is the density of states.

electronic states of an optical transition have essentially the same momentum. Therefore, one talks of a **vertical transition**.

color	red	orange	yellow	green	cyan	blue	violet
energy/eV	1.65-1.98	1.98-2.10	2.10-2.19	2.19-2.48	2.48-2.56	2.56-2.75	2.75-3.26

Source: https://en.wikipedia.org/wiki/Visible_spectrum, retrieved Dec. 3, 2020)

Light is usually absorbed by producing electron-hole pairs. That is, an electron from the valence band is lifted into the empty conduction states. The first observation we make, is that there are no intraband transitions in the s-band, because there are no two states at the same k-point. Also there are no transitions within the d-bands, because they are all occupied. Thus, we look for transitions between d- and s-states.² The lowest unoccupied s-states are located close to the X-point in Fig. 9.4. Thus, the absorption edge is approximately the distance of the upper band edge of the d-states from the Fermi level. For copper this absorption edge allows red light to be reflected, whereas photons with higher energy are (partly) absorbed. The reflected red light gives copper the red shine. In contrast, for silver the d-band lies further below the Fermi level, so that also green and blue light is reflected as well. For gold the green and blue photons are absorbed, so that it obtains a yellowish shine.

A relativistic effect: A surprising observation is that the absorption edge does not vary smoothly from copper to gold according to their increasing atomic number. Following the sequence copper (Cu), silver (Ag), gold (Au), we would expect gold to have a white color. The reason for the yellow color of gold is a relativistic effect: The s-electrons close to the nucleus of Au become so fast, that they obtain a relativistic mass enhancement. In turn, the increased mass shrinks the wave function. Because the s-electrons are now closer to the nucleus, their energy is lowered. This is the so-called **Darwin shift**. The Darwin shift moves the Fermi level, which is tied to the s-band, towards lower energies and thus closer to the d-band. Hence the absorption edge moves again towards lower energies from silver to gold.

²Note that the nominal d-states have a small admixture of s- and p-states.

9.3 Transition metals

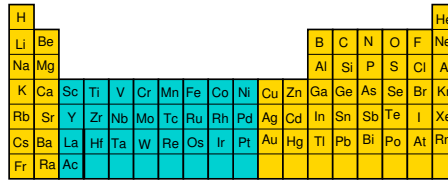


Fig. 9.6: Location of transition metals in the periodic table marked in green.

The final epoch of the prehistory of humanity, the iron age, is named after a transition metal. **Steel**, an iron-carbon alloy, is one of the most important materials for today’s technology.

Band width of d-bands

The band structure of the transition metals is determined by the narrow d-bands. Below and above the d-states, one finds the free-electron like s-p bands. At the Fermi level, these free-electron bands are not important because of level-repulsion.

The d-electrons of the transition metal series are very localized, similar to the s and p states with the same main quantum number, which are core states. In the 3d-transition metal series the 3d-states are in the valence electron shell, together with the 4s and 4p states. The 3s and 3p states, on the other hand are core states. The radial extent of the wave functions is, however, similar with other states of the same main quantum number. Because the d-electrons are so localized, the form narrow bands. The valence s- and p-electron levels, on the other hand lie several eV above the Fermi level. They overlap energetically with the d-band, because of the large s-band width.

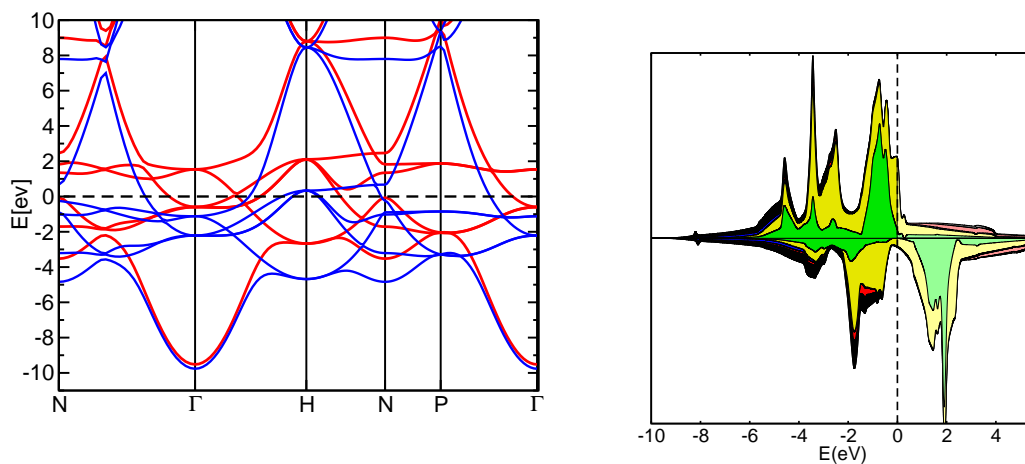


Fig. 9.7: Band structure and density of states of iron (Fe). The energy zero is the Fermi level.

bcc vs. closed packed structures: The transition metals form either closed-packed lattices such as **fcc** and **hcp**³ or, in the middle of the transition metal series, the **bcc**-lattice⁴. The origin of this behavior can be understood from the density of states. The d-density of states in the closed packed lattices is block-like. In contrast, the density of states of d-electrons in the body-centered lattice

³fcc denotes the face-centered cubic lattice, hcp denotes the hexagonal closed-packed lattice, and bcc stands for body-centered cubic lattice.

⁴bcc stands for body-centered cubic lattice.

consists of two main peaks with high density of states, which are separated by a region of low density of states. In the middle of the transition-metal series, the Fermi level lies in the quasi band gap of the bcc structure. When this happens, the filled states are further below the Fermi level, which stabilizes the bcc structure compared to the closed-packed structures such as fcc and hcp.

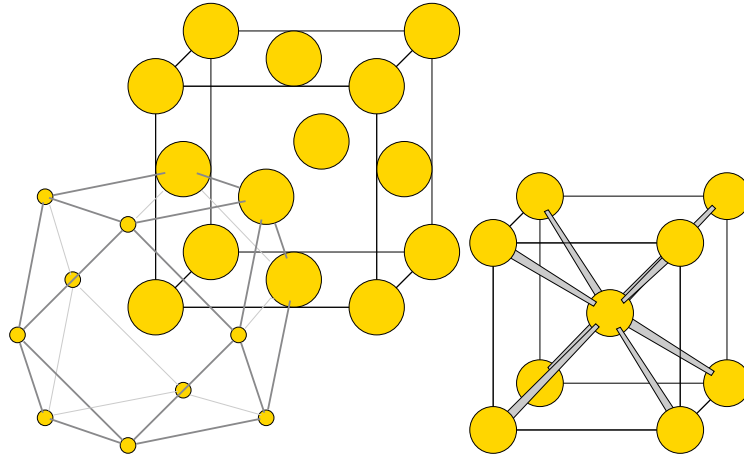


Fig. 9.8: Atomic structure of the face-centered cubic (fcc) lattice and the body-centered cubic (bcc) lattice. An atom in the face centered cubic lattice has 12 nearest neighbors, while that of the bcc structure has 8 nearest neighbors and 6 next nearest neighbors.

Electron correlation: The quasi-particle picture is useful, when the kinetic energy dominates over the electron-electron interaction. The energy scale for the kinetic energy is the band width, respectively the hopping parameter $|t|$, while the energy scale for the interaction is the Coulomb parameter U . The Coulomb parameter is large, for orbitals that are localized in small spatial region such as the d-electrons.

When the band width is small compared to the band width as for the d-electrons of the transition metals, the Coulomb interaction becomes more important in comparison to the kinetic energy. In the extreme case, the band width is considered as a small perturbation, which lead us to the atomic limit, where the electron-electron interaction dominates over the kinetic energy. In between these two extreme cases, one expects strong correlations between electrons, which leads to a range of interesting and exotic many-particle effects.

Magnetism: One such interaction effect is magnetism. Magnetism for elements occurs in the 3d-transition metal series for Cr, Fe, Ni. Magnetism is the result of Hund's rule, which says that, for atoms, electrons in the same angular momentum shell tend to align their spins.

While this effect is the origin of magnetism, it is driven by the Coulomb interaction and the Pauli principle. For the same electron density, electrons with the same spin stay further away due to the Pauli principle, as compared to electrons with opposite spin. This reduces the Coulomb interaction for electrons with parallel spin. Due to the small band width of the d-electron shell and small spatial extent of the d-electrons, this atomic correlation effect survives when the crystal is formed. This Coulomb effect is with several eV much larger than typical energies from the magnetic field $-\mu_e \vec{B}$, where the B is the magnetic field and μ_e is the magnetic moment of an electron. Magnetic energies are in the milli-eV energy range and below.

A magnetic system can be ferromagnetic (the spin orientation of all atoms are aligned), antiferromagnetic (the spin orientations of the atoms compensate each other) or ferrimagnetic (there is a net magnetic moment, but the atoms have different magnitude and/or orientation.).

When the system becomes magnetic, electrons in the majority-spin direction experience a different effective potential than those of the minority-spin direction. As a consequence one obtains different band structures and densities of states for the two spin orientation. In the energy region, where the

d-electrons dominate, the spin-up and spin-down electrons have similar band structures, but displaced relative to each other. The sp-electrons, which are located away further away from the atom, have a smaller Coulomb interaction and, therefore, they experience a smaller energy shift. The same effect is seen in the density of states.

Let us turn to iron, for which the bands are shown in Fig. 9.7. Without magnetism, the Fermi level would lie in the upper peak of the canonical density of states of the d-electrons. This would be very unfavorable compared to the closed packed structures. There is also a non-magnetic high-temperature phase of iron, named **austenite** or γ -iron, which assumes the fcc structure. The stable form of iron is the magnetic form of iron, named α -iron or **ferrite**. Ferrite has the bcc structure. The magnetic transition positions the Fermi level in the quasi gap of the minority spin direction and above the d-density of states for the majority spin direction.

Editor: The relation between stability and quasi-band gap has not been explained in a sound fashion.

The holes come in two variants, namely there are two **heavy holes** (small curvature) and one **light hole** (high curvature). The conduction electrons are located on the Γ -X line next to the X-point.

The conduction band minimum in silicon lies away from the Γ -point, which is unusual for the semiconductors. Silicon has six symmetry-related conduction band minima at the Γ -X line in reciprocal space, close to the X-point. It is often referred to as “**camel back**”. The mass of the conduction electrons is not isotropic but it has a large longitudinal mass in the direction of the X-point, and small transversal effective masses in the direction perpendicular to the Γ -X line. The longitudinal mass is in the range of the free-electron mass. The transversal masses are much smaller, which can be seen from the large curvature of the conduction band along the X-W and X-K lines of the band structure shown in Fig. 9.10.

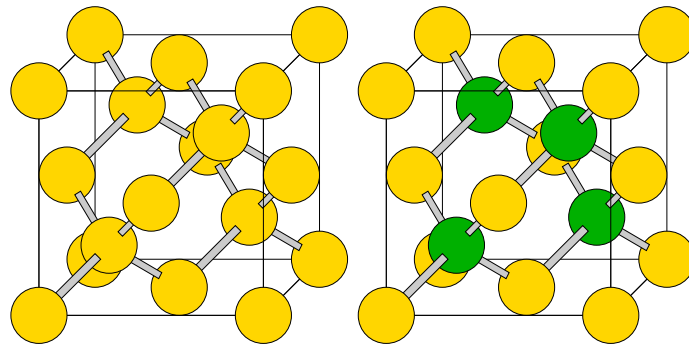


Fig. 9.11: Diamond structure (left) and zinc-blende structure (right).

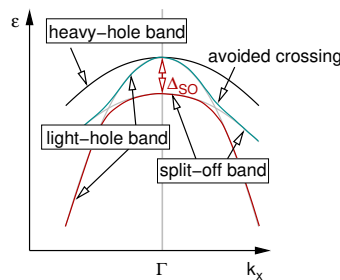


Fig. 9.12: Close-up of the valence band top in zinc-blende semiconductors with heavy atoms. Schematic drawing of the bands and their splitting due to spin-orbit coupling. Δ_{SO} is the spin-orbit splitting. Spin-orbit coupling has not been considered in the calculated band structure of silicon shown in Fig. 9.10.

For the semiconductors with heavier elements, relativistic effects, namely **spin-orbit coupling** split the three-fold degenerate valence band top into a **heavy-hole band**, a **light-hole band** and a **split-off band**. The valence band top is made from the p-states. At the Γ -point the three p-states are degenerate as a consequence of the cubic symmetry. In a non-relativistic description spin and orbital angular momentum are strictly decoupled. Spin-orbit coupling $-\frac{\Delta_{SO}}{\hbar^2} \hat{L} \hat{S}$ is a relativistic effect, which favors an anti-parallel alignment of spin and orbital angular momentum. As a result, the three p-states split into a singlet and a doublet.

- In the singly degenerate state, spin and orbital angular momentum are antiparallel. This state has a total spin $j = \frac{1}{2} \hbar$. Considering the spin multiplicity, there are actually two states, one with $j_z = -\frac{1}{2} \hbar$ and another one with $j_z = +\frac{1}{2} \hbar$. This band is called the split-off band.
- In the doubly degenerate state spin and orbital angular momentum are parallel and the total spin

is $j = \frac{3}{2}\hbar$. Including spin multiplicity there are four states with $j_z \in \{-\frac{3}{2}\hbar, -\frac{2}{2}\hbar, +\frac{2}{2}\hbar, \frac{3}{2}\hbar\}$. These states belong to the heavy- and light-hole bands.

There is a subtle point that often is not obvious from most representations, but which can clearly be seen in the calculated band structures of semiconductors[?]: There is an **avoided crossing** of a light hole band and the split-off band. The two heavy holes from the non-relativistic description are split into the final heavy-hole band and the split off band. The light hole band undergoes an avoided crossing with the split off band and connects to the upper heavy hole band. For atoms with a large atomic number, the relativistic effects become more important. When the spin orbit splitting exceeds thermal energies, i.e. $k_B T$, the split-off band does not hold any holes and, thus, it does not contribute to charge transport.

Doping: Electrons and holes can be formed in silicon as thermal electron-hole pairs by heating the sample or photo-induced electron-hole pairs by shining light on the sample. Then most important way of introducing charge carriers is doping. In silicon the most well known **dopants** are phosphorus as **electron donors** and boron as **electron acceptors**.

Phosphorus atoms in silicon can be considered like a quasi hydrogen atom, where the P^+ ion assumes the role of the proton of the hydrogen atom, while the electron is the additional electron in the conduction band. The measured binding energy of 45 meV⁶ can be estimated roughly from the 1s level $\epsilon_s[H] = -\frac{1}{2} \frac{m_e e^4}{(4\pi\epsilon_0 \hbar)^2} \approx -13.303$ eV of hydrogen atom after scaling the mass to the effective mass of the conduction electron and the dielectric constant to that of silicon.⁷ The effective Bohr radius is approximately 2 nm, which is much larger than the interatomic distance of two silicon atoms.[65]

The binding energy of the electron to the phosphorus ion is in the range of thermal energies $k_B T = 25$ meV at room temperature, which implies that most phosphorus ions are ionized and the electron is separated from the ion. Thus, the doped silicon behaves like a metal with a very small electron concentration, which is proportional to the dopant concentration.

Compound semiconductors: Silicon is only one member of a large class of semiconductors that form the diamond- or zincblende (ZnS) structure. Besides using four-valent elements, it is also possible to form compounds which are, on average, four valent such as GaAs. This means that As, which is five-valent gives one electron to the tri-valent Ga, so that both ions have four electrons, which they contribute to the tetrahedral network. If the two atom types occupy neighboring lattice positions of the diamond structure, the zinc-blende structure is obtained. The large variability of similar materials allows one to combine these materials to form complicated structured materials on the nanometer length scale such as a semiconductor chip.

When ions from the third column of the periodic table such as Ga are combined with atoms of the fifth column such as As one speaks of a III-V semiconductor. Other well-known III-V semiconductor is GaN, which is the material for blue light-emitting diodes (LED). When atoms from the second column such as Zn are combined with atoms from the sixth row such as Se one speaks of II-VI semiconductors.

Other tetrahedrally coordinated networks: There is also a hexagonal variation of the diamond structure, the **wurtzite** lattice. Also in the wurtzite lattice, the atoms are tetrahedrally coordinated. The difference to the diamond lattice becomes evident only in the second nearest neighbor shell. Therefore, the properties in the cubic and the hexagonal variants are very similar.

Amorphous silicon there are many tetrahedral networks, which are all good candidates for accommodating four-valent atoms.

Other tetrahedral networks are formed by SiO_2 , in which each Si-Si bond is replaced by a Si-O-Si bridge. There are crystalline variants such as α -quartz, also in the form of quartz sand. Amorphous SiO_2 is essentially the same as window glass.

Another tetrahedral network is water: In water, the oxygen ions are connected via hydrogen bonds. Each oxygen ion in a water molecule is bound to two hydrogen atoms. They can form weak

⁶Source: C. Jagannath, Z. W. Grabowski, and A. K. Ramdas, Physical Review B 23, 2082 (1981)

⁷Relative dielectric constant $\epsilon_r = 11.9$, longitudinal effective electron mass $m_l^* = 0.98 m_e$, transversal electron mass $m_t = 0.19 m_e$, effective heavy-hole mass $m_{hh}^* = -0.49 m_e$ effective light-hole mass $m_{lh}^* = 0.16 m_e$ (Source: <http://www.virginiasemi.com/pdf/generalpropertiesSi62002.pdf> retrieved Dec.3, 2020)

hydrogen bonds with the back-side of the H₂O molecule.

9.5 Simple oxides

Oxides are a tremendously important class of materials. They are the major corrosion end products under atmospheric conditions, and thus they are the major component of rocks. They also include a wide range of functional materials such as the high- T_c superconductors. You look at them when you stare out of the window, you lie on them on the beach, because glass and sand are both the oxide of silicon. The most simple oxides are, as the name says, **simple oxides**. They are the oxides of the most electropositive elements, for which the cations do not contain transition metals, and for which the valence electrons are used up completely to form O^{2-} anions.

Examples for simple oxides are MgO, Al_2O_3 . Other ionic compounds, such as NaCl follow the same principle. What I consider as non-simple oxides, are many transition-metal oxides, because their properties are largely determined by the d-electrons of the transition metals. Also SiO_2 is an oxide, which I would not consider as “simple” in the current sense. It forms a tetrahedral network of corner-connected SiO_4 -tetrahedra and such networks exhibit a large structural variety compared to the simple oxides.

Simple oxides form typically a closed packed lattice of oxygen ions, with cations in the voids, between the anion spheres.

These materials are a good starting point for understanding the more complicated oxides. One can simplify them even further, by making the same trick as for the jellium model: when we smear out the cation cores to a homogeneous positive charge background and leave only the electrons to saturate the oxygen valence shell, we obtain, what I call **jellium oxide** or **jelly-O**. The oxygen ions form a closed packed lattice. The electronic structure of Jelly-O is almost indistinguishable to those of the simple oxides.

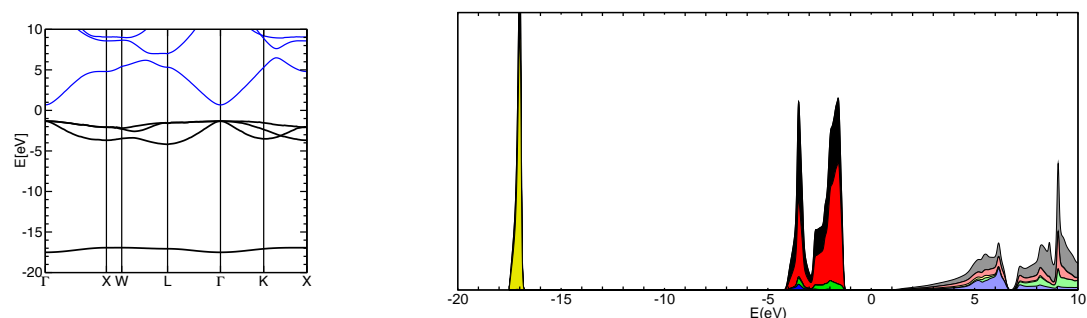


Fig. 9.13: Electronic structure of jellium oxide, an fcc array of O^{2-} ions with a homogeneous positive charge background. Left: band structure. The filled bands are black, the empty ones are blue. Right: Density of states. Based on density functional calculations using the CP-PAW code.

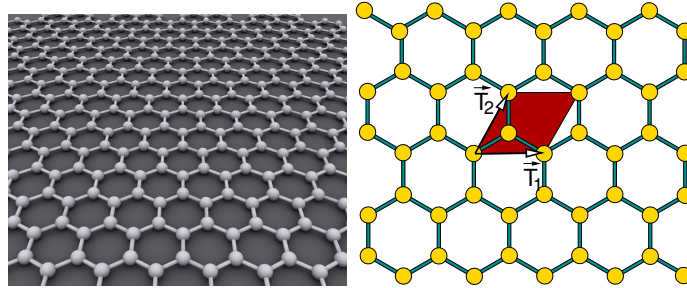
The band structure is characterized by a low lying band of oxygen s-character. Above, and well separated from the s-band one finds the oxygen p-band which forms the valence shell. In contrast to the semiconductors, the s and p-bands are now well separated. This is, on the one hand, due to the large s-p splitting of the atom, and on the other hand it is due to the smaller band width of the oxygen p-band caused by the larger distance between oxygen ions.

Very characteristic for the oxygen valence band is the double-peaked structure. It is caused entirely by the hopping between the oxygen ions and is not to be mistaken by a bond to the cations.

The empty conduction band is very similar to a free-electron like band.

9.6 Graphene

Graphite is the stable configuration of carbon. It consists of monolayers of atoms. While the carbon atoms in each sheet form strong covalent bonds, the layers are bonded among each other only by weak van-der Waals forces. A single such sheet is called graphene. The atoms in a graphene sheet arrange in a honeycomb lattice as shown below.



The band structure can be described as follows. Carbon forms sp_2 hybrid orbitals which lie in the plane of the graphene sheet and which form an angle of 120° . The bonding orbitals are filled and the antibonding orbitals are empty. This explains that the carbon atoms form a honeycomb lattice. The corresponding states are shown as yellow and green areas in the density of states shown in figure 9.14.

The remaining orbital of the carbon atom is a p-orbital standing perpendicular to the graphene sheet. These are the states that determine the band structure near the Fermi level. The band structure of this single band is shown in figure 9.14 below. The band structure of graphene has been the topic of the practice section 4.6.1 on p. 145.

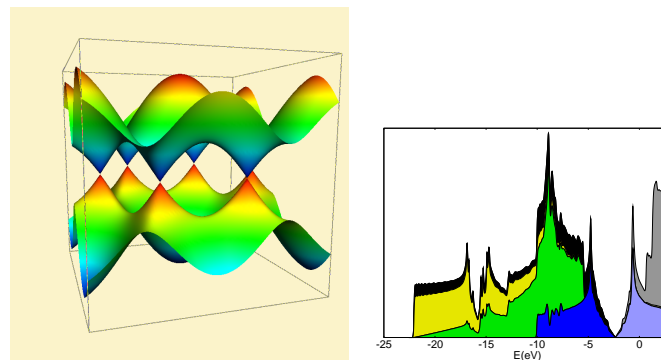


Fig. 9.14: Left: Band structure $\epsilon_n(\vec{k})$ of the perpendicular p-orbitals of graphene. The two bands shown in the 2-dimensional reciprocal space touch at the Dirac points, which lie exactly at the Fermi level. The band structure has been calculated analytically using a tight-binding model. Right: Density of states of a graphene sheet. The blue area is the density of states projected onto the p_z orbitals perpendicular to the graphene sheet. The yellow area is the density of states projected onto s states and the green area is the one projected onto the p-orbitals in the plane. The black area which reaches to the bottom behind the projected density of states is the total density of states. The density of states are obtained with density-functional calculations using the CP-PAW code.

The band structure of a graphene sheet has an interesting property, namely that the bands form Dirac points right at the Fermi level. At the Dirac points \vec{k}_0 the dispersion relation $\epsilon(\vec{k}) = v|\vec{k} - \vec{k}_0|$ is linear. It has the form of a conical intersection, which we became familiar with in the context of the Born-Oppenheimer framework. A linear dispersion relation is characteristic for mass-less particles such as the photon (light) or the phonon (lattice vibration). These particles are usually bosons, that have integral spin. Here we obtain mass-less quasi particles that have spin $\frac{1}{2}\hbar$.

The nearly abrupt increase of the density of states at the band edges is characteristic for two-dimensional bands with a parabolic dispersion relation. The density of states of the Dirac cones behave very differently near the Fermi level from that of particles with mass.

9.7 Parent compound of high-temperature superconductors

In 1986, Georg Bednorz and Alex. Müller from the IBM Zurich Research Laboratory in Rüschlikon, Switzerland detected the first high- T_c superconductors.[34] While the transition temperature of conventional superconductors are limited to about 30 K, the high- T_c compounds increased this limit to 150 K, well above the liquid nitrogen temperature of 77 K.

The materials in this class are called **cuprates**. The parent compound of these materials is La_2CuO_4 . Hole doping of this material by replacing some of the trivalent La ions by divalent Ba ions makes this compound superconducting.

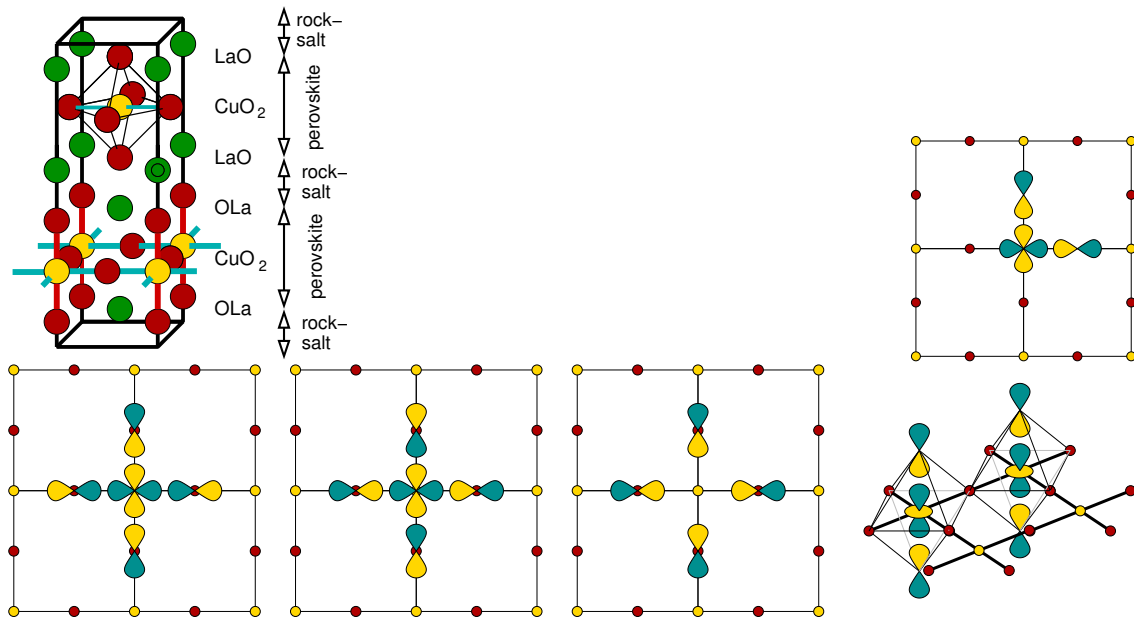


Fig. 9.15: Atomic structure of La_2CuO_4 , the parent compound of the high- T_c superconductors invented by Bednorz and Müller. Cu is shown in yellow, oxygen in red and La in green. The unit cell contains two CuO_2 planes. We used the upper one to show the octahedron, and the lower one to demonstrate the connectivity in the CuO_2 plane. In the upper right, the three orbitals responsible for the most important features of the bandstructure are shown, namely the Cu-centered $d_{x^2-y^2}$ orbital and the two O- $2p$ orbitals connecting two Cu ions. The lower graph shows on the left a set of three symmetry adapted orbitals, and, at the very right, another orbital which connects to the axial oxygen neighbors.

The component relevant for superconductivity are the CuO_2 planes, while the LaO-layers in between the CuO_2 planes are considered as spacers that donate two electrons per Cu site.

The charge count on the ions is $\text{La}_2^{3+}\text{Cu}^{2+}(\text{O}^{2-})_4$, which leaves the copper ion in a configuration with nine electrons (d^9 configuration). That is, one electron per Cu ion is missing to fill the Cu-d shell. The spins of the missing electrons order antiferromagnetically, which results in an insulating antiferromagnet.

The electronic structure can be described[66]⁸ by a limited orbital set containing only the Cu- $d_{x^2-y^2}$ in the CuO_2 plane, and one p-orbital per oxygen atom in the plane pointing towards the Cu-neighbors. These orbitals are shown in the upper right of fig. 9.15.

These three orbitals, plus one additional one, can be transformed into

⁸Chen et al.[67] discuss the three-band model mentioned here. Editor: See this paper also for a reference of the Zhang-Rice singlet. The Zhang-Rice singlet corresponds to the hole in half-filled antibonding Cu- $d_{x^2-y^2}$ orbital in the non-spin polarized calculation. See also Santoso et al.[68]

- a bonding $d_{x^2-y^2}$ orbital, i.e. a σ -bonding combination of a Cu- $d_{x^2-y^2}$ orbital in the center with four O-p orbitals on the four neighbors. The orbital is shown at the very left at the bottom of fig. 9.15.
- a antibonding $d_{x^2-y^2}$ orbital, i.e. an σ^* -anti-bonding combination of a Cu- $d_{x^2-y^2}$ orbital in the center with O-p orbitals on the four neighbors. The orbital is shown as second from left at the bottom of fig. 9.15.
- A symmetric combination of O-p orbitals in the CuO_2 plane pointing towards the central Cu-site. The orbital is shown as third from left at the bottom of fig. 9.15.
- $d_{3z^2-r^2}$ orbital, i.e. an Cu-d orbital perpendicular to the plane, which is σ^* -antibonding with the axial oxygen neighbors. The orbital is shown at the very right at the bottom of fig. 9.15.

The last two orbitals can be combined again into a bonding and antibonding superposition. We refer to them as the bonding and antibonding $d_{3z^2-r^2}$ orbitals.

The density of states are shown in fig. 9.16. The non-spin polarized calculation on the right of fig. 9.16 exhibits a metallic band (yellow) crossing the Fermi level. This band is half filled, because it contains one hole.

Compared to the non-spin polarized state, the system can lower its energy by introducing an antiferromagnetic order in the antibonding $d_{x^2-y^2}$ band, which doubles the unit cell. This antiferromagnetic order splits the metallic band and produces an insulator as shown on the left of fig. 9.16. Thus, the material is an antiferromagnetic insulator. The antibonding Cu-d state splits into a so-called upper Hubbard band (UHB) and the Zhang-Rice singlet (ZRS)[66].⁹

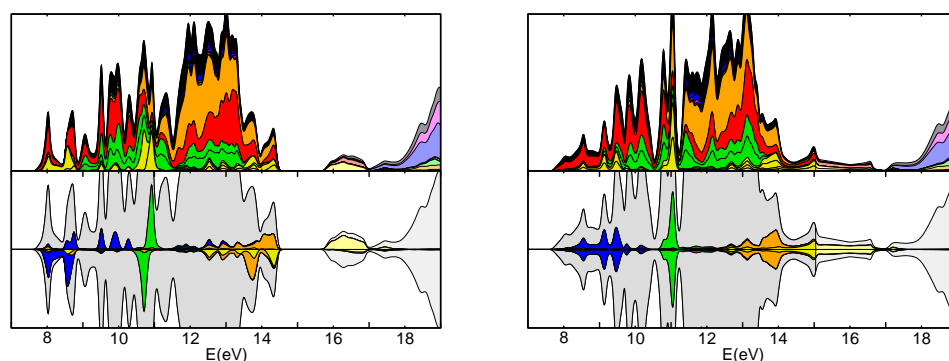


Fig. 9.16: Density of states of antiferromagnetic (left) and paramagnetic (right) La_2CuO_4 . For the paramagnetic calculation any spin dependence is suppressed. The upper graph shows the Cu-eg orbitals in yellow, and the t_{2g} orbitals in green. The projected density of states from the oxygen-p-orbitals in the CuO_2 plane are shown in red and those from the LaO planes are shown in orange. The density of states projected onto the s-, p-, d- and f- states of La are drawn in green, magenta, blue and magenta and are visible on the very right of the respective graph. The lower graph shows the density of states projected onto the bonding Cu- $d_{x^2-y^2}$ states (blue), antibonding Cu- $d_{x^2-y^2}$ states (yellow), the bonding Cu- $d_{3z^2-r^2}$ states (green), antibonding Cu- $d_{3z^2-r^2}$ states (orange). For the definition of the orbitals, see text. The spin-up density of states points upward and the spin-down density of states points downward. The projected density of states is shown only one of the two atoms. **Editor: The calculations has been done with too few k-points for a good-quality density of states.**

⁹Assignment of UHM and ZRS from Matsubayashi and Ishihara[69]

9.8 What band structures are good for

From ΦSX:Quantum mechanics of the chemical bond[3]

9.8.1 Chemical stability

Jahn-Teller distortion, Peierls distortion (polyacetylene, silicon)

Abrupt interfaces

While a dispersion relation is strictly defined only for translationally invariant systems, where the energy eigenstates are also momentum eigenstates, we can also understand what happens at the interface between materials. As a particle passes from one material to the other, it may gain or lose momentum perpendicular to the interface, but we can use energy conservation and conservation of the momentum parallel to the interface to obtain some information on the interface crossing.

Lifetime broadening

Sometimes the material has some randomness or other interactions that break translational symmetry. If these perturbations of translational symmetry are small, the eigenstates of the Hamiltonian are no more momentum eigenstates. If we still project the energy eigenstates onto momentum eigenstates, each momentum will obtain contribution from several energies. Instead of sharp energies for each momentum we have a broadened distribution. The width of the energy distribution is a measure for the life time of a momentum: Scattering processes will redirect the particle.

9.9 Home study and practice

9.9.1 Bandstructure and lifetime broadening

Editor: Caution: In preparation. It requires second-order perturbation theory, rather than first-order perturbation theory. When the orbitals do not adjust to the thermally perturbed potential, the energy shifts average out for large systems. The result may be analogous to an interaction??

Editor: The goal is to introduce the spectral function and lifetime broadening without electron-electron interaction.

When we discuss bandstructures, we assume that there is a fixed relation $\epsilon_n(\vec{k})$. For real systems, the bands are not “sharp”, but they have a finite width. This can be described in terms of the **spectral function** $A_n(\vec{k}, \epsilon)$. The spectral function for a pair of orbitals $|\chi_\alpha\rangle$ and $|\chi_\beta\rangle$ is, according to Eq. 9.32 in ΦSX:Advanced Solid-State Theory[2].

$$A_{\alpha,\beta}(\epsilon) = \sum_{m,n} (P_n + P_m) \langle \Phi_n | \hat{c}_\alpha | \Phi_m \rangle \langle \Phi_m | \hat{c}_\beta^\dagger | \Phi_n \rangle \delta(\epsilon - (E_m - E_n)) \quad (9.1)$$

where the $|\Phi_n\rangle$ are the many-electron energy eigenstates with energies E_n . Each many-particle state can have a different number of particles N_n . Together with their probabilities P_n , they define an ensemble of electronic states. In thermal equilibrium,¹⁰ the probabilities are $P_n = \frac{1}{Z_{T,\mu}} e^{-\beta(E_n - \mu N_n)}$

¹⁰When the Hamilton operator is not particle-number conserving, the energy eigenstates are not particle-number eigenstates, so that N_n is undefined. However, in that case, there is not particle reservoir, which can be accounted for by setting the chemical potential μ to zero.

with the partition function $Z_{T,\mu} = \sum_n e^{-\beta(E_n - \mu N_n)}$. \hat{c}_α^\dagger and \hat{c}_α are creation and annihilation operators for the one-particle orbital $|\chi_\alpha\rangle$.

The spectral function can be considered as a generalization of the density of states

$$\hat{D}(\epsilon) = \sum_{\alpha,\beta} |\chi_\alpha\rangle A_{\alpha,\beta}(\epsilon) \langle \chi_\beta| \quad (9.2)$$

Let us choose a one-particle basisset of Bloch waves, which may, for example, be the natural orbitals of a crystal. Even for the natural orbitals the spectral functions is not necessarily diagonal.

Nevertheless, let us investigate the diagonal elements of the spectral function.

For sharp bands, the spectral function has the form

$$A_n(\vec{k}, \epsilon) = \delta(\epsilon - \epsilon_n(\vec{k})) \quad (9.3)$$

When the system is perturbed, the spectral function broadens and the broadening can be interpreted as a lifetime broadening.

We start with the Hamiltonian for a linear Holstein chain, which describes a linear chain of electron orbitals, coupled to a local phonon on each site.¹¹

$$\hat{H} = \underbrace{\sum_{j=1}^N \frac{\hat{p}_j^2}{2M}}_{\text{phonons}} + \underbrace{\sum_j \frac{1}{2} C (\hat{R}_j - \bar{R}_j)}_{\text{electrons}} - \underbrace{\sum_j t (\hat{c}_{j+1}^\dagger \hat{c}_j + \hat{c}_{j+1} \hat{c}_j^\dagger)}_{\text{electron-phonon coupling}} + \sum_j \gamma (\hat{R}_j - \bar{R}_j) \hat{c}_j^\dagger \hat{c}_j \quad (9.4)$$

Editor: Mention that only one spin direction is used. *spin-less electrons*. Editor: Mention periodic boundary conditions. Editor: Describe all parameters M, C, t, γ, \dots

We use the Gauß integral

$$\int_{-\infty}^{\infty} dx e^{-x^2} = \sqrt{\pi} \quad (9.5)$$

- Calculate the spectral function at finite temperature up to liner order in the electron-phonon coupling.
- Use the broadening of the spectral function to estimate the lifetime of the electron states.

Editor: Interesting would also be to investigate the band structure undergoing period doubling as for polyacetylene. The band structure would be evaluated in the high-symmetry unit cell, and both distortions are permitted in the average.

In first order, we only need to evaluate the expectation value of the perturbed Hamiltonian for the unperturbed wave function. Thus, we determine the probability for a given atomic displacement in thermal equilibrium in the absence of electron-phonon coupling. Then we determine the electronic wave functions in the absence of the electron phonon coupling. Evaluation of the matrix elements with the electron-phonon coupling term in the Hamiltonian provides the energy shifts due to the presence of the phonon oscillations.

Unperturbed eigenstates of the electronic system

In the absence of the electron phonon coupling, the electrons experience the Hamiltonian

$$\hat{H}_{\gamma=0}^{el}(\vec{R}_j) = - \sum_{j=1}^N t (\hat{c}_{j+1}^\dagger \hat{c}_j + \hat{c}_{j+1} \hat{c}_j^\dagger) \quad (9.6)$$

¹¹This system has some pathological features, because undergoes a symmetry breaking already in the ground state. This behavior does not become evident because of the approximations we make.

This is a non-interacting Hamiltonian, which can be diagonalized with the help of the one-particle eigenstates.

$$|\varphi(k)\rangle = \frac{1}{\sqrt{N}} \sum_{j=1}^N |\chi_j\rangle e^{ik a_{\text{lat}} j} \quad (9.7)$$

and their one-particle energies

$$\epsilon_k = -2t \cos(ka_{\text{lat}}) \quad (9.8)$$

Note, that for s-orbitals, the hopping parameter is positive, so that the lower band edge is at the Γ -point ($k = 0$).

The k-points are selected by the boundary conditions. We choose them to be periodic boundary conditions with N beads in the repeat unit.

$$e^{ik a_{\text{lat}} N} = 1 \quad \Rightarrow \quad k_n = \frac{2\pi}{a_{\text{lat}}} n \quad \text{with} \quad -\frac{N}{2} < n \leq \frac{N}{2} \quad (9.9)$$

The many-particle eigenstates of the non-interacting electronic Hamiltonian are

$$|\vec{\sigma}\rangle = \prod_n \left(\frac{1}{\sqrt{N}} \sum_{j=1}^N \hat{c}_j^\dagger e^{ik_n a_{\text{lat}} j} \right)^{\sigma_n} |\mathcal{O}\rangle \quad \text{with energy} \quad E_{\vec{\sigma}} = \sum_n \sigma_n \epsilon_{k_n} \quad (9.10)$$

where $|\mathcal{O}\rangle$ is the electronic vacuum state. For each non-zero occupation number σ_n , an electron is created in the Bloch state $|\varphi(k_n)\rangle$.

Unperturbed phonons in thermal equilibrium

In the absence of electron-phonon coupling, the nuclear motion are governed by the Hamiltonian function

$$H^{nuc} = \sum_j \frac{P_j^2}{2M} + \frac{1}{2} \sum_j C(R_j - \bar{R}_j) \quad (9.11)$$

The probability distribution of the atomic displacements in thermal equilibrium can be calculated using the Boltzmann factor. (Section 6.6 in Φ SX: Statistical Physics.[38].

The displacement of the atoms in the absence of electron-phonon coupling have the probability distribution

$$P(\vec{R}) = \frac{e^{-\beta \frac{1}{2} C \sum_j (R_j - \bar{R}_j)^2}}{\int d^N R_j e^{-\beta \frac{1}{2} C \sum_j (R_j - \bar{R}_j)^2}} = \prod_j \frac{e^{-\beta \frac{1}{2} C (R_j - \bar{R}_j)^2}}{\int_{-\infty}^{\infty} du e^{-\beta \frac{1}{2} C u^2}} = \prod_j \left[\sqrt{\frac{\beta C}{2\pi}} e^{-\beta \frac{1}{2} C (R_j - \bar{R}_j)^2} \right] \quad (9.12)$$

Energy displacements due to the presence of phonons

In first order, we can estimate the displacement of the energy levels due to the phonons in first order

$$\begin{aligned} \delta\epsilon_k(R_j) &= \langle \varphi_k | \left(\sum_j |\chi_j\rangle \gamma(R_j - \bar{R}_j) \langle \chi_j| \right) | \varphi_k \rangle = \sum_j \gamma(R_j - \bar{R}_j) \underbrace{\langle \varphi_k | \chi_j \rangle \langle \chi_j | \varphi_k \rangle}_{1/N} \\ &= \frac{1}{N} \sum_j \gamma(R_j - \bar{R}_j) \end{aligned} \quad (9.13)$$

Editor: This factor $1/N$ makes sense.

$$\begin{aligned}
 \langle \delta \epsilon_k^2 \rangle_T &= \int d^N R P(\vec{R}) \left(\frac{1}{N} \sum_j \gamma(R_j - \bar{R}_j) \right)^2 \\
 &= \int d^N R \prod_n \left[\sqrt{\frac{\beta C}{2\pi}} e^{-\beta \frac{1}{2} C (R_n - \bar{R}_n)^2} \right] \left(\frac{1}{N} \sum_j \gamma(R_j - \bar{R}_j) \right)^2 \\
 &= \frac{1}{N^2} \gamma^2 \sum_{j,j'} \int d^N R \prod_n \left[\sqrt{\frac{\beta C}{2\pi}} e^{-\beta \frac{1}{2} C (R_n - \bar{R}_n)^2} \right] (R_j - \bar{R}_j)(R_{j'} - \bar{R}_{j'}) \\
 &= \frac{1}{N^2} \gamma^2 \sum_j \int dR_j \left[\sqrt{\frac{\beta C}{2\pi}} e^{-\beta \frac{1}{2} C (R_j - \bar{R}_j)^2} \right] (R_j - \bar{R}_j)^2 \\
 &\quad + \frac{\gamma^2}{N^2} \sum_{j,j':j \neq j'} \underbrace{\left[\int dR_j \sqrt{\frac{\beta C}{2\pi}} e^{-\beta \frac{1}{2} C (R_j - \bar{R}_j)^2} (R_j - \bar{R}_j) \right]}_{=0} \underbrace{\left[\int dR_{j'} \sqrt{\frac{\beta C}{2\pi}} e^{-\beta \frac{1}{2} C (R_{j'} - \bar{R}_{j'})^2} (R_{j'} - \bar{R}_{j'}) \right]}_{=0} \\
 &= \gamma^2 \frac{1}{\sqrt{\pi}} \frac{2}{\beta C} \frac{1}{N^2} \sum_j \int \underbrace{d\left(\sqrt{\frac{\beta C}{2}} R_j \right)}_{dx} \underbrace{e^{-\frac{\beta C}{2} (R_j - \bar{R}_j)^2}}_{e^{-x^2}} \underbrace{\frac{\beta C}{2} (R_j - \bar{R}_j)^2}_{x^2} \\
 &= \gamma^2 \frac{1}{\sqrt{\pi}} \frac{2}{\beta C} \frac{1}{N} \underbrace{\int dx e^{-x^2} x^2}_{\sqrt{\pi}/2} = \frac{1}{N} \frac{\gamma^2}{C} k_B T \tag{9.14}
 \end{aligned}$$

Editor: The factor $1/N$ seems incorrect! Maybe, however, this is related to the central-limit theorem, which describes that the width falls off with system size, because more and more displacements add in random directions. This implies that thermal motion contributes to the lifetime of electrons only for finite systems. That is where the energy levels (the k-points) are discrete.

9.9.2 Peierls transition

Editor: Caution: In preparation

The band structures of independent particles are continuous throughout the Brillouin zone. For interacting systems on the other hand one obtains at times bands that seem to end somewhere inside the Brillouin zone, while another band suddenly seem to start in the same region. This effect, which, at first, is quite stunning can be traced to phenomenon that can easily be understood.

Imagine a molecule such as polyacetylene $(\text{CH})_n$, which forms a zig-zag chain of carbon atoms, that lie in a common plane. The p_z orbitals perpendicular to the chain, form a half-filled band.

These orbitals are well described by a half-filled linear chain of hydrogen atoms. This will be the model we will investigate. **Peierls' theorem** says that a one-dimensional equally spaced chain with one electron per ion is unstable.

$$\hat{H}^{BO}(\vec{x}) = - \sum_{j=1}^N t \left[1 - \gamma(x_{j+1} - x_j) \right] \left(\hat{c}_j^\dagger \hat{c}_{j+1} + \hat{c}_{j+1} \hat{c}_j^\dagger \right) + \underbrace{\sum_{j=1}^N \frac{1}{2} C x_j^2}_{\text{restoring term}} \tag{9.15}$$

In second-order perturbation theory, the energy shift is obtained as follows: The perturbation \hat{W} is scaled by a parameter λ . The λ -dependent Schrödinger equation is derived two times with respect to the parameter, which yields the first two λ -derivatives of the one-particle energies. Next

the derivatives are taken at $\lambda = 0$, and the second-order Taylor expansion of the energies is evaluated at $\lambda = 1$.

$$\begin{aligned}
 & [\hat{h} + \lambda \hat{W} - \epsilon_k(\lambda)] |\varphi_k(\lambda)\rangle = 0 \\
 \Rightarrow & \left[\hat{W} - \frac{d\epsilon_k}{d\lambda} \right] |\varphi_k(\lambda)\rangle + [\hat{h} + \lambda \hat{W} - \epsilon_k(\lambda)] \left| \frac{d\varphi_k}{d\lambda} \right\rangle = 0 \\
 \Rightarrow & \left[-\frac{d^2\epsilon_k}{d\lambda^2} \right] |\varphi_k(\lambda)\rangle + 2 \left[\hat{W} - \frac{d\epsilon_k}{d\lambda} \right] \left| \frac{d\varphi_k}{d\lambda} \right\rangle + [\hat{h} + \lambda \hat{W} - \epsilon_k(\lambda)] \left| \frac{d^2\varphi_k}{d\lambda^2} \right\rangle = 0
 \end{aligned} \tag{9.16}$$

From the first derivative, I obtain

$$\begin{aligned}
 & \langle \phi(k') | [\hat{W} - \frac{d\epsilon_k}{d\lambda}] |\varphi_k(\lambda)\rangle + \underbrace{\langle \phi(k') | [\hat{h} + \lambda \hat{W} - \epsilon_k(\lambda)]}_{\langle \phi(k') | \epsilon_{k'}(\lambda)} \left| \frac{d\varphi_k}{d\lambda} \right\rangle = 0 \\
 \left| \frac{d\varphi_k}{d\lambda} \right\rangle &= \sum_{k'(\neq k)} |\varphi_{k'}\rangle \langle \varphi_{k'} | \frac{d\varphi_k}{d\lambda} \rangle = \sum_{k'(\neq k)} |\varphi_{k'}\rangle \frac{1}{\epsilon_k - \epsilon_{k'}} \langle \varphi_{k'} | [\hat{W} - \frac{d\epsilon_k}{d\lambda}] |\varphi_k\rangle \\
 \frac{d\epsilon_k}{d\lambda} &= \langle \phi_k | \hat{W} | \varphi_k \rangle
 \end{aligned} \tag{9.17}$$

The exclusion of the terms $k = k'$ is to ensure orthonormality of the perturbed states

From the second derivative, I obtain

$$\begin{aligned}
 & \left[-\frac{d^2\epsilon_k}{d\lambda^2} \right] + 2 \langle \varphi_k(\lambda) | [\hat{W} - \frac{d\epsilon_k}{d\lambda}] \left| \frac{d\varphi_k}{d\lambda} \right\rangle + \underbrace{\langle \varphi_k(\lambda) | [\hat{h} + \lambda \hat{W} - \epsilon_k(\lambda)]}_{=0} \left| \frac{d^2\varphi_k}{d\lambda^2} \right\rangle = 0 \\
 \frac{d^2\epsilon_k}{d\lambda^2} &= 2 \langle \varphi_k(\lambda) | \hat{W} - \frac{d\epsilon_k}{d\lambda} \left| \frac{d\varphi_k}{d\lambda} \right\rangle \\
 &= 2 \sum_{k'(\neq k)} \langle \varphi_k | [\hat{W} - \frac{d\epsilon_k}{d\lambda}] |\varphi_{k'}\rangle \frac{1}{\epsilon_k - \epsilon_{k'}} \langle \varphi_{k'} | [\hat{W} - \frac{d\epsilon_k}{d\lambda}] |\varphi_k\rangle \\
 &= 2 \sum_{k'(\neq k)} \frac{|\langle \varphi_k | \hat{W} | \varphi_{k'} \rangle|^2}{\epsilon_k - \epsilon_{k'}}
 \end{aligned} \tag{9.18}$$

Thus, the energy levels in second-order perturbation theory are

$$\epsilon_k + \delta\epsilon_k = \epsilon_k + \langle \phi_k | \hat{W} | \varphi_k \rangle + \sum_{k'(\neq k)} \frac{|\langle \varphi_k | \hat{W} | \varphi_{k'} \rangle|^2}{\epsilon_k - \epsilon_{k'}} \tag{9.19}$$

Let me now evaluate the matrix elements

$$\begin{aligned}
 \langle \varphi_k | \hat{W} | \varphi_{k'} \rangle &= \langle \varphi_k | \sum_j |\chi_j\rangle \gamma (R_j - \bar{R}_j) \langle \chi_j | \varphi_{k'} \rangle \\
 &= \frac{1}{N} \sum_{j=1}^N \gamma (R_j - \bar{R}_j) e^{i(k-k')j a_{\text{lat}}} \\
 \langle \varphi_k | \hat{W} | \varphi_{k+q} \rangle &= \gamma \cdot \frac{1}{N} \sum_{j=1}^N (R_j - \bar{R}_j) e^{-iq a_{\text{lat}} \cdot j}
 \end{aligned} \tag{9.20}$$

The matrix elements are thus proportional to the Fourier transform of the displacements.

Part II

Additional topics

Editor: These topics are not part of the lecture. The material was too much. Also, I am still in the process of writing material up in a more organized manner and to place it into the proper context.

Chapter 10

Phonon scattering

Editor: This chapter is yet a collection of notes. It is not in a stage ready reading

In a previous chapter, chapter 7, we discussed the description of phonons. The focus of this section was on non-interacting phonons. We arrived at phonon modes analogous to one-electron wave functions of electrons. We obtained a dispersion relation for phonons similarly to the dispersion relation of electrons. The description of electrons began with the idea of quantum particles, for which the expectation values and dynamics are expressed by one-particle wave functions. For phonons we investigated the cooperative vibration, the classical atomic displacements, which are described by a wave equation. Out of this wave-description the picture of a new particle, the phonon, emerged. There is one aspect missing for a complete particle description of phonons, namely the particle-number quantization. The particle-number quantization is a direct consequence of the quantization of the motion of the nuclei.

The quantization of classical particles is called **first quantization** and leads to a quantum theory of particles, which is equivalent to a **classical field theory**. The quantization of wave functions is called **second quantization** and leads to a **quantum field theory**.

In the following, we will study the interaction of phonons. The interaction of phonons is described as phonon-phonon scattering. The main goal of this section is to obtain the collision term of the Boltzmann equation. Apart from completing the investigation of the Boltzmann equation, it also prepares us for the study of interacting particles, which is the central subject of the next course, ΦSX: Advanced solid-state theory[2].

10.1 Sketch of the derivation of the collision term of the Boltzmann equation for phonons

Editor: This section is a copy of a part in the appendix.

Before getting into the details let me sketch the main steps ahead:

1. Set up Newton's equations of motion for the distortions $Q_\lambda(t)$.
2. Introduce **phonon amplitudes** $b_\lambda^\pm(t)$

$$Q_\lambda(t) = b_\lambda^+(t)e^{i\omega_\lambda t} + b_\lambda^-(t)e^{-i\omega_\lambda t}$$

The state can be described alternatively by the phonon amplitudes or by the **density matrix**

$$\rho_{\lambda,\lambda'}(t) = b_\lambda^+(t)b_{\lambda'}^-(t)$$

Both, phonon amplitudes and density matrix, contain the full information of trajectories. The off-diagonal elements of the density matrix describe the entanglement of the phonons.

3. Perturbation expansion in the anharmonic terms (We go to second order, which is the minimum to obtain forward- and back-reaction.) The perturbation expansion is not necessary for a derivation of the Boltzmann equation, but it ensures a simple form of the scattering operator.
4. **Initial random-phase approximation:** The initial random-phase approximation removes the off-diagonal elements from the initial density matrix.

The state is now an ensemble described by an average density matrix

$$\left\langle \rho_{\lambda,\lambda'}(t) \right\rangle = \left\langle b_{\lambda}^{+}(t)b_{\lambda'}^{-}(t) \right\rangle_{\text{initial phases}} = 0 \quad \text{for } \lambda \neq \lambda'$$

5. Long-time limit, which turns the oscillatory functions into delta functions of the frequency difference. The result is **energy conservation**. The initial random-phase approximation is required to obtain the desired form of the long-time limit.
6. **Final random-phase approximation:** The final randomization of the phases deletes the off-diagonal elements of the density matrix after the scattering event. This is the point where irreversibility is introduced.

The final random-phase approximation is, in my opinion, the critical approximation of the Boltzmann equations. It is the condition to describe the particles by their density rather than by their wave functions. The process of decoherence is likely to provide a physical mechanism for the loss of phase information.

7. Formulation of a **rate equation:** Let us combine the occupations $n_{\lambda}(t) = \rho_{\lambda,\lambda}(t)$ into a vector $\vec{n}(t)$. A rate equation gives

$$\partial_t \vec{n}(t) = -\mathbf{A}(\vec{n}(t) - \vec{n}^{eq}) \quad \Leftrightarrow \quad \vec{n}(t) = \vec{n}^{eq} + e^{-\mathbf{A}t}(\vec{n}(0) - \vec{n}^{eq})$$

The diagonal elements of the density matrix as obtained from a more rigorous theory, obey the mapping

$$\rho_{\lambda,\lambda}(t) = \rho_{\lambda,\lambda}^{eq} + \sum_{\lambda'} M_{\lambda,\lambda'}(t) (\rho_{\lambda',\lambda'}(0) - \rho_{\lambda',\lambda'}^{eq})$$

For sufficiently large times, the mapping shall be of exponential form $\mathbf{M}(t) = e^{-\mathbf{A}t}$ (assumption), that is

$$\mathbf{A}(t) = -\frac{1}{t} \ln[\mathbf{M}(t)] \quad \text{for } t > T_{decoh}$$

The resulting equation has the general form of the linearized collision term in the Boltzmann equation.

10.2 Equation of motion for the phonon amplitudes

Let us now derive the equations of motion in terms of phonon amplitudes for the anharmonic case. We start from the definition of the phonon amplitudes Eq. U.23 and use the equation of motion Eq. 7.74 for the normal coordinates $Q_n(\vec{k}, t)$.

Let me start forming the time derivative of the phonon amplitudes

$$\begin{aligned}
b_{n,\sigma}(\vec{k}) &\stackrel{\text{Eq. U.23}}{=} e^{-i\sigma\omega_n(\vec{k})t} \sqrt{\frac{\mathcal{N}}{2\hbar\omega_n(\vec{k})}} \left(\omega_n(\vec{k})Q_n(\vec{k}) - i\sigma\dot{Q}_n(\vec{k}) \right) \\
\Rightarrow i\hbar\dot{b}_{n,\sigma}(\vec{k}) &= i\hbar e^{-i\sigma\omega_n(\vec{k})t} \sqrt{\frac{\mathcal{N}}{2\hbar\omega_n(\vec{k})}} \left[-i\sigma\omega_n(\vec{k}) \left(\omega_n(\vec{k})Q_n(\vec{k}) - i\sigma\dot{Q}_n(\vec{k}) \right) + \left(\omega_n(\vec{k})\dot{Q}_n(\vec{k}) - i\sigma\ddot{Q}_n(\vec{k}) \right) \right] \\
&= i\hbar e^{-i\sigma\omega_n(\vec{k})t} \sqrt{\frac{\mathcal{N}}{2\hbar\omega_n(\vec{k})}} \left[-i\sigma \left(\omega_n^2(\vec{k})Q_n(\vec{k}) + \ddot{Q}_n(\vec{k}) \right) \right] \\
&\stackrel{\text{Eq. 7.74}}{=} \sigma\hbar e^{-i\sigma\omega_n(\vec{k})t} \sqrt{\frac{\mathcal{N}}{2\hbar\omega_n(\vec{k})}} \left[- \sum_{\vec{k}', \vec{k}'' \in \Omega_G} \sum_{l,m} \frac{1}{2} X_{n,l,m}(-\vec{k}, \vec{k}', \vec{k}'') Q_l(\vec{k}') Q_m(\vec{k}'') \right] \\
&\stackrel{\text{Eq. U.24}}{=} \sigma\hbar e^{-i\sigma\omega_n(\vec{k})t} \sqrt{\frac{\mathcal{N}}{2\hbar\omega_n(\vec{k})}} \left[- \sum_{\vec{k}', \vec{k}'' \in \Omega_G} \sum_{l,m} \frac{1}{2} X_{n,l,m}(-\vec{k}, \vec{k}', \vec{k}'') \right. \\
&\quad \times \left(\frac{\hbar}{\sqrt{2\mathcal{N}\hbar\omega_l(\vec{k}')}} \sum_{\sigma' \in \pm} b_{l,\sigma'} e^{i\sigma'\omega_n(\vec{k}')t} \right) \left(\frac{\hbar}{\sqrt{2\mathcal{N}\hbar\omega_m(\vec{k}'')}} \sum_{\sigma'' \in \pm} b_{m,\sigma''} e^{i\sigma''\omega_m(\vec{k}'')t} \right) \left. \right] \\
&= -\sigma \left[\sum_{\vec{k}', \vec{k}'' \in \Omega_G} \sum_{l,m} \frac{\mathcal{N}}{2} \left(\frac{\hbar}{2\mathcal{N}} \right)^{\frac{3}{2}} \frac{X_{n,l,m}(-\vec{k}, \vec{k}', \vec{k}'')}{\sqrt{\omega_n(\vec{k})\omega_l(\vec{k}')\omega_m(\vec{k}'')}} \right. \\
&\quad \times \left. \sum_{\sigma', \sigma'' \in \pm} b_{l,\sigma'} b_{m,\sigma''} e^{i[\sigma'\omega_n(\vec{k}') + \sigma''\omega_m(\vec{k}'') - \sigma\omega_n(\vec{k})]t} \right]
\end{aligned} \tag{10.1}$$

Editor: In the derivation above there has been a sign mistake! It is marked by the red underbrace. The correction has been carried up to this point, but no further.

EQUATION OF MOTION FOR THE PHONON AMPLITUDES

The phonon amplitudes follow the equation of motion[70]^a

$$i\hbar\dot{b}_{n,\sigma}(\vec{k}) = -\sigma \sum_{\vec{k}', \vec{k}'' \in \Omega_G} \sum_{l,m} Y_{n,l,m}(-\vec{k}, \vec{k}', \vec{k}'') \sum_{\sigma', \sigma'' \in \{+, -\}} e^{i[\sigma'\omega_l(\vec{k}') + \sigma''\omega_m(\vec{k}'') - \sigma\omega_n(\vec{k})]t} b_{l,\sigma'}(\vec{k}') b_{m,\sigma''}(\vec{k}'') \quad (10.2)$$

with

$$Y_{n,l,m}(\vec{k}, \vec{k}', \vec{k}'') = \frac{\mathcal{N}}{2} \left(\frac{\hbar}{2\mathcal{N}} \right)^{\frac{3}{2}} \frac{X_{n,l,m}(\vec{k}, \vec{k}', \vec{k}'')}{\sqrt{\omega_n(\vec{k})\omega_l(\vec{k}')\omega_m(\vec{k}'')}} \quad (10.3)$$

where X is given by Eq. 7.66 on p. 230.

$$X_{l,m,n}(\vec{k}, \vec{k}', \vec{k}'') \stackrel{\text{def}}{=} \left(\sum_{\vec{G}} \delta_{\vec{k} + \vec{k}' + \vec{k}'' - \vec{G}} \right) \times \sum_{\alpha, \beta, \gamma} \left[\sum_{\vec{t}, \vec{t}', \vec{t}''} \frac{W_{\alpha, \vec{0}, \beta, \vec{t}, \gamma, \vec{t}''}}{\sqrt{M_\alpha M_\beta M_\gamma}} e^{i\vec{k}'\vec{t}} e^{i\vec{k}''\vec{t}''} \right] U_{\alpha,l}(\vec{k}) U_{\beta,m}(\vec{k}') U_{\gamma,n}(\vec{k}'') \quad (10.4)$$

The requirement that the displacements are real-valued translates into

$$b_{n,\sigma}(\vec{k}) \stackrel{\text{Eq. U.25}}{=} \left(b_{n,-\sigma}(-\vec{k}) \right)^* \quad (10.5)$$

^aEq.20 of ref. [70]. Compare also with Eq.1.2 of Brout and Prigogine[71]. (The paper of Brout and Prigogine is one in a sequence [72, 73, 74, 75, 71]) Note that the frequencies occur with opposite sign. The different sign can be traced to the notation adopted by Ziman.[76]

An interesting side aspect is that start from a second-order differential equation for the displacements $\delta R_{\alpha,t}$ and we arrive at a first-order differential equation of a complex-valued variable $b(t)$. Eq. 10.2 has some analogy with the Schrödinger equation.

$$i\hbar\dot{\psi}(\vec{r}, t) = \hat{H}\psi(\vec{r}, t) \quad (10.6)$$

The difference is that the Schrödinger equation is a linear equation, while the equation of motion for the phonon amplitudes is nonlinear. The non-linearity is a consequence of the interaction, that is, scattering between particles.

Two further aspects of Eq. 10.2 are surprising: Firstly, the lack of a an energy term describing the harmonic energy contribution and, secondly, the appearance of the phase factors. They are due to the classical pendant of the **interaction picture** of quantum mechanics:¹ The propagator of the non-interacting system is incorporated into the dynamical variable, which gets the non-interacting energy term out of the picture. Let me undo this transformation and define a kind of phonon amplitude without the phase factor.

$$B_{n,\sigma}(\vec{k}, t) \stackrel{\text{def}}{=} b_{n,\sigma}(\vec{k}, t) e^{i\sigma\omega_n(\vec{k})t} \quad (10.7)$$

¹The interaction picture with wave functions $|\psi_I(t)\rangle$ and operators $\hat{A}_I(t)$ eliminates the unperturbed Hamiltonian \hat{h} from the Schrödinger equation. This is suitable for a perturbation expansion in \hat{W} . The "normal representation is the Schrödinger picture indicated by a subscript S . One begins the argument with the propagator $\hat{U}_0(t,0)$ of the

In terms of the variables $B_{n,\sigma}(\vec{k})$, Eq. 10.2 obtains the form

$$i\hbar\dot{B}_{n,\sigma}(\vec{k}) \stackrel{\text{Eq. 10.2}}{=} -\sigma\hbar\omega_n(\vec{k})B_{n,\sigma}(\vec{k}) - \sigma \sum_{\vec{k}', \vec{k}'' \in \Omega_G} \sum_{l,m} Y_{n,l,m}(-\vec{k}, \vec{k}', \vec{k}'') \sum_{\sigma', \sigma'' \in \{+,-\}} B_{l,\sigma'}(\vec{k}') B_{m,\sigma''}(\vec{k}'') \quad (10.8)$$

Editor: The following is only a sketch: The connection to antiparticles needs to be established. When we interpret the harmonic term as the energy analogous to a Schrödinger equation $i\hbar\dot{\psi}(\vec{r}, t) = \hat{H}\psi(\vec{r}, t)$. We recognize that there are positive and negative energies $\sigma\hbar\omega_n(\vec{k})$. The corresponding terms could be attributed to particles and antiparticles. One does not speak of phonons and antiphonons, because they cannot exist independently. Once the phonon amplitudes $\{b_{n,-}(\vec{k})\}$ are known, the requirement of real-valued displacements $b_{n,+}(-\vec{k}) = (b_{n,-}(\vec{k}))^*$ determines the amplitudes of the antiphonons $\{b_{n,+}(\vec{k})\}$.

10.3 Momentum and energy conservation

10.3.1 Momentum conservation

Important is the selection rule via the factor

$$\left(\sum_{\vec{G}} \delta_{\vec{k} + \vec{k}' + \vec{k}'' - \vec{G}} \right) \quad (10.9)$$

in Eq. 10.4. This term vanishes unless the wave vectors obey a selection rule. This selection rule implies that phonons can scatter only, if they obey **momentum conservation**. Momentum conservation is a result of the lattice translation symmetry. The momentum $\hbar\vec{G}$ is a momentum that is transferred to the crystal as a whole.

For each pair of wave vectors \vec{k}', \vec{k}'' in the reciprocal unit cell, there is exactly one reciprocal lattice vector \vec{G} of the crystal, which selects a third wave vector \vec{k} in the first reciprocal unit cell.

It is interesting how the momentum conservation emerged out of the crystal symmetry. Note, that this momentum is not related to the momenta of the atoms. The momentum of a mode has the form²

$$\vec{P}_n(\vec{k}, t) = \sum_{\alpha, \vec{r}} M_{\alpha, \vec{r}} \delta \dot{R}_{\alpha, \vec{r}} = \sum_{\alpha, \vec{r}} \sqrt{M_{\alpha}} U_{\alpha, n} e^{-i\vec{k}\vec{r}} \dot{Q}_n(\vec{r}) = \mathcal{N} \delta_{\vec{k}, \vec{0}} \left(\sum_{\alpha} \sqrt{M_{\alpha}} U_{\alpha, n} \right) \dot{Q}_n(\vec{r}) \quad (10.10)$$

unperturbed system.

$$\begin{aligned} i\hbar\partial_t \hat{U}_0(t, 0) &= \hat{h}_S \hat{U}_0(t, 0) \rightsquigarrow \hat{U}_0(t, 0) \\ |\psi_I(t)\rangle &\stackrel{\text{def}}{=} \hat{U}_0^{-1}(t, 0) |\psi_S(t)\rangle \Leftrightarrow |\psi_S(t)\rangle = \hat{U}_0(t, 0) |\psi_I(t)\rangle \\ \hat{A}_I(t) &\stackrel{\text{def}}{=} \hat{U}_0^{-1}(t, 0) \hat{A}_S \hat{U}_0(t, 0) \\ i\hbar\partial_t |\psi_S(t)\rangle &= (\hat{h}_S + \hat{W}_S) |\psi_S(t)\rangle \\ \Rightarrow i\hbar\partial_t \underbrace{\hat{U}_0(t, 0) |\psi_I(t)\rangle}_{|\psi_S(t)\rangle} &= \underbrace{(i\hbar\partial_t \hat{U}_0(t, 0))}_{\hat{h}_S \hat{U}_0(t, 0)} |\psi_I(t)\rangle + \hat{U}_0(t, 0) i\hbar\partial_t |\psi_I(t)\rangle \stackrel{!}{=} (\hat{h}_S + \hat{W}_S) \underbrace{\hat{U}_0(t, 0) |\psi_I(t)\rangle}_{|\psi_S(t)\rangle} \\ \Rightarrow i\hbar\partial_t |\psi_I(t)\rangle &= \underbrace{\hat{U}_0^{-1}(t, 0) \hat{W}_S \hat{U}_0(t, 0)}_{\hat{W}_I} |\psi_I(t)\rangle = \hat{W}_I |\psi_I(t)\rangle \end{aligned}$$

The oscillations of the wave function in the interaction picture are much slower than those of the Schrödinger picture. The wave functions of the interaction picture are constants of motion in the absence of a perturbation.

Similarly, the contribution of the harmonic energy $-\sigma\hbar\omega$ is eliminated from Eq. 10.8 to Eq. 10.2 by including the unperturbed (harmonic) propagator $e^{-i\sigma\omega t}$ in the phonon amplitudes $B_{n,\sigma}(t)$.

²Without restriction of generality, we consider here a complex-valued partial wave.

Thus, only the modes with $\vec{k} = 0$ can have a nonzero true momentum, while the phonons with a finite wave vector \vec{k} have vanishing true momentum $\vec{P}_n(\vec{k})$.

This is a nice illustration that the momentum conservation follows from a symmetry, and not from some god-given fundamental momentum conservation.

Normal and umklapp processes: A scattering event where the crystal momentum \vec{G} in Eq. 10.9 vanishes is called a **normal process**, while one with a finite crystal momentum in Eq. 10.9 is called an **umklapp process**. The term “umklapp process” has been coined by Peierls implying that the total momentum of the phonons in the scattering event may “flip over”. See also Fig. 10.1 (same as Fig. 7.4 on p. 230.)

The umklapp processes are important to bring a system into thermal equilibrium.

When umklapp processes are excluded, the total momentum of the phonons is conserved and can not relax to its equilibrium value, namely zero. Umklapp processes exchange momentum of phonons with the rigid lattice, which opens the required relaxation channels. Umklapp processes are effectively suppressed at low temperatures, because the wave vector of most phonons is too small to allow combinations that add up to a reciprocal lattice vector.

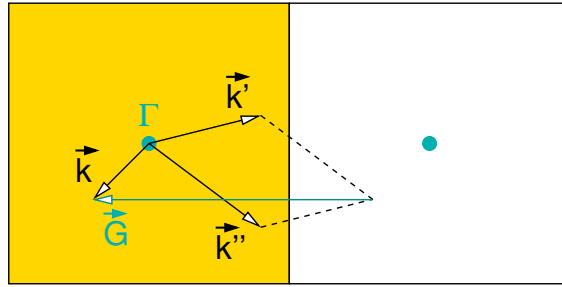


Fig. 10.1: Sketch to show that three wave vectors in the Brillouin zone can add up to a reciprocal lattice vector $\vec{G} = \vec{k} - \vec{k}' - \vec{k}''$. Scattering processes, which involve reciprocal lattice vectors \vec{G} to conserve momentum, are called **umklapp processes**.

10.3.2 Energy conservation

The factor

$$e^{i[\sigma'\omega_l(\vec{k}') + \sigma''\omega_m(\vec{k}'') - \sigma\omega_n(\vec{k})]t} \tag{10.11}$$

in Eq. 10.2 is responsible for energy conservation. If the frequencies do not add up to zero, this factor oscillates rapidly in time, so that the net effect on the phonon amplitude nearly cancels. If the frequencies add up to zero, i.e. $\sigma\omega_n(\vec{k}) = \sigma'\omega_l(\vec{k}') + \sigma''\omega_m(\vec{k}'')$ the factor is a constant, so that the oscillations are in resonance and the response has time to build up.

At this point it is a hand-waving argument. In the following, we will obtain a more precise meaning of it.

10.4 Scattering

10.4.1 Compact notation

For the following discussion it will be convenient to use a more compressed notation, namely to integrate the mode index n , the wave vector \vec{k} and the index σ into a single variable $\lambda \stackrel{\text{def}}{=} (\vec{k}_\lambda, n_\lambda, \sigma_\lambda)$.

The phonon amplitudes in the extended notation have been defined in terms of normal coordinates in Eq. U.23 on p. 562. The choice of the compact notation aims at simplifying the equation of motion Eq. 10.2 on p. 330 for the phonon amplitudes.

COMPACT NOTATION FOR THE PHONON AMPLITUDES

$$\begin{aligned}
 \lambda &\stackrel{\text{def}}{=} (\vec{k}_\lambda, n_\lambda, \sigma_\lambda) \\
 -\lambda &\stackrel{\text{def}}{=} (-\vec{k}_\lambda, n_\lambda, -\sigma_\lambda) \\
 b_\lambda &\stackrel{\text{def}}{=} b_{n_\lambda, \sigma_\lambda}(\vec{k}_\lambda) \\
 \omega_\lambda &\stackrel{\text{def}}{=} \sigma_\lambda \omega_{n_\lambda}(\vec{k}_\lambda) \\
 Y_{\lambda, \lambda', \lambda''} &\stackrel{\text{def}}{=} -\sigma_\lambda Y_{n_\lambda, n_{\lambda'}, n_{\lambda''}}(\vec{k}_\lambda, \vec{k}_{\lambda'}, \vec{k}_{\lambda''}) \\
 \Rightarrow Y_{-\lambda, \lambda', \lambda''} &= \sigma_\lambda Y_{n_\lambda, n_{\lambda'}, n_{\lambda''}}(-\vec{k}_\lambda, \vec{k}_{\lambda'}, \vec{k}_{\lambda''}) \\
 U_{\alpha, \lambda} &\stackrel{\text{def}}{=} U_{\alpha, n_\lambda}(\vec{k}_\lambda)
 \end{aligned} \tag{10.12}$$

Editor: change the definition from $Y = -\sigma Y$ to $Y = +\sigma Y$

Notice the definition of the “negative index” $-\lambda$.

Let me now list a few properties in the compact notation, that we may use later on

$$\begin{aligned}
 U_{\alpha, -\lambda} &\stackrel{\text{Eq. 7.59}}{=} U_{\alpha, \lambda}^* \\
 Y_{-\lambda, -\lambda', -\lambda''} &\stackrel{\text{Eq. 10.3}}{=} -Y_{\lambda, \lambda', \lambda''}^* \\
 \sigma_1 Y_{\lambda_1, \lambda_2, \lambda_3} &\stackrel{\text{Eq. 10.3}}{=} \sigma_2 Y_{\lambda_2, \lambda_3, \lambda_1} = \sigma_3 Y_{\lambda_3, \lambda_1, \lambda_2} = \sigma_3 Y_{\lambda_3, \lambda_2, \lambda_1} = \sigma_2 Y_{\lambda_2, \lambda_1, \lambda_3} = \sigma_1 Y_{\lambda_1, \lambda_3, \lambda_2} \\
 \omega_\lambda &\stackrel{\text{Eq. 7.58}}{=} -\omega(-\lambda)
 \end{aligned} \tag{10.13}$$

The displacements in the new notation are

$$\delta R_{\alpha, \vec{r}}(t) \stackrel{\text{Eq. U.27}}{=} \sum_{\lambda} \frac{1}{\sqrt{M_\alpha}} U_{\alpha, \lambda} \sqrt{\frac{\hbar}{2N\hbar|\omega_\lambda|}} b_\lambda(t) e^{i[\vec{k}_\lambda \vec{r} + \omega_\lambda t]} \tag{10.14}$$

Like other summations, the λ -sum includes a sum over all (positive) band indices, the two values of σ , and the k -point sum. The terms with λ and $-\lambda$ add up to a real number.

The total energy, including the kinetic energy, is

$$E = \underbrace{\frac{1}{2} \sum_{\lambda} \sigma_\lambda \hbar \omega_\lambda b_{+\lambda} b_{-\lambda}}_{E_{kin} + E_{harm} \text{ Eq. U.33}} + \underbrace{\sum_{\lambda, \lambda', \lambda''} \frac{2}{3!} \frac{-\sigma_\lambda Y_{\lambda, \lambda', \lambda''}}{\sqrt{|\omega_\lambda \omega_{\lambda'} \omega_{\lambda''}|}} b_\lambda b_{\lambda'} b_{\lambda''} e^{i[\omega_\lambda + \omega_{\lambda'} + \omega_{\lambda''}]t}}_{E_{anharm} \text{ Eq. 7.134}} \tag{10.15}$$

The factor 1/2 in the harmonic term accounts for the fact that the sum contains each pair $(\lambda, -\lambda)$ twice.

With these definitions, the equations of motion Eq. 10.2 obtain the form

EQUATION OF MOTION FOR PHONON AMPLITUDES IN THE COMPACT NOTATION

$$i\hbar\dot{b}_\lambda \stackrel{\text{Eq. 10.2}}{=} - \sum_{\lambda', \lambda''} Y_{-\lambda, \lambda', \lambda''} e^{i[\omega_{\lambda'} + \omega_{\lambda''} + \omega_{-\lambda}]t} b_{\lambda'} b_{\lambda''} \quad (10.16)$$

The requirement that the displacements are real-valued translates into

$$b_\lambda \stackrel{\text{Eq. U.25}}{=} (b_{-\lambda})^* \quad (10.17)$$

10.4.2 Perturbation theory

Now, we can integrate the equation of motion. First we bring the equation of motion Eq. 10.16 into its integral form

$$b_\lambda(t) \stackrel{\text{Eq. 10.16}}{=} \frac{i}{\hbar} \int_0^t dt' \sum_{\lambda', \lambda''} \gamma Y_{-\lambda, \lambda', \lambda''} e^{i[\omega_{\lambda'} + \omega_{\lambda''} + \omega_{-\lambda}]t'} b_{\lambda'}(t') b_{\lambda''}(t') \quad (10.18)$$

Let us tackle this problem by perturbation theory, that is, we scale the scattering matrix by a scale factor γ and expand the solutions in orders of γ .

$$b_\lambda(t) = \sum_{n=0}^{\infty} \gamma^n b_\lambda^{(n)}(t) \quad (10.19)$$

We insert the Taylor expansion in to the expression for the phonon amplitudes Eq. 10.18, sort the terms according to powers of γ . Each order of γ yields an equation connecting the expansion coefficients for the phonon amplitudes. We use them to calculate the expansion coefficients sequentially. Finally, the scale factor γ in the perturbation expansion is set to unity.

The key to the perturbation expansion is the Taylor expansion. A Taylor expansion can have a finite convergence radius. Beyond this convergence radius, the Taylor expansion has no relation to the correct result, even if a truncated Taylor expansion provides a defined value. The convergence radius is often related by a singularity or another point where the result is not analytic.

Editor: (1) Describe that it does not help to go away from the singularity. (2) Describe that it helps to move the expansion center

Phonon amplitudes in zeroth order

In the absence of scattering, the phonon amplitudes do not change and they are related directly to the initial conditions.

$$b_\lambda^{(0)}(t) = b_\lambda^{(0)}(0) =: b_\lambda^{(0)} \quad (10.20)$$

Thus, we can drop the time argument from the phonon amplitudes in zeroth order.

Phonon amplitudes in first order

The phonon amplitudes in first order are

$$b_\lambda^{(1)}(t) = \frac{i}{\hbar} \sum_{\mu, \mu'} Y_{-\lambda, \mu, \mu'} \underbrace{\left[\int_0^t dt' e^{i[\omega_\mu + \omega_{\mu'} + \omega_{-\lambda}]t'} \right]}_{tF^{(1)}([\omega_\mu + \omega_{\mu'} + \omega_{-\lambda}]t)} b_\mu^{(0)} b_{\mu'}^{(0)} \quad (10.21)$$

We will see that two the time dependence enters via two functions,

$$F^{(1)}(\omega t) \stackrel{\text{def}}{=} \frac{1}{t} \int_0^t dt' e^{i\omega t'} \quad (10.22)$$

and

$$F^{(2)}(\omega t, \omega' t) \stackrel{\text{def}}{=} \frac{1}{t^2} \int_0^t dt' e^{i\omega t'} \int_0^{t'} dt'' e^{i\omega' t''} \quad (10.23)$$

We will discuss their properties later in section 10.4.6, where we will see that they lead to an effective energy conservation law for the phonon scattering events.

Phonon amplitudes in second order

The phonon amplitudes in second order are³

$$\begin{aligned} b_\lambda^{(2)}(t) &= \frac{2i}{\hbar} \int_0^t dt' \sum_{\mu, \mu'} Y_{-\lambda, \mu, \mu'} e^{i[\omega_\mu + \omega_{\mu'} + \omega_{-\lambda}]t'} b_\mu^{(0)} b_{\mu'}^{(1)}(t) \\ &= \frac{2i}{\hbar} \int_0^t dt' \sum_{\mu, \mu'} Y_{-\lambda, \mu, \mu'} e^{i[\omega_\mu + \omega_{\mu'} + \omega_{-\lambda}]t'} b_\mu^{(0)} \left\{ \frac{i}{\hbar} \sum_{\nu, \nu'} Y_{-\mu', \nu, \nu'} \left[\int_0^{t'} dt'' e^{i[\omega_\nu + \omega_{\nu'} + \omega_{-\mu'}]t''} \right] b_\nu^{(0)} b_{\nu'}^{(0)} \right\} \\ &= -\frac{2}{\hbar^2} \sum_{\mu, \mu', \nu, \nu'} Y_{-\lambda, \mu, \mu'} Y_{-\mu', \nu, \nu'} \underbrace{\left[\int_0^t dt' e^{i[\omega_\mu + \omega_{\mu'} + \omega_{-\lambda}]t'} \int_0^{t'} dt'' e^{i[\omega_\nu + \omega_{\nu'} + \omega_{-\mu'}]t''} \right]}_{t^2 F^{(2)}([\omega_\mu + \omega_{\mu'} + \omega_{-\lambda}]t, [\omega_\nu + \omega_{\nu'} + \omega_{-\mu'}]t)} b_\mu^{(0)} b_\nu^{(0)} b_{\nu'}^{(0)} \end{aligned} \quad (10.24)$$

The result is a product of two or three initial phonon amplitudes, a frequency-dependent term from the time integration and a product of the anharmonic terms. Let us deal with those contributions one-by-one in the following sections.

10.4.3 Density matrix

Our goal is to predict the time evolution of the phonon numbers. This will allow us to understand how heat, carried by phonons, is redistributed inside the material. For this purpose the relevant quantity is the number of phonons. The phonon number in turn is related to products of two phonon amplitudes.

$$n_\lambda(t) = b_\lambda^*(t) b_\lambda(t) = b_{-\lambda}(t) b_\lambda(t) \quad (10.25)$$

Therefore, we evaluate the one-phonon-reduced density matrix

$$\rho_{\lambda, \lambda'}(t) \stackrel{\text{def}}{=} b_\lambda(t) b_{\lambda'}(t) \quad (10.26)$$

for a given initial state after a certain time interval.

Up to second order in the anharmonicity, the density matrix is

$$\begin{aligned} \rho_{\lambda, \lambda'}(t) &= \sum_{n=0}^{\infty} \rho_{\lambda, \lambda'}^{(n)}(t) \\ &= b_\lambda^{(0)}(t) b_{\lambda'}^{(0)}(t) \\ &\quad + b_\lambda^{(1)}(t) b_{\lambda'}^{(0)}(t) + b_\lambda^{(0)}(t) b_{\lambda'}^{(1)}(t) \\ &\quad + b_\lambda^{(2)}(t) b_{\lambda'}^{(0)}(t) + b_\lambda^{(1)}(t) b_{\lambda'}^{(1)}(t) + b_\lambda^{(0)}(t) b_{\lambda'}^{(2)}(t) + \dots \end{aligned} \quad (10.27)$$

³compare Eq. 3.1 of Brout and Prigogine[71].

In zeroth order, we obtain the initial value,

$$\rho_{\lambda,\lambda'}^{(0)}(t) \stackrel{\text{Eq. 10.27}}{=} b_{\lambda}^{(0)} b_{\lambda'}^{(0)} \quad (10.28)$$

which does not depend on time.

In first order, we obtain

$$\begin{aligned} \rho_{\lambda,\lambda'}^{(1)}(t) &\stackrel{\text{Eq. 10.27}}{=} b_{\lambda}^{(0)} b_{\lambda'}^{(1)}(t) + b_{\lambda}^{(1)}(t) b_{\lambda'}^{(0)} \\ &\stackrel{\text{Eq. 10.21}}{=} \frac{i}{\hbar} \sum_{\mu,\mu'} Y_{-\lambda,\mu,\mu'} t F^{(1)}([\omega_{\mu} + \omega_{\mu'} + \omega_{-\lambda}]t) b_{\mu}^{(0)} b_{\mu'}^{(0)} b_{\lambda'}^{(0)} + (\lambda \leftrightarrow \lambda') \end{aligned} \quad (10.29)$$

The term denoted with $(\lambda \leftrightarrow \lambda')$ indicates that the same expression as above needs to be added with the two indices interchanged.

For the second order, we obtain

$$\begin{aligned} \rho_{\lambda,\lambda'}^{(2)}(t) &\stackrel{\text{Eq. 10.27}}{=} b_{\lambda}^{(2)}(t) b_{\lambda'}^{(0)}(t) + b_{\lambda}^{(1)}(t) b_{\lambda'}^{(1)}(t) + b_{\lambda}^{(0)}(t) b_{\lambda'}^{(2)}(t) \\ &= \underbrace{-\frac{2}{\hbar^2} \sum_{\mu,\mu',\nu,\nu'} Y_{-\lambda,\mu,\mu'} Y_{-\mu',\nu,\nu'} \left(t^2 F^{(2)}([\omega_{\mu} + \omega_{\mu'} + \omega_{-\lambda}]t, [\omega_{\nu} + \omega_{\nu'} + \omega_{-\mu'}]t) \right)}_{b_{\lambda}^{(2)}(t) \text{ from Eq. 10.24}} b_{\mu}^{(0)} b_{\nu}^{(0)} b_{\mu'}^{(0)} b_{\lambda'}^{(0)} \\ &+ \underbrace{\frac{1}{2} \left(\frac{i}{\hbar} \right)^2 \sum_{\mu,\mu'} \sum_{\nu,\nu'} Y_{-\lambda,\mu,\mu'} Y_{-\lambda',\nu,\nu'} \left(t^2 F^{(1)}([\omega_{\mu} + \omega_{\mu'} + \omega_{-\lambda}]t) F^{(1)}([\omega_{\nu} + \omega_{\nu'} + \omega_{-\lambda'}]t) \right)}_{\frac{1}{2} b_{\lambda}^{(1)}(t) b_{\lambda'}^{(1)}(t) \text{ Eq. 10.21}} b_{\mu}^{(0)} b_{\mu'}^{(0)} b_{\nu}^{(0)} b_{\nu'}^{(0)} \\ &+ (\lambda \leftrightarrow \lambda') \end{aligned} \quad (10.30)$$

The term denoted with $(\lambda \leftrightarrow \lambda')$ indicates that the both terms of the expression as above need to be added with the two indices interchanged.

10.4.4 Initial random-phase approximation

The initial conditions for a trajectory, that is positions and velocities of all atoms are uniquely determined by the set of phonon amplitudes. The phonon amplitude $b_{\lambda} = \sqrt{n_{\lambda}} e^{i\phi_{\lambda}}$ consists of an absolute value, which reflects the phonon number $n_{\lambda} = b_{\lambda}^* b_{\lambda}$, and a phase ϕ_{λ} .

If one is only interested in the phonon number, it seems appropriate to average over all phases ϕ_{λ} of the initial state. This is the so-called **initial random-phase approximation** [70].

Not all phases are independent. The phases ϕ_{λ} of b_{λ} and $b_{-\lambda}$ are opposite, because the phonon amplitudes b_{λ} and $b_{-\lambda}$ are complex conjugates of each other.⁴ States with opposite indices λ have opposite phases.⁵

$$\phi_{\lambda} = -\phi_{-\lambda} \quad \Leftrightarrow \quad \phi_{n_{\lambda}}(\vec{k}_{\lambda}) = -\phi_{n_{\lambda}}(-\vec{k}_{\lambda}) \quad (10.31)$$

When we average over all initial phases, the products with independent phases in two terms average to zero, and only products that can be decomposed into **contractions**, that is pairs with canceling phases, i.e. opposite indices, contribute to a final result.

⁴The fact $b_{\lambda} = -b_{-\lambda}^*$ is a consequence of the fact that displacements are real. See Eq. U.8 and Eq. U.18

⁵The compact notation is described in section 10.4.1 on p. 332.

We obtain

$$\begin{aligned}
 \langle b_{\lambda}^{(0)} b_{\lambda'}^{(0)} \rangle_{\vec{\phi}} &= \delta_{\lambda+\lambda'} n_{\lambda}^{(0)} \\
 \langle b_{\lambda}^{(0)} b_{\lambda'}^{(0)} b_{\lambda''}^{(0)} \rangle_{\vec{\phi}} &= 0 \\
 \langle b_{\lambda}^{(0)} b_{\lambda'}^{(0)} b_{\lambda''}^{(0)} b_{\lambda'''}^{(0)} \rangle_{\vec{\phi}} &= \underbrace{\delta_{\lambda+\lambda'} \delta_{\lambda''+\lambda'''} (1 - \delta_{\lambda+\lambda'''})}_{(a,-a,b,-b)-(a,-a,a,-a)} n_{\lambda}^{(0)} n_{\lambda''}^{(0)} \\
 &\quad + \underbrace{\delta_{\lambda+\lambda''} \delta_{\lambda'+\lambda'''} (1 - \delta_{\lambda+\lambda'})}_{(a,b,-a,-b)-(a,-a,-a)} n_{\lambda}^{(0)} n_{\lambda'}^{(0)} \\
 &\quad + \underbrace{\delta_{\lambda+\lambda'''} \delta_{\lambda'+\lambda''} (1 - \delta_{\lambda+\lambda''})}_{(a,b,-b,-a)-(a,a,-a,-a)} n_{\lambda}^{(0)} n_{\lambda'}^{(0)} \tag{10.32}
 \end{aligned}$$

The terms connected to the Kronecker deltas are the **double-counting correction**. Without them we would count certain terms twice. Let me explain how they come about: The term with four amplitudes can be contracted in three possible ways as indicated in the following sketch:

$$\begin{array}{ccc}
 \begin{array}{c} \overbrace{(\lambda, \lambda', \lambda'', \lambda''')} \\ \underbrace{(a, -a, b, -b)} \\ \underbrace{(a, -a, a, -a)}_{(A)\text{-delete}} \end{array} & \text{and} & \begin{array}{c} \overbrace{(\lambda, \lambda', \lambda'', \lambda''')} \\ \underbrace{(a, -a, -a, a)}_{(B)} \end{array} \\
 \begin{array}{c} \overbrace{(\lambda, \lambda', \lambda'', \lambda''')} \\ \underbrace{(a, b, -a, -b)} \\ \underbrace{(a, a, -a, -a)}_{(C)} \end{array} & \text{and} & \begin{array}{c} \overbrace{(\lambda, \lambda', \lambda'', \lambda''')} \\ \underbrace{(a, b, -b, -a)} \\ \underbrace{(a, -a, -a, a)}_{(B)\text{-delete}} \end{array} \\
 \begin{array}{c} \overbrace{(\lambda, \lambda', \lambda'', \lambda''')} \\ \underbrace{(a, b, -b, -a)} \\ \underbrace{(a, a, -a, -a)}_{(C)\text{-delete}} \end{array} & \text{and} & \begin{array}{c} \overbrace{(\lambda, \lambda', \lambda'', \lambda''')} \\ \underbrace{(a, b, -b, -a)} \\ \underbrace{(a, -a, a, -a)}_{(A)} \end{array}
 \end{array}$$

connect the first amplitude to any of the three remaining ones and pair the remaining two. This gives three different possibilities, namely $(a, -a, b, -b)$, $(a, b, -a, -b)$, and $(a, b, -b, -a)$. If there are four phonons with the same “absolute index” $|a|$, that is, two equal phonons and two opposite ones such as $(a, a, -a, -a)$, $(a, -a, a, -a)$, and $(a, -a, -a, a)$, they occur each in two of the three terms considered so far $(a, a, -a, -a) \in \{(a, b, -a, -b), (a, b, -b, -a)\}$, $(a, -a, a, -a) \in \{(a, -a, b, -b), (a, b, -b, -a)\}$, and $(a, -a, -a, a) \in \{(a, -a, b, -b), (a, b, -a, -b)\}$. Thus, they are accounted twice, so that one needs to be removed again. We choose to integrate $(a, -a, a, -a)$ into the pattern $(a, -a, b, -b)$, $(a, -a, -a, a)$ into $(a, b, -a, -b)$ and $(a, a, -a, -a)$ into $(a, b, -b, -a)$.

We can convince ourselves of the need to take the double counting into account. For that purpose we consider a specific example, namely

$$\begin{aligned}
 \langle b_a^{(0)} b_{-a}^{(0)} b_a^{(0)} b_{-a}^{(0)} \rangle_{\vec{\phi}} &\stackrel{\text{Eq. 10.32}}{=} \underbrace{\delta_{a-a} \delta_{a-a}}_{=1} \underbrace{(1 - \delta_{a-a})}_{=0} n_a^{(0)} n_a^{(0)} + \underbrace{\delta_{a+a} \delta_{-a-a}}_{=0} \underbrace{(1 - \delta_{a-a})}_{=0} n_a^{(0)} n_{-a}^{(0)} \\
 &\quad + \underbrace{\delta_{a-a} \delta_{-a+a}}_{=1} \underbrace{(1 - \delta_{a+a})}_{=1} n_a^{(0)} n_{-a}^{(0)} = n_a^{(0)} n_a^{(0)} \tag{10.33}
 \end{aligned}$$

Without the double-counting correction, an additional, erroneous factor two would have occurred.

Eq. 10.32 shows that the random-phase approximation eliminates the first order terms for the density matrix Eq. 10.27.

In the following, I indicate the *initial* random-phase approximation by a subscript $\vec{\phi}_i$ in order to discriminate the symbols from those with an initial and a final random phase approximation, which will be denoted by two sets of phases $\vec{\phi}_i, \vec{\phi}_f$.

With the initial random-phase approximation, the second-order term Eq. 10.30 of the density matrix reduces to⁶

$$\begin{aligned}
\left\langle \rho_{\lambda, \lambda'}^{(2)}(t) \right\rangle_{\bar{\phi}_i} &\stackrel{\text{Eq. 10.30}}{=} -\frac{2}{\hbar^2} \sum_{\mu, \mu', \nu, \nu'} Y_{-\lambda, \mu, \mu'} Y_{-\mu', \nu, \nu'} t^2 F^{(2)}([\omega_\mu + \omega_{\mu'} + \omega_{-\lambda}]t, [\omega_\nu + \omega_{\nu'} + \omega_{-\mu'}]t) \\
&\quad \times \left\langle b_\mu^{(0)} b_\nu^{(0)} b_{\nu'}^{(0)} b_{\lambda'}^{(0)} \right\rangle_{\bar{\phi}_i} \\
&+ \frac{1}{2} \left(\frac{i}{\hbar} \right)^2 \sum_{\mu, \mu'} \sum_{\nu, \nu'} Y_{-\lambda, \mu, \mu'} Y_{-\lambda, \nu, \nu'} t^2 F^{(1)}([\omega_\mu + \omega_{\mu'} + \omega_{-\lambda}]t) F^{(1)}([\omega_\nu + \omega_{\nu'} + \omega_{-\lambda}]t) \\
&\quad \times \left\langle b_\mu^{(0)} b_{\mu'}^{(0)} b_\nu^{(0)} b_{\nu'}^{(0)} \right\rangle_{\bar{\phi}_i} \\
&+ (\lambda \leftrightarrow \lambda') \\
&\stackrel{\text{Eq. 10.32}}{=} -\frac{2}{\hbar^2} \sum_{\zeta, \mu'} Y_{-\lambda, \zeta, \mu'} Y_{-\mu', -\zeta, -\lambda'} t^2 F^{(2)}([\omega_\zeta + \omega_{\mu'} + \omega_{-\lambda}]t, [\omega_{-\zeta} + \omega_{-\lambda'} + \omega_{-\mu'}]t) \\
&\quad \times \left(1 - \delta_{\zeta + \lambda'} \right) n_\zeta^{(0)} n_{\lambda'}^{(0)} \quad \leftarrow \boxed{\text{(A): } (\mu, \nu, \nu', \lambda') \rightarrow (\zeta, -\zeta, -\lambda', \lambda')} \\
&- \frac{2}{\hbar^2} \sum_{\zeta, \mu'} Y_{-\lambda, \zeta, \mu'} Y_{-\mu', -\lambda', -\zeta} t^2 F^{(2)}([\omega_\zeta + \omega_{\mu'} + \omega_{-\lambda}]t, [\omega_{-\lambda'} + \omega_{-\zeta} + \omega_{-\mu'}]t) \\
&\quad \times \left(1 - \delta_{\zeta - \lambda'} \right) n_\zeta^{(0)} n_{\lambda'}^{(0)} \quad \leftarrow \boxed{\text{(B): } (\mu, \nu, \nu', \lambda') \rightarrow (\zeta, -\lambda', -\zeta, \lambda')} \\
&- \frac{2}{\hbar^2} \sum_{\zeta, \mu'} Y_{-\lambda, -\lambda', \mu'} Y_{-\mu', \zeta, -\zeta} t^2 F^{(2)}([\omega_{-\lambda'} + \omega_{\mu'} - \omega_\lambda]t, [\underbrace{\omega_\zeta + \omega_{-\zeta} - \omega_{\mu'}}_{=0}]t) \\
&\quad \times \left(1 - \delta_{\zeta + \lambda'} \right) n_\zeta^{(0)} n_{\lambda'}^{(0)} \quad \leftarrow \boxed{\text{(C): } (\mu, \nu, \nu', \lambda') \rightarrow (-\lambda', \zeta, -\zeta, \lambda')} \\
&\text{-----} \\
&- \frac{1}{2} \frac{1}{\hbar^2} \sum_{\zeta, \zeta'} Y_{-\lambda, \zeta, -\zeta} Y_{-\lambda', \zeta', -\zeta'} t^2 F^{(1)}([\underbrace{\omega_\zeta + \omega_{-\zeta} - \omega_\lambda}_{=0}]t) F^{(1)}([\underbrace{\omega_{\zeta'} + \omega_{-\zeta'} - \omega_{\lambda'}}_{=0}]t) \\
&\quad \times \left(1 - \delta_{\zeta - \zeta'} \right) n_\zeta^{(0)} n_{\zeta'}^{(0)} \quad \leftarrow \boxed{\text{(D): } (\mu, \mu', \nu, \nu') \rightarrow (\zeta, -\zeta, \zeta', -\zeta')} \\
&- \frac{1}{2} \frac{1}{\hbar^2} \sum_{\zeta, \zeta'} Y_{-\lambda, \zeta, \zeta'} Y_{-\lambda', -\zeta, -\zeta'} t^2 F^{(1)}([\omega_\zeta + \omega_{\zeta'} - \omega_\lambda]t) F^{(1)}([\omega_{-\zeta} + \omega_{-\zeta'} - \omega_{\lambda'}]t) \\
&\quad \times \left(1 - \delta_{\zeta + \zeta'} \right) n_\zeta^{(0)} n_{\zeta'}^{(0)} \quad \leftarrow \boxed{\text{(E): } (\mu, \mu', \nu, \nu') \rightarrow (\zeta, \zeta', -\zeta, -\zeta')} \\
&- \frac{1}{2} \frac{1}{\hbar^2} \sum_{\zeta, \zeta'} Y_{-\lambda, \zeta, \zeta'} Y_{-\lambda', -\zeta', -\zeta} t^2 F^{(1)}([\omega_\zeta + \omega_{\zeta'} - \omega_\lambda]t) F^{(1)}([\omega_{-\zeta'} + \omega_{-\zeta} - \omega_{\lambda'}]t) \\
&\quad \times \left(1 - \delta_{\zeta - \zeta'} \right) n_\zeta^{(0)} n_{\zeta'}^{(0)} \quad \leftarrow \boxed{\text{(F): } (\mu, \mu', \nu, \nu') \rightarrow (\zeta, \zeta', -\zeta', -\zeta)} \\
&\text{-----} \\
&+ (\lambda \leftrightarrow \lambda') \tag{10.34}
\end{aligned}$$

- terms (A) and (B) are identical except for the double counting correction. (We use $Y_{a,b,c}$ ^{Eq. 10.13})
- terms (E) and (F) are identical except for the double counting correction. (We use $Y_{a,b,c}$ ^{Eq. 10.13})

⁶The boxes indicate how the indices have been renamed in the corresponding step. The letters further identify terms so that we can follow them during the following equations.

$$\begin{aligned}
\left\langle \rho_{\lambda, \lambda'}^{(2)}(t) \right\rangle_{\bar{\phi}_i} &\stackrel{\text{Eq. 10.34}}{=} -\frac{2}{\hbar^2} \sum_{\zeta, \mu'} Y_{-\lambda, \zeta, \mu'} Y_{-\mu', -\zeta, -\lambda'} \underbrace{t^2 F^{(2)}([\omega_\zeta + \omega_{\mu'} - \omega_\lambda]t, [\omega_{-\zeta} + \omega_{-\lambda'} - \omega_{\mu'}]t)} \\
&\quad \times (2 - \delta_{\zeta+\lambda'} - \delta_{\zeta-\lambda'}) n_\zeta^{(0)} n_{\lambda'}^{(0)} \quad \leftarrow \boxed{\text{(A)+(B)}} \\
&- \frac{2}{\hbar^2} \sum_{\zeta, \mu'} Y_{-\lambda, -\lambda', \mu'} Y_{-\mu', \zeta, -\zeta} \underbrace{t^2 F^{(2)}([\omega_{-\lambda'} + \omega_{\mu'} - \omega_\lambda]t, -\omega_{\mu'} t)} (1 - \delta_{\zeta+\lambda'}) n_\zeta^{(0)} n_{\lambda'}^{(0)} \quad \leftarrow \boxed{\text{(C)}} \\
&\text{-----} \\
&- \frac{1}{2} \frac{1}{\hbar^2} \sum_{\zeta, \zeta'} Y_{-\lambda, \zeta, -\zeta} Y_{-\lambda', -\zeta', -\zeta'} t^2 F^{(1)}(-\omega_\lambda t) F^{(1)}(-\omega_{\lambda'} t) (1 - \delta_{\zeta-\zeta'}) n_\zeta^{(0)} n_{\zeta'}^{(0)} \quad \leftarrow \boxed{\text{(D)}} \\
&- \frac{1}{2} \frac{1}{\hbar^2} \sum_{\zeta, \zeta'} Y_{-\lambda, \zeta, \zeta'} Y_{-\lambda', -\zeta, -\zeta'} t^2 F^{(1)}([\omega_\zeta + \omega_{\zeta'} - \omega_\lambda]t) F^{(1)}([\omega_{-\zeta} + \omega_{-\zeta'} - \omega_{\lambda'}]t) \\
&\quad \times (2 - \delta_{\zeta+\zeta'} - \delta_{\zeta-\zeta'}) n_\zeta^{(0)} n_{\zeta'}^{(0)} \quad \leftarrow \boxed{\text{(E)+(F)}} \\
&\text{-----} \\
&+ (\lambda \leftrightarrow \lambda') \tag{10.35}
\end{aligned}$$

The expression obtained here is valid in the second-order of the anharmonicity. The second-order perturbation theory implies that the anharmonic terms must be weak. Higher-order terms such as quartic interactions, describing scattering events in four phonons, are not included for the sake of keeping things simple.

The initial random-phase approximation implies that we start from a specific set of phonon numbers $\{n_\lambda^{(0)}\}$, but there is already a statistical average over the phases of the initial states. As a consequence, the initial density matrix has nonzero elements $\rho_{\lambda, \lambda'}$ only if $\lambda' = -\lambda$

What are the phase factors?

Consider a wave packet $f(x, t)$ with a narrow spectral width, that is $a_{\vec{k}}$ contributes only near \vec{k}_0 .

$$\begin{aligned}
f(x, t) &= \sum_{\vec{k}} a_{\vec{k}} e^{i[\vec{k}\vec{r} - \omega(\vec{k})t]} \\
&= e^{i[\vec{k}_0\vec{r} - \omega(\vec{k}_0)t]} \sum_{\vec{k}} a_{\vec{k}} e^{i(\vec{k} - \vec{k}_0)[\vec{r} - \nabla_{\vec{k}}\omega(\vec{k})t] + O(|\vec{k} - \vec{k}_0|^2)} \\
&\approx e^{i[\vec{k}_0\vec{r} - \omega(\vec{k}_0)t]} \underbrace{\sum_{\vec{k}} a_{\vec{k}} e^{i(\vec{k} - \vec{k}_0)[\vec{r} - \vec{v}_g t]}_{\chi(\vec{r} - \vec{v}_g t)} \\
&= e^{i[\vec{k}_0\vec{r} - \omega(\vec{k}_0)t]} \chi(\vec{r} - \vec{v}_g t) \tag{10.36}
\end{aligned}$$

where $\chi(\vec{r})$ is the envelope function, which modulates the leading wave $e^{i[\vec{k}_0\vec{r} - \omega(\vec{k}_0)t]}$. The wave packet moves with the group velocity \vec{v}_g .

1. Multiplication of the wave packet with a constant phase factor $e^{i\phi}$ leaves the position and the shape of the envelope function unchanged but it displaces the leading wave.
2. Multiplication of the wave packet with a phase factor that changes linearly with \vec{k} , i.e. $\phi = \vec{d}(\vec{k} - \vec{k}_0)$ leaves the shape of the envelope function unchanged but it displaces the envelope function in space by \vec{d} as shown below:

$$\begin{aligned}
\chi(r) &= \sum_{\vec{k}} a(k) e^{i(\vec{k} - \vec{k}_0)\vec{r}} \quad \text{and} \quad a'(\vec{k}) = a(\vec{k}) e^{i(\vec{k} - \vec{k}_0)\vec{d}} \\
\Rightarrow \chi'(\vec{r}) &\stackrel{\text{def}}{=} \sum_{\vec{k}} a'(k) e^{i(\vec{k} - \vec{k}_0)\vec{r}} = \sum_{\vec{k}} a(k) e^{-i(\vec{k} - \vec{k}_0)\vec{d}} e^{i(\vec{k} - \vec{k}_0)\vec{r}} = \sum_{\vec{k}} a(k) e^{i(\vec{k} - \vec{k}_0)(\vec{r} - \vec{d})} = \chi(\vec{r} - \vec{d})
\end{aligned}$$

When we identify a wave packet with a phonon with a position and a momentum, this implies that the phase average includes an average over the initial positions.

3. Other phase factors will change the shape of the envelope function. If the phases are continuous⁷ functions of \vec{k} , however, these terms will only affect envelope functions that are “not very smooth”. That is, their effect vanishes in the limit of extremely broad envelope functions.

10.4.5 Repeated random-phase approximation

While the phonons are propagated, they scatter among each other. After a certain while, a new density matrix Eq. 10.35 in terms of phonon numbers is obtained. In contrast to the initial density matrix $\rho_{\lambda,\lambda'}(0) = n_{\lambda}(0)\delta_{\lambda+\lambda'}$ obtained after the initial random-phase approximation, this final density matrix $\rho_{\lambda,\lambda'}(t)$ is no more diagonal. This implies that the relative phase factors between the phonons are important to describe the final state. The central approximation of the Boltzmann equation is that the relative phases are ignored repeatedly in very short time intervals.

The relevance of phase factors is usually attributed to quantum effects. Note, however, that our theory of phonons is purely classical. The role of phase factors emerges naturally from the wave nature of the underlying theory, be it classical or quantum in nature.

Consequence of the final random phase approximation

Starting from Eq. 10.35, we multiply the density matrix with phase factors

$$\begin{aligned}
 \left\langle \rho_{\lambda,\lambda'}^{(2)}(t) \right\rangle_{\vec{\phi}_i, \vec{\phi}_f} &= \frac{1}{2\pi} \int d\phi_{f,\lambda} \frac{1}{2\pi} \int d\phi_{f,\lambda'} e^{i\phi_{f,\lambda}} \left\langle \rho_{\lambda,\lambda'}^{(2)}(t) \right\rangle_{\vec{\phi}} e^{i\phi_{f,\lambda'}} \\
 &= \delta_{\lambda,-\lambda'} \left\langle \rho_{\lambda,-\lambda}^{(2)}(t) \right\rangle_{\vec{\phi}_i} \\
 &= \delta_{\lambda,-\lambda'} n_{\lambda}^{(2)}(t)
 \end{aligned} \tag{10.38}$$

The phase average reduces the information of the density matrix to that of the phonon occupations, which is directly related to the distribution function of the Boltzmann equation.

After the final random-phase approximation, only the phonon-numbers survive and Eq. 10.35

⁷This assumption is not necessarily valid.

results in

$$\begin{aligned}
 n_{\lambda}^{(2)}(t) &= \left\langle \rho_{\lambda, -\lambda}^{(2)}(t) \right\rangle_{\bar{\phi}_i, \bar{\phi}_f} \\
 &= -\frac{2}{\hbar^2} \sum_{\zeta, \mu'} Y_{-\lambda, \zeta, \mu'} Y_{-\mu', -\zeta, \lambda} \underbrace{t^2 F^{(2)}([\omega_{\zeta} + \omega_{\mu'} - \omega_{\lambda}]t, [\omega_{-\zeta} + \omega_{\lambda} - \omega_{\mu'}]t)}_{\rightarrow \pi t \delta(\omega_{\zeta} + \omega_{\mu'} - \omega_{\lambda}) \text{ for } t \rightarrow \infty; \text{ see Eq. 10.47}}^{\overbrace{-(\omega_{\zeta} + \omega_{\mu'} - \omega_{\lambda})}} \\
 &\quad \times \left(2 - \delta_{\zeta - \lambda} - \delta_{\zeta + \lambda} \right) n_{\zeta}^{(0)} n_{-\lambda}^{(0)} \quad \leftarrow \boxed{\text{(A)+(B)}} \\
 &\quad - \frac{2}{\hbar^2} \sum_{\zeta, \mu'} Y_{-\lambda, \lambda, \mu'} Y_{-\mu', \zeta, -\zeta} \underbrace{t^2 F^{(2)}([\omega_{\lambda} + \omega_{\mu'} - \omega_{\lambda}]t, -\omega_{\mu'} t)}_{\rightarrow \pi t \delta(\omega_{\mu'}) \text{ for } t \rightarrow \infty; \text{ see Eq. 10.47}}^{\overbrace{\omega_{\mu'}}} (1 - \delta_{\zeta - \lambda}) n_{\zeta}^{(0)} n_{-\lambda}^{(0)} \quad \leftarrow \boxed{\text{(C)}} \\
 &\quad \text{-----} \\
 &\quad - \frac{1}{2} \frac{1}{\hbar^2} \sum_{\zeta, \zeta'} Y_{-\lambda, \zeta, -\zeta} Y_{+\lambda, \zeta', -\zeta'} \underbrace{t^2 F^{(1)}(-\omega_{\lambda} t) F^{(1)}(\overbrace{-\omega_{-\lambda} t}^{+\omega_{\lambda}})}_{\rightarrow 2\pi t \delta(\omega_{\lambda}) \text{ for } t \rightarrow \infty; \text{ see Eq. 10.45}} (1 - \delta_{\zeta - \zeta'}) n_{\zeta}^{(0)} n_{\zeta'}^{(0)} \quad \leftarrow \boxed{\text{(D)}} \\
 &\quad - \frac{1}{2} \frac{1}{\hbar^2} \sum_{\zeta, \zeta'} Y_{-\lambda, \zeta, \zeta'} Y_{+\lambda, -\zeta, -\zeta'} \underbrace{t^2 F^{(1)}([\omega_{\zeta} + \omega_{\zeta'} - \omega_{\lambda}]t) F^{(1)}(\overbrace{[\omega_{-\zeta} + \omega_{-\zeta'} - \omega_{-\lambda}]t}^{\overbrace{-(\omega_{\zeta} + \omega_{\zeta'} - \omega_{\lambda})}})}_{\rightarrow 2\pi t \delta(\omega_{\zeta} + \omega_{\zeta'} - \omega_{\lambda}) \text{ for } t \rightarrow \infty; \text{ see Eq. 10.45}} \\
 &\quad \times \left(2 - \delta_{\zeta + \zeta'} - \delta_{\zeta - \zeta'} \right) n_{\zeta}^{(0)} n_{\zeta'}^{(0)} \quad \leftarrow \boxed{\text{(E)+(F)}} \\
 &\quad \text{-----} \\
 &\quad + (\lambda \leftrightarrow -\lambda) \tag{10.39}
 \end{aligned}$$

In the equation above, $F^{(2)}$ occurs always in the form $F^{(2)}(\omega t, -\omega t)$ and the products of $F^{(1)}$ occur always in the form $F^{(1)}(\omega t)F^{(1)}(-\omega t)$. This simplifies the expressions and allows to relate both time-dependent functions to a δ -function as shown below in Eq. 10.47 and Eq. 10.45. For easier comparison, I already inserted the δ -functions in the underbraces of the above expression.

Editor: Does the full time dependence for $F^{(2)}(\omega t, \omega' t)$ with $\omega \neq \omega'$ already produce oscillatory terms that average out? This would provide a justification for the repeated random-phase approximation.

Relation to the Boltzmann equation

With the initial random phase approximation, we selected an ensemble, which does not contain the knowledge of the relative phases.

Eq. 10.35 maps these initial occupations onto a final density matrix. The final phase average removes the information, but leaves the information on the phonon numbers $n_{\lambda}(t)$ intact. Thus, we arrive at a mapping Eq. 10.39 from initial phonon numbers onto final phonon numbers at time t .

$$n_{\lambda}(0) \xrightarrow{\text{Eq. of motion}} \rho_{\lambda, \lambda'}(t) \xrightarrow{\text{phase average}} n_{\lambda}(t) \tag{10.40}$$

We arrived at a mapping from initial phonon numbers $n_{\lambda}(0)$ onto the phonon numbers $n_{\lambda}(t)$ at a later time t . The approximation made is perturbation theory. This approximation is done for convenience and the derivation can be extended beyond it. Other than this we have not introduced any approximations to the equations of motion for the atoms, we started from. We have given up some of the information of the original equations of motion by averaging over phases, but that is not an approximation.

Besides this approximation, Eq. 10.39 predict the phonon number arbitrarily far into the future. Thus, this mapping could replace the Boltzmann equation, which does exactly the same, namely to provide a mapping from an initial distribution to final distribution.

However, the outcome of the Boltzmann equation and that of Eq. 10.39 is not necessarily the same. When they are not the same, the Boltzmann equation is invalid.

The Boltzmann equation rests on the **repeated random-phase approximation** [70]. It implies using the mapping $n_\lambda(0) \rightarrow n_\lambda(t)$ via Eq. 10.39, for short time intervals Δ to build up a trajectory for a large time period. This implies that after a time interval Δ the phase information is discarded. Such a step is only justified beyond what is called the decoherence time τ_{decoh} . The rationale is that there is a physical process, which leads to an effective loss the phase decoherence. Whether this rationale is justified, needs to be shown.

The Boltzmann equation then performs some course graining, and replaces the finite difference quotient by the time derivative

$$\frac{n_\lambda(t + \Delta) - n_\lambda(t)}{\Delta} = \frac{n_\lambda^{(2)}(\Delta)}{\Delta} \xrightarrow{\text{Boltzmann eq}} \partial_t n_\lambda(t) \quad (10.41)$$

A worthwhile remark is that taking the time derivative of $n_\lambda^{(2)}(t)$ is a poor idea, because it implies discarding the phase information on a much shorter than the physical decoherence process.

The loss of phase information is at the origin of the second law of thermodynamics. Since entropy is the lack of knowledge on the state of the system, loss of information implies an entropy increase.

The question regarding the origin of the entropy growth is very fundamental and of great interest: Namely it can be shown that the entropy for a closed quantum system is a constant of motion, that is, it does not grow. Because this question is far from being settled I will leave the subject and refer to the scientific literature. Van Hove[77, 78] has been one of the pioneers of this topic. See also Spohn[79].

As a side remark, I want to mention that the phase randomization depends on the choice of the one-particle basisset. In this case the normal modes correspond to the one-particle basisset. While it is reasonable to select normal modes, the phase average could have been done after a unitary transformation onto any other basisset. The new basis functions are just superposition of phonon modes. After the phase average is performed in the new basisset, one would transform the result back into the original basis. Considering the flexibility regarding the choice of the random-phase approximation, we might also look for the “best possible” random phase approximation. The criterion would be that the random phase approximation has the least impact on the long term dynamics of the phonon numbers.

10.4.6 Long-time limit, energy conservation and Fermi’s golden rule

Time dependence

As shown in appendix P, the integrations in Eq. 10.21 and Eq. 10.24 can be expressed for large times in terms of delta functions.

The first time integral has the form

$$F^{(1)}(\omega t) \stackrel{\text{def}}{=} \frac{1}{t} \int_0^t dt' e^{i\omega t'} \quad (10.42)$$

It has the form

$$F^{(1)}(x) \stackrel{\text{Eq. ??}}{=} \frac{\sin(x)}{x} - i \frac{\cos(x) - 1}{x} \quad (10.43)$$

For large times we use the limiting expression

$$\lim_{t \rightarrow \infty} t F^{(1)}(\omega t) \stackrel{\text{Eq. ??}}{=} \pi \delta(\omega) \quad (10.44)$$

For the second-order terms we will use

$$\lim_{t \rightarrow \infty} t^2 F^{(1)}(\omega t) F^{(1)}(-\omega t) \stackrel{\text{Eq. P.15}}{=} 2\pi t \delta(\omega) \quad (10.45)$$

The second time integral is⁸

$$F^{(2)}(\omega t, \omega' t) \stackrel{\text{def}}{=} \frac{1}{t^2} \int_0^t dt' e^{i\omega t'} \int_0^{t'} dt'' e^{i\omega' t''} \quad (10.46)$$

In the large-time limit it has the form

$$\lim_{t \rightarrow \infty} t^2 F^{(2)}(\omega t, -\omega t) \stackrel{\text{Eq. P.15}}{=} \pi t \delta(\omega) \quad (10.47)$$

Editor: The following belongs somewhere below: “Some caution is required, because we treat the sum over phonons as discrete sum, and at the same time we use the delta function, which requires a continuous integral over frequencies. This problem disappears, when we make the limit of an infinitely large system, where the spectrum is continuous. This problem hints at an important difference between finite and infinite systems that is important for the approach to thermal equilibrium.”

Large-time limit

The time evolution of the phonon numbers is given by Eq. 10.39. Here, I take the large-time limits for the time dependence, namely Eq. ?? , i.e. $t^2 F^{(2)}(\omega t, -\omega t) \rightarrow \pi t \delta(\omega)$ and Eq. 10.45, i.e. $t^2 F^{(1)}(\omega t) F^{(1)}(-\omega t) \rightarrow 2\pi t \delta(\omega)$.

Below, I start from Eq. 10.39, insert the δ -functions and combine the terms obtained by interchange $\lambda \rightarrow -\lambda$.

$$\begin{aligned} n_\lambda^{(2)}(t) &\stackrel{\text{Eq. 10.39}}{=} \left\langle \rho_{\lambda, -\lambda}^{(2)}(t) \right\rangle_{\vec{\phi}_i, \vec{\phi}_f} \\ &= -\frac{2\pi t}{\hbar^2} \sum_{\zeta, \zeta'} \underbrace{Y_{-\lambda, \zeta, \zeta'} Y_{-\zeta', -\zeta, \lambda}}_{\sigma_\lambda \sigma_{\zeta'} |Y_{-\lambda, \zeta, \zeta'}|^2} \delta(\omega_\zeta + \omega_{\zeta'} - \omega_\lambda) (2 - \delta_{\zeta-\lambda} - \delta_{\zeta+\lambda}) n_\zeta^{(0)} n_\lambda^{(0)} \quad \leftarrow \boxed{\text{(A)+(B)}} \\ &\quad -\frac{2\pi t}{\hbar^2} \sum_{\zeta, \zeta'} \underbrace{Y_{\lambda, -\zeta, -\zeta'} Y_{\zeta', \zeta, -\lambda}}_{\sigma_\lambda \sigma_{\zeta'} |Y_{-\lambda, \zeta, \zeta'}|^2} \underbrace{\delta(\omega_{-\zeta} + \omega_{-\zeta'} - \omega_{-\lambda})}_{\delta(\omega_\zeta + \omega_{\zeta'} - \omega_\lambda)} \underbrace{(2 - \delta_{-\zeta+\lambda} - \delta_{-\zeta-\lambda})}_{2 - \delta_{\zeta-\lambda} - \delta_{\zeta+\lambda}} n_\zeta^{(0)} n_\lambda^{(0)} \quad \leftarrow \boxed{\text{(A')+(B')}} \\ &\quad -\frac{2\pi t}{\hbar^2} \sum_{\zeta, \zeta'} \underbrace{Y_{-\lambda, \zeta, \zeta'} Y_{+\lambda, -\zeta, -\zeta'}}_{-|Y_{-\lambda, \zeta, \zeta'}|^2} \delta(\omega_\zeta + \omega_{\zeta'} - \omega_\lambda) (2 - \delta_{\zeta+\zeta'} - \delta_{\zeta-\zeta'}) n_\zeta^{(0)} n_{\zeta'}^{(0)} \quad \leftarrow \boxed{\text{(E)+(F)+(E')+(F')}} \\ &\quad -\frac{2\pi t}{\hbar^2} \sum_{\zeta, \zeta'} Y_{-\lambda, \lambda, \zeta'} Y_{-\zeta', \zeta, -\zeta} \delta(\omega_{\zeta'}) (1 - \delta_{\zeta-\lambda}) n_\zeta^{(0)} n_\lambda^{(0)} \quad \leftarrow \boxed{\text{(C)}} \\ &\quad -\frac{2\pi t}{\hbar^2} \sum_{\zeta, \zeta'} \underbrace{Y_{\lambda, -\lambda, -\zeta'} Y_{\zeta', -\zeta, \zeta}}_{Y_{-\lambda, \lambda, \zeta'}^* Y_{-\zeta', \zeta, -\zeta}^*} \underbrace{\delta(\omega_{-\zeta'})}_{\delta(\omega_{\zeta'})} \underbrace{(1 - \delta_{-\zeta+\lambda})}_{1 - \delta_{\zeta-\lambda}} n_\zeta^{(0)} n_\lambda^{(0)} \quad \leftarrow \boxed{\text{(C')}} \\ &\quad -\frac{2\pi t}{\hbar^2} \sum_{\zeta, \zeta'} Y_{-\lambda, \zeta, -\zeta} Y_{+\lambda, \zeta', -\zeta'} \delta(\omega_\lambda) (1 - \delta_{\zeta-\zeta'}) n_\zeta^{(0)} n_{\zeta'}^{(0)} \quad \leftarrow \boxed{\text{(D)+(D')}} \end{aligned} \quad (10.48)$$

We used $Y_{\lambda, \lambda', \lambda''} = -Y^*(-\lambda, -\lambda', -\lambda'')$ and that $\sigma_\lambda Y_{\lambda, \lambda', \lambda''}$ is invariant under interchange of the indices.

The primed terms (A')+(B'), (C'), (D'), (E')+(F') are the terms obtained by interchanging λ and λ' in of the density matrix. In the occupation number Eq. 10.39, the interchange of λ and λ' translates into a inversion of the index λ , respectively an interchange of λ and $-\lambda$.

The terms (E)+(F) and (D) are already symmetric under interchange of λ and $-\lambda$ so that (E'), (F') and (D') are accounted for simply by multiplication of (E)+(F) and (D) by a factor of two.

⁸ $\frac{1}{2} F^{(2)}$ is the average of a plane wave $e^{i(\omega t' + \omega' t'')}$ with wave vector (ω, ω') over a triangle in the t', t'' -plane with corners $(0, 0)$, $(t, 0)$, (t, t) .

For the terms (A')+(B') and (C'), the sum indices ζ, ζ' have been inverted alongside with the index λ . This does not change the result, because positive and negative terms are both included in the sum.

$$\begin{aligned}
n_{\lambda}^{(2)}(t) = & -\frac{4\pi t}{\hbar^2} \sum_{\zeta, \zeta'} \sigma_{\lambda} \sigma_{\zeta'} |Y_{-\lambda, \zeta, \zeta'}|^2 \delta(\omega_{\zeta} + \omega_{\zeta'} - \omega_{\lambda}) (2 - \delta_{\zeta-\lambda} - \delta_{\zeta+\lambda}) n_{\zeta}^{(0)} n_{\lambda}^{(0)} \quad \leftarrow \boxed{(A)+(B)+(A')+(B')} \\
& + \frac{2\pi t}{\hbar^2} \sum_{\zeta, \zeta'} |Y_{-\lambda, \zeta, \zeta'}|^2 \delta(\omega_{\zeta} + \omega_{\zeta'} - \omega_{\lambda}) (2 - \delta_{\zeta+\zeta'} - \delta_{\zeta-\zeta'}) n_{\zeta}^{(0)} n_{\zeta'}^{(0)} \quad \leftarrow \boxed{(E)+(F)+(E')+(F')} \\
& - \frac{4\pi t}{\hbar^2} \sum_{\zeta, \zeta'} \text{Re}[Y_{-\lambda, \lambda, \zeta'} Y_{-\zeta', \zeta, -\zeta}] \delta(\omega_{\zeta'}) (1 - \delta_{\zeta-\lambda}) n_{\zeta}^{(0)} n_{\lambda}^{(0)} \quad \leftarrow \boxed{(C)+(C')} \\
& - \frac{2\pi t}{\hbar^2} \sum_{\zeta, \zeta'} \text{Re}[Y_{-\lambda, \zeta, -\zeta} Y_{+\lambda, \zeta', -\zeta'}] \delta(\omega_{\lambda}) (1 - \delta_{\zeta-\zeta'}) n_{\zeta}^{(0)} n_{\zeta'}^{(0)} \quad \leftarrow \boxed{(D)+(D')} \quad (10.49)
\end{aligned}$$

The term (A) + (B) can be compared with Eq. 3.7 of Brout and Prigogine[71]. **Editor: There is a discrepancy of a factor of two. There may be a mistake regarding the definition of the phonon number including both λ and $-\lambda$.**

Now, we can limit λ to values with $\sigma_{\lambda} = +$.

$$\begin{aligned}
n_{\lambda}^{(2)}(t) \stackrel{\sigma_{\lambda}=+}{=} & -\frac{4\pi t}{\hbar^2} \sum_{\zeta} \left[\sum_{\zeta'} \sigma_{\zeta'} |Y_{-\lambda, \zeta, \zeta'}|^2 \delta(\omega_{\zeta} + \omega_{\zeta'} - \omega_{\lambda}) \right] (2 - \delta_{\zeta-\lambda} - \delta_{\zeta+\lambda}) n_{\zeta}^{(0)} n_{\lambda}^{(0)} \quad \leftarrow \boxed{(A)+(B)+(A')+(B')} \\
& + \frac{2\pi t}{\hbar^2} \sum_{\zeta, \zeta'} |Y_{-\lambda, \zeta, \zeta'}|^2 \delta(\omega_{\zeta} + \omega_{\zeta'} - \omega_{\lambda}) (2 - \delta_{\zeta+\zeta'} - \delta_{\zeta-\zeta'}) n_{\zeta}^{(0)} n_{\zeta'}^{(0)} \quad \leftarrow \boxed{(E)+(F)+(E')+(F')} \\
& - \frac{4\pi t}{\hbar^2} \sum_{\zeta, \zeta'} \text{Re}[Y_{-\lambda, \lambda, \zeta'} Y_{-\zeta', \zeta, -\zeta}] \delta(\omega_{\zeta'}) (1 - \delta_{\zeta-\lambda}) n_{\zeta}^{(0)} n_{\lambda}^{(0)} \quad \leftarrow \boxed{(C)+(C')} \\
& - \frac{2\pi t}{\hbar^2} \sum_{\zeta, \zeta'} \text{Re}[Y_{-\lambda, \zeta, -\zeta} Y_{+\lambda, \zeta', -\zeta'}] \delta(\omega_{\lambda}) (1 - \delta_{\zeta-\zeta'}) n_{\zeta}^{(0)} n_{\zeta'}^{(0)} \quad \leftarrow \boxed{(D)+(D')} \quad (10.50)
\end{aligned}$$

Editor: Do not read! This is a small calculation for a check: Check whether the delta-terms cancel

$$\begin{aligned}
0_{\lambda}^{(2)}(t) \overset{\sigma_{\lambda} \equiv +}{=} & + \frac{4\pi t}{\hbar^2} \sum_{\zeta} \left[\sum_{\zeta'} \sigma_{\zeta'} |Y_{-\lambda, \zeta, \zeta'}|^2 \delta(\omega_{\zeta} + \omega_{\zeta'} - \omega_{\lambda}) \right] \delta_{\zeta-\lambda} n_{\zeta}^{(0)} n_{\lambda}^{(0)} \quad \leftarrow \boxed{(A)+(B)+(A')+(B')} \\
& + \frac{4\pi t}{\hbar^2} \sum_{\zeta} \left[\sum_{\zeta'} \sigma_{\zeta'} |Y_{-\lambda, \zeta, \zeta'}|^2 \delta(\omega_{\zeta} + \omega_{\zeta'} - \omega_{\lambda}) \right] \delta_{\zeta+\lambda} n_{\zeta}^{(0)} n_{\lambda}^{(0)} \quad \leftarrow \boxed{(A)+(B)+(A')+(B')} \\
& - \frac{2\pi t}{\hbar^2} \sum_{\zeta, \zeta'} |Y_{-\lambda, \zeta, \zeta'}|^2 \delta(\omega_{\zeta} + \omega_{\zeta'} - \omega_{\lambda}) \delta_{\zeta+\zeta'} n_{\zeta}^{(0)} n_{\zeta'}^{(0)} \quad \leftarrow \boxed{(E)+(F)+(E')+(F')} \\
& - \frac{2\pi t}{\hbar^2} \sum_{\zeta, \zeta'} |Y_{-\lambda, \zeta, \zeta'}|^2 \delta(\omega_{\zeta} + \omega_{\zeta'} - \omega_{\lambda}) \delta_{\zeta-\zeta'} n_{\zeta}^{(0)} n_{\zeta'}^{(0)} \quad \leftarrow \boxed{(E)+(F)+(E')+(F')} \\
& + \frac{4\pi t}{\hbar^2} \sum_{\zeta, \zeta'} \text{Re}[Y_{-\lambda, \lambda, \zeta'} Y_{-\zeta', \zeta, -\zeta}] \delta(\omega_{\zeta'}) \delta_{\zeta-\lambda} n_{\zeta}^{(0)} n_{\lambda}^{(0)} \quad \leftarrow \boxed{(C)+(C')} \\
& + \frac{2\pi t}{\hbar^2} \sum_{\zeta, \zeta'} \text{Re}[Y_{-\lambda, \zeta, -\zeta} Y_{+\lambda, \zeta', -\zeta'}] \delta(\omega_{\lambda}) \delta_{\zeta-\zeta'} n_{\zeta}^{(0)} n_{\zeta'}^{(0)} \quad \leftarrow \boxed{(D)+(D')} \\
\overset{\sigma_{\lambda} \equiv +}{=} & + \frac{4\pi t}{\hbar^2} \left[\sum_{\zeta'} \sigma_{\zeta'} |Y_{-\lambda, \lambda, \zeta'}|^2 \delta(\omega_{\zeta'}) \right] n_{\lambda}^{(0)} n_{\lambda}^{(0)} \quad \leftarrow \boxed{(A)+(B)+(A')+(B')} \\
& + \frac{4\pi t}{\hbar^2} \left[\sum_{\zeta'} \sigma_{\zeta'} |Y_{-\lambda, -\lambda, \zeta'}|^2 \delta(\underbrace{\omega_{-\lambda} + \omega_{\zeta'} - \omega_{\lambda}}_{\omega_{\zeta'} - 2\omega_{\lambda}}) \right] \underbrace{n_{-\lambda}^{(0)}}_{n_{\lambda}^{(0)}} n_{\lambda}^{(0)} \quad \leftarrow \boxed{(A)+(B)+(A')+(B')} \\
& - \frac{2\pi t}{\hbar^2} \sum_{\zeta} |Y_{-\lambda, \zeta, -\zeta}|^2 \delta(-\omega_{\lambda}) n_{\zeta}^{(0)} \underbrace{n_{-\zeta}^{(0)}}_{n_{\zeta}^{(0)}} \quad \leftarrow \boxed{(E)+(F)+(E')+(F')} \\
& - \frac{2\pi t}{\hbar^2} \sum_{\zeta} |Y_{-\lambda, \zeta, \zeta}|^2 \delta(2\omega_{\zeta} - \omega_{\lambda}) n_{\zeta}^{(0)} n_{\zeta}^{(0)} \quad \leftarrow \boxed{(E)+(F)+(E')+(F')} \\
& + \frac{4\pi t}{\hbar^2} \sum_{\zeta'} \text{Re}[Y_{-\lambda, \lambda, \zeta'} Y_{-\zeta', \lambda, -\lambda}] \delta(\omega_{\zeta'}) n_{\lambda}^{(0)} n_{\lambda}^{(0)} \quad \leftarrow \boxed{(C)+(C')} \\
& + \frac{2\pi t}{\hbar^2} \sum_{\zeta} \text{Re}[Y_{-\lambda, \zeta, -\zeta} Y_{+\lambda, \zeta, -\zeta}] \delta(\omega_{\lambda}) n_{\zeta}^{(0)} n_{\zeta}^{(0)} \quad \leftarrow \boxed{(D)+(D')} \tag{10.51}
\end{aligned}$$

10.4.7 Phonon scattering without lattice expansion

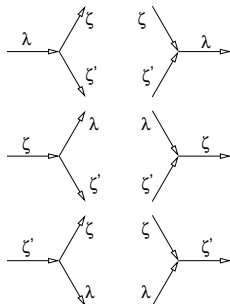
The terms (C),(C'),(D),(D') describe the interaction of the phonon gas with a homogeneous expansion or contraction of the lattice. These effects differ from the phonon-phonon scattering. Let me therefore divide the change of occupation into two terms $n^{(2a)}$, which describes phonon-phonon scattering, while $n^{(2b)}$ describes the interaction of the phonon gas with an expansion of the lattice.

Let me consider the first two terms only. In order to make the equations more transparent, all

terms will be expressed by those with $\sigma > 0$.

$$\begin{aligned}
 n_{\lambda}^{(2a)}(t) &= -\frac{4\pi t}{\hbar^2} \sum_{\zeta, \zeta'} \sigma_{\zeta'} |Y_{-\lambda, \zeta, \zeta'}|^2 \delta(\omega_{\zeta} + \omega_{\zeta'} - \omega_{\lambda}) (2 - \delta_{\zeta-\lambda} - \delta_{\zeta+\lambda}) n_{\zeta}^{(0)} n_{\lambda}^{(0)} \leftarrow \boxed{(A)+(B)+(A')+(B')} \\
 &\quad + \frac{2\pi t}{\hbar^2} \sum_{\zeta, \zeta'} |Y_{-\lambda, \zeta, \zeta'}|^2 \delta(\omega_{\zeta} + \omega_{\zeta'} - \omega_{\lambda}) (2 - \delta_{\zeta+\zeta'} - \delta_{\zeta-\zeta'}) n_{\zeta}^{(0)} n_{\zeta'}^{(0)} \leftarrow \boxed{(E)+(F)+(E')+(F')} \\
 &= -\frac{4\pi t}{\hbar^2} \sum_{\zeta, \zeta': \sigma_{\zeta} = \sigma_{\zeta'} = +} \\
 &\quad \times \left\{ |Y_{-\lambda, \zeta, \zeta'}|^2 \delta(\omega_{\zeta} + \omega_{\zeta'} - \omega_{\lambda}) \left[\underbrace{(2 - \delta_{\zeta-\lambda})}_{(a)} n_{\lambda}^{(0)} - \frac{1}{2} \underbrace{(2 - \delta_{\zeta-\zeta'})}_{(b)} n_{\zeta'}^{(0)} \right] n_{\zeta}^{(0)} \right. \\
 &\quad + |Y_{-\lambda, -\zeta, \zeta'}|^2 \delta(\omega_{-\zeta} + \omega_{\zeta'} - \omega_{\lambda}) \left[\underbrace{(2 - \delta_{\zeta-\lambda})}_{(c)} n_{\lambda}^{(0)} - \frac{1}{2} \underbrace{(2 - \delta_{\zeta-\zeta'})}_{(d)} n_{\zeta'}^{(0)} \right] n_{\zeta}^{(0)} \\
 &\quad + |Y_{-\lambda, \zeta, -\zeta'}|^2 \delta(\omega_{\zeta} + \omega_{-\zeta'} - \omega_{\lambda}) \left[-\underbrace{(2 - \delta_{\zeta-\lambda})}_{(e)} n_{\lambda}^{(0)} - \frac{1}{2} \underbrace{(2 - \delta_{\zeta-\zeta'})}_{(f)} n_{\zeta'}^{(0)} \right] n_{\zeta}^{(0)} \\
 &\quad \left. + |Y_{-\lambda, -\zeta, -\zeta'}|^2 \underbrace{\delta(\omega_{-\zeta} + \omega_{-\zeta'} - \omega_{\lambda})}_{=0} \left[-\underbrace{(2 - \delta_{\zeta-\lambda})}_{(e)} n_{\lambda}^{(0)} - \frac{1}{2} \underbrace{(2 - \delta_{\zeta-\zeta'})}_{(f)} n_{\zeta'}^{(0)} \right] n_{\zeta}^{(0)} \right\} \\
 &= \frac{4\pi t}{\hbar^2} \sum_{\zeta, \zeta': \sigma_{\zeta} = \sigma_{\zeta'} = +} \left\{ |Y_{-\lambda, \zeta, \zeta'}|^2 \delta(\omega_{\zeta} + \omega_{\zeta'} - \omega_{\lambda}) \left[\underbrace{-(2 - \delta_{\zeta-\lambda})}_{(a)} n_{\lambda}^{(0)} n_{\zeta}^{(0)} + \frac{1}{2} \underbrace{(2 - \delta_{\zeta-\zeta'})}_{(b)} n_{\zeta'}^{(0)} n_{\zeta}^{(0)} \right] \right. \\
 &\quad \left. + |Y_{-\lambda, \zeta, -\zeta'}|^2 \delta(\omega_{\zeta} - \omega_{\zeta'} - \omega_{\lambda}) \left[\underbrace{(2 - \delta_{\zeta'-\lambda})}_{(c)} n_{\lambda}^{(0)} n_{\zeta'}^{(0)} - \underbrace{(2 - \delta_{\zeta-\lambda})}_{(e)} n_{\lambda}^{(0)} n_{\zeta}^{(0)} - \underbrace{(2 - \delta_{\zeta-\zeta'})}_{(d)+(f)} n_{\zeta}^{(0)} n_{\zeta'}^{(0)} \right] \right\}
 \end{aligned} \tag{10.52}$$

- terms (d) and (f) are identical because they only differ by an exchange of ζ with ζ'
- The term (a) describes the loss of phonons λ as they collide with a phonon σ and form a new phonon σ'
-



Interpretation: Editor: This is in preparation

- The terms (A) + (B) + (A') + (B') describe for ...

10.4.8 Phonons coupling to elastic distortions

Editor: This is no properly explained.

The terms (C),(C'),(D),(D') couple phonons with frequency close to zero. Those are the acoustic phonons, which also describe the elastic constants. I believe that these terms describe thermal expansion of the lattice, respectively the cooling of the phonon-gas upon expansion of the lattice. The cooling effect can occur in two ways, namely by (C)+(C') changing the phonon numbers or by (D)+(D') reducing the energy of existing phonons. **Editor:** check this!

Here, I collect the terms of Eq. 10.50, which have not been included in $n_\lambda^{(2a)}(t)$, Eq. 10.52. They will be denoted as $n_\lambda^{(2b)}(t)$.

$$\begin{aligned} n_\lambda^{(2b)}(t) = & -\frac{4\pi t}{\hbar^2} \sum_{\zeta, \zeta'} \operatorname{Re}[Y_{-\lambda, \lambda, \zeta'} Y_{-\zeta', \zeta, -\zeta}] \delta(\omega_{\zeta'}) (1 - \delta_{\zeta-\lambda}) n_\zeta^{(0)} n_\lambda^{(0)} \quad \leftarrow \boxed{(C)+(C')} \\ & -\frac{2\pi t}{\hbar^2} \sum_{\zeta, \zeta'} \operatorname{Re}[Y_{-\lambda, \zeta, -\zeta} Y_{+\lambda, \zeta', -\zeta'}] \delta(\omega_\lambda) (1 - \delta_{\zeta-\zeta'}) n_\zeta^{(0)} n_{\zeta'}^{(0)} \quad \leftarrow \boxed{(D)+(D')} \end{aligned} \quad (10.53)$$

10.5 Kinetic equation

Now, we are ready to write down a kinetic equation that determines the dynamics of the phonon numbers. We extract the derivative Eq. 10.41, albeit in the long-time limit, and obtain for the terms in $n^{(2a)}$, Eq. 10.53.

$$\begin{aligned} \partial_t n_\lambda = & \frac{4\pi}{\hbar^2} \sum_{\zeta, \zeta': \sigma_\zeta = \sigma_{\zeta'} = +} \left\{ \underbrace{|Y_{-\lambda, \zeta, \zeta'}|^2 \delta(\omega_\zeta + \omega_{\zeta'} - \omega_\lambda)}_{\frac{\hbar^2}{4\pi} L_{\zeta, \zeta'}^\lambda} \left[\underbrace{-(2 - \delta_{\zeta-\lambda}) n_\lambda^{(0)} n_\zeta^{(0)}}_{(a)} + \frac{1}{2} \underbrace{(2 - \delta_{\zeta-\zeta'}) n_{\zeta'}^{(0)} n_\zeta^{(0)}}_{(b)} \right] \right. \\ & \left. + |Y_{-\lambda, \zeta, -\zeta'}|^2 \delta(\omega_\zeta - \omega_{\zeta'} - \omega_\lambda) \left[\underbrace{(2 - \delta_{\zeta'-\lambda}) n_\lambda^{(0)} n_{\zeta'}^{(0)}}_{(c)} - \underbrace{(2 - \delta_{\zeta-\lambda}) n_\lambda^{(0)} n_\zeta^{(0)}}_{(e)} - \underbrace{(2 - \delta_{\zeta-\zeta'}) n_\zeta^{(0)} n_{\zeta'}^{(0)}}_{(d)+(f)} \right] \right\} \\ = & \frac{4\pi}{\hbar^2} \sum_{\lambda', \lambda'': \sigma_{\lambda'} = \sigma_{\lambda''} = +} \left\{ |Y_{-\lambda, \lambda', \lambda''}|^2 \delta(\omega_{\lambda'} + \omega_{\lambda''} - \omega_\lambda) \left[\underbrace{-(2 - \delta_{\lambda'-\lambda}) n_\lambda^{(0)} n_{\lambda'}^{(0)}}_{(a)} + \frac{1}{2} \underbrace{(2 - \delta_{\lambda'-\lambda''}) n_{\lambda''}^{(0)} n_{\lambda'}^{(0)}}_{(b)} \right] \right. \\ & \left. + |Y_{-\lambda, \lambda', -\lambda''}|^2 \delta(\omega_{\lambda'} - \omega_{\lambda''} - \omega_\lambda) \left[\underbrace{(2 - \delta_{\lambda''-\lambda}) n_\lambda^{(0)} n_{\lambda''}^{(0)}}_{(c)} - \underbrace{(2 - \delta_{\lambda'-\lambda}) n_\lambda^{(0)} n_{\lambda'}^{(0)}}_{(e)} - \underbrace{(2 - \delta_{\lambda'-\lambda''}) n_{\lambda'}^{(0)} n_{\lambda''}^{(0)}}_{(d)+(f)} \right] \right\} \end{aligned} \quad (10.54)$$

$$\partial_t n_\lambda = \sum_{\zeta, \zeta'} \left(L_{\zeta, \zeta'}^\lambda n_\zeta n_{\zeta'} + L_{\zeta'}^\lambda n_{\zeta'} (n_{\zeta'} + n_\zeta n_{\zeta'} + n_\lambda n_{\zeta'}) - \frac{1}{2} L_{\lambda}^{\zeta, \zeta'} (n_\lambda + n_\lambda n_\zeta + n_\lambda n_{\zeta'}) - L_{\lambda, \zeta}^{\zeta'} (n_\lambda n_\zeta) \right) \quad (10.55)$$

where

$$L_{\lambda', \lambda''}^\lambda = -L_{\lambda}^{\lambda', \lambda''} \stackrel{\text{def}}{=} \frac{4\pi}{\hbar^2} Y_{-\lambda, \lambda', \lambda''} \delta(\omega_{\lambda'} + \omega_{\lambda''} + \omega_{-\lambda}) \quad (10.56)$$

The matrix elements Y have been defined in Eq. 10.3 on p. 330. The conversion into the compact notation is given in Eq. 10.12 and Eq. 10.13.

Editor: DEMONSTRATE HOW TO GET FROM THE PREVIOUS TO THIS EQUATION: It seems that the δ -terms cancel, but I need to show how. Consider also that one need to consider both terms $n^{(2a)}$ and $n^{(2b)}$ for the cancellation.

Editor: The argument to drop the Kronecker deltas rests probably that the delta functions make the problem overdetermined, so that they do not contribute. There is a 6-dimensional k -integration. On the other hand there is momentum and energy conservation, converting it into a 2-dimensional integration. If we then introduce an additional constraint constraining two momenta, we would attempt to constrain more degrees of freedom than there are. I have not found a cancellation without this argument.

$$\begin{aligned} \partial_t n_\lambda = & \frac{8\pi}{\hbar^2} \sum_{\lambda', \lambda''; \sigma_\lambda > 0, \sigma_\lambda > 0} \delta(\omega_{\lambda'} + \omega_{\lambda''} - \omega_\lambda) |Y_{\lambda, \lambda', \lambda''}|^2 \left[\frac{1}{2} n_{\lambda'} n_{\lambda''} - n_\lambda n_{\lambda''} \right] \\ & + \frac{8\pi}{\hbar^2} \sum_{\lambda', \lambda''; \sigma_\lambda > 0, \sigma_\lambda > 0} \delta(\omega_{\lambda'} - \omega_{\lambda''} - \omega_\lambda) |Y_{\lambda, \lambda', -\lambda''}|^2 \left[n_{\lambda'} n_{\lambda''} - n_\lambda n_{\lambda''} - n_\lambda n_{\lambda'} \right] \end{aligned} \quad (10.57)$$

CLASSICAL KINETIC EQUATION FOR PHONON NUMBERS

The kinetic equation is simply the scattering of the (phonon)-Boltzmann equation without the drift term.

$$\begin{aligned}
\partial_t n_\sigma(k) = & + \frac{\hbar\pi}{4} \sum_{\vec{k}_1, \vec{k}_2, \sigma_1 > 0, \sigma_2 > 0} \delta \left(\sum_{j \in \{1,2\}} \omega_{\sigma_j}(\vec{k}_j) - \omega_\sigma(\vec{k}) \right) \frac{|A_{\sigma, \sigma_1, \sigma_2}(-\vec{k}, \vec{k}_1, \vec{k}_2)|^2 / \mathcal{N}}{\omega_\sigma(\vec{k}) \omega_{\sigma_1}(\vec{k}_1) \omega_{\sigma_2}(\vec{k}_2)} \\
& \times \left[\underbrace{\frac{1}{2} n_{\sigma_1}^{(0)}(\vec{k}_1) n_{\sigma_2}^{(0)}(\vec{k}_2)}_{(1)} - \underbrace{n_\sigma^{(0)}(\vec{k}) n_{\sigma_2}^{(0)}(\vec{k}_2)}_{(2)} \right] \\
& + \frac{\hbar\pi}{4} \sum_{\vec{k}_1, \vec{k}_2, \sigma_1 > 0, \sigma_2 > 0} \delta \left(\omega_{\sigma_1}(\vec{k}_1) - \omega_{\sigma_2}(\vec{k}_2) - \omega_\sigma(\vec{k}) \right) \frac{|A_{\sigma, \sigma_1, \sigma_2}(-\vec{k}, \vec{k}_1, -\vec{k}_2)|^2 / \mathcal{N}}{\omega_\sigma(\vec{k}) \omega_{\sigma_1}(\vec{k}_1) \omega_{\sigma_2}(\vec{k}_2)} \\
& \times \left[\underbrace{n_{\sigma_1}^{(0)}(\vec{k}_1) n_{\sigma_2}^{(0)}(\vec{k}_2)}_{(3)} - \underbrace{n_\sigma^{(0)}(\vec{k}) n_{\sigma_2}^{(0)}(\vec{k}_2)}_{(4)} + \underbrace{n_\sigma^{(0)}(\vec{k}) n_{\sigma_1}^{(0)}(\vec{k}_1)}_{(5)} \right] \quad (10.58)
\end{aligned}$$

The processes can all be described as the collision of two phonons or antiphonons that result in a third phonon or antiphonon. ^a

1. $1 + 2 \rightarrow 0$: create a particle $\underbrace{(\vec{k}, \sigma)}_{\text{"0"}}$ from two particles, $\underbrace{(\vec{k}_1, \sigma_1)}_{\text{"1"}}$ and $\underbrace{(\vec{k}_2, \sigma_2)}_{\text{"2"}}$.
2. $0 + 2 \rightarrow 1$: annihilate a particle $\underbrace{(\vec{k}, \sigma)}_{\text{"0"}}$ by a collision with $\underbrace{(\vec{k}_2, \sigma_2)}_{\text{"2"}}$ to form $\underbrace{(\vec{k}_1, \sigma_1)}_{\text{"1"}}$.
3. $1 + \bar{2} \rightarrow 0$ create a particle $\underbrace{(\vec{k}, \sigma)}_{\text{"0"}}$ from a particle $\underbrace{(\vec{k}_1, \sigma_1)}_{\text{"1"}}$ and an antiparticle $\underbrace{(-\vec{k}_2, \sigma_2)}_{\text{"2"}}$.
4. $0 + \bar{2} \rightarrow 1$ annihilate a particle $\underbrace{(\vec{k}, \sigma)}_{\text{"0"}}$ by a collision with antiparticle $\underbrace{(-\vec{k}_2, \sigma_2)}_{\text{"2"}}$ to form $\underbrace{(\vec{k}_1, \sigma_1)}_{\text{"1"}}$.
5. $0 + \bar{1} \rightarrow \bar{2}$ create a particle $\underbrace{(\vec{k}, \sigma)}_{\text{"0"}}$ by a collision with an antiparticle $\underbrace{(-\vec{k}_1, \sigma_1)}_{\text{"1"}}$ to form an antiparticle $\underbrace{(\vec{k}_2, \sigma_2)}_{\text{"2"}}$. **Editor: check this!**

Editor: Clean the descriptions up

Editor: There is a sign error!

^aWith antiphonon we simply denote a phonon with a negative energy $\hbar\omega_\lambda$. The term antiphonon is not common practice. However, for particle with mass, the negative energy solutions are identified with antiparticles.

For an easier comparison with the quantum expression Eq. 10.93 derived later, when we express the result with the **intrinsic probabilities of transition** defined in Eq. 10.94. **Editor: There is probably a factor 2 between the definition here and the one in the section Boltzmann equation.**

$$\begin{aligned}
\partial_t n_\sigma(k) = & \sum_{\vec{k}_1, \vec{k}_2, \sigma_1 > 0, \sigma_2 > 0} L_{\vec{k}_1, \sigma_1; \vec{k}_2, \sigma_2}^{\vec{k}, \sigma} \left[\frac{1}{2} n_{\sigma_1}^{(0)}(\vec{k}_1) n_{\sigma_2}^{(0)}(\vec{k}_2) - n_\sigma^{(0)}(\vec{k}) n_{\sigma_2}^{(0)}(\vec{k}_2) \right] \\
& + \sum_{\vec{k}_1, \vec{k}_2, \sigma_1 > 0, \sigma_2 > 0} L_{\vec{k}_1, \sigma_1}^{\vec{k}, \sigma; \vec{k}_2, \sigma} \left[n_{\sigma_1}^{(0)}(\vec{k}_1) n_{\sigma_2}^{(0)}(\vec{k}_2) - n_\sigma^{(0)}(\vec{k}) n_{\sigma_2}^{(0)}(\vec{k}_2) + n_\sigma^{(0)}(\vec{k}) n_{\sigma_1}^{(0)}(\vec{k}_1) \right]
\end{aligned}$$

10.5.1 Units of quantities

For testing purposes, I list here the units of the quantities involved:

UNITS

$u_{j,\vec{r}}$	$\sim m$	displacement
c	$\sim \frac{kg}{s^2}$	force constant
d	$\sim \frac{kg}{ms^2}$	anharmonicity
D	$\sim \frac{1}{s^2}$	dynamical matrix
u	$\sim \frac{1}{\sqrt{kg}}$	eigenmode
Q	~ 1	amplitude
A	$\sim \frac{1}{ms^2\sqrt{kg}}$	anharmonic coupling
\hbar	$\sim \frac{kgm^2}{s}$	Planck quantum
Y	$\sim \frac{1}{s^2}$	anharmonic coupling
b^\pm	~ 1	phonon amplitude
Γ	$\sim \frac{1}{s}$	rate constant

10.6 Quantum derivation of the collision term

In chapter 8 on the Boltzmann equation we introduced quantum effects in section 8.2.4 by including a factor $(1 \pm f_n(\vec{p}, \vec{r}))$ with the occupation of the final state in the intrinsic scattering probability. This was based on a plausibility argument. The goal here is to extend the theory to nuclei treated quantum mechanically. As a result we will see how this factor emerges naturally.

By quantizing the nuclear motion, we effectively do the step to a quantum field theory. This is only one of many possible routes to quantum field theory. While the principles of second quantization are analogous for phonons and electrons, the route presented here is most natural for phonons, because it emerges naturally out of the first quantization we are familiar with.

10.6.1 From the Lagrangian to ladder operators

In this section, I will walk you through the main steps from a classical Lagrange function to the quantum-mechanical description of the phonon modes. I will emphasize the steps from a classical to a quantum description and the relation between normal coordinates and phonon amplitudes. In order to simplify the derivation, I drop the anharmonicity and the sum over phonons. Hence we deal with a simple one-dimensional harmonic oscillator. Otherwise I will adhere to the notation used in this book.

We begin with the Lagrangian Eq. 7.67, without anharmonic terms at first, which has the simplified form⁹

$$\mathcal{L}(Q, V, t) = \frac{1}{2} \frac{\hbar}{2\omega} V^2 - \frac{1}{2} \frac{\hbar\omega}{2} Q^2 \quad (10.60)$$

From the Lagrange function, we obtain the Hamilton function, which we need to obtain the Hamilton operator.

$$\mathcal{H}(P, Q, t) = \text{stat}_V (PV - \mathcal{L}(Q, V, t)) \quad (10.61)$$

The symbol stat_V implies that the value is to be taken at a point of the following expression, where the derivative with respect to V vanish. Thus, it is similar but also more general than the min or max symbols.

The canonical momentum is defined by the stationary condition of Eq. 10.61

$$P(Q, V, t) = \frac{\partial \mathcal{L}}{\partial V} = \frac{\hbar}{2\omega} V \quad (10.62)$$

This expression is inverted to obtain the velocity V at the stationary point in terms of coordinates Q and momenta P .

$$V(Q, P, t) = \frac{2\omega}{\hbar} P \quad (10.63)$$

⁹Normally, one writes \dot{Q} instead of V . While I frequently use it myself to avoid introduction of a new symbol, I consider this sloppy notation. The reason is that the action is defined

$$S[Q(t)] = \int_{[Q(t)]} dt \mathcal{L}(Q(t), \dot{Q}(t), t) \quad (10.59)$$

with $\dot{Q}(t)$ as value of the second argument V of the Lagrange function. Nevertheless, the Lagrange function is a normal function of regular numbers. The Euler-Lagrange equation $\partial_t \frac{\partial \mathcal{L}}{\partial V} = \frac{\partial \mathcal{L}}{\partial Q}$ obtains a second equation $\dot{Q} = V$ as partner. The two equations are equivalent to Hamilton's equations.

This result is used to obtain a closed expression for the Hamilton function

$$\begin{aligned}
\mathcal{H}(Q, P, t) &= PV(Q, P, t) - \mathcal{L}(Q, V(Q, P, t), t) \\
&= \frac{2\omega}{\hbar} P^2 - \frac{1}{2} \frac{\hbar}{2\omega} \left(\frac{2\omega}{\hbar} P \right)^2 + \frac{1}{2} \frac{\hbar\omega}{2} Q^2 \\
&= \frac{1}{2} \frac{2\omega}{\hbar} P^2 + \frac{1}{2} \frac{\hbar\omega}{2} Q^2 \\
&= \hbar\omega \left[\frac{1}{\hbar^2} P^2 + \frac{1}{4} Q^2 \right]
\end{aligned} \tag{10.64}$$

The quantization, that is the transition from a Hamilton function to a Hamilton operator is done by replacing the coordinates and momenta by the corresponding operators, which obey the commutator relations $[\hat{P}, \hat{Q}]_- = \frac{\hbar}{i}$.

Before doing this step, let me transform the Hamilton functions onto what I denoted the phonon amplitudes, which will turn into creation and annihilation operators.

Let me introduce the variables Eq. ??

$$\begin{aligned}
b^* &= \frac{1}{2} \left(Q + \frac{1}{i\omega} V \right) = \frac{1}{2} \left(Q + \frac{2}{i\hbar} P \right) \\
b &= \frac{1}{2} \left(Q - \frac{1}{i\omega} V \right) = \frac{1}{2} \left(Q - \frac{2}{i\hbar} P \right)
\end{aligned} \tag{10.65}$$

which correspond to our $b^* = b_{+\sigma}^f e^{i\omega\sigma t}$ and $b = b_{-\sigma}^f e^{-i\omega\sigma t}$.

Now, we do the quantization by replacing momentum and coordinates by operators.

$$\begin{aligned}
\hat{b}^\dagger &= \frac{1}{2} \left(\hat{Q} + \frac{2}{i\hbar} \hat{P} \right) \\
\hat{b} &= \frac{1}{2} \left(\hat{Q} - \frac{2}{i\hbar} \hat{P} \right)
\end{aligned} \tag{10.66}$$

Next we will require the commutator and anticommutator relations. For that purpose, I work out the products of the phonon amplitudes

$$\begin{aligned}
\hat{b}^\dagger \hat{b} &= \frac{1}{2} \left(\hat{Q} + \frac{2}{i\hbar} \hat{P} \right) \frac{1}{2} \left(\hat{Q} - \frac{2}{i\hbar} \hat{P} \right) = \frac{1}{4} \left(\hat{Q}^2 + \frac{4}{\hbar^2} \hat{P}^2 + \frac{2}{i\hbar} [\hat{P}, \hat{Q}]_- \right) \\
&= \frac{1}{4} \hat{Q}^2 + \frac{1}{\hbar^2} \hat{P}^2 - \frac{1}{2} \\
\hat{b} \hat{b}^\dagger &= \frac{1}{2} \left(\hat{Q} - \frac{2}{i\hbar} \hat{P} \right) \frac{1}{2} \left(\hat{Q} + \frac{2}{i\hbar} \hat{P} \right) = \frac{1}{4} \left(\hat{Q}^2 + \frac{4}{\hbar^2} \hat{P}^2 - \frac{2}{i\hbar} [\hat{P}, \hat{Q}]_- \right) \\
&= \frac{1}{4} \hat{Q}^2 + \frac{1}{\hbar^2} \hat{P}^2 + \frac{1}{2}
\end{aligned} \tag{10.67}$$

which are combined to yield the known commutator relations

$$\begin{aligned}
[\hat{b}^\dagger, \hat{b}]_+ &= 2 \left(\frac{1}{4} \hat{Q}^2 + \frac{1}{\hbar^2} \hat{P}^2 \right) = \frac{2}{\hbar\omega} \hat{H} \\
[\hat{b}, \hat{b}^\dagger]_- &= 1
\end{aligned} \tag{10.68}$$

The anticommutator yields the Hamiltonian

$$\hat{H} = \frac{\hbar\omega}{2} [\hat{b}^\dagger, \hat{b}]_+ = \frac{\hbar\omega}{2} \left(\hat{b}^\dagger \hat{b} + \underbrace{\hat{b} \hat{b}^\dagger}_{1 - \hat{b}^\dagger \hat{b}} \right) = \hbar\omega \left(\hat{b}^\dagger \hat{b} + \frac{1}{2} \right) \tag{10.69}$$

From here on, we proceed analogously to the quantum treatment of a harmonic oscillator. It is described for example in section 5.6 of ΦSX : Quantum theory[4].

The basis of energy eigenstates can be constructed from the ground state $|0\rangle$ via

$$|n\rangle = \frac{1}{\sqrt{n!}} (\hat{b}^\dagger)^n |0\rangle$$

with

$$\hat{H}|n\rangle = |n\rangle \hbar\omega \left(n + \frac{1}{2} \right)$$

10.6.2 The phonon Hamiltonian

Let us return again to the Lagrangian Eq. 7.67, expressed in terms of in normal modes. Now, we also consider the anharmonicity and the phonons.

This will allow us to write down the many-phonon Hamiltonian.

$$\begin{aligned} \mathcal{L}(\vec{Q}, \vec{V}, t) &= \frac{1}{2} \sum_{k,\sigma} \frac{\hbar}{2\omega_\sigma(\vec{k})} V_\sigma(\vec{k}) V_\sigma^*(\vec{k}) - \frac{1}{2} \sum_{\vec{k},\sigma} \frac{\hbar\omega_\sigma(\vec{k})}{2} Q_\sigma(\vec{k}) Q_\sigma^*(\vec{k}) \\ &- \frac{1}{3!} \left(\frac{\hbar}{2} \right)^{\frac{3}{2}} \sum_{\vec{k},\vec{k}',\vec{k}''} \sum_{\sigma,\sigma',\sigma''} \frac{A_{\sigma,\sigma',\sigma''}(\vec{k},\vec{k}',\vec{k}'')/\sqrt{\mathcal{N}}}{\sqrt{\omega_\sigma(\vec{k})\omega_{\sigma'}(\vec{k}')\omega_{\sigma''}(\vec{k}'')}} Q_\sigma(\vec{k}, t) Q_{\sigma'}(\vec{k}') Q_{\sigma''}(\vec{k}'') \end{aligned} \quad (10.70)$$

The argument \vec{Q} implies the dependence on all components $Q_\sigma(\vec{k})$ for all k-points. Similarly, \vec{V} is the vector of velocities $V_\sigma(\vec{k})$ of the normal modes of all components for all k-points.

Now, we construct the Hamiltonian by introducing the canonical momentum

$$P_\sigma(\vec{k}, \vec{Q}, \vec{V}, t) = \frac{\partial \mathcal{L}(\vec{Q}, \vec{V}, t)}{\partial V_\sigma(\vec{k})} = \frac{\hbar}{4\omega_\sigma(\vec{k})} V_\sigma^*(\vec{k}) \quad (10.71)$$

so that we arrive at the Hamilton function

$$\begin{aligned} \mathcal{H}(\vec{Q}, \vec{P}, t) &= \sum_{k,\sigma} P_\sigma(\vec{k}) V_\sigma(\vec{k}) + P_\sigma^*(\vec{k}) V_\sigma^*(\vec{k}) - \mathcal{L}(\vec{Q}, \vec{V}, t) \\ &= \frac{1}{2} \sum_{k,\sigma} \frac{8\omega_\sigma(\vec{k})}{\hbar} P_\sigma(\vec{k}) P_\sigma(\vec{k}) + \frac{1}{2} \sum_{\vec{k},\sigma} \frac{\hbar\omega_\sigma(\vec{k})}{2} Q_\sigma(\vec{k}) Q_\sigma^*(\vec{k}) \\ &+ \frac{1}{6} \left(\frac{\hbar}{2} \right)^{\frac{3}{2}} \sum_{\vec{k},\vec{k}',\vec{k}''} \sum_{\sigma,\sigma',\sigma''} \frac{A_{\sigma,\sigma',\sigma''}(\vec{k},\vec{k}',\vec{k}'')/\sqrt{\mathcal{N}}}{\sqrt{\omega_\sigma(\vec{k})\omega_{\sigma'}(\vec{k}')\omega_{\sigma''}(\vec{k}'')}} Q_\sigma(\vec{k}, t) Q_{\sigma'}(\vec{k}') Q_{\sigma''}(\vec{k}'') \end{aligned} \quad (10.72)$$

We can quantize the atomic motion, simply by replacing each normal coordinate $Q_\sigma(\vec{k})$ and the corresponding canonical momentum $P_\sigma(\vec{k})$ into operators $\hat{Q}_\sigma(\vec{k})$ and $\hat{P}_\sigma(\vec{k})$ which obey the commutator relations

$$[\hat{P}_\sigma(\vec{k}), \hat{Q}_{\sigma'}(\vec{k}')]_- = \frac{\hbar}{i} \delta_{\sigma,\sigma'} \cdot \delta(\vec{k} - \vec{k}') \quad (10.73)$$

Because the coordinates and momenta depend on a continuous variable, the wave vector, the quantization leads to a quantum theory. Interesting is to understand what the operators act on. Apparently the wave function

$$|\Phi\rangle = \int d^\infty Q |\vec{Q}\rangle \underbrace{\langle \vec{Q} | \Phi \rangle}_{\Phi(\vec{Q})} = \int \mathcal{D}[\vec{Q}(\vec{k})] \underbrace{|[\vec{Q}(\vec{k})]\rangle}_{\Phi[\vec{Q}]} \langle [\vec{Q}(\vec{k})] | \Phi \rangle \quad (10.74)$$

is a functional of the normal-mode coordinates, rather than a function. We use the symbol $\mathcal{D}[Q]$ to indicate that we integrate over all possible fields.

Before proceeding along this direction of quantizing the fields, let me transform the normal coordinates to phonon amplitudes. From Eq. U.23 and Eq. U.24 we defined the phonon amplitudes as

$$b_{n,\sigma}(\vec{k}) \stackrel{\text{Eq. U.23}}{=} e^{-i\sigma\omega_n(\vec{k})t} \sqrt{\frac{\mathcal{N}}{2\hbar\omega_n(\vec{k})}} \left(\omega_n(\vec{k})Q_n(\vec{k}) - i\sigma V_n(\vec{k}) \right) \quad (10.75)$$

$$Q_n(\vec{k}) \stackrel{\text{Eq. U.24}}{=} \frac{\hbar}{\sqrt{2\mathcal{N}\hbar\omega_n(\vec{k})}} \sum_{\sigma \in \pm} b_{n,\sigma}(\vec{k}) e^{i\sigma\omega_n(\vec{k})t} \quad (10.76)$$

$$\hat{Q}_\sigma(\vec{k}) = \hat{b}_\sigma^\dagger(\vec{k}) + \hat{b}_\sigma(-\vec{k}) \quad (10.77)$$

$$\hat{P}_\sigma(\vec{k}) = 2i\hbar \left(\hat{b}_\sigma^\dagger(\vec{k}) - \hat{b}_\sigma(-\vec{k}) \right) \Rightarrow [\hat{P}, \hat{Q}]_- = \frac{\hbar}{i} \quad \text{with} \quad [\hat{b}, \hat{b}^\dagger] = 1 \quad (10.78)$$

$$\begin{aligned} \mathcal{H} &= \sum_{\vec{k}, \sigma} P_\sigma(\vec{k}) \dot{Q}_\sigma^*(\vec{k}) + P_\sigma^*(\vec{k}) \dot{Q}_\sigma(\vec{k}) - \mathcal{L} \\ &= \frac{1}{2} \sum_{\vec{k}, \sigma} \frac{8\omega_\sigma(\vec{k})}{\hbar} P_\sigma(\vec{k}) P_\sigma^*(\vec{k}) + \frac{1}{2} \sum_{\vec{k}, \sigma} \frac{\hbar\omega_\sigma(\vec{k})}{2} Q_\sigma(\vec{k}) Q_\sigma^*(\vec{k}) \\ &\quad + \frac{1}{6} \left(\frac{\hbar}{2} \right)^{\frac{3}{2}} \sum_{\vec{k}, \vec{k}', \vec{k}''} \sum_{\sigma, \sigma', \sigma''} \frac{A_{\sigma, \sigma', \sigma''}(\vec{k}, \vec{k}', \vec{k}'') / \sqrt{\mathcal{N}}}{\sqrt{\omega_\sigma(\vec{k})\omega_{\sigma'}(\vec{k}')\omega_{\sigma''}(\vec{k}'')}} Q_\sigma(\vec{k}, t) Q_{\sigma'}(\vec{k}', t) Q_{\sigma''}(\vec{k}'', t) \end{aligned}$$

With the transformation

$$Q_\sigma(\vec{k}, t) = b_\sigma^+(\vec{k}, t) e^{+i\omega_\sigma(\vec{k})t} + b_\sigma^-(\vec{k}, t) e^{-i\omega_\sigma(\vec{k})t}$$

defined and the condition for real-valued amplitudes Eq. ?? $b_\sigma^-(\vec{k}) \stackrel{\text{def}}{=} \left(b_\sigma^+(\vec{k}) \right)^*$, we may translate

$$\begin{aligned} \hat{Q}_\sigma(\vec{k}, t) &= \hat{b}_{l,\sigma}^\dagger(\vec{k}, t) e^{+i\omega_\sigma(\vec{k})t} + \hat{b}_{l,\sigma}(-\vec{k}, t) e^{-i\omega_\sigma(\vec{k})t} \\ &= e^{\frac{i}{\hbar} \hat{H}_0 t} \hat{b}_{l,\sigma}^\dagger(\vec{k}, t) e^{-\frac{i}{\hbar} \hat{H}_0 t} + e^{\frac{i}{\hbar} \hat{H}_0 t} \hat{b}_{l,\sigma}(-\vec{k}, t) e^{-\frac{i}{\hbar} \hat{H}_0 t} \end{aligned}$$

which expresses the operators \hat{b}_l in the interaction picture with the harmonic terms defining the unperturbed Hamiltonian \hat{H}_0 .

The corresponding Hamiltonian is¹⁰

$$\begin{aligned}
\mathcal{H} &= \sum_{k,\sigma} \hbar\omega_\sigma(\vec{k}) \left(\hat{b}_\sigma^\dagger(\vec{k}) \hat{b}_\sigma(\vec{k}) + \frac{1}{2} \right) + \frac{1}{6} \left(\frac{\hbar}{2} \right)^{\frac{3}{2}} \sum_{\vec{k},\vec{k}',\vec{k}''} \sum_{\sigma,\sigma',\sigma''} \\
&\quad \frac{A_{\sigma,\sigma',\sigma''}(\vec{k},\vec{k}',\vec{k}'')/\sqrt{N}}{\sqrt{\omega_\sigma(\vec{k})\omega_{\sigma'}(\vec{k}')\omega_{\sigma''}(\vec{k}'')}} \left(\hat{b}_\sigma^\dagger(\vec{k}) + \hat{b}_\sigma(\vec{k}) \right) \left(\hat{b}_{\sigma'}^\dagger(\vec{k}') + \hat{b}_{\sigma'}(\vec{k}') \right) \left(\hat{b}_{\sigma''}^\dagger(\vec{k}'') + \hat{b}_{\sigma''}(\vec{k}'') \right) \\
&= \sum_{k,\sigma}^{\pm} \frac{1}{2} \hbar\omega_\sigma(\vec{k}) \hat{b}_{-\sigma}(\vec{k}) \hat{b}_\sigma(\vec{k}) \\
&\quad + \frac{1}{6} \left(\frac{\hbar}{2} \right)^{\frac{3}{2}} \sum_{\vec{k},\vec{k}',\vec{k}''} \sum_{\sigma,\sigma',\sigma''}^{\pm} \frac{A_{\sigma,\sigma',\sigma''}(\vec{k},\vec{k}',\vec{k}'')/\sqrt{N}}{\sqrt{\omega_\sigma(\vec{k})\omega_{\sigma'}(\vec{k}')\omega_{\sigma''}(\vec{k}'')}} \hat{b}_\sigma(\vec{k}) \hat{b}_{\sigma'}(\vec{k}') \hat{b}_{\sigma''}(\vec{k}'')
\end{aligned} \tag{10.79}$$

We have extended the sum over positive and negative values of σ , where we introduced

$$\hat{b}_\sigma = \begin{cases} \hat{b}_\sigma^\dagger(\vec{k}) & \text{for } \sigma > 0 \\ \hat{b}_\sigma(-\vec{k}) & \text{for } \sigma < 0 \end{cases}$$

The many-phonon wave function has the form

$$\begin{aligned}
|\Phi(t)\rangle &= \sum_{\vec{n}} |\vec{n}\rangle c_{\vec{n}}(t) = \sum_{\vec{m}} \prod_{\vec{k},\sigma>0} \left(\hat{b}_\sigma^\dagger(\vec{k}) \right)^{m_{\vec{k},\sigma}} |\mathcal{O}\rangle c_{\vec{m}}(t) \\
|\vec{n}\rangle &= \prod_{\vec{k},\sigma>0} \left(\hat{b}_\sigma^\dagger(\vec{k}) \right)^{n_{\vec{k},\sigma}} |\mathcal{O}\rangle
\end{aligned} \tag{10.80}$$

where $|\vec{n}\rangle$ is the number representation forming the many-particle basis set and $|\mathcal{O}\rangle$ is the vacuum state.

10.6.3 Random-phase approximation and rate equation

The random-phase approximation for quantum systems is derived in the appendix I, '*Random-Phase approximation*' of *ΦSX:Quantum Theory*[4]. In our case, the perturbation is the interaction between the phonons. While the interaction is time-independent we make a Gedankenexperiment, where the interaction is switched on and switched off at some later time. We choose $\omega = 0$ and \hat{W} the phonon-phonon interaction operator.

In the limit of the Fermi's golden rule we obtain

¹⁰Compared to Eq. Chernatynskiy-B4 the creation and annihilation operators translate as

$$\hat{b}_\sigma^\dagger(\vec{k}) \rightarrow i a_{-\vec{k},\sigma}^* \quad \text{and} \quad \hat{b}_\sigma(\vec{k}) \rightarrow -i a_{\vec{k},\sigma}$$

In addition there is an unexplained factor $\sqrt{\frac{V}{N}}$. Note also that the k-vectors in our notation differ in sign from those of Chernatynskiy and Ziman.

RATE EQUATION USING FERMI'S GOLDEN RULE

$$\partial_t P_{\vec{n}}(t) = \sum_{\vec{m}} \left(\Gamma_{\vec{n} \leftarrow \vec{m}} P_{\vec{m}}(t) - \Gamma_{\vec{m} \leftarrow \vec{n}} P_{\vec{n}}(t) \right) \quad (10.81)$$

with

$$\Gamma_{\vec{n} \leftarrow \vec{m}} = \frac{2\pi}{\hbar} \left| \langle \vec{n} | \hat{W} | \vec{m} \rangle \right|^2 \delta(E_{\vec{n}} - E_{\vec{m}} - \hbar\omega) = \Gamma_{\vec{m} \leftarrow \vec{n}} \quad (10.82)$$

Note that this approximation rests on a number of seemingly contradicting assumptions. The transition probability is symmetric

$$\Gamma_{\vec{n} \leftarrow \vec{m}} = \Gamma_{\vec{m} \leftarrow \vec{n}} \quad (10.83)$$

Here $P_{\vec{n}}(t)$ are the probabilities of many-phonon states $|\vec{n}\rangle$. In our case the interaction is time independent and therefore $\hbar\omega = 0$.

In the random-phase approximation the phonon density matrix collapses into a diagonal matrix in the phonon-number representation. As in the classical case the random-phase approximation additionally ensures that the off-diagonal elements do not develop. This approximation implies the absence of entangled phonons.

The change of occupations $f_{\lambda}(t) = \sum_{\vec{n}} P_{\vec{n}}(t) n_{\lambda}$ can be obtained from the rate equation

$$\begin{aligned} \frac{\partial f_{\lambda}}{\partial t} &= \sum_{\vec{n}} n_{\lambda} \partial_t P_{\vec{n}}(t) \stackrel{\text{Eq. 10.81}}{=} \sum_{\vec{n}, \vec{m}} n_{\lambda} \left(\Gamma_{\vec{n} \leftarrow \vec{m}} P_{\vec{m}}(t) - \Gamma_{\vec{m} \leftarrow \vec{n}} P_{\vec{n}}(t) \right) \\ &= \sum_{\vec{n}, \vec{m}} (n_{\lambda} - m_{\lambda}) \Gamma_{\vec{n} \leftarrow \vec{m}} P_{\vec{m}} \end{aligned} \quad (10.84)$$

Thus, a transition $\vec{n} \leftarrow \vec{m}$ only contributes when $n_{\lambda} = m_{\lambda} + 1$ and it contributes with negative sign when $n_{\lambda} = m_{\lambda} - 1$.

$$\frac{\partial f_{\lambda}}{\partial t} = \sum_{\vec{m}} P_{\vec{m}} \sum_{\vec{n}} \left(\delta_{m_{\lambda}, n_{\lambda}+1} - \delta_{m_{\lambda}, n_{\lambda}-1} \right) \underbrace{\frac{2\pi}{\hbar} \left| \langle \vec{n} | \hat{W} | \vec{m} \rangle \right|^2 \delta(E_{\vec{n}} - E_{\vec{m}} - \hbar\omega)}_{\Gamma_{\vec{n} \leftarrow \vec{m}}} \quad (10.85)$$

Let us now consider all the potential transitions from a given configuration $|\vec{n}\rangle$ that change the occupation number of the phonon λ :

- There is one matrix element having a product of three creation operators and one with three annihilation operators. Because the argument of $\delta(\hbar\omega_{\lambda} + \hbar\omega_{\lambda'} + \hbar\omega_{\lambda'})$ never vanishes, these matrix elements do not contribute. In other words such a process always violates energy conservation.
- There are matrix elements where two phonons are created and one is annihilated. There are two possibilities, namely that phonon λ is created or that it is annihilated.
- There are matrix elements where two phonons are annihilated and one is created. There are two possibilities, namely that phonon λ is created or that it is annihilated.

$$\begin{aligned}
\frac{df_\lambda}{dt} = & \frac{1}{2} \sum_{\lambda', \lambda''} \sum_{\vec{n}} P_{\vec{n}} \\
& \times \left\{ \frac{2\pi}{\hbar} \left| \langle n_\lambda + 1, n_{\lambda'} - 1, n_{\lambda''} - 1 | \hat{W} | n_\lambda, n_{\lambda'}, n_{\lambda''} \rangle \right|^2 \delta(\hbar\omega_\lambda - \hbar\omega_{\lambda'} - \hbar\omega_{\lambda''}) \right. \\
& + \frac{2\pi}{\hbar} \left| \langle n_\lambda + 1, n_{\lambda'} + 1, n_{\lambda''} - 1 | \hat{W} | n_\lambda, n_{\lambda'}, n_{\lambda''} \rangle \right|^2 \delta(\hbar\omega_\lambda + \hbar\omega_{\lambda'} - \hbar\omega_{\lambda''}) \\
& + \frac{2\pi}{\hbar} \left| \langle n_\lambda + 1, n_{\lambda'} - 1, n_{\lambda''} + 1 | \hat{W} | n_\lambda, n_{\lambda'}, n_{\lambda''} \rangle \right|^2 \delta(\hbar\omega_\lambda - \hbar\omega_{\lambda'} + \hbar\omega_{\lambda''}) \\
& - \frac{2\pi}{\hbar} \left| \langle n_\lambda - 1, n_{\lambda'} + 1, n_{\lambda''} + 1 | \hat{W} | n_\lambda, n_{\lambda'}, n_{\lambda''} \rangle \right|^2 \delta(-\hbar\omega_\lambda + \hbar\omega_{\lambda'} + \hbar\omega_{\lambda''}) \\
& - \frac{2\pi}{\hbar} \left| \langle n_\lambda - 1, n_{\lambda'} - 1, n_{\lambda''} + 1 | \hat{W} | n_\lambda, n_{\lambda'}, n_{\lambda''} \rangle \right|^2 \delta(-\hbar\omega_\lambda - \hbar\omega_{\lambda'} + \hbar\omega_{\lambda''}) \\
& \left. - \frac{2\pi}{\hbar} \left| \langle n_\lambda - 1, n_{\lambda'} + 1, n_{\lambda''} - 1 | \hat{W} | n_\lambda, n_{\lambda'}, n_{\lambda''} \rangle \right|^2 \delta(-\hbar\omega_\lambda + \hbar\omega_{\lambda'} - \hbar\omega_{\lambda''}) \right\}
\end{aligned}$$

The factor $\frac{1}{2}$ compensates the double counting of pairs (λ', λ'') and (λ'', λ') . The transitions 3 and 4 as well as the transitions 5 and 6 can be combined into the same term after exchanging λ' and λ'' in one of the terms.

NEGLECT OF DOUBLE EXCITATIONS AND ELASTIC DISTORTIONS

In the above equation we implicitly assumed that all three participating phonons are distinct, that is $\lambda \neq \lambda' \neq \lambda''$. This implies that we ignore cases where two phonons with the same quantum number are simultaneously deleted or created.

Respectively we ignore that a three-phonon process creates and annihilates the same phonon, resulting in an effective single phonon scattering event. because of the energy and momentum conservation the latter effect does only occur for phonons at the Gamma point with zero energy. This it is probably a process such as thermal expansion.

The Hamiltonian Eq. 10.79 is of the form

$$\hat{W} = \sum_{\lambda, \lambda', \lambda''} X_{\lambda, \lambda', \lambda''} (\hat{b}_\lambda^\dagger + \hat{b}_{-\lambda}) (\hat{b}_{\lambda'}^\dagger + \hat{b}_{-\lambda'}) (\hat{b}_{\lambda''}^\dagger + \hat{b}_{-\lambda''}) \quad (10.86)$$

where $-\lambda$ stands for $-\vec{k}, \sigma$.

We need to evaluate matrix elements of the form

$$\begin{aligned}
\langle n_\lambda + 1, n_{\lambda'} + 1, n_{\lambda''} - 1 | \hat{b}_\lambda^\dagger \hat{b}_{\lambda'}^\dagger \hat{b}_{\lambda''} | n_\lambda, n_{\lambda'}, n_{\lambda''} \rangle &= \sqrt{(n_\lambda + 1)(n_{\lambda'} + 1)n_{\lambda''}} \\
\langle n_\lambda + 1, n_{\lambda'} + 1, n_{\lambda''} - 1 | \hat{b}_\lambda^\dagger \hat{b}_{\lambda'} \hat{b}_{\lambda''} | n_\lambda, n_{\lambda'}, n_{\lambda''} \rangle &= \sqrt{(n_\lambda + 1)n_{\lambda'} n_{\lambda''}}
\end{aligned}$$

where we used

$$\begin{aligned}
|n\rangle &= \frac{1}{\sqrt{n!}} (\hat{b}^\dagger)^n |0\rangle \\
\hat{b}^\dagger |n\rangle &= \frac{1}{\sqrt{(n+1)!}} (\hat{b}^\dagger)^{n+1} |0\rangle \sqrt{n+1} = |n+1\rangle \sqrt{n+1} \\
\hat{b} |n\rangle &= \frac{1}{\sqrt{(n-1)!}} (\hat{b}^\dagger)^{n-1} |0\rangle \sqrt{n} = |n-1\rangle \sqrt{n} \\
\hat{b}^2 |n\rangle &= \hat{b} |n-1\rangle \sqrt{n} = |n-2\rangle \sqrt{n(n-1)}
\end{aligned}$$

but we ignored matrix elements where two or more operators act on the same phonon.

$$\begin{aligned} \frac{df_{\lambda}}{dt} = \frac{1}{2} \sum_{\lambda', \lambda''} \sum_{\vec{n}} P_{\vec{n}} \left\{ \frac{2\pi}{\hbar} \left| 6X_{\lambda, -\lambda', -\lambda''} \right|^2 (n_{\lambda} + 1) n_{\lambda'} n_{\lambda''} \delta(\hbar\omega_{\lambda} - \hbar\omega_{\lambda'} - \hbar\omega_{\lambda''}) \right. \\ + \frac{2\pi}{\hbar} \left| 6X_{\lambda, \lambda', -\lambda''} \right|^2 (n_{\lambda} + 1)(n_{\lambda'} + 1) n_{\lambda''} \delta(\hbar\omega_{\lambda} + \hbar\omega_{\lambda'} - \hbar\omega_{\lambda''}) \\ - \frac{2\pi}{\hbar} \left| 6X_{-\lambda, \lambda', \lambda''} \right|^2 n_{\lambda} (n_{\lambda'} + 1)(n_{\lambda''} + 1) \delta(\hbar\omega_{\lambda} - \hbar\omega_{\lambda'} - \hbar\omega_{\lambda''}) \\ \left. - \frac{2\pi}{\hbar} \left| 6X_{-\lambda, -\lambda', \lambda''} \right|^2 n_{\lambda} n_{\lambda'} (n_{\lambda''} + 1) \delta(\hbar\omega_{\lambda} + \hbar\omega_{\lambda'} - \hbar\omega_{\lambda''}) \right\} \end{aligned}$$

We have changed the sign of the arguments of the delta functions in the last two terms. The factor six enters because there are several terms of the Hamiltonian connecting initial and final states. They differ in the permutation of the three indices.

ASSUMPTION OF UNCORRELATED PHONON OCCUPATIONS

Next we assume that the mean occupation numbers of the phonons are uncorrelated, that is

$$\begin{aligned} \langle n_{\lambda} n_{\lambda'} \rangle &= \sum_{\vec{n}} P_{\vec{n}} n_{\lambda} n_{\lambda'} = \left(\sum_{\vec{n}} P_{\vec{n}} n_{\lambda} \right) \left(\sum_{\vec{n}} P_{\vec{n}} n_{\lambda'} \right) = \langle n_{\lambda} \rangle \langle n_{\lambda'} \rangle \quad \text{for } \lambda \neq \lambda' \\ &= f_{\lambda} f_{\lambda'} \quad \text{for } \lambda \neq \lambda' \end{aligned} \quad (10.87)$$

respectively,

$$\begin{aligned} \langle n_{\lambda} n_{\lambda'} n_{\lambda''} \rangle &= \sum_{\vec{n}} P_{\vec{n}} n_{\lambda} n_{\lambda'} n_{\lambda''} = \left(\sum_{\vec{n}} P_{\vec{n}} n_{\lambda} \right) \left(\sum_{\vec{n}} P_{\vec{n}} n_{\lambda'} \right) \left(\sum_{\vec{n}} P_{\vec{n}} n_{\lambda''} \right) \\ &= \langle n_{\lambda} \rangle \langle n_{\lambda'} \rangle \langle n_{\lambda''} \rangle \quad \text{for } \lambda \neq \lambda' \neq \lambda'' \neq \lambda \\ &= f_{\lambda} f_{\lambda'} f_{\lambda''} \quad \text{for } \lambda \neq \lambda' \neq \lambda'' \neq \lambda \end{aligned} \quad (10.88)$$

Editor: The following statement is not a good idea and shall be removed, after all symbols are adjusted. "The mean occupation number will be described by the same symbol as the occupation number because the correct meaning becomes obvious from the context."

This yields

$$\begin{aligned}
\frac{df_\lambda}{dt} = \frac{1}{2} \sum_{\lambda', \lambda''} & \left\{ \underbrace{\frac{2\pi}{\hbar} \left| 6X_{\lambda, -\lambda', -\lambda''} \right|^2}_{L_{\lambda', \lambda''}^\lambda} \delta(\hbar\omega_\lambda - \hbar\omega_{\lambda'} - \hbar\omega_{\lambda''}) (f_\lambda + 1) f_{\lambda'} f_{\lambda''} \right. \\
& + 2 \underbrace{\frac{2\pi}{\hbar} \left| 6X_{\lambda, \lambda', -\lambda''} \right|^2}_{L_{\lambda''}^{\lambda, \lambda'}} \delta(\hbar\omega_\lambda + \hbar\omega_{\lambda'} - \hbar\omega_{\lambda''}) (f_\lambda + 1) (f_{\lambda'} + 1) f_{\lambda''} \\
& - \underbrace{\frac{2\pi}{\hbar} \left| 6X_{-\lambda, \lambda', \lambda''} \right|^2}_{L_\lambda^{\lambda', \lambda''}} \delta(\hbar\omega_\lambda - \hbar\omega_{\lambda'} - \hbar\omega_{\lambda''}) f_\lambda (f_{\lambda'} + 1) (f_{\lambda''} + 1) \\
& \left. - 2 \underbrace{\frac{2\pi}{\hbar} \left| 6X_{-\lambda, -\lambda', \lambda''} \right|^2}_{L_{\lambda, \lambda'}^{\lambda''}} \delta(\hbar\omega_\lambda + \hbar\omega_{\lambda'} - \hbar\omega_{\lambda''}) f_\lambda f_{\lambda'} (f_{\lambda''} + 1) \right\} \quad (10.89)
\end{aligned}$$

This result can be expressed in a more convenient form

$$\begin{aligned}
\frac{df_\lambda}{dt} = \sum_{\lambda', \lambda''} & \left\{ \frac{1}{2} L_{\lambda', \lambda''}^\lambda (f_\lambda + 1) f_{\lambda'} f_{\lambda''} + L_{\lambda''}^{\lambda, \lambda'} (f_\lambda + 1) (f_{\lambda'} + 1) f_{\lambda''} \right. \\
& \left. - \frac{1}{2} L_\lambda^{\lambda', \lambda''} f_\lambda (f_{\lambda'} + 1) (f_{\lambda''} + 1) - L_{\lambda, \lambda'}^{\lambda''} f_\lambda f_{\lambda'} (f_{\lambda''} + 1) \right\} \quad (10.90)
\end{aligned}$$

where the L , defined below in Eq. 10.91, are called **intrinsic probabilities of transition**. (Compare with Chernatynski Gl. A5.)

$$\begin{aligned}
L_{\lambda', \lambda''}^\lambda &= \frac{2\pi}{\hbar} \left| 6X_{\lambda, -\lambda', -\lambda''} \right|^2 \delta(\hbar\omega_\lambda - \hbar\omega_{\lambda'} - \hbar\omega_{\lambda''}) \\
L_{\lambda''}^{\lambda, \lambda'} &= \frac{2\pi}{\hbar} \left| 6X_{\lambda, \lambda', -\lambda''} \right|^2 \delta(\hbar\omega_\lambda + \hbar\omega_{\lambda'} - \hbar\omega_{\lambda''}) \\
L_\lambda^{\lambda', \lambda''} &= \frac{2\pi}{\hbar} \left| 6X_{-\lambda, \lambda', \lambda''} \right|^2 \delta(\hbar\omega_\lambda - \hbar\omega_{\lambda'} - \hbar\omega_{\lambda''}) \\
L_{\lambda, \lambda'}^{\lambda''} &= \frac{2\pi}{\hbar} \left| 6X_{-\lambda, -\lambda', \lambda''} \right|^2 \delta(\hbar\omega_\lambda + \hbar\omega_{\lambda'} - \hbar\omega_{\lambda''})
\end{aligned}$$

It may be helpful to notice that the lower indices of L obtain a negative index of X and a negative sign for $\hbar\omega$ in the delta function.

With

$$X_{\lambda, \lambda', \lambda''} \stackrel{\text{Eq. 10.86}}{=} \frac{1}{6} \left(\frac{\hbar}{2} \right)^{\frac{3}{2}} \frac{A_{\lambda, \lambda', \lambda''} / \sqrt{\mathcal{N}}}{\sqrt{\omega_\lambda \omega_{\lambda'} \omega_{\lambda''}}}$$

we obtain the **intrinsic probabilities of transition**. (Compare with Chernatynski Gl. A5.)

$$\begin{aligned}
L_{\lambda', \lambda''}^\lambda &= \frac{2\pi}{\hbar} \left(\frac{\hbar}{2} \right)^3 \frac{|A_{\lambda, -\lambda', -\lambda''}|^2 / \mathcal{N}}{\omega_\lambda \omega_{-\lambda'} \omega_{-\lambda''}} \delta(\hbar\omega_\lambda - \hbar\omega_{\lambda'} - \hbar\omega_{\lambda''}) \\
L_\lambda^{\lambda', \lambda''} &= \frac{2\pi}{\hbar} \left(\frac{\hbar}{2} \right)^3 \frac{|A_{-\lambda, \lambda', \lambda''}|^2 / \mathcal{N}}{\omega_{-\lambda} \omega_{\lambda'} \omega_{\lambda''}} \delta(\hbar\omega_\lambda - \hbar\omega_{\lambda'} - \hbar\omega_{\lambda''}) \quad (10.91)
\end{aligned}$$

Using the symmetry property that the three phonon scattering matrix A becomes complex conjugate, when the sign of all k -vectors is reversed, we find that the two remaining intrinsic scattering probabilities are identical, that is

$$L_{\lambda',\lambda''}^{\lambda} = L_{\lambda}^{\lambda',\lambda''} \quad (10.92)$$

QUANTUM PHONON-BOLTZMANN EQUATION

$$\partial_t f_{\lambda} + \vec{v}_{\lambda} \vec{\nabla} f_{\lambda} = \sum_{\lambda',\lambda''} \left\{ \frac{1}{2} L_{\lambda',\lambda''}^{\lambda} (f_{\lambda} + 1) f_{\lambda'} f_{\lambda''} + L_{\lambda''}^{\lambda,\lambda'} (f_{\lambda} + 1) (f_{\lambda'} + 1) f_{\lambda''} - \frac{1}{2} L_{\lambda}^{\lambda',\lambda''} f_{\lambda} (f_{\lambda'} + 1) (f_{\lambda''} + 1) - L_{\lambda,\lambda'}^{\lambda''} f_{\lambda} f_{\lambda'} (f_{\lambda''} + 1) \right\} \quad (10.93)$$

with $\lambda = (\vec{k}, \sigma)$, $\lambda' = (\vec{k}', \sigma')$, and $\lambda'' = (\vec{k}'', \sigma'')$, $\vec{v}_{\lambda} := \vec{\nabla}_{\vec{k}} \omega_{\lambda}$, and

$$L_{\vec{k},\sigma}^{\vec{k}',\sigma',\vec{k}'',\sigma''} \stackrel{\text{Eq. 10.91}}{=} \frac{2\pi}{\hbar} \left(\frac{\hbar}{2} \right)^3 \frac{|A_{\sigma,\sigma',\sigma''}(\vec{k}, -\vec{k}', -\vec{k}'')|^2 / \mathcal{N}}{\omega_{\sigma}(\vec{k}) \omega_{\sigma'}(-\vec{k}') \omega_{\sigma''}(-\vec{k}'')} \delta(\hbar \omega_{\sigma}(\vec{k}) - \hbar \omega_{\sigma'}(\vec{k}') - \hbar \omega_{\sigma''}(\vec{k}''))$$

$$L_{\vec{k},\sigma}^{\vec{k}',\sigma',\vec{k}'',\sigma''} \stackrel{\text{Eq. 10.91}}{=} \frac{2\pi}{\hbar} \left(\frac{\hbar}{2} \right)^3 \frac{|A_{\sigma,\sigma',\sigma''}(-\vec{k}, \vec{k}', \vec{k}'')|^2 / \mathcal{N}}{\omega_{\sigma}(-\vec{k}) \omega_{\sigma'}(\vec{k}') \omega_{\sigma''}(\vec{k}'')} \delta(-\hbar \omega_{\sigma}(\vec{k}) + \hbar \omega_{\sigma'}(\vec{k}') + \hbar \omega_{\sigma''}(\vec{k}'')) \quad (10.94)$$

Eq. 10.93 is identical to Chernatynskiy-A5. The different signs are explained by his definition resulting in $\partial_t f_{\lambda} + \vec{v}_{\lambda} \vec{\nabla} f_{\lambda} = - \sum_{\lambda',\lambda''} P_{\lambda,\lambda',\lambda''}$.

Editor: Caution!!!! there is a symbol switch from f to n from here onward.

10.6.4 Classical limit

The classical limit of the phonon Boltzmann equation is obtained for dilute phonon gases, that is if $n_{\lambda} \ll 1$. In this case all triple products of phonon occupations are ignored.

$$\partial_t n_{\lambda} + \vec{v}_{\lambda} \vec{\nabla} n_{\lambda} = \sum_{\lambda',\lambda''} \left\{ \frac{1}{2} L_{\lambda',\lambda''}^{\lambda} n_{\lambda'} n_{\lambda''} + L_{\lambda''}^{\lambda,\lambda'} \left[n_{\lambda}'' + n_{\lambda'} n_{\lambda''} + n_{\lambda} n_{\lambda''} \right] - \frac{1}{2} L_{\lambda}^{\lambda',\lambda''} \left[n_{\lambda} + n_{\lambda} n_{\lambda'} + n_{\lambda} n_{\lambda''} \right] - L_{\lambda,\lambda'}^{\lambda''} n_{\lambda} n_{\lambda'} \right\} \quad (10.95)$$

Pay attention to the terms linear in the occupations!!!

Normally the high-temperature limit is identical to the classical limit. Here, the opposite seems to be true. Only at low temperatures the phonon gas is dilute.

A good description of the classical limit seems appropriate for the optical phonons below the Debye temperature. The current-carrying acoustic modes have occupations that are larger than classical result.

10.6.5 Linearized Boltzmann equation

We introduce a new variable Φ_{λ} (Chernatynsky A6), which plays the role of a quasi Fermi level.

$$n_{\lambda} = n^{eq}(\epsilon_{\lambda} - \Phi_{\lambda}) \approx n_{\lambda}^{eq} - \Phi_{\lambda} \frac{\partial n_{\lambda}^{eq}}{\partial \epsilon_{\lambda}}$$

where

$$n^{eq} = \begin{cases} (e^{\beta(\epsilon-\mu)} - 1)^{-1} & \text{for Bosons} \\ (e^{\beta(\epsilon-\mu)} + 1)^{-1} & \text{for Fermions} \\ (e^{\beta(\epsilon-\mu)})^{-1} & \text{for a Boltzmann gas} \end{cases}$$

is the Bose, Fermi or Boltzmann distribution.

For phonons we use the Bose distribution with $\mu = 0$ and $\epsilon_\lambda = \hbar\omega_\lambda$.

$$\partial_\epsilon n_\lambda^{eq} = \partial_\epsilon \frac{1}{e^{\beta(\epsilon-\mu)} - 1} = -\beta e^{\beta(\epsilon-\mu)} \frac{1}{(e^{\beta(\epsilon-\mu)} - 1)^2} = -\beta (n^{eq})^2 \left((n^{eq})^{-1} + 1 \right) = -\beta n^{eq} (n^{eq} + 1)$$

so that

$$n_\lambda = n^{eq}(\epsilon_\lambda - \Phi_\lambda) \approx n_\lambda^{eq} + \underbrace{\beta \Phi_\lambda n_\lambda^{eq} (1 + n_\lambda^{eq})}_{\delta n_\lambda}$$

This yields

$$\begin{aligned} \delta n_\lambda &= \left[\beta \Phi_\lambda (1 + n_\lambda^{eq}) \right] n_\lambda^{eq} \\ \delta(1 + n_\lambda) &= \left[\beta \Phi_\lambda n_\lambda^{eq} \right] (1 + n_\lambda^{eq}) \\ \delta \left[(1 + n_\lambda^{eq}) n_{\lambda'}^{eq} n_{\lambda''}^{eq} \right] &= \beta \left[\Phi_\lambda n_\lambda^{(eq)} + \Phi_{\lambda'} (1 + n_{\lambda'}^{(eq)}) + \Phi_{\lambda''} (1 + n_{\lambda''}^{(eq)}) \right] (1 + n_\lambda^{eq}) n_{\lambda'}^{eq} n_{\lambda''}^{eq} \\ \delta \left[(1 + n_\lambda)(1 + n_{\lambda'}) n_{\lambda''} \right] &= \beta \left[\pm \Phi_\lambda n_\lambda^{(eq)} \pm \Phi_{\lambda'} n_{\lambda'}^{(eq)} + \Phi_{\lambda''} (1 + n_{\lambda''}^{(eq)}) \right] (1 + n_\lambda^{eq})(1 + n_{\lambda'}^{eq}) n_{\lambda''}^{eq} \end{aligned}$$

Following Chernatynskiy (Eq. Chernatynskiy-B10), we define the **equilibrium transition rate** Λ

$$\begin{aligned} \Lambda_{\lambda',\lambda''}^\lambda &:= L_{\lambda',\lambda''}^\lambda (n_\lambda^{eq} + 1) n_{\lambda'}^{eq} n_{\lambda''}^{eq} \\ \Lambda_{\lambda}^{\lambda',\lambda''} &:= L_{\lambda}^{\lambda',\lambda''} n_\lambda^{eq} (n_{\lambda'}^{eq} + 1) (n_{\lambda''}^{eq} + 1) \end{aligned} \quad (10.96)$$

The intrinsic probabilities of transition L have been defined in Eq. 10.91.

We obtain Eq. 10.93 to first order in the shift of the quasi-chemical potential in the form

$$\begin{aligned} \partial_t n_\lambda &\stackrel{\text{Eq. 10.93}}{=} \sum_{\lambda',\lambda''} \left[+ \frac{1}{2} L_{\lambda',\lambda''}^\lambda (n_\lambda + 1) n_{\lambda'} n_{\lambda''} - L_{\lambda,\lambda'}^{\lambda''} n_\lambda n_{\lambda'} (n_{\lambda''} + 1) \right. \\ &\quad \left. + L_{\lambda''}^{\lambda,\lambda'} (n_\lambda + 1) (n_{\lambda'} + 1) n_{\lambda''} - \frac{1}{2} L_{\lambda}^{\lambda',\lambda''} n_\lambda (n_{\lambda'} + 1) (n_{\lambda''} + 1) \right] \\ &= \sum_{\lambda',\lambda''} \left[+ \frac{1}{2} \Lambda_{\lambda',\lambda''}^\lambda - \Lambda_{\lambda,\lambda'}^{\lambda''} + \Lambda_{\lambda''}^{\lambda,\lambda'} - \frac{1}{2} \Lambda_{\lambda}^{\lambda',\lambda''} \right] \\ &\quad + \beta \sum_{\lambda',\lambda''} \left[+ \frac{1}{2} \Lambda_{\lambda',\lambda''}^\lambda \left(\Phi_\lambda n_\lambda^{(eq)} + \Phi_{\lambda'} (1 + n_{\lambda'}^{(eq)}) + \Phi_{\lambda''} (1 + n_{\lambda''}^{(eq)}) \right) \right. \\ &\quad - \Lambda_{\lambda,\lambda'}^{\lambda''} \left(\Phi_{\lambda''} n_{\lambda''}^{(eq)} + \Phi_\lambda (1 + n_\lambda^{(eq)}) + \Phi_{\lambda'} (1 + n_{\lambda'}^{(eq)}) \right) \\ &\quad + \Lambda_{\lambda''}^{\lambda,\lambda'} \left(\Phi_\lambda n_\lambda^{(eq)} + \Phi_{\lambda'} n_{\lambda'}^{(eq)} + \Phi_{\lambda''} (1 + n_{\lambda''}^{(eq)}) \right) \\ &\quad \left. - \frac{1}{2} \Lambda_{\lambda}^{\lambda',\lambda''} \left(\Phi_{\lambda'} n_{\lambda'}^{(eq)} + \Phi_{\lambda''} n_{\lambda''}^{(eq)} + \Phi_\lambda (1 + n_\lambda^{(eq)}) \right) \right] + O(\Phi^2) \\ &= \beta \sum_{\lambda',\lambda''} \left[+ \frac{1}{2} \Lambda_{\lambda',\lambda''}^\lambda \left(\Phi_{\lambda'} + \Phi_{\lambda''} \right) - \Lambda_{\lambda,\lambda'}^{\lambda''} \left(\Phi_\lambda + \Phi_{\lambda'} \right) + \Lambda_{\lambda''}^{\lambda,\lambda'} \Phi_{\lambda''} - \frac{1}{2} \Lambda_{\lambda}^{\lambda',\lambda''} \Phi_\lambda \right] + O(\Phi^2) \end{aligned}$$

In the last step we exploited the equilibrium condition that says that the equilibrium distribution is stationary so that the zeroth order term vanishes. Using exactly the same condition all terms proportional to n^{eq} cancel as well.

As a consequence of detailed balance Eq. 8.46 and the restriction to elastic (energy-conserving) scattering processes, we have the condition.

$$\Lambda_{\lambda',\lambda''}^{\lambda} = \Lambda_{\lambda}^{\lambda',\lambda''} \quad (10.97)$$

Proof: We start with the definition of the equilibrium transition rate Eq. 10.96.

$$L_{\lambda',\lambda''}^{\lambda}(n_{\lambda}^{eq} + 1)n_{\lambda'}^{eq}n_{\lambda''}^{eq} \stackrel{\text{Eq. 10.96}}{=} \Lambda_{\lambda',\lambda''}^{\lambda} \stackrel{?}{=} \Lambda_{\lambda}^{\lambda',\lambda''} \stackrel{\text{Eq. 10.96}}{=} L_{\lambda}^{\lambda',\lambda''}n_{\lambda}^{eq}(n_{\lambda'}^{eq} + 1)(n_{\lambda''}^{eq} + 1)$$

The intrinsic probabilities of transition are invariant against replacing upper and lower indices according to Eq. 10.92. Thus, we need to show

$$(n_{\lambda}^{eq} + 1)n_{\lambda'}^{eq}n_{\lambda''}^{eq} \stackrel{?}{=} n_{\lambda}^{eq}(n_{\lambda'}^{eq} + 1)(n_{\lambda''}^{eq} + 1) \quad \Leftrightarrow \quad \frac{n_{\lambda}^{eq} + 1}{n_{\lambda}^{eq}} \frac{n_{\lambda'}^{eq}}{n_{\lambda'}^{eq} + 1} \frac{n_{\lambda''}^{eq}}{n_{\lambda''}^{eq} + 1} \stackrel{?}{=} 1$$

For the Bose distribution $\frac{n_{\lambda}^{eq} + 1}{n_{\lambda}^{eq}} = e^{\beta\hbar\omega_{\lambda}}$. Thus

$$e^{\beta(\hbar\omega_{\lambda} - \hbar\omega_{\lambda'} - \hbar\omega_{\lambda''})} = 1 \quad \Leftrightarrow \quad \hbar\omega_{\lambda} - \hbar\omega_{\lambda'} - \hbar\omega_{\lambda''} = 0$$

This is nothing but the energy conservation condition inherent in the definition of the intrinsic probabilities of transition L . This completes the proof of Eq. 10.97.

Eq. 10.97 simplifies the expression further to the collision term in the linearized Phonon Boltzmann equation

LINEARIZED QUANTUM PHONON-BOLTZMANN EQUATION

$$\begin{aligned} & \underbrace{\beta\hbar\omega_{\lambda}n_{\lambda}^{eq}(1+n_{\lambda}^{eq})\beta k_B}_{\partial_T n_{\lambda}^{eq}} \left(\partial_t T + \vec{v}_{\lambda} \vec{\nabla} T \right) + \underbrace{\beta n_{\lambda}^{eq}(1+n_{\lambda}^{eq})}_{\partial_{\epsilon} n_{\lambda}^{eq}} \left(\partial_t \Phi_{\lambda} + \vec{v}_{\lambda} \vec{\nabla} \Phi_{\lambda} \right) \\ & = \beta \sum_{\lambda',\lambda''} \left[\Lambda_{\lambda,\lambda'}^{\lambda''} \left(\Phi_{\lambda''} - \Phi_{\lambda} - \Phi_{\lambda'} \right) + \frac{1}{2} \Lambda_{\lambda}^{\lambda',\lambda''} \left(\Phi_{\lambda'} + \Phi_{\lambda''} - \Phi_{\lambda} \right) \right] \end{aligned} \quad (10.98)$$

with $\lambda = (\vec{k}, \sigma)$, $\lambda' = (\vec{k}', \sigma')$, and $\lambda'' = (\vec{k}'', \sigma'')$, and

$$\begin{aligned} \Lambda_{\vec{k}',\sigma',\vec{k}'',\sigma''}^{\vec{k},\sigma} & \stackrel{\text{Eq. 10.96}}{=} \frac{2\pi}{\hbar} \left(\frac{\hbar}{2} \right)^3 \frac{|A_{\sigma,\sigma',\sigma''}(\vec{k}, -\vec{k}', -\vec{k}'')|^2 / \mathcal{N}}{\omega_{\sigma}(\vec{k})\omega_{\sigma'}(-\vec{k}')\omega_{\sigma''}(-\vec{k}'')} \\ & \times \delta \left(\hbar\omega_{\sigma}(\vec{k}) - \hbar\omega_{\sigma'}(\vec{k}') - \hbar\omega_{\sigma''}(\vec{k}'') \right) (n_{\sigma}^{eq}(\vec{k}) + 1)n_{\sigma'}^{eq}(\vec{k}')n_{\sigma''}^{eq}(\vec{k}'') \\ \Lambda_{\vec{k},\sigma}^{\vec{k}',\sigma',\vec{k}'',\sigma''} & \stackrel{\text{Eq. 10.96}}{=} \frac{2\pi}{\hbar} \left(\frac{\hbar}{2} \right)^3 \frac{|A_{\sigma,\sigma',\sigma''}(-\vec{k}, \vec{k}', \vec{k}'')|^2 / \mathcal{N}}{\omega_{\sigma}(-\vec{k})\omega_{\sigma'}(\vec{k}')\omega_{\sigma''}(\vec{k}'')} \\ & \times \delta \left(-\hbar\omega_{\sigma}(\vec{k}) + \hbar\omega_{\sigma'}(\vec{k}') + \hbar\omega_{\sigma''}(\vec{k}'') \right) n_{\sigma}^{eq}(\vec{k})(n_{\sigma'}^{eq}(\vec{k}') + 1)(n_{\sigma''}^{eq}(\vec{k}'') + 1) \end{aligned} \quad (10.99)$$

This equation Eq. 10.98 compares to Eq. (Chernatynskiy-A9) and Eq. (Chernatynskiy-B10). Note that his P is defined with the opposite sign. There is a deviation between our Eq. 10.99 and

Eq. (Chernatinskyi-B10): In the matrix element with one lower index the argument of the Delta function has the opposite sign for $\hbar\omega_{\lambda'}$ and $\hbar\omega_{\lambda''}$, while we obtain the same sign. Our sign stems from the fact that one phonon with λ is annihilated, while two phonons with λ', λ'' are created. The expression of Chernatinskyi is derived from his Eq. (Chernatinskyi-B9), where the sign convention is similar to our expression. This error may be caused by copying the delta function term from B9 without changing the indices.

The equation Eq. 10.98 is also equivalent to Eq. (Broido-3)[80], if we translate

$$W_{\lambda,\lambda',\lambda''}^+ = \Lambda_{\lambda,\lambda'}^{\lambda''} \quad \text{and} \quad W_{\lambda,\lambda',\lambda''}^- = \Lambda_{\lambda'}^{\lambda,\lambda''}$$

This translation is reversed in the definition of Broido's W^\pm Eq. (Broido-4) when compared to our Λ . This can be done on the basis of detailed balance, which has been applied in the derivation before. Note that there is an error in Eq. (Broido-4), which is corrected in Eq.2 of a later of his papers[81]. Therefore, we compare to the latter paper.

$$W_{\lambda,\lambda',\lambda''}^+ = \frac{2\pi}{\hbar\mathcal{N}} \left(\frac{\hbar}{2}\right)^3 \frac{|A_{-\lambda,-\lambda',\lambda''}|^2}{\omega_\lambda\omega_{\lambda'}\omega_{\lambda''}} \delta(\hbar\omega_\lambda + \hbar\omega_{\lambda'} - \hbar\omega_{\lambda''}) (n_\lambda^{eq} + 1)(n_{\lambda'}^{eq} + 1)n_{\lambda''}^{eq} (= \Lambda_{\lambda'}^{\lambda,\lambda''})$$

$$W_{\lambda,\lambda',\lambda''}^- = \frac{2\pi}{\hbar\mathcal{N}} \left(\frac{\hbar}{2}\right)^3 \frac{|A_{-\lambda,\lambda',\lambda''}|^2}{\omega_\lambda\omega_{\lambda'}\omega_{\lambda''}} \delta(\hbar\omega_\lambda - \hbar\omega_{\lambda'} - \hbar\omega_{\lambda''}) (n_\lambda^{eq} + 1)n_{\lambda'}^{eq}n_{\lambda''}^{eq} (= \Lambda_{\lambda',\lambda''}^\lambda)$$

The agreement is there when the sign of the indices of the three-phonon scattering matrix elements are given the opposite sign. Such a change does not affect the result, because the three phonon scattering matrix elements are only made complex conjugate by such a sign change. Broido furthermore assumes inversion symmetry of the frequencies in k-space.

Chapter 11

Density-functional theory

Density-functional theory[82, 83] is an extremely powerful technique. It is based on an exact theorem that the ground-state energy is determined solely by the density alone.

The theorem says

- that all ground-state properties are unique functionals of the electron density and
- that the electron density can be obtained from a Schrödinger equation in an effective potential.

density-functional theory maps the interacting electron system onto a system of non-interacting electrons in an effective potential. The effective potential depends in turn on the electron distribution and describes the interacting between the electrons in an effective way.

density-functional theory provides a total-energy functional of the form

$$E[n(\vec{r})] = \underbrace{\sum_n f_n \langle \phi_n | \frac{\hat{p}^2}{2m_e} | \phi_n \rangle}_{T_s[n(\vec{r})]} + \int d^3r n(\vec{r}) v_{\text{ext}}(\vec{r}) + \underbrace{\frac{1}{2} \int d^3r \int d^3r' \frac{e^2 n(\vec{r}) n(\vec{r}')}{4\pi\epsilon_0 |\vec{r} - \vec{r}'|}}_{E_{\text{Hartree}}} + E_{xc}[n(\vec{r})]$$

T_s is not the kinetic energy of the many-electron system, but the one of the non-interacting reference system with density $n(\vec{r})$. We will see later that it can be written as functional of the density. E_{xc} is another functional of the density, called the exchange and correlation energy functional. This functional is not known in practice. Therefore, one uses approximate functionals, that are derived from known analytical properties of the functional and/or even experimental data.

As a result of the minimum principle we obtain the following Kohn-Sham equation for the one-particle orbitals

$$\left[\frac{\hat{p}^2}{2m_e} + v_{\text{eff}}(\hat{r}) - \epsilon_n \right] |\phi_n\rangle = 0$$

where the effective potential is defined as

$$v_{\text{eff}}(\vec{r}) = v_{\text{ext}}(\vec{r}) + \frac{e^2}{4\pi\epsilon_0} \int d^3r' \frac{n(\vec{r}')}{|\vec{r} - \vec{r}'|} + \underbrace{\frac{\delta E_{xc}}{\delta n(\vec{r})}}_{\mu_{xc}(\vec{r})}$$

The proofs will be given later. Let us start out with the language used in the field of density-functional theory and the physical pictures that emerge.

11.1 One-particle and two-particle densities

In order to get used with the terminology, let me introduce a number of definitions related to density matrices[84].

11.1.1 N-particle density matrix

Let us start with the **N-particle density matrix** of an N-particle system

$$\rho^{(N)}(\vec{x}_1, \dots, \vec{x}_N; \vec{x}'_1, \dots, \vec{x}'_N) \stackrel{\text{def}}{=} \Psi(\vec{x}_1, \dots, \vec{x}_N) \Psi^*(\vec{x}'_1, \dots, \vec{x}'_N)$$

The N-particle density matrix is formed from the matrix elements

$$\rho^{(N)}(\vec{x}_1, \dots, \vec{x}_N; \vec{x}'_1, \dots, \vec{x}'_N) = \langle \vec{x}_1, \dots, \vec{x}_N | \hat{\rho}^{(N)} | \vec{x}'_1, \dots, \vec{x}'_N \rangle$$

of the **density operator**

$$\hat{\rho}^{(N)} \stackrel{\text{def}}{=} |\Psi\rangle \langle \Psi| \quad (11.1)$$

This is the same density operator, that has been used in statistical mechanics a lot. In Eq. 11.1, however, we restricted ourselves to the density matrix of a pure state. A pure state can be described by a single many-particle wave function, whereas a statistical mixture is an ensemble of many-particle states, of which each contributes with a certain probability.

The N-particle density matrix contains all the information of the wave function itself, because one can determine the expectation value of any operator from it:

We use the representation of the unity operator in a N-particle Hilbert space of spin-orbitals

$$\hat{1} = \int d^4x_1 \cdots \int d^4x_N |\vec{x}_1, \dots, \vec{x}_N\rangle \langle \vec{x}_1, \dots, \vec{x}_N|$$

and obtain

$$\begin{aligned} \langle \Psi | \hat{A} | \Psi \rangle &= \langle \Psi | \hat{A} | \Psi \rangle = \langle \Psi | \hat{1} \hat{A} \hat{1} | \Psi \rangle \\ &= \int d^4x_1 \cdots \int d^4x_N \int d^4x'_1 \cdots \int d^4x'_N \\ &\quad \cdot \underbrace{\langle \vec{x}_1, \dots, \vec{x}_N | \Psi \rangle \langle \Psi | \vec{x}'_1, \dots, \vec{x}'_N \rangle}_{\rho^{(N)}} \langle \vec{x}'_1, \dots, \vec{x}'_N | \hat{A} | \vec{x}_1, \dots, \vec{x}_N \rangle \\ &= \int d^4x_1 \cdots \int d^4x_N \int d^4x'_1 \cdots \int d^4x'_N \\ &\quad \cdot \rho^{(N)}(\vec{x}_1, \dots, \vec{x}_N; \vec{x}'_1, \dots, \vec{x}'_N) \langle \vec{x}'_1, \dots, \vec{x}'_N | \hat{A} | \vec{x}_1, \dots, \vec{x}_N \rangle \end{aligned} \quad (11.2)$$

For us the expectation value of the Hamilton operator plays a special role. The energy expectation value can be constructed from the N-particle density matrix. However, the special form of the Hamilton operator relevant to us allows to use simpler, so-called reduced density matrices. We will define those in the following.

Fertig: WS06/07 8 Doppelstunde 27.Nov.06

11.1.2 One-particle reduced density matrix

From the N-particle density matrix we can form several **contractions** that are physically important, because they allow to represent expectation values of one-particle operators and the Coulomb interaction in an elegant fashion.

For example, we do not need the full N -particle density matrix to determine the expectation value of a one-particle operator, if we know the so-called one-particle density matrix.

A general one-particle operator has the matrix elements

$$\langle \vec{x}_1, \dots, \vec{x}_N | \hat{A} | \vec{x}'_1, \dots, \vec{x}'_N \rangle = \sum_{i=1}^N A(\vec{x}_i, \vec{x}'_i) \prod_{k(k \neq i)}^N \delta(\vec{x}_k - \vec{x}'_k) \quad (11.3)$$

This allows one to simplify the expression for the expectation value as follows

$$\begin{aligned} \langle \Psi | \hat{A} | \Psi \rangle &\stackrel{\text{Eqs. 11.2, 11.3}}{=} \int d^4 x_1 \cdots \int d^4 x_N \int d^4 x'_1 \cdots \int d^4 x'_N \\ &\quad \rho^{(N)}(\vec{x}_1, \dots, \vec{x}_N; \vec{x}'_1, \dots, \vec{x}'_N) \sum_{i=1}^N A(\vec{x}_i, \vec{x}'_i) \prod_{k(k \neq i)}^N \delta(\vec{x}_k - \vec{x}'_k) \\ &\stackrel{(1)}{=} \int d^4 x_1 \cdots \int d^4 x_N \int d^4 x'_1 \cdots \int d^4 x'_N \\ &\quad \rho^{(N)}(\vec{x}_1, \dots, \vec{x}_N; \vec{x}'_1, \dots, \vec{x}'_N) N A(\vec{x}_1, \vec{x}'_1) \prod_{k=2}^N \delta(\vec{x}_k - \vec{x}'_k) \\ &= \int d^4 x_1 \int d^4 x'_1 A(\vec{x}_1, \vec{x}'_1) \\ &\quad \cdot N \int d^4 x_2 \cdots \int d^4 x_N \int d^4 x'_2 \cdots \int d^4 x'_N \\ &\quad \cdot \rho^{(N)}(\vec{x}_1, \dots, \vec{x}_N; \vec{x}'_1, \dots, \vec{x}'_N) \prod_{k=2}^N \delta(\vec{x}_k - \vec{x}'_k) \\ &= \int d^4 x_1 \int d^4 x'_1 A(\vec{x}_1, \vec{x}'_1) \\ &\quad \cdot \underbrace{N \int d^4 x_2 \cdots \int d^4 x_N \rho^{(N)}(\vec{x}_1, \vec{x}_2, \dots, \vec{x}_N; \vec{x}'_1, \vec{x}_2, \dots, \vec{x}_N)}_{\rho^{(1)}(\vec{x}_1, \vec{x}'_1)} \quad (11.4) \end{aligned}$$

In (1), we exploited that the density matrix describes identical particles. Thus, it is invariant under permutation of two particle indices. (Simultaneously on both sides.)

Thus, if we define the **one-particle reduced density matrix**¹ $\rho^{(1)}(\vec{x}, \vec{x}')$, as²

$$\begin{aligned} \rho^{(1)}(\vec{x}, \vec{x}') &\stackrel{\text{def}}{=} N \int d^4 x_2 \cdots \int d^4 x_N \rho^{(N)}(\vec{x}, \vec{x}_2, \dots, \vec{x}_N; \vec{x}', \vec{x}_2, \dots, \vec{x}_N) \\ &= N \int d^4 x_2 \cdots \int d^4 x_N \Psi(\vec{x}, \vec{x}_2, \dots, \vec{x}_N) \Psi^*(\vec{x}', \vec{x}_2, \dots, \vec{x}_N) \quad (11.5) \end{aligned}$$

we can determine the expectation values of any one-particle operator as

$$\langle \Psi | \hat{A} | \Psi \rangle \stackrel{\text{Eq. 11.4}}{=} \int d^4 x \int d^4 x' \rho^{(1)}(\vec{x}, \vec{x}') A(\vec{x}', \vec{x}) \quad (11.6)$$

The integral in the first equation of the definition Eq. 11.5 provides the density of a single electron. This density is the same for all the electrons. Therefore, we obtain the total density by multiplication by the number N of electrons, which explains the factor in front of the integral.

¹The word "reduced" is usually dropped. However the context must avoid confusion with the density matrix of a one-particle system.

²Note that this definition only holds for density matrices of indistinguishable particles.

Electron density

The operator for the electron density at a position \vec{r} is

$$\hat{n}(\vec{r}) = \sum_{\sigma} |\vec{r}, \sigma\rangle \langle \vec{r}, \sigma| \quad (11.7)$$

It has the matrix elements

$$\langle \vec{r}, \sigma | \hat{n}(\vec{r}_0) | \vec{r}', \sigma' \rangle = \delta(\vec{r} - \vec{r}_0) \delta(\vec{r}' - \vec{r}_0) \delta_{\sigma, \sigma'} \quad (11.8)$$

in a one-particle, real-space and spin representation.

The matrix elements of the operator in a N-particle, real-space and spin representation are

$$\langle \vec{x}_1, \dots, \vec{x}_N | \hat{n}(\vec{r}_0) | \vec{x}'_1, \dots, \vec{x}'_N \rangle \stackrel{\text{Eq. 11.3}}{=} \sum_{i=1}^N \delta(\vec{r}_i - \vec{r}_0) \delta(\vec{r}'_i - \vec{r}_0) \delta_{\sigma_i, \sigma'_i} \prod_{k(k \neq i)} \delta(\vec{x}_k - \vec{x}'_k)$$

Thus, we obtain the electron density as

$$\begin{aligned} n(\vec{r}_0) &= \langle \Psi | \hat{n}(\vec{r}_0) | \Psi \rangle \stackrel{\text{Eq. 11.6}}{=} \int d^4x \int d^4x' \hat{\rho}^{(1)}(\vec{x}, \vec{x}') \delta(\vec{r} - \vec{r}_0) \delta(\vec{r}' - \vec{r}_0) \delta_{\sigma, \sigma'} \\ &= \sum_{\sigma} \hat{\rho}^{(1)}(\vec{r}_0, \sigma, \vec{r}_0, \sigma) \end{aligned} \quad (11.9)$$

Magnetization

The magnetization operator has the form

$$\hat{m} = \frac{q}{m_e} \hat{S} = \frac{\hbar q}{2m_e} \hat{\sigma} \quad (11.10)$$

Its matrix elements in a one-particle real-space representation are

$$\langle \vec{r}, \sigma | \hat{m}_j | \vec{r}', \sigma' \rangle = \frac{\hbar q}{2m_e} \delta(\vec{r} - \vec{r}') \sigma_{j, \sigma, \sigma'} \quad (11.11)$$

where \hat{S} is the spin operator, q is the electron charge and m_e is its mass. With σ_j we denote the Pauli matrices defined in Eq. 3.4 for $j \in \{x, y, z\}$. Unfortunately, it is a little difficult not to get confused by the many σ 's.

The matrix elements in the N-particle Hilbert space are

$$\langle \vec{x}_1, \dots, \vec{x}_N | \hat{m}_n(\vec{r}) | \vec{x}'_1, \dots, \vec{x}'_N \rangle \stackrel{\text{Eq. 11.3}}{=} \sum_{i=1}^N \underbrace{\delta(\vec{r}_i - \vec{r}) \frac{\hbar q}{2m_e} \sigma_{j, \sigma, \sigma'}}_{\langle \vec{r}_i, \sigma_i | \hat{m}_j | \vec{r}_i, \sigma'_i \rangle} \prod_{k(k \neq i)} \delta(\vec{x}_k - \vec{x}'_k)$$

Thus, we obtain the magnetization as

$$\begin{aligned} \vec{m}(\vec{r}_0) &= \langle \Psi | \hat{m}(\vec{r}_0) | \Psi \rangle = \int d^4x \int d^4x' \hat{\rho}^{(1)}(\vec{x}, \vec{x}') \delta(\vec{r}_0 - \vec{r}) \vec{\sigma}_{\sigma, \sigma'} \\ &= \sum_{\sigma, \sigma'} \hat{\rho}^{(1)}(\vec{r}_0, \sigma, \vec{r}_0, \sigma') \vec{\sigma}_{\sigma, \sigma'} \end{aligned}$$

Kinetic energy

The matrix elements for the operator that provides the kinetic energy in a given direction at a given point are

$$\langle \vec{x}_1, \dots, \vec{x}_N | \hat{T} | \vec{x}'_1, \dots, \vec{x}'_N \rangle = \sum_{i=1}^N \delta(\vec{x}_i - \vec{x}'_i) \frac{-\hbar^2}{2m_e} \vec{\nabla}_i'^2 \prod_{k(k \neq i)} \delta(\vec{x}_k - \vec{x}'_k)$$

This expression is weird: The matrix element is a differential operator that points no-where! Not really. Let us investigate the meaning of this expression:

Consider a one-particle state $|f\rangle$ and let us define a second one as $|g\rangle \stackrel{\text{def}}{=} \frac{\hat{p}^2}{2m_e} |f\rangle$. Then we find

$$g(\vec{r}) = \langle \vec{r} | g \rangle = \langle \vec{r} | \frac{\hat{p}^2}{2m_e} | f \rangle = \langle \vec{r} | \frac{\hat{p}^2}{2m_e} \underbrace{\int d^3 r' |\vec{r}'\rangle \langle \vec{r}' | f \rangle}_{\hat{1}} = \int d^3 r' \langle \vec{r} | \frac{\hat{p}^2}{2m_e} | \vec{r}' \rangle \underbrace{\langle \vec{r}' | f \rangle}_{f(\vec{r}')}$$

On the other hand, we know that $g(\vec{r}) = \frac{-\hbar^2}{2m_e} \vec{\nabla}^2 f(\vec{r})$, so that we can formally identify the kinetic energy operator in a one-particle Hilbert space as

$$\langle \vec{r} | \frac{\hat{p}^2}{2m_e} | \vec{r}' \rangle = \delta(\vec{r} - \vec{r}') \frac{-\hbar^2}{2m_e} \vec{\nabla}^2$$

It is, however, important that the gradient stands in front of the function depending on \vec{r}' . I do not recommend to use tricks like this, because one has to be awfully careful.

The gradient $\vec{\nabla}'_i$ acts exclusively on the i -th primed position \vec{r}'_i . Note that the gradient cannot be interchanged with the δ -function preceding it, because a gradient does not commute with a function of the corresponding coordinate.

Thus, we obtain the kinetic energy T as

$$\begin{aligned} T &\stackrel{\text{def}}{=} \langle \Psi | \hat{T} | \Psi \rangle = \int d^4 x \int d^4 x' \delta(\vec{x} - \vec{x}') \frac{-\hbar^2}{2m_e} (\vec{\nabla}')^2 \hat{\rho}^{(1)}(\vec{x}', \vec{x}) \\ &= \sum_{\sigma} \int d^3 r \lim_{\vec{r} \rightarrow \vec{r}'} \frac{-\hbar^2}{2m_e} \vec{\nabla}'^2 \hat{\rho}^{(1)}(\vec{r}', \sigma, \vec{r}, \sigma) \end{aligned}$$

11.1.3 Two-particle density

In order to evaluate the Coulomb interaction energy between electrons, we need to know the two-particle density.

The matrix elements of the interaction in a real-space representation are

$$\langle \vec{x}_1, \dots, \vec{x}_N | \hat{W} | \vec{x}'_1, \dots, \vec{x}'_N \rangle = \frac{1}{2} \sum_{i \neq j} w(\vec{x}_i, \vec{x}_j) \prod_{i=1}^N \delta(\vec{x}_i - \vec{x}'_i)$$

where $w(x, x') = \frac{e^2}{4\pi\epsilon_0 |\vec{r} - \vec{r}'|}$.

$$\begin{aligned}
\langle \Psi | \hat{W} | \Psi \rangle &= \int d^4 x_1 \cdots \int d^4 x_N \int d^4 x'_1 \cdots \int d^4 x'_N \\
&\quad \rho^{(N)}(\vec{x}_1, \dots, \vec{x}_N; \vec{x}'_1, \dots, \vec{x}'_N) \langle \vec{x}'_1, \dots, \vec{x}'_N | \hat{W} | \vec{x}_1, \dots, \vec{x}_N \rangle \\
&= \int d^4 x_1 \cdots \int d^4 x_N \int d^4 x'_1 \cdots \int d^4 x'_N \\
&\quad \rho^{(N)}(\vec{x}_1, \dots, \vec{x}_N; \vec{x}'_1, \dots, \vec{x}'_N) \frac{1}{2} \sum_{i \neq j} w(\vec{x}_i, \vec{x}_j) \prod_{i=1}^N \delta(\vec{x}_i - \vec{x}'_i) \\
&= \int d^4 x_1 \cdots \int d^4 x_N \rho^{(N)}(\vec{x}_1, \dots, \vec{x}_N; \vec{x}_1, \dots, \vec{x}_N) \frac{1}{2} \sum_{i \neq j} w(\vec{x}_i, \vec{x}_j) \\
&= \int d^4 x_1 \cdots \int d^4 x_N \rho^{(N)}(\vec{x}_1, \dots, \vec{x}_N; \vec{x}_1, \dots, \vec{x}_N) \frac{N(N-1)}{2} w(\vec{x}_1, \vec{x}_2) \\
&= \frac{1}{2} \int d^4 x \int d^4 x' w(\vec{x}, \vec{x}') \\
&\quad \underbrace{N(N-1) \int d^4 x_1 \cdots \int d^4 x_N \rho^{(N)}(\vec{x}_1, \dots, \vec{x}_N; \vec{x}_1, \dots, \vec{x}_N) \delta(\vec{x} - \vec{x}_1) \delta(\vec{x}' - \vec{x}_2)}_{n^{(2)}(\vec{x}, \vec{x}')} \\
&= \frac{1}{2} \int d^4 x \int d^4 x' n^{(2)}(\vec{x}, \vec{x}') w(\vec{x}, \vec{x}')
\end{aligned}$$

Thus, we define the **two-particle density**³ $n^{(2)}(\vec{x}, \vec{x}')$ as

$$\begin{aligned}
n^{(2)}(\vec{x}, \vec{x}') &\stackrel{\text{def}}{=} N(N-1) \int d^4 x_1 \cdots \int d^4 x_N \\
&\quad \rho^{(N)}(\vec{x}_1, \dots, \vec{x}_N; \vec{x}_1, \dots, \vec{x}_N) \delta(\vec{x} - \vec{x}_1) \delta(\vec{x}' - \vec{x}_2)
\end{aligned} \tag{11.12}$$

so that we can determine the interaction energy as

$$\langle \Psi | \hat{W} | \Psi \rangle = \frac{1}{2} \int d^4 x \int d^4 x' n^{(2)}(\vec{x}, \vec{x}') w(\vec{x}, \vec{x}')$$

The two-particle density can also be expressed as expectation value as follows

$$\begin{aligned}
n^{(2)}(\vec{x}, \vec{x}') \text{ Eq. 11.12} &= \int d^4 x_1 \cdots \int d^4 x_N \Psi(\vec{x}_1, \dots, \vec{x}_N) \sum_{i \neq j} \delta(\vec{x} - \vec{x}_i) \delta(\vec{x}' - \vec{x}_j) \Psi^*(\vec{x}_1, \dots, \vec{x}_N) \\
&= \langle \Psi | \sum_{i \neq j} \delta(\vec{x} - \vec{x}_i) \delta(\vec{x}' - \vec{x}_j) | \Psi \rangle
\end{aligned} \tag{11.13}$$

The two-particle density describes the probability density that there is one electron at \vec{r} and another one at \vec{r}' . It integrates up to the number of ordered pairs, namely $N(N-1)$.

Note that the two-particle density is often confused with the one-particle density matrix. Both have the same number of arguments, but they are fundamentally different quantities.

The q -particle densities contain the information only about the probability to find a q -tuple of electrons with a given set of coordinates. It is, however, not possible to extract for example the momentum or the kinetic energy from a given q -particle density. In contrast, the q -electron density

³There are different conventions in use, which differ by a factor 1/2. We follow here the choice of McWeeny[84], who does not have the factor $\frac{1}{2}$. Here, the factor $\frac{1}{2}$, which compensates for the double counting of two pairs at \vec{x} and \vec{x}' (one obtained by exchanging the two particles from the other) must be done explicitly. On the other hand the two-particle density as defined by McWeeny has the simple physical interpretation of a density for one particle at \vec{x} and another one at \vec{x}' , irrespective of their order.

matrix contains the complete information on q -tuple of electrons. For a q -particle system, the q -particle density matrix contains the complete information on the system, that is the same information contained in the wave function. Already from the one-particle density matrix we can determine the momentum or the kinetic energy.

In the following, we list various densities and density-matrices in comparison, to show the difference

- one-particle density matrix

$$\rho^{(1)}(\vec{x}_1, \vec{x}'_1) = N \int d^4x_2 \cdots \int d^4x_N \rho^{(N)}(\vec{x}_1, \vec{x}_2, \dots, \vec{x}_N; \vec{x}'_1, \vec{x}_2, \dots, \vec{x}_N)$$

- two-particle density matrix

$$\rho^{(2)}(\vec{x}_1, \vec{x}_2, \vec{x}'_1, \vec{x}'_2) = N(N-1) \int d^4x_3 \cdots \int d^4x_N \rho^{(N)}(\vec{x}_1, \vec{x}_2, \vec{x}_3, \dots, \vec{x}_N; \vec{x}'_1, \vec{x}'_2, \vec{x}_3, \dots, \vec{x}_N)$$

- one-particle density

$$n^{(1)}(\vec{x}_1) = N \int d^4x_2 \cdots \int d^4x_N \rho^{(N)}(\vec{x}_1, \dots, \vec{x}_N; \vec{x}_1, \dots, \vec{x}_N)$$

- two-particle density

$$n^{(2)}(\vec{x}_1, \vec{x}_2) = N(N-1) \int d^4x_3 \cdots \int d^4x_N \rho^{(N)}(\vec{x}_1, \dots, \vec{x}_N; \vec{x}_1, \dots, \vec{x}_N)$$

- N -particle density

$$n^{(N)}(\vec{x}_1, \dots, \vec{x}_N) = \rho^{(N)}(\vec{x}_1, \dots, \vec{x}_N; \vec{x}_1, \dots, \vec{x}_N)$$

The q -particle density can directly be obtained from the q -particle density matrix

$$n^{(q)}(\vec{x}_1, \dots, \vec{x}_q) = \rho^{(q)}(\vec{x}_1, \dots, \vec{x}_q, \vec{x}_1, \dots, \vec{x}_q)$$

The density matrix has always two arguments per particle while the density has only one per particle.

The two-particle density is so important for many-particle physics, because we can directly express the interaction energy by the two-particle density. The Coulomb interaction between electrons can be written as

$$E_H + E_X = \langle \Psi | \frac{1}{2} \sum_{i \neq j} \frac{e^2}{4\pi\epsilon_0 |\vec{r} - \vec{r}'|} | \Psi \rangle = \frac{1}{2} \sum_{\sigma, \sigma'} \int d^3r \int d^3r' \frac{e^2 n^{(2)}(\vec{x}, \vec{x}')}{4\pi\epsilon_0 |\vec{r} - \vec{r}'|} \quad (11.14)$$

In chapter ?? we derived the expression for the expectation value of a two-particle operator with a Slater determinant. According to Eq. 11.13, the two-particle density can be expressed as an expectation value. For a single Slater determinant, the two-particle density would have the form

$$\begin{aligned} n^{(2)}(\vec{r}, \vec{r}') &\stackrel{Eqs. \text{??}, 11.13}{=} \sum_{i,j}^N \int d^4x_1 \int d^4x_2 \phi_i^*(\vec{x}_1) \phi_j^*(\vec{x}_2) \delta(\vec{r} - \vec{r}_1) \delta(\vec{r}' - \vec{r}_2) \phi_i(\vec{x}_1) \phi_j(\vec{x}_2) \\ &- \sum_{i,j}^N \int d^4x_1 \int d^4x_2 \phi_i^*(\vec{x}_1) \phi_j^*(\vec{x}_2) \delta(\vec{r} - \vec{r}_1) \delta(\vec{r}' - \vec{r}_2) \phi_j(\vec{x}_1) \phi_i(\vec{x}_2) \\ &= n(\vec{r})n(\vec{r}') - \sum_{i,j}^N \sum_{\sigma, \sigma'} \phi_i^*(\vec{r}, \sigma) \phi_j(\vec{r}, \sigma) \phi_j^*(\vec{r}', \sigma') \phi_i(\vec{r}', \sigma') \end{aligned} \quad (11.15)$$

11.1.4 Two-particle density of the free-electron gas

Let us work out the two-particle density of the free-electron gas in the Hartree-Fock approximation:
 For the free-electron gas the one-particle orbitals are, according to Eq. 4.32,

$$\phi_{\vec{k},\sigma}(\vec{r},\sigma') = \frac{1}{\sqrt{\Omega}} e^{i\vec{k}\vec{r}} \delta_{\sigma,\sigma'}$$

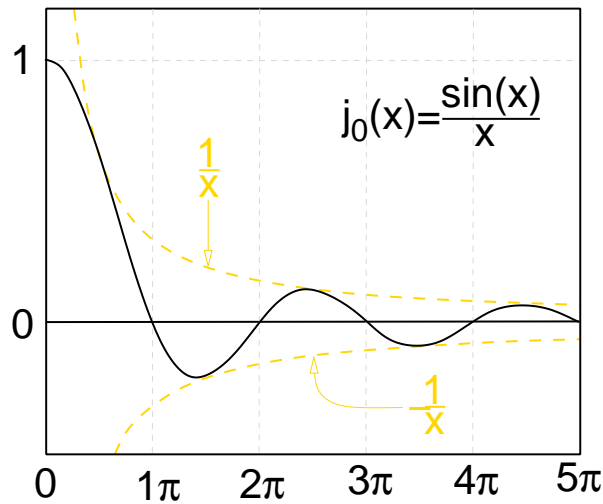
Now, we need to determine the two-particle density according to Eq. 11.15. The first term is trivial because the density is constant. The exchange term is more complicated. let us therefore work out the expression $C(\vec{x},\vec{x}')$ which occurs in the exchange term of Eq. 11.15.

$$\begin{aligned} C(\vec{x},\vec{x}') &\stackrel{\text{def}}{=} \sum_{i,j}^N \phi_i^*(\vec{x})\phi_j(\vec{x})\phi_j^*(\vec{x}')\phi_i(\vec{x}') \\ \text{Eq. 5.13} &= \sum_{\sigma_1,\sigma_2} \Omega^2 \int_{|\vec{k}_1|<k_F} \frac{d^3k_1}{(2\pi)^3} \int_{|\vec{k}_2|<k_F} \frac{d^3k_2}{(2\pi)^3} \phi_{\vec{k}_1,\sigma_1}^*(\vec{r},\sigma)\phi_{\vec{k}_2,\sigma_2}(\vec{r},\sigma)\phi_{\vec{k}_2,\sigma_2}^*(\vec{r}',\sigma')\phi_{\vec{k}_1,\sigma_1}(\vec{r}',\sigma') \\ \text{Eq. 4.32} &= \int_{|\vec{k}_1|<k_F} \frac{d^3k_1}{(2\pi)^3} \int_{|\vec{k}_2|<k_F} \frac{d^3k_2}{(2\pi)^3} e^{i(\vec{k}_2-\vec{k}_1)(\vec{r}-\vec{r}')} \underbrace{\sum_{\sigma_1,\sigma_2} \delta_{\sigma,\sigma_1}\delta_{\sigma,\sigma_2}\delta_{\sigma',\sigma_2}\delta_{\sigma',\sigma_1}}_{=\delta_{\sigma,\sigma'}\delta_{\sigma',\sigma}=\delta_{\sigma,\sigma'}} \\ &= \delta_{\sigma,\sigma'} \left(\int_{|\vec{k}_1|<k_F} \frac{d^3k_1}{(2\pi)^3} e^{-i\vec{k}_1(\vec{r}-\vec{r}')} \right) \left(\int_{|\vec{k}_2|<k_F} \frac{d^3k_2}{(2\pi)^3} e^{i\vec{k}_2(\vec{r}-\vec{r}')} \right) \\ &\stackrel{\vec{k}_1 \rightarrow \vec{k}}{=} \delta_{\sigma,\sigma'} \left| \int_{|\vec{k}|<k_F} \frac{d^3k}{(2\pi)^3} e^{i\vec{k}(\vec{r}-\vec{r}')} \right|^2 \end{aligned}$$

Now, we use a tremendously useful theorem, that allows to decompose plane waves into radial functions and spherical harmonics $Y_{\ell,m}$

$$e^{i\vec{k}\vec{r}} = 4\pi \sum_{\ell=0}^{\infty} \sum_{m=-\ell}^{\ell} i^{\ell} j_{\ell}(|\vec{k}||\vec{r}|) Y_{\ell,m}(\vec{r}) Y_{\ell,m}^*(\vec{k}) \tag{11.16}$$

where the $j_{\ell}(z)$ are the **spherical Bessel functions**, also named **Bessel functions of half-integer order**. The Bessel function $j_0(x)$ is shown in the following figure



In the last result we see that it depends only on the relative positions for the two electrons. Therefore, we introduce

$$\vec{u} \stackrel{\text{def}}{=} \vec{r} - \vec{r}'$$

Since we integrate over a spherical volume in reciprocal space, only the terms with $\ell = 0$ contribute a finite value, because all other spherical harmonics integrate to zero.

$$\begin{aligned}
 C(\vec{x}, \vec{x}') &\stackrel{\vec{r}-\vec{r}'\rightarrow\vec{u}}{=} \delta_{\sigma,\sigma'} \left| \int_{|\vec{k}<k_F} \frac{d^3k}{(2\pi)^3} e^{i\vec{k}\vec{u}} \right|^2 \\
 &\stackrel{\text{Eq. 11.16}}{=} \delta_{\sigma,\sigma'} \left| \int_{|\vec{k}<k_F} \frac{d^3k}{(2\pi)^3} 4\pi \sum_{\ell=0}^{\infty} \sum_{m=-\ell}^{\ell} i^{\ell} j_{\ell}(|\vec{k}||\vec{u}|) Y_{\ell,m}(\vec{u}) Y_{\ell,m}^*(\vec{k}) \right|^2 \\
 &= \delta_{\sigma,\sigma'} \left| \frac{1}{(2\pi)^3} \int_{k<k_F} dk k^2 4\pi j_0(|\vec{k}||\vec{u}|) \underbrace{\frac{1}{4\pi}}_{Y_{0,0}(\vec{u})Y_{0,0}^*(\vec{k})} \right|^2 \\
 &\stackrel{|\vec{k}|\rightarrow k}{=} \delta_{\sigma,\sigma'} \frac{1}{(2\pi)^6} \left(4\pi \int_{k<k_F} dk k^2 \frac{\sin(k|\vec{u}|)}{k|\vec{u}|} \right)^2 \\
 &\stackrel{k|\vec{u}|\rightarrow x}{=} \delta_{\sigma,\sigma'} \frac{1}{(2\pi)^6} \left(\frac{4\pi}{|\vec{u}|^3} \int_{x<k_F|u|} dx x \sin(x) \right)^2
 \end{aligned}$$

The integral can be solved using

$$\frac{d}{dx} (x \cos(x) - \sin(x)) = \cos(x) - x \sin(x) - \cos(x) = x \sin(x)$$

Now, we continue

$$\begin{aligned}
 C(\vec{x}, \vec{x}') &\stackrel{k|\vec{u}|\rightarrow x}{=} \delta_{\sigma,\sigma'} \frac{1}{(2\pi)^6} \left| \frac{1}{|\vec{u}|^3} (k_F|\vec{u}| \cos(k_F|\vec{u}|) - \sin(k_F|\vec{u}|)) \right|^2 \\
 &= \frac{\delta_{\sigma,\sigma'} k_F^6}{(2\pi)^6} \left(\frac{k_F|\vec{u}| \cos(k_F|\vec{u}|) - \sin(k_F|\vec{u}|)}{(k_F|\vec{u}|)^3} \right)^2
 \end{aligned}$$

For the sake of aesthetics⁴, let scale the expression in parenthesis such that it starts with value 1 at $u = 0$. (See footnote below⁵)

$$\begin{aligned}
 \lim_{x\rightarrow 0} \frac{x \cos(x) - \sin(x)}{x^3} &= \lim_{x\rightarrow 0} \sum_{n=0}^{\infty} \left(\frac{(-1)^n}{2n!} x^{2n-2} - \frac{(-1)^n}{(2n+1)!} x^{2n-2} \right) \\
 &= \lim_{x\rightarrow 0} \sum_{n=0}^{\infty} \left(\frac{1}{(2n)!} - \frac{1}{(2n+1)!} \right) (-1)^n x^{2n-2} \\
 &= \lim_{x\rightarrow 0} \sum_{n=0}^{\infty} (1-1) x^{-2} - \left(\frac{1}{2} - \frac{1}{6} \right) x^0 + O(x^2) = \frac{1}{3}
 \end{aligned}$$

⁴aesthetics=Ästetik”
⁵

$$\begin{aligned}
 e^x &= \sum_{n=0}^{\infty} \frac{1}{n!} x^n \\
 \Rightarrow e^{ix} &= \sum_{n=0}^{\infty} \frac{1}{n!} i^n x^n = \sum_{n=0}^{\infty} \left(\frac{1}{(2n)!} (-1)^n x^{2n} + i \frac{1}{(2n+1)!} (-1)^n x^{2n+1} \right) = \cos(x) + i \sin(x) \\
 \Rightarrow \cos(x) &= \sum_{n=0}^{\infty} \frac{(-1)^n}{2n!} x^{2n} \quad ; \quad \sin(x) = \sum_{n=0}^{\infty} \frac{(-1)^{n+1}}{(2n+1)!} x^{2n+1}
 \end{aligned}$$

We rescale the term in parenthesis and obtain

$$C(\vec{x}, \vec{x}') = \delta_{\sigma, \sigma'} \underbrace{\left(\frac{1}{(2\pi)^3} \frac{4\pi}{3} k_F^3 \right)^2}_{\frac{1}{2}n} \left(3 \frac{k_F |\vec{u}| \cos(k_F |\vec{u}|) - \sin(k_F |\vec{u}|)}{(k_F |\vec{u}|)^3} \right)^2$$

With $n = 2 \cdot \frac{1}{(2\pi)^3} \frac{4\pi}{3} k_F^3$ we obtain the final result

$$\begin{aligned} n^{(2)}(\vec{r}, \vec{r}') &= n^2 - \sum_{\sigma, \sigma'} C(\vec{x}, \vec{x}') \\ &= \sum_{\sigma, \sigma'} \left(\frac{n_{\uparrow} + n_{\downarrow}}{2} \right)^2 \left(1 - \delta_{\sigma, \sigma'} \left(3 \frac{k_F |\vec{r} - \vec{r}'| \cos(k_F |\vec{r} - \vec{r}'|) - \sin(k_F |\vec{r} - \vec{r}'|)}{(k_F |\vec{r} - \vec{r}'|)^3} \right)^2 \right) \\ &= (n_{\uparrow} + n_{\downarrow})^2 \left(1 - \frac{1}{2} \left(3 \frac{k_F |\vec{r} - \vec{r}'| \cos(k_F |\vec{r} - \vec{r}'|) - \sin(k_F |\vec{r} - \vec{r}'|)}{(k_F |\vec{r} - \vec{r}'|)^3} \right)^2 \right) \end{aligned}$$

The result is shown in Fig. 11.1. We observe that the two-particle density for identical spin direction vanishes at small distances in accordance with the Pauli principle, which excludes that two identical particles can be at the same position. The two-particle density for opposite spin is that of two uncorrelated electrons, namely the product of the two spin densities. For large distances the two-particle densities for both spin directions approach the uncorrelated value.

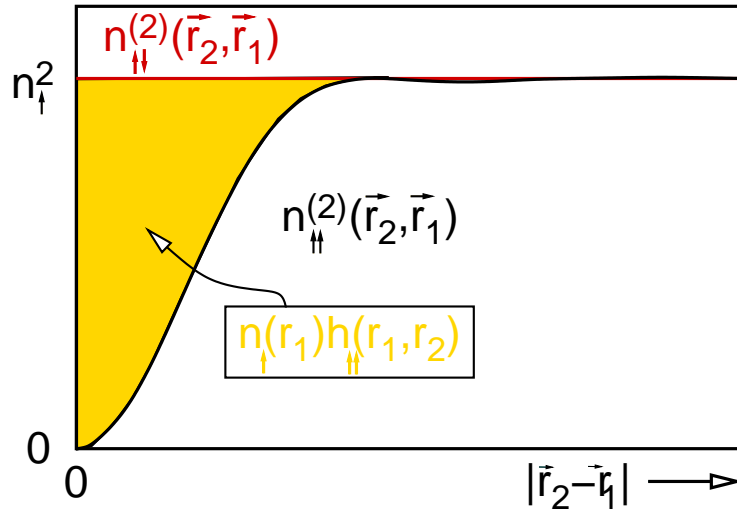


Fig. 11.1: Two-particle density of the non-interacting free-electron gas.

11.1.5 Pair-correlation function and hole function

Another quantity that is useful is the **pair-correlation function**

PAIR-CORRELATION FUNCTION

$$g(\vec{x}, \vec{x}_0) = \frac{n^{(2)}(\vec{x}, \vec{x}_0)}{n(\vec{x}_0)}$$

The pair-correlation function describes the probability to find an electron with coordinates \vec{x} , given that there is one at \vec{x}_0 . The pair-correlation function is the electron density seen by one electron that is located at \vec{x}_0 . Consider an N -electron system. Pick out one electron and determine the density of the remaining $N - 1$ electrons.

Given that an electron will see at large distances nothing but the charge density itself, it makes sense to define a more short-ranged quantity, namely the **exchange-correlation hole function** $h(\vec{x}, \vec{x}_0)$

HOLE FUNCTION $H(\vec{X}, \vec{X}_0)$

$$g(\vec{x}, \vec{x}_0) = n(\vec{x}) + h(\vec{x}, \vec{x}_0)$$

The physical picture of the hole function is that each electron “sees” the total density $n(\vec{x})$ and the density $h(\vec{x}, \vec{x}')$ of “one missing electron”. The density $h(\vec{x}, \vec{x}')$ is like a hole in the total charge density due to the fact that the remaining electrons do not come near to the electron in question. Thus, the Coulomb repulsion between the electrons is reduced relative to the Hartree energy by the attraction of the electron to its exchange-correlation hole.

Accurate calculations of the exchange-correlation hole have been obtained by quantum Monte-Carlo calculations[85].

The two-particle density can now be expressed by the density and the exchange-correlation hole function as

$$n^{(2)}(\vec{x}, \vec{x}_0) = n(\vec{x}_0) [n(\vec{x}) + h(\vec{x}, \vec{x}_0)]$$

Now, we can also rewrite the interaction energy Eq. 11.14

$$E_{int} = \underbrace{\frac{1}{2} \sum_{\sigma, \sigma'} \int d^3 r \int d^3 r' \frac{e^2 n(\vec{x}) n(\vec{x}')}{4\pi\epsilon_0 |\vec{r} - \vec{r}'|}}_{E_H} + \underbrace{\sum_{\sigma} \int d^3 r n(\vec{x}) \frac{1}{2} \sum_{\sigma'} \int d^3 r' \frac{e^2 h(\vec{x}', \vec{x})}{4\pi\epsilon_0 |\vec{r} - \vec{r}'|}}_{U_{xc}}$$

11.2 Self-made density functional

In order to understand, how density functionals are made, let us demonstrate the principle on a simple example. We will make our own, first-principles, density functional. It will not be terribly good, but it will not be a complete disaster either. However, it will be our own!

The typical process of creating a density functional is that we take all available information on the hole function, that may be relevant, and find an expression that reproduces this information as best as possible. As more and more information about the hole function becomes available, the functionals are continuously improved.

Apparently all the information about the interaction is contained in the hole function $h(\vec{r}, \vec{r}')$. Let us collect all we know so far about the hole function:

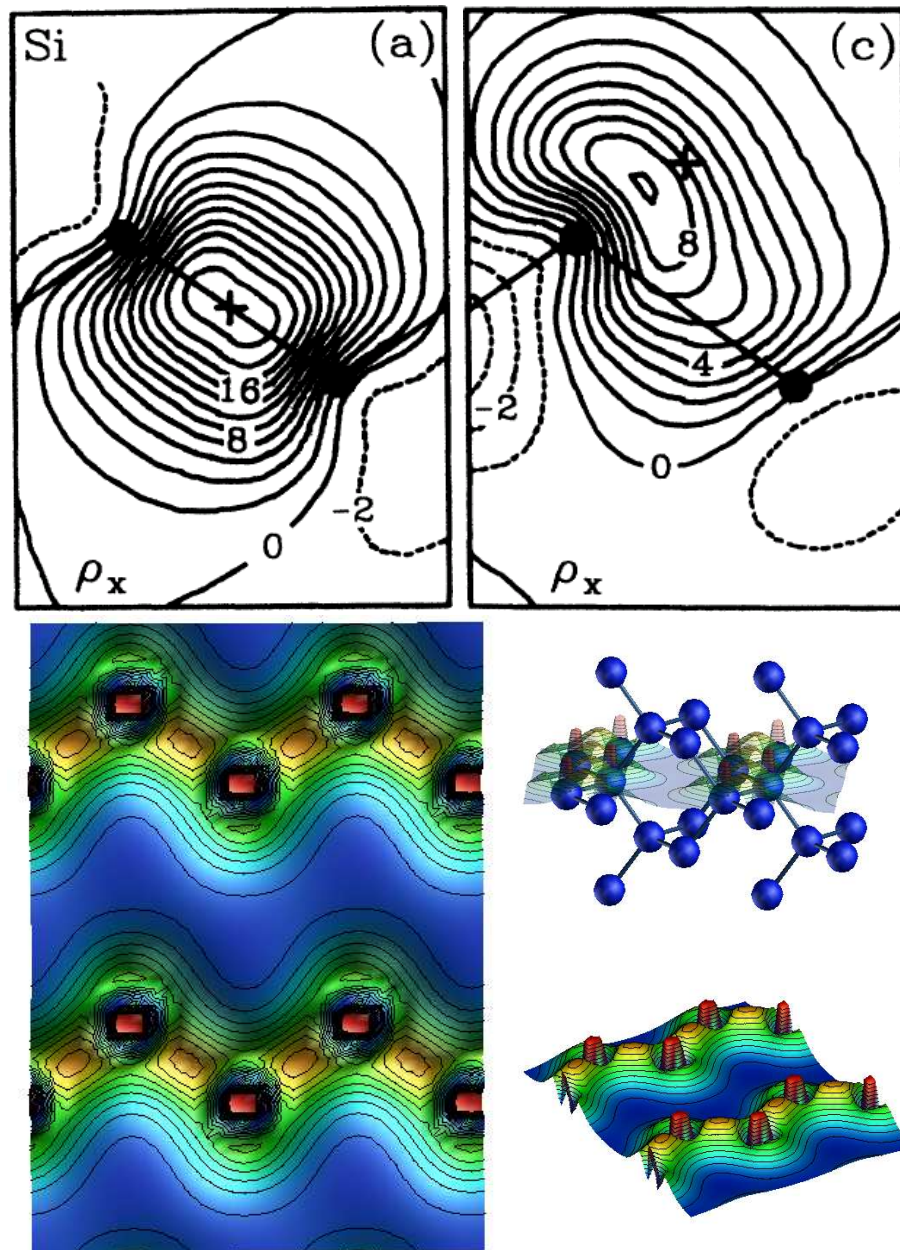


Fig. 11.2: Top: Exchange-correlation hole in the 110 plane of silicon[86]. The cross indicates the position of the reference electron. In the bond, the exchange-correlation hole is centered on the reference electron, while in the tail region it is located off-center. Bottom: Valence charge density of silicon in the (110) plane.

KNOWN PROPERTIES OF THE HOLE FUNCTION

- The hole function vanishes for large distances between the electrons

$$\lim_{|\vec{r}-\vec{r}_0|\rightarrow\infty} h(\vec{x}, \vec{x}_0) = 0$$

- The integral over the hole function with equal spins is equal to one, that is

$$\int d^3r h(\vec{x}, \vec{x}_0) = -\delta_{\sigma,\sigma_0}$$

This statement follows from the fact that an electron in an N -electron system, always sees the $N - 1$ other electrons. Thus, the correlation function \bar{g} integrates to $N - 1$ and the hole function integrates to -1 . The argument is easily extended to different spin directions.

The hole function is not a probability density function, but it is a probability density function.

Thus, we know the height, the width and the volume of the hole function. What is unknown is the shape. Let us assume the most simple shape, namely a spherical box centered at the reference electron, that is

$$h(\vec{x}, \vec{x}_0) = -n(\vec{x}_0)\theta\left(\sqrt[3]{\frac{3}{4\pi n(\vec{x}_0)}} - |\vec{r} - \vec{r}_0|\right)\delta_{\sigma,\sigma_0} \tag{11.17}$$

where $\theta(x)$ is the Heaviside function.⁶

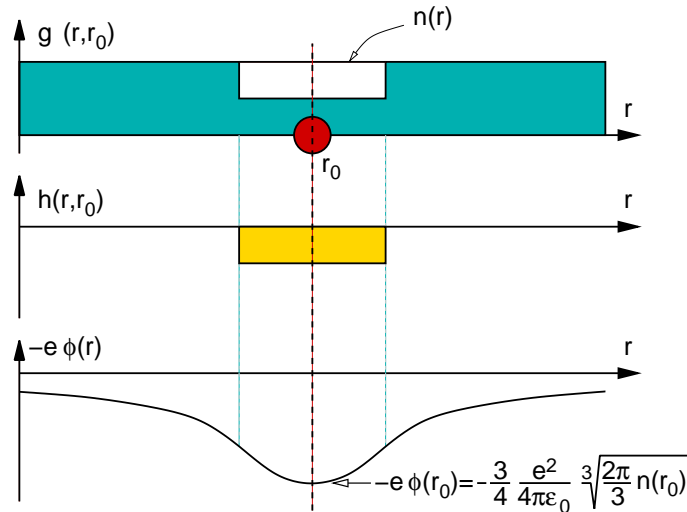


Fig. 11.3: Schematic representation of the xc-hole and the xc-potential energy. The electron density $n(\vec{r})$ is assumed to be constant. The electron shall be located at \vec{r}_0 . The two-particle density $n(\vec{r}, \vec{r}_0)$ describes the density of the $N - 1$ electrons as experienced from the reference electron at \vec{r}_0 . The two-particle density differs from the total density by the exchange hole $h(\vec{r} - \vec{r}_0)$. If we use the model that the exchange hole is a homogeneously charged sphere, the interaction energy of the reference electron and the exchange hole can be calculated as $v(\vec{r}_0)$.

⁶The Heaviside function is defined by

$$\theta(x) = \begin{cases} 0 & \text{for } x < 0 \\ \frac{1}{2} & \text{for } x = 0 \\ 1 & \text{for } x > 0 \end{cases}$$

Now, we can determine the exchange energy as

$$\begin{aligned}
E_{xc} &= \int d^3r \sum_{\sigma} n(\vec{x}) \frac{1}{2} \sum_{\sigma'} \int d^3r' \frac{e^2 h(\vec{x}', \vec{x})}{4\pi\epsilon_0 |\vec{r} - \vec{r}'|} \\
&= \int d^3r \sum_{\sigma} n(\vec{x}) \frac{1}{2} \sum_{\sigma'} \int d^3r' \frac{e^2}{4\pi\epsilon_0} \frac{-n(\vec{x}) \delta_{\sigma, \sigma'} \theta \left(\sqrt[3]{\frac{3}{4\pi n(\vec{x})}} - |\vec{r}' - \vec{r}| \right)}{|\vec{r}' - \vec{r}|} \\
&= \int d^3r \frac{1}{2} \frac{e^2}{4\pi\epsilon_0} \sum_{\sigma} n(\vec{x}) \int d^3r' \frac{-n(\vec{x}) \theta \left(\sqrt[3]{\frac{3}{4\pi n(\vec{x})}} - |\vec{r}' - \vec{r}| \right)}{|\vec{r}' - \vec{r}|} \\
&= \int d^3r \frac{1}{2} \frac{e^2}{4\pi\epsilon_0} \sum_{\sigma} n(\vec{x}) \left[-\frac{3}{2 \sqrt[3]{\frac{3}{4\pi n(\vec{x})}}} \right] \\
&= - \int d^3r \frac{3}{4} \sqrt[3]{\frac{4\pi}{3}} \frac{e^2}{4\pi\epsilon_0} \sum_{\sigma} n(\vec{x})^{\frac{4}{3}}
\end{aligned}$$

The integral over \vec{r}' is easily solved directly. Here, we take a little detour, that may add some physical insight. The integral corresponds to the potential in the center of a homogeneously charged sphere with radius $s_0 = \sqrt[3]{\frac{3}{4\pi n}}$, with a total charge of one electron. The potential of a homogeneously charged sphere can be determined by fitting the potential outside and inside.

$$\Phi(\vec{s}) = \int d^3s' \frac{en\theta(s_0 - |\vec{s}'|)}{4\pi\epsilon_0 |\vec{s}'|} = \frac{e}{4\pi\epsilon_0} \begin{cases} \frac{1}{|\vec{s}|} & \text{for } s > s_0 \\ \frac{1}{s_0} \left[\frac{3}{2} - \frac{1}{2} \left(\frac{|\vec{s}|}{s_0} \right)^2 \right] & \text{for } s < s_0 \end{cases}$$

Thus, we obtain the exchange-correlation energy per electron within our model as

$$\epsilon_{xc}(n(\vec{r}, \uparrow), n(\vec{r}, \uparrow)) = -\frac{3}{4} \sqrt[3]{\frac{4\pi}{3}} \frac{e^2}{4\pi\epsilon_0} \frac{\sum_{\sigma} n(\vec{r}, \sigma)^{\frac{4}{3}}}{\sum_{\sigma} n(\vec{r}, \sigma)}$$

If the spin-densities of both spin directions are equal, we obtain, introducing the symbol $n_t(\vec{r})$ for the total electron density,

$$\epsilon_{xc}\left(\frac{1}{2}n_t(\vec{r}), \frac{1}{2}n_t(\vec{r})\right) = -\frac{3}{4} \sqrt[3]{\frac{4\pi}{3}} \frac{e^2}{4\pi\epsilon_0} \cdot \left(\frac{n_t(\vec{r})}{2}\right)^{\frac{1}{3}}$$

and if the all electrons have the same spin, we obtain

$$\epsilon_{xc}(n_t(\vec{r}), 0) = -\frac{3}{4} \sqrt[3]{\frac{4\pi}{3}} \frac{e^2}{4\pi\epsilon_0} \cdot n_t(\vec{r})^{\frac{1}{3}}$$

The exchange-correlation energy is more favorable, if the electrons are all parallel. This is a reflection of **Hund's rule**.

In Fig. 11.4 the exchange-correlation energy per electron as function of the electron density is compared to the Hartree-Fock and the numerically correct result. Note that our model approaches the exact result for low densities. The deviation of our model is somewhat better than the Hartree-Fock result. Still, the errors are of order few eV, which is in the range of to binding energies. In an actual calculation of bond formation or bond-breaking the density changes only by a small amount and only in a local region, so that the errors will be acceptable.

Since we can now determine the interaction energy, at least in our model, we can write down a

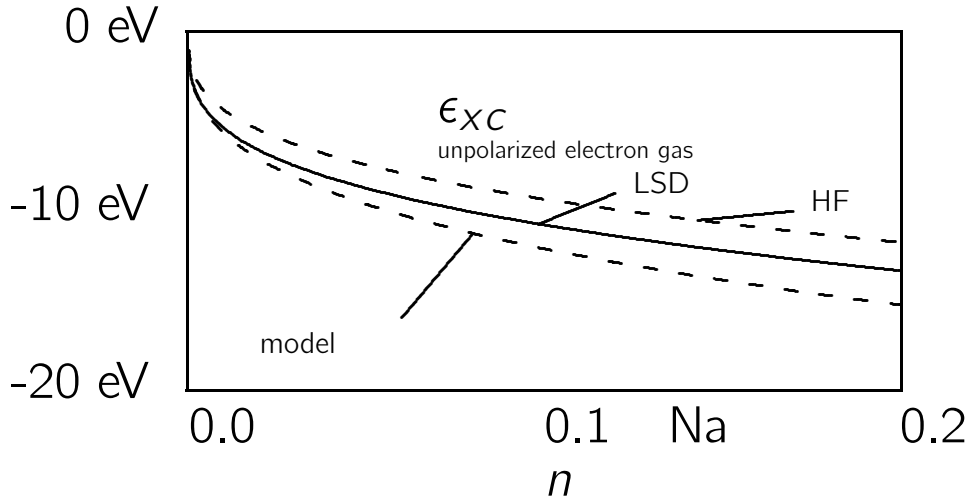


Fig. 11.4: Exchange-correlation energy per electron for a free-electron gas as function of the density. The density is given in Hartree atomic units. The dashed line denoted “model” denotes the result obtained from the model of a homogeneously charged sphere as exchange-correlation hole. The dashed line denoted “HF” is the result obtained from Hartree-Fock. The correct result, which is the result from density-functional theory is denoted by “LSD”. Note that the hard-sphere model describes the exchange-correlation energy per electron well in the low-density region, where the electrostatic repulsion dominates over the kinetic energy cost required to deform the exchange-correlation hole. The correct result lies in between the hard-sphere model and the Hartree-Fock result. This can be understood as follows: The exchange hole of the free-electron gas (Hartree-Fock) does not yet adjust to the interaction. It corresponds to the limit where the kinetic energy determines the shape of the hole. The interaction makes the hole more compact than the true exchange-correlation hole and thus lowers the total energy. In the hard-sphere model, the hole is chosen to optimize the interaction energy. It corresponds to the limit where the kinetic energy cost to deform the hole is negligible. However, it does not consider the kinetic energy cost at all. Thus, it underestimates the true exchange-correlation energy.

total-energy expression

$$\begin{aligned}
 E[n(\vec{x})] = & \underbrace{\sum_n f_n \langle \psi_n | \frac{\hat{p}^2}{2m_e} | \psi_n \rangle}_{E_{kin}} + \int d^3r n_t(\vec{r}) v_{ext}(\vec{r}) \\
 & + \underbrace{\frac{1}{2} \int d^3r \int d^3r' \frac{e^2 n_t(\vec{r}) n_t(\vec{r}')}{4\pi\epsilon_0 |\vec{r} - \vec{r}'|}}_{Hartree} - \underbrace{\int d^3r \frac{3}{4} \sqrt{\frac{4\pi}{3}} \frac{e^2}{4\pi\epsilon_0} \sum_{\sigma} n(\vec{r}, \sigma)^{\frac{4}{3}}}_{E_{xc}}
 \end{aligned}$$

The effective potential is obtained as the derivative of the potential energy

$$v_{eff}(\vec{x}) = \frac{\delta E_{pot}}{\delta n(\vec{x})} = v_{ext}(\vec{r}) + \int d^3r' \frac{e^2 n_t(\vec{r}')}{4\pi\epsilon_0 |\vec{r} - \vec{r}'|} - \underbrace{\frac{e^2}{4\pi\epsilon_0} \sqrt{\frac{4\pi}{3}} n(\vec{x})^{\frac{1}{3}}}_{\mu_{xc}(\vec{x})}$$

Note, that the exchange-correlation potential differs from the exchange-correlation energy per electron. Both scale in the same way, but they differ by a factor.

There is a second observation. The effective potential is spin dependent. This spin dependence is responsible that we can calculate whether materials are magnetic or not. The potential has nothing to do with a magnetic interaction, even though it looks exactly like a magnetic field in the Pauli equation.

In fact the origin for the magnetization of materials is unrelated to the magnetic interactions. Its true origin is the so-called **exchange interaction**, which again roots in the Pauli principle. Note, however, that the exchange interaction is not a new physical form of interaction between particles.

Fertig: WS06/07 9 Doppelstunde 4.Dec.06

11.3 Constrained search

Density-functional theory says that all ground-state properties can be expressed, at least in principle, as functionals of the charge density alone. This is a nontrivial statement, because the wave function contains far more information than the density. It also provides a dramatic simplification as the density, in contrast to the wave function, can be handled on a computer: The density is a function in three dimensions, while the wave function is a function in 3^N dimensions.

The original proof of existence for density functionals goes back to Hohenberg and Kohn[87]. Later, Levy[88, 89] and Lieb[90] have given a recipe how the density functional can actually be constructed. This proof contains the proof of existence. For this reason, I will not present the original proof of Hohenberg and Kohn, but show the one by Levy.

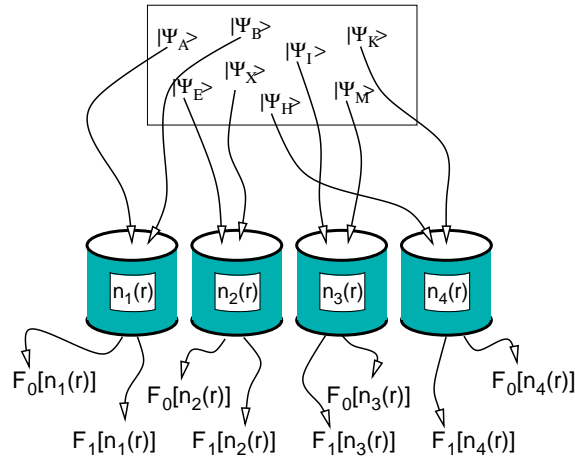


Fig. 11.5: Sketch of Levy's derivation of a density functional.

Let us start with a Hamilton operator

$$\hat{H}_\lambda = \hat{T} + \hat{V}_{ext} + \lambda \hat{W}$$

where

$$\hat{T} = \int d^4x_1 \cdots \int d^4x_N |\vec{x}_1, \dots, \vec{x}_N\rangle \left(\sum_{i=1}^N \frac{-\hbar^2}{2m_e} \vec{\nabla}_i^2 \right) \langle \vec{x}_1, \dots, \vec{x}_N|$$

is the kinetic energy operator,

$$\hat{V} = \int d^4x_1 \cdots \int d^4x_N |\vec{x}_1, \dots, \vec{x}_N\rangle \left(\sum_{i=1}^N v_{ext}(\vec{r}_i) \right) \langle \vec{x}_1, \dots, \vec{x}_N|$$

represents the external potential, and

$$\hat{W} = \int d^4x_1 \cdots \int d^4x_N |\vec{x}_1, \dots, \vec{x}_N\rangle \left(\frac{1}{2} \sum_{i \neq j} \frac{e^2}{4\pi\epsilon_0 |\vec{r}_i - \vec{r}_j|} \right) \langle \vec{x}_1, \dots, \vec{x}_N|$$

is the interaction energy operator. We have scaled the electron-electron interaction by a coupling parameter λ , which allows us later to switch the electron-electron interaction on and off. This is not required for the proof of Levy, but later on, we will often refer to Hamiltonians without interaction.

The idea of the proof is very simple:

1. Group all normalized, antisymmetric many-particle wave functions $\{|\Psi\rangle\}$ according to their density. Each such subset $\mathcal{A}[n(\vec{r})]$ contains all wave functions in the **Fock space** \mathcal{F} with the same density.

$$\mathcal{A}[n(\vec{r})] = \{|\Psi\rangle \in \mathcal{F} : \langle \Psi | \hat{n}(\vec{r}) | \Psi \rangle = n(\vec{r})\}$$

The Fock space is the union⁷ of all N -particle Hilbert spaces \mathcal{H}^N , that is

$$\mathcal{F} \stackrel{\text{def}}{=} \bigcup_{N=0}^{\infty} \mathcal{H}^N$$

The Fock space will be introduced in more detail later. If the reader feels uncomfortable with this concept, he may replace the Fock space with the N -particle Hilbert space for a specific N .

2. For each subset $\mathcal{A}[n(\vec{r})]$, that is for each density, we determine that wave function $|\Psi_{\lambda}^{(0)}[n(\vec{r})]\rangle$ that provides the lowest energy $\langle \Psi | \hat{H}_{\lambda} | \Psi \rangle$. The minimum of the total energy defines the total-energy functional $E_{\lambda}[n(\vec{r})]$ of the electron density.

$$E_{\lambda}[n(\vec{r})] = \min_{|\Psi\rangle \in \mathcal{A}[n(\vec{r})]} \langle \Psi | \hat{H}_{\lambda} | \Psi \rangle = \langle \Psi_{\lambda}^{(0)}[n(\vec{r})] | \hat{H}_{\lambda} | \Psi_{\lambda}^{(0)}[n(\vec{r})] \rangle$$

3. The energy can be divided into **universal density functional** $F_{\lambda}[n(\vec{r})]$, which is a general property of the electron gas, and a system-specific term, that depends on the external potential.

$$E_{\lambda}[n(\vec{r})] = \underbrace{F_{\lambda}[n(\vec{r})]}_{\langle \Psi_{\lambda}^{(0)}[n] | \hat{T} + \lambda \hat{W} | \Psi_{\lambda}^{(0)}[n] \rangle} + \underbrace{\int d^3r n(\vec{r}) v_{\text{ext}}(\vec{r})}_{\langle \Psi_{\lambda}^{(0)}[n] | \hat{V} | \Psi_{\lambda}^{(0)}[n] \rangle}$$

Because the energy related to the external potential only depends on the density, it is a constant within each group of a given density. Thus, we can directly determine the universal functional $F_{\lambda}[n(\vec{r})]$ as minimum of $\langle \Psi | \hat{T} + \lambda \hat{W} | \Psi \rangle$ for all wave functions with the specified density.

UNIVERSAL DENSITY FUNCTIONAL

$$F_{\lambda}[n(\vec{r})] \stackrel{\text{def}}{=} \min_{|\Psi\rangle \in \mathcal{A}[n(\vec{r})]} \langle \Psi | \hat{T} + \lambda \hat{W} | \Psi \rangle$$

4. To find the ground-state energy $E_{\lambda}^{(0)}$ of an electron gas with N electrons in a given external potential, we minimize the total-energy functional under the constraint of a specified total number of electrons.

$$E_{\lambda}^{(0)} = \min_{n(\vec{r}): \int d^3r n(\vec{r}) = N} \left\{ F_{\lambda}[n(\vec{r})] + \int d^3r n(\vec{r}) v_{\text{ext}}(\vec{r}) \right\}$$

The Lagrange parameter μ is the chemical potential of the electrons. This minimization with respect to the density provides us with the ground-state density and the ground-state energy. If we have remembered the wave function $|\Psi^0[n(\vec{r})]\rangle$ that minimized the total-energy within a group with given density $n(\vec{r})$, we can, in principle work our way back to the ground-state wave function, which contains all information about the electronic ground state.

⁷germ.: union=Vereinigung

This concludes the proof by Levy on the existence of a universal functional of the density, that allows to determine the ground-state energy and, in principle, all other properties of the electronic ground state.

11.4 Self-consistent equations

In the following, I will discuss, how this proof can be used for a practical scheme to find the electronic ground-state energy and density under the assumption that the universal functional is known.

We will be lead to a system of equations, that must be fulfilled simultaneously for the electronic ground state. Then we will show, how this system of equations can be solved iteratively.

11.4.1 Universal functional

Let us write down the universal functional $F_\lambda[n(\vec{r})]$ discussed in the proof of Levy more explicitly.

$$F_\lambda[n(\vec{r})] = \text{extr}_{\eta} \text{extr}_{\gamma(\vec{r})} \min_{|\Psi\rangle} \left\{ \langle \Psi | \hat{T} + \lambda \hat{V} | \Psi \rangle + \int d^3r \gamma(\vec{r}) \left[\langle \Psi | \hat{n}(\vec{r}) | \Psi \rangle - n(\vec{r}) \right] - \eta \left[\langle \Psi | \Psi \rangle - 1 \right] \right\}$$

Instead of explicitly grouping the wave functions we enforce the constraints by the method of Lagrange multipliers $\gamma(\vec{r})$ and η . Note, that we need not specify the chemical potential here, because the particle number is fixed by the specification of the density $n(\vec{r})$.

The operator $\hat{n}(\vec{r})$ yields the one-particle density of a many-particle wave function.⁸ It is defined by

$$\hat{n}(\vec{r}) = \int d^4x_1 \cdots \int d^4x_N |\vec{x}_1, \dots, \vec{x}_N\rangle \left(\sum_{i=1}^N \delta(\vec{r} - \vec{r}_i) \right) \langle \vec{x}_1, \dots, \vec{x}_N |$$

This means that we minimize the total energy $\langle \Psi | \hat{H}_\lambda | \Psi \rangle$ under the constraint that the density of the wave function is identical to $n(\vec{r})$ specified beforehand, namely.

$$\langle \Psi | \hat{n}(\vec{r}) | \Psi \rangle = n(\vec{r})$$

The corresponding Lagrange multiplier is $\gamma(\vec{r})$. It is position dependent, because there is a constraint for every position. In addition, we need to impose the constraint that the wave function is normalized, that is

$$\langle \Psi | \Psi \rangle = 1$$

This normalization condition is automatically fulfilled only if we restrict the search to N particle wave function and the density $n(\vec{r})$ integrates to N . However, if we allow for wave functions with variable particle number, the norm-condition must be imposed as an extra condition.

⁸Thus

$$\begin{aligned} \langle \Psi | \hat{n}(\vec{r}) | \Psi \rangle &= \int d^4x_1 \cdots \int d^4x_N \langle \Psi | \vec{x}_1, \dots, \vec{x}_N \rangle \left(\sum_{i=1}^N \delta(\vec{r} - \vec{r}_i) \right) \langle \vec{x}_1, \dots, \vec{x}_N | \Psi \rangle \\ &= \sum_{i=1}^N \int d^4x_1 \cdots \int d^4x_N \Psi^*(\vec{x}_1, \dots, \vec{x}_N) \delta(\vec{r} - \vec{r}_i) \Psi(\vec{x}_1, \dots, \vec{x}_N) \end{aligned}$$

The equilibrium condition results in a Schrödinger equation

$$\left[\hat{T} + \lambda \hat{W} + \int d^3r \gamma(\vec{r}) \hat{n}(\vec{r}) - \eta \right] |\Psi\rangle = 0$$

The wave function obeys a Schrödinger equation in an external potential $\gamma(\vec{r})$. The energy in that potential is η .

11.4.2 Exchange-correlation functional

Now, we split off from the functional $F_1[n]$, that is the universal density functional of the interacting electron gas, two terms that are fairly easy to evaluate. One is the Hartree energy E_H and the other is the kinetic energy of a non-interacting electron gas with the same density, which is simply $F_0[n]$. As a result, we obtain the **exchange and correlation energy**

EXCHANGE-CORRELATION FUNCTIONAL

$$E_{xc}[n(\vec{r})] \stackrel{\text{def}}{=} F_1[n(\vec{r})] - F_0[n(\vec{r})] - \underbrace{\frac{1}{2} \int d^3r \int d^3r' \frac{e^2 n(\vec{r}) n(\vec{r}')}{4\pi\epsilon_0 |\vec{r} - \vec{r}'|}}_{E_H}$$

Note that F_1 contains the kinetic energy of the interacting electron system and the electrostatic interaction energy, while F_0 is the kinetic energy of a non-interacting electron gas with the same density. Even though the wave functions of the interacting and the non-interacting electron gases have the same density, they are different, because they minimize different Hamiltonians.

The total-energy functional of the interacting electron system can be written with the help of the exchange and correlation energy as

$$E_1[n(\vec{r})] = F_0[n(\vec{r})] + \frac{1}{2} \int d^3r \int d^3r' \frac{e^2 n(\vec{r}) n(\vec{r}')}{4\pi\epsilon_0 |\vec{r} - \vec{r}'|} + \int d^3r n(\vec{r}) v_{\text{ext}}(\vec{r}) + E_{xc}[n(\vec{r})] \quad (11.18)$$

It seems as if we have not gained much because now we have to deal with two functionals F_0 and E_{xc} . The advantage is that F_0 is the functional for non-interacting electrons, which we can evaluate, and that E_{xc} is a small term that can be approximated. Important is also the E_{xc} can be expressed in physically intuitive terms, so that we can make reasonable assumptions about it.

11.4.3 The self-consistency condition

In order to determine the minimum of the total energy, we need to be able to determine the density which fulfills

$$\frac{\delta E_1}{\delta n(\vec{r})} \stackrel{\text{Eq. 11.18}}{=} \frac{\delta F_0}{\delta n(\vec{r})} + \int d^3r' \frac{e^2 n(\vec{r}')}{4\pi\epsilon_0 |\vec{r} - \vec{r}'|} + v_{\text{ext}}(\vec{r}) + \mu_{xc}(\vec{r}) - \mu = 0 \quad (11.19)$$

where the exchange-correlation potential is defined as

$$\mu_{xc}(\vec{r}) \stackrel{\text{def}}{=} \frac{\delta E_{xc}}{\delta n(\vec{r})}$$

The exchange-correlation potential μ_{xc} should not be confused with the chemical potential μ .

We can form all the functional derivatives of Eq. 11.19 with the exception of the functional derivative of F_0 . In the following, we will determine it.

We will make use of a **Legendre transform** of the universal density functional of the non-interacting electron gas.

As a reminder of the Legendre transform, let us take a little detour and repeat as example for a Legendre transform. We look into how the enthalpy $H(p)$, which is a function of the pressure, is constructed from the total energy $E(V)$, given as function of the volume. We start to define the enthalpy as the minimum total energy of a system connected to a volume reservoir. The latter is characterized by a pressure.

$$H(p) = \min_V E(V) + pV$$

as minimum condition we obtain

$$\frac{dE}{dV} + p = 0 \quad \Rightarrow \quad p(V^{(0)}) = - \left. \frac{dE}{dV} \right|_{V^{(0)}}$$

This equation is resolved to obtain the optimum volume $V^{(0)}(p)$ for a given pressure. Thus, we can express the enthalpy as a function of the pressure alone, namely

$$H(p) = E(V^{(0)}(p)) + pV^{(0)}(p)$$

Similarly we can obtain the energy from the enthalpy by a Legendre backtransform.

$$E(V) = \max_p H(p) - pV$$

which yields the minimum condition

$$\frac{dH}{dp} - V = 0$$

from which we obtain the pressure for a given volume $p^{(0)}(V)$, which we insert to obtain the energy as function of volume

$$E(V) = H(p^{(0)}(V)) - p^{(0)}(V)V$$

Thus, we showed how the Legendre transform works back and forth. The Legendre transform is unique if the function is either fully concave or fully convex.

After this little detour, let us Legendre transform the universal density functional.

$$Q[u(\vec{r})] = \min_{n(\vec{r})} \left\{ F_0[n] + \int d^3r n(\vec{r})u(\vec{r}) \right\}$$

The minimum condition with respect to the density yields

$$\left. \frac{\delta F_0}{\delta n(\vec{r})} \right|_{n^{(0)}([u], \vec{r})} + u(\vec{r}) = 0$$

which specifies a density $n^{(0)}([u], \vec{r})$ for each $u(\vec{r})$, so that

$$Q[u] = F_0[n^{(0)}] + \int d^3r n^{(0)}(\vec{r}) u(\vec{r})$$

The functional $Q[u]$ has an intuitive interpretation and can be calculated in a straightforward manner. It is simply the ground-state total energy of a non-interacting electron gas in an external potential $v_{eff}(\vec{r}) \stackrel{\text{def}}{=} u(\vec{r}) + \mu$, where the one-particle orbitals are occupied up to the chemical potential

μ . Because the ground state of a non-interacting system is represented by a Slater determinant we can express Q by one-particle orbitals.

$$Q[u] = \sum_n \langle \phi_n | \frac{\hat{p}^2}{2m_e} + \hat{v}_{eff} | \phi_n \rangle = \sum_n \epsilon_n$$

where the one-particle orbitals obey the Schrödinger equation

$$\left[\frac{-\hbar^2}{2m_e} \nabla^2 + v_{eff}(\vec{r}) - \epsilon_n \right] \phi_n(\vec{r}) = 0$$

and have energies smaller than the chemical potential μ . Note that the chemical potential drops out of the equation. It has been introduced here to draw the connection to the known physical quantities.

After we know how to obtain the Legendre transform $Q[u]$, the universal density functional of the non-interacting electron gas F_0 can be obtained by a Legendre backtransform

$$F_0[n] = \max_u \left\{ Q[u] - \int d^3r n(\vec{r})u(\vec{r}) \right\} \quad (11.20)$$

We see again that F_0 corresponds to the kinetic energy of a non-interacting electron gas.

The minimum condition defines an effective potential $u^{(0)}([n], \vec{r})$ as function of the density

$$\left. \frac{\delta Q}{\delta u(\vec{r})} \right|_{u^{(0)}(\vec{r})} - n(\vec{r}) = 0 \quad (11.21)$$

so that

$$F_0[n(\vec{r})] = Q[u^{(0)}([n], \vec{r})] - \int d^3r n(\vec{r})u^{(0)}([n], \vec{r})$$

Now, we can form the derivative with respect to the density

$$\begin{aligned} \frac{\delta F_0}{\delta n(\vec{r})} &= \int d^3r' \underbrace{\left(\frac{\delta Q}{\delta u(\vec{r}')} - n(\vec{r}') \right)}_{=0} \frac{\delta u^{(0)}(\vec{r}')}{\delta n(\vec{r})} - u^{(0)}(\vec{r}) \\ &\stackrel{\text{Eq. 11.21}}{=} -u^{(0)}(\vec{r}) \end{aligned} \quad (11.22)$$

Thus, we found an expression for the derivative of $F_0[n]$ and a recipe for constructing it by solving a Schrödinger equation for a non-interacting electron gas.

Now, we can insert this result, namely Eq. 11.22, into the minimum condition Eq. 11.19 of the total energy

$$\frac{\delta E}{\delta n(\vec{r})} = \underbrace{-u^{(0)}([n], \vec{r})}_{\frac{\delta F_0}{\delta n(\vec{r})}} + \int d^3r' \frac{e^2 n(\vec{r}')}{4\pi\epsilon_0 |\vec{r} - \vec{r}'|} + v_{ext}(\vec{r}) + \mu_{xc}(\vec{r}) - \mu = 0 \quad (11.23)$$

which is an equation that specifies the effective potential $v_{eff}(\vec{r}) = u(\vec{r}) + \mu$, that yields the ground-state density, as

$$\underbrace{v_{eff}(\vec{r})}_{u(\vec{r})+\mu} = v_{ext}(\vec{r}) + \int d^3r' \frac{e^2 n(\vec{r}')}{4\pi\epsilon_0 |\vec{r} - \vec{r}'|} + \mu_{xc}(\vec{r}) \quad (11.24)$$

where $n(\vec{r})$ is the ground-state density of the non-interacting electron gas in the potential $v_{eff}(\vec{r})$ and a chemical potential μ .

11.4.4 Flow chart for a conventional self-consistency loop

Thus, we can now list the equation system that defines the ground-state energy

$$\left[\frac{\hat{p}^2}{2m_e} + v_{eff}(\hat{r}) - \epsilon_n \right] |\phi_n\rangle = 0$$

$$n(\vec{r}) = \sum_{n=1}^N \phi_n^*(\vec{r}) \phi_n(\vec{r})$$

$$v_{eff}(\vec{r}) = v_{ext}(\vec{r}) + \int d^3r' \frac{e^2 n(\vec{r}')}{4\pi\epsilon_0 |\vec{r} - \vec{r}'|} + \mu_{xc}(\vec{r})$$

In Fig. 11.6 the steps required to solve this coupled system of equations is shown.

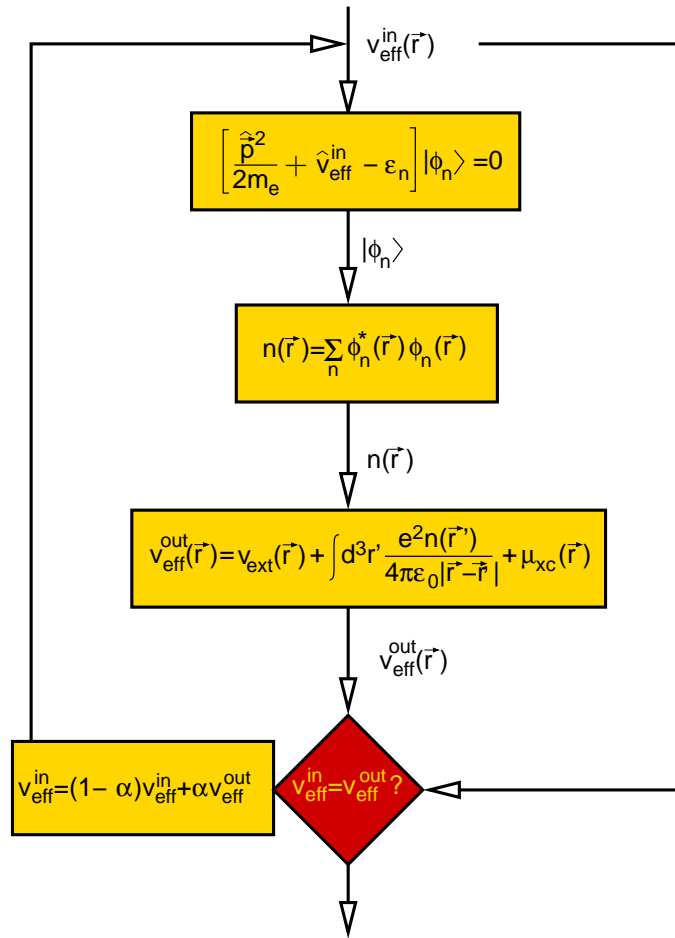


Fig. 11.6: Self-consistency cycle

11.4.5 Another minimum principle

The total-energy functional has the form

$$E_1[n] = F_0[n] + \frac{1}{2} \int d^3r \int d^3r' \frac{e^2 n(\vec{r}) n(\vec{r}')}{4\pi\epsilon_0 |\vec{r} - \vec{r}'|} + \int d^3r n(\vec{r}) v_{ext}(\vec{r}) + E_{xc}[n(\vec{r})]$$

Because the ground state of a non-interacting electron gas is a Slater determinant, we can define the functional $F_0[n]$ by minimizing over Slater determinants only. This allows us to describe F_0 as minimum over one-particle wave functions.

The functional F_0 can therefore be written as

$$F_0[\vec{n}] = \text{extr}_{\Lambda_{n,m}} \text{extr}_{v_{eff}(\vec{r})} \min_{|\phi_n\rangle} \left\{ \sum_n \langle \phi_n | \frac{\hat{p}^2}{2m_e} | \phi_n \rangle + \int d^3r v_{eff}(\vec{r}) \left[\sum_n \phi_n^*(\vec{r}) \phi_n(\vec{r}) - n(\vec{r}) \right] - \sum_{n,m} (\langle \phi_n | \phi_m \rangle - \delta_{n,m}) \Lambda_{m,n} \right\}$$

where v_{eff} plays the role of a Lagrange multiplier. This allows us to express the derivative of the universal density functional of the non-interacting electrons as

$$\frac{\delta F_0}{\delta n(\vec{r})} = v_{eff}(\vec{r})$$

In practical calculation we (1) chose an arbitrary potential v_{eff} . Then (2) we solve the Schrödinger equation, to obtain the one-particle wave functions, and the kinetic energy of the non-interacting electrons. Now, (3) we evaluate the density. The kinetic energy and the density allows us (4) to evaluate the total energy. The density provides us (5) with a new expression for v_{eff} . Out of the last and the new effective potential one creates (6) a better choice for the effective potential, which is used as new start potential for (1). If the effective potentials, the one used for the Schrödinger equation and the one obtained from the density, are identical, we have found the desired ground-state energy and density.

Fertig: WS06/07 10 Doppelstunde 10.Dec.06

11.5 Adiabatic connection

We have seen so far that one can reasonably estimate the exchange-correlation hole, and evaluate the energy of the electron in the potential of the exchange-correlation hole. However, it is nearly hopeless to estimate the kinetic energy contribution to the exchange-correlation energy.

If there would be no cost to deform the exchange-correlation hole, the latter would simply adjust such that the electrostatic energy is optimized. One can easily estimate how the hole would look like: It would have the shape of a hard sphere centered at the reference electron. Its radius would be determined by the sum rule that says that there is exactly one positive charge in the exchange-correlation hole. The reason for this shape is that the electron would repel its neighbors as much as possible, in order to reduce its electrostatic interaction.

However as the exchange-correlation hole is deformed, there is a price to pay, namely that the kinetic energy goes up. In the extreme case of a hard-sphere like hole, the wave functions would have steps, that is infinite curvature. The kinetic energy is just a measure of the curvature of the wave function. Thus, the deformation of the hole costs kinetic energy. The final shape of the XC-hole is therefore a balance between electrostatic gain and kinetic energy cost.

The **adiabatic connection** [91, 92, 93] is a theorem that allows to relate the net energy gain, including the kinetic energy cost, to the electrostatic energy gain only, but for variable strengths of the interaction energy. While this theorem looks like mystery, it cannot be applied directly. Nevertheless it provides an important route that allows important approximations to be made. The theorem is demonstrated in the following:

We consider a given electron density for which the non-interacting functional $F_0[n(\vec{r})]$ is exactly known.

$$F_\lambda[n(\vec{r})] = \langle \Psi_\lambda | \hat{T} + \lambda \hat{W} | \Psi_\lambda \rangle + \int d^3r \mu_\lambda(\vec{r}) (\langle \Psi_\lambda | \hat{n}(\vec{r}) | \Psi_\lambda \rangle - n(\vec{r})) - E_\lambda (\langle \Psi_\lambda | \Psi_\lambda \rangle - 1)$$

where $|\Psi_\lambda\rangle$ is the many electron wave function that minimizes F_λ under the constraint that the density of the wave function is equal to $n(\vec{r})$. The function $\mu_\lambda(\vec{r})$ represents the Lagrange parameters. The operator

$$\hat{n}(\vec{r}) \stackrel{\text{def}}{=} \int d^4x_1 \cdots \int d^4x_N |\vec{x}_1, \dots, \vec{x}_N\rangle \left(\sum_{i=1}^N \delta(\vec{r} - \vec{r}_i) \right) \langle \vec{x}_1, \dots, \vec{x}_N|$$

is the operator that extracts the electron density from the wave function.

The wave functions that minimize the functional obey the Schrödinger equation

$$\left[\hat{T} + \lambda \hat{W} + \int d^3r \mu_\lambda(\vec{r}) \hat{n}(\vec{r}) - E_\lambda \right] |\Psi_\lambda\rangle = 0 \quad (11.25)$$

This means that as the interaction strength is increased, a local potential, $\mu_\lambda(\vec{r})$, is switched on that ensures that the electron density remains unchanged.

If we know the derivatives of the functional with respect to the interaction strength λ , and if we know the functional for the non-interacting electron gas, we can determine the functional for the interacting electron gas as

$$\begin{aligned} F_1[n(\vec{r})] &= F_0[n(\vec{r})] + \int_0^1 d\lambda \frac{dF_\lambda[n(\vec{r})]}{d\lambda} \\ &= \langle \Psi_0 | \hat{T} | \Psi_0 \rangle + \int_0^1 d\lambda \frac{dF_\lambda[n(\vec{r})]}{d\lambda} \end{aligned}$$

The first term is simply the kinetic energy of the non-interacting electron gas with the same density as the interacting system.

Now, we can show that the derivative of the functional with respect to the interaction strength can be determined from the interaction energy alone. The proof rests on the **Hellmann-Feynman theorem**.

$$\begin{aligned} \frac{dF_\lambda[n(\vec{r})]}{d\lambda} &= \frac{d}{d\lambda} \left[\langle \Psi_\lambda | \hat{T} + \lambda \hat{W} | \Psi_\lambda \rangle \right. \\ &\quad \left. + \int d^3r \mu_\lambda(\vec{r}) \left(\langle \Psi_\lambda | \hat{n}(\vec{r}) | \Psi_\lambda \rangle - n(\vec{r}) \right) - E_\lambda \left(\langle \Psi_\lambda | \Psi_\lambda \rangle - 1 \right) \right] \\ &= \left\langle \frac{d\Psi_\lambda}{d\lambda} \right| \hat{T} + \lambda \hat{W} | \Psi_\lambda \rangle + \langle \Psi_\lambda | \hat{W} | \Psi_\lambda \rangle + \langle \Psi_\lambda | \hat{T} + \lambda \hat{W} | \frac{d\Psi_\lambda}{d\lambda} \rangle \\ &\quad + \int d^3r \frac{d\mu_\lambda(\vec{r})}{d\lambda} \underbrace{\left(\langle \Psi_\lambda | \hat{n}(\vec{r}) | \Psi_\lambda \rangle - n(\vec{r}) \right)}_{=0} \\ &\quad + \int d^3r \mu_\lambda(\vec{r}) \left(\left\langle \frac{d\Psi_\lambda}{d\lambda} \right| \hat{n}(\vec{r}) | \Psi_\lambda \rangle + \langle \Psi_\lambda | \hat{n}(\vec{r}) | \frac{d\Psi_\lambda}{d\lambda} \right) \\ &\quad - \frac{dE_\lambda}{d\lambda} \underbrace{\left(\langle \Psi_\lambda | \Psi_\lambda \rangle - 1 \right)}_{=0} - E_\lambda \left(\left\langle \frac{d\Psi_\lambda}{d\lambda} \right| \Psi_\lambda \right) + \langle \Psi_\lambda | \frac{d\Psi_\lambda}{d\lambda} \rangle \\ &= \langle \Psi_\lambda | \hat{W} | \Psi_\lambda \rangle \\ &\quad + \left\langle \frac{d\Psi_\lambda}{d\lambda} \right| \underbrace{\left[\hat{T} + \lambda \hat{W} + \int d^3r \mu_\lambda(\vec{r}) \hat{n}(\vec{r}) - E_\lambda \right]}_{=0} | \Psi_\lambda \rangle \\ &\quad + \underbrace{\langle \Psi_\lambda | \left[\hat{T} + \lambda \hat{W} + \int d^3r \mu_\lambda(\vec{r}) \hat{n}(\vec{r}) - E_\lambda \right]}_{=0} \left| \frac{d\Psi_\lambda}{d\lambda} \right\rangle \end{aligned}$$

$$\stackrel{\text{Eq. 11.25}}{=} \langle \Psi_\lambda | \hat{W} | \Psi_\lambda \rangle$$

Thus, we can express the functional for the finite interaction strength as

$$F_1[n(\vec{r})] = \langle \Psi_0 | \hat{T} | \Psi_0 \rangle + \underbrace{\int_0^1 d\lambda \langle \Psi_\lambda | \hat{W} | \Psi_\lambda \rangle}_{E_H[n(\vec{r})] + E_{xc}[n(\vec{r})]}$$

Thus, we have obtained an explicit expression for the exchange-correlation energy, that does not directly refer to the kinetic energy.

$$E_{xc}[n(\vec{r})] = \int_0^1 d\lambda \langle \Psi_\lambda | \hat{W} | \Psi_\lambda \rangle - \underbrace{\frac{1}{2} \int d^3 r \int d^3 r' \frac{e^2 n(\vec{r}) n(\vec{r}')}{4\pi\epsilon_0 |\vec{r} - \vec{r}'|}}_{E_H}$$

This expression has the problem that we still need the wave functions $|\Psi_\lambda\rangle$ for all possible values for the interaction strength.

The interaction energy can further be expressed by the exchange-correlation hole for a given value of the interaction, namely

$$\langle \Psi_\lambda | \hat{W} | \Psi_\lambda \rangle = \frac{1}{2} \int d^3 r \int d^3 r' \frac{e^2 n(\vec{r}) n(\vec{r}')}{4\pi\epsilon_0 |\vec{r} - \vec{r}'|} + \int d^3 r n(\vec{r}) \frac{1}{2} \int d^3 r' \frac{e^2 h_\lambda(\vec{r}, \vec{r}')}{4\pi\epsilon_0 |\vec{r} - \vec{r}'|}$$

so that

$$E_{xc} = \int d^3 r n(\vec{r}) \underbrace{\int_0^1 d\lambda \frac{1}{2} \int d^3 r' \frac{e^2 h_\lambda(\vec{r}, \vec{r}')}{4\pi\epsilon_0 |\vec{r} - \vec{r}'|}}_{=: \epsilon_{xc}} \quad (11.26)$$

The variable ϵ_{xc} , which itself is a functional of the density is the exchange-correlation energy per electron.

11.5.1 Screened interaction

It is possible⁹ to reformulate the exchange-correlation energy by the exchange-only energy with a screened interaction. This is a form that reminds of the so-called **GW approximation**, where the self-energy is expressed by Green's-function times screened interaction.

$$\begin{aligned} E_{xc} &\stackrel{\text{Eq. 11.26}}{=} \frac{1}{2} \int d^3 r \int d^3 r' n(r) h_0(r, r') \underbrace{\int d\lambda \frac{h_\lambda(\vec{r}, \vec{r}')}{h_0(\vec{r}, \vec{r}')}}_{v_{scr}(\vec{r} - \vec{r}')} \frac{e^2}{4\pi\epsilon_0 |\vec{r} - \vec{r}'|} \\ &= \frac{1}{2} \sum_{ij} \int d^3 r \int d^3 r' \phi_i^*(\vec{r}) \phi_j(\vec{r}) v_{scr}(\vec{r} - \vec{r}') \phi_j^*(\vec{r}') \phi_i(\vec{r}') \end{aligned}$$

where the screened interaction is defined as

$$v_{scr}(\vec{r} - \vec{r}') \stackrel{\text{def}}{=} \int d\lambda \frac{h_\lambda(\vec{r}, \vec{r}')}{h_0(\vec{r}, \vec{r}')} \frac{e^2}{4\pi\epsilon_0 |\vec{r} - \vec{r}'|}$$

Note that, in contrast to the GW approximation, our expression is exact, but, on the other hand, it is limited to the ground state.

Note also that the screened interaction in this formulation only enters the exchange term, but not the Hartree term. It also includes the kinetic energy correction.

The qualitative behavior can be understood easily:

⁹This is an idea from the author, that has not been crosschecked properly. Therefore, some caution is required.

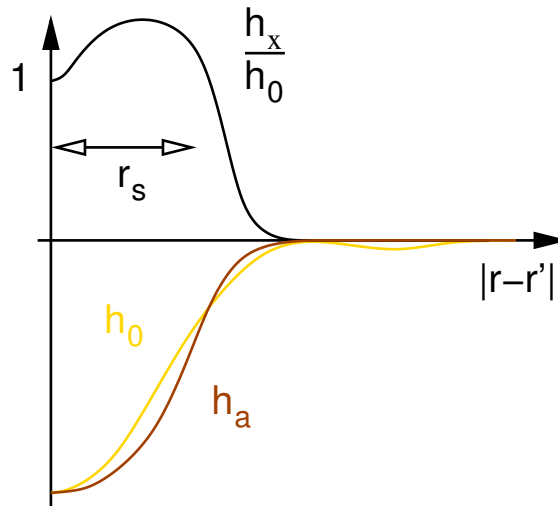


Fig. 11.7: Schematic diagram of the effect of the screening of the interaction. The golden line h_0 is the hole function of the non-interacting reference system, while the red line h_λ is the hole function in presence of a scaled interaction. The ratio scaled the Coulomb interaction in the exchange term. It suppresses the long-range tail of the interaction, and enhances the interaction for intermediate distances. r_s is the average electron radius $\frac{4\pi}{3}r_s^2 * n = 1$. (h_a and h_x should be h_λ ; Problem with the drawing program.)

- The hole function $h_\lambda(\vec{r}, \vec{r}')$ for a finite interaction is generally more compact than the one obtained without interaction. Thus, the screened interaction v_{scr} is generally more short ranged than the unscreened interaction.
- The screened interaction for $\vec{r} = \vec{r}'$ is identical to the unscreened interaction, because the hole function cancels exactly the spin density, independent of the strength of the interaction.
- Due to the compression of the hole upon increasing interaction and because of the sum-rule that the hole integrates to exactly one positive charge, the interaction must be enhanced for intermediate distances.
- The screening will be more effective, if the price for the distortion of the wave function is low, that is for a low density. This implies that the unscreened interaction is a reasonable approximation in the high-density region around the atomic center, while the tail region of a molecule is better described by a more short-ranged interaction.

11.5.2 Hybrid functionals

The adiabatic connection scheme is exploited in the construction of so-called **hybrid functionals**. These density functionals describe the exchange-correlation energy as a mixture of the correct exchange, obtained as in the Hartree-Fock method and another local or gradient corrected functional.

The performance of the hybrid functionals is probably among the best. They have the disadvantage that they require that the Hartree-Fock exchange must be evaluated, which is computationally more challenging than the evaluation of the regular density functionals.

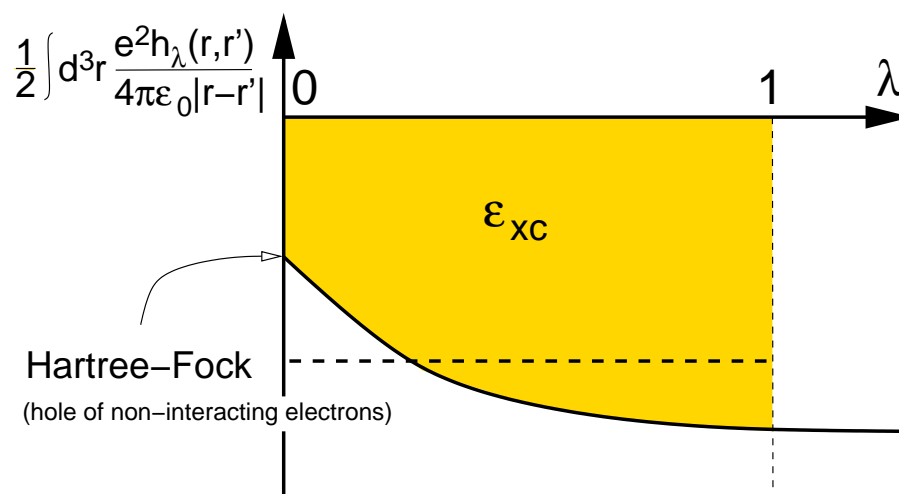
The idea behind the hybrid functionals is that the local functionals are appropriate if the interaction energy is very large. However if the interaction energy is small, the exchange hole is given by Hartree-Fock exchange.

If for example the kinetic energy dominates, the shape of the exchange-correlation hole cannot adjust, and we can approximate $h_\lambda(\vec{r}, \vec{r}') \approx h_0(\vec{r}, \vec{r}')$ by the hole of the non-interacting electron gas.

Thus, we obtain

$$\epsilon_{xc} \approx \frac{1}{2} \int d^3r' \frac{e^2 h_0(\vec{r}, \vec{r}')}{4\pi\epsilon_0 |\vec{r} - \vec{r}'|}$$

If the electrostatic interaction dominates over the kinetic energy then $h_1(\vec{r}, \vec{r}')$ would be a hard sphere, and therefore fairly local. Therefore, the hybrid functionals try to approximate the integral by a superposition of HF-exchange and a local density functional.



11.6 Functionals

According to the Bible, Jacob had a dream in which he saw a ladder descending from Heaven to Earth and angels climbing and descending the ladder¹⁰. In John Perdew's dream, the angels are users of DFT who climb the ladder to gain greater precision (at greater cost), but who also need to be able to descend the ladder depending upon their needs[94].

¹⁰Jacob's ladder has been described in the Book of Genesis (28:11-19). It is a ladder from earth to heaven on which the angels descend and ascend.

JACOB'S LADDER OF DENSITY FUNCTIONALS

The different stairs of Jacob's Ladder of density functionals are

1. LDA (local density approximation): the exchange-correlation hole is taken from the free-electron gas. These functionals exhibit strong overbinding. While the van-der Waals bond is not considered in these functionals, the overbinding mimicked van-der-Waals bonding, albeit for the wrong reason.
2. GGA (generalized gradient approximation): These functionals not only use the electron density but also its gradient to estimate the asymmetry of the exchange-correlation hole with respect to the reference electrons. As a result, surfaces are energetically favored compared to LDA and the overbinding is strongly reduced.
3. meta-GGA: in addition to the gradient also the kinetic energy density is used as a parameter. The kinetic energy is a measure for the flexibility of the electron gas.
4. Hybrid functionals: Hybrid functionals include a fraction of exact exchange. These functionals improve the description of left-right correlations.
5. Exact: An exact density functional can be obtained using the constrained search formalism using many-particle techniques.

11.7 X_α method

Even before the invention of density-functional theory per se, the so-called X_α method has been introduced. Today, the X_α method has mostly historical value. The X_α method uses the expression for the exchange of a homogeneous electron gas instead of the exchange-correlation energy. However, the exchange energy has been scaled with a parameter, namely X_α , that has been adjusted to Hartree-Fock calculations. The results are shown in Fig. 11.8.

The rationale behind the X_α -method is a dimensional argument. Choose a given shape for the exchange-correlation hole, but scale it according to the density and the electron sum rule. Then the exchange-correlation energy per electron always scales like $n^{\frac{1}{3}}$. Each shape corresponds to a pre-factor.

Consider a given shape described by a function $f(\vec{r})$ with

$$\begin{aligned} f(\vec{0}) &= 1 \\ \int d^3r f(\vec{r}) &= 1 \end{aligned}$$

Now, we express the hole function by the function f by scaling its magnitude at the origin such that the amplitude of the hole cancels the electron density. Secondly, we stretch the function in space so that the sum rule, which says that the hole must integrate to -1 , is fulfilled. These conditions yield the model for the exchange correlation hole.

$$h(\vec{r}_0, \vec{r}) = -n(\vec{r}_0) f\left(\frac{\vec{r} - \vec{r}_0}{n(\vec{r}_0)^{\frac{1}{3}}}\right)$$

The corresponding exchange-correlation energy per electron is

$$\epsilon_{xc}(\vec{r}) = -\frac{1}{2} \int d^3r' \frac{e^2}{4\pi\epsilon_0|\vec{r} - \vec{r}'|} f\left(\frac{\vec{r} - \vec{r}'}{n(\vec{r})^{\frac{1}{3}}}\right)$$

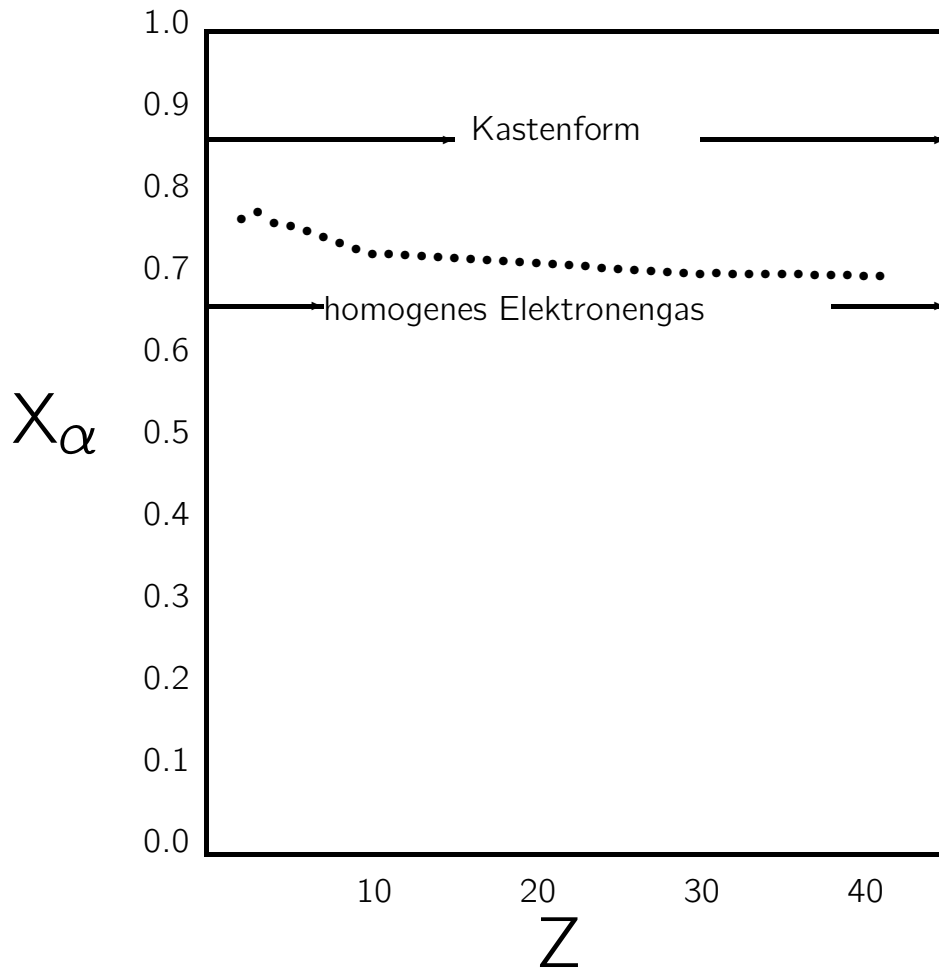


Fig. 11.8: X_α value obtained by comparison of the atomic energy with exact Hartree-Fock calculations as function of atomic number of the atom.[95, 96]

If we introduce a variable transform

$$\vec{y} = \frac{\vec{r} - \vec{r}'}{n(\vec{r})^{\frac{1}{3}}}$$

we obtain

$$\epsilon_{xc}(\vec{r}) = -\frac{n(\vec{r})^{\frac{1}{3}}}{2} \int d^3y' \frac{e^2}{4\pi\epsilon_0|\vec{y}'|} f(\vec{y}') = -Cn^{\frac{1}{3}}$$

where C is a constant that is entirely defined by the shape function $f(\vec{r})$.

In general, the X_α method yields larger band gaps than density functional theory. The latter severely underestimates band gaps. This is in accord with the tendency of Hartree-Fock to overestimate band gaps. In contrast to Hartree-Fock, however, the X_α method is superior for the description of metals because it does not lead to a vanishing density of states at the Fermi level.

11.8 Local density functionals

The first true density functionals were constructed for the homogeneous electron gas, by extracting the exchange-correlation energy per electron ϵ_{xc} from a calculation of the interacting homogeneous electron gas.

A breakthrough came about when Ceperley and Alder[97] performed quantum Monte-Carlo calculations of the homogeneous electron gas as function of the density. Quantum Monte-Carlo calculations are computationally expensive, but provide the energy of an interacting electron gas in principle exactly, that is with the exceptions of numerical errors. These results have been parameterized by Perdew and Zunger[98] and combined with so-called RPA results for the high-density limit. **RPA** stands for **Random-Phase Approximation** [99], which is accurate in the high density limit.

These density functionals exhibit very good results for solids. Electron densities are nearly perfect. Bond distances are typically underestimated by 1-3 % and bond angles agree with experiment within few degrees. Binding energies, on the other hand, are strongly overestimated. The errors are in the range of electron volts and thus comparable to bond energies. Thus, these functionals have been useless for studying chemical reactions. However, the results for solid-state processes such as diffusion have been very good. This has led to a long-standing misunderstanding between solid-state physicists and chemists about the usefulness of density-functional theory. The density functionals worked fine for solids, which was what the physicists are interested in, while they were a disaster for the binding energies of molecules, the major interest of chemists. This difficulty has been overcome by the gradient corrected density functionals discussed later.

The overestimate of the binding energies covers up the lack of van-der-Waals interactions. For example, the binding energy and the bond distances of noble gases are in very good agreement with experiment. However, the agreement is good for the wrong reason. The weak van-der-Waals interaction is not described properly in local density functionals, but the overbinding compensates for this fact.

For a long time it was surprising that the approximate density functionals work at all. They have been derived from a completely homogeneous electron gas and are applied to an electron density of real materials, which are far from homogeneous. Jones and Gunnarsson gave one explanation, namely that density functionals observe an important sum rule, namely that the exchange-correlation hole integrates to minus one electron charge. Fig. 11.9 compares the exchange hole of a free-electron gas with that of a nitrogen atom, demonstrating that despite their very different shape, their contributions to the exchange energy are similar.

11.9 Local spin-density approximation

In order to describe magnetic systems, or so-called open-shell molecules, one uses the local spin-density approximation, where the spin-dependent density $n(\vec{x}) = n(\vec{r}, \sigma)$ is used instead of the total density $n(\vec{r}) = \sum_{\sigma} n(\vec{x})$. As a result, we obtain one-particle wave functions with spin up and spin down character and one obtains two effective potentials, one for the spin-up electrons and another for the spin-down electrons.

The difference between the effective potentials acts like a magnetic field, even though its origin is purely electrostatic, namely exchange and correlation also called the **exchange interaction**.

11.10 Non-collinear local spin-density approximation

While the local spin-density formalism only allows one-particle wave function to have either purely spin-up or purely spin down character, the non-collinear formulation allows the wave functions to have a mixed spin-up and spin-down character. As a result, the magnetization can not only vary in magnitude but also in direction.

11.11 Generalized gradient functionals

For a long time one has hoped to obtain better functionals by including also a dependence on the gradient of the density. The first attempts started from a model with a weakly oscillating electron

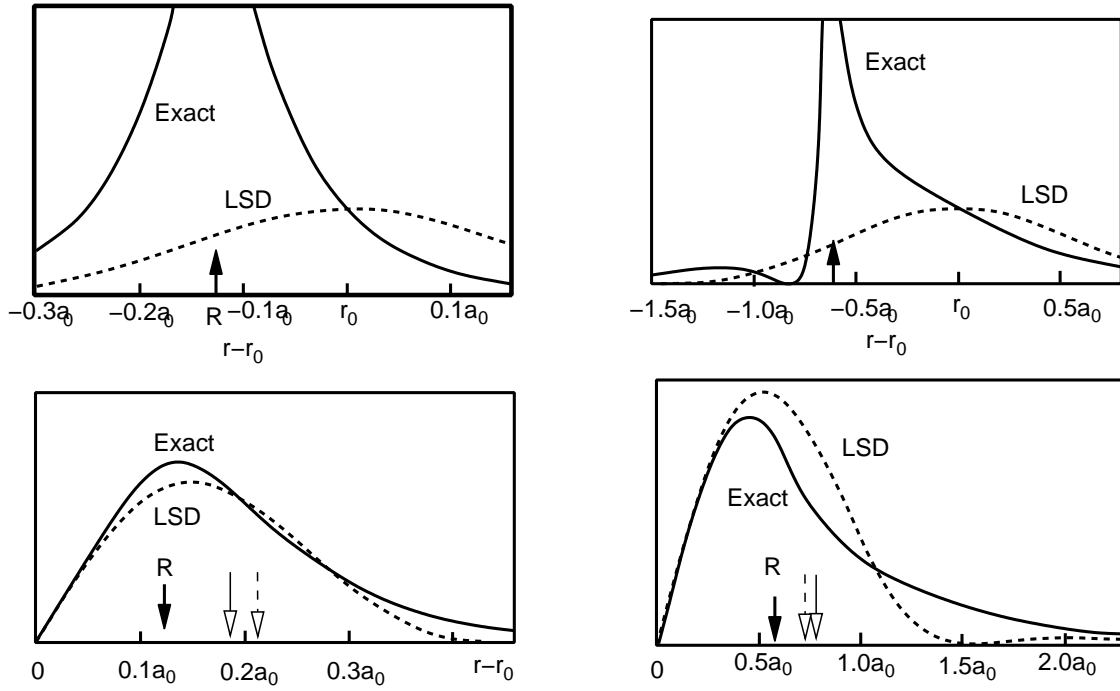


Fig. 11.9: exchange-correlation hole of an electron in the nitrogen atom (full line) and in the local density-functional approximation (dashed) [100]. In the left row, the reference electron is located $0.13 a_0$ from the nucleus and on the right it is located further, at $0.63 a_0$. Even though the shape of the DFT-exchange hole deviates grossly from the correct exchange hole, the spherical averages shown in the bottom figures are similar, which is attributed to the particle sum rule, obeyed in the local density approximation (LDA). The arrows pointing down indicate the exact and the DFT result of $\left[\int d^3r \frac{|\psi(\vec{r}, \vec{r}_0)|}{|\vec{r}-\vec{r}_0|} \right]^{-1}$. Similar results are available for neon [98].

density. The resulting functionals however were worse than the local functionals.

The reason for this failure was that when the expansion for slowly varying densities are extrapolated to strongly oscillating densities, the density of the exchange-correlation hole was overcompensating the total density.

Later one realized that one should introduce a dimension-less scaled gradient defined as

$$s = \frac{r_s |\vec{\nabla} n|}{n}$$

The scaled gradient allows to switch off the gradient corrections in a physical sense, that is if the hole runs into the danger of producing a negative correlation function $g(\vec{x}', \vec{x})$.

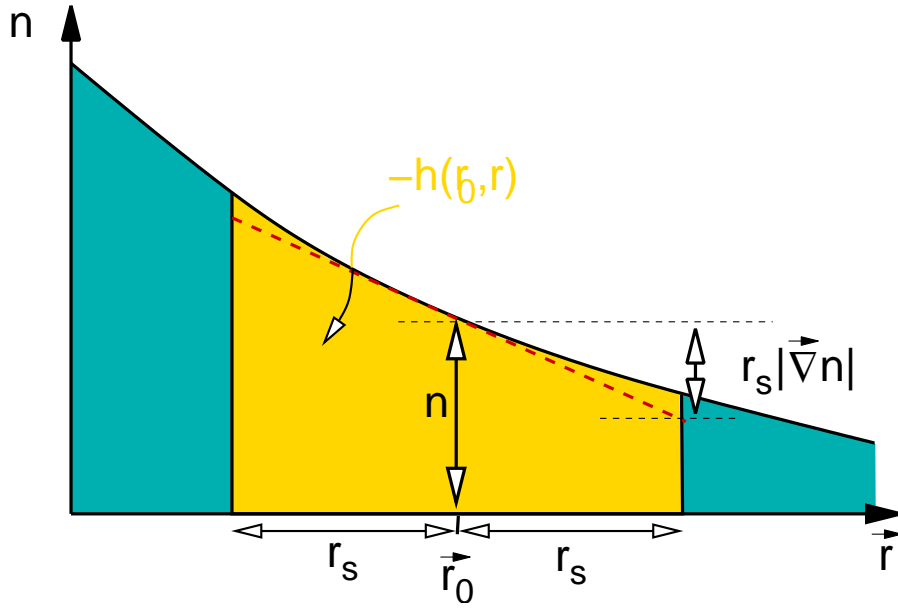
One way to construct the density is to use the results for slowly varying densities, which provides the parameter β .

$$\epsilon_{xc}(n, s) = \epsilon_{xc}^{hom} \left[1 + \beta(n) s^2 \right] \quad \text{for} \quad s \ll 1 \quad (11.27)$$

Surprisingly, the scaled gradient is largest in the tails of the wave functions, where the density falls off exponentially, that is

$$n(\vec{r}) \approx A e^{-\lambda \vec{e} \cdot \vec{r}}$$

where \vec{e} is the unit vector pointing into the direction in which the density falls off. Let us determine



the scaled gradient for this density

$$s = \sqrt[3]{\frac{3}{4\pi} \frac{A\lambda \exp(-\lambda \vec{e}\vec{r})}{A^{\frac{4}{3}} \lambda \exp(-\frac{4}{3}\lambda \vec{e}\vec{r})}} = \sqrt[3]{\frac{3}{4\pi}} \lambda n^{-\frac{1}{3}} \rightarrow \infty$$

If we use only the gradient correction with the small- s expansion, the exchange-correlation energy per particle clearly becomes infinite.

However, in the tail region we can make use of other information. Consider an electron that is far outside of a molecule. It is clear that it “sees” a molecule with $N - 1$ electrons. Thus, the hole is entirely localized on the molecule and the center of the hole is far from the reference electron. If the hole is at the molecule and the reference electron is far from it, we can estimate its interaction by

$$\epsilon_{xc} = \frac{1}{2r} \quad (11.28)$$

where r is the distance of the electron from the molecule.

Let me demonstrate the construction of such a gradient corrected functional using the example of Becke’s gradient correction for exchange[101]. We make an ansatz for the exchange energy per electron as

$$\epsilon_{xc} = C n^{\frac{1}{3}} F(s) \quad (11.29)$$

where C is the pre-factor for the exchange energy. The function $F(s)$ is determined such that small gradient expansion, Eq. 11.27, is reproduced, and that the exchange energy per electron in the tail region is correct.

To consider the tail region we require

$$\epsilon_{xc} \stackrel{\text{Eq. 11.29}}{=} C n^{\frac{1}{3}} F(s) \stackrel{\text{Eq. 11.28}}{=} \frac{1}{2r} \quad \Rightarrow \quad F(s) = \frac{1}{2C r n^{\frac{1}{3}}} \quad \text{for } s \rightarrow \infty$$

First, we express the radius by the density and insert the result in Eq. 11.30 to obtain an expression for $F(n(s))$.

$$\begin{aligned} n(r) = A e^{-\lambda r} &\quad \Rightarrow \quad r(n) = -\frac{1}{\lambda} \ln \left[\frac{n}{A} \right] \\ \Rightarrow F(s) = \frac{1}{2C r n^{\frac{1}{3}}} &= \frac{-\lambda}{2C n^{\frac{1}{3}} (\ln[n] - \ln[A])} \end{aligned}$$

Next we express the density by the scaled gradient and insert the result in the above equation to obtain an expression for $F(s)$.

$$\begin{aligned}
 s(n) &= \sqrt[3]{\frac{3}{4\pi}} \lambda n^{-\frac{1}{3}} \quad \Rightarrow \quad n(s) = \frac{3\lambda^3}{4\pi} s^{-3} \\
 \Rightarrow F(s) &= \frac{-\lambda}{2Cn^{\frac{1}{3}} (\ln[n] - \ln[A])} \\
 &= \frac{-\lambda}{2C\sqrt[3]{\frac{3\lambda^3}{4\pi}} \frac{1}{s} \left(\ln\left[\frac{3\lambda^3}{4\pi} s^{-3}\right] - \ln[A] \right)} \\
 &= \frac{-s}{2C\sqrt[3]{\frac{3}{4\pi}} \left(\ln\left[\frac{3\lambda^3}{4\pi A^3} s^{-3}\right] - 3\ln[s] \right)} \\
 &\stackrel{s \rightarrow \infty}{\approx} \frac{1}{6C} \sqrt[3]{\frac{4\pi}{3}} \frac{s^2}{s \ln[s]}
 \end{aligned}$$

This equation gives us the large gradient limit of $F(s)$.

In order to connect the low gradient limit with the large gradient limit we choose

$$F(s) = 1 + \frac{\beta s^2}{1 + 6C\beta s \sinh^{-1}(s)}$$

The result is shown in Fig. 11.10.

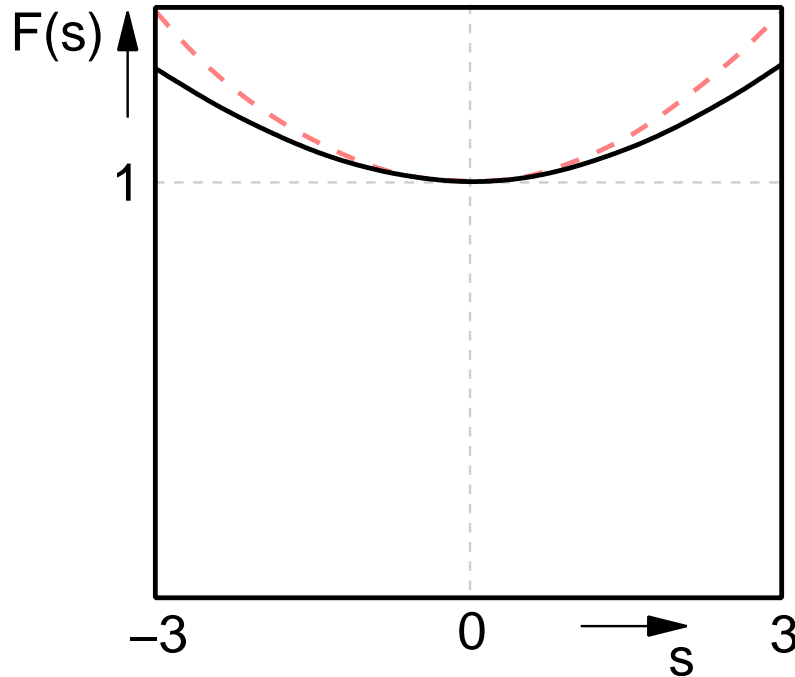


Fig. 11.10: The function $F(s)$ from Becke's gradient corrected functional [101] for the exchange energy and from the small gradient expansion (dashed). Note that the gradient correction of Becke is smaller than the expansion for large gradients.

The gradient correction plays the role of a surface energy, as it contributes mostly in the tail region. While the exchange-correlation energy per electron falls off exponentially in the local functionals, it falls off as $\frac{1}{2r}$ in the gradient corrected functionals. This effect lowers the energy in the tail region

of a molecule compared to the local functionals. If we break a bond, the surface area of a molecule increases, because the bond is transformed into a tail region. Thus, the gradient correction favors the dissociation of the bonds. As a consequence, gradient corrected functionals avoid the artificial overbinding of the local functionals. This argument also explains that local functionals perform fairly well in solids: If an atom diffuses, there is no additional surface created so that the gradient correction is minor.

Up to now there is an entire suite of different gradient corrected functionals. They are called **Generalized Gradient Approximations (GGA)** to differentiate them from the gradient expansions. The most common functionals are the Perdew-Wang-91-GGA, which has been superseded by the simpler Perdew-Burke-Ernzerhof functional. Both yield nearly identical results.

As shown in Fig. 11.11, the performance of gradient corrected functionals is extremely good also for binding energies, which were unsatisfactory in the local density functionals. This has drawn also the chemists into the field of density-functional calculations.

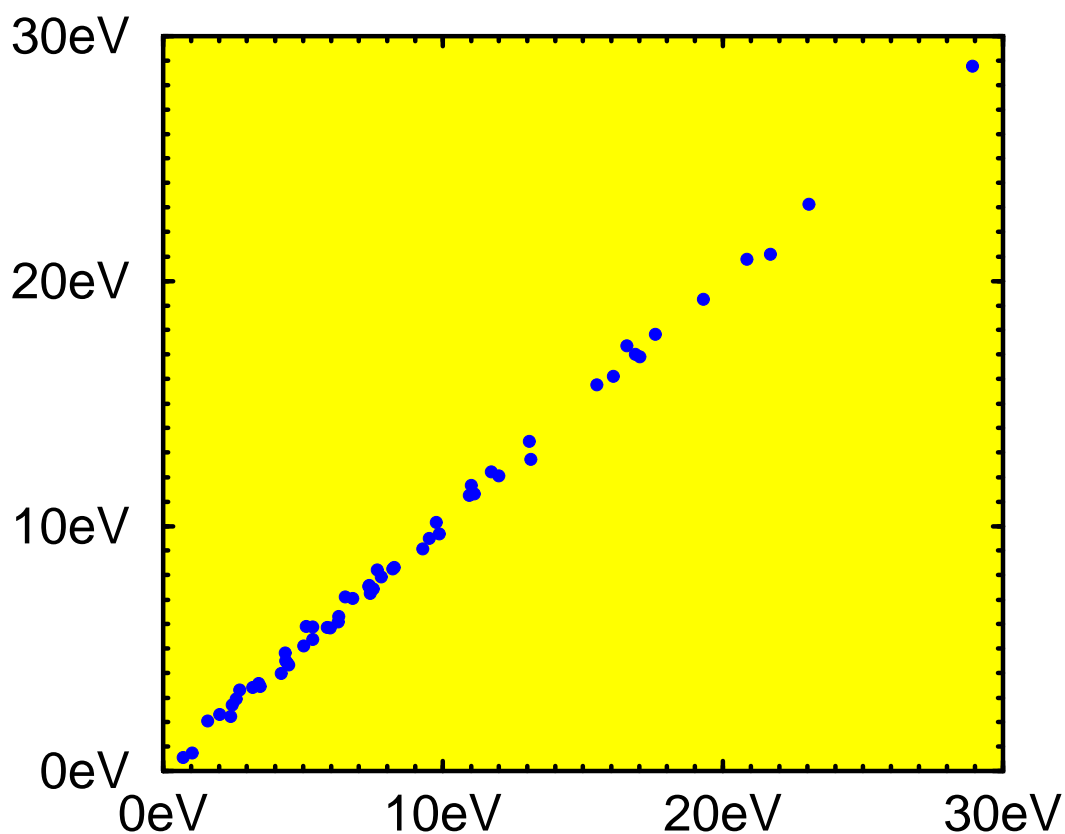


Fig. 11.11: Accuracy of the atomization energies calculated with the Becke88-Perdew86 density functional compared to experiment.

11.12 Additional material

11.12.1 Relevance of the highest occupied Kohn-Sham orbital

According to Perdew[102?], the energy of the highest occupied Kohn Sham orbital is the ionization potential of the material.

This statement has been disputed by Kleinman[103].

11.12.2 Correlation inequality and lower bound of the exact density functional

11.13 Functionals

- **[X- α]** Uses a local expression for exchange as derived from the free-electron gas, and scaled with a factor α .
- **[Barth-Hedin]**
- **[PZ (Perdew-Zunger)]** parameterization of Ceperley and Alder's quantum Monte Carlo data of the free-electron gas.
- **[BP86 (Becke-Perdew)]**
- **[PW91 (Perdew-Wang)]** First completely parameter free version of a gradient corrected density functional
- **[PBE (Perdew-Burke-Ernzerhof)]**
- **[B3LYP (Becke-Lee-Yang-Parr)]** Hybrid functional.
- **[GGA (Generalized gradient approximation)]** General expression for gradient corrected functionals.
- **[Hybrid functionals]** General expression functionals employing a mixture of Hartree-Fock and a density functional

Fertig: WS06/07 11 Doppelstunde 13.Dec.06

11.14 Reliability of DFT

If we knew the exact density functional, we would be able to determine exactly

- the total energy
- the electron density and
- the energy of the highest occupied orbital

The argument that DFT predicts the highest occupied orbital, while the orbital energies of all other one-particle orbitals are, in principle, without physical meaning goes as follows: Far from the surface of a crystal the density of a one-particle orbital falls off as $e^{-\lambda z}$ where λ is related to the orbital energy by $\lambda = \frac{1}{\hbar} \sqrt{-2m_e \epsilon}$, where the orbital energy is measured relative to the vacuum level, that is $\lim_{z \rightarrow \infty} V_{eff}(\vec{r})$. For large distances the highest occupied orbital, which has the slowest decay, will dominate the electron density. Thus, if we would know the electron density very accurately far from a surface, we would be able to determine the dominant exponential decay constant and thus

the energy of the highest occupied orbital.¹¹ Thus, the energy of the highest occupied orbital can be determined from the density, which is an exact prediction of DFT.

Of course, even though exact DFT predicts these quantities accurately, it remains to be seen in each case if that also holds for the approximate functionals used in practice.

- **Bond energies:** Local functionals overestimate binding by often more than 1 eV. Energies are fairly good as long as the effective surface area of the system is not changed. This poor result is dramatically improved by the GGA's.
- **Structures:** bond lengths are underestimated in LDA by 0-2 %. They are overestimated by GGA's by 0-2 %.
- **Dipole moments** standard deviation 0.1 Debye[104]

11.15 Deficiencies of DFT

- **Missing van-der-Waals interaction:** The van-der-Waals interaction is not included. Surprisingly the description of van-der-Waals bonds is nearly perfect with truly local density functionals. This however is an artifact of the tendency to overbinding in truly local density functionals on the one hand, and the lack of van-der-Waals interactions on the other. Since the overbinding of covalent bonds introduces errors in the range of 1 eV, it is generally not a good idea to use truly local density functionals instead of their gradient corrected counterparts.

A density functional for the van-der-Waals interaction has been developed by Dion et al.[105]. It is named vdWDF (van-der-Waals density functional).

- **Band-gap Problem:** If we compare the spectrum of Kohn Sham states with optical absorption spectra we observe that the band gaps are too small. This is not a deficiency of density-functional theory, but an over-interpretation of the Kohn Sham spectrum. The excited states should not be calculated from the same potential as the ground state.
- **Reduced band width:** Band width of alkaline metals.
- **Mott insulators**
- **unstable negative ions**
- **Broken symmetry spin states:** singlet O₂ Molecule
- **Transition states:**
- **High-energy spectrum:** The high-energy part of the Kohn-Sham spectrum is too low compared to the measured optical spectrum. The reason is that the exchange-correlation hole cannot follow the very fast electrons.????

¹¹There is a caveat in the argument. Consider an insulator which may have surface states in the band gap. In that case the density would probe the highest occupied surface state, which may lie above the highest occupied bulk state.

Chapter 12

Magnetism

Noncollinear magnetism See (1) C.Herring, *Magnetism, exchange interactions among itinerant electrons*, Academic press, New York and London 1966. (2) L. Sandratskii, Phys Stat Sol. (b) 135, p.167 (1986) (3) L. Sandratskii J. Phys. F: Metal Phys. 15. L43 (1986) (4) Lizarraga Jurado, R., *Non-collinear Magnetism, in d- and f-electron systems*, PhD Thesis, Upsala University (2006), ISBN 91-554-6540-4, <https://www.diva-portal.org/smash/get/diva2:168187/FULLTEXT01.pdf> [106]

12.1 Charged particles in a magnetic field

12.2 Dirac equation and magnetic moment

Spin-orbit coupling responsible for magnetic anisotropy.

- Non-relativistic magnetic moment \vec{m} of a charge rotating about a center

$$\vec{m}_{cl} = \frac{q}{2m} \vec{L} \quad (12.1)$$

- Dirac equation defines the gyro-magnetic ratio of $g = 2$.
- Quantum field theory leads to $g = 2.00232\dots$

12.3 Magnetism of the free-electron gas

Landau levels

12.4 Magnetic order

Stoner criterion, Pauli paramagnetism,

ferromagnetism, ferrimagnetism, antiferromagnetism, Ising model, Heisenberg model, Weiss regions.

Part III

Appendices

Appendix A

Organization

A.1 Some ideas on the examination

Here I am collecting some material that could be relevant for the examination. When it is complete it should cover the main points conveyed in the lecture. **Editor: It is still far from complete!** As student you may orient yourself on this list while preparing for the lecture. However, you cannot rely on it!

I recommend to not use this as the sole approach to prepare because this will accumulate disconnected knowledge. Disconnected knowledge is of little practical value and it is rapidly forgotten. Rather, the student is encouraged to consult this list during learning the material to remind himself and to gain confidence.

- Calculate band structures for electrons and phonons from specified lattice vectors and parameters for the Hamiltonian.
- Do everything with two-by-two matrices: Know the inverse, determinant, hermitian conjugate, transpose, complex conjugate. Be able to diagonalize a two-by-two matrix and to identify a unitary matrix.
- What is level repulsion?
- What is an avoided crossing?
- Standard Hamiltonian of solid state physics and its limitations.
- Born-Huang ansatz and its interpretation, Born-Oppenheimer equation and nuclear Schrödinger equation. Know the meaning of all indices in the nuclear Schrödinger equation. Explain!
- Born-Oppenheimer approximation and its limitations.
- Pauli principle. Understand particle exchange symmetry.
- What is a conical intersection. Why are conical intersections important?
- calculate the magnetization and the charge density from a two-component Pauli spinor wave function and for a Slater-determinant made from a set of Pauli-spinor wave functions.
- What is the non-crossing theorem? (Statement without proof)
- Provide the general expression for the charge density $\rho(\vec{r})$ and the magnetization $\vec{m}(\vec{r})$, respectively the electron density $n(\vec{r})$ and the spin density $\vec{s}(\vec{r})$. Given are the occupations and natural orbitals, which are a two-component Pauli spinor wave functions.

- determine the electron wave function of a one-electron system with a given spatial one-particle wave function $|\varphi\rangle$ and the requirement that the spin points in x -direction.
- Slater determinant.
- occupation-number representation, general wave function. Fock space. Vacuum state.
- creation and annihilation operators, anti-commutator relations. Express a Slater determinant given in occupation number representation into creation and annihilation operators.
- Given a one-particle Hamiltonian \hat{h} , its eigenvalues ϵ_n and eigenstates $|\psi_n\rangle$ specify the eigenstates of total energy and particle-number eigenvalues of non-interacting electrons in this Hamiltonian.
- Fermi distribution, Bose distribution and Boltzmann distribution. Know the functional expression and be able to describe its graph.
- Be able to translate a Slater determinant from the wave function representation to the occupation number representation to the second quantization notation with creation and annihilation operators.
- Interpretation of dispersion relations: one-particle energy and circular frequency, momentum, wave vector, group velocity, particle velocity, effective mass, electrons and holes, Fermi velocity, optical excitation.
- Specify reciprocal lattice vectors from real lattice vectors.
- Physical meaning of a reciprocal lattice vector, i.e length and direction.
- Bloch theorem
- Again: know how to calculate band structures and how to make sense out of them.
- given the one-particle operator \hat{A} and the Bloch states $|\psi_n(\vec{k}, \sigma)\rangle$ specify the expectation value $\langle A \rangle$ in thermal equilibrium for a given temperature and Fermi level. Give the expression in integral form. Specify the chosen normalization of the wave function used uniquely in real space.
- What is the density of states. Projected density of states. (General formula and description).
- Transform the expression for an expectation value of a non-interacting electron system using a discrete set of k -points

$$A_{T,\mu} = \sum_{n,\vec{k}} f_{T,\mu}(\epsilon_{n,\vec{k}}) \langle \psi_{\vec{k},n} | \hat{A} | \psi_{\vec{k},n} \rangle \quad (\text{A.1})$$

into a continuous Brillouin-zone integration. (Section 5.1.2)

- Density of states. Work out the density of states of free electrons in various dimensions. Make the spin indices explicit. What is the energy of non-interacting electrons with a specified density of states?
- Specify the Boltzmann equation including drift and collision term. The latter shall describe impurity scattering. Consider the case of Fermions and Bosons.
- What is "detailed balance"?
- evaluate linear transport coefficients from the linearized Boltzmann equation in the relaxation time approximation.
- What is a dynamical matrix?

- Know the harmonic oscillator up and down. Multi-dimensional, quantum mechanical and classical, with friction, with driving force. Know what the trajectories of damped and overdamped dynamics, as well as of critical damping.
- Obtain phonon frequencies from the masses and second derivatives of the total energy with respect to atomic positions
- sketch a longitudinal and transversal acoustic phonon. Same for optical phonons.
- describe the Debye model for phonons.
- calculate the phonon density of states from the Debye model.
- calculate the phonon density of states for atoms connected by springs in various geometries.

A.2 Timing

Nr	Date	Ch	Topic
1a	27.10.2021	1	Standard model of solid state physics
1b	28.10.2021	2	Born-Huang Ansatz
2a	03.11.2021	2	Nuclear equation of motion
2b	04.11.2021	2	Non-adiabatic terms, Non-crossing theorem
3a	10.11.2021	2	Jahn-Teller model
3b	11.11.2021	2	Nuclear Trajectories
4a	17.11.2021	3	Spin orbitals
4b	18.11.2021	3	Permutation/Slater determinants
5a	24.11.2021	3	Occupation number representation/ 2nd quantization
5b	25.11.2021	3	Non-interacting electrons
6a	01.12.2021	4	Dispersion relations/Bloch theorem/Slater Koster
6b	02.12.2021	4	Tight-binding band structure
7a	08.12.2021	5	Expectation values/Density of states
7b	09.12.2021	6	Tour of band structures
8a	15.12.2021	?	?
8b	16.12.2021	?	?
9a	22.12.2021	11	Thermodynamics
9b	23.12.2021	12	ausgefallen
10a	12.01.2022	9	Phonons from Born-Oppenheimer
10b	13.01.2022	9	Bloch theorem for phonons
11a	19.01.2022	9	Phonon amplitudes
11b	20.01.2022	9	Phonon band structures
12a	26.01.2022	8	Boltzmann equation: General form
12b	27.01.2022	8	Boltzmann equation: Collisions
13a	02.02.2022	8	Boltzmann equation: Thermal equilibrium/ Inherent approximations
13b	03.02.2022	8	Boltzmann equation, Linearized, relaxation time approx.
14a	09.02.2022	8	Boltzmann equation, Linearized, relaxation time approx.
14b	10.02.2022	–	Review

Appendix B

More on the Born-Huang Ansatz

B.1 Combined systems

In the Born-Huang Ansatz, we divide the Hilbert space for electron and nuclei into two different spaces. In order to make the distinction more evident, I use the abstract bra-ket notation for the electrons and the real-space wave function notation for the nuclei. In this section, I present translations of this problem into different notations.

B.1.1 Coupled systems

Consider two coupled systems A and B . Let $A = \{|\alpha\rangle\}$ be a complete, orthonormal basisset in A and let $B = \{|\beta\rangle\}$ be a complete, orthonormal basisset in B . The product states $|\alpha, \beta\rangle$ form a basisset of the combined system AB . Product states are often written in the form $|\alpha, \beta\rangle = |\alpha\rangle \otimes |\beta\rangle$

A general wave function $|\psi\rangle$ in the combined system AB is a superposition of all product states $|\psi\rangle = \sum_{\alpha \in A; \beta \in B} |\alpha, \beta\rangle c_{\alpha, \beta}$ with complex-valued coefficients $c_{\alpha, \beta}$.

An operator for the the combined system can be written in the form

$$\hat{H}^{AB} = \sum_{\substack{\alpha, \alpha' \in A \\ \beta, \beta' \in B}} |\alpha, \beta\rangle H_{(\alpha, \beta), (\alpha', \beta')}^{AB} \langle \alpha', \beta'| \quad (\text{B.1})$$

As a guide to the eye, I have placed parenthesis around the index pairs, which would not be necessary.

To familiarize you with operators acting in product spaces let me use a special Hamiltonian, that allows me to demonstrate classes of terms.

$$\begin{aligned} \hat{H}^{AB} &= \sum_{\alpha, \alpha' \in A; \beta, \beta' \in B} |\alpha, \beta\rangle \left(H_{\alpha, \alpha'}^A \delta_{\beta, \beta'} + \delta_{\alpha, \alpha'} H_{\beta, \beta'}^B + C_{\alpha, \alpha'}^A C_{\beta, \beta'}^B + V_{(\alpha, \beta), (\alpha', \beta')}^{AB} \right) \langle \alpha', \beta'| \\ &= \underbrace{\left(\sum_{\alpha, \alpha' \in A} |\alpha\rangle H_{\alpha, \alpha'}^A \langle \alpha'| \right)}_{\hat{H}^A} \underbrace{\left(\sum_{\beta \in B} |\beta\rangle \langle \beta| \right)}_{\hat{1}^B} + \underbrace{\left(\sum_{\alpha \in A} |\alpha\rangle \langle \alpha| \right)}_{\hat{1}^A} \underbrace{\left(\sum_{\beta, \beta' \in B} |\beta\rangle H_{\beta, \beta'}^B \langle \beta'| \right)}_{\hat{H}^B} \\ &\quad + \underbrace{\left(\sum_{\alpha, \alpha' \in A} |\alpha\rangle C_{\alpha, \alpha'}^A \langle \alpha'| \right)}_{\hat{C}^A} \underbrace{\left(\sum_{\beta, \beta' \in B} |\beta\rangle C_{\beta, \beta'}^B \langle \beta'| \right)}_{\hat{C}^B} + \underbrace{\sum_{\alpha, \alpha' \in A; \beta, \beta' \in B} |\alpha, \beta\rangle V_{(\alpha, \beta), (\alpha', \beta')}^{AB} \langle \alpha', \beta'|}_{\hat{V}^{AB}} \\ &= \hat{H}^A + \hat{H}^B + \hat{C}^A \hat{C}^B + \hat{V}^{AB} \quad (\text{B.2}) \end{aligned}$$

The first term, \hat{H}^A , acts only on subsystem A . It consists of the product of a Hamiltonian in A and the unit operator in B . The second term is similar to the first acting on subsystem B . In the last

line, we observe that the unit operator is often not made explicit, but that it is implicitly assumed. The third term is a product of two operators, one of which acts in A and the other acts in B . I included product operators, because they are fairly abundant. The electron-phonon coupling in the Holstein dimer or the Jahn-Teller model is an example. The last term is a general operator in the combined system.

B.1.2 Brackets and real-space wave functions

In chapter Eq. 2 about the Born-Huang framework, I use the bracket notation for the electrons and real-space wave functions for the nuclei.

Let me start with a general wave function $|\Psi\rangle$ describing electrons and nuclei. First I represent it in the real-space-and-spin representation. Then I introduce a basiset $|\alpha\rangle$ for the electrons.

$$\begin{aligned}
 |\Psi\rangle &= \int d^{4N}x \int d^{3M}R |\vec{x}, \vec{R}\rangle \Psi(\vec{x}, \vec{R}) \\
 &= \int d^{4N}x \int d^{3M}R \underbrace{\left(\sum_{\alpha} |\alpha\rangle \langle \alpha| \right)}_{\hat{1}^A} \underbrace{|\vec{x}\rangle \otimes |\vec{R}\rangle}_{|\vec{x}, \vec{R}\rangle} \Psi(\vec{x}, \vec{R}) \\
 &= \sum_{\alpha} \int d^{3M}R |\alpha\rangle \otimes |\vec{R}\rangle \underbrace{\int d^{4N}x \underbrace{\langle \alpha | \vec{x} \rangle}_{\Phi_{\alpha}^*(\vec{x})} \Psi(\vec{x}, \vec{R})}_{\Theta_{\alpha}(\vec{R})} \\
 &= \int d^{3M}R |\vec{R}\rangle \left(\sum_{\alpha} |\alpha\rangle \Theta_{\alpha}(\vec{R}) \right) \tag{B.3}
 \end{aligned}$$

In the Born-Huang framework, we have the additional complication that the states in the electronic Hilbert space, the Born-Oppenheimer wave functions, depend themselves on the nuclear positions. One could now introduce this position dependence explicitly as follows

$$|\Psi\rangle = \int d^{3M}R |\vec{R}\rangle \left(\sum_{\alpha} |\alpha, \vec{R}\rangle \Theta_{\alpha}(\vec{R}) \right) \tag{B.4}$$

where $|\alpha, \vec{R}\rangle$ corresponds to our Born-Oppenheimer wave function $|\alpha, \vec{R}\rangle = |\Phi_{\alpha}^{BO}(\vec{R})\rangle$.¹

B.2 Non-uniqueness of the nuclear wave function

The Born-Huang Ansatz Eq. 2.6 allows for some variations: The Born-Oppenheimer wave functions and the nuclear wave functions can be transformed simultaneously such that the final nuclear-electronic wave function remains unchanged. This transformation leads to a new nuclear Schrödinger equation, which has the same structure as the original one, albeit with transformed derivative couplings and a matrix-object replacing the Born-Oppenheimer surfaces. This transformation can be exploited to bring the nuclear wave function into a more convenient form.

The transformation is analogous to the gauge transformation of electromagnetic potentials and the electronic wave function of the quantum electrodynamics. (see Eq. 9.5 and Eq. 13.20 of Φ SX: Electrodynamics[107].)

¹As a curiosity, one may also use, for one atomic configuration \vec{R} , the Born-Oppenheimer wave function of another configuration $\vec{R}' = \vec{Q}(\vec{R})$.

$$|\Psi\rangle = \int d^{3M}R |\vec{R}\rangle \left(\sum_{\alpha} |\alpha, \vec{Q}(\vec{R})\rangle \Theta_{\alpha}(\vec{R}) \right) \tag{B.5}$$

This is indeed also used in the literature, even though it is a bit weird.

To arrive at such a more general formulation, let me start with the Ansatz for the nuclear-electronic wave function in terms of a transformed set of electronic and nuclear wave functions. For this purpose, we introduce a unitary transformation matrix $\mathbf{S}(\vec{R}, t)$, which depends on nuclear coordinates and time. Thus, I can rewrite the Born-Huang Ansatz Eq. 2.6 in the form

$$\begin{aligned} \Phi(\vec{x}, \vec{R}, t) &\stackrel{\text{Eq. 2.6}}{=} \sum_n \langle \vec{x} | \Psi_n^{BO}(\vec{R}) \rangle \underbrace{\sum_k S_{n,k}(\vec{R}, t) S_{k,m}^\dagger(\vec{R}, t)}_{\delta_{n,m}} \Theta_m(\vec{R}, t) \\ &= \sum_k \langle \vec{x} | \tilde{\Psi}_k^e(\vec{R}, t) \rangle \tilde{\Theta}_k(\vec{R}, t) \end{aligned} \quad (\text{B.6})$$

In the second line, I introduced the new electronic wave functions $|\tilde{\Psi}_k^e(\vec{R}, t)\rangle$ and the new nuclear wave functions $\tilde{\Theta}_k(\vec{R}, t)$, which are identified by the tilde. They are defined by

$$\langle \vec{x} | \tilde{\Psi}_k^e(\vec{R}, t) \rangle \stackrel{\text{def}}{=} \sum_n \langle \vec{x} | \Psi_n^{BO}(\vec{R}) \rangle S_{n,k}(\vec{R}, t) \quad (\text{B.7})$$

$$\tilde{\Theta}_k(\vec{R}, t) \stackrel{\text{def}}{=} \sum_m S_{k,m}^\dagger(\vec{R}, t) \Theta_m(\vec{R}, t) \quad (\text{B.8})$$

The requirement² is that the matrix $\mathbf{S}(\vec{R}, t)$ is unitary, i.e.

$$\sum_k S_{n,k}(\vec{R}, t) S_{k,m}^\dagger(\vec{R}, t) = \delta_{n,m} \quad (\text{B.9})$$

Now, we can work out the equation of motion for the transformed nuclear wave function. We start from the equation of motion Eq. 2.27 for the original (multi-valued) nuclear wave function with components $\Theta_n(\vec{R}, t)$

$$i\hbar \partial_t \Theta_m \stackrel{\text{Eq. 2.27}}{=} \sum_n \left[\frac{1}{2} \sum_k \left(\delta_{m,k} \hat{P} + \vec{A}_{m,k} \right) \mathbf{M}^{-1} \left(\delta_{k,n} \hat{P} + \vec{A}_{k,n} \right) + \delta_{m,n} E_m^{BO} \right] \Theta_n \quad (\text{B.10})$$

²The condition follows from the requirement that the Born-Oppenheimer wave functions remain orthonormal and that the norm of the nuclear wave functions remains unchanged under the transformation.

and insert the transformation of the nuclear wave function $\Theta_k(\vec{R}, t) = \sum_k S_{k,m}(\vec{R}, t)\tilde{\Theta}_m(\vec{R}, t)$.

$$\begin{aligned}
\Rightarrow i\hbar\partial_t\tilde{\Theta}_j &\stackrel{\text{Eq. B.8}}{=} i\hbar\partial_t\left(\sum_m S_{j,m}^\dagger\Theta_m\right) = \sum_m S_{j,m}^\dagger\left(i\hbar\partial_t\Theta_m\right) + \sum_m i\hbar\left(\partial_t S_{j,m}^\dagger\right)\Theta_m \\
&\stackrel{\text{Eq. B.10}}{=} \sum_m S_{j,m}^\dagger\sum_n\left[\frac{1}{2}\sum_q\left(\delta_{m,q}\hat{P} + \vec{A}_{m,q}\right)\mathbf{M}^{-1}\left(\delta_{q,n}\hat{P} + \vec{A}_{q,n}\right)\right. \\
&\quad \left. + \delta_{m,n}E_m^{BO} + \sum_q S_{m,q}i\hbar\left(\partial_t S_{q,n}^\dagger\right)\right]\underbrace{\sum_k S_{n,k}\tilde{\Theta}_k}_{\Theta_n} \\
&= \sum_k\left\{\frac{1}{2}\sum_q\left[\sum_m S_{j,m}^\dagger\left(\delta_{m,q}\hat{P} + \vec{A}_{m,q}\right)\right]\underbrace{\sum_p S_{q,p}S_{p,r}^\dagger\mathbf{M}^{-1}\left[\left(\delta_{r,n}\hat{P} + \vec{A}_{r,n}\right)S_{n,k}\right]}_{\delta_{q,r}}\right. \\
&\quad \left. + \left(\sum_{m,n} S_{j,m}^\dagger\delta_{m,n}E_m^{BO}S_{n,k}\right) + \sum_n i\hbar\left(\partial_t S_{j,n}^\dagger\right)S_{n,k}\right\}\tilde{\Theta}_k \\
&= \sum_k\left\{\frac{1}{2}\sum_p\left[\underbrace{\sum_{m,q} S_{j,m}^\dagger\left(\delta_{m,q}\hat{P} + \vec{A}_{m,q}\right)S_{q,p}}_{\delta_{j,p}\hat{P} + \vec{A}_{j,p}}\right]\mathbf{M}^{-1}\left[\underbrace{\sum_{r,n} S_{p,r}^\dagger\left(\delta_{r,n}\hat{P} + \vec{A}_{r,n}\right)S_{n,k}}_{\delta_{p,k}\hat{P} + \vec{A}_{p,k}}\right]\right. \\
&\quad \left. + \left[\sum_m\left(S_{j,m}^\dagger E_m^{BO}S_{m,k} - \underbrace{S_{j,m}^\dagger i\hbar\left(\partial_t S_{m,k}\right)}_{\leftarrow\partial_t(S^\dagger S)=0}\right)\right]\right\}\tilde{\Theta}_k \tag{B.11} \\
&\quad \underbrace{\hspace{10em}}_{=:\tilde{V}_{j,k}}
\end{aligned}$$

We observe that the Born-Oppenheimer surfaces have been replaced by a more general matrix³

$$\tilde{V}_{j,k} \stackrel{\text{def}}{=} \sum_m S_{j,m}^\dagger\left(E_m^{BO} - i\hbar\partial_t\right)S_{m,k} \tag{B.12}$$

in the space of the electronic wave functions. The tilde indicates that the matrix refers to the transformed state.

We still need to simplify the kinetic energy in the above equation Eq. B.11:

$$\begin{aligned}
\sum_{r,n} S_{p,r}^\dagger\left(\delta_{r,n}\hat{P} + \vec{A}_{r,n}\right)S_{n,k} &= \sum_n S_{p,n}^\dagger\hat{P}S_{n,k} + \sum_{r,n} S_{p,r}^\dagger\vec{A}_{r,n}S_{n,k} \\
&= \underbrace{\sum_n S_{p,n}^\dagger S_{n,k}}_{\delta_{p,k}}\hat{P} + \underbrace{\frac{\hbar}{i}\sum_n S_{p,n}^\dagger\left(\vec{\nabla}S_{n,k}\right) + \sum_{r,n} S_{p,r}^\dagger\vec{A}_{r,n}S_{n,k}}_{\vec{A}_{p,n}} \\
&\stackrel{\text{Eq. B.14}}{=} \delta_{p,k}\hat{P} + \vec{A}_{p,k} \tag{B.13}
\end{aligned}$$

This implies that the derivative couplings transform as

$$\vec{A}_{p,k} \stackrel{\text{def}}{=} \sum_{r,n} S_{p,r}^\dagger\left(\vec{A}_{r,n} + \delta_{r,n}\frac{\hbar}{i}\vec{\nabla}_R\right)S_{n,k} \tag{B.14}$$

Taking all this together, we obtain the transformed nuclear Schrödinger equation. It has the same structure as the original version with the exception that $\tilde{\mathbf{V}}^{BO}$ is no more diagonal.

³In the following equation Eq. B.12, the right parenthesis does not stop the time derivative

TRANSFORMED NUCLEAR SCHRÖDINGER EQUATION

$$i\hbar\partial_t\tilde{\Theta}_m = \sum_n \left[\frac{1}{2} \sum_k \left(\delta_{m,k} \hat{P} + \vec{A}_{m,k} \right) \mathbf{M}^{-1} \left(\delta_{k,n} \hat{P} + \vec{A}_{k,n} \right) + \tilde{V}_{m,n}^{BO} \right] \tilde{\Theta}_n \quad (\text{B.15})$$

with

$$|\tilde{\Psi}_k^e(\vec{R}, t)\rangle \stackrel{\text{Eq. B.7}}{=} \sum_n |\Psi_n^{BO}(\vec{R})\rangle S_{n,k}(\vec{R}, t) \quad (\text{B.16})$$

$$\vec{A}_{k,n}(\vec{R}, t) \stackrel{\text{Eq. B.14}}{=} \sum_{i,j} S_{k,i}^\dagger(\vec{R}, t) \left(\vec{A}_{i,j}(\vec{R}) + \delta_{ij} \frac{\hbar}{i} \vec{\nabla} \right) S_{j,n}(\vec{R}, t) \quad (\text{B.17})$$

$$= \langle \tilde{\Psi}_k^e(\vec{R}, t) | \frac{\hbar}{i} \vec{\nabla}_R | \tilde{\Psi}_n^e(\vec{R}, t) \rangle \quad (\text{B.18})$$

$$\tilde{V}_{j,k}(\vec{R}, t) \stackrel{\text{Eq. B.12}}{=} \sum_m S_{j,m}^\dagger(\vec{R}, t) \left(E_m^{BO}(\vec{R}) - i\hbar\partial_t \right) S_{m,k}(\vec{R}, t) \quad (\text{B.19})$$

$$= \langle \tilde{\Psi}_j^e(\vec{R}, t) | \hat{H}^{BO}(\vec{R}) - i\hbar\partial_t | \tilde{\Psi}_k^e(\vec{R}, t) \rangle \quad (\text{B.20})$$

Rather than transforming the equations from the Born-Oppenheimer transformation, we may as well choose an arbitrary set of orthonormal electronic wave functions $|\tilde{\Psi}_n^e(\vec{R}, t)\rangle$. From this set of wave functions, the matrix elements \tilde{V} and derivative couplings \vec{A} are evaluated, which are used to set up the corresponding nuclear Schrödinger equation.

Above, we started from the Born-Oppenheimer framework and introduced a transformation of the electronic and nuclear wave functions. It is also possible, to directly start with a final set of position-dependent electronic wave functions, and obtain the corresponding potential \tilde{V} and derivative couplings \vec{A} .

GENERAL NUCLEAR SCHRÖDINGER EQUATION

In the most general representation, we can choose any complete, orthonormal set of electronic wave functions $|\Psi_n^e(\vec{R}, t)\rangle$, which may depend on the nuclear coordinates \vec{R} and time t . The nuclear-electronic wave function is then obtained as

$$\Phi(\vec{x}, \vec{R}, t) = \sum_n \langle \vec{x} | \Psi_n^e(\vec{R}, t) \rangle \tilde{\Theta}_n(\vec{R}, t) \quad (\text{B.21})$$

where the nuclear wave function $\tilde{\Theta}_n(\vec{R}, t)$ satisfies the Schrödinger equation

$$i\hbar\partial_t\tilde{\Theta}_m(\vec{R}, t) = \sum_n \left[\frac{1}{2} \sum_k \left(\delta_{m,k} \frac{\hbar}{i} \vec{\nabla}_R + \vec{A}_{m,k}(\vec{R}, t) \right) \mathbf{M}^{-1} \left(\delta_{k,n} \frac{\hbar}{i} \vec{\nabla}_R + \vec{A}_{k,n}(\vec{R}, t) \right) + \tilde{V}_{m,n}(\vec{R}, t) \right] \tilde{\Theta}_n(\vec{R}, t) \quad (\text{B.22})$$

with

$$\vec{A}_{k,n}(\vec{R}, t) = \langle \tilde{\Psi}_k^e(\vec{R}, t) | \frac{\hbar}{i} \vec{\nabla}_R | \tilde{\Psi}_n^e(\vec{R}, t) \rangle \quad (\text{B.23})$$

$$\tilde{V}_{j,k}(\vec{R}, t) = \langle \tilde{\Psi}_j^e(\vec{R}, t) | \hat{H}^{BO}(\vec{R}) - i\hbar\partial_t | \tilde{\Psi}_k^e(\vec{R}, t) \rangle \quad (\text{B.24})$$

The Born-Huang Ansatz makes a special choice for the electronic wave functions, namely ones that

- do not depend on time, and that
- diagonalize $\tilde{V}(\vec{R}, t)$. The eigenvalues are the Born-Oppenheimer surfaces $E^{BO}(\vec{R})$.

This representation chosen by Born and Oppenheimer is also called the **adiabatic representation**. In this adiabatic representation, the coupling between different components of the nuclear wave function is small except for certain points in phase space. This is exploited in the widely used Born-Oppenheimer approximation.

An alternative representation, which is often discussed is the **diabatic representation**. In the diabatic approximation, the derivative couplings vanish identically. As shown by Mead and Truhlar[13] an exact diabatic basis does not exist in general, except for a trivial solution. Nevertheless, the diabatic representation forms the starting point for a number of theoretical considerations. More on the diabatic representation can be found in appendix B.3.

B.3 Diabatic picture

In the field of non-adiabatic effects, the diabatic picture is often used in the scientific literature as an alternative description to the adiabatic/non-adiabatic description discussed above. Therefore, I briefly describe the principle underlying the diabatic picture.

In section B.2 on p. 410 it has been shown, how the Born-Huang ansatz can be generalized by a unitary transformation of the Born-Oppenheimer wave functions. The diabatic picture is the attempt to remove the derivative couplings from the nuclear Schrödinger equation by choosing a suitable unitary transformation between the Born-Oppenheimer wave functions. Unfortunately, the construction of such a transformation is not strictly possible in the presence of conical intersections.[13].

The price to be paid, is that the set of Born-Oppenheimer surfaces are replaced by a non-diagonal matrix. The off-diagonal matrix elements are responsible for the electronic transitions.

The diabatic representation has been described well in the paper by Baer [108], which I follow here. The reader is encouraged to review section B.2 before reading on.

The transformation of the Born-Oppenheimer wave functions $|\Psi_n^{BO}(\vec{R})\rangle$ and the corresponding nuclear wave function $\phi_n^{adia}(\vec{R}, t)$

$$|\tilde{\Psi}_n^{e,dia}(\vec{R})\rangle \stackrel{\text{Eq. B.7}}{=} \sum_m |\Psi_m^{BO}(\vec{R})\rangle S_{m,n}(\vec{R}) \quad (\text{B.25})$$

$$\tilde{\phi}_n^{dia}(\vec{R}, t) \stackrel{\text{Eq. B.8}}{=} \sum_m S_{n,m}^\dagger(\vec{R}) \phi_m^{adia}(\vec{R}, t) \quad (\text{B.26})$$

with a position dependent, but time-independent, unitary matrix $S_{m,n}(\vec{R})$, leads to the diabatic electronic wave function $|\tilde{\Psi}_n^{e,dia}(\vec{R})\rangle$ and the corresponding diabatic nuclear wave function $\tilde{\phi}_n^{dia}(\vec{R}, t)$. The transformation leaves the complete electron-nuclear wave function $\sum_n |\tilde{\Psi}_n^{e,dia}(\vec{R})\rangle \tilde{\phi}_n^{dia}(\vec{R}, t)$ invariant, but it changes the form for the derivative couplings and the energy surfaces for the nuclear Schrödinger equation.

The transformed derivative couplings and energy surfaces are given in Eq. B.17 and Eq. B.19 on p. 413 as

$$\begin{aligned} \vec{A}_{k,n}^{dia}(\vec{R}) &\stackrel{\text{Eq. B.17}}{=} \sum_{i,j} S_{k,i}^\dagger(\vec{R}) \left(\vec{A}_{i,j}^{adia}(\vec{R}) + \delta_{i,j} \frac{\hbar}{i} \vec{\nabla} \right) S_{j,n}(\vec{R}) \\ \tilde{V}_{j,k}^{dia}(\vec{R}) &\stackrel{\text{Eq. B.19}}{=} \sum_m S_{j,m}^\dagger(\vec{R}) E_m^{BO}(\vec{R}) S_{m,k}(\vec{R}) \end{aligned} \quad (\text{B.27})$$

The requirement that the diabatic derivative couplings \vec{A}^{dia} vanish leads to the condition

$$\frac{\hbar}{i} \vec{\nabla}_j S_{n,o}(\vec{R}) + \sum_m \vec{A}_{n,m,j}^{dia} S_{m,o}(\vec{R}) = 0 \quad (\text{B.28})$$

for the transformation matrix $\mathbf{S}(\vec{R})$. A formal solution of Eq. B.28 is

$$S_{m,n}(\vec{R}) = \sum_o \left[\exp \left(-\frac{i}{\hbar} \sum_{j=1}^M \int_{\vec{R}_0}^{\vec{R}} dR'_j \mathbf{A}_j^{dia}(\vec{R}') \right) \right]_{m,o} S_{o,n}(\vec{R}_0) \quad (\text{B.29})$$

The integral is performed along a line connecting \vec{R}_0 and \vec{R} .

Unfortunately, the line integral in Eq. B.29 is not always independent of the path taken and the solution is thus ill-defined. When the path of the integral winds around a conical intersection, the integral picks up the geometric phase of the conical intersection. Thus, the presence of a conical intersections, conflicts with a transformation to a diabatic picture. Unfortunately, the diabatic representation is problematic exactly, where one would want to use it, namely to study electronic transitions, which take place predominantly at conical intersections.

In the diabatic picture, the nuclear Schrödinger equation Eq. B.22 has the simple form

NUCLEAR HAMILTONIAN IN THE DIABATIC REPRESENTATION

$$i\hbar \partial_t \tilde{\phi}_n^{dia}(\vec{R}, t) = \left[\sum_{j=1}^M \frac{-\hbar^2}{2M_j} \nabla_{R_j}^2 + E_n^{BO}(\vec{R}) \right] \phi_n(\vec{R}, t) + \sum_m W_{n,m}(\vec{R}) \phi_m(\vec{R}, t) \quad (\text{B.30})$$

where

$$W_{n,m}(\vec{R}) \stackrel{\text{def}}{=} \sum_k S_{n,k}^\dagger(\vec{R}) E_k^{BO}(\vec{R}) S_{k,m}(\vec{R}) - E_n^{BO}(\vec{R}) \delta_{n,m} \quad (\text{B.31})$$

captures the non-adiabatic effects.

The non-adiabatic effects are reflected now in the potential-energy terms rather than being described by the derivative couplings. The potential energy is no more diagonal in the band indices.

After sketching the main idea behind the diabatic picture, I will stop and refer to the literature. I recommend to follow the paper by Baer [108], and for references to newer developments the review by Worth and Robb[7].

Appendix C

Non-crossing theorem

Here, I provide the proof of the non-crossing theorem discussed in section 2.4.1 on p. 55. The **non-crossing theorem** has been derived by von Neumann and Wigner[18].

NON-CROSSING THEOREM

Consider a Hamiltonian $H(Q_1, \dots, Q_m)$ which depends on m parameters Q_1, \dots, Q_m . The subspace with a degeneracy $E_m(\vec{Q}) = E_n(\vec{Q})$ for a pair (m, n) is called the **degenerate seam**.

- For each point (Q_1, \dots, Q_m) with an **accidental** crossing, there is a three-dimensional subspace of the parameter space in which the degeneracy is lifted except for a single point. The degenerate seam is a $(m - 3)$ -dimensional hypersurface.

For the point with the degeneracy, one can find three orthogonal vectors in the parameter space that are directions that lift the degeneracy. The remaining $m - 3$ orthonormal vectors are tangential to the degenerate seam.

- If the Hamiltonian is real-valued for all parameters, the subspace where the degeneracy is lifted has two dimensions and the degenerate seam is a $m - 2$ dimensional hypersurface.

C.1 Proof of the non-crossing theorem

The proof of the non-crossing theorem is a generalization of the simple example described in the previous section 2.4.2 on p. 56.

The underlying idea of the proof is to compare the number of degrees of freedom of a Hamiltonian $H(\vec{Q})$ with and without a degeneracy. The number of degrees of freedom of a Hamiltonian with specific properties is equal to the dimension of the parameter space that can change the Hamiltonian without violating those properties. The dimension of the coordinate space, which also maintains a certain degeneracy, is smaller than that of a general Hamiltonian because of the additional requirement. By counting the number of degrees of freedom in a Hamiltonian with a given multiplet structure¹, we can estimate the dimension of the hypersurface that maintains the multiplet structure. This hypersurface is the degenerate seam.

Number of degrees of freedom and dimension of the coordinate space: The proof rests on counting the number of degrees of freedom for a Hamiltonian with certain properties. Therefore, we need a clear understanding of what we mean with degrees of freedom.

¹A **multiplet** is a set of degenerate states. The multiplet structure describes the groups of degenerate eigenvalues.

Let me consider a Hamiltonian with certain properties. For example, we may require that two eigenvalues of the Hamiltonian shall be degenerate. Imagine a magic formula, which sets up such a Hamiltonian from a set \vec{Q} of parameters. The formula shall establish a bijective (one-to-one) relationship $\vec{Q} \leftrightarrow H$ between parameter sets and the Hamiltonian with the specified properties. In other words,

- distinct sets of parameters produce distinct Hamiltonians, i.e. $H(\vec{Q}) \neq H(\vec{Q}')$ if $\vec{Q} \neq \vec{Q}'$.
- every Hamiltonian with the specified properties can be constructed by one parameter set \vec{Q} .

If these requirements are satisfied, the number of parameters in the set \vec{Q} is equal to the number of degrees of freedom.

Multiplet structure: Let us now determine the number of degrees of freedom of a Hamiltonian with a specified multiplet structure. What is a multiplet structure? A Hamiltonian may have a ℓ distinct eigenvalues with degeneracies (g_1, \dots, g_ℓ) . The **multiplet structure** is defined by the set of degeneracies $\{g_1, \dots, g_\ell\}$.²

Let $D(g_1, \dots, g_\ell)$ be the number of degrees of freedom of a Hamiltonian with a given multiplet structure. The number d of conditions on the Hamiltonian, which are relaxed, when a double degeneracy is lifted, is

$$d = D(g_1, \dots, g_q, 1, 1) - D(g_1, \dots, g_q, 2) \quad (\text{C.1})$$

$D(g_1, \dots, g_q, 2)$ gives the number of degrees of freedom for a matrix with degeneracies (g_1, \dots, g_q) and the requirement that the last two eigenvalues are two-fold degenerate as well. $D(g_1, \dots, g_q, 1, 1)$ corresponds to the same situation, but there is no requirement that the last two eigenvalues are degenerate. Because this requirement is missing, the situation without degeneracy is expected to have more degrees of freedom compared to the former.

For each point in phase space with a double degeneracy, there is a d -dimensional hypersurface (d from Eq. C.1) on which (1) the degeneracy is lifted and on which (2) there is only one point where the degeneracy is intact. In other words, if the Hamiltonian depends on M coordinates, the degeneracy is intact on a $M - d$ dimensional hypersurface in the coordinate space.

As a first thought, one might expect that there is one additional degree of freedom, i.e. $d = 1$, because one condition is relaxed. However, the non-crossing theorem says that there are two, respectively three, additional degrees of freedom.

We will see below, that $d = 2$ for real-valued Hamiltonians and $d = 3$ for complex-valued Hamiltonians. This implies that two Born-Oppenheimer surfaces touch in the form of a **conical intersection** in two, respectively three, dimensions.

Free parameters of a Hamiltonian with a specified multiplet structure: What is left, is to determine the number $D(g_1, \dots, g_\ell)$ of independent parameters of a Hamiltonian with a given multiplet structure (g_1, \dots, g_ℓ) .

Every Hamiltonian can be constructed from its eigenvalues E_k and eigenvectors.³ The eigenvec-

²The degeneracies can be combined into a vector, but the specific order of vector components does not distinguish multiplet structures.

³The Hamiltonian can be represented by its eigenstates $|\psi_n\rangle$ and its eigenvalues E_n as

$$\begin{aligned} \hat{H} &= \sum_n |\psi_n\rangle E_n \langle \psi_n| \quad \text{with} \quad \langle \psi_m | \psi_n \rangle = \delta_{m,n} \\ H_{\alpha,\beta} &\stackrel{\text{def}}{=} \langle \chi_\alpha | \hat{H} | \chi_\beta \rangle = \sum_n \langle \chi_\alpha | \psi_n \rangle E_n \langle \psi_n | \chi_\beta \rangle \quad \text{with} \quad \sum_\alpha \langle \psi_m | \chi_\alpha \rangle \langle \chi_\alpha | \psi_n \rangle = \delta_{m,n} \\ U_{\alpha,n} &\stackrel{\text{def}}{=} \langle \chi_\alpha | \psi_n \rangle \quad \text{and} \quad U_{n,\alpha}^\dagger = \langle \psi_n | \chi_\alpha \rangle \end{aligned} \quad (\text{C.2})$$

tors form the unitary matrix \mathbf{U}

$$H_{\alpha,\beta} = \sum_{n=1}^N U_{\alpha,n} E_n U_{n,\beta}^\dagger \tag{C.3}$$

Below (in Eq. C.7 and Eq. C.8), we will determine the number $\kappa(n)$ of free parameters for a unitary matrix of dimension n . In the following, we assume that $\kappa(n)$ is known.

The number of degrees of freedom for a general Hamiltonian is the sum of

1. the number ℓ of (distinct) eigenvalues and
2. the number $\kappa(n)$ of degrees of freedom for the eigenvectors, respectively for the unitary matrix \mathbf{U} . $\kappa(n)$ is different for real-valued and complex-valued matrices.
3. As shown below, we need to subtract for each multiplet with degeneracy g_j the number $\kappa(g_j)$ of possible unitary transformations within this multiplet.

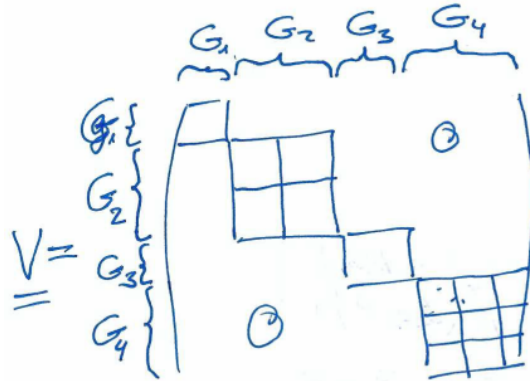
$$D(g_1, \dots, g_\ell) = \ell + \kappa(N) - \sum_{j=1}^{\ell} \kappa(g_j) \quad \text{where } N = \sum_{j=1}^{\ell} g_j \tag{C.4}$$

Let me explain the third point regarding the individual multiplets: When eigenvalues are degenerate, many unitary matrices in place of a specific \mathbf{U} produce the same Hamiltonian. This flexibility must be subtracted from the first estimate $\ell + \kappa(N)$ for the number of degrees of freedom $D(g_1, \dots, g_\ell)$.

The overcounting can be quantified as the number of independent unitary transformations that leave the Hamiltonian invariant. Any block-diagonal unitary matrix \mathbf{V} , which transforms only states within the same multiplet into each other, leaves the multiplet structure invariant.⁴

$$H_{\alpha,\beta} = \sum_{i,j} U_{\alpha,i} \underbrace{\sum_{n=1}^N V_{i,n} E_n V_{n,j}^\dagger}_{H'_{i,j}} U_{j,\beta}^\dagger \tag{C.5}$$

This is true, because $\sum_n V_{i,n} E_n V_{n,j}^\dagger = E_i \delta_{i,j}$, which is shown next.



The block-diagonal form of \mathbf{V} implies that $V_{i,j} = 0$ unless i and j are from the same set G_p of degenerate orbitals. The Hamilton matrix \mathbf{H}' obtained after the transformation \mathbf{V} is diagonal as shown below

$$H'_{i,j} = \sum_{n=1}^N V_{i,n} E_n V_{n,j}^\dagger = \sum_{p=1}^{\ell} \sum_{n \in G_p} V_{i,n} E_n V_{n,j}^\dagger = \sum_{p=1}^{\ell} \sum_{n \in G_p} \overbrace{E_n \delta_{i,j}}^{E_j \delta_{i,j}} = \delta_{i,j} E_j \tag{C.6}$$

⁴This implies that $V_{i,j} = 0$ if i and j are indices from different multiplets.

We exploited that the energies in one multiplet G_p are the same so that they the energies can be taken out of the sum. Then we exploit $V_{i,n} = 0$ when i and n are not in the same multiplet, to obtain $\sum_{n \in G_p} V_{i,n} V_{n,j}^\dagger = \sum_n V_{i,n} V_{n,j}^\dagger = \delta_{i,j}$. This completes the proof of Eq. C.5.

With Eq. C.4, we can work out Eq. C.1 to obtain the number d of independent directions, that lift the degeneracy. What is left to do, is to work out $\kappa(n)$, which is done next:

Degrees of freedom in a general real-valued unitary matrix Let me work out the number $\kappa^{\text{real}}(n)$ of a real-valued, unitary matrix with dimension n . A real-valued unitary matrix with matrix elements $U_{\alpha,j} = \langle \chi_\alpha | \psi_j \rangle$ can be expressed by a set of orthonormal real-valued vectors. The number of degrees of freedom is obtained by the number of independent elements for the eigenvectors minus the number of orthonormality conditions.

1. A set of n real-valued vectors with dimension n contains n^2 real numbers and thus has n^2 degrees of freedom.
2. the orthogonality requirement accounts for $\frac{n(n-1)}{2}$ real-valued conditions: There is one condition for each pair of vectors (i, j) with $i > j$ and there are $n(n-1)/2$ such pairs.
3. the normalization of the n vectors adds n additional conditions.

Thus, the number of degrees of freedom to fix a general real-valued unitary matrix is

$$\kappa^{\text{real}}(n) = n^2 - \frac{1}{2}n(n-1) - n = \frac{n(n-1)}{2} \quad (\text{C.7})$$

Degrees of freedom in a general a complex-valued unitary matrix Let me work out the number $\kappa^{\text{complex}}(n)$ of a complex-valued unitary matrix with dimension n . A complex-valued unitary matrix of dimension n is expressed by n complex-valued orthonormal vectors.

1. the n complex-valued vectors have n^2 elements and thus have $2n^2$ real-valued degrees of freedom,
2. the orthonormality requirement accounts for $\frac{n(n-1)}{2}$ complex-valued conditions. Each complex-valued condition corresponds to two degrees of freedom. Thus, the orthonormality corresponds to $n(n-1)$ degrees of freedom.
3. the normalization condition contributes n real-valued conditions.

Thus, the number of degrees of freedom of a general complex-valued unitary matrix is

$$\kappa^{\text{complex}}(n) = 2n^2 - n(n-1) - n = n^2 \quad (\text{C.8})$$

Compare parameters with and without degeneracy: We obtained the number of degrees of freedom for a real-valued or complex-valued Hamiltonian with a specific multiplet structure as

$$\begin{aligned} D(g_1, \dots, g_\ell) &\stackrel{\text{Eq. C.4}}{=} \ell + \kappa \left(\sum_{p=1}^{\ell} g_p \right) - \sum_{p=1}^{\ell} \kappa(g_p) \\ &= \begin{cases} \ell + \frac{N(N+1)}{2} - \sum_{p=1}^{\ell} \frac{g_p(g_p+1)}{2} & \text{for real-valued Hamiltonians} \\ \ell + N^2 - \sum_{p=1}^{\ell} g_p^2 & \text{for complex-valued Hamiltonians} \end{cases} \quad (\text{C.9}) \end{aligned}$$

with $N(g_1, \dots, g_\ell) = \sum_{p=1}^{\ell} g_p$ being the dimension of the Hamiltonian.

Now, we need to understand how the number of free parameters changes when a doubly degenerate state splits into two non-degenerate levels. The number d of additional degrees of freedom is given Eq. C.1.

In the presence of the double degeneracy, there shall be p multiplets plus one doublet. When the degeneracy is lifted, the doublet splits into two singlets. Thus, the number of multiplets is increased from $\ell = p + 1$ to $\ell = p + 2$. The dimension of both Hamiltonians remains unchanged, i.e. $N = 2 + \sum_{p=1}^{\ell} g_p$.

This determines the number d of degrees of freedom, which are gained by relaxing the condition for one double degeneracy as

$$\begin{aligned}
 d &\stackrel{\text{Eq. C.1}}{=} D(g_1, \dots, g_p, 1, 1) - D(g_1, \dots, g_p, 2) \\
 &\stackrel{\text{Eq. C.4}}{=} 1 - 2\kappa(1) + \kappa(2) \\
 &\stackrel{\text{Eqs. C.7, C.8}}{=} \begin{cases} 2 & \text{for a real-valued Hamiltonian} \\ 3 & \text{for a complex-valued Hamiltonian} \end{cases} \quad (\text{C.10})
 \end{aligned}$$

This is what had to be shown to prove the non-crossing theorem.

Appendix D

Adiabatic decoupling in the Born-Oppenheimer approximation

D.1 Adiabatic theorem

Editor: The proof of the adiabatic theorem shall be included.

The **adiabatic theorem** goes back to Ehrenfest.[?]] A mathematically rigorous proof has been provided by Born and Fock[109] in 1928.

ADIABATIC THEOREM

"A physical system remains in its instantaneous eigenstate if a given perturbation is acting on it slowly enough and if there is a gap between the eigenvalue and the rest of the Hamiltonian's spectrum."
[109]^a

Let me define the adiabatic states $|\Phi_n(t)\rangle$ as the instantaneous eigenstates of a time-dependent Hamiltonian.

$$\hat{H}(t)|\Phi_n(t)\rangle = |\Phi_n(t)\rangle E_n(t) \quad (\text{D.1})$$

and $E_n(t)$ the adiabatic energies. Note that the adiabatic eigenstates do not satisfy the time-dependent Schrödinger equation.

The wave function of the physical system evolves under the time-dependent Schrödinger equation

$$i\hbar\partial_t|\Psi(t)\rangle = \hat{H}(t)|\Psi(t)\rangle \quad (\text{D.2})$$

The adiabatic theorem claims that the transition probability

$$P_{m,n}(t) = |\langle\Phi_m(t)|\Psi(t)\rangle|^2 \quad \text{for } \langle\Phi_n(0)|\Psi(0)\rangle = 1 \quad (\text{D.3})$$

from one adiabatic state to another one becomes infinitely small, if (1) the time-dependent Hamiltonian $\hat{H}(t)$ evolves infinitely slowly, and if (2) the states are separated by a finite band gap $E_m(t) - E_n(t)$.

^aFormulierung von https://en.wikipedia.org/wiki/Adiabatic_theorem, retrieved Nov 23, 2017

D.2 Justification for the Born-Oppenheimer approximation

In the following, I will present an argument, that I **believe** is close to the original proof of Born and Oppenheimer. We will investigate an artificial model that we can solve exactly and compare the results of the Born-Oppenheimer approximation with the exact result.

Imagine a Hamiltonian in which all interactions are harmonic instead of Coulombic. Secondly, consider only a one-dimensional electron and a one-dimensional nucleus. The electron coordinate is denoted by x and the nuclear coordinate by R . The corresponding momenta are p_{el} for the electron coordinate and P_{nuc} for the nuclear coordinate. Thus, the full Hamiltonian is

$$\begin{aligned}\hat{H} &= \frac{\hat{P}_{nuc}^2}{2M} + \frac{\hat{p}_{el}^2}{2m} + \frac{1}{2}a\hat{x}^2 + b\hat{x}\hat{R} + \frac{1}{2}c\hat{R}^2 \\ &= \frac{m}{M} \frac{\hat{P}_{nuc}^2}{2m} + \frac{\hat{p}_{el}^2}{2m} + \frac{1}{2}a\hat{x}^2 + b\hat{x}\hat{R} + \frac{1}{2}c\hat{R}^2\end{aligned}\quad (\text{D.4})$$

Exact solution of the model system

From the description of the multidimensional harmonic oscillator (see section 5.6 of $\Phi\text{SX:Quantum Theory}$ [4] and section 3.8 of $\Phi\text{SX:Klassische Mechanik}$ [110]), we know that we need to know only the two classical eigenfrequencies ω_+ and ω_- to specify the spectrum of the two-dimensional quantum-mechanical harmonic oscillator.

$$E_{j,n} = \hbar\omega_+ \left(n + \frac{1}{2} \right) + \hbar\omega_- \left(j + \frac{1}{2} \right) \quad (\text{D.5})$$

In order to obtain the classical frequencies ω_{\pm} , let us consider the classical harmonic oscillator, which has the Hamilton function

$$H(P_{nuc}, p_{el}, R, x) \stackrel{\text{Eq. D.4}}{=} \frac{P_{nuc}^2}{2M} + \frac{p_{el}^2}{2m} + \frac{1}{2}ax^2 + bxR + \frac{1}{2}cR^2 \quad (\text{D.6})$$

Hamilton's second equation yield

$$\begin{pmatrix} \dot{p}_{el} \\ \dot{P}_{nuc} \end{pmatrix} = \begin{pmatrix} m\ddot{x} \\ M\ddot{R} \end{pmatrix} = - \begin{pmatrix} a & b \\ b & c \end{pmatrix} \begin{pmatrix} x \\ R \end{pmatrix} = \begin{pmatrix} F_{el} \\ F_{nuc} \end{pmatrix} \quad (\text{D.7})$$

By diagonalizing the dynamical matrix D

$$D = \frac{1}{m} \begin{pmatrix} a & \sqrt{\frac{m}{M}}b \\ \sqrt{\frac{m}{M}}b & \frac{m}{M}c \end{pmatrix} \quad (\text{D.8})$$

we obtain the eigenvalues ω^2 of the dynamical matrix

$$m\omega_{\pm}^2 = \frac{a + \frac{m}{M}c}{2} \pm \sqrt{\left(\frac{a - \frac{m}{M}c}{2}\right)^2 + \frac{m}{M}b^2} \quad (\text{D.9})$$

Let us investigate first two terms in an expansion in orders of $\frac{m}{M}$.

$$\begin{aligned}m\omega_+^2 &= a + \frac{m}{M} \frac{b^2}{a} + O\left(\frac{m}{M}\right)^2 \\ m\omega_-^2 &= \frac{m}{M} \left(c - \frac{b^2}{a} \right) - \left(\frac{m}{M}\right)^2 \left(\frac{c^2}{2a} + \frac{a}{2} \left(\frac{2b^2 - ac}{2a^2} \right)^2 \right) + O\left(\frac{m}{M}\right)^4\end{aligned}\quad (\text{D.10})$$

The higher frequency ω_+ can be attributed to electronic excitation energies $\Delta E = \hbar\omega_+$. Thus, $\hbar\omega_+$ is similar size as excitation energies, that is typically in the range of few eV. The lower frequency

ω_- can be attributed to the atomic motion. The energy $\hbar\omega_-$ is comparable to vibrational excitation energies, that is in the range of about 10 meV.

Thus, the eigenvalue spectrum is

$$E_{j,n} \stackrel{\text{Eq. D.5}}{=} \hbar \sqrt{\frac{c - \frac{b^2}{a} - \frac{m}{M} \left[\frac{2c^2}{a} + \frac{a}{2} \left(\frac{2b^2 - ac}{2a^2} \right)^2 \right]}{M}} \left(j + \frac{1}{2} \right) + \hbar \sqrt{\frac{a + \frac{m}{M} \frac{b^2}{a}}{m}} \left(n + \frac{1}{2} \right) + O\left(\left(\frac{m}{M} \right)^2 \right) \quad (\text{D.11})$$

Born-Oppenheimer solution of the model system

We can now apply the Born-Oppenheimer approximation in order to see how it deviates from the exact result:

$$\begin{aligned} \hat{H}^{BO} &= \frac{\hat{p}_{el}^2}{2m} + \frac{1}{2}ax^2 + bRx + \frac{1}{2}cR^2 \\ &= \frac{\hat{p}_{el}^2}{2m} + \frac{1}{2}a\left(x + \frac{b}{a}R\right)^2 + \frac{1}{2}\left(c - \frac{b^2}{a}\right)R^2 \end{aligned} \quad (\text{D.12})$$

The force constant for the electrons is a , so that we obtain a frequency $\omega_+^{BO} = \sqrt{\frac{a}{m}}$. Knowing that the energy eigenvalues of the harmonic oscillator are $\hbar\omega_+^{BO}(n + \frac{1}{2})$ we can immediately determine the Born-Oppenheimer energy surfaces.

$$E_n^{BO}(R) = \frac{1}{2}\left(c - \frac{b^2}{a}\right)R^2 + \hbar\sqrt{\frac{a}{m}}\left(n + \frac{1}{2}\right) \quad (\text{D.13})$$

Now, we can determine the eigenvalues of the nuclear Hamiltonian

$$H^{nuc} = \frac{P_{nuc}^2}{2M} + E_n^{BO}(R) \quad (\text{D.14})$$

which has eigenvalues

$$E_{j,n} = \hbar\sqrt{\frac{c - \frac{b^2}{a}}{M}}\left(j + \frac{1}{2}\right) + \hbar\sqrt{\frac{a}{m}}\left(n + \frac{1}{2}\right) \quad (\text{D.15})$$

We see that the spectrum obtained from the Born-Oppenheimer approximation Eq. D.15 provides the correct result, Eq. D.11, if $\frac{m}{M}$ vanishes.

The corrections to the Born-Oppenheimer approximations, that is the difference between Eq. D.11 and Eq. D.15, are of order $\frac{m}{M}$.

This ratio, namely $\frac{m}{M}$, is typically in of order 10^{-4} and definitely smaller than 10^{-3} , because the mass of a single nucleon (proton or neutron) is about 1823 times the mass of an electron. Therefore, we can assume that the Born-Oppenheimer corrections can be ignored in most cases.

The underlying reason for the validity of the Born-Oppenheimer approximation is that oscillators do not affect each other strongly, if they are out of resonance. In a solid, the oscillators are the electronic excitations and the phonons, that is lattice vibrations. Electronic excitation energies are larger than the optical band gap of the material, which is typically in the range of 1 eV. Lattice vibrations have wavenumbers below than 800 cm^{-1} and thus their energies lie below 10 meV. Except for metals or molecules with a nearly degenerate ground state this separation of frequencies is real.

Illustration of the out-of-resonance condition

To illustrate this effect let us consider the classical model of two coupled harmonic oscillators shown in Fig. D.1. The large pendulum represents the nuclear vibrations, while the small pendulum represents

the electronic degrees of freedom. For the electrons, the nuclei seem static. The dynamics of the nuclei is perturbed little, because the forces from the electrons are almost averaged out. Two effects must be considered though: Only the center of gravity of electrons and nuclei performs a smooth oscillation, that is unperturbed by the electrons. The nucleus has in addition a small high-frequency oscillation with small amplitude. The long oscillation period is not given by the mass of the nucleus alone, but by the total mass of electrons and nucleus.

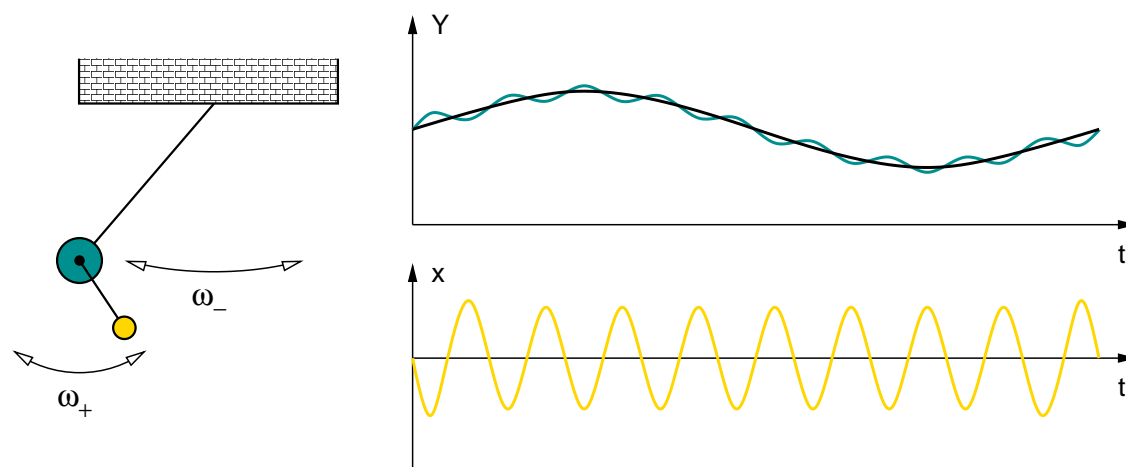


Fig. D.1: Schematic demonstration of the classical analog for the Born-Oppenheimer approximation

Appendix E

Trajectories and non-adiabatic effects

This section contains some derivations to which we refer in the section on non-adiabatic effects.

In order to demonstrate non-adiabatic effects, we consider the dynamics of nuclei treated as classical particles under the influence of non-adiabatic effects. Firstly, I consider the dynamics on a single Born-Oppenheimer surface.

E.1 Nuclear trajectories

A complete quantum-mechanical treatment of the nuclear dynamics is often not adequate, because the quantum effects are usually relevant only next to conical intersections. Practical calculations rely on a classical or semi-classical treatment of the nuclei.

Editor: Include a graph sketching an avoided crossing and the splitting of a wave packet.

The first quantum effect that comes into one's mind is that a localized wave packet tends to broaden.¹ A much more severe quantum effect is the splitting of a wave packet. While a wave packet can be approximated reasonably well by a classical trajectory, this is no more possible for a superposition of two wave packets.

The splitting of a wave packet is well known from an example in elementary quantum mechanics, namely the partial reflection of a wave packet at a potential step. A reasonable simplified description for a split wave packet is an ensemble of independent trajectories (see e.g. chapter 5 of [111]), namely a set of classical trajectories weighted by their probabilities. As shown in appendix K.1 in Φ SX: Quantum Physics[4] such a description is rigorously valid in the semi-classical approximation, when only one Born-Oppenheimer surface is taken into account.² The quantum-mechanical transmission coefficient determines the probabilities that the particle is either transmitted or reflected. Replacing the split wave packet by an ensemble of trajectories discards the information on the relative phases of the wave packets. In reality, the wave packets are still **entangled** and this phase relation is lost by choosing trajectories.

Is the loss of entanglement a severe problem? In most cases it is not a problem. The reason is **decoherence**. Any coupling to an environment will destroy the phase relationship between transmitted and reflected waves. Decoherence acts like randomizing the relative phases of the wave packets. Thus, in **open systems**, there is a physical process that destroys the phase relationship between

¹In section 4.4.1 of Φ SX:Quantum Theory[4], we estimated this broadening $d(t)$ in Eq. 4.13 as

$$d(t) = d(0) \sqrt{1 + \left(\frac{\hbar t}{2m[d(0)]^2} \right)^2} \quad (\text{E.1})$$

where m is the mass of the particle and t is the time. $d(0)$ is the smallest broadening along the trajectory.

²One would simulate this by a random process, which produces a transmitted or reflected trajectory with probabilities based in the transmission coefficient.

split wave packets. The result is an ensemble of wave packets without phase relations, which can be approximated by classical trajectories. The discussion of decoherence is non-trivial. More can be found in chapter 5 of *ΦSX: Statistical properties of matter*[25].

The concept of representing split wave packets by an ensemble of trajectories is rather fundamental. It is important for the practical simulation of non-adiabatic effects of real systems. However, it probably is a key element of understanding quantum effects in general. The arguments underlying the Boltzmann equation are of a similar nature.

Editor: Consult Tully,98[112] for this section. (Classical Limit, Ehrenfest, Surface Hopping.)

E.1.1 Born-Oppenheimer dynamics

The most simple approach towards a description with classical trajectories is to take the Hamilton operator in the Born-Oppenheimer approximation from Eq. 2.30, constrain it to a particular total-energy surface specified by n , and to form the corresponding Hamilton function for the nuclei.

$$H_n(\vec{P}, \vec{R}) = \sum_j \frac{\vec{P}_j^2}{2M_j} + E_n^{BO}(\vec{R}) \quad (\text{E.2})$$

The Hamilton function defines the classical Hamilton equations of motion

$$\begin{aligned} \partial_t \vec{R}_j &= \vec{\nabla}_{\vec{P}_j} H_n(\vec{P}, \vec{R}, t) = \frac{1}{M_j} \vec{P}_j \\ \partial_t \vec{P}_j &= -\vec{\nabla}_{\vec{R}_j} H_n(\vec{P}, \vec{R}, t) = -\vec{\nabla}_{\vec{R}_j} E_n^{BO}(\vec{R}) \end{aligned} \quad (\text{E.3})$$

This, in turn, leads to Newton's equations of motion for the nuclei

$$M_j \partial_t^2 \vec{R}_j = -\vec{\nabla}_{\vec{R}_j} E_n^{BO}(\vec{R}) \quad (\text{E.4})$$

This is the approximation that is most widely used to study the dynamics of the atoms in a molecule or a solid. A simulation of classical atoms using some kind of parameterized Born-Oppenheimer surface is called **molecular dynamics simulation**³. When the Born-Oppenheimer surface is obtained on the fly from a quantum-mechanical electronic-structure method, the method is called **ab-initio molecular dynamics**[113]. The method of determining the nuclear trajectories in the Born-Oppenheimer approximation for the ground-state Born-Oppenheimer surface is called **Born-Oppenheimer dynamics**.

Unless one is specifically interested in the excited-state dynamics as for photochemistry, the ground-state Born-Oppenheimer surface is selected.

The Born-Oppenheimer surface $E_n^{BO}(\vec{R})$ acts just like a total-energy surface for the motion of the nuclei. Once $E_n^{BO}(\vec{R})$ is known, the electrons are taken completely out of the picture. Within the Born-Oppenheimer approximation, no transitions between the ground-state and the excited-state surface take place. This implies not only that a system in the electronic ground state remains in the ground state. It also implies that a system in the excited state will remain there for ever. Transitions between different sheets $E_n^{BO}(\vec{R})$ of the Born-Oppenheimer energy are only possible when non-adiabatic effects are included.

The simple picture of the Born-Oppenheimer dynamics as replacing a wave packet by a point in phase space is oversimplified. As shown in appendix K.1 in *ΦSX: Quantum Physics*[4], the Born-Oppenheimer dynamics is equivalent to the semi-classical approximation, which describes amplitude and phase of the wave function to leading order in \hbar . This comparison of a wave function and an ensemble of trajectories is important when one tries to compare the dynamics obtained from Born-Oppenheimer dynamics with that of a quantum description of the nuclei.

³Editor: First publication on an application of the molecular dynamics method: B. J. Alder and T. E. Wainwright. Phase transition for a hard sphere system. *J. Chem. Phys.*, 27:1208-1209, 1957. Description of the method: B. J. Alder and T. E. Wainwright. *Studies in molecular dynamics. I. General method.* *J. Chem. Phys.*, 31:459, 1959.

E.1.2 Electron dynamics for nuclear trajectories

Let me analyze the electron dynamics for a given nuclear trajectory $\vec{R}(t)$. The electron motion is determined by the time-dependent Schrödinger equation.

$$i\hbar\partial_t|\Psi(t)\rangle = \hat{H}^{BO}(\vec{R}(t))|\Psi(t)\rangle \quad (\text{E.5})$$

The electron wave function $|\Psi(t)\rangle$ can be represented in any basis set and we choose the basis set of Born-Oppenheimer states.

$$|\Psi(t)\rangle = \sum_n |\Psi_n^{BO}(\vec{R}(t))\rangle C_n(t) \quad (\text{E.6})$$

defined by

$$\hat{H}^{BO}(\vec{R})|\Psi_n^{BO}(\vec{R})\rangle \stackrel{\text{Eq. 2.4}}{=} |\Psi_n^{BO}(\vec{R})\rangle E_n^{BO}(\vec{R}) \quad (\text{E.7})$$

Note the difference between the electronic wave function $|\Psi(t)\rangle$ and the Born-Oppenheimer states $|\Psi_n^{BO}(\vec{R})\rangle$.

With the Ansatz Eq. E.6, the Schrödinger equation Eq. E.5 translates into an equation of motion for the coefficients $C_n(t)$

$$\begin{aligned} \sum_n \left\{ |\Psi_n^{BO}(\vec{R}(t))\rangle \left[i\hbar\partial_t C_n(t) - E_n^{BO}(\vec{R}(t))C_n(t) \right] + C_n(t) i\hbar\partial_t |\Psi_n^{BO}(\vec{R}(t))\rangle \right\} &= 0 \\ \stackrel{\langle \Psi_m^{BO} | \times}{\Rightarrow} & i\hbar\partial_t C_m(t) - E_m^{BO}(\vec{R}(t))C_m(t) + \sum_n i\hbar\dot{\vec{R}} \langle \Psi_m^{BO} | \vec{\nabla}_R | \Psi_n^{BO} \rangle C_n(t) = 0 \\ \stackrel{\text{Eq. 2.29}}{\Rightarrow} & i\hbar\partial_t C_m(t) - E_m^{BO}(\vec{R}(t))C_m(t) - \sum_n \dot{\vec{R}} \vec{A}_{m,n}(\vec{R}(t))C_n(t) = 0 \quad (\text{E.8}) \end{aligned}$$

where I used Eq. 2.29 for the derivative couplings

$$\vec{A}_{m,n}(\vec{R}) \stackrel{\text{Eq. 2.29}}{=} \left\langle \Psi_m^{BO}(\vec{R}) \left| \frac{\hbar}{i} \vec{\nabla}_R \right| \Psi_n^{BO}(\vec{R}) \right\rangle \quad (\text{E.9})$$

Let me separate out the rapid oscillations of the **dynamical phase** with the Ansatz

$$C_n(t) = \underbrace{\exp\left(-\frac{i}{\hbar} \int_0^t dt' E_n^{BO}(\vec{R}(t'))\right)}_{\text{dynamical phase}} \Gamma_n(t) \quad (\text{E.10})$$

which yields an equation of motion for the new variables $\Gamma_m(t)$

$$i\hbar\partial_t \Gamma_m(t) = \sum_n \dot{\vec{R}} \vec{A}_{m,n}(\vec{R}(t)) \exp\left(-\frac{i}{\hbar} \int_0^t dt' (E_n^{BO}(\vec{R}(t')) - E_m^{BO}(\vec{R}(t')))\right) \Gamma_n(t) \quad (\text{E.11})$$

When derivative couplings vanish as in the Born-Oppenheimer approximation, the coefficients $\Gamma_m(t)$ are time independent.

ELECTRONIC WAVE FUNCTION FOR A CLASSICAL NUCLEAR TRAJECTORY

Given a nuclear trajectory $\vec{R}(t)$, the electronic wave function $|\Psi(t)\rangle$, which evolves under the time-dependent Schrödinger equation with the Hamiltonian $\hat{H}^{BO}(\vec{R}(t))$, is

$$|\Psi(t)\rangle \stackrel{\text{Eq. E.6}}{=} \sum_n |\Psi_n^{BO}(\vec{R}(t))\rangle \exp\left(-\frac{i}{\hbar} \int_0^t dt' E_n^{BO}(\vec{R}(t'))\right) \Gamma_n(t) \quad (\text{E.12})$$

with

$$i\hbar\partial_t \Gamma_m(t) = \sum_n \dot{\vec{R}} \vec{A}_{m,n}(\vec{R}(t)) \exp\left(-\frac{i}{\hbar} \int_0^t dt' (E_n^{BO}(\vec{R}(t')) - E_m^{BO}(\vec{R}(t')))\right) \Gamma_n(t) \quad (\text{E.13})$$

where $|\Psi_n^{BO}(\vec{R}(t))\rangle$ are the eigenvectors, $E_n^{BO}(\vec{R}(t))$ are energy eigenvalues of the instantaneous Hamiltonian $\hat{H}^{BO}(\vec{R}(t))$, and $\vec{A}_{m,n}(\vec{R}(t))$ are the first-derivative couplings defined in Eq. 2.29 and Eq. E.9.

Let us inspect Eq. E.13 and rationalize some of the observations we made earlier for the full description.

- When the derivative couplings vanish, that is in the Born-Oppenheimer approximation, the coefficients $\Gamma_m(t)$ are time independent. This reproduces the notion that there are no transitions in the Born-Oppenheimer approximation.
- The dynamical phase oscillates rapidly if the two Born-Oppenheimer surfaces are far apart. When the prefactor $\dot{\vec{R}} \vec{A}_{mn}(\vec{R}(t)) \Gamma_n(t)$ is approximately constant, the phase factor in Eq. E.13 averages out and does not have a net effect. This supports the notion that transitions between Born-Oppenheimer surfaces are important, whenever two Born-Oppenheimer surfaces come close to each other.

With Eq. E.9 and Eq. 2.31, we can rewrite the equation of motion Eq. E.13 in a form that uses the Born-Oppenheimer wave functions rather than the derivative couplings. We also exploit the normalization condition of the Born-Oppenheimer wave functions $\langle \Psi_m^{BO} | \Psi_m^{BO} \rangle = 1$

$$\begin{aligned} i\hbar\partial_t \Gamma_m(t) &= \hbar \underbrace{\text{Im} \left\langle \Psi_m^{BO}(\vec{R}(t)) \left| \frac{d\Psi_m^{BO}(\vec{R}(t))}{dt} \right\rangle}_{=0 \text{ for real-valued } \langle \vec{x} | \Psi_m^{BO} \rangle} \Gamma_m(t) \\ &+ \sum_{n;n \neq m} \left\langle \Psi_m^{BO}(\vec{R}(t)) \left| \frac{d\hat{H}^{BO}(\vec{R}(t))}{dt} \right| \Psi_n^{BO}(\vec{R}(t)) \right\rangle \\ &\times \frac{\exp\left(-\frac{i}{\hbar} \int_0^t dt' (E_n^{BO}(\vec{R}(t')) - E_m^{BO}(\vec{R}(t')))\right)}{\frac{i}{\hbar} (E_n^{BO}(\vec{R}(t)) - E_m^{BO}(\vec{R}(t)))} \Gamma_n(t) \end{aligned} \quad (\text{E.14})$$

The diagonal term in Eq. E.14 describes a time-dependent phase factor $e^{i\phi_n(t)}$ for the wave functions. It vanishes for real-valued Born-Oppenheimer wave functions.

Geometric phase

When the system moves adiabatically, so that it stays on one Born-Oppenheimer surface, the wave function picks up a phase $\varphi(t)$. The phase for a closed trajectory is the geometric phase. This is the original physical picture for the concept of a geometric phase.

The phase difference of the wave function for a trajectory is obtained from the equation of motion for $\Gamma_n(t) = e^{i\varphi(t)}$

$$\begin{aligned}
 i\hbar\partial_t\Gamma_n(t) &\stackrel{\text{Eq. E.13}}{=} \dot{\vec{R}}\vec{A}_{n,n}(\vec{R})\Gamma_n(t) \\
 \Rightarrow \partial_t\varphi(t) &= -i\partial_t\ln(\Gamma_n(t)) = -i\frac{1}{i\hbar}\frac{1}{\Gamma(t)}i\hbar\partial_t\Gamma_n(t) = -\frac{1}{\hbar}\dot{\vec{R}}\vec{A}_{n,n}(\vec{R}) \\
 \Rightarrow \varphi(t) &= \varphi(0) - \frac{1}{\hbar}\int_0^t dt' \dot{\vec{R}}(t')\vec{A}_{m,m}(\vec{R}(t')) = \varphi(0) - \frac{1}{\hbar}\int_{\vec{R}(0)}^{\vec{R}(t)} d\vec{R}'\vec{A}_{m,m}(\vec{R}') \quad (\text{E.15})
 \end{aligned}$$

Eq. E.15 leads to the expression for the geometric phase[114] as

$$\Delta\varphi = -\frac{1}{\hbar}\oint d\vec{R}\vec{A}_{m,m}(\vec{R}). \quad (\text{E.16})$$

which corresponds to Eq. H.33 in the case of the Jahn-Teller model.

Landau-Zener formula

Using the picture of an electronic wave function following a nuclear trajectory underlies a simple intuitive expression for the transition probability, the **Landau-Zener formula**. A derivation is provided in appendix F on p. 453.

$$P = \exp\left(-2\pi\frac{|H_{12}|}{\hbar}\frac{|H_{12}|}{V|F_1 - F_2|}\right) \quad (\text{E.17})$$

E.1.3 Ehrenfest dynamics

We can now use the instantaneous wave function to evaluate the forces acting on the nuclei. With the wave function Eq. E.12, the forces are a weighted average from all Born-Oppenheimer surfaces, with the weights $|\Gamma_n(t)|^2$. When these forces are entered into Newton's equations of motion for the nuclear trajectories, the description corresponds to Ehrenfest dynamics. As described in appendix E.3.2 on p. 435, Ehrenfest dynamics can be described in terms of a Lagrangian for electronic wave functions and atomic trajectories.

Ehrenfest's theorem[115]. establishes that the expectation values of positions and momenta evolve according to Hamilton's equations of motion with the expectation values of the forces. Ehrenfest theorem is described in section 8.3 of Φ SX: Quantum Physics[4].

$$\begin{aligned}
 \frac{d}{dt}\langle\Phi(t)|\hat{R}|\Phi(t)\rangle &= \langle\Phi(t)|\vec{\nabla}_P\hat{H}(\hat{P}, \hat{R})|\Phi(t)\rangle \\
 \frac{d}{dt}\langle\Phi(t)|\hat{P}|\Phi(t)\rangle &= -\langle\Phi(t)|\vec{\nabla}_R\hat{H}(\hat{P}, \hat{R})|\Phi(t)\rangle \quad (\text{E.18})
 \end{aligned}$$

These equations are the quantum-mechanical analogue of **Hamilton's equations of motion**

$$\begin{aligned}
 \dot{\vec{R}} &= \vec{\nabla}_P H(\vec{P}, \vec{R}) \\
 \dot{\vec{P}} &= -\vec{\nabla}_R H(\vec{P}, \vec{R}). \quad (\text{E.19})
 \end{aligned}$$

Ehrenfest dynamics is a technique, which identifies the quantum expectation value of momenta and positions with momenta and positions of a trajectory. Thus, the positions and momenta of the nuclei evolve under the forces obtained as expectation value with the electronic wave function. The electronic wave function is obtained from Eq. E.12 as solution of the time-dependent Schrödinger equation along the nuclear trajectory.

There is, however, a fundamental flaw in Ehrenfest dynamics, which becomes evident if the wave function splits into several wave packets: In reality, each wave packet evolves under its own set of forces, which have little to do with the mean value of the forces for several wave packets. If the wave function is a superposition of several separated wave packets, Ehrenfest's theorem is useful to describe the trajectory of each individual wave packet in phase space, separately. The dynamics of the average positions and momenta, which is given by Ehrenfest's theorem, is, however, of limited value to construct the trajectories of the nuclei.

E.1.4 Surface hopping

The two techniques, Born-Oppenheimer dynamics and Ehrenfest dynamics, are suitable in different occasions and one fails, when the other performs well.

- The Born-Oppenheimer dynamics performs well as long as (1) the Born-Oppenheimer energies are well separated and (2) when the wave function contributes only to one specific Born-Oppenheimer surface. The Born-Oppenheimer dynamics fails at conical intersections and avoided or true crossings, because it cannot describe the transition between different Born-Oppenheimer surfaces.
- Ehrenfest dynamics works well as the trajectory corresponds to a single wave packet. It describes the electronic transitions at a conical intersection. However, when the wave function has important contributions from several Born-Oppenheimer surfaces, the true dynamics would split the wave packet in configuration space. This splitting can not be described with a single trajectory employed in the Ehrenfest dynamics. Rather the system experiences the average forces of several Born-Oppenheimer surfaces.

The **surface-hopping method** invented by John Tully [116] provides a pragmatic approach out of this dilemma. In its modern version, the surface hopping employs the so-called *fewest switching criterion*. [117]

In this method, the forces acting on the atoms are determined from a specific sheet of the Born-Oppenheimer surfaces. Let us name its index n . The wave functions coefficients $\Gamma_n(t)$ are propagated according to Eq. E.13.

The transition probabilities $T_{m \leftarrow n}$ for a time interval Δ are evaluated in each time step.

$$T_{m \leftarrow n} = \begin{cases} \frac{|\Gamma_m(t+\Delta)|^2 - |\Gamma_m(t)|^2}{|\Gamma_n(t)|^2} & \text{for } m \neq n \\ 1 - \sum_{j:j \neq n} \frac{|\Gamma_j(t+\Delta)|^2 - |\Gamma_j(t)|^2}{|\Gamma_n(t)|^2} & \text{for } m = n \end{cases} \quad (\text{E.20})$$

A random process is established to select a transition consistent with the transition probabilities.

The electronic wave function remains unchanged during the surface hop. However, after the hop, it is propagated with the Hamiltonian of the new Born-Oppenheimer surface.

Modifications of the surface hopping have been suggested to introduce decoherence of the electronic wave functions [117].

E.1.5 Statistical mixtures

Editor: This is in preparation. Do not read

It is sensible to approximate such a composite wave function, which consists of several wave packets, by a statistical ensemble of wave packets. Each of these wave packets is then approximated by a classical trajectory, which evolves according to Ehrenfest dynamics.

The information lost in this approximation is the phase-relation between the wave packets. If the wave packets meet again they would undergo constructive or destructive interference, which is no more possible, when they are described by a set of trajectories. We will come to that during this section.

Let me consider a single trajectory, and perform the step from one multi-valued wave function which evolves according to Eq. E.12 to a statistical **ensemble** of wave functions $|\Psi^{(q)}(t)\rangle$ and their probabilities P_q .

Such an ensemble can be described by the **density matrix** $\hat{\rho}(t)$, which is a time-dependent operator in the electronic Hilbert space.

$$\hat{\rho}(t) = \sum_q |\Psi^{(q)}(t)\rangle P_q \langle \Psi^{(q)}(t)| \quad (\text{E.21})$$

Using the expansion in Born-Oppenheimer wave functions

$$|\Psi^{(q)}(t)\rangle = \sum_n |\Psi_n^{BO}(\vec{R}(t))\rangle \Gamma_n^{(q)}(t), \quad (\text{E.22})$$

we obtain

$$\hat{\rho}(t) \stackrel{\text{Eq. E.12}}{=} \sum_{m,n} |\Psi_m^{BO}(\vec{R}(t))\rangle \rho_{m,n}(t) \langle \Psi_n^{BO}(\vec{R}(t))| \quad (\text{E.23})$$

with the matrix elements

$$\rho_{m,n}(t) \stackrel{\text{Eq. E.12}}{=} \left(\sum_q P_q \Gamma_m^{(q)}(t) \Gamma_n^{(q)}(t) \right) \exp \left(-\frac{i}{\hbar} \int_0^t dt' \left(E_m^{BO}(\vec{R}(t')) - E_n^{BO}(\vec{R}(t')) \right) \right) \quad (\text{E.24})$$

Now, we do an approximation, which I will call the **random-phase approximation**. This approximation is not to be confused with the random-phase approximation (RPA) of many-particle physics, which describes the screening of the Coulomb interaction by electron-hole pairs. The random-phase approximation can be justified in several different ways. Therefore, let me explain first what it is and later give possible justifications for it.

The random-phase approximation discards the off-diagonal elements of the density matrix in a given representation of the wave functions.

$$\rho_{m,n}(t) \approx \delta_{m,n} \left(\sum_q P_q \Gamma_n^{(q)}(t) \Gamma_n^{(q)}(t) \right) \quad (\text{E.25})$$

In the present case, the basisset chosen are the Born-Oppenheimer wave functions. The question, in which basisset the off-diagonal elements are discarded, is non-trivial and has a fundamental effect on the effect of the approximation. We need to return to this point later.

The expression in parenthesis in Eq. E.25 can be identified as probability that the system is on a certain Born-Oppenheimer surface.

Justifications: There are several possible justifications of the random-phase approximation. Here, I will give two of them.

- **Time average:** The time evolution of $\Gamma_n(t)$ is slow, when the derivative coupling is small. If a measurement determines an expectation value⁴ of an observable A with a process that averages over a time interval Δ , the dynamical phase factors collapse into a Kronecker delta.

$$\frac{1}{\Delta} \int_{t_0-\Delta/2}^{t_0+\Delta/2} dt \exp \left(-\frac{i}{\hbar} \int_0^t dt' \left(E_m^{BO}(\vec{R}(t')) - E_n^{BO}(\vec{R}(t')) \right) \right) \approx \delta_{m,n} \quad (\text{E.26})$$

if $(E_m^{BO} - E_n^{BO})\Delta \gg 2\pi$. Thus, Eq. E.24 will be converted into Eq. E.25. If (1) the Born-Oppenheimer surfaces are well separated, if at the same time (2) the derivative couplings are small and if (3) the experiment does a time average, the experiment is not sensitive to the phase relations, which are discarded in the random-phase approximation.

⁴ $A = \text{Tr}[\hat{\rho}\hat{A}]$

- **Decoherence:** If the system is coupled to an environment, the Born-Oppenheimer surfaces are themselves a statistical ensemble over different environments or better different states of the environment. The ensemble over environments can be translated into an ensemble of relative phases.

$$\Delta\varphi_{m,n}(t) = -\frac{i}{\hbar} \int_0^t dt' \left(\Delta E_m^{BO}(\vec{R}(t')) - \Delta E_n^{BO}(\vec{R}(t')) \right) \quad (\text{E.27})$$

Taking the average over $e^{\Delta\varphi_{m,n}}$ removes the off-diagonal elements after a sufficient long time because $\langle e^{\Delta\varphi_{m,n}} \rangle \rightarrow \delta_{m,n}$. This is the origin for the name “*random-phase approximation*”.

Choice of the representation: In the complete description, the Born-Oppenheimer states are just one basis set of many. As discussed in section B.2, other choices are possible. The justifications of the random-phase approximation are based on physical processes. These processes also determine, which basis set shall be chosen.

There are good reasons for choosing the Born-Oppenheimer wave functions. Start with a wave packet which is localized in the nuclear coordinate space, but which is distributed over several Born-Oppenheimer surfaces. The contributions from different Born-Oppenheimer surfaces experience different forces and thus will evolve into different directions. Thus, the wave function splits into different wave packets, each of which can be assigned to a distinct Born-Oppenheimer surface. As a consequence of the **adiabatic theorem** (see section D.1), the wave packets from different Born-Oppenheimer surfaces do not affect each other strongly as long as the Born-Oppenheimer surfaces are well separated and the velocity of the wave packets is sufficiently slow. The wave packets which are separate into different spatial regions, will couple differently to an environment and thus pick up different phase shifts. Therefore, the phase average should be taken in a basis set of Born-Oppenheimer surfaces. *Editor: This argument is still a bit hand-waving. I am looking for a more rigorous discussion.*

From wave packets to trajectories:

After discarding the information on the phases of the wave packets, we can describe each wave packet by a trajectory. Thus, the description of an ensemble of wave packets is translated into an ensemble of trajectories.

$$\vec{R}^{(n)}(t) \quad (\text{E.28})$$

with initial probabilities

$$P_n(0) = \left(\sum_q P_q \Gamma_n^{(q)}(0) \Gamma_n^{(q)}(0) \right) \quad (\text{E.29})$$

and initial electronic wave function

$$|\psi^{(n)}(0)\rangle = |\psi_n^{BO}(\vec{R}(0))\rangle \quad (\text{E.30})$$

E.2 Further reading

Here, a few reviews and other articles related to non-adiabatic effects. I have not read all of them carefully yet myself.

- A good introduction given in the special volume of the Journal “Advances in Chemical Physics” from 2002[118]. In particular, I liked the article of Child[119] and that by Worth and Robb[7]
- Introductory lecture by Jasper et al.[111]

- the book “Beyond Born-Oppenheimer: Conical Intersections and Electronic Nonadiabatic Coupling Terms” by Michael Baer[120]. Baer uses a very compact notation, but he describes the topological effects in a very elegant manner.
- Non-adiabatic effects can lead to damping of the atomic motion due to the energy-loss due to to excitation of electron-hole pairs. Persson and Helsing[121] report the first-principles calculations of vibrational damping. Li and Wahnstrom[122] investigate the non-adiabatic effects by extending Newton’s equations of motion for the atoms by a Langevin equation, i.e. by adding a friction and a stochastic fluctuation term.

E.3 Ehrenfest dynamics

E.3.1 Lagrangian for the Schrödinger equation

As a prelude, let me introduce here the action principle for the Schrödinger equation.⁵ The Lagrangian for which the action principle yields the Schrödinger equation as Euler-Lagrange equation is

$$\mathcal{L}[|\psi\rangle, |\dot{\psi}\rangle] = i\hbar\langle\psi|\dot{\psi}\rangle - \langle\psi|\hat{H}|\psi\rangle \quad (\text{E.31})$$

The wave function $|\Psi\rangle$ may be the electron-nuclear wave function. While the Lagrangian appears to be different for Bras and Kets, the Euler-Lagrange equations nevertheless produce the Schrödinger equation and its hermitian conjugate

$$\begin{aligned} 0 &= \frac{\partial\mathcal{L}}{\partial\langle\psi|} - \frac{d}{dt}\frac{\partial\mathcal{L}}{\partial\langle\dot{\psi}|} = i\hbar\partial_t|\psi\rangle - \hat{H}|\psi\rangle \\ 0 &= \frac{\partial\mathcal{L}}{\partial|\psi\rangle} - \frac{d}{dt}\frac{\partial\mathcal{L}}{\partial|\dot{\psi}\rangle} = -\langle\psi|\hat{H} - i\hbar\partial_t\langle\psi| \end{aligned} \quad (\text{E.32})$$

E.3.2 Lagrangian for Ehrenfest dynamics

In section E.1.3, **Ehrenfest dynamics** has been introduced. It describes the atoms by classical trajectories and the wave functions on a quantum-mechanical level.

Let me postulate here a Lagrangian for nuclei following classical trajectories $\vec{R}(t)$ and electronic wave functions $|\Psi^e(t)\rangle$

$$\mathcal{L} = \frac{1}{2}\sum_{j=1}^{3M} M_j \dot{R}_j^2 + \langle\Psi^e(t)|i\hbar\partial_t|\Psi^e(t)\rangle - \langle\Psi^e(t)|\hat{H}^{BO}(\vec{R})|\Psi^e(t)\rangle \quad (\text{E.33})$$

According to Eq. 2.2, the Coulomb repulsion between nuclei is included in the Born-Oppenheimer Hamiltonian. The electronic wave functions $|\Psi^e(t)\rangle$ are many-electron wave functions.

Remark: The Lagrangian Eq. E.33 above has not been constructed as the quasi-classical limit of the full electron-nuclear Lagrangian, which also treats the nuclei quantum mechanically.

The expression $\langle\Psi^e(t)|i\hbar\partial_t|\Psi^e(t)\rangle$ is a kinetic energy for the wave function dynamics, which is not to be confused with the true kinetic energy of the electrons. It produces the Schrödinger equation as Euler-Lagrange equation. It is a consequence of the non-relativistic limit of a term containing two time derivatives.

⁵The Lagrangian in quantum mechanics, Paul A.M. Dirac Phys.Z.Sowjetunion 3, 64-72 (1933) https://doi.org/10.1142/9789812567635_0003

The Lagrangian Eq. E.33 describes **Ehrenfest dynamics**: The Euler-Lagrange equations are

$$0 = \frac{d}{dt} \frac{\partial \mathcal{L}}{\partial \dot{R}_j} - \frac{\partial \mathcal{L}}{\partial R_j} = M_j \ddot{R}_j - \underbrace{\left\langle \Psi^e(t) \left| -\frac{\partial \hat{H}^{BO}}{\partial R_j} \right| \Psi^e(t) \right\rangle}_{\text{Force}}$$

$$0 = \frac{\partial \mathcal{L}}{\partial \langle \Psi^e |} - \frac{d}{dt} \frac{\partial \mathcal{L}}{\partial \langle \dot{\Psi}^e |} = i\hbar \partial_t |\Psi^e\rangle - \hat{H}^{BO}(\vec{R}) |\Psi^e\rangle \quad (\text{E.34})$$

The atoms experience the expectation value of the force, and the electrons experience the electronic Hamiltonian for the instantaneous atomic configuration. This is the essence of Ehrenfest dynamics.

EHRENFEST DYNAMICS

Ehrenfest dynamics propagates the electronic wave function $|\Psi^e(t)\rangle$ with the Born-Oppenheimer Hamiltonian, which depends on the instantaneous atom positions. The atom positions evolve according to Newton's equations of motion following the *expectation value* of the forces.

$$M_j \ddot{R}_j(t) = \underbrace{\left\langle \Psi^e(t) \left| -\frac{\partial \hat{H}^{BO}}{\partial R_j} \right| \Psi^e(t) \right\rangle}_{\text{Force}}$$

$$i\hbar \partial_t |\Psi^e(t)\rangle = \hat{H}^{BO}(\vec{R}(t)) |\Psi^e(t)\rangle \quad (\text{E.35})$$

E.3.3 Ehrenfest dynamics in terms of the Born-Oppenheimer framework

The set of equations Eq. E.35 is sufficient to define Ehrenfest dynamics. In order to understand the resulting dynamics, it is convenient to rewrite these equations in the spirit of the Born-Oppenheimer framework presented in chapter 2. While the equations of motion become, at first sight, more complicated, they (1) hide the electronic structure problem and they separate the BO-dynamics from the electronic transitions.

I expand the electronic wave functions in terms of Born-Oppenheimer wave functions

$$|\Psi^e(t)\rangle \stackrel{\text{Eq. E.6}}{=} \sum_{n=1}^{\infty} |\Psi_n^{BO}(\vec{R}(t))\rangle C_n(t) \quad (\text{E.36})$$

The coefficients $C_n(t)$ are related to the nuclear wave functions in the Born-Huang formalism. Because we describe the nuclei classical rather than quantum mechanical, the coefficients do not depend only on time, but not on the nuclear coordinates.

Insertion of the Ansatz Eq. E.36 into the Lagrangian Eq. E.33 yields

$$\begin{aligned} \mathcal{L} &= \frac{1}{2} \sum_{j=1}^{3M} M_j \dot{R}_j^2 + \sum_{m,n=1}^{\infty} C_m^* \langle \Psi_m^{BO} | i\hbar \partial_t | \Psi_n^{BO} \rangle C_n - \sum_{m,n=1}^{\infty} C_m^* \langle \Psi_m^{BO} | \hat{H}^{BO} | \Psi_n^{BO} \rangle C_n \\ &= \frac{1}{2} \sum_{j=1}^{3M} M_j \dot{R}_j^2 + \sum_{m,n=1}^{\infty} C_m^* \underbrace{\langle \Psi_m^{BO} | \Psi_n^{BO} \rangle}_{\delta_{m,n}} (i\hbar \partial_t C_n) + \sum_{m,n=1}^{\infty} C_m^* \underbrace{\langle \Psi_m^{BO} | i\hbar \sum_{j=1}^{3M} \dot{R}_j \partial_{R_j} | \Psi_n^{BO} \rangle}_{- \dot{\vec{R}} \vec{A}_{m,n}} C_n - \sum_{n=1}^{\infty} C_n^* E_n^{BO} C_n \\ &= \frac{1}{2} \sum_{j=1}^{3M} M_j \dot{R}_j^2 + \sum_{n=1}^{\infty} C_n^* (i\hbar \partial_t C_n) - \sum_{n=1}^{\infty} C_n^* E_n^{BO} C_n - \sum_{m,n=1}^{\infty} C_m^* \left(\sum_{j=1}^{3M} \dot{R}_j A_{j;m,n} \right) C_n \end{aligned} \quad (\text{E.37})$$

Thus, we arrive at the Lagrangian for the nuclear positions and the wave function coefficients in terms of Born-Oppenheimer wave functions.

$$\mathcal{L} = \frac{1}{2} \sum_{j=1}^{3M} M_j \dot{R}_j^2 + \sum_{n=1}^{\infty} C_n^* (i\hbar \partial_t C_n) - \sum_{n=1}^{\infty} C_n^* E_n^{BO} C_n - \sum_{m,n=1}^{\infty} C_m^* \left(\sum_{j=1}^M \dot{R}_j A_{j;m,n} \right) C_n \quad (\text{E.38})$$

The physical content of this Lagrangian is identical of that provided for the Ehrenfest dynamics given above in Eq. E.33.

The Euler-Lagrange equations for the nuclei are

$$\begin{aligned} 0 &= \frac{d}{dt} \frac{\partial \mathcal{L}}{\partial \dot{R}_j} - \frac{\partial \mathcal{L}}{\partial R_j} \\ &= M_j \ddot{R}_j + \sum_n C_n^* C_n \left(\partial_{R_j} E_n^{BO}(\vec{R}) \right) \\ &\quad - \sum_{m,n} A_{j,m,n} \frac{d}{dt} (C_m^* C_n) - \sum_{k=1}^M \dot{R}_k \partial_{R_k} \sum_{m,n} C_m^* A_{j;m,n} C_n + \sum_{k=1}^M \dot{R}_k \partial_{R_j} \sum_{m,n} C_m^* A_{k;m,n} C_n \\ &= M_j \ddot{R}_j + \sum_n C_n^* C_n \left(\partial_{R_j} E_n^{BO}(\vec{R}) \right) \\ &\quad - \sum_{m,n} A_{j,m,n} \frac{d}{dt} (C_m^* C_n) - \sum_{k=1}^M \dot{R}_k \left(\partial_{R_k} A_j^{eff} - \partial_{R_j} A_k^{eff} \right) \end{aligned} \quad (\text{E.39})$$

In the last equation above, I introduced an “effective” derivative coupling $A_j^{eff}(t)$ defined by

$$A_j^{eff}(t) \stackrel{\text{def}}{=} \sum_{m,n} C_m^* A_{j;m,n} C_n. \quad (\text{E.40})$$

The physical interpretation is that the nuclei experience the forces from the Born-Oppenheimer surfaces and a velocity-dependent force from the effective derivative couplings. These terms are very similar to the dynamics of a particle in a electromagnetic field, albeit in higher dimensions.

One additional term comes from a change of the electronic density matrix $\rho_{m,n} = C_m^* C_n$. This term gives the atoms an additional “kick” during a transition between two Born-Oppenheimer surfaces. This kick apparently compensates the gain or loss of electronic energy (and momentum?) during a transition, by transferring this energy to the nuclear kinetic energy.⁶

The Euler-Lagrange equations for the wave-function coefficients are obtained as follows

$$\begin{aligned} 0 &= \frac{d}{dt} \frac{\partial \mathcal{L}}{\partial \dot{C}_n^*} - \frac{\partial \mathcal{L}}{\partial C_n^*} = -(i\hbar \partial_t C_n) + E_n^{BO}(\vec{R}) C_n + \sum_m \left(\sum_j \dot{R}_j A_{j;n,m} \right) C_m \\ 0 &= \frac{d}{dt} \frac{\partial \mathcal{L}}{\partial \dot{C}_n} - \frac{\partial \mathcal{L}}{\partial C_n} = i\hbar \partial_t C_n^* + E_n^{BO}(\vec{R}) C_n^* + \sum_m C_m^* \left(\sum_j \dot{R}_j A_{j;m,n} \right) \end{aligned} \quad (\text{E.41})$$

The derivatives with respect to C_n and C_n^* are Wirtinger derivatives, rather than real and imaginary part of C_n . The equations of motion for C_n and C_n^* are complex conjugates of each other. The equation of motion is equivalent to Eq. E.13 for the coefficients $\Gamma_n(t)$ defined in Eq. E.10.

⁶This argument rests on the energy conservation, which results from the action principle with a time-independent Lagrangian. (See Noether theorem)

LAGRANGIAN FOR CLASSICAL NUCLEI AND QUANTUM ELECTRONS

The Lagrangian for a systems of M classical nuclei with positions $\vec{R}(t)$ and coefficients of the electronic wave functions Eq. E.36 is

$$\mathcal{L} = \frac{1}{2} \sum_{j=1}^{3M} M_j \dot{R}_j^2 + \sum_{n=1}^{\infty} C_n^* (i\hbar \partial_t C_n) - \sum_{n=1}^{\infty} C_n^* E_n^{BO}(\vec{R}) C_n - \sum_{m,n=1}^{\infty} C_m^* \left(\sum_{j=1}^{3M} \dot{R}_j A_{j,m,n}(\vec{R}) \right) C_n \quad (\text{E.42})$$

The resulting equations of motion are

$$i\hbar \partial_t C_n = E_n^{BO}(\vec{R}) C_n + \sum_m \left(\sum_{j=1}^{3M} \dot{R}_j A_{j,n,m} \right) C_m \quad (\text{E.43})$$

$$M_j \ddot{R}_j = \sum_n C_n^* C_n \left(-\partial_{R_j} E_n^{BO}(\vec{R}) \right) + \sum_{k=1}^M \dot{R}_k \left(\partial_{R_k} A_j^{eff} - \partial_{R_j} A_k^{eff} \right) + \sum_{m,n} A_{j,m,n} \frac{d}{dt} (C_m^* C_n) \quad (\text{E.44})$$

The effective derivative couplings \vec{A}^{eff} are defined in Eq. E.40

Because the equations of motion have been derived from a Lagrangian formulation, the energy conservation for these equations of motion are strictly satisfied.

Let me discuss the equation of motion for the nuclei:

1. the first term $\sum_n C_n^* C_n \left(-\partial_{R_j} E_n^{BO}(\vec{R}) \right)$ describes forces as a weighted average over all Born-Oppenheimer surfaces. This is a kind of mean-field approximation and it is the main approximation of Ehrenfest dynamics. A better description would offer a distinct atom trajectory for each Born-Oppenheimer surface, so that each trajectory represents a wave packet on a single Born-Oppenheimer surface. These wave packets experience different forces and thus follow different trajectories.

Ehrenfest dynamics will be reliable if the electrons reside on a single Born-Oppenheimer surface, or if the forces from the contributing Born-Oppenheimer surfaces are similar. If the forces from the relevant Born-Oppenheimer surfaces are different, the system may evolve with Ehrenfest dynamics into regions of configuration space, which none of the wave packets would choose.

2. The second term $\sum_{k=1}^M \dot{R}_k \left(\partial_{R_k} A_j^{eff} - \partial_{R_j} A_k^{eff} \right)$ behaves like a magnetic field, albeit in $3M$ dimensions. Like a magnetic field it does not add or remove energy.
3. The third term describes a force which results from the electronic transition. The energy gained as an electron makes a transition to a lower Born-Oppenheimer surface, is compensated by an accelerating force on the atom trajectory.

E.4 Quasi-classical approximation for the nuclear wave functions

Editor: This section ‘‘Quasi-classical Limit: From wave functions to trajectories’’ is in preparation. Do not read.

Editor: Consult Tully,98[112] for this section. (Classical Limit, Ehrenfest, Surface Hopping.)

1. From the Schrödinger equation to the Hamilton-Jacobi equation.
2. Trajectories to solve the Hamilton-Jacobi equation.

3. Lagrangian for the trajectories.

Let me start from the electron-nuclear Schrödinger equation with Hamiltonian $\frac{1}{2}\vec{P}\mathbf{M}^{-1}\vec{P}\hat{1} - \hat{H}^{BO}(\vec{R})$ and construct the corresponding Lagrangian for $\Phi(\vec{r}, \vec{R}, t)$. Then, I represent the wave function in terms of Born-Oppenheimer wave functions $\Phi(\vec{r}, \vec{R}, t) = \sum_n \langle \vec{r} | \Psi_n^{BO}(\vec{R}) \rangle \Theta_n(\vec{R}, t)$

$$\begin{aligned}
 \mathcal{L}^\Phi &= \langle \Phi | i\hbar\partial_t - \hat{H} | \Phi \rangle \\
 &= \sum_{m,n} \int d^{3N}R \Theta_m^*(\vec{R}, t) \langle \Psi_m^{BO}(\vec{R}) | \left[i\hbar\partial_t \hat{1} - \underbrace{\frac{1}{2} \left(\frac{\hbar}{i} \vec{\nabla}_R \right) \mathbf{M}^{-1} \left(\frac{\hbar}{i} \vec{\nabla}_R \right)}_{-\hat{H} \text{ for electrons and nuclei}} - \hat{H}^{BO}(\vec{R}) \right] | \Psi_n^{BO}(\vec{R}) \rangle \Theta_n(\vec{R}, t) \\
 &\stackrel{\text{Eq. 2.27}}{=} \sum_{m,n} \int d^{3N}R \Theta_m^*(\vec{R}, t) \\
 &\quad \times \left[i\hbar\delta_{m,n}\partial_t \hat{1} - \frac{1}{2} \sum_k \left(\delta_{m,k} \frac{\hbar}{i} \vec{\nabla}_R + \vec{A}_{m,k}(\vec{R}) \right) \mathbf{M}^{-1} \left(\delta_{k,n} \frac{\hbar}{i} \vec{\nabla}_R + \vec{A}_{k,n}(\vec{R}) \right) - \delta_{m,n} E_m^{BO}(\vec{R}) \right] \Theta_n(\vec{R}, t) \\
 &= \int d^{3N}R \left[\sum_n \left(-\partial_t S_n - E_n^{BO}(\vec{R}) \right) \right. \\
 &\quad - \sum_{m,n} e^{\frac{i}{\hbar}(S_m - S_n)} \frac{1}{2} \sum_k \left(\delta_{m,k} (\vec{\nabla}_R S_n) + \vec{A}_{m,k}(\vec{R}) \right) \mathbf{M}^{-1} \left(\delta_{k,n} (\vec{\nabla}_R S_n) + \vec{A}_{k,n}(\vec{R}) \right) \\
 &\quad \left. - \sum_{m,n} e^{\frac{i}{\hbar}(S_m - S_n)} \frac{1}{2} \frac{\hbar}{i} \vec{\nabla}_R \mathbf{M}^{-1} \left(\delta_{m,n} (\vec{\nabla}_R S_n) + \vec{A}_{m,n}(\vec{R}) \right) \right] \\
 &\approx - \int d^{3N}R \sum_n \left[\partial_t S_n + \frac{1}{2} \sum_k \left(\delta_{n,k} (\vec{\nabla}_R S_n) + \vec{A}_{n,k}(\vec{R}) \right) \mathbf{M}^{-1} \left(\delta_{k,n} (\vec{\nabla}_R S_n) + \vec{A}_{k,n}(\vec{R}) \right) + E_n^{BO}(\vec{R}) \right. \\
 &\quad \left. + \frac{1}{2} \frac{\hbar}{i} \vec{\nabla}_R \mathbf{M}^{-1} \left((\vec{\nabla}_R S_n) + \vec{A}_{n,n}(\vec{R}) \right) \right]
 \end{aligned} \tag{E.45}$$

In the last step, I removed the terms proportional to $e^{\frac{i}{\hbar}(S_m - S_n)}$ with $m \neq n$.

$$\begin{aligned}
 0 &= \frac{\partial \mathcal{L}^\Theta}{\partial \Theta_m^*(\vec{R})} - \frac{d}{dt} \frac{\partial \mathcal{L}^\Theta}{\partial \dot{\Theta}_m^*(\vec{R})} \\
 &= \sum_n \left[i\hbar\partial_t \hat{1} \delta_{m,n} - \frac{1}{2} \langle \Psi_m^{BO}(\vec{R}) | \left(\frac{\hbar}{i} \vec{\nabla}_R \right) \mathbf{M}^{-1} \left(\frac{\hbar}{i} \vec{\nabla}_R \right) | \Psi_n^{BO}(\vec{R}) \rangle \right. \\
 &\quad \left. - \langle \Psi_m^{BO}(\vec{R}) | \hat{H}^{BO}(\vec{R}) | \Psi_n^{BO}(\vec{R}) \rangle \right] \Theta_n(\vec{R}, t)
 \end{aligned} \tag{E.46}$$

We make the Ansatz for the quasiclassical approximation for the nuclear wave function $\Theta_n(\vec{R}, t)$

$$\begin{aligned}
 \Theta_n(\vec{R}, t) &= e^{\frac{i}{\hbar} S_n(\vec{R}, t)} \quad \text{with} \quad S_n = S_{0,n} + \frac{\hbar}{i} S_{1,n} \\
 |\Theta_n(\vec{R}, t)|^2 &= e^{2S_{1,n}(\vec{R}, t)} \rightsquigarrow S_{1,n} \\
 \frac{\Theta_n(\vec{R}, t)}{|\Theta_n(\vec{R}, t)|} &= e^{\frac{i}{\hbar} S_{0,n}(\vec{R}, t)} \rightsquigarrow S_{0,n}
 \end{aligned} \tag{E.47}$$

We will use

$$\begin{aligned}
 e^{-\frac{i}{\hbar} S_n} i\hbar\partial_t \Theta_n &= -\partial_t S_n + i\hbar\partial_t \\
 e^{-\frac{i}{\hbar} S_n} \frac{\hbar}{i} \vec{\nabla} \Theta_n &= \vec{\nabla} S_n + \frac{\hbar}{i} \vec{\nabla}
 \end{aligned} \tag{E.48}$$

This Ansatz is inserted into Eq. 2.27 on p. 50.

$$\begin{aligned}
0 &= \partial_t S_m + \sum_n e^{\frac{i}{\hbar}(S_n - S_m)} \\
&\quad \times \left[\frac{1}{2} \sum_k \left(\delta_{m,k} \vec{\nabla} S_n + \delta_{m,k} \frac{\hbar}{i} \vec{\nabla} + \vec{A}_{m,k} \right) \mathbf{M}^{-1} \left(\delta_{k,n} \vec{\nabla} S_n + \delta_{k,n} \frac{\hbar}{i} \vec{\nabla} + \vec{A}_{k,m} \right) + \delta_{m,n} E_m^{BO} \right] \\
&= \partial_t S_m + \sum_n e^{\frac{i}{\hbar}(S_n - S_m)} \\
&\quad \times \left[\frac{1}{2} \sum_k \left(\delta_{m,k} \vec{P}_n + \vec{A}_{m,k} \right) \mathbf{M}^{-1} \left(\delta_{k,n} \vec{P}_n + \vec{A}_{k,m} \right) + \delta_{m,n} E_m^{BO} + \frac{1}{2} \frac{\hbar}{i} \vec{\nabla} \left(\delta_{m,n} \vec{P}_n - \vec{A}_{m,n} \right) \right]
\end{aligned} \tag{E.49}$$

The gradient in $\vec{\nabla} S_n$ does not act beyond S_n . In order to make the notation more concise in this respect, I introduced the momentum $\vec{P}_n(\vec{R}, t) \stackrel{\text{def}}{=} \vec{\nabla} S_n(\vec{R}, t)$.

In the next step we split off the terms coupling the wave functions on different Born-Oppenheimer surfaces and combine them into a source term $Q_m(\vec{R}, t)$.

$$\begin{aligned}
0 &= \partial_t S_m + \frac{1}{2} \sum_k \left(\delta_{m,k} \vec{P}_m + \vec{A}_{m,k} \right) \mathbf{M}^{-1} \left(\delta_{k,m} \vec{P}_m + \vec{A}_{k,m} \right) + E_m^{BO} + \frac{\hbar}{2i} \vec{\nabla} \left(\vec{P}_m + \vec{A}_{m,m} \right) + Q_m \\
Q_m &= \sum_{n;n \neq m} e^{\frac{i}{\hbar}(S_n - S_m)} \left[\vec{A}_{m,n} P_n + \frac{1}{2} \sum_k \vec{A}_{m,k} \vec{A}_{k,n} + \frac{\hbar}{2i} \vec{\nabla} \vec{A}_{m,n} \right] \\
\vec{P}_n &= \vec{\nabla} S_n
\end{aligned} \tag{E.50}$$

So-far we only rewrote the nuclear Schrödinger equation. Now, we introduce the expansion of the action $S_n(\vec{R}, t)$ in orders of \hbar .

$$\begin{aligned}
0 &= \partial_t S_{0,m} + \frac{1}{2} \sum_k \left(\delta_{m,k} \vec{P}_{0,m} + \vec{A}_{m,k} \right) \mathbf{M}^{-1} \left(\delta_{k,m} \vec{P}_{0,m} + \vec{A}_{k,m} \right) + E_m^{BO} + Q_{0,m} \\
Q_{0,m} &= \sum_{n;n \neq m} e^{\frac{i}{\hbar}(S_n - S_m)} \left[\vec{A}_{m,n} \vec{P}_{0,n} + \frac{1}{2} \sum_k \vec{A}_{m,k} \vec{A}_{k,n} \right] \\
\vec{P}_{0,n} &= \vec{\nabla} S_{0,n}
\end{aligned} \tag{E.51}$$

The factor $e^{\frac{i}{\hbar}(S_n - S_m)}$ depends on the full action and not the zero-th order approximation of the action.

In the quasi-classical limit, $\hbar \rightarrow 0$, the factor $e^{\frac{i}{\hbar}(S_n - S_m)}$ contributes only, when $\vec{P}_n - \vec{P}_m$ vanishes approximately. In all other cases the factor oscillates rapidly and thus averages out the result to zero.

The source term $Q_m(\vec{R}, t)$ is complex and thus contributes both to the zeroth and the first order.

E.5 Diagonal terms of the derivative couplings

As we have seen, the non-adiabatic effects are determined entirely by the derivative couplings $\vec{A}_{m,n,j}(\vec{R})$ defined in Eq. 2.29 on p. 50.

The off-diagonal terms are responsible for relaxation processes, the most evident physical effect due to non-adiabatic effects. Even if we suppress all transitions between the Born-Oppenheimer surfaces, non-adiabatic effects are present. These can be investigated by including only the diagonal terms of the first-derivative couplings.⁷

⁷In this approximation, the nuclear motion on the different Born-Oppenheimer surfaces are decoupled as in the Born-Oppenheimer approximation. This can be seen by inspecting Eq. 2.29: The derivative couplings are the only non-diagonal terms.

We will see that the diagonal derivative couplings act in a way similar to magnetic fields. We will also see the analogy of the geometrical phase and the Aharonov-Bohm effect in electrodynamics. Let me therefore revisit the most relevant equations we will need from electrodynamics.

Reminder of electrodynamics The equation of motion of a charged particle in a magnetic field is

$$M_j \ddot{\vec{R}}_j = q \left(\vec{E}(\vec{R}) + \dot{\vec{R}} \times \vec{B}(\vec{R}) \right) = q \left(\vec{E} + \dot{\vec{R}} \mathbf{F} \right) \quad (\text{E.52})$$

The magnetic field \vec{B} and the electric field \vec{E} are connected to the vector potential \vec{A} and the electric potential ϕ by

$$\begin{aligned} \vec{B} &= \vec{\nabla} \times \vec{A} \\ \vec{E} &= -\vec{\nabla} \phi - \dot{\vec{A}} \end{aligned} \quad (\text{E.53})$$

The electric field-strength tensor^a \mathbf{F} is

$$\mathbf{F} = \left(\vec{\nabla} \otimes \vec{A} \right) - \left(\vec{\nabla} \otimes \vec{A} \right)^\dagger = \begin{pmatrix} 0 & B_z & -B_y \\ B_y & 0 & B_x \\ B_y & -B_x & 0 \end{pmatrix} \quad (\text{E.54})$$

The components the field-strength tensor are

$$F_{i,j} = \partial_i A_j - \partial_j A_i \quad (\text{E.55})$$

and those of the magnetic field are

$$B_i = \sum_{j,k} \epsilon_{i,j,k} \partial_j A_k \quad (\text{E.56})$$

where $\epsilon_{i,j,k}$ is the Levi-Civita symbol or fully antisymmetric tensor.

The Lorentz force can be written in terms of the field strength tensor using

$$\dot{\vec{R}} \mathbf{F} = \dot{\vec{R}} \times \vec{B} \quad (\text{E.57})$$

^aWhat we call the electric field-strength tensor is actually the spatial part of the four-dimensional electric field-strength tensor in relativistic description. The corresponding space-time elements contain the electric fields. We kept the name used in a relativistic description.

Within the diagonal approximation, we can do the classical approximation. Each sheet of the Born-Oppenheimer approximation contributes a Hamilton function $H_n(\vec{P}, \vec{R})$ for the motion of the nuclei.

$$H_n(\vec{P}, \vec{R}) = \sum_{j=1}^{3M} \frac{1}{2M_j} \left(\vec{P}_j + \vec{A}_{n,n,j}(\vec{R}) \right)^2 + E_n^{BO}(\vec{R}) \quad (\text{E.58})$$

In the following, I will drop the index n , which refers to a particular sheet of the Born-Oppenheimer surfaces. Thus, we work with the Hamiltonian

$$H(\vec{P}, \vec{R}) = \sum_{j=1}^{3M} \frac{1}{2M_j} \left(\vec{P}_j + \vec{A}_j(\vec{R}) \right)^2 + E^{BO}(\vec{R}) \quad (\text{E.59})$$

For convenience, we use $3M$ dimensional vectors \vec{R}, \vec{P} for the momenta and coordinates of the nuclei. However, we will also use the three-dimensional vectors \vec{R}_j and \vec{P}_j for the j -th atom. Similarly, we use the mass M_j of the j -th atom. I will indicate the gradients with respect to momenta by $\vec{\nabla}_{\vec{P}_j}$ and the ones to positions either explicitly by $\vec{\nabla}_{\vec{R}_j}$ and simply by $\vec{\nabla}_j$.

Hamilton's equations for this system have the form

$$\dot{\vec{P}}_j = -\vec{\nabla}_{\vec{R}_j} H(\vec{R}, \vec{P}) = -\underbrace{\frac{1}{M_k} (\vec{P}_k + \vec{A}_k)}_{\dot{\vec{R}}_k} \sum_k (\vec{\nabla}_j \otimes \vec{A}_k) - \vec{\nabla}_j E^{BO} \quad (\text{E.60})$$

$$\dot{\vec{R}}_j = \vec{\nabla}_{\vec{P}_j} H(\vec{R}, \vec{P}) = \frac{1}{M_j} (\vec{P}_j + \vec{A}_j) \quad (\text{E.61})$$

With \otimes I denote the dyadic or outer product defined by $(\vec{a} \otimes \vec{b})_{ij} = a_i b_j$.

The two Hamilton's equations Eq. E.60 and Eq. E.61 can be combined into the form of Newton's equations

$$\begin{aligned} M_j \ddot{\vec{R}}_j &\stackrel{\text{Eq. E.61}}{=} \dot{\vec{P}}_j + \sum_k (\dot{\vec{R}}_k \vec{\nabla}_{\vec{R}_k}) \vec{A}_j(\vec{R}) \\ &\stackrel{\text{Eq. E.60}}{=} \underbrace{-\sum_k (\vec{\nabla}_j \otimes \vec{A}_k) \frac{1}{M_k} (\vec{P}_k + \vec{A}_k) - \vec{\nabla}_j E_n^{BO}}_{\dot{\vec{R}}_k} + \sum_k (\dot{\vec{R}}_k \vec{\nabla}_k) \vec{A}_j(\vec{R}) \\ &\stackrel{\text{Eq. E.61}}{=} \sum_k (\dot{\vec{R}}_k \vec{\nabla}_k) \vec{A}_j(\vec{R}) - \sum_k (\vec{\nabla}_j \otimes \vec{A}_k) \dot{\vec{R}}_k - \vec{\nabla}_j E_n^{BO} \\ &\stackrel{\text{Eq. E.61}}{=} \sum_k \dot{\vec{R}}_k \mathbf{F}_{k,j} - \vec{\nabla}_j E_n^{BO} \end{aligned} \quad (\text{E.62})$$

where $\mathbf{F}_{k,j}$ is something like a **generalized field-strength tensor**, which captures the non-adiabatic effects

$$\mathbf{F}_{k,j} = (\vec{\nabla}_k \otimes \vec{A}_j) - (\vec{\nabla}_j \otimes \vec{A}_k)^\dagger \quad (\text{E.63})$$

In order to make the structure of the velocity-dependent term in Eq. E.62 evident, let me use the bac-cab rule⁸ for a velocity vector \vec{v} and a vector field $\vec{A}(\vec{r})$

$$\vec{v} \times \underbrace{(\vec{\nabla} \times \vec{A})}_{\vec{B}} \stackrel{\text{bac-cab rule}}{=} \vec{\nabla} (\vec{v} \cdot \vec{A}) - (\vec{v} \cdot \vec{\nabla}) \vec{A} = \sum_j \underbrace{(\partial_i A_j - \partial_j A_i)}_{F_{ij}} v_j \quad (\text{E.64})$$

This shows that the velocity dependent force in Eq. E.62 is formally analogous to the Lorentz force $\vec{v} \times \vec{B}$ with $\vec{B} = \vec{\nabla} \times \vec{A}$ of a charged particle in a magnetic field. The physical origin is, however, very different.

Like the Hamilton function, also the equation of motion has great similarities with equation of motion of a charged particle (with charge $q = -1$) in an electromagnetic field. There, is however a major difference, namely that the velocity of one particle contributes to the force acting on another. There would be generalized magnetic field for each pair of atoms. The field strength tensor is not a three-by-three matrix, but a $3M \times 3M$ -matrix, where M is the number of nuclei.

We can work out the analogue of the field-strength tensor using the notation with $3M$ dimensional vectors that combine Cartesian coordinate with the particle index.

$$\begin{aligned} \partial_i A_{n,n,j} - \partial_j A_{n,n,i} &= \partial_{R_i} \langle \Psi_n^{BO} | \frac{\hbar}{i} \partial_{R_j} | \Psi_n^{BO} \rangle - \partial_{R_j} \langle \Psi_n^{BO} | \frac{\hbar}{i} \partial_{R_i} | \Psi_n^{BO} \rangle \\ &= \frac{\hbar}{i} \left(\langle \partial_{R_i} \Psi_n^{BO} | \partial_{R_j} \Psi_n^{BO} \rangle - \langle \partial_{R_j} \Psi_n^{BO} | \partial_{R_i} \Psi_n^{BO} \rangle \right) \\ &= 2\hbar \text{Im} \left(\langle \partial_{R_i} \Psi_n^{BO} | \partial_{R_j} \Psi_n^{BO} \rangle \right) \end{aligned}$$

⁸The bac-cab rule is $\vec{a} \times (\vec{b} \times \vec{c}) = \vec{b}(\vec{a} \cdot \vec{c}) - \vec{c}(\vec{a} \cdot \vec{b})$

Using again the vector-matrix notation for Cartesian coordinates and indices for the atoms, we obtain

$$F_{k,j} = 2\hbar \operatorname{Im} \langle \vec{\nabla}_k \Psi_n^{BO} | \otimes | \vec{\nabla}_j \Psi_n^{BO} \rangle \quad (\text{E.65})$$

This result seems to indicate that the non-adiabatic effects can be made to vanish by choosing real-valued Born-Oppenheimer wave functions.

This is, however, not so: While real-valued wave functions can be chosen in the absence of magnetic fields as a consequence of time-inversion symmetry⁹, the choice of real-valued wave functions unavoidably produces a step in the wave function when there is a conical intersection. We have encountered this effect in the Jahn-Teller model. This is related to the existence of a **geometrical phase**. Key words related to the geometrical phase is the **Jahn-Teller effect** and the **Berry phase**.

E.5.1 Example: Jahn-Teller model

For the lower Born-Oppenheimer surface of the Jahn-Teller model, we obtained with $\vec{R} = (X, Z)$

$$\begin{aligned} E_-^{BO}(\vec{R}) &\stackrel{\text{Eq. H.17}}{=} -g|\vec{R}| + w\vec{R}^2 \\ \vec{A}_{--}(\vec{R}) &\stackrel{\text{Eq. H.31}}{=} \frac{\hbar}{2\vec{R}^2} \begin{pmatrix} Z \\ -X \end{pmatrix} \end{aligned} \quad (\text{E.66})$$

The generalized field strength tensor $F_{k,j}$ is

$$\begin{aligned} \mathbf{F} &\stackrel{\text{Eq. E.63}}{=} \begin{pmatrix} \partial_x \\ \partial_z \end{pmatrix} \otimes \frac{\hbar}{2\vec{R}^2} \begin{pmatrix} Z \\ -X \end{pmatrix} - \left[\begin{pmatrix} \partial_x \\ \partial_z \end{pmatrix} \otimes \frac{\hbar}{2\vec{R}^2} \begin{pmatrix} Z \\ -X \end{pmatrix} \right]^\dagger \\ &= -\frac{\hbar}{4\vec{R}^4} \begin{pmatrix} X \\ Z \end{pmatrix} \otimes \begin{pmatrix} Z \\ -X \end{pmatrix} + \frac{\hbar}{2\vec{R}^2} \begin{pmatrix} \partial_x \\ \partial_z \end{pmatrix} \otimes \begin{pmatrix} Z \\ -X \end{pmatrix} - [\dots]^\dagger \\ &= -\frac{\hbar}{4\vec{R}^4} \begin{pmatrix} XZ & -X^2 \\ Z^2 & -XZ \end{pmatrix} + \frac{\hbar}{2\vec{R}^2} \begin{pmatrix} 0 & -1 \\ 1 & 0 \end{pmatrix} - [\dots]^\dagger \\ &= -\frac{\hbar}{4\vec{R}^4} \begin{pmatrix} 0 & -X^2 - Z^2 \\ X^2 + Z^2 & 0 \end{pmatrix} + \frac{\hbar}{\vec{R}^2} \begin{pmatrix} 0 & -1 \\ 1 & 0 \end{pmatrix} \\ &= \frac{3\hbar}{4\vec{R}^2} \begin{pmatrix} 0 & -1 \\ 1 & 0 \end{pmatrix} \end{aligned} \quad (\text{E.67})$$

Next we can evaluate the equation of motion as

$$\begin{aligned} M \begin{pmatrix} \ddot{X} \\ \ddot{Z} \end{pmatrix} &= \begin{pmatrix} \dot{X} \\ \dot{Z} \end{pmatrix} \frac{3\hbar}{4\vec{R}^2} \begin{pmatrix} 0 & -1 \\ 1 & 0 \end{pmatrix} + \frac{g}{|\vec{R}|} \begin{pmatrix} X \\ Z \end{pmatrix} - 2w \begin{pmatrix} X \\ Z \end{pmatrix} \\ &= \frac{3\hbar}{4\vec{R}^2} \begin{pmatrix} \dot{Z} \\ -\dot{X} \end{pmatrix} + \frac{g}{|\vec{R}|} \begin{pmatrix} X \\ Z \end{pmatrix} - 2w \begin{pmatrix} X \\ Z \end{pmatrix} \end{aligned} \quad (\text{E.68})$$

The system experiences¹⁰ a quasi-magnetic field $B_Y = \frac{-3\hbar}{4\vec{R}^2}$. The quasi-magnetic field B_Y for a two-dimensional system is a scalar. It can also be considered as the Y-component of the quasi-magnetic field in a three dimensional (X, Y, Z) -space, where the derivative couplings have components (A_X, A_Y, A_Z) .

⁹See appendix ??

¹⁰The Lorentz force of a charged particle in an electromagnetic field is $\vec{F} = q\vec{E}(\vec{r})q\vec{v} \times \vec{B}(\vec{r})$, where \vec{F} is the force acting on a particle with charge q with position \vec{r} and velocity \vec{v} , \vec{E} is the electric field and \vec{B} is the magnetic field.

Because of the factor \hbar , this field B_Y vanishes in the classical limit, except for the conical intersection.¹¹ There is a region with radius $R_c = \sqrt{3\hbar|\vec{V}|/(4g)}$ centered at the conical intersection, where the forces from the quasi-magnetic field even dominate over the forces from the Born-Oppenheimer surfaces. The size of this region depends on the velocity $\vec{V} = (\dot{X}, \dot{Z})$ of the nuclear coordinates.

Editor: The following is not finished. I am attempting to understand (1) whether the conical intersection in this limit can be considered as a hard sphere and (2) if I can extract a finite transfer of angular momentum during the collision with a conical intersection. It should be noted that transitions through the conical intersection cannot be ignored in this region.

While the quasi-magnetic field near the conical intersection is far from constant, let me remind us of the trajectories in a constant magnetic field. The trajectory for the equations of motion

$$M\ddot{X} = B_Y\dot{Z} \quad \text{and} \quad M\ddot{Z} = -B_Y\dot{X} \quad (\text{E.69})$$

are

$$\begin{aligned} X(t) &= X_C + (X(0) - X_C) \cos(\omega t) + \frac{V_x(0)}{\omega} \sin(\omega t) \\ Z(t) &= X_C + (Z(0) - Z_C) \cos(\omega t) + \frac{V_z(0)}{\omega} \sin(\omega t) \end{aligned} \quad (\text{E.70})$$

where $\omega = B_Y/M$. The trajectory proceeds in a circle centered at $(X_C, Z_C) = (X(0) + V_z B_Y/M, Z(0) - V_x B_Y/M)$. The radius is $B_Y|\vec{V}|/M$.

E.6 Geometric phase

E.6.1 Aharonov-Bohm effect

Imagine the following experiment: An electron beam is split into two coherent electron beams. The two beams pass on either side of a magnetic coil without entering the inside of the coil. The magnetic coil produces a magnetic field inside the coil, but none outside. The electron beams are then joined again and brought into interference. The surprising observation is that the interference pattern of the two electron beams depends on the magnetic field inside the coil, even though none of the electron beams experiences the magnetic field.

The explanation is that the phase of the electronic wave function is affected by the vector potential. Unlike the magnetic field, the vector potential is not restricted to the inside of the coil. The relative phase shift of the two electron beams can be expressed by a contour integral of the vector potential around the coil. This contour integral is related to the magnetic flux in the coil and thus proportional to the magnetic field inside the coil.

Even though the vector potential is not an observable quantity, because it is changed under a gauge transformation, the contour integral is gauge invariant and therefore observable.

E.6.2 Geometric phase

Editor: Under construction: do not read

The adiabatic theorem[109] states that a quantum system returns to its original state under the dynamics with a time-dependent Hamiltonian $\hat{H}(t)$, which changes slowly and returns to the original state. Michael Berry showed that in this process the initial and final state may differ by a phase factor, the so-called Berry phase[114]. **Editor:** Statement from Wikipedia. check!

¹¹The limit of \hbar/\vec{R}^2 for $\hbar \rightarrow 0$ and $\vec{R} \rightarrow 0$ is undefined. The limit $|\vec{R}| \rightarrow 0$ needs to be taken first, because in reality \hbar will be very small, but never really zero.

Berry describes the electronic wave function for classical nuclear trajectory as described in section E.1.2 on p. 429.

ELECTRONIC WAVE FUNCTION FOR A CLASSICAL NUCLEAR TRAJECTORY

Given a nuclear trajectory $\vec{R}(t)$, the electronic wave function $|\Phi(t)\rangle$, which evolves under the time-dependent Schrödinger equation with the Hamiltonian $\hat{H}(\vec{R}(t))$ is

$$|\Phi(t)\rangle \stackrel{\text{Eq. E.12}}{=} \sum_n |\psi_n^{BO}(\vec{R}(t))\rangle \exp\left(-\frac{i}{\hbar} \int_0^t dt E_n^{BO}(\vec{R}(t))\right) \Gamma_n(t) \quad (\text{E.71})$$

with

$$i\hbar\partial_t \Gamma_m(t) \stackrel{\text{Eq. E.13}}{=} \sum_n \dot{\vec{R}} \vec{A}_{m,n}(\vec{R}(t)) \exp\left(-\frac{i}{\hbar} \int dt (E_n^{BO}(t) - E_m^{BO}(t))\right) \Gamma_n(t) \quad (\text{E.72})$$

where $|\psi_n^{BO}(\vec{R}(t))\rangle$ are the eigenvectors and $E_n^{BO}(\vec{R}(t))$ are energy eigenvalues of the instantaneous Hamiltonian $\hat{H}(\vec{R}(t))$.

Adiabatic approximation

For an infinitely slow, that is adiabatic, trajectory, the oscillations of the dynamical phase factor average out so that the terms connecting different Born-Oppenheimer surfaces do not contribute. The basis for this argument is the adiabatic theorem[109] given in appendix D.1 on p. 423.

With the Ansatz

$$\Gamma_n(t) = e^{-i\gamma_n(t)} \quad (\text{E.73})$$

for the coefficients $\Gamma_n(t)$, we obtain in the adiabatic approximation

$$\hbar\partial_t \gamma_m \approx \dot{\vec{R}} \vec{A}_{m,m}(\vec{R}(t)) \quad (\text{E.74})$$

so that

$$\gamma_m(T) \approx \frac{1}{\hbar} \int_0^T dt \dot{\vec{R}} \vec{A}_{m,m}(\vec{R}(t)) \stackrel{\text{Eq. 2.29}}{=} \frac{1}{\hbar} \int_{\vec{R}(0)}^{\vec{R}(T)} d\vec{R} \vec{A}_{m,m}(\vec{R}) \quad (\text{E.75})$$

Note, that the factor \hbar cancels with the corresponding factor in the derivative couplings. Therefore, we can expect a finite limiting value for γ in the limit $\hbar \rightarrow 0$.

Independence of the choice of Born-Oppenheimer wave functions

While the derivative couplings depend on the phases used for the Born-Oppenheimer wave functions, it can be shown that the phase for a closed contour \mathcal{C} is independent of the phases. This is also the main result of Berry on the existence of a geometrical phase.

We use Stokes theorem to map the contour integral for a closed contour onto a surface integral over the area \mathcal{P} enclosed by the contour \mathcal{C} . In order to simplify the equations, I will limit the derivation to three dimensions.

$$\gamma_m(\mathcal{C}) = \frac{1}{\hbar} \oint_{\mathcal{C}} d\vec{R} \vec{A}_{m,m}(\vec{R}) = \frac{1}{\hbar} \int_{\mathcal{P}} d^2\vec{A} \vec{\nabla} \times \vec{A}_{m,m}(\vec{R}) \quad (\text{E.76})$$

The vector $d^2\vec{A}$ is the surface element and stands perpendicular to the surface. Please use caution because we use the same symbol A for the surface element $d\vec{A}$ and the derivative couplings $\vec{A}_{m,m}$.

The resulting equation reminds of the one for the magnetic flux through an area.

We can now rewrite the result

$$\begin{aligned}
\gamma_m(\mathcal{C}) &\stackrel{\text{def}}{=} \frac{1}{\hbar} \oint d\vec{R} \vec{A}_{m,m}(\vec{R}) \\
&\stackrel{\text{Eq. 2.29}}{=} \frac{1}{\hbar} \int_{\mathcal{P}} d^2\vec{A} \vec{\nabla}_R \times \left\langle \Psi_m^{BO}(\vec{R}) \left| \frac{\hbar}{i} \vec{\nabla}_R \right| \Psi_m^{BO}(\vec{R}) \right\rangle \\
&= \frac{1}{\hbar} \int_{\mathcal{P}} d^2\vec{A} \left\langle \vec{\nabla}_R \Psi_m^{BO}(\vec{R}) \left| \times \frac{\hbar}{i} \vec{\nabla}_R \right| \Psi_m^{BO}(\vec{R}) \right\rangle + \left\langle \vec{\nabla} \Psi_m^{BO}(\vec{R}) \left| \frac{\hbar}{i} \underbrace{\vec{\nabla}_R \times \vec{\nabla}_R}_{=0} \right| \Psi_m^{BO}(\vec{R}) \right\rangle \\
&= \frac{1}{\hbar} \int_{\mathcal{P}} d^2\vec{A} \sum_n \left\langle \vec{\nabla}_R \Psi_m^{BO}(\vec{R}) \left| \Psi_n^{BO}(\vec{R}) \right\rangle \times \left\langle \Psi_n^{BO}(\vec{R}) \left| \frac{\hbar}{i} \vec{\nabla}_R \right| \Psi_m^{BO}(\vec{R}) \right\rangle
\end{aligned} \tag{E.77}$$

We exploit that the Born-Oppenheimer wave functions are orthonormal, so that

$$\begin{aligned}
0 &= \vec{\nabla}_R \left\langle \Psi_n^{BO}(\vec{R}) \left| \Psi_m^{BO}(\vec{R}) \right\rangle \right. \\
&= \left\langle \vec{\nabla}_R \Psi_n^{BO}(\vec{R}) \left| \Psi_m^{BO}(\vec{R}) \right\rangle + \left\langle \Psi_n^{BO}(\vec{R}) \left| \vec{\nabla}_R \Psi_m^{BO}(\vec{R}) \right\rangle \right. \\
\left\langle \vec{\nabla}_R \Psi_n^{BO}(\vec{R}) \left| \Psi_m^{BO}(\vec{R}) \right\rangle &= - \left\langle \Psi_n^{BO}(\vec{R}) \left| \vec{\nabla}_R \Psi_m^{BO}(\vec{R}) \right\rangle
\end{aligned} \tag{E.78}$$

This yields

$$\gamma_m(\mathcal{C}) = \frac{-i}{\hbar^2} \int_{\mathcal{P}} d^2\vec{A} \sum_n \left\langle \Psi_m^{BO}(\vec{R}) \left| \frac{\hbar}{i} \vec{\nabla}_R \right| \Psi_n^{BO}(\vec{R}) \right\rangle \times \left\langle \Psi_n^{BO}(\vec{R}) \left| \frac{\hbar}{i} \vec{\nabla}_R \right| \Psi_m^{BO}(\vec{R}) \right\rangle \tag{E.79}$$

Because the vector product of two identical vectors vanishes, the term with $n = m$ vanishes. The other terms can be rewritten with the help of Eq. 2.31 (p. 53) in terms of expectation values of the gradient of the Born-Oppenheimer Hamiltonian.

$$\begin{aligned}
\gamma_m(\mathcal{C}) &= \frac{-i}{\hbar^2} \int_{\mathcal{P}} d^2\vec{A} \sum_{n;n \neq m} \frac{\left\langle \Psi_m^{BO}(\vec{R}) \left| \left(\frac{\hbar}{i} \vec{\nabla}_R \hat{H} \right) \right| \Psi_n^{BO}(\vec{R}) \right\rangle}{E_n^{BO}(\vec{R}) - E_m^{BO}(\vec{R})} \times \frac{\left\langle \Psi_n^{BO}(\vec{R}) \left| \left(\frac{\hbar}{i} \vec{\nabla}_R \hat{H} \right) \right| \Psi_m^{BO}(\vec{R}) \right\rangle}{E_m^{BO}(\vec{R}) - E_n^{BO}(\vec{R})} \\
&= \frac{+i}{\hbar^2} \int_{\mathcal{P}} d^2\vec{A} \sum_{n;n \neq m} \frac{\left\langle \Psi_m^{BO}(\vec{R}) \left| \left(\frac{\hbar}{i} \vec{\nabla}_R \hat{H} \right) \right| \Psi_n^{BO}(\vec{R}) \right\rangle \times \left\langle \Psi_n^{BO}(\vec{R}) \left| \left(\frac{\hbar}{i} \vec{\nabla}_R \hat{H} \right) \right| \Psi_m^{BO}(\vec{R}) \right\rangle}{\left(E_n^{BO}(\vec{R}) - E_m^{BO}(\vec{R}) \right)^2}
\end{aligned} \tag{E.80}$$

While the Born-Oppenheimer wave function have a phase that can be chosen arbitrary for each set of atomic coordinates, this phase factor drops out of the equation in the expression given above.

The phase is a real-valued quantity: taking the complex conjugate of the expression above is equivalent to exchanging the two terms in the numerator and an additional sign change. This interchange in a vector product changes the sign of the expression, which absorbs the sign change. Hence the expression is identical to its complex conjugate, and hence it is real-valued.

Berry introduced the object

$$\vec{V}_m(\vec{R}) = \frac{-i}{\hbar^2} \sum_{n;n \neq m} \frac{\left\langle \Psi_m^{BO}(\vec{R}) \left| \left(\frac{\hbar}{i} \vec{\nabla}_R \hat{H} \right) \right| \Psi_n^{BO}(\vec{R}) \right\rangle \times \left\langle \Psi_n^{BO}(\vec{R}) \left| \left(\frac{\hbar}{i} \vec{\nabla}_R \hat{H} \right) \right| \Psi_m^{BO}(\vec{R}) \right\rangle}{\left(E_n^{BO}(\vec{R}) - E_m^{BO}(\vec{R}) \right)^2} \tag{E.81}$$

which yields

$$\gamma_m(\mathcal{C}) = - \int_{\mathcal{P}} d^2\vec{A} \vec{V}_m(\vec{R}) \tag{E.82}$$

The object $\vec{V}_m(\vec{R})$ is analogous to a magnetic field. It is purely real-valued and independent of the phases chosen for the Born-Oppenheimer surfaces. Thus, it is a gauge invariant quantity.

E.6.3 Generalization to more than three dimensions

Editor: Do not read: unfinished!

Stokes theorem in 3 dimensions has the form

$$\oint_{\mathcal{C}} d\vec{R} \vec{Y}(\vec{R}) = \int_{\mathcal{P}} d^2\vec{A} \left(\vec{\nabla} \times \vec{Y}(\vec{R}) \right) \quad (\text{E.83})$$

The M -dimensional generalization of Stokes theorem has the form

$$\oint_{\mathcal{C}} d\vec{R} \vec{Y}(\vec{R}) = \sum_{j_1, j_2, \dots, j_M=1}^M \epsilon_{j_1, \dots, j_M} \int_{\mathcal{P}} d^2 a_{j_1, \dots, j_{M-2}} \left(\partial_{j_{M-1}} Y_{j_M}(\vec{R}) \right) \quad (\text{E.84})$$

where $\epsilon_{j_1, \dots, j_M}$ is the fully-antisymmetric tensor or Levi-Civita symbol in M dimensions.

E.6.4 Berry phase and polarization

Let me refer here to an excellent pedagogical introduction by N. A. Spaldin[123].

Editor: The following are some notes taken some time ago while going through the work of King-Smith and Vanderbilt[124]. I need to check, whether it adds important aspects to the ‘Beginner’s Guide’ by Spaldin[123].

Editor: The following is not proofread and is under construction

The change of polarization due to an infinitesimal electric field is

$$\frac{d\vec{P}}{d\lambda} = -i \frac{ifq\hbar}{N\Omega m_e} \sum_k \sum_{n \in \text{occ.}} \sum_{m \in \text{unocc.}} \frac{\langle \Psi_{k,n} | \hat{p} | \Psi_{k,m} \rangle \langle \Psi_{k,m} | \frac{dV}{d\lambda} | \Psi_{k,n} \rangle}{(\epsilon_{k,i} - \epsilon_{k,j})^2} + c.c.$$

The wave functions are represented as Bloch states

$$|\Psi_{k,n}\rangle = e^{i\vec{k}\vec{r}} |u_{k,n}\rangle$$

Correspondingly we define a k -dependent Hamiltonian.

$$\begin{aligned} \hat{p}_k &= e^{-ikr} \vec{p} e^{ikr} = \vec{p} + \hbar\vec{k} \\ \hat{H}_k &= e^{-ikr} \left[\frac{\vec{p}^2}{2m} + V \right] e^{ikr} = \frac{(\vec{p} + \hbar\vec{k})^2}{2m} + V = \frac{\vec{p}_k^2}{2m} + V \end{aligned}$$

We can express the momentum by the Hamiltonian as

$$[\vec{\nabla}_k, \hat{H}_k] = \frac{\hbar}{m} (\vec{p} + \hbar\vec{k}) = \frac{\hbar}{m} \vec{p}_k$$

Therefore,

$$\begin{aligned}
\langle \Psi_{k,n} | \hat{p} | \Psi_{k,m} \rangle &= \langle u_{k,n} | \hat{p}_k | u_{k,m} \rangle = \frac{m}{\hbar} \langle u_{k,n} | [\partial_k, \hat{H}_k] | u_{k,m} \rangle \\
&= \frac{m}{\hbar} [\langle u_{k,n} | \partial_k \hat{H}_k | u_{k,m} \rangle - \langle u_{k,n} | \hat{H}_k \partial_k | u_{k,m} \rangle] \\
&= \frac{m}{\hbar} [\langle u_{k,n} | \partial_k | u_{k,m} \rangle \epsilon_{k,m} - \langle u_{k,n} | \partial_k | u_{k,m} \rangle \epsilon_{k,n}] \\
&= \frac{m}{\hbar} \langle u_{k,n} | \partial_k | u_{k,m} \rangle (\epsilon_{k,m} - \epsilon_{k,n}) \\
&= \frac{m}{\hbar} (\epsilon_{k,m} - \epsilon_{k,n}) \left[\underbrace{(\partial_k \langle u_{k,n} | u_{k,m} \rangle)}_{=0} - \langle \partial_k u_{k,n} | u_{k,m} \rangle \right] \\
&= -\frac{m}{\hbar} (\epsilon_{k,m} - \epsilon_{k,n}) \langle \partial_k u_{k,n} | u_{k,m} \rangle
\end{aligned}$$

Now, we rewrite the second term as

$$\begin{aligned}
\langle \Psi_{k,m} | \frac{dV}{d\lambda} | \Psi_{k,n} \rangle &= \langle u_{k,m} | [\partial_\lambda, \hat{H}] | u_{k,n} \rangle \\
&= \langle u_{k,m} | \partial_\lambda \hat{H} | u_{k,n} \rangle - \langle u_{k,m} | \hat{H} \partial_\lambda | u_{k,n} \rangle \\
&= (\epsilon_{k,n} - \epsilon_{k,m}) \langle u_{k,m} | \partial_\lambda u_{k,n} \rangle
\end{aligned}$$

$$\begin{aligned}
\frac{d\vec{P}}{d\lambda} &= -i \frac{ifq}{N\Omega} \sum_k \sum_{n \in occ} \sum_{m \in unocc} \langle \partial_k u_{k,n} | u_{k,m} \rangle \langle u_{k,m} | \partial_\lambda u_{k,n} \rangle + c.c. \\
&= -i \frac{ifq}{N\Omega} \sum_k \sum_{n \in occ} \sum_{m=1}^{\infty} \langle \partial_k u_{k,n} | u_{k,m} \rangle \langle u_{k,m} | \partial_\lambda u_{k,n} \rangle + c.c. \\
&\quad + i \frac{ifq}{N\Omega} \sum_k \sum_{n \in occ} \sum_{m \in occ} \langle \partial_k u_{k,n} | u_{k,m} \rangle \langle u_{k,m} | \partial_\lambda u_{k,n} \rangle + c.c. \\
&= -i \frac{ifq}{N\Omega} \sum_k \sum_{n \in occ} [\langle \partial_k u_{k,n} \partial_\lambda u_{k,n} \rangle - \langle \partial_k u_{k,n} \partial_\lambda u_{k,n} \rangle^*] \\
&\quad + i \frac{ifq}{N\Omega} \sum_k \sum_{n \in occ} \sum_{m \in occ} [\langle \partial_k u_{k,n} | u_{k,m} \rangle \langle u_{k,m} | \partial_\lambda u_{k,n} \rangle - \langle u_{k,m} | \partial_k u_{k,n} \rangle \langle \partial_\lambda u_{k,n} | u_{k,m} \rangle]
\end{aligned}$$

Now, we use

$$\begin{aligned}
\langle \partial_k u_{k,n} | u_{k,m} \rangle &= \underbrace{\partial_k \langle u_{k,n} | u_{k,m} \rangle}_{=0} - \langle u_{k,n} | \partial_k u_{k,m} \rangle \\
\langle \partial_\lambda u_{k,n} | u_{k,m} \rangle &= \underbrace{\partial_\lambda \langle u_{k,n} | u_{k,m} \rangle}_{=0} - \langle u_{k,n} | \partial_\lambda u_{k,m} \rangle
\end{aligned}$$

in order to get rid of the second term

$$\begin{aligned}
&+ i \frac{ifq}{N\Omega} \sum_k \sum_{n \in occ} \sum_{m \in occ} [\langle \partial_k u_{k,n} | u_{k,m} \rangle \langle u_{k,m} | \partial_\lambda u_{k,n} \rangle - \langle u_{k,m} | \partial_k u_{k,n} \rangle \langle \partial_\lambda u_{k,n} | u_{k,m} \rangle] \\
&+ i \frac{ifq}{N\Omega} \sum_k \sum_{n \in occ} \sum_{m \in occ} [-\langle u_{k,n} | \partial_k u_{k,m} \rangle \langle u_{k,m} | \partial_\lambda u_{k,n} \rangle + \langle u_{k,m} | \partial_k u_{k,n} \rangle \langle u_{k,n} | \partial_\lambda u_{k,m} \rangle] \\
&= 0
\end{aligned}$$

The sum over k-points can be transformed into a Brillouin zone integral

$$\int d^3k = \frac{(2\pi)^3}{N\Omega_0} \sum_k$$

Thus, we obtain the result for a finite polarization as

$$\begin{aligned}
 \Delta \vec{P} &= \int_0^1 d\lambda \frac{d\vec{P}}{d\lambda} \\
 &= -i \frac{ifq}{N\Omega} \sum_k \int_0^1 d\lambda \sum_{n \in occ.} [\langle \partial_k u_{k,n} | \partial_\lambda u_{k,n} \rangle - \langle \partial_k u_{k,n} | \partial_\lambda u_{k,n} \rangle^*] \\
 &= -i \frac{ifq}{(2\pi)^3} \int d^3k \int_0^1 d\lambda \sum_{n \in occ.} [\langle \partial_k u_{k,n} | \partial_\lambda u_{k,n} \rangle - \langle \partial_\lambda u_{k,n} | \partial_k u_{k,n} \rangle]
 \end{aligned}$$

Now, we can express the term as rotation of a vector field in the k_j, λ plane.

$$\begin{aligned}
 &\langle \partial_k u_{k,n} | \partial_\lambda u_{k,n} \rangle - \langle \partial_\lambda u_{k,n} | \partial_k u_{k,n} \rangle \\
 &= \partial_k \langle u_{k,n} | \partial_\lambda u_{k,n} \rangle - \langle u_{k,n} | \partial_k \partial_\lambda u_{k,n} \rangle - \partial_\lambda \langle u_{k,n} | \partial_k u_{k,n} \rangle + \langle u_{k,n} | \partial_\lambda \partial_k u_{k,n} \rangle \\
 &= \partial_k \langle u_{k,n} | \partial_\lambda u_{k,n} \rangle - \partial_\lambda \langle u_{k,n} | \partial_k u_{k,n} \rangle \\
 &= \partial_k A_\lambda - \partial_\lambda A_k
 \end{aligned}$$

with $\vec{A} = \begin{pmatrix} \langle u_{k,n} | \partial_k u_{k,n} \rangle \\ \langle u_{k,n} | \partial_\lambda u_{k,n} \rangle \end{pmatrix}$

E.7 Exact factorization

Editor: Do not read!

This is an attempt to understand the ‘‘Exact Factorization’’ approach by Abedi et al. [125, 126]. The goal of this approach is to rewrite the time electronic-nuclear wave function with a single-valued nuclear wave function. The electronic wave function is time dependent and normalized for each set of nuclear positions and time.

We use mass-weighted coordinates.

One starts with an Ansatz for the electronic-nuclear wave function as a single product.

$$\Psi(\vec{x}, \vec{R}, t) = \Phi^e(\vec{x}, \vec{R}, t) \chi(\vec{R}, t) \tag{E.85}$$

We insert the time-dependent Schrödinger equation.

$$i\hbar \partial_t \Psi(\vec{x}, \vec{R}, t) = \left(\frac{1}{2} \vec{P}^2 + \hat{H}^{BO} \right) \Psi(\vec{x}, \vec{R}, t) \tag{E.86}$$

and obtain one equation for the nuclear wave function and one for the electronic wave function.

Differential equation for the nuclear wave function

We insert the Ansatz Eq. E.85 into the Schrödinger equation Eq. E.86, multiply from the left with $\langle \Phi^e |$ and divide by the norm $\langle \Phi^e | \Phi^e \rangle$.

$$\begin{aligned}
i\hbar\partial_t\chi &= -\chi \frac{\langle \Phi^e | i\hbar\partial_t | \Phi^e \rangle}{\langle \Phi^e | \Phi^e \rangle} + \frac{1}{2} \hat{P}^2 \chi + \frac{\langle \Phi^e | \hat{P} | \Phi^e \rangle}{\langle \Phi^e | \Phi^e \rangle} \hat{P} \chi + \chi \frac{\langle \Phi^e | \frac{1}{2} \hat{P}^2 + \hat{H}^{BO} | \Phi^e \rangle}{\langle \Phi^e | \Phi^e \rangle} \\
&= \frac{1}{2} \hat{P}^2 \chi + \frac{\langle \Phi^e | \hat{P} | \Phi^e \rangle}{\langle \Phi^e | \Phi^e \rangle} \hat{P} \chi + \chi \frac{\langle \Phi^e | -i\hbar\partial_t + \frac{1}{2} \hat{P}^2 + \hat{H}^{BO} | \Phi^e \rangle}{\langle \Phi^e | \Phi^e \rangle} \\
&= \left[\frac{1}{2} \left(\hat{P} + \frac{\langle \Phi^e | \hat{P} | \Phi^e \rangle}{\langle \Phi^e | \Phi^e \rangle} \right)^2 + E \right] \chi \\
&\quad + \chi \frac{\langle \Phi^e | -i\hbar\partial_t + \frac{1}{2} \hat{P}^2 + \hat{H}^{BO} - E | \Phi^e \rangle}{\langle \Phi^e | \Phi^e \rangle} - \chi \frac{1}{2} \left(\frac{\langle \Phi^e | \hat{P} | \Phi^e \rangle}{\langle \Phi^e | \Phi^e \rangle} \right)^2 - \chi \frac{1}{2} \left(\frac{\hat{P} \langle \Phi^e | \hat{P} | \Phi^e \rangle}{\langle \Phi^e | \Phi^e \rangle} \right) \\
&= \left[\frac{1}{2} \left(\hat{P} + \frac{\langle \Phi^e | \hat{P} | \Phi^e \rangle}{\langle \Phi^e | \Phi^e \rangle} \right)^2 + E \right] \chi \\
&\quad + \chi \left\{ \frac{\langle \Phi^e | -i\hbar\partial_t + \frac{1}{2} \hat{P}^2 + \hat{H}^{BO} - E | \Phi^e \rangle}{\langle \Phi^e | \Phi^e \rangle} - \frac{1}{2} \left(\frac{\langle \Phi^e | \hat{P} | \Phi^e \rangle}{\langle \Phi^e | \Phi^e \rangle} \right)^2 \right. \\
&\quad \left. - \frac{1}{2} \left[-\frac{\langle \hat{P} \Phi^e | \hat{P} \Phi^e \rangle}{\langle \Phi^e | \Phi^e \rangle} + \frac{\langle \Phi^e | \hat{P}^2 | \Phi^e \rangle}{\langle \Phi^e | \Phi^e \rangle} - \left(\frac{\langle \Phi^e | \hat{P} | \Phi^e \rangle}{\langle \Phi^e | \Phi^e \rangle} \right)^2 + \frac{\langle \Phi^e | \hat{P} | \Phi^e \rangle \langle \hat{P} \Phi^e | \Phi^e \rangle}{\langle \Phi^e | \Phi^e \rangle^2} \right] \right\} \\
&= \left[\frac{1}{2} \left(\hat{P} + \frac{\langle \Phi^e | \hat{P} | \Phi^e \rangle}{\langle \Phi^e | \Phi^e \rangle} \right)^2 + E \right] \chi \\
&\quad + \chi \left\{ \frac{\langle \Phi^e | -i\hbar\partial_t + \hat{H}^{BO} - E | \Phi^e \rangle}{\langle \Phi^e | \Phi^e \rangle} + \frac{1}{2} \frac{\langle \hat{P} \Phi^e | \hat{P} \Phi^e \rangle}{\langle \Phi^e | \Phi^e \rangle} - \frac{1}{2} \left| \frac{\langle \Phi^e | \hat{P} | \Phi^e \rangle}{\langle \Phi^e | \Phi^e \rangle} \right|^2 \right\} \quad (E.87)
\end{aligned}$$

We define $E(\vec{R}, t)$ so that the second line vanishes. This defined E as¹²

$$E(\vec{R}, t) \stackrel{\text{def}}{=} \frac{\langle \Phi^e | -i\hbar\partial_t + \hat{H}^{BO} | \Phi^e \rangle}{\langle \Phi^e | \Phi^e \rangle} + \frac{1}{2} \frac{\langle \hat{P} \Phi^e | \hat{P} \Phi^e \rangle}{\langle \Phi^e | \Phi^e \rangle} - \frac{1}{2} \left| \frac{\langle \Phi^e | \hat{P} | \Phi^e \rangle}{\langle \Phi^e | \Phi^e \rangle} \right|^2 \quad (E.88)$$

with¹³

$$\vec{A}(\vec{R}, t) \stackrel{\text{def}}{=} \frac{\langle \Phi^e | \hat{P} | \Phi^e \rangle}{\langle \Phi^e | \Phi^e \rangle} \quad (E.89)$$

Then the nuclear Schrödinger equation Eq. E.87 is¹⁴

$$i\hbar\partial_t\chi \stackrel{\text{Eq. E.87}}{=} \left[\frac{1}{2} \left(\hat{P} + \vec{A} \right)^2 + E \right] \chi \quad (E.90)$$

¹²Compare this with Eq. 64 of Abedi[126].

¹³Compare this with Eq. 33 of Abedi[126].

¹⁴compare with Eq. 43 of Abedi[126].

Differential equation for the electronic wave function

We insert the Ansatz Eq. E.85 into the Schrödinger equation Eq. E.86, and divide by the nuclear waver function $\chi(\vec{R}, t)$.

$$\begin{aligned}
 i\hbar\partial_t|\Phi^e\rangle &= |\phi^e\rangle \left[\frac{-i\hbar\partial_t\chi}{\chi} + \frac{1}{2} \frac{\hat{P}^2\chi}{\chi} \right] + \left(\frac{\hat{P}\chi}{\chi} \right) \hat{P}|\phi^e\rangle + \frac{1}{2} \hat{P}^2|\phi^e\rangle + \hat{H}^{BO}|\phi^e\rangle \\
 &\stackrel{\text{Eq. E.90}}{=} |\phi^e\rangle \left[-\frac{1}{2\chi} (\hat{P} + \vec{A})^2 \chi - E + \frac{1}{2} \frac{\hat{P}^2\chi}{\chi} \right] + \left(\frac{\hat{P}\chi}{\chi} \right) \hat{P}|\phi^e\rangle + \frac{1}{2} \hat{P}^2|\phi^e\rangle + \hat{H}^{BO}|\phi^e\rangle \\
 &= |\phi^e\rangle \left[-\frac{1}{2} (\hat{P}\vec{A}) - \vec{A} \frac{\hat{P}\chi}{\chi} - \frac{1}{2} \vec{A}^2 \right] + \left(\frac{\hat{P}\chi}{\chi} \right) \hat{P}|\phi^e\rangle + \frac{1}{2} \hat{P}^2|\phi^e\rangle + (\hat{H}^{BO} - E)|\phi^e\rangle \\
 &= |\phi^e\rangle \left[\underbrace{-\frac{1}{2} (\hat{P}\vec{A})}_{(-B)} - \vec{A} \frac{\hat{P}\chi}{\chi} - \underbrace{\frac{1}{2} \vec{A}^2}_{(A)} \right] + \left(\frac{\hat{P}\chi}{\chi} \right) \hat{P}|\phi^e\rangle \\
 &\quad + \frac{1}{2} (\hat{P} - \vec{A})^2|\phi^e\rangle + \underbrace{\frac{1}{2} (\hat{P}\vec{A})}_{(B)}|\phi^e\rangle + \vec{A} \hat{P}|\phi^e\rangle - \underbrace{\frac{1}{2} \vec{A}^2}_{(A)}|\phi^e\rangle + (\hat{H}^{BO} - E)|\phi^e\rangle \\
 &= |\phi^e\rangle \left[-\left(\frac{\hat{P}\chi}{\chi} + \vec{A} \right) \vec{A}|\phi^e\rangle \right] + \left(\frac{\hat{P}\chi}{\chi} + \vec{A} \right) \hat{P}|\phi^e\rangle + \frac{1}{2} (\hat{P} - \vec{A})^2|\phi^e\rangle + (\hat{H}^{BO} - E)|\phi^e\rangle \\
 &= \left(\frac{\hat{P}\chi}{\chi} + \vec{A} \right) (\hat{P} - \vec{A})|\phi^e\rangle + \frac{1}{2} (\hat{P} - \vec{A})^2|\phi^e\rangle + (\hat{H}^{BO} - E)|\phi^e\rangle \tag{E.91}
 \end{aligned}$$

For the first line, see Eq. 39 of Abedi[126]. For the last line see Eq. 42 of Abedi[126].

Abedi introduces the electron-nuclear coupling potential

$$\hat{U}_{en} \stackrel{\text{def}}{=} \left(\frac{\hat{P}\chi}{\chi} + \vec{A} \right) (\hat{P} - \vec{A}) + \frac{1}{2} (\hat{P} - \vec{A})^2 \tag{E.92}$$

and the electronic Hamiltonian

$$H_{el} \stackrel{\text{def}}{=} \hat{U}_{en} + \hat{H}^{BO} \tag{E.93}$$

so that the electronic Schrödinger equation Eq. E.91 obtains the form

$$i\hbar\partial_t|\Phi^e\rangle \stackrel{\text{Eq. E.91}}{=} (\hat{H}_{el} - E)|\Phi^e\rangle \tag{E.94}$$

Let me work out the expectation value of the electron nuclear coupling potential

$$\begin{aligned}
\langle \Phi^e | \hat{U}_{en} | \Phi^e \rangle &= \langle \Phi^e | \left(\frac{\hat{P}\chi}{\chi} + \vec{A} \right) (\hat{P} - \vec{A}) + \frac{1}{2} (\hat{P} - \vec{A})^2 | \Phi^e \rangle \\
&= \left(\frac{\hat{P}\chi}{\chi} + \vec{A} \right) \underbrace{\langle \Phi^e | (\hat{P} - \vec{A}) | \Phi^e \rangle}_{=0} + \frac{1}{2} \langle \Phi^e | \hat{P}^2 | \Phi^e \rangle - \frac{1}{2} \langle \Phi^e | \Phi^e \rangle (\hat{P}\vec{A}) - \vec{A} \langle \Phi^e | \hat{P} | \Phi^e \rangle + \frac{1}{2} \vec{A}^2 \langle \Phi^e | \Phi^e \rangle \\
&= \frac{1}{2} \langle \Phi^e | \hat{P}^2 | \Phi^e \rangle - \frac{1}{2} \langle \Phi^e | \Phi^e \rangle (\hat{P}\vec{A}) - \frac{1}{2} \vec{A}^2 \langle \Phi^e | \Phi^e \rangle \\
&= \frac{1}{2} \hat{P} \langle \Phi^e | \hat{P} | \Phi^e \rangle + \frac{1}{2} \langle (\hat{P}\Phi^e) | (\hat{P}\Phi^e) \rangle - \frac{1}{2} \langle \Phi^e | \Phi^e \rangle (\hat{P}\vec{A}) - \frac{1}{2} \vec{A}^2 \langle \Phi^e | \Phi^e \rangle \\
&= \frac{1}{2} \hat{P} (\langle \Phi^e | \Phi^e \rangle \vec{A}) + \frac{1}{2} \langle (\hat{P}\Phi^e) | (\hat{P}\Phi^e) \rangle - \frac{1}{2} \langle \Phi^e | \Phi^e \rangle (\hat{P}\vec{A}) - \frac{1}{2} \vec{A}^2 \langle \Phi^e | \Phi^e \rangle \\
&= \frac{1}{2} \vec{A} \hat{P} \langle \Phi^e | \Phi^e \rangle + \frac{1}{2} \langle (\hat{P}\Phi^e) | (\hat{P}\Phi^e) \rangle - \frac{1}{2} \vec{A}^2 \langle \Phi^e | \Phi^e \rangle \\
&= -\frac{1}{2} \vec{A} \langle (\hat{P}\Phi^e) | \Phi^e \rangle + \frac{1}{2} \vec{A} \langle \Phi^e | \hat{P} | \Phi^e \rangle + \frac{1}{2} \langle (\hat{P}\Phi^e) | (\hat{P}\Phi^e) \rangle - \frac{1}{2} \vec{A}^2 \langle \Phi^e | \Phi^e \rangle \\
&= -\frac{1}{2} |\vec{A}|^2 \langle \Phi^e | \Phi^e \rangle + \frac{1}{2} \langle (\hat{P}\Phi^e) | (\hat{P}\Phi^e) \rangle \\
\frac{\langle \Phi^e | \hat{U}_{en} | \Phi^e \rangle}{\langle \Phi^e | \Phi^e \rangle} &= -\frac{1}{2} |\vec{A}|^2 + \frac{1}{2} \frac{\langle (\hat{P}\Phi^e) | (\hat{P}\Phi^e) \rangle}{\langle \Phi^e | \Phi^e \rangle} \tag{E.95}
\end{aligned}$$

Inserting this result in Eq. E.88, I obtain the energy as

$$E(\vec{R}, t) \stackrel{\text{Eq. E.88}}{=} \frac{\langle \Phi^e | -i\hbar\partial_t + \hat{H}_{el} | \Phi^e \rangle}{\langle \Phi^e | \Phi^e \rangle} \tag{E.96}$$

Flow chart

We obtained two coupled differential equations. We need to show that this is a closed set of equations, which uniquely determines the time evolution.

1. Given a set of $\chi(\vec{R}, t = 0)$ and $|\Phi^e(\vec{R}, t)\rangle$, for all configurations (impossible, but still...),
2. calculate \vec{A} from Eq. E.89.
3. calculate \hat{U}_{en} from Eq. E.92.
4. calculate $\hat{H}_{el} = \hat{H}^{BO} + \hat{U}_{en}$ from Eq. E.93.
5. propagate $|\Phi^e\rangle$ with Eq. E.94. Adjust the energy $E(\vec{R}, t)$ so that the norm of the wave function remains constant. Eq. E.96 is then automatically satisfied.
6. iterate the nuclear Schrödinger equation Eq. E.90.
7. The electronic and nuclear wave functions are now available for the next time step. Proceed to the top of the list and iterate the next step.

Appendix F

Landau-Zener formula

F.1 Landau-Zener formula

The transition between two adiabatic total-energy surfaces has been analyzed by Landau and Zener¹ [19, 127, 20]. for a one-dimensional model. Here, we follow the analysis of Wittig[20].

Editor: See also Vutha[128]

The model of Landau and Zener describes a system with one nuclear coordinate Q and two electronic states $\{|\chi_1\rangle, |\chi_2\rangle\}$. The electronic Hamiltonian

$$\hat{H}^{BO}(Q) = \begin{pmatrix} |\chi_1\rangle \\ |\chi_2\rangle \end{pmatrix} \begin{pmatrix} -F_1Q & H_{12} \\ H_{12}^* & -F_2Q \end{pmatrix} \begin{pmatrix} \langle\chi_1| \\ \langle\chi_2| \end{pmatrix} \quad (\text{F.1})$$

exhibits an avoided crossing at $X = 0$ with a minimum level splitting² $2|H_{12}|$. The symbols $F_{1/2}$ describe a force $F_j = -\frac{\partial H(\vec{p}, \vec{r})}{\partial r_j}$ acting on the generalized nuclear coordinate Q . It describes the negative slopes of the energy surfaces away from the avoided crossing.

The Born-Oppenheimer Hamiltonian is specified in a basisset $\{|\chi_1\rangle, |\chi_2\rangle\}$ for the electronic Hilbert space, which does not depend on the nuclear positions. Such a basisset is called a trivial **diabatic** basisset.³ Note that the approach used here differs from that in section E.1.2.

The assumption of the Landau-Zener model are

1. the nuclei are classical particles.
2. the electrons follow the nuclei according to Ehrenfest dynamics.
3. the nuclear trajectory has a constant velocity V .
4. the transition probability is sufficiently small that multiple transitions can be ignored.

The atoms are moving with a constant velocity, i.e. $\partial_t Q(t) = V$, that is $Q(t) = Vt$. This turns the position-dependent Hamiltonian into an effectively time-dependent Hamiltonian.

$$\hat{H}(t) = \hat{H}^{BO}(Q(t)) = \begin{pmatrix} |\chi_1\rangle \\ |\chi_2\rangle \end{pmatrix} \begin{pmatrix} -F_1Vt & H_{12} \\ H_{12}^* & -F_2Vt \end{pmatrix} \begin{pmatrix} \langle\chi_1| \\ \langle\chi_2| \end{pmatrix} \quad (\text{F.2})$$

¹According to Wittig[20] the result of Landau[127] has an error of 2π

²I avoid the symbol t for the hopping matrix element to avoid confusion with the symbol for time.

³A diabatic basisset is one for which the derivative couplings vanish. The derivative couplings vanish for any position independent basisset, which is called a trivial diabatic basisset. A trivial diabatic basisset does not adapt to the atomic structure, which makes it inefficient. An exact non-trivial diabatic basisset does not exist for the general case as discussed in appendix B.3.

The time-dependent electronic wave function is described by the following Ansatz

$$|\Psi_e(t)\rangle = \sum_{j \in \{1,2\}} |\chi_j\rangle e^{-\frac{i}{\hbar} \int dt H_{jj}^{BO}(Q(t))} \Gamma_j(t) \quad (\text{F.3})$$

with

$$\begin{pmatrix} \Gamma_1(t) e^{-\frac{i}{\hbar} \int dt H_{1,1}^{BO}(Q(t))} \\ \Gamma_2(t) e^{-\frac{i}{\hbar} \int dt H_{2,2}^{BO}(Q(t))} \end{pmatrix} = \begin{pmatrix} \Gamma_1(t) e^{+\frac{i}{\hbar} \int dt F_1 V t} \\ \Gamma_2(t) e^{+\frac{i}{\hbar} \int dt F_2 V t} \end{pmatrix} = \begin{pmatrix} \Gamma_1(t) e^{+\frac{i}{\hbar} \frac{F_1 V}{2} t^2} \\ \Gamma_2(t) e^{+\frac{i}{\hbar} \frac{F_2 V}{2} t^2} \end{pmatrix} \quad (\text{F.4})$$

The lower bound of the time integral has been absorbed in the initial conditions.

Insertion into the time-dependent Schrödinger equation yield

$$\begin{aligned} i\hbar \partial_t |\Psi_e(t)\rangle &= \hat{H}^{BO}(Q(t)) |\Psi_e(t)\rangle \\ \stackrel{\text{Eq. F.3}}{\Rightarrow} i\hbar \partial_t \begin{pmatrix} \Gamma_1(t) e^{iF_1 V t^2 / (2\hbar)} \\ \Gamma_2(t) e^{iF_2 V t^2 / (2\hbar)} \end{pmatrix} &= \begin{pmatrix} -F_1 V t & H_{12} \\ H_{12}^* & -F_2 V t \end{pmatrix} \begin{pmatrix} \Gamma_1(t) e^{iF_1 V t^2 / (2\hbar)} \\ \Gamma_2(t) e^{iF_2 V t^2 / (2\hbar)} \end{pmatrix} \\ &\Rightarrow \begin{pmatrix} \partial_t \Gamma_1(t) \\ \partial_t \Gamma_2(t) \end{pmatrix} = \begin{pmatrix} -\frac{i}{\hbar} H_{12} \Gamma_2(t) e^{i(F_2 - F_1) V t^2 / (2\hbar)} \\ -\frac{i}{\hbar} H_{12}^* \Gamma_1(t) e^{-i(F_2 - F_1) V t^2 / (2\hbar)} \end{pmatrix} \quad (\text{F.5}) \end{aligned}$$

thus

$$\begin{aligned} \partial_t \Gamma_1(t) &= -\frac{i}{\hbar} H_{12} \Gamma_2(t) e^{i(F_2 - F_1) V t^2 / (2\hbar)} \\ \partial_t \Gamma_2(t) &= -\frac{i}{\hbar} H_{12}^* \Gamma_1(t) e^{-i(F_2 - F_1) V t^2 / (2\hbar)} \quad \Rightarrow \quad \Gamma_1(t) = -\frac{\hbar}{i} \underbrace{\frac{H_{12}}{|H_{12}|^2}}_{1/H_{12}^*} e^{i(F_2 - F_1) V t^2 / (2\hbar)} \partial_t \Gamma_2(t) \end{aligned} \quad (\text{F.6})$$

Insertion of the second equation into the first yields a differential equation for $\Gamma_2(t)$.

$$\begin{aligned} \partial_t \left(\underbrace{-\frac{\hbar}{i} \frac{H_{12}}{|H_{12}|^2} e^{i(F_2 - F_1) V t^2 / (2\hbar)} \partial_t \Gamma_2(t)}_{\Gamma_1(t)} \right) &= -\frac{i}{\hbar} H_{12} \Gamma_2(t) e^{i(F_2 - F_1) V t^2 / (2\hbar)} \\ \Rightarrow -\frac{H_{12}}{|H_{12}|^2} (F_2 - F_1) V t e^{i(F_2 - F_1) V t^2 / (2\hbar)} \partial_t \Gamma_2(t) + \\ &+ \left(-\frac{\hbar}{i} \frac{H_{12}}{|H_{12}|^2} e^{i(F_2 - F_1) V t^2 / (2\hbar)} \partial_t^2 \Gamma_2(t) \right) = -\frac{i}{\hbar} H_{12} \Gamma_2(t) e^{i \frac{(F_2 - F_1) V}{2\hbar} t^2} \\ \Rightarrow -\frac{1}{|H_{12}|^2} (F_2 - F_1) V t \partial_t \Gamma_2(t) + \left(-\frac{\hbar}{i} \frac{1}{|H_{12}|^2} \partial_t^2 \Gamma_2(t) \right) &= -\frac{i}{\hbar} \Gamma_2(t) \\ \Rightarrow \frac{i}{\hbar} (F_2 - F_1) V t \partial_t \Gamma_2(t) + \partial_t^2 \Gamma_2(t) &= -\frac{1}{\hbar^2} |H_{12}|^2 \Gamma_2(t) \\ \Rightarrow \partial_t^2 \Gamma_2(t) + \frac{i}{\hbar} (F_2 - F_1) V t \partial_t \Gamma_2(t) + \frac{1}{\hbar^2} |H_{12}|^2 \Gamma_2(t) &= 0 \quad (\text{F.7}) \end{aligned}$$

Thus, we have a differential equation for the probability amplitude $\Gamma_2(t)$ on the second energy sheet $-F_2 Q$.

The initial conditions are chosen so that we describe a transition from the upper energy sheet (on the left side) to the lower one (on the right side) as the atom passes the avoided crossing from left to right. Thus, we look for the probability for the system to stay on the second energy sheet $-F_2 Q$. The corresponding initial conditions are (for $V > 0$)

$$Q(-\infty) = -\infty \quad \text{and} \quad \Gamma_1(-\infty) = 0 \quad \text{and} \quad \Gamma_2(-\infty) = 1 \quad (\text{F.8})$$

The transition probability is then $|\Gamma_2(+\infty)|^2$

The differential equation for $\Gamma_2(t) = x(t)$ is of the form

$$\ddot{x} + i\alpha t \dot{x} + \beta x = 0 \tag{F.9}$$

with $\alpha \stackrel{\text{def}}{=} \frac{(F_2 - F_1)V}{\hbar}$ and $\beta \stackrel{\text{def}}{=} \frac{|H_{12}|^2}{\hbar^2}$.

So far, the derivation is standard. Wittig[20] showed a solution to the problem using contour integrals.

$$\begin{aligned} \frac{1}{t} \frac{\ddot{x}}{x} + i\alpha \frac{\dot{x}}{x} + \frac{\beta}{t} &= 0 \\ i\alpha \int_{t_i}^{t_f} dt \partial_t \ln[x(t)] &= -\beta \int_{t_i}^{t_f} dt \frac{1}{t} - \int_{t_i}^{t_f} dt \frac{1}{t} \frac{\ddot{x}}{x} \\ i\alpha \ln\left(\frac{x_f}{x_i}\right) &= -\beta \int_{-\infty}^{\infty} dt \frac{1}{t} - \int_{-\infty}^{\infty} dt \frac{1}{t} \frac{\ddot{x}}{x} \end{aligned} \tag{F.10}$$

The integral of the first term on the right-hand side yields[20]

$$\int_{-\infty}^{\infty} dt \frac{1}{t} = \pm i\pi \tag{F.11}$$

depending on whether the integration is performed in the upper or lower half of the complex plane.

Thus, we obtain

$$\begin{aligned} \ln[x_f] &= \ln[x_i] \mp \pi \frac{\beta}{\alpha} + \frac{i}{\alpha} \int_{-\infty}^{\infty} dt \frac{1}{t} \frac{\ddot{x}}{x} \\ x_f &= x_i e^{\mp \pi \beta / \alpha} \exp\left(\frac{i}{\alpha} \int_{-\infty}^{\infty} dt \frac{1}{t} \frac{\ddot{x}}{x}\right) \end{aligned} \tag{F.12}$$

If the transition probability at the avoided crossing is large, that is $x_f - x_i \approx 1$, we can ignore the last term and obtain the estimate

$$x_f \approx x_i e^{\mp \pi \beta / \alpha} \tag{F.13}$$

When we insert the parameters $\alpha = \frac{(F_2 - F_1)V}{\hbar}$ and $\beta = \frac{|H_{12}|^2}{\hbar^2}$, we obtain the Landau-Zener estimate for the transition probability $P = \left|\frac{x_f}{x_i}\right|^2$.

LANDAU-ZENER FORMULA

The transition probability between two Born-Oppenheimer surfaces is given by the **Landau-Zener formula**(Eq. 16 of Wittig)

$$P = \exp\left(-2\pi \underbrace{\frac{|H_{12}|}{\hbar}}_{\text{Rabi frequency } \omega_{12}} \underbrace{\frac{|H_{12}|}{V|F_1 - F_2|}}_{\tau}\right) \tag{F.14}$$

where V is the velocity and H_{12} is the coupling between the two crossing total-energy surfaces. ω_{12} is the **Rabi frequency** at the crossing point and τ is a measure for the duration of the interaction between the surfaces.

F.1.1 Relation to the Landau-Zener formula

Let me do a sanity check and compare the Landau-Zener formula Eq. F.14 with the expressions in the literature.[Editor: This needs more work](#)

The level splitting at the avoided crossing of the Born-Oppenheimer surfaces along a given trajectory is $2t = 2gZ_0$. Thus, we can identify the Rabi frequency as $\hbar\omega_{Rabi} = gZ_0$. The transition time is $\tau = \frac{t}{2gV} = \frac{Z_0}{V}$.

Thus, we obtain $\omega_{Rabi}\tau = \frac{gZ_0^2}{\hbar V}$. The Landau Zener formula gives an exponential law

$$P = \exp(-2\pi\omega_{Rabi}\tau) \quad (F.15)$$

Zener's transition probability[19] is

$$P = 1 - \exp\left(\frac{|H_{1,2}|^2}{\partial_t(H_{11} - H_{22})}\right) = 1 - \exp\left(-2\pi\frac{gZ_0^2}{2\hbar V}\right) \quad (F.16)$$

Question: The difference between my result and that of the Landau-Zener approach may also be that they describe the transition probability in the original, diabatic basis, which does not depend on the position, while we chose the adiabatic basis. In the original basis, the coefficients would see a time-dependent Hamiltonian

$$H(R(t)) = g \begin{pmatrix} Vt & X_0 \\ X_0 & Vt \end{pmatrix} \quad (F.17)$$

for a path $\vec{R} = (X_0, Vt)$.

F.2 Size of a conical intersection

In order to understand relaxation processes, it is vital to understand the transition through a conical intersection. Unfortunately, a full treatment of the dynamics next to a conical intersection is very complicated. Therefore, we try to arrive here at a reasonable approximate expression for the transition probability between two Born-Oppenheimer surfaces, as a system passes by a conical intersection. We will see that the conical interaction can be described by a cross section, which is proportional to the velocity of the nuclear coordinates.

I study a system, which passes by a conical intersection and thus undergoes, with a certain probability, an electronic transition from one Born-Oppenheimer surface to another one.

In order to simplify the problem we make a set of assumptions:

- we consider a spherical conical intersection
- nuclei are treated as classical particles
- nuclei move on a straight line with constant velocity.
- the electronic wave functions obey the time-dependent Schrödinger equation.

This is the approach taken in the original paper by Edward Teller[129] in 1937.

The conical intersection is described by the electron-nuclear Schrödinger equation Eq. H.10, keeping only the linear terms in the nuclear coordinates,

$$i\hbar\partial_t|\Psi(t)\rangle = \left\{ \frac{\hat{P}_X^2 + \hat{P}_Z^2}{2M} + g \begin{pmatrix} |\chi_1\rangle \\ |\chi_2\rangle \end{pmatrix} \begin{pmatrix} \hat{Z} & \hat{X} \\ \hat{X} & -\hat{Z} \end{pmatrix} \begin{pmatrix} \langle\chi_1| \\ \langle\chi_2| \end{pmatrix} \right\} |\Psi(t)\rangle \quad (F.18)$$

where a general wave function has the form

$$\Psi(\vec{x}, \vec{R}, t) = \langle\vec{x}, \vec{R}|\Phi(t)\rangle = \sum_{j=1}^2 \langle\vec{x}|\chi_j\rangle c_j(\vec{R}, t) \quad (F.19)$$

with $\vec{R} = (X, Z)$. Thus, the nuclear-electronic Hilbert space is spanned by a 2-dimensional electronic Hilbert space and a two-dimensional real-space basis $\{|X, Z\rangle\}$ for the nuclei.

The conical intersection is at $\vec{R} = \vec{0}$ in the X, Z -plane. The system shall pass the conical intersection at a distance Z_0 with uniform velocity V .

$$\vec{R}(t) = \begin{pmatrix} Vt \\ Z_0 \end{pmatrix} \quad (\text{F.20})$$

For the electronic wave function⁴ $|\Psi(t)\rangle = \sum_j |\chi_j\rangle c_j(t)$, we make the Ansatz that it obeys the time-dependent Schrödinger equation. (This is also used in the surface hopping approach)

$$i\hbar\partial_t|\Psi\rangle = \hat{H}^{BO}(\vec{R}(t))|\Psi\rangle \quad (\text{F.21})$$

The wave function is expanded in Born-Oppenheimer wave functions, so that we can extract the transition probability from their coefficients $C_n(t)$.

$$|\Psi(t)\rangle = \sum_n |\Psi_n^{BO}(\vec{R}(t))\rangle C_n(t) \quad (\text{F.22})$$

The path $\vec{R}(t)$ is prescribed and the wave function amplitudes follow the time-dependent Schrödinger equation. As described in section E.1.2, the wave function coefficients obey

$$i\hbar\partial_t C_m(t) \stackrel{\text{Eq. E.8}}{=} \sum_n \left[\dot{\vec{R}} \vec{A}_{m,n}(\vec{R}(t)) + U_{m,n}(\vec{R}(t)) \right] C_n(t) \quad (\text{F.23})$$

The Born-Oppenheimer energies are

$$\mathbf{U}(X, Z) \stackrel{\text{Eq. H.17}}{=} g\sqrt{X^2 + Z^2} \begin{pmatrix} 1 & 0 \\ 0 & -1 \end{pmatrix} \Rightarrow \mathbf{U}(\vec{R}(t)) = g\sqrt{Z_0^2 + V^2 t^2} \begin{pmatrix} 1 & 0 \\ 0 & -1 \end{pmatrix} \quad (\text{F.24})$$

and the derivative couplings are

$$V\mathbf{A}_X(X, Z) \stackrel{\text{Eq. H.31}}{=} \frac{\hbar V Z_0}{X^2 + Z^2} \begin{pmatrix} 1 & i \\ -i & 1 \end{pmatrix} \Rightarrow \dot{\vec{R}} \vec{A}(\vec{R}(t)) = \frac{\hbar V Z_0}{Z_0^2 + V^2 t^2} \begin{pmatrix} 1 & i \\ -i & 1 \end{pmatrix} \quad (\text{F.25})$$

Thus, we obtain the time-dependent Schrödinger equation

$$i\hbar\partial_t C_m(t) = \sum_n H_{m,n}(t) C_n(t) \quad (\text{F.26})$$

with

$$\begin{pmatrix} H_{11}(t) & H_{12}(t) \\ H_{21}(t) & H_{22}(t) \end{pmatrix} = \frac{\hbar V}{Z_0} \frac{1}{1 + (Vt/Z_0)^2} \begin{pmatrix} 1 & i \\ -i & 1 \end{pmatrix} + gZ_0 \sqrt{1 + (Vt/Z_0)^2} \begin{pmatrix} 1 & 0 \\ 0 & -1 \end{pmatrix} \quad (\text{F.27})$$

From here on, we deviate slightly from the procedure in section E.1.2, because we can exploit the special properties of the problem at hand. Namely, we absorb the diagonal elements of the derivative couplings into the dynamical phase. We get rid of the diagonal terms of the Hamiltonian

$$C_j(t) = \bar{C}_j(t) e^{-\frac{i}{\hbar} \int_0^t dt' H_{jj}(t')} \quad (\text{F.28})$$

⁴Before we used the coefficients $c_j(\vec{R}, t)$. For classical nuclei on a trajectory $\vec{R}(t)$, the coefficients are $c_j(\vec{R}(t), t)$, which we describe as in a short-hand notation as $c_j(t)$.

which

$$\begin{aligned} i\hbar\partial_t\bar{C}_1 &= H_{1,2} \exp\left(-\frac{i}{\hbar}\int_0^t dt' (H_{2,2}(t') - H_{1,1}(t'))\right) \bar{C}_2 \\ i\hbar\partial_t\bar{C}_2 &= H_{2,1} \exp\left(+\frac{i}{\hbar}\int_0^t dt' (H_{2,2}(t') - H_{1,1}(t'))\right) \bar{C}_1 \end{aligned} \quad (\text{F.29})$$

$$\begin{aligned} i\hbar\partial_t\bar{C}_{1/2} &= \pm \frac{i\hbar V}{Z_0} \frac{1}{1+(Vt/Z_0)^2} \exp\left(\mp \frac{i}{\hbar} 2gZ_0 \int_0^t dt' \sqrt{1+\left(\frac{Vt'}{Z_0}\right)^2}\right) \bar{C}_{2/1} \\ &= \pm \frac{i\hbar V}{Z_0} \frac{1}{1+(Vt/Z_0)^2} \exp\left(\mp \frac{i}{\hbar} \frac{2gZ_0^2}{V} \int_0^{Vt/Z_0} dx \sqrt{1+x^2}\right) \bar{C}_{2/1} \\ &= \pm \frac{i\hbar V}{Z_0} \frac{1}{1+(Vt/Z_0)^2} \exp\left(\mp \frac{i}{\hbar} \frac{2gZ_0^2}{V} \frac{1}{2} \left(x\sqrt{1+x^2} + \operatorname{asinh}(x)\right)_0^{Vt/Z_0}\right) \bar{C}_{2/1} \\ &= \pm \frac{i\hbar V}{Z_0} \frac{1}{1+(Vt/Z_0)^2} \exp\left(\mp \frac{i}{\hbar} \frac{gZ_0^2}{V} \left(\frac{Vt}{Z_0} \sqrt{1+(Vt/Z_0)^2} + \operatorname{asinh}(Vt/Z_0)\right)\right) \bar{C}_{2/1} \end{aligned} \quad (\text{F.30})$$

We used $\frac{d}{dx} \left[\frac{1}{2} \left(x\sqrt{1+x^2} + \operatorname{asinh}(x) \right) \right] = \sqrt{1+x^2}$.

The function in the exponential has the following properties

$$x\sqrt{1+x^2} + \operatorname{asinh}(x) \rightarrow \begin{cases} -x^2 & \text{for } x \rightarrow -\infty \\ 2x & \text{for } x \rightarrow 0 \\ x^2 & \text{for } x \rightarrow +\infty \end{cases} \quad (\text{F.31})$$

We transform the differential equation onto a dimension-less time variable

$$T(t) \stackrel{\text{def}}{=} \frac{Vt}{Z_0} \quad (\text{F.32})$$

which yields

$$\partial_T \bar{C}_{1/2} = \pm \frac{1}{1+T^2} \exp\left(\mp \frac{i}{\hbar} \frac{gZ_0^2}{V} \left(T\sqrt{1+T^2} + \operatorname{asinh}(T)\right)\right) \bar{C}_{2/1} \quad (\text{F.33})$$

The transition probability between two Born-Oppenheimer surfaces is obtained from the squared coefficients.

$$P_{2 \rightarrow 1} = |\bar{C}_1(+\infty)|^2 \quad \text{with} \quad \bar{C}_1(-\infty) = 0 \quad \text{and} \quad \bar{C}_2(-\infty) = 1 \quad (\text{F.34})$$

Eq. F.33 tells us that the transition probability is a function only of $\frac{gZ_0^2}{\hbar V}$. As we expect the transition probability to vanish for $Z_0 \rightarrow \infty$, it thus vanishes also for $V \rightarrow 0$. Thus, the transition probability vanishes for very slow motion of the nuclei, which is consistent with the adiabatic theorem.

The transition probability $P_{2 \rightarrow 1}(x)$ as function of $z \stackrel{\text{def}}{=} \frac{gZ_0^2}{\hbar V}$ is shown in figure F.1. They have been obtained by numerical integration of the differential equation Eq. F.33 using second-order Runge Kutta.

A fit yields the approximative formula Eq. F.35. (The fit is so good that it might be exact.)

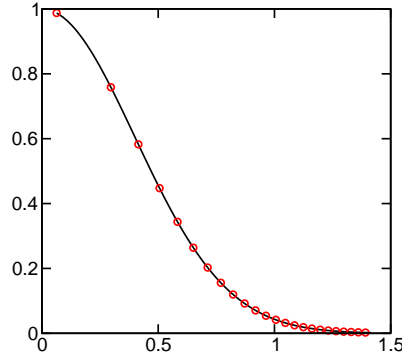


Fig. F.1: Transition probability $P_{2 \rightarrow 1}$ as function $\sqrt{\frac{gZ_0^2}{\hbar V}}$. The black line is obtained numerically. The red symbols is the approximate formula Eq. F.35.

TRANSITION PROBABILITY NEXT TO A CONICAL INTERSECTION

The transition probability at a symmetric conical intersection calculated with the Landau-Zener formula is

$$P_{2 \rightarrow 1}(g, Z_0, V) = \exp\left(-\frac{\pi g}{\hbar V} Z_0^2\right) \quad (\text{F.35})$$

where g is the electron-phonon coupling constant as defined in Eq. F.18, V is the velocity of the atomic trajectory and Z_0 is the distance of the trajectory from the conical intersection at the point of closest approach.

The transition probability falls off like a Gaussian (e^{-x^2}) with increasing distance from the conical intersection. The region with significant transition probability shrinks with decreasing velocity, which is consistent with the adiabatic limit.

Cross section of the conical intersection: Let me try to extract an approximate cross section r_c for the conical intersection. For this purpose, I replace the probability $P_{2 \rightarrow 1}(Z_0)$ by a rectangular one with the same integral, i.e.

$$P'(Z) = \begin{cases} 1 & \text{for } Z_0 < r_c \\ 0 & \text{else} \end{cases} \quad \text{and} \quad \int_{-\infty}^{\infty} dZ P(Z) = \int_{-\infty}^{\infty} dZ P'(Z) \quad (\text{F.36})$$

This yields with Eq. F.35

$$r_c = \frac{1}{2} \sqrt{\frac{\hbar V}{g}} \quad (\text{F.37})$$

SCATTERING CROSS SECTION OF A CONICAL INTERSECTION

The scattering cross section $2r$ of a spherical conical intersection is

$$2r_c \approx \sqrt{\frac{\hbar V}{g}} \tag{F.38}$$

where V is the velocity of the nuclei perpendicular to the degenerate seam and g describes the steepness of the conical intersection. Trajectories that pass the conical intersection within the distance r_c will undergo a transition.

Teller's approach[129], which has been presented here, has been generalized[130] to conical intersections with distinct topography, for example by adding a sloped linear potential to the Hamiltonian.

Sanity check (not for the reader): Comparison with Eq. 7 of Teller[129]: In order to enforce circular symmetry in Teller's calculation, we set his $a = b$ and $\beta = 0$. Our derivation above considers only spherical conical intersections. The parameters $a = b$ correspond to my parameter g . Teller's Eq. 5

$$P = \underbrace{e^{-2\pi \frac{\epsilon_{12}^2}{\hbar q v}}}_{\text{Teller Eq. 5}} \stackrel{?}{=} \underbrace{e^{-2\pi \frac{|H_{12}|^2}{\hbar v |F_1 - F_2|}}}_{\text{our Eq. F.14}}$$

is the Landau-Zener expression Eq. F.14, where $\epsilon_{12} = H_{12}$, $v = V$, $q = F_1 - F_2$. There is a discrepancy in that Teller uses h , where we (and Wittig) have \hbar . Teller's Eq. 6

$$\bar{P} = \underbrace{\sqrt{\frac{\hbar a v}{b^2}}}_{\text{Teller Eq. 6}} \stackrel{?}{=} \underbrace{\sqrt{\frac{\hbar V}{g}}}_{\text{our Eq. F.38}} = 2r_c$$

translates the expression of his Eq.5 with $q = 2a$, $\epsilon_{12} = by$. The results agree up to the same confusion of h and \hbar , that has been observed in Teller's Eq. 5.

F.2.1 Landau-Zener formula in terms of Born-Oppenheimer states

Editor: Caution! unfinished! This is an attempt to derive the Landau-Zener formula in terms of Born-Oppenheimer states as described in section E.1.2 on p.429. It turns out to be much more complicated than the derivation using a diabatic basisset.

$$H^{BO}(Q) = \begin{pmatrix} |\chi_1\rangle \\ |\chi_2\rangle \end{pmatrix} \begin{pmatrix} -F_1 Q & \Delta \\ \Delta & -F_2 Q \end{pmatrix} \begin{pmatrix} \langle \chi_1 | \\ \langle \chi_2 | \end{pmatrix} \tag{F.39}$$

Born-Oppenheimer surfaces

$$E_{\pm}^{BO}(Q) = -\frac{F_1 + F_2}{2} Q \pm \sqrt{\left(\frac{F_1 - F_2}{2} Q\right)^2 + \Delta^2} \tag{F.40}$$

Born-Oppenheimer wave functions The wave functions are described by

$$|\Psi_{-}^{BO}(Q)\rangle = \begin{pmatrix} |\chi_1\rangle \\ |\chi_2\rangle \end{pmatrix} \begin{pmatrix} \cos(\gamma(Q)) \\ \sin(\gamma(Q)) \end{pmatrix} \quad \text{and} \quad |\Psi_{+}^{BO}(Q)\rangle = \begin{pmatrix} |\chi_1\rangle \\ |\chi_2\rangle \end{pmatrix} \begin{pmatrix} -\sin(\gamma(Q)) \\ \cos(\gamma(Q)) \end{pmatrix} \tag{F.41}$$

$$\begin{aligned}
 & (-F_1 Q - E_-^{BO}(Q)) \cos(\gamma(Q)) + \Delta \sin(\gamma(Q)) = 0 \\
 \tan(\gamma(Q)) &= \frac{1}{\Delta} (F_1 Q + E_-^{BO}(Q)) \\
 &= \frac{1}{\Delta} \left(\frac{F_1 - F_2}{2} Q - \sqrt{\left(\frac{F_1 - F_2}{2} Q \right)^2 + \Delta^2} \right) \\
 &= \frac{F_1 - F_2}{2\Delta} Q - \sqrt{1 + \left(\frac{F_1 - F_2}{2\Delta} Q \right)^2} \quad (F.42)
 \end{aligned}$$

Below we will need the derivative of $\gamma(Q)$:

$$\begin{aligned}
 \partial_Q \tan(\gamma(Q)) &= \partial_Q \frac{\sin(\gamma(Q))}{\cos(\gamma(Q))} = \left(\frac{\cos(\gamma(Q))}{\cos(\gamma(Q))} + \frac{\sin^2(\gamma(Q))}{\cos^2(\gamma(Q))} \right) \partial_Q \gamma(Q) = (1 + \tan^2(\gamma(Q))) \partial_Q \gamma(Q) \\
 \partial_Q \gamma(Q) &= \frac{\partial_Q \tan(\gamma(Q))}{1 + \tan^2(\gamma(Q))} = \frac{1}{1 + \tan^2(\gamma(Q))} \frac{1}{Q} \left(a - \frac{2a^2}{2\sqrt{1+a^2}} \right) \\
 &= \frac{1}{1 + a^2 - 2a\sqrt{1+a^2} + 1 + a^2} \frac{a}{Q} \left(1 - \frac{a}{\sqrt{1+a^2}} \right) \\
 &= \frac{1}{2} \frac{1}{1 + a^2 - a\sqrt{1+a^2}} \frac{a}{Q} \left(1 - \frac{a}{\sqrt{1+a^2}} \right) = \frac{1}{2Q} \frac{a}{1 + a^2} = \frac{1}{2Q} \frac{\frac{F_1 - F_2}{2\Delta} Q}{1 + \left(\frac{F_1 - F_2}{2\Delta} Q \right)^2} \quad (F.43)
 \end{aligned}$$

I used $a = \frac{F_1 - F_2}{2\Delta} Q$.

Derivative couplings The derivative couplings are

$$\begin{aligned}
 A_{m,n}(Q) &= \left\langle \Psi_m^{BO}(\gamma(Q)) \left| \frac{\hbar}{i} \partial_\gamma \right|_{\gamma(Q)} \Psi_n^{BO}(\gamma) \right\rangle \frac{d\gamma(Q)}{dQ} \\
 A_{-,-}(Q) &= \left(-\cos(\gamma) \sin(\gamma) + \sin(\gamma) \cos(\gamma) \right) \frac{\hbar}{i} \frac{d\gamma(Q)}{dQ} = 0 \\
 A_{+,+}(Q) &= \left(\sin(\gamma) \cos(\gamma) - \cos(\gamma) \sin(\gamma) \right) \frac{\hbar}{i} \frac{d\gamma(Q)}{dQ} = 0 \\
 A_{-,+}(Q) &= \left(-\cos^2(\gamma) - \sin^2(\gamma) \right) \frac{\hbar}{i} \frac{d\gamma(Q)}{dQ} = -\frac{\hbar}{i} \frac{d\gamma(Q)}{dQ} \\
 A_{+,-}(Q) &= A_{-,+}^*(Q) = -A_{-,+}(Q) = \frac{\hbar}{i} \frac{d\gamma(Q)}{dQ} \quad (F.44)
 \end{aligned}$$

Equations of motion The equations of motion or the coefficients are

$$\begin{aligned}
 i\hbar \partial_t \Gamma_+(t) &= V A_{+,-}(Q) \exp\left(\frac{i}{\hbar} \int dt' (E_+^{BO}(Q(t)) - E_-^{BO}(Q(t))) \right) \Gamma_-(t) \\
 i\hbar \partial_t \Gamma_-(t) &= \underbrace{-V A_{+,-}(Q)}_{V A_{-,+}(Q)} \exp\left(-\frac{i}{\hbar} \int dt' (E_+^{BO}(Q(t)) - E_-^{BO}(Q(t))) \right) \Gamma_+(t) \quad (F.45)
 \end{aligned}$$

Note, that the coefficients Γ_\pm differ from those in the previous section, because they relate to the basis of Born-Oppenheimer states rather than the trivial diabatic basis used before.

I resolve the second equation for $\Gamma_+(t)$ and insert it into the first

$$\begin{aligned}
 \Gamma_-(t) &= \exp\left(-\frac{i}{\hbar} \int dt' (E_+^{BO}(Q(t)) - E_-^{BO}(Q(t))) \right) \frac{1}{V A_{+,-}(Q)} i\hbar \partial_t \Gamma_+(t) \\
 \Gamma_+(t) &= \exp\left(\frac{i}{\hbar} \int dt' (E_+^{BO}(Q(t)) - E_-^{BO}(Q(t))) \right) \frac{1}{-V A_{+,-}(Q)} i\hbar \partial_t \Gamma_-(t) \quad (F.46)
 \end{aligned}$$

$$\begin{aligned}
i\hbar\partial_t \left\{ e^{\frac{i}{\hbar} \int dt' (E_+^{BO}(Q(t)) - E_-^{BO}(Q(t)))} \frac{i\hbar\partial_t \Gamma_-(t)}{-VA_{+,-}(Q)} \right\} &= VA_{+,-}(Q) e^{\frac{i}{\hbar} \int dt' (E_+^{BO}(Q(t)) - E_-^{BO}(Q(t)))} \Gamma_-(t) \\
i\hbar\partial_t \left\{ e^{-\frac{i}{\hbar} \int dt' (E_+^{BO}(Q(t)) - E_-^{BO}(Q(t)))} \frac{i\hbar\partial_t \Gamma_+(t)}{VA_{+,-}(Q)} \right\} &= \underbrace{-VA_{+,-}(Q)}_{VA_{-+}(Q)} e^{-\frac{i}{\hbar} \int dt' (E_+^{BO}(Q(t)) - E_-^{BO}(Q(t)))} \Gamma_+(t)
\end{aligned} \tag{F.47}$$

$$\begin{aligned}
-\left(E_+^{BO}(Q(t)) - E_-^{BO}(Q(t))\right) \frac{i\hbar\partial_t \Gamma_-(t)}{-VA_{+,-}(Q)} + i\hbar\partial_t \frac{i\hbar\partial_t \Gamma_-(t)}{-VA_{+,-}(Q)} &= VA_{+,-}(Q) \Gamma_-(t) \\
\left(E_+^{BO}(Q(t)) - E_-^{BO}(Q(t))\right) \frac{i\hbar\partial_t \Gamma_+(t)}{VA_{+,-}(Q)} + i\hbar\partial_t \frac{i\hbar\partial_t \Gamma_+(t)}{VA_{+,-}(Q)} &= -VA_{+,-}(Q) \Gamma_+(t)
\end{aligned} \tag{F.48}$$

$$\begin{aligned}
i\hbar\partial_t \ln(\Gamma_-(t)) &= \frac{1}{E_+^{BO}(Q(t)) - E_-^{BO}(Q(t))} \left\{ \left(VA_{+,-}(Q) \right)^2 + \frac{VA_{+,-}(Q)}{\Gamma_-(t)} i\hbar\partial_t \frac{i\hbar\partial_t \Gamma_-(t)}{VA_{+,-}(Q)} \right\} \\
&= \frac{1}{2\Delta \sqrt{1 + \left(\frac{F_1 - F_2}{2\Delta} Q \right)^2}} \left\{ \left(V \frac{\hbar}{i} \frac{1}{2Q} \frac{\frac{F_1 - F_2}{2\Delta} Q}{1 + \left(\frac{F_1 - F_2}{2\Delta} Q \right)^2} \right)^2 + \dots \right\} \\
&= -\frac{V^2 \hbar^2 |F_1 - F_2|^2}{8\Delta^2} \frac{1}{\left[1 + \left(\frac{F_1 - F_2}{2\Delta} Q \right)^2 \right]^{5/2}} + \dots \\
i\hbar\partial_t \ln(\Gamma_+(t)) &= -\frac{1}{E_+^{BO}(Q(t)) - E_-^{BO}(Q(t))} \left\{ \left(VA_{+,-}(Q) \right)^2 + \frac{VA_{+,-}(Q)}{\Gamma_+(t)} i\hbar\partial_t \frac{i\hbar\partial_t \Gamma_+(t)}{VA_{+,-}(Q)} \right\}
\end{aligned} \tag{F.49}$$

Appendix G

Optical excitations in the Holstein dimer

G.1 Optic transitions

Editor: The section on optic transitions need more explanations or shall be removed. It does not connect to the non-adiabatic effects covered in the text.

Three dipole allowed transition are possible in the Holstein dimer.

- The vertical optic transition between two Born-Oppenheimer surfaces proceeds at fixed atomic positions. The transition is so rapid that the atoms cannot move appreciably during this process.
- The tunneling transition at low frequencies between minima in the same Born-Oppenheimer surface.
- The thermally activated transition is an interband transition, which requires a thermal activation to reach a region with a strong optical absorption matrix element.

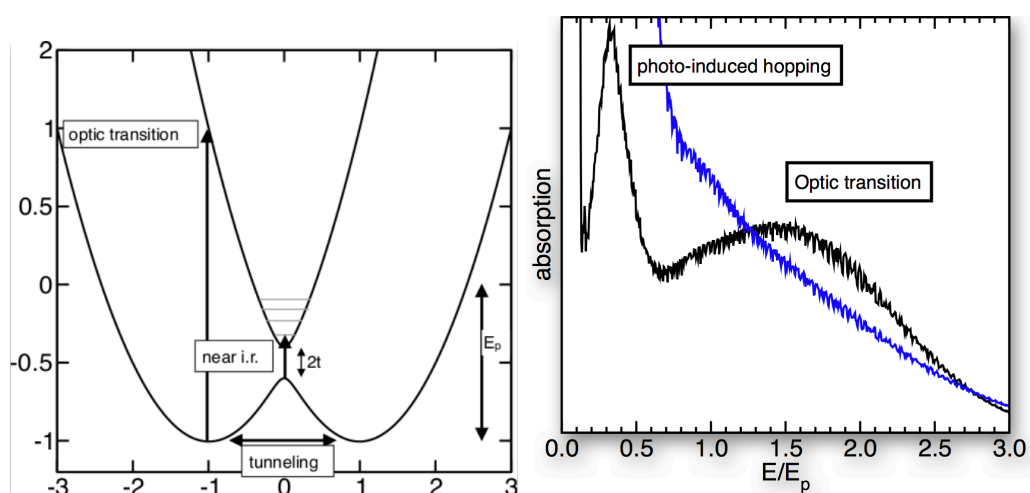


Fig. G.1: Left: Sketch of the major optic transitions in the Holstein dimer. Editor: Remove the incorrect notation "near i.r.". Right: calculated absorption spectra for two different temperatures. Editor: Check whether photo-induced hopping is the correct term.

In the calculated spectra of Fig. G.1, we notice that the optic transition energy is lower than the energy expected from the distance of the Born-Oppenheimer surfaces. ($1.5 E_P$ rather than $2E_P$). This is due to the fact that the optic transition matrix element peaks at the avoided crossing. Thus, the transition is shifted towards the avoided crossing, which reduces the excitation energy.

In Figure G.2, we can understand these effects on the level of the nuclear wave functions. Shown in blue is the ground state¹. The black and orange curve are the two components of the nuclear wave functions of the excited state. The black line is the component of the lower Born-Oppenheimer surface. Relevant is the component on the upper Born-Oppenheimer surface. It has a strong overlap with the ground-state wave function at the classical turning point of the vibration on the upper Born-Oppenheimer surface. This large overlap is the true reason why the optic transition reaches up to the Born-Oppenheimer surface and not higher.

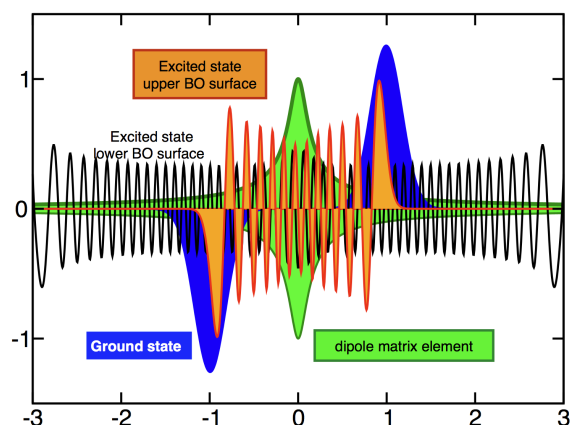


Fig. G.2: Wave functions and matrix elements involved in the optic transition of the Holstein dimer.

Editor: Here should be the expression of the tunneling transition.

¹Being antisymmetric, it is probably the first excited state rather than the true ground state. The energy difference is however negligible because it is determined by the tunneling between the two minima of the Born-Oppenheimer surface.

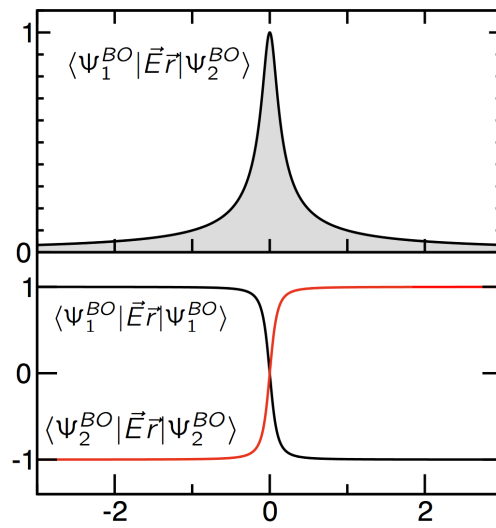


Fig. G.3: The matrix elements of the dipole operator of the Holstein dimer.

Appendix H

Jahn-Teller model

H.1 Jahn-Teller model as minimal model with a conical intersection

How to arrive at a minimal model for a conical intersection? We require a system with two Born-Oppenheimer surfaces, so that we can describe a crossing. According to the non-crossing theorem, we need at least two nuclear coordinates $\vec{R} = (X, Z)$.

1. We start (2×2) matrix as the Born-Oppenheimer Hamiltonian

$$H^{BO}(X, Z) = \begin{pmatrix} \bar{\epsilon}_1(X, Z) & t(X, Z) \\ t(X, Z) & \bar{\epsilon}_2(X, Z) \end{pmatrix} \quad (\text{H.1})$$

2. We choose a real-valued Hamiltonian, so that we obtain a conical intersection in two dimensions according to the non-crossing theorem, that is $\text{Im}[t] = 0$.
3. The eigenvalues of the Born-Oppenheimer Hamiltonian are

$$\epsilon_{\pm} = \frac{\bar{\epsilon}_1 + \bar{\epsilon}_2}{2} \pm \sqrt{\left(\frac{\bar{\epsilon}_1 - \bar{\epsilon}_2}{2}\right)^2 + |t|^2} \quad (\text{H.2})$$

The two Born-Oppenheimer surface shall touch. At that point, the hopping and the difference of the diagonal elements vanish. This is the position of the conical intersection. Near the conical intersection the two Born-Oppenheimer surfaces look like two cones that touch with their tips.

Let us position the origin of the nuclear coordinate system so that the conical intersection lies in the origin. Let us furthermore shift the energy axis so that the energy at the conical intersection is zero. This implies $\bar{\epsilon}_1(\vec{0}) = \bar{\epsilon}_2(\vec{0}) = 0$ and $|t(\vec{0})| = 0$.

4. Let me include for the Hamiltonian only the highest order in the displacement (X, Z) from the position $(0, 0)$ of the conical intersection.
5. The linear term in the distance $\sqrt{X^2 + Z^2}$ from the conical intersection contains three independent directions: One, the gradient of $\frac{\bar{\epsilon}_1 + \bar{\epsilon}_2}{2}$, describes a position-independent force, which acts on the nuclei irrespective of the Born-Oppenheimer surface. The other two directions describe a non-spherical deformation of the cones.

We can simplify the problem by removing the nonspherical terms, i.e. the force at the origin and the deformations of the cones.

Then, we can rotate the coordinate system so that $t(X, Z)$ vanishes so that the gradient of t is perpendicular to the Z coordinate.

$$H^{BO}(X, Z) = g \begin{pmatrix} Z & X \\ X & Z \end{pmatrix} \quad (\text{H.3})$$

6. The spherical Hamiltonian, we arrived so-far is not bounded from below. In order to introduce a lower bound to the energy, we stabilize the system by adding a parabolic potential.

$$H^{BO}(X, Z) = w(X^2 + Z^2) \begin{pmatrix} 1 & 0 \\ 0 & 1 \end{pmatrix} + g \begin{pmatrix} Z & X \\ X & -Z \end{pmatrix} \quad (\text{H.4})$$

H.2 Jahn-Teller model and manganites

The Jahn-Teller model can be used to describe the Jahn-Teller effect in doped manganites. Manganites such as $\text{Ca}_x\text{La}_{1-x}\text{MnO}_3$ form a very interesting class of materials with a complicated phase diagram and enormous variety of different physical properties that can be controlled by doping, temperature, magnetic fields, etc. Their main structural element is a network of corner-sharing MnO_6 octahedra. If Mn is in the 4+ charge state (Mn^{IV}) as in CaMnO_3 , the Mn ions in the center of the octahedra exhibit two degenerate d-orbitals of e_g symmetry, which are unoccupied. (see figure H.1, upper right)

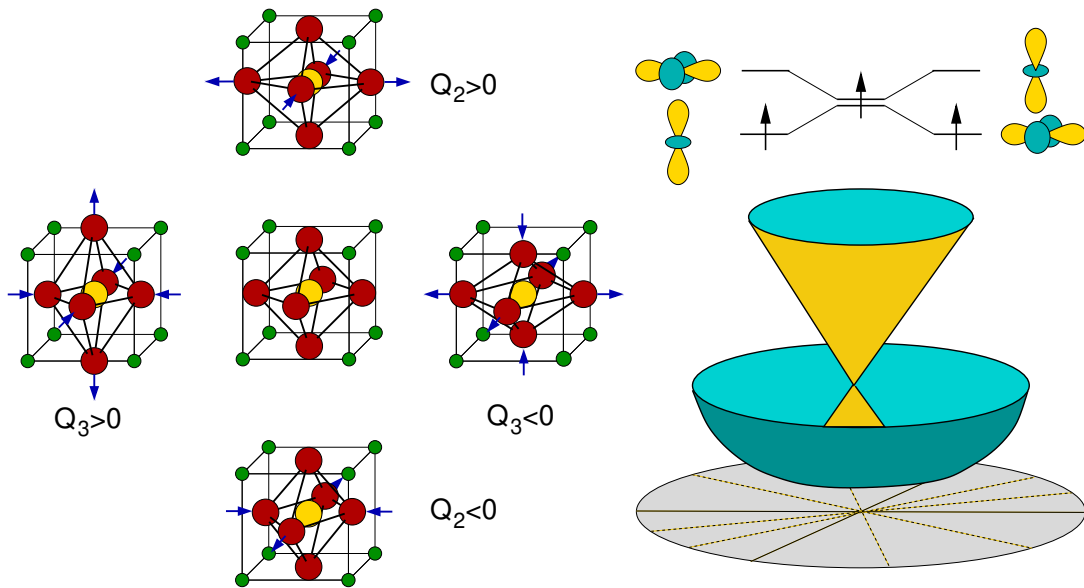


Fig. H.1: Left: the two Jahn-Teller active modes of the octahedron in a perovskite ABO_3 . The red spheres represent oxygen ions, the yellow atom in the center is the transition metal ion (B-type ion) on which the two e_g orbitals reside. The green spheres are the A-type ions. The undistorted octahedron is drawn in the center. Along the horizontal axis the positive and negative distortions of the Q_2 mode are drawn. Along the vertical axis the positive and negative distortions of the Q_3 mode are drawn. Right top: Jahn-Teller splitting of the two e_g orbitals under the influence of a positive and negative distortion of the Q_3 mode. Left bottom: The two Born-Oppenheimer surfaces of the Jahn-Teller model in the two-dimensional coordinate space of the two Jahn-Teller active modes. The point of contact of the two Born-Oppenheimer surfaces is a conical intersection.

In the doped materials, electrons can be added to these pair of degenerate states. This electron in a given orbital induces a structural distortion of the octahedra, which lowers the filled orbital and

raises the empty orbital. The distortions are the elongation and compression of the octahedra along one axis into a prolate (cigar-shaped) and an oblate (pancake-shaped) form. (see figure H.1, left)

One can say that the electron and the octahedral distortion (a phonon) form a bound state. This bound state is called a **polaron**.

The Jahn-Teller distortions can be expressed in terms of the outward displacements a_x , a_y and a_z of the oxygen ligands in x, y, and z directions, respectively. These can be combined into a vector (a_x, a_y, a_z) . The two Jahn-Teller active displacements are [131] $Q_2 = \frac{1}{\sqrt{2}}(1, -1, 0)$ and $Q_3 = \frac{1}{\sqrt{6}}(-1, -1, 2)$. The positive and negative distortions Q_3 can be described by a **prolate** (cigar-shaped) and an **oblate** (pancake-shaped) distortion. The Jahn-Teller distortions span a two-dimensional parameter space. They can be described by an amplitude $\sqrt{Q_2^2 + Q_3^2}$ and an angle parameter α specifying the type of the distortion pattern.

α	(a_x, a_y, a_z)	(Q_2, Q_3)	
0°	$\frac{1}{\sqrt{2}}(1, -1, 0)$	(1, 0)	
30°	$\frac{1}{\sqrt{6}}(1, -2, 1)$	$(\frac{1}{2}\sqrt{3}, \frac{1}{2})$	oblate along y
60°	$\frac{1}{\sqrt{2}}(0, 1, -1)$	$(\frac{1}{2}, \frac{1}{2}\sqrt{3})$	
90°	$\frac{1}{\sqrt{6}}(-1, -1, 2)$	(0, 1)	prolate along z
120°	$\frac{1}{\sqrt{2}}(-1, 0, 1)$	$(-\frac{1}{2}, \frac{1}{2}\sqrt{3})$	
150°	$\frac{1}{\sqrt{6}}(-2, 1, 1)$	$(-\frac{1}{2}\sqrt{3}, \frac{1}{2})$	oblate along x
180°	$\frac{1}{\sqrt{2}}(-1, 1, 0)$	(-1, 0)	
210°	$\frac{1}{\sqrt{6}}(-1, 2, -1)$	$(-\frac{1}{2}\sqrt{3}, -\frac{1}{2})$	prolate along y
240°	$\frac{1}{\sqrt{2}}(0, 1, -1)$	$(-\frac{1}{2}, -\frac{1}{2}\sqrt{3})$	
270°	$\frac{1}{\sqrt{6}}(1, 1, -2)$	(0, 1)	oblate along z
300°	$\frac{1}{\sqrt{2}}(1, 0, -1)$	$(\frac{1}{2}, -\frac{1}{2}\sqrt{3})$	
330°	$\frac{1}{\sqrt{6}}(2, -1, -1)$	$(\frac{1}{2}\sqrt{3}, -\frac{1}{2})$	prolate along x

Table H.1: Jahn-Teller active distortions of the octahedron as function of the angular coordinate α . The second row (a_x, a_y, a_z) describes the bond expansions in x,y,z directions and the third describes the mode amplitudes.

In the following, we discuss the conical intersection at a single octahedron. The relevant structural distortions of the octahedra are described by the generalized nuclear coordinates X, Z . The electronic wave function is described as a vector in a two-dimensional Hilbert space of the two e_g orbitals. I label the two e_g orbitals as $|a\rangle$ and $|b\rangle$.

The atomic coordinates, that is the generalized coordinates for the two octahedral distortions, which couple to the two e_g states are denoted by the two-dimensional vector¹ $\vec{R} = (X, Z) \stackrel{\text{def}}{=} (Q_2, Q_3)$.

H.3 Jahn-Teller model

The **Jahn-Teller model** [129, 132] is a minimal model for a **conical intersection**. It is thus ideally suited to investigate the generic properties of a conical intersection respectively a relaxation process.

In appendix H.1 it is described how one arrives at the Jahn-Teller model as minimal model for a conical intersection. That section shall serve as motivation for the Jahn-Teller model. Furthermore it makes the simplifying assumptions evident.

¹I am using uppercase symbols as these are nuclear coordinates. X and Z are used rather than X and Y , because of the two non-imaginary Pauli matrices σ_x and σ_z .

The Jahn-Teller model has been developed to study manganites, a material class with a variety of unusual and interesting effects. A brief sketch of manganites and how they relate to the Jahn-Teller model is given in appendix H.2.

Let me mention for the interested reader the relation of the Jahn-Teller model with the **Higgs mechanism**[133], discussed in elementary particle physics as origin of the particle mass. The Higgs mechanism postulated a Mexican-hat potential which results from a spontaneous symmetry breaking. In the symmetry-broken state, the particle has two modes, of which the radial mode has a finite curvature and is identified with the Higgs mode, while the motion into the other direction has no curvature and is identified with the “mass-less” Nambu-Goldstone boson.

In the following, we will determine the Born-Oppenheimer surfaces, the Born-Oppenheimer wave functions and derivative couplings. The procedure to solve the nuclear Schrödinger equation is given in appendix H on p. 467.

The Jahn-Teller model acts for us as a worked example to practice the workings of the Born-Huang framework and to determine the nuclear wave function and their ingredients. The solution of the nuclear Schrödinger equation is discussed in the appendix for the interested reader, but it not part of the lecture.

The Jahn Teller model shall also elucidate some surprising properties, related to a geometric phase. Specifically, it will be shown, that the Born-Oppenheimer wave function can not be described as real-valued wave functions, that are continuous in the nuclear coordinate space. This inevitably produces serious problems for setting up the derivative couplings which enter the nuclear Hamiltonian. However, there is a remedy of that problem in terms of a gauge transformation, which makes the Born-Oppenheimer wave functions complex-valued but continuous everywhere, except right at the conical intersection. The findings related to the geometric phase is relevant for a wider class of problems including the so-called topological insulators.

H.3.1 Jahn-Teller model

For a conical intersection we require at least two Born-Oppenheimer surfaces, and two coordinates for the nuclei.

- Let me describe the two-dimensional Hilbert space for the electronic degrees of freedom by two orbitals, which we denote as $|d_1\rangle$ and $|d_2\rangle$. A general electronic wave function is a superposition of these two orbitals. A general electronic wave function is therefore

$$|\psi^{el}\rangle = |d_1\rangle \underbrace{\langle d_1|\psi^{el}\rangle}_{c_1} + |d_2\rangle \underbrace{\langle d_2|\psi^{el}\rangle}_{c_2} = \int d^4x |\vec{x}\rangle \underbrace{\left(\overbrace{d_1(\vec{x})}^{\langle \vec{x}|d_1\rangle} c_1 + \overbrace{d_2(\vec{x})}^{\langle \vec{x}|d_2\rangle} c_2 \right)}_{=\psi^{el}(\vec{x})=\langle \vec{x}|\psi^{el}\rangle} \quad (\text{H.5})$$

While we consider here only one-electron wave functions, the electronic wave function in the Born-Huang framework is a general many-electron wave function. For manganites, the two orbitals are the two relevant d-orbitals shown in the upper right of fig. H.1.

- Let me denote the relevant nuclear degrees of freedom by $\vec{R} = (X, Z)$. A general nuclear wave function with two spatial degrees of freedom (X, Z) has the form

$$|\psi^{nuc}\rangle = \int dX \int dZ |X, Z\rangle \underbrace{\psi^{nuc}(X, Z)}^{\langle X, Z|\psi^{nuc}\rangle} \quad (\text{H.6})$$

- the combined wave functions for electrons and nuclear can be described in a basisset $|d_m, \vec{R}\rangle \stackrel{\text{def}}{=} |d_m\rangle \otimes |X, Z\rangle$, which are products of electronic and nuclear wave functions. A general combined wave function has the form

$$|\Phi\rangle = \int dX \int dZ \sum_{m=1}^2 |d_m, X, Z\rangle \underbrace{C_m(X, Z)}_{\langle d_m, X, Z|\Phi\rangle} \quad (\text{H.7})$$

The coefficients $C_m(X, Z)$ can be regarded as components of a multi-valued nuclear wave functions. However, they differ from the nuclear wave functions $\Theta_m(\vec{R})$ defined in the Born-Huang framework. This is why I am using different symbols.²

The time-dependent nuclear-electronic Schrödinger equation of the Jahn-Teller model is³

$$i\hbar\partial_t|\Phi(t)\rangle = \left[\underbrace{\frac{\hat{P}^2}{2M}}_{E_{kin}^{nuc}} + w(\hat{X}^2 + \hat{Z}^2) + g \underbrace{\begin{pmatrix} |d_1\rangle \\ |d_2\rangle \end{pmatrix} \begin{pmatrix} \hat{Z} & \hat{X} \\ \hat{X} & -\hat{Z} \end{pmatrix} \begin{pmatrix} \langle d_1| \\ \langle d_2| \end{pmatrix}}_{\text{electron-phonon coupling}} \right] |\Phi(t)\rangle \quad (\text{H.10})$$

where g is the electron-phonon coupling parameter and w is the force constant for the restoring force. $\hat{R} = (\hat{X}, \hat{Z})$ and $\hat{P} = (\hat{P}_X, \hat{P}_Z)$ are the operators describing the nuclear degrees of freedom and their momenta.

Insertion of the ansatz Eq. H.7 in Eq. H.10 yields the equation for the the wave-function components

$$i\hbar\partial_t \begin{pmatrix} C_1(X, Z, t) \\ C_2(X, Z, t) \end{pmatrix} \stackrel{\text{Eq. H.10}}{=} \left[\frac{-\hbar^2}{2M} (\partial_X^2 + \partial_Z^2) + w(X^2 + Z^2) \right] \begin{pmatrix} C_1(X, Z, t) \\ C_2(X, Z, t) \end{pmatrix} + g \begin{pmatrix} Z & X \\ X & -Z \end{pmatrix} \begin{pmatrix} C_1(X, Z, t) \\ C_2(X, Z, t) \end{pmatrix} \quad (\text{H.11})$$

H.3.2 Born-Oppenheimer Hamiltonian and Born-Oppenheimer surfaces

The Born-Oppenheimer Hamiltonian is obtained by stripping the terms containing the nuclear momenta from the many-particle Hamiltonian.⁴ The Hamilton matrix in the basisset of the two electronic orbitals $|d_1\rangle$ and $|d_2\rangle$ is

$$\mathbf{H}^{BO}(\vec{R}) = g \begin{pmatrix} Z & X \\ X & -Z \end{pmatrix} + w(X^2 + Z^2) \begin{pmatrix} 1 & 0 \\ 0 & 1 \end{pmatrix} \quad (\text{H.12})$$

The first term describes the electronic Hamiltonian, that is the splitting of the degenerate electronic states upon distortion, while the second term is a simple restoring potential for the nuclear distortions.

Polar coordinates are convenient due to the circular symmetry of the problem.

$$X(R, \alpha) = R \sin(\alpha) \quad \text{and} \quad Z(R, \alpha) = R \cos(\alpha) \quad (\text{H.13})$$

²The reader may wonder why one uses the Born-Oppenheimer wave functions instead of a position independent electronic basisset as in the present example. There are two answers to this: Firstly, position independent basissets work well for model systems such as a Jahn-Teller model. For the description of real systems, they are inefficient, because very many basisfunctions are required to describe the electrons with the same basisset for all possible nuclear configurations. The second answer is that transitions between different Born-Oppenheimer surfaces are limited to special regions, where they become close. For a basisset such as $\{|d_1\rangle, |d_2\rangle\}$, the system is always in a superposition of all basis functions.

³Using the Pauli matrices Eq. H.10 can be written in the form

$$i\hbar\partial_t|\Phi(t)\rangle = \left[\frac{\hat{P}^2}{2M} + w\hat{R}^2 + g\hat{R}\hat{\sigma} \right] |\Phi(t)\rangle \quad (\text{H.8})$$

The components of $\hat{\sigma}$,

$$\begin{aligned} \hat{\sigma}_x &= |\chi_1\rangle\langle\chi_2| + |\chi_2\rangle\langle\chi_1| \quad \text{and} \\ \hat{\sigma}_z &= |\chi_1\rangle\langle\chi_1| - |\chi_2\rangle\langle\chi_2|, \end{aligned} \quad (\text{H.9})$$

are represented by the Pauli matrices σ_x and σ_z , defined below in Eq. 3.4 on p. 86.

$${}^4\vec{R}\hat{\sigma} = X\sigma_x + Z\sigma_z = \begin{pmatrix} Z & X \\ X & -Z \end{pmatrix}.$$

and

$$\alpha(X, Z) = \text{atan}\left(\frac{Z}{X}\right) - \frac{\pi}{2}(\text{sgn}(Z) - 1) \quad \text{and} \quad R(X, Z) = \sqrt{X^2 + Z^2} \quad (\text{H.14})$$

In polar coordinates the Born-Oppenheimer Hamiltonian is

$$\mathbf{H}^{BO} = \begin{pmatrix} gR \cos(\alpha) + wR^2 & gR \sin(\alpha) \\ gR \sin(\alpha) & -gR \cos(\alpha) + wR^2 \end{pmatrix} \quad (\text{H.15})$$

The Born-Oppenheimer equation Eq. 2.8 for the eigenvalues $E_{\pm}^{BO}(\vec{R})$ is

$$\begin{pmatrix} gR \cos(\alpha) + wR^2 - E_{\pm}^{BO}(R, \alpha) & gR \sin(\alpha) \\ gR \sin(\alpha) & -gR \cos(\alpha) + wR^2 - E_{\pm}^{BO}(R, \alpha) \end{pmatrix} \begin{pmatrix} \langle d_1 | \Psi_{\pm}^{BO}(R, \alpha) \rangle \\ \langle d_2 | \Psi_{\pm}^{BO}(R, \alpha) \rangle \end{pmatrix} = 0 \quad (\text{H.16})$$

where the Born-Oppenheimer wave functions are $|\Psi_{\pm}^{BO}(\vec{R})\rangle = \sum_{m=1}^2 |d_m\rangle \langle d_m | \Psi_{\pm}^{BO}(\vec{R})\rangle$. The Born-Oppenheimer equation yields the two Born-Oppenheimer surfaces $E_{\pm}^{BO}(\vec{R})$ of the Jahn-Teller model.

BORN-OPPENHEIMER SURFACES OF THE JAHN-TELLER MODEL

$$E_{\pm}^{BO}(\vec{R}) = \pm g|\vec{R}| + w\vec{R}^2 \quad (\text{H.17})$$

The Born-Oppenheimer surfaces are shown in Fig. H.2. The two surfaces meet at a single point, which is the **conical intersection**. The lower Born-Oppenheimer surface has the shape of a Mexican hat.

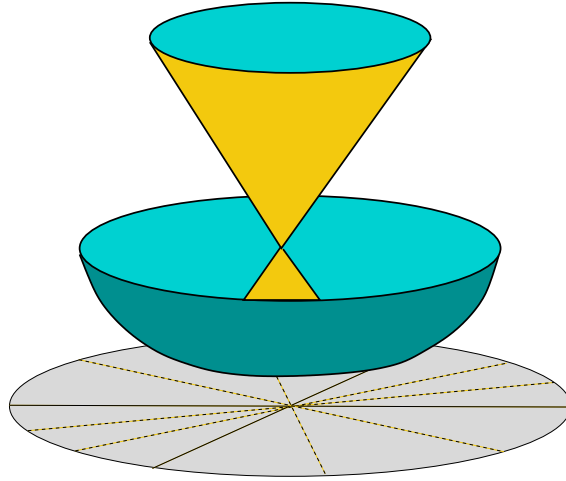


Fig. H.2: Born-Oppenheimer surfaces $E_{\pm}^{BO}(X, Z)$ of the Jahn-Teller model as function of the two nuclear degrees of freedom.

H.3.3 Born-Oppenheimer wave functions: real-valued, but discontinuous

When we insert the Born-Oppenheimer surfaces into Eq. H.16, we obtain

$$gR \begin{pmatrix} \cos(\alpha) \mp 1 & \sin(\alpha) \\ \sin(\alpha) & -\cos(\alpha) \mp 1 \end{pmatrix} \begin{pmatrix} \langle d_1 | \Psi_{\pm}^{BO}(R, \alpha) \rangle \\ \langle d_2 | \Psi_{\pm}^{BO}(R, \alpha) \rangle \end{pmatrix} = 0$$

To construct the eigenstates, we take the first line of Eq. H.16. We construct the vector orthogonal to $(u, v) = (\cos(\alpha) \mp 1, \sin(\alpha))$ according to the rule $(u, v) \perp (-v, u)$, and then we normalize it. This will produce the eigenvector of the Born-Oppenheimer Hamiltonian.

This yields the Born-Oppenheimer states $|\bar{\Psi}_{\pm}^{BO}\rangle$. The bar on top of the symbol for the Born-Oppenheimer state is there to distinguish it from the final result, which is multiplied with an additional phase factor.

$$\begin{aligned} \begin{pmatrix} \langle d_1 | \bar{\Psi}_{\pm}^{BO} \rangle \\ \langle d_2 | \bar{\Psi}_{\pm}^{BO} \rangle \end{pmatrix} &= \begin{pmatrix} -\sin(\alpha) \\ \cos(\alpha) \mp 1 \end{pmatrix} \frac{1}{\sqrt{\sin^2(\alpha) + (\cos(\alpha) \mp 1)^2}} \\ &= \begin{pmatrix} -\sin(\alpha) \\ \cos(\alpha) \mp 1 \end{pmatrix} \frac{1}{\sqrt{2(1 \mp \cos(\alpha))}} \end{aligned} \quad (\text{H.18})$$

This expression is defined only for $\cos(\alpha) \neq \pm 1$.

We use the trigonometric identities

$$\begin{aligned} \cos(x) + 1 &= +2 \cos^2\left(\frac{x}{2}\right) \quad \Rightarrow \quad \left| \cos\left(\frac{x}{2}\right) \right| = \sqrt{\frac{1}{2}(1 + \cos(x))} \\ \cos(x) - 1 &= -2 \sin^2\left(\frac{x}{2}\right) \quad \Rightarrow \quad \left| \sin\left(\frac{x}{2}\right) \right| = \sqrt{\frac{1}{2}(1 - \cos(x))} \\ \sin(x) &= 2 \sin\left(\frac{x}{2}\right) \cos\left(\frac{x}{2}\right) \end{aligned} \quad (\text{H.19})$$

to obtain

$$\begin{pmatrix} \langle d_1 | \bar{\Psi}_{+}^{BO} \rangle \\ \langle d_2 | \bar{\Psi}_{+}^{BO} \rangle \end{pmatrix} = \begin{pmatrix} -2 \sin\left(\frac{\alpha}{2}\right) \cos\left(\frac{\alpha}{2}\right) \\ -2 \sin^2\left(\frac{\alpha}{2}\right) \end{pmatrix} \frac{1}{2|\sin\left(\frac{\alpha}{2}\right)|} = \begin{pmatrix} -\cos\left(\frac{\alpha}{2}\right) \\ -\sin\left(\frac{\alpha}{2}\right) \end{pmatrix} \text{sgn}\left(\sin(\alpha/2)\right) \quad (\text{H.20})$$

and

$$\begin{pmatrix} \langle d_1 | \bar{\Psi}_{-}^{BO} \rangle \\ \langle d_2 | \bar{\Psi}_{-}^{BO} \rangle \end{pmatrix} = \begin{pmatrix} -2 \sin\left(\frac{\alpha}{2}\right) \cos\left(\frac{\alpha}{2}\right) \\ 2 \cos^2\left(\frac{\alpha}{2}\right) \end{pmatrix} \frac{1}{2|\cos\left(\frac{\alpha}{2}\right)|} = \begin{pmatrix} -\sin\left(\frac{\alpha}{2}\right) \\ \cos\left(\frac{\alpha}{2}\right) \end{pmatrix} \text{sgn}\left(\cos(\alpha/2)\right) \quad (\text{H.21})$$

where the sign function "sgn" is positive for positive arguments and negative for negative arguments.⁵ The resulting functions are sketched in Fig. H.3.

The Born-Oppenheimer wave functions are discontinuous⁶ because of the sign function in Eq. H.21. Without the sign-term in Eq. H.21, the Born-Oppenheimer wave functions are periodic with 4π , that is, they change sign with every full turn and they are periodic only after two full turns around the conical intersection. Thus, the Born-Oppenheimer wave functions would be double valued. This double periodicity is reminiscent of the half-integer angular momentum eigenvalues of spin $\frac{1}{2}$ systems. The sign term in Eq. H.21 restores the original 2π periodicity of the problem at the cost of introducing discontinuities.

The Born-Oppenheimer wave function are not defined uniquely. We are free to multiply each Born-Oppenheimer by an arbitrary, position dependent complex-valued phase factor $e^{iX_{\pm}(X,Z)}$. Thus, there are several alternative descriptions

- The Born-Oppenheimer wave functions are real, but discontinuous in the nuclear coordinates as in the example above.

⁵For an argument zero, the sgn function vanishes. Here we will not discuss this isolated point which will not cause problems.

⁶At the point of the discontinuity, the wave function is undefined. See section H.5.1 on p. 500 and fig H.8 therein.

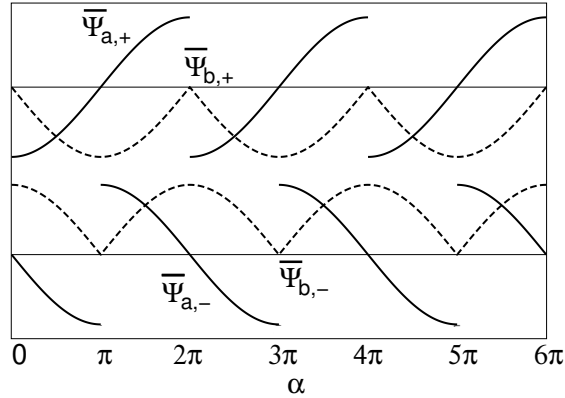


Fig. H.3: Orbital coefficients $\bar{\Psi}_{j,n}^{BO}(\alpha)$ of the discontinuous, real-valued Born-Oppenheimer wave functions $|\Psi_{\pm}^{BO}(\alpha)\rangle = \sum_{j \in \{a,b\}} |d_j\rangle \bar{\Psi}_{j,\pm}^{BO}(\alpha)$ at a conical intersection from Eq. H.21 as function of the angular coordinate α in the (X, Z) -plane of the nuclear coordinates. Upper graph: components of the excited-state BO wave function $|\Psi_{+}^{BO}(\alpha)\rangle$, namely $\bar{\Psi}_{a,+}^{BO}$ (filled) and $\bar{\Psi}_{b,+}^{BO}$ (dashed). Lower graph: components of the ground-state BO wave function $|\Psi_{-}^{BO}(\alpha)\rangle$, namely $|\bar{\Psi}_{a,-}^{BO}$ (filled) $|\bar{\Psi}_{b,-}^{BO}$ (dashed). Apparent are the discontinuities at $\alpha = 2\pi n + 1$ for the ground-state wave function and at $\alpha = 2\pi n$ for the excited-state wave function. In the model considered, the orbital coefficients do not depend on the distance $|(X, Z)|$ from the conical intersection. **Editor: Fix the notation: Here I use $|\Psi_{a,\pm}^{BO}$ for $\langle d_1 | \Psi_{\pm}^{BO} \rangle$ and similar**

- The Born-Oppenheimer wave functions are real-valued and continuous, but double valued. Double valued means that they change sign with each full turn around the conical intersection and they obtain the original value only after two full turns. This result would be obtained if one drops the sign term in the above equation.
- The Born-Oppenheimer wave function is continuous and single valued, but complex-valued. This is obtained from the above result by replacing the sign term with a smooth phase factor with the same periodicity as the sign function. This representation is created below.

H.3.4 Continuous, but complex-valued Born-Oppenheimer wave functions

The discontinuities of the real-valued Born-Oppenheimer wave functions can be removed by a gauge transformation. By replacing the sign function in Eq. H.21 by a complex-valued phase factor⁷ $\mp e^{i\alpha/2}$, I obtain a new set of Born-Oppenheimer wave functions. This amounts to gauge transformation Eq. 2.34.

$$|\Psi_{\pm}^{BO}(\vec{R})\rangle \stackrel{\text{def}}{=} |\bar{\Psi}_{\pm}^{BO}(\vec{R})\rangle e^{\frac{i}{\hbar}\chi_{\pm}(\vec{R})} \quad (\text{H.22})$$

with the gauge potential defined by

$$\begin{aligned} e^{\frac{i}{\hbar}\chi_{+}(\alpha)} &= -\text{sgn}\left[\sin\left(\frac{\alpha}{2}\right)\right] e^{i\alpha/2} &\Rightarrow & \frac{1}{\hbar}\chi_{+}(R, \alpha) = \frac{\alpha}{2} + \frac{\pi}{2} \left[1 + \text{sgn}\left[\sin\left(\frac{\alpha}{2}\right)\right]\right] \\ e^{\frac{i}{\hbar}\chi_{-}(\alpha)} &= +\text{sgn}\left[\cos\left(\frac{\alpha}{2}\right)\right] e^{i\alpha/2} &\Rightarrow & \frac{1}{\hbar}\chi_{-}(R, \alpha) = \frac{\alpha}{2} + \frac{\pi}{2} \left[1 - \text{sgn}\left[\cos\left(\frac{\alpha}{2}\right)\right]\right] \end{aligned} \quad (\text{H.23})$$

The two sets of wave functions are distinguished by the (missing) bar on top of the symbol.

⁷The additional sign change has been introduced to make the equations appear simpler. It is permitted because it is a global sign change.

The gauge transform applied to the wave functions Eq. H.21 on p. 473 yields⁸ the new Born-Oppenheimer states

$$\begin{pmatrix} \langle d_1 | \Psi_+^{BO} \rangle \\ \langle d_2 | \Psi_+^{BO} \rangle \end{pmatrix} = \begin{pmatrix} \cos(\alpha/2) \\ \sin(\alpha/2) \end{pmatrix} e^{i\alpha/2} = \frac{1}{2} \begin{pmatrix} e^{i\alpha} + 1 \\ -i(e^{i\alpha} - 1) \end{pmatrix}$$

$$\begin{pmatrix} \langle d_1 | \Psi_-^{BO} \rangle \\ \langle d_2 | \Psi_-^{BO} \rangle \end{pmatrix} = \begin{pmatrix} -\sin(\alpha/2) \\ \cos(\alpha/2) \end{pmatrix} e^{i\alpha/2} = \frac{1}{2} \begin{pmatrix} +i(e^{i\alpha} - 1) \\ e^{i\alpha} + 1 \end{pmatrix} \tag{H.24}$$

BORN-OPPENHEIMER STATES OF THE JAHN-TELLER MODEL

Orbital coefficients of the continuous but complex-valued Born-Oppenheimer wave functions.

$$\begin{pmatrix} \langle d_1 | \Psi_+^{BO} \rangle \\ \langle d_2 | \Psi_+^{BO} \rangle \end{pmatrix} = \frac{1}{2} \begin{pmatrix} e^{i\alpha} + 1 \\ -i(e^{i\alpha} - 1) \end{pmatrix} \quad \text{and} \quad \begin{pmatrix} \langle d_1 | \Psi_-^{BO} \rangle \\ \langle d_2 | \Psi_-^{BO} \rangle \end{pmatrix} = \frac{1}{2} \begin{pmatrix} +i(e^{i\alpha} - 1) \\ e^{i\alpha} + 1 \end{pmatrix} \tag{H.25}$$

The coefficients are shown in Fig. H.4 on p. 475.

The abstract states are obtained from these coefficients as

$$|\Psi_{\pm}^{BO}(\vec{R})\rangle = |d_1\rangle \langle d_1 | \Psi_{\pm}^{BO}(\vec{R})\rangle + |d_2\rangle \langle d_2 | \Psi_{\pm}^{BO}(\vec{R})\rangle \tag{H.26}$$

where α is determined by the nuclear coordinates \vec{R} via Eq. H.13

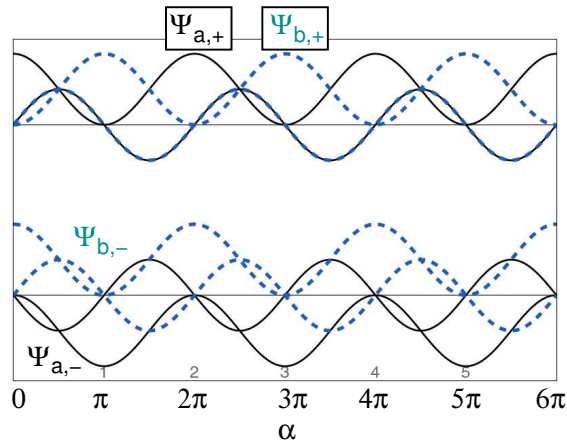


Fig. H.4: Orbital coefficients $\Psi_{j,n}^{BO}(\alpha)$ of the continuous, complex-valued Born-Oppenheimer wave functions $|\Psi_{\pm}^{BO}(\alpha)\rangle = \sum_{j \in \{a,b\}} |\chi_j\rangle \Psi_{j,\pm}^{BO}(\alpha)$ next to a conical intersection from Eq. H.25 as function of the angular coordinate α in the (X, Z) -plane of the nuclear coordinates. Upper graph: complex-valued components of the excited-state BO wave function $|\Psi_+^{BO}(\alpha)\rangle$, namely $\Psi_{a,+}^{BO}$ (filled) and $\Psi_{b,+}^{BO}$ (dashed). Each component has a real and an imaginary part. Lower graph: components of the ground-state BO wave function $|\Psi_-^{BO}(\alpha)\rangle$, namely $|\Psi_{a,-}^{BO}$ (filled) $|\Psi_{b,-}^{BO}$ (dashed). In the model considered, the orbital coefficients do not depend on the distance $|(X, Z)|$ from the conical intersection. Compare with Fig. H.3.

Eq. H.22 is a gauge transformation, which removes the discontinuities except for the one at the conical intersection, i.e. for at the origin $R = 0$. At the conical intersection, the Born-Oppenheimer

⁸Using $\cos(x) = \frac{1}{2}(e^{ix} + e^{-ix})$ and $\sin(x) = \frac{1}{2i}(e^{ix} - e^{-ix})$

wave function is undetermined, which reflects that any unitary transformation of a degenerate set of eigenstates produces another, equally valid, set of eigenstates. We may fix this ambiguity by the choice that for $R = 0$ the value $\alpha = 0$ is taken.

Nevertheless the discontinuity at the origin remains. Discontinuities in the Born-Oppenheimer wave functions lead to δ -function-like contributions in the derivative couplings.

The important message is that the Born-Oppenheimer wave function near a conical intersection cannot be chosen real-valued without introducing steps in the wave function. This invalidates many arguments which indicate that the derivative couplings may be negligible.

Derivative couplings

The next step towards the equation of motion for the nuclear wave functions is to evaluate the derivative couplings.⁹

$$\vec{A}_{m,n}(X, Z) \stackrel{\text{Eq. 2.29}}{=} \left\langle \Psi_m^{BO}(\vec{R}) \left| \frac{\hbar}{i} \vec{\nabla}_{\vec{R}} \right| \Psi_n^{BO}(\vec{R}) \right\rangle \stackrel{\text{Eq. H.25}}{=} \left\langle \Psi_m^{BO}(\alpha) \left| \frac{\hbar}{i} \partial_\alpha \right| \Psi_n^{BO}(\alpha) \right\rangle \underbrace{\frac{1}{R^2} \begin{pmatrix} Z \\ -X \end{pmatrix}}_{\vec{\nabla}_{\vec{R}}\alpha(X,Z)} \tag{H.29}$$

With the Born-Oppenheimer wave functions from Eq. H.25 we obtain

$$\begin{aligned} \left\langle \Psi_+^{BO}(\vec{R}) \left| \partial_\alpha \right| \Psi_+^{BO}(\vec{R}) \right\rangle &= \left(\frac{1}{2}(e^{i\alpha} + 1) \right)^* \left(\frac{i}{2}e^{i\alpha} \right) + \left(-\frac{i}{2}(e^{i\alpha} - 1) \right)^* \left(\frac{1}{2}e^{i\alpha} \right) = \frac{i}{2} \\ \left\langle \Psi_+^{BO}(\vec{R}) \left| \partial_\alpha \right| \Psi_-^{BO}(\vec{R}) \right\rangle &= \left(\frac{1}{2}(e^{i\alpha} + 1) \right)^* \left(-\frac{1}{2}e^{i\alpha} \right) + \left(-\frac{i}{2}(e^{i\alpha} - 1) \right)^* \left(\frac{i}{2}e^{i\alpha} \right) = -\frac{1}{2} \\ \left\langle \Psi_-^{BO}(\vec{R}) \left| \partial_\alpha \right| \Psi_+^{BO}(\vec{R}) \right\rangle &= \left(\frac{i}{2}(e^{i\alpha} - 1) \right)^* \left(\frac{i}{2}e^{i\alpha} \right) + \left(\frac{1}{2}(e^{i\alpha} + 1) \right)^* \left(\frac{1}{2}e^{i\alpha} \right) = \frac{1}{2} \\ \left\langle \Psi_-^{BO}(\vec{R}) \left| \partial_\alpha \right| \Psi_-^{BO}(\vec{R}) \right\rangle &= \left(\frac{i}{2}(e^{i\alpha} - 1) \right)^* \left(-\frac{1}{2}e^{i\alpha} \right) + \left(\frac{1}{2}(e^{i\alpha} + 1) \right)^* \left(\frac{i}{2}e^{i\alpha} \right) = \frac{i}{2} \end{aligned} \tag{H.30}$$

which yields, with Eq. H.29, the first-derivative couplings

FIRST-DERIVATIVE COUPLINGS OF THE JAHN-TELLER MODEL

$$\vec{A}_{m,n}(\vec{R}) \stackrel{\text{Eq. H.29}}{=} \frac{\hbar}{2R^2} \begin{pmatrix} Z \\ -X \end{pmatrix} \times \begin{cases} 1 & \text{for } (m, n) = (+, +) \\ i & \text{for } (m, n) = (+, -) \\ -i & \text{for } (m, n) = (-, +) \\ 1 & \text{for } (m, n) = (-, -) \end{cases} \tag{H.31}$$

The derivative couplings are shown in fig. H.5.

⁹ use $\partial_x \text{atan}(x) = (1 + x^2)^{-1}$ and Eq. H.14

$$\alpha(X, Z) \stackrel{\text{Eq. H.14}}{=} \text{atan}\left(\frac{X}{Z}\right) - \frac{\pi}{2}(\text{sgn}(Z) - 1) \tag{H.27}$$

to obtain the gradient of α

$$\frac{\partial \alpha(X, Z)}{\partial X} = \left(1 + \left(\frac{X}{Z} \right)^2 \right)^{-1} \frac{1}{Z} = \frac{Z}{X^2 + Z^2} \quad \text{and} \quad \frac{\partial \alpha(X, Z)}{\partial Z} = \left(1 + \left(\frac{X}{Z} \right)^2 \right)^{-1} \frac{-X}{Z^2} = \frac{-X}{X^2 + Z^2} \tag{H.28}$$

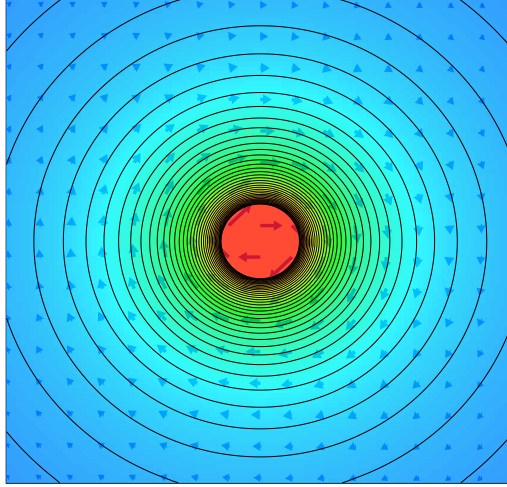


Fig. H.5: Derivative couplings $\vec{A}_{+,+}(X, Z) = \vec{A}_{-,-}(X, Z) = -i\vec{A}_{+,-}(X, Z) = +i\vec{A}_{-,+}(X, Z)$ of the Jahn-Teller model from Eq. H.31. The color-coding indicates the size of the derivative couplings, which falls off like $1/R$ from the conical intersection. The derivative couplings point along the circles in a clock-wise manner. The red plateau is due to a cutoff introduced for drawing purposes.

Geometric phase

The curl of the derivative couplings for a specific Born-Oppenheimer surface vanishes except for the conical intersection

$$\begin{aligned}\vec{\nabla} \times \vec{A} &= \partial_X A_{Z,n,n} - \partial_Z A_{X,n,n} \\ &= \partial_X \left(\frac{-\hbar X}{2R^2} \right) - \partial_Z \left(\frac{\hbar Z}{2R^2} \right) = -\frac{\hbar}{2} \left(\partial_X \frac{X}{R^2} + \partial_Z \frac{Z}{R^2} \right) \\ &\stackrel{R \neq 0}{=} -\frac{\hbar}{2} \left(\frac{1}{R^2} + \frac{1}{R^2} - \frac{2X X}{R^3} - \frac{2Z Z}{R^3} \right) = 0\end{aligned}\quad (\text{H.32})$$

The circular integral of the derivative couplings around the intersection is finite and independent of the distance.

$$\frac{1}{\hbar} \oint d\vec{R} \vec{A}_{n,n} = \frac{1}{\hbar} (2\pi R) \frac{\hbar}{2R} = \pi \quad (\text{H.33})$$

This is the so-called **geometric phase** or **Berry phase**[114].

Using Stokes' theorem¹⁰ we can show that the curl has the form of a delta function at the conical intersection

$$\vec{\nabla} \times \vec{A} = \hbar \pi \delta(\vec{R}) \quad (\text{H.35})$$

¹⁰Stokes' theorem

$$\int_F d\vec{A} \cdot \vec{\nabla} \times \vec{A}_{n,n} = \oint_{\partial F} d\vec{R} \vec{A}_{nn} \quad (\text{H.34})$$

Editor: This footnote ¹¹ is for later.

H.3.5 Nuclear Schrödinger equation

So-far we have worked out the ingredients for the nuclear Schrödinger equation of the Jahn-Teller model, namely the Born-Oppenheimer surfaces and the derivative couplings.

$$i\hbar\partial_t\Theta_m(\vec{R}, t) \stackrel{\text{Eq. 2.27}}{=} \sum_n \left[\frac{1}{2} \sum_k \left(\delta_{m,k} \frac{\hbar}{i} \vec{\nabla}_R + \vec{A}_{m,k}(\vec{R}) \right) \mathbf{M}^{-1} \left(\delta_{k,n} \frac{\hbar}{i} \vec{\nabla}_R + \vec{A}_{k,n}(\vec{R}) \right) + \delta_{m,n} E_m^{BO}(\vec{R}) \right] \Theta_n(\vec{R}, t) \quad (\text{H.37})$$

For the sake of completeness, let me write down the nuclear Schrödinger equation. The purpose of this is to provide a glimpse of the complexity and the overall structure of it. This Schrödinger equation contains a lot of interesting aspects, which are described in appendix H.4 on p. 479.

$$i\hbar\partial_t\Theta_{\pm}(\vec{R}, t) = \left[\frac{1}{2M} \left(\frac{\hbar}{i} \vec{\nabla}_R + \vec{A}_{\pm,\pm}(\vec{R}) \right)^2 + \frac{1}{2M} \left| \vec{A}_{\pm,\mp}(\vec{R}) \right|^2 + E_{\pm}^{BO}(\vec{R}) \right] \Theta_{\pm}(\vec{R}, t) + \underbrace{\left[\frac{1}{2M} \left(\frac{\hbar}{i} \vec{\nabla}_R + \vec{A}_{\pm,\pm}(\vec{R}) \right) \vec{A}_{\pm,\mp}(\vec{R}) + \frac{1}{2M} \vec{A}_{\pm,\mp}(\vec{R}) \left(\frac{\hbar}{i} \vec{\nabla}_R + \vec{A}_{\mp,\mp}(\vec{R}) \right) \right]}_{\frac{1}{2M} \left[\frac{\hbar}{i} \vec{\nabla}_R, \vec{A}_{\pm,\mp}(\vec{R}) \right] + \frac{1}{M} \vec{A}_{\pm,\mp}(\vec{R}) \left(\frac{\hbar}{i} \vec{\nabla}_R + \vec{A}_{\mp,\mp}(\vec{R}) \right)} \Theta_{\mp}(\vec{R}, t) \quad (\text{H.38})$$

Let me introduce a short-hand

$$\begin{aligned} \vec{a}(\vec{R}) &= \vec{A}_{\pm,\pm} = \vec{A}_{\mp,\mp} \\ \vec{A}_{\pm,\mp} &= i\vec{a}(\vec{R}) \\ \vec{A}_{\mp,\pm} &= -i\vec{a}(\vec{R}) \end{aligned} \quad (\text{H.39})$$

$$\begin{aligned} \vec{a} &= \frac{\hbar}{R^2} \begin{pmatrix} Z \\ -X \end{pmatrix} = \frac{\hbar}{2} \begin{pmatrix} \partial_Z \\ -\partial_X \end{pmatrix} \ln(X^2 + Z^2) = \frac{\hbar}{2} \vec{e}_y \times \vec{\nabla} \ln(X^2 + Z^2) \\ \vec{a} &= \frac{\hbar}{2} \vec{\nabla}_R \alpha(\vec{R}) \\ \vec{\nabla} \vec{a} &= \frac{\hbar}{2} \vec{\nabla} (\vec{e}_y \times \vec{\nabla}) \ln(X^2 + Z^2) = \frac{\hbar}{2} \vec{e}_y (\vec{\nabla} \times \vec{\nabla}) \ln(X^2 + Z^2) = 0 \quad \text{for } \vec{R} \neq \vec{0} \\ \vec{a}^2 &= \frac{\hbar^2}{4R^2} \end{aligned} \quad (\text{H.40})$$

¹¹

$$\begin{pmatrix} 0 \\ 1 \\ 0 \end{pmatrix} \times \begin{pmatrix} \partial_X \\ \partial_Y \\ \partial_Z \end{pmatrix} \ln(|\vec{R}|) = \begin{pmatrix} \partial_Z \\ 0 \\ -\partial_X \end{pmatrix} \ln(|\vec{R}|) = \frac{1}{|\vec{R}|} \begin{pmatrix} \partial_Z \\ 0 \\ -\partial_X \end{pmatrix} |\vec{R}| = \frac{1}{R^2} \begin{pmatrix} Z \\ 0 \\ -X \end{pmatrix} = \vec{\nabla}_R \alpha(X, Z) \quad (\text{H.36})$$

$$\begin{aligned}
 i\hbar\partial_t\Theta_{\pm}(\vec{R}, t) &= \left[\frac{1}{2M} \left(\frac{\hbar}{i} \vec{\nabla}_R + \vec{a}(\vec{R}) \right)^2 + \frac{\hbar^2}{8MR^2} + wR^2 \pm g|R| \right] \Theta_{\pm}(\vec{R}, t) \\
 &\quad + \frac{i}{M} \left[\vec{a}(\vec{R}) \frac{\hbar}{i} \vec{\nabla}_R + \frac{\hbar^2}{4R^2} \right] \Theta_{\mp}(\vec{R}, t) \\
 \text{with } \vec{a} &= \frac{\hbar}{2} \vec{\nabla} \alpha(\vec{R})
 \end{aligned} \tag{H.41}$$

Once the nuclear wave function has been obtained, it is combined with the Born-Oppenheimer wave function to the full nuclear-electronic wave function.

H.4 Nuclear wave function of the Jahn-Teller model

H.4.1 Nuclear Schrödinger equation of the Jahn-Teller model

In section H.3 on p. 469 we evaluated the Born-Oppenheimer surfaces from Eq. H.17, the electronic Born-Oppenheimer wave functions from Eq. H.25 and the derivative couplings from Eq. H.31. Thus, we can set up the Schrödinger equation Eq. 2.27 for the nuclei.

$$\begin{aligned}
 i\hbar\partial_t\Theta_{\pm} \stackrel{\text{Eq. 2.27}}{=} &\left\{ \frac{1}{2M} \left[\frac{\hbar}{i} \vec{\nabla} + \vec{A}_{\pm,\pm} \right]^2 + \frac{1}{2M} \vec{A}_{\pm,\mp} \vec{A}_{\mp,\pm} + E_{\pm}^{BO} \right\} \Theta_{\pm} \\
 &+ \frac{1}{2M} \left\{ \left[\frac{\hbar}{i} \vec{\nabla} + \vec{A}_{\pm,\pm} \right] \vec{A}_{\pm,\mp} + \vec{A}_{\pm,\mp} \left[\frac{\hbar}{i} \vec{\nabla} + \vec{A}_{\mp,\mp} \right] \right\} \Theta_{\mp}
 \end{aligned} \tag{H.42}$$

Let me translate the Schrödinger equation into polar coordinates defined in Eq. H.13 with Eq. ???. This yields

$$\frac{\hbar}{i} \vec{\nabla} + \vec{A}_{n,n} = \underbrace{\begin{pmatrix} \sin(\alpha) \\ \cos(\alpha) \end{pmatrix} \frac{\hbar}{i} \partial_R}_{(a)} + \underbrace{\begin{pmatrix} \cos(\alpha) \\ -\sin(\alpha) \end{pmatrix} \frac{\hbar}{iR} \partial_{\alpha}}_{(b)} + \underbrace{\frac{\hbar}{2R} \begin{pmatrix} \cos(\alpha) \\ -\sin(\alpha) \end{pmatrix}}_{(c)} \tag{H.43}$$

so that

$$\begin{aligned}
 \left(\frac{\hbar}{i} \vec{\nabla} + \vec{A}_{n,n} \right)^2 &= \underbrace{-\hbar^2 \partial_R^2}_{(aa)} - \underbrace{\frac{\hbar^2}{R} \partial_R}_{ba} - \underbrace{\frac{\hbar^2}{R^2} \partial_{\alpha}^2}_{bb} + \underbrace{\frac{\hbar^2}{iR^2} \partial_{\alpha}}_{bc+cb} + \underbrace{\frac{\hbar^2}{4R^2}}_{cc} \\
 &= \frac{-\hbar^2 (R^2 \partial_R^2 + R \partial_R + \partial_{\alpha}^2)}{R^2} + \frac{\hbar^2}{R^2} \left(-i \partial_{\alpha} + \frac{1}{4} \right)
 \end{aligned} \tag{H.44}$$

$$\begin{aligned}
 \vec{A}_{\pm,\mp} \left(\frac{\hbar}{i} \vec{\nabla} + \vec{A}_{\mp,\mp} \right) &= \pm \frac{i\hbar}{2R} \begin{pmatrix} \cos(\alpha) \\ -\sin(\alpha) \end{pmatrix} \cdot \underbrace{\begin{pmatrix} \sin(\alpha) \\ \cos(\alpha) \end{pmatrix} \frac{\hbar}{i} \partial_R}_{=0} \pm \left(\frac{\hbar^2}{2R^2} \partial_{\alpha} + \frac{i\hbar^2}{4R^2} \right) \\
 &= \pm i \frac{\hbar^2}{2R^2} \left(-i \partial_{\alpha} + \frac{1}{2} \right)
 \end{aligned} \tag{H.45}$$

$$\left(\frac{\hbar}{i} \vec{\nabla} + \vec{A}_{\pm,\pm} \right) \vec{A}_{\pm,\mp} = \pm \left(\frac{\hbar^2}{2R^2} \partial_{\alpha} + \frac{i\hbar^2}{4R^2} \right) = \pm i \frac{\hbar^2}{2R^2} \left(-i \partial_{\alpha} + \frac{1}{2} \right) \tag{H.46}$$

$$\vec{A}_{\pm,\mp} \vec{A}_{\mp,\pm} = \frac{\hbar^2}{4R^2} \tag{H.47}$$

In polar coordinates, Eq. H.42 has thus the form

$$i\hbar\partial_t\Theta_{\pm} = \left\{ \underbrace{\frac{-\hbar^2(R^2\partial_R^2 + R\partial_R + \partial_{\alpha}^2)}{2MR^2}}_{-\hbar^2\bar{\nabla}^2/2M} + \underbrace{\frac{\hbar^2(-i\partial_{\alpha} + \frac{1}{4})}{2MR^2}}_{\text{nonBO}} \right\} + \underbrace{\frac{\hbar^2}{8MR^2}}_{\text{nonBO}} \underbrace{\pm gR + wR^2}_{E_{\pm}^{BO}} \Theta_{\pm}(R, \alpha, t) \\ \pm i \underbrace{\frac{\hbar^2(-i\partial_{\alpha} + \frac{1}{2})}{2MR^2}}_{\text{nonBO}} \Theta_{\mp}(R, \alpha, t) \quad (\text{H.48})$$

This equation can be rewritten in two-component form

$$\Rightarrow i\hbar\partial_t \begin{pmatrix} \Theta_+ \\ \Theta_- \end{pmatrix} = \underbrace{\frac{-\hbar^2(R^2\partial_R^2 + R\partial_R + \partial_{\alpha}^2)}{2MR^2}}_{-\hbar^2\bar{\nabla}^2/(2M)} \begin{pmatrix} \Theta_+ \\ \Theta_- \end{pmatrix} + \begin{pmatrix} (+gR + wR^2)\Theta_+ \\ (-gR + wR^2)\Theta_- \end{pmatrix} \\ + \underbrace{\frac{\hbar^2(-i\partial_{\alpha} + \frac{1}{2})}{2MR^2}}_{\text{nonBO}} \begin{pmatrix} 1 & i \\ -i & 1 \end{pmatrix} \begin{pmatrix} \Theta_+ \\ \Theta_- \end{pmatrix} \quad (\text{H.49})$$

Now, I shift a factor i into Θ_+ , because this will lead to a radial Schrödinger equation with real-valued coefficients. $i\Theta_+$, being a real-valued function, implies that Θ_+ is purely imaginary.

$$i\hbar\partial_t \begin{pmatrix} i\Theta_+ \\ \Theta_- \end{pmatrix} = \underbrace{\frac{-\hbar^2(R^2\partial_R^2 + R\partial_R + \partial_{\alpha}^2)}{2MR^2}}_{-\hbar^2\bar{\nabla}^2/(2M)} \begin{pmatrix} i\Theta_+ \\ \Theta_- \end{pmatrix} + \begin{pmatrix} (+gR + wR^2)i\Theta_+ \\ (-gR + wR^2)\Theta_- \end{pmatrix} \\ + \frac{\hbar^2(-i\partial_{\alpha} + \frac{1}{2})}{2MR^2} \begin{pmatrix} 1 & -1 \\ -1 & 1 \end{pmatrix} \begin{pmatrix} i\Theta_+ \\ \Theta_- \end{pmatrix} \\ = \left\{ \underbrace{\frac{-\hbar^2(R^2\partial_R^2 + R\partial_R + \partial_{\alpha}^2)}{2MR^2}}_{-\hbar^2\bar{\nabla}^2/(2M)} \mathbf{1} + gR\sigma_z + wR^2\mathbf{1} + \underbrace{\frac{\hbar^2(-i\partial_{\alpha} + \frac{1}{2})}{2MR^2}}_{\text{nonBO}} (\mathbf{1} - \sigma_x) \right\} \begin{pmatrix} i\Theta_+ \\ \Theta_- \end{pmatrix} \quad (\text{H.50})$$

This nuclear Schrödinger equation has a rotational symmetry, because the angular coordinate α does not enter in the differential operator. Only the angular derivative ∂_{α} enters. Therefore, I decompose the nuclear wave function into angular-momentum eigenstates. The angular-momentum eigenstates are further divided into the eigenstates of the nuclear Hamiltonian.¹²

$$\Theta_{\pm}(\alpha, R, t) = \sum_m e^{im\alpha} \sum_j e^{-\frac{i}{\hbar}\mathcal{E}_{j,m}t} \mathcal{R}_{\pm,j,m}(R) c_{j,m} \quad (\text{H.51})$$

The energies $\mathcal{E}_{m,j}$ are the those of the complete system including electronic and nuclear degrees of freedom. The angular-momentum quantum numbers m extend from $-\infty$ to $+\infty$. They are integer, so that the wave function is single valued.

Once the radial functions $\mathcal{R}_{\pm,m,j}(R)$ and its energies $\mathcal{E}_{m,j}$ are known, we can reconstruct the full wave function by multiplying this nuclear wave function with the Born-Oppenheimer wave functions.

$$|\Phi(t)\rangle = \sum_{\pm,m,j} \int dX \int dZ \left(|a, X, Z\rangle \Psi_{a,\pm}^{BO}(R, \alpha) + |b, X, Z\rangle \Psi_{b,\pm}^{BO}(R, \alpha) \right) \mathcal{R}_{\pm,j,m}(R) e^{im\alpha} e^{-\frac{i}{\hbar}\mathcal{E}_{j,m}t} c_{j,m} \quad (\text{H.52})$$

¹²Another way of looking at this is: After multiplication with $2MR^2$, the Hamiltonian is the sum of an angular and a radial Hamiltonian. This allows to separate the angular and radial variables (see section 4.3 of Φ SX:Quantum Theory [4]) and use a product ansatz.

Here, $R = \sqrt{X^2 + Z^2}$ and $\alpha = \text{atan}\left(\frac{X}{Z}\right)$ are direct functions of the nuclear coordinates (X, Z) .

We insert the Born-Oppenheimer wave functions from Eq. H.25 to obtain the final form of the electronic-nuclear wave function.

ELECTRONIC-NUCLEAR WAVE FUNCTION FOR THE JAHN-TELLER MODEL

The complete electronic nuclear wave functions expressed in terms of the two electronic e_g orbitals $|\vec{a}\rangle$ and $|\vec{b}\rangle$ and the generalized nuclear coordinates (X, Z) . Eq. H.13 connects the angular and radial variables α and R to (X, Z) .

$$|\Phi(t)\rangle = \sum_{m,j} |\Phi_{j,m}\rangle e^{-\frac{i}{\hbar} \mathcal{E}_{j,m} t} c_{j,m} \quad (\text{H.53})$$

The complex-valued coefficients $c_{j,m} = \langle \Phi_{j,m} | \Phi(0) \rangle$ are defined by the initial conditions. The eigenstates of the Hamiltonian are

$$|\Phi_{j,m}\rangle = \int dX \int dZ \frac{1}{2} \left(|a, X, Z\rangle \left[(e^{i\alpha} + 1) \mathcal{R}_{+,j,m}(R) + i(e^{i\alpha} - 1) \mathcal{R}_{-,j,m}(R) \right] \right. \\ \left. + |b, X, Z\rangle \left[-i(e^{i\alpha} - 1) \mathcal{R}_{+,j,m}(R) + (e^{i\alpha} + 1) \mathcal{R}_{-,j,m}(R) \right] \right) e^{im\alpha} \quad (\text{H.54})$$

The radial components are obtained from Eq. H.50 with the ansatz Eq. H.51 for the nuclear wave functions. Thus, the defining equation is

$$\left\{ \underbrace{\frac{-\hbar^2 (R^2 \partial_R^2 + R \partial_R - m^2)}{2MR^2}}_{-\hbar^2 \vec{\nabla}^2 / (2M)} \mathbf{1} + \underbrace{gR\sigma_z + wR^2 \mathbf{1}}_{E^{BO}} - \mathcal{E}_{j,m} \mathbf{1} \right. \\ \left. + \underbrace{\frac{\hbar^2 (m + \frac{1}{2})}{2MR^2} (\mathbf{1} - \sigma_x)}_{\text{nonBO}} \right\} \begin{pmatrix} i\mathcal{R}_{+,j,m}(R) \\ \mathcal{R}_{-,j,m}(R) \end{pmatrix} \stackrel{\text{Eq. H.50}}{=} 0 \quad (\text{H.55})$$

The radial equation is a two-component system of coupled ordinary differential equations. It can be solved either by a power-series ansatz, or by numerical integration of the differential equation.

The radial nuclear wave functions are shown in Fig. H.6. For low energies, the wave packet lies in the circular valley of the ground-state Born-Oppenheimer surface. With increasing energy, the number of radial nodes increases. At the same time, also the contribution of the excited-state Born-Oppenheimer surface grows. At higher energies, the wave function looks like a combination of a ground-state and an excited-state Born-Oppenheimer wave function at about the same energy. Thus, the ground-state contribution is spread over a wide region and has short oscillations due to the high kinetic energy. The excited-state surface has no or less nodes and it is localized around the center, which is the minimum of the excited-state Born-Oppenheimer surface.

What can be learned from this equation?

- At first we see that the eigenstates have contribution on both the upper and the lower sheet of the Born-Oppenheimer surface. This coupling, indicated in Eq. H.55 as “nonBO”, is scaled with the inverse mass. This seems to indicate that non-adiabatic effects become less important when the nuclear masses are large (in comparison to the electron mass.) However, the non-adiabatic coupling also diverges at the position of the conical intersection. That is, it cannot be ignored however large the nuclear masses are.
- An important observation is that the eigenstates are no angular-momentum eigenstates. In addition to the term $e^{im\alpha}$ related to the nuclear wave function, there are also terms $e^{i\alpha}$ from the Born-Oppenheimer wave function. Taken together, this implies that the eigenstates contain components from two angular momenta, namely $L_z = \hbar m$ and $L_z = \hbar(m + 1)$. It is as if the

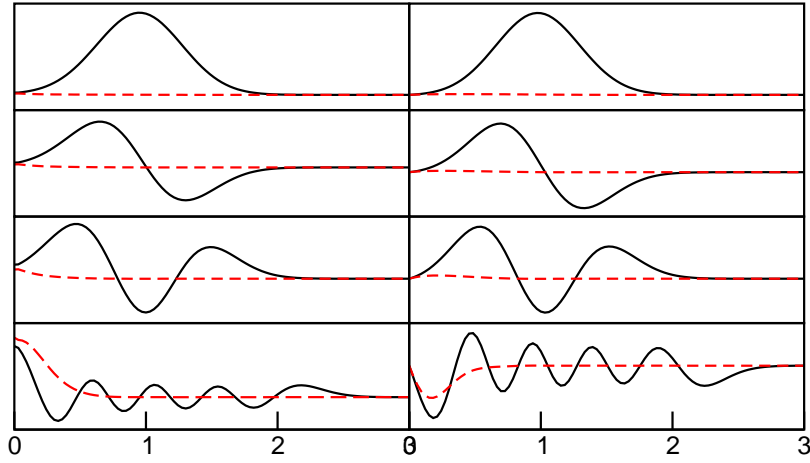


Fig. H.6: Radial nuclear wave functions $\mathcal{R}_{\pm j,m}(R)$ for the Jahn-Teller model for $j = 0, 1, 2$ and $j = 9$ from top to bottom and for $m = 0$ left and $m = 1$ right. The ground-state component is shown as black full line, and the component on the excited Born-Oppenheimer surface is shown as red dashed line. The energies for $m = 0$ are $E_{j,m} = -0.89705, -0.69574, -0.49290, +0.80876$ for $j = 0, 1, 2, 9$ and $m = 0$ and $E_{j,m} = -0.87415, -0.66431, -0.44920, +0.98900$ for $j = 0, 1, 2, 9$ and $m = 1$. The model parameters are $M = \frac{1}{2}$, $g_{JT} = 2$ and $w_{JT} = 1$. The conical intersection is at $E = 0$ and the minimum of the ground-state Born-Oppenheimer surface lies at $E = -1$ and $R = 1$.

conical intersection would have its own pseudo-spin of $\pm \frac{1}{2} \hbar$, which may interact with the nuclear “orbital motion”.

- Even though the Schrödinger equation is purely real-valued, the Born-Oppenheimer wave functions at a conical intersection cannot be chosen real-valued and at the same time continuous.
- The stationary wave functions for m and $-m - 1$ are complex conjugates of each other, i.e.

$$\Phi_{j,-m-1}(\vec{r}, X, Z) = \Phi_{j,m}^*(\vec{r}, X, Z) \quad (\text{H.56})$$

and the same holds for the radial functions

$$\left(\mathcal{R}_{\pm j,-m-1}(R) \right)^* = \mathcal{R}_{\pm j,m}(R) \quad \Leftrightarrow \quad \begin{cases} \mathcal{R}_{-j,-m-1}(R) = -\mathcal{R}_{-j,m}(R) \\ \mathcal{R}_{+j,-m-1}(R) = +\mathcal{R}_{+j,m}(R) \end{cases} \quad (\text{H.57})$$

and the energies are related by $\mathcal{E}_{j,-m-1} = \mathcal{E}_{j,m}$. This implies that the corresponding solutions of the stationary Schrödinger equation are complex conjugates of each other. The derivation of Eq. H.56 and Eq. H.57 is given in Appendix H.4.2 on p. 482.

H.4.2 Relation of stationary wave functions for m and $-m - 1$

In Eq. H.56 and Eq. H.57 on p. 482 we mentioned that the electron-nuclear wave functions $\Phi_{j,m}(\vec{x}, X, Z)$ and $\Phi_{j,-m-1}(\vec{x}, X, Z)$ are complex conjugates of each other.¹³

$$\Phi_{j,-m-1}(\vec{x}, X, Z) = \Phi_{j,m}^*(\vec{x}, X, Z) \quad (\text{H.58})$$

¹³More precisely, they can be chosen to be complex conjugates of each other.

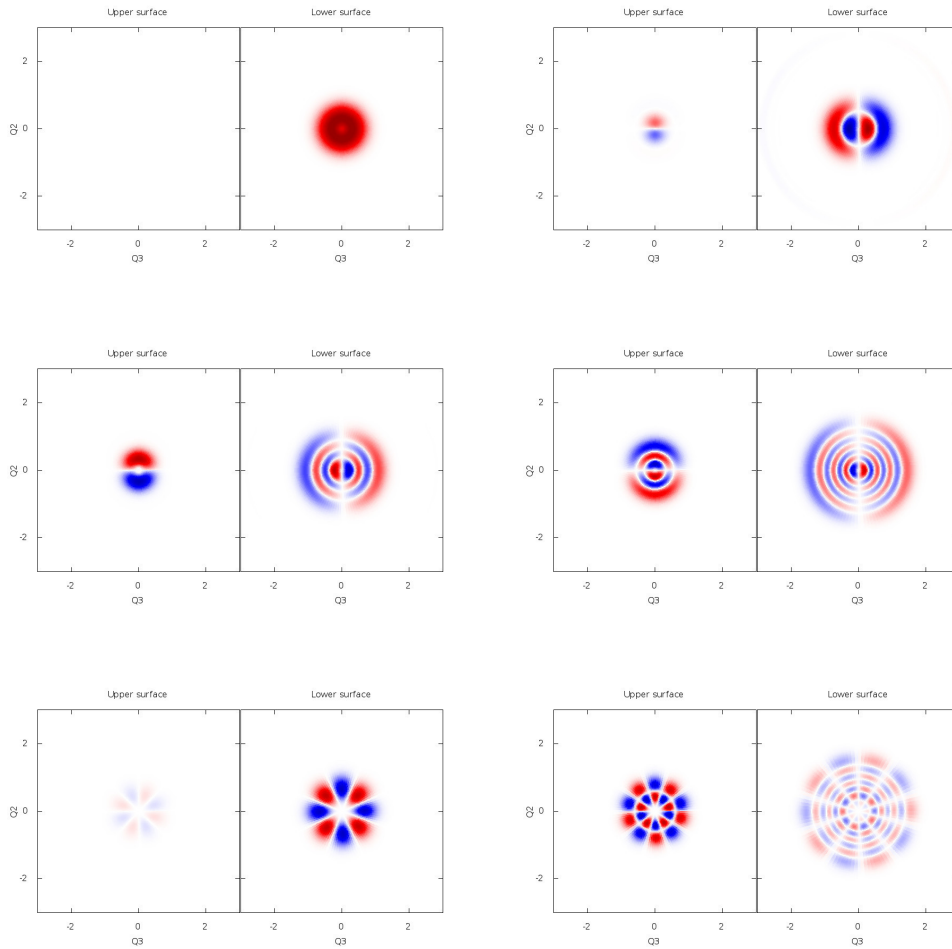


Fig. H.7: Nuclear wave functions of the Jahn-Teller model at specific energies and with given angular momenta. Each graph as two squares, one (left) for the ground-state contribution and another one n(right) for the first excited-state contribution. Blue and read intensities mark positive and negative amplitudes of the wave function. (With friendly permission of M. Ten Brink.)

and that the same holds for the radial functions

$$\left(\mathcal{R}_{\pm j, -m-1}(R)\right)^* = \mathcal{R}_{\pm j, m}(R) \quad \Leftrightarrow \quad \begin{cases} \mathcal{R}_{-j, -m-1}(R) = -\mathcal{R}_{-j, m}(R) \\ \mathcal{R}_{+j, -m-1}(R) = +\mathcal{R}_{+j, m}(R) \end{cases} \quad (\text{H.59})$$

Here, we provide the detailed derivation.

Complex conjugation of the radial nuclear wave function: We start from the equation Eq. H.50 for $\mathcal{R}_{\pm j, -m-1}$

$$\begin{aligned}
& \left\{ \underbrace{\frac{-\hbar^2 (R^2 \partial_R^2 + R \partial_R - (-m-1)^2)}{2MR^2}}_{-\hbar^2 \nabla^2 / (2M)} \mathbf{1} + \underbrace{gR\sigma_z + wR^2 \mathbf{1}}_{E^{BO}} \right. \\
& \left. + \underbrace{\frac{\hbar^2 ((-m-1) + \frac{1}{2})}{2MR^2} (\mathbf{1} - \sigma_x) - \mathcal{E}_{j,m} \mathbf{1}}_{\text{nonBO}} \right\} \begin{pmatrix} i\mathcal{R}_{+j, -m-1}(R) \\ \mathcal{R}_{-j, -m-1}(R) \end{pmatrix} \stackrel{\text{Eq. H.55}}{=} 0 \\
\Rightarrow & \left\{ \frac{-\hbar^2 (R^2 \partial_R^2 + R \partial_R - m^2) + \overbrace{2\hbar^2 (m + \frac{1}{2})}^{2A}}{2MR^2} \mathbf{1} + gR\sigma_z + wR^2 \mathbf{1} \right. \\
& \left. + \frac{\hbar^2 (m + \frac{1}{2})}{2MR^2} \underbrace{(-\mathbf{1})}_{-A} + \underbrace{\sigma_x}_B - \mathcal{E}_{j,m} \mathbf{1} \right\} \begin{pmatrix} i\mathcal{R}_{+j, -m-1}(R) \\ \mathcal{R}_{-j, -m-1}(R) \end{pmatrix} = 0
\end{aligned} \tag{H.60}$$

The term denoted $2A$ combines with the term $-A$. The term B is the only coupling term between the two components of the wave function. A sign change of this term can be absorbed by a sign change of one component relative to the other. Thus, we arrive at

$$\begin{aligned}
& \left\{ \frac{-\hbar^2 (R^2 \partial_R^2 + R \partial_R - m^2)}{2MR^2} \mathbf{1} + gR\sigma_z + wR^2 \mathbf{1} \right. \\
& \left. + \frac{\hbar^2 (m + \frac{1}{2})}{2MR^2} (\mathbf{1} - \sigma_x) - \mathcal{E}_{j,m} \mathbf{1} \right\} \begin{pmatrix} -i\mathcal{R}_{+j, -m-1}(R) \\ \mathcal{R}_{-j, -m-1}(R) \end{pmatrix} = 0
\end{aligned} \tag{H.61}$$

This is the equation for the index m . Thus, if the solution for m is known, we immediately know the solution for $-m-1$ by the transformation Eq. H.57, which completes the proof of Eq. H.59.

Complex conjugation of the electron-nuclear wave function: Next, we need to show that also the electron nuclear wave function Eq. H.54 obey

$$\langle \vec{x}, X, Z | \Phi_{j,m} \rangle = \langle \vec{x}, X, Z | \Phi_{j, -m-1} \rangle^* \tag{H.62}$$

We start with Eq. H.54 with m replaced by $-m-1$. We use that $\mathcal{R}_{+j,m}$ is purely imaginary and that $\mathcal{R}_{-j,m}$ is purely real.

$$\begin{aligned}
\langle \vec{x}, X, Z | \Phi_{j, -m-1} \rangle & \stackrel{\text{Eq. H.54}}{=} \frac{1}{2} \left(\langle \vec{x} | a \rangle \left[(e^{i\alpha} + 1) \mathcal{R}_{+j, -m-1}(R) + i(e^{i\alpha} - 1) \mathcal{R}_{-j, -m-1}(R) \right] \right. \\
& \left. + \langle \vec{x} | b \rangle \left[-i(e^{i\alpha} - 1) \underbrace{\mathcal{R}_{+j, -m-1}(R)}_{\mathcal{R}_{+j,m}^*(R)} + (e^{i\alpha} + 1) \underbrace{\mathcal{R}_{-j, -m-1}(R)}_{\mathcal{R}_{+j,m}^*(R)} \right] \right) e^{i(-m-1)\alpha} \\
& \stackrel{\text{Eq. H.59}}{=} \left[\frac{1}{2} \left(\langle \vec{x} | a \rangle^* \left[(e^{-i\alpha} + 1) \mathcal{R}_{+j,m}(R) - i(e^{-i\alpha} - 1) \mathcal{R}_{-j,m}(R) \right] \right. \right. \\
& \left. \left. + \langle \vec{x} | b \rangle^* \left[i(e^{-i\alpha} - 1) \mathcal{R}_{+j, -m-1}(R) + (e^{-i\alpha} + 1) \mathcal{R}_{-j, -m-1}(R) \right] \right) e^{i(m+1)\alpha} \right]^* \\
& = \left[\frac{1}{2} \left(\langle \vec{x} | a \rangle^* \left[(e^{i\alpha} + 1) \mathcal{R}_{+j,m}(R) + i(e^{i\alpha} - 1) \mathcal{R}_{-j,m}(R) \right] \right. \right. \\
& \left. \left. - \langle \vec{x} | b \rangle^* \left[+i(e^{i\alpha} - 1) \mathcal{R}_{+j,m}(R) + (e^{i\alpha} + 1) \mathcal{R}_{-j,m}(R) \right] \right) e^{i m \alpha} \right]^* \\
& \stackrel{\text{Eq. H.54}}{=} \langle \vec{x}, X, Z | \Phi_{j,m} \rangle^*
\end{aligned} \tag{H.63}$$

which completes the proof that the electron-nuclear wave functions for m and $-m - 1$ are complex conjugates of each other.

H.4.3 Behavior of the radial nuclear wave function at the origin

In order to obtain a solution of a radial Schrödinger equation such as Eq. H.55, it is always helpful to know the behavior at the origin, which will be shown here.

At the origin the derivative couplings and the kinetic energy dominate the behavior of the wave function. Let me analyze this behavior. We start with a Taylor expansion:

$$\mathcal{R}_{\pm} = \sum_n a_{\pm,n} R^n \quad (\text{H.64})$$

Insertion of the power-series ansatz into Eq. H.55 yields

$$\begin{aligned} 0 &= \left\{ \frac{-\hbar^2 (n(n-1) + n - m^2)}{2M} \mathbf{1} + \underbrace{\frac{\hbar^2 (m + \frac{1}{2})}{2M} (\mathbf{1} - \sigma_x)}_{\text{nonBO}} \right\} \begin{pmatrix} ia_{+,n} \\ a_{-,n} \end{pmatrix} \\ &\quad + g\sigma_z \begin{pmatrix} ia_{+,n-3} \\ a_{-,n-3} \end{pmatrix} + w \begin{pmatrix} ia_{+,n-4} \\ a_{-,n-4} \end{pmatrix} - \mathcal{E} \begin{pmatrix} ia_{+,n-2} \\ a_{-,n-2} \end{pmatrix} \\ &= \frac{\hbar^2}{2M} \left\{ (-n^2 + m^2) \mathbf{1} + \underbrace{\left(m + \frac{1}{2}\right) (\mathbf{1} - \sigma_x)}_{\text{nonBO}} \right\} \begin{pmatrix} ia_{+,n} \\ a_{-,n} \end{pmatrix} \\ &\quad + g\sigma_z \begin{pmatrix} ia_{+,n-3} \\ a_{-,n-3} \end{pmatrix} + w \begin{pmatrix} ia_{+,n-4} \\ a_{-,n-4} \end{pmatrix} - \mathcal{E} \begin{pmatrix} ia_{+,n-2} \\ a_{-,n-2} \end{pmatrix} \end{aligned} \quad (\text{H.65})$$

This equation can be written as a recursive equation for the coefficients with increasing order

$$\begin{aligned} \begin{pmatrix} ia_{+,n} \\ a_{-,n} \end{pmatrix} &= \frac{2M}{\hbar^2} \left\{ (-n^2 + m^2) \mathbf{1} + \underbrace{\left(m + \frac{1}{2}\right) (\mathbf{1} - \sigma_x)}_{\text{nonBO}} \right\}^{-1} \\ &\quad \times \left\{ w \begin{pmatrix} ia_{+,n-4} \\ a_{-,n-4} \end{pmatrix} + g\sigma_z \begin{pmatrix} ia_{+,n-3} \\ a_{-,n-3} \end{pmatrix} - \mathcal{E} \begin{pmatrix} ia_{+,n-2} \\ a_{-,n-2} \end{pmatrix} \right\} \end{aligned} \quad (\text{H.66})$$

We start the expansion with zero coefficients, i.e. $a_{\pm,n} = 0$ for all n below a minimum. The iteration produces non-zero elements only if the inverted matrix is singular. Thus, we need to look for the indices where an eigenvalue of $(-n^2 + m^2) \mathbf{1} + (m + \frac{1}{2}) (\mathbf{1} - \sigma_x)$ vanishes.

Thus, the leading order of the nuclear wave function is determined by the zero of the determinant of the above matrix.

$$\begin{aligned} \det \begin{vmatrix} -n^2 + m^2 + m + \frac{1}{2} & -(m + \frac{1}{2}) \\ -(m + \frac{1}{2}) & -n^2 + m^2 + m + \frac{1}{2} \end{vmatrix} &= 0 \\ \Rightarrow \left(-n^2 + m^2 + m + \frac{1}{2}\right)^2 - \left(m + \frac{1}{2}\right)^2 &= 0 \\ \Rightarrow n^2 = m^2 + m + \frac{1}{2} \pm \left(m + \frac{1}{2}\right) & \\ \Rightarrow n = \pm(m + 1) \quad \text{or} \quad n = \pm m & \end{aligned} \quad (\text{H.67})$$

Thus, we obtain four solutions for the leading order n , of which two correspond to regular solutions of the differential equation and two further ones correspond to the irregular solutions.

m	$n_{reg,1}$	$n_{reg,2}$	$n_{irr,1}$	$n_{irr,2}$
$m \geq 0$	m	$m+1$	$-m$	$-m+1$
2	2	3	-2	-3
1	1	2	-1	-2
0	0	1	0	-1
-1	0	1	0	-1
-2	1	2	-1	-2
-3	2	3	-2	-3
$- m $	$ m -1$	$ m $	$- m +1$	$- m $

What is the meaning of having two orders where the power series may start? They correspond to two independent solutions. Two independent solutions rather than one occur because the nuclear Schrödinger equation of the Jahn-Teller problem is a two-component equation. Giving the leading order n_0 the next higher power determined by the recursion Eq. H.66 is n_0+2 . An independent power series expansion can be started with n_0+1 .

Next we need to determine the null vectors. We distinguish the cases with $m \geq 0$ and with $m < 0$. (Note that the eigenvectors of the inverse are the eigenvectors of the original matrix.)

- first we consider $m \geq 0$:

$$\begin{aligned}
 0 &= (-n^2 + m^2) \mathbf{1} + \underbrace{\left(m + \frac{1}{2}\right) (\mathbf{1} - \sigma_x)}_{\text{nonBO}} \begin{pmatrix} ia_{+,n} \\ a_{-,n} \end{pmatrix} \\
 \stackrel{n=m}{=} &\left(m + \frac{1}{2}\right) \begin{pmatrix} 1 & -1 \\ -1 & 1 \end{pmatrix} \begin{pmatrix} ia_{+,m} \\ a_{-,m} \end{pmatrix} \Rightarrow \begin{pmatrix} ia_{+,m} \\ a_{-,m} \end{pmatrix} = \begin{pmatrix} 1 \\ 1 \end{pmatrix} A_m \quad (\text{H.68})
 \end{aligned}$$

where A_m is an arbitrary coefficient. Now, we consider the second regular solution

$$\begin{aligned}
 0 &= (-n^2 + m^2) \mathbf{1} + \underbrace{\left(m + \frac{1}{2}\right) (\mathbf{1} - \sigma_x)}_{\text{nonBO}} \begin{pmatrix} ia_{+,n} \\ a_{-,n} \end{pmatrix} \\
 \stackrel{n=m+1}{=} &\left(m + \frac{1}{2}\right) \begin{pmatrix} 1 & 1 \\ 1 & 1 \end{pmatrix} \begin{pmatrix} ia_{+,m} \\ a_{-,m} \end{pmatrix} \Rightarrow \begin{pmatrix} ia_{+,m} \\ a_{-,m} \end{pmatrix} = \begin{pmatrix} -1 \\ 1 \end{pmatrix} B_m \cdot A_m \quad (\text{H.69})
 \end{aligned}$$

where B is another arbitrary coefficient.

Thus, the wave function for $m \geq 0$ has the form

$$\begin{pmatrix} i\mathcal{R}_+(R) \\ \mathcal{R}_-(R) \end{pmatrix} = AR^m \begin{pmatrix} 1 - BR + O(R^2) \\ 1 + BR + O(R^2) \end{pmatrix} \quad (\text{H.70})$$

- now we consider $m < 0$:

$$\begin{aligned}
 0 &= (-n^2 + m^2) \mathbf{1} + \underbrace{\left(m + \frac{1}{2}\right) (\mathbf{1} - \sigma_x)}_{\text{nonBO}} \begin{pmatrix} ia_{+,n} \\ a_{-,n} \end{pmatrix} \\
 \stackrel{n=-m-1}{=} &\left(m + \frac{1}{2}\right) \begin{pmatrix} 1 & 1 \\ 1 & 1 \end{pmatrix} \begin{pmatrix} ia_{+,m} \\ a_{-,m} \end{pmatrix} \Rightarrow \begin{pmatrix} ia_{+,m} \\ a_{-,m} \end{pmatrix} = \begin{pmatrix} -1 \\ 1 \end{pmatrix} A_m \quad (\text{H.71})
 \end{aligned}$$

where A_m is an arbitrary coefficient.

$$\begin{aligned}
 0 &= (-n^2 + m^2) \mathbf{1} + \underbrace{\left(m + \frac{1}{2}\right) (\mathbf{1} - \sigma_x)}_{\text{nonBO}} \left\{ \begin{pmatrix} ia_{+,n} \\ a_{-,n} \end{pmatrix} \right\} \\
 \stackrel{n=-m}{=} \left(m + \frac{1}{2}\right) \begin{pmatrix} 1 & -1 \\ 1 & -1 \end{pmatrix} \begin{pmatrix} ia_{+,m} \\ a_{-,m} \end{pmatrix} &\Rightarrow \begin{pmatrix} ia_{+,m} \\ a_{-,m} \end{pmatrix} = \begin{pmatrix} 1 \\ 1 \end{pmatrix} B_m \cdot A_m \quad (\text{H.72})
 \end{aligned}$$

where B_m is another arbitrary coefficient.

Thus, the wave function for $m \geq 0$ has the form

$$\begin{pmatrix} i\mathcal{R}_+(R) \\ \mathcal{R}_-(R) \end{pmatrix} = A_m R^m \begin{pmatrix} -1 + B_m R + O(R^2) \\ 1 + B_m R + O(R^2) \end{pmatrix} \quad (\text{H.73})$$

We observe that we can choose the coefficients A_m , B_m such that the first terms of the power series expansion for m and $-m - 1$ are complex conjugates of each other. We will see below in section H.4.2 that this is a general property of the solutions.

Another observation is that the nuclear wave function is not differentiable in all orders at the origin. Rather the $m =$ solution exhibits a kink at the origin.

H.4.4 Optimization of the radial wave functions

There are different ways to solve the nuclear radial Schrödinger equation numerically, which are discussed in the following two sections.

The one described here exploits Ritz' variational principle. It starts from an expression for the total energy as functional of a nuclear wave function. By minimizing this energy we obtain the ground state. Minimizing the same functional again again, but with the restriction that it is orthogonal to the ground state, will yield the first excited state. Similarly, we can successively build up all radial wave functions.

We write down the total energy of an ensemble of electron and nuclear states. The states can be expressed entirely by the nuclear radial functions. The occupations, which are denoted as P_{mj} . They are Boltzmann weights.

In order to deal with real-valued functions, we introduce

$$\begin{pmatrix} f_+ \\ f_- \end{pmatrix} \stackrel{\text{def}}{=} \begin{pmatrix} i\mathcal{R}_+ \\ \mathcal{R}_- \end{pmatrix} \quad (\text{H.74})$$

The total-energy functional to be minimized is obtained from the differential equation. Here we include all excited states, but give them probabilities P_{mj} . The probabilities can be chosen fairly arbitrarily. While they are inspired by the expressions for a thermal ensemble, they are used here only as a numerical tool. Without proof let me state the following: (1) If all probabilities differ from each other, the resulting wave functions are eigenstates of the stationary Schrödinger equation. (2) The states are ordered such that the energies for states with higher probability are lower.

$$\begin{aligned}
 E[\vec{f}_{j,m}(R)] &= \sum_{m,j} P_{mj} \int_0^\infty dR \underbrace{(2\pi R)}_{\text{ang. integr.}} \\
 &\times \left\{ \vec{f}_{j,m}^*(R) \left[\frac{-\hbar^2 (R^2 \partial_R^2 + R \partial_R - m^2)}{2MR^2} \mathbf{1} + gR \sigma_z + wR^2 \mathbf{1} + \frac{\hbar^2 (m + \frac{1}{2})}{2MR^2} (\mathbf{1} + \sigma_x) \right] \vec{f}_{j,m}(R) \right\} \\
 &+ \sum_m \sum_{j,j'} \Lambda_{mj',j} \left\{ \left[\int_0^\infty dR \underbrace{(2\pi R)}_{\text{ang. integr.}} \vec{f}_{j,m}^* \vec{f}_{j',m} \right] - \delta_{jj'} \right\} \quad (\text{H.75})
 \end{aligned}$$

This expression acts as potential energy in a fictitious Lagrangian

$$\mathcal{L}[\{\vec{f}_{j,m}(R), \dot{\vec{f}}_{j,m}(R)\}] = \left\{ \sum_{m,j} P_{m,j} \int dr m_f \dot{\vec{f}}_{j,m}(R) \dot{\vec{f}}_{j,m}(R) \right\} - E[\{\vec{f}_{j,m}(R)\}] \quad (\text{H.76})$$

and derive an equation of motion for the radial wave function in the spirit of the Car-Parrinello method[113]. The time defining the “velocity of $\vec{f}_{m,j}$ ”, is not a real time but simply a coordinate describing dynamics of the wave functions during the optimization process.

The first variation of the total energy with respect to the radial functions is

$$dE = \sum_{m,j} P_{m,j} \int_0^\infty dR (2\pi R) d\vec{f}_{j,m}^* \vec{y}_{j,m} + \text{c.c.} \quad (\text{H.77})$$

which yields an effective gradient of the functional

$$\vec{y}_{j,m} = \left\{ \left[\frac{-\hbar^2 (R^2 \partial_R^2 + R \partial_R - m^2)}{2MR^2} \mathbf{1} + gR \boldsymbol{\sigma}_z + wR^2 \mathbf{1} + \frac{\hbar^2 (m + \frac{1}{2})}{2MR^2} (\mathbf{1} + \boldsymbol{\sigma}_x) \right] \vec{f}_{j,m}(R) + \sum_{j'} \vec{f}_{j',m} \Lambda_{m,j',j} \right\} \quad (\text{H.78})$$

The Euler-Lagrange equations for the Lagrangian Eq. H.76 produce an equation of motion

$$m_f \ddot{\vec{f}}_{m,j}(R) = -\vec{y}_{j,m}(R) \quad (\text{H.79})$$

We did not consider here the constraint term, because we will enforce this constraint separately. This equation of motion is augmented by a friction term and discretized using the Verlet algorithm[134].

In the **Verlet algorithm**[134] a differential equation is discretized by replacing the first and second derivatives by the differential quotients

$$\begin{aligned} \dot{x} &\rightarrow \frac{x(t+\Delta) - x(t-\Delta)}{2\Delta} \\ \ddot{x} &\rightarrow \frac{x(t+\Delta) - 2x(t) + x(t-\Delta)}{\Delta^2} \end{aligned} \quad (\text{H.80})$$

This allows to iteratively obtain the solution of a differential equation $m\ddot{x} = F(x) - \gamma\dot{x}$ for $x(j\Delta)$.

$$x(t+\Delta) = x(t) \frac{2}{1+a} - x(t-\Delta) \frac{1-a}{1+a} + F \frac{\Delta^2}{m(1+a)} \quad (\text{H.81})$$

with $a = \frac{\gamma\Delta}{2m}$.

We start from an arbitrary wave function $\vec{f}_{j,m}(R)$ for each m and j . The wave function is first orthogonalized to all functions with lower j , and then it is normalized. Starting from this initial wave function we perform a Car-Parrinello like optimization in the space orthogonal to the lower-lying states.

1. calculate the gradient $\vec{y}_{j,m}(R)$

$$\vec{y}_{j,m} = \left\{ \left[\frac{-\hbar^2 (R^2 \partial_R^2 + R \partial_R - m^2)}{2MR^2} \mathbf{1} + gR \boldsymbol{\sigma}_z + wR^2 \mathbf{1} + \frac{\hbar^2 (m + \frac{1}{2})}{2MR^2} (\mathbf{1} + \boldsymbol{\sigma}_x) \right] \vec{f}_{j,m}(R) \right\} \quad (\text{H.82})$$

2. orthogonalize $\vec{y}_{j,m}(R)$ to all lower-lying functions

$$\vec{y}_{j,m} \leftarrow \vec{y}_{j,m} - \sum_{j'=1}^{j-1} \vec{f}_{j',m} \left(\int_0^\infty dR R \vec{f}_{j',m}^*(R) \vec{y}_{j,m}(R) \right) \quad (\text{H.83})$$

3. propagate with the Verlet algorithm

$$\vec{f} = \vec{f}(t) \frac{2}{1+a} - \vec{f}(t-\Delta) \frac{1-a}{1+a} - \vec{y} \frac{\Delta^2}{2m_f(1+a)} \quad (\text{H.84})$$

4. normalize

$$\begin{aligned} \vec{f}(t+\Delta) &= \vec{f} + \vec{f}(t)\lambda \\ 1 &\stackrel{!}{=} 2\pi \int_0^\infty dR R \vec{f}^*(+) \vec{f}(+) \\ &= \underbrace{\left(2\pi \int_0^\infty dR R \vec{f}^* \vec{f}(+)\right)}_C - 1 + 2\lambda \underbrace{\text{Re}\left(2\pi \int_0^\infty dR R \vec{f}^* \vec{f}(0)\right)}_B + \lambda^2 \underbrace{2\pi \int_0^\infty dR R \vec{f}^*(0) \vec{f}(0)}_A \\ \lambda &= -\frac{B}{A} \left[1 - \sqrt{1 - \frac{A^2 C}{B^2}}\right] \end{aligned} \quad (\text{H.85})$$

Since the function is known for the next time step, we can begin again with the first point of the iteration sequence.

H.4.5 Integration of the Schrödinger equation for the radial nuclear wave functions

Editor: This is not finished!

$$\begin{aligned} 0 &= \left\{ -\frac{\hbar^2}{2M} \partial_R^2 - \frac{\hbar^2}{2MR} \partial_R + \frac{\hbar^2 \left[m(m+1) + \frac{1}{2} \right]}{2MR^2} \pm g|\bar{R}| + w\bar{R}^2 - \mathcal{E}_{m,j} \right\} \mathcal{R}_{\pm,m,j} \pm \frac{i\hbar^2 \left(m + \frac{1}{2} \right)}{2MR^2} \mathcal{R}_{\mp,m,j} \\ 0 &= \left\{ -R^2 \partial_R^2 - R \partial_R + \left[m(m+1) + \frac{1}{2} \right] + \frac{2M}{\hbar^2} \left[-\mathcal{E}_{m,j} R^2 \pm gR^3 + wR^4 \right] \right\} \mathcal{R}_{\pm,m,j} \pm i \left(m + \frac{1}{2} \right) \mathcal{R}_{\mp,m,j} \end{aligned}$$

Now, we introduce an exponential Ansatz $R(x) = e^x$

$$\mathcal{R}_{\pm,m,j}(e^x) = f_{\pm,m,j}(x) \quad (\text{H.86})$$

$$\begin{aligned} R(x) = e^x &\Rightarrow \frac{dR}{dx} = e^x = R \Rightarrow \frac{dx}{dR} = 1/R \\ R \partial_R &= \partial_x \\ R^2 \partial_R^2 &= R^2 \partial_R \frac{1}{R} R \partial_R = R^2 \partial_R \frac{1}{R} \partial_x = R^2 \left(-\frac{1}{R^2} + \frac{1}{R^2} R \partial_R \right) \partial_x = -\partial_x + \partial_x^2 \\ R^2 \partial_R^2 + R \partial_R &= \partial_x^2 \end{aligned} \quad (\text{H.87})$$

This yields

$$0 = \left\{ -\partial_x^2 + \left[m(m-1) + \frac{1}{2} \right] + \frac{2M}{\hbar^2} \left[-\mathcal{E}_{m,j} R^2 \pm gR^3 + wR^4 \right] \right\} f_{\pm,m,j}(x) \mp i \left(m + \frac{1}{2} \right) f_{\mp,m,j}(x)$$

We solve this equation numerically on a grid using the Verlet algorithm[134], which replaces the second derivative with the differential quotient

$$\partial_x^2 f = \frac{f(+)-2f(0)+f(-)}{\alpha^2} \quad (\text{H.88})$$

where α is the grid spacing.

An important aspect is that one needs to integrate from the outside inward. The reason is that in the outer region, there is one solution that falls off towards the outside and one solution that increases exponentially. We are interested in the solution falling off.

When we integrate outward, any little numerical error will admit a fraction of the exponentially increasing solution. This small fraction will now be exponentially amplified, leading to a poor solution. On the other hand, when we integrate inward, every error will admit a partial solution that falls off in the inward direction, so that any error heals immediately.

Editor: Reread the remainder of this section: It is unclear.

Therefore, we choose the strategy to integrate from the outside inward and match the solutions in the center.

For a given energy, we calculate the Schrödinger equation outward from the inside with two distinct boundary conditions and obtain $(f_{1,1}^{(i)}(x), f_{2,1}^{(i)}(x))$ and $(f_{1,2}^{(i)}(x), f_{2,2}^{(i)}(x))$. At the same time, I evaluate the energy derivatives $\dot{f}_{m,n}^{(i)}(x, \epsilon) := \partial_\epsilon f_{m,n}^{(i)}(x, \epsilon)$ yielding $(\dot{f}_{1,1}^{(i)}(x), \dot{f}_{2,1}^{(i)}(x))$ and $(\dot{f}_{1,2}^{(i)}(x), \dot{f}_{2,2}^{(i)}(x))$. The boundary conditions are $(f_{1,1}^{(i)}(x), f_{2,1}^{(i)}(x)) = (1, 0)$ and $(f_{1,2}^{(i)}(x), f_{2,2}^{(i)}(x)) = (0, 1)$ at the first grid point. The derivatives are set to zero. For the energy derivative functions value and derivative at the first grid points are set to zero.

The condition that the two functions match with value and derivative can be approximated by the condition that the two functions match on two subsequent points x_k on the grid.

$$\sum_{\alpha=1}^2 \left(f_{i,\alpha}^{(i)}(x_k) + (\epsilon - \epsilon_0) \dot{f}_{i,\alpha}^{(i)}(x_k) \right) c_\alpha = \sum_{\alpha=1}^2 \left(f_{i,\alpha}^{(o)}(x_k) + (\epsilon - \epsilon_0) \dot{f}_{i,\alpha}^{(o)}(x_k) \right) c_{\alpha+2} \quad (\text{H.89})$$

This value must be fulfilled for $k = 1, 2$ and $i = 1, 2$. This is an eigenvalue equation **Editor:** There is something wrong. Are the eigenvectors missing?

$$\begin{pmatrix} f_{1,1}^{(i)}(x_a) & f_{1,2}^{(i)}(x_a) & -f_{1,1}^{(o)}(x_a) & -f_{1,2}^{(o)}(x_a) \\ f_{2,1}^{(i)}(x_a) & f_{2,2}^{(i)}(x_a) & -f_{2,1}^{(o)}(x_a) & -f_{2,2}^{(o)}(x_a) \\ f_{1,1}^{(i)}(x_b) & f_{1,2}^{(i)}(x_b) & -f_{1,1}^{(o)}(x_b) & -f_{1,2}^{(o)}(x_b) \\ f_{2,1}^{(i)}(x_b) & f_{2,2}^{(i)}(x_b) & -f_{2,1}^{(o)}(x_b) & -f_{2,2}^{(o)}(x_b) \end{pmatrix} + (\epsilon - \epsilon_0) \begin{pmatrix} \dot{f}_{1,1}^{(i)}(x_a) & \dot{f}_{1,2}^{(i)}(x_a) & -\dot{f}_{1,1}^{(o)}(x_a) & -\dot{f}_{1,2}^{(o)}(x_a) \\ \dot{f}_{2,1}^{(i)}(x_a) & \dot{f}_{2,2}^{(i)}(x_a) & -\dot{f}_{2,1}^{(o)}(x_a) & -\dot{f}_{2,2}^{(o)}(x_a) \\ \dot{f}_{1,1}^{(i)}(x_b) & \dot{f}_{1,2}^{(i)}(x_b) & -\dot{f}_{1,1}^{(o)}(x_b) & -\dot{f}_{1,2}^{(o)}(x_b) \\ \dot{f}_{2,1}^{(i)}(x_b) & \dot{f}_{2,2}^{(i)}(x_b) & -\dot{f}_{2,1}^{(o)}(x_b) & -\dot{f}_{2,2}^{(o)}(x_b) \end{pmatrix} = 0 \quad (\text{H.90})$$

We define the matrix

$$\mathbf{A} \stackrel{\text{def}}{=} \begin{pmatrix} \dot{f}_{1,1}^{(i)}(x_a) & \dot{f}_{1,2}^{(i)}(x_a) & -\dot{f}_{1,1}^{(o)}(x_a) & -\dot{f}_{1,2}^{(o)}(x_a) \\ \dot{f}_{2,1}^{(i)}(x_a) & \dot{f}_{2,2}^{(i)}(x_a) & -\dot{f}_{2,1}^{(o)}(x_a) & -\dot{f}_{2,2}^{(o)}(x_a) \\ \dot{f}_{1,1}^{(i)}(x_b) & \dot{f}_{1,2}^{(i)}(x_b) & -\dot{f}_{1,1}^{(o)}(x_b) & -\dot{f}_{1,2}^{(o)}(x_b) \\ \dot{f}_{2,1}^{(i)}(x_b) & \dot{f}_{2,2}^{(i)}(x_b) & -\dot{f}_{2,1}^{(o)}(x_b) & -\dot{f}_{2,2}^{(o)}(x_b) \end{pmatrix}^{-1} \begin{pmatrix} f_{1,1}^{(i)}(x_a) & f_{1,2}^{(i)}(x_a) & -f_{1,1}^{(o)}(x_a) & -f_{1,2}^{(o)}(x_a) \\ f_{2,1}^{(i)}(x_a) & f_{2,2}^{(i)}(x_a) & -f_{2,1}^{(o)}(x_a) & -f_{2,2}^{(o)}(x_a) \\ f_{1,1}^{(i)}(x_b) & f_{1,2}^{(i)}(x_b) & -f_{1,1}^{(o)}(x_b) & -f_{1,2}^{(o)}(x_b) \\ f_{2,1}^{(i)}(x_b) & f_{2,2}^{(i)}(x_b) & -f_{2,1}^{(o)}(x_b) & -f_{2,2}^{(o)}(x_b) \end{pmatrix} \quad (\text{H.91})$$

and diagonalize it using the LAPACK routine ZGEEV. The eigenvalues are an estimate for the next energy eigenvalue. The eigenvalues are $\epsilon - \epsilon_0$. Using the eigenvalues only one can zoom into the correct energy. That is, ϵ_0 is adjusted to the new estimate for the energy eigenvalue until $\epsilon - \epsilon_0$ nearly vanishes for the chosen eigenvector.

Finally, one can evaluate the right-hand eigenvector, which provides the coefficients of the inner and outer partial solutions.

The final solution is then constructed

$$\begin{aligned} \vec{f}(x) &= \left(\vec{f}_1^{(i)} + (\epsilon - \epsilon_0) \dot{\vec{f}}_1^{(i)} \right) c_1 + \left(\vec{f}_2^{(i)} + (\epsilon - \epsilon_0) \dot{\vec{f}}_2^{(i)} \right) c_2 \\ \vec{f}(x) &= \left(\vec{f}_1^{(o)} + (\epsilon - \epsilon_0) \dot{\vec{f}}_1^{(o)} \right) c_3 + \left(\vec{f}_2^{(o)} + (\epsilon - \epsilon_0) \dot{\vec{f}}_2^{(o)} \right) c_4 \end{aligned} \quad (\text{H.92})$$

Depending on the value of x , either the equation with the inner or the outer partial solutions is used.

The solution is then normalized so that

$$\begin{aligned}
 2\pi \int dR R \cdot R^{2m} \left(f_{+,m,j}^*(x(R)) f_{+,m,j}(x(R)) + f_{-,m,j}^*(x(R)) f_{-,m,j}(x(R)) \right) &= 1 \\
 2\pi \int_{-\infty}^{\infty} dx \frac{dR}{dx} R \cdot R^{2m} \left(f_{+,m,j}^*(x(R)) f_{+,m,j}(x(R)) + f_{-,m,j}^*(x(R)) f_{-,m,j}(x(R)) \right) &= 1 \\
 2\pi \int_{-\infty}^{\infty} dx e^{(2m+2)x} \left(f_{+,m,j}^*(x) f_{+,m,j}(x) + f_{-,m,j}^*(x) f_{-,m,j}(x) \right) &= 1 \\
 2\pi \alpha \sum_{x_i} e^{(2m+2)x_i} \left(f_{+,m,j}^*(x_i) f_{+,m,j}(x_i) + f_{-,m,j}^*(x_i) f_{-,m,j}(x_i) \right) &= 1 \quad (\text{H.93})
 \end{aligned}$$

The factor $2\pi r$ results from the angular integration. Please check!

H.4.6 FORTRAN code

I am including here the FORTRAN code that calculates the Born-Oppenheimer surfaces and the radial wave functions for the Jahn-Teller model.

The first file is an executable, which that compiles and runs the code. It requires the FORTRAN code below as `jt.f90`. Furthermore, it requires the FORTRAN compiler `gfortran` and the linear-algebra library `LAPACK`. Both are available in the public domain.

The file uses the compiler option `-framework accelerate`, which is specific for MacOS. Its function is to link to the LAPACK Library.

```

#!/bin/bash
#
echo compiling $X ...
gfortran -Wall -fdollar-ok -framework accelerate -o jt.x jt.f90
RC=$?
if [[ $RC -ne 0 ]] ; then echo "error in $0: compile error"; exit 1 ; fi
#
#
#
echo "executing $X ..."
jt.x
if [[ $RC -ne 0 ]] ; then echo "error in $0: execution error"; exit 1 ; fi
echo "... execution of $X finished"
#
#
#
xmgrace -free -noask -nxy ebo.dat &
xmgrace -free -noask -nxy phi0_1.dat &

```

The code produces the

- the file `ebo.dat` contains the two Born-Oppenheimer surfaces as function of the radius R .
- the files `phi0_1.dat` containing the two radial components of the nuclear wave functions. The first number, in this case 0, describes the angular momentum, while the second one, in this case 1 denotes the band index for this angular momentum. The values for the angular momentum range from $m = 0$ to $m = 2$, the state index ranges from 1 to 20.

Below is the FORTRAN code. The parameters of the calculations can be adjusted in the `MODULE JAHNTPELLER_MODULE`.

```

MODULE JAHNTELLER_MODULE
!**
!** RADIAL GRID Q(I)=(I-1)*DQ FOR I
!**
INTEGER(4),PARAMETER :: MX=2      ! MAX ANGULAR MOMENTUM
INTEGER(4),PARAMETER :: JX=20     ! #(STATES PER ANGULAR MOMENTUM)
INTEGER(4),PARAMETER :: NP=100    ! #(SPATIAL GRID POINTS)
REAL(8)  ,PARAMETER  :: QX=3.DO   ! Q-RANGE: [0,QX]
REAL(8)  ,PARAMETER  :: QMASS=5.D+1 ! MASS OF THE COORDINATE Q
REAL(8)  ,PARAMETER  :: GJT=2.DO  ! ELECTRON-PHONON COUPLING
REAL(8)  ,PARAMETER  :: WJT=0.5D0*GJT ! RESTORING FORCE CONSTANT
REAL(8)  ,PARAMETER  :: DT=1.D-1  ! TIME STEP FOR CP DYNAMICS
REAL(8)  ,PARAMETER  :: ANNE=0.DO  ! CP FRICTION
REAL(8)  ,PARAMETER  :: MPSI=1.D+2 ! FICTITIOUS WAVE FUNCTION MASS
LOGICAL(4),PARAMETER :: TBO=.FALSE. ! BORN OPPENHEIMER APPROXIMATION
END MODULE JAHNTELLER_MODULE
!
!.1.....2.....3.....4.....5.....6.....7.....8
MODULE STRINGS_MODULE
!*****
!**                                     **
!** NAME: STRINGS                       **
!**                                     **
!** PURPOSE: DEFINE CASING OPERATORS FOR STRING MANIPULATIONS **
!**                                     **
!** FUNCTIONS:                           **
!** '+'  UPPERCASE A STRING              **
!** '-'  LOWERCASE A STRING              **
!**                                     **
!*****
PUBLIC
INTERFACE OPERATOR (-)
  MODULE PROCEDURE LOWER_CASE
END INTERFACE
INTERFACE OPERATOR (+)
  MODULE PROCEDURE UPPER_CASE
END INTERFACE
CONTAINS
!
!.1.....2.....3.....4.....5.....6.....7.....8
FUNCTION LOWER_CASE(OLD) RESULT(NEW)
  IMPLICIT NONE
  CHARACTER(*), INTENT(IN):: OLD
  CHARACTER(LEN(OLD))    :: NEW
  INTEGER(4)             :: I,ISVAR
!
  *****
  NEW=OLD
  DO I=1,LEN(TRIM(OLD))
    ISVAR=IACHAR(OLD(I:I))
    IF(ISVAR.GE.65.AND.ISVAR.LE.90) NEW(I:I)=ACHAR(ISVAR+32)
  ENDDO
  RETURN
END FUNCTION LOWER_CASE
!
!.1.....2.....3.....4.....5.....6.....7.....8
FUNCTION UPPER_CASE(OLD) RESULT(NEW)

```



```

      IMPLICIT NONE
      CHARACTER(*), INTENT(IN):: OLD
      CHARACTER(LEN(OLD))      :: NEW
      INTEGER(4)                :: I, ISVAR
! *****
      NEW=OLD
      DO I=1,LEN(TRIM(OLD))
        ISVAR=IACHAR(OLD(I:I))
        IF(ISVAR.GE.97.AND.ISVAR.LE.122) NEW(I:I)=ACHAR(ISVAR-32)
      ENDDO
      END FUNCTION UPPER_CASE
END MODULE STRINGS_MODULE
!
!
! ..1.....2.....3.....4.....5.....6.....7.....8
PROGRAM MAIN
USE JAHNTPELLER_MODULE , ONLY : JX,MX,NP,QX
IMPLICIT NONE
REAL(8)                :: E(JX,MX+1)
REAL(8)                :: PHI(2,NP,JX,MX+1)
INTEGER(4)             :: M
! *****
!
! =====
! == WRITE BORN-OPPENHEIMER SURFACES TO FILE "EBO.DAT"
! =====
CALL WRITEEBO()
!
! =====
! == DETERMINE NUCLEAR WAVE FUNCTIONS AND ENERGIES
! =====
DO M=0,MX
  WRITE(*,FMT='(80(=""),T10," STATES FOR ANGULAR MOMENTUM ",A5," ")')
  CALL ITERATE(M,JX,NP,QX,E(:,M+1),PHI(:, :, :, M+1))
ENDDO
WRITE(*,FMT='(80(=""),T10," CALCULATION COMPLETED ")')
STOP
END
!
! ..1.....2.....3.....4.....5.....6.....7.....8
SUBROUTINE ITERATE(M,NSTATE,NP,QX,E,PHI)
! *****
! **
! *****
USE STRINGS_MODULE
USE JAHNTPELLER_MODULE, ONLY : DT,ANNE,MPSI
IMPLICIT NONE
INTEGER(4),INTENT(IN)  :: M          ! ANGULAR MOMENTUM
INTEGER(4),INTENT(IN)  :: NSTATE     ! NUMBER OF GRID POINTS
INTEGER(4),INTENT(IN)  :: NP        ! NUMBER OF GRID POINTS
REAL(8) ,INTENT(IN)    :: QX        ! GRID BOUNDARIES [-QX,QX]
REAL(8) ,INTENT(OUT)   :: E(NSTATE)
REAL(8) ,INTENT(OUT)   :: PHI(2,NP,NSTATE)
INTEGER(4),PARAMETER   :: NITER=1000000

```

```

REAL(8)          :: TOL=1.D-10
CHARACTER(32)    :: STRING
CHARACTER(32)    :: STRING2
REAL(8)          :: PHIO(2,NP)
REAL(8)          :: PHIP(2,NP)
REAL(8)          :: PHIM(2,NP)
REAL(8)          :: HPHI(2,NP)
REAL(8)          :: EPOT,EKIN
REAL(8)          :: SVAR1,SVAR2,SVAR3
REAL(8)          :: A,B,C
REAL(8)          :: LAMBDA
REAL(8)          :: X
REAL(8)          :: EPOTLAST
REAL(8)          :: DQ
REAL(8)          :: CVEC(2)
REAL(8) ,PARAMETER :: PI=4.DO*ATAN(1.DO)
INTEGER(4)       :: IP,ITER,ISTATE,I
LOGICAL(4)       :: CONVG
! *****
OPEN(UNIT=12,FILE='- 'OUT.DAT')
REWIND(12)
DQ=QX/REAL(NP-1,KIND=8)
DO ISTATE=1,NSTATE
! =====
! == CONSTRUCT INITIAL STATE ==
! =====
CVEC=(/1.DO,1.DO/) !EVEN PLUS ODD
PHIO=0.DO
DO IP=1,NP
  X=PI*REAL(IP-1,KIND=8)/REAL(NP-1,KIND=8)
  PHIO(1,IP)=CVEC(1)*SIN(X) +CVEC(2)*SIN(2.DO*X)
ENDDO
! __ AVOID NUMERICAL PROBLEMS DUE TO SLIGHTLY NONZERO VALUES__
PHIO(:,NP)=0.DO
IF(M.NE.0) PHIO(:,1)=0.DO

! __ ORTHOGONALIZE TO PREVIOUS STATES__
DO I=1,ISTATE-1
  CALL SCALARPRODUCT(NP,DQ,PHI(:, :, I),PHIO,X)
  PHIO=PHIO-PHI(:, :, I)*X
ENDDO
! __ NORMALIZE__
CALL SCALARPRODUCT(NP,DQ,PHIO,PHIO,X)
PHIO=PHIO/SQRT(X)
CALL SCALARPRODUCT(NP,DQ,PHIO,PHIO,X)

! =====
! == OPTIMIZE STATE ==
! =====
EPOTLAST=HUGE(EPOTLAST)
PHIM=PHIO
DO ITER=1,NITER
!
! == TOTAL ENERGY AND FORCE =====

```

```

CALL ETOT(M,NP,PHIO,EPOT,HPHI)
!
!   == STOP WAVE FUNCTION OF ENERGY GOES UP =====
IF(EPOTLAST.LT.EPOT) THEN
    PHIM=PHIO
END IF
!
!   == ORTHOGONALIZE FORCE TO PREVIOUS STATES =====
DO I=1, ISTATE-1
    CALL SCALARPRODUCT(NP,DQ,PHI(:, :, I),HPHI,X)
    HPHI=HPHI-PHI(:, :, I)*X
ENDDO
!
!   == PROPAGATE WITHOUT CONSTRAINTS =====
SVAR1=2.DO/(1.DO+ANNE)
SVAR2=1.DO-SVAR1
SVAR3=DT**2/MPSI/(1.DO+ANNE)
PHIP = PHIO*SVAR1 + PHIM*SVAR2 - HPHI*SVAR3
!
!   == ENFORCE CONSTRAINTS =====
CALL SCALARPRODUCT(NP,DQ,PHIP,PHIP,C)
CALL SCALARPRODUCT(NP,DQ,PHIP,PHIO,B)
CALL SCALARPRODUCT(NP,DQ,PHIO,PHIO,A)
!   __ A*X^2+B*X+C=1
C=C-1.DO
B=2.DO*B
C=C/A
B=B/A
A=A/A
!   __ X^2+2BX+C=0
LAMBDA=-B+SQRT(B**2-C)
PHIP=PHIP+PHIO*LAMBDA
!
!   == ORTHOGONALIZE TO PREVIOUS STATES=====
DO I=1, ISTATE-1
    CALL SCALARPRODUCT(NP,DQ,PHI(:, :, I),PHIP,X)
    PHIP=PHIP-PHI(:, :, I)*X
ENDDO
CALL SCALARPRODUCT(NP,DQ,PHIP,PHIP,X)
PHIP=PHIP/SQRT(X)
!
!   == KINETIC ENERGY =====
CALL SCALARPRODUCT(NP,DQ,PHIP-PHIM,PHIP-PHIM,EKIN)
EKIN=MPSI*EKIN/(2.DO*DT)**2
WRITE(12,FMT='(I10,3F20.10,2I5)') ITER,EKIN,EPOT,EKIN+EPOT, ISTATE,M
WRITE(*,FMT='(I10,3F20.10,2I5)') ITER,EKIN,EPOT,EKIN+EPOT, ISTATE,M
!
!   == CHECK CONVERGENCE AND EXIT =====
CONVG=.TRUE.
CONVG=CONVG.AND.(EKIN.LT.TOL)
CONVG=CONVG.AND.(ABS(EPOT-EPOTLAST).LT.TOL)
IF(CONVG) EXIT
!
!   == SWITCH =====

```

```

        EPOTLAST=EPOT
        PHIM=PHIO
        PHIO=PHIP
        ENDDO ! END OF LOOP OVER ITERATIONS
        PHI(:,: ,ISTATE)=PHIO
        ENDDO ! END OF LOOP OVER STATES
        CLOSE(12)

!
!
! =====
! == DIAGONALIZE ==
! =====
        CALL DIAGONA(M,NSTATE,NP,DQ,PHI,E)
!
!
! =====
! == WRITE RESULT TO FILE ==
! =====
        WRITE(String2,*)M
        String2='ENERGIES'//TRIM(ADJUSTL(String2))//'.DAT'
        OPEN(UNIT=12,FILE=-TRIM(String2))
        WRITE(String2,*)M
        String2='PHI'//TRIM(ADJUSTL(String2))//'_ '
        DO ISTATE=1,NSTATE
            WRITE(12,FMT='(I5,F10.5,3F10.5)')ISTATE,E(ISTATE)
            WRITE(String,*)ISTATE
            String=TRIM(ADJUSTL(String2))//TRIM(ADJUSTL(String))//'.DAT'
            OPEN(10,FILE=-TRIM(String))
            DO IP=1,NP
                WRITE(10,*)DQ*REAL(IP-1),PHI(: ,IP,ISTATE)
            ENDDO
            CLOSE(10)
        ENDDO
        CLOSE(12)
        RETURN
        END

!
! ..1.....2.....3.....4.....5.....6.....7.....8
SUBROUTINE DIAGONA(M,NSTATE,NP,DQ,PHI,E)
!
! *****
! **
! *****
        IMPLICIT NONE
        INTEGER(4),INTENT(IN)      :: M ! ANGULAR MOMENTUM
        INTEGER(4),INTENT(IN)      :: NSTATE
        INTEGER(4),INTENT(IN)      :: NP
        REAL(8) ,INTENT(IN)        :: DQ
        REAL(8) ,INTENT(INOUT)     :: PHI(2,NP,NSTATE)
        REAL(8) ,INTENT(OUT)       :: E(NSTATE)
        INTEGER(4)                 :: I,J
        REAL(8)                    :: EPOT
        REAL(8)                    :: H(NSTATE,NSTATE)
        REAL(8)                    :: U(NSTATE,NSTATE)
        REAL(8)                    :: HPHI(2,NP)
        REAL(8)                    :: PHI1(2,NP,NSTATE)

```

```

REAL(8)                :: WORK(3*NSTATE)
INTEGER(4)             :: INFO
! *****
DO I=1,NSTATE
  CALL ETOT(M,NP,PHI(:, :, I),EPOT,HPHI)
  DO J=I,NSTATE
    CALL SCALARPRODUCT(NP,DQ,PHI(:, :, J),HPHI,H(I,J))
    H(J,I)=H(I,J)
  ENDDO
ENDDO

!
! =====
! == DIAGONALIZE USING LAPACK ==
! =====

U=0.5DO*(H+TRANPOSE(H))
CALL DSYEV('V','U',NSTATE,U,NSTATE,E,WORK,3*NSTATE,INFO )
IF(INFO.NE.0) THEN
  IF(INFO.LT.0) THEN
    PRINT*, 'I-TH ARGUMENT HAD AN ILLEGAL VALUE'
    PRINT*, 'I', -INFO
    STOP 'IN DIAGONA'
  ELSE
    PRINT*, 'THE ALGORITHM FAILED TO CONVERGE'
    PRINT*, 'OFF-DIAGONAL ELEMENTS OF AN INTERMEDIATE'
    PRINT*, 'TRIDIAGONAL FORM DID NOT CONVERGE TO ZERO'
    PRINT*, 'I', INFO
    STOP 'IN DIAGONA'
  END IF
END IF

!
! =====
! == DIAGONALIZE USING LAPACK ==
! =====

DO I=1,NSTATE
  PHI1(:, :, I)=0.DO
  DO J=1,NSTATE
    PHI1(:, :, I)=PHI1(:, :, I)+PHI(:, :, J)*U(J,I)
  ENDDO
ENDDO
PHI=PHI1
RETURN
END

!
! ..1.....2.....3.....4.....5.....6.....7.....8
SUBROUTINE SCALARPRODUCT(NP,DQ,PHI1,PHI2,SP)
! *****
! ** CALCULATE THE SCALAR PRODUCT OF TWO FUNCTIONS **
! ** INCLUDING ANGULAR PART (2*PI*R) **
! *****
IMPLICIT NONE
INTEGER(4),INTENT(IN) :: NP          ! NUMBER OF GRID POINTS
REAL(8)  ,INTENT(IN)  :: DQ          ! GRID SPACING
REAL(8)  ,INTENT(IN)  :: PHI1(2,NP)
REAL(8)  ,INTENT(IN)  :: PHI2(2,NP)

```

```

REAL(8)    ,INTENT(OUT)  :: SP
REAL(8)    ,PARAMETER   :: PI=4.DO*ATAN(1.DO)
REAL(8)    :: Q
INTEGER    :: IP
! *****
SP=0.DO
DO IP=1,NP
  Q=DQ*REAL(IP-1,KIND=8) !RADIAL POSITION
  SP=SP+Q*(PHI1(1,IP)*PHI2(1,IP)+PHI1(2,IP)*PHI2(2,IP))
ENDDO
SP=2.DO*PI*SP*DQ
RETURN
END
!
! ..1.....2.....3.....4.....5.....6.....7.....8
SUBROUTINE ETOT(M,NP,PHI,EPOT,HPhi)
! *****
! **
! *****
USE JAHNTPELLER_MODULE , ONLY : TBO,QX,QMASS,GJT,WJT
IMPLICIT NONE
INTEGER(4),INTENT(IN)  :: M          ! ANGULAR MOMENTUM
INTEGER(4),INTENT(IN)  :: NP          ! NUMBER OF GRID POINTS
REAL(8)    ,INTENT(IN)  :: PHI(2,NP)
REAL(8)    ,INTENT(OUT) :: EPOT
REAL(8)    ,INTENT(OUT) :: HPhi(2,NP)
INTEGER(4)  :: IP
REAL(8)     :: MPLUSHALF ! (M+1/2)
REAL(8)     :: DQ ! SPACING ON RADIAL GRID
REAL(8)     :: Q ! RADIAL GRID COORDINATE
REAL(8)    ,PARAMETER  :: PI=4.DO*ATAN(1.DO)
! *****
DQ=QX/REAL(NP-1,KIND=8)
MPLUSHALF=REAL(M,KIND=8)+0.5DO
HPhi=0.DO
DO IP=2,NP-1
  Q=REAL(IP-1,KIND=8)*DQ
  HPhi(:,IP)=-Q**2*( PHI(:,IP+1)-2.DO*PHI(:,IP)+PHI(:,IP-1) )/DQ**2 &
&              -Q*( PHI(:,IP+1)-PHI(:,IP-1) )/(2.DO*DQ) &
&              +REAL(M**2,KIND=8)*PHI(:,IP)
! == NONADIABATIC TERMS =====
  IF(.NOT.TBO) THEN
    HPhi(1,IP)=HPhi(1,IP)+MPLUSHALF*(PHI(1,IP)-PHI(2,IP))
    HPhi(2,IP)=HPhi(2,IP)+MPLUSHALF*(PHI(2,IP)-PHI(1,IP))
  END IF
! == MULTIPLY FACTOR =====
  HPhi(:,IP)=HPhi(:,IP)/(2.DO*QMASS*Q**2)
! == ADD BORN-OPPENHEIMER POTENTIAL =====
  HPhi(:,IP)=HPhi(:,IP)+WJT*Q**2*PHI(:,IP)
  HPhi(1,IP)=HPhi(1,IP)-GJT*Q*PHI(1,IP)
  HPhi(2,IP)=HPhi(2,IP)+GJT*Q*PHI(2,IP)
ENDDO
IF(M.EQ.0) THEN
  IP=1

```

```

      HPHI(:,IP)=- ( PHI(:,IP+1)-2.DO*PHI(:,IP)+PHI(:,IP+1) )/DQ**2 / (2*QMASS)
    ELSE
      HPHI(:,1)=0.DO
    END IF
    HPHI(:,NP)=0.DO
    CALL SCALARPRODUCT(NP,DQ,PHI,HPHI,EPOT)
    RETURN
  END

!
! ..1.....2.....3.....4.....5.....6.....7.....8
SUBROUTINE WRITEEBO()
USE STRINGS_MODULE
USE JAHNTELLER_MODULE , ONLY : NP,QX,GJT,WJT
IMPLICIT NONE
INTEGER(4)          :: NFIL=10
INTEGER(4)          :: IP
REAL(8)             :: Q
REAL(8)             :: EBO(2)
! *****
OPEN(NFIL,FILE='-EBO.DAT')
DO IP=1,NP
  Q=QX*REAL(IP-1,KIND=8)/REAL(NP-1,KIND=8)
  EBO(1)=-GJT*Q+WJT*Q**2
  EBO(2)=+GJT*Q+WJT*Q**2
  WRITE(NFIL,*)Q,EBO
ENDDO
CLOSE(NFIL)
RETURN
END

```

H.5 From a conical intersection to an avoided crossing

We have seen that avoided crossings and conical intersections are the points where non-adiabatic effects become important. In order to learn about the relation between the two, it is possible within the Jahn-Teller model to change the conical intersection into an avoided crossing with a single parameter. Here, I only point out how one arrives at it. Its investigation is left to the interested reader.

The Jahn-Teller model can easily be extended to a three-dimensional parameter space by adding the third Pauli matrix in the Schrödinger equation Eq. H.10.

$$i\hbar\partial_t|\Phi(t)\rangle = \left[\frac{\hat{P}_x^2 + \hat{P}_y^2 + \hat{P}_z^2}{2M} + w\hat{R}^2 + g\hat{X}\hat{\sigma}_x + g\hat{Y}\hat{\sigma}_y + g\hat{Z}\hat{\sigma}_z \right] |\Phi(t)\rangle \quad (\text{H.94})$$

The conical intersection in the Born-Oppenheimer surface is at $(X, Y, Z) = \vec{0}$.

In the next step we can treat Y as a parameter, so that we obtain a two-dimensional model in the coordinate space (X, Z) but an additional parameter $Y = \lambda$

$$i\hbar\partial_t|\Phi(t)\rangle = \left[\frac{\hat{P}_x^2 + \hat{P}_y^2}{2M} + w\hat{R}^2 + g\hat{X}\hat{\sigma}_x + g\hat{Z}\hat{\sigma}_z + \lambda\hat{\sigma}_y \right] |\Phi(t)\rangle \quad (\text{H.95})$$

For $\lambda = 0$ we obtain the Jahn-Teller model with the conical intersection. For non-zero values of λ the conical intersection is converted into an avoided crossing with a gap of $2|\lambda|$.

The case of an “avoided” conical intersection is of special interest to understand the derivative derivative couplings of the Jahn-Teller model. There is a puzzle that the diagonal derivative couplings vanish for real-valued wave function, but not its curl.

Considering the conical intersection as limiting case of an avoided conical intersection, I will show below that the derivative coupling exhibits a delta-function-like contribution where the real-valued wave functions exhibit a jump. Depending on the side from which the limit is taken the derivative couplings change sign. Using perfect real-valued wave functions without taking the limit produces “the average” of both limits, and this leads to vanishing derivative couplings.

H.5.1 Conical intersection as limit of an avoided intersection

Introduce polar coordinates

$$\begin{aligned}
 i\hbar\partial_t|\Phi(t)\rangle &\stackrel{\text{Eq. H.95}}{=} \left[\frac{\hat{p}_x^2 + \hat{p}_y^2}{2M} + w\hat{R}^2 + g\hat{X}\hat{\sigma}_x + g\hat{Z}\hat{\sigma}_z + \lambda\hat{\sigma}_y \right] |\Phi(t)\rangle \\
 \hat{H}_\lambda^{BO}(X, Z) &= \left[w\vec{R}^2 + gX\hat{\sigma}_x + gZ\hat{\sigma}_z + \lambda\hat{\sigma}_y \right] \\
 &= \left[wR^2 + gR\sin(\alpha)\hat{\sigma}_x + gR\cos(\alpha)\hat{\sigma}_z + \lambda\hat{\sigma}_y \right] \\
 &= \begin{pmatrix} wR^2 + gR\cos(\alpha) & gR\sin(\alpha) - i\lambda \\ gR\sin(\alpha) + i\lambda & wR^2 - gR\cos(\alpha) \end{pmatrix} \quad (\text{H.96})
 \end{aligned}$$

The eigenvalues are

$$\begin{aligned}
 (wR^2 - E)^2 - (gR\cos(\alpha))^2 - (gR\sin^2(\alpha))^2 - \lambda^2 &= 0 \\
 E = wR^2 \pm \sqrt{(gR\cos(\alpha))^2 + (gR\sin^2(\alpha))^2 + \lambda^2} \\
 &= wR^2 \pm \sqrt{\lambda^2 + (gR)^2} \quad (\text{H.97})
 \end{aligned}$$

The eigenstates are

$$\begin{aligned}
 &= \begin{pmatrix} -gR\sin(\alpha) + i\lambda \\ gR\cos(\alpha) \mp \sqrt{(gR)^2 + \lambda^2} \end{pmatrix} \frac{1}{\sqrt{g^2R^2\sin^2(\alpha) + \lambda^2 + (gR\cos(\alpha) \mp \sqrt{(gR)^2 + \lambda^2})^2}} \\
 &= \begin{pmatrix} -gR\sin(\alpha) + i\lambda \\ gR\cos(\alpha) \mp \sqrt{(gR)^2 + \lambda^2} \end{pmatrix} \frac{1}{\sqrt{(gR\sin(\alpha))^2 + \lambda^2 + (gR\cos(\alpha))^2 \mp 2gR\cos(\alpha)\sqrt{(gR)^2 + \lambda^2} + (gR)^2 + \lambda^2}} \\
 &= \begin{pmatrix} -gR\sin(\alpha) + i\lambda \\ gR\cos(\alpha) \mp \sqrt{(gR)^2 + \lambda^2} \end{pmatrix} \frac{1}{\sqrt{2(g^2R^2 + \lambda^2 \mp gR\cos(\alpha)\sqrt{(gR)^2 + \lambda^2})}} \\
 &= \begin{pmatrix} -\sin(\alpha) + i\frac{\lambda}{gR} \\ \cos(\alpha) \mp \sqrt{1 + \left(\frac{\lambda}{gR}\right)^2} \end{pmatrix} \frac{1}{\sqrt{2\left(1 + \left(\frac{\lambda}{gR}\right)^2 \mp \cos(\alpha)\sqrt{1 + \left(\frac{\lambda}{gR}\right)^2}\right)}} \quad (\text{H.98})
 \end{aligned}$$

This equations shows, that the wave functions become real-valued only for $\lambda = 0$, and that the imaginary part changes sign with the sign of λ . This indicates already that the derivative couplings change sign with the sign of λ .

In order to calculate the derivative couplings We need to evaluate

$$\begin{aligned}
 & \frac{f^*}{\sqrt{f^*f + g^*g}} \partial_x \frac{f}{\sqrt{f^*f + g^*g}} + \frac{g^*}{\sqrt{f^*f + g^*g}} \partial_x \frac{g}{\sqrt{f^*f + g^*g}} \\
 &= \frac{f^* \partial_x f + g^* \partial_x g}{f^*f + g^*g} + \frac{f^*f + g^*g}{f^*f + g^*g} \sqrt{f^*f + g^*g} \partial_x \frac{1}{\sqrt{f^*f + g^*g}} \\
 &= \frac{f^* \partial_x f + g^* \partial_x g}{f^*f + g^*g} - \frac{1}{2} \frac{\partial_x (f^*f + g^*g)}{f^*f + g^*g}
 \end{aligned} \tag{H.99}$$

where $f = -gR \sin(\alpha) + i\lambda$ and $g = gR \cos(\alpha) \mp \sqrt{(gR)^2 + \lambda^2}$ and x is either α or R .

$$\begin{aligned}
 & \Psi_a^{BO,*}(R, \alpha) \frac{\hbar}{i} \partial_\alpha \Psi_a^{BO}(R, \alpha) + \Psi_b^{BO,*}(R, \alpha) \frac{\hbar}{i} \partial_\alpha \Psi_b^{BO}(R, \alpha) \\
 &= \frac{\hbar}{i} \left[\left(-\sin(\alpha) - i \frac{\lambda}{gR} \right) \left(-\cos(\alpha) \right) + \left(\cos(\alpha) \mp \sqrt{1 + \left(\frac{\lambda}{gR} \right)^2} \right) \left(-\sin(\alpha) \right) \right] \\
 & \quad \frac{1}{2 \left(1 + \left(\frac{\lambda}{gR} \right)^2 \mp \cos(\alpha) \sqrt{1 + \left(\frac{\lambda}{gR} \right)^2} \right)} \\
 &= \frac{\frac{1}{2} \frac{\hbar}{i} \left(\pm 2 \sin(\alpha) \sqrt{1 + \left(\frac{\lambda}{gR} \right)^2} \right)}{2 \left(1 + \left(\frac{\lambda}{gR} \right)^2 \mp \cos(\alpha) \sqrt{1 + \left(\frac{\lambda}{gR} \right)^2} \right)} \\
 &= \frac{\frac{\hbar}{i} \left[\left(i \cos(\alpha) \frac{\lambda}{gR} \right) + \left(\pm \sin(\alpha) \sqrt{1 + \left(\frac{\lambda}{gR} \right)^2} \right) - \frac{1}{2} \left(\pm 2 \sin(\alpha) \sqrt{1 + \left(\frac{\lambda}{gR} \right)^2} \right) \right]}{2 \left(1 + \left(\frac{\lambda}{gR} \right)^2 \mp \cos(\alpha) \sqrt{1 + \left(\frac{\lambda}{gR} \right)^2} \right)} \\
 &= \frac{\frac{\hbar}{2} \frac{\cos(\alpha) \frac{\lambda}{gR}}{1 + \left(\frac{\lambda}{gR} \right)^2 \mp \cos(\alpha) \sqrt{1 + \left(\frac{\lambda}{gR} \right)^2}}}{2}
 \end{aligned} \tag{H.100}$$

This term produces a non-zero contribution, where the $\cos(\alpha) = \pm 1$, which looks like a δ -function. It changes sign with the sign of λ . Hence it also vanishes for $\lambda = 0$. However, the derivative couplings are non-differentiable with λ so that the limits for $\lambda = 0$ from both sides are finite and different.

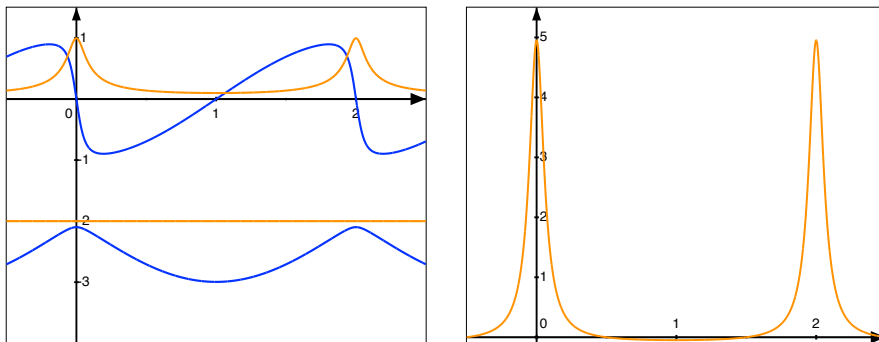


Fig. H.8: Left: upper Born-Oppenheimer wave function ($\Psi_{a,+}^{BO}(\alpha)$, $\Psi_{b,+}^{BO}(\alpha)$) of the Jahn-Teller model with a lifted conical intersection for $\lambda(gR) = 0.2$. Real (blue) and imaginary parts (orange) of the component $\Psi_{b,+}^{BO}(\alpha)$ are displaced by -2 along the ordinate. Compare with fig. H.3 on p. 474. Right graph: real part of the angular component of the derivative coupling.

The relevant limit for a true conical intersection is if $gR \gg \lambda$ and $\lambda \rightarrow 0$, that is $\lambda/(gR) \rightarrow 0$.

$$\begin{aligned} & \Psi_a^{BO,*}(R, \alpha) \frac{\hbar}{i} \partial_\alpha \Psi_a^{BO}(R, \alpha) + \Psi_b^{BO,*}(R, \alpha) \frac{\hbar}{i} \partial_\alpha \Psi_b^{BO}(R, \alpha) \\ &= \frac{\hbar}{2} \frac{\cos(\alpha) \frac{\lambda}{gR}}{1 + \left(\frac{\lambda}{gR}\right)^2 \mp \cos(\alpha) \sqrt{1 + \left(\frac{\lambda}{gR}\right)^2}} \end{aligned} \quad (\text{H.101})$$

To work out the geometric phase, use Bronstein p56, Eq.348

$$\begin{aligned} \int dx \frac{\cos(x)}{b + c \cos(x)} &= \frac{x}{c} - \frac{b}{c} \int dx \frac{1}{b + c \cos(x)} \\ \int dx \frac{1}{b + c \cos(x)} &= \begin{cases} \frac{2}{\sqrt{b^2 - c^2}} \operatorname{atan} \left(\frac{(b-c) \tan(x/2)}{\sqrt{b^2 - c^2}} \right) & \text{for } b^2 > c^2 \\ \frac{1}{c^2 - b^2} \ln \left(\frac{(c-b) \tan(x/2) + \sqrt{c^2 - b^2}}{(c-b) \tan(x/2) - \sqrt{c^2 - b^2}} \right) & \text{for } b^2 < c^2 \end{cases} \end{aligned} \quad (\text{H.102})$$

Appendix I

Quick peek on creation and annihilation operators

The language of second quantization in terms of creation and annihilation operators is covered in detail in Φ SX:Advanced Solid State Theory[2]. This notation can just as well be used for non-interacting particles. However, this is not required and therefore I leave that complication away from the current lecture.

Nevertheless, there are students who already had some contact with creation and annihilation operators and who would like to make contact between the different notations. Therefore, I have copied the relevant material into this appendix.

The chapter rests on the occupation-number representation described in section 3.4 on p. 98. In the occupation number representation the Slater determinants expressed in some ordered one-particle basisset $\{|\phi_j\rangle\}$ are expressed in terms of a vector $\vec{\sigma}$ containing the occupation numbers $\sigma_j \in \{0, 1\}$ of the one-particle orbitals.

I.1 Creation and annihilation operators, the language of second quantization

We can express Slater determinants in terms of a **vacuum state** $|\mathcal{O}\rangle$ and **creation operators** \hat{a}_α^\dagger and their hermitian conjugate **annihilation operators** \hat{a}_α . The vacuum state $|\mathcal{O}\rangle = |000000\dots\rangle$ is a state without particles. Note, that the vacuum state $|\mathcal{O}\rangle$ differs from the **zero state** $|\emptyset\rangle$ obtained by multiplying a state with zero. While a vacuum state describes a physical situation, namely space without particles, the zero state does not describe any physics. *“The zero state is not even nothing!”*

The **creation operators** \hat{a}_j^\dagger adds a particle to a given state containing zero or more particles. Using creation operators we can create all many-particle states from the vacuum state.

CREATION OPERATOR

We define the creation operator \hat{a}_j^\dagger for a particular one-particle orbital $|\phi_j\rangle$ as follows:

When we apply a creation operator to a Slater determinant, it adds a row with the new orbital at the top of the corresponding matrix, and introduces a column with a new coordinate to the right.

It is important to watch the sign of the state. Let us consider an example where a third particle in the one-particle orbital $|\phi_2\rangle$ is added to a many-particle state that already contains two particles,

one in $|\phi_1\rangle$ and one in $|\phi_3\rangle$.

$$\begin{aligned}
 \hat{a}_2^\dagger \left(\overbrace{\frac{1}{\sqrt{2!}} \det \begin{vmatrix} \phi_1(\bar{x}_1) & \phi_1(\bar{x}_2) \\ \phi_3(\bar{x}_1) & \phi_3(\bar{x}_2) \end{vmatrix}}^{|1,0,1,0,\dots\rangle} \right) &= \overbrace{\frac{1}{\sqrt{3!}} \det \begin{vmatrix} \phi_2(\bar{x}_1) & \phi_2(\bar{x}_2) & \phi_2(\bar{x}_3) \\ \phi_1(\bar{x}_1) & \phi_1(\bar{x}_2) & \phi_1(\bar{x}_3) \\ \phi_3(\bar{x}_1) & \phi_3(\bar{x}_2) & \phi_3(\bar{x}_3) \end{vmatrix}}^{\hat{a}_2^\dagger |1,0,1,0,\dots\rangle} \\
 &= (-1) \cdot \overbrace{\frac{1}{\sqrt{3!}} \det \begin{vmatrix} \phi_1(\bar{x}_1) & \phi_1(\bar{x}_2) & \phi_1(\bar{x}_3) \\ \phi_2(\bar{x}_1) & \phi_2(\bar{x}_2) & \phi_2(\bar{x}_3) \\ \phi_3(\bar{x}_1) & \phi_3(\bar{x}_2) & \phi_3(\bar{x}_3) \end{vmatrix}}^{|1,1,1,0,\dots\rangle}} \quad (1.1)
 \end{aligned}$$

That is

$$\hat{a}_2^\dagger |1, 0, 1, 0, 0, \dots\rangle = -|1, 1, 1, 0, 0, \dots\rangle \quad (1.2)$$

We realize that

- we need to introduce a sign change, because we need to bring the new row in the matrix of the Slater determinant into the correct position. Every permutation of two rows introduces a sign change.
- creating an electron into a one-particle orbital that is already occupied produces a zero state $|\emptyset\rangle$, because a determinant of a matrix with two identical rows vanishes.

Generalizing this principle leads to

$$\begin{aligned}
 \hat{a}_i^\dagger |\sigma_1, \sigma_2, \dots, \underbrace{0}_{\sigma_i}, \dots\rangle &= |\sigma_1, \sigma_2, \dots, \underbrace{1}_{\sigma_i}, \dots\rangle \left[(-1)^{\sum_{j=1}^{i-1} \sigma_j} \right] \\
 \hat{a}_i^\dagger |\sigma_1, \sigma_2, \dots, \underbrace{1}_{\sigma_i}, \dots\rangle &= |\emptyset\rangle \\
 \hat{a}_i |\sigma_1, \sigma_2, \dots, \underbrace{1}_{\sigma_i}, \dots\rangle &= |\sigma_1, \sigma_2, \dots, \underbrace{0}_{\sigma_i}, \dots\rangle \left[(-1)^{\sum_{j=1}^{i-1} \sigma_j} \right] \\
 \hat{a}_i |\sigma_1, \sigma_2, \dots, \underbrace{0}_{\sigma_i}, \dots\rangle &= |\emptyset\rangle \quad (1.3)
 \end{aligned}$$

In short, we may write

FERMIONIC CREATION AND ANNIHILATION OPERATORS

The definition of Fermionic creation and annihilation operators is

$$\begin{aligned}
 \hat{a}_i^\dagger |\sigma_1, \sigma_2, \dots, \sigma_i, \dots\rangle &= |\sigma_1, \sigma_2, \dots, \sigma_i + 1, \dots\rangle \left[(-1)^{\sum_{j=1}^{i-1} \sigma_j} \right] \sqrt{1 - \sigma_i} \\
 \hat{a}_i |\sigma_1, \sigma_2, \dots, \sigma_i, \dots\rangle &= |\sigma_1, \sigma_2, \dots, \sigma_i - 1, \dots\rangle \left[(-1)^{\sum_{j=1}^{i-1} \sigma_j} \right] \sqrt{\sigma_i} \quad (1.4)
 \end{aligned}$$

which implies that the sign changes, whenever the new electron is shifted to the right of an already occupied orbital.

A state with a occupation number σ_i different from zero or one is a zero state $|\emptyset\rangle$, that is

$$|\sigma_1, \sigma_2, \dots\rangle \stackrel{\text{def}}{=} |\emptyset\rangle \quad \text{if there is an } \sigma_i \notin \{0, 1\} \quad (1.5)$$

This requirement is additionally imposed by the factors ^a $\sqrt{1 - \sigma_i}$ and $\sqrt{\sigma_i}$.

^aThe square-root is irrelevant for fermions, and it is chosen in analogy with bosons.

Anticommutator relations: The creation and annihilation operators of Fermions obey anticommutator relations¹

$$\begin{aligned} [\hat{a}_j^\dagger, \hat{a}_k^\dagger]_+ &= 0 \\ [\hat{a}_j, \hat{a}_k]_+ &= 0 \\ [\hat{a}_j^\dagger, \hat{a}_k]_+ &= \delta_{j,k} \end{aligned} \tag{1.6}$$

The anticommutator relations follow directly from the definition.² They are, however, not derived here. See for example section 3 in *ΦSX: Advanced Solid-State Theory*[2].

From states to operators: Every Slater determinant $|\vec{\sigma}\rangle$ can be built up from the vacuum state by creating particles successively using Eq. 1.4. Sign changes can be avoided when we start creating particles in the one-particle orbitals with the highest quantum number. This provides us with yet another way of expressing a Slater determinant:

NUMBER REPRESENTATION AND CREATION OPERATORS

A state characterized in the occupation number representation by a string $\vec{\sigma}$ of occupation numbers can be constructed by successively applying creation operators to the vacuum state $|\mathcal{O}\rangle$ in the form

$$|\vec{\sigma}\rangle = \prod_{j=1}^{\infty} (\hat{a}_j^\dagger)^{\sigma_j} |\mathcal{O}\rangle = (\hat{a}_1^\dagger)^{\sigma_1} (\hat{a}_2^\dagger)^{\sigma_2} \dots (\hat{a}_\infty^\dagger)^{\sigma_\infty} |\mathcal{O}\rangle \tag{1.8}$$

- Like the occupation-number representation, the meaning of the creation and annihilation operators depends on the choice of the one-particle basisset.
- The indices in the product increase from the left to the right. That is, the first electron is created in the one-particle orbital with the highest quantum number.
- remember that the construction of a bra requires the order of operators to be interchanged, i.e.

$$\langle \vec{\sigma} | = \langle \mathcal{O} | \prod_{j=\infty}^1 (\hat{a}_j)^{\sigma_j} = \langle \mathcal{O} | (\hat{a}_\infty)^{\sigma_\infty} \dots (\hat{a}_2)^{\sigma_2} (\hat{a}_1)^{\sigma_1} \tag{1.9}$$

Fermions and Bosons: The creation and annihilation operators differ in several points:

- Instead of anticommutator relations, bosonic creation and annihilation operators obey analogous commutator relations. This implies that the interchange of two bosonic creation operators does not change the sign.
- the occupation numbers can be any non-negative integer.

1.1.1 Hamilton operator with creation and annihilation operators (Optional)

In this section, I will translate the main results just discussed into the language of creation and annihilation operators. While trying to be precise in the statements, I will also try to be as brief as

¹An **anticommutator** is defined as $[\hat{A}, \hat{B}]_+ \stackrel{\text{def}}{=} \hat{A}\hat{B} + \hat{B}\hat{A}$.

²One plausibility argument is that interchanging creation operators interchanges the two particles. For Fermions, Pauli principle says that this changes the sign of the state.

$$\hat{a}_j^\dagger \hat{a}_k^\dagger |\Phi\rangle = -\hat{a}_k^\dagger \hat{a}_j^\dagger |\Phi\rangle \quad \rightarrow \quad [\hat{a}_j^\dagger, \hat{a}_k^\dagger]_+ = 0 \tag{1.7}$$

possible. Furthermore, I will not attempt to be comprehensive. A more detailed exposition of the material can be found in $\Phi\text{SX}:\text{Advanced Solid-State Theory}[2]$.

So far, we can represent the Hamiltonian in a Hilbert space with a fixed number N of particles. Let me now write down the Hamiltonian for an arbitrary many-particle wave function.

Here, I make use of the **occupation-number operator** $\hat{a}_n^\dagger \hat{a}_n$, which has the eigenvalue equation

$$\hat{a}_n^\dagger \hat{a}_n |\vec{\sigma}\rangle = |\vec{\sigma}\rangle \sigma_n \quad (1.10)$$

We will also need the representation of the identity

$$\hat{1} = \sum_{\vec{\sigma}} |\vec{\sigma}\rangle \langle \vec{\sigma}| \quad (1.11)$$

in terms of Slater determinants. Slater determinants can also be *defined* as the eigenstates of the occupation-number operators.

The operators \hat{a}_n^\dagger and \hat{a}_n are defined in a basiset of eigenstates of the one-particle Hamiltonian. This yields

$$\begin{aligned} \hat{H} &= \sum_{\vec{\sigma}} \hat{H} |\vec{\sigma}\rangle \langle \vec{\sigma}| = \sum_{\vec{\sigma}} |\vec{\sigma}\rangle E_{\vec{\sigma}} \langle \vec{\sigma}| = \sum_{\vec{\sigma}} |\vec{\sigma}\rangle \underbrace{\left(\sum_n \epsilon_n \sigma_n \right)}_{E_{\vec{\sigma}}} \langle \vec{\sigma}| \\ &= \sum_{\vec{\sigma}} \left(\sum_n \epsilon_n \underbrace{|\vec{\sigma}\rangle \sigma_n}_{\hat{a}_n^\dagger \hat{a}_n |\vec{\sigma}\rangle} \right) \langle \vec{\sigma}| = \sum_n \epsilon_n \hat{a}_n^\dagger \hat{a}_n \underbrace{\sum_{\vec{\sigma}} |\vec{\sigma}\rangle \langle \vec{\sigma}|}_{\hat{1}} \\ &= \sum_n \epsilon_n \hat{a}_n^\dagger \hat{a}_n \end{aligned} \quad (1.12)$$

Analogously, we obtain the **particle-number operator** \hat{N} . Instead of the energy eigenvalue ϵ_n in the Hamilton operator the one-particle eigenvalue of the particle-number operator is 1. Therefore

$$\hat{N} = \sum_{\vec{\sigma}} |\vec{\sigma}\rangle N_{\vec{\sigma}} \langle \vec{\sigma}| = \sum_{\vec{\sigma}} |\vec{\sigma}\rangle \left(\sum_{n=1}^{\infty} \sigma_n \right) \langle \vec{\sigma}| = \sum_n \hat{a}_n^\dagger \hat{a}_n \quad (1.13)$$

Creation and annihilation operators for an arbitrary one-particle basis: So far, a special one-particle basiset $\{|\varphi_n\rangle\}$ has been chosen, namely the eigenstates of Hamiltonian. Let me now start with an arbitrary, but still complete and orthonormal one-particle basiset $\{|\chi_\alpha\rangle\}$. The eigenstates $|\varphi_j\rangle$ of the Hamiltonian can be built from this basiset by a unitary transformation

$$|\varphi_n\rangle = \sum_{\alpha} |\chi_\alpha\rangle \langle \chi_\alpha | \varphi_n\rangle = \sum_{\alpha} |\chi_\alpha\rangle U_{\alpha,n} \quad (1.14)$$

where \mathbf{U} is the unitary matrix formed by the eigenvectors of \mathbf{h} in the new basiset $|\chi_\alpha\rangle$

Now, I choose the creation operators so that

$$|\varphi_n\rangle = \hat{a}_n^\dagger |\mathcal{O}\rangle \quad (1.15)$$

$$|\chi_\alpha\rangle = \hat{c}_\alpha^\dagger |\mathcal{O}\rangle \quad (1.16)$$

which yields

$$\begin{aligned} \hat{a}_n^\dagger |\mathcal{O}\rangle &\stackrel{\text{Eq. 1.15}}{=} |\varphi_n\rangle \stackrel{\text{Eq. 1.14}}{=} \underbrace{\sum_{\alpha} |\chi_\alpha\rangle \langle \chi_\alpha | \varphi_n\rangle}_{\hat{1}} \stackrel{\text{Eq. 1.16}}{=} \sum_{\alpha} \underbrace{\hat{c}_\alpha^\dagger |\mathcal{O}\rangle}_{|\chi_\alpha\rangle} \underbrace{\langle \chi_\alpha | \varphi_n\rangle}_{U_{\alpha,n}} = \left(\sum_{\alpha} \hat{c}_\alpha^\dagger \underbrace{\langle \chi_\alpha | \varphi_n\rangle}_{U_{\alpha,n}} \right) |\mathcal{O}\rangle \\ \Leftrightarrow \hat{a}_n^\dagger &= \sum_{\alpha} \hat{c}_\alpha^\dagger \underbrace{\langle \chi_\alpha | \varphi_n\rangle}_{U_{\alpha,n}} \end{aligned} \quad (1.17)$$

Thus, we learned how to transform creation operators between different one-particle basis sets.

This allows one to express the Hamiltonian in the basisset $|\chi_\alpha\rangle$. That is $h_{\alpha,\beta} \stackrel{\text{def}}{=} \langle\chi_\alpha|\hat{h}|\chi_\beta\rangle$.

$$\begin{aligned} \hat{H} \stackrel{\text{Eq. 1.12}}{=} \sum_n \epsilon_n \hat{a}_n^\dagger \hat{a}_n &= \sum_n \left(\sum_\alpha \hat{c}_\alpha^\dagger \underbrace{\langle\chi_\alpha|\varphi_n\rangle}_{U_{\alpha,n}} \right) \epsilon_n \left(\sum_\beta \underbrace{\langle\varphi_n|\chi_\beta\rangle}_{U_{n,\beta}^\dagger} \hat{c}_\beta \right) = \sum_{\alpha,\beta} \hat{c}_\alpha^\dagger \underbrace{\langle\chi_\alpha| \left(\sum_n |\varphi_n\rangle \epsilon_n \langle\varphi_n| \right) |\chi_\beta\rangle}_{h_{\alpha,\beta}} \hat{c}_\beta \\ &= \sum_{\alpha,\beta} h_{\alpha,\beta} \hat{c}_\alpha^\dagger \hat{c}_\beta \end{aligned} \quad (1.18)$$

The many-particle eigenstates of a Hamiltonian for non-interacting electrons are

$$|\vec{\sigma}\rangle = \left[\prod_{n=1}^{\infty} \left(\sum_\alpha \hat{c}_\alpha^\dagger \underbrace{\langle\chi_\alpha|\varphi_n\rangle}_{U_{\alpha,n}} \right)^{\sigma_n} \right] |\mathcal{O}\rangle \quad (1.19)$$

The states $|\vec{\sigma}\rangle$ are still Slater determinants expressed in the basis of $|\varphi_n\rangle$, while the creation operators \hat{c}_α refer to another (orthonormal) one-particle basis $\{|\chi_\alpha\rangle\}$.

This result can be generalized to any hermitian one-particle operator \hat{A} in the form

$$\hat{A} = \sum_{\alpha,\beta} \underbrace{A_{\alpha,\beta}}_{\langle\chi_\alpha|\hat{A}|\chi_\beta\rangle} \hat{c}_\alpha^\dagger \hat{c}_\beta \quad (1.20)$$

Noteworthy is that a state, which can be represented as a single Slater determinant in one representation, is a superposition over many Slater determinants, once expressed in terms of another one-particle basisset. The occupations, however, are indicator of whether the state can be represented as Slater determinant in any representation are the occupations: When they are all integers, i.e. zero or one, the state is a single Slater determinant in the basis of its natural orbitals.

HAMILTONIAN AND EIGENSTATES FOR INDEPENDENT ELECTRONS

Using the occupation-number representation in a basisset of a one-particle Hamiltonian \hat{h} , i.e. $\hat{h}|\varphi_n\rangle = |\varphi_n\rangle\epsilon_n$ with $\langle\varphi_m|\varphi_n\rangle = \delta_{m,n}$, the corresponding Hamiltonian of (many) independent particles is

$$\hat{H} = \sum_{\vec{\sigma}} |\vec{\sigma}\rangle \left(\sum_{n=1}^{\infty} \epsilon_n \sigma_n \right) \langle\vec{\sigma}| \quad \text{and} \quad \hat{N} = \sum_{\vec{\sigma}} |\vec{\sigma}\rangle \left(\sum_{n=1}^{\infty} \sigma_n \right) \langle\vec{\sigma}| \quad (1.21)$$

with eigenstates $|\vec{\sigma}\rangle$ and energy eigenvalues $E_{\vec{\sigma}} = \sum_n \epsilon_n \sigma_n$. The particle-number eigenvalues are $N_{\vec{\sigma}} = \sum_n \sigma_n$.

With the creation operators for energy eigenstates $\hat{a}_n^\dagger|\mathcal{O}\rangle = |\varphi_n\rangle$ and for some other orthonormal one-particle basis set with orbitals $\hat{c}_\alpha^\dagger|\mathcal{O}\rangle = |\chi_\alpha\rangle$.

$$\hat{H} = \sum_n \epsilon_n \hat{a}_n^\dagger \hat{a}_n = \sum_{\alpha,\beta} h_{\alpha,\beta} \hat{c}_\alpha^\dagger \hat{c}_\beta \quad \text{and} \quad \hat{N} = \sum_n \hat{a}_n^\dagger \hat{a}_n = \sum_{\alpha,\beta} \delta_{\alpha,\beta} \hat{c}_\alpha^\dagger \hat{c}_\beta \quad (1.22)$$

The eigenstates are of Hamiltonian and particle number are

$$|\vec{\sigma}\rangle = \left[\prod_{n=1}^{\infty} \left(\hat{a}_n^\dagger \right)^{\sigma_n} \right] |\mathcal{O}\rangle = \left[\prod_{n=1}^{\infty} \left(\sum_\alpha \hat{c}_\alpha^\dagger \langle\chi_\alpha|\varphi_n\rangle \right)^{\sigma_n} \right] |\mathcal{O}\rangle \quad (1.23)$$

Appendix J

Some group theory for symmetries

Symmetry operators are important to break down a Hamiltonian into a block diagonal matrix, which greatly simplifies the construction of the Hamilton eigenvalues. For this purpose we need to determine distinct sets of states which are eigenstates with respect to the symmetry operators of the Hamiltonian.

The following follows closely the Chemwiki
http://chemwiki.ucdavis.edu/Theoretical_Chemistry/Symmetry/Group_Theory%3A_Theory

J.1 Definition of a group

The symmetry operators form a **group**.

A group consists of a set of elements and an operation. In our case the elements are the symmetry operations and the operations is the operator multiplication. To be a group the following properties need to be fulfilled.

- **Closure:** For any two members \hat{A} and \hat{B} of the group, their product $\hat{C} = \hat{A}\hat{B}$ is a member of the group.
- **Associativity:** The order in which the multiplications are performed does not affect the result.

$$\forall_{\hat{A}, \hat{B}, \hat{C} \in G} (\hat{A}\hat{B})\hat{C} = \hat{A}(\hat{B}\hat{C}) \quad (\text{J.1})$$

- **Identity:** There is one element $\hat{1}$ in the group, called identity, which leaves all elements in the group unchanged when operated on it from the left or from the right.

$$\exists_{\hat{1} \in G} \forall_{\hat{A} \in G} \hat{1}\hat{A} = \hat{A}\hat{1} \quad (\text{J.2})$$

- **Inverse:** For each element \hat{A} in the group, there is one element in the group, called the inverse \hat{A}^{-1} of \hat{A} , which produces the identity when operated on \hat{A} .

$$\forall_{\hat{A} \in G} \exists_{\hat{A}^{-1} \in G} \hat{A}^{-1}\hat{A} = \hat{A}\hat{A}^{-1} = \hat{1} \quad (\text{J.3})$$

J.2 Symmetry class

A **similarity transform**¹ with an invertible operator \hat{X} transforms an operator \hat{A} into an operator \hat{B} by

$$\hat{X}^{-1}\hat{A}\hat{X} = \hat{B} \quad (\text{J.4})$$

¹Source: https://en.wikipedia.org/wiki/Matrix_similarity,
<http://mathworld.wolfram.com/SimilarityTransformation.html>.

To construct the symmetry class C_A containing operator A , calculate all operators obtained by a similarity transform with any of the operators in the group.

$$C_A = \{\hat{X}^{-1}\hat{A}\hat{X}\}_{\forall \hat{X} \in G} \quad (\text{J.5})$$

If \hat{B} is in the symmetry class C_A containing \hat{A} , then \hat{A} is member of the symmetry class C_B .

Proof: If \hat{B} is member of \hat{C}_A , then there is one group operation \hat{X} so that $\hat{B} = \hat{X}^{-1}\hat{A}\hat{X}$. Thus, also $\hat{A} = \hat{X}\hat{B}\hat{X}^{-1}$. Because also the inverse \hat{X}^{-1} is member of the group, \hat{A} is member of the class C_B containing \hat{B} .

The classes produced by two operators in the same class are identical.

$$\hat{B} \in C_A \Rightarrow C_B = C_A \quad (\text{J.6})$$

Appendix K

Thermodynamic relations

K.1 Thermal expectation values from the grand potential

Here we derive the expression of the thermal expectation value of a one-particle operator \hat{A} in system of a non-interacting fermions,

THERMAL EXPECTATION VALUE

$$\langle \hat{A} \rangle = \int_{-\infty}^{\infty} d\epsilon f_{T,\mu}(\epsilon) \text{Tr} [\hat{D}(\epsilon) \hat{A}] \quad (\text{K.1})$$

from fundamental thermodynamic principles.

Relation Eq. K.1 follows from the thermodynamic relations: For an extended Hamiltonian $H(\gamma) = H_0 + \gamma \hat{A}$, one obtains the extended grand potential

$$\Omega(\gamma) \stackrel{\text{Eq. 6.10}}{=} -k_B T \ln \text{Tr} \left[e^{-\beta(\hat{H}_0 + \gamma \hat{A} - \mu \hat{N})} \right] \quad (\text{K.2})$$

The thermal expectation value of any operator can be generated as derivative of the extended grand potential with the coupling parameter.

$$\left. \frac{\partial \Omega}{\partial \gamma} \right|_{\gamma=0} = \lim_{\gamma \rightarrow 0} -k_B T \underbrace{\frac{1}{\text{Tr} \left[e^{-\beta(\hat{H}_0 + \gamma \hat{A} - \mu \hat{N})} \right]}}_{1/Z} \text{Tr} \left[-\beta \hat{A} e^{-\beta(\hat{H}_0 + \gamma \hat{A} - \mu \hat{N})} \right] = \text{Tr} \left[\hat{A} \hat{\rho}^{eq} \right] = \langle \hat{A} \rangle \quad (\text{K.3})$$

We used the expression for the equilibrium density matrix $\hat{\rho}^{eq}$ from Eq. 6.8. The identity Eq. K.3 is very general: it holds for all thermal equilibrium states and for any operator, be it a one-particle or a many-particle operator.

For non-interacting particles we can make use of the grand potential given in Eq. 6.25.

$$\Omega(\gamma) \stackrel{\text{Eq. 6.25}}{=} \int_{-\infty}^{\infty} d\epsilon D_{tot}(\epsilon, \gamma) \left[-k_B T \ln \left(1 + e^{-\beta(\epsilon - \mu)} \right) \right] \quad (\text{K.4})$$

Because this expression is restricted to non-interacting systems, the operator \hat{A} is required to be a one-particle operator as well.

The coupling constant γ enters only via the total density of states

$$D_{tot}(\epsilon, \gamma) \stackrel{\text{Eq. 5.22}}{=} \sum_n \delta(\epsilon - \epsilon_n(\gamma)) \quad (\text{K.5})$$

Its coupling-constant derivative is ¹

$$\begin{aligned} \frac{\partial D_{tot}(\epsilon, \gamma)}{\partial \gamma} &= \sum_n \frac{d\delta(\epsilon - \epsilon_n(\gamma))}{d\epsilon} \underbrace{\left(-\frac{d\epsilon_n}{d\gamma}\right)}_{-\langle \psi_n | \hat{A} | \psi_n \rangle} = \frac{d}{d\epsilon} \text{Tr} \left[\sum_n |\psi_n\rangle \delta(\epsilon - \epsilon_n) \langle \psi_n | \hat{A} \right] \\ &\stackrel{\text{Eq. 5.16}}{=} \frac{d}{d\epsilon} \text{Tr} \left[\hat{D}(\epsilon) \hat{A} \right] \end{aligned} \quad (\text{K.6})$$

We used the eigenstates $|\psi_n\rangle$ of the Hamiltonian.

Thus,

$$\begin{aligned} \langle \hat{A} \rangle &\stackrel{\text{Eq. K.3}}{=} \left. \frac{\partial \Omega}{\partial \gamma} \right|_{\gamma=0} \stackrel{\text{Eq. K.4}}{=} \int_{-\infty}^{\infty} d\epsilon \frac{\partial D_{tot}(\epsilon, \gamma)}{\partial \gamma} \left[-k_B T \ln \left(1 + e^{-\beta(\epsilon - \mu)} \right) \right] \\ &= \int_{-\infty}^{\infty} d\epsilon \left(\frac{d}{d\epsilon} \text{Tr} \left[\hat{D}(\epsilon) \hat{A} \right] \right) \left[-k_B T \ln \left(1 + e^{-\beta(\epsilon - \mu)} \right) \right] \\ &= - \int_{-\infty}^{\infty} d\epsilon \text{Tr} \left[\hat{D}(\epsilon) \hat{A} \right] \underbrace{\frac{d}{d\epsilon} \left[-k_B T \ln \left(1 + e^{-\beta(\epsilon - \mu)} \right) \right]}_{-f_{T,\mu}(\epsilon)} \\ &= \int_{-\infty}^{\infty} d\epsilon f_{T,\mu}(\epsilon) \text{Tr} \left[\hat{D}(\epsilon) \hat{A} \right] \quad q.e.d. \end{aligned} \quad (\text{K.7})$$

which proves Eq. K.1.

One remark is still required regarding the partial energy integration in the step to Eq. K.7 above. In order to perform the partial integration leading to Eq. K.7, the term

$$\text{Tr} \left[\hat{D}(\epsilon) \hat{A} \right] \left[-k_B T \ln \left(1 + e^{-\beta(\epsilon - \mu)} \right) \right] \quad (\text{K.8})$$

need to vanish at $\epsilon = \pm\infty$. The term vanishes at $\epsilon = -\infty$, if the Hamiltonian is bounded from below, so that the density of states vanishes at low energies. It vanishes for $\epsilon = \infty$ because $\ln \left(1 + e^{-\beta(\epsilon - \mu)} \right)$ approaches zero for large positive energies.

K.2 Sommerfeld expansion

Here we sketch the derivation for the Sommerfeld expansion we refer to in section 6.5.2 on p. 194.

Many integrations involving the Fermi functions have the form

$$I = \int_{-\infty}^{\infty} d\epsilon g(\epsilon) f(\epsilon) \quad (\text{K.9})$$

where $f(\epsilon) = (1 + e^{\beta(\epsilon - \mu)})^{-1}$ is the Fermi function and $g(\epsilon)$ is some other function which is differentiable to infinite order.²

The **Sommerfeld expansion** is a method to evaluate these integrals given that integral and the derivatives of $g(\epsilon)$ are known at the Fermi level. The Sommerfeld expansion is a low-temperature expansion.

Let us define the integrand of $g(\epsilon)$

$$G(\epsilon) \stackrel{\text{def}}{=} \int_{-\infty}^{\epsilon} d\epsilon' g(\epsilon') \quad (\text{K.10})$$

¹Editor: Look for a sign error in the second equal sign below. Explain why it is correct, if it is.

²This may apply to some models. For real systems this assumption is not obeyed.

Then

$$\begin{aligned}
I &= \int_{-\infty}^{\infty} d\epsilon g(\epsilon) f(\epsilon) \\
&= \int_{-\infty}^{\infty} d\epsilon \left[\partial_{\epsilon} \left(G(\epsilon) f(\epsilon) \right) - G(\epsilon) \partial_{\epsilon} f(\epsilon) \right] \\
&= G(\infty) \underbrace{f(\infty)}_{=0} - G(-\infty) \underbrace{f(-\infty)}_{=1} - \int_{-\infty}^{\infty} d\epsilon G(\epsilon) \partial_{\epsilon} f(\epsilon) \\
&= -G(-\infty) - \sum_{n=0}^{\infty} \frac{1}{n!} \left(\partial_{\epsilon}^n \Big|_{\mu} G \right) \int_{-\infty}^{\infty} d\epsilon (\epsilon - \mu)^n \partial_{\epsilon} \underbrace{\frac{1}{1 + e^{\beta(\epsilon - \mu)}}}_{f(\epsilon)} \\
&= -G(-\infty) - \sum_{n=0}^{\infty} \frac{1}{n!} \left(\partial_{\epsilon}^n \Big|_{\mu} G \right) (k_B T)^n \int_{-\infty}^{\infty} dx x^n \partial_x \frac{1}{1 + e^x} \\
&= G(\mu) - G(-\infty) - \sum_{n=1}^{\infty} \frac{(k_B T)^{2n}}{(2n)!} \left(\partial_{\epsilon}^{2n} \Big|_{\mu} G \right) \int_{-\infty}^{\infty} dx x^{2n} \partial_x \frac{1}{1 + e^x} \\
&= \left(\int_{-\infty}^{\mu} d\epsilon g(\epsilon) \right) + \underbrace{\sum_{n=1}^{\infty} (k_B T)^{2n} \left(-\frac{1}{(2n)!} \int_{-\infty}^{\infty} dx x^{2n} \partial_x \frac{1}{1 + e^x} \right)}_{a_n} \left(\partial_{\epsilon}^{2n-1} \Big|_{\mu} g \right) \quad (\text{K.11})
\end{aligned}$$

Following Ashcroft and Mermin[135] (Ashcroft-Eq. 2.70 and Appendix C)

$$a_n = -\frac{1}{(2n)!} \int_{-\infty}^{\infty} dx x^{2n} \partial_x \frac{1}{1 + e^x} = \left(2 - \frac{1}{2^{2n-2}} \right) 2^{2n-1} \frac{\pi^{2n}}{(2n)!} B_n \quad (\text{K.12})$$

with the Bernoulli numbers $B_1 = \frac{1}{6}$ and $B_2 = \frac{1}{30}$.

$$\begin{aligned}
a_1 &= -\frac{1}{2!} \int dx x^2 \partial_x \frac{1}{1 + e^x} = \frac{\pi^2}{6} \\
a_2 &= -\frac{1}{4!} \int dx x^4 \partial_x \frac{1}{1 + e^x} = \frac{7\pi^4}{360} \quad (\text{K.13})
\end{aligned}$$

Thus, we obtain

SOMMERFELD EXPANSION

$$\int_{-\infty}^{\infty} d\epsilon g(\epsilon) f(\epsilon) = \left(\int_{-\infty}^{\mu} d\epsilon g(\epsilon) \right) + \frac{(\pi k_B T)^2}{6} \left(\partial_{\epsilon} \Big|_{\mu} g \right) + \frac{7(\pi k_B T)^4}{360} \left(\partial_{\epsilon}^3 \Big|_{\mu} g \right) + O\left((k_B T)^6 \right) \quad (\text{K.14})$$

which is equivalent to Eq. 6.46 on p. 195.

Appendix L

Why is the effective mass of semiconductors much smaller than that of metals?

Let me respond to the question why the effective masses of metals are comparable to the free-electron mass, while the effective masses of the semiconductors are usually much larger.

The first part of the answer is that the two masses are different concepts.

- The effective mass of a semiconductor is related to the curvature at the band edges and therefore describes the transport properties of charge carriers in the valence and conduction band.
- the effective mass of metals is related to the heat capacity, which in turn is a measure of the density of states at the Fermi level.

For the elemental metals such as Na(1e), K(1e), Al(3e), Cu(1e), Ag(1e), Au(1e) etc. the electronic structure is a variation of the free-electron band structure. Thus, one expects their effective masses to be similar (order of magnitude...) to that of a free electron.

The following discussion shall rationalize the underlying process leading from free electrons to the band gap of semiconductors. While I believe that the underlying concepts are more or less valid, please take the discussion with a grain of salt. I have not spent too much time on it.

The concepts can be followed from the band structures of the free-electron metal aluminium and the semiconductor silicon shown in Fig. L.1. If one follows the lowest bands from Γ to X and back, one will see some similarities between the two band structures. The uppermost green band of aluminium at the Γ point (at about +12 eV) translates into the valence band top of silicon (at 0 eV).¹ The band gap of silicon can loosely be attributed to an avoided crossing of the free-electron bands.

Let us try to model this: For the semiconductors the band gap develops out of an avoided crossing of "free-electron-like" bands, and this determines the effective mass. A true free electron would have a true band crossing. The resulting curvature of the bands is infinite. Hence the effective mass would vanish completely.

Let us make a crude model to elucidate the principles. Consider a free-electron band

$$E(k) = \frac{\hbar^2 k^2}{2m_e} \quad (\text{L.1})$$

The Fermi level shall be at the Fermi momentum p_F . The Fermi velocity is thus $v_F = \frac{\partial E}{\partial p} = \frac{p_F}{m_e}$.

¹The Fermi level in silicon is higher up because it has 8 electrons in the unit cell instead of the three electrons of aluminium.

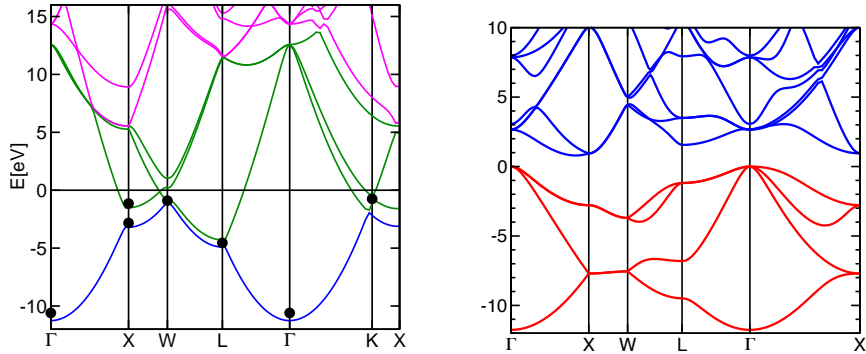


Fig. L.1: Comparison of the band structure of aluminium (left) and that of silicon (right). The Fermi level is at energy zero.

Now, we introduce a lattice so that p_F is equal to one-half of the reciprocal lattice vector. Because the band structure is periodically folded in, the Fermi momentum will be folded onto the Gamma point ($\vec{G} = 0$). Furthermore, there will be several bands crossing at Γ . If the lattice potential lifts the degeneracy, the band crossing will turn into an avoided crossing with some band gap E_g .

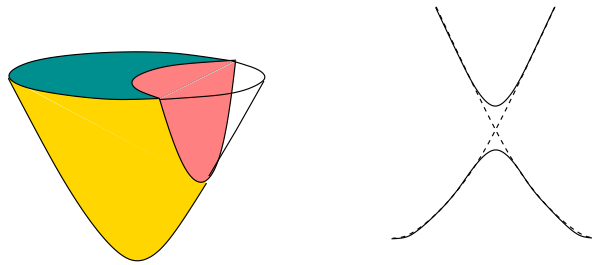


Fig. L.2: Intersection of two free-electron dispersions $\epsilon(\vec{k} - \vec{G})$ for two different reciprocal lattice vectors \vec{G} . At their intersection the upper and lower bands are formed. The sharp edge of the upper band will turn into an avoided crossing with a large curvature, i.e. light effective mass.

Imagine an avoided crossing of two bands in one dimension with the slope given by some Fermi velocity v_F and a band gap E_g . Let the avoided crossing be at $k = 0$.

$$E_{\pm}(k) = \pm \sqrt{(\hbar v_F k)^2 + \left(\frac{1}{2} E_g\right)^2} \quad (\text{L.2})$$

The curvature at the band edges is $\left. \frac{\partial^2 E}{\partial k^2} \right|_{k=0} = 2(\hbar v_F)^2 / E_g = \frac{\hbar^2}{m^*}$, so that the effective mass is

$$m^* = \frac{E_g}{2v_F^2} = \frac{E_g m_e^2}{2p_F^2} \quad (\text{L.3})$$

In this model, the effective mass is about proportional to the band gap, even though the “free-electron band” has a curvature determined by the true free-electron mass. It is also clear that the effective mass is much larger than the free-electron mass.

For similar semiconductors with a direct band gap at Gamma, I expect that the effective mass will be approximately proportional to the band gap.

For band gaps such as silicon which has the band minimum near the *X*-point, an analogous construction tells that the longitudinal effective electron mass should be similar to the free-electron mass, while the transversal mass should again be very small.

518 L WHY IS THE EFFECTIVE MASS OF SEMICONDUCTORS MUCH SMALLER THAN THAT OF METALS?

Appendix M

Brillouin-zone integrations

M.1 Solid in a box

In section 5.1.1 we described the counting of states for periodic boundary conditions. One may be concerned that periodic boundary conditions produce artifacts. Therefore, I show here for a simple example that the same state counting is obtained for a finite system. As example, I will use particles in a box.

One way to do the transition from a finite system to an infinite solid is to enclose the solid into a box Ω and then let the box grow to infinite size. Inside the box, the potential is equal to that of the crystal, and outside the box the potential is infinite.

Let us consider the box with side-lengths L_x, L_y, L_z along the three Cartesian coordinates.¹ The box shall occupy the volume with

$$\vec{r} \in \Omega \quad \Leftrightarrow \quad \left[0 < x < L_x \quad \text{and} \quad 0 < y < L_y \quad \text{and} \quad 0 < z < L_z \right] \quad (\text{M.1})$$

It may be useful to introduce a step function $\theta_\Omega(\vec{r})$ which equals one inside the box and which vanishes outside.

$$\theta_\Omega(\vec{r}) = \begin{cases} 1 & \text{for } \vec{r} \in \Omega \\ 0 & \text{for } \vec{r} \notin \Omega \end{cases} \quad (\text{M.2})$$

Because the Schrödinger equation inside the box Ω is that of a free particle, the wave functions inside the box are plane waves. The boundary conditions of vanishing wave function at the boundary of the box, are satisfied by

$$\psi_{\vec{\sigma}}(\vec{r}, \sigma) = \delta_{\sigma, \vec{\sigma}} \theta_\Omega(\vec{r}) \sqrt{\frac{8}{|\Omega|}} \sin(k_x x) \sin(k_y y) \sin(k_z z) \quad (\text{M.3})$$

with

$$\vec{k}_{i,j,k} = \begin{pmatrix} \frac{\pi}{L_x} i \\ \frac{\pi}{L_y} j \\ \frac{\pi}{L_z} k \end{pmatrix} \quad (\text{M.4})$$

with positive integers i, j, k .

We learned that the states for a finite box correspond to a discrete grid of k-points. In the case of a box, the k-points are restricted to have positive indices i, j, k .

¹I allow for different side lengths to allow for the study of quasi-one-dimensional or quasi-two-dimensional systems.

The reciprocal-space volume related to a k -point is $(2\pi)^3/|\Omega|$ with the box-volume $|\Omega|$. When we divide up the reciprocal-space volume between the k -points we obtain only π^3/Ω for each k -point. Because the k -point indices are all positive, we also need to consider the regions of reciprocal space for which one or more of the three k -point indices are negative. This contributes a factor 8 to each k -point.

Below, we will find that another set of boundary conditions produces a different set of k -points albeit with exactly the same reciprocal space volume attributed to each k -point.

Considering the solid in a finite box with surfaces has the disadvantage that the problem becomes inhomogeneous. As a consequence, it is hardly possible to construct the wave functions of a solid in a box from the Bloch states of the infinite system. This difficulty is one motivation for using the periodic boundary conditions.

Appendix N

Minimal models for phonon-phonon scattering

In this section I plan to explore the workings of phonon-phonon scattering using minimal models. Each phonon is replaced by a harmonic oscillator. The phonons will be coupled by an additional anharmonic term.

- first, I study a simple anharmonic oscillator.
- secondly we study three harmonic oscillators, which can convert into each other by phonon-phonon scattering.

Editor: This is not finished.

N.1 Anharmonic oscillator

Let us start from the Lagrangian of an anharmonic oscillator

$$\mathcal{L}(x, v) = \frac{1}{2}mv^2 - \frac{1}{2}m\omega_0^2x^2 - \frac{1}{3!}gx^3 - \frac{1}{4!}\frac{3g^2}{8c}x^4 \quad (\text{N.1})$$

The fourth-order term has been added to the potential energy to avoid that the energy becomes unbound from below. The prefactor is chosen equal to the minimum value, which guarantees that there is only a single minimum.

The Euler-Lagrange equations are

$$\begin{aligned} \frac{d}{dt} \left(\frac{\partial \mathcal{L}}{\partial v} \right) &= \frac{\partial \mathcal{L}}{\partial x} \quad \text{and} \quad \dot{x} = v \\ \Rightarrow m\ddot{x} &= -m\omega_0^2x - \frac{g}{2}x^2 - \frac{g^2}{16c}x^3 \quad \Rightarrow \quad \ddot{x} + \omega_0^2x = -\frac{g}{2m}x^2 - \frac{g^2}{16mc}x^3 \end{aligned} \quad (\text{N.2})$$

The anharmonic effects changes the period of the oscillation. We can describe this by a frequency shift from ω_0 to ω_g . On the other hand we may also perform a Fourier transform of the coordinate $x(t) = \sum_{n=1}^{\infty} 2\text{Re} [e^{-in\omega_g t} X_n]$. The anharmonicity leads to a set of **overtones**.

We introduce the “phonon” amplitudes

$$b_{\sigma}(t) = e^{-i\sigma\omega_0 t} \frac{1}{\sqrt{2m\hbar\omega_0}} (\omega_0 - i\sigma\partial_t) x(t) \quad (\text{N.3})$$

for which

$$x(t) = \frac{\sqrt{2m\hbar\omega_0}}{2\omega_0} \sum_{\sigma} b_{\sigma}(t) e^{i\sigma\omega_0 t} \quad (\text{N.4})$$

If we ignore the overtones, $x(t) = 2\text{Re}(X_1 e^{-i\omega_g t})$, so that

$$b_1(t) = \frac{\omega_0 + \omega_g}{\sqrt{2m\hbar\omega_0}} e^{i(\omega_g - \omega_0)t} X_1 + \frac{\omega_0 - \omega_g}{\sqrt{2m\hbar\omega_0}} e^{-i(\omega_g + \omega_0)t} X_1^* \quad (\text{N.5})$$

The amplitude undergoes a large oscillation with frequency $\omega - \omega_g$. This describes the frequency change due to the anharmonic effects. Overlaid is a weaker high-frequency oscillation.

$$\begin{aligned} i\hbar\partial_t b_\sigma(t) &\stackrel{\text{Eq. N.3}}{=} e^{-i\sigma\omega_0 t} \frac{1}{\sqrt{2m\hbar\omega_0}} \left[-i\sigma\omega_0 (\omega_0 x(t) - i\sigma\partial_t x(t)) + (\omega_0\partial_t x(t) - i\sigma\partial_t^2 x(t)) \right] \\ &= e^{-i\sigma\omega_0 t} \frac{1}{\sqrt{2m\hbar\omega_0}} \left[-i\sigma\omega_0^2 x(t) \underbrace{-\omega_0\dot{x}(t) + \omega_0\dot{x}(t)}_{=0} - i\sigma\partial_t^2 x(t) \right] \\ &\stackrel{\text{Eq. N.2}}{=} -i\sigma e^{-i\sigma\omega_0 t} \frac{1}{\sqrt{2m\hbar\omega_0}} \left[-\frac{g}{2m} x^2(t) \right] \\ &\stackrel{\text{Eq. N.4}}{=} i\sigma e^{-i\sigma\omega_0 t} \frac{1}{\sqrt{2m\hbar\omega_0}} \frac{g}{2m} \left[\left(\frac{\sqrt{2m\hbar\omega_0}}{2\omega_0} \right)^2 \sum_{\sigma, \sigma'} b_\sigma b_{\sigma'} e^{i[\sigma\omega_0 + \sigma'\omega_0]t} \right] \\ &= i\sigma \frac{g\sqrt{2m\hbar\omega_0}}{8m\omega_0^2} \sum_{\sigma', \sigma''} b_{\sigma'} b_{\sigma''} e^{i[\sigma'\omega_0 + \sigma''\omega_0 - \sigma\omega_0]t} \quad (\text{N.6}) \end{aligned}$$

In fig. N.1 the time evolution of the phonon amplitude is shown under the influence of an anharmonicity, which is switched on for a finite interval. It is apparent that the phonon amplitude remains constant in the absence of an anharmonic term. With the anharmonicity, the phonon amplitude undergoes a slow phase rotation. The slow phase rotation is superimposed with a smaller oscillation, which is due to the coupling of the mode with itself, resulting in an overtone.

N.2 First- and second-order approximation

We start with the equation of motion for the phonon amplitudes

$$i\hbar\partial_t b_\sigma(t) = i\sigma \frac{g\sqrt{2m\hbar\omega_0}}{8m\omega_0^2} \sum_{\sigma', \sigma''} b_{\sigma'}(t) b_{\sigma''}(t) e^{i[\sigma'\omega_0 + \sigma''\omega_0 - \sigma\omega_0]t} \quad (\text{N.7})$$

which yields

$$\Rightarrow b_\sigma(t) = b_\sigma(0) + \frac{1}{\hbar} \sigma \frac{g\sqrt{2m\hbar\omega_0}}{8m\omega_0^2} \sum_{\sigma', \sigma''} \int_0^t dt' b_{\sigma'}(t') b_{\sigma''}(t') e^{i[\sigma'\omega_0 + \sigma''\omega_0 - \sigma\omega_0]t'} \quad (\text{N.8})$$

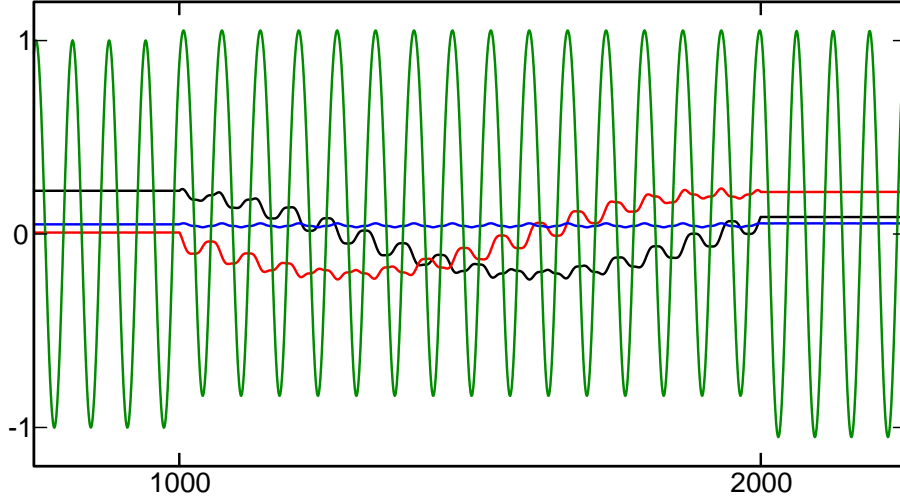


Fig. N.1: Dynamics of the phonon amplitudes $b_+(t)$ of a one-dimensional anharmonic oscillator as function of time for $\omega_0 = 0.1$, $g = -0.007$, $m = 1$, $g_4 = \frac{3}{8}g^2/(m\omega_0^2)$. The anharmonicity is switched on between $t = 1000$ and $t = 2000$. The large oscillation in green is the displacement $x(t)$, the blue line is the absolute value $|b_+(t)|$ of the phonon amplitude, the black and red lines are the real and imaginary part of the phonon amplitude $b_+(t)$. The calculation used the Verlet algorithm for $x(t)$ and recalculated the phonon amplitude from the distortion.

Next we divide the expression into orders of the anharmonicity g

$$\begin{aligned}
 \Rightarrow b_{\sigma}^{(0)}(t) &= b_{\sigma}(0) \\
 b_{\sigma}^{(1)}(t) &= \left(\frac{1}{\hbar}\sigma\frac{g\sqrt{2m\hbar\omega_0}}{8m\omega_0^2}\right)\sum_{\sigma',\sigma''}\int_0^t dt' e^{i[\sigma'\omega_0+\sigma''\omega_0-\sigma\omega_0]t'} b_{\sigma'}^{(0)}(t') b_{\sigma''}^{(0)}(t') \\
 &= \left(\frac{1}{\hbar}\sigma\frac{g\sqrt{2m\hbar\omega_0}}{8m\omega_0^2}\right)\sum_{\sigma',\sigma''}\frac{e^{i[\sigma'\omega_0+\sigma''\omega_0-\sigma\omega_0]t}-1}{i[\sigma'\omega_0+\sigma''\omega_0-\sigma\omega_0]} b_{\sigma'}(0) b_{\sigma''}(0) \\
 b_{\sigma}^{(2)}(t) &= \left(\frac{1}{\hbar}\sigma\frac{g\sqrt{2m\hbar\omega_0}}{8m\omega_0^2}\right)\sum_{\sigma',\sigma''}\int_0^t dt' e^{i[\sigma'\omega_0+\sigma''\omega_0-\sigma\omega_0]t'} \left(b_{\sigma'}^{(1)}(t') b_{\sigma''}^{(0)}(t') + b_{\sigma'}^{(0)}(t') b_{\sigma''}^{(1)}(t')\right) \\
 &= 2\left(\frac{1}{\hbar}\sigma\frac{g\sqrt{2m\hbar\omega_0}}{8m\omega_0^2}\right)\sum_{\sigma',\sigma''}\int_0^t dt' e^{i[\sigma'\omega_0+\sigma''\omega_0-\sigma\omega_0]t'} b_{\sigma'}^{(0)}(t') b_{\sigma''}^{(1)}(t') \\
 &= 2\left(\frac{1}{\hbar}\sigma\frac{g\sqrt{2m\hbar\omega_0}}{8m\omega_0^2}\right)^2\sum_{\sigma',\sigma''}\int_0^t dt' e^{i[\sigma'\omega_0+\sigma''\omega_0-\sigma\omega_0]t'} b_{\sigma'}(0) \\
 &\quad \times \sum_{\bar{\sigma}',\bar{\sigma}''}\frac{e^{i[\bar{\sigma}'\omega_0+\bar{\sigma}''\omega_0-\sigma''\omega_0]t'}-1}{i[\bar{\sigma}'\omega_0+\bar{\sigma}''\omega_0-\sigma''\omega_0]} b_{\bar{\sigma}'}(0) b_{\bar{\sigma}''}(0) \\
 &= 2\left(\frac{1}{\hbar}\sigma\frac{g\sqrt{2m\hbar\omega_0}}{8m\omega_0^2}\right)^2\sum_{\sigma',\bar{\sigma}',\bar{\sigma}''} b_{\sigma'}(0) b_{\bar{\sigma}'}(0) b_{\bar{\sigma}''}(0) \\
 &\quad \times \int_0^t dt' \left[\sum_{\sigma''}\frac{e^{i[\bar{\sigma}'\omega_0+\bar{\sigma}''\omega_0+\sigma'\omega_0-\sigma\omega_0]t'}-e^{i[\sigma'\omega_0+\sigma''\omega_0-\sigma\omega_0]t'}}{i[\bar{\sigma}'\omega_0+\bar{\sigma}''\omega_0-\sigma''\omega_0]}\right] \\
 &= 2\left(\frac{1}{\hbar}\sigma\frac{g\sqrt{2m\hbar\omega_0}}{8m\omega_0^2}\right)^2\sum_{\sigma',\bar{\sigma}',\bar{\sigma}''} b_{\sigma'}(0) b_{\bar{\sigma}'}(0) b_{\bar{\sigma}''}(0) \\
 &\quad \sum_{\sigma''}\frac{1}{i[\bar{\sigma}'\omega_0+\bar{\sigma}''\omega_0-\sigma''\omega_0]}\left[\frac{e^{i[\bar{\sigma}'\omega_0+\bar{\sigma}''\omega_0+\sigma'\omega_0-\sigma\omega_0]t}-1}{i[\bar{\sigma}'\omega_0+\bar{\sigma}''\omega_0+\sigma'\omega_0-\sigma\omega_0]}-\frac{e^{i[\sigma'\omega_0+\sigma''\omega_0-\sigma\omega_0]t}-1}{i[\sigma'\omega_0+\sigma''\omega_0-\sigma\omega_0]}\right] \\
 &\quad 2\left(\frac{1}{\hbar}\sigma\frac{g\sqrt{2m\hbar\omega_0}}{8m\omega_0^2}\right)^2\sum_{\sigma',\bar{\sigma}',\bar{\sigma}''} b_{\sigma'}(0) b_{\bar{\sigma}'}(0) b_{\bar{\sigma}''}(0)
 \end{aligned}$$

When we inspect the terms we observe that they all oscillate to finite values and back to zero, except for those with

$$\bar{\sigma}' + \bar{\sigma}'' + \sigma' - \sigma = 0 \quad (\text{N.10})$$

For these terms we obtain a contribution to $b^{(2)}$ which increases linearly with time.

$\bar{\sigma}'$	$\bar{\sigma}''$	σ'	σ
-	+	+	+
+	-	+	+
+	+	-	+
+	-	-	-
-	+	-	-
-	-	+	-

$$\begin{aligned}
\Rightarrow b_{\sigma}^{(0)}(t) &= b_{\sigma}(0) + \frac{2}{i\omega_0} \left(\frac{1}{\hbar} \sigma \frac{g\sqrt{2m\hbar\omega_0}}{8m\omega_0^2} \right)^2 \sum_{\sigma', \bar{\sigma}', \bar{\sigma}''} b_{\bar{\sigma}'}(0) b_{\bar{\sigma}''}(0) b_{\sigma'}(0) \\
&\times \sum_{\sigma''} \frac{1}{\bar{\sigma}' + \bar{\sigma}'' - \sigma''} \left[\frac{e^{i[\bar{\sigma}'\omega_0 + \bar{\sigma}''\omega_0 + \sigma'\omega_0 - \sigma\omega_0]t} - 1}{i[\bar{\sigma}'\omega_0 + \bar{\sigma}''\omega_0 + \sigma'\omega_0 - \sigma\omega_0]} - \frac{e^{i[\sigma'\omega_0 + \sigma''\omega_0 - \sigma\omega_0]t} - 1}{i[\sigma'\omega_0 + \sigma''\omega_0 - \sigma\omega_0]} \right] \\
&\approx b_{\sigma}(0) + \frac{2t}{i\omega} \left(\frac{1}{\hbar} \sigma \frac{g\sqrt{2m\hbar\omega_0}}{8m\omega_0^2} \right)^2 \left\{ b_{-\sigma}(0) b_{+\sigma}(0) b_{+\sigma}(0) \underbrace{\sum_{\sigma''} \frac{1}{-1 + 1 - \sigma''}}_{=0} \right. \\
&\quad \left. + b_{+\sigma}(0) b_{-\sigma}(0) b_{+\sigma}(0) \underbrace{\sum_{\sigma''} \frac{1}{+1 - 1 - \sigma''}}_{=0} + b_{+\sigma}(0) b_{+\sigma}(0) b_{-\sigma}(0) \underbrace{\sum_{\sigma''} \frac{1}{2 - \sigma''}}_{=4/3} \right\} \\
&= b_{\sigma}(0) - it \frac{8}{3\omega} \left(\frac{1}{\hbar} \sigma \frac{g\sqrt{2m\hbar\omega_0}}{8m\omega_0^2} \right)^2 |b_{+\sigma}(0)|^2 b_{+\sigma}(0) \quad (\text{N.11})
\end{aligned}$$

Now, we can try to form a new differential equation in this approximation

$$\begin{aligned}
i\hbar\partial_t b_{\sigma}(t) &= \hbar \frac{8}{3\omega} \left(\frac{1}{\hbar} \sigma \frac{g\sqrt{2m\hbar\omega_0}}{8m\omega_0^2} \right)^2 |b_{+\sigma}(0)|^2 b_{+\sigma}(0) \\
&= \frac{1}{12} \frac{g^2}{m\omega_0^4} |b_{+\sigma}(0)|^2 b_{+\sigma}(0) \quad (\text{N.12})
\end{aligned}$$

Appendix O

Boltzmann equation

O.1 Boltzmann equation constructed from a specified equilibrium distribution

In chapter 8, we discussed the stationary distribution of a given Boltzmann equation. That is, we considered the mapping $(H_n, Q_n) \rightarrow f_n^{eq}$. Now, we investigate the inverse mapping. Given an equilibrium distribution $\{f_n^{eq}\}$, obtained for example from an independent calculation, can we find the Boltzmann equation that yields this particular static distribution? The answer is useful to set up a Boltzmann equation.

The idea is to start from a Boltzmann equation with a modified Hamilton function $H_n(\vec{r}, \vec{p}) + \Sigma_n(\vec{r}, \vec{p})$. We call the additional term **self energy** in loose analogy with the self-energy from many-particle physics. The self-energy term $\Sigma(\vec{r}, \vec{p})$ accounts, like the collision term, for the interaction between particles. Rather than describing specific collisions, however, this term describes the interaction with an unspecific continuum of other particles. It may for example describe an increase of the effective mass of particles, when the particle is dressed by a continuum of other particles. In this fashion it may account for multiple-scattering events, which are usually ignored in the collision term.¹

The Boltzmann equation with the self-energy term has the form

$$\left[\partial_t + \left(\vec{\nabla}_p H_n(\vec{r}, \vec{p}, t) + \vec{\nabla}_p \Sigma_n(\vec{r}, \vec{p}, t) \right) \vec{\nabla}_r + \left(-\vec{\nabla}_r H_n(\vec{r}, \vec{p}, t) - \vec{\nabla}_r \Sigma_n(\vec{r}, \vec{p}, t) \right) \vec{\nabla}_p \right] f_n(\vec{r}, \vec{p}, t) = \Delta Q_n(\vec{r}, \vec{p}, t) \quad \text{with } \Delta Q_n(\vec{r}, \vec{p}, t) = 0 \text{ in equilibrium (i.e. for } f_n^{eq}) \quad (\text{O.1})$$

From what we learned, we can write down the equilibrium distribution as

$$f_n^{eq}(\vec{r}, \vec{p}) = \begin{cases} e^{-\beta[H_n(\vec{r}, \vec{p}) + \Sigma_n(\vec{r}, \vec{p}) - \mu]} & \text{for distinguishable particles} \\ \left(e^{\beta[H_n(\vec{r}, \vec{p}) + \Sigma_n(\vec{r}, \vec{p}) - \mu]} - 1 \right)^{-1} & \text{for Bosons} \\ \left(e^{\beta[H_n(\vec{r}, \vec{p}) + \Sigma_n(\vec{r}, \vec{p}) - \mu]} + 1 \right)^{-1} & \text{for Fermions} \end{cases} \quad (\text{O.2})$$

The ansatz Eq. O.2 can be inverted, so that $\Sigma_n(\vec{r}, \vec{p})$ is obtained from the specified equilibrium distribution $f_n^{eq}(\vec{r}, \vec{p})$.

$$\Sigma_n(\vec{r}, \vec{p}) = -H_n(\vec{r}, \vec{p}) + \mu + k_B T \begin{cases} \ln \left(\left[f_n^{eq}(\vec{r}, \vec{p}) \right]^{-1} \right) & \text{for distinguishable particles} \\ \ln \left(\left[f_n^{eq}(\vec{r}, \vec{p}) \right]^{-1} + 1 \right) & \text{for bosons} \\ \ln \left(\left[f_n^{eq}(\vec{r}, \vec{p}) \right]^{-1} - 1 \right) & \text{for fermions} \end{cases} \quad (\text{O.3})$$

¹Multiple-scattering events would lead to complicated collision terms.

Finally, we combine the self-energy terms in the Boltzmann equation Eq. O.1 with the collision term ΔQ_n on the right-hand side of Eq. O.1,

$$\left[\partial_t + \vec{\nabla}_p H_n(\vec{r}, \vec{p}, t) \vec{\nabla}_r - \vec{\nabla}_r H_n(\vec{r}, \vec{p}, t) \vec{\nabla}_p \right] f_n(\vec{r}, \vec{p}, t) \\ \stackrel{\text{Eq. O.1}}{=} \underbrace{- \left[\vec{\nabla}_p \Sigma_n(\vec{r}, \vec{p}, t) \vec{\nabla}_r - \vec{\nabla}_r \Sigma_n(\vec{r}, \vec{p}, t) \vec{\nabla}_p \right] f_n(\vec{r}, \vec{p}, t) + \Delta Q_n(\vec{r}, \vec{p}, t)}_{Q_n(\vec{r}, \vec{p}, t)} \quad (\text{O.4})$$

which yields a collision term of the form²

$$Q_n(\vec{r}, \vec{p}, t) = - \left[\left(\vec{\nabla}_p \Sigma_n(\vec{r}, \vec{p}) \right) \vec{\nabla}_r + \left(-\vec{\nabla}_r \Sigma_n(\vec{r}, \vec{p}) \right) \vec{\nabla}_p \right] f_n(\vec{r}, \vec{p}, t) + \Delta Q_n(\vec{r}, \vec{p}, t) \\ \stackrel{\text{Eq. O.3}}{=} \underbrace{\left[\left(\vec{\nabla}_p H_n(\vec{r}, \vec{p}) \right) \vec{\nabla}_r + \left(-\vec{\nabla}_r H_n(\vec{r}, \vec{p}) \right) \vec{\nabla}_p \right] f_n^{eq}(\vec{r}, \vec{p})}_{Q^{eq}(\vec{r}, \vec{p})} + \Delta Q_n(\vec{r}, \vec{p}, t) \\ - \left[\left(\vec{\nabla}_p \Sigma_n(\vec{r}, \vec{p}) \right) \vec{\nabla}_r + \left(-\vec{\nabla}_r \Sigma_n(\vec{r}, \vec{p}) \right) \vec{\nabla}_p \right] \left(f_n(\vec{r}, \vec{p}, t) - f_n^{eq}(\vec{r}, \vec{p}) \right) \quad (\text{O.6})$$

By ignoring the non-equilibrium contribution of the self-energy term (last line in Eq. O.6), we obtain

BOLTZMANN EQUATION FOR A SPECIFIED EQUILIBRIUM DISTRIBUTION

For a given equilibrium distribution $f_n^{eq}(\vec{r}, \vec{p})$ and the Hamilton functions $H_n(\vec{r}, \vec{p})$, that govern the dynamics in the absence of interactions, respectively collisions, the Boltzmann equation has the form

$$\left[\partial_t + \vec{v}_n(\vec{r}, \vec{p}) \vec{\nabla}_r + \vec{F}_n(\vec{r}, \vec{p}) \vec{\nabla}_p \right] f_n(\vec{r}, \vec{p}, t) = Q_n(\vec{r}, \vec{p}, t) \quad (\text{O.7})$$

with

$$\vec{v}_n(\vec{r}, \vec{p}) = +\vec{\nabla}_p H_n(\vec{r}, \vec{p}) \\ \vec{F}_n(\vec{r}, \vec{p}) = -\vec{\nabla}_r H_n(\vec{r}, \vec{p}) \\ Q_n(\vec{r}, \vec{p}, t) = \left[\left(\vec{\nabla}_p H_n(\vec{r}, \vec{p}) \right) \left(\vec{\nabla}_r f_n^{eq}(\vec{r}, \vec{p}) \right) - \left(\vec{\nabla}_r H_n(\vec{r}, \vec{p}) \right) \left(\vec{\nabla}_p f_n^{eq}(\vec{r}, \vec{p}) \right) \right] \\ + \Delta Q_n(\vec{r}, \vec{p}, t) \quad (\text{O.8})$$

where $\Delta Q_n(\vec{r}, \vec{p}, t)$ is an additional collision term, which is a functional of the instantaneous distribution $f_n(\vec{r}, \vec{p}, t)$, and that vanishes for the specified equilibrium distribution $f_n^{eq}(\vec{r}, \vec{p})$.

Eq. O.7 differs from Eq. O.1 by the non-equilibrium contribution of the self-energy term.

The relevance of this section is the following: Usually, one considers only cases, for which the net collision term Q_n vanishes for the equilibrium distribution f^{eq} . I consider this unnecessarily restrictive. With the construction presented in this section, we can relax this requirement: The general Hamiltonian can, for example, be divided into a non-interacting part, which governs the collision-less dynamics via the Hamilton functions H_n , and an interaction part, which describes the interaction via the collision term Q_n . The equilibrium distribution is not determined by the non-interacting Hamiltonian H_n alone. Collisions take place also in thermal equilibrium and drive the distribution away from the equilibrium distribution of non-interacting particles.

²We exploited

$$\left(\vec{\nabla}_p f(\vec{r}, \vec{p}) \right) \left(\vec{\nabla}_r Y(f(\vec{r}, \vec{p})) \right) - \left(\vec{\nabla}_r f(\vec{r}, \vec{p}) \right) \left(\vec{\nabla}_p Y(f(\vec{r}, \vec{p})) \right) \\ \stackrel{\text{Eq. O.4}}{=} \left(\vec{\nabla}_p f(\vec{r}, \vec{p}) \right) \frac{dY}{df} \left(\vec{\nabla}_r f(\vec{r}, \vec{p}) \right) - \left(\vec{\nabla}_r f(\vec{r}, \vec{p}) \right) \frac{dY}{df} \left(\vec{\nabla}_p f(\vec{r}, \vec{p}) \right) = 0 \quad (\text{O.5})$$

which is valid for any function $f(\vec{r}, \vec{p})$ and $Y(f)$.

Of course, one is free to shift $\Sigma(\vec{r}, \vec{p})$ from the collision term into Hamilton functions. This corresponds to a redefinition of the particles: They are no more non-interacting particles, called bare particles, but quasi particles, which are dressed by a cloud of other particles effectively tied to them by the interaction.³

Whatever the equilibrium distribution of the system is, there is a multitude of collision terms obeying $\Delta Q^{eq}[f^{eq}] = 0$, and all these collision terms produce the same stationary distribution.

O.2 Self energy from a density-matrix functional

Editor: Not ready yet

Let me step away from the empirical approach towards the Boltzmann equation and connect it to many-particle wave functions. Specifically in this section I want to show, how to interpret that we obtain an equilibrium distribution of non-interacting particles. If the equilibrium distribution deviates from that of non-interacting particles, a self energy is introduced. What is the nature of that self energy.

In order to arrive at the Boltzmann equation, we need a specific setting⁴: Real space is partitioned into small regions. In each of these regions, we determine the one-particle eigenstates of a one-particle Hamiltonian. The regions shall be sufficiently large that the energy quantization of the one-particle states can be ignored. On the other hand, the regions are treated as infinitesimally small and are identified by the real-space coordinate \vec{r} . Thus, one obtains a one-particle basisset $|\phi_{n,\vec{r}}\rangle$. Note that \vec{r} plays the role of a quantum number, which specifies a region centered at \vec{r} . This one-particle basisset shall be complete.

Editor: This should be formulated with Wigner functions.

We construct a many-particle basis from this one-particle basis. The many-particle basis functions can be represented in a occupation-number representation. The states are $|\vec{\sigma}\rangle$, where the component σ_j is the occupation number of the j -th one-particle orbital $|\phi_{n,\vec{r}}\rangle$. The occupation number is integer. For Fermions the many-particle states are Slater determinants. For Bosons they are permanents and for distinguishable particles they are product states.

The density matrix of the system can be expressed in this basis in the form

$$\hat{\rho} = \sum_{\vec{\sigma}, \vec{\sigma}'} |\vec{\sigma}\rangle \rho_{\vec{\sigma}, \vec{\sigma}'} \langle \vec{\sigma}'| \tag{O.9}$$

The occupations in the basis of the chosen one-particle orbitals are

$$f_n(\vec{p}, \vec{r}) = \text{Tr}(\hat{\rho} \hat{c}_n^\dagger(\vec{p}, \vec{r}) \hat{c}_n(\vec{p}, \vec{r})) = \sum_{\vec{\sigma}, \vec{\sigma}'} \rho_{\vec{\sigma}, \vec{\sigma}'} \langle \vec{\sigma}' | \hat{c}_n^\dagger(\vec{p}, \vec{r}) \hat{c}_n(\vec{p}, \vec{r}) | \vec{\sigma} \rangle = \sum_{\vec{\sigma}, \vec{\sigma}'} \rho_{\vec{\sigma}, \vec{\sigma}'} \delta_{\sigma_n, \sigma_n} \sigma_n \tag{O.10}$$

They are expressed with creation and annihilation operators in the one-particle basisset $|\phi_{m,\vec{p},\vec{r}}\rangle$.

It is obvious, that many density matrices will have the same set of occupations as defined above. In order to assign a unique density matrix to every set of occupations, we perform a **constrained search** and impose additional constraints to the **maximum-entropy principle**. Let me define what I will call the **density-matrix functional** $Q_T[f]$.⁵

³This should not be taken literally, but be considered as an intuitively accessible picture.

⁴The reader will notice that this setting involves some contradicting properties.

⁵Note, that there are several variants of density matrix functionals. We call Q_T a density matrix functional despite the fact that it depends only on the diagonal elements of the reduced density matrix. The reason is that the generalization to reduced density matrices of the form $\rho_{m,n}^{red}(\vec{r}, \vec{p})$ is fairly straightforward.

We rewrite the grand potential with an external potential $v_n(\vec{p}, \vec{r})$ in the form

$$\begin{aligned}
\Omega_{T,\mu}[v] &= E - \mu N - TS \\
&= \min_{\hat{\rho}} \text{stat}_{\lambda} \left\{ \underbrace{k_B T \text{Tr}[\hat{\rho} \ln(\hat{\rho})]}_{-TS} + \underbrace{\text{Tr}[\hat{\rho} \hat{H}[v]]}_E - \underbrace{\mu \text{Tr}[\hat{\rho} \hat{N}]}_{\mu N} + \lambda \left(\text{Tr}[\hat{\rho}] - 1 \right) \right\} \\
&= \min_{f_n(\vec{p}, \vec{r}) \geq 0} \left\{ \sum_{n, \vec{p}, \vec{r}} f_n(\vec{p}, \vec{r}) \left(\epsilon_n(\vec{p}, \vec{r}) + v_n(\vec{p}, \vec{r}) - \mu \right) + Q_T[f] - T \sum_{n, \vec{r}, \vec{p}} X(f_n(\vec{r}, \vec{p})) \right\}
\end{aligned} \tag{O.11}$$

with the functional

$$\begin{aligned}
Q_T[f_n(\vec{p}, \vec{r})] &= T \sum_{n, \vec{r}, \vec{p}} X(f_n(\vec{r}, \vec{p})) + \max_{\hat{\rho}, \bar{\epsilon}, \lambda} \text{stat} \left\{ \underbrace{k_B T \text{Tr}[\hat{\rho} \ln(\hat{\rho})]}_{-TS[\hat{\rho}]} + \lambda \left(\text{Tr}[\hat{\rho}] - 1 \right) \right. \\
&\quad \left. + \text{Tr} \left[\hat{\rho} \left(\hat{H} - \underbrace{\sum_{n, \vec{p}, \vec{r}} \epsilon_n(\vec{p}, \vec{r}) \hat{c}_n^\dagger(\vec{p}, \vec{r}) \hat{c}_n(\vec{p}, \vec{r})}_{\hat{W}} \right) \right] \right. \\
&\quad \left. - \sum_{n, \vec{p}, \vec{r}} \bar{\epsilon}_n(\vec{p}, \vec{r}) \left[\text{Tr} \left(\hat{\rho} \hat{c}_n^\dagger(\vec{p}, \vec{r}) \hat{c}_n(\vec{p}, \vec{r}) \right) - f_n(\vec{p}, \vec{r}) \right] \right\}
\end{aligned} \tag{O.12}$$

where $\epsilon_n(\vec{p}, \vec{r})$ are the energies of the non-interacting Hamiltonian and $\sum_{n, \vec{r}, \vec{p}} X(f_n(\vec{r}, \vec{p}))$ is the entropy of non-interacting electrons with the specified occupations. $X(f)$ is defined as

$$\begin{aligned}
X(f) &= -k_B \left(f \ln(f) - \eta (1 + \eta f) \ln(1 + \eta f) \right) \\
&= -k_B \begin{cases} f \ln(f) & \text{for distinguishable particles} \\ f \ln(f) - (1 + f) \ln(1 + f) & \text{for bosons} \\ f \ln(f) + (1 - f) \ln(1 - f) & \text{for fermions} \end{cases}
\end{aligned} \tag{O.13}$$

For Fermions the occupations must not only be non-negative, but also smaller than one.

The minimum in Eq. O.12 establishes a unique mapping from a distribution $f_n(\vec{p}, \vec{r})$ to a specific many-particle density matrix $\hat{\rho}$. The value of the functional Q_T contains the energy related to the collision term, that is the interaction energy, and the difference of the entropies of the interacting system and that of a non-interacting system with the same distribution function. This definition ensures that it vanishes for a system of non-interacting particles.

The equilibrium condition with respect to the occupations yields

$$\bar{\epsilon}_n(\vec{p}, \vec{r}) + v_n(\vec{p}, \vec{r}) - \mu + \frac{\partial Q_T}{\partial f_n(\vec{p}, \vec{r})} - T \frac{\partial X}{\partial f} \Big|_{[f]} = 0 \tag{O.14}$$

which results the Fermi-, Bose- or Boltzmann distributions with energies

$$\bar{\epsilon}_n([v], \vec{p}, \vec{r}) = \epsilon_n(\vec{p}, \vec{r}) + v_n(\vec{p}, \vec{r}) + \frac{\partial Q_T}{\partial f_n(\vec{p}, \vec{r})} \tag{O.15}$$

The energies $\bar{\epsilon}_n([v=0], \vec{r}, \vec{p})$ are called **quasi-particle energies**.

The **self energy shifts**, Eq. O.3, can now be extracted from a microscopic description as

$$\Sigma_n(\vec{p}, \vec{r}) = \frac{\partial Q_T}{\partial f_n(\vec{p}, \vec{r})} \tag{O.16}$$

If we apply the maximum-entropy principle to determine the grand-canonical equilibrium probabilities with such a form of the total energy, we arrive at the distribution functions

$$f_n(\vec{r}, \vec{p}) = \begin{cases} e^{-\beta(\bar{\epsilon}_n(\vec{r}, \vec{p})-\mu)} & \text{for distinguishable particles} \\ [1 + e^{\beta(\bar{\epsilon}_n(\vec{r}, \vec{p})-\mu)}]^{-1} & \text{for Fermions} \\ [e^{\beta(\bar{\epsilon}_n(\vec{r}, \vec{p})-\mu)} - 1]^{-1} & \text{for Bosons} \end{cases} \quad (O.17)$$

That is, distinguishable particles attain the Boltzmann distribution, Fermions attain the Fermi distribution and Bosons attain the Bose distribution. In all three cases the entropy can be expressed in terms of the occupations themselves, which yields Eq. ??.

This result demonstrates an important point: Either we set up the Boltzmann equation with the quasi-particle energies $\bar{\epsilon}_n(\vec{r}, \vec{p})$, and obtain a stationary distribution of non-interacting particles. Or we use the bare energies, but obtain an equilibrium distribution, which depends on the collision term.

The quasi-particle energies $\bar{\epsilon}_n(\vec{r}, \vec{p})$ differ from the energies $\epsilon_n(\vec{r}, \vec{p})$ of the non-interacting (bare) particles in the dispersion relation. They include additional terms which are related to the collision terms. Note, that the collision term is a result of the interaction of particles.

O.3 Wigner functions

Editor: do not read. The factors are still wrong. This is only a note for myself to get started. See for example: William B. Case, *Wigner functions and Weyl transforms for pedestrians*, Am. J.Phys.76, 937 (2008) doi: 10.1119/1.295788

$$\begin{aligned} \langle A \rangle &= \sum_q P_q \langle \psi_q | \hat{A} | \psi_q \rangle \\ &= \sum_q P_q \langle \psi_q | \underbrace{\int d^3r |\vec{r}\rangle \langle \vec{r}|}_{=1} \hat{A} \underbrace{\int d^3r' |\vec{r}'\rangle \langle \vec{r}'|}_{=1} | \psi_q \rangle \\ &= \int d^3r \int d^3r' \underbrace{\sum_q \langle \vec{r}' | \psi_q \rangle P_q \langle \psi_q | \vec{r} \rangle}_{\langle \vec{r}' | \hat{\rho} | \vec{r} \rangle} \langle \vec{r} | \hat{A} | \vec{r}' \rangle \\ &= \int d^3r \int d^3z \sum_q \langle \vec{r} - \frac{\vec{z}}{2} | \psi_q \rangle P_q \langle \psi_q | \vec{r} + \frac{\vec{z}}{2} \rangle \langle \vec{r} + \frac{\vec{z}}{2} | \hat{A} | \vec{r} - \frac{\vec{z}}{2} \rangle \\ &= \int d^3r \int d^3z \int d^3z' \underbrace{\int \frac{d^3p}{(2\pi\hbar)^3} e^{i\vec{p}(\vec{z}-\vec{z}')} \delta(\vec{z}-\vec{z}')}_{\rho_W(\vec{r}, \vec{p})=2\pi\hbar W(\vec{r}, \vec{p})} \sum_q \langle \vec{r} - \frac{\vec{z}}{2} | \psi_q \rangle P_q \langle \psi_q | \vec{r} + \frac{\vec{z}}{2} \rangle \langle \vec{r} + \frac{\vec{z}}{2} | \hat{A} | \vec{r} - \frac{\vec{z}}{2} \rangle \\ &= \int d^3r \int \frac{d^3p}{(2\pi\hbar)^3} \left(\underbrace{\int d^3z e^{i\vec{p}\vec{z}} \sum_q \langle \vec{r} - \frac{\vec{z}}{2} | \psi_q \rangle P_q \langle \psi_q | \vec{r} + \frac{\vec{z}}{2} \rangle}_{\rho_W(\vec{r}, \vec{p})=2\pi\hbar W(\vec{r}, \vec{p})} \right) \\ &\quad \times \underbrace{\left(\int d^3z' e^{-i\vec{p}\vec{z}'} \langle \vec{r} + \frac{\vec{z}}{2} | \hat{A} | \vec{r} - \frac{\vec{z}}{2} \rangle \right)}_{A_W(\vec{r}, \vec{p})} \end{aligned} \quad (O.18)$$

The Wigner function is defined as

$$W(\vec{r}, \vec{p}) \stackrel{\text{def}}{=} \frac{1}{(2\pi\hbar)^3} \int d^3z e^{i\vec{p}\vec{z}} \sum_q \langle \vec{r} - \frac{\vec{z}}{2} | \psi_q \rangle P_q \langle \psi_q | \vec{r} + \frac{\vec{z}}{2} \rangle \quad (O.19)$$

Expectation values are obtained by a phase-space integral

$$\langle A \rangle = \text{Tr}[\hat{\rho}\hat{A}] = \int d^3r \int d^3p W(\vec{r}, \vec{p}) A_W(\vec{r}, \vec{p}) \tag{O.20}$$

O.4 Generating functional:

The condition of detailed balance Eq. 8.50 implies that the collision terms can be derived from a single functional of the distribution function.

Editor: This paragraph is in preparation. Do not read! It is still wrong!
 The condition of detailed balance implies that the intrinsic scattering probabilities can be derived as derivatives of a functional

$$\begin{aligned} Q_{T,\mu}[\vec{f}] &= \sum_{M,N} \frac{1}{(N+M)!} \sum_{o_1, \dots, o_N} \sum_{i_1, \dots, i_M} L^{o_1, \dots, o_N}_{i_1, \dots, i_M} e^{-\beta(\sum_{k=1}^M (H_{i_k} + \Sigma_{o_k}) - \mu)} f_1, \dots, f_{N+M} \\ L^{o_1, \dots, o_N}_{i_1, \dots, i_M} &= \left. \frac{\partial^{N+M} Q_{T,\mu}[\vec{f}]}{\partial f_{o_1} \dots \partial f_{i_N}} \right|_{\vec{f}=0} e^{+\beta(\sum_{k=1}^M (H_{i_k} + \Sigma_{i_k}) - \mu)} \end{aligned} \tag{O.21}$$

The source term Q_n can be obtained ??? from the functional Q as

$$Q_n[\vec{f}] = - \frac{\partial Q_{T,\mu}[\vec{f}]}{\partial f_n} \quad ??? \tag{O.22}$$

If this is true, the extremum of $Q_{T,\mu}(f) - \vec{f}\vec{Q}[f]$ identifies the equilibrium distribution. \vec{f}^{eq} . This in turn defines a few functional $P_{T,\mu}[\vec{Q}] := \text{extr}_{\vec{f}} [Q_{T,\mu}(f) - \vec{f}\vec{Q}]$ of the source term. The functional $P_{T,\mu}(Q)$ is the Legendre transform of $Q_{T,\mu}[\vec{f}]$. From $P_{T,\mu}[\vec{Q}]$ one should be able to obtain the equilibrium distribution as minimizer or maximizer of $\vec{f}^{eq} = \vec{\nabla}_S P_{T,\mu}[\vec{Q}]$

O.5 Functional form of Boltzmann's entropy

BOLTZMANN ENTROPY

Boltzmann's entropy $S^B[\vec{f}]$ has been defined in Eq. 8.39 on p. 269 as the maximum von-Neumann entropy for a specified set \vec{f} of (one-particle) occupations. Its functional form is

$$\begin{aligned} S^B[\vec{f}] &= -k_B \sum_{n=1}^{\infty} (f_n \ln(f_n) - \eta(1 + \eta f_n) \ln(1 + \eta f_n) + (\eta^2 - 1)f_n) \\ &= -k_B \sum_{n=1}^{\infty} \begin{cases} f_n \ln(f_n) + (1 - f_n) \ln(1 - f_n) & \text{for fermions } (\eta = -1) \\ f_n \ln(f_n) - (1 + f_n) \ln(1 + f_n) & \text{for bosons } (\eta = +1) \\ f_n \ln(f_n) - f_n & \text{for distinguishable particles } (\eta = 0) \end{cases} \end{aligned} \tag{O.23}$$

The occupations f_n of an ensemble $\{|\Phi_q\rangle, P_q\}$ are defined as $f_n = \sum_q P_q \langle \Phi_q | \hat{c}_n^\dagger \hat{c}_n | \Phi_q \rangle$. The entropy is maximized over ensembles of arbitrary many-particle wave functions $|\Phi_q\rangle$, having the correct symmetry properties under particle exchange for fermions, bosons and distinguishable particles, respectively. That is, the proof is not limited to non-interacting particles. The Boltzmann-entropy functional $S[\vec{f}]$ is independent of the one-particle basisset chosen to define the occupations. The corresponding optimum ensemble, on the other hand, does depend on the one-particle basisset.

I will show this connection Eq. O.23 between Boltzmann and von-Neumann entropy for identical particles using the creation and annihilation operators for an orthonormal and complete set of one-particle orbitals. Let \hat{c}_n^\dagger be the creation operator for a particle in the one-particle orbital $|\chi_n\rangle = \hat{c}_n^\dagger|\mathcal{O}\rangle$.

The maximum von-Neumann entropy for a given set of occupations is

$$S[\vec{f}] = \max_{\hat{\rho}, \vec{\gamma}, \lambda} \text{stat} \left\{ \underbrace{-k_B \text{Tr}[\hat{\rho} \ln(\hat{\rho})] - \sum_{n=1}^{\infty} k_B \gamma_n (\text{Tr}[\hat{\rho} \hat{c}_n^\dagger \hat{c}_n] - f_n)}_{S(\hat{\rho}, \vec{f}, \vec{\gamma}, \lambda)} - k_B \lambda (\text{Tr}[\hat{\rho}] - 1) \right\} \quad (\text{O.24})$$

$k_B \gamma_n$ and $k_B \lambda_n$ are the Lagrange parameters enforcing the constraints. The Lagrange multipliers are defined with factors k_B to simplify the following expressions. The density matrix $\hat{\rho}$ can be expressed for an ensemble of probabilities P_q and normalized many-particle wave functions $|\Phi_q\rangle$ as $\hat{\rho} = \sum_q |\Phi_q\rangle P_q \langle \Phi_q|$.

The variation of the entropy S in Eq. O.24 is

$$\begin{aligned} \frac{1}{k_B} dS = & \text{Tr} \left[\underbrace{\left\{ -\ln(\hat{\rho}) - \hat{1} - \sum_{n=1}^{\infty} \gamma_n \hat{c}_n^\dagger \hat{c}_n - \lambda \hat{1} \right\}}_{\frac{1}{k_B} \partial S / \partial \hat{\rho}} d\hat{\rho} \right] - \sum_{n=1}^{\infty} \underbrace{\left\{ \text{Tr}[\hat{\rho} \hat{c}_n^\dagger \hat{c}_n] - f_n \right\}}_{-\frac{1}{k_B} \partial S / \partial \gamma_n} d\gamma_n \\ & - \underbrace{\left\{ \text{Tr}[\hat{\rho}] - 1 \right\}}_{-\frac{1}{k_B} \partial S / \partial \lambda} d\lambda + \text{higher orders} \end{aligned} \quad (\text{O.25})$$

Setting the variation with respect to the density matrix to zero is the equilibrium condition, which yields an ansatz for the von-Neumann density matrix

$$\frac{dS}{d\hat{\rho}} = 0 \quad \Rightarrow \quad \hat{\rho} = e^{-(\lambda+1)} e^{-\sum_{n=1}^{\infty} \gamma_n \hat{c}_n^\dagger \hat{c}_n} \underset{\text{Tr}[\hat{\rho}]=1}{=} \frac{1}{\text{Tr}[e^{-\sum_{n=1}^{\infty} \gamma_n \hat{c}_n^\dagger \hat{c}_n}]} e^{-\sum_{n=1}^{\infty} \gamma_n \hat{c}_n^\dagger \hat{c}_n} \quad (\text{O.26})$$

It turns out that the density matrix is a function of a one-particle-at-a-time operator, namely $\sum_n \gamma_n \hat{c}_n^\dagger \hat{c}_n$. The density matrix is given as function of $\vec{\gamma}$, which itself must be determined by the constraint condition $\text{Tr}[\hat{\rho} \hat{c}_n^\dagger \hat{c}_n] = f_n$.

Because the operator $\sum_n \gamma_n \hat{c}_n^\dagger \hat{c}_n$ is a one-particle-at-a-time operator, its eigenstates are Slater-determinants $|\vec{\sigma}\rangle$ in the one-particle basis, that define the creation and annihilation operators. These Slater determinants satisfy the eigenvalue equations

$$\hat{c}_n^\dagger \hat{c}_n |\vec{\sigma}\rangle = |\vec{\sigma}\rangle \sigma_n \quad (\text{O.27})$$

The von-Neumann density matrix Eq. O.26 can thus be written as

$$\hat{\rho}(\vec{\gamma}) = \sum_{\vec{\sigma}} |\vec{\sigma}\rangle P_{\vec{\sigma}}(\vec{\gamma}) \langle \vec{\sigma}| \quad (\text{O.28})$$

with probabilities $P_{\vec{\sigma}}(\vec{\gamma})$ and the partition function $Z(\vec{\gamma})$

$$P_{\vec{\sigma}}(\vec{\gamma}) = \frac{1}{Z(\vec{\gamma})} e^{-\sum_{n=1}^{\infty} \sigma_n \gamma_n} \quad (\text{O.29})$$

$$Z(\vec{\gamma}) = \sum_{\vec{\sigma}} e^{-\sum_{n=1}^{\infty} \sigma_n \gamma_n} \quad (\text{O.30})$$

The partition function is chosen to satisfy the constraint $\text{Tr}[\hat{\rho}] = \sum_{\vec{\sigma}} P_{\vec{\sigma}} = 1$.

For the following step, we require a few identities related to geometric sums. I consider only the two cases relevant for Fermions and for Bosons. For Fermions, $\eta = -1$ and the σ -sum extends from zero to one. For Bosons, $\eta = +1$ and the σ -sum extends from zero to infinity. For any real-valued number with $|x| < 0$, we obtain

$$\sum_{\sigma} x^{\sigma} = (1 - \eta x)^{-\eta} \quad (\text{O.31})$$

$$\sum_{\sigma} \sigma x^{\sigma} = x \partial_x \sum_{\sigma} x^{\sigma} \quad (\text{O.32})$$

$$\begin{aligned} \frac{\sum_{\sigma} \sigma x^{\sigma}}{\sum_{\sigma} x^{\sigma}} &\stackrel{\text{Eq. O.32}}{=} x \partial_x \ln \left(\sum_{\sigma} x^{\sigma} \right) \stackrel{\text{Eq. O.31}}{=} x \partial_x \ln \left((1 - \eta x)^{-\eta} \right) = -\eta \frac{-\eta x}{1 - \eta x} \\ &= (x^{-1} - \eta)^{-1} \end{aligned} \quad (\text{O.33})$$

The values of γ_n are obtained from the constraints for the occupations.

$$\begin{aligned} f_n(\vec{\gamma}) &\stackrel{!}{=} \text{Tr} \left[\hat{\rho} \hat{c}_n^{\dagger} \hat{c}_n \right] \stackrel{\text{Eq. O.28}}{=} \sum_{\vec{\sigma}} P_{\vec{\sigma}}(\vec{\gamma}) \underbrace{\langle \vec{\sigma} | \hat{c}_n^{\dagger} \hat{c}_n | \vec{\sigma} \rangle}_{\sigma_n} \stackrel{\text{Eq. O.29}}{=} \frac{\sum_{\vec{\sigma}} \sigma_n e^{-\sum_{n=1}^{\infty} \sigma_n \gamma_n}}{\sum_{\vec{\sigma}} e^{-\sum_{n=1}^{\infty} \sigma_n \gamma_n}} \\ &= \frac{\sum_{\sigma} \sigma e^{-\gamma_n \sigma}}{\sum_{\sigma} e^{-\gamma_n \sigma}} \stackrel{\text{Eq. O.33}}{=} (e^{\gamma_n} - \eta)^{-1} \\ \Rightarrow \quad \gamma_n(\vec{f}) &= \ln \left(\frac{1 + \eta f_n}{f_n} \right) \end{aligned} \quad (\text{O.34})$$

where $\eta = -1$ for Fermions and $\eta = +1$ for Bosons.

The normalization factor Eq. O.30 can be evaluated as

$$\begin{aligned} Z(\vec{\gamma}) &\stackrel{\text{Eq. O.30}}{=} \sum_{\vec{\sigma}} e^{-\sum_{n=1}^{\infty} \gamma_n \sigma_n} = \prod_{n=1}^{\infty} \sum_{\sigma_n} (e^{-\gamma_n})^{\sigma_n} \stackrel{\text{Eq. O.31}}{=} \prod_{n=1}^{\infty} (1 - \eta e^{-\gamma_n})^{-\eta} \\ \ln[Z(\vec{\gamma})] &= -\sum_{n=1}^{\infty} \eta \ln(1 - \eta e^{-\gamma_n}) \stackrel{\text{Eq. O.34}}{=} \eta \sum_{n=1}^{\infty} \ln(1 + \eta f_n) =: \ln(Z(\vec{f})) \end{aligned} \quad (\text{O.35})$$

Using the optimized probabilities and wave functions, the entropy is

$$\begin{aligned} S^B(\vec{f}) &= -k_B \sum_{\vec{\sigma}} P_{\vec{\sigma}} \ln(P_{\vec{\sigma}}) \\ &\stackrel{\text{Eq. O.29}}{=} -k_B \sum_{\vec{\sigma}} P_{\vec{\sigma}} \ln \left(\frac{1}{Z(\vec{\gamma})} e^{-\sum_n \gamma_n \sigma_n} \right) \\ &= -k_B \sum_{\vec{\sigma}} P_{\vec{\sigma}} \left(-\ln(Z(\vec{\gamma})) - \sum_n \gamma_n \sigma_n \right) \\ &\stackrel{\text{Eq. O.34}}{=} -k_B \left\{ -\ln(Z(\vec{\gamma})) - \sum_n \underbrace{\ln \left(\frac{1 + \eta f_n}{f_n} \right)}_{\gamma_n} \underbrace{\sum_{\vec{\sigma}} P_{\vec{\sigma}} \sigma_n}_{f_n} \right\} \\ &\stackrel{\text{Eq. O.35}}{=} -k_B \sum_{n=1}^{\infty} \left\{ -\eta \ln(1 + \eta f_n) - \ln \left(\frac{1 + \eta f_n}{f_n} \right) f_n \right\} \\ &= -k_B \sum_{n=1}^{\infty} \left\{ (-\eta - f_n) \ln(1 + \eta f_n) + f_n \ln(f_n) \right\} \\ &= -k_B \sum_{n=1}^{\infty} \begin{cases} f_n \ln(f_n) + (1 - f_n) \ln(1 - f_n) & \text{for fermions} \\ f_n \ln(f_n) - (1 + f_n) \ln(1 + f_n) & \text{for bosons} \end{cases} \end{aligned} \quad (\text{O.36})$$

This determined the desired expression for the Boltzmann entropy for Bosons and Fermions.

The Boltzmann entropy for non-interacting electrons is obtained from the dilute limit for fermions and bosons, namely⁶

$$S^B[\vec{f}] = -k_B \sum_{n=1}^{\infty} \left\{ f_n \ln(f_n) - f_n \right\} \quad \text{for distinguishable particles} \quad (O.39)$$

O.6 H-theorem

Here, I show that the Boltzmann entropy increases with time under the Boltzmann equation. It is shown that the entropy growth is due to the collision term. I need to make two basic assumption, namely that of **elastic collisions** and that of **positive intrinsic scattering probabilities**.

I will first show that the drift term conserves Boltzmann's entropy. The entropy growth is hence entirely due to the collision term. To show the entropy growth, I first demonstrate it on a simple case, the collision on an obstacle, before I present the derivation for a general collision term.

O.6.1 The drift term conserves the Boltzmann entropy

Let me investigate the time evolution of the Boltzmann entropy

$$S^B(t) \stackrel{\text{Eq. 8.41}}{=} \int \frac{d^3r d^3p}{(2\pi\hbar)^3} \sum_n X(f_n(\vec{r}, \vec{p}, t)) \quad (O.40)$$

with $X(f)$ defined in Eq. ??.

⁶In the dilute limit, the particle distribution is small, which implies that $\epsilon - \mu \gg k_B T$. In this limit, the Fermi-, Bose- and Boltzmann distributions become identical.

$$f_{T,\mu}^{(\eta)}(\epsilon) = 1 / \left[\underbrace{e^{\beta(\epsilon-\mu)}}_{\gg 1 \text{ if dilute}} - \eta \right] = e^{-\beta(\epsilon-\mu)} = f_{T,\mu}^{(0)}(\epsilon) . \quad (O.37)$$

Alternatively we can also rewrite the entropy

$$\begin{aligned} f \ln(f) - \eta(1 + \eta f) \ln(1 + \eta f) &= f \ln(f) - \eta(1 + \eta f) \left(- \sum_{j=1}^{\infty} \frac{1}{j} (-\eta f)^j \right) \\ &= f \ln(f) - \eta \left(- \sum_{j=1}^{\infty} \frac{1}{j} (-\eta f)^j + \sum_{j=1}^{\infty} \frac{1}{j} (-\eta f)^{j+1} \right) \\ &= f \ln(f) - \eta \left(- \sum_{j=1}^{\infty} \frac{1}{j} (-\eta f)^j + \sum_{j=2}^{\infty} \frac{1}{j-1} (-\eta f)^j \right) \\ &= f \ln(f) - \eta \left(\eta f - \sum_{j=2}^{\infty} \frac{1}{j} (-\eta f)^j + \sum_{j=2}^{\infty} \frac{1}{j-1} (-\eta f)^j \right) \\ &= f \ln(f) - f + \eta \sum_{j=2}^{\infty} \frac{1}{j(j-1)} (-\eta f)^j \end{aligned} \quad (O.38)$$

Editor: The meaning of the next term as in $S^B[f_n] = -k_B \sum_n [f_n \ln(f_n) - f_n]$ is not clear to me, neither why it is ignored

I begin with the contribution of a particular orbital

$$\begin{aligned}
& \frac{d}{dt} X(f_n(\vec{r}, \vec{p}, t)) \\
&= \left. \frac{dX}{df} \right|_{f_n(\vec{r}, \vec{p}, t)} \partial_t f_n(\vec{r}, \vec{p}, t) \\
&= \left. \frac{dX}{df} \right|_{f_n(\vec{r}, \vec{p}, t)} \left(-\vec{v}_n \vec{\nabla}_r f_n(\vec{r}, \vec{p}, t) - \vec{F}_n \vec{\nabla}_p f_n(\vec{r}, \vec{p}, t) + Q_n(\vec{r}, \vec{p}) \right) \\
&= -\vec{v}_n \vec{\nabla}_r X(f_n(\vec{r}, \vec{p}, t)) - \vec{F}_n \vec{\nabla}_p X(f_n(\vec{r}, \vec{p}, t)) + Q_n(\vec{r}, \vec{p}) \left. \frac{dX}{df} \right|_{f_n(\vec{r}, \vec{p}, t)} \\
&= -\vec{\nabla}_r \left[\vec{v}_n X(f_n(\vec{r}, \vec{p}, t)) \right] - \vec{\nabla}_p \left[\vec{F}_n X(f_n(\vec{r}, \vec{p}, t)) \right] + X(f_n(\vec{r}, \vec{p}, t)) \underbrace{\left[\vec{\nabla}_r \vec{v}_n + \vec{\nabla}_p \vec{F}_n \right]}_{= 0 \text{ Liouville Eq. 8.10}} + Q_n(\vec{r}, \vec{p}) \left. \frac{dX}{df} \right|_{f_n(\vec{r}, \vec{p}, t)} \\
&= -\vec{\nabla}_r \left[\vec{v}_n X(f_n(\vec{r}, \vec{p}, t)) \right] - \vec{\nabla}_p \left[\vec{F}_n X(f_n(\vec{r}, \vec{p}, t)) \right] + Q_n(\vec{r}, \vec{p}) \left. \frac{dX}{df} \right|_{f_n(\vec{r}, \vec{p}, t)} \tag{O.41}
\end{aligned}$$

Integration over a phase-space region Ω yields the change of the Boltzmann entropy

$$S_\Omega^B(t) = \sum_n \int_\Omega \frac{d^3 r d^3 p}{(2\pi\hbar)^3} X(f_n(\vec{r}, \vec{p}, t)) \tag{O.42}$$

as

$$\begin{aligned}
& \frac{dS_\Omega^B}{dt} + \left(\frac{1}{(2\pi\hbar)^3} \oint_{\partial\Omega} d\vec{A}_r \sum_n \vec{v}_n X_n \right) + \left(\frac{1}{(2\pi\hbar)^3} \oint_{\partial\Omega} d\vec{A}_p \sum_n \vec{F}_n X_n \right) \\
& \stackrel{\text{Eq. O.41}}{=} \sum_n \int_\Omega \frac{d^3 r d^3 p}{(2\pi\hbar)^3} \frac{\partial X_n}{\partial f_n(\vec{r}, \vec{p})} Q_n(\vec{r}, \vec{p}) \tag{O.43}
\end{aligned}$$

where the surface integrals are done at the boundary $\partial\Omega$ of the phase-space region Ω .

Under normal circumstances, the surface integral vanishes: For a finite system, we can assume that the distribution function vanishes when either $|\vec{r}| \rightarrow \infty$ or $|\vec{p}| \rightarrow \infty$. In this case the surface integrations vanish. For spatially extended systems, one can use periodic boundary conditions to show that the spatial surface integrations vanish, even though the distribution does not vanish for $|\vec{r}| \rightarrow \infty$.

If the surface integrations vanish, we obtain

$$\frac{dS_\infty^B}{dt} = \sum_n \int_\infty \frac{d^3 r d^3 p}{(2\pi\hbar)^3} \frac{\partial X_n}{\partial f_n(\vec{r}, \vec{p})} Q_n(\vec{r}, \vec{p}) \tag{O.44}$$

where ∞ indicates that the integration is performed over the entire phase space.

The result of Eq. O.44 is that the drift term conserves the entropy and the changes of the Boltzmann entropy are entirely due to the collision term.

It is clear that the Boltzmann entropy is conserved in the absence of collisions. In the next section, we investigate whether the scattering term leads to an increase or decrease of the Boltzmann entropy.

O.6.2 Entropy growth for scattering at obstacles

Let me first investigate the entropy growth for the most simple scattering term, namely scattering at obstacles. This provides a blueprint for the proof of entropy growth for general scattering terms, discussed later.

Sketch: We combine momentum and band index into one index. We assume that both the Hamiltonian and the distribution are translationally invariant in time, so that the change of the distribution f_n is only due to the collision term.

$$\frac{dS^B}{dt} \stackrel{\text{Eq. O.44}}{=} \sum_n \frac{\partial X}{\partial f_n} Q_n \tag{O.45}$$

Let me first investigate the collision term for obstacles. We consider the occupation of the final state of the scattering process with the factor $(1 + \eta f_n)$, where η has been defined in Eq. 8.29 on p. 265. The function $X(f)$ is a short hand for the contribution of a single one-particle state to the Boltzmann entropy

$$X(f) \stackrel{\text{Eq. ??}}{=} -k_B \left(f \ln(f) - \eta(1 + \eta f) \ln(1 + \eta f) + (\eta^2 - 1)f \right) \tag{O.46}$$

Q_n is the source term describing the collisions.

Below we will need the derivatives (for $\eta \in \{-1, 0, 1\}$)

$$\begin{aligned} \frac{dX}{df} &= -k_B \left(\underbrace{\ln(f) + 1}_{\partial_f f \ln(f)} - \underbrace{\eta^2 \ln(1 + \eta f) - \eta^2}_{-\partial_f \eta(1 + \eta f) \ln(1 + \eta f)} + (\eta^2 - 1) \right) \\ &= k_B \left(-\ln(f) + \eta^2 \ln(1 + \eta f) \right) \\ &= k_B \left(-\ln(f) + \ln(1 + \eta f) \right) \end{aligned} \tag{O.47}$$

The factor η^2 has been dropped, because it is unity for the quantum case $\eta \neq 0$ and because $\ln(1 + \eta f) = \ln(1) = 0$ for the classical case with $\eta = 0$.

The change of the Boltzmann entropy-functional S^B is

$$\begin{aligned} \frac{dS^B}{dt} &\stackrel{\text{Eq. O.45}}{=} \sum_n \frac{\partial X}{\partial f_n} Q_n \\ &\stackrel{\text{Eq. 8.31}}{=} \sum_n \frac{\partial X}{\partial f_n} \sum_a \left((1 + \eta f_n) L^n_a f_a - (1 + \eta f_a) L^a_n f_n \right) \\ &= \sum_{n,a} \frac{1}{2} \left[\frac{\partial X}{\partial f_n} \left((1 + \eta f_n) L^n_a f_a - (1 + \eta f_a) L^a_n f_n \right) + \frac{\partial X}{\partial f_a} \left((1 + \eta f_a) L^a_n f_n - (1 + \eta f_n) L^n_a f_a \right) \right] \\ &= \frac{1}{2} \sum_{n,a} \left[(1 + \eta f_n) L^n_a f_a - (1 + \eta f_a) L^a_n f_n \right] \left(\frac{\partial X}{\partial f_n} - \frac{\partial X}{\partial f_a} \right) \\ &\stackrel{\text{Eq. O.47}}{=} \frac{k_B}{2} \sum_{n,a} \underbrace{f_n f_a}_{\geq 0} \left(\frac{1 + \eta f_n}{f_n} L^n_a - \frac{1 + \eta f_a}{f_a} L^a_n \right) \left[\ln \left(\frac{1 + \eta f_n}{f_n} \right) - \ln \left(\frac{1 + \eta f_a}{f_a} \right) \right] \end{aligned} \tag{O.48}$$

From here on, I need to limit the discussion to elastic processes, for which detailed balance Eq. 8.49 implies

$$L^n_a = L^a_n \tag{O.49}$$

so that, for $\eta \neq 0$,

$$\frac{dS^B}{dt} = \frac{k_B}{2} \sum_{n,a} \underbrace{f_n f_a}_{\geq 0} L^n_a \underbrace{\left(\frac{1 + \eta f_n}{f_n} - \frac{1 + \eta f_a}{f_a} \right)}_{\substack{x \\ y}} \underbrace{\left[\ln \left(\frac{1 + \eta f_n}{f_n} \right) - \ln \left(\frac{1 + \eta f_a}{f_a} \right) \right]}_{\substack{\ln(x) \\ \ln(y)}} \tag{O.50}$$

Next, we can use the inequality $(x - y)(\ln(x) - \ln(y)) \geq 0$, for $x, y \geq 0$, where the identity holds for $x = y$. This inequality follows from the fact that $(1 + \eta f)/f$ and $\ln[(1 + \eta f)/f]$ are monotonously

falling functions with f for positive f . For positive intrinsic scattering probabilities the entropy grows until $\frac{1+\eta f_n}{f_n} = \text{const}$. The intrinsic scattering probabilities are positive because they are probabilities.

This shows that impurity scattering term results in a growth of the Boltzmann entropy.

0.6.3 Entropy growth for complicated scattering processes

In the following, we will show that the entropy growth for obstacles can be generalized to complicated scattering processes.

Time reversibility of the scattering process implies that an interchange of indices of absorbed and emitted particles does not change the scattering probability.

$$\begin{aligned} L^a_{b,c} &= L^{b,c}_a \\ L^{a,b}_{c,d} &= L^{b,c}_{a,b} \\ L^{o_1, \dots, o_N}_{i_1, \dots, i_M} &= L^{i_1, \dots, i_M}_{o_1, \dots, o_N} \end{aligned} \quad (O.51)$$

Higher-order scattering processes behave analogously. The scattering probability is symmetric with respect to an interchange of indices of emitting particles among each other, and the same holds for the absorbing particles.

Editor: Below, only $\eta = \pm 1$ is considered, but distinguishable particles are excluded. This needs to be checked and then mentioned accordingly.

$$\begin{aligned} \frac{dS^B}{dt} &\stackrel{\text{Eq. O.45}}{=} \sum_n \frac{\partial X}{\partial f_n} Q_n \\ &\stackrel{\text{Eq. 8.34}}{=} \sum_n \frac{\partial X}{\partial f_n} \sum_{N,M} \sum_{o_1, \dots, o_N} \sum_{i_1, \dots, i_M} \left(\sum_{j=1}^N \delta_{n, o_j} - \sum_{k=1}^M \delta_{n, i_k} \right) \left[\prod_{j=1}^N (1 + \eta f_{o_j}) \right] L^{o_1, \dots, o_N}_{i_1, \dots, i_M} \left[\prod_{k=1}^M f_{i_k} \right] \\ &= \sum_{N,M} \sum_{o_1, \dots, o_N} \sum_{i_1, \dots, i_M} \left(\sum_{j=1}^N \frac{\partial X}{\partial f_{o_j}} - \sum_{k=1}^M \frac{\partial X}{\partial f_{i_k}} \right) \left[\prod_{j=1}^N (1 + \eta f_{o_j}) \right] L^{o_1, \dots, o_N}_{i_1, \dots, i_M} \left[\prod_{k=1}^M f_{i_k} \right] \\ &\stackrel{\text{Eq. ??}}{=} k_B \sum_{N,M} \sum_{o_1, \dots, o_N} \sum_{i_1, \dots, i_M} \ln \left(\left[\prod_{j=1}^N \frac{1 + \eta f_{o_j}}{f_{o_j}} \right] \left[\prod_{k=1}^M \frac{f_{i_k}}{1 + \eta f_{i_k}} \right] \right) L^{o_1, \dots, o_N}_{i_1, \dots, i_M} \left[\prod_{j=1}^N (1 + \eta f_{o_j}) \right] \left[\prod_{k=1}^M f_{i_k} \right] \\ &= k_B \sum_{N,M} \sum_{o_1, \dots, o_N} \sum_{i_1, \dots, i_M} \underbrace{\left[\prod_{j=1}^N f_{o_j} \right] \left[\prod_{k=1}^M f_{i_k} \right]}_{\geq 0} L^{o_1, \dots, o_N}_{i_1, \dots, i_M} \\ &\quad \times \left[\ln \left(\prod_{j=1}^N \frac{1 + \eta f_{o_j}}{f_{o_j}} \right) - \ln \left(\prod_{k=1}^M \frac{1 + \eta f_{i_k}}{f_{i_k}} \right) \right] \left[\prod_{j=1}^N \frac{1 + \eta f_{o_j}}{f_{o_j}} \right] \end{aligned} \quad (O.52)$$

Next, we average the term where the sets of incoming and outgoing indices are reversed. We furthermore exploit detailed balance and we limit the discussion to elastic collisions.

$$\begin{aligned} \frac{dS^B}{dt} &= \frac{1}{2} k_B \sum_{N,M} \sum_{o_1, \dots, o_N} \sum_{i_1, \dots, i_M} \underbrace{\left[\prod_{j=1}^N f_{o_j} \right] \left[\prod_{k=1}^M f_{i_k} \right]}_{\geq 0} L^{o_1, \dots, o_N}_{i_1, \dots, i_M} \\ &\quad \times \left[\underbrace{\ln \left(\prod_{j=1}^N \frac{1 + \eta f_{o_j}}{f_{o_j}} \right)}_{\ln(x)} - \underbrace{\ln \left(\prod_{k=1}^M \frac{f_{i_k}}{1 + \eta f_{i_k}} \right)}_{\ln(y)} \right] \underbrace{\left[\prod_{j=1}^N \frac{1 + \eta f_{o_j}}{f_{o_j}} \right]}_x \underbrace{\left[\prod_{k=1}^M \frac{1 + \eta f_{i_k}}{f_{i_k}} \right]}_y \end{aligned} \quad (O.53)$$

Because the logarithm is monotonically increasing, the identity $(x - y)(\ln(x) - \ln(y)) \geq 0$ holds. The identity holds exactly for $x = y$. With

$$\begin{aligned} x &= \prod_{j=1}^N \frac{1 + \eta f_{o_j}}{f_{o_j}} \\ y &= \prod_{k=1}^M \frac{1 + \eta f_{i_k}}{f_{i_k}} \end{aligned} \tag{O.54}$$

we see that $dS/dt \geq 0$. This proves that the collision term leads to an increase of the Boltzmann entropy, if all collisions are elastic. Together with the finding that the drift term does not increase the entropy this proves the second law of thermodynamics for the Boltzmann equation.

Appendix P

Time integrals for the phonon-phonon scattering elements

In the perturbation expansion of the phonon amplitudes, the time dependence enters via two functions, namely

$$F^{(1)}(\omega t) \stackrel{\text{Eq. 10.22}}{=} \frac{1}{t} \int_0^t dt' e^{i\omega t'} \quad (\text{P.1})$$

and

$$F^{(2)}(\omega t, \omega' t) \stackrel{\text{Eq. 10.23}}{=} \frac{1}{t^2} \int_0^t dt' e^{i\omega t'} \int_0^{t'} dt'' e^{i\omega' t''} \quad (\text{P.2})$$

In the density matrix the first term occur as product

$$F^{(1)}(\omega t)F^{(1)}(\omega' t) = \frac{1}{t^2} \int_0^t dt' e^{i\omega t'} \int_0^t dt'' e^{i\omega' t''} \quad (\text{P.3})$$

which differs from $F^{(2)}(\omega t, \omega' t)$ only in the upper bound of the inner integral.

P.1 Integrations have only two arguments

$$F^{(2)}(\omega t, \omega' t) \stackrel{\text{Eq. 10.23}}{=} \frac{1}{t^2} \int_0^t dt' e^{i\omega t'} \int_0^{t'} dt'' e^{i\omega' t''} \quad (\text{P.4})$$

Let me introduce two new symbols, namely $x \stackrel{\text{def}}{=} \omega t$ and $x' = \omega' t$. Let me furthermore introduce two new integration variables, namely $\tau = t'/t$ and $\tau' = t''/t$. This leads to $\omega t' = x\tau$ and $\omega' t'' = x'\tau'$.

$$F^{(2)}(x, x') = \int_0^1 d\tau e^{ix\tau} \int_0^\tau d\tau' e^{ix'\tau'} = \int_0^1 d\tau \int_0^1 d\tau' \theta(\tau - \tau') e^{i(x\tau + x'\tau')} \quad (\text{P.5})$$

The same variable transform converts

$$F^{(1)}(\omega t)F^{(1)}(\omega' t) = \frac{1}{t^2} \int_0^t dt' e^{i\omega t'} \int_0^t dt'' e^{i\omega' t''} \quad (\text{P.6})$$

into

$$F^{(1)}(x)F^{(1)}(x') = \int_0^1 d\tau e^{ix\tau} \int_0^1 d\tau' e^{ix'\tau'} = \int_0^1 d\tau \int_0^1 d\tau' e^{i(x\tau + x'\tau')} \quad (\text{P.7})$$

The integrand $e^{i(x\tau+x'\tau')}$ is a plane wave in the two dimensional τ, τ' -plane with wave vector (x, x') . This plane wave is integrated over the unit square for $F^{(1)}(x)F^{(1)}(x')$ and over a triangle for $F^{(2)}(x, x')$.

P.2 Integrations relevant for the occupations

In the expression for the second-order contribution to the occupations, the two functions mentioned above occur only with opposite arguments, that is as $F^{(1)}(x)F^{(1)}(-x)$ and $F^{(2)}(x, -x)$.

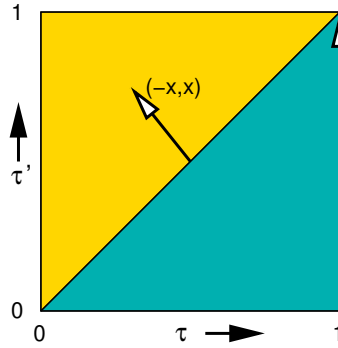


Fig. P.1: Integration area in the τ, τ' -plane. The integration area for $F^{(2)}(x, -x)$ is the lower-right triangle (green). The integral for the upper left triangle is the complex conjugate of the one in the lower right triangle, because the plane wave becomes complex conjugate upon inversion on the main diagonal. $F^{(1)}(x)F^{(1)}(-x)$ is the sum over both integrals.

On the one hand, we observe that inversion of x turns the integral into its complex conjugate.

$$F^{(2)}(x, -x) \stackrel{\text{Eq. P.5}}{=} \int_0^1 d\tau \int_0^1 d\tau' \theta(\tau - \tau') e^{ix(\tau - \tau')} = \left(F^{(2)}(-x, x) \right)^* \quad (\text{P.8})$$

On the other hand, a mirror operation on the main diagonal reverts the wave vector $(-x, x)$ back into the original orientation $(x, -x)$ and also interchanges the two triangles. This mirror operation leaves the integral $\left(F^{(2)}(-x, x) \right)^*$ unchanged. Thus, the integral over the upper triangle is the complex conjugate of the lower triangle.

The product $F^{(1)}(x)F^{(1)}(-x)$ is the integral over both triangles, so that

$$F^{(1)}(x)F^{(1)}(-x) = F^{(2)}(x, -x) + \left(F^{(2)}(-x, x) \right)^* = 2\text{Re}\left[F^{(2)}(x, -x) \right] \quad (\text{P.9})$$

We will see furthermore, that $F^{(2)}(x, -x)$ always occurs in pairs with opposite arguments, so that the imaginary parts cancel.

$$\begin{aligned}
 F^{(2)}(x, -x) &= \stackrel{\text{Eq. P.5}}{=} \int_0^1 d\tau \int_0^1 d\tau' \theta(\tau - \tau') e^{ix(\tau - \tau')} \\
 &= \int_0^1 d\tau e^{ix\tau} \int_0^\tau d\tau' e^{-ix\tau'} = \int_0^1 d\tau e^{ix\tau} \frac{e^{-ix\tau} - 1}{-ix} \\
 &= \frac{1}{-ix} \int_0^1 d\tau (1 - e^{ix\tau}) = \frac{1}{-ix} \left(1 - \frac{e^{ix} - 1}{ix} \right) \\
 &= \frac{1}{-ix} - \frac{\cos(x) + i \sin(x) - 1}{x^2} \\
 &= \overbrace{\left(\frac{1 - \cos(x)}{x^2} \right)}^{2 \sin^2(x/2)} + i \left(\frac{1}{x} - \frac{\sin(x)}{x^2} \right) \\
 &= \frac{1}{2} \left(\frac{\sin(x/2)}{x/2} \right)^2 + i \left(\frac{x - \sin(x)}{x^2} \right) \tag{P.10}
 \end{aligned}$$

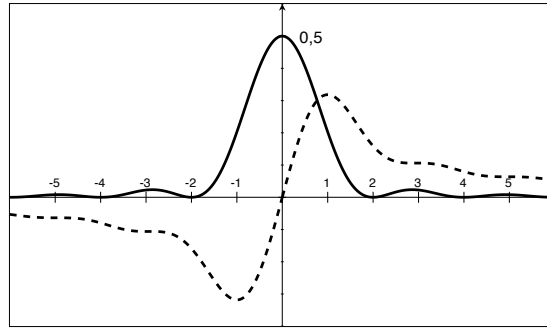


Fig. P.2: Real part (full line) and imaginary part (dashed) of $F^{(2)}(\pi x, -\pi x)$.

Let me now determine the integral over the real part ¹

$$\int_{-\infty}^{\infty} dx \operatorname{Re} \left[F^{(2)}(x, -x) \right] = \int_{-\infty}^{\infty} dx \frac{1}{2} \left(\frac{\sin(x/2)}{x/2} \right)^2 = \int_{-\infty}^{\infty} dy \left(\frac{\sin(y)}{y} \right)^2 = \pi \tag{P.12}$$

The integral

$$\int dw t \operatorname{Re} \left[F^{(2)}(wt, -wt) \right] \int dx \operatorname{Re} \left[F^{(2)}(x, -x) \right] = \pi \delta(t) \tag{P.13}$$

is invariant with t . This and the property that the function vanishes everywhere except the origin indicates the relation to the *delta*-function

$$\lim_{T \rightarrow \infty} t \operatorname{Re} \left[F^{(2)}(wt, -wt) \right] = \pi \delta(t) \tag{P.14}$$

¹See Bronstein-Eq.19 in Bronstein-Section 1.1.3.4 "Tabelle einiger Bestimmter Integrale"[48] or follow the derivation to the sine integral $\operatorname{Si}(x) = \int_0^x dt \frac{\sin(t)}{t}$, which obeys $\operatorname{Si}(\infty) - \operatorname{Si}(0) = \pi/2$.

$$\begin{aligned}
 \int_0^{\infty} dx \frac{1}{x} \underbrace{\sin(2x)}_{2 \sin(x) \cos(x) = \partial_x \sin^2(x)} &= \int_0^{\infty} dx \underbrace{\frac{1}{x}}_f \underbrace{\partial_x \sin^2(x)}_{g'} = \underbrace{\left[\frac{\sin^2(x)}{x} \right]_0^{\infty}}_{fg=0} - \int_0^{\infty} dx \underbrace{\left(-\frac{1}{x^2} \sin^2(x) \right)}_{f'g} = \int_0^{\infty} dx \frac{\sin^2(x)}{x^2} \\
 \Rightarrow \int_0^{\infty} dx \frac{\sin^2(x)}{x^2} &= \int_0^{\infty} d(2x) \frac{\sin(2x)}{2x} = \int_0^{\infty} du \frac{\sin(u)}{u} = \operatorname{Si}(x) \Big|_0^{\infty} = \frac{\pi}{2} \tag{P.11}
 \end{aligned}$$

Thus, we arrive at

$$\lim_{t \rightarrow \infty} 2t \operatorname{Re} \left[F^{(2)}(\omega t, -\omega t) \right] = \lim_{t \rightarrow \infty} t F^{(1)}(\omega t) F^{(1)}(-\omega t) = 2\pi\delta(\omega) \quad (\text{P.15})$$

We can still multiply this equation with t to obtain for example

$$\lim_{T \rightarrow \infty} t^2 \operatorname{Re} \left[F^{(2)}(\omega t, -\omega t) \right] = \pi t \delta(t) \quad (\text{P.16})$$

Appendix Q

Additional material for the Phonon Boltzmann equation

Q.1 Sketch of the derivation of the Phonon Boltzmann equation

1. Set up Newton's equations of motion for the distortions $Q_\lambda(t)$.
2. Introduce **phonon amplitudes** $b_\lambda^\pm(t)$

$$Q_\lambda(t) = b_\lambda^+(t)e^{i\omega_\lambda t} + b_\lambda^-(t)e^{-i\omega_\lambda t}$$

The state can be described alternatively by the phonon amplitudes, or by the **density matrix**

$$\rho_{\lambda,\lambda'}(t) = b_\lambda^+(t)b_{\lambda'}^-(t)$$

Both contain the full information of trajectories. The off-diagonal elements of the density matrix describe the entanglement of the phonons.

3. Perturbation expansion in the anharmonic terms (We go to second order, which is the minimum to obtain forward and back-reaction.) This is not required for a derivation of the Boltzmann equation, but it ensures a simple scattering operator.
4. **Initial random-phase approximation:** The initial random phase approximation removes the off-diagonal elements from the initial density matrix.

The state is now an ensemble described by a density matrix average

$$\langle \rho_{\lambda,\lambda'}(t) \rangle = \langle b_\lambda^+(t)b_{\lambda'}^-(t) \rangle_{\text{initial phases}}$$

5. Long-time limit, which turns the oscillatory functions into delta functions of the frequency difference. The result is **energy conservation**. The initial random-phase approximation is required to obtain the desired form of the long-time limit.
6. **Final random-phase approximation:** The final randomization of the phases deletes the off-diagonal elements of the density matrix. This is the point where irreversibility is introduced.

A thorough derivation should analyze $\rho_{\lambda,\lambda'}(t)$.

- After a decoherence time the off-diagonal elements should vanish

- the diagonal elements obey the mapping

$$\rho_{\lambda,\lambda}(t) = \sum_{\lambda'} M_{\lambda,\lambda'}(t) \rho_{\lambda',\lambda'}(0)$$

The mapping shall be of exponential form $\mathbf{M}(t) = e^{-\mathbf{A}t}$, that is

$$\mathbf{A}(t) = -\frac{1}{t} \ln[\mathbf{M}(t)] \quad \text{for } t > T_{decoh}$$

It is possible that a unitary transformation of the phonons fulfills the requirements, if this is not the case in the original basis.

7. Formulation of a **rate equation**: Let us combine the occupations $n_{\lambda}(t) = \rho_{\lambda,\lambda}(t)$ into a vector $\vec{n}(t)$. A rate equation gives

$$\partial_t \vec{n}(t) = -\mathbf{A} \vec{n}(t) \quad \Leftrightarrow \quad \vec{n}(t) = e^{-\mathbf{A}t} \vec{n}(0)$$

Q.2 Equations of motion of phonon amplitudes

Editor: This is in progress: It aims at deriving the equations of motion in an alternative way. The main purpose is to crosscheck all signs and factors. It may however also turn out to be the more elegant derivation.

Q.2.1 Obtain Lagrangian in terms of phonon amplitudes

We start from the Lagrangian Eq. 7.67 in normal coordinates

$$\begin{aligned} \mathcal{L} \stackrel{\text{Eq. 7.67}}{=} \mathcal{N} \left\{ \sum_{\vec{k} \in \Omega_G, n} \left(\frac{1}{2} \dot{Q}_n^*(\vec{k}) \dot{Q}_n(\vec{k}) - \frac{1}{2} \omega_n^2(\vec{k}) Q_n^*(\vec{k}) Q_n(\vec{k}) \right) \right. \\ \left. - \sum_{\vec{k}, \vec{k}', \vec{k}'' \in \Omega_G} \sum_{l, m, n} \frac{1}{3!} X_{l, m, n}(\vec{k}, \vec{k}', \vec{k}'') Q_l(\vec{k}) Q_m(\vec{k}') Q_n(\vec{k}'') \right\} \end{aligned} \quad (\text{Q.1})$$

which is converted into phonon amplitudes using

$$Q_n(\vec{k}) \stackrel{\text{Eq. U.24}}{=} \frac{\hbar}{\sqrt{2N\hbar\omega_n(\vec{k})}} \sum_{\sigma \in \pm} b_{n,\sigma}(\vec{k}) e^{i\sigma\omega_n(\vec{k})t} \quad (\text{Q.2})$$

Kinetic energy of free phonons

$$\begin{aligned}
 E^{kin} &= \mathcal{N} \sum_{\vec{k} \in \Omega_G} \sum_n \frac{1}{2} \dot{Q}_n^*(\vec{k}) \dot{Q}_n(\vec{k}) \\
 &= \frac{1}{2} \mathcal{N} \sum_{\vec{k} \in \Omega_G} \sum_n \left(\frac{\hbar}{\sqrt{2\mathcal{N}\hbar\omega_n(\vec{k})}} \sum_{\sigma \in \pm} \left(\partial_t b_{n,\sigma}(\vec{k}) + i\sigma\omega_n(\vec{k})b_{n,\sigma}(\vec{k}) \right) e^{i\sigma\omega_n(\vec{k})t} \right)^* \\
 &\quad \times \left(\frac{\hbar}{\sqrt{2\mathcal{N}\hbar\omega_n(\vec{k})}} \sum_{\sigma' \in \pm} \left(\partial_t b_{n,\sigma'}(\vec{k}) + i\sigma'\omega_n(\vec{k})b_{n,\sigma'}(\vec{k}) \right) e^{i\sigma'\omega_n(\vec{k})t} \right) \\
 &= \sum_{\vec{k} \in \Omega_G} \sum_n \frac{\hbar}{4\omega_n(\vec{k})} \sum_{\sigma, \sigma' \in \pm} \left(\dot{b}_{n,\sigma}^*(\vec{k}) - i\sigma\omega_n(\vec{k})b_{n,\sigma}^*(\vec{k}) \right) \left(\dot{b}_{n,\sigma'}(\vec{k}) + i\sigma'\omega_n(\vec{k})b_{n,\sigma'}(\vec{k}) \right) \\
 &\quad \times e^{-i[\sigma\omega_n(\vec{k}) - \sigma'\omega_n(\vec{k})]t} \\
 &= \sum_{\vec{k} \in \Omega_G} \sum_n \frac{\hbar}{4\omega_n(\vec{k})} \sum_{\sigma, \sigma' \in \pm} e^{-i[\sigma - \sigma']\omega_n(\vec{k})t} \\
 &\quad \times \left(\dot{b}_{n,\sigma}^*(\vec{k}) \dot{b}_{n,\sigma'}(\vec{k}) + \sigma\sigma'\omega_n^2(\vec{k})b_{n,\sigma}^*(\vec{k})b_{n,\sigma'}(\vec{k}) + i\sigma'\omega_n(\vec{k})\dot{b}_{n,\sigma}^*(\vec{k})b_{n,\sigma'}(\vec{k}) - i\sigma\omega_n(\vec{k})\dot{b}_{n,\sigma'}(\vec{k})b_{n,\sigma}^*(\vec{k}) \right)
 \end{aligned} \tag{Q.3}$$

Potential energy of free phonons

Let us work out the potential energy of the phonons without anharmonic terms.

$$\begin{aligned}
 E^{harm} &= \mathcal{N} \sum_{\vec{k} \in \Omega_G} \sum_n \frac{1}{2} \omega_n^2(\vec{k}) Q_n^*(\vec{k}) Q_n(\vec{k}) \\
 &= \mathcal{N} \frac{1}{2} \sum_{\vec{k} \in \Omega_G} \sum_n \omega_n^2(\vec{k}) \left(\frac{\hbar}{\sqrt{2\mathcal{N}\hbar\omega_n(\vec{k})}} \sum_{\sigma \in \pm} b_{n,\sigma}(\vec{k}) e^{i\sigma\omega_n(\vec{k})t} \right)^* \left(\frac{\hbar}{\sqrt{2\mathcal{N}\hbar\omega_n(\vec{k})}} \sum_{\sigma \in \pm} b_{n,\sigma}(\vec{k}) e^{i\sigma\omega_n(\vec{k})t} \right) \\
 &= \frac{1}{4} \sum_{\vec{k} \in \Omega_G} \sum_n \hbar\omega_n(\vec{k}) \sum_{\sigma, \sigma' \in \pm} b_{n,\sigma}^*(\vec{k}) b_{n,\sigma'}(\vec{k}) e^{-i[\sigma - \sigma']\omega_n(\vec{k})t}
 \end{aligned} \tag{Q.4}$$

Interaction energy of phonons

The energy due to the anharmonic terms have been obtained in Eq. 7.134 on p. 244

$$\begin{aligned}
 E^{anharm} &\stackrel{\text{Eq. 7.134}}{=} \mathcal{N} \sum_{\vec{k}, \vec{k}', \vec{k}'' \in \Omega_G} \sum_{l, m, n} \frac{1}{3!} \left(\frac{\hbar}{2\mathcal{N}} \right)^{\frac{3}{2}} \frac{X_{l, m, n}(\vec{k}, \vec{k}', \vec{k}'')}{\sqrt{\omega_l(\vec{k})\omega_m(\vec{k}')\omega_n(\vec{k}'')}} \\
 &\quad \times \sum_{\sigma, \sigma', \sigma'' \in \pm} b_{l,\sigma}(\vec{k}) b_{m,\sigma'}(\vec{k}') b_{n,\sigma''}(\vec{k}'') e^{i[\sigma\omega_l(\vec{k}) + \sigma'\omega_m(\vec{k}') + \sigma''\omega_n(\vec{k}'')]t}
 \end{aligned} \tag{Q.5}$$

Q.3 Comparison of formulas

Q.3.1 Comparison with Peierls work

In ref.[70], Peierls describes the phonon-Boltzmann equation similar to the present text. Let me therefore make a comparison.

Peierls starts with a simple one-dimensional chain of atoms with an energy

$$E = \sum_n \underbrace{\frac{1}{2} m \dot{u}^2 + \omega_0 (u_n - u_{n-1})^2}_{\text{Peierls-Eq.1}} + \epsilon \underbrace{\frac{M}{3} \omega_0^2 (u_n - u_{n-1})^3}_{\text{Peierls-Eq.16}} \tag{Q.6}$$

In Peierls-Eq.6, Peierls introduces normal coordinates

$$u_n = \sum \xi_f e^{ifn} \tag{Q.7}$$

which, in three dimensions translates into Peierls-Eq.6'.

$$\vec{r}_{n_1, n_2, n_3} = \sum \vec{\xi}_{f, g, h} e^{i(fn_1 + gn_2 + hn_3)} \tag{Q.8}$$

where $\vec{\xi}$ is the polarization vector for the wave vector $(f, g, h)/a$.

He arrives at the equation of motion (Peierls-Eq.20.)

$$\dot{b}_{fghj} = \frac{i}{M\omega_f} \sum_{f', f''} V_{-f, f', f''} b_{f'} b_{f''} e^{i(\omega_{f'} + \omega_{f''} - \omega_f)t} \tag{Q.9}$$

	Peierls	this text
displacement	$u_n, (x, y, z)_{n_1, n_2, n_3}$	$\delta \vec{R}_{\alpha, t}$
mass	m	M_α
Nr. of atoms	N	–
total mass	$M = Nm$	–
wave vector	f	$\vec{k} \vec{T}$
normal coordinate	ξ_f	$Q_n(\vec{k})$
complex conjugate	\bar{x}	x^*

Q.3.2 Equation of motion of the phonon amplitudes

On p. 330 we arrive at the equation of motion for the phonon amplitudes Eq. 10.2.

Appendix R

Slater determinants for parallel and antiparallel spins

Why can spin-up and spin-down electrons be treated as non-identical particles, even though they are only spinor-components of identical particles.

Here, we try to give an answer by showing that a one-particle orbitals can be occupied independently of each other with one spin-up and one spin-down electron. That is, for each placement of the two electrons into one-particle orbitals there is a Slater determinant. For two spin-up electrons or for two spin-down electrons, the same one-particle orbital can only be occupied once.

This implies that the statistics of spin up and spin-down electrons is such that spin up electrons are treated as a class of identical particles and spin-down electrons are treated as a different class of independent particles.

Let us consider two spatial one-particle orbitals $\chi_a(\vec{r})$ and $\chi_b(\vec{r})$. The two orbitals shall be orthonormal. Out of these two orbitals, we construct four spin orbitals, namely

$$\begin{aligned}\phi_{a\uparrow}(\vec{r}, \sigma) &= \chi_a(\vec{r})\delta_{\sigma,\uparrow} \\ \phi_{a\downarrow}(\vec{r}, \sigma) &= \chi_a(\vec{r})\delta_{\sigma,\downarrow} \\ \phi_{b\uparrow}(\vec{r}, \sigma) &= \chi_b(\vec{r})\delta_{\sigma,\uparrow} \\ \phi_{b\downarrow}(\vec{r}, \sigma) &= \chi_b(\vec{r})\delta_{\sigma,\downarrow}\end{aligned}$$

or using $\alpha \in \{a, b\}$ and $s \in \{\uparrow, \downarrow\}$.

$$\phi_{\alpha,s}(\vec{r}, \sigma) = \chi_\alpha(\vec{r})\delta_{s,\sigma}$$

Out of these one-particle spin orbitals, we construct the Slater determinants

$$\begin{aligned}\Phi_{\alpha,\beta,s,s'}(\vec{r}, \sigma, \vec{r}', \sigma') &= \frac{1}{\sqrt{2}} \left(\phi_{\alpha,s}(\vec{r}, \sigma)\phi_{\beta,s'}(\vec{r}', \sigma') - \phi_{\beta,s'}(\vec{r}, \sigma)\phi_{\alpha,s}(\vec{r}', \sigma') \right) \\ &= \frac{1}{\sqrt{2}} \left(\chi_\alpha(\vec{r})\chi_\beta(\vec{r}')\delta_{s,\sigma}\delta_{s',\sigma'} - \chi_\beta(\vec{r})\chi_\alpha(\vec{r}')\delta_{s,\sigma'}\delta_{s',\sigma} \right)\end{aligned}$$

Some of these Slater determinants are zero states, but that does not matter at the moment.

These Slater determinants are products of a spatial two-particle wave function and a two-particle wave function in the spin space. It will be convenient to introduce such two-particle states that are

symmetric and antisymmetric under particle exchange. (Exchange of the arguments.) These are

$$\begin{aligned}\Psi_{\alpha,\beta}^+(\vec{r}, \vec{r}') &\stackrel{\text{def}}{=} \frac{1}{\sqrt{2}} \left(\chi_{\alpha}(\vec{r})\chi_{\beta}(\vec{r}') + \chi_{\beta}(\vec{r})\chi_{\alpha}(\vec{r}') \right) \\ \Psi_{\alpha,\beta}^-(\vec{r}, \vec{r}') &\stackrel{\text{def}}{=} \frac{1}{\sqrt{2}} \left(\chi_{\alpha}(\vec{r})\chi_{\beta}(\vec{r}') - \chi_{\beta}(\vec{r})\chi_{\alpha}(\vec{r}') \right) \\ G_{s,s'}^+(\sigma, \sigma') &\stackrel{\text{def}}{=} \frac{1}{\sqrt{2}} \left(\delta_{s,\sigma}\delta_{s',\sigma'} + \delta_{s',\sigma'}\delta_{s,\sigma} \right) \\ G_{s,s'}^-(\sigma, \sigma') &\stackrel{\text{def}}{=} \frac{1}{\sqrt{2}} \left(\delta_{s,\sigma}\delta_{s',\sigma'} - \delta_{s',\sigma'}\delta_{s,\sigma} \right)\end{aligned}$$

The Slater determinants have the form

$$\begin{aligned}\Phi_{\alpha,\beta,s,s'}(\vec{r}, \sigma, \vec{r}', \sigma') &= \frac{1}{\sqrt{2}} \left[\frac{1}{2} \left(\Psi_{\alpha,\beta}^+ + \Psi_{\alpha,\beta}^- \right) \left(G_{s,s'}^+ + G_{s,s'}^- \right) - \frac{1}{2} \left(\Psi_{\alpha,\beta}^+ - \Psi_{\alpha,\beta}^- \right) \left(G_{s,s'}^+ - G_{s,s'}^- \right) \right] \\ &= \frac{1}{\sqrt{2}} \left[\Psi_{\alpha,\beta}^+(\vec{r}, \vec{r}') G_{s,s'}^-(\sigma, \sigma') + \Psi_{\alpha,\beta}^-(\vec{r}, \vec{r}') G_{s,s'}^+(\sigma, \sigma') \right]\end{aligned}\quad (\text{R.1})$$

Now, we can analyze the result using

$$\begin{aligned}G_{s,s'}^-(\sigma, \sigma') &\equiv 0 & \text{for } s &= s' \\ \Psi_{\alpha,\beta}^-(\vec{r}, \vec{r}') &\equiv 0 & \text{for } \alpha &= \beta\end{aligned}$$

Let us now consider two spin up electrons. Because of Eq. R.1 and $G_{\uparrow,\uparrow}^- = 0$, there is only a single non-zero Slater determinant, namely

$$|\Phi_{a,b,\uparrow,\uparrow}\rangle = \Psi_{a,b}^- \left(\frac{1}{\sqrt{2}} G_{s,s'}^+ \right)$$

The Slater determinant $|\Phi_{b,a,\uparrow,\uparrow}\rangle$ differs from $|\Phi_{a,b,\uparrow,\uparrow}\rangle$ only by a sign change. Thus, we see that the spatial wave function is antisymmetric. Hence, the Pauli principle exists in the spatial coordinates.

To show the difference let us investigate the states with different spin.

$$\begin{aligned}|\Phi_{a,a,\uparrow,\downarrow}\rangle &= \left(\frac{1}{\sqrt{2}} \Psi_{a,a}^+ \right) G_{\uparrow,\downarrow}^- \\ |\Phi_{a,b,\uparrow,\downarrow}\rangle &= \frac{1}{\sqrt{2}} \left(\Psi_{a,b}^+ G_{\uparrow,\downarrow}^- + \Psi_{a,b}^- G_{\uparrow,\downarrow}^+ \right) \\ |\Phi_{b,a,\uparrow,\downarrow}\rangle &= \frac{1}{\sqrt{2}} \left(\Psi_{a,b}^+ G_{\uparrow,\downarrow}^- - \Psi_{a,b}^- G_{\uparrow,\downarrow}^+ \right) \\ |\Phi_{b,b,\uparrow,\downarrow}\rangle &= \left(\frac{1}{\sqrt{2}} \Psi_{b,b}^+ \right) G_{\uparrow,\downarrow}^-\end{aligned}$$

We see that the two electrons with different spin can be placed without restriction into the two spatial one-particle orbitals.

This indicates that the statistics of electrons with different spin is identical to that of two non-identical particles. The statistics of electrons with like spin is like identical particles.

R.1 Spatial symmetry for parallel and antiparallel spins

Here, we show that

- the spatial wave functions for two electrons with parallel spin is antisymmetric
- the spatial wave functions for two electrons with anti-parallel spin is symmetric

under exchange of the coordinates.

A common misconception is that the Slater determinant of two one-particle spin-orbitals with opposite spin describes two electrons with anti-parallel spin. For such a state the z-component of the spin vanishes, but it is a superposition of a two states with $S_z = 0$, namely one with antiparallel spin and the other with parallel spin with a total spin lying in the xy-plane.

In order to determine states with parallel and antiparallel spin, we need to determine the spin eigenstates and eigenvalues. If the eigenvalue for $\hat{S}_{tot}^2 = (\hat{S}_1 + \hat{S}_2)^2$ vanishes, the wave function has antiparallel spin. If the eigenvalue is $2\hbar^2$ the spins are parallel.

Using the ladder operators \hat{S}_{\pm} we write the total spin as

$$\begin{aligned}\hat{S}_{tot}^2 &= (\hat{S}_1 + \hat{S}_2)^2 \\ &= \hat{S}_1^2 + \hat{S}_2^2 + 2\hat{S}_1\hat{S}_2 \\ &= \hat{S}_1^2 + \hat{S}_2^2 + 2\left[\frac{1}{2}\hat{S}_{1,+}\hat{S}_{2,-} + \frac{1}{2}\hat{S}_{1,-}\hat{S}_{2,+} + \hat{S}_{1,z}\hat{S}_{2,z}\right] \\ &= \hat{S}_1^2 + \hat{S}_2^2 + \hat{S}_{1,+}\hat{S}_{2,-} + \hat{S}_{1,-}\hat{S}_{2,+} + 2\hat{S}_{1,z}\hat{S}_{2,z}\end{aligned}$$

The ladder operators are defined as

$$\begin{aligned}\hat{S}_+ &= \hat{S}_x + i\hat{S}_y \\ \hat{S}_- &= \hat{S}_x - i\hat{S}_y\end{aligned}$$

and obey

$$\begin{aligned}\hat{S}_-|\uparrow\rangle &= |\downarrow\rangle\hbar & \text{and} & \quad \hat{S}_-|\downarrow\rangle = |\emptyset\rangle \\ \hat{S}_+|\uparrow\rangle &= |\emptyset\rangle & \text{and} & \quad \hat{S}_+|\downarrow\rangle = |\uparrow\rangle\hbar\end{aligned}$$

Thus

$$\begin{aligned}(\hat{S}_{1+}\hat{S}_{2-} + \hat{S}_{1-}\hat{S}_{2+})|G_{\uparrow,\downarrow}^{\pm}\rangle &= (\hat{S}_{1+}\hat{S}_{2-} + \hat{S}_{1-}\hat{S}_{2+})\frac{1}{\sqrt{2}}(|\uparrow,\downarrow\rangle \pm |\downarrow,\uparrow\rangle) \\ &= \frac{1}{\sqrt{2}}(|\downarrow,\uparrow\rangle \pm |\uparrow,\downarrow\rangle)\hbar^2 \\ &= |G_{\uparrow,\downarrow}^{\pm}\rangle(\pm\hbar^2)\end{aligned}$$

$$(\hat{S}_{1+}\hat{S}_{2-} + \hat{S}_{1-}\hat{S}_{2+})|G_{\uparrow,\uparrow}^{\pm}\rangle = |\emptyset\rangle$$

$$(\hat{S}_{1+}\hat{S}_{2-} + \hat{S}_{1-}\hat{S}_{2+})|G_{\downarrow,\downarrow}^{\pm}\rangle = |\emptyset\rangle$$

$$\hat{S}_{1,z}\hat{S}_{2,z}|G_{\uparrow,\downarrow}^{\pm}\rangle = |G_{\uparrow,\downarrow}^{\pm}\rangle\left(-\frac{\hbar^2}{4}\right)$$

$$\hat{S}_{1,z}\hat{S}_{2,z}|G_{\uparrow,\uparrow}^{\pm}\rangle = |G_{\uparrow,\uparrow}^{\pm}\rangle\left(+\frac{\hbar^2}{4}\right)$$

$$\hat{S}_{1,z}\hat{S}_{2,z}|G_{\downarrow,\downarrow}^{\pm}\rangle = |G_{\downarrow,\downarrow}^{\pm}\rangle\left(+\frac{\hbar^2}{4}\right)$$

$$\hat{S}_i^2|G_{s,s'}^{\pm}\rangle = |G_{s,s'}^{\pm}\rangle\frac{3\hbar^2}{4}$$

$$\hat{S}_{tot}^2|G_{\uparrow,\downarrow}^{\pm}\rangle = |G_{\uparrow,\downarrow}^{\pm}\rangle\left[\frac{3\hbar^2}{4} + \frac{3\hbar^2}{4} \pm \hbar^2 - \frac{\hbar^2}{2}\right] = |G_{\uparrow,\downarrow}^{\pm}\rangle(1 \pm 1)\hbar^2$$

$$\hat{S}_{tot}^2|G_{\uparrow,\uparrow}^{\pm}\rangle = |G_{\uparrow,\uparrow}^{\pm}\rangle\left[\frac{3\hbar^2}{4} + \frac{3\hbar^2}{4} + \frac{\hbar^2}{2}\right] = |G_{\uparrow,\uparrow}^{\pm}\rangle 2\hbar^2$$

$$\hat{S}_{tot}^2|G_{\downarrow,\downarrow}^{\pm}\rangle = |G_{\downarrow,\downarrow}^{\pm}\rangle\left[\frac{3\hbar^2}{4} + \frac{3\hbar^2}{4} + \frac{\hbar^2}{2}\right] = |G_{\downarrow,\downarrow}^{\pm}\rangle 2\hbar^2$$

Thus, we see that $|G_{\uparrow,\downarrow}^+\rangle$, $|G_{\uparrow,\uparrow}^+\rangle$ and $|G_{\downarrow,\downarrow}^+\rangle$ describe two electrons with parallel spin. Note that $|G_{s,s'}^-\rangle$ vanishes for parallel spin.

The only solution with antiparallel spin is $|G_{\uparrow,\downarrow}^-\rangle$.

From Eq. R.1 we know that the antisymmetric spin wave function is always combined with the symmetric spatial orbital and vice versa. Hence, the wave functions describing two electrons with anti-parallel spin are symmetric in their spatial coordinates, while the ones with parallel spin have an antisymmetric spatial wave function.

R.2 An intuitive analogy for particle with spin

Consider balls that are painted on the one side green and on the other side red.

If we place two such balls on a table with the green side up, turn around and look at them again, we cannot tell if the two balls have been interchanged.

Now we place them with opposite colors up. If we only allow that the positions of the two balls are interchanged, but exclude that they are turned around, we can tell the two spheres apart from their orientation. Hence, we can treat them as non-identical spheres.

However, if we consider exchanges of position *and* orientation, we are again unable to tell, whether the spheres have been interchanged or not.

Thus, if we can exclude that the spins of the particles –or the orientation of our spheres– change, we can divide electrons into two classes of particles, namely spin-up and spin-down electrons. Particles within each class are indistinguishable, but spin-up and spin-down electrons can be distinguished. When the spin is preserved, the Hamiltonian is invariant with respect to spin-rotation, and spin is a good quantum number.

However, if there is a magnetic field, which can cause a rotation of the spin direction, the division into spin-up and spin-down particles is no more a useful concept. In our model, if the orientation of the spheres can change with time, we cannot use it as distinguishing feature.

Appendix S

Lagrange formalism and action principle

Hamilton's principle says that the action functional defined as

$$S[x(t)] = \int dt \mathcal{L}(\vec{x}, \dot{\vec{x}}, t) \quad (\text{S.1})$$

is at a stationary point for the physical path $\vec{x}(t)$. Only paths with given boundary conditions $\vec{x}(t_i) = \vec{x}_i$ and $\vec{x}(t_f) = \vec{x}_f$.

The action is defined via the Lagrange function $\mathcal{L}(\vec{x}, \vec{v}, t)$.

In the following, I use the short-hand notation

$$\frac{\partial \mathcal{L}}{\partial \vec{x}} \stackrel{\text{def}}{=} \vec{\nabla}_x \mathcal{L} \quad \text{and} \quad \frac{\partial \mathcal{L}}{\partial \vec{v}} \stackrel{\text{def}}{=} \vec{\nabla}_v \mathcal{L} \quad (\text{S.2})$$

$$\begin{aligned} \delta S[x(t)] &= \int_{x_i, t_i}^{x_f, t_f} dt \left(\frac{\partial \mathcal{L}}{\partial \vec{x}} \delta \vec{x}(t) + \frac{\partial \mathcal{L}}{\partial \vec{v}} \delta \dot{\vec{x}}(t) \right) \\ &= \int_{x_i, t_i}^{x_f, t_f} dt \left(\frac{\partial \mathcal{L}}{\partial \vec{x}} \delta \vec{x} + \frac{d}{dt} \left(\frac{\partial \mathcal{L}}{\partial \vec{v}} \delta \vec{x} \right) - \delta \vec{x} \frac{d}{dt} \frac{\partial \mathcal{L}}{\partial \vec{v}} \right) \\ &= \left[\frac{\partial \mathcal{L}}{\partial \vec{v}} \delta \vec{x} \right]_{x_i, t_i}^{x_f, t_f} + \int_{x_i, t_i}^{x_f, t_f} dt \delta \vec{x}(t) \left(\frac{\partial \mathcal{L}}{\partial \vec{x}} - \frac{d}{dt} \frac{\partial \mathcal{L}}{\partial \vec{v}} \right) \end{aligned} \quad (\text{S.3})$$

The first term vanishes because of the boundary conditions, which enforce $\delta \vec{x}(t_i) = \delta \vec{x}(t_f) = 0$. The variation of the action vanishes only for all possible variations $\delta \vec{x}(t)$, if the Euler-Lagrange equations

$$\frac{\partial \mathcal{L}(\vec{x}, \vec{v}, t)}{\partial \vec{x}} - \frac{d}{dt} \frac{\partial \mathcal{L}(\vec{x}, \vec{v}, t)}{\partial \vec{v}} = 0 \quad \text{and} \quad \frac{d\vec{x}}{dt} = \vec{v} \quad (\text{S.4})$$

are satisfied.

From Euler-Lagrange equations to Hamilton's equations

With the definition

$$\vec{p}(\vec{x}, \vec{v}, t) = \frac{\partial \mathcal{L}(\vec{x}, \vec{v}, t)}{\partial \vec{v}} \quad (\text{S.5})$$

The Euler-Lagrange equations Eq. S.4 have the form

$$\frac{d}{dt} p(\vec{x}, \vec{v}, t) = \frac{\partial \mathcal{L}(\vec{x}, \vec{v}, t)}{\partial \vec{x}} \quad \text{and} \quad \frac{d\vec{x}}{dt} = \vec{v} \quad (\text{S.6})$$

This is already close to Hamilton's equations of motion. Unfortunately the condition for the momentum needs to be satisfied. The condition implies that one looks for the value \vec{v} such that the gradient of the Lagrangian has a certain value, namely the momentum. Problems of this sort are best solved by a **Legendre transform**.

The definition for the canonical momentum can also be written in the form

$$\vec{\nabla}_v \left(\vec{p}\vec{v} - \mathcal{L}(\vec{x}, \vec{v}, t) \right) = 0 \quad (\text{S.7})$$

Furthermore, we find

$$\begin{aligned} \vec{\nabla}_p \left(\vec{p}\vec{v} - \mathcal{L}(\vec{x}, \vec{v}, t) \right) &= \vec{v} \\ \vec{\nabla}_x \left(\vec{p}\vec{v} - \mathcal{L}(\vec{x}, \vec{v}, t) \right) &= -\frac{\partial \mathcal{L}}{\partial \vec{x}} \end{aligned} \quad (\text{S.8})$$

This implies that the right-hand sides of both equations can be expressed in terms of derivatives of this new object.

If I define the Hamilton function as

$$\mathcal{H}(\vec{p}, \vec{x}, t) = \text{stat}_{\vec{v}} \left\{ \vec{p}\vec{v} - \mathcal{L}(\vec{x}, \vec{v}, t) \right\} \quad (\text{S.9})$$

I can rewrite the Euler-Lagrange equations in the form

$$\frac{d\vec{p}}{dt} = -\frac{\partial \mathcal{H}(\vec{x}, \vec{v}, t)}{\partial \vec{x}} \quad \text{and} \quad \frac{d\vec{x}}{dt} = \frac{\partial \mathcal{H}(\vec{x}, \vec{v}, t)}{\partial \vec{p}} \quad (\text{S.10})$$

which are Hamilton's equations.

Legendre transform and Lagrange multipliers

Editor: The following is a sketch to motivate Hamilton functions and momenta. So-far it has not been successful. Do not read!

The Hamilton's equations are first-order differential equations in phase space while the Lagrange equations are second-order differential equations in coordinate space. However, also the Lagrange equations can be formulated as first-order equations in an expanded space, which will make the analogy with phase space more apparent.

Let me expand the action functional by a velocity trajectory, and a Lagrange multiplier, which will enforce that $\vec{v}(t)$ is the time-derivative of the position-trajectory

$$S[\vec{v}(t)] = \text{stat}_{\vec{x}(t), \vec{p}(t)} \int dt \left\{ \mathcal{L}(\vec{x}, \vec{v}, t) - \vec{p} \left(\dot{\vec{x}} - \vec{v} \right) \right\} \quad (\text{S.11})$$

For a given velocity trajectory $\vec{v}(t)$, the position and momenta obey

$$\begin{aligned} \frac{\partial \mathcal{L}}{\partial \vec{x}} + \frac{d\vec{p}}{dt} &= 0 \\ \dot{\vec{x}}(t) - v(t) = 0 &\Rightarrow \vec{x}(t) = \vec{x}_i + \int_{t_i}^t dt \vec{v}(t) \end{aligned} \quad (\text{S.12})$$

The boundary condition requires

$$\int_{t_i}^{t_f} dt \vec{v}(t) = \vec{x}_f - \vec{x}_i \quad (\text{S.13})$$

By choosing a velocity path $\vec{v}(t)$, we also select a real-space path. In order to obtain the stationary trajectory, I need to set the first variation of $S[v(t)]$ to zero. This implies that the

$$S = \text{stat}_{\vec{x}(t), \vec{v}(t), \vec{p}(t)} \int dt \left\{ \mathcal{L}(\vec{x}, \vec{v}, t) + \vec{p} \left(\dot{\vec{x}} - \vec{v} \right) \right\} \quad (\text{S.14})$$

- When we do set the variation of the momenta to zero at first, we obtain the action expressed by the Lagrange function.

$$S = \text{stat}_{\vec{x}(t)} \int dt \mathcal{L}(\vec{x}, \dot{\vec{x}}, t) \quad (\text{S.15})$$

Apparently, I can drop the trajectory $\vec{v}(t)$ altogether and get the velocity directly from the trajectory

- When we do the variation of the velocities first, we obtain

$$S = \text{stat}_{\vec{x}(t), \vec{p}(t)} \int dt \left\{ \vec{p} \dot{\vec{x}} - \mathcal{H}(\vec{x}, \vec{p}, t) \right\} \quad (\text{S.16})$$

where

$$\mathcal{H}(\vec{p}, \vec{x}, t) = \text{stat}_{\vec{v}} \left\{ \vec{p} \vec{v} - \mathcal{L}(\vec{x}, \vec{v}, t) \right\} \quad (\text{S.17})$$

or

$$\mathcal{H}(\vec{p}, \vec{x}, t) = \vec{p} \vec{v} - \mathcal{L}(\vec{x}, \vec{v}, t) \quad \text{with} \quad \vec{p} = \frac{\partial \mathcal{L}(\vec{x}, \vec{v}, t)}{\partial \vec{v}} \quad (\text{S.18})$$

Appendix T

Recommended reading

- William Jones and Norman H. March, *Theoretical Solid-State Physics, Volume 1: Perfect lattices in Equilibrium*
- Ashcroft Mermin, *Solid-State Physics*, 1976
- Michael P. Marder, *Condensed Matter Physics*, 2nd Ed. 2015.[62]
- A standard reference for the Boltzmann equation is the book of Haug and Jauho[136].

Appendix U

Additional notes for the chapter on phonons

This chapter is not for the reader. It is a collection of notes intended for future changes of the lecture notes in the phonon amplitudes.

U.1 Vibrational amplitudes

Editor: This material was intended to be introduced in or after the section ‘Harmonic oscillator revisited’ in chapter Phonons. This option would introduce the concept of phonon amplitudes before introducing Bloch’s theorem.

Editor: This is under construction

$$\begin{aligned} H(\vec{P}, \vec{X}, t) &= \text{stat}_{\vec{V}} \left(\vec{P}\vec{V} - \mathcal{L}(\vec{V}, \vec{X}, t) \right) \\ \mathcal{L}(\vec{V}, \vec{X}, t) &= \text{stat}_{\vec{P}} \left(\vec{P}\vec{V} - H(\vec{P}, \vec{X}, t) \right) \\ S[\vec{X}(t)] &= \min_{[\vec{X}(t)]} \int_{\vec{X}_1, t_1}^{\vec{X}_2, t_2} dt \mathcal{L}(\dot{\vec{X}}, \vec{X}, t) \end{aligned} \tag{U.1}$$

$$\begin{aligned}
\vec{b}(\vec{V}, \vec{X}) &= \frac{1}{\sqrt{2\omega}} \left(i\mathbf{U}^\dagger \mathbf{M}^{\frac{1}{2}} \vec{V} + \omega \mathbf{U}^\dagger \mathbf{M}^{\frac{1}{2}} \vec{X} \right) \\
\vec{b} + \vec{b}^* &= \sqrt{2\omega} \mathbf{U}^\dagger \mathbf{M}^{\frac{1}{2}} \vec{X} \quad \Rightarrow \quad \vec{X} = \frac{1}{\sqrt{2}} \mathbf{M}^{-\frac{1}{2}} \mathbf{U} \frac{1}{\sqrt{\omega}} (\vec{b} + \vec{b}^*) \\
\vec{b} - \vec{b}^* &= \frac{i\sqrt{2}}{\sqrt{\omega}} \mathbf{U}^\dagger \mathbf{M}^{\frac{1}{2}} \vec{V} \quad \Rightarrow \quad \vec{V} = \frac{-i}{\sqrt{2}} \mathbf{M}^{-\frac{1}{2}} \mathbf{U} \sqrt{\omega} (\vec{b} - \vec{b}^*) \\
\vec{b}^* \omega \vec{b} &= \left(\left(\vec{X} \mathbf{M}^{\frac{1}{2}} \mathbf{U} \omega - i \vec{V} \mathbf{M}^{\frac{1}{2}} \mathbf{U} \right) \frac{1}{\sqrt{2\omega}} \right) \omega \left(\frac{1}{\sqrt{2\omega}} \left(i\mathbf{U}^\dagger \mathbf{M}^{\frac{1}{2}} \vec{V} + \omega \mathbf{U}^\dagger \mathbf{M}^{\frac{1}{2}} \vec{X} \right) \right) \\
&= \frac{1}{2} \vec{X} \underbrace{\mathbf{M}^{\frac{1}{2}} \mathbf{U} \omega^2 \mathbf{U}^\dagger \mathbf{M}^{\frac{1}{2}}}_{\substack{D \\ C}} \vec{X} + \frac{1}{2} \vec{V} \underbrace{\mathbf{M}^{\frac{1}{2}} \mathbf{U} \mathbf{U}^\dagger \mathbf{M}^{\frac{1}{2}}}_{\substack{1 \\ M}} \vec{V} \\
&+ \\
&= E_{\text{kin}} + E_{\text{pot}} \\
E_{\text{pot}} &= \frac{1}{2} \vec{X} \mathbf{C} \vec{X} \\
&= (\vec{b} + \vec{b}^*) \frac{1}{\sqrt{\omega}} \mathbf{U}^\dagger \underbrace{\mathbf{M}^{-\frac{1}{2}} \mathbf{C} \mathbf{M}^{-\frac{1}{2}}}_{\substack{D \\ \omega^2}} \mathbf{U} \frac{1}{\sqrt{\omega}} (\vec{b} + \vec{b}^*) \\
&= (\vec{b} + \vec{b}^*) \omega (\vec{b} + \vec{b}^*) \\
E_{\text{kin}} &= \frac{1}{2} \vec{V}^* \mathbf{M} \vec{V} = (\vec{b}^* - \vec{b}) \sqrt{\omega} \underbrace{\mathbf{U}^\dagger \mathbf{M}^{-\frac{1}{2}} (i) \mathbf{M} (-i) \mathbf{M}^{-\frac{1}{2}} \mathbf{U}}_{\substack{1 \\ \omega}} \sqrt{\omega} (\vec{b} - \vec{b}^*) \\
&= (\vec{b}^* - \vec{b}) \omega (\vec{b} - \vec{b}^*) \\
&= -(\vec{b} - \vec{b}^*) \omega (\vec{b} - \vec{b}^*) \\
E_{\text{kin}} + E_{\text{pot}} &= (\vec{b} + \vec{b}^*) \omega (\vec{b} + \vec{b}^*) - (\vec{b} - \vec{b}^*) \omega (\vec{b} - \vec{b}^*) \\
&= 2(\vec{b} \omega \vec{b}^* + \vec{b}^* \omega \vec{b}) = 4\vec{b}^* \omega \vec{b} \\
E_{\text{kin}} - E_{\text{pot}} &= 4\vec{b}^* \omega \vec{b} - 2(\vec{b} + \vec{b}^*) \omega (\vec{b} + \vec{b}^*) = -2(\vec{b} \omega \vec{b} + \vec{b}^* \omega \vec{b}^*)
\end{aligned} \tag{U.2}$$

The coefficients of the partial solutions can be evaluated at any time from

$$A_n = e^{i\omega t} \frac{1}{2\omega_n} (i\partial_t + \omega_n) Z(t) \tag{U.3}$$

which is verified by applying the expression to the general solution

$$\begin{aligned}
e^{i\omega t} \frac{1}{2\omega_n} (i\partial_t + \omega_n) \underbrace{\left(A_n e^{-i\omega_n t} + B_n e^{i\omega_n t} \right)}_{Z(t)} &= e^{i\omega t} \frac{1}{2\omega_n} \left(A_n \omega e^{-i\omega_n t} - B_n \omega e^{i\omega_n t} + A_n \omega_n e^{-i\omega_n t} + B_n \omega_n e^{i\omega_n t} \right) \\
&= A_n
\end{aligned} \tag{U.4}$$

Thus, we obtained a variable, which is a constant of motion for the harmonic oscillator.

$$\begin{aligned}
\vec{X}(t) &= \sum_n \mathbf{M}^{-\frac{1}{2}} \mathbf{U} e^{-i\omega_n(t-t')} \frac{1}{2\omega_n} (i\partial_{t'} + \omega_n) \mathbf{U}^\dagger \mathbf{M}^{\frac{1}{2}} \vec{X}(t') \\
&+ \sum_n \mathbf{M}^{-\frac{1}{2}} \mathbf{U} e^{+i\omega_n(t-t')} \frac{1}{2\omega_n} (-i\partial_{t'} + \omega_n) \mathbf{U}^\dagger \mathbf{M}^{\frac{1}{2}} \vec{X}(t')
\end{aligned} \tag{U.5}$$

$$\begin{aligned}
 b_n(t) &= \frac{1}{2\omega_n} (i\partial_t + \omega_n) \mathbf{U}^\dagger \mathbf{M}^{\frac{1}{2}} \vec{X}(t) \\
 \vec{b}(\vec{V}, \vec{X}) &= \frac{1}{2\omega} \left(i\mathbf{U}^\dagger \mathbf{M}^{\frac{1}{2}} \vec{V} + \omega \mathbf{U}^\dagger \mathbf{M}^{\frac{1}{2}} \vec{X} \right) \\
 \vec{b}(\vec{V}, \vec{X}) &= \frac{1}{2\omega} \left(i\mathbf{U}^\dagger \mathbf{M}^{\frac{1}{2}} \vec{V} + \omega \mathbf{U}^\dagger \mathbf{M}^{\frac{1}{2}} \vec{X} \right) \\
 i\dot{b} &= \frac{\partial b}{\partial V} \ddot{X} + \frac{\partial b}{\partial X} \dot{X} \\
 \vec{X} &= \frac{1}{\sqrt{M_\alpha}} U_{\alpha,n} e^{-i\omega t} A_n(t')
 \end{aligned} \tag{U.6}$$

U.2 Backup material on phonon amplitudes

U.2.1 Left- and right-moving waves

The distortions resulting from Eq. ?? are composed of two terms, one of which has a phase velocity parallel to the wave vector, and a second term with a phase velocity in the opposite direction.

We divide the displacements Eq. 7.49 into left and right-moving partial waves

$$\begin{aligned}
 \delta R_{\alpha,\vec{r}} &\stackrel{Eqs. ??, 7.61}{=} \sum_{\vec{k} \in \Omega_G} \sum_n \frac{1}{\sqrt{M_\alpha}} U_{\alpha,n}(\vec{k}) e^{i[\vec{k}\vec{r} - \omega_n(\vec{k})t]} A_n(\vec{k}) \\
 &+ \underbrace{\sum_{\vec{k} \in \Omega_G} \sum_n \frac{1}{\sqrt{M_\alpha}} U_{\alpha,n}(\vec{k}) e^{i[\vec{k}\vec{r} + \omega_n(\vec{k})t]} B_n(\vec{k})}_{\underbrace{U_{\alpha,n}^*(-\vec{k}) \left(e^{i[-\vec{k}\vec{r} - \omega_n(\vec{k})t]} \right)^*}_{\left(U_{\alpha,n}(-\vec{k}) e^{i[-\vec{k}\vec{r} - \omega_n(\vec{k})t]} B_n^*(-\vec{k}) \right)^*}} \\
 &\stackrel{-\vec{k} \rightarrow \vec{k}}{=} \sum_{\vec{k}} \sum_n \frac{1}{\sqrt{M_\alpha}} U_{\alpha,n}(\vec{k}) e^{i[\vec{k}\vec{r} - \omega_n(\vec{k})t]} A_n(\vec{k}) + \sum_{\vec{k}} \sum_n \left(\frac{1}{\sqrt{M_\alpha}} U_{\alpha,n}(\vec{k}) e^{i[\vec{k}\vec{r} - \omega_n(\vec{k})t]} B_n^*(-\vec{k}) \right)^*
 \end{aligned} \tag{U.7}$$

We have rearranged the terms so that each wave vector contains the contributions propagating with a phase velocity in the direction of the wave vector.

We impose the requirement that the distortions are real-valued by requiring

$$A_n(\vec{k}) = B_n^*(-\vec{k}). \tag{U.8}$$

Thus, the trajectories are

$$\delta R_{\alpha,\vec{r}} = 2\text{Re} \left[\sum_{\vec{k} \in \Omega_G} \sum_n \frac{1}{\sqrt{M_\alpha}} U_{\alpha,n}(\vec{k}) e^{i[\vec{k}\vec{r} - \omega_n(\vec{k})t]} A_n(\vec{k}) \right] \tag{U.9}$$

U.2.2 From normal coordinates to phonon amplitudes

Eq. U.9 gives us the trajectories for a known set of coefficients $A_n(\vec{k})$. Now, we approach the inverse problem, namely to calculate the coefficients from a given trajectory. This will be important to decompose the trajectories into its components after a scattering event.

We start from a trajectory of the normal coordinates $Q_n(\vec{k}, t)$ and decompose it into traveling Bloch waves. For this purpose, we do the following thought experiment: At a specific time t_0 , we

switch the anharmonic terms off and inspect the time evolution of the resulting trajectory $\bar{Q}_n(t, t_0)$. We use a bar on top of the symbol to distinguish this fictitious trajectory \bar{Q}_n , with the anharmonic terms switched off, from the true trajectory Q_n with intact anharmonic terms. This fictitious trajectory $\bar{Q}(t, t_0)$ describes free phonons and has, for $t > t_0$, the form

$$\bar{Q}_n(\vec{k}, t, t_0) = A_n(\vec{k}, t_0)e^{-i\omega_n(\vec{k})t} + B_n(\vec{k}, t_0)e^{i\omega_n(\vec{k})t} \quad (\text{U.10})$$

For $t > t_0$, i.e. when scattering is absent, the decomposition of the trajectory into phonons, i.e. the plane waves, is straightforward.

The coefficients $A_n(\vec{k}, t_0)$ and $B_n(\vec{k}, t_0)$ for the travelling waves are obtained by matching the trajectory $Q_n(\vec{k}, t)$ at time t_0 with value and time derivative to the trajectory $\bar{Q}_n(\vec{k}, t, t_0)$ of Eq. U.10. The matching conditions are

$$\begin{aligned} Q_n(\vec{k}, t_0) &= \bar{Q}_n(\vec{k}, t_0, t_0) \\ \dot{Q}_n(\vec{k}, t_0) &= \dot{\bar{Q}}_n(\vec{k}, t_0, t_0) \end{aligned} \quad (\text{U.11})$$

which translates with Eq. U.10 into

$$\begin{aligned} Q_n(\vec{k}, t_0) &= A_n(\vec{k}, t_0)e^{-i\omega_n(\vec{k})t_0} + B_n(\vec{k}, t_0)e^{i\omega_n(\vec{k})t_0} \\ \dot{Q}_n(\vec{k}, t_0) &= -i\omega_n(\vec{k})A_n(\vec{k}, t_0)e^{-i\omega_n(\vec{k})t_0} + i\omega_n(\vec{k})B_n(\vec{k}, t_0)e^{i\omega_n(\vec{k})t_0} \end{aligned} \quad (\text{U.12})$$

where $B_n(\vec{k}, t_0) = A_n^*(-\vec{k}, t_0)$ (Eq. U.8). The time argument t_0 for the coefficients refers to the time at which the modes are matched to the trajectory.

The matching condition can be inverted to obtain the coefficients $A_n(\vec{k}(t_0))$ and $B_n(\vec{k}(t_0))$ from the trajectory and its time derivatives.

$$\begin{aligned} \begin{pmatrix} Q_n(\vec{k}, t_0) \\ \dot{Q}_n(\vec{k}, t_0) \end{pmatrix} &= \begin{pmatrix} e^{-i\omega_n(\vec{k})t_0} & e^{i\omega_n(\vec{k})t_0} \\ -i\omega_n(\vec{k})e^{-i\omega_n(\vec{k})t_0} & i\omega_n(\vec{k})e^{i\omega_n(\vec{k})t_0} \end{pmatrix} \begin{pmatrix} A_n(\vec{k}, t_0) \\ B_n(\vec{k}, t_0) \end{pmatrix} \\ \Rightarrow \begin{pmatrix} A_n(\vec{k}, t_0) \\ B_n(\vec{k}, t_0) \end{pmatrix} &= \frac{1}{2i\omega_n(\vec{k})} \begin{pmatrix} i\omega_n(\vec{k})e^{i\omega_n(\vec{k})t_0} & -e^{i\omega_n(\vec{k})t_0} \\ i\omega_n(\vec{k})e^{-i\omega_n(\vec{k})t_0} & e^{-i\omega_n(\vec{k})t_0} \end{pmatrix} \begin{pmatrix} Q_n(\vec{k}, t_0) \\ \dot{Q}_n(\vec{k}, t_0) \end{pmatrix} \\ &= \frac{1}{2} \begin{pmatrix} e^{i\omega_n(\vec{k})t_0} & -e^{i\omega_n(\vec{k})t_0} \\ e^{-i\omega_n(\vec{k})t_0} & e^{-i\omega_n(\vec{k})t_0} \end{pmatrix} \begin{pmatrix} Q_n(\vec{k}, t_0) \\ \frac{1}{i\omega_n(\vec{k})}\dot{Q}_n(\vec{k}, t_0) \end{pmatrix} \end{aligned} \quad (\text{U.13})$$

We can extract the coefficients via

$$A_n(\vec{k}, t) = e^{i\omega_n(\vec{k})t} \frac{1}{2} \left(1 - \frac{1}{i\omega_n(\vec{k})} \partial_t \right) Q_n(\vec{k}, t) \quad (\text{U.14})$$

$$B_n(\vec{k}, t) = e^{-i\omega_n(\vec{k})t} \frac{1}{2} \left(1 + \frac{1}{i\omega_n(\vec{k})} \partial_t \right) Q_n(\vec{k}, t) \stackrel{\text{Eq. U.8}}{=} A_n^*(-\vec{k}) \quad (\text{U.15})$$

The matching can be performed at any time t_0 , so that we obtain time-dependent coefficients $A_n(\vec{k}, t)$ and $B_n(\vec{k}, t)$. Therefore, we do no more use a separate symbol t_0 for the matching time.

The procedure used here provides a physical picture for collisions in the Boltzmann equation. One starts with free phonons, that is without anharmonic terms. Then one switches the anharmonic terms on for a short time slice. After that the anharmonic terms are set to zero. This experiment connects outgoing to incoming phonons. By repeating this thought experiment for different sets of incoming phonons, we can extract the collision matrix, which yields the intrinsic scattering probabilities of the Boltzmann equation. Note, however, that the description presented here still maintains the phase relations between the particles unlike the Boltzmann equation.

Harmonic oscillator: The coefficients Eq. U.14 and Eq. U.15 are closely related to quantum mechanical creation and annihilation operators for phonons. The creation and annihilation operators, in turn, are closely related to the ladder operators of the quantum mechanical harmonic oscillator.

Let us consider the algebraic treatment of the quantum-mechanical harmonic oscillator. The standard approach is to introduce creation and annihilation operators which are expressed in terms of momentum and position operators. Here we do the analogous transformation as in quantum mechanics, but we do it on the level of classical mechanics.

We start from the Hamilton function of the harmonic oscillator

$$H(p, x) = \frac{p^2}{2m} + \frac{1}{2}m\omega_0^2 x^2 = \frac{1}{2m}(-ip + m\omega_0 x)(+ip + m\omega_0 x) + m\hbar\omega_0 \frac{i}{\hbar}[p, x]_- = \hbar\omega_0 b_+(b_1.16)$$

where ω_0 is the eigenfrequency of the harmonic oscillator and

$$\begin{aligned} b_- &\stackrel{\text{def}}{=} e^{i\omega_0 t} \frac{1}{\sqrt{2m\hbar\omega_0}} (ip + m\omega_0 x) \stackrel{p=m\dot{x}}{=} e^{i\omega_0 t} \frac{1}{\sqrt{2m\hbar\omega_0}} (im\dot{x} + m\omega_0 x) \\ &= e^{i\omega_0 t} \sqrt{\frac{m}{2\hbar\omega_0}} (\omega_0 + i\partial_t) x(t) \\ b_+ &\stackrel{\text{def}}{=} e^{-i\omega_0 t} \frac{1}{\sqrt{2m\hbar\omega_0}} (-ip + m\omega_0 x) \\ &= e^{-i\omega_0 t} \sqrt{\frac{m}{2\hbar\omega_0}} (\omega_0 - i\partial_t) x(t) \end{aligned} \quad (\text{U.17})$$

The requirement that the energy is real-valued is imposed by

$$b_+ = b_-^* \quad (\text{U.18})$$

$b_{\pm}(t)$ are constants of motion of the harmonic oscillator. This can be verified by evaluating it for a general trajectory.

$$\begin{aligned} b_-(t) &= e^{i\omega_0 t} \sqrt{\frac{m}{2\hbar\omega_0}} (\omega_0 + i\partial_t) \underbrace{(Ae^{i\omega_0 t} + Be^{-i\omega_0 t})}_{x(t)} \\ &= e^{i\omega_0 t} \sqrt{\frac{m}{2\hbar\omega_0}} (A(\omega_0 - \omega_0)e^{i\omega_0 t} + (\omega_0 + \omega_0)Be^{-i\omega_0 t}) \\ &= \frac{1}{\hbar} \sqrt{2m\hbar\omega_0} B \\ b_+(t) &= e^{-i\omega_0 t} \sqrt{\frac{m}{2\hbar\omega_0}} (\omega_0 - i\partial_t) \underbrace{(Ae^{i\omega_0 t} + Be^{-i\omega_0 t})}_{x(t)} \\ &= e^{-i\omega_0 t} \sqrt{\frac{m}{2\hbar\omega_0}} (A(\omega_0 + \omega_0)e^{i\omega_0 t} + (\omega_0 - \omega_0)Be^{-i\omega_0 t}) \\ &= \frac{1}{\hbar} \sqrt{2m\hbar\omega_0} A \end{aligned} \quad (\text{U.19})$$

The variables $b_{\pm}(t)$ are, up to a constant, identical to A , B of the trajectory. Thus, the trajectory has the form

$$x(t) = \frac{\hbar}{\sqrt{2m\hbar\omega_0}} (b_+(t)e^{i\omega_0 t} + b_-(t)e^{-i\omega_0 t}) \quad (\text{U.20})$$

The introduction of the coordinates $b_{\pm}(t)$ is first and foremost a variable transform from $x(t)$ to $b_{\pm}(t)$. While the transform has been motivated by a specific physical system, the harmonic oscillator,

it can be used irrespective of whether the Hamilton function describes a harmonic oscillator or whether it also includes higher-order terms in x . Beyond this, the new variables have the special property that they are constants of motion for the harmonic system.

The occurrence of \hbar does not indicate, that we consider any quantum effects. We introduced \hbar merely to show the analogy to quantum mechanics. The factor \hbar cancels out of our final result for the atomic displacements. Our treatment of phonons is, so far, completely classical.

Back to phonons: We can use the same procedure for the phonons by introducing

$$b_{n,-}(\vec{k}, t) \stackrel{\text{def}}{=} \frac{1}{\hbar} \sqrt{2\mathcal{N}\hbar\omega_n(\vec{k})} A_n(\vec{k}, t) \quad (\text{U.21})$$

$$\stackrel{\text{Eq. U.14}}{=} e^{i\omega_n(\vec{k})t} \sqrt{\frac{2\mathcal{N}}{\hbar\omega_n(\vec{k})}} \frac{1}{2} (\omega_n(\vec{k}) + i\partial_t) Q_n(\vec{k}, t)$$

$$b_{n,+}(\vec{k}, t) \stackrel{\text{def}}{=} \frac{1}{\hbar} \sqrt{2\mathcal{N}\hbar\omega_n(\vec{k})} B_n(\vec{k}, t)$$

$$\stackrel{\text{Eq. U.15}}{=} e^{-i\omega_n(\vec{k})t} \sqrt{\frac{2\mathcal{N}}{\hbar\omega_n(\vec{k})}} \frac{1}{2} (\omega_n(\vec{k}) - i\partial_t) Q_n(\vec{k}, t) \quad (\text{U.22})$$

For later reference, let me mention that the amplitude $b_{n,-}(\vec{k})$ will turn into the **annihilation operator** $\hat{b}_n(\vec{k})$, while the **creation operator** $\hat{b}_n^\dagger(\vec{k})$ corresponds to $b_{n,-}^*(\vec{k}) = b_{n,+}(-\vec{k})$.

PHONON AMPLITUDES

The phonon amplitudes are ^a with $\sigma \in \{+, -\}$

$$b_{n,\sigma}(\vec{k}) = e^{-i\sigma\omega_n(\vec{k})t} \sqrt{\frac{\mathcal{N}}{2\hbar\omega_n(\vec{k})}} (\omega_n(\vec{k})Q_n(\vec{k}) - i\sigma\dot{Q}_n(\vec{k})) \quad (\text{U.23})$$

$$Q_n(\vec{k}) = \frac{\hbar}{\sqrt{2\mathcal{N}\hbar\omega_n(\vec{k})}} \sum_{\sigma \in \pm} b_{n,\sigma}(\vec{k}) e^{i\sigma\omega_n(\vec{k})t} \quad (\text{U.24})$$

Each set has an additional requirement, which ensures that the atomic displacements are real, namely

$$Q_n(\vec{k}, t) \stackrel{\text{Eq. 7.75}}{=} Q_n^*(-\vec{k}, t) \\ b_{n,+}(\vec{k}, t) = (b_{n,-}(-\vec{k}, t))^* \quad (\text{U.25})$$

It seems as if we have doubled the number of degrees of freedom from the complex-valued normal coordinates $Q_n(\vec{k}, t)$ to the doubled set of complex-valued phonon amplitudes $b_{n,-}(\vec{k}, t)$ and $b_{n,+}(\vec{k}, t)$. The reason for this is that the phonon amplitudes encode, for a given time t , both, value and time derivative of the normal coordinates. A result of this is that the equation of motion for the phonon amplitudes Eq. 10.2 is a first-order, rather than a second-order differential equation as the equation of motion Eq. 7.74 for the normal coordinates.

^acompare with Eq. 11 of Peierls[70].

For the derivation of the back transformation Eq. U.24, see below.¹

Trajectories: The displacement vectors for a given set of phonon amplitudes are then obtained using Eq. U.9 and Eq. U.21.

$$\begin{aligned}
 \delta R_{\alpha, \vec{k}}(t) &\stackrel{\text{Eq. 7.61}}{=} \sum_{\vec{k}} \sum_n \frac{1}{\sqrt{M_\alpha}} U_{\alpha, n}(\vec{k}) e^{i\vec{k}\vec{r}} Q_n(\vec{k}, t) \\
 &\stackrel{\text{Eq. U.24}}{=} \sum_{\vec{k}} \sum_n \frac{1}{\sqrt{M_\alpha}} U_{\alpha, n}(\vec{k}) e^{i\vec{k}\vec{r}} \left[\frac{\hbar}{\sqrt{2\mathcal{N}\hbar\omega_n(\vec{k})}} \sum_n \sum_{\sigma \in \pm} b_{n, \sigma}(\vec{k}) e^{i\sigma\omega_n(\vec{k})t} \right] \\
 &= \sum_{\vec{k}} \sum_n \frac{1}{\sqrt{M_\alpha}} U_{\alpha, n}(\vec{k}) \left[\frac{\hbar}{\sqrt{2\mathcal{N}\hbar\omega_n(\vec{k})}} \sum_{\sigma \in \pm} b_{n, \sigma}(\vec{k}) e^{i[\vec{k}\vec{r} + \sigma\omega_n(\vec{k})t]} \right] \quad (\text{U.27})
 \end{aligned}$$

Each phonon amplitude is the prefactor of a well-defined displacement wave moving (with phase velocity) into the direction of the wave vector if $\sigma = -$ and opposite to the wave vector for $\sigma = +$.

The condition that the trajectories are real-valued imposes $b_{n, +}(\vec{k}) = b_{n, -}^*(-\vec{k})$, so that the trajectory can be expressed with the help of Eq. 7.70 as

$$\delta R_{\alpha, \vec{k}}(t) = 2\text{Re} \left\{ \sum_{\vec{k}} \sum_n \frac{1}{\sqrt{M_\alpha}} U_{\alpha, n}(\vec{k}) \left[\frac{\hbar}{\sqrt{2\mathcal{N}\hbar\omega_n(\vec{k})}} b_{n, -}(\vec{k}) e^{i[\vec{k}\vec{r} - \omega_n(\vec{k})t]} \right] \right\} \quad (\text{U.28})$$

In this way, we recognize again that the general solution consists of wave with a phase velocity $\vec{v}_{ph}(\vec{k}) = \frac{\vec{k}\omega(\vec{k})}{|\vec{k}|^2}$ in the direction of the wave vector.

The ratio between displacements $\delta R_{\alpha, t}$ and phonon amplitudes $b_{n, \sigma}(\vec{k})$ depends on the frequency. This is a result of the convention used in quantum mechanics. I do not believe that it has any significance.

¹The back transformation Eq. U.24 is obtained as follows

$$\begin{aligned}
 b_n^*(-\vec{k}) &\stackrel{\text{Eq. U.23}}{=} e^{-i\omega_n(\vec{k})t} \sqrt{\frac{\mathcal{N}}{2\hbar\omega_n(\vec{k})}} (\omega_n(\vec{k})Q_n^*(-\vec{k}) - i\dot{Q}_n^*(-\vec{k})) \\
 &\stackrel{\text{Eq. 7.69}}{=} e^{-i\omega_n(\vec{k})t} \sqrt{\frac{\mathcal{N}}{2\hbar\omega_n(\vec{k})}} (\omega_n(\vec{k})Q_n(\vec{k}) - i\dot{Q}_n(\vec{k})) \\
 \Rightarrow b_n(\vec{k})e^{-i\omega_n(\vec{k})t} + b_n^*(-\vec{k})e^{i\omega_n(\vec{k})t} &= \sqrt{\frac{\mathcal{N}}{2\hbar\omega_n(\vec{k})}} 2\omega_n(\vec{k})Q_n(\vec{k}) \\
 \Rightarrow Q_n(\vec{k}) &= \frac{\hbar}{\sqrt{2\mathcal{N}\hbar\omega_n(\vec{k})}} (b_n(\vec{k})e^{-i\omega_n(\vec{k})t} + b_n^*(-\vec{k})e^{i\omega_n(\vec{k})t}) \quad (\text{U.26})
 \end{aligned}$$

Phonon energy:

$$\begin{aligned}
\hbar\omega_n(\vec{k})b_{n,-}^*(\vec{k})b_{n,-}(\vec{k}) &\stackrel{\text{Eq. U.23}}{=} \hbar\omega_n(\vec{k}) \left[e^{-i\omega_n(\vec{k})t} \sqrt{\frac{\mathcal{N}}{2\hbar\omega_n(\vec{k})}} \left(\omega_n(\vec{k})Q_n^*(\vec{k}) - i\dot{Q}_n^*(\vec{k}) \right) \right] \\
&\quad \times \left[e^{+i\omega_n(\vec{k})t} \sqrt{\frac{\mathcal{N}}{2\hbar\omega_n(\vec{k})}} \left(\omega_n(\vec{k})Q_n(\vec{k}) + i\dot{Q}_n(\vec{k}) \right) \right] \\
&= \frac{\mathcal{N}}{2} \left(\omega_n(\vec{k})Q_n(-\vec{k}) - i\dot{Q}_n(-\vec{k}) \right) \left(\omega_n(\vec{k})Q_n(\vec{k}) + i\dot{Q}_n(\vec{k}) \right) \\
&= \frac{\mathcal{N}}{2} \underbrace{\left[\dot{Q}_n(-\vec{k})\dot{Q}_n(\vec{k}) + \omega_n^2(\vec{k})Q_n(-\vec{k})Q_n(\vec{k}) \right]}_{\text{compare with Eq. 7.72}} \\
&\quad - i\omega_n(\vec{k}) \left(\dot{Q}_n(-\vec{k})Q_n(\vec{k}) - Q_n(-\vec{k})\dot{Q}_n(\vec{k}) \right) \quad (\text{U.29})
\end{aligned}$$

When we perform the \vec{k} -sum, the last term drops out because it changes sign upon inverting the wave vector.

Thus, we obtain the total energy of the harmonic system as a sum of phonon contributions. The energy is the value of the Hamilton function, which we obtain from the Lagrange function by a Legendre transform.²

$$\begin{aligned}
E_{tot}^{harm} &= \sum_{\vec{k},n} \frac{\partial \mathcal{L}^{harm}}{\partial \dot{Q}_n(\vec{k})} \dot{Q}_n(\vec{k}) - \mathcal{L}^{harm} \\
&\stackrel{\text{Eq. ??}}{=} \mathcal{N} \sum_{\vec{k},n} \frac{1}{2} \left[\dot{Q}_n(-\vec{k})\dot{Q}_n(\vec{k}) + \omega_n^2(\vec{k})Q_n(-\vec{k})Q_n(\vec{k}) \right] \\
&\stackrel{\text{Eq. U.29}}{=} \sum_{\vec{k},n} \hbar\omega_n(\vec{k})b_{n,-}^*(\vec{k})b_{n,-}(\vec{k}) \quad (\text{U.33})
\end{aligned}$$

This is the total energy for non-interacting phonons in a rigorously classical treatment. Note that this term includes kinetic and potential energy for the harmonic system.

Eq. U.33 looks like a quantum expression

$$E_{tot}^{QM} = \sum_{\vec{k},\vec{n}} \hbar\omega_n(\vec{k}) \left(\hat{b}_n^\dagger(\vec{k})\hat{b}_n(\vec{k}) + \frac{1}{2} \right) \quad (\text{U.34})$$

which is that of a harmonic oscillator for each phonon. From the quantum-mechanical treatment of the harmonic oscillator, we know that the spacing of the energy levels, as well as the zero-point energy, vanish in the classical limit $\hbar \rightarrow 0$. This is exactly what happens in our classical equation Eq. U.33, for which the phonon amplitudes are complex numbers rather than operators. Note, that

²The energy, respectively the Hamilton function $H(\vec{p}, \vec{x}, t)$, is obtained by a Legendre transform from the Lagrange function $\mathcal{L}(\vec{x}, \vec{v}, t)$. The Legendre transform can be expressed in terms of a stationary principle.

$$E = H(\vec{p}, \vec{x}, t) = \text{stat}_{\vec{v}} \left[\vec{p}\vec{v} - \mathcal{L}(\vec{x}, \vec{v}, t) \right] \quad (\text{U.30})$$

The symbol $\text{stat}_{\vec{v}}$ implies that the value is obtained at a stationary point (minimum, maximum or saddle point) with respect to the velocities \vec{v} . The stationary condition defines the **canonical momentum** \vec{p} as

$$p_j = \frac{\partial \mathcal{L}}{\partial v_j} \quad (\text{U.31})$$

so that the energy at a certain point of the trajectory $\vec{x}(t)$ is

$$E(t) = \sum_j \frac{\partial \mathcal{L}}{\partial v_j} v_j - \mathcal{L}(\vec{x}, \vec{v}, t) \quad \text{with} \quad \vec{v} = \dot{\vec{x}} \quad (\text{U.32})$$

the factor \hbar is inconsequential, as it is absorbed by a factor $\hbar^{-\frac{1}{2}}$ in the definition of the variables $b_n(\vec{k})$.

In analogy with the quantum expression we can identify $\hat{n}_n(\vec{k}) \stackrel{\text{def}}{=} b_{n,-}^*(\vec{k})b_{n,-}(\vec{k})$ with the **number of bosons**. In the classical theory, we consider here, the number of bosons is a continuous number. The concept of individual particles is a result of quantization and emerges only in the quantum theory.

Appendix V

Dictionary

caveat	Vorbehalt
coincidence	Übereinstimmung
convolution	Faltung
cross section	Wirkungsquerschnitt
aesthetics	Ästetik
factorial	Fakultät (mathematische Operation)
faculty	Fakultät (akademische Verwaltungseinheit)
for the sake of ...	um ... willen (gen)
formidable	gewaltig, eindrucksvoll
propagator	Zeitentwicklungsoperator
commutate	kommutieren
rank	Rang
scattering amplitude	Streuamplitude
without loss of generality	ohne Beschränkung der Allgemeinheit
wlog	oBdA (ohne Beschränkung der Allgemeinheit)

V.1 Explanations

- caveat: Latin, a modifying or cautionary detail to be considered

V.2 Symbols

A list of mathematical symbols can be found on the internet https://en.wikipedia.org/wiki/List_of_mathematical_symbols_by_subject. While it is the goal to adhere to a standard set of symbols, this may not have been achieved.

- A vector is represented as \vec{a} , a matrix is shown as bold-face symbol \mathbf{a} and an operator is indicated by a hat \hat{a} .
- **Natural numbers:** \mathbb{N} , **integer numbers** \mathbb{Z} , **real numbers** \mathbb{R} , **complex numbers** \mathbb{C} .
- c^* complex conjugate of the complex-valued number c .
- $O(x^n)$ stands for all terms of order n and higher of x .
- \mathbf{A}^\dagger is the **hermitian conjugate** or **adjunct** of the matrix \mathbf{A}

- A^T is the **transpose** of matrix A
- $\theta(x)$ **Heaviside function**.
- $\forall_x \dots$ "for all $x \dots$ ". $\exists_x \dots$ "there exists one x with \dots ".
- $[A, B]_- = [A, B] = AB - BA$ **commutator** of A and B . A and B may be matrices or operators.
- $[A, B]_+ = AB + BA$ **anti-commutator** of A and B . A and B may be matrices or operators.
- $\vec{a} \cdot \vec{b}$ **scalar product** between two vectors.
- $\vec{a} \times \vec{b}$ **vector product** between two three dimensional vectors \vec{a} and \vec{b} .

$$\vec{a} \times \vec{b} = \begin{pmatrix} a_y b_z - a_z b_y \\ a_z b_x - a_x b_z \\ a_x b_y - a_y b_x \end{pmatrix} \quad (\text{V.1})$$

- $\vec{a} \otimes \vec{b}$ **outer product** or **dyadic product** of two vectors \vec{a} and \vec{b} .

$$\left(\vec{a} \otimes \vec{b} \right)_{ij} = a_i b_j \quad (\text{V.2})$$

- $\det |\mathbf{A}|$ **determinant** of matrix \mathbf{A}
- $\text{perm} |\mathbf{A}|$ **permanent** of matrix \mathbf{A} . The permanent is computed like the determinant with the exceptions that all terms are summed up without the sign changes for permutations.
- δ_{ij} **Kronecker delta**

$$\delta_{ij} = \begin{cases} 1 & \text{for } i = j \\ 0 & \text{else} \end{cases} \quad (\text{V.3})$$

- $\delta(\vec{x})$ **Dirac's delta function** defined by

$$\forall_{f(x)} \int dx f(x) \delta(x) = f(0) \quad (\text{V.4})$$

which holds for all differentiable functions $f(x)$. The delta function of a vector is the product of the delta functions of its components.

- $\epsilon_{i_1, \dots, i_N}$ **Levy-Civita Symbol** or **fully-antisymmetric tensor**
- Fundamental variables:
 - e electron charge
 - m_e electron mass
 - \hbar reduced Planck constant $h/(2\pi)$
 - ϵ_0 vacuum dielectric constant
 - a_B Bohr radius $a_B = 4\pi\epsilon_0\hbar^2/(m_e e^2)$
 - H Hartree $m_e e^4/(4\pi\epsilon\hbar)^2$
 - μ_B Bohr magneton $\mu_B = e\hbar/(2m_e)$
 - k_B Boltzmann constant

Other, more special symbolsEditor: [incomplete](#)

c_s	speed of sound
c	speed of light (sometimes also speed of sound)
\vec{j}_X	current density of observable X
Ψ, Φ	many-particle wave function
ϕ, ψ	one-particle wave function
$\Theta_n(\vec{R})$	nuclear wave function
\vec{x}	combined index of spin and electronic position
\vec{r}	position
σ	spin, also occupation number, Pauli matrix
\vec{p}	momentum
\vec{R}	atomic position
\hat{H}^{BO}	Born-Oppenheimer Hamiltonian
\hat{E}^{BO}	Born-Oppenheimer surface
$ \Psi^{BO}\rangle$	Born-Oppenheimer wave function
ϵ_n	one-particle energy
E_n	many-particle energy
P_n	probability
\vec{A}	derivative couplings
$ \chi\rangle$	local orbital
ρ	density matrix, charge density
\hat{P}_j	permutation operator
v_g	group velocity
v_{ph}	phase velocity
ω	circular frequency
\vec{k}	wave vector
\vec{t}	general lattice translation vector
\vec{T}_j	primitive lattice translation vectors
\vec{g}_j	primitive reciprocal lattice vectors
\vec{G}	general reciprocal lattice vectors
\hat{S}	spin operator, symmetry operator
$f_{T,\mu}(\epsilon)$	Fermi distribution function $f_{T,\mu}(\epsilon) = 1/[1 + e^{-\frac{1}{k_B T}(\epsilon - \mu)}]$
β	thermodynamic β ; $\beta = 1/(k_B T)$
T	temperature
Ω_T, V_T	region or volume of the primitive unit cell
$\Omega(T, V, \mu)$	grand potential
$U(S, V, N)$	internal energy
p	pressure
V_g	region or volume of the primitive reciprocal unit cell
Ω	integration volume for the normalization of the wave function
$D(\epsilon)$	density of states
S	entropy
S^B	Boltzmann entropy
μ	chemical potential

Appendix W

Greek Alphabet

<i>A</i>	α	alpha	<i>N</i>	ν	nu
<i>B</i>	β	beta	Ξ	ξ	ksi
Γ	γ	gamma	<i>O</i>	$o,$	omicron
Δ	δ	delta	Π	π, ϖ	pi
<i>E</i>	ϵ, ε	epsilon	<i>P</i>	ρ, ϱ	rho
<i>Z</i>	ζ	zeta	Σ	σ, ς	sigma
<i>H</i>	η	eta	<i>T</i>	τ	tau
Θ	θ, ϑ	theta	Υ	υ	upsilon
<i>I</i>	ι	iota	Φ	ϕ, φ	phi
<i>K</i>	κ	kappa	<i>X</i>	χ	chi
Λ	λ	lambda	Ψ	ψ	psi
<i>M</i>	μ	mu	Ω	ω	omega

Appendix X

Philosophy of the Φ SX Series

In the Φ SX series, I tried to implement what I learned from the feedback given by the students which attended the courses and that relied on these books as background material.

The course should be **self-contained**. There should not be any statements “as shown easily...” if, this is not true. The reader should not need to rely on the author, but he should be able to convince himself, if what is said is true. I am trying to be as complete as possible in covering all material that is required. The basis is the mathematical knowledge. With few exceptions, the material is also developed in a sequence so that the material covered can be understood entirely from the knowledge covered earlier.

The derivations shall be **explicit**. The novice should be able to step through every single step of the derivation with reasonable effort. An advanced reader should be able to follow every step of the derivations even without paper and pencil.

All **units** are explicit. That is, formulas contain all fundamental variables, which can be inserted in any desirable unit system. Expressions are consistent with the SI system, even though I am quoting some final results in units, that are common in the field.

The equations that enter a specific step of a derivation are noted as **hyperlinks** on top of the equation sign. The experience is that the novice does not immediately memorize all the material covered and that he is struggling with the math, so that he spends a lot of time finding the rationale behind a certain step. This time is saved by being explicit about it. The danger that the student gets dependent on these indications, is probably minor, as it requires some effort for the advanced reader to look up the assumptions, an effort he can save by memorizing the relevant material.

Important results and equations are highlighted by including them in **boxes**. This should facilitate the preparations for examinations.

Portraits of the key researchers and short biographical notes provide independent associations to the material. A student may not memorize a certain formula directly, but a portrait. From the portrait, he may associate the correct formula. The historical context provides furthermore an independent structure to organize the material.

The two first books are in German (That is the intended native language) in order to not add complications to the novice. After these first books, all material is in English. It is mandatory that the student masters this language. Most of the scientific literature is available only in English. English is currently the language of science, and science is absolutely dependent on international contacts.

I tried to include many graphs and figures. The student shall become used to use all his senses in particular the **visual sense**.

I have slightly modified the selection of the material commonly taught in most courses. Some topics, which I consider of mostly historical relevance I have removed. Others such as the Noether theorem, I have added. Some, like chaos, stochastic processes, etc. I have not added yet.

X.1 Todo

- The overview gets easily lost when the mathematical derivations become lengthy. In that case it is helpful to reserve one-half blackboard for (1) definition of symbols, (2) list of assumptions, (3) brief list of main steps.
- start the lecture with a 5-min review of the previous lecture.
- present typical example calculations in the class rather than leaving it to the homework entirely. Homework examples can be integrated directly into the lecture notes.
- To bring back the context, it has been useful to summarize the topics and place them into experimental or other context. This can be done on a “shallow” level in a beamer presentation.
- Literature recommendation to wrap up the material and to provide a direction for further study.
- direct connection between lectures and exercises
- Potential theme: magnetic properties
- Thermodynamics: keep as extensive in the lecture notes and exercises, but short in teaching. (Sommerfeld expansion is known from Introduction to Solid State Physics.)
- Include a short summary at the end of each chapter
- Include a appendix with teaching goals and hints what should be known for the examination. (See Chapter 18 in Advanced Solid State Theory.)
- When teaching in presence: Require that the lecture notes are read before the lecture. Keep the notes ready on the beamer, so that one can refer to specific positions in the text.

Appendix Y

About the Author

Prof. Dr. rer. nat Peter E. Blöchl studied physics at Karlsruhe University of Technology in Germany. Subsequently he joined the Max Planck Institutes for Materials Research and for Solid-State Research in Stuttgart, where he developed of electronic-structure methods related to the LMTO method and performed first-principles investigations of interfaces. He received his doctoral degree in 1989 from the University of Stuttgart.

Following his graduation, he joined the renowned T.J. Watson Research Center in Yorktown Heights, NY in the US on a World-Trade Fellowship. In 1990 he accepted an offer from the IBM Zurich Research Laboratory in Ruschlikon, Switzerland, which had just received two Nobel prizes in Physics (For the Scanning Tunneling Microscope in 1986 and for the High-Temperature Superconductivity in 1987). He spent the summer term 1995 as visiting professor at the Vienna University of Technology in Austria, from where he was later awarded the habilitation in 1997. In 2000, he left the IBM Research Laboratory after a 10-year period and accepted an offer to be professor for theoretical physics at Clausthal University of Technology in Germany. Since 2003, Prof. Blöchl is member of the Braunschweigische Wissenschaftliche Gesellschaft (Academy of Sciences).

The main thrust of Prof. Blöchl's research is related to ab-initio simulations, that is, parameter-free simulation of materials processes and molecular reactions based on quantum mechanics. He developed the Projector Augmented Wave (PAW) method, one of the most widely used electronic structure methods to date. This work has been cited over 45,000 times.¹ It is among the 100 most cited scientific papers of all times and disciplines², and it is among the 10 most-cited papers out of more than 500,000 published in the 120-year history of Physical Review.³ Next to the research related to simulation methodology, his research covers a wide area from biochemistry, solid state chemistry to solid state physics and materials science. Prof. Blöchl contributed to 8 Patents and published about 100 research publications, among others in well-known Journals such as "Nature". The work of Prof. Blöchl has been cited over 60,000 times, and he has an H-index of 44.⁴

¹Researcher ID: B-3448-2012

²R. van Noorden, B. Maher and R. Nuzzo, Nature 514, 550 (2014)

³Oct. 15, 2014, search in the Physical Review Online Archive with criteria "a-z".

⁴Researcher ID: B-3448-2012

Bibliography

- [1] P.W. Anderson. More is different. Science, 177:393, 1972.
- [2] Peter E. Blöchl. ΦSX: Advanced Solid State Theory. Blöchl, 2017. URL <https://phisx.org/>.
- [3] Peter E. Blöchl. ΦSX: Quantum Mechanics of the Chemical Bond. Blöchl, 2015. URL <https://phisx.org/>.
- [4] Peter E. Blöchl. ΦSX: Theoretical Physics III, Quantum Theory. Blöchl, 2015. URL <https://phisx.org/>.
- [5] M. Born and R. Oppenheimer. Zur quantentheorie der molekeln. Ann. Phys., 84:457, 1927.
- [6] M. Born and K. Huang. Dynamical Theory of Crystal Lattices. Oxford University Press, Oxford, 1954.
- [7] G.A. Worth and M.A. Robb. Applying direct molecular dynamics to non-adiabatic systems. Adv. Chem. Phys., 124:355, 2002.
- [8] Felix T. Smith. Diabatic and adiabatic representations for atomic collision problems. Phys. Rev., 179:111–123, Mar 1969. doi: 10.1103/PhysRev.179.111. URL <http://link.aps.org/doi/10.1103/PhysRev.179.111>.
- [9] F. Dufey. Störungsreihen für die nichtadiabatische Kopplung mit durchschneidenden Potentialflächen. PhD thesis, Technische Universität München, 2002.
- [10] M. Baer, Á. Vibok, G. J. Halaász, and D. J. Kouri. The electronic non-adiabatic coupling terms: On the connection between molecular physics and field theory. Adv. Quantum Chem., 44:103, 2003.
- [11] Y. Aharonov and D. Bohm. Significance of electromagnetic potentials in the quantum theory. Phys. Rev., 115:485–491, Aug 1959. doi: 10.1103/PhysRev.115.485. URL <http://link.aps.org/doi/10.1103/PhysRev.115.485>.
- [12] C. N. Yang and R. L. Mills. Conservation of isotopic spin and isotopic gauge invariance. Phys. Rev., 96:191–195, Oct 1954. doi: 10.1103/PhysRev.96.191. URL <http://link.aps.org/doi/10.1103/PhysRev.96.191>.
- [13] C. Alden Mead and Donald G. Truhlar. Conditions for the definition of a strictly diabatic electronic basis for molecular systems. J. Chem. Phys., 77:6090, 1982.
- [14] Donald G. Truhlar and C. Alden Mead. Relative likelihood of encountering conical intersections and avoided intersections on the potential energy surfaces of polyatomic molecules. Phys. Rev. A, 68:032501, Sep 2003. doi: 10.1103/PhysRevA.68.032501. URL <http://link.aps.org/doi/10.1103/PhysRevA.68.032501>.
- [15] D.R. Yarkony. Diabolical conical intersections. Rev. Mod. Phys., 68:985, 1996.

- [16] C. Alden Mead. Electronic hamiltonian, wave functions, and energies, and derivative coupling between born-oppenheimer states in the vicinity of a conical intersection. J. Chem. Phys., 78: 807, 1983.
- [17] Kilian Hader, Julian Albert, E. K. U. Gross, and Volker Engel. Electron-nuclear wave-packet dynamics through a conical intersection. J. Chem. Phys., 146:74304, 2017.
- [18] J. v. Neumann and E.P. Wigner. über das verhalten von eigenwerten bei adiabatischen prozessen. Phys. Z., 30:467, 1929.
- [19] C. Zener. Non-adiabatic crossing of energy levels. Proc. Roy. Soc. A, 137:696, 1932.
- [20] C. Wittig. The landau-zener formula. J. Phys. Chem., 109:8428, 2005.
- [21] T. Holstein. Studies of polaron motion. part i. the molecular crystal model. Ann. Phys., 8: 325, 1959.
- [22] T. Holstein. Studies of polaron motion: Part ii. the "small" polaron. Ann. Phys., 8:343, 1959.
- [23] Yu A. Firsov and E.K. Kudinov. The polaron state of a crystal. Physics of the Solid State, 43: 447, 2001.
- [24] G.H. Wannier. The structure of electronic excitation levels in insulating crystals. Phys. Rev., 52:191, 1937.
- [25] Peter E. Blöchl. ΦSX: Advanced Topics of Theoretical Physics II, The statistical properties of matter. Blöchl, 2015. URL <https://phisx.org/>.
- [26] Carl D. Anderson. The positive electron. Phys. Rev., 43:491, 1933.
- [27] Peter J. Mohr, Barry N. Taylor, and David B. Newell. CODATA recommended values of the physical constants: 2010. Rev. Mod. Phys., 84:1527, 2012.
- [28] J.C. Slater. The theory of complex spectra. Phys. Rev., 34:1293, 1929.
- [29] J.C. Slater. Cohesion in monovalent metals. Phys. Rev., 35:509, 1930.
- [30] M.I. Aroyo, editor. International Tables for Crystallography, volume A. Wiley, second edition, 2016. doi: doi:10.1107/97809553602060000114. URL <http://it.iucr.org/Ac/>.
- [31] J.C. Slater and G.F. Koster. Simplified LCAO method for the periodic potential problem. Phys. Rev., 94:1498, 1954.
- [32] Ole K. Andersen and Ove Jepsen. Explicit, first-principles tight-binding theory. Phys. Rev. Lett., 53:2571, 1984.
- [33] P. R. Wallace. The band theory of graphite. Phys. Rev., 71:622, 1947.
- [34] J.G. Bednorz and K.A. Müller. Possible high T_c superconductivity in the Ba-La-Cu-O system. Z. Phys., 64:189, 1986. Original paper on High- T_c superconductors.
- [35] N. F. Mott. Rare-earth compounds with mixed valencies. Phil. Mag., 30:403, 1974.
- [36] B. Coqblin and A. Blandin. Stabilité des moments magnétiques localisés dans les métaux. Adv. Phys., 17:281, 1968.
- [37] Mohsen Sotoudeh, Sangeeta Rajpurohit, Peter Blöchl, Daniel Mierwaldt, Jonas Norpoth, Vladimir Roddatis, Stephanie Mildner, Birte Kressdorf, Benedikt Iffland, and Christian Jooss. Electronic structure of $\text{Pr}_{1-x}\text{Ca}_x\text{MnO}_3$. Phys. Rev. B, 95:235150, Jun 2017. doi: 10.1103/PhysRevB.95.235150. URL <https://link.aps.org/doi/10.1103/PhysRevB.95.235150>.

- [38] Peter E. Blöchl. ΦSX: Theoretical Physics IV, Statistical Physics. Blöchl, 2015. URL <https://phisx.org/>.
- [39] R. Hoffmann. Nobel Lectures Chemistry, 1981-1990, chapter Building Bridges between inorganic and Organic Chemistry. World Scientific, Singapore, 1992.
- [40] R. Hoffmann. A chemical and theoretical way to look at bonding on surfaces. Rev. Mod. Phys., 60:601, 1988.
- [41] R. Dronskowski and P.E. Blöchl. Crystal orbital Hamilton populations (COHP). Energy-resolved visualization of chemical bonding in solids based on density-functional calculations. J. Phys. Chem., 97:8617, 1993.
- [42] John P. Perdew, Kieron Burke, and Matthias Ernzerhof. Generalized gradient approximation made simple. Phys. Rev. Lett, 77:3865, 1996.
- [43] E.T. Jaynes. Information theory and statistical mechanics. Phys. Rev., 106:620, 1957.
- [44] E.T. Jaynes. Information theory and statistical mechanics ii. Phys. Rev., 108:171, 1957.
- [45] C.E. Shannon. A mathematical theory of computation. Bell. Syst. Techn. J., 22:379, 1948.
- [46] A. D. McNaught and A. Wilkinson, editors. IUPAC Compendium of Chemical Terminology. Blackwell Scientific Publications, Oxford, 2 edition, 1997. doi: doi:10.1351/goldbook. URL <http://goldbook.iupac.org>.
- [47] E.R. Cohen and P. Giamoco. Symbols, units, nomenclature and fundamental constants in physics 1987 revision. Physica, 146A:1, 1987. URL iupap.org/wp-content/uploads/2014/05/A4.pdf.
- [48] I.N. Bronstein and K.A. Semendjajew. Taschenbuch der Mathematik. BSB B.G. eubner Verlagsgesellschaft, Leipzig, 1983.
- [49] W. Jones and N.H. March. Theoretical Solid State Physics: Perfect Lattices in Equilibrium, volume 1. Dover, 1985.
- [50] J. W. Lynn, H. G. Smith, and R. M. Nicklow. Lattice dynamics of gold. Phys. Rev. B, 8: 3493–3499, Oct 1973. doi: 10.1103/PhysRevB.8.3493. URL <http://link.aps.org/doi/10.1103/PhysRevB.8.3493>.
- [51] Werner Weber. Adiabatic bond charge model for the phonons in diamond, si, ge, and $\alpha - \text{Sn}$. Phys. Rev. B, 15:4789–4803, May 1977. doi: 10.1103/PhysRevB.15.4789. URL <http://link.aps.org/doi/10.1103/PhysRevB.15.4789>.
- [52] Albert Einstein. Die plancksche theorie der strahlung und die theorie der spezifischen wärme. Annalen der Physik, 327(1):180–190, 1907. ISSN 1521-3889. doi: 10.1002/andp.19063270110. URL <http://dx.doi.org/10.1002/andp.19063270110>.
- [53] Manuel Cardona. Albert einstein as the father of solid state physics. ArXiv Physics e-prints, 2005.
- [54] Lars Onsager. Reciprocal relations in irreversible processes i. Phys. Rev., 37:405, 1931.
- [55] Lars Onsager. Reciprocal relations in irreversible processes ii. Phys. Rev., 38:2265, 1931.
- [56] Paul Ehrenfest and Tatjana Ehrenfest. **Enzyklopädie der Mathematischen Wissenschaften**, volume IV:32, chapter Begriffliche Grundlagen der statistischen Auffassung in der Mechanik. 1907. URL <https://gdz.sub.uni-goettingen.de/id/PPN360619320?tfify=%7B%22pages%22%3A%5B789%5D%2C%22view%22%3A%22scan%22%7D>.

- [57] E. T. Jaynes. Gibbs vs boltzmann entropies. Am. J. Phys., 33:391, 1965.
- [58] von Neumann. Mathematische Grundlagen der Qantenmechanik. Springer, Berlin, 1932.
- [59] Cédric Villani. Handbook of Mathematical Fluid Dynamics, volume 1, chapter A review of mathematical topics in collisional kinetic theory, pages 71–305. North Holland, Amsterdam, 2002. URL https://cedricvillani.org/sites/dev/files/old_images/2012/07/B01.Handbook.pdf.
- [60] Cédric Villani. Mathematics of granular materials. Technical report. URL https://www.cedricvillani.org/sites/dev/files/old_images/2012/08/B06.Granular1.pdf.
- [61] David Pines and David Bohm. A collective description of electron interactions: li. collective vs individual particle aspects of the interactions. Phys. Rev., 85:338, 1952.
- [62] Michael O. Marder. Condensed Matter Physics. John Wiley and Sons, 2000. ISBN 0-471-17779-2.
- [63] O.K. Andersen and O. Jepsen. Advances in the theory of one-electron energy states. Physica B+C, 91:317 – 328, 1977. ISSN 0378-4363. doi: [https://doi.org/10.1016/0378-4363\(77\)90200-5](https://doi.org/10.1016/0378-4363(77)90200-5). URL <http://www.sciencedirect.com/science/article/pii/0378436377902005>.
- [64] Arnaud Manas. Fifty shades of yellow: a color model for gold-silver-copper alloys. Gold Bulletin, 51:205, 2018.
- [65] J. S. Smith, A. Budi, M. C. Per, N. Vogt, D. W. Drumm, L. C. L. Hollenberg, J. H. Cole, and S. P. Russo. Ab initio calculation of energy levels for phosphorus donors in silicon. Scientific Reports, 7:6010, 2017.
- [66] F. C. Zhang and T. M. Rice. Effective hamiltonian for the superconducting cu oxides. Phys. Rev. B, 37:3759–3761, Mar 1988. doi: 10.1103/PhysRevB.37.3759. URL <https://link.aps.org/doi/10.1103/PhysRevB.37.3759>.
- [67] C.-C. Chen, M. Sentef, Y. F. Kung, C. J. Jia, R. Thomale, B. Moritz, A. P. Kampf, and T. P. Devereaux. Doping evolution of the oxygen k -edge x-ray absorption spectra of cuprate superconductors using a three-orbital hubbard model. Phys. Rev. B, 87:165144, Apr 2013. doi: 10.1103/PhysRevB.87.165144. URL <https://link.aps.org/doi/10.1103/PhysRevB.87.165144>.
- [68] Iman Santoso, Wei Ku, Tomonori Shirakawa, Gerd Neuber, Xinmao Yin, M. Enoki, Masaki Fujita, Ruixing Liang, T. Venkatesan, George A. Sawatzky, Aleksei Kotlov, Seiji Yunoki, Michael Rübhausen, and Andrivo Rusydi. Unraveling local spin polarization of zhang-rice singlet in lightly hole-doped cuprates using high-energy optical conductivity. Phys. Rev. B, 95:165108, 2017.
- [69] Yukihiro Matsubayashi and Sumio Ishihara. Numerical study of resonant inelastic x-ray scattering at the oxygen k edge in insulating cuprates. Phys. Rev. Lett., 107:075121, 2023.
- [70] R. Peierls. Zur kinetischen theorie der wärmeleitung in kristallen. Ann. Phys., 3:1055, 1929.
- [71] R. Brout and I. Prigogine. Statistical mechanics of irreversible processes. Physica, 22:35, 1956.
- [72] G. Klein and I. Prigogine. Sur la mécanique statistique des phénomènes irréversibles i. Physica, 19:74, 1953.
- [73] G. Klein and I. Prigogine. Sur la mécanique statistique des phénomènes irréversibles ii. Physica, 19:89, 1953.

- [74] G. Klein and I. Prigogine. Sur la mécanique statistique de phénomènes irréversibles iii. Physica, 19:1053, 1953.
- [75] I. Prigogine and R. Bingen. Sur la mécanique statistique des phénomènes irréversibles iv. Physica, 21:299, 1955.
- [76] J.M. Ziman. Electrons and Phonons: The Theory of Transport Phenomena in Solids. Oxford at the Clarendon Press, 1960.
- [77] L. van Hove. Quantum-mechanical perturbations giving rise to a statistical transport equation. Physica, 21:517, 1955.
- [78] L. van Hove. The approach to equilibrium in quantum statistics. Physica, 23:441, 1957.
- [79] Herbert Spohn. Kinetic equations for quantum many-particle systems. Arxiv, 0706:0807, 2007.
- [80] D.A. Broido, A. Ward, and N. Mingo. Lattice thermal conductivity of silicon from empirical interatomic potentials. Phys. Rev. B, 72:14308, 2005.
- [81] D. A. Broido, M. Malorny, G. Birner, Natalio Mingo, and D. A. Stewart. Intrinsic lattice thermal conductivity of semiconductors from first principles. Appl. Phys. Lett., 91:231922, 2007.
- [82] Pierre Hohenberg and Walter Kohn. Inhomogeneous electron gas. Phys. Rev., 136:B864, 1964. doi: 10.1103/PhysRev.136.B864. URL <http://link.aps.org/doi/10.1103/PhysRev.136.B864>.
- [83] Walter Kohn and Lu J. Sham. Self-consistent equations including exchange and correlation effects. Phys. Rev., 140:A1133, 1965. doi: 10.1103/PhysRev.140.A1133. URL <http://link.aps.org/doi/10.1103/PhysRev.140.A1133>.
- [84] R. McWeeny. Some recent advances in density matrix theory. Rev. Mod. Phys., 32:334, 1960.
- [85] A. Puzder, M.Y. Chou, and R.Q. Hood. Exchange and correlation in the Si atom: A quantum monte carlo study. Phys. Rev. A, 64:22501, 2001.
- [86] Mark S. Hybertsen and Steven G. Louie. Electron correlation in semiconductors and insulators: Band gaps and quasiparticle energies. Phys. Rev. B, 34:5390, 1986.
- [87] Pierre Hohenberg and Walter Kohn. Inhomogeneous electron gas. Phys. Rev., 136:B864, 1964. doi: 10.1103/PhysRev.136.B864. URL <http://link.aps.org/doi/10.1103/PhysRev.136.B864>.
- [88] Mel Levy. Universal variational functionals of electron densities, first order density matrixes and natural spin-orbitals and solution of the v-representability problem. Proc. Nat'l Acad. Sci. USA, 76:6062, 1979. URL <http://www.pnas.org/content/76/12/6062.abstract>.
- [89] M. Levy. Electron densities in search of hamiltonians. Phys. Rev. A, 26:1200, 1982.
- [90] Elliott H. Lieb. Density functionals for coulomb systems. Int. J. Quantum Chem., 24(3): 243–277, 1983. ISSN 1097-461X. doi: 10.1002/qua.560240302. URL <http://dx.doi.org/10.1002/qua.560240302>.
- [91] J. Harris and R.O. Jones. The surface energy of a bounded electron gas. J. Phys. F: Met. Phys., 4:1170, 1974.
- [92] David C. Langreth and John P. Perdew. The exchange–correlation energy of a metallic surface. Sol. St. Commun., 17:1425, 1975.
- [93] Olle Gunnarsson and Bengt I. Lundquist. Exchange and correlation in atoms, molecules, and solids by the spin-density-functional formalism. Phys. Rev. B, 13:4274, 1976.

- [94] John P. Perdew and Karla Schmidt. Jacob's ladder of density functional approximations for the exchange-correlation energy. AIP Conf. Proc., 577:1, 2001.
- [95] K. Schwarz. Optimization of the statistical exchange parameter α for the free atoms through nb. Phys. Rev. B, 5:2466, 1971.
- [96] I. Lindgren and K. Schwarz. Analysis of the electronic exchange in atoms. Phys. Rev. A, 5: 542, 1972.
- [97] D.M. Ceperley and B.J. Alder. Ground state of the electron gas by a stochastic method. Phys. Rev. Lett., 45:566, 1980.
- [98] J.P. Perdew and A. Zunger. Self interaction correction to density-functional approximations for many-electron systems. Phys. Rev. B, 23:5048, 1981.
- [99] David Bohm and David Pines. A collective description of electron interactions: iii. coulomb interactions in a degenerate electron gas. Phys. Rev., 92:609, 1953.
- [100] Robert O. Jones and Olle Gunnarsson. The density functional formalism, its applications and prospects. Rev. Mod. Phys., 61:689, 1989.
- [101] A. D. Becke. Density-functional exchange energy with correct asymptotic behavior. Phys. Rev. A, 38:3098, 1988.
- [102] John P. Perdew, Robert G. Parr, Mel Levy, and Jose L. Balduz. Density-functional theory for fractional particle number: Derivative discontinuities of the energy. Phys. Rev. Lett., 49: 1691–1694, Dec 1982. doi: <http://dx.doi.org/10.1103/PhysRevLett.49.1691>. URL <http://link.aps.org/doi/10.1103/PhysRevLett.49.1691>.
- [103] Leonard Kleinman. Reply to "comment on 'significance of the highest occupied kohn-sham eigenvalue' ". Phys. Rev. B, 56:16029–16030, Dec 1997. doi: 10.1103/PhysRevB.56.16029. URL <https://link.aps.org/doi/10.1103/PhysRevB.56.16029>.
- [104] A. Klamt, V. Jonas, T. Bürger, and J.W. Lohrenz. Refinement and parameterization of cosmo-rs. J. Phys. Chem. A, 102:5074, 1998.
- [105] M. Dion, H. Rydberg, E. Schröder, D. C. Langreth, and B. I. Lundqvist. Van der waals density functional for general geometries. Phys. Rev. Lett, 92:246401, 2004.
- [106] R. Lizarraga Jurado. Non-collinear Magnetism, in d- and f-electron systems. PhD thesis, Upsala University, 2002. URL <https://www.diva-portal.org/smash/get/diva2:168187/FULLTEXT01.pdf>.
- [107] Peter E. Blöchl. ΦSX: Theoretische Physik II, Elektrodynamik. Blöchl, 2015. URL <https://phix.org/>.
- [108] M. Baer. Topological effects in molecular systems: an attempt towards a complete theory. Chem. Phys., 259:123, 2000.
- [109] M. Born and V. Fock. Beweis des adiabatenatzes. Z. Phys., 51:165, 1928.
- [110] Peter E. Blöchl. ΦSX: Theoretische Physik I, Klassische Mechanik. Blöchl, 2015. URL <https://phix.org/>.
- [111] Ahren W. Jasper, Chaoyuan Zhu, Shikha Nangia, and Donald G. Truhlar. Introductory lecture: Nonadiabatic effects in chemical dynamics. Faraday Discuss., 127:1, 2004.
- [112] John C. Tully. Mixed quantum-classical dynamics. Faraday Discuss., 110:407, 1998. doi: <https://doi.org/10.1039/A801824C>.

- [113] Roberto Car and Michele Parrinello. Unified approach for molecular dynamics and density-functional theory. *Phys. Rev. Lett.*, 55:2471, 1985. doi: 10.1103/PhysRevLett.55.2471. URL <http://link.aps.org/doi/10.1103/PhysRevLett.55.2471>.
- [114] M.V. Berry. Quantal phase factors accompanying adiabatic changes. *Proc. Roy. Soc. A*, 392:45, 1984.
- [115] P. Ehrenfest. Bemerkung über die angenäherte Gültigkeit der klassischen mechanik innerhalb der Quantenmechanik. *Zeitschr. Phys.*, 45:455, 1927.
- [116] John C. Tully and Richard K. Preston. Trajectory surface hopping approach to nonadiabatic molecular collisions: The reaction of H^+ with D_2 . *J. Chem. Phys.*, 55:562, 1971.
- [117] John C. Tully. Molecular dynamics with electronic transitions. *J. Chem. Phys.*, 92:1061, 1990.
- [118] M. Baer and G.D. Billing, editors. *The role of degenerate states in chemistry*, volume 124 of *Adv. Chem. Phys.* John Wiley and Sons, 2002.
- [119] M.S. Child. Early perspectives on geometric phase. *Adv. Chem. Phys.*, 124:1, 2002.
- [120] Michael Baer. *Beyond Born-Oppenheimer: Conical Intersections and Electronic Nonadiabatic Coupling Terms*. John Wiley, 2006.
- [121] M. Persson and B. Hellsing. Electronic damping of adsorbate vibrations on metal surfaces. *Phys. Rev. Lett.*, 49:662, 1982.
- [122] Yinggang Li and Göran Wahnström. Molecular-dynamics simulation of hydrogen diffusion in palladium. *Phys. Rev. B*, 46:14528, 1992.
- [123] Nicola A. Spaldin. A beginner's guide to the modern theory of polarization. *J. Solid State Chem.*, 195:2, 2012. doi: 10.1016/j.jssc.2012.05.010. URL <https://arxiv.org/abs/1202.1831>.
- [124] R.D. King-Smith and D. Vanderbilt. Theory of polarization of crystalline solids. *Phys. Rev. B*, 47:1651, 1993.
- [125] Ali Abedi, Neepa T. Maitra, and E. K. U. Gross. Exact factorization of the time-dependent electron-nuclear wave function. *Phys. Rev. Lett.*, 105:123002, 2010.
- [126] Ali Abedi, Neepa T. Maitra, and E. K. U. Gross. Correlated electron-nuclear dynamics: Exact factorization of the molecular wavefunction. *J. Chem. Phys.*, 137:22a530, 2012.
- [127] L. Landau. Zur Theorie der Energieübertragung II. *Phys. Z.*, 2:46, 1932. Landau-Zener Caution: error of error by 2π .
- [128] Amar C. Vutha. A simple approach to the Landau-Zener formula. *Eur. J. Phys.*, 31:389, 2010. doi: 10.1088/0143-0807/31/2/016.
- [129] E. Teller. Crossing of potential surfaces. *J. Phys. Chem.*, 41:109, 1937. doi: 10.1021/j150379a010.
- [130] Joao Pedro Malhado and James T. Hynes. Non-adiabatic transition probability dependence on conical intersection topography. *J. Chem. Phys.*, 145:194104, 2016.
- [131] J. H. Van Vleck. The Jahn-Teller effect and crystalline Stark splitting for clusters of the form XY_6 . *J. Chem. Phys.*, 7:72, 1939.
- [132] H.C. Longuet-Higgins, U. Opik, M.H.L. Pryce, and R.A. Sack. Studies of the Jahn-Teller effect II. The dynamical problem. *Proc. Roy. Soc. A*, 244:1, 1958.

- [133] P.W. Higgs. Broken symmetries and the masses of gauge bosons. Phys. Rev. Lett, 13:508, 1964.
- [134] L. Verlet. Computer "experiments" on classical fluids i. thermodynamical properties of lennard-jones molecules. Phys. Rev., 159:98, 1967.
- [135] N.W. Ashcroft and N.D. Mermin. Solid State Physics. Thomson Learning, 1987.
- [136] H. Haug and A.-P. Jauho. Quantum Kinetics in Transport and Optics of Semiconductors, volume 2. Springer, 1996.

Index

- acceptor
 - electron, 310
- acoustic branch, 245
- action, 70
- action principle, 220
- adiabatic principle, 51
- adiabatic connection, 387
- adiabatic representation, 414
- adiabatic theorem, 423
- adibatic theorem, 434
- adjacent, 27
- adjunct, 567
- Aharonov-Bohm effect, 52
- anharmonic terms, 216
- annihilation operator, 562
- annihilation operator, 242
- annihilation operators, 503
- anticommutator, 505
- antisymmetric tensor, 94
- Arrhenius law, 64
- austenite, 307
- avoided crossing, 310
- avoided crossing, 59

- band structure, 121, 180
- bare, 273
- bcc, 305
- Berry phase, 443, 477
- Besselfunction
 - half-integer order, 372
 - spherical, 372
- bi-orthonormality condition, 38
- biorthogonality, 282
- Bloch vector, 130
- Bloch's theorem, 132
- body-centered cubic, 305
- Bohr magneton, 202, 205, 209
- Bohr magneton, 89
- Boltzmann constant, 187
- Boltzmann distribution, 190
- Boltzmann entropy, 269
- Boltzmann equation, 262, 276
- Born-Huang framework, 43, 44
- Born-Huang expansion, 45
- Born-Oppenheimer dynamics:, 58
- Born-Oppenheimer dynamics, 428
- Born-Oppenheimer approximation, 43, 51
- Born-Oppenheimer equation, 45
- Born-Oppenheimer surface, 44, 45, 51
- Born-Oppenheimer wave functions, 44, 45
- Bose distribution, 251
- Bose-Einstein condensation, 190
- Bose distribution, 190
- Boson, 93
- boson, 85
- Brillouin zone, 134, 224
- Brillouin-zone integration, 176
- bucky ball, 145
- bulk modulus, 202

- camel back, 309
- canonical momentum, 70
- canonical transform, 70
- carbon nanotube, 145
- chemical potential, 187
- coherence time, 278
- COHP, 178
- collision term, 262
- commutator, 568
- complex number
 - set of, 567
- conductivity
 - electric, 285
- conductivity
 - electric, 298
- conical intersection, 55, 56, 418, 469, 472
- conical intersections, 43
- constrained search, 527
- contraction, 336, 366
- COOP, 178
- coordinates
 - relative, 128
- correspondence principle, 261
- correspondence principle, 126
- correspondence principle, 125
- covalent bond, 24
- creation operator, 562
- creation operator, 242, 503
- crystal-orbital Hamilton population, 178
- crystal-orbital overlap population, 178

- crystallographic space groups, 127
- cuprate, 315
- current
 - thermo-electric, 294
- Darwin shift, 304
- Debye frequency, 249
- Debye temperature, 250
- degenerate
 - Fermi gas, 190
- degenerate electron gas, 203
- degenerate seam, 417
- degenerate seam, 57
- delta function, 568
- density
 - two-particle, 370
- density of states, 176
- density of states
 - free-electron gas, 182
 - total, 178
- density of states
 - operator, 177
 - projected, 178
- density-matrix functional, 527
- density matrix, 433
 - von Neumann, 183
 - N-particle, 366
 - one-particle reduced, 367
- density matrix
 - one-particle reduced, 101
- density matrix
 - von Neumann, 268
- density operator, 183, 366
- derivative coupling, 48
 - first, 48
 - second, 48
- detailed balance, 271
- determinant, 568
- diabatic representation, 54, 414, 453
- diagonalizable, 282
- dimensional bottleneck, 19
- Dirac comb, 32
- Dirac atom, 32
- Dirac sea, 123, 124
- Dirac's delta function, 568
- Dirac equation, 86
- dispersion relation, 121
- dispersion relation, 180
- dispersion relation
 - phonons, 228
- donor
 - electron, 310
- dopant, 310
- dressed, 273
- drift term, 262
- dyadic product, 568
- dynamical matrix
 - k-dependent, 227
- dynamical phase, 429
- effective mass, 308
- Ehrenfest dynamics, 58
- Ehrenfest dynamics, 431, 435, 436
- Ehrenfest theorem, 431
- eigenvalue problem
 - generalized, 21
- eigenvector
 - left-handed, 38
- eigenvector
 - right-handed, 38
- eigenvectors
 - left-handed, 282
 - right-handed, 282
- Einstein frequency, 248
- elastic, 272
- electric conductivity, 294
- electric conductivity, 285
- electric resistance, 285
- electron gas
 - degenerate, 203
- electron-gas parameter, 182, 204, 207
- electron-phonon coupling, 214
- electron-phonon coupling
 - adiabatic, 217
 - non-adiabatic, 217
- electron-phonon coupling
 - adiabatic, 217
- electron-phonon coupling, 62
- electrons
 - conduction, 124
- ensemble, 101, 183, 433
- ensemble
 - thermal, 101
- entanglement, 427
- entropy
 - Boltzmann, 269
 - Shannon, 268
 - von Neumann, 184, 268
- exchange-correlation hole, 109
- exchange-correlation hole function, 375
- exchange and correlation energy, 383
- exchange energy, 119
- exchange interaction, 380, 394
- excitations
 - electronic, 217
- exclusion principle, 265
- expectation value
 - thermal, 183

- extended zone scheme, 134
 extended zone scheme, 295
- face-centered cubic, 305
 fcc, 305
 Fermi distribution, 101
 Fermi energy, 182, 189
 Fermi level, 124, 189
 Fermi momentum, 182
 Fermi velocity, 204, 205
 Fermi wave vector, 182
 Fermi-distribution function, 188
 Fermion, 85, 93
 Fermi distribution, 190
 Fermi distribution function, 37
 Fermi gas
 - degenerate, 190
 field-strength tensor, 54
 field-strength tensor
 - generalized, 442
 Fock space, 381
 force, 123
 Franck-Condon principle, 46
 free-electron gas, 179
 free-electron gas
 - density of states, 182
 Friedel oscillations, 108
 fullerene, 145
 fully-antisymmetric tensor, 568
 fully-antisymmetric tensor, 94
- g-factor, 88, 202
 gauge transformation, 54
 Generalized gradient approximations, 398
 geometric phase, 57
 geometrical phase, 443
 geometric phase, 477
 GGA, 398
 grand canonical ensemble, 187
 grand potential, 185, 187, 270
 graphene, 145
 graphite, 145
 ground-state energy, 216
 ground-state energy, 214
 group, 509
 GW approximation, 389
 gyro-magnetic ratio, 202, 205, 209
- Hamilton function, 122
 Hamilton's equations, 122
 Hamilton's equations of motion, 431
 harmonic oscillator, 220
 Hartree energy, 118
 heat, 185
 heat capacity, 199, 290
 Heaviside function, 568
 heavy hole, 309
 heavy-hole band, 203, 309
 Hellmann-Feynman theorem, 388
 hermitian conjugate, 567
 hexagonally closed packed, 305
 hfp, 305
 Higgs mechanism, 470
 high- T_c superconductor, 151
 high-symmetry points, 138
 hole, 124
 hopping parameter, 64
 Hund's rule, 104
 Hund's rule, 119, 378
 hybrid functionals, 390
 hypotenuse, 27
- Impurity scattering, 266
 impurity scattering, 264
 incompressible flow, 260
 inelastic, 272
 inelastic process, 272
 integer number
 - set of, 567
 interaction
 - screened, 20
 interaction picture, 330
 interaction picture
 - classical, 242
 intrinsic scattering probabilities, 264
 intrinsic scattering probability, 265
 intrinsic probabilities of transition, 349, 359
 irreducible zone, 138
- Jacob's ladder, 392
 Jahn-Teller effect, 443
 Jahn-Teller model, 43, 57, 469
 jellium oxide, 312
 jellium model, 103, 179
 jelly-O, 312
- Kronecker delta, 568
- Lagrange function, 70
 Landau-Zener formula, 58
 Landau-Zener formula, 431
 law of thermodynamics
 - second, 268
 LCAO method, 135
 Legendre transform, 185, 552
 Legendre transform, 384
 level repulsion, 303
 level repulsion, 132

- level repulsion, 21–24
- Levi-Civita symbol, 94
- Levy-Civita Symbol, 568
- lifetime, 20, 125, 281
- light hole, 309
- light-hole band, 203, 309
- Liouville operator, 282
- Liouville's theorem, 260
- longitudinal
 - waves, 245
- magnetic susceptibility, 202
- magnetic anisotropy, 19
- magnetic moment, 88
- mass, 123
 - effective, 20
- mass
 - effective, 124
- maximum-entropy principle, 184
- maximum-entropy principle, 269, 527
- molecular chaos, 265, 268
- molecular chaos hypothesis, 277
- molecular dynamics, 43, 77, 428
 - ab-initio, 428
- momentum conservation
 - phonons, 331
- momentum
 - canonical, 564
- multiplet, 417
- multiplet structure, 418
- natural numbers
 - set of, 567
- natural orbitals, 101
- nesting, 156
- non-adiabatic effects, 43
- non-adiabatic effects, 51
- non-collinear, 87
- non-crossing theorem, 43, 55, 417
- non-radiative transition, 52
- normal coordinates, 227, 228
- number of bosons, 565
- number representation, 186
- oblate, 469
- occupation, 101
- occupation numbers, 186
- occupation-number operator, 506
- occupation-number representation, 99
- Ohm's law, 285, 290
- one-particle operator, 99
- one-particle wave function, 94
- open system, 427
- opposite, 27
- optic branch, 245
- orbital populations, 178
- orbital-mixing angle, 25
- orbital sum rule, 21
- outer product, 568
- P-wave, 246
- pair-correlation function, 374
- particle-number operator, 506
- partition function, 184
- Pauli equation, 86
- Pauli matrix, 86
- Pauli principle, 18, 265
- Peierls' theorem, 320
- periodic boundary conditions, 173
- periodic zone scheme, 134
- permanent, 568
- permutation operator, 93, 94
- phase
 - geometric, 477
- phase space, 260
- phonon, 43, 62
- phonon amplitude, 232
- phonon amplitudes, 562
- phonon band structure, 213
- phonon number, 232
- phonon-phonon coupling, 216
- phonons, 213
- point-group symmetry, 127
- polariton
 - phonon, 247
- polaron, 62, 469
- polaron
 - large, 65
- polaron
 - large, 65
- polaron binding energy, 62, 63, 72
- polaron hopping, 63
- positron, 86
- positron annihilation, 123
- pressure, 185, 201
- pressure wave, 246
- product state, 96
- product wave function, 94
- projector functions, 177
- prolate, 469
- pseudopotential method, 131
- quantization
 - second, 233
- quantum field theory, 213
- quantum numbers, 91
- quasi particles, 99
- quasi-particle, 273

- quasi-particle energies, 528
 quasiparticles, 122
- Rabi frequency, 58, 59, 455
 random-phase approximation, 277, 394, 433
 initial, 336
 repeated, 342
 rank, 94
 real number
 set of, 567
 reciprocal lattice vectors, 128
 reduced zone scheme, 134
 reduced zone scheme, 295
 relaxation time, 280
 resistance
 electric, 285
 resistivity, 285
 reststrahl absorption, 246
 Riemann series theorem, 219
 RPA, 394
- S-wave, 246
 scalar product, 568
 scattering
 impurities, 264
 scattering probability
 intrinsic, per unit time, 264
 screening, 20
 seam
 degenerate, 55
 second quantization, 213
 secular equation, 73
 Seebeck coefficient, 290, 294
 Seitz radius, 182, 204, 207
 self energy, 528
 self-energy correction, 273
 self-polarization, 63
 self energy
 classical, of charges, 119
 self energy
 Boltzmann equation, 525
 separation of variables, 100
 shear wave, 246
 simple oxides, 312
 singular-value decomposition, 287
 sink, 260
 Slater determinant, 186
 Slater determinant, 97
 Sommerfeld expansion, 194
 Sommerfeld coefficient, 201
 Sommerfeld expansion, 512
 sound waves, 246
 source, 260
 source density, 260
- spectral function, 275, 317
 spin, 86
 spin susceptibility
 Pauli, 202
 spin-orbit coupling, 309
 spinor, 85
 spin orbitals, 85
 split-off band, 309
 standard model, 17
 steel, 305
 stray fields, 19
 strong correlations, 99
 sum rule
 orbital, 21
 trace, 21
 Surface hopping, 59
 surface-hopping method, 432
 susceptibility
 magnetic, 202
 spin, Pauli, 202
 symmetry, 90
- tangent half-angle formula, 74
 tensor
 fully-antisymmetric, 94, 568
 thermo-electric current, 294
 thermodynamic beta, 187
 thermoelectric coefficient, 298
 thermoelectric coefficient, 294
 thermoelectric current, 298
 tight-binding orbitals
 ab-initio, 135
 time-inversion symmetry, 56
 trace sum rule, 21
 transformation operator, 90
 transition
 vertical, 304
 transition-state theory, 64
 transition rate
 equilibrium, 361
 transpose, 568
 transversal
 waves, 246
 two-particle density, 370
- umklapp process, 230, 332
 umklapp process, 332
 unit cell
 primitive, 127
 universal density functional, 381
- vacuum state, 503
 vector product, 568
 velocity, 123

velocity

 group velocity, 126

Verlet algorithm, 488

vertical process, 125

vertical transition, 304

Wigner Seitz cell, 134

Yang-Mills fields, 52

Zeeman splitting, 202

zero state, 503

zone scheme

 extended, 295

zone scheme, reduced, 295